

Rohana Hassan · Marina Yusoff
Anizahyati Alisibramulisi · Norliyati Mohd Amin
Zulhabri Ismail *Editors*

InCIEC 2014

Proceedings of the International
Civil and Infrastructure Engineering
Conference 2014

InCIEC 2014

Rohana Hassan · Marina Yusoff
Anizahyati Alisibramulisi
Norliyati Mohd Amin · Zulhabri Ismail
Editors

InCIEC 2014

Proceedings of the International Civil
and Infrastructure Engineering
Conference 2014

Editors

Rohana Hassan
Institute for Infrastructure Engineering
and Sustainable Management (IIESM)
Universiti Teknologi MARA
Shah Alam, Selangor
Malaysia

Marina Yusoff
IIESM
Universiti Teknologi MARA
Shah Alam, Selangor
Malaysia

Anizahyati Alisibramulisi
Faculty of Civil Engineering
Universiti Teknologi MARA
Shah Alam, Selangor
Malaysia

Norliyati Mohd Amin
IIESM
Universiti Teknologi MARA
Shah Alam, Selangor
Malaysia

Zulhabri Ismail
Faculty of Architecture, Planning
and Surveying
Universiti Teknologi MARA
Shah Alam, Selangor
Malaysia

ISBN 978-981-287-289-0

ISBN 978-981-287-290-6 (eBook)

DOI 10.1007/978-981-287-290-6

Library of Congress Control Number: 2015932473

Springer Singapore Heidelberg New York Dordrecht London

© Springer Science+Business Media Singapore 2015

This work is subject to copyright. All rights are reserved by the Publisher, whether the whole or part of the material is concerned, specifically the rights of translation, reprinting, reuse of illustrations, recitation, broadcasting, reproduction on microfilms or in any other physical way, and transmission or information storage and retrieval, electronic adaptation, computer software, or by similar or dissimilar methodology now known or hereafter developed.

The use of general descriptive names, registered names, trademarks, service marks, etc. in this publication does not imply, even in the absence of a specific statement, that such names are exempt from the relevant protective laws and regulations and therefore free for general use.

The publisher, the authors and the editors are safe to assume that the advice and information in this book are believed to be true and accurate at the date of publication. Neither the publisher nor the authors or the editors give a warranty, express or implied, with respect to the material contained herein or for any errors or omissions that may have been made.

Printed on acid-free paper

Springer Science+Business Media Singapore Pte Ltd. is part of Springer Science+Business Media (www.springer.com)

Welcome Message

The Institute for Infrastructure Engineering and Sustainable Management (IIESM), Universiti Teknologi MARA (UiTM) has over the years been instrumental in providing a platform for several collaboration research program and publications involving all Civil Engineering disciplines. IIESM has so far focused on research with the aims to solve infrastructure and environmental engineering problems with a more sustainable way.

IIESM in collaboration with Universitas Gadjah Mada, Indonesia; Mahatma Gandhi University, India and BRE Centre for Innovative Construction Materials, UK are organizing a 3-day “International Civil and Infrastructure Engineering Conference 2014, (InCIEC 2014)”. The conference is supported by IEEE Malaysia IE/IA Joint Chapter dated from 28th September to 1st October 2014 in Kota Kinabalu, Sabah, Malaysia.

It is hoped that InCIEC 2014 will be a useful platform for researchers to present their findings in the areas of multidisciplinary related to civil engineering issues emphasizes on concrete waste and earthquake engineering, construction project management, fluvial and river engineering dynamics, geotechnical engineering, innovative construction materials and structures, micro and nanotechnology in construction and civil engineering, sustainable environment, timber engineering and transportation systems, infrastructure and intelligent transport. Besides, this conference is also a platform for researchers to establish new interfaces, compare the findings, benchmark their work, exchange views, and widen the scope and range of their research activities. The conference is also looking forward to new peers in diverse areas of expertise.

On behalf of the organising committee we would like to take this opportunity to express our gratitude to all reviewers and participants for their support to ensure the success of this event. We also would like to thank all the authors, session chairpersons, and delegates for the great support and contribution given. Last but not least, a special thank goes to the organising committee, who have been working

hard toward the success of this event. Without their cooperation, hard work, and dedication, this event would simply not be possible.

We wish all participants and presenters, have a very pleasure stay in Kota Kinabalu and do enjoy the conference.

Rohana Hassan
General Chair, InCIEC 2014

Advisory Committee:

Zakiah Ahmad
IIESM, Universiti Teknologi MARA, Malaysia

Simon Aicher
Materials Testing Institute University of Stuttgart, Germany

Sabu Thomas
Mahatma Gandhi University, India

Pete Walker
BRE Centre for Innovative Construction Materials, UK

Mustafa Kamal Hamzah
IEEE Malaysia IE/IA Joint Chapter

A.S.M. Abdul Awal
Universiti Teknologi Malaysia

Azmi Ibrahim
Faculty of Civil Engineering, Universiti Teknologi MARA, Malaysia

Agus Kurniawan
Universitas Gadjah Mada, Indonesia

Hadariah Bahron
Research Management Institute (RMI), Universiti Teknologi MARA, Malaysia

Rugayah Hashim
Research Management Institute (RMI), Universiti Teknologi MARA, Malaysia

Issam A. Al-Khatib
Berzeit University, West Bank, Palestine



About IIESM

The Institute for Infrastructure Engineering and Sustainable Management (IIESM) was officially approved by the Universiti Teknologi MARA, Malaysia as an Institute on the 7th of January 2009. The formation of this Institute would further expedite research and publication activities at the university. IIESM focuses on research in all civil engineering disciplines that enlighten a broader scope in research and engineering education. Our aim is to solve infrastructure and environmental engineering problems in a more sustainable way and introduce new state-of-the-art technology.

It is a merger of 10 research excellence centres which are:

1. Timber Engineering Research Centre (TEReC)
2. Concrete Waste Engineering and Earthquake Research Centre (CWE²C)
3. Flood Management and Intelligence Development Centre (FloodMind)
4. Fluvial and River Engineering Dynamics Centre (FRiEnD)
5. Geotechnical Forensic Research Centre (GEOFORENSIC)
6. Innovative Construction Materials and Structures Centre (ICMSC)
7. Bioremediation Research Centre (mybioREC)
8. Geotechnical Engineering and Georisk Management Centre (myGERMEC)
9. Synergistic Innovative Management Research Centre (SIMReC)
10. Transportation Systems, Infrastructure and Intelligent Transport Research Centre (TransIIT)

Vision

To establish the institute as a premier entity to provide leadership in the scholarship of research and consultancy.

Mission

To be the excellence centre and an engine of growth for new knowledge to solve future problem.

Institute for Infrastructure Engineering and Sustainable Management (IIESM)

Level 3, Block 1, Engineering Complex,

Universiti Teknologi MARA, 40450 Shah Alam, Selangor, Malaysia

Phone: + (6) 03 5544 2780/5521 1910

Fax: + (6) 03 5521 1911

E-mail: iiesm.fka@gmail.com

Website: <http://iiesm.uitm.edu.my>

Venue



The Pacific Sutera Hotel

The luxurious five-star The Pacific Sutera Hotel features 500 immaculately appointed rooms and suites with contemporary décor and dramatic views of either the sprawling golf course or of the sea and nearby tropical islands.

The grand entrance and high-ceiling lobby lounge offer an uninterrupted, panoramic view of the ocean and is a popular meeting point for leisure and business travelers. The Pacific Club guests enjoy the magnificent views from the top floors where breakfast and cocktails are served in the exclusive Pacific Club Lounge.

Sutera Harbour Resort
1 Sutera Harbour Boulevard Malaysia
T. (6088) 318 888
E. reservations@suteraharbour.com.my



Organising Committee

International Advisory/Liason

Pete Walker, BRE Center for Innovative Construction Materials, United Kingdom
Simon Aicher, Materials Testing Institute University of Stuttgart, Germany
Sabu Thomas, Mahatma Gandhi University, India
Agus Kurniawan, Universitas Gadjah Mada, Indonesia
Issam A. Al-Khatib, Berzeit University, West Bank, Palestine

Advisor

Mustafar Kamal Hamzah, IEEE Malaysia IE/IA Joint Chapter
Hadariah Bahron, Research Management Institute (RMI), UiTM, Malaysia
Rogayah Hashim, Research Management Institute (RMI), UiTM, Malaysia
Azmi Ibrahim, Faculty of Civil Engineering, UiTM, Malaysia
Zakiah Ahmad, IIESM, UiTM, Malaysia

General Chair

Rohana Hassan, UiTM, Malaysia

General Co-Chair

Marina Yusoff, UiTM, Malaysia

Technical Program Chair

Zulhabri Ismail, UiTM, Malaysia

Publication and Finance Chair

Anizahyati Alisibramulisi, UiTM, Malaysia
Norliyati Mohd Amin, UiTM, Malaysia
Mohd Fadzil Arshad, UiTM, Malaysia

Website Chair

Marina Yusoff, UiTM, Malaysia

Secretariat

Mohd Shafee Harun, IIESM, UiTM, Malaysia
Rosnani Md Saini, IIESM, UiTM, Malaysia
Wan Nina Nabella Wan Azlan Hafifi, IIESM, UiTM, Malaysia
Kamisah Yahaya, IIESM, UiTM, Malaysia

Reviewers

Abdul Halim Ghazali, Universiti Putra Malaysia
Abdul Omar, Universiti Kebangsaan Malaysia
Abdul Samad Abdul Rahman, Universiti Teknologi MARA
Abu Sufian Muhammad Abdul Awal, Universiti Teknologi Malaysia
Adnan Zainorabidin, Universiti Tun Hussein Onn Malaysia
Aeslina Abdul Kadir, Universiti Tun Hussien Onn Malaysia
Aftab Hameed Memon, Quaid-e-Awam University of Engineering, Science
and Technology, Nawabshah Sindh Pakistan
Afzan Ahmad Zaini, Universiti Teknologi MARA
Agus Kurniawan, Universitas Gadjah Mada, Indonesia
Ahmad Kamil Arshad, Universiti Teknologi MARA
Aidah Jumahat, Universiti Teknologi MARA
Ali Akbar Firoozi, Universiti Kebangsaan Malaysia
Ali Rafiei, University of Technology Sydney, Australia
Amily Fikry, Universiti Teknologi MARA
Amin Azdarpour, Universiti Teknologi MARA
Aminaton Marto, Universiti Teknologi Malaysia
Amir Zahedi, Sahand University of Technology, Iran
Amiruddin Ismail, Universiti Kebangsaan Malaysia
Amit Bhardwaj, Lovely Professional University, India
Amiza Rasmi, TM Research and Development, Malaysia
Amnorzahira Amir, Universiti Teknologi MARA
Andrew Thomson, University of Bath, United Kingdom
Andy Bery, Universiti Sains Malaysia
Aniza Ibrahim, Universiti Pertahanan Nasional Malaysia
Anizahyati Alisibramulisi, Universiti Teknologi MARA
Anuar Bin Mohamed Kassim, Universiti Teknikal Malaysia Melaka
Aryani Ahmad Latiffi, Universiti Tun Hussein Onn Malaysia
Azinoor Azida Abu Bakar, Universiti Teknologi MARA
Azizul Mohamad, Universiti Malaysia Perlis
Azlinda Saadon, Universiti Teknologi MARA

Badorul Hisham Abu Bakar, Universiti Sains Malaysia
Behrouz Gordan, Universiti Teknologi Malaysia
Bemgba Nyakuma, Universiti Teknologi Malaysia
Bilal Beydoun, Lebanese University, Lebanon
Brij Gupta, National Institute of Technology Kurukshetra, India
Chao Wang, Georgia Institute of Technology, USA
Che Maznah Mat Isa, Universiti Teknologi MARA
Chee-Ming Chan, Universiti Tun Hussien Onn Malaysia
Cheng-Ta Chiang, National Chia Yi University, Taiwan
Chengzong Pang, Wichita State University, USA
Chien-Ping Chang, Chien Hsin University of Science and Technology, Taiwan
Chin Han Chan, Universiti Teknologi MARA
Christy Gomez, Universiti Tun Hussein Onn Malaysia
Deepak Choudhary, LPU, India
Dhaval Bhati, Indian Institute of Technology Madras, India
Ebenezer Oluwasola, Universiti Teknologi Malaysia
Eduard Babulak, Sungkyunkwan University, USA
Ekarizan Shaffie, Universiti Teknologi MARA
Emilio Jiménez Macías, University of La Rioja, Spain
Fadzil Arshad, Universiti Teknologi MARA
Faizah Kamarudin, Universiti Teknologi MARA
Farid Ezanee Mohamed Ghazali, Universiti Sains Malaysia
Farzad Hejazi, Universiti Putra Malaysia
Fauzan Mohd. Jakarni, Universiti Putra Malaysia
Fauzi Baharudin, Universiti Teknologi MARA
Fauziah Ahmad, Universiti Sains Malaysia
Fauzilah Ismail, Universiti Teknologi MARA
Grzegorz Debita, Wroclaw University of Technology, Poland
Hamidah Mohd Saman, Universiti Teknologi MARA
Hammad Aziz, Universiti Teknologi PETRONAS
Hanizam Awang, Universiti Sains Malaysia
Hartini Kasmin, Universiti Tun Hussien Onn Malaysia
Haryati Awang, Universiti Teknologi MARA
Heng Ly, Chulalongkorn University, Thailand
Hilton Ahmad, Universiti Tun Hussein Onn Malaysia
Hing Keung Lau, The Open University of Hong Kong, Hong Kong
Hj Harizan Che Mat Haris, Universiti Teknologi MARA
Honghai Liu, University of Cincinnati, USA
Houman Ebrahimpour, Shahid Bahonar University of Kerman, Iran
Hui Hwang Goh, Universiti Tun Hussein Onn Malaysia
Hussain Hamid, Universiti Putra Malaysia
Ibrahim Ali Noorbacha, International Islamic University Malaysia
Ibrahim Salihi, Universiti Teknologi PETRONAS
Ishtiaque Ahmed, Universiti Teknologi Malaysia
Ismacahyadi Bagus Mohd Jais, Universiti Teknologi MARA

Issam Al-Khatib, Birzeit University, Palestine
Ivson dos Anjos, UFPB-Federal University of Paraíba, Brazil
Izwan Johari, Universiti Sains Malaysia
Jalina Kassim, Universiti Teknologi MARA
Jamaluddin Mahmud, Universiti Teknologi MARA
Juraidah Ahmad, Universiti Teknologi MARA
Kartini Kamaruddin, Universiti Teknologi MARA
Khairul Salleh Baharudin, Infrastructure University Kuala Lumpur Malaysia
Khairulzan Yahya, Universiti Teknologi Malaysia
Khalida Muda, Universiti Teknologi Malaysia
Koay Mei Hye, Universiti Teknologi MARA
Lee Wei Koon, Universiti Teknologi MARA
Lee Yee Loon, Universiti Tun Hussein Onn Malaysia
Mahmood Anwar, Hitachi CFP Pte Ltd., Singapore
Mahmood Md Tahir, Universiti Teknologi Malaysia
Maisarah Ali, International Islamic University Malaysia
Manir Zaman, Universiti Teknologi Malaysia
Marfiah Ab. Wahid, Universiti Teknologi MARA
Maria Grazia D'Elia, University of Salerno, Italy
Marina Yusoff, Universiti Teknologi MARA
Masumeh Dodel, Amirkabir University of Technology, Iran
Mazidah Mukri, Universiti Teknologi MARA
Mazlina Mohamad, Universiti Teknologi MARA
Md Azlin Md Said, Universiti Sains Malaysia
Megat Ahmad Kamal Megat Hanafiah, Universiti Teknologi MARA
Megat Azmi Megat Johari, Universiti Sains Malaysia
Meonghun Lee, Sunchon National University, Korea
Meor Othman Hamzah, Universiti Sains Malaysia
Mohamad Razip Selamat, Universiti Sains Malaysia
Mohammad Rashed Iqbal Faruque, Space Science Center (ANGKASA), Malaysia
Mohd Azrizal Fauzi, Universiti Teknologi MARA
Mohd Idrus Mohd Masirin, Universiti Tun Hussein Onn Malaysia
Mohd Jamil Abdul Wahab, Forest Research Institute Malaysia
Mohd Nazree Derman, Universiti Malaysia Perlis
Mohd Reeza Yusof, Universiti Teknologi MARA
Mohd Zulham, Universiti Malaysia Perlis
Muhammad Akram Adnan, Universiti Teknologi MARA
Muhammad Aslam, Universiti Teknologi PETRONAS
Muhammad Fauzinizam Razali, Universiti Sains Malaysia
Muhammad Naufal Mansor, Universiti Malaysia Perlis
Muhammad Rafi Raza, Universiti Kebangsaan Malaysia
Narayan Dungana College of Science and Technology, Bhutan
Nik Norsyahariati Nik Daud, Universiti Putra Malaysia
Noor Ahmad Tajedi, Syarikat Prasarana Negara Berhad, Malaysia
Noor Aisyah Asyikin Mahat, Universiti Teknologi MARA

Noor Elaiza Abd Khalid, Universiti Teknologi MARA
Noor Faizah Fitri Md. Yusof, Universiti Sains Malaysia
Noor Izzri Abdul Wahab, Universiti Putra Malaysia
Noorsuhada Md Nor, Universiti Teknologi MARA
Nor Azizi Safiee, Universiti Putra Malaysia
Nor Azura Md Ghani, Universiti Teknologi MARA
Nor Hayati Saad, Universiti Teknologi MARA
Nor Zaidi Haron, Universiti Teknikal Malaysia Melaka
Noraiham binti Mohamad, Universiti Teknikal Malaysia Melaka
Norashidah Abd Rahman, Universiti Tun Hussien Onn Malaysia
Norazlan Khalid, Universiti Teknologi MARA
Norhazilan Md Noor, Universiti Teknologi Malaysia
Noridah Mohamad, Universiti Tun Hussein Onn Malaysia
Norlia Mohamad Ibrahim, Universiti Malaysia Perlis
Norliyati Mohd Amin, Universiti Teknologi MARA
Norshuhaila Mohamed Sunar, Universiti Tun Hussien Onn Malaysia
Norsuzailina Mohamed Sutan, Universiti Malaysia Sarawak
Nur Asmaliza Mohd Noor, Universiti Teknologi MARA
Nur Sabahiah Abdul Sukor, Universiti Sains Malaysia
Nurul Fadly Habidin, Universiti Pendidikan Sultan Idris
Oskar Hassan, Universiti Teknologi MARA
Othman Che Puan, Universiti Teknologi Malaysia
Petr Máca, Czech Technical University, Czech Republic
Pooya Saffari, Universiti Teknologi MARA
Rahmat Sanudin, Universiti Tun Hussien Onn Malaysia
Rakesh Raut, Post-Doc. Research Fellow, Switzerland
Ramlah Mohd Tajuddin, Universiti Teknologi MARA
Razi Ahmad, Universiti Malaysia Perlis
Rehan Masood, The University of Lahore, Pakistan
Ricky Lee Nyuk San, Universiti Malaysia Sabah
Ridzuan Ali, Universiti Teknologi MARA
Rohana Hassan, Universiti Teknologi MARA
Rosnawati Buhari, Universiti Tun Hussein Onn Malaysia
Rozaina Ismail, Universiti Teknologi MARA
S. Vijaykumar, 6th Sense Advanced Research Foundation, India
Sabariah Arbai, Universiti Teknologi MARA
Saidatulakmar Shamsuddin, Universiti Teknologi MARA
Saurdi Ishak, Universiti Teknologi MARA
Shaharin Hamid, Universiti Teknologi MARA
Shahida Begum, Universiti Tenaga Nasional
Shahiron Shahidan, Universiti Tun Hussien Onn Malaysia
Shamsul Rahman Kutty, Universiti Teknologi PETRONAS
Shan Huang, Georgia Institute of Technology, USA
Shilpa Mehta, Electronics and Communication, FACULTY, India
Shun-Wen Cheng, Far East University, Taiwan

Sing Sing Wong, University College of Technology Sarawak
Sinin Hamdan, Universiti Malaysia Sarawak
Siotai Cheong, Macao Polytechnic Institute, Macao
Siti Akhtar Mahayuddin, Universiti Teknologi MARA
Siti Azlina Rosli, Universiti Teknologi MARA
Siti Fatin Mohd Razali, Universiti Kebangsaan Malaysia
Siti Hawa Hamzah, Universiti Teknologi MARA
Siti Kartina Abdul Karim, Universiti Teknologi MARA
Sivakumar Dhar Malingam, Universiti Teknikal Malaysia Melaka
Sulaiman Hasim, Universiti Teknologi MARA
Sunitha Doraisamy, Universiti Tun Hussien Onn Malaysia
Suraya Hani Adnan, Universiti Tun Hussein Onn Malaysia
Suzana Ramli, Universiti Teknologi MARA
Syed Burhanuddin Hilmi Syed Mohamad, Universiti Tun Hussein Onn Malaysia
T. Manjunath, Principal HKBK College of Engineering, Bangalore
Karnataka, India
Tehmina Ayub, Universiti Teknologi PETRONAS
Tengku Amran Tengku Mohd, Universiti Teknologi MARA
Tien Choon Toh, Universiti Tunku Abdul Rahman
Tomoko Saiki, Saiki Patent, Japan
Tshewang Rinzin, College of Science and Technology, Bhutan
Tuan Asmaa Tuan Resdi, Universiti Teknologi MARA
Ummi Kalthum Ibrahim, Universiti Teknologi MARA
Vikrant Bhateja, Shri Ramswaroop Memorial Group of Professional Colleges,
Lucknow (UP), India
Vishnu Satya Chaitanya, Manipal University, India
Wan Zuki Azman Wan Muhamad, Universiti Malaysia Perlis
Wardah Tahir, Universiti Teknologi MARA
Wei Wen Liu, Universiti Malaysia Perlis
Wei-Koon Lee, Universiti Teknologi MARA
Wu Chia-Ching, Kao Yuan University, Taiwan
Yiming Li, National Chiao Tung University, Taiwan
Yingqiong Gu, University of Notre Dame, USA
Ying-Ren Chien, National I-Lan University, Taiwan
Yong Chua Bon, Universiti Teknologi MARA
Yu Kuang, University of Nevada, Las Vegas, USA
Zainal Ahmad, Universiti Sains Malaysia
Zainorizuan Mohd Jaini, Universiti Tun Hussein Onn Malaysia
Zainudin Kornain, Universiti Kuala Lumpur British Malaysian Institute, Malaysia
Zakiah Ahmad, Universiti Teknologi MARA
Zaliman Sauli, Universiti Malaysia Perlis
Zanariah Abd Rahman, Universiti Teknologi MARA
Zhe-Yang Huang, Industrial Technology Research Institute, Taiwan
Zuhaida Mohd Zaki, Universiti Teknologi MARA
Zulhabri Ismail, Universiti Teknologi MARA

Zulkiflee Abd Latif, Universiti Teknologi MARA
Zuriati Zakaria, Universiti Teknologi Malaysia

Contents

Part I Concrete Waste and Earthquake Engineering

Analysis of the Effect of Vibration from Footfalls on Office Building	3
Tuan Norhayati Tuan Chik, Shurl Yabi, Nor Azizi Yusoff and Mohd. Imran Ghazali	
Shear Resistance Analysis of Rebar Connector in RC Stocky Wall Panel Using Lusas 3D Modelling	17
Noraspalela Abdullah, Mohd Suhelmiey Sobri and Siti Hawa Hamzah	
Determination of Modulus Elasticity and Poison Ratio of Expanded Polystyrene (EPS) Lightweight Concrete (LWC) Enhanced with Steel Fiber	29
Jamilah Abd. Rahim, Siti Hawa Hamzah and Hamidah Mohd Saman	
Structural Performance of Steel Fibre Reinforced Concrete Three-Ribbed Wall Panel on Compression	37
Mohd Maiziz Bin Fishol Hamdi, Siti Hawa Binti Hamzah and Mohd Hisbany Bin Mohd Hashim	
Compressive Strength and Water Absorption Characteristics of Brick Using Quarry Dust.	51
Maureena Jurliel Abdullah, Zakiah Ahmad, Atikah Fatma Md. Daud and Nur Kamaliah Mustaffa	
Enhancing the Performance of Recycled Aggregate Concrete Using Micronized Biomass Silica	65
A. Suraya Hani, Ismail Abdul Rahman and Hamidah Mohd Saman	

An Evaluation of High-Rise Concrete Building Performance Under Low Intensity Earthquake Effects	79
Rozaina Ismail and Nurul Fasihah Zamahidi	
Strength of Various Densities of Lightweight Coir Fiber Concrete Containing Protein and Synthetic Foam	87
Mazlina Mohamad, Mohd Fadzil Arshad and Nur Amalina Abdul Hamid	
An Experimental Study on the Fracture Energy of Foamed Concrete Using V-Notched Beams	97
Norashidah Abd. Rahman, Zainorizuan Mohd Jaini, Nor Azira Abd. Rahim and Siti Aisyah Abd. Razak	
Strength and Deformation Behaviour of Concrete Incorporating Steel Fibre from Recycled Tyre	109
A.S.M. Abdul Awal, Mariyana Aida Ab Kadir, Lim Lion Yee and Neelam Memon	
 Part II Construction Project Management	
Using PLS-SEM Path Modeling to Determine Factors Influencing Performance of Malaysian Construction Firms in International Markets	121
Che Maznah Mat Isa, Hamidah Mohd Saman, Siti Rashidah Mohd Nasir, Christopher Nigel Preece and Nur Izzati Ab. Rani	
Study on Flow Improvement of Brick Laying Operations in a Residential Construction Project	137
Muhamad Abduh and Aditya Pratama	
The Implication of the Standard Method of Measurement (SMMs) for Building Works Toward Contractors' Works	149
Anis Rosniza Nizam Akbar, Mohammad Fadhil Mohammad, Noor Amalia Talib and Mysarah Maisham	
The Way Forward for Industrialised Building System (IBS) in Malaysia	163
Muhamad Faiz Musa, Mohammad Fadhil Mohammad, Mohd Reeza Yusof and Rohana Mahbub	

A Review of the Maintenance Performance Factors for Heritage Buildings 177
 Syed Burhanuddin Hilmi Syed Mohamad, Zainal Abidin Akasah and Mohammad Ashraf Abdul Rahman

Strategies in Dealing with Cost Overrun Issues: Perspective of Construction Stakeholders 189
 Kai Chen Goh, Aaron Boon Kian Yap, Ta Wee Seow, Md Asrul Nasid Masrom, Hui Hwang Goh and Jia Sin Tey

Risk Level of Factors Contributing to Waste Generation in Construction Phase 199
 Ismail Abdul Rahman, Nor Solehah Md Akhir, Aftab Hameed Memon and Sasitharan Nagapan

Building Sustainable Design Performance Through Integrated Value Management Practice 211
 Mohd Nasrun Mohd Nawi, Faizatul Akmar Abdul Nifa and Siti Halipah Ibrahim

Homeowner’s Prevalence Upkeep Behavior Towards Implementation of Home Maintenance Manual for Residential Building 219
 Ahmad Sharim Abdullah, Nor Rima Mohd Ariff, Robiah Abdul Rashid, Norsalisma Ismail and Nur Nabila Mohd Tamim

Green Roofs Benefits; Perception by Malaysian Residential Highrise End Users 231
 Wan Zuriea Wan Ismail, Sabarinah Sh. Ahmad, Hikmah Kamarudin and Zarina Ithnin

Critical Review on the Theoretical Framework and Critical Success Factors in Green Construction 243
 Afzan Ahmad Zaini and Intan Rohani Endut

A Review in Developing a High Rise Building Construction Safety and Health Risk Model 253
 Afzan Binti Ahmad Zaini, Intan Rohani Endut and Nurzawani Binti Md Sofwan

Evaluating Importance Level of Buildability Factors in Cambodian Construction Projects 263
 Heng Ly, Tanit Tongthong and Vachara Peansupap

Developing an Accident Causation Model for Accident Prevention at Building Construction Sites 273
 Amran Asan and Zainal Abidin Akasah

Identification of Malaysian Contractors with Sustained International Operations (CSIO) 287
 Che Maznah Mat Isa, Nur Izzati Abd. Rani, Christopher Nigel Preece and Hamidah Mohd Saman

Problems Associated with Delay Analysis Methodology in Malaysian Construction Delay Practice 301
 Nurul Huda Muhamad, Mohammad Fadhil Mohammad, Asmalia Che Ahmad and Edelin Hussein

An Overview on the Issue of Delay in the Construction Industry 313
 Sunitha V. Doraisamy, Zainal Abidin Akasah and Riduan Yunus

Propelling Site Safety Through Accident Causation Models 321
 Noor Aisyah Asyikin Mahat, Faridah Ismail and Sharifah Nur Aina Syed Alwee

Ventilation Performance Assessment of an Educational Building in a Hot and Humid Climate 333
 Maisarah Ali, Majeed Oladokun, Samsul Baharin Osman, Niza Samsuddin, Hairul Aini Hamzah and Md Noor Salleh

Part III Fluvial and River Engineering Dynamic

Nutrient Uptake and Growth of Bovine Rectal Bacteria in Application of Textile Wastewater Bioremediation 347
 N.M. Sunar, A.S.M. Kassim and N.M. Noor

Neural Network Hydrological Modeling for Kemaman Catchment 359
 Tuan Asmaa Tuan Resdi and Wei-Koon Lee

Hydrodynamic Model for the Investigation of Environmental Flow in Johor River Estuary 373
 Wei-Koon Lee and NurHidayah Aqilla binti Zaharuddin

A Conceptual Review of Tsunami Models Based on Sumatara-Andaman Tsunami Event 387
 N.H. Mardi, M.A. Malek, M.S. Liew and H.E. Lee

Heavy Metal Removal Using *Cabomba Caroliniana* as Submerged Vegetation Species in Constructed Wetland. 397
 A.K. Nur Fadzeelah, J. Lynna Juliana and A. Muhammad Habibuddin

Effect of Vibration on Hydraulic Conductivity of Clogged Soil. 407
 Fauzi Baharudin, Mohd Shafee Harun and Nur Syafiqah Roslee

Investigation of pH Impacts on Mineralization of CO₂ in Conditions Representative of the Malay Basin. 417
 Erfan Mohammadian, Hossien Hamidi, Amin Azdarpour and Radzuan Junin

Part IV Geotechnical Engineering

The Engineering Properties of Dredged Marine Soil Solidified with Activated Steel Slag 427
 Chee-Ming Chan and Nor Hanisah Hamzah

SOFT Soil Subgrade Stabilization Using Waste Paper Sludge Ash (WPSA) Mixtures 439
 Norazlan Khalid, Mazidah Mukri, Faizah Kamarudin, Abdul Halim Abdul Ghani, Mohd Fadzil Arshad and Fauzi Baharudin

Prediction of Inundation Settlement Using Rotational Multiple Yield Surface Framework in Unsaturated Granite Residual Soil 447
 M.J. Md. Noor, I.B. Mohamed Jais and Y. Ashaari

Enhancement in Electrical Resistivity Tomography Resolution for Environmental and Engineering Geophysical Study. 459
 Andy Anderson Bery and Rosli Saad

Geophysical Characterisation of Road Subsurface. 469
 Haryati Awang and Alicia David

Data Acquisition Challenges on Peat Soil Using Seismic Refraction 477
 Mohd Jazlan Mad Said, Adnan Zainorabidin and Aziman Madun

The Characteristics of Pontian Peat Under Dynamic Loading 487
 Siti Nurul Aini Zolkefle, Adnan Zainorabidin and Habib Musa Mohamad

Assessment of Riverbank Soil Properties at Sg. Damansara	501
Fauzi Baharudin, Mohd Shafee Harun, Norazlan Khalid and Zulina Mohd Yusof	
Stress-Strain Behavior of Parit Nipah Peat	515
Siti Hajar Binti Mansor and Adnan Bin Zainorabidin	
Effect of Fines Content on Liquefaction Susceptibility of Sand-Kaolin Mixtures	525
Aminaton Marto, Choy Soon Tan, Ahmad Mahir Makhtar, Lim Mei Yen and Ung Shu Wen	
An Evaluation of Shrinkage Measurement on Undisturbed Peat Soil Using Modified Techniques	533
Nursyahidah Binti Saedon, Adnan Bin Zainorabidin and Ismail Bin Bakar	
Rainfall Infiltration into Unsaturated Soil	545
Aniza Ibrahim, Muhammad Mukhlisin and Othman Jaafar	
Predicting Uniaxial Compression Strength (UCS) Using Bulk Density for Kuala Lumpur Granite and Limestone	557
Haryati Awang and Noor Akma Mohd Naru	
Laboratory Test Methods for Shear Strength Behavior of Unsaturated Soils Under Suction Control, Using Triaxial Apparatus	567
Pooya Saffari, Mohd Jamaludin Md Noor, Basharudin Abdul Hadi and Shervin Motamedi	
The Study of Interface Shear Strength Between Geotextile and Soil Liner Containing Different Percentage of Sodium Bentonite	577
M. Mukri, A. Azmi, S. Hashim, S. Aziz, F.H. Ahmad and N. Khalid	
 Part V Innovative Construction Materials and Structures	
Experimental Investigation on Shear Strengthening of RC Continuous T-Beams with Different Layer of CFRP Schemes	589
M.B.S. Alferjani, A.A. Abdul Samad, Blkasem S. Elrawaff, Omer Elzaroug and N. Mohamad	

Bending Strength of Pre-tensioned (PRT) Concrete Beam 605
 Nurul Huda binti Suliman, Siti Hawa binti Hamzah,
 Afidah binti Abu Bakar and Norliyati Mohd Amin

**Chloride Permeability of Nanoclayed Ultra-High Performance
 Concrete** 613
 M.J. Mohd Faizal, M.S. Hamidah, M.S. Muhd Norhasri,
 I. Noorli and M.P. Mohamad Ezad Hafez

**2D Multi-scale Simulation and Homogenization of Foamed
 Concrete Containing Rubber Bars** 625
 Zainorizuan Mohd Jaini, Shahrul Niza Mokhatar,
 Yuantian Feng and Mazlan Abu Seman

**Qualitative Fault Tree and Event Tree Model of Bridge
 Defect for Reinforced Concrete Highway Bridge** 639
 Wan Safizah Wan Salim, Mohd Shahir Liew and A'fza Shafie

**Experimental Investigation of Cold-formed Steel (CFS)
 Channel Material at Post Elevated Temperature** 651
 Fadhluhartini Muftah, Mohd Syahrul Hisyam Mohd Sani,
 Ahmad Rasidi Osman, Mohd Azran Razlan and Shahrin Mohammad

The Thermal Stability Property of Bio-composites: A Review 667
 Z.A. Rasid

**Finite Element Analysis of Staggered Micro Couple Resonant
 Sensor Structure** 681
 N.A. Shuib, A.F. Zubair, N.H. Saad, A.A. Bakir,
 M.F. Ismail and I.P. Almanar

**An Experimental Study of Reinforced Concrete Beams
 with Artificial Aggregate Concrete Infill Under Impact Loads** 691
 Shahrul Niza Mokhatar, Zainorizuan Mohd Jaini,
 Mohd Khairy Burhanudin, Mohamad Luthfi Ahmad Jeni
 and Mohd Nasrul Naim Ismail

**Factors Effecting the Thermal and Microstructures
 of Recycled Glass Concrete** 703
 Renga Rao Krishnamoorthy and Ridzuan Mohd Ali

**Determination of Rayleigh Damping Coefficient for Natural
 Damping Rubber Plate Using Finite Element Modal Analysis** 713
 Ahmad Idzwan Yusuf and Norliyati Mohd Amin

Construction of Roller Compacted Concrete Dam in Malaysia: A Case Study at Batu Hampar Dam.	727
Assrul Reedza Zulkifli, Abdul Rahim Abdul Hamid, Mohd Fadhil Arshad and Juhaizad Ahmad	
Partial Replacement of Glass Fiber with Kenaf Waste in Cement Board Production	741
Zakiah Ahmad, Mohd Fadzil Arshad and Afifah Azrae	
A New Method to Treat Oily Water Using Rice Husk Ash Onboard Vessel	757
M.R. Zoolfakar and M.S.M. Shukor	
Influence of Different Fillers on the Tensile Properties of 50/50 NR/NBR Blend.	767
Nurul Husna Rajhan, Rozaina Ismail, Hanizah Ab. Hamid and Azmi Ibrahim	
The Effect of Rolling Direction to the Tensile Properties of AA5083 Specimen	779
Latifah Mohd Najib, Anizahyati Alisibramulisi, Norliyati Mohd Amin, Ilyani Akmar Abu Bakar and Sulaiman Hasim	
Multicriteria Assessment of Ageing Civil and Structure Facilities in Onshore Process Plants	789
Dabo Baba Hammad, Nasir Shafiq and Muhd Fadhil Nuruddin	
Comments on Structural Reliability for Design and Construction as Per Eurocode	801
K.A. Al Sanjery and J.Y. Sia	
 Part VI Micro and Nano Technology in Constructions and Civil Engineering	
Influence of Ionic Substitution on the Mechanical Properties of Nanosized Biphasic Calcium Phosphates.	811
Mohamad Firdaus Abdul Wahid, Koay Mei Hyie, Mardziah Che Murad and N.R. Nik Roselina	
Performance of Carbon Nanotubes (CNT) Based Natural Rubber Composites: A Review.	821
Rozaina Ismail, Azmi Ibrahim, Hanizah Ab. Hamid, Mohamad Rusop Mahmood and Azlan Adnan	

Nano Filler Reinforced Intumescent Fire Retardant Coating for Protection of Structural Steel 831
 Hammad Aziz, Faiz Ahmad and M. Zia-ul-Mustafa

Deposition Behavior of Titanium Dioxide Nanoparticles During Electrophoretic Deposition: Effect on Particle Size. 845
 Norain Ramli and Noorsuhana Mohd Yusof

Preparation and Characterization of Corn Starch Nanocrystal Reinforced Natural Rubber Nanocomposites via Co-coagulation Process. 855
 K.R. Rajisha, L.A. Pothan, S. Thomas and Z. Ahmad

Low Dense CNT for Ultra-Sensitive Chemoresistive Gas Sensor Development 865
 Amirul Abd Rashid, Nor Hayati Saad, Daniel Bien Chia Sheng, Teh Aun Shih, Muhammad Aniq Shazni, Mohammad Haniff and Mai Woon Lee

Stripping Performance and Volumetric Properties Evaluation of Hot Mix Asphalt (HMA) Mix Design Using Natural Rubber Latex Polymer Modified Binder (NRMB) 873
 E. Shaffie, J. Ahmad, A.K. Arshad, D. Kamarun and F. Kamaruddin

Effect of Sintering Temperature on V₂O₅ Doped Barium Zinc Tantalate (BZT) Dielectric Properties 885
 H. Jaafar

Fabrication of a-C:B/n-Si Solar Cells with Low Positive Bias by Using Palm Oil Precursor 895
 A. Ishak, K. Dayana, I. Saurdi and M. Rusop

Effect of Nanoclay in Soft Soil Stabilization 905
 Norazlan Khalid, Mazidah Mukri, Faizah Kamarudin, Abdul Halim Abdul Ghani, Mohd Fadzil Arshad, Norbaya Sidek, Ahmad Zulfaris Ahmad Jalani and Benard Bilong

Compatibility of Plastomeric Modified Bituminous Blends: Its Effect on the Performance Behavior of Modified Bituminous Mixture. 915
 Noor Zainab Habib, Ibrahim Kamaruddin and Madzalan Napiiah

Effects of Residual Carbon on Microstructure and Surface Roughness of PIM 316L Stainless Steel. 927
 Muhammad Rafi Raza, Faiz Ahmad, Norhamidi Muhamad, Abu Bakar Sulong, M.A. Omar, Majid Niaz Akhtar, Muhammad Shahid Nazir, Ali S. Muhsan and Muhammad Aslam

Structural, Optical and Electrical Properties of Nano-structured Sn-doped ZnO Thin Film via Sol Gel Spin Coating Technique 937
 I. Saurdi, M.H. Mamat, A. Ishak and M. Rusop

Part VII Sustainable Environment

Stakeholder Roles in Building Integrated Photovoltaic (BIPV) Implementation 951
 Aaron Boon Kian Yap, Kai Chen Goh, Ta Wee Seow and Hui Hwang Goh

Removal of Oil from Water by Column Adsorption Method Using Microwave Incinerated Rice Husk Ash (MIRHA) 963
 Alina. M. Faizal, Shamsul Rahman Mohamed Kutty and Ezerie Henry Ezechi

Biomass as Low-Cost Adsorbents for Removal of Heavy Metals from Aqueous Solution: A Review of Some Selected Biomass. 973
 Salihi Ibrahim Umar, Shamsul Rahman Mohamed Kutty, Mohamed Hasnain Isa, Nasiru Aminu, Ezerie Henry and Ahmad Fitri B. Abd Rahim

Partly Decomposed Empty Fruit Bunch Fiber as a Potential Adsorbent for Ammonia-Nitrogen from Urban Drainage Water 989
 A.Y. Zahrim, L.N.S. Ricky, Y. Shahril, S. Rosalam, B. Nurmin, A.M. Harun and I. Azreen

A Study on Artificial Hexavalent Chromium Removal by Using Zero Valent Iron Reactor and Sand Filter in Electrochemical Reduction Process. 1003
 Babby Freskayani Izyani Kaliwon

Antibiotic Resistance Bacteria in Coastal Shrimp Pond Water and Effluent 1011
 Marfiah Ab. Wahid, Zummy Dahria Mohamed Basri, Azianabiha A. Halip, Fauzi Baharudin, Janmaizatulriah Jani and Mohd Fozi Ali

Assessment and Reduction of Carbon Footprint: An Approach via Best Management Practices in a Construction Site. 1019
 Amirhossein Malakahmad, Nur Arinah Binti Hisham Albakri and Nasir Shafiq

Effect of Kenaf Water Retting Process by *Bacillus Macerans* ATCC 843 on the pH of Retting Water 1031
 Mohd Nazrin Othman, Ramlah Mohd Tajuddin and Zakiah Ahmad

Pollutants Removal in Storm Water Pond. 1037
 Z. Mohd-Zaki, N. Manan, A. Amir and A. Baki

Removal of Nitrate by *Eichhornia crassipes* sp. in Landfill Leachate 1043
 N. Jaya, A. Amir and Z. Mohd-Zaki

Building Facilities for Autistic Children in Malaysia 1053
 Nurul Aida Nazri and Zulhabri Ismail

Adsorption of Metals (Zn, Ca and B) in Used Engine Oil by Using Microwave Incinerated Rice Husk Ash (MIRHA) 1065
 Amir Izzuddin Habib, Shamsul Rahman Mohd Kutty, Nasir Shafiq and Mohd Fadil Nuruddin

Influence of Indoor Microclimate Distribution on Mould Infestation in a University Library 1075
 Maisarah Ali, Majeed Oladokun, Samsul Baharin Osman, Niza Samsuddin, Hairul Aini Hamzah and Md Noor Salleh

Palm Oil Fuel Ash and Ceramic Sludge as Partial Cement Replacement Materials in Cement Paste 1087
 Nurliyana Ismail, Mohd Fadzil Arshad, Hamidah Mohd Saman and Mazni Mat Zin

Part VIII Timber Engineering

Analysis of Pre-fabricated Timber Roof Truss 1095
 Khairul Salleh Baharudin, Zakiah Ahmad, Azmi Ibrahim and Mohamed Rassam

Charring Rate of Glued Laminated Timber (Glulam) Made from Selected Malaysian Tropical Timber 1107
 Atikah Fatma Md Daud, Zakiah Ahmad and Rohana Hassan

Derivation of Grade Stresses of Malaysian Tropical Timber in Structural Size.	1117
M.B.F.M. Puaad, Z. Ahmad and S.A.K. Yamani	
Bending Strength Performance of Selected Timber Species with Different GFRP Strips Pattern	1129
Rohana Hassan, Norilmi Ghazali and Abdullah Omar Abdullah Zamli	
Computational Approach for Timber and Composite Material Connection Using Particle Swarm Optimization	1141
Marina Yusoff, Ili Izdhar Roslan, Anizahyati Alisibramulisi and Rohana Hassan	
A Review of Dowel Connection for Glulam Timber Strengthening with GFRP	1153
Nurul Atikah Seri, Rohana Hassan and Shaharin Hamid	
A Review of Connections for Glulam Timber	1163
Nurain Rosdi, Rohana Hassan and Mohd Hanafie Yasin	
 Part IX Transportation Systems Infrastructure and Intelligent Transport	
Investigation of Patching Road Defect with Relation to Soil and Pavement Parameter: A Case Study at Bukit Beruntung	1177
Ab. Mughni B. Ab Rahim, Muhammad Akram Adnan, Norliana Sulaiman and Mohd Azda B. Nordin	
Rheological Evaluation of High Reclaimed Asphalt Content Modified with Warm Mix Additive.	1187
Lillian Gungat and Meor Othman Hamzah	
Effect of Aging on the Resilient Modulus of Stone Mastic Asphalt Incorporating Electric Arc Furnace Steel Slag and Copper Mine Tailings	1199
Ebenezer Akin Oluwasola, Mohd Rosli Hainin, Md. Maniruzzaman A. Aziz and Santokh Singh A/L Mahinder Singh	
A Comparative Study on the Behaviour of Motorcyclists on Exclusive Motorcycle Lane at Merging Section Under Different Configuration of Road Marking.	1209
Muhammad Hazmi Bin Ilias and Muhammad Akram Adnan	

Differences in Pedestrian Profile Pattern During Weekdays and Weekends in Central Business District Kuala Lumpur 1221
Noor Iza Bahari, Ahmad Kamil Arshad and Zahrullaili Yahya

Performance Tests of Porous Asphalt Mix—A Review. 1231
K.A. Masri and A.K. Arshad

Assessing Pedestrian Behavioral Pattern at Rail Transit Terminal: State of the Art 1245
Masria Mustafa and Yasmin Ashaari

Pedestrian Behaviour at Stairways and Escalator: A Review 1255
Mohd Khairul Afzan Mohd Lazi and Masria Mustafa

Federal Road Profile Model Generation Based on Road Scanner Data 1269
Rosnawati Buhari, Azali Akhbar Seblan, Munzilah Md Rohani and Saifullizam Puteh

Author Index 1279

About the Editors



Dr. Rohana Hassan is a Head of Research (Science and Technology) at Research Management Unit (RMI), Universiti Teknologi MARA (UiTM), Malaysia. Currently, she also works as Senior Lecturer at Faculty of Civil Engineering, UiTM and actively doing research in the field of fracture and impact energy for building material, timber engineering, engineered wood product, timber design, and composites materials. Thus, she has become a regular invited speaker in the same field and acted as the Chairman for InCIEC 2013 and 2014 and Technical Program Chair for various Civil Engineering conferences. In addition, she is one of the

Editors for InCIEC 2013. Her research papers and journals have been published locally and internationally. And she has received numerous awards through her research products.



Dr. Marina Yusoff is the fellow researcher and Coordinator of Quality and Standard of Institute for Infrastructure Engineering and Sustainability Management, Faculty of Civil Engineering and Senior Lecturer of Faculty of Computer and Mathematical Sciences, Universiti Teknologi MARA. She holds a PhD in Information Technology and Quantitative Sciences (Intelligent System) from Universiti Teknologi MARA. She previously worked as a senior executive of Information Technology in SIRIM Berhad, Malaysia. She also holds a Bachelor Degree in Computer

Science from the University of Science Malaysia, and Master of Science in Information Technology from Universiti Teknologi MARA. She is currently an active researcher in floods management, graphology, image processing, and developed many intelligent systems. She has published journals and presented her research in many conferences locally and internationally.



Dr. Anizahyati Alisibramulisi worked with Jurutera Perunding Zaaba before joining Universiti Teknologi MARA (UiTM) in 2001. She holds a Bachelor Degree in Civil Engineering from UiTM, Master in Structural Engineering from Universiti Teknologi Malaysia (UTM) and PhD in Structural Engineering from Norwegian University of Science and Technology (NTNU), Norway. At the moment, she is working as a Lecturer at Faculty of Civil Engineering, UiTM. She is also a Senior Member of Universal Association of Civil, Structural and Environmental Engineers (UASCE) United States, Member of Board of Engineers Malaysia (BEM), Graduate Member of Institute of Engineers Malaysia (IEM), Member of Malaysian Structural Steel Association (MSSA), Honorary Treasurer of Concrete Society of Malaysia (CSM), and Fellow Researcher of Institute for Infrastructure Engineering and Sustainable Management (IIESM) Malaysia. She has published a few articles, books, and proceedings locally and internationally. In addition, she has also involved as Technical Program Chair for various IEEE conferences. Her interest areas are in through process modeling, welded aluminum, steel, concrete, corrosion, and structural engineering.



Dr. Norliyati Mohd Amin has been working as a lecturer at Universiti Teknologi MARA (UiTM), Shah Alam Malaysia for 12 years. She completed her PhD from Kyushu University Japan in 2011. She received her Master of Science in Civil Engineering (Structure) from Universiti Teknologi MARA (UiTM), Shah Alam, Malaysia in 2007 and obtained her BEng (Civil Engineering) from Kyushu University in 1999. Her research interest includes computational mechanics, model analysis, dynamic analysis, model order reduction, and seismic isolation system. Currently, she has been appointed as Fellow at Institute Infrastructure Engineering and Sustainable Management (IIESM), UiTM, Shah Alam, Malaysia.



Dr. Zulhabri Ismail is currently attached to the Faculty of Architecture Planning and Surveying (FSPU), Universiti Teknologi MARA (UiTM). Dr. Zulhabri holds Doctor of Philosophy in Built Environment (Construction Law). Dr. Zulhabri is a Member of the Chartered Institute of Arbitrators United Kingdom and Institution of Electrical and Electronics Engineers. Dr. Zulhabri is the Head of Legal Aspects in Built Environment Initiative Group has published more than 60 papers in which most of them are indexed publications. Dr. Zulhabri is one of the UiTM's vanguard researchers with cumulative of more than RM1.2 M worth of

research grant, more than 20 research projects and more than 20 postgraduate students under his research supervision. Dr. Zulhabri is one of a few being selected to sit as a panel of assessors for Society of Construction Law Essay Writing Competition for the Vincent Powell Smith Prize (Malaysia). He is a Chairman/Technical Program Chair/Advisory Committee/Editorial Review Board for more than 20 indexed/non-indexed conferences and more than 15 journals.

Part I
Concrete Waste and Earthquake
Engineering

Analysis of the Effect of Vibration from Footfalls on Office Building

Tuan Norhayati Tuan Chik, Shurl Yabi, Nor Azizi Yusoff
and Mohd. Imran Ghazali

Abstract Human footfalls are the main source of vibration in office building and it could affect the structure of the building as well as causing discomfort and annoyance to the occupants of the building when the vibration level inside the building exceeds the recommended level. The objectives of the study are to determine the level of vibration on each floor of a multi-storey building due to footfalls and to perform structural response on the multi-storey building due to footfalls input. The selected building for this study is Registrar Office building located in Universiti Tun Hussein Onn Malaysia (UTHM). The scope of study is focused on the effect of vibration induced by footfalls on multi-storey building and analyzing the data using MATLAB and ANSYSv14. The real inputs of vibration induced by footfalls were measured and obtained using Laser Doppler Vibrometer (LDV). The vibration level induced by footfalls on the multi-storey office building can be determined using Vibration Criteria (VC) guidelines. Finally, from the study, the vibration level achieved for this Registrar Office building is in ISO level range which is still under the acceptable limit for office building.

Keywords Vibration · Footfalls · Multi-storey · Dynamic analysis

T.N.T. Chik (✉) · S. Yabi (✉) · N.A. Yusoff
Department of Structures and Materials Engineering,
Universiti Tun Hussein Onn Malaysia, Johor, Malaysia
e-mail: thayati@uthm.edu.my

S. Yabi
e-mail: shurl_y@yahoo.com

N.A. Yusoff
e-mail: azizy@uthm.edu.my

Mohd. Imran Ghazali
Department of Engineering Mechanics,
Universiti Tun Hussein Onn Malaysia, Johor, Malaysia
e-mail: imran@uthm.edu.my

1 Introduction

Vibration in buildings is a common problem and concern especially in big cities because of the daily activities such as road traffic, construction work and even from internal vibration, such as from machinery and human itself. In 1831, in Manchester, England, the Broughton Suspension Bridge had collapsed due to vibration when soldier were marching over it [1].

Vibration in building could reach a level that may not be acceptable to the building occupants and may have an effect such as annoying physical sensations, interference with activities such as work, annoying noise caused by rattling of window panes, walls and loose objects and also interference with proper operation of sensitive instruments.

Vibration can also effect sensitive equipment due to transmission of vibration which will cause interference with its proper operation. Computers and scanners are examples of sensitive equipment normally located in the office building. The Registrar Office building is selected because it is a multi-storey building with occupants and computers on each floor level. The effect of vibration induced by footfalls will be investigated in this study.

There are two objectives in this study, the first one is to perform structural response on the Registrar Office building under vibration due to footfalls input and secondly is to determine the level of vibration due to footfalls on Registrar Office.

2 Internal Vibration Induced by Footfalls

Internal sources are a set of vibration sources acting inside a building, such as from mechanical excitation like washing machine or human activity itself by proving either continuous or transitory types of vibration. However, the possibility of internal vibration can be felt by residents in a building depends on the frequency source and resonance frequency and damping of the structural elements that propagate the vibration through the building. Thus, this problem is more common in high rise building [2].

Davenny [3] concluded that internal vibration from footfall is often the major source of floor vibration compare to machinery. In a word, building floor will vibrate at its natural frequency in response to a footstep impulse and is most severe at the middle of the floor and least severe near the columns.

Vibration from footfall is induced from the movement phases of legs and feet during walking. Hence, the body weight is transferred to the floor. Figure 1 shows the movement phases of legs and feet during walking.

Fig. 1 Phases of legs and feet during walking [4]

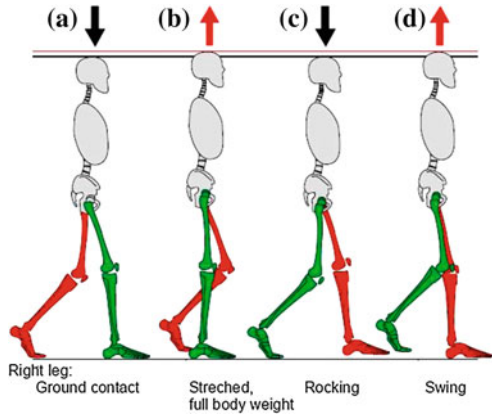


Table 1 Footfalls rate [5]

Frequency (Hz)	Designation
1.5–1.8	“Normal walking” for cellular areas
1.8–2.0	“Someone who is in hurry”
2.0–2.4	“A very brisk pace” considered likely in corridors

When the right foot touches the ground with the heel, this is the starting point of the contact forces and when the right leg is stretched, the full body weight is transmitted to the floor. Next, the right foot will rock while the left leg swings forward. This is called “Rocking”. And finally, the left foot touches the ground while the right leg swings forward.

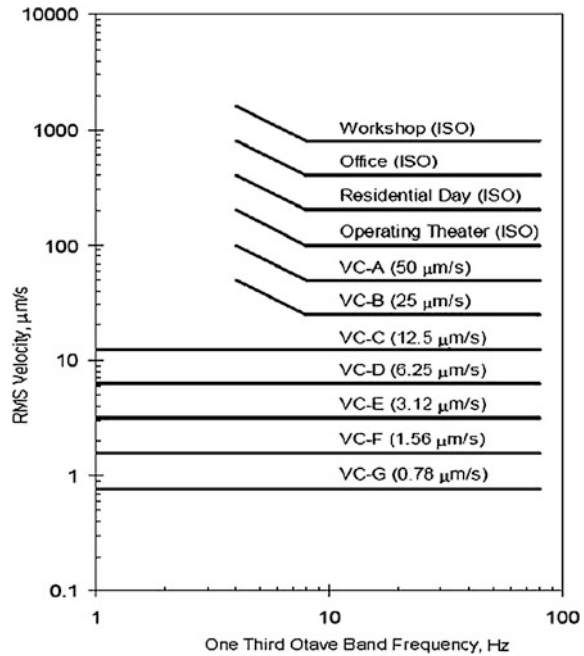
However, the vibrations due to footfalls also depend on the speed of walking. A more general footfall rate classification prepared by Arup [5] is presented in Table 1.

3 Vibration Criteria (VC) Curve

In this study, a specific vibration criteria guideline was used in order to investigate and obtain the performance of the structures. The curves and descriptions were intended to meet the needs of all tools within each category as the previous researchers could judge based on experience mingled with tool-specific specifications [6].

Vibration criteria curves is important as a guideline in designing facilities such as buildings and instruments that are sensitive to vibrations [4]. Each curve of the criteria are associated with line width or size detail which is a representation of the device capabilities [7] as shown in Fig. 2. The form of the criteria is taken through a

Fig. 2 Generic vibration criteria (VC) curves for vibration sensitive equipment [7]



set of one-third octave band velocity where the generic vibration criteria ranges from ISO for the effects of vibration on human occupants in building to VC-G for evaluation only [4].

Table 2 shows the application and range of the vibration criteria limits including ISO criteria for human taking into account through experience on past and present projects [7].

4 Field Measurement at Site

Field measurement was conducted to obtain the signal data for this study by using the Vibrometer equipment. The amplitude of the vibration produced by footfalls is measured during office hour on working days. Figure 3a shows the Vibrometer equipment used in this study, Laser Doppler Vibrometer (LDV 100) and Fig. 3b shows the location of the measurement in the office building, while Fig. 4 shows the side view of the Registrar office building.

The footfall vibration measurement conducted inside the building produced the vibration waves as shown in Fig. 5. Next, this raw data must be processed and analyzed using specific algorithm in Mathematics Laboratory (MATLAB) to obtain

Table 2 Application and range of the vibration criteria curve [7]

Vibration curve	Amplitude (µm/s)	Detail size (µm/s)	Application and experience
<i>a</i>			
Workshop (ISO)	800	N/A	Distinctly perceptible vibration. Appropriate to workshops and no sensitive areas
Office (ISO)	400	N/A	Perceptible vibration. Appropriate to offices and no sensitive areas
Residential day (ISO)	200	75	Barely perceptible vibration. Appropriate to sleep areas in most instances. Usually adequate for computer equipment, hospital recovery rooms, semiconductor probe test equipment and microscopes less than 40×
Operating theatre (ISO)	100	25	Vibration not perceptible. Suitable in most instances for surgical suites microscopes to 100× and other equipment of low sensitivity
<i>b</i>			
VC-A	50	8	Adequate in most instances for optical microscope to 400×, microbalances, optical balances, proximity and projection aligners, etc.
VC-B	25	3	Appropriate for inspection and lithography equipment (including steppers) to 3 µm line widths
VC-C	12.5	1–3	Appropriate standard for optical microscopes to 1,000×, lithography and inspection equipment (including moderately sensitive electron microscopes) to 1 µm line widths. TFT-LCD stepper/scanner processes
VC-D	6.25	0.1–0.3	Suitable in most instances for demanding equipment, including electron microscopes (TEMs and SEMs) and E-beam systems
VC-E	3.12	<0.1	A difficult criterion to achieve in most instances. Assumed to be adequate for the most demanding of sensitive systems including long path, laser-based, small target systems. E-beam lithography systems working at nanometer scales and other systems requiring extraordinary dynamic stability
VC-F	1.56	N/A	Not recommended for use as a design criterion, only for evaluation
VC-G	0.78	N/A	Not recommended for use as a design criterion, only for evaluation

N/A not available

a signal input which can be used to further analyzed in finite element modeling using ANSYS software to obtain the natural frequency, mode shapes and time history of the building.



Fig. 3 a Laser Doppler vibrometer (LDV 100). b Measurement at site



Fig. 4 Registrar office building (side view)

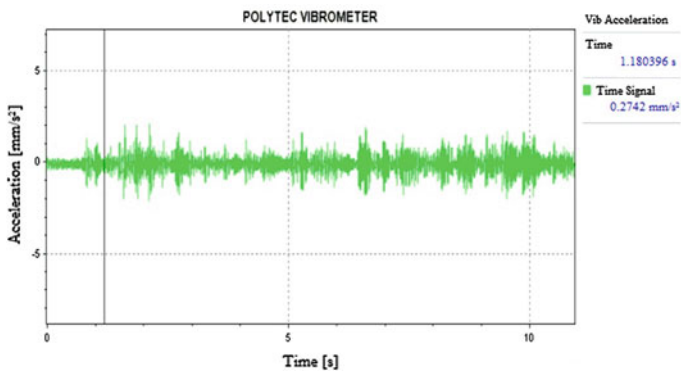


Fig. 5 Vehicles vibration waves measured by LDV 100

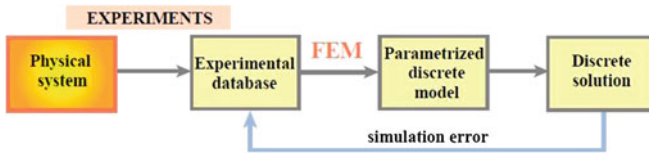


Fig. 6 Finite element method process [8]

5 Finite Element Method (FEM)

The process of FEM is shown in Fig. 6, and it is applied using the ANSYS and MATLAB software. In this study, the numerical simulation of vibration response on the Registrar office building was carried out by using ANSYS, finite element package software and a tool developed using MATLAB interface and algorithm known as Vibration Serviceability Assessment Tools (VSATs).

All relevant outputs from ANSYS were processed in MATLAB programs, where it will analyze the data from ANSYS and the output produced will be used to determine the level of vibration subjected by the building. Next, the data will then be compared to the vibration criteria curves which are used as a guideline in this study.

6 Results and Discussions

6.1 Mode Shape Analysis

Mode shape analysis was performed to determine the condition of the floor structure of the Registrar office building when subjected to different frequency modes. The first tenth modes are shown in Fig. 7. The fundamental mode of the building has a natural frequency of 1.02 Hz and shows no obvious deformation for the rest of the modes. Changes in the horizontal direction are not taken into account as the displacement at the column is not considered in this study. Only the vertical direction which shows changes on floor behaviour is taken into consideration.

The highest peak displacement for both directions is represented by the red area while the minimum displacement is represented by the blue area. For areas with the highest deflection, it is not recommended for sensitive equipment. The occupants in that area may also be affected.

A detailed description for each mode as shown in Fig. 7 is described in Table 3 for both horizontal and vertical directions. The model was analyzed under 100 modes to obtain the peak response of natural frequency and vertical behavior of the building floor structure.

Mode shape analysis is used to determine the condition of the floor structure of the building when subjected to different frequency modes. Highest peak displacement is

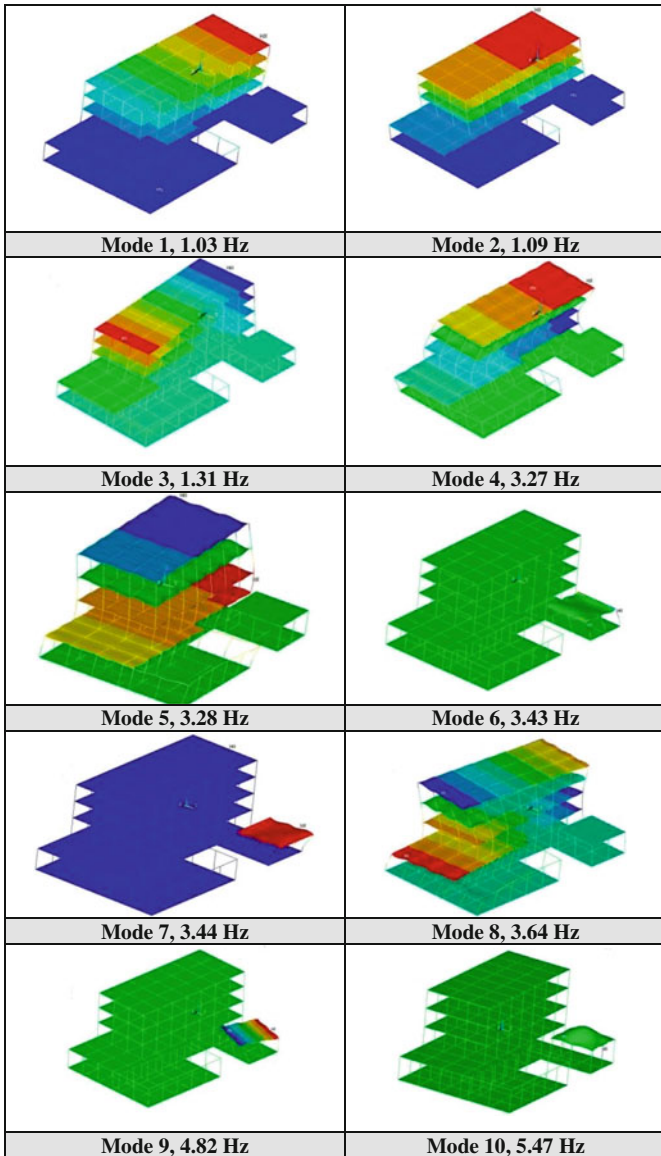


Fig. 7 First ten mode shapes of the Registrar office building

represented by the red area while the minimum displacement is represented by the blue area. Green areas shows a little displacement and not so obvious. For areas with the maximum deflection, that area is not suitable for sensitive equipment and people in this area may also be affected.

Table 3 Mode description for first ten modes

Mode/frequency (Hz)	Mode description	Displacement value (mm)
<i>a</i>		
Mode 1/1.03	Horizontal: small displacement	0.429
	Vertical: small displacement	1.543
Mode 2/1.09	Horizontal: small displacement	1.067
	Vertical: very small displacement	0.269
Mode 3/1.31	Horizontal: very small displacement	0.631
	Vertical: medium displacement	2.056
Mode 4/3.27	Horizontal: small displacement	0.856
	Vertical: small displacement	0.802
Mode 5/3.28	Horizontal: very small displacement	0.661
	Vertical: small displacement	0.931
<i>b</i>		
Mode 6/3.43	Horizontal: medium displacement	3.747
	Vertical: very small displacement	0.0159
Mode 7/3.44	Horizontal: very small displacement	0.0175
	Vertical: medium displacement	3.753
Mode 8/3.65	Horizontal: very small displacement	0.55
	Vertical: medium displacement	1.719
Mode 9/4.82	Horizontal: small displacement	4.064
	Vertical: small displacement	8.089
Mode 10/5.47	Horizontal: very small displacement	0.579
	Vertical: very small displacement	0.584

6.2 Vibration Serviceability Assessment Tools (VSATs)

VSATs is a MATLAB based GUI driven software developed to analyze and assess the vibration serviceability state of large structures such as footbridges. The software enables results from different models to be compared and can also be used for assessing vibration serviceability of structures where the model properties and serviceability is known [9].

Figure 8 shows the mode shapes of the first tenth modes obtained using VSATs analysis. Results obtained from VSATs in Fig. 8 shows the mode shape of each floor be identical or almost identical with the mode shape obtained in Fig. 7.

6.3 Vibration Criteria (VC) Analysis

Vibration serviceability analysis was carried out on each floor using VSATs. Figure 9a shows the vibration input and Fig. 9b shows the response after applying the input from field measurement on the third floor of the Registrar Office building.

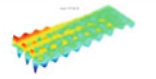
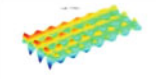
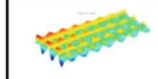
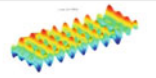
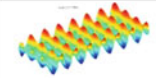
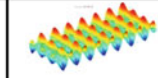
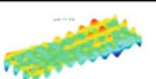
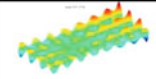
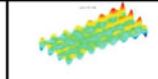
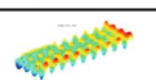
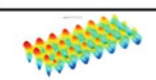
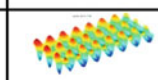
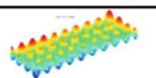
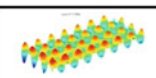
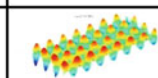
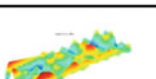
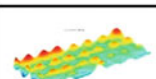
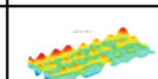
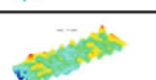
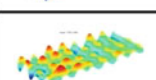
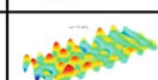
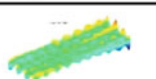
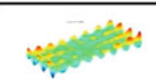
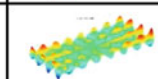
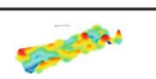
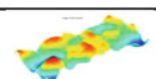
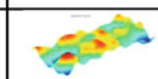
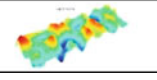
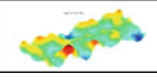
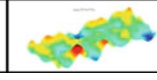
Mode/ Frequency (Hz)	First Floor	Second Floor	Third Floor
1/ 1.03			
2/ 1.09			
3/ 1.31			
4/3.27			
5/ 3.28			
6/ 3.43			
7/ 3.44			
8/ 3.64			
9/ 4.82			
10/ 5.47			

Fig. 8 Deform shape in VSATs, **a** first floor, **b** second floor, and **c** third floor

The dark blue areas represent the highest VC level which is above ISO standard, unsuitable for area with sensitive equipment while the light blue areas represent the ISO standard VC level, appropriate for office and no sensitive areas. The brown area represents VC-E, the lowest VC level.

All three floors show almost the same vibration response where the response obtained for each respective floor is in ISO standard range when referred to the

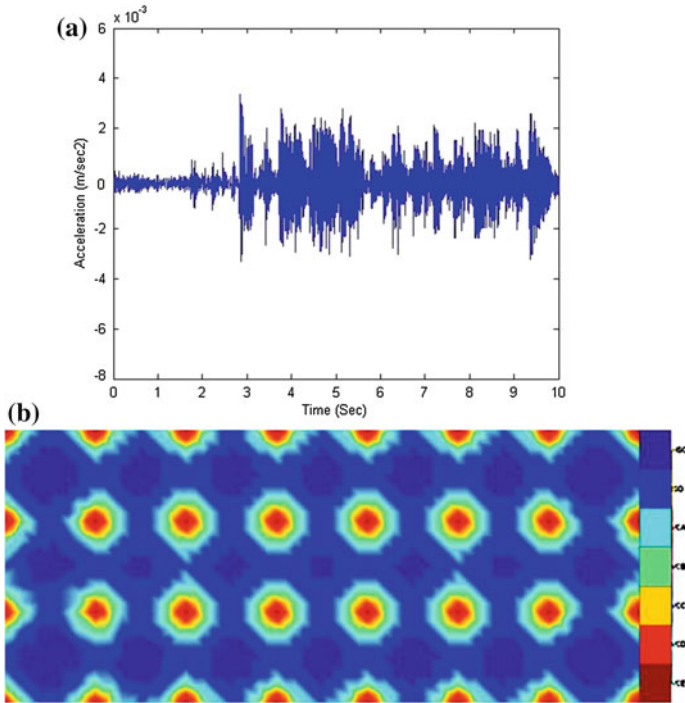


Fig. 9 a Vibration input and b response on the third floor of the Registrar office building

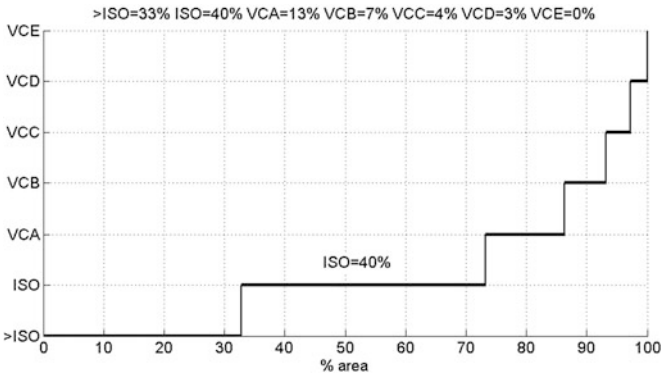


Fig. 10 The vibration criteria value on the third floor of Registrar office building

generic criteria guideline [4], 38 % ISO for first floor, 39 % ISO for second floor and 40 % ISO for the third floor. The vibration response for third floor is shown in Fig. 10.

7 Conclusion

The average value for the vibration criteria of the Registrar office floors are ISO level with the percentage of 38 % for the first floor, 39 % for the second floor and 40 % for the third floor. For the above ISO level, the percentage for first floor is 34 and 33 % for both the second and third floor. Referring to Table 2, the maximum value of amplitude for ISO level is 400 $\mu\text{m/s}$, which is appropriate for office building with no sensitive equipment. Whereas, the maximum value of amplitude for above ISO level is 800 $\mu\text{m/s}$, which is appropriate for workshop. Therefore, the maximum response value obtained from footfall is acceptable as the response obtained is mainly at the range of ISO and below. Thus, the vibration level would not affect the building structure, occupants and any electronic office equipment in this office.

It is really important to ensure that vibration level in building does not exceed the recommended standard to avoid costly repair of structure damage, replacement of electronic equipment and annoyance to the occupants in building. The objectives were achieved where the structural response on the UTHM's Registrar office building subjected to the footfalls vibration input was obtained and it was within the acceptable limit based on the generic vibration criteria.

Acknowledgments The authors would like to thank the staff at the Development and Property Management Office (PPH) UTHM for supplying the structural drawing of Registrar office building. This research is funded by Multi-Disciplinary Research (MDR) research grant Vot 1310 at Universiti Tun Hussein Onn Malaysia (UTHM). Also thank you to all those who were involved in this study.

References

1. Broughton Suspension Bridge, http://en.wikipedia.org/wiki/Broughton_Suspension_Bridge. Retrieved date: 16.10.2012, Time: 2015 hours
2. N. Sylvestre-Williams, B. Rimrott, J. Cho, The vibration of a high rise building's columns due to rhythmic activity internoise, in *Inter Noise*, Lisbon, 15–16 June 2010, pp. 1–8
3. B. Davenny, Footfall induced vibrations healthcare facilities. *Health Care Des. Mag.* (2010), <http://www.healthcaredesignmagazine.com/blogs/acentech/footfall-inducedvibrations-healthcare-facilities>. Retrieved date: 13 Dec 2012, time: 1544 h
4. H. Amick, M. Gendreau, T. Busch, C.G. Gordon, Evolving criteria for research facilities: I-vibration, in *SPIE Conference 5933: Buildings for Nanoscale Research and Beyond*, San Diego, California (2005)
5. O. Arup, *Hospital Floor Vibration Study, Comparison of Possible Hospital Floor Structures with Respect to NHS Vibration Criteria* (Ove Arup & Partners Ltd., London, 2004)
6. H. Amick, On generic vibration criteria for advanced technology facilities: with a tutorial on vibration data representation. *J. Inst. Environ. Sci.* **XL**, 35–44 (1997)

7. C.G. Gordon, Generic criteria for vibration sensitive equipment, in *Proceedings of the International Society for Optical Engineering*, San Jose, United States (1991)
8. C.A. Felippa, *Introduction to Finite Element Methods* (University of Colorado, Boulder, 2004)
9. A. Pavic, J.M.W. Brownjohn, S. Zivanovic, VSATs Software for assessing and visualizing floor vibration serviceability based on first principles. *Structures Congress 2010*. American Society of Civil Engineers, Orlando, Florida. 902–913 (2010)

Shear Resistance Analysis of Rebar Connector in RC Stocky Wall Panel Using Lusas 3D Modelling

Noraspaleta Abdullah, Mohd Suhelmiey Sobri and Siti Hawa Hamzah

Abstract Reinforced concrete (RC) stocky wall panel is a new innovation to the construction industry. To-date, studies on the RC stocky wall panel are under progress. This paper is analyzed shear resistance of rebar connector in RC stocky wall panels using LUSAS 3D model. Four (4) number of model have been analyzed using finite element analysis with varies size of rebar connector which is T12, T16, T20 and T25. These models of RC stocky wall panel was constructed in same dimension, 125 mm × 1,000 mm × 500 mm (Thickness:Length:Height). This paper was concerned with a finite element model to determine the maximum deflection of the RC stocky wall panel in resisting lateral load. These four (4) models are being analyzed to observe its deflection, stress and strain. The result was illustrated and discussed in graphs namely stress-strain relationship and also load versus displacement contour. The size of rebar connectors are affected the shear resistance results in term of lateral deflection, stress and strain. From this study, it can be concluded that, the larger diameter of rebar size has give the less displacement in model.

Keywords RC stocky wall panel • Rebar connector • Shear resistance • Deflection

N. Abdullah · M.S. Sobri (✉) · S.H. Hamzah
Faculty of Civil Engineering, Universiti Teknologi MARA (UiTM), Shah Alam,
Selangor, Malaysia
e-mail: suhelmiey_sobri@yahoo.com

N. Abdullah
e-mail: noraspalela.abdullah@yahoo.com

S.H. Hamzah
e-mail: shh@salam.uitm.edu.my

1 Introduction

Wall can be categorized in many types with different function. The reinforced concrete (RC) wall is one of the type walls that is categories as load bearing or non-load bearing. Load bearing wall caters the load from its own weight and the load from the main structure such as beam and slab followed by transmitting the load to the foundation. Non-load bearing wall only uphold its own weight, then all load transfer to the column and proceed to the foundation.

In Malaysia the wall panels are widely used and have already been used in numerous projects, including the construction of residential houses, hotels and commercial buildings. RC wall panel is usually design and manufacturer in rectangular shape. The RC stocky wall panels are same like shear wall panels in term of function but different in dimension size of wall.

Nowadays the Industrialised building system (IBS) is compulsory to be used in all the Malaysian government's projects which must not be less than 70 % of the all building works. Based on the structure scopes IBS can be divided into five major parts;

- Precast concrete framings, panel and box systems,—The common group of IBS products is the pre-cast concrete elements which is precast concrete columns, beams, slabs, walls and lightweight precast concrete and etc.
- Steel framework systems; example of steel framework systems are tunnel forms, tilt-up systems, beams and columns moulding forms, and permanent steel formworks (metal decks).
- Prefabricated timber framings systems—Commonly used with pre-cast concrete slabs, steels columns and beams, steel framing systems.
- Framing systems—Among the products listed in this category are timber building frames and timber roof trusses.
- Blockwork systems—The construction method of using conventional bricks has been revolutionized by the development and usage of interlocking concrete masonry units (CMU) and lightweight concrete blocks.

The RC stocky wall panels can be categorized as precast concrete and are one of the elements in the IBS. The stocky wall panels was categories as precast concrete framings, panel and box systems. The products of IBS are encouraged to be used in the construction industries to speed up the delivery time and built affordable and quality of project.

The precast RC wall panels are manufactured in factories, and mobilized to the site. Generally to easier mobilize to the site, the manufacturer will design the components of wall with a certain fixed length and shall be connected at the site. The workers at site must connect the RC wall to the main structure such as column and beam. The connection from one wall panel with other panel is importance because the lower workmanship at final work will make the lower performance in structure serviceability.

The innovation in stocky wall panels as load bearing wall have been most helpful in the construction industry to achieve that short time frame in work and on the other hand will make much energy efficiency benefits in construction. The minimum wastage on the rebar used in the site project will contribute to energy efficiency. The use of rebar's to link these stocky wall panels as the main wall structures is the main focus of this study.

Rebar also known as reinforcement bar, reinforcing steel or deformed bar. Normally rebar formed from the carbon steel, the normal reinforcement bar used in Malaysia's industries is mild steel round bar (Grade 250) and high tensile deformed bar (Grade 460) but in certain special construction, the contractor was used special grade of high tensile bar for minimize the number of reinforcement bars example Grade 500.

The RC stocky wall panels with rebar connector is a newbie in construction industries, which is more research should be done to this wall in order to make it useable to construction industries in future. The new finding and research about the RC stocky wall panels will make the industries become more effective and competitive.

2 Theoretical Wall Design Using British Standard (BS 8110: Part 1: 1997)

According to BS 8110, a wall is defined as a vertical load- bearing member whose length on plan exceeds four times its thickness and on the other hand the member can call as a column [1]. A reinforced wall with minimum amount of vertical reinforcement used can be categorised as plain concrete wall. According to BS 8110 (clauses 3.9.4), it recommends that the design ultimate axial force in a plain concrete wall may be calculated on the assumption that the members transmitting forces on the walls are simply supported. Summary for design requirement for reinforced concrete wall are given in Table 1.

3 Finding from Previous Research

RC Wall panel is commonly used in construction industries. Basic functions of wall are partition of area, separator for interior space, some time as fire wall and etc. RC walls have three main structural functions where are listed below;

- Resist gravity loads applied through floor framing systems.
- Resist lateral loading imposed by earth pressure or liquid pressure.
- Resisting lateral resistance from wind or earthquake forces and/or promotes lateral stability to a building.

Table 1 Data properties preparation

	Area of steel reinforcement ($A_{sc} \geq 4 h \text{ mm}^2/\text{m}$)
Unbraced walls	Effective Height
	l_e to be determined as for columns (refer BS 8110, Clause 3.8.1.6.1)
	Stocky Wall ($l_e/h \leq 15$, where h is wall thickness)
	Design unit length of wall as a short column bent about the minor axis, with $e_{min} = 0.05 h \leq 20 \text{ mm}$ (refer to BS 8110 design chart for rectangular column)
	Alternatively, for a wall supporting an approximately symmetrical arrangement of slabs (uniform load and spans differing by no more than 15 %)
	Design ultimate axial load per unit length is given by
	Slender Wall ($15 < l_e/h \leq 40$ for $A_{sc} < 10 h$, 45 otherwise)
	Design unit length of wall as a slender column bent about the minor axis. If only one layer of centrally placed reinforcement is provided, double the additional moment
Unbraced walls	Effective Height
	l_e to be determined as for columns (refer BS 8110, Clause 3.8.1.6.1)
	Stocky Wall ($l_e/h \leq 10$, where h is wall thickness)
	Considered as for braced column
	Slender Wall ($10 < l_e/h \leq 30$)
	Design unit length of wall as a slender column bent about the minor axis. If only one layer of centrally placed reinforcement is provided, double the additional moment due to slenderness

RC wall Panel is suitable for using as components in Industrialize Building System (IBS). Steel fibre reinforced concrete wall panel with aspect ratio (h/l) and slenderness ratio (h/t) are 1.5 and 20 respectively shall be sustained more capacity and advantages in terms of crack compared with the normal reinforced concrete wall, [2]. The reinforced concrete stocky wall panel by using recycled aggregate with double layers steel fabric can achieved high ultimate strength compared with the theoretical results [3].

Study on the nonlinear behavior of reinforced concrete slit wall with shear connection using finite element software ANSYS 12. The study has founded that the finite element analysis was simulated accurate and realistic the behavior of the reinforced concrete walls [4]. On the other hand, the slender and stocky reinforced concrete walls shall be started flexural and deform when the walls nominal shear strength of approximately twice the lateral force [5]. The nonlinear behavior of composite shear walls with vertical steel encased profiles is believed that the shear failure can be avoided if the composite elements in the shear wall are designed to bending and shear at the associated shear force of the capable bending moment [6]. On the contrary, the nonlinearities are caused by the steel yielding which occurred in steel profiles and vertical reinforcement, plastic deformations occurred in concrete, steel concrete connection and due to shear stud connector's behavior [7]. The ultimate shear resistance of the multiple shears key connection mainly depends on the load was acted to the connection, and the hearing stresses and shear friction along the slip surfaces [8].

4 Methodology

Generally, this research was used LUSAS software version 14.7 to identify the solutions and get the results and achieve the objective for this research.

4.1 Analysis

The main focus of this research to investigate and analysis the behavior of rebars connector in RC stocky wall panel by using Finite Element Method (FEM) in non linear method. From the analysis, the maximum deflection, maximum stresses and strains of the RC stocky wall panel using LUSAS 3D has been discussed. Finite element methods can make advanced computing facilities in obtaining safe and optimum building solutions without the need for expensive and time consuming laboratory testing and at the same time his was stated that the finite element method is innovative and efficient building products [9].

4.2 Computer Modelling Using LUSAS Software

Linear and nonlinear finite element analysis can be prepared using LUSAS computer program. The LUSAS program shall be capable to provide 3-Dimensional graphical modeling for the sample of RC stocky wall panel. Finite Element Analysis was modeling in three (3) stages of works, which is:

1. Pre-Processing/Modelling
2. Finite Element Solver/Running the analysis
3. Results-Processing/Viewing the results

4.3 RC Stocky Wall Panel

Four (4) models of Reinforced concrete (RC) Stocky Wall Panel with dimensions 125 mm × 1,000 mm × 500 mm (Thickness:Length:Height) has been modeled by using LUSAS 3D program. The RC stocky wall panel was modeled by using concrete Grade 30 ($f_{cu} = 30 \text{ N/mm}^2$) and double layer steel fabric types B385 (B7) as the main reinforcement. Rebar connector with sizes of T12, T16, T20 and T25 are defined in the four numbers of RC short wall panel models respectively. The rebar connector has been modeled in vertically between the two RC stocky wall panels and analysed using the LUSAS software. Figure 1 shows the detailed models dimensions of RC stocky wall panel. The lateral global load distributed 0.2858 kN/m was used in the modeling. The load is converted based on the basic wind speed 100 years return periods for Ipoh. The data from Ipoh was used because their give

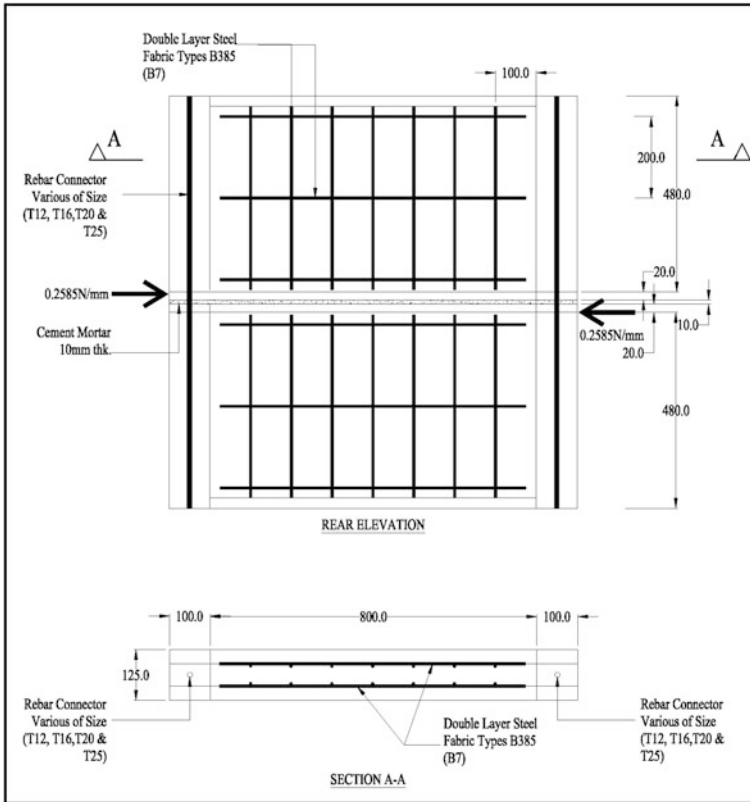


Fig. 1 RC stocky wall detailing model with rebar connector of various size

critical values for wind speed in Malaysia. The data has been founded from the Jabatan Meteorologi Malaysia.

4.4 Data Used in LUSAS Modeling

The double layer of rectangular steel fabric mesh type B385 or B7 with 7 mm diameter of wire has been used to reinforce the samples [10]. The mesh size nominal pitch of wires for main wire is 100 mm spacing centre to centre and for the cross wire is 200 mm centre to centre. The cross section area per meter width for the main wire is 385 mm^2 and for the cross wire is 193 mm^2 . The yield stress for the steel fabric mesh and the reinforcement bars is 485 and 460 N/mm^2 respectively. Furthermore, the other properties of the materials used for the steel fabric mesh and rebar connector are the Young's modulus specified as $209,000 \text{ N/mm}^2$, Poisson's

Table 2 Data properties preparation

1. Grade of concrete	30 N/mm ²
2. Grade of reinforcement	
(a) Nominal reinforcement	460 N/mm ²
(b) Welded steel fabric	485 N/mm ²
3. Density of concrete	24 kN/mm ³
4. Dimension of wall	125 mm × 1,000 mm × 500 mm (Thickness:Length:Height)
5. Concrete cover to reinforcement	25 mm
6. Reinforcement bar @ rebar connector size	
(a) Model 1	12 mm
(b) Model 2	16 mm
(c) Model 3	20 mm
(d) Model 4	25 mm
7. Steel fabric types	B 385 (B7) 7 mm diameter
8. Selfweight-gravity load	9.81 N/mm ²
9. Mortar thickness	10 mm

ratio 0.3, mass density specified as 7,800 kg/m³ and coefficient of thermal expansion 0.011E-3. Tables 2 are shown the data that used in LUSAS Modeling.

The concrete properties material has been assigned based on the BS 8110 for concrete Grade 30 with Young's modulus specified as 26,000 N/mm², Poisson's ratio 0.2, mass density specified as 24 kg/m³. Mortar with 10 mm thickness was used in the model as a join for RC stocky wall panels. The properties materials used for mortar are the Young's modulus specified as 15,000 N/mm², Poisson's ratio 0.25, mass density specified as 24 kg/m³. LUSAS elements are classified into groups according to their function. Two types of elements has been used in modeled RC stocky wall panels, there are bar element, BRS2 and 3D continuum element, HX8M. The bar elements BRS2 were selected for the steel fabric mesh while on the other hand the elements HX8M were used for the concrete section. BRS2 are three-dimensional bar elements comprising of 2 nodes each with 3 degrees of freedom and the geometric properties of this element is constant along the length of the bar. In the analysis, BRS2 can be deformed perfectly. HX8M elements are three dimensional solid hexahedral elements comprising 8 nodes each with 3 degrees of freedom moreover the HX8M elements are linear with respect to geometry. The displacement contour variations along the length of the element are linear axial, linear rotational and cubic transverse displacement contour. Figure 2 shows the LUSAS element used in modeling the RC stocky wall panel. All the RC stocky wall panels have been assigned with fully fixed supports at the top and bottom of the wall. Figures 3 and 4 show the support conditions, load applied location on wall panel and mortar location that has been modeled in LUSAS software.

Fig. 2 LUSAS elements used in modelling

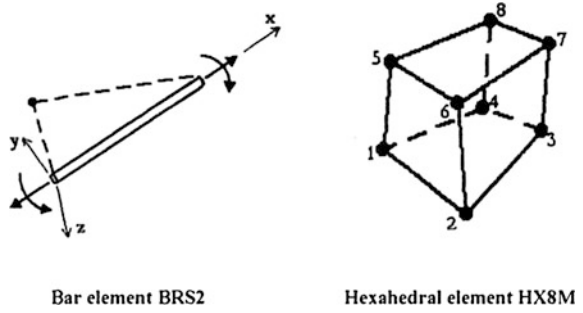


Fig. 3 RC stocky wall panel-LUSAS model

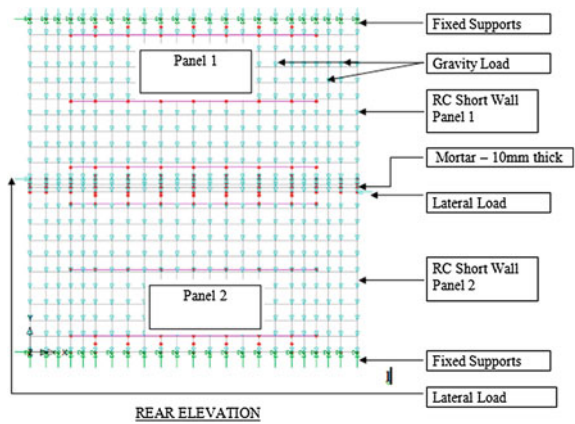
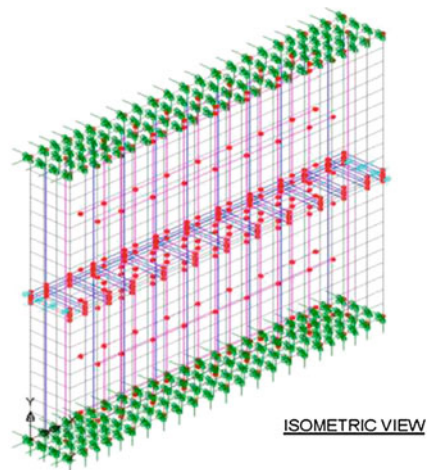


Fig. 4 RC stocky wall panel-LUSAS model



5 Result and Discussion

Four (4) models of RC stocky wall panels was modeled and analysed under horizontal load condition. All the models was modeled using difference size of rebar connector which is T12, T16, T20 and T25 and the cross section area of reinforcement bar is 113.10, 201.061, 314.161 and 490.871 mm² respectively. RC stocky wall panel Model 1, Model 2, Model 3 and Model 4 are representative the RC stocky wall panels with the rebar connector size T12, T16, T20, and T25 respectively. Tables 3, 4 and 5 shown the maximum displacement in x-direction, maximum and minimum stress in x-plane, and maximum and minimum strain in x-plane was occurred on Model 1, Model 2, Model 3 and Model 4.

5.1 Graph of Load Versus Displacement

Figure 5 show load in x-direction versus displacement in x-direction for Model 1, Model 2, Model 3 and Model 4 as model with T12, T16, T20 and T25 respectively.

Table 3 Maximum displacement in x-direction

Model number	Elastic condition – max displacement in x-direction (mm)	Plastic condition – max displacement in x-direction (mm)
Model 1	0.0392×10^{-3}	0.242
Model 2	0.0382×10^{-3}	0.243
Model 3	0.0373×10^{-3}	0.213
Model 4	0.0366×10^{-3}	0.239

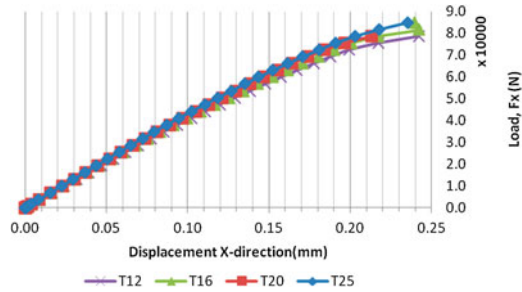
Table 4 Maximum and minimum stress in X-plane

Model number	Elastic condition – max stress in x-plane (N/mm ²)	Elastic condition – min stress in x-plane (N/mm ²)	Plastic condition – max stress in x-plane (N/mm ²)	Plastic condition – min stress in x-plane (N/mm ²)
Model 1	3.236e-3	-8.200e-3	36.729	-65.918
Model 2	3.180e-3	-9.815e-3	64.262	-80.845
Model 3	2.556e-3	-9.093e-3	64.262	-80.845
Model 4	2.035e-3	-8.665e-3	18.125	-47.557

Table 5 Maximum and minimum strain in X-plane

Model number	Elastic condition – max strain in x-plane (N/mm ²)	Elastic condition – min strain in x-plane (N/mm ²)	Plastic condition – max strain in x-plane (N/mm ²)	Plastic condition – min strain in x-plane (N/mm ²)
Model 1	0.067e-6	-0.267e-6	0.469e-3	-1.698e-3
Model 2	0.068e-6	-0.316e-6	0.844e-3	-2.048e-3
Model 3	0.066e-6	-0.295e-6	0.642e-3	-1.790e-3
Model 4	0.068e-6	-0.281e-6	0.591e-3	-2.246e-3

Fig. 5 Load displacement relationship of RC stocky wall panel for model 1, 2, 3, and 4

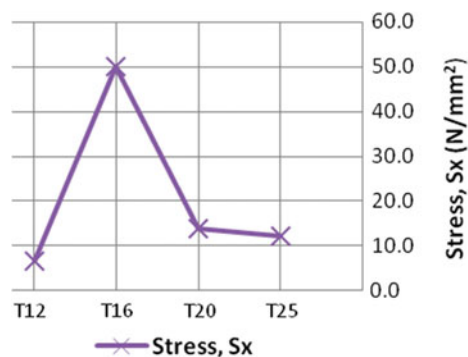


From the graph, the rebar connector T25 give less displacement on the higher load. The maximum load for model 1 (T12), model 2 (T16), model 3 (T20), and model 4 (T25) before the model yielded are 78.64, 81.765, 78.64 and 84.89 kN respectively. When comparing displacement with size of rebars connector, it can clearly be seen that the bigger size of rebar connector will give less displacement.

5.2 Graph of Stress Versus Strain

Figures 6 and 7 are showing the graph of stress-strain curve for RC stocky wall panel for all models. However in Fig. 6 shows the graph of maximum stress and size of rebar connector relationship. The maximum stress occurred on model with the rebar connector of size T16 and the value 49.895 N/mm². In the other hand, the Fig. 7 shows the graph of stress in Sx-plane versus strain in Ez-plane. Based on the analysis, these three types of plane give the maximum value of stress and strain because the shear resistance was occurred in this plane area. From the analysis the maximum stress and strain was occurred at the location of the applied load position. When the RC stocky wall panel was loading beyond the proportional limit, the elongation increases more rapidly and reached the elastic limit.

Fig. 6 Maximum stress versus size of rebar connector



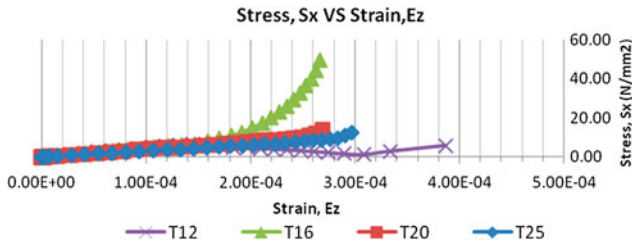


Fig. 7 Graph of stress (Sx) versus strain (Ex) of RC stocky wall panel for model 1, 2, 3 and 4

6 Conclusion

From this study, it can be concluded that there are some differences of structural behavior of reinforced concrete shear wall by using different size of rebar connector. In this paper the parameter of different size of rebar has been considered with function as rebar connector between the top and bottom connection of RC stocky wall panels. Based on the lateral load applied to the RC stocky wall models, the displacement contour were determined in all directions, and the maximum is found to be 0.243 mm which occurred in x-direction. The maximum displacement occurred in model 1 with rebar connector of size T12. Based on the results the maximum values for stress is $49.895 \text{ N/mm}^2 > 30 \text{ N/mm}^2$ and occur in x-plane of model 2 with rebar connector T16.

From this research, it can be concluded that the size of rebar connector used in the model of RC stocky wall panels affect the values of displacement, stress and also strain. Based on the results, RC stocky wall panels size $125 \text{ mm} \times 1,000 \text{ mm} \times 500 \text{ mm}$ (Thickness:Length:Height) with rebar connector size T20 is suitable to be used in the design because the stress from the modeling is 13.793 N/mm^2 , which is not exceed the concrete strength has been used (30 N/mm^2) in this design and moreover at same time to avoid crack problem to the RC stocky wall panel. Based on calculation using BS 8110, the shear stress for model 3 with rebar connector T20 is 1.258 N/mm^2 and less than the maximum shear stress which is 5 N/mm^2 or $0.85\sqrt{f_{cu}}$. The shear resistance of RC stocky wall panel with rebar connector T20 also fulfills the requirement was stated in BS 8110.

Acknowledgments The authors express their sincere gratitude to the Concrete, Fabrication and Heavy Structure Laboratory Faculty of Civil Engineering, UiTM Malaysia for providing the laboratory and testing facilities during the conduct of this research and Ministry of Science, Technology and Innovation (MOSTI) for their invaluable help and funding support while conducting this research.

References

1. BS 8110, *Structural Use of Concrete, Part 1, Code of Practice for Design and Construction* (British Standards Institution, London, 1997)
2. A.R Nurharniza, H. Siti Hawa, E.T. Wong, Effective performance of steel fibre reinforced concrete wall panel for IBS component, in *International Conference on Construction and building technology, ICCBT*, C-(18), pp. 203–212 (2008)
3. S. Mohd Suhelmiey, H. Siti Hawa, M.R. Ahmad Ruslan, Ultimate strength of steel fabric reinforced concrete short wall panel using crushed concrete waste aggregate (CCWa). *Int. J. Civil Environ. Eng. IJCEE-IJENS* **11**(01), 64–80 (2011)
4. B. Sergiu, C. Ioan-Petru, *Nonlinear Finite Element Analysis of Reinforced Concrete Slit Walls with ANSYS (I)*. *Buletinul Institutului Politehnic Din Iasi*, pp. 31–55 (2011)
5. M.M. Leonardo, O. Kutay, W.W. John, Flexural and shear responses in slender Rc shear walls, in *13th World Conference on Earthquake Engineering, Vancouver*, 1–6 Aug 2004, Paper No. 1067, B.C., Canada (2004)
6. D. Dan, A. Fabian, V. Stoian, Nonlinear behavior of composite shear walls with vertical steel encased profiles. *Eng. Struct.* **33**, 2794–2804 (2011)
7. V. Stoian, D. Dan, A. Fabian, Composite shear walls with encased profiles, new solution for buildings placed in seismic area. *Acta Technica Napocensis Civ. Eng. Archit.* **54**(1), 6–12 (2011)
8. H.R. Sarni, L.S.J. Reynaud, H. Scott, K.A. Emmanuel, Multiple shear key connections for precast shear wall panels. *PCI J.* 104–120 (1989)
9. M. Mahendran, Applications of finite element analysis in structural engineering, in *Proceedings International Conference on Computer Aided Engineering*, Chennai, India, eds. by P.N. Siva, A.S. Sekar, S. Krishnapillai (2007), pp. 38–46
10. BS 8666, *Scheduling, Dimensioning, Bending and Cutting of Steel Reinforcement for Concrete-Specification* (British Standards Institution, London, 2005)

Determination of Modulus Elasticity and Poison Ratio of Expanded Polystyrene (EPS) Lightweight Concrete (LWC) Enhanced with Steel Fiber

Jamilah Abd. Rahim, Siti Hawa Hamzah and Hamidah Mohd Saman

Abstract Nowadays lightweight concrete (LWC) is used on a large scale for structural purposes. The application of structural LWC in the construction industry has many advantages such as saving in dead load for structural design and foundation, reduce the risk of earthquake damage to structure, and good tensile strain capacity. Modulus of elasticity of concrete has been considered as a vital factor in designing concrete structures. However, in practice, the concrete modulus usually not measured, but estimated from the concrete compressive strength using empirical. Therefore, this study is conducted to determine the modulus elasticity of lightweight concrete by stress-strain in lateral and longitudinal direction. Hence, the poison ratio of LWC also determined. From this research, it was found that Poison ratio for the EPS-LWC enhanced with steel fiber is 0.17. Meanwhile, the modulus of elasticity is 13.79 GPa.

Keywords Poison ratio · Modulus of elasticity · Expanded polystyrene (EPS) · Steel fiber · Lightweight concrete

1 Introduction

In 21st century, engineers are challenged to build taller and skyscrapers to be an iconic to the country. This situation challenges development of new light weight material with superior strength to enhance the carrying capacity of the structural death in the build design.

J. Abd. Rahim (✉) · S.H. Hamzah · H.M. Saman
Faculty of Civil Engineering, Universiti Teknologi MARA,
40450 Shah Alam, Selangor, Malaysia
e-mail: jamilahabdrahim@yahoo.com

S.H. Hamzah
e-mail: shh@salam.uitm.edu.my

H.M. Saman
e-mail: hamid929@salam.uitm.edu.my

Lightweight concrete (LWC) is one of the favourable material to be used as it has low density with acceptable high strength, good tensile strain capacity, low coefficient of thermal expansion due to the voids present in the LWC. The LWC have density from 1,000 to 2,000 kg/m³ and compression strength from 1 to 100 MPa [1]. From literature, it is has indicated that there are three (3) categorize of LWC namely no fines concrete, aeration or foam concrete and lightweight aggregate concrete. There are two (2) type of lightweight aggregate: natural and artificial. Expanded Polystyrene (EPS) is one of the artificial lightweight aggregate types with low density of only 10–30 kg/m³ and strength of EPS lightweight aggregate is almost zero (0).

Nevertheless, in certain applications, such as ocean platforms and long-span bridges, the need higher for durability and toughness concrete because important and must be given appropriate attention. Structures from LWC mixture can design to have similar strength and mechanical characteristic as in normal concrete.

Unfortunately, the aggregate used to reduce the unit weight of concrete also typically degrade its elastic properties, in particular the Young's Modulus and strength [2, 3]. To improve it tensile and strength, concrete may be reinforced with suitable fibers. Steel fibers are especially effective. However, most studies on steel fiber reinforced concrete have neglected lightweight concrete. Therefore, expanded polystyrene (EPS) beads have been used as lightweight aggregate and enhanced with steel fibre to produce light weight concrete. For a given type of aggregate, there is a strong correlation between the cement content, aggregate volume fraction, fiber content, compressive strength and elastic properties.

2 Modulus Elasticity

The modulus of elasticity and Poisson ratio of concrete are fundamental parameters necessary in structural analysis for the determination of the strain distributions and displacements especially when the design process is based on elasticity considerations. According to the results given in literature and in design standards [4, 5] the modulus of elasticity and Poisson ratio are estimated from compressive strength of concrete, which increases with age. Modulus of elasticity was also determined from the empirical formula. Concrete modulus generally increases with strength. The composite modulus will therefore also increase. Compression strength also influences the value of Young's Modulus. The modulus of the elasticity of lightweight concrete is lower than normal concrete [6]. This obviously showed by using polystyrene as a lightweight aggregate will reduce the structural strength of concrete. Therefore, there is need to determine the Modulus elasticity and Poisson ration by using empirical formula and experimental works.

The bond between fibres and cement paste matrix depends on the ability of the fibres to absorb water. Modulus of elasticity indicate that the steel fibres were able to sustain higher load at given deformation compared with the polyethylene fibres (PF). This is because steel fibres can ensure more effective stress transfer and

develop better bonding over crack opening. From the experiment, the value Modulus of elasticity for steel fiber-high strength concrete is 38.1 GPa and for PF- high strength concrete is 37.0 GPa [7]. Compression strength also influences the value of modulus of elasticity. The different of water cement ratio affect the compression strength of the concrete [8]. The research shown lowest water cement ratio gives the highest value of compression strength. Therefore, to achieve the highest strength of EPS concrete the water cement ratio should be kept as low as possible to increase the entrapped air content due to incomplete compaction.

3 Empirical Formula

In practice, the concrete modulus is usually not measured, but estimated from the concrete compressive strength using empirical formula. According to ACI Building CODE 318-83, the Young's Modulus of normal concrete is:

$$E_c = 4.7f_c^{0.5} \quad (1)$$

where, f_c is cylinder compressive strength. For concrete with density from 1,500 to 2,500 kg/m³, the relationship changes to:

$$E_c = 43\rho^{1.5}f_c^{0.5} \times 10^{-6} \quad (2)$$

while Poison ratio can be determine by:

$$\text{Poisson's Ratio, } \nu = \frac{\text{lateral strain}}{\text{longitudinal strain}} \quad (3)$$

4 Experimental Works

4.1 Material and Mix Proportion

Following the general usage in real construction, ordinary portland cement (OPC) was used as cementing material coarse aggregate with size of passing 10 mm, and fine aggregate that passing 2.36 mm were used. Size of EPS beads is 3.0 mm diameter. Steel fiber with hooked ends type with size of 60 mm length and 1 mm diameter was incorporated in EPS-LWC.

There are three concrete mix proportion which is normal concrete, expanded polystyrene lightweight concrete (EPS-LWC), and expanded polystyrene enhance with steel fiber lightweight concrete (EPS-SF LWC). Details of concrete mix proportion are shown in Table 1. There are six (6) cylinders were casted for each mix proportion.

Table 1 Mix proportion details

Material	Weight per m ³ (kg)		
	Series 1	Series 2	Series 3
OPC cement	376	263	262
Water	233	163	162
Fine aggregate	1,003	701	696
Coarse aggregate	788	701	696
30 % EPS beads	–	4.93	4.94
0.5 % steel fiber	–	–	41.3
No. of samples	6	6	6
Size of cylinder (mm)	150 × 300	150 × 300	150 × 300

Fig. 1 Strain gauge placed on the cylindrical surface

4.2 Sample Preparation

The fresh concrete directly transferred into cylindrical steel mould after the mixing process already completed. The cylindrical mould was filled with 1/3 of fresh concrete and vibrated using vibration table for several times. However, only slow vibration was applied for series 2 and series 3 to avoid segregation of EPS beads. This step will repeat until the cylindrical mould was fully filled. After 24 h casted, all the samples were immersed into the water tank for 28 days as the curing process. The samples were tested using 1,000 kN Universal Testing Machine (UTM). Strain gauge was placed on the cylindrical surface to measure the stress- strain in lateral and longitudinal direction and connected to the data logger. Figure 1 shows the lateral and longitudinal strain gauge placing on the cylindrical surface to measure the poison ratio for each mix proportion series.

5 Result and Discussion

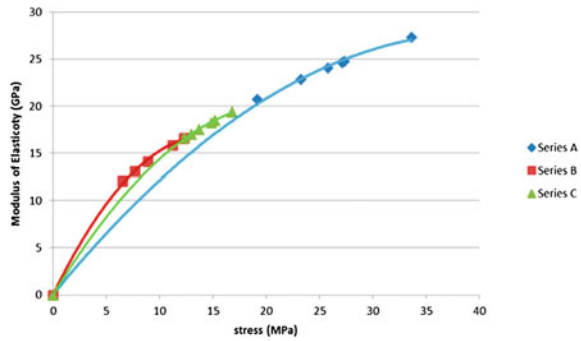
5.1 Stress-Strain Lateral and Longitudinal Direction

Table 2 shown the summarization data from the experiment that has been done to determine stress-strain in lateral and longitudinal direction for three different mix

Table 2 Poison ration and modulus elasticity

Series	Stress (MPa)	Poison ratio	Modulus elasticity
A	26.05	0.21	23.90
B	9.81	0.15	10.82
C	14.28	0.17	13.79

Fig. 2 Relationship between modulus elasticity and compressive strength



proportion of concrete. For series A, which is normal concrete value of poison’s ratio obtained is 0.21. The value is accepted because the range of poison’s ratio for normal concrete is 0.18–0.22. Meanwhile for series B, gives the lowest value of Poison’s ratio which is 0.15. This is because by using EPS as the lightweight aggregate in a concrete mixing will produce low Poison’s ratio value. For series C, the proportion of lightweight concrete with 0.5 % of steel fiber the compressive strength increased. Hence, the result of Poison’s ratio for series C was increased to 0.17.

Figure 2 shows the relationship between modulus of elasticity and compression stress of the three series. Sample in series A was recorded the highest modulus of elasticity which is 23.90 GPa. It is because series A is normal concrete. Modulus elasticity from series C was higher than samples in series B. This is because the presence of steel fibre in EPS-LWC were able to sustain high load at given deformation compared to the composition in series B which is consist of expanded polystyrene beads only. The average value of Modulus of Elasticity for series C is 13.79 GPa while in series B is 10.82 GPa only. The graph also describes when the compression stress increased, the modulus of elasticity also increased. Concrete in series C gives high compression stress result compared to concrete in series B. By adding polymer material such as polystyrene, it weaken the modulus of elasticity [9].

5.2 Cracks Pattern

Crack pattern of each series mix proportion was figure out after compression load applied to determine stress-strain of the sample. There are different pattern that was produced from three (3) different mix proportion as shown in Fig. 3. Based on the

Fig. 3 Crack pattern for each mix proportion

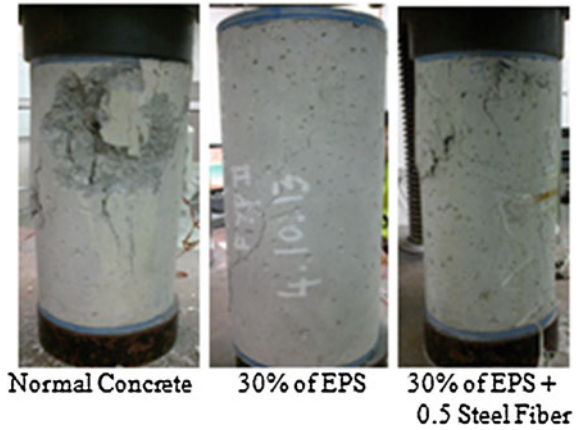


Table 3 Force and deformation for each series

Series	No. of sample	Force (kN)	Deformation (mm)
A	6	338.900	4.298
		410.793	2.441
		451.791	3.143
		594.264	2.689
		482.732	2.324
	Average	459.605	3.084
B	6	157.032	1.880
		114.452	3.314
		135.028	3.697
		197.803	5.463
		216.604	3.686
	217.676	3.368	
Average	173.099	3.568	
C	6	156.600	6.635
		216.991	4.737
		241.575	4.259
		227.963	6.302
		145.947	5.155
	261.576	7.947	
Average	208.442	5.839	

figure above, control sample was rupture after axial force was applied on that sample. The maximum applied force is 458.161 kN. Whereas, for sample which is containing 30 % of EPS was cracking at mid height at the 173.099 kN maximum applied load. The sample is slowly cracking but not rupture like control sample. This is because the EPS has ductility characteristic which is ability to deform under

compressive stress that applied [10]. However, the maximum force is less than control sample since by using polystyrene as a lightweight aggregate will make structural strength of concrete more weaker [6].

For sample mix using 30 % of EPS enhanced 0.5 % of SF, the cracking occur at the top of the sample and stop spreading before arrive at the middle of the sample. By adding of steel fiber into concrete mix will be resulted arresting growth of cracks based on the bond of steel fiber and cement paste. Steel fiber also can transfer more effective stress and develop better bonding over cracking [11]. So, the length of the crack is shorter than sample containing only EPS. In addition, it seems that control sample was crack in longitudinal axis. Whereas, others two samples crack in lateral axis. This is because EPS and steel fiber tends to absorbing the force that have been imposed. The concrete specimen of higher density generally presented side longitudinal cracking pattern with a great explosion because the concrete are more brittle than those concrete containing EPS as their aggregate proportion. The force and deformation of the samples were tabulated in Table 3.

6 Conclusion

Poison's ratio for proportion C (EPS and steel fiber) is 0.17 and it is higher than EPS-LWC. This is because it is related with the strength of the concrete. By adding EPS-LWC with steel fiber the strength of the concrete can be increased as well as the Poison's ratio increased. Besides, the strength of concrete also related to the modulus of elasticity of the concrete. Results showed the modulus of elasticity EPS-LWC with steel fiber is 13.79 GPa which is higher than LWC without steel fiber.

The modulus of elasticity is a property of a material that needs sufficient tension to make it a little bit longer or shorter. If the modulus of elasticity is high, therefore the peak stresses will be high. These means that the higher of the modulus of elasticity in concrete, the sooner cracks will appear.

Acknowledgments The greatest gratitude expressed to all technicians in Concrete laboratory Universiti Teknologi MARA (UITM) for their assistance in conducting this research and the Ministry of Education (MOE) for providing the research fund of Exploratory Research Grant Scheme (ERGS).

References

1. H.N. Muhammad, Bond high strength concrete with high strength reinforcing steel. *Open Civ. Eng. J.*, pp. 143–147
2. A.M. Neville, *Properties of Concrete*. Pearson Education Limited; 200, p. 844
3. S. Popovics, History of mathematical model for strength development of Portland cement concrete. *ACI Mater J* **95**(5), 593–600 (1998)

4. American Concrete Institute 318-95/318R-85. Building Code requirements for structural concrete. ACI manual of concrete practice. Part 3: Use of concrete in buildings–Design, Specifications and related topics, Detroit, p. 345 (1996)
5. American Concrete Institute 363R-92. State of the art report on high strength concrete. ACI manual of concrete, Detroit, p. 55 (1994)
6. L.R. Robert, P. Edouard, B. Claude, Taking into account the inclusions' size in lightweight concrete compressive strength prediction. *Cem. Concr. Res.* **35**, 770–775 (2004)
7. W. Shasha, Z. Min-Hong, T.Q. Ser, Mechanical behaviour of fiber-reinforced high-strength concrete subjected to high strain-rate compressive loading. *Constr. Build. Mater.* **31**, 1–11 (2012)
8. R.S. Ravindrarajah, A.J. Tuck, Properties of hardened concrete containing treated expanded polystyrene beads. *Cem. Concr. Compos.* **16**, 273–277 (1994)
9. S. Kurugol, L. Tanacan, H.Y. Ersoy, Young's modulus of fiber-reinforced and polymer-modified lightweight concrete composites. *Constr. Build. Mater.* **22**, 1019–1028 (2008)
10. P.C. Ryan, Relationship between Young Modulus's, Compressive Strength, Poisson's Ratio and Time for Early Age Concrete, Master Thesis of Swarthmore College (2009)
11. W. Shasha, Z. Min-Hong, T.Q. Ser, Mechanical behaviour of fiber-reinforced and polymer-modified lightweight concrete composites. *Constr. Build. Mater.* **22**, 1019–1028 (2012)

Structural Performance of Steel Fibre Reinforced Concrete Three-Ribbed Wall Panel on Compression

Mohd Maiziz Bin Fishol Hamdi, Siti Hawa Binti Hamzah
and Mohd Hisbany Bin Mohd Hashim

Abstract Precast reinforced concrete wall offer many advantages during construction stage. One of the advantages is fast and economical. Despite that, the structure strength is carefully design in order to provide strong and reliable elements that made up the whole building. This research focus on the structural performance of three-ribbed wall reinforced with steel fibre and apart from steel fabric as the main reinforcement (WSF). In contrast, another typical wall was constructed without using steel fabric (WOSF). The wall dimensions were 1,600 mm × 1,000 mm × 100 mm (height × length × width) reinforced with B7 of steel fabric size as well as steel fibre HE 0.75/60 using concrete grade 30. Both walls were set up as pinned-fixed at the top and bottom end. The loading consist of uniformly distributed axial load connected to hydraulic jack and has 2,000 kN capacity limit. Analysis of results was done based on the ultimate load carrying capacity, wall displacement, mode of failure and cracking pattern. The location of the maximum displacement was located at 1,450 mm from the bottom while wall WOSF occurs approximately at 1,150 mm (about 0.7 H of the wall height). Wall WSF fails by crushing as indicates due to slenderness ratio 16 less than 20 and it experienced crushing at the top end along load distribution area. Load appliance to the WOSF wall was stopped as no sign of failure can be identified as the machine already reached its capacity.

Keywords Steel fibre · Concrete wall · Rib

M.M.B.F. Hamdi (✉) · S.H.B. Hamzah · M.H.B.M. Hashim
Faculty of Civil Engineering, Universiti Teknologi MARA,
Shah Alam, Selangor, Malaysia
e-mail: mohd.maiziz@gmail.com

S.H.B. Hamzah
e-mail: shh@salam.uitm.edu.my

M.H.B.M. Hashim
e-mail: hisbany@salam.uitm.edu.my

1 Introduction

In Malaysia, industrial building system (IBS) has been practiced as one of the methods to obtain fast and economical construction process which is precasting is one of the available methods that can be used. Developers prefer fast construction method to save time, avoid variation order and cut cost [1]. To ensure this method can be achieved, the industry needs to make sure both party; workers and professionals team able to yield productivity in terms of worker and competency in order to reduce dependence on foreign labours. Precast concrete wall is one of the most commonly used IBS components as a structural member due to its ability to transfer load from above to footing effectively [2].

Basically, a wall reinforced with steel fabric is much stronger in terms of its load capacity, crack controls and buckling mode. A difference between wall with and without steel fabric would give significant impact to industry whether the strength of the wall is capable to transport load. However this structural component still require high amount of concrete which causes high self-weight loading to the structure and will slow down the construction work. For this research, precast ribbed wall is introduced as a new design of load bearing wall. Ribbed wall as load bearing structure not only gives aesthetic appearance of the wall but it also provide reasonable strength with proper design and calculation. Even though the volume of concrete is reduced due to the ribbed section, the precast wall can be reinforced with fibres to impart addition strength of the structure. Steel fibre is use because it improved flexural toughness, flexural fatigue resistance as well as good durability and crack control [3].

In this study, precast ribbed wall with and without steel fabric were constructed with an addition of steel fibre as a reinforcing element. The load carrying capacity, displacement profile and stress-strain reading of the walls will be analysed to indicate the significance of having steel fabric and steel fibre as reinforcement. It will also acknowledge the ability of three-ribbed wall and its structural capability (with and without steel fabric) to act as a load bearing structure where the reduction of concrete volume gives sustainable element in construction as well as to reduce construction time and cost incurred.

2 Theoretical Background

2.1 Steel Fibre Reinforced Concrete

Steel fibre reinforced concrete is a combination of cement and aggregates reinforced with short steel fibres. Many previous researchers has study the application of steel fibre in concrete mixture. Raman et al. [4] indicates that steel fibre was designed with end cones or completely corrugated and hooked ends, to improve adhesion and anchorage within the mix. Moreover steel fibres are supplied as single strands but

some are glued together or magnetically aligned to reduce “fibre balling” or clumping to ensure a good uniform distribution during mixing. Addition of steel fibre will be randomly distributed in the concrete mix and act as crack arrestors.

Increase of steel fibre properties such as modulus of elasticity (E) to 75 % will help to reduce deflection of the concrete structure component. Concrete is known to have weak tensile strength and the addition of steel fibres during mixing will increase the mechanical properties and later effect on post failure behaviour. Johnston [5] discussed the content of steel fibre by 0.5 % of volume result in concrete matrix strength to increase and it will cause significant increase in residual load of deflections at unstable strain softening zone. After composite strength has been reached steel fibres will enhance the capacity of concrete to dissipate energy [6] while [7] conclude that ultimate and flexural capacity is increased when steel fibres is introduced to plain concrete. Figure 1 shows the various types of steel fibre available.

2.2 Reinforced Concrete Wall

Previous research has been done regarding the application of reinforced concrete wall. Oberlender and Everard [8] tested 54 wall panels under eccentric loadings and uniformly distributed axial load. The effect of load eccentricity, geometric condition, slenderness and aspect ratio was investigated. Rectangular steel fabric of uniform spacing was used to reinforce the wall. The result has shown slenderness ratio of wall panel less than 20 was failed by crushing and if more than 20 it failed by buckling under eccentric and axial loading. Lateral deflection for slenderness ratio less than 20 was not increase at the time of failure but for slenderness ratio more than 20 it shown an increase in lateral deflection. Strength reduction also recorded ranging from 18 to 50 % for slenderness ratio between 8 and 28 under effect of eccentricity loading at $t/6$ of the walls.

Abdul Rahman et al. [3] studied on structural behaviour of concrete reinforced steel fibre wall panel under eccentric loading. A total sample of eight walls are casted using concrete Grade 30 with size 1,000 mm \times 1,500 mm \times 75 mm and reinforced with double layer steel fabric of grade B7 with 510 N/mm² yield

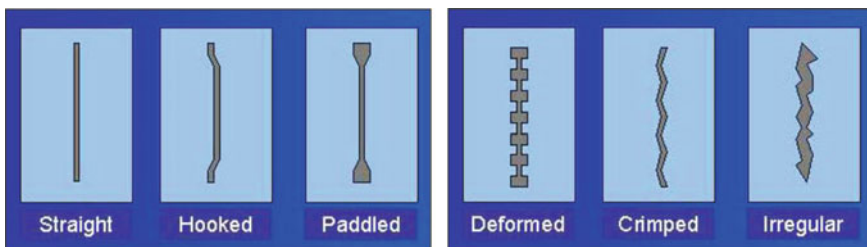


Fig. 1 Various types of steel fibre shape [2]

strength. An axial load is imposed on the wall with 12.5 mm eccentricity under support condition of pinned-fixed at the upper and lower end. From the result, all walls failed by compression shear and it shows similar pattern of curvature where the bend can be seen towards rear side.

British Standards Association [9] conducted research on the comparison of steel fibre reinforced wall panel with steel fabric and another one is only reinforced with steel fabric. Two sample of wall panels measured 1,500 mm × 1,000 mm × 75 mm was casted using cement grade C 40 and the wall is set up using pinned-fixed support and tested under compressive axial load. The experimental result shown that steel fibre improves the structural properties of wall compared to normal wall. There was an increase of 41 % in term of ultimate load of steel fibre wall panel compared to steel fabric reinforced wall. The second wall panel also showed an increase of 45 % higher than normal wall. It can be conclude that mixing of steel fibre with concrete helps the uniformity of distribution in wall panel so that it can absorb more energy over the deformation range.

3 Method

For this research, two walls consist of three-ribbed with and without steel fabric were and both concrete mixtures were added with steel fibre. The dimension of precast concrete three-ribbed walls were 1,600 × 1,000 × 100 mm (height × length × thickness) (Fig. 2) with 1,600 mm × 200 mm × 50 mm (height × length × thickness) of ribbed segment size as shown in Fig. 3. The samples were tested under uniform axial

Fig. 2 Ribbed wall sample dimension

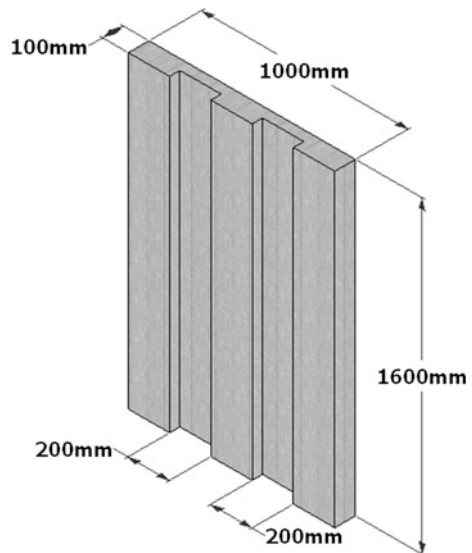
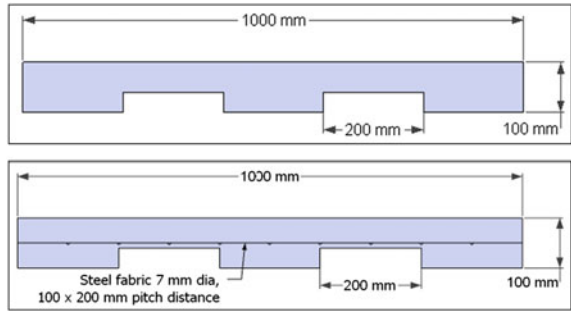


Fig. 3 Rib measurement on wall samples



load with 2,000 kN capacity limit. One wall sample were reinforced with steel fabric B7 grade (MS 145:2006) with 100 mm × 200 mm in size and steel fibre grade HE 0.75/60 (hooked end steel fibre) strength of 1,200 MPa. The wall support conditions were pinned at the upper end while the lower end is fixed support. The concrete target mean strength used for the wall samples was 30 N/mm² with an addition of 0.5 % by volume of steel fibre.

The schematic experimental set up was shown in Fig. 4. The wall was painted using white colour to ensure all cracks are visible and easily to be marked. The set up consist of rigid based at bottom end and a movable load at the top end. The ribbed wall panel is placed vertically as shown with upper support was set as pinned while the lower end was set as fixed. A steel plate is welded to steel bar to ensure uniform distribution of load across the wall dimension. Steel bracing was placed at each side of the wall panel to act as a bracing in order to prevent lateral movement at the upper end of the structure and to maintain the vertical alignment of the wall as safety precaution. The wall samples were tested under uniformly distributed top-to-bottom compression axial load by means of hydraulic jack connects to the loading machine as shown in Fig. 5.

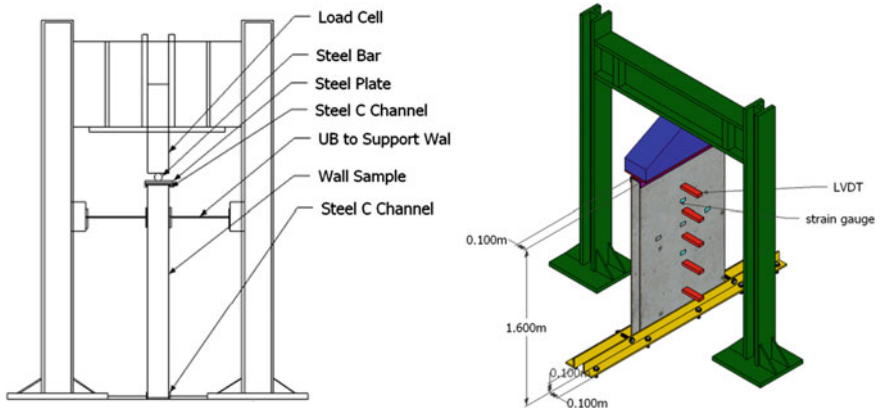


Fig. 4 Schematic wall panel compression testing setup

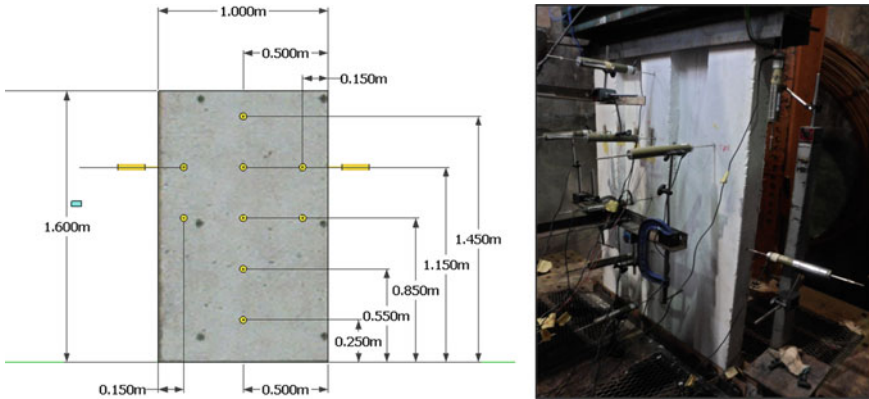


Fig. 5 Linear variable displacement transducer (LVDT) allocation

Linear variable displacement transducers (LVDT) were placed at various location horizontally and vertically to check the displacement profile of the wall (Fig. 5). Horizontal LVDT's locations were positioned at 0.7, 0.5, 0.3, and 0.1 H as well as at the centre height of the wall. Meanwhile, the vertical transducer was placed at the upper end of the wall. The LVDT were calibrated, labelled and installed properly according to the location and position as shown in Fig. 5. All strain gauges and the LVDT's were labelled and were connected to the data logger where the data was recorded. The load cell is set to give a maximum 2,000 kN of compression axial force to the wall sample. The compression load was applied incrementally until the walls fail and the load applied was stopped immediately. Any visible crack on the wall surface were observed and recorded.

4 Result Analysis

4.1 *Three-Ribbed Walls with Steel Fabric (WSF) and Without Steel Fabric (WOSF)*

The structural behaviour of the walls were clearly observed by using the LVDT's; positioned at various locations horizontally and vertically as well as the strain gauges. The deformation of the strain gauges installed inside at the steel fabric and on the surface of the wall were also observed and interpreted to gain an understanding about the wall performance. The data obtained were analyzed and study in terms of ultimate load bearing capacity, displacement profile, crack pattern and modes of failure.

4.2 Displacements

The walls were analysed based on the displacement profile consist of horizontal and vertical LVDT’s position at the wall. Vertical transducer measures the wall displacement when axial load was applied while horizontal transducer measures the lateral wall deformation. Table 1 illustrates the corresponding load and vertical displacement for WSF and WOSF wall. The relationship between vertical transducer reading and correspond load were plotted as shown in Fig. 6. Based on the graph, the displacement of WSF was higher compared to WOSF due to the bigger curve pattern of the wall. The load increases linearly with respect to the vertical displacement until it reaches the peak load where it failed and the load were consequently decreased. The highest vertical displacements occur at the ultimate load capacity where the recorded readings are 5.67 and 4.57 mm respectively. The graph patterns of the wall were similar from the previous study.

The wall WSF in Fig. 7 shows a double curvature profile as illustrate and it fail by crushing due to design slenderness ratio of 16 (less than 20) as mentioned by Oberlender and Everard [8]. Based on visual observation on the wall condition, it was found that the top end suffer massive crack and crush all along its length, but no cracks are spotted on the surface. From the load percentage below, the maximum displacement were found at location T1 where the highest reading recorded was 11.67 mm at the ultimate load. Meanwhile, data in Table 2 shows the negative value at 100, 75, 50 and 25 %P as it can be seen happen at T3 location (half the wall height).

Table 1 Load and vertical displacement

Load percentage (%P)	WSF		WOSF	
	Load (kN)	T7 (mm)	Load (kN)	T7 (mm)
25	432.28	3.24	492.08	2.32
50	864.55	4.01	984.15	3.17
75	1,296.83	4.71	1,476.23	3.87
100	1,729.1	5.67	1,968.3	4.57

Fig. 6 Load versus vertical displacement of three-ribbed wall panel

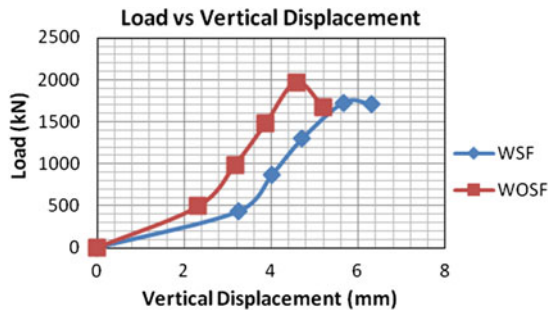


Fig. 7 Lateral displacement profile of three-ribbed WSF wall panel

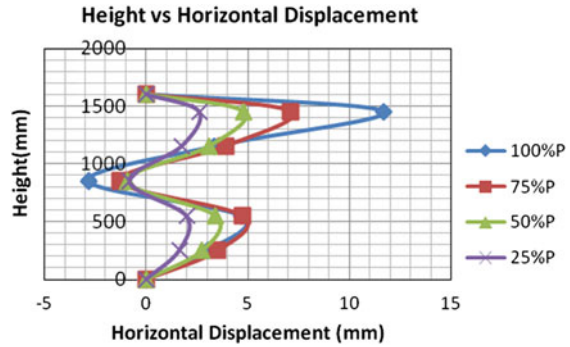


Table 2 Increment of lateral displacement by percentage of loading on WSF panel

LVDT	Height (mm)	100 %P (mm)	75 %P (mm)	50 %P (mm)	25 %P (mm)
T1	1,450	11.67	7.11	4.78	2.61
T2	1,150	3.37	3.91	3.08	1.76
T3	850	-2.81	-1.28	-0.92	-0.82
T4	550	4.67	4.75	3.42	1.99
T5	250	3.03	3.51	2.74	1.63

This indicates the wall action trying to return to its normal condition. The buckling curve justify with the Euler buckling theory where it happens at the 0.7 H of the wall. The curve pattern shows constant profile displacement indicates that the steel fibre helps load distribution to be widely spread across its concrete composite, thus prevent crack propagation towards bottom end of the wall. The addition of steel fibre in the mix for WSF and WOSF wall helps concrete to dissipate energy around its matrix as reported by Oliveira et al. [6] and the ultimate load and flexural capacity also increased as agreed to Altoubat et al. [7]. Table 2 shows the increment of lateral displacement by percentage of loading applied.

WOSF shows similar pattern of displacement where it only buckles on one side (single curvature) as shown in Fig. 8. It buckles approximately at 0.7 H of the wall due to the support condition and show similar profile to Abdul Rahman et al. [3]. The designed slenderness ratio of the wall was 16 and it was expected to fail by crushing; unfortunately the wall did not fail during the experimental test and subsequently was stopped to prevent any further damage on the machine. The highest displacement occurs at 1,150 mm of the wall height where the largest displacement was 10.2 mm. It can be concluded that the relationship between loads are correspond to the value of displacement. The addition of steel fibre also imparts strength to the wall by increasing the concrete ductility and fracture energy resulted the ultimate strength of WOSF is higher than the WSF wall. Table 3 shows the increment of lateral displacement by percentage of loading applied for three-ribbed WOSF wall panel.

Fig. 8 Lateral displacement profile of three-ribbed WOSF wall panel

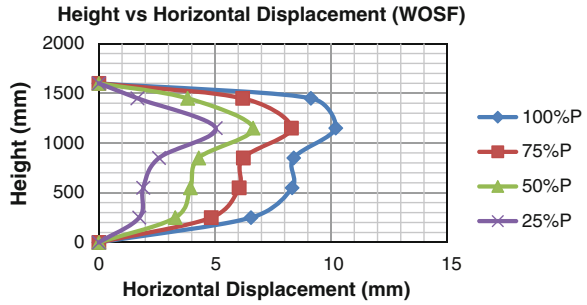


Table 3 Increment of lateral displacement by percentage of loading on WOSF panel

LVDT	Height (mm)	100 %P (mm)	75 %P (mm)	50 %P (mm)	25 %P (mm)
T1	1,450	9.13	6.19	3.82	1.66
T2	1,150	10.2	8.29	6.64	5.03
T3	850	8.39	6.22	4.3	2.59
T4	550	8.32	6.04	3.94	1.91
T5	250	6.55	4.84	3.29	1.74

The load versus horizontal displacement as illustrates in Fig. 9 shows the effect of adding steel fabric on the ultimate load carrying capacity of the wall. LVDT of T1, T2, T4 and T5 shows a linear line up to the 50 % of the maximum load before it gradually increase and stopped. Meanwhile at T3, the reading shows negative values to indicate the inward displacement of the wall.

For wall WOSF, the graph in Fig. 10 shows a linearity of displacement throughout the whole experiment. It can be concluded that the displacement increase linearly to the load. The maximum displacement occurs at T2 location approximately 1,150 mm from the wall height. As agreed along with the theoretical assumption, it is proven the displacements are clearly seen at the 0.7 H of the wall height.

Fig. 9 Lateral displacement increment on each transducer for three-ribbed WSF wall panel

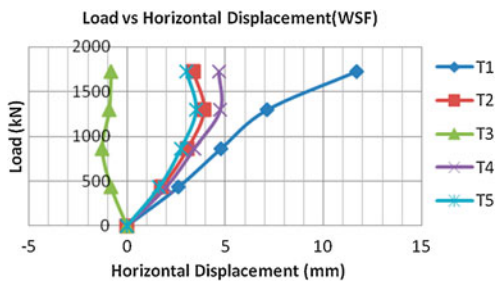
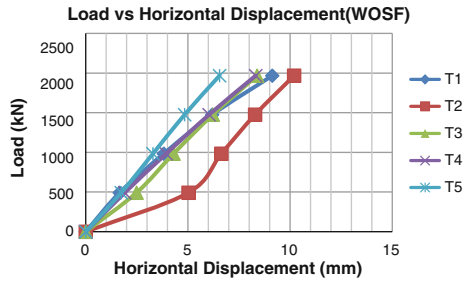


Fig. 10 Lateral displacement increment on each transducer for three-ribbed WOSF wall panel



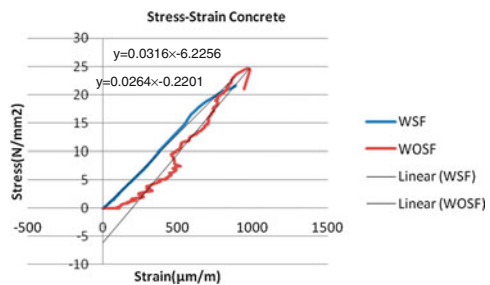
4.3 Stress-Strain

Graph in Fig. 11 shows the stress-strain relationship of both walls. Note that the strain gauges values were taken at the 0.7 H of the wall height. This was where the critical deformation of the wall as stated in Euler buckling theory. The elastic modulus of concrete for WSF wall was 0.0264 N/mm^2 and also equivalent to $26,400 \text{ N/m}^2$. Meanwhile, for WOSF wall the elastic modulus was 0.0316 N/mm^2 and equivalent to $31,600 \text{ N/m}^2$. This value was not significant to be used providing that elastic modulus of concrete at 28 days is 33 GPa according to British Standards Association [10]. From the experiment, the value should be higher than the code provision because both walls are reinforced with steel fabric and steel fibre which in general gives more strength to the concrete composition.

Meanwhile, Fig. 12 shows the stress-strain profile of steel fabric in wall WSF. The steel fabric elastic modulus was obtained from the graph equation. It is equivalent to 7,111 kPa. This value is lower than code provision of 200 GPa as stated in [10].

During the experiment progress, no visible cracks can be found on the wall surface whether at the ribbed segment or at the normal surface. As shown in Fig. 13, the cracks only happen at the top end of the wall where uniformly axial load were applied. At the bottom end of the wall no visible cracks were found. This indicates the usage of steel fibres do increase the concrete strength and ductility where the

Fig. 11 Stress versus strain relationship on concrete surface of both three-ribbed wall panel samples



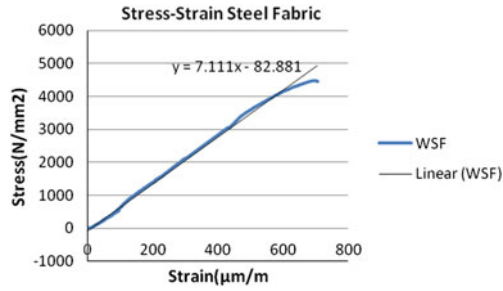


Fig. 12 Stress versus strain relationship on steel fabric surface of both three-ribbed wall panel samples



Fig. 13 Crushing failure occurred at the top of three-ribbed WSF wall

load distribution are absorbed by the steel fibres matrix. The use of hot rolled steel fabric has developed the ductility of the wall as stated by Sorelli et al. [11]. The wall failed after the top end experience total crushed and the experimental work was stopped. Furthermore, the wall WOSF crack pattern was not visible at all through out the entire experiment process. When the load has reached 1,968.3 kN, the loading machine was stopped to avoid any equipment failure because the machine capacity was limited to 2,000 kN. There are several reason why it happens. The wall was kept for dry curing about 180 days compare to wall WSF (150 days)

before test was assembled. As time passes it develops enough strength through bonding of steel fibre with concrete and able to absorb as well as dissipate the energy across its composite. Then, it was found that on the testing day, the concrete cube strength for WOSF was higher than the WSF cube strength.

5 Conclusion

Supposedly, the ultimate load of wall WSF must be higher than wall WOSF due to the addition of steel fabric reinforcement. The theoretical calculation has proved the difference between ultimate loads of those two walls. But after experimental work, it was found that the ultimate load of wall WOSF was higher than the WSF due to the certain factors as mentioned previously. Nevertheless, the new finding of the wall WOSF ultimate strength is higher than wall WSF need to be study vigorously by another researcher. More wall sample need to be tested to give accurate and significant result. The supports condition must be properly set according to its function thus prevent any rotation and movement that will change the result. This is the new gap a researcher must filled in order to approve the theoretical assumption.

Furthermore, both walls buckle at 0.7 H as specified in the theoretical Euler buckling mode. Wall WSF buckle the highest at T1 location (1,450 mm) and the highest value is 11.67 mm respectively. Meanwhile, wall WOSF buckle at T2 location (1,150 mm) with the highest reading is 10.2 mm. The buckling curve in WSF is different from WOSF due to several reasons. It can be concluded that WSF experienced a double curvature towards inside at certain load before return to normal positions. In wall WOSF, the buckling curves are freely towards one side as specified in the theory.

Crack pattern for both walls are not visible during the testing procedure. Only in wall WSF a crushing and cracking pattern was visible at the top end where uniformly distributed load was applied. Due to the wall thickness of 100 mm, the heavyweight aggregates in mix design and the addition of steel fibres are the main reason why there are no visible cracks on the wall surface. High density of wall contributes to the high strength concrete as well as the function of steel fibre that control crack propagations and the bond strength between steel fibre with concrete helps to stitch small crack thus limiting the cracks as compared to conventional reinforcements.

Acknowledgments Special thanks to Faculty of Civil Engineering, Universiti Teknologi MARA (UiTM) Malaysia in providing the computer and software facilities used and Ministry of Science, Technology and Innovation (MOSTI) for their invaluable help and funding support while conducting this research.

References

1. W.A.M. Thanoon, L.W. Peng, M.R. Abdul Kadir, M.S. Jaafar, M.S. Salit, The Experiences of Malaysia and Other Countries in Industrialised Building System in Malaysia. Proceeding on IBS Seminar, UPM, Malaysia (2003)
2. R. Supinyeh, S.H. Hamzah, Structural behaviour of steel fabric reinforced concrete wall panel under eccentric loading. *Int. J. Civ. Environ. Eng. IJCEE-IJENS*, 10(04) (2010)
3. N. Abdul Rahman, S.H. Hamzah, E.T.Wong, Effective Performance of Steel Fibre Reinforced Concrete Wall Panel for IBS Component. International Conference of Construction and Building Technology (ICCBT), ICCBT. 2008-C-18, pp. 203–212 (2008)
4. S.N. Raman, M.Z. Jumaat, H. Mahmud, M.F. Mohd Zain, Fibre reinforced concrete and high performance fibre reinforced cementitious composites: an overview. *IEM JURUTERA Bull.* **2007**(7), 32–35 (2007)
5. C.D. Johnston, Fibre-reinforced cements and concretes, *J. Constr. Build. Mater.* 228–285 (2000)
6. J. Oliveira, D.L. Araújo, E.A. Guerra, F.M.P. Gomes, The influence of steel fibre aspect ratio on the mechanical performance of concrete. *J. Constr. Build. Mater.* **2007**, 1–6 (2007)
7. S.A. Altoubat, J.R. Roesler, D.A. Lange, K. Rieder, Simplified method for concrete pavement design with discrete structural fibers, *J. Constr. Build. Mater.*, 1–10 (2005)
8. G.D. Oberlender, N.J. Everard, Investigation of reinforced concrete walls. *ACI J. Proc.* **74**(6), 256–263 (1977)
9. British Standards Association, BS 8110: Part 1. Structural Use of Concrete, British Standard Institution (1997)
10. British Standards Association, BS 8110: Part 1. Structural Use of Concrete, British Standard Institution (1997)
11. L. Sorelli, A. Meda, G.A. Plizzari, Bending and uni-axial tensile tests on concrete reinforced with hybrid steel fibres. *ASCE Mater. J. Struct. Eng.* **15**(5), 519–527 (2005)

Compressive Strength and Water Absorption Characteristics of Brick Using Quarry Dust

Maureena Jurliel Abdullah, Zakiah Ahmad, Atikah Fatma Md. Daud and Nur Kamaliah Mustaffa

Abstract This paper reports the investigation made on the suitability and the optimum ratio of quarry dust in replacing river sand for brick production. A series of mix proportions for different ratio of cement:sand:quarry dust were prepared. Five types of mix proportions were practiced in the production of brick specimens were 1:10:0, 1:7.5:2.5, 1:5:5, 1:2.5:7.5 and 1:0:10 (Cement:Sand:Quarry Dust) and denoted as B1, B2, B3, B4 and B5 respectively. The curing method applied in this study was air dry as this type of curing was widely used in the manufacturing of bricks. The compressive strength of the samples was determined at 7, 28 and 45 days. Compressive strength tests were conducted in accordance with BS 3921:1985. Water absorptions of the samples were determined by using 24 h cold immersion test and 5 h boiling test. Bricks with mix ratio 1:0:10 (B5) containing 100 % quarry dust in replacing the sand gave the highest strength and the lowest water absorption compared to other ratios. All the quarry dust-sand-cement bricks exhibited a compressive strength much higher than the minimum requirement for standard bricks (5 N/mm²) according to British Standard (BS 3921:1985). Bricks B5 can be considered to be in 'severe weathering' grade and the other bricks are in 'moderate weathering' grade in accordance with ASTM C62.

Keywords Bricks · Cement bricks · Quarry dust · Compressive strength · Water absorption · Initial rate of suction

M.J. Abdullah · A.F.Md. Daud (✉) · N.K. Mustaffa
Faculty of Civil Engineering, Universiti Teknologi Mara, Shah Alam, Malaysia
e-mail: fatikah@psa.edu.my; fatikah5488@gmail.com

M.J. Abdullah
e-mail: 2012961663@isiswa.uitm.edu.my

N.K. Mustaffa
e-mail: nurkamaliah@salam.uitm.edu.my

Z. Ahmad
Institute of Infrastructure Engineering, Universiti Teknologi Mara, Shah Alam, Malaysia
e-mail: zakiah@salam.uitm.edu.my

1 Introduction

The worldwide consumption of sand as fine aggregate in construction is very high, and several developing countries have encountered some strain in the supply of natural sand in order to meet the increasing demand of infrastructural development in recent years. River sand has been one of the key ingredients as the fine aggregate component of concrete and overuse of the material has led to environmental concern, the depleting of securable river sand deposits and a concomitant price increase in the material. To overcome these problems there is a need to find for cost effective alternative and innovative materials. There were some alternatives that have been used in concrete mixing such as crush recycle aggregate, sheet glass powder, foundry sand, cupola slag and etc.

Other alternative material is quarry dust. It has very recently gained good attention to be used as an effective filler material instead of fine aggregate. Quarry dust can be defined as residue, tailing or other non-volatile waste material after the extraction and processing of rocks to form fine particles less than 6 mm [1]. Also, the use of quarry dust as the fine aggregate in concrete has decreases the cost of concrete production in terms of the partial replacement for natural river sand.

Researchers had investigated the potential of using quarry waste and its effect on the strength, workability and the durability of concrete as well as the cost of concrete production [2–4]. The use of quarry dust in concrete has shown to improve strength properties and increase the workability of concrete Kapgate and Satone [5] and Shakir et al. [6], investigated the fly ash brick and the incorporation of 50 % quarry dust by weight has significantly improved the compressive strength. Meanwhile, Sahu et al. [7] reported significant increase in flexural strength, compressive strength, and split tensile strength of concrete with 40 % quarry dust replacement. Nagaraj [8] has proposed a mix design that ensuring good workability by using combination of quarry dust, sand and super plasticizer with optimum water content. Quarry dust does not contain silt or organic impurities and can be produced to meet desired gradation and fineness as per requirement. Consequently, it improves the strength of concrete [9]. Ilangoan and Nagamani [1] suggested that concrete with quarry dust as full replacement for sand is possible but requires proper treatment of quarry dust.

As most of the studies on the use of quarry dust are on concrete, therefore this study is aimed to investigate the mechanical and water absorption properties of sand cement brick with quarry dust as sand replacement.

2 Experimental Works

2.1 Materials

2.1.1 Cement

Ordinary Portland Cement (OPC) conforming to MS522 Part1: 2006 was used in this study.

2.1.2 Sand

River sand as received was dried in the room temperature. The basic physical tests were conducted and its specific gravity was around 3.0, density of $1,460 \text{ kg/m}^3$ and fine modulus of 2.9.

2.1.3 Quarry Dust

The quarry dust was supplied by factory ID Interlocking Brick Sdn Bhd., Terengganu. The specific gravity of quarry dust was 2.69 and the fineness modulus was 2.8 with density of $1,630 \text{ kg/m}^3$. The quarry dust of size 6 mm after sieving was used. The quarry dust was then dried in the room temperature before used.

2.1.4 Water

Tap water available in the laboratory was used in the samples preparation.

2.2 Mix Design

To investigate the effect of quarry dust on brick properties, five different group mixtures were prepared. The design proportion of control cement:sand:brick was 1:10 which followed the mix proportion of commercial cement- sand bricks produced by factory ID Interlocking Brick Sdn Bhd. Terengganu. In the samples preparation, proportion of sand was replaced by quarry dust by weight of sand. The percentages for quarry dust replacement were 25, 50, 75 and 100 %. The different series of mixtures are denoted as B1 for ratio 1:10:0 (cement:sand:quarry dust) that is 0 % quarry dust content, B2: 1:7.5:2.5 (25 % quarry dust); B3: 1:5:5 (50 % quarry dust); B4: 1:2.5:7.5 (75 % quarry dust); B5: 1:0:100 (100 % quarry dust) respectively. Table 1 shows the mix design for the bricks.

Table 1 Mix design

Sample label	Ratio (Cement: Sand: Quarry Dust)	No. of samples	Cement (kg)	Sand		Quarry dust	
				kg	%	kg	%
B1	1:10:0	24	8.8	87.2	100	0	0
B2	1:7.5:2.5	24	8.8	65.4	75	21.8	25
B3	1:5:5	24	8.8	43.6	50	43.6	50
B4	1:2.5:7.5	24	8.8	21.8	25	65.4	75
B5	1:0:10	24	8.8	0	0	87.2	100
Total		120	44	218		218	

2.3 Casting and Batching

Sand, cement and quarry dust were placed in a mixer and dry mixed for 2 min. Water was then added and the contents were mixed for another 2 min. The mixture was then tested for flow consistency in accordance with ASTM D6103 [10] with spread



Fig. 1 Manufacturing of bricks

diameter of 200 + 20 mm [11]. Water content was adjusted until the required consistency has been achieved. The mixture was then poured into the brick moulds of size 230 mm × 120 mm × 70 mm. The preparations of the samples are shown in Fig. 1.

A total of 120 samples of bricks were prepared. The bricks were covered with wet gunny sacks overnight and then air dried until testing.

3 Test Methods

The densities of the bricks were determined for each series. The quarry dust bricks were tested for compressive strength, Initial Rate Suction (IRS) and water absorption. All test procedures have been done according to British Standard and ASTM.

3.1 Density

Firstly, the bricks were pre-conditioned by drying in a ventilated oven at a temperature of 105 ± 5 °C for the first 24 h and the weighing of the specimens was then carried out. The drying and weighing process for the second 24 h was repeated. The repeated process is needed for ensuring the constant mass is reached by measuring the loss in mass between two determinations is not more than 0.2 % of the total mass. The bricks were left to cool for 4 h 10 bricks were used for every mix ratios. The dimensions of the bricks were measured. The density of brick specimens was measured by dividing the weight with the volume of the brick samples.

3.2 Compressive Strength

For compression test, the bricks were first soaked in the water for 16 h. The bricks were pad dried and placed on the compression machine with the bed face perpendicular to the direction of application of the load of the testing machine (Fig. 2). The compressive strength test was performed on the bricks after 7, 28 and 45 days of curing in accordance with ASTM C67-07a [12].

3.3 Initial Rate Suction

Initial Rate Suction (IRS) is a test to determine the amount of water sucked by the brick upon contact with mortar during brick laying in 1 min and the results depend on capillary mechanism of small pores in the bricks. The amount of water absorbed by the bricks will affect the strength between unit and mortar. IRS can be used as a

Fig. 2 Compressive strength test



factor in the design of mortars that will bond strongly with units. IRS test was performed in accordance with BS3921 [13].

The bricks were dried in similar manner as the preparation for density measurement. The weights of the bricks were taken prior to IRS test. The bricks were placed on their bed face downwards on metal plates in water dish as shown in Fig. 3.

The depth of immersion of the brick was maintained at 3 mm. After 60 s, the bricks were removed and quickly wiped off the surplus water with a damp cloth and reweighed the brick to the nearest gram. IRS was determined by subtracting the weight of the bricks before and after immersion in the water dish for 60 s.

3.4 Water Absorption Test

Water absorption of a brick is defined as the weight of water absorbed by the brick which is expressed as a percentage of the dry weight of the brick. The determination of water absorption was done according to BS3921 [13].

Fig. 3 Initial rate suction test



3.4.1 24 h Cold Immersion Test

Again, the bricks were pre-conditioned in similar manner as the density measurement. Five (5) replicates were prepared for each mix ratio. The dry mass d_m , of the bricks was measured. The bricks were submerged in clean tap water for 24 h. Then the bricks were removed and wiped dry and weighed. The water absorption was determined using Eq. (1).

$$\text{Absorption by immersion} = 100[(W_{sc} - W_d)/W_d] \quad (1)$$

where

W_d mass of the dry brick (in gram)

W_{sc} mass of the wet brick (in gram)

3.4.2 5 h Boiling Test

A 5 replicates per brick types were used in this test to satisfy the minimum requirement as stated in standard. The bricks were pre-conditioned as described in density measurement to determine the initial mass. Then the bricks were placed into a tank of water where the water was already heated to the boiling point (100 °C) as shown in Fig. 4.

Fig. 4 5 h hot water immersion test



The bricks were arranged with spaces in between bricks and tiers. The water was boiled continuously for 5 h and then allowed cooling to room temperature for 16 h. The specimens were then removed from the water tank and wiped out any traces of water with damp cloth and the weights were measured. Water absorption, in percentage was calculated and recorded.

4 Results and Discussion

The results of mechanical properties and water absorption test are shown in Table 2. The detailed discussions are given in the following sections.

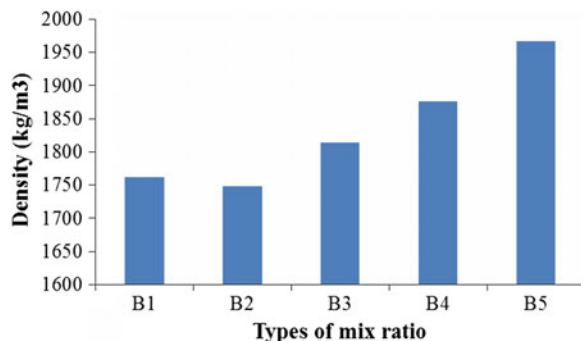
4.1 Brick Density

The density of bricks influences the weight of walls and the variation in weight has implications on structural, acoustical and thermal design of the wall [14]. Figure 5 shows that the density of all the bricks. It can be seen that as the amount of quarry dust increases the density of the brick increases which is due to the density of quarry dust ($1,630 \text{ kg/m}^3$) which is higher than the density of sand ($1,460 \text{ kg/m}^3$).

Table 2 Mechanical and water absorption properties of quarry dust bricks

Brick types	Density (kg/m^3)	Compressive strength at 28 days (N/mm^2)	IRS ($\text{kg/m}^2 \text{ min}$)	Water absorption (cold water) (%)	Water absorption (hot water) (%)
B1	1,761.7	6.0	2.48	9.1	10.9
B2	1,748.2	5.3	1.21	9.4	11.3
B3	1,813.8	7.6	1.23	8.6	11.1
B4	1,876.1	9.5	1.26	8.5	10.2
B5	1,967.1	12.1	1.26	7.3	9.0

Fig. 5 The average density of bricks with different percentages of quarry dust



4.2 Compressive Strength

In this study, the compressive strength was determined at 7, 28 and 45 days. The test results show that compressive strength increases as days of curing increases (Fig. 6).

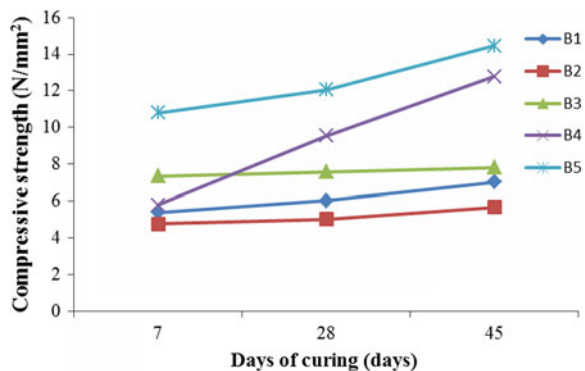
For B1, B2 and B3 bricks the strength increased marginally while the compressive strength of B4 increased quite substantially, i.e. 65 % at 28 days followed by B5 bricks at 11 % when compared to the strength at 7 days. However the compressive strength of B4 is still lower than the compressive strength of B5. B5 has the highest compressive strength and the strength at 28 days is 12 N/mm² and it is a 100 % increased from control bricks (6 N/mm²).

From Table 2, it is clear that the compressive strength increases as the amount of quarry dust increases which is well correlated with the density of the bricks. This is due to the fineness of the quarry dust which has filled the voids and hence enhances the compressive strength of the bricks [15].

Result for compressive strength at 28 days for all types of mix ratio ranged between 5.3 and 12 N/mm². According to British Standard [13], the minimum requirement for compressive strength is 5 N/mm², ASTM standard, the minimum strength is 2.5 N/mm², Australian standard AS 1225 [16], the strength is 4 N/mm². In Malaysia, for any bricks to be used as construction materials, the minimum permissible average compressive strength specified by Public Works Department is 5.2 N/mm² for bricks and 2.8 N/mm² for hollow blocks per 10 samples taken at random from the Contractor's stock pile of 1,000 or part thereof [15].

As the bricks can be used as an in-filled material, therefore they do not really need to have the strength of an engineering bricks thus; the compressive strength of bricks for all types of mix ratios determined in this study fulfilled the requirement of the standards and can be used in construction as common bricks. However when compared to the compressive strength of conventional bricks such as clay brick and cement bricks that available in the market, the compressive strengths of those bricks are 12–15 N/mm² and 8–10 N/mm² respectively. It can be seen that only M5 that falls within the standard limits and the strength of conventional bricks. Therefore bricks with 100 % quarry dust as sand replacement can be proposed to be used in the construction.

Fig. 6 Compressive strength at 7, 28 and 45 days for different types of mix ratio



4.3 Initial Rate Suction

Initial Rate Suction (IRS) is the rate at which brick sucks water from mortar through the bed face of the bricks in 1 min during laying. ASTM recommends that bricks to be wetted before laying if the IRS is higher than $1.5 \text{ kg/m}^2 \text{ min}$.

From Fig. 7, bricks B2, B3, B4 and B5 with IRS 1.21, 1.23, 1.26 and $1.26 \text{ kg/m}^2 \text{ min}$ respectively fit the acceptable IRS value below $1.5 \text{ kg/m}^2 \text{ min}$ as stated in the standard ASTM C67-07a [12].

Meanwhile control bricks B1 showed the average IRS value of $2.48 \text{ kg/m}^2 \text{ min}$ which is higher than $1.5 \text{ kg/m}^2 \text{ min}$ as recommended. Therefore this B1 bricks are recommended to be wetted before laying. Since B1 brick is the least dense compared to other bricks, thus may contained more pores which did not filled by fine particles of quarry dust and this has allowed more water to sip through.

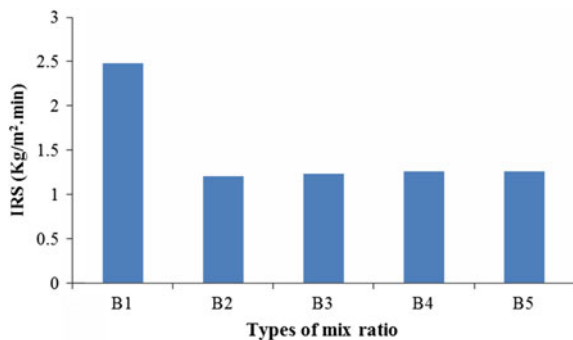
4.4 Water Absorption

Two types of methods used for measuring water absorption used in this research, 24 h cold immersion test and 5 h boiling test. The 5 h boiling test provides results for saturated condition while 24 h cold immersion gives partial saturation. Figure 8 shows the results for cold and hot water immersion tests.

Results for water absorption of bricks ranged from 7.3 to 9.0 % for cold water immersion test and 9.0 to 10.9 % for hot water immersion, as given in Table 2. Figure 8 shows the relationship between the percentages of quarry dust replacement and the water absorption and the relationship and it is clear that the water absorption decreased as the percentages of quarry dust replacement increased for both types of water absorption tests.

The trend in the increase and decrease of the water absorption very much related with the density of the bricks as can be seen in Fig. 9. For example, the water absorption for B2 bricks is the highest while the density is the lowest. At the same time the water absorption of B2 is lower than control bricks B1. These findings also

Fig. 7 Initial rate of suction (IRS) for bricks with different types of mix ratio



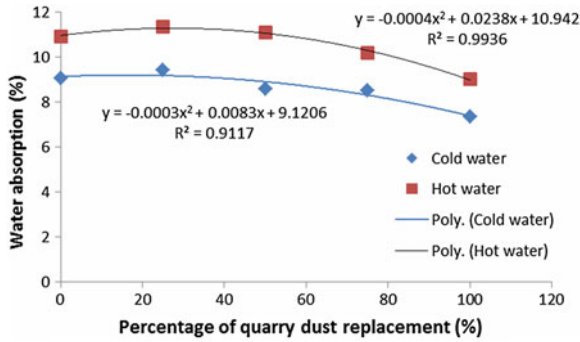


Fig. 8 Relationship of percentage of water absorption and water absorption for different percentages of quarry dust replacement

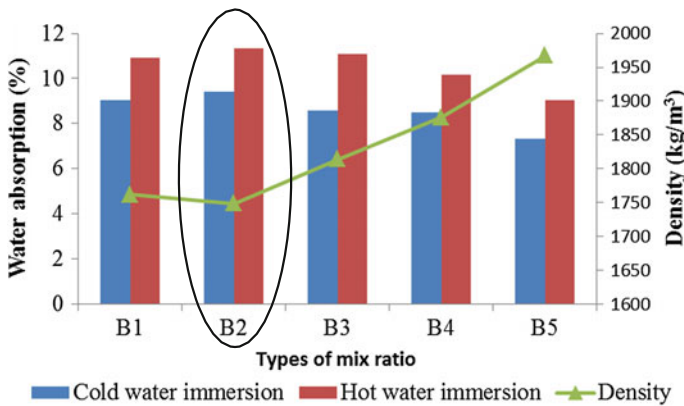


Fig. 9 Relationship between density and water absorption for different types of ratio

tally with the results of compressive strength which also show that as the density increases the compressive strength increases and the compressive strength of B2 is the lowest.

This may be due to the physical size and shape of quarry dust which is rough, sharp and angular, hence causes a gain in strength due to better interlocking between each brick constituents and resulted in less porously compared to natural sand. Therefore by added more quarry dust in the mix proportion has shown to increase the compressive strength of brick specimens and on the same time the water absorption of bricks to decrease.

According to ASTM C62 [17] specification for building bricks, the requirement for water absorptions for building bricks is categorized according to Table 3.

Table 3 Water absorption limit based on ASTM C62

ASTM C26 class specification	Maximum 24-h cold water absorption, 8 % ^a			
	Maximum 5 h boiling		Maximum saturation	
	Water absorption (%)		Coefficient	
	5 bricks average	Individual bricks	5 bricks average	Individual bricks
SW	17	20	0.78	0.80
MW	25	25	0.88	0.90
NM	No limit		No limit	

SN, MW and NW denote severe, moderate and normal weathering respectively

^a If the cold water absorption does not exceed 8 % wt, then the boiling water absorption and saturation coefficient specification are waived

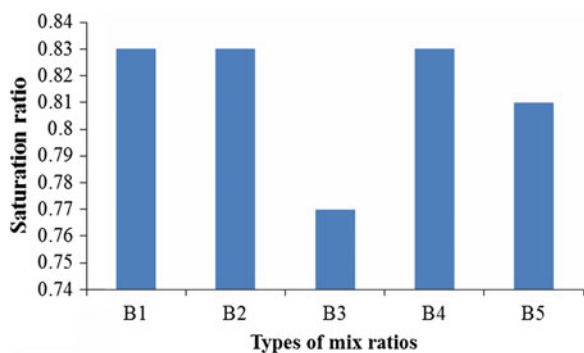
Based on Table 2, the water absorption for B5 is less than 8 % which fit the requirement of ASTM C62 as re-tabulated here in Table 3 and the boiling water absorption and saturation coefficient specification can be waived.

The rest of the bricks have moisture absorption percentages higher than 8 % therefore need to look at the requirement for 5-h boiling water absorption limits. From Table 2, the percentages of absorption after 5-h boiling test for all the bricks for different mix ratios are higher than 8 % but lower than 17 %.

To further quantify the durability of the bricks, saturation coefficients were determined. Saturation coefficient is the ratio of absorption by 24 h immersion in cold water to the absorption after 5 h submersion in boiling water. The saturation coefficient is traditionally used to measure the durability of brick. The lower the saturation coefficient the less likely that brick will damaged. The saturation coefficient ranges from 0.4 to 0.95; the lower value around 0.4 indicates high durability and the higher value around 0.95, low durability [18]. Figure 10 shows the saturation coefficient of all the bricks.

From Fig. 10, the saturation coefficient for bricks B1, B2 and B4 are similar that is 0.83 and they are higher than the saturation coefficient for B3 (0.77). Based on Table 3, bricks B5 falls in the class ‘severe weathering’ since the water absorption (7.3 %) less than 8 % requirement for cold water immersion. Although bricks B3

Fig. 10 Saturation coefficient for different types of mix ratio



have the absorption of 11.1 % in 5-h boiling water which less than 17 % as per requirement and the saturation coefficient of 0.77 which is at par with the requirement of 0.78, this bricks B3 will be considered as ‘moderate weathering’ grade similar to B1, B2 and B4 since the saturation coefficient is at the highest side of the limit.

5 Conclusion

From the various laboratory investigations made on the mechanical properties and water absorption characteristics of quarry dust bricks, the following conclusions can be drawn.

1. The dry densities of the bricks increases as the amount of quarry dust increases the density of the brick increases which seems to be influenced by the densities of the quarry dust ($1,630 \text{ kg/m}^3$) and sand ($1,460 \text{ kg/m}^3$) as the density of cement was hold constant.
2. The compressive strength of the bricks also increases as the amount of quarry dust increases. The compressive strength of all types of bricks meet all the relevant standards on building bricks however these bricks are not suitable for engineering bricks. Although all bricks for different types of mix ratio meet the requirement of building bricks, only bricks M5 that falls within the standard limits and the strength of conventional bricks that currently used in the construction industry.
3. The water absorption characteristics of all bricks improved when the sand is replaced by higher percentages of quarry dust. Based on the results of water absorption in cold water and 5-h boiling water as well as saturation coefficient, bricks B5 falls in the class ‘severe weathering’ and bricks B1, B2 and B4 are considered ‘moderate weathering’ grade in accordance with ASTM C62.

Acknowledgments Our highest appreciation to ID Interlocking Bricks Sdn Bhd, Terengganu for the supply of the quarry dust as well as for their support and guidance during this project. We wish to thank the technicians of Faculty of Civil Engineering, Universiti Teknologi Mara for their assistance and support. The work reported here was financially supported by Ministry of Higher Education (Grant: 600-RMI/RAGS 5/3 (53/2012)) is greatly acknowledged.

References

1. R. Ilangovan, K. Nagamani, Studies on strength and behavior of concrete by using quarry dust as fine aggregate. CE CR J. 40–42 (2006)
2. K.K. Babu, R. Radhakrishnan, E.K.K. Nambiar, Compressive strength of brick masonry with alternative-aggregate mortar. CE CR J. 25–29 (1997)

3. T.S. Nagaraj, Z. Banu, Efficient utilization of rock dust and pebbles as aggregates in Portland cement concrete. *Indian Conc. J.* 53–56 (1996)
4. C. Narasimahan, B.T. Patil, S.H. Sanni, Performance of concrete with quarry dust as fine aggregate—an experimental study. *CE CR J.* 19–24 (1999)
5. S.S. Kapgate, S.R. Satone, Effect of quarry dust as partial replacement of sand in concrete. *Indian Streams Res. J.* 3(5), 1–8 (2013)
6. A.A. Shakir, S. Naganathan, K.N. Mustapha, Effect of quarry dust and billet scale additions on the properties of fly ash bricks. *IJST, Trans. Civil Eng.* 38(1), 51–60 (2014)
7. A.K. Sahu, S. Kumar, A.K. Sachan, Quarry stone waste as fine aggregate for concrete. *Indian Concr. J.* 845–848 (2003)
8. T.S. Nagaraj, Proportioning concrete mix with rock dust as fine aggregate. *CE CR J.* 27–31 (2000)
9. M.S. Hameed, A.S.S. Sekar, Properties of green concrete containing quarry rock dust and marbel sludge powder as fine aggregate. *ARPN J. Eng. Appl. Sci.* 81–89 (2009)
10. ASTM D 6103-00, Standard test method for flow consistency of controlled low-strength material (CLSM). American Society for Testing and Materials, PA, USA (2000)
11. S. Naganathan, H. Abdul Razak, S. Nadzriah, Effects of Kaolin on the performance of controlled low-strength material using industrial waste incineration bottom ash. *Waste Manage. Res.* 28, 848–860 (2010)
12. ASTM C67-07a, Standard test methods for sampling and testing of clay brick and tile masonry units and related units. American Society for Testing and Materials, PA, USA (2003)
13. BS 3921, Specifications for clay brick. British Standard Institute, UK (1985)
14. C.T. Grimm, Clay brick masonry weight variation. *J. Arch. Eng.* 2(4), 135–137 (1996)
15. MS 27:1971, *Malaysian Standard: Specification of Precast Concrete Block*
16. AS 1225, *Clay Building Bricks*. Standards Association of Australia, Australia (1984)
17. ASTM C62, *Standard Specification for Building Bricks (Solid masonry units)*. ASTM International, West Conshohocken, PA (2005)
18. F.M. Khalaf, A.W. Hendry, D.R. Fairbairn, Study of the compressive strength of blockwork masonry. *ACI Struct. J.* 91(4), 367–375 (1994)
19. K. Sunil, A perspective study on fly ash–lime–gypsum bricks and hollow blocks for low cost housing development. *Constr. Build. Mater.* 16, 519–525 (2002)
20. BS EN 771-3:2003, *Specification for Masonry Units*. Aggregate Concrete Masonry Units (Dense and Light-weight Aggregates) (2003)

Enhancing the Performance of Recycled Aggregate Concrete Using Micronized Biomass Silica

A. Suraya Hani, Ismail Abdul Rahman and Hamidah Mohd Saman

Abstract Utilization of Recycled Aggregate (RA) in concrete is due to the awareness of society in preserving natural resources for future generation. RA application as coarse aggregate in concrete mixes initiation is to make use effectively of the waste materials. The purpose of this study is to improve the Recycled Aggregate Concrete (RAC) by using the Micronized Biomass Silica (MBS). Concrete cube specimens containing various percentages of RA and MBS were prepared and tested. The results indicated that after 28 days curing, concrete containing 12 % of MBS and 100 % RA enables to enhance the compressive strength up to 17.20 % and reduce the water permeability coefficient and water penetration up to 47.10 and 7.5 % respectively. It can be concluded that RAC containing MBS perform significantly better RAC without MBS.

Keywords Recycled aggregate • Micronized biomass silica • Compressive strength • Water permeability coefficient • Water penetration

1 Introduction

Although, Recycled Aggregate (RA) is widely used in some developed countries such as United Kingdom, United States and Denmark [1], however it's utilization in Malaysia is still assumed as new material in construction industry [2]. Less interest in using RA is due to factors such as lack of information on RA performance in

A. Suraya Hani (✉)

Faculty of Technology, University Tun Hussein Onn Malaysia, Batu Pahat, Johor, Malaysia
e-mail: suraya@uthm.edu.my

I.A. Rahman

Faculty of Civil and Environmental Engineering, University Tun Hussein Onn Malaysia, Batu Pahat, Johor, Malaysia

H.M. Saman

Faculty of Civil Engineering, UiTM, Shah Alam, Selangor, Malaysia

concrete and there is still sufficient supply in natural resources. Besides that, landfill area is still able to receive construction waste in Malaysia. However, as a responsibility society, Malaysia should apply RA in the construction industry to protect its natural resources for future generation.

Construction industry is very active in Malaysia due to rapid development for achieving developed country in 2020. However, there is a sign of scarcity in reducing of natural resources for producing concrete like gravel and crushed granite which played a role as coarse aggregate. Thus, to preserve this source, the application of RCA for producing concrete is vital.

Even though RA is becoming a good alternative material, there is still a weakness on its performance in concrete. For fresh concrete performance, it was found that concrete containing RA or known as Recycled Aggregate Concrete (RAC) has lower workability as compared to concrete containing Natural Aggregate or known as Natural Aggregate Concrete (NAC) [3, 4]. For hardened concrete performance, RAC compressive strength is still lower to NAC [3, 5–7].

Thus, this study applies Micronized Biomass Silica (MBS) as cement replacement material in RAC mixes for improving the performance of RAC. It focused on the influence of various percentages of MBS in RAC for its performance in compressive strength, water permeability coefficient and water penetration of RAC.

2 Experimental Work

2.1 Materials

2.1.1 Physical Properties of the Ordinary Portland Cement (OPC)

The cement used for this study is an ordinary Portland cement with a brand name of HOLCIM. The cement is stored in airtight steel drum in the Material Laboratory of Universiti Tun Hussein Onn Malaysia (UTHM). The chemical compositions of OPC are shown in Table 3. The chemical analysis on the OPC was carried out using X-Ray Fluorescence (XRF) analysis.

2.1.2 Aggregates

Fine aggregate and coarse aggregate was used for producing concrete specimens for this study. For fine aggregate, the mining sand with maximum size of 5 mm was used. The sand was sieved prior to casting concrete.

For this study, two types of coarse aggregate were used namely the Natural Aggregate (NA) and Recycled Aggregate (RA). For NA, the crushed granite with maximum size of 20 mm was used. For RA, it was prepared by crushing the waste cubes dumped at the outside of Material Laboratory of Universiti Tun Hussein Onn

Table 1 Physical properties of aggregate used for the study

Physical properties		NA	RA
Specific gravity	SSD	2.48	2.39
	Oven dried	2.46	2.31
	Apparent	2.51	2.5
Aggregate crushing value (ACV)		17.25	35.86
Water absorption		0.83	3.34

Malaysia (UTHM). The waste cubes were randomly collected without considering the age of the cubes. It was broken into smaller pieces by using hammer and then crushed in jaw crusher for the size between 5 and 20 mm. The physical properties for NA and RA are tabulated in Table 1.

2.1.3 Superplasticizer

In this study, superplasticizer was used as to improve the workability performance of concrete mix. The superplasticizer with a brand name CONPLAST AP used for all concrete mix is water reducing admixture which is known as modified naphthalene sulfonate (without chloride).

2.1.4 Micronized Biomass Silica (MBS)

Micronized Biomass Silica (MBS) [8] was prepared by burning the rice husk in rotary reactor furnace in the Material Laboratory for enabling to synthesis any biomass silica material at different temperature regime. This is to obtain an amorphous characteristic for the burnt rice husk. For this work, the temperature of the rotary furnace was fixed at 500 °C where an off white amorphous material is obtained after 1 h duration and about 50 g of ash has been produced. Then, the ash was fed to Jar Mill for producing finer biomass silica. The Mill was rotating for 1 h. In the jar mill apparatus, 50 balls mill were used for grinding the MBS to finer particles. The final product of ash has a mean diameter of 25.77 μm which was used for this study as cement replacement material.

2.1.5 Characterization of MBS

In order to determine the characterization of MBS, several testing were carried out such as surface area, microscopic image and chemical composition. The surface area was identified by using surface area analyzer. This testing was conducted in accordance to ASTM C 204-94 and EN 196-6. The microscopic image was observed and captured by using SEM (JEOL JSM-638 OLA Analytical Scanning Electron Microscope).

2.2 Concrete Mixtures

Twenty concrete mixtures were prepared and Table 2 illustrates the mix proportions for each series of concrete mix. Target strength of the concrete at 28 days is 25 MPa, its water-cement ratio is 0.5 and its slump value is designed for 60–180 mm. The proportion of MBS replacement is 0, 4, 8 and 12 % by weight of cement. These proportions were chosen based on the performance of MBS concrete in terms of compressive strength and water permeability in preliminary works. For each replacement level of MBS, different percentages replacement of RA as coarse aggregate to NA was employed. The replacement percentages are 0, 25, 50, 75 and 100 %. Superplasticizer is also been used to maintain the workability of concrete. For each concrete mix, three cubes were prepared where an average reading was taken as data for interpretation. The concrete cubes had been cured in water until testing time.

Table 2 Mix proportions for concrete mix

Concrete series	RA (%)	MBS (%)	Cement (kg/m ³)	Water (kg/m ³)	CA (kg/m ³)		FA (kg/m ³)	SP (ml/kg ³)
					NA (kg/m ³)	RA (kg/m ³)		
Control concrete	0	0	450	225	1,115	0	892	4,500
RA25	25	0	450	225	836	279	892	4,500
RA50	50	0	450	225	558	558	892	4,500
RA75	75	0	450	225	279	836	892	4,500
RA100	100	0	450	225	0	1,115	892	4,500
M4	0	4	432	225	1,115	0	892	4,320
M4-RA25	25	4	432	225	836	279	892	4,320
M4-RA50	50	4	432	225	558	558	892	4,320
M4-RA75	75	4	432	225	279	836	892	4,320
MBS4-RA100	100	4	432	225	0	1,115	892	4,320
M8	0	8	414	225	1,115	0	892	4,140
M8-RA25	25	8	414	225	836	279	892	4,140
M8-RA50	50	8	414	225	558	558	892	4,140
M8-RA75	75	8	414	225	279	836	892	4,140
M8-RA100	100	8	414	225	0	1,115	892	4,140
M12	0	12	396	225	1,115	0	892	3,960
M12-RA25	25	12	396	225	836	279	892	3,960
M12-RA50	50	12	396	225	558	558	892	3,960
M12-RA75	75	12	396	225	279	836	892	3,960
M12-RA100	100	12	396	225	0	1,115	892	3,960

RA RA content

M MBS content

CA coarse aggregate

FA fine aggregate

2.2.1 Testing of Fresh Concrete

Slump test was applied to determine workability of the fresh concrete. The test was conducted in accordance to BS 1881: Part 102: 1983.

2.2.2 Testing of Hardened Concrete

Performance of hardened concrete was assessed using three tests which are compressive strength, water permeability coefficient and water penetration tests.

(i) *Compressive Strength*

The compressive strength of the concrete cubes was determined according to BS EN 12390-3 (2002). Cube sized 100 mm × 100 mm × 100 mm was used as specimen testing. The cube specimens were tested at 7, 14 and 28 days.

(ii) *Water Permeability Coefficient*

The water permeability coefficient for concrete was determined by using German Water Permeability Test (GWT) apparatus and conducted according to ISO/DIS 7031 (1983). The GWT test was chosen as this test is non-destructive, convenient and reliable for assessing concrete water permeability in the laboratory [9]. The cube specimens were tested at 7, 14, 28 and 90 days.

(iii) *Water Penetration*

This test was conducted by using Water Impermeability Apparatus Three-Place Model Test. The test was conducted according to DIN 1048 (1972) which requires the sample cube of 200 mm size. However, for this experiment the concrete sample size was modified to cater 100 mm cube. This modification gave convenient in handling during the testing due to large number of samples used. Ahmad et al. [10] has also modified the size of sample to 150 mm cube in their studies. Previously, as according to DIN 1048 (1972), the original gasket made for 200 mm was applied. The gasket which located below the concrete sample was required to prevent the leakage of water and to ensure the water penetrated into concrete specimens. In this study, the rubber gasket with diameter 100 mm was fabricated. The cube specimens were tested at 28 and 90 days.

3 Results and Discussion

3.1 Properties of Raw Materials

The calculated surface area of MBS and cement are found to be 24.4039 and 2.693 m²/g respectively. These results indicate that MBS has larger surface area compared to cement or nine times finer than that of cement. This also means that MBS has more tendencies to absorb more water and thus hydrate more as compared to cement during the hydration process.

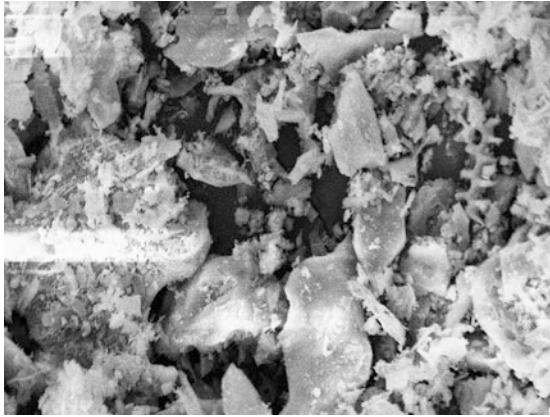


Fig. 1 Scanning electron microscopic image of MBS under $\times 2,000$ magnification

The purpose of microscopy image is to give a better understanding of MBS shape and the captured image of MBS sample is as shown in Fig. 1. The image indicates that MBS particles are angular, rough and crushed in shape. There are also tiny hollow spaces within the particles. The figure also shows that MBS has variable size particles. As a comparison, the cement microscopic image is as shown in Fig. 2, it shows that cement has more irregular and crushed shape particles. Table 3 provides the chemical composition of MBS. As seen in Table 3, the total percentage of main oxides for MBS which are $\text{SiO}_2 + \text{Al}_2\text{O}_3 + \text{Fe}_2\text{O}_3$ is found to be 88.544 %.

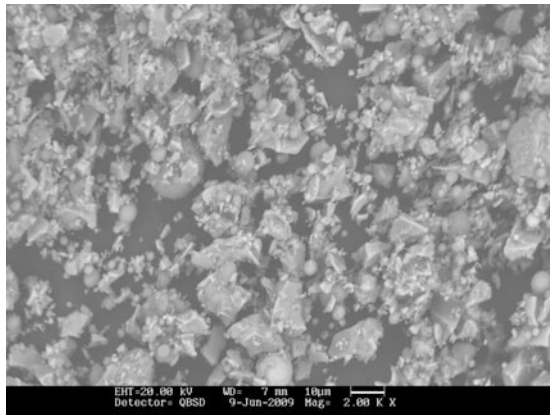


Fig. 2 Scanning electron microscopic image of cement under $\times 2,000$ magnification

Table 3 Chemical composition of MBS and OPC

Chemical composition	SiO ₂	Al ₂ O ₃	Fe ₂ O ₃	CaO	MgO	K ₂ O	SO ₃	LOI
MBS	87.67	0.343	0.531	1.18	0.872	5.08	0.59	1.22
OPC	17.91	4.69	2.97	65.93	1.19	0.41	3.67	1.46

This total percentage fulfils the requirement for pozzolans material as stated by ASTM C 618-08a which specifies the total percentage of SiO₂ + Al₂O₃ + Fe₂O₃ must be more than 70 % of its contents in order to classify as pozzolanic material. Thus MBS fulfils the requirement as pozzolanic material.

3.2 Workability

The results of workability of the concrete mix are illustrated in Fig. 3. The figure shows that slump of the fresh concrete mix decreases with respect to the increases of RA content. These results are expected because RA possesses high capacity to absorb water as shown in Table 2. Remaining mortar in RA attributed to that phenomenon and makes the concrete mixes harsher and less cohesive. The angular (crushed) shape of RA cause larger specific surface area as noted by Taylor [11] and thus can absorb more water for about 15–20 % increases from those of round shape.

Furthermore, the decrease in slump was also observed when MBS was included as depicted in Fig. 3. From these results it can be said that concrete containing MBS attained lower in slump value compared to concrete without MBS. This is due to cellular characteristic of MBS which lead into high absorption capacity in concrete containing MBS and less water available for workability in the mix. This high absorption characteristic is also found for other pozzolanic material like silica fume [12] and rice husk ash [13, 14].

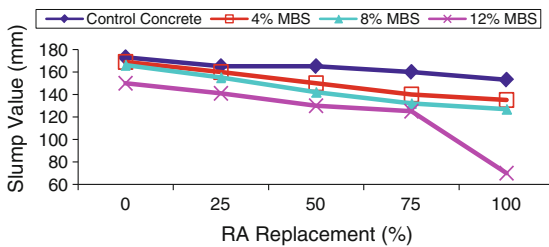


Fig. 3 Slump value of concrete mixes with various percentages of RA and MBS

3.3 Compressive Strength

The results of compressive strength of concrete cubes are presented in Table 4. This table indicates that the control concrete (with NA) has higher compressive strength as compared to other concrete that contained RA. This is due to the presence of RA which is weaker aggregate than NA. These findings are in agreement with the research work from Poon et al. [7] and Tangchirapart et al. [15]. According to Poon et al. [7] and Olorunsogo [16], the weaker compressive strength is due to the higher percentage of fine particles and higher porosity of RA. As an agreement to these, Kong et al. [17] and Otsuki et al. [18] have recognised that RAC has two Interfacial Transition Zone (ITZ). The first ITZ is between RA and new cement paste namely as new ITZ and second ITZ, is between RA and old cement mortar attached namely as old ITZ. Because of these ITZ presences in concrete, the large amount of pores and cracks were created which contribute into low strength of concrete. Other research study conducted by Topcu and Guncan [19] indicates that for RAC the compressive strength achieved about 80–95 % of that Natural Aggregate Concrete (NAC). This study found that RAC with 25 % of RA managed the equivalent achieve of 80–95 % of NAC as found by Topcu and Guncan [19].

It is apparent from Table 4, the compressive strength of concrete contained MBS has higher value than control concrete. The graph clearly shows the trend of increase in compressive strength with respect to increase of MBS content. Based on the table, at early age (7 days), replacement of 12 % MBS replacement compressive strengths contributes to large percentage difference increment (about 49 %) of that control concrete. It is evident that MBS does behave like other high pozzolanic reactivity of Supplementary Cementitious Material (SCM) namely silica fume and metakolin as that MBS is in agreement with Mazloom et al. [12], Poon et al. [20], Wong and Abdul Razak [21] and Zhang et al. [22] which shows the enhancement in compressive strength of concrete as SCM was included in the concrete mixes.

The results also revealed that the NAC with MBS concrete attain higher compressive strength value compared to those of RAC with MBS. This confirmed that the presence of RA in the concrete contributes to the decrease of compressive strength even though MBS was included in the mix. High porosity of RA decreases the bond strength of Interfacial Transition Zone (ITZ) in concrete [23]. Nevertheless, with 4 % of MBS content, the RAC with 25 % of RA can attain similar compressive strength of control concrete. By increasing 8–12 % of MBS, the concrete improve its compressive strength significantly. Thus, it can be concluded that MBS has the pozzolanic characteristics and be able to increase compressive strength of RAC. As pozzolana, inclusion of MBS forms additional C-S-H gel that densifying the cement matrix and improves the ITZ between new cement matrix and NA. Thus, MBS is a great potential of new pozzolana to be used and compensated the reduction in compressive strength of RAC.

Table 4 Compressive strength of concrete with various percentages of RA and MBS

Mixes	Compressive strength (MPa)		
	7 days	28 days	90 days
Control concrete	20.00	30.20	31.90
25 % RA	19.20	26.20	31.30
50 % RA	15.50	25.10	29.00
75 % RA	16.00	22.00	28.50
100 % RA	16.50	23.60	28.00
4 % MBS	24.00	32.40	35.10
4 % MBS-25 % RA	18.10	29.10	34.10
4 % MBS-50 % RA	23.30	30.40	33.90
4 % MBS-75 % RA	26.00	31.60	33.70
4 % MBS-100 % RA	25.00	30.50	32.10
8 % MBS	24.80	37.50	39.60
8 % MBS-25 % RA	19.00	32.30	36.70
8 % MBS-50 % RA	24.80	33.90	34.80
8 % MBS-75 % RA	21.00	32.00	33.80
8 % MBS-100 % RA	25.60	31.70	33.70
12 % MBS	29.80	39.00	45.70
12 % MBS-25 % RA	26.70	34.30	39.30
12 % MBS-50 % RA	28.20	36.10	36.10
12 % MBS-75 % RA	23.00	33.90	34.20
12 % MBS-100 % RA	27.80	35.40	35.70

3.4 Water Permeability Coefficient

It is proven that MBS inclusion could further enhance the permeability of RAC. Low water permeability coefficient characteristic is required for concrete so that the water is not easily permeated into concrete. Based on Table 5, it is identified that inclusion of 4 % MBS into the RAC containing either 25 % RA, 50 % RA or 75 % RA cause water permeability coefficient of the resulted concrete to be lower as compared to control concrete. Same trend was observed when 8 and 12 % MBS were employed. Therefore, it is evident that inclusion of MBS into the RAC reduces its water permeability characteristic. This is due to calcium silicate hydrate, C-S-H gel acts as a binder to fill-up the pores and Interfacial Transition Zone (ITZ) in concrete. As the pores and ITZ in the concrete was filled, it protects the concrete from water entering into that cause concrete to be prone to water permeability.

Table 5 also depicts that increase in RA content in concrete increase the water permeability coefficient of MBS concrete. This can be seen as NAC attained lower in water permeability coefficient compared to RAC. This is due to high porosity of RA which is associated with mortar attached to it. On the other hand, Kong et al. [17] has recognised that RAC having two types of ITZ, i.e. old ITZ (of RA and mortar) and new ITZ. Thus, when two (2) ITZ's exist in RAC, more pores are created as concrete made of only NA and hence, high water absorption capacity is resulted in RAC.

Table 5 Water permeability coefficient of concrete with various percentages of RA and MBS

Mixes	Water permeability coefficient (m/s)			
	7 days	14 days	28 days	90 days
Control concrete	1.04E-10	3.87E-11	1.50E-11	9.58E-12
25 % RA	1.10E-10	4.12E-11	1.85E-11	6.88E-12
50 % RA	1.21E-10	6.11E-11	1.98E-11	7.31E-12
75 % RA	1.77E-10	6.27E-11	2.15E-11	8.08E-12
100 % RA	2.08E-10	7.98E-11	2.40E-11	8.13E-12
4 % MBS	1.02E-10	2.67E-11	7.51E-12	9.01E-12
4 % MBS-25 % RA	1.13E-10	3.20E-11	8.62E-12	6.11E-12
4 % MBS-50 % RA	1.16E-10	4.03E-11	8.72E-12	6.20E-12
4 % MBS-75 % RA	2.41E-10	4.95E-11	8.84E-12	6.93E-12
4 % MBS-100 % RA	2.85E-10	2.92E-11	9.54E-12	7.61E-12
8 % MBS	9.39E-11	2.56E-11	6.25E-12	7.25E-12
8 % MBS-25 % RA	7.84E-11	6.26E-11	6.99E-12	4.28E-12
8 % MBS-50 % RA	4.71E-11	1.03E-11	7.46E-12	4.84E-12
8 % MBS-75 % RA	3.53E-10	6.65E-11	7.81E-12	4.92E-12
8 % MBS-100 % RA	1.99E-10	1.24E-11	7.88E-12	5.62E-12
12 % MBS	3.60E-11	7.69E-12	4.56E-12	6.83E-12
12 % MBS-25 % RA	4.43E-11	9.38E-12	5.15E-12	9.58E-12
12 % MBS-50 %RA	4.57E-11	8.92E-12	6.26E-12	6.88E-12
12 % MBS-75 % RA	2.54E-10	6.95E-11	6.99E-12	7.31E-12
12 % MBS-100 % RA	1.06E-10	7.78E-12	7.94E-12	8.08E-12

3.5 Water Penetration

Based on Table 6, it is revealed that MBS has an ability to increase resistance to the water penetration of RAC. The concrete is identified as good and durable concrete when its water penetration is low. From this table, it is identified that concrete specimens containing 8 % MBS and 12 % MBS produce the lower depth water penetration of concrete specimens containing 25 % RA. This is due to pozzolanic reaction which was occurred between silicon dioxide, SiO_2 from MBS and calcium hydroxide, $\text{Ca}(\text{OH})_2$ from cement hydration process which producing calcium silicate hydrate, C-S-H gel. This gel functions to fill up the micropores and ITZ between the aggregate surface and the cement paste in concrete that resisting the water from entering the concrete [17]. Utilisation of MBS in RAC also does densify the pore concrete which leads into high resistance of water to penetrating into concrete.

It is also revealed that concrete containing RA lead into high water penetration. As seen in figures, concrete specimens containing MBS with NA as concrete specimens attained lower in water penetration compared to RAC. The reason is may be attributed to that RAC of having two ITZ. First ITZ is between RA and new

Table 6 Water penetration for MBS-RA concrete

Mixes	Water penetration (mm)	
	28 days	90 days
Control concrete	60	51
25 % RA	53	48
50 % RA	60	56
75 % RA	67	64.5
100 % RA	70.1	67.5
4 % MBS	72.5	70
4 % MBS-25 % RA	50	48.5
4 % MBS-50 % RA	54.5	50
4 % MBS-75 % RA	62	60
4 % MBS-100 % RA	65	62
8 % MBS	68.5	65.5
8 % MBS-25 % RA	45.5	43
8 % MBS-50 %RA	50	47.5
8 % MBS-75 % RA	60.5	55
8 % MBS-100 % RA	62.5	57
12 % MBS	64.5	60
12 % MBS-25 % RA	60	51
12 % MBS-50 %RA	53	48
12 % MBS-75 % RA	60	56
12 % MBS-100 % RA	67	64.5

cement paste namely as new ITZ and second ITZ, is between RA and old cement mortar attached namely as old ITZ [17]. Because of these ITZ presences in concrete, the large amount of pores and cracks were created which contribute into high water absorption. High water content requirement in new ITZ of RAC was resulted from this phenomenon which leads into high water permeability of the resulted concrete. However, MBS could overcome the inferiority performance due to RA inclusion by C-S-H gel formation which has an ability to fill up the ITZ and strengthen the ITZ [7, 24] thus increase the resistance to water penetration.

Besides, according to Ann et al. [23], RA has high porous characteristic. Thus, this characteristic leads into higher water penetration in RAC than those of NAC. Mortar attached on RA has influenced the porosity and high water absorption in RA which led into high water penetration in concrete [25].

4 Conclusion

This study illustrates the performance of Recycled Aggregate Concrete (RAC) containing Micronized Biomass Silica (MBS). It can be concluded that with the presence of 12 % MBS as a partial cement replacement in the concrete with 25 %

RA can cause to lower slump value of the fresh concrete by an average of 81.5 % of control concrete. However, MBS enables to strengthen compressive strength of the harden concrete by an average of 13.60 %. Beside, MBS also offers better water permeability coefficient and water penetration of RAC by 65.70 and 16.7 % respectively. It can be recommended that the further study can be conducted by adding other pozzolans materials such as fly ash, silica fume in RAC.

References

1. F.T. Olorunsogo, N. Padayachee, Performance of recycled aggregate concrete monitored by durability indexes. *Cem. Concr. Res.* **32**(2), 179–185 (2002)
2. A.R.M. Ridzuan, M.F. Nuruddin, A.B.M. Diah, K.B. Kamarulzaman, Early compressive strength and drying shrinkage of recycled aggregate concrete, in *Proceeding of Seventh International Conference on Concrete Engineering and Technology*, Selangor, Malaysia (2001), pp. 51–58
3. I.B. Topcu, S. Sengel, Properties of concretes produced with waste concrete aggregate. *Cem. Concr. Res.* **34**(8), 1307–1312 (2004)
4. M.C. Limbachiya, Coarse recycled aggregates for use in new concrete. *Proc. Inst. Civil Eng., Eng. Sustain.* **157**(ES2), 99–106 (2004)
5. A.L. Fraaij, H.S. Pietersen, J.Vries, Performance of concrete with recycled aggregates, in *Proceedings of International Conference on Sustainable Concrete Construction*, University of Dundee, Scotland, UK (2002), pp. 187–198
6. S. Kenai, F. Debieb, L. Azzouz, Mechanical properties and durability of concrete made with coarse and fine recycled aggregate, in *Proceedings of International Conference on Sustainable Concrete Construction*, University of Dundee, Scotland, UK (2002), pp. 383–392
7. C.S. Poon, Z.H. Shui, L. Lam, Effect of microstructure of ITZ on compressive strength of concrete prepared with recycled aggregates. *Constr. Build. Mater.* **18**(6), 461–468 (2004)
8. A. Suraya Hani, A.R., Ismail, M.S. Hamidah, L. Yee Loon, Pozzolanic properties of micronized biomass silica in enhancing compressive strength and water permeability of concrete. *Mod. Appl. Sci.* **6**(11), 1–8 (2012)
9. Y.L. Lee, K.O. Khoo, S. Chong, M.W. Hussin, Strength development and water permeability of high strength TIA concrete, in *Proceedings of the International Conference of Modern Concrete Materials: Binders, Additions and Admixtures*, University of Dundee (1999), pp. 175–181
10. S. Ahmad, W.A. Al-Kutti, O.S.B. Al-Amoudi, M. Maslehuddin, Compliance criteria for quality concrete. *Constr. Build. Mater.* **22**(6), 1029–1036 (2008)
11. G.D. Taylor, *Materials in Construction—An Introduction* (Pearson Education Limited, 2000)
12. M. Mazloom, A.A. Ramezaniapour, J.J. Brooks, Effect of silica fume on mechanical properties of high-strength concrete. *Cement Concr. Compos.* **26**(4), 347–357 (2004)
13. M. Nehdi, J. Duquette, A.E. Damatty, Performance of rice husk ash produced using a new technology as a mineral admixture in concrete. *Cem. Concr. Res.* **33**(8), 1203–1210 (2003)
14. K. Kartini, *Mechanical, Time-Dependent and Durability Properties of Grade 30 Rice Husk Ash Concrete*. Ph.D. Thesis, Universiti Malaya (2009)
15. W. Tangchirapat, R. Buranasing, C. Jaturapitakkul, P. Chindaprasirt, Influence of rice husk-bark ash on mechanical properties of concrete containing high amount of recycled aggregate. *Constr. Build. Mater.* **22**(8), 1812–1819 (2008)
16. F.T. Olorunsogo, Early Age properties of recycled aggregate concrete, in *Proceedings of the International Seminar on Exploiting Wastes in Concrete*, University of Dundee, Scotland, UK (1999), pp.163–170

17. D. Kong, T. Lei, J. Zheng, C. Ma, J. Jiang, J. Jiang, Effect and mechanism of surface-coating pozzolanics materials around aggregate on properties and ITZ microstructure of recycled aggregate concrete. *Constr. Build. Mater.* **24**(5), 701–708 (2010)
18. N. Otsuki, S. Miyazato, W. Yodsudjai, Influence of recycled aggregate on interfacial transition zone, strength, chloride penetration and carbonation of concrete. *J. Mater. Civil Eng.* 443–451 (2003)
19. I.B. Topcu, N.F. Guncan, Using waste concrete as aggregate. *Cem. Concr. Res.* **25**(7), 1385–1390 (1995)
20. C.S. Poon, S.C. Kou, L. Lam, Compressive strength, chloride diffusivity and pore structure of high performance metakaolin and silica fume concrete. *Constr. Build. Mater.* **20**, 858–865 (2006)
21. H.S. Wong, H. Abdul Razak, Efficiency of calcined kaolin and silica fume as cement replacement material for strength performance. *Cem. Concr. Res.* **35**, 696–702 (2005)
22. M.H. Zhang, R. Lastra, V.M. Malhotra, Rice-husk ash paste and concrete: Some aspects of hydration and the microstructure of the interfacial zone between the aggregate and paste. *Cem. Concr. Res.* **26**(6), 963–977 (1996)
23. K.Y. Ann, H.Y. Moon, Y.B. Kim, J. Ryou, Durability of recycled aggregate concrete using pozzolanic materials. *Waste Manage.* **28**(6), 993–999 (2008)
24. J. Li, H. Xiao, Y. Zhou, Influence of coating recycled aggregate surface with pozzolanic powder on properties of recycled aggregate concrete. *Constr. Build. Mater.* **23**(3), 1287–1291 (2009)
25. H.J. Chen, T. Yen, K.H. Chen, Use of building rubbles as recycled aggregates. *Cem. Concr. Res.* **33**(1), 125–132 (2003)

An Evaluation of High-Rise Concrete Building Performance Under Low Intensity Earthquake Effects

Rozaina Ismail and Nurul Fasihah Zamahidi

Abstract The paper presents an evaluation of high rise building in Kedah which subjected to low intensity earthquakes effects. The earthquake study is relevant even though Malaysia is outside the earthquake region but still had experienced and did suffered from major cases in the past like Tsunami. Engineers should concern and consider the loading for reinforced concrete building due to earthquake in Malaysia's building design procedure. The study addresses on the earthquake study due to performance of critical frame reinforced concrete building. The Quarters Tentera Laut Diraja Malaysia (TLDM) Langkawi, Kedah was chosen as a main model for this study. The building was analyzed using Finite Element Modelling (FEM) under different types of analyses using IDARC 2D depend on variety of earthquake intensities from Time History Analysis (THA) considering low to medium earthquake intensities. The yield point at beam-column connections was analyzed to determine the damage index and damage level of the building. The building performed the early yielding point at 3.115 s for beam element at intensity 0.20 g. Based on result, the critical frame 2A/F-B of the building can stand an earthquake happen with intensity up to 0.20 g. There is no structural damage but some non-structural damage is expected in the non-linear analysis of modal frames which indicates that the building was categorized in the light damage level.

Keywords Building performance • Damage index • Low intensity • Dynamic analysis • Non-linear analysis

R. Ismail (✉) · N.F. Zamahidi
Faculty of Civil Engineering, Universiti Teknologi MARA (UiTM),
Shah Alam, Selangor, Malaysia
e-mail: rozaina_fka_uitm@yahoo.com

N.F. Zamahidi
e-mail: nfasihah_zamahidi@yahoo.com

1 Introduction

The reinforced concrete frame is easy to be affected due to the earthquake impact. Most of structural damages are results from inability of structural to perform under larger forces, also due to failure from surrounding soil and surface ruptures. It is essential to have a proper design detailing and selection of materials so that the reinforced concrete structure can withstand under severe combination of loadings such as dead load, imposed load, and earthquake loading. Malaysia is located at the low intensity of earthquake region and surrounded by major tectonic plates. Engineers should concern and consider the earthquake impacts of buildings in Malaysian's building design procedure due to the past incident like Tsunami. According to Li et al. [1], the reinforced concrete frame has to meet the requirements of performance-based earthquake engineering when conducting a structural performance assessment.

Moreno-Gonzalez and Bairan [2] presented the performance of the building in low to moderate earthquake regions. The results show that the buildings expected to have damages due to its poor expected performance. Ditommaso et al. [3] estimated the period of reinforced concrete buildings to start damage structurally and also identified the non-structural elements that were expected to damage due to earthquake event. IDARC 2D performs the non linear analysis. Barron and Hueste [4] found that the flexible model results more displacement and interstory drift than that of the rigid frame by using the IDARC 2-Dimensional software for reinforced concrete building [5]. The performance normally involves a qualitative process of measurement. Due to the reflection and expectation of the damage state, the values and parameters should be taken place in order to measure quantitatively due to the performance level. Table 1 shows the ATC-13 damage level [6] in [7] to define the level of the damage state was which adopted in this study.

Table 1 ATC-13 the structural engineers association of California (SEAOC) damage levels [6]

SEAOC earthquake level	SEAOC damage	ATC-13 damage factors (state)
Minor	Without any damage	D.F.* = 0 (none) D.F. <0.01 (slight)
Moderate	No structural damage, some non-structural damage	0.01 < D.F. ≤0.10 (light) 0.01 < D.F. ≤0.30 (moderate)
Major	No collapse, some structural damage, non-structural damage considerable	0.30 < D.F. ≤0.60 (heavy) 0.60 < D.F. <1.0 (major)
Collapse	Collapse	D.F. = 1.0 (destroyed)

D.F.* = damage factor = damage index

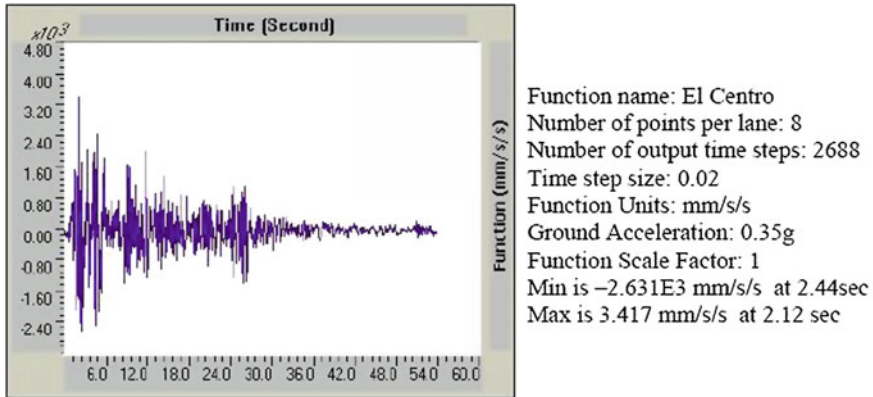


Fig. 1 Time history record of imperial valley earthquake (May 18, 1940—El Centro) [7]

2 Dynamic Non-linear Analysis

The El-Centro time history record is shown in Fig. 1 with 2,688 number of outputs within 0.02 time steps with the maximum acceleration of 0.35 g. This time history was adopted from Ismail et al. [7]. The El-Centro earthquake occurred in May 18, 1940 at Imperial Valley with magnitude 7.1 on the Richter scale. The acceleration is simulated to four variation of low earthquake intensities; 0.05, 0.10, 0.15, and 0.2 g. This study used 5 % damped spectral acceleration.

3 Modeling Concept

Table 2 shows the properties of columns and beams. Figure 2 shows the elevation view of the Quarters Tentera Laut Diraja Malaysia (TLDM) Langkawi, Kedah. A critical main frame classified as concrete moment resisting frame was chosen from the building for the finite element modeling analysis purpose. The structural framing system consists of 2 bays of 4.68 and 4.58 m in length. The building height is equal to 18.8 m which is categorized as a high-rise building (6 stories).

British Standard [8] is referred to determine the loadings applied to the structure in the analysis steps to be applied as nodal loading in the modeling steps as shown in Fig. 3. Fortran based program developed by the University of Buffalo called IDARC 2D was then used to carry out two dimensional analyses on selected frames from each building. This program is able to compute what is known as “structural damage index” which can be defined as a way of quantifying numerically the seismic damage suffered by buildings. Details of structural members such sizes of

Table 2 Columns and beams properties

Column types	Size (mm)	No. of bars and diameter bar	Hoops and spacing (mm)
C1	300 × 600	12 @ 20	8 @ 225
C2	300 × 600	10 @ 20	8 @ 225
C3	250 × 450	10 @ 16	8 @ 175
C4	250 × 450	8 @ 16	8 @ 175
B1	200 × 500	Top&bottom = 2 @ 12	8 @ 250
B2	200 × 500	Top&bottom = 2 @ 25	8 @ 250
B3	200 × 500	Top&bottom = 2 @ 16	8 @ 250

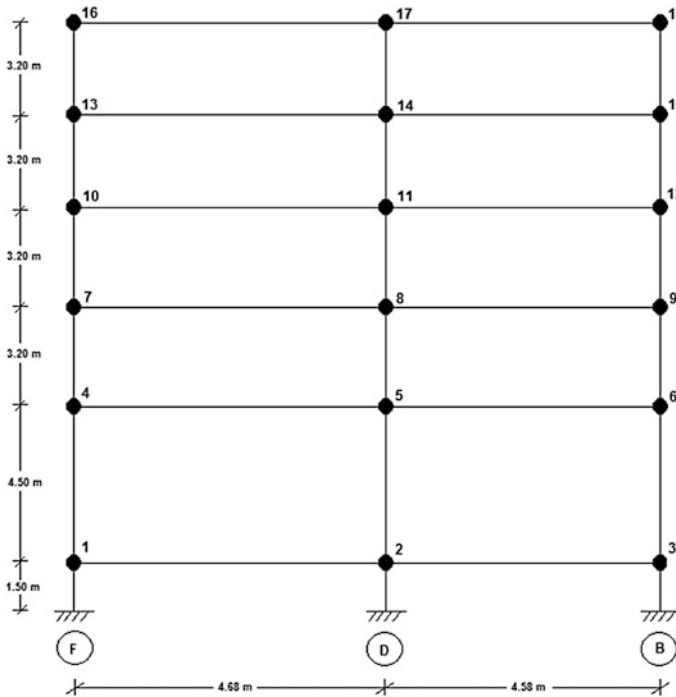
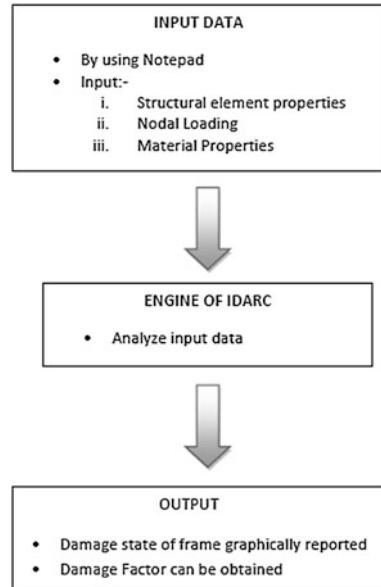


Fig. 2 An elevation view of quarters tentera laut diraja malaysia (TLDM) Langkawi, Kedah

columns and beams, their steel reinforcements and the cumulative column axial loads are taken from the results that calculate by manual calculation and entered as input data in IDARC 2D. Nodal weights were calculated and were based on tributary areas to the node and frame in question. The models were analyzed using the modified design response spectra. The computed damage indices were tabulated for easy reference and comparison.

Fig. 3 Flowchart of modeling steps



4 Result and Discussion

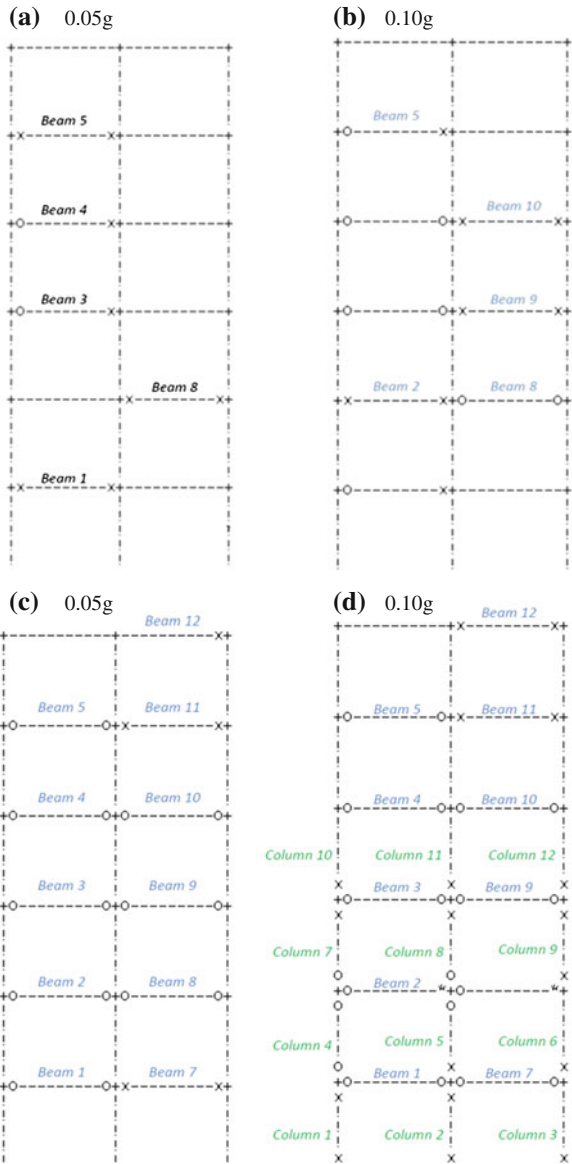
The term plastic hinge is used to describe the deformation of a section of a frame which consist of beams and columns where the plastic bending occurs. Normally, the plastic hinges for moment resisting frame type of buildings due to structural local failures occur either at beam or column connection. Figure 4 shows the formation of the damage state location and plastic hinge of the moment resistance frame with four different intensities of ground acceleration. These represent the sequences of damage state of frames under earthquake loading.

4.1 Damage Pattern Due to Plastic Hinge

The study focus on the damage level and plastic hinge of the building. In damage pattern, the frame show where the locations of element structural start yielding, cracking or collapse. From the results, the modal frame experienced cracking and yielding at the beam and column elements.

The “x” symbol shows the occurrence of crack for concrete frame and the “o” symbol shows the yield of plastic hinge developed. For intensity 0.05 the damage pattern show the frame has started experienced yielding and cracking. For example at intensity 0.05 g, the cracking happen at right and left on the first floor and initial yield of the plastic hinge starts to develop at the left of beam at fourth floor.

Fig. 4 Damage state frame under 0.05, 0.10, 0.15 and 0.20 g earthquake intensity for the building



4.2 Damage Analysis

The program developed by Park et al. [9] is used in this study to provide a measure of the accumulated damage index sustained by the components of the building included the maximum to ultimate deformations ratio. Table 3 shows in detail the summary of overall damage index of Quarters TLDM, Langkawi various intensity.

Table 3 Summarization of first yielding point and damage level

Intensity (g)	Floor level	Location	Time when start yielding (sec)	Overall damage index	Damage level
0.05	3	Beam 3-left	4.420	0.015	Moderate
0.10	3	Beam 3-left	3.660	0.029	Moderate
0.15	3	Beam 3-left	3.215	0.043	Moderate
0.20	3	Beam 3-left	3.115	0.034	Moderate

The overall damage index for the building which can be referred to the SEAOC Damage Level in Table 1. The overall damage index for intensity 0.05, 0.10, 0.15 and 0.20 g categorized at moderate (light) level that means no structural damage, some non-structural damage but at this intensity no structural element yielding.

5 Conclusion

The conclusion of this topic can be obtained from the result of the IDARC 2D analysis. The overall damage index was increased due to increment of intensity. From the result, the damage level is moderate for intensities 0.05, 0.10, 0.15 and 0.20 g. There is no structural damage but some non-structural is damage. The location of structural element starts yielding at Beam 3 at the left position at level 3. For intensity 0.05 g, at time 4.42 s the Beam 3 start yielding. While, the yielding start occur for intensity 0.10, 0.15 and 0.20 g at 3.66, 3.215 and 3.115 s. So, that can be concluded the higher intensity may result the quicker time for structural element start yielding. The damages are mostly developed at beam connection followed by column connection. From the overall analyses, it can be concluded that the building samples have no structural element damages even the high intensity of earthquake 0.20 g is occur to the building.

Acknowledgments The authors would like to acknowledge Ministry of Education (MOE) for providing financial support under project RAGS and support from Research Management Institute (RMI), Universiti Teknologi MARA (UiTM).

References

1. G. Li, Y. Zhang, H. Li, Seismic damage analysis of reinforced concrete frame using the force analogy method. *J. Eng. Mech.* **139**(12), 1780–1789 (2013)
2. R. Moreno-Gonzalez, J.M. Bairan, Seismic damage assessment for waffled-slabs reinforced concrete (RC) buildings in Barcelona. *Int. J. Architectural Heritage: Conserv. Anal. Restor.* **7** (1), 116–134 (2013)

3. R. Ditommaso, M. Vona, M.R. Gallipoli, M. Mucciarelli, Evaluation and considerations about fundamental periods of damaged reinforced concrete buildings. *Nat. Hazards Earth Syst. Sci.* **13**, 1903–1912 (2013)
4. J.M. Barron, M.B.D. Hueste, Diaphragm effects in rectangular reinforced concrete buildings. *ACI Struct J. Tech. Pap.* **3**, 89–98 (2004)
5. S.K. Kunnath, A.M. Reinhorn, R.F. Lobo, *IDARC Version 3.0: A Program for the Inelastic Damage Analysis of Reinforced Concrete Structures*, Report no. NCEER-92-0022 (National Center for Earthquake Engineering Research, State University of New York at Buffalo, 1992)
6. S.K.V. Gunturi, *Building Specific Earthquake Damage Estimation*, Doctor of Philosophy Dissertation, Stanford University, San Francisco, 1992
7. R. Ismail, A. Adnan, A. Ibrahim, Vulnerability of public buildings in sabah subjected to earthquake by finite element modeling. The 2nd international building control conference 2011. *Procedia Engineering* **20**, 54–60 (2011)
8. BS 6399: Part 1, Loading for Building, Part 1. Code of Practice for Dead and Imposed Loads (1996)
9. Y.J. Park, A.H.S. Ang, Y.K. Wen, *Seismic Damage Analysis and Damage-Limiting design of R/C Buildings*, Civil Engineering Studies, Technical report no. SRS 516 (University of Illinois, Urbana, 1984)

Strength of Various Densities of Lightweight Coir Fiber Concrete Containing Protein and Synthetic Foam

Mazlina Mohamad, Mohd Fadzil Arshad
and Nur Amalina Abdul Hamid

Abstract Lightweight concrete which was proposed normally to reduce the dead load of ordinary concrete has become very popular among researcher. One of the lightweight concrete is known as lightweight foam concrete. This type of concrete can support lesser load compared to ordinary concrete. Thus, a lot of study has been conducted to increase the strength of lightweight foam concrete. Fiberglass has been introduced to increase the strength of lightweight foam concrete, however, it is not an environmental friendly product. Therefore, in this study natural fiber named as coir fiber has been used to strengthen the foam concrete. A total of 18 cube samples with $100 \times 100 \times 100$ mm size have been produced. The samples have been produced using protein and synthetic foaming agent and comparison on compressive strength have been made. Different densities of concrete were considered in this study which are 1400, 1600 and 1800 kg/m^3 . A compressive strength testing machine was used to obtain the strength of these 18 cube samples at 28 days of water curing. Results on compressive strength have been compared between the lightweight coir fiber concrete containing protein and synthetic foam of various densities. The relationships indicate that the increment of concrete density has increased the strength of lightweight fiber concrete containing protein and synthetic foam. Besides, the strength of lightweight fiber concrete containing synthetic foam is higher than protein foam.

Keywords Foam concrete · Coir fiber · Synthetic foam · Protein foam · Lightweight concrete

M. Mohamad (✉) · M.F. Arshad · N.A.A. Hamid
Institute of Infrastructure Engineering and Sustainable Management,
Universiti Teknologi MARA, 40450 Shah Alam, Selangor, Malaysia
e-mail: mazlina9090@salam.uitm.edu.my

M.F. Arshad
e-mail: fadiil2013@yahoo.com

N.A.A. Hamid
e-mail: hamid.amalina@gmail.com

1 Introduction

Lightweight concrete is part of concrete that has a lower density than normal concrete. The range of densities of lightweight concrete is between 300 and 1850 kg/m³. According to Neville [1], there are three types of lightweight concrete that can be obtained by replacing some of the solid materials in the mix with air voids. Three possible placements of the air voids are in the aggregates particles known as lightweight aggregate, in between coarse aggregate particles where the fine aggregates being excluded known as no-fines concrete and in the cement paste known as cellular concrete.

Based on Nooraini et al. [2], cellular concrete or also called foam concrete is a versatile material that consists of Portland cement paste or mortar mixed with at least 20 % by volume air in the form of small bubbles introduced by a foaming agent. Integrating the air-voids in the form of foam into the mix will cause production of void in the concrete once it is hardened. Yet, according to Mydin and Wang [3], the occurrence of voids in concrete can cause reduction of concrete densities within range of 400–1600 kg/m³.

Other than economical, lightweight foam concrete also has a number of undoubted advantages in providing high workability, excellent thermal conductivity, high impact resistance, good freeze thaw resistance, and low self-density [4]. Besides, it is suitable to be applied for both cast-in-place and precast and it is easy to be fabricated anywhere in any shape or building unit size on a small scale.

However, foam concrete is not applicable to be used as structural material as it has low compressive strength. Addition of fine aggregates in the mortar matrix could help to enhance the mechanical properties of the foam concrete. Several studies on this matter have been carried out by few researchers [5, 6]. Thus, there are still lacks of information and limited studies have been conducted on the uses of fiber as reinforced materials in foam concrete.

Zollo [7, 8] have found that there is enhancement in the impact and mechanical properties with the application of polypropylene fiber in cellular concrete with density of 640 kg/m³. Zollo [8] mentioned that the typical behavior of cellular concrete can be transformed from brittle to ductile elastic-plastic behavior by reinforcing concrete with fiber. Furthermore, Jones and McCarthy [5] have found about 52 % increments in compressive strength when comparison of foam concrete with and without reinforcement was made. The usage of steel fibers in reinforcing lightweight concrete also has been observed by researchers [9]. Steel and polypropylene fiber is good but they are not environmental friendly. Therefore the use of natural fiber is proposed.

Paramasivam et al. [10] reported that coir fibers are cheaper in most tropical countries as it can be easily found and also fairly inexpensive to be treated. Therefore, coir fiber is a good choice as it can be easily obtained and this kind of waste will lead

to open burning and greenhouse effect. According to Nooraini et al. [2], reusing of waste materials which is happening in concrete construction industries lately can lead towards having a sustainable development for the country. Based on Majid et al. [11], brown fibers are mostly applied in engineering field. This is because brown coir fibers are good abrasion resistant compared to white coir fibers.

Protein foams and synthetic foams are normally used to produce foam. Protein foam is a natural type of foam while synthetic foam is a man-made chemical. According to Mydin and Norizal [12], foams that produced from protein based have smaller size of bubbles and it is more stable and has a stronger closed bubble formation compared to the foams from synthetic based. Thus, it is good to study how protein and synthetic foam will react with the present of natural fiber.

Foam concrete is known as self-compacting concrete. Therefore, it cannot be imposed to any types of compaction or even vibration as it might affect the design density. Hence, the significant characteristics of fresh state for the foam concrete are flow ability and self-compatibility [5, 13–19]. The properties of hardened foam concrete can be distinguished into two distinct ways. First is the physical properties comprise of density, air-void system and porosity. The second property of hardened foam concrete is the mechanical properties which consist of compressive strength, tensile strength and modulus elasticity [12].

Based on Hanizam et al. [4], the densities of lightweight foam concrete influenced the mechanical properties by the pores production. Different density of foam concrete will give different production of pores in term of the size and amount of the pores. As more foam added into the mix, less density that the foam concrete would be and more voids and pores will be produced. Research on the effect of fiber to the properties of foam concrete a very limited being carried out. This research was carried out with attention to identify the effect of coir fiber to the compressive strength of concrete containing different type of foaming agent at 28 days curing age. The lightweight concrete containing coir fiber and different type of foaming agent at different density has been analysed and compared on their compressive strength performance.

2 Materials and Method

2.1 Coir Fiber

The brown coir fiber used in this study has a length ranging between 4 and 8 cm. The brown coir fiber has been chosen as it was found to be good in withstanding abrasion compared to white coir fiber [11].

2.2 Foaming Agent

Two types of foaming agent have been used in this study. The protein foam that was used was a palm oil based chemical polyurethane (PU). The storage of the natural protein foam cannot be too long as it can easily affect the concrete performance. The synthetic foaming agent that has been used was MEYCO SLF 30 supplied by BASF.

2.3 Cement Composite

1. Binders

In this study, ordinary Portland cement, sand, coir fiber and foaming agents were used as cement-binders constituents. The sand used was passing 600 μm during sieve analysis as required by BS 882:1992 [20].

2. Mixing and Casting

In order to identify compressive strengths of samples, $100 \times 100 \times 100$ mm cube samples have been prepared. The sample has 0.5 water cement ratio. The preparation of the mix design proportion in this study is based on the proportion of 1 m^3 concrete. Amount of foam that has been used in this study was differing according to different densities which are 1400, 1600 and 1800 kg/m^3 . Details on the mix proportion of lightweight coir fiber concrete containing protein and synthetic foam for cube sample have been summarized in Table 1.

The mixing process starts by combining all the basic materials and mixing them thoroughly in the concrete mixer. The coir fibers were then been added into the concrete mix before adding the foam. Preparation of foam was done separately. The fresh concrete mix was poured into a mould of $100 \times 100 \times 100$ mm in size. The mixture was left in the mould for about 24 h before removed. Vibration process is not required as it may cause damage to the foam structure and affect the density of foam concrete. The samples then undergo normal curing which is curing by water for 28 days.

Table 1 Mix proportion for lightweight coir fiber concrete containing protein and synthetic foam for cube sample

Materials	Cube 1 1400 (kg/m^3)	Cube 2 1600 (kg/m^3)	Cube 3 1800 (kg/m^3)
Cement (kg)	5.57	6.37	6.63
Water (kg)	2.78	3.15	2.90
Finest river sand (kg)	8.34	9.55	9.96
Coir fiber (kg)	0.11	0.13	0.13
Foam mix (1:30) (L)	0.04	0.03	0.02
protein/synthetic foam water	1.20	0.90	0.60

2.4 Compression Test

A total of 18 samples have been tested for compressive strength. BS1881: Part 116: 1983 [21] has been used in conducting testing for compressive strength.

3 Results and Discussion

3.1 Comparison in Compressive Strength Between LCF Concrete Containing Protein and Synthetic Foams

Figure 1 presents the compressive strength of concrete containing coir fiber with different type of foaming agent. From Fig. 1, the compressive strength of lightweight coir fiber concrete with protein foaming agent found to be increased as the density of concrete increased. At a density of 1400, 1600 and 1800 kg/m³, a compressive strength of lightweight coir fiber concrete with protein foam is 4.8, 6.88 and 12.47 N/mm² respectively. While for lightweight coir fiber concrete containing synthetic foam, the compressive strength was found to be 11.02, 11.71 and 16.09 N/mm² for 1400, 1600 and 1800 kg/m³ respectively.

From the analysis, it has been found that the increments on compressive strengths for lightweight concrete with protein foam between 1400–1600 and 1600–1800 kg/m³ densities were found to be 43.3 and 81.3 % respectively. The increment of compressive strength for lightweight concrete consists of synthetic foam between 1400–1600 kg/m³ is 6.3 % and for 1600–1800 kg/m³ is 37.4 %. The effect of foaming agent type to the percentage increment of compressive strength has been summarized in Table 2.

Fig. 1 Compressive strength against density at 28 curing days

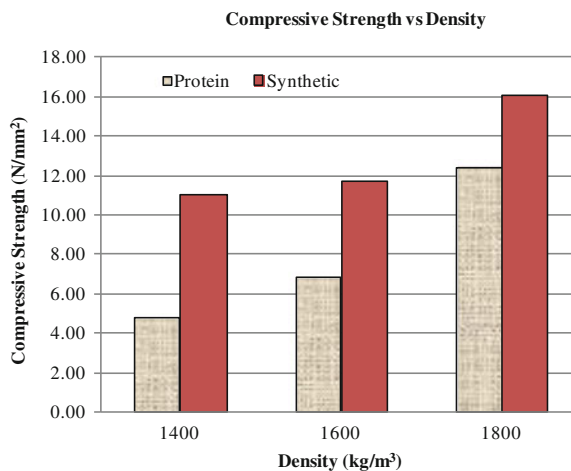


Table 2 Effect of foaming agent type to the percentage increment of compressive strength

Density (kg/m ³)	Protein foam (%)	Synthetic foam (%)
1400–1600	43.3	6.3
1600–1800	81.3	37.4

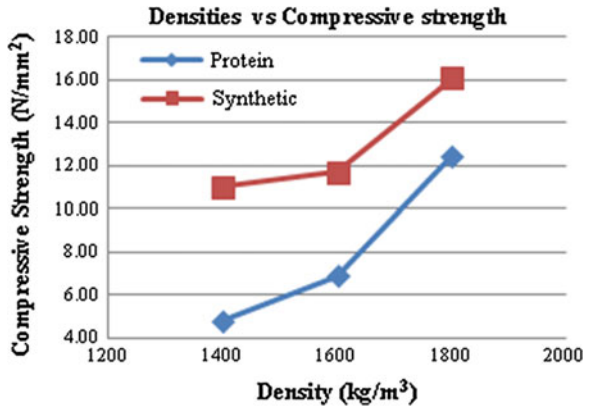
Based on Table 2, it can be seen that the highest increment occurred between 1600–1800 kg/m³ densities of lightweight concrete with protein foam. Comparison on the percentage increment of compressive strength between protein and synthetic foaming agents shows that protein foaming agent obtained higher increment compared to synthetic. It shows that the addition of coir fiber in the lightweight foam concrete containing protein foaming agent affected a lot in the concrete strength development as the density increased. In the case of synthetic foam, higher compressive strength has been achieved for 1400 kg/m³ density compared to protein foaming agent which lead to small difference in percentage of compressive strength for 1400–1600 kg/m³. However, the increment in compressive strength is higher between 1600–1800 kg/m³.

The comparison in compressive strength for various densities of LCF concrete containing Protein and Synthetic foams has been made at 28 days curing age only and presented in Fig. 1. It was found that the compressive strengths of lightweight coir fiber concrete containing synthetic foam are higher compared to LCF containing protein foam. In both foaming agent, the strength will increased as the density increased. The highest compressive strength occurs at 1800 kg/m³. Based on findings by Mydin and Norzila [12], foam produce from protein based is more stable compared to synthetic. However, in this research, when these foams being combine with coir fiber which is a natural fiber, the synthetic foam was found to be more stable as it obtained higher compressive strength.

3.2 Comparison of Relationship Between Compressive Strength and Various Densities of Lightweight Coir Fiber Concrete Containing Protein and Synthetic Foam

In lightweight foamed concrete, curing plays an important role for strength development. Foam concrete gives different strength depending on its density. For densities higher than 1000 kg/m³, as the air-voids are far apart to have an influence on the compressive strength, the composition of the paste determines the compressive strength. Besides, the longer the curing process, the crystallization process has enhanced the bond between molecules inside the concrete matrix even more. The relationship of compressive strength of lightweight coir fiber concrete containing protein and synthetic foam only done based on the 28 days of curing age because in 28 days the strength value is the most applicable and optimum age of curing to be referred for as suggested by Neville [1]. The result for the relationship

Fig. 2 Densities against compressive strength of lightweight coir fiber concrete containing protein and synthetic foam at 28 days



between compressive strength and density of lightweight coir fiber concrete containing synthetic and protein foam is shown in Fig. 2.

Based on Fig. 2, the value of slopes between 1400–1600 and 1600–1800 kg/m³ LCF concrete with synthetic foam are found to be 0.0035 and 0.0219 respectively. Lightweight coir fiber concrete with protein foaming agent obtained higher value of slopes between 1400–1600 and 1600–1800 kg/m³ which are 0.0104 and 0.0280. The slopes between 1600–1800 kg/m³ show higher value in both LCF concrete containing different foaming agent. It shows rapid increment in compressive strength between these densities.

From Fig. 2, the compressive strength of lightweight coir fiber concrete which contains protein and synthetic foam show the same relationship between density and compressive strength. There is an increment in compressive strength as the density increased. Generally, the density of a porous media is dependent on the amount of pores and pore size distribution in the media. It would have been expected therefore, that a higher density foamed concrete would record a higher compressive strength due to its lower porosity as suggested by Narayanan and Ramamurthy [22] that the compressive strength is dependent on the amount or distribution of pores and pore sizes. The size and the amount of pores influence the compressive strength of a porous material, which a smaller size of air pores lead to higher compressive strength. During the experimental process it is concluded that less pores available in lightweight coir fiber concrete containing synthetic foam as it shows higher strength value in 28 days of curing compared to other curing days.

Figure 3 shows the densities against percentage differ for LCF concrete with different foaming agents at 28 days. It can be seen that the percentage differ decreasing as the density increased. The percentage differ on the compressive strength of synthetic over protein foaming agent for 1400, 1600 and 1800 kg/m³ are 129.6, 70.2 and 29 % respectively.

As the density increase, the difference in strength will decrease. According to Awang et al. [4] and Narayanan and Ramamurthy [22], the density of lightweight foam concrete influence the compressive strength produced. It is affected by the size

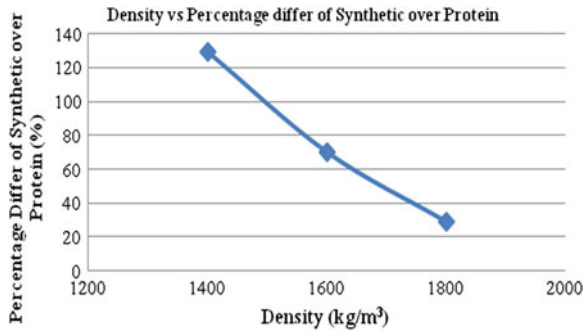


Fig. 3 Density against percentage differ of compressive strength of lightweight coir fiber concrete containing synthetic over protein foam at 28 days

and amount of pores produce. Lesser density will require more foam which will lead to more formation of voids and pores. As can be seen in Table 1, the amount of foam for 1400 kg/m^3 is greater than 1800 kg/m^3 specimen.

4 Conclusion

Based on the study on compressive strength of lightweight coir fiber concrete containing protein and synthetic foam, the following conclusions can be drawn:

- In the addition of coir fiber, LCF concrete containing synthetic foaming agent was found to be better compared to LCF concrete with protein foam. At 28 days, the compressive strengths of coir fiber containing synthetic foaming agent are 129.6, 70.2 and 29 % greater compared to protein.
- For the relationship between compressive strength and the various densities of lightweight coir fiber concrete containing protein and synthetic foam, it was found that as the density increase, the compressive strength will increase as well. This behavior complies with the theory of concrete strength development.
- Foam concrete and fiber can be blended together. In the occurrence of fiber the production of lower concrete density is still possible.

Acknowledgments This research work is funded by Institute for Infrastructure Engineering and Sustainable Management and Faculty of Civil Engineering, Universiti Teknologi MARA, Malaysia.

References

1. A.M. Neville, *Properties of Concrete*, 4th edn. (Longman Group Limited Essex, England, 1995)
2. M.Z. Nooraini, A.R. Ismail, A.Z. Ahmad Mujahid, Potential application in thermal insulation, in *Proceedings of MUCEET2009, Malaysian Technical Universities Conference on Engineering and Technology*, Malaysia, 20–22 June 2009
3. M.A.O. Mydin, Y.C. Wang, Mechanical properties of foamed concrete exposed to high temperatures. *Constr. Build. Mater.* **26**, 638–654 (2012)
4. H. Awang, M.A.O. Mydin, A.F. Roslan, Effect of additives on mechanical and thermal properties of lightweight foamed concrete. *Pelagia Res. Libr.* **3**(5), 3326–3338 (2012)
5. M.R. Jones, A. McCarthy, Utilising unprocessed low-lime coal fly ash in foamed concrete. *Fuel* **84**(11), 1398–1409 (2005)
6. K. Ramamurthy, E.K. Kunhanandan Nambiar, G. Indu Siva Ranjani, A classification of studies on properties of foam concrete. *Cem. Concr. Compositions* **31**(6), 388–396 (2009)
7. R.F. Zollo, Fiber-reinforced concrete: an overview after 30 years of development. *Cem. Concr. Composites* **997**(19), 107–122 (1997)
8. R.F. Zollo, Engineering material properties of a fiber reinforced cellular concrete. *ACI Mater J.* **95**(5), 631–635 (1998)
9. O. Kayali, M.N. Haque, B. Zhu, Some characteristics of high strength fiber reinforced lightweight aggregate concrete. *Cem. Concr. Composites* **25**(2), 207–213 (2003)
10. P. Paramasivam, G.K. Nathan, N.C.D. Gupta, Coconut fibre reinforced corrugated slabs. *Int. J. Cem. Compos. Lightweight Concr.* **6**(1), 19–27 (1984)
11. A. Majid, L. Anthony, S. Hou, C. Nawawi, Mechanical and dynamic properties of coconut fibre reinforced concrete. *Constr. Build. Mater.* **30**, 814–825 (2012)
12. M.A.O. Mydin, M.N. Norizal, *Mechanical, Thermal and Functional Properties of Green Lightweight Foamcrete* (Analele Universitat. Anul XIX, NR. 1, 2012), ISSN 1453-7297
13. E.P. Kearsley, P.J. Wainwright, Porosity and permeability of foamed concrete. *Cem. Concr. Res.* **31**(5), 805–812 (2001)
14. E.P. Kearsley, P.J. Wainwright, The effect of high fly ash content on the compressive strength of foamed concrete. *Cem. Concr. Res.* **31**(1), 105–112 (2001)
15. E.P. Kearsley, P.J. Wainwright, The effect of porosity on the strength of foamed concrete. *Cem. Concr. Res.* **32**(2), 233–239 (2002)
16. E.P. Kearsley, P.J. Wainwright, Ash content for optimum strength of foamed concrete. *Cem. Concr. Res.* **32**(2), 241–246 (2002)
17. M.R. Jones, A. McCarthy, Preliminary views on the potential of foamed concrete as structural material. *Mag. Concr. Res.* **57**(1), 21–31 (2005)
18. E.K.K. Nambiar, K. Ramamurthy, Influence of filler type on the properties of foam concrete. *Cem. Concr. Compositions* **28**(5), 475–480 (2006)
19. E.K.K. Nambiar, K. Ramamurthy, Models relating mixture composition to the density and strength of foam concrete using response surface methodology. *Cem. Concr. Compositions* **28**, 752–760 (2006)
20. BS 882, *Specification for Aggregates from Natural Sources for Concrete* (British Standard Institution, London, 1992)
21. BS 1881: Part 116, *Testing Concrete: Method for Determination of Compressive Strength of Concrete Cubes* (British Standard Institution, London, 1983)
22. N. Narayanan, K. Ramamurthy, Structure and properties of aerated concrete: a review. *Cem. Concr. Compos.* **22**, 321–329 (2000)

An Experimental Study on the Fracture Energy of Foamed Concrete Using V-Notched Beams

Norashidah Abd. Rahman, Zainorizuan Mohd Jaini,
Nor Azira Abd. Rahim and Siti Aisyah Abd. Razak

Abstract Foamed concrete has recently gained attention as an alternative to normal concrete in structural engineering. Foamed concrete with a low range of densities can be obtained for various applications. As a structural component, foamed concrete is mainly advantageous given characteristics such as high strength with low density, good serviceability, and light weight. Therefore, many studies have investigated its strength and mechanical properties. However, these investigations did not examine the fracture energy of foamed concrete, which is the main parameter that governs damage and crack mechanisms. Therefore, the present study aims to experimentally investigate the fracture energy of foamed concrete using beam specimens with V-notches through the three-point bending test. Beam specimens of foamed concrete were cast and prepared at densities of 1,400 and 1,600 kg/m³. Moreover, the designed V-notch was 30 mm long and was positioned at the center of the beam. The beam specimens were then assessed to generate the strength-displacement profiles. Consequently, fracture energy was determined based on the Hillerborg, Bazant, and Comite Euro-International du Beton models. Results showed that cracks propagated from the tip of the notch to the upper surface of the beam. Surprisingly, the fracture energy of the foamed concrete were relatively high at approximately 18–25 N/m given compressive strengths of 6.4 and 14 MPa. Furthermore, the fracture energy of foamed concrete was only a fraction of that of normal concrete.

Keywords Fracture energy · Foamed concrete · Beam V-notch · Three-point bending test

N.Abd. Rahman (✉) · Z.M. Jaini
Jamilus Research Center, Universiti Tun Hussein Onn Malaysia,
86400 Parit Raja, Batu Pahat, Johor, Malaysia
e-mail: nrashida@uthm.edu.my

Z.M. Jaini
e-mail: rizuan@uthm.edu.my

N.A. Abd. Rahim · S.A. Abd. Razak
Faculty of Civil and Environmental Engineering, Universiti Tun Hussein Onn Malaysia,
86400 Parit Raja, Batu Pahat, Johor, Malaysia
e-mail: zirarahim@yahoo.com

S.A. Abd. Razak
e-mail: ctaisyahrazak@gmail.com

1 Introduction

Foamed concrete is also called cellular lightweight concrete or aerated concrete. It is produced by mixing Portland cement, sand with or without additives, water, and preformed stable foam. This type of concrete is a non-homogenous material that displays complex mechanical behavior. Many experimental studies have investigated the strengths of concrete through tensile, compression, and flexural tests, which are conducted under static loaded state. Already in the unloaded state, concrete contains micro-cracks that are initiated during softening by reduced material stiffness. This reduced stiffness is a form of mechanical damage and can be detected by evaluating fracture energy [1]. The damage either remains distributed or is localized under the influence of fracture energy depending on the size, structure shape, loading type, and the presence or absence of reinforcement [2]. Therefore, fracture energy is a dominant factor that governs the initiation, growth, and coalescence of micro-cracks, as well as macroscopic crack propagation, fracture and progressive damage of brittle materials.

Fracture energy is an important material behavior that should be studied when foamed concrete is utilized as a structural component. Fracture energy is often covered by the constitutive law during computational modeling to ensure the accurate modeling of structural behavior and damage mechanisms. However, previous studies do not investigate the fracture energy of foamed concrete; rather, most of the literature on foamed concrete has focused on its elastic properties, tensile and compressive strengths, and permeability. Thus, these studies have not examined in-depth the material behavior that governs structural failure under applied load. Therefore, the present study investigates the fracture energy of foamed concrete through experimentation.

2 Fracture Energy

Previous studies have experimentally investigated the fracture energy in conventional and lightweight aggregate concrete. Conventional concrete has a fracture energy level of approximately 75–100 N/m depending on grade [3]. However, the fracture energy of lightweight concrete, including most cellular concrete, is expected to be less than 30–50 % that of conventional concrete. Mier [4] suggested that the fracture energy of foamed concrete is roughly 25 N/m given a compressive strength of 2.9 MPa and at densities that range between 400 and 1,200 kg/m³. This finding indicates that foamed concrete has a relatively high fracture energy level despite its compressive strength. Meanwhile, Rahman and Jaini [5] reported that foamed concrete has a fracture energy level of 15 N/m during the modeling of a

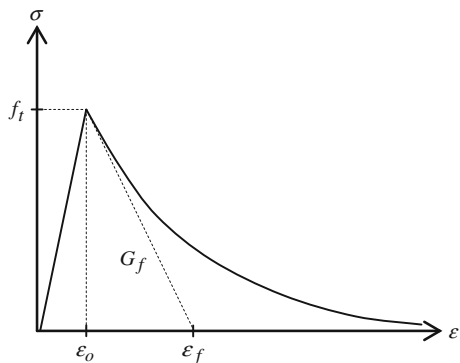
sandwich-foamed concrete wall. The results of their study agreed numerically and experimentally with respect to damage behavior. On the other hand, Wang and Li [6] suggested that the fracture energy level of foamed concrete is only a fraction of that of normal concrete if this foamed concrete references lightweight aggregate concrete in terms of strength and density. Voids or air bubbles typically affect the strength of foamed concrete, consequently reducing fracture energy. The strength of foamed concrete depends mainly on its density, which varies from 800 to 1,800 kg/m³. As a result, fracture energy levels vary with different foamed concrete strengths given strength conditions.

Fracture energy is simply the total amount of work required to break a specimen completely per unit ligament area. It can also be referred to as the energy required in the incarnation and formation of cracks as dissipated per unit area [7, 8]. Fracture energy basically corresponds to the area of the softening phase at a stress-strain curve, as shown in Fig. 1. The area under the curve represents the energy dissipated during the complete separation (formation of the stress-free surface) of a unit area of plain concrete. The area under the initial tangent of the softening curve is a fraction of the total fracture energy, which is significant in the calculation of the failure loads of test specimens. This definition relies on the assumption that all of the energy required to break the specimen is transformed into surface energy. However, energy dissipation outside of the fracture zone is also often considered in the determination of fracture energy and should not be overlooked.

Mathematically, fracture energy can simply be defined as follows:

$$G_f = \int \sigma du \tag{1}$$

Fig. 1 Fracture energy at the stress-strain curve



The following equation for constant slope softening is generated through integration over the localization band width of the crack:

$$E = -\frac{f_t^2 l_c}{2G_f} \quad (2)$$

Rearranging the above equation simplifies the expression of fracture energy as follows:

$$G_f = \frac{K_{IC}^2}{E} \quad (3)$$

where G_f is fracture energy; σ is stress strength; f_t is tensile strength; l_c is crack length; K_{IC} is the stress intensity of the fracture toughness that can be obtained through an experimental study of indentation strength; and E is Young's modulus.

However, the fracture toughness of concrete is difficult to determine and is convoluted because of its quasi-brittleness. Thus, fracture energy must be comprehensively investigated especially with respect to the foamed concrete, which is more brittle than conventional concrete. In addition, the fracture energy formula, which is based on the stress intensity of fracture toughness and the Young's modulus, is valid only when the material is presumably fully isotropic and homogeneous. As a result, this formula is invalid for foamed concrete. If the Hillerborg model [9] is used to experimentally investigate conventional concrete, then fracture energy can be determined using the following equation:

$$G_f = \frac{U_o + m_g d_o}{B(W - a_o)} \quad (4)$$

where U_o is the area under the softening phase of the stress-strain curve; B is specimen width; W is specimen depth; a_o is notch depth; m_g is specimen weight; and d_o is the load-point deflection at the fracture.

Fracture energy can also be predicted based on aggregate size, compressive strength, and water-cement ratio, as suggested by the Bazant [10] and Comite Euro-International du Beton (CEB) models [11]. In these models, the fracture energy of concrete is governed principally by the properties of the aggregate, and strong concrete produces high fracture energy. Moreover, the energy stored in the concrete with maximum tensile strength increases with compressive strength, but the energy dissipation capability of this concrete remains approximately constant [12]. In the Bazant model, fracture energy also depends on the water-cement ratio, which influences concrete strength considerably. Martin et al. [13] used both the Bazant and the CEB models to predict fracture energy in concrete. The predicted results accorded with those obtained using the Hillerborg model. Equations as stated in (5) and (6) express the formula used to determine fracture energy according to the Bazant and CEB models, respectively:

$$G_F = 2.5 \alpha_0 \left(\frac{f_c}{0.058} \right)^{0.40} \left(1 + \frac{D_{max}}{1.94} \right)^{0.43} \left(\frac{w}{c} \right)^{-0.18} \tag{5}$$

$$G_F = 0.0143 \alpha_0 (D_{max})^2 - 0.5 D_{max} + 26 \times \left(\frac{f_c}{10} \right)^{0.7} \tag{6}$$

where α_0 is an aggregate shape factor ($\alpha_0 = 1$ for the rounded aggregate, $\alpha_0 = 1.12$ for the angular aggregate); f_c is the compressive strength of concrete; D_{max} is the maximum aggregate size; and w/c is the water-cement ratio of concrete.

3 Experimental Study

The experimental study of the fracture energy in foamed concrete involves material preparation, the casting of cube and beam specimens, compression tests, and the three-point bending tests. Fracture energy is computed based on the procedures suggested by the fracture mechanics of the concrete-test method presented by Reunion Internationale des Laboratoires et Experts des Materiaux (RILEM) [14, 15]. This type of experimental study must be conducted carefully and be measured accurately because foamed concrete is weaker than normal concrete and can fail easily under direct loading.

3.1 Mixed Design and Material Preparation

The mixed design based on the Department of Environment (DOE) was utilized to evaluate the proportions of foamed and normal concrete. The proposed densities of the foamed concrete are 1,400 and 1,600 kg/m³. Normal concrete has a density of 2,400 kg/m³ and a target grade of 25. Table 1 shows the mixed design of foamed and normal concrete in terms of the proportions of cement, sand, water, aggregate, and foam agents. This study uses ordinary ASTM type 1 Portland cement. The maximum diameters of the aggregate and of the sand are 20 and 3 mm, respectively. The water-cement ratio for normal concrete is 0.5.

Table 1 Mixed design of foamed and normal concrete

Type of concrete	Density (kg/m ³)	Ratio		
		C/S	F/C	W/C
Foamed concrete	1,400	1:2	0.85	0.55
	1,600	1:2	0.70	0.55
Normal concrete	2,400	<i>Sand</i>	<i>Cement</i>	<i>Aggregate</i>
		1	2	4

Ratio C/S = Cement-sand; F/C = foam-cement and W/C = water-cement

3.2 Cube and Beam Specimens

A total of 18 cube specimens were cast for the compressive test. Six foamed concrete specimens had densities of 1,400 and 1,600 kg/m³, whereas another six specimens were composed of normal concrete. Beam specimens with V-notches were designed according to the size standard of the three-point bending test. The beam is 700 mm long, 150 mm deep, and 150 mm wide. The notch is located at the center of the beam and is 30 mm deep. The schematic of the beam is detailed in Fig. 2. In this experimental study, six beam specimens of foamed concrete with densities 1,400 and 1,600 kg/m³ were casting. In addition, three normal concrete beam specimens were also prepared to calibrate the three-point bending test procedure for accurate application to foamed concrete.

3.3 Test Procedures

All cube specimens were placed under compression loading after 7, 14, and 28 days long curing processes to determine compressive strength. Figure 3 depicts the compressive test on the cube specimens of foamed and normal concrete. Meanwhile, all beam specimens were subjected to the three-point bending test, as exhibited in Fig. 4. The machine was set to the minimum speed at 0.5 mm/min to provide sufficient time during which the propagation of the crack tip can be detected and to prevent sudden catastrophic failure in the beam specimens. Beam displacement was measured based on the slope of the machine. The obtained measurements were similar to that obtained with a linear variable displacement transducer.

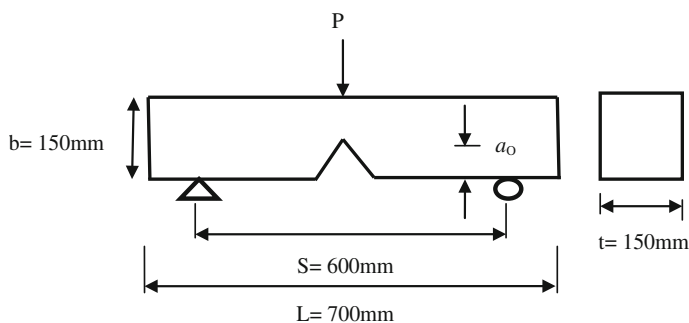


Fig. 2 Schematic of the beam specimens with V-notches

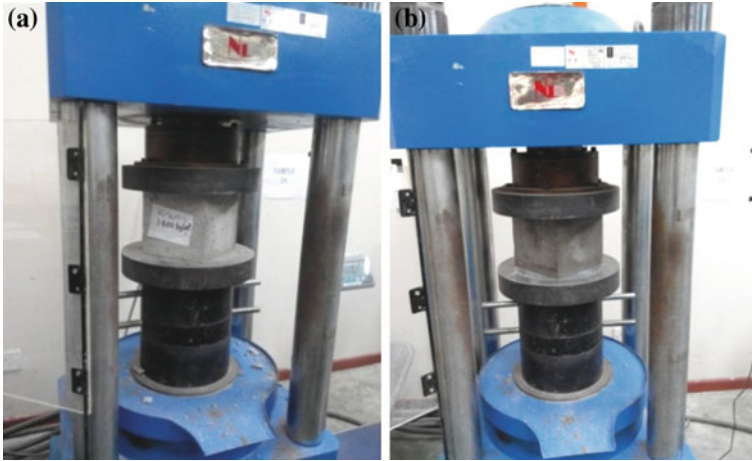


Fig. 3 Compression test: **a** foamed concrete and **b** normal concrete

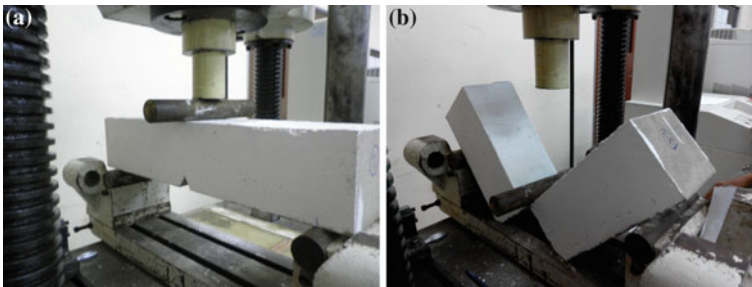


Fig. 4 Three-point bending test: **a** test setup and **b** failure of the beam specimen

4 Experimental Results

The experimental study obtains the compressive strengths and strength-displacement profiles that are paramount to the determination of fracture energy. In the process, crack tip, length, and propagation were also determined.

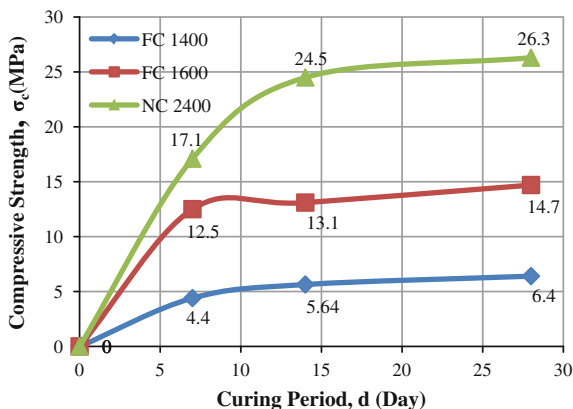
4.1 Compressive Strength

The compressive strength results for foamed and normal concrete at 7, 14, and 28 days are presented in Table 2 and in Fig. 5. Foamed concrete displayed the

Table 2 Compressive strengths of foamed concrete and normal concrete

Type of concrete	Density (kg/m ³)	Compressive strength (MPa)		
		7 days	14 days	28 days
Foamed concrete	1,400	4.4	5.64	6.4
	1,600	12.5	13.1	14.7
Normal concrete	2,400	17.1	24.5	26.3

Fig. 5 Compressive strengths of the cube specimens of foamed concrete with densities of 1,400 (FC 1400) and 1,600 kg/m³ (FC 1600), as well as those of the cube specimens of normal concrete (NC 2400)

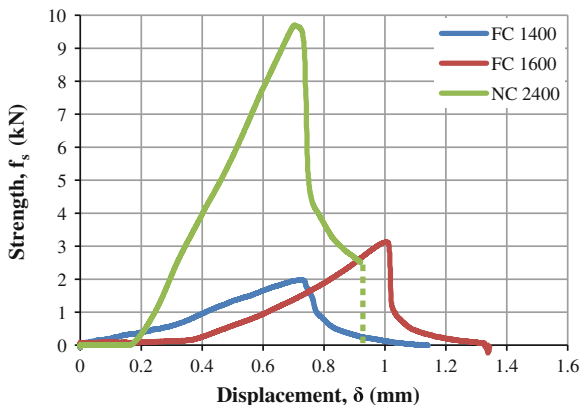


standard compressive strength given densities of 1,400 and 1,600 kg/m³. However, its strength rarely reached 14.7 MPa at a density of 1,600 kg/m³. Similarly, normal concrete achieved the target compressive strength at a concrete grade of 25.

4.2 Strength-Displacement Profile

Figure 6 displays the strength-displacement profiles of foamed and normal concrete as obtained during the three-point bending test. The normal concrete ruptured suddenly during the softening phase because it is quasi-brittle. Therefore, it retains little residual strength after meeting the yield condition. The maximum strength and displacement of normal concrete are 9,704.69 N and 0.707 mm, respectively. Meanwhile, the beam specimens of foamed concrete completed the softening phase under the slow loading applied during the three-point bending test. The foamed concrete retained residual strength even after reaching the maximum strength values of 1,978.13 and 3,128.13 N at densities of 1,400 and 1,600 kg/m³, respectively, because of the presence of air bubbles and the complex mechanical behavior of this concrete type. Foamed concrete is weaker than normal concrete by almost 70 %; thus, the area of the strength-displacement profiles of foamed concrete is also smaller than those of the profiles of normal concrete. This finding significantly affects fracture energy.

Fig. 6 Strength—displacement profiles of the beam specimens of foamed concrete at densities of 1,400 (FC 1400) and 1,600 kg/m³ (FC 1600), as well as those of the beam specimens of normal concrete (NC 2400)



4.3 Fracture Energy

Fracture energy can be determined using the Hillerborg model and the three-point bending test. The area under the strength-displacement profile is a dominant factor in this case. In addition, fracture energy can also be predicted with the Bazant and CEB models. The fracture energy levels of foamed and normal concrete are indicated in Table 3; the fracture energy level of normal concrete is 83.36 N/m. This level is presumably within the acceptable range for concrete grade 25. The Hillerborg model alone generated accurate results with regard to the fracture energy of concrete. However, the fracture energy level of foamed concrete can be accurately determined using the Hillerborg, Bazant, and CEB models given that their results are close to one another. The fracture energy levels of foamed concrete were 18 and 25 N/m at densities of 1,400 and 1,600 kg/m³, respectively. Thus, the fracture energy levels of foamed concrete vary according to density and strength.

4.4 Crack Propagation

Figures 7 and 8 show the crack propagation in foamed and normal concrete, respectively. The crack was initiated at the notch tip and propagated to the loaded area. The initial crack was approximately 51–54 mm long in the foamed concrete

Table 3 Fracture energy levels of foamed concrete and normal concrete

Type of concrete	Density (kg/m ³)	Fracture energy (N/m)		
		Hillerborg	Bazant	CEB
Foamed concrete	1,400	18.13	18.27	19.00
	1,600	25.38	25.50	34.04
Normal concrete	2,400	83.36	36.79	51.11

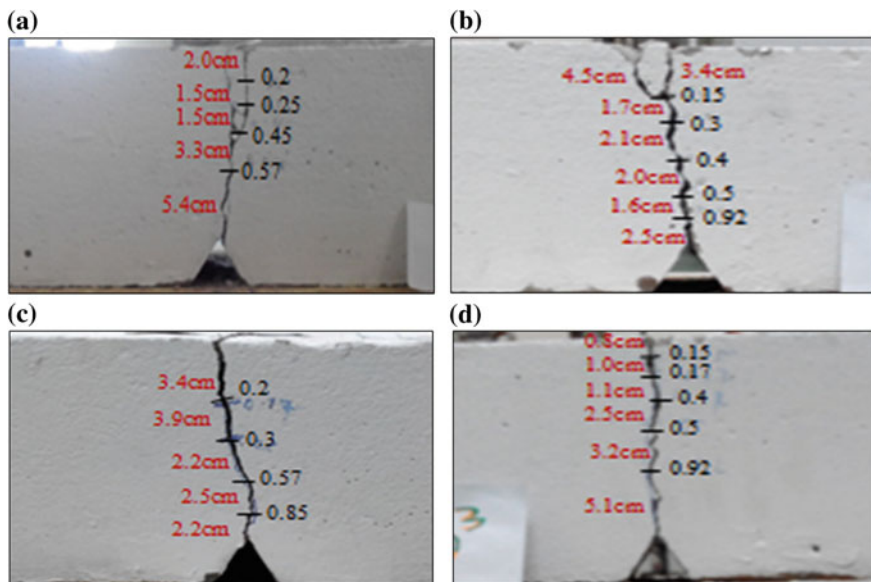


Fig. 7 Crack propagation from the tip to the upper surface of the foamed concrete. **a** Sample 1: front. **b** Sample 2: front. **c** Sample 1: rear. **d** Sample 2: rear

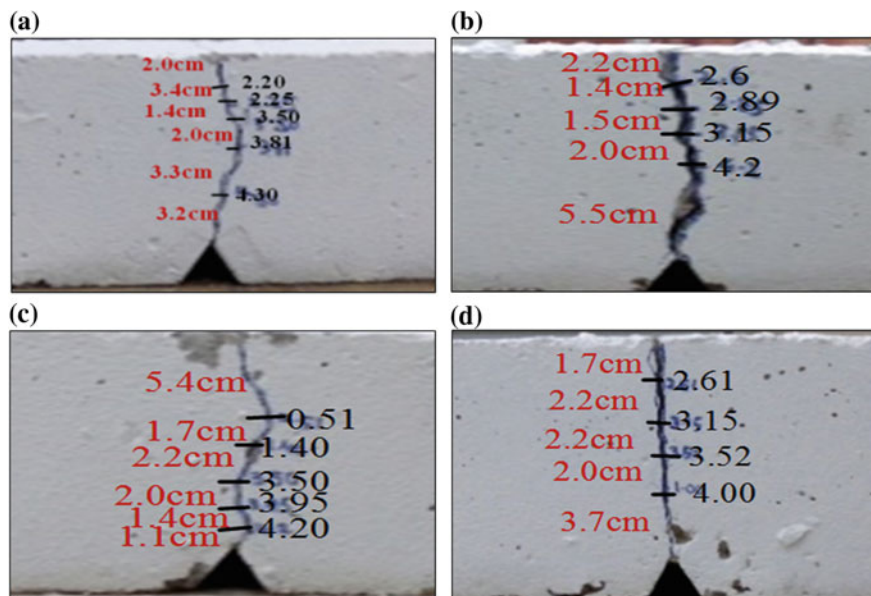


Fig. 8 Crack propagation from the tip to the upper surface of the normal concrete. **a** Sample 1: front. **b** Sample 2: front. **c** Sample 1: rear. **d** Sample 2: rear

and was roughly 10–30 mm in the normal concrete. Moreover, crack propagation was deliberately slow and almost invisible at the initial stage of the softening phase in the foamed concrete. The cracks also propagated as dowel and flexure tensile cracks.

5 Conclusion

An experimental study was conducted on the fracture energy of foamed concrete using the three-point bending test. This test mainly measured the amount of energy absorbed when the beam specimen broke in half. Compression strengths and strength-displacement profiles were obtained and analyzed, and the Hillerborg, Bazant, and CEB models were used to determine fracture energy level. In the Hillerborg model, the areas under the strength-displacement profiles and maximum displacement are the predominant parameters. The Bazant and CEB models consider compressive strength, maximum aggregate size, and the water-cement ratio of concrete. In addition, the fracture energy level of foamed concrete ranged from 18–25 N/m. This range of values was considerably lower than that for normal concrete. Furthermore, the fracture energy levels of foamed concrete varied according to density and strength. In the future, the effect of the dimensions of beam specimens should be investigated under different notch lengths.

Acknowledgments The authors would like to thank the Ministry of Education and University Tun Hussein Onn Malaysia for funding and the use of the facilities. This study was conducted under the grant scheme of FRGS Code 1219.

References

1. H. Cifuentes, M. Alcalde, F. Medina, Measuring the size-independent fracture energy of concrete. *Int. J. Exp. Mech.* **49**(1), 54–59 (2012)
2. S.T. Yang, X.Z. Hu, Z.M. Wu, Influence of local fracture energy distribution on maximum fracture load of three-point bending notched concrete beams. *J. Eng. Fract. Mech.* **78**(18), 3289–3299 (2011)
3. S. Muralidhara, B.K.R. Prasad, B.L. Karihaloo, R.K. Singh, Size independent fracture energy in plain concrete beams using tri-linear model. *J. Constr. Build. Mater.* **25**(7), 3051–3058 (2011)
4. J.G.M. van Mier, *Fracture Processes of Concrete, Florida* (CRP Press, United States, 1997)
5. M.H.A. Rahman, Z.M. Jaini, The combined finite-discrete element analysis of precast lightweight foamed concrete sandwich panel (PLFP) under axial load, in *Proceedings of the International Conference on Advances in Structural*. Kuala Lumpur, Malaysia: Civil and Environmental Engineering (2013)
6. S. Wang, V.C. Li, Lightweight engineered cementitious composites (ECC), in *Proceedings 4th International RILEM Workshop on High Performance Fiber-Reinforced Cement Composites*. Michigan, United States: Ann Arbor (2003)

7. Y.N. Li, A.P. Hong, Z.P. Bazant, Initiation of parallel cracks from surface of elastic half-plane. *Int. J. Fract.* **69**, 357–369 (1995)
8. M. Jirasek, S. Rolshoven, P. Grassl, Size effect on fracture energy induced by non-locality. *Int. J. Numer. Anal. Methods Geomech.* **28**, 653–670 (2004)
9. A. Hillerborg, The theoretical basis of a method to determine the fracture energy G_F of concrete. *Mater. Struct.* **18**(4), 291–296 (1985)
10. Z.P. Bazant, Concrete fracture models: testing and practice. *Eng. Fract. Mech.* **69**, 165–205 (2002)
11. Comite Euro-International du Beton, *CEB-FIB Model Code 1990* (Thomas Telford Service Ltd, Switzerland, 1993)
12. B. Trunk, F.H. Wittmann, Experimental investigation into the size dependence of fracture mechanics parameters, in: *Proceedings of Third International Conference of Fracture Mechanics of Concrete Structures*, Gifu, Japan (1998)
13. J. Martin, J. Stanton, N. Mitra, L.N. Lowes, Experimental testing to determine concrete fracture energy using simple laboratory test setup. *ACI Mater. J.* **104**(6), 575–584 (2007)
14. RILEM TC 89-FMT Fracture Mechanics of Concrete-Test Methods, Determination of fracture parameters (K_{IC} and $CTOD_c$) of plain concrete using three-point bend tests. *Mater. Struct.* **23**, 457–460 (1990)
15. RILEM TC 89-FMT Fracture Mechanics of Concrete-Test Methods, Size effect method for determining fracture energy and process zone size of concrete. *Mater. Struct.* **23**, 461–465 (1990)

Strength and Deformation Behaviour of Concrete Incorporating Steel Fibre from Recycled Tyre

A.S.M. Abdul Awal, Mariyana Aida Ab Kadir, Lim Lion Yee and Neelam Memon

Abstract This paper presents experimental results on strength and deformation behaviour of concrete reinforced with steel fibre from recycled tyre. Various concrete mixes were made where steel fibres were used at volume fractions ranging from 0 to 2 % by volume of concrete mix. Test specimens comprising of cube, cylinder and prism were prepared and tested for strength after 28 days of curing in water. It has been found that the compressive strength of concrete was slightly increased by the incorporation of recycled steel fibre. However, the tensile and flexural strength of concrete was remarkably improved with the increase of fibre content. Laboratory investigation further revealed that the addition of steel fibre had no influence on drying shrinkage; the creep of concrete, however, was found to be lower in concrete with fibre reinforcement than that in the control specimen.

Keywords Concrete · Recycled tyre · Steel fibre · Strength · Shrinkage · Creep

1 Introduction

The idea of reinforcing building materials with fibres has been known and practised since ancient times. The basic principle in both historic and recent examples is to enhance the properties of an inherently weak and brittle cementitious matrix by adding fibres to increase tensile strength and ameliorate brittleness giving improved ductility and toughness. Although this principle remains largely unchanged today, the diversity in fibre types, shapes and sizes has broadened greatly in recent years [1–3].

Fibres commonly used in concrete are steel fibres, synthetic fibres, glass fibres, and natural fibres. Since the advent of fibre reinforcing of concrete, a great deal of testing has been conducted on various fibrous materials to determine the actual

A.S.M. Abdul Awal (✉) · M.A.A. Kadir · L.L. Yee · N. Memon
Faculty of Civil Engineering, Universiti Teknologi Malaysia, Johor Bahru, Malaysia
e-mail: abdulawal@utm.my

characteristics and advantages for each product. Over the decades different types of steel fibres have been successfully used to reinforce concrete [4].

In recent years, there has been an increased interest in using the recycled steel waste especially from tire products. In all parts of the world large quantities of scrap tires are generated annually resulting in environmental hazards. It has been estimated that over 8 million units of scrap tire are generated in Malaysia, and 60 % of the scrap tires are disposed via unknown route [5]. These scrap tires are dangerous not only due to potential environmental threat, but also from fire hazards and provide breeding grounds for rats, mice, and mosquitoes. Today, scrap tire disposal has become a serious issue, and research works have been devoted to the use of steel fibres recovered from waste tires in concrete. Concrete obtained by adding recycled steel fibres has evidenced a satisfactory improvement of the fragile matrix, mostly in terms of toughness and post-cracking behaviour [6, 7]. However, very little is known about the deformation behaviour, particularly drying shrinkage and creep of concrete. This paper highlights the use of recycled steel fibre from scrap tires as reinforcement of normal concrete and discusses strength and deformation characteristics of concrete with this steel fibre.

2 Materials and Test Methods

2.1 Concrete Materials

In this study ordinary Portland cement (ASTM Type I) was used throughout the experimental work. The coarse aggregate used was crushed granite with a maximum size of 20 mm. Natural river sand with fineness modules of 2.5 was used as fine aggregate. Both coarse and fine aggregates were batched in a saturated surface dry condition. Supplied tap water was used throughout the study in mixing, curing and other purposes. RHEOBUILD 1100, a commercial polynaphthalene sulfonate type superplasticiser was utilized as high range water reducing agent in the concrete. The dosage of superplasticiser was kept constant for all concrete mixes in order to eliminate any probable effect of this parameter on the properties of hardened concrete.

2.2 Preparation of Steel Fibre from Recycled Tire

Steel fibres used in this research were recovered by a shredding process of waste tires. The steel was successively separated from rubber by a pyrolysis process. The steel fibres, shown in Fig. 1, are characterized by different diameters and length. The diameter of each fibre was recorded by a micrometer and determined averaging three measures, namely at the two extremities of the fibre and at the midpoint. The average fibre length was 30 mm with an average tensile strength of 1,030 MPa.



Fig. 1 Recycled steel fibre before and after shredding

2.3 Preparation of Concrete Mix

Various concrete mixes were made where steel fibres were used at different volume fractions of 1.0, 1.5 and 2.0 %. The mix proportions of recycled steel fibre reinforced concrete (SFRC) are shown in Table 1. It is to note that except for fibre contents, all the ingredients of concrete were kept constant in all mixes. The mixing procedure was divided into three stages. In the first stage cement, fine and coarse aggregates were weighed and mixed by hand until all the constituents are mixed uniformly. In the second stage, the recycled steel fibres were added slowly and uniformly to eliminate the clumping of steel fibres. In the final stage, measured water and superplasticiser were added and mixed thoroughly until a homogeneous mix is obtained.

2.4 Testing of Concrete Specimens

The production and testing of concrete samples were carried out in the Structure and Materials laboratory of the Faculty of Civil Engineering, Universiti Teknologi Malaysia. In order to investigate the compressive strength of concrete, uniaxial compression test was carried out on 100 mm cube specimen following BS 1881-116 [8]. The splitting tensile test was, however, performed on the standard

Table 1 Mix proportion of recycled steel fibre reinforced concrete

Mixture code	Fibre content (%)	Cement (kg/m ³)	Water (kg/m ³)	Coarse aggregate (kg/m ³)	Fine aggregate (kg/m ³)	Fibre (kg/m ³)	SP (kg/m ³)
Control	–	562	225	925	670	–	5.62
SFRC-1	1	562	225	925	670	25	5.62
SFRC-2	1.5	562	225	925	670	37.5	5.62
SFRC-3	2	562	225	925	670	50	5.62



Fig. 2 Sample preparation for creep and shrinkage

test cylinders measuring 100×200 mm conforming BS 1881-117 [9]. The flexural strength test was conducted using $100 \times 100 \times 500$ mm beams under third point loading following the BS 1881-118 [10]. The modulus of elasticity, and drying shrinkage and creep were tested on 100×200 mm cylindrical specimens following ASTM C469 [11] and ASTM C512 [12] standards respectively. The sample preparation for creep and shrinkage and the test arrangement for creep test are shown in Figs. 2 and 3. As recorded, the average temperature and the relative humidity in the test laboratory are 27 ± 2 °C and 85 ± 5 % respectively.

3 Test Results and Discussion

3.1 Compressive Strength

The 28-day compressive strength values of concrete specimens having various amount of fibre are presented in Table 2. Among the three volume fractions, concrete with fibre volume fraction of 1.5 % showed the highest strength gain. It can be seen that on average, compressive strength of SFRC are about 2–6 % higher than that of control mixture. A close observation has been made by Modtrifi et al. [13] who reported that an addition of 0.7 % recycled steel fibres in concrete resulted in an increase of approximately 12 % in compressive strength. This is to note that the failure mode exhibited a considerable change from fragile to ductile state. Due to bridging effect of the fibre, the cubic specimens did not crush suddenly but held their integrity up to the end of the test. Figure 4 illustrates the typical failure mode of plain concrete and recycled steel fibre reinforced concrete.

Fig. 3 Creep test rigs showing concrete samples



Table 2 Mechanical properties of different concrete mixes

Mixture code	Fibre content (%)	Compressive strength (MPa)	Tensile strength (MPa)	Flexural strength (MPa)	Modulus of elasticity (GPa)
Control	–	55.85	3.80	4.60	22.35
SFRC-1	1.0	58.20	7.10	5.75	24.10
SFRC-2	1.5	59.00	8.15	6.15	26.50
SFRC-3	2.0	58.70	9.45	6.95	26.70

3.2 Splitting Tensile Strength

Along with compressive strength, the splitting tensile strength values of concrete are shown in Table 2. Apparently, the tensile strength of SFRS was found to increase with the increasing amount of fibre. The test results presented in the table indicate that splitting tensile strength of SFRCs is about 70–149 % higher than that of the control mix. Indeed, recycled steel fibres significantly improved the

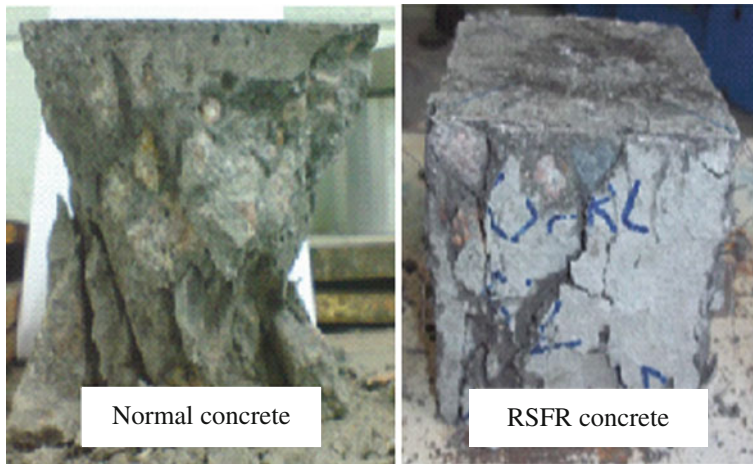


Fig. 4 Typical failure pattern of normal and recycled steel fibre reinforced concrete cube

splitting tensile strength of concrete as compared to compressive strength. The observations made in this study are consistent with the results obtained in previous studies [13–15].

The recycled steel fibre did not only affect the splitting tensile strength but also appeared to control the cracking of SFRC and alter the post cracking behaviour. The recycled steel fibres seemed to provide a load redistribution mechanism after initial cracking. Unlike in normal concrete, it was difficult to separate the fractured specimens easily, because the recycled steel fibres were bridging the gap that kept the two concrete parts together, as shown in Fig. 5a. Figure 5b illustrates the distribution of fibres at the cracked section of a broken cylinder. It can be seen that the distribution of fibres in SFRC specimens is quite homogeneous. Some recycled steel fibres were broken and a number of effective fibres can be observed on the surface of the split specimens.



Fig. 5 **a** Concrete cylinder after splitting tensile test. **b** Distribution of steel fibre in broken cylinder

3.3 Flexural Strength

Experimental data given in Table 2 reveals that on average flexural strength of SFRC is about 14–52 % higher than the control sample. The flexural strength of control specimen, for example, is 4.60 MPa. For the volume fractions of 1, 1.5 and 2 % the flexural strength values were 5.75, 6.15 and 6.95 MPa respectively.

Evidently, the flexural strength of concrete has significantly been improved by incorporating recycled steel fibres; higher the volume fraction, higher was the strength gain.

3.4 Modulus of Elasticity

The value of modulus of elasticity was calculated as slope of the axial stress-strain curve at 40 % of the ultimate strength using extensometers on 100×200 mm cylindrical specimens. Data presented in Table 2 reveals that the elastic modulus of concrete increased with the increase in fibre content.

The 28-day modulus of elasticity of the control specimen, for instance, was 22.35 GPa while higher values of 24.10, 26.50 and 26.70 GPa were recorded for concrete with 1, 1.5 and 2 % fibre content respectively. This is to be expected as, in general, modulus of elasticity is largely influenced by the strength value for a particular concrete mix.

3.5 Shrinkage and Creep

Tests on shrinkage and creep of concrete were conducted on samples prepared from concrete mixes with 1.5 % recycled steel. The values of drying shrinkage, measured over a period of 100 days, are plotted in Fig. 6. The test data clearly reveals that the shrinkage values of both the concrete specimens i.e. concrete with or without steel fibre did not show any difference throughout the period of study. Figure 7 illustrates the creep strain measured over the same period. It can be seen that the inclusion of steel fibre reduced the creep strain in concrete. Experimental data on the time dependent deformation properties of concrete containing recycled steel fibre are scarce as to compare the findings of the research work. The test results obtained by Chern and Young [16], however, indicate that the optimum volume content of steel fibres to reduce shrinkage of concrete is less than 2 % and that shrinkage was comparably less for concrete containing fibres with a large aspect ratio.

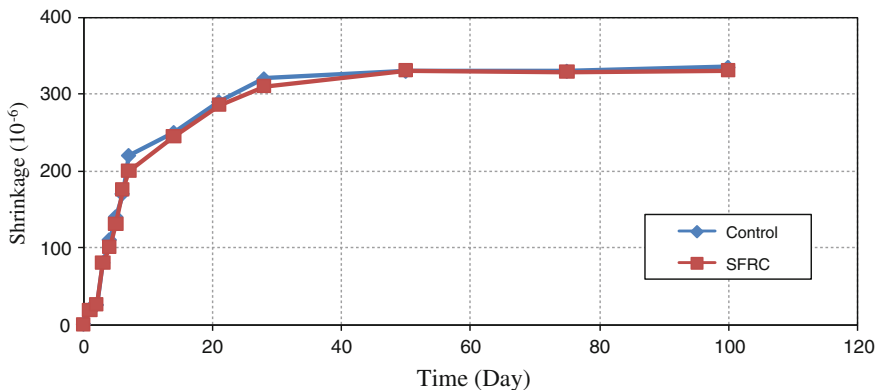


Fig. 6 Drying shrinkage of concrete

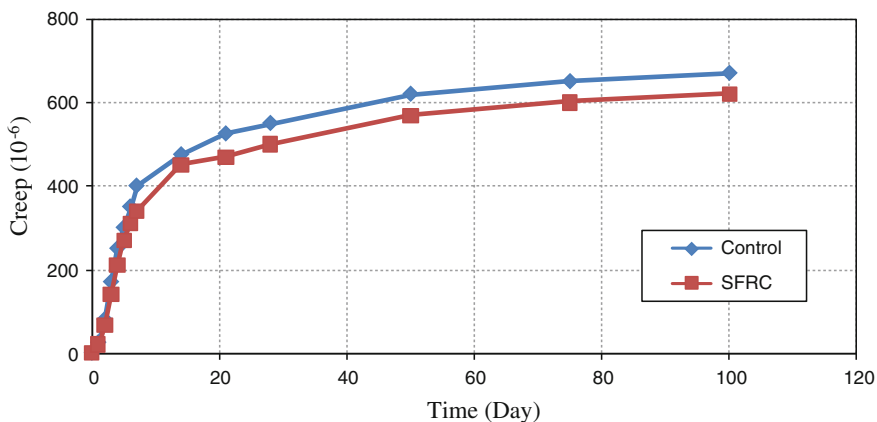


Fig. 7 Creep in control and SFRC concrete

4 Conclusion

The results obtained and the observation made in this study draw some conclusions. These are:

- Recycled steel fibre has been found to improve the overall strength performance of concrete. This improvement has been shown to be prominent in case of tensile and flexural strength as compared to that of compressive strength.
- The modulus of elasticity of concrete was increased with the increase in the corresponding strength value.
- The addition of recycled steel fibre did not influence the shrinkage value of concrete. No significant change had been shown to occur in concrete with or

without recycled steel fibres. Unlike shrinkage strain, creep of concrete with recycled steel fibres was lower than in concrete without any reinforcement.

- The overall findings in this study suggest that the steel fibre from recycled tyre has a good potential as a reinforcing material. Long-term investigation including durability aspects, however, has been put forward as recommendation for future study to obtain better understanding of this material in concrete.

References

1. C.D. Johnston, Fibre-reinforced cement and concrete, in *Advances in Concrete Technology*, 2nd edn, ed. by V.M. Malhotra (CANMET Natural Resources Canada, 1994), pp. 603–674
2. S. Mindess, J.F. Young, D. Darwin, *Concrete* (Pearson Education, New Jersey, 1996)
3. A.M. Neville, J.J. Brooks, *Concrete Technology*, ELBS edn. (Longman Group UK Ltd., London, 1994)
4. D.J. Colin, Steel fibre-reinforced concrete-present and future in engineering construction. *Composites* **13**, 113–121 (1982)
5. M.A. Jalil, Sustainable development in Malaysia: a case study on household waste management. *J. Sustain. Dev.* **3**(3), 91–102 (2010)
6. H. Tlemat, K. Pilakoutas, K. Neocleous, Design issues for concrete reinforced with steel fibre recovered from waste tyres. *J. Mater. Civ. Eng.* **18**, 677–685 (2006)
7. T.R. Naik, S.S. Singh, Utilization of discarded tires as construction materials for transportation facilities. Report No. CBU-1991-02, UMW Centre for by-products utilization, University of Wisconsin-Milwaukee, 1991, p. 16
8. BS1881-116, *Testing Concrete: Method for Determination of Compressive Strength of Concrete Cubes* (British Standards Institution, London, 1983)
9. BS 1881-117, *Testing Concrete: Method for Determination of Tensile Splitting Strength* (British Standards Institution, London, 1983)
10. BS 1881-118, *Testing Concrete: Method for Determination of Flexural Strength* (British Standards Institution, London, 1983)
11. ASTM C469, *Test for Static Modulus of Elasticity and Poisson's Ratio of Concrete in Compression*. Annual Book of ASTM Standards (American Society for Testing and Materials, West Conshohocken, 1994)
12. ASTM C512/C512M, *Standard Test Method for Creep of Concrete*. Annual Book of ASTM Standards (American Society for Testing and Materials, West Conshohocken, 2010)
13. N. Modtrifi, I.S. Ibrahim, A.B. Rahman, Mechanical properties of concrete containing recycled steel fibres, in *Proceedings of the Third International Conference of EACEF (European Asian Civil Engineering Forum)* (Universitas Atma Jaya, Yogyakarta, Indonesia, B-135-B140, 2011)
14. A.S.M.A. Awal, D. Mazlan, M.L. Mansur, Utilisation of soft drink can as reinforcement in concrete, in *Proceedings of the Third International Conference of EACEF (European Asian Civil Engineering Forum)* (Universitas Atma Jaya, Yogyakarta, Indonesia, B15-B20, 2011)
15. C.G. Papakonstantinou, M.J. Tobolski, Use of waste tyre steel beads in Portland cement concrete. *Cem. Concr. Res.* **36**, 1686–1691 (2006)
16. J.C. Chern, C.H. Young, Compressive creep and shrinkage of steel fibre reinforced concrete. *Int. J. Cem. Compos. Lightweight Concr.* **11**(4), 205–214 (1989)

Part II
Construction Project Management

Using PLS-SEM Path Modeling to Determine Factors Influencing Performance of Malaysian Construction Firms in International Markets

**Che Maznah Mat Isa, Hamidah Mohd Saman,
Siti Rashidah Mohd Nasir, Christopher Nigel Preece
and Nur Izzati Ab. Rani**

Abstract International market expansion into foreign markets has become increasingly important for construction firms. In this borderless world, no market is safe from foreign competition. This situation is also evident for the construction firms, as international construction is not a new phenomenon. Hence, firms have to be prepared and adopt effective strategies to face various challenges in unfamiliar environments and most importantly be able to sustain and perform in new business ventures. The main aim of this research is to determine the factors influencing the performance of the Malaysian construction firms in international markets. Questionnaire surveys were sent to 115 construction companies registered with CIDB Malaysia. A structural equation modeling (SEM) using partial least square (SMART PLS 2.0) was used to determine significant factors influencing performance of the firms. The confirmatory factor analysis carried out through SEM-PLS analysis has revealed that firm factors have significantly influenced the firm's performance. The findings based on loadings generated by the PLS-SEM model revealed the eleven significant factors influencing the firm's performance are the firm's ability to assess market signals and opportunities, long-term and strong management strategic orientation and objectives, superior management and organizational dynamic capabilities, firm's financing capacity and competencies, strong

C.M.M. Isa (✉) · H.M. Saman · S.R.M. Nasir
Faculty of Civil Engineering, UiTM, Shah Alam, Selangor, Malaysia
e-mail: chema982@salam.uitm.edu.my

H.M. Saman
e-mail: hamid929@salam.uitm.edu.my

C.N. Preece · N.I.Ab. Rani
UTM RAZAK School of Engineering and Advanced Technology,
UTM, Kuala Lumpur, Malaysia
e-mail: chrispreece@ic.utm.my

N.I.Ab. Rani
e-mail: nizzati237@live.utm.my

resources related to level of knowledge and Research and Development, profit targets, level of knowledge and international experience, product differentiation (strong brand name), reputation, good track record and competitive advantage. The five significant performance factors are based on the acquirements of competitive advantages, return of investment, prestige, stability, business expansion and security of the firm.

Keywords Factors · Performance · Malaysian construction firms · PLS-SEM path modeling

1 Introduction

International market expansion into foreign markets has become increasingly important for construction related firms [1–3]. Despite the worldwide trend towards globalization and increased research efforts on this field, relatively few Malaysian construction firms have been consistently successful in international markets. There are obviously risks and challenges which contribute to the lack of performance of the Malaysian construction firms. Thus, the ability to sustain and perform internationally may be determined by different sets of factors from within and outside of the firm's environment [4].

The reviews of relevant literature suggest that a model or theory related to performance in international markets for construction firms is still lacking [5]. Therefore, this study aims to investigate the factors influencing the performance of Malaysian construction firms in international projects.

2 Literature Review

2.1 Research Context

This paper constitutes part of a larger research which examined construction firms and the factors influencing the firms' performance in international markets.

Performance can be measured using indicators such as return on investment (ROI), financial gain or loss, longevity, overall client satisfaction, achievement on strategic objectives and multidimensional measures, including financial and operational [6]. However, the current literature largely concentrates on manufacturing sectors, while theories have not been investigated empirically in construction industry, except few studies on factors affecting construction with the exception of few studies on factors affecting firms' performance in international markets [7, 8]. An earlier study has revealed and ranked the important factors related to the Malaysian contractors' performance in the international market namely;

technological, firm size, firm reputation, project management expertise, specialist expertise, strong equipment support and international experience [7]. Hence, these factors have been identified to ensure favorable results or performance for construction industry. While, another study focused on the Malaysian firms' motives to pursue international joint ventures, mainly to expedite profit generation and market penetration together with the factors which affect their performance for developed countries [9]. Since construction projects are highly sensitive to external risks, the effect of location in which the firm operates also significantly influenced the firm performance. Hence, the selection of the host country location is one of the most crucial decisions due to the financial and resource constraints and also the multitude of potential risks arising from poor market selection [10] and the host government attitude [11]. Thus, the firms must be aware of the political stability of the host country, tax policies and employment laws, which would include environmental and industrial safety regulations and acts accordingly, to safeguard their interest.

International market expansion must be based on good understanding of the external factors such as the opportunities and threats, industry or market conditions due to currency fluctuation, currency exchange, restrictions, cultural differences and problems related to the host country rules and regulations, as well as the internal factors based on the firm's preparedness to venture abroad [12]. Another factor is the growth of construction operations in the international market which are due to the lowering of trade barriers, the movements of funds and the setting up of new operations globally. This has created a platform for interested construction companies to penetrate the international construction market [13].

Firm capabilities related technologies, reputation and management are other distinct factors to compete in the international market [14]. In addition, the firms' international experience with good track record are the competitive advantages acquired by the firms [12] including project management capability, top management support, project managers coordinating and leadership skills, monitoring and feedback by the clients, decision making, coordination among project participants, owner's competence, social condition, economic condition and climatic condition state [15]. Working in the international setting often requires a much wider view of the project's context than domestic projects where the project expertise is often disconnected from other aspects of the business and international projects manifest more types of risk than domestic projects [7]. At the same time, many projects report poor performance due to many evidential project causes such as unavailability of materials, poor coordination among participants, ineffective monitoring and feedback and lack of project leadership skills [15]. In summary, the literature reviews revealed four major constructs influencing the performance of firms in the international market which are the country, market, firm and project factors as shown in Table 1.

Table 1 Constructs for factors and performance

Construct	Factors
COUN01	Attitude and intervention of host government
COUN02	Similarity of host country/market (social/cultural/religious)
COUN03	Proximity to host country
COUN04	Anticipated noneconomic risk (political risk, technological)
COUN05	Anticipated economic risk (currency fluctuation, interest rate)
COUN06	Other foreign competitors in the host country
COUN07	Promotion of export efforts of home government
COUN08	Financial support from home country banks
COUN09	Trade relationship between two countries
COUN10	Diplomatic relationship between two countries
COUNT11	Host government control: licensing, restrictions and FDI rqmts
MARK1	Market profit potential/attractiveness
MARK2	Market intensity of competition
MARK3	Product/service market growth
MARK3	Market entry barriers
MARK4	Availability of innovative and entrepreneurial opportunities
MARK4	Construction demand: finance, labor, material, transport etc.
FIRM01	Firm size
FIRM02	Firm ability to assess market signals and opportunities
FIRM03	Firm level of international experience
FIRM04	Long-term and strong management strategic orientation/objectives
FIRM05	Superior management and organizational dynamic capabilities
FIRM06	Firm financing capacity
FIRM07	Firm competencies: project management, specialist expertise and technology
FIRM08	Firm resources (level of knowledge and R&D)
FIRM09	Firm management risk attitude
FIRM10	Management quality (product, service, human resource)
FIRM11	Firm performance: profit targets (return on investment/sales/assets)
FIRM12	Firm performance: level of knowledge and international experience
FIRM13	Uncertainty avoidance
FIRM14	Int. I business network: relationship with foreign partners
FIRM15	Product differentiation: strong brand name
FIRM16	Firm reputation
FIRM17	Firm good track record/competitive advantage
PROJ01	Project size
PROJ02	Project types (e.g., building, manufacturing)
PROJ03	Technical complexity of projects
PROJ04	Type of clients (public vs. private)
PROJ05	Availability of funds for projects
PROJ06	Contract types/procurement methods

(continued)

Table 1 (continued)

Construct	Factors
PROJ07	Experience of firm in similar works
PROJ08	Existence of strict time limitations
PROJ09	Existence of strict quality requirements
PROJ10	Availability of partner/alliance
PERF01	Competitive advantages
PERF02	Return of investment (ROI) and assets
PERF03	Prestige
PERF04	Stability
PERF05	Business expansion
PERF06	Utilization of resources
PERF07	Security

2.2 Research Model

The literature on factors related to firm, market country and project influencing the performance of firms in the international market also lends support to the formulation of the research conceptual framework for examining the relationship between the dependent and independent variables as shown in Fig. 1. The PLS-SEM was used in this study to answer the objective that focuses on the prediction and explaining the variance of key target construct (performance) by different

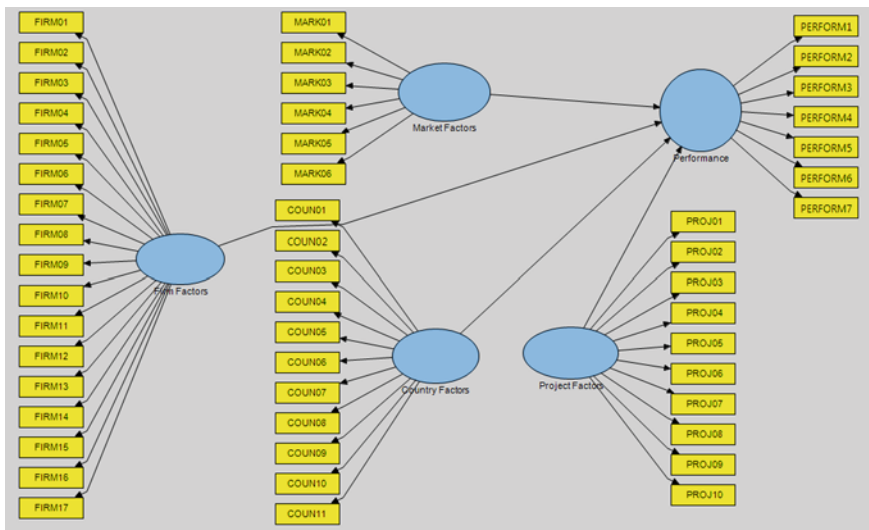


Fig. 1 Research model using PLS path modeling for factors influencing performance of Malaysian construction firms in international market

explanatory constructs (firm, market, country and project factors) and also due to the relatively small sample size. Moreover, the formatively measured construct (performance) is particularly useful for explanatory constructs (factors).

From the reviews, hypotheses were formed in this study to examine the relationship between the factors and the performance of the construction firms in international market operation as follows:

Hypothesis 1 (H1) There is a significant relationship between country factors and firm performance.

Hypothesis 2 (H2) There is a significant relationship between the firm factors and firm performance.

Hypothesis 3 (H3) There is a significant relationship between the market factors and firm performance.

Hypothesis 4 (H4) There is a significant relationship between the project factors and firm performance.

3 Methodology

This section explains the methodology related to the measurements for the constructs based on the target population and respondents, design of survey, methods of analysis adopted together with the analysis and discussions of the findings.

3.1 Target Respondents

Based on the general rule, the minimum number of respondents or sample size is five-to-one ratio of the number of independent variables to be tested. However, Hair et al. [16] proposed that the acceptable ratio is ten-to-one. Nonprobability purposive sampling was used in this study. Since the total population of construction firms working internationally is unknown, a sampling frame consists of the firms listed under CIDB of Malaysia directory for 2012/13 comprised of 115 firms registered under the Grade 7 and Class A categories was used. The sampling units were the directors, managers and executives in these firms. Their involvements in international projects and experience in different countries and in various sectors such as building, infrastructure, branches of engineering, mechanical, electrical and power transmission.

3.2 Data Collection and Respondents' Profile

The findings in this research are presented based only on two parts of the questionnaire. The first part enquires on the respondents' name, designation, firms' international experience and the business locations (s). Part two enquires the respondents' opinion on the level of significant of the factors influencing the firms' performance based on 5-point Likert scale.

3.3 Measures and Assessment of Goodness of Measures

A questionnaire using a five-point Likert scale was used to gather data for each construct of the research model. The respondents were requested to evaluate forty four (44) factors related to performance based on the level of influence (1: No significant influence; 2: Less Influence; 3: Influence; 4: Significant Influence; and 5: Very significant influence). The questionnaires were adapted from previous literatures and were modified to suit the objectives of this study [17]. The two main criteria used for testing goodness of measures are validity and reliability. Reliability is a test of how consistently a measuring instrument measures whatever concept it is measuring, whereas validity is a test of how well an instrument that is developed measures the particular concept it is intended to measure [18].

4 Analysis and Results

4.1 Response Rate and Respondents' Profile

One hundred and fifteen self-administered questionnaires were used for gathering data from the respondents. A multiple method of data collection was employed, whereby some questionnaires were mailed to the respondents, some were e-mailed and some were personally administered. Fifty one (N = 51) firms have responded resulting in a response rate of 44 %. The response rate is considered high. Most surveys carried out in Malaysia on average only achieve between 10 and 20 % response rates [18]. In addition, the ratio of ten to 1 of the respondents is fulfilled for this study [19].

The respondents' designations are those of general/senior/project managers (N = 11), senior/project/design engineers (N = 7), project/architecture coordinators (N = 2), quantity surveyors (N = 3), vice presidents (N = 2), general/HR managers (N = 3), managing/technical directors (N = 5), project planner (N = 1) and quality/contract/financial managers (N = 11). The respondents' international experience show that approximately 50 % have more than 10 years, 15 % between 5 and 10 year and the rest (37 %) have less than 5 years of experience. For the firms'

business locations, it was found that 29 % have penetrated the ASEAN countries (Singapore, Indonesia, Thailand, Vietnam, Myanmar, Brunei, Philippines, Cambodia) with the majority of the firms (71 %) venturing to the non-ASEAN countries. Hence, the profile findings indicate that the respondents have the required international construction background to participate and give reliable opinions in the survey. In order to determine the most significant factors influencing the firm's performance in international market, a structural equation modeling using SMART PLS-SEM was adopted in this study. The purpose of each analysis, the results and discussion are outlined in the next sections.

4.2 Construct Validity

Construct validity testifies to how well the results obtained from the use of the measure fit the theories around which the test is designed [18]. In order to determine that the instrument adopts the concept as theorized, an assessment through convergent and discriminant validity was carried out. First, the respective loadings and cross loadings were examined if there are problems with any particular items. A cut-off value for loadings at 0.5 as significant [16] was used in which, if any items has a loading of higher than 0.5 on two or more factors, they are deemed to have significant cross loadings. It was observed that all the items measuring a particular construct loaded highly on that construct thus confirming construct validity.

4.3 Convergent Validity

Next, the convergent validity was tested, to ensure the degree to which multiple items to measure the same concept are in agreement. As suggested by [16] the factor loadings, composite reliability and average variance extracted were the indicators to assess convergence validity. Table 2 (third column) depicts loadings for all items exceeded the recommended value of 0.5 [16]. While, the composite reliability (CR—refer to fourth column) values which depict the degree to which the construct indicators indicate the latent construct ranged from 0.889 to 0.950, which exceed the recommended value of 0.5 [16]. The average variance extracted (AVE) measures the variance captured by the indicators relative to measurement error, and it should be greater than 0.50 to justify using a construct [20]. The results show that average variance extracted, were in the range of 0.525 and 0.607. Table 2 summarizes the results of the measurement model. In addition, the last column shows the results from the t-values which indicate all factors (country, firm, market and project) are valid measures with their respective constructs based on their parameter estimates and statistical significance [21]. The t-values were extracted from the structural model developed in this study (refer to Fig. 3).

Table 2 Results of measurement model

Model construct	Measurement item	Loadings	CR ^a	AVE ^b	t-values
Country factors	COUN02	0.733	0.918	0.583	9.439
	COUN04	0.759			8.679
	COUN05	0.784			8.245
	COUN06	0.723			8.044
	COUN08	0.731			8.342
	COUN09	0.794			7.779
	COUN10	0.771			8.698
	COUN11	0.810			9.536
Firm factors	FIRM02	0.702	0.941	0.594	10.360
	FIRM04	0.705			7.660
	FIRM05	0.870			16.334
	FIRM06	0.832			13.886
	FIRM07	0.736			5.862
	FIRM08	0.807			9.792
	FIRM11	0.704			7.436
	FIRM14	0.734			7.658
	FIRM15	0.769			13.474
	FIRM16	0.850			12.573
	FIRM17	0.747			9.108
Market factors	MARK01	0.802	0.911	0.719	8.289
	MARK02	0.918			11.662
	MARK03	0.863			11.375
	MARK04	0.805			9.103
Project factors	PROJ02	0.745	0.938	0.627	8.144
	PROJ03	0.769			12.694
	PROJ04	0.777			11.956
	PROJ05	0.791			13.113
	PROJ06	0.846			16.605
	PROJ07	0.815			9.737
	PROJ08	0.867			20.215
	PROJ09	0.786			11.230
	PROJ10	0.719			7.811

^a Composite reliability (CR) = (square of the summation of the factor loadings)/{(square of the summation of the factor loadings) + (square of the summation of the error variances)}

^b Average variance extracted (AVE) = (summation of the square of the factor loadings)/{(summation of the square of the factor loadings) + (summation of the error variances)}

t-values > 2.58 ($p < 0.01$)

Table 3 Discriminant validity of constructs

Factors	Country	Firm	Market	Project
Country	0.764			
Firm	0.599	0.771		
Market	0.579	0.413	0.848	
Project	0.753	0.760	0.453	0.819

Diagonals (in bold) represent the square root of the AVE (variance extracted) while the off-diagonals represent the correlations

4.4 Discriminant Validity

The discriminant validity of constructs is the extent to which the measures do not reflect other variables and it is indicated by low correlations between the measures of interest and of other constructs [21, 22]. Items should load more strongly on their own constructs in the model, and the average variance shared between each construct and its measures should be greater than the variance shared between the construct and other constructs.

As shown in Table 3, the correlations for each construct are less than the squared average variance extracted by the indicators measuring that construct indicating adequate discriminant validity. Thus, the measurement model demonstrates adequate convergent and discriminant validity.

4.5 Reliability Analysis

The Cronbach’s alpha coefficients to assess the inter item consistency in the measurement items were also measured. Table 4 summarizes the loadings and

Table 4 Results of loadings and alpha values

Model construct	Measurement item	Cronbach alpha	Loading range	^a No. of items
Country factors	COUN02, COUN04, COUN05, COUN06, COUN08, COUN09, COUN10, COUN11	0.898	0.723–0.810	8(11)
Firm factors	FIRM02, FIRM04, FIRM05, FIRM06, FIRM07, FIRM08, FIRM11, FIRM14, FIRM15, FIRM16, FIRM17	0.931	0.702–0.870	11(17)
Market factors	MARK01, MARK02, MARK03, MARK04	0.871	0.802–0.918	4(6)
Project factors	PROJ02, PROJ03, PROJ04, PROJ05, PROJ06, PROJ07, PROJ08, PROJ09, PROJ10	0.925	0.719–0.867	9(10)
				32(44)

^a Final items numbers (initial numbers)

shows that all alpha values are above 0.6 as suggested by Nunnally and Berstein [23]. The CR values ranged from 0.911 to 0.941 and interpreted like a Cronbach’s alpha for internal consistency reliability estimate where a CR of 0.70 or greater is considered acceptable [23]. Hence, the measurements are reliable.

4.6 Hypotheses Testing

In order test the four hypotheses generated earlier, path analysis was used. The extracted results are shown in Fig. 2 and Table 5 results. Figure 2 shows the structural model with results of the path analysis for factors affecting performance with loadings and β values. The structural model indicates the causal relationships among the constructs (factors) in the model, which includes the estimates of the path coefficients and the R^2 value, which determine the power of the model. Table 5 indicates the presents the results of the hypotheses testing. Hypotheses H1, H2, H3 and H4 examine the relationships between each factor and the firm’s performance. A non-parametrical test to determine the coefficient R^2 was applied to evaluate the structural model’s quality, where a logical metric for judging the inner model is the endogenous variables’ determination coefficient (R^2). It reflects the level or share of the latent constructs’ explained variance. Therefore, it measures the regression function’s “goodness-of-fit” (GoF) against the empirically obtained manifest items.

The R^2 can assume values between 0 and 1. The larger the value, the larger the percentage of variance explained. Figure 2 shows an R^2 value of 0.468 which suggests that 46.8 % of the variance in extent of performance can be explained by

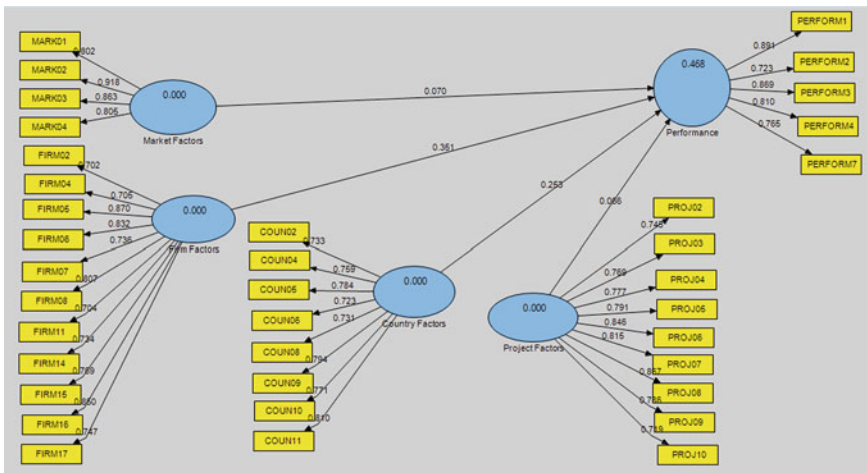


Fig. 2 The structural model with results of the path analysis for factors affecting performance with loadings and β values

Table 5 Path coefficients and hypothesis testing

Hypothesis	Relationship	β coefficient	SE	t-values	Supported
H1	Country factor \rightarrow performance	0.253	0.285	0.890	No
H2	Firm factor \rightarrow performance	0.351	0.179	1.958	Yes
H3	Market factor \rightarrow performance	0.070	0.232	0.302	No
H4	Project factor \rightarrow performance	0.066	0.267	0.246	No

t-values > 1.671 ($p < 0.05$)

the country, firm, market and project factors. The R^2 values of 0.02, 0.13 and 0.26 indicate the endogenous latent variables' weak, moderate or substantial influence on the particular latent exogenous variable. Hence, the model indicates that the endogenous latent variables (factors) have substantially influenced the latent exogenous variable (performance). In addition, GoF was also used to judge the overall fit of the PLS model. On the basis of the results, the GoF value (calculated) of 0.374 (R^2 was 0.468) for the research model was obtained, which exceeds the cut-off value of 0.26 for large R^2 . Hence, it has confirmed the adequate support to validate the PLS model globally [24, 25]. Figure 3 shows the structural model with results of the path analysis with t-values between constructs.

Results show that only one out of four constructs namely the firm factor demonstrates a significant relationship with the firm's performance. Hence, the firm factors ($\beta = 0.351, p < 0.05$) was positively related to performance of the firms explaining 46.8 % of the variance, thus supporting H1 in this study. Hence, the following discussion focuses only on the eleven significant firm factors influencing the five significant performance indicators generated by PLS path analysis.

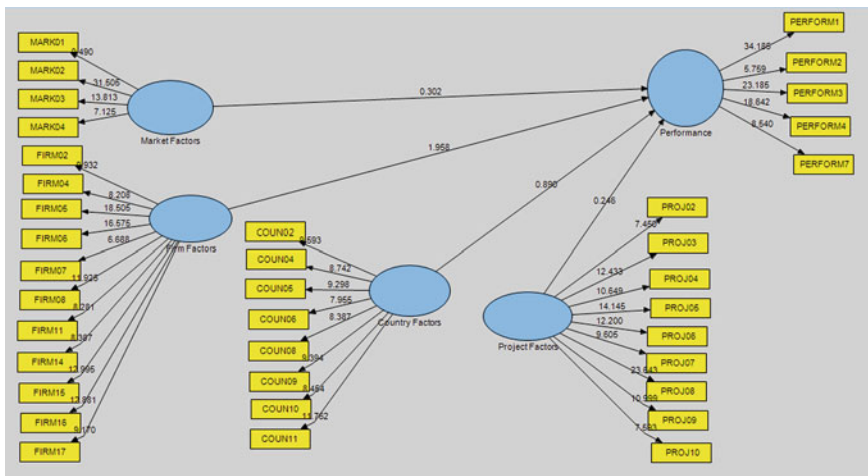


Fig. 3 The structural model with results of the path analysis with t-values between constructs

5 Discussions

The empirical results show that the ability of firms to assess market signal and opportunities have motivated them to be successful in their international operations. It was argued that the firms' perceptions about the level of competition have affected their performance based on the uncertainty of the market environment and lack of information related to the opportunities [20]. However, the findings indicate that the performance was influenced by the long term and strong management strategic orientation and objectives. Despite the high initial financial and operating risks, the firms' with strong management having set mission and vision have bravely entered the unfamiliar markets by absorbing risks and costs associated with product/service and market development [21]. The next findings reveal that sufficient financial capacity have significantly influenced the firm's performance in the foreign market place. The findings are in line with few studies where the Vietnamese contractors were found to be lagging behind their competitors due to their weak financial capacity [4] and shortage of working capital experienced by the Chinese contractors [22]. Since international projects are valuable in price with complex undertaking, the construction firms must acquire a strong financial capacity to secure the material resources and be able to overcome the increased cost of labor, material, equipment which is critical to project delivery and the firm's performance. Thus, the Malaysian firms seemed to be aware of the requirement of having a comprehensive and strong financial package before participating in international market [22, 26]. The next significant factor influencing the firm's performance is having strong competencies in project management with specialist expertise and technology. Hence, to successfully perform in the international market or to be distinct from other foreign competitors, Malaysian firms must acquire comprehensive and specific technical and management expertise and capabilities [13]. Expertise in terms of technology also enhances their capability when handling international projects. Another similar study found that the Chinese contractors' preferred to adopt more sophisticated technology and methodology that were easier to be transferred into international markets [22]. These competencies are required by the firms to endure the increasing threats and uncertainties in the rapid changing international market environment [12, 23, 27]. It would seem to be recommended that the Malaysian firms offer their strengths in distinguished products and services, thus complementing the host country contractors those were behind in design and technical capability, project management skills and financial capacity. In return, the operation costs were lowered and at the same time they adapted comfortably with the host country cultures and industry practices [27].

The next prominent factors contributing to the firms' performance are having strong resource related to their level of knowledge with research and development (R&D) capability. It is noticeable that construction firms may establish or learn about the technological innovation for overseas activities. The limited use of ICT by Chinese contractors restrains them from achieving better performance in international market [24, 25]. Hence, by applying advanced ICT, Malaysian firms can

either integrate with local partners in order to increase their technological capability to achieve better performance. However, for continual improvement it would seem to be necessary for the Malaysian construction firms to keep up with the emerging technology and participate in technology R&D.

The profit target based on the return on investment, sales and assets was another key factor in which the expansion of the Malaysian firms' to overseas locations offers profitable opportunities [12]. Similarly, another study also revealed that 'long term profitability' was the firms' reasons to operate and be successful internationally [28] which may be due to the fact that firms need higher profitability to counterbalance the greater risks and efforts in setting up their international operations. Hence, the decision to enter a new foreign market is of critical importance for the company's profit making ability and sustainable growth [29]. The findings indicate that level of international experience have significantly influenced their performance in the international market which is line with a study stating that as firms accumulate international experience, they develop a capability and perform in the foreign markets. However, it seem that Malaysian firms need sufficient time to gain more international experience which may lead to their lack of performance as they require more preparation to overcome constraints and risks in international construction. Thus, the findings indicate that acquired experience is very important to solve similar problems that might be encountered in their future projects. As the level of experience in similar jobs gets higher, then the ability to take the job increases, its competitive position gets stronger and the performance is improved [8]. Finally, the findings show that the firms that have ventured abroad have good track records by successfully completing overseas projects. Through involvement in these projects, they have gained useful experience, knowledge, skills, technology and expertise. Hence, the performance of past successes creates recognition, high reputation and provides motivational factors for the firms to be successful in their ventures [12].

6 Conclusions

This research has revealed that the firm factors have significantly influenced the performance of the Malaysian construction firms in international markets. Firms with superior management and dynamic capabilities have moved forward to achieve their long term and strategic objectives by targeting profits based on high return of investment, sales and assets. In order to achieve the firm's strategic objective it has been found that they must have strong resources in terms of financial, technical competencies, technology, knowledge and experience. This would seem to have resulted in the firm's reputation and recognition with strong brand name in the international construction markets. It is hoped that the results can assist the construction firms in their pursuit of global market ventures.

Acknowledgments We would like to thank the Faculty of Civil Engineering, UiTM, for giving support and to the Research Management Institute, UiTM, Malaysia and Ministry of Science, Technology and Innovation (MOSTI) for providing the financial support (E-science fund: 100-RMI/SF 16/6/2 (33/2012)). We are also grateful to the professionals and managers from Malaysian construction firms, CIDB Malaysia and other institutions for their participation in this research.

References

1. Y. Lan, *The Expansion of Chinese Construction Companies in the Global Market* (2011)
2. A.A. Usman, A. Abdul-Aziz, International markets: Malaysian construction contractors and the stage theory. *Aust. J. Constr. Econ. Build.* **2**(1), 94–106 (2001)
3. A. Abdul-Aziz, D.P. Ngau, Y.M. Lim, A.R. Nuruddin, Internationalization of Malaysian quantity surveying firms: exploring the best fit models. *Const. Manage. Econ.* **29**(1), 49–58 (2011)
4. F. Yean, Y. Ling, V. Min, C. Pham, T.P. Hoang, Strengths, weaknesses, opportunities, and threats for AEC firms: case study of Vietnam. *J. Constr. Eng. Manage.* **135**, 1105–1113 (2009)
5. A. Abdul-Aziz, S. Wong, A. Awil, Formulating a holistic model to describe international diversification of construction companies. In: *Conference on Building Abroad: Procurement of Construction and Reconstruction Projects in the International Context*, vol. 9, no. 1. University of Montreal, Montreal, Canada, pp. 27–36, 23–25 Oct 2008
6. B. Ozorhon, D. Arditi, M. Asce, I. Dikmen, M.T. Birgonul, Performance of international joint ventures in construction. *J. Civ. Eng. Manag.* **26**(4), 209–222 (2010)
7. Z.U. Ahmed, O. Mohamad, B. Tan, J.P. Johnson, International risk perceptions and mode of entry: a case study of Malaysian multinational firms. *J. Bus. Res.* **55**(10), 805–813 (2002)
8. B. Ozorhon, I. Dikmen, M.T. Birgonul, Using analytic network process to predict the performance. *J. Manage. Eng.* **23**(3), 156–163 (2007)
9. A. Idris, L.S. Tey, Exploring the motives and determinants of innovation performance of Malaysian offshore international joint ventures. *Manage. Decis.* **49**(10), 1623–1641 (2011)
10. C.K.I. Ibrahim, M. Othman, A.M. Baki, M.K. Ghani, Location consideration in international construction market by Malaysian firms: specific locale perspective. In *CSSR* (2009)
11. N. Pangarkar, H. Lim, Performance of foreign direct investment from Singapore. *Int. Bus. Rev.* **12**, 601–624 (2003)
12. S. Gunhan, D. Arditi, Factors affecting international construction. *J. Constr. Eng. Manage.* **131**(3), 273–282 (2005)
13. A.B. Ngowi, E. Pienaar, A. Talukhaba, J. Mbachu, The globalisation of the construction industry—a review. *Build. Environ.* **40**(1), 135–141 (2005)
14. S.Z. Ahmad, P.J. Kitchen, International expansion strategies of Malaysian construction firms: entry mode choice and motives for investment. *Probl. Perspect. Manage.* **6**(3), 15–23 (2008)
15. A. Enshassi, S. Mohamed, S. Abushaban, Factors affecting the performance of construction projects in the Gaza strip. *J. Civ. Eng. Manage.* **15**(3), 269–280 (2009)
16. J.F. Hair, W.C. Black, B.J. Babin, R.E. Anderson, *Multivariate Data Analysis* (Prentice-Hall, Upper Saddle River, 2010)
17. J. Nunnally, *Psychometric Theory*, 2nd edn. (McGraw-Hill, NY, 1978)
18. T. Ramayah, O. Mohamad, Internationalisation of Malaysian contractors. *J. Int. Bus. Entrep. Dev.* **5**(1), 18–27 (2010)
19. U. Sekaran, R. Bougie, *Research Method for Business: A Skill Building Approach*, 5th edn. (Wiley, New York, 2009)
20. D. Barclay, R. Thompson, C. Higgins, The partial least squares approach to causal modeling: personal computer adoption and use as an illustration. *Technol. Stud. Spec. Issue Res. Methodol.* **2**(2), 285–324 (1995)

21. W.S. Chow, L.S. Chan, Social network and shared goals in organizational knowledge sharing. *Inf. Manage.* **45**(7), 24–30 (2008)
22. C.M.K. Cheung, M.K.O. Lee, A theoretical model of intentional social action in online social networks. *Decis. Support Syst.* **49**(1), 24–30 (2010)
23. J. Nunnally, I. Berstein, *Psychometric Theory* (McGraw-Hill, NY, 1994)
24. M. Wetzels, G. Odekerken-Schroder, C. van Oppen, Using PLS path modeling for assessing hierarchical construct models: guidelines and empirical illustration. *MIS Quarterly* **33**(1), 177–195 (2009)
25. M. Wetzels, G. Odekerken-Schroder, C. van Oppen, Using PLS path modeling for assessing hierarchical construct models: guidelines and empirical illustration. *MIS Quarterly* **136**(1), 127–135 (2010)
26. D. Compeau, C.A. Higgins, S. Huff, Social cognitive theory and individual reactions to computing technology: a longitudinal study. *MIS Q.* **23**(2), 145–158 (1999)
27. C. Fornell, D.F. Larcker, Evaluating SEM models with unobservable variables and measurement error. *J. Market Res.* **18**(1), 39–50 (1981)
28. J.-M. Becker, K. Klein, M. Wetzels, Hierarchical latent variable models in PLS-SEM: guidelines for using reflective-formative type models. *Long Range Plann.* **45**(5–6), 359–394 (2012)
29. P.M.G. Villaverde, M.J.R. Ortega, Determinants of entry timing: firm capabilities and environmental conditions. *Manage. Res.* **5**(2), 101–112 (2007)

Study on Flow Improvement of Brick Laying Operations in a Residential Construction Project

Muhamad Abduh and Aditya Pratama

Abstract Construction has been acknowledged as a production process with much inefficiency related to various generated wastes during the process. Lean construction initiative is attempting to mitigate this problem by reducing waste generating processes and, on the other hand, trying to increase the value the customer needs. There have been many successful applications of the lean construction principles in many countries that encourage the adoption of the principles in Indonesia. One of the efforts in implementing one of the lean construction principles in the Indonesia construction industry was conducted in an action research and is reported in this paper. The research was aiming to implement flow improvement approaches to reduce the waste in a three-unit residential construction project, and focusing only on brick laying operations of three different materials for three different houses: clay brick, concrete brick, and light-weight brick. Durations, sequences, and resources related to each task in each operation were collected using a video camera to calculate their performances such as productivities, idleness of resources, and cycle times during the beginning phase of the operations and then considered as existing conditions. Based on existing performances, especially related to non-productive activities, analyses and recommendations were made to improve the flow of each brick laying operation. The recommendations were then implemented to the next phase of all three operations, and resulted in reduced waste, potentially better productivity, cycle time, and labor utilization factors of those three brick laying operations.

Keywords Brick laying · Cycle time · Flow · Residential · Productivity · Waste

M. Abduh (✉) · A. Pratama
Faculty of Civil and Environmental Engineering, Institut Teknologi Bandung,
Bandung, Indonesia
e-mail: abduh@si.itb.ac.id

A. Pratama
e-mail: apratama@rocketmail.com

1 Introduction

In Indonesia, lean construction concept has been introduced since early 2000s, but it is still considered as a new paradigm among Indonesian construction practitioners as well as academia. Although some lean construction principles and techniques are already adopted and implemented by construction practitioners in their day-to-day activities, understanding of lean construction as an integrated concept is still not yet sufficient. Therefore, the efforts to spread the word of lean construction concept, principles, and techniques have been an agenda for research and education in Indonesia, such as what so called 'a roadmap towards lean construction in Indonesia' in 2005 [1]. The agenda is still relevant until now since there are not much supports given from the related parties to implement it, especially from the contractors' and government's sides, and only academia's efforts to improve the awareness of the lean construction concepts were consistently performed.

In the meantime, Indonesian contractors still face problem of inefficiencies in their business processes. The inefficiencies found in Indonesian contractor's operations were mostly in the forms of delays of schedule, repairs on finishing works, damaged materials on site, waiting for equipment repair and to arrive, and equipment frequently breaks down. Identified factors causing such wastes were lots of design changes, lack of trades' skill, slow in making decision, poor coordination among project participants, poor planning and control, delays on delivery of materials to site, and inappropriate construction methods [2].

Realizing the importance role of contractors in adopting and implementing the lean construction concept, an assessment model was developed to measure the readiness of contractors towards lean construction for validating the research agenda [3]. The six case studies to measure the readiness of Indonesian contractors towards lean construction revealed that Indonesian big contractors already implemented macro lean construction principles, such as the policy to have continuous improvement and to increase transparency. Meanwhile, on micro principles of lean construction, such as reduction of cycle time and reduction of variability, the Indonesian big contractors still lack of awareness and ability to implement the principles and techniques. It is also found from the case studies that contractors lack of the capability to plan good work flow of their construction operations [4].

Moreover, based on the findings, an agenda was proposed to improve the readiness of Indonesian big contractors toward lean construction, especially to improve the capability of Indonesian big contractors to plan good workflow of their construction processes [5]. Three topics of the agenda are planning production processes, making the processes flow, and analysis and evaluation of the processes. The developed agenda was intended for Indonesia big-size contractors to reap the benefit of lean construction principles and techniques. Yet the agenda would not be successfully implemented only by the contractors. The agenda needs more participations and contributions from academia and also the Indonesian government to accelerate and to support the efforts made by the contractors.

Challenged by the aforementioned agenda and also encouraged by many successful applications of the lean construction principles in many countries [6], an action research was conducted to implement flow improvement approaches in reducing the waste in a residential construction project by the Faculty of Civil and Environmental Engineering, ITB, in collaboration with the Research Institute for Human Settlement (RIHS). The action research was enabled to design the construction operations on the pilot project, monitor, evaluate, suggest the improvement and implement it. The research as well as the recommendations gathered from it is reported in this paper.

2 Research Objective and Methods

2.1 Research Problem and Design

A three-unit of modest residential construction project was selected for the research and specially designed to study productivity related issues by the RIHS. Fortunately, the project could also be used as a research project to implement one of the important techniques in the lean construction concept, that are flow improvement to reduce the waste of the construction operation through flow of resources and information [7–9], for the project.

The research limited the scope to focus only on the brick laying operations of three different materials for three simple six-by-six square meters houses: clay brick (B1), concrete brick (B2), and light-weight brick (B3). All three houses themselves had simple and similar architectural design as depicted in Fig. 1. All three houses are located side-by side and surrounded by other existed residential houses as depicted in Fig. 2.

Considering the location of the project was not easy to access in term of transporting material to the site, the materials were stored in the open space near the house 3 where the workshop was also located. Physical flows of materials, equipment and labors were the concern to the success of the project. Moreover, the flow of the brick laying operation on each house was another concern to the study;

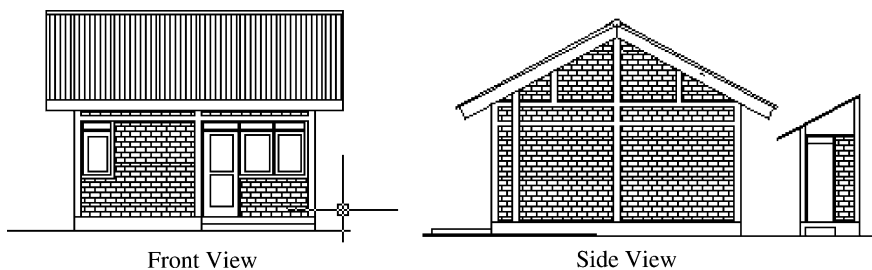
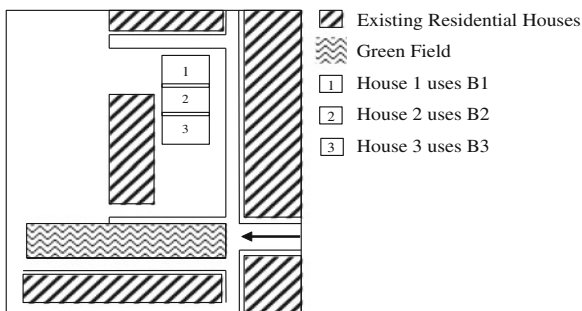


Fig. 1 Front and side views of the six-by-six square meters house

Fig. 2 The pilot project site



to the extent whether the different type of materials would differ the performance of the brick laying operation assuming the labors had the same average skills and was supervised by the same foreman. Brick laying operation was chosen since the operation was considered a common operation in Indonesian residential construction and therefore abundant number of labors would be available have the same average skill. B1 and B2 materials are very common for Indonesian houses, yet B1 has smaller dimension compared to B2. On the other hand, the dimension of B2 and B3 almost the same, yet B3 is lighter than B2.

2.2 Objective of Research

The research itself was aiming to implement flow improvement approaches to reduce the identified waste of brick laying operation in the three houses. The research will demonstrate the effectiveness of the use of one of important techniques introduced in the lean construction concept, that is flow improvement, as means to reduce the waste of construction operation. Three different materials used in three different houses were meant to check the effect of material technology as well as workmanship associated with it to the flow improvement.

2.3 Research Methods

The brick laying operation was firstly designed to determine the production unit, operation’s cycle, processes and tasks related to the operation, and also resources to support the operation. Since the materials investigated were different in size and weight, it was expected that the difference between three materials was only on duration of the operation’s cycle.

As far as an action research’s concern, the research team was also involved in the project like the owner (RIHS) and the contractor. However, the involvement of the research team was limited to the data acquisition, evaluation, recommendation,

Table 1 Project's participants involvement

Activity	Involvement		
	Owner	Contractor	Research team
Design of operation	Approve	Conduct	
Resources procurement		Conduct	
Data acquisition I		Assist	Conduct
Evaluation and recommendation	Approve		Conduct
Improvements	Order	Conduct	Assist
Data acquisition II		Assist	Conduct
Evaluation and report	Receive		Conduct

implementation of the improvement, and re-evaluation after the improvement as can be seen in Table 1. The contractor was entitled to conduct the initial design of the operation based on its experiences and standard practices to meet the given technical specification of the brick laying operation in the contract. Moreover, the contractor should procure the resources needed, assist the research team in data acquisition, and conduct the improvements. While the owner was taking important role in approving the initial design of the operation and the improvement, and ordering the contractor to accommodate the recommendation of improvements.

The research team set up video recording system for data acquisition. Durations, sequences, problems, resources related to each process and task of the brick laying operation of each house were collected in 10 days for the first data acquisition using 3 video cameras. Only 2 h recording during morning and afternoon sessions were collected, since the two-hour window of optimal productivity for both sessions was assumed to be applicable in this case: 09.00–11.00 in the morning and 13.30–15.30 in the afternoon. Number of labors conducting each brick laying operation was the same.

Then, the research team analyzed the gathered data to determine the operations' performances, such as productivities, idleness of resources, and cycle times during the beginning phase of the operations and then considered as existing conditions. Based on existing performances, especially related to non-productive activities, analyses and recommendations were made to improve the flow of each brick laying operation. The recommendations were then implemented by the contractor, and the research team conducted the second data acquisition in 2-day operation. The follow-up evaluation was done afterward for measuring the effectiveness of the flow improvement in reducing the waste that was found in the existing conditions.

3 Existing Brick Laying Operations' Performances

Based on the recorded video, the existing three brick laying operations that were designed by the contractor can be generalized and they consisted of three categories of processes. They are productive processes: mixing mortar, and laying the bricks; supporting processes: preparation, mortar transportation, measuring, instruction,

and finishing; and non-productive process: idleness and personal time. The performance of the existing three brick laying operations will be discussed based on the proportion of productive and non-productive processes, average productivity, and average cycle time.

3.1 Productive, Supporting, and Non-productive Processes

The following table will show the comparison between performances of brick laying operation using B1, B2, and B3 materials in terms of proportion productive, supporting, and non-productive processes.

It can be seen from Table 2 that labors working for B1 and B3 brick laying operations used mostly of their time to do productive processes as much as to do non-productive processes. Meanwhile, the labors of B2 brick laying operation used most of their time for doing non-productive processes. But in general, it can be concluded that the non-productive processes are commonly found in all operations and consumed about 40 % of the cycle time. Those performances were considered as common in Indonesian construction industry.

From the information related to the supporting processes, it can be concluded that bigger dimension of brick, and of course also heavier the brick, would need more time to do supporting processes.

3.2 Average Productivity and Cycle Time

The average productivity and cycle time of each brick laying operation is depicted in Table 3.

Due to difference dimension and weight of brick, the productivity and cycle time of each brick laying process was affected. B1 is small in dimension and consumes 60 units of bricks to fill up 1 square meter of wall. B2 is larger and heavier than B1 and consumes 12 units of bricks to fill up 1 square meter of wall. On the other hand, B3 is even larger but lighter than B2 and consumes 8 units of bricks to fill up 1 square meter of wall. It can be concluded here that the B3 brick laying operation is the most productive, and the B1 brick laying operation is the worst due to their dimensions.

Table 2 Proportion of productive, supporting and non-productive processes (existing)

Process category	Existing brick laying operation		
	B1 (%)	B2 (%)	B3 (%)
Productive	40	29	37
Supporting	19	30	25
Non-productive	41	41	38
Total	100	100	100

Table 3 Average productivity and cycle time (existing)

Indicator	Existing brick laying operation		
	<i>B1</i>	<i>B2</i>	<i>B3</i>
Average productivity (unit/h)	48	15.6	16.2
Units needed per m ² (unit)	60	12	8
Average productivity (m²/h)	0.80	1.30	2.03
Average cycle time (min)	0.59	1.68	1.32

Based on the average cycle time, it can be concluded that the lighter brick will need less time to finish its cycle. B3 material is then very superior in terms of dimensions and weight and could improve the productivity of its laying operation.

4 Recommended Flow Improvements

The performances of the existing three brick laying operations suggested that the potential area of improvement was on the supporting and the non-productive processes. The non-productive processes of all brick laying operations consumed the same amount of time of the operation which mean averagely similar problem faced by the individual and the team during the operation.

Further analysis on the supporting and non-productive processes for each brick laying operation was showing the needed improvements as depicted in Tables 4 and 5. There were four areas that were worthy to be improved from the tables: preparation and measurement process, transportation process, more strict supervision to reduce the ‘not-active’ process, and flow of material. The two first processes to be improved

Table 4 Proportion of supporting processes

Process	Existing brick laying operation		
	<i>B1</i> (%)	<i>B2</i> (%)	<i>B3</i> (%)
Preparation and measurement	59	64	51
Transportation	39	28	18
Instruction	1	4	20
Finishing	1	4	11

Table 5 Proportion of non-productive processes

Process	Existing brick laying operation		
	<i>B1</i> (%)	<i>B2</i> (%)	<i>B3</i> (%)
Not active	89	85	88
Wait for materials	6	12	3
Personal time	5	3	9

Table 6 Labor utilization factor

Indicator	Existing brick laying operation		
	B1 (%)	B2 (%)	B3 (%)
Labor utilization factor (existing)	64.4	32.6	60.6
Labor utilization factor (potential)	90.1	59.1	81.5

related to the supporting process, and therefore could increase the cycle time of the operations. Meanwhile the two last ones were related to the non-productive process and the improvement on it will improve the flow of three brick laying operations.

Using the process, cycle and crew balance charts, the potential improvements in term of labor utilization factor (LUF), as defined in (1), can be determined and compared to the existing LUF, as depicted in Table 6.

$$LUF = \frac{(productive\ Time) + (Supporting\ Time \times 0.5)}{Total\ Observation\ Time} \times 100\% \quad (1)$$

Based on Table 6 and the results of process, cycle and crew balance charts (not provided in this paper), the most potential improvement can be done in B1 and B3 brick laying operation was by stricter supervision and more precise and reliable information of the operation method to the labors.

Based on those analyses, some of improvements were identified:

1. To improve the flow of the operation by reducing the time spent by the labors for being not active during the operation due to unacceptable reasons. This can be done by stricter supervision by the foreman and the owner.
2. To make the flow of material more streamlined, by providing a temporary location of the bricks that was closer to the location of the operations. By doing so, the effort would improve the transportation time and also in the same time would reduce the time needed to wait refilled materials.
3. To improve the operation method by providing more clear explanation on the sequences, techniques and specification of the three brick laying operations to the labors. More clear instruction was needed for B3 since this material required more strict specification and more skill compared to the others. In order to do this, then the work-structuring should be done first, and then clearer instructions should be delivered to the foreman and the labors.

The following table summarizes the flow improvements that are resources and information, for all three brick laying operations. Those were then recommended to the owner to be implemented in the field by the contractor. The owner approved it and the contractor conducted the recommendation for improvements.

Table 7 Recommended flow improvements

Flow improvement	Existing brick laying operation		
	<i>B1</i>	<i>B2</i>	<i>B3</i>
Resources	Material temporary location	Material temporary location	Stricter supervision
	Stricter supervision		
Information	Work structuring	Work structuring	Clearer instruction
	Clearer instruction	Clearer instruction	

5 Improved Brick Laying Operations' Performances

As recommended in Table 7, the contractor tried to accommodate all of the flow improvements. However, as the project progressed and more operations conducted simultaneously, the available space for locating temporary storage for bricks materials was rare. This implicated that the improvement of providing temporary location for material storage could not be implemented as recommended by the contractor. The performances provided in the following sections are limited to that condition and only based on data collected in two-day operation.

Moreover, since the evaluation and analysis of the existing operation took more than 3 days to finish, to get approval, and to be implemented, the improved brick laying operations that were investigated already approached almost-finished state. Therefore, the improved brick laying operations were conducted on the higher level than the existing brick laying operations. Due to this situation, comparing the average productivity and cycle time between the improved and existing operations was not relevant. The higher the location of the operation, the less the productivity of the operation would be.

5.1 Productive, Supporting, and Non-productive Processes

In terms of proportion between productive, supporting, and non-productive processes, the performances of the improved brick laying operations were better than the existing ones. As depicted in Table 8, the improvements for all brick materials are significant. From the Table 9, it can be concluded that all three brick laying operations gained the impact of the flow improvements. However, the most impacted operations would be the B1 and B3 brick laying operations. The waste for all operations was reduced as much as 25 % by introducing flow improvement in resources and information.

Table 8 Proportion of productive, supporting and non-productive processes (improved)

Process category	Improved brick laying operation		
	<i>B1</i> (%)	<i>B2</i> (%)	<i>B3</i> (%)
Productive	77	45	65
Supporting	10	41	21
Non-productive	13	14	14
Total	100	100	100

Table 9 Improvement of proportion of productive, supporting and non-productive processes

Process category	Improved brick laying operation		
	<i>B1</i> (%)	<i>B2</i> (%)	<i>B3</i> (%)
Productive	+37	+16	+28
Supporting	-9	+11	-4
Non-productive	-28	-27	-24

5.2 Productivity, Cycle Time, and LUF

As stated before, the comparisons of productivity and cycle time are not relevant here. However, for accountability, the following table shows the average productivity and cycle time of the improved brick laying operations. Moreover, other indicator, that is LUF, is combined in the following table.

Based on Table 10, the productivities of all the improved brick laying operations decreased, and their cycle time increased. This was caused by the higher location of the improved operations compared to the existing ones. The higher the location, more efforts, tools, equipment for vertical transportation of the materials are needed. Moreover, the bricklayer would be more careful in doing the operation in higher place especially working in a high platform or scaffolding.

Table 10 Average productivity, cycle time, and LUF (improved)

Indicator	Improved brick laying operation		
	<i>B1</i>	<i>B2</i>	<i>B3</i>
Average productivity (unit/h)	32.4	9	13.8
Units needed per m ² (unit)	60	12	8
Average productivity (m²/h)	0.54	0.75	1.73
Average cycle time (min)	0.71	2.93	1.67
Labor utilization factor	81.6 %	65.6 %	56.7 %

In addition to that, potential increments of LUFs were not as high as expected. B1 brick laying operation achieved 17.2 % increment, B2 brick laying operation achieved 33 % increment, and the B3 brick laying operation merely decreased (3.9 %). This situation could be easily explained as the B2 increased the supporting process proportion significantly compared to its productive process. For B1, the high increment proportion of productive processes was reduced by the decrement of supporting processes. Meanwhile, B3 experience almost the same situation as B1, except that its decrement of supporting processes and increment of productive processes were modest.

A special attention needs to be given to the B3 brick laying operation. Even though, the impact of the flow improvement was considered modest compared to the B1 and B2, its productivity and cycle time were not severely decreased compare to the others. Since the beginning to the improvement state, the productivity, cycle time, and also the LUF of this B3 operation have been stable. The research team expected that this is due to more robust method and system provided by the B3 material, that is lightweight brick. This will implicate to the easiness of performing the operation by the skilled and experienced labors. Even though in nature the productivity of higher location operation would decrease, the flow improvement made to the B3 operation could also maintain the productivity and cycle time, not only reducing the waste. This finding would become a positive marketable feature of the lightweight bricks.

6 Conclusions

This paper demonstrates the benefit of flow improvement, especially resources and information flows, to be implemented in brick laying operations to reduce the waste identified in the existing operations. The flow improvements introduced in this paper are work structuring, stricter inspection, better layout of material storage, and clearer instruction to the workers. The benefit of the flow improvements would also affect the productivity, cycle time and LUF of the operation.

The results of the research would be very useful for the Indonesian construction industry as it will be the proof of the usefulness of the lean construction techniques. The research team is very keen and looking forward to seeing more action researches conducted to encourage the Indonesian construction practitioners in adopting the lean construction paradigm to their day-to-day construction operations.

Acknowledgments The authors thank to the Research Institute for Human Settlement (RIHS) of the Indonesian Ministry of Public Works for inviting the authors to join the research related to the construction productivity and providing the pilot project for fulfilling the research objective.

References

1. M. Abduh, S. Syachrani, H.A. Roza, Research agenda of lean construction (in Indonesian). In *Proceedings of the 25th Anniversary of Construction Engineering and Management Education in Indonesia*, School of Civil and Environmental Engineering, Institut Teknologi Bandung, Indonesia, Aug 2005
2. S. Alwi, K. Hampson, S. Mohamed, Non value-adding activities: a comparative study of Indonesian and Australian construction projects. In *Proceedings of the 10th annual conference of the IGLC*, Gramado, Brazil (2002)
3. H.A Roza, Development of assessment model to measure readiness of Indonesian contractors towards lean construction (in Indonesian). Master's Thesis, School of Civil and Environmental Engineering, Institut Teknologi Bandung, Indonesia (2006)
4. M. Abduh, H.A Roza, Indonesian contractors' readiness towards lean construction. In *Proceedings of the 14th Annual Conference of International Group for Lean Construction*, Santiago, Chile, 2006
5. M. Abduh, H.A. Roza, Toward lean construction: an agenda for Indonesian contractors. In *Proceedings of the 10th East Asia-Pacific Conference on Structural Engineering and Construction (EASEC 10)*, Bangkok, Thailand, 3–5 Aug 2006
6. M.M.S. Bernardes, C.T. Formoso, Contributions to the evaluation of production planning and control systems in companies. In *Proceedings of the 10th Annual Conference of the IGLC*, Gramado, Brazil (2002)
7. A. Serpell, A. Venturi, J. Contreras, Characterization of waste in building construction projects. In *Proceedings of the 3rd Workshop on Lean Construction*, Albuquerque (1995)
8. A. dos Santos, Application of flow principles in the production management of construction sites. Ph.D. Dissertation, School of Construction and Property Management, the University of Salford, UK (1999)
9. L. Koskela, An Exploration Towards a Production Theory and Its Application to Construction. (VVT Technical Research Center of Finland, Finland, 2000)

The Implication of the Standard Method of Measurement (SMMs) for Building Works Toward Contractors' Works

Construction Contract Management

Anis Rosniza Nizam Akbar, Mohammad Fadhil Mohammad,
Noor Amalia Talib and Mysarah Maisham

Abstract Standard Method of Measurement (SMM) is a reference document used to determine a localized technique of construction measurement protocol needed in producing a good Bills of Quantities (BQ) which is then incorporated into the contract document for the project. The preparation of the BQ based on SMM that is reflective of the actual work will actually help the contractor to price the tender realistically. Tendering is a serious business, whereby failure to properly price it at a realistic and profitable level can give a bad impact to the contractor's organization. Thus, it is crucial to conduct research which aimed to investigate the two edition of the SMM for building works between the SMM1 and SMM2 version in the preparation of the BQs, focusing towards improving the appreciation of the contractors during the course of tender and construction. In view of the above matter, this paper will attempt to identify a few differences on the method of measurement between SMM1 and SMM2 and to analyze the contractors' perception on the application of the SMM in determining the tender realistically and reflective of the work on site. Triangular data collection approach was used in order to obtain a

Research Acculturation Grant Scheme (RAGS) by the Universiti Teknologi MARA (UiTM).

A.R.N. Akbar (✉) · M.F. Mohammad · N.A. Talib · M. Maisham
Construction Economics and Procurement Research Group,
Centre of Studies for Quantity Surveying, University Teknologi MARA (UiTM),
40450 Shah Alam, Selangor, Malaysia
e-mail: anis.rosniza@gmail.com

M.F. Mohammad
e-mail: fadhilnavy@yahoo.com

M. Maisham
e-mail: mysarah_maisham@yahoo.com

variety of information on the same issues. It comprises a literature review followed by document analysis, a questionnaire survey which was then supported by semi-structured interviews. However, due to the limitation of the space, this paper will only focus on one major element which is the excavation work. There are three differences identified between the SMM1 and SMM2, which are; unit of measurement, method of measurement and additional new items/elements. There were also a few items the contractor prefers to be measured according to the SMM1. Thus, an improvement is needed in order fill in the gap identified between the two SMMs.

Keywords Bill of quantities • Contract document • Contractor • SMM

1 Introduction

The construction industry is flooded with the involvement of many key players in developing and improving the industry. Quantity Surveyors (QS) is one of the key players who are needed before the initiation or inception stage start. Generally QS offer its clients a wide range of professional services from contractual matters to costs estimation, evaluation and control. Preparing a Bill of Quantities (BQ) is one of the core services provided by the QS for the purpose of project cost control and management [1, 2]. BQ is a document containing a detailed list of works and the quantities required for a building or other civil engineering project used during pre and post contract stages [3–5]. Through the BQ, the needs and requirements of the clients will be transformed from drawings, schedule and specification produced by the architects and Engineers into a tender document which are fully described and accurately represented, the quantity and quality of the works [1, 6–11].

In order to produce an appropriate BQ which is properly measured, determined and quantified [12], a Standard Method of Measurements (SMMs) protocol has been developed and used [13]. The Standard Method of Measurement for building works (SMM2) which is the revision from the first edition is the current standardized references used in Malaysia for the measurement of the building works which will eventually turned into a BQ that form part of the procurement or contract document. In order to clarify the readers on the relationship between the SMM and the BQ, Fig. 1 illustrates the significance and importance of SMM on the roles and activities of key players who are involved in both traditional procurement and non-traditional procurement systems. It clearly shows that in both procurement systems, the SMMs are used by the QS to standardize the method of preparing the measurement for building and civil engineering works to be incorporated in the contract document. During the tender stage, the contractors will be using the BQ as a medium in submitting a reliable and competitive tender in their bid for the project.

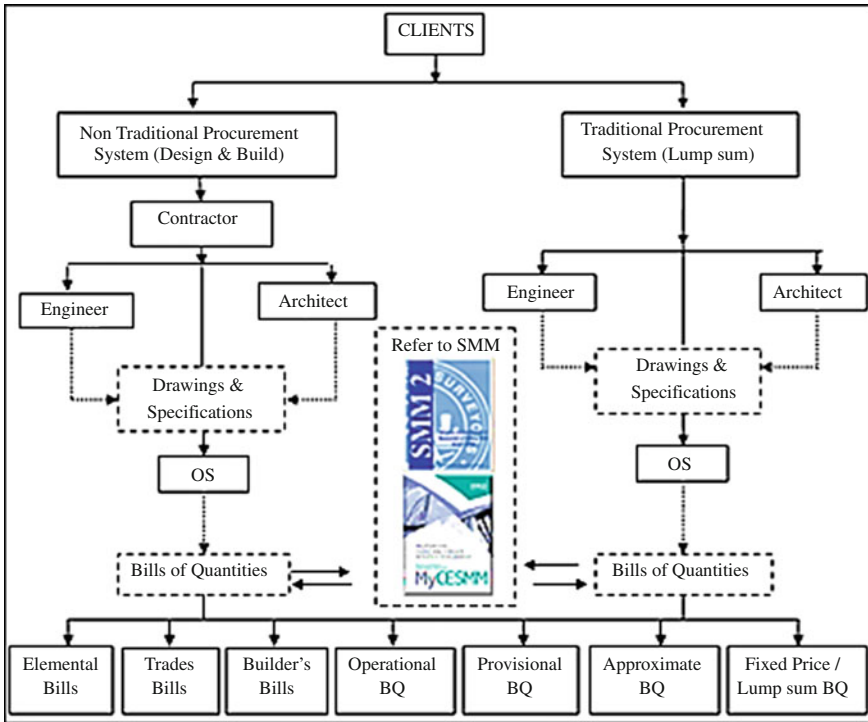


Fig. 1 The significance and importance of the SMM on the key players both in the traditional and non-traditional procurement systems

Although the SMM2 is the current standardized reference used in Malaysia for the purpose of measurement for building works, there are still a handful of firms who do not use this measurement protocol as a whole. This statement supported by a study done by [14], listed current industry issues which are currently surrounding the application of current Malaysian Standard Method of Measurement (SMM) as a single standard system of measurement. During the measurement process, a Quantity Surveyor should ensure that the work measured are to be arranged in a sequence that can be easily understood by all parties and easily priced by the Contractor. This process is very dependent on which method of measurement to be used, because the SMM1 and SMM2 will produce a different form of protocols and coverage of the Bills of Quantities. Then the questions also arise as to what extent are the SMM being used to assist the contractor to bid and complete his work during the pre-contract and post contract stages? Furthermore, between the SMM1 and SMM2, which methods will better facilitate a contractor? Moreover what are the pros and cons both of these SMMs have that could be the underlying principles in the preparation of the Bills of Quantities? Circuitously, this inquiry will give an

answer as to how the correct application of the SMM could allow a BQ to be very functional to a contractor. Comparative studies are important in realizing the shift in the consumption of the SMM1 and SMM2. In this regard, a comparison will be made for these items as building elements and trades in SMM1 and SMM2. The conclusions thereof will be made to answer the research objectives which include to investigate the differences on method of measurement between the SMM1 and SMM2 and to analyze the contractors' perception on the application of the standard method of measurement in appreciating the tender realistically and reflective of the work on site. Besides that, the outcome of this paper is expected to be used as a supporting and fundamental data to be carried along to the next level of the main research which aims to develop a more accepted and practical Standard Method of Measurement for construction works in Malaysia.

2 Literature Review

(A) *Justification for the Changes in SMM1 and SMM2*

After the application of the SMM1 for such a long period of time in the industry, a plan for its improvements was being discussed and later on agreed by players in the industry. This is necessary as the result of the changes in the industry's needs and in line with the technical advancement and development. Various techniques and materials of construction have changed throughout the decades and, therefore, changes to the SMM1 is inevitable.

In May 2000, the SMM2 were published by the Association of Surveyors, Malaysia, which was later known as the Institution of Surveyors, Malaysia. Unfortunately, most of the potential users either the contractors or quantity surveyors do not adopt it as a whole. Throughout the study of the SMM2 formation from 1984 to 2000, there were three groups of committee members responsible for getting the work completed. Key reference at that time was made to the SMM6, which was previously used in the U.K. In the early stages of the research, SMM6 was the most recent at that time, while SMM7 is still on the draft plan stage. Hence, reference was made only to the SMM6 and it was modified and adapted to meet the needs of local practitioners and industry players.

However, the period from completing the preliminary research up to the publishing of the SMM2 has taken quite a long time. In the midst of it, the SMM7 was published in the UK. Many users voiced out why SMM7 was not being used instead since it is more recent, and its tabulated form is more convenient as a guide to would be users. Many argued that the structure of the SMM2 original draft that is based on the SMM6 should also be changed to a tabulated form. However, this will require more time to complete which the industry just do not have. The decision was finally made to refer only to the format and content of the SMM6 with the necessary modifications to meet the local practice and requirement.

(B) *Contractors perception on the application of SMM for building works*

One of the main responsibilities of the QS is to prepare the BQ and the contract document while the contractors are responsible for completing a project with a realistic and profitable cost, time and quality. Although the contractors do not have a choice as well as the responsibility to use the SMM in creating a BQ, the understanding and applicability of this document is necessary to enable them to appreciate this document. The contractors need to understand the description as well as familiar with the quantities provided by a QS through the taking off process using the SMM in order to have a realistic and profitable project [15]. A good take—offs will attempt to expose everything necessary in preparing the estimated contract sum [16]. There are three basic rules for taking off quantities [16]: measure everything as it shows, take off everything that can be seen and if it is different, keep it separate. In order to organize the protocol of the taking off work, they need to refer to the standard method of measurement. Thus, the need of the SMM as a guideline in preparing the taking off of works in the preparation of the BQ.

The SMM is the key reference document that will guide the QS in the preparation of producing a BQ. The provisions of goods and services presented in a BQ are based on an accurate measurement and a good description. Good description is based on a good and detailed SMM. The SMM is considered to be good when it is able to produce a description that can be easily understood [17], easily priced [4] and represents the work carried out on site [1, 4]. It is, therefore, important to produce a good SMM that can describe the contractor's work well and clearly.

Unfortunately, when the item description provided in the BQ was based on an individual method of measurement without the use of a set of standard and established rules, the quantity of measurement can vary widely [4, 18–20]. This will contribute to the non-uniformity of the bills of quantities [18]. There could also be a description that may not represent the work to be carried out on site [4, 11, 19]. To make matter worst, certain items that have been measured cannot be priced realistically due to its unclear description in relation to the actual scope of work. This can contribute to wrong interpretation and can lead to non-accurate bidding price. As a result, it will end up being disqualified or becoming a non-competitive tender. A BQ is a part of the contract document and will become the basis for disbursing interim payments to the contractor. Due to this reason, the process of restructuring the BQ becomes very important and cannot be neglected.

Cooperation from both the QS and the contractor in using the SMM2 is very important especially to agree on the use of the document as a measurement reference. If the QS uses the right references for each item and the contractor can well understand it, then it is an open shut case. However, on the other hand, the QS should have the ability to better understand the issues on labor productivity, plant and machinery performance and should also comprehend the works to be carried out on site during construction [21].

In conclusion, it can be deduced that a good QS is a person who not only well versed with the work to be carried out on site, but also the necessary plants to be used and the labour performance. When they fully understand the scope of work, they will be able to prepare a reliable and integrated BQ that reflects the work to be carried out on site. Hence, the preparation of a BQ in accordance to the work to be carried out on site is very important to ensure that contractors can appreciate each quantity realistically. The actual measurement of work should also take into account the complexity of the work to be performed. As far as the contractor is concern, the BQ should be closely related to the methodology and construction activities. All the measurement rules where possible should reflect the works to be carried out on site and must consider all the critical factors related to the final cost of the item in the BQ.

3 Research Methodology

In order to achieve the objectives of this paper, the primary data were gathered through the means of document analysis, a questionnaire survey and then supported by face to face interviews with selected respondents. The professionals targeted for both questionnaire survey and face to face interviews are QSs who are working in the contracting organization. Table 1 below show the number of respondents for both methods used. Only 32 copies of questionnaires were returned (out of 50), and a total of seven (7) interviews were conducted. Out of the 32 respondents received from the survey, only 18 were accounted for, and analysed based on their (1) academic qualification; a degree in QS, who are considered as a qualified person to be dealing with the SMM and (2) working experience; more than 5 years. Respondents for the face to face interviews are selected based on their experience and willingness to be interviewed.

4 Research Findings

(A) Document Analysis

The analysis was made on the differences in the SMM clauses and the principles of measurement in both the SMM1 and SMM2. The selected clauses examined are the major changes made on excavation items between the SMM1 and SMM2. Tables 2 and 3 presented the summary of the differences between the two SMMs.

Table 1 Number of respondents

Method used	Number of respondent
Questionnaire survey	18
Face to face interview	7

Table 2 Summary of comparison for the excavation and earthwork item in SMM1 and SMM2

SMM1		SMM2		Adjustment made
Clause	Items	Clause	Items	
iii	Excavator	D	Excavation and earthwork	
1(f)	General	D.10	Excavation	Principle of measurement—stages in the depth of excavation
	Depth of excavation work in 1.50 m stages		Depth of excavation shall be measured and be classified as the maximum depth not exceeding	
			0.25 m	
			1.00 m	
			2.00 m	
			4.00 m	
		And thereafter in 2.00 m stages		
3(a)	Surface excavation	D.12.4	Excavate to reduce level	Unit of measurement depends on the average depth
	Average depth shall be given in the description and the measurement unit:		Measurement unit—m ³	
	<300 mm—m ²			
	>300 mm—m ³			

Table 3 Summary of comparison for the excavation and earthwork item in SMM1 and SMM2

SMM1		SMM2		Adjustment made
Clause	Items	Clause	Items	
iii	Excavator	D	Excavation and earthwork	
11(a)	Disposal of excavated material	D.17–18	Disposal of excavated material	New clauses
	– To be included with the items of excavation or measured separately		– Have own clauses for excavated material	
	– Nonexistence of multiple handling items		– Multiple handling items introduced	
	Filling to excavation work and excavation work are combined under one item	D.24–25	Filling to excavations	New clauses
			– Filling to excavation work being measured separately from excavation work	
6(a)	Forming embankments and treatment surface	D.26	Filling to make up level	Unit of measurement
	Measurement unit—m ³		– The average work shall be given in the description and the measurement unit for it is	
			<250 mm—m ²	
			>250 mm—m ³	

(B) *Questionnaire survey is supported by face to face interview*

The primary objective of the questionnaire survey is to measure the level of the standard method of measurement that reflects the work to be carried out on site and to enable it to be priced realistically. The respondents were asked to rate the level of SMM that they preferred more. They were also asked to rate their level of perception on the application of SMM, which help their job during tendering and construction process. Face to face interview approach was used in order to make the analysis and findings more robust and conclusive on the choice of answers given by the respondents.

1. *Division of work that is more appropriate for construction work*

Respondents were asked on their opinion on which division of work that is more appropriate for construction. 83 % of the respondents (15 out of 18 numbers of respondents) choose trades as the most appropriate method in dividing or categorizing construction work. Only 17 % (3 respondents) believes that the division of work by elemental is more appropriate in categorizing construction work due to the nature of our construction industry practice, whereby work done by sub-contractors are normally based on trades and not by elements.

2. *Comparison between SMM1 and SMM2 on measurement rules that reflected the work carried out on site*

The level of measurement for excavation works that reflect the works to be carried out on site based on SMM1 and SMM2 were examined. There are 5 clauses that are different in the measurement rules between the SMM1 and SMM2. Figure 2 shows a comparison of the mean value on the excavation works between SMM1 and SMM2. Based on the mean value, the measurement rules using the SMM1 are considered to be more reflective to the

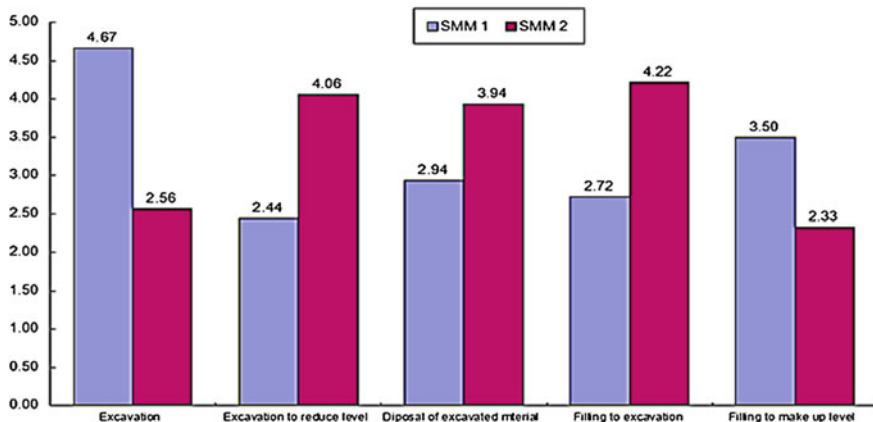


Fig. 2 Comparison of the mean value in excavation works between the SMM1 and SMM2 that actually reflects the works carried out on site

works compared to the SMM2 rules in the case of excavation and filling to make up level. From the interviews, the respondents claimed that, the rules in the SMM should reflect the method of construction to be used on site. However, it should not be too precise such as incorporating the different stages of excavation depth due to the nature of excavation work that just could not be undertaken accurately. The excavation to reduce level as indicated in the measurement rules in the SMM2 is highly reflective of the work on site where there are no stages of excavation depth being applied on site. Two other items introduced in the SMM2 which are the disposal of excavated material (3.94) and filling to make up level (4.22) gives the impression that the measurement rules in the SMM2 are more reflective of the works carried out on site. Most respondents also agreed that when it comes to important and critical elements, they should be clearly highlighted by creating their own measurement rules and clearly explained in the SMM.

3. *Comparison between SMM1 and SMM2 on the measurement of items that would enable the pricing of the works be done realistically*

Figure 3 indicated that three (3) items out of the five (5) excavation works which are measured using the SMM2 were highly acceptable in pricing of the works. They include the items on excavation to reduce level, disposal of excavated material and filling to excavation. In excavation work, it would be much easier to measure it in bulk or m³ because it actually reflects how the earthwork is being handled on site. Although most of the respondents agree with the 1.5 m depth for the different stages of excavation, some of them preferred to change it to 2.0 m stages since it is in line

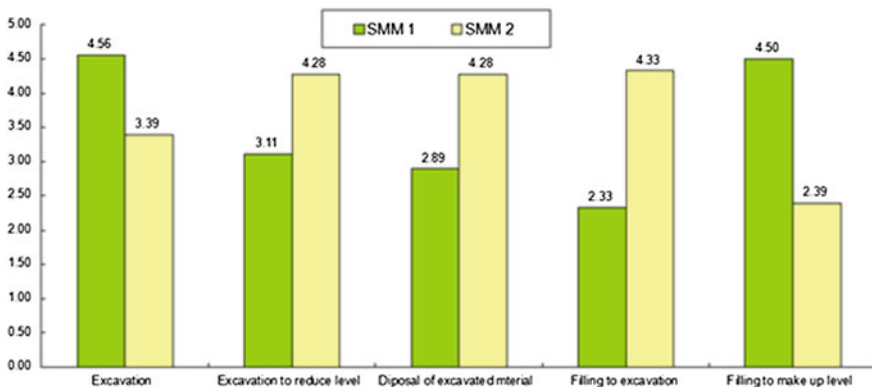


Fig. 3 Comparison between SMM1 and SMM2 on measurement items which will assist more in pricing realistically for excavation works

Table 4 Comparison between SMM1 and SMM2 on the level of assistance during the tendering stage

Description	SMM1	SMM2
Clarity of item description on the nature of works to be carried out	2.56	3.94
Easy to recognize the required items for each element of works	2.89	3.78
Easy to price the items for each element of works	4.40	3.28

Table 5 Comparison between the SMM1 and SMM2 on the level of assistance during the construction stage

Description	SMM1	SMM2
Easy in the quantification of works	4.34	3.38
Easy in the quantification of ordering materials	3.00	4.33
Easy in the quantification of the required plants and equipments	3.04	4.06
Easy in the quantification of labours and related worker and specialist	4.03	2.83
Easy in preparing claims	2.72	4.24

with the current plant and machinery capacity (bulldozer, wheel dozer and wheel loader).

4. Contractor's Perception

In this section, the contractor's perception on which SMM that could assist them more during tendering and construction process are being examined.

(a) During the Tendering Stage

From the overall findings (as show in table 4), the contractor's general perceptions on the SMM based on the comparisons made of during the tendering stage have found that the SMM2 is much more preferred to than the SMM1. However, the SMM1 is more preferable than SMM2 on the level of understanding and the ease of pricing on the items for each element of works. This is because the pricing of the BQ could become complicated when too many trades are combined together under one element. Although the SMM2 is considered to be better than SMM1 in terms of the clarity of the item description on the nature of works to be carried out (3.78) and can be easily recognized for the required items on each element of works (3.94), the value of the means is still considered to be fair. Most respondents reiterated that the SMM2 still needs to be adjusted and modified accordingly to make it clearer and structured while being more user friendly in which all parties can adopt it easily and effectively.

(b) *During the Construction Stage*

According to Table 5 below, during the construction stage, adopting the SMM1 would ease the task of performing the quantification of works as well as identifying the related labour and specialist. According to most of the respondents, the contractors usually price the tender based on the labour rates that are involved in that particular work. This is why most of the respondents in the survey agree that the arrangement by trades in the SMM1 is more appropriate for the quantification of construction works. Nonetheless, the quantification of items in relation to ordering of materials, plant and equipments and in preparing claims, using the SMM2 seems to be more convenient and practical to most respondents.

5 Conclusion and Recommendations

The study has identified some potential areas on what needs to be improved in the current SMM in order to assist the contractors during the course of tender and construction stages.

1. The amendments for the upcoming SMM should include a full review, design and introduction of more item descriptions in accordance to the work to be carried out on site to allow the contractor to price the bills of quantity more realistically. Major items for excavation and excavation to reduce level, for example should follow the measurement rules provided in the SMM1 whereby the staging in 1.50 m depth of excavation is much easier to price although it may not really reflect the work that is carried out on site.
2. Important measurement rules should be highlighted by creating their stand alone clause. This will lessen the possibility of missing those important items in the BQ. It would not assist the contractor either in the pricing, when the important items are being combined under one description.
3. When dealing with items in excavation work, it would be easier and actually reflecting the cost of the earthwork when it is being measured in bulk (m³). Although most of the respondents agree with the 1.5 m depth stages for excavation, some of them would prefer to change it to 2.0 m stages since it is in tandem with the current plant and machinery capacity (bulldozer, wheel dozer and wheel loader).
4. Finally, most of the respondents claimed that the SMM2 needed some adjustments and refinements to make it clearer and structured as well as being more users friendly whereby all parties can benefit from its use easily and effectively. It should also include providing more clarity on the item description to allow easy recognition and consideration on the critical factors required for costing of items in each element or trades of the works.

Acknowledgments The Author is appreciative of the expertise of the supervisory committee and to industry collaborators for their practical and applied evaluations. A remark of indebtedness is also owed to the Research Acculturation Grant Scheme (RAGS) by the Universiti Teknologi MARA (UiTM), for its grant award.

References

1. R. Abd Rashid, M. Mustapa, S.N. Abd Wahid, Bills of Quantities—Are They Usefull and Relevant Today? in *International Conference on Construction Industry* (2006 June), pp. 1–10
2. A.R. Abdul Aziz, N. Ali, Outsourcing and quality performance: malaysia's public works department. *Struct. Surv.* **22**(1), 53–60 (2004)
3. M. Brook, *Estimating and Tendering for Construction Work* (Butterworth Heinemann, Oxford, 1998)
4. H. Adnan, A.H. Mohd Nawawi, S.M. Mohd Akhir, A. Supardi, H. Chong, Bills of quantities: perspectives of contractor in Malaysia. *Aust. J. Basic Appl. Sci.* **5**(11), 863–873 (2011)
5. P.R. Davis, P.E.D. Love, D. Baccarini, Bills of quantities: nemesis or nirvana? *Emerald J.* **27** (2), 99–108 (2009)
6. K. Abd Rashid, In Need of Studies to Assess the Effectiveness of Bills of Quantities, in *10th Management in Construction Research (MiCRA) Conference* (2011)
7. K. Abd. Latif, Standardising and Enhancing Bills of Quantities for Civil Engineering Works using Malaysian Standard Method of Measurement using Malaysian Standard Method of Measurement (CESMM). Seminar on SMM in construction presented on 31 March 2010 (Kuala Lumpur, 2010)
8. P.R. Davis, D. Baccarini, The Use of Bills of Quantities in Construction Projects—An Australian Survey, in *Proceedings of COBRA* (2004)
9. N.S. Kamaruddin, Bill of Quantity (BQ) and Preparation of BQ (2010)
10. T.R. Myles, Bills of what?—The Origin of Bills of Quantities, Hanscomb/Means Reports (2006)
11. A. Razali, K. Abd Rashid, Applicability of Bill of Quantities in Today's Construction Industry, in *10th Management in Construction Research (MiCRA) Conference* (2011)
12. A.K. Mohd Din, An Introduction of Roles and Responsibilities of Pengurusan Aset Air Berhad in Water Industry and why WWSMM? Seminar on Standard of Measurement in Construction Procurement Presented on 2 July (2009)
13. M.F. Mohammad, Standard Method of Measurement: A Review of Its Importance and Relevance in Quantity Surveying Practice, in *International Seminar 2012: Responding to Global Challenges—The Need for Quantity Surveyor Professional Standard* (2012)
14. A.R. Nizam Akbar, M.F. Mohammad, N. Ahmad, M. Mysham, Adopting Standardization in Construction Environment: Standard Method of Measurement (SMMs), in *Procedia Social and Behavioral Sciences* (2014)
15. R. Hussin, F. Ishak, Contractors' Professionalism: Fundamental Mistakes and Ignorance During Costing and Tendering, *RISM* (Kuala Lumpur, Jan 2004), pp. 28–34
16. N. Foster, T.J. Trauner, R.R. Vespe, W.M. Chapman, *Construction Estimates From Take-Off to Bid* (McGraw-Hill, USA, 1995)
17. M. Cutts, How to make laws easier to read and understand, in *Laws for Citizens* (2008), pp. 1–10
18. M.M. Che Mat, The Need to Standardise the Bill of Quantities for Civil Engineering Works. Seminar on Standard of Measurement in Construction Procurement (Kuala Lumpur, 2010)

19. S. Hassan, "Evolving SMM", CPD talk development from board of quantity surveyors, Malaysia (BQSM) and construction industry development board Malaysia (CIDB). Presented at Taylor's University College on **15**, 2011 (2011)
20. S. Hassan, Role of SMM in Construction Industry, Seminar on SMM in Construction Procurement presented on 2 July 2009 (Kuala Lumpur, 2009)
21. A. Ashworth, K. Hogg, *Willis's Practice and Procedure for the Quantity Surveyor*, 11th ed. (Blackwell Science, UK, 2002)

The Way Forward for Industrialised Building System (IBS) in Malaysia

Muhamad Faiz Musa, Mohammad Fadhil Mohammad,
Mohd Reeza Yusof and Rohana Mahbub

Abstract Industrialised Building System (IBS) is a construction process that uses standardised building components mass produced in a factory or on site, then transported and assembled into a structure using appropriate machinery and equipment with minimal workers on site with proper planning and integration. IBS is the term used to represent the prefabrication concept in Malaysian construction industry. IBS contributes to sustainability, improves site safety, quality and productivity in the built environment. Since the move towards industrialisation in the construction industry is a global phenomenon, the definitions, classifications, characteristics and concepts of IBS needs to evolve and in line with the global understanding. The main objective of this paper is to study the way forward for IBS (adopting sustainability, degree of industrialisation and modular construction) and revisit the current definitions, classifications, characteristics and concepts in IBS based on comprehensive reviews of previous researches with an explanatory method. Better understanding on the fundamentals and future improvement of IBS will encourage construction industry players to adopt IBS and increase the awareness on IBS.

Keywords Industrialised building system (IBS) · Definitions · Classifications · Characteristics · Concepts · Sustainability · Degree of industrialisation · Modular construction

1 Introduction

The IBS agenda in Malaysia began in the early 1960s, whereby the Malaysian government initiated IBS pilot project aiming to speed up the delivery time of the project [1]. Even though the introduction of IBS in Malaysia is over 40 years ago, its

M.F. Musa (✉) · M.F. Mohammad · M.R. Yusof · R. Mahbub
Construction Economics and Procurement Research Group,
Centre of Studies for Quantity Surveying, Faculty of Architecture, Planning and Surveying,
Universiti Teknologi MARA (UiTM), 40450 Shah Alam, Selangor, Malaysia
e-mail: faeezz@yahoo.com

acceptance was not widespread, and the IBS implementation is still slow. Despite the potential of IBS, the adoption and uptake on IBS in the Malaysian construction industry are low [2]. Now days there are many industrialisations, off-site manufacturing, and prefabrication terminologies in the construction industry, but IBS had become a term to represent those terminologies in the Malaysian construction industry. The term IBS is widely used by Malaysian government; academicians and construction industry players to represent industrialisation in construction [3].

In an attempt to address the IBS agenda in Malaysia, the Malaysian government through Construction Industry Development Board (CIDB), encourages a paradigm shift in the construction industry from the traditional and conventional approach to industrialisation perspective by promoting IBS [4]. In order to promotes IBS in Malaysian construction industry, the Malaysian government and CIDB introduced plans and policies to encourage the implementation of IBS. The introduction of Construction Industry Master Plan (CIMP 2006–2015) is a guide for the future direction of Malaysian construction industry by the Malaysian government has highlighted the importance of IBS and sustainability for Malaysian construction industry [5]. In addition, IBS Roadmap introduced to steer the direction of IBS implementation and addressing issues related to IBS. IBS Roadmap 2003–2010 was the first IBS Roadmap and replaced by IBS Roadmap 2011–2015. The objectives of the new IBS Roadmap 2011–2015 are to impose high level intended outcome of implementing IBS. The objectives are sustainability, quality, efficiency and competency [6]. Levy exemption as an incentive for IBS adopters that have used IBS more than 50 % of the building components for residential buildings and projects. The introduction of IBS Score is also essential for the development of IBS in Malaysia. Furthermore, the Malaysian Treasury Circular (SSP7/2008) is an important milestone to increase the adoption and implementation of IBS in the construction of public buildings in Malaysia [7].

The broader view and key factors of IBS implementation in Malaysia are about changing of the conventional mindset, reengineering of human capital development, improving trust and cooperation, promoting integrity and transparency [8]. There is a raise of consensus amongst Malaysian industry players on IBS; however, the move towards industrialisation of the construction industry is global and worldwide initiative. Hence the fundamentals of IBS (definition, classification, characteristics and concepts) need to be evolved and incorporated with global views and understanding. It will give a new perspective and enriches ones understanding on IBS as a whole.

2 Definition of IBS

IBS is a construction method or technique that uses pre-fabricated components, where project clients and developers can gain benefits from many ways. This paper revisits the definition of IBS from 2003 until present. The definitions are listed on the Table 1.

The move towards industrialisation of the construction industry is not only in Malaysia, its also a global phenomenon. The definitions need to be evolved and

Table 1 Definitions of IBS

Authors	Definitions
Richard [13]	Industrialisation has demonstrated a high capacity to reduce costs, improve quality and make complex products available for the vast majority people
Richard [22]	Industrialisation is a generic organisation based on quantity and offering an individualised finished product: (a) a generic organisation (b) based on the quantity (c) offering an individualised finished product
CIDB [12], Kamar et al. [23]	A construction technique in which components are manufactured in a controlled environment (on or off site), transported, positioned and assembled into a structure with minimal additional works
Abdullah and Egbu [24]	A method of construction developed due to human investment in innovation and on rethinking the best ways of work deliveries. It was developed based on categories which can be classified as pre-building system, modern construction, advanced automation and volumetric
Hassim et. al. [25]	IBS is an organisational process continuity of production implying a steady flow of demand, standardisation, integration of different stages of the whole production process, a high degree of organisation of work, mechanisation to replace human labour wherever possible
Abdullah et al. [26]	IBS is a process in which components are manufactured, positioned and assembled as a structure with minimal additional site works both off-site and on-site

incorporated with global understanding and views. Literatures highlighted several key fundamentals of IBS definition. Based on the reviewed information from relevant literature, a comprehensive definition of IBS can be deduced as:

“Industrialised Building System (IBS) is a construction process that uses standardised building components mass produced in a factory or on site then transported and assembled into a structure using appropriate machinery and equipment with minimal workers on site with proper planning and integration.”

3 Classification of IBS

IBS has various classification based on the material, process and system. For further exploration and discussion between academicians and researchers in this field, a general classification for IBS is as the followings [9]:

- Frame system (pre-cast or steel)
- Panel system
- Onsite fabrication
- Sub-assembly and components
- Block work system
- Hybrid system
- Volumetric/modular system

Table 2 List of IBS classifications in Malaysia

IBS introduce in	Classifications of IBS	Types of IBS classifications
Early 60s	Badir et al. [27]	<ol style="list-style-type: none"> 1. Frame system 2. Panel system 3. Box system
Early 90s	Badir et al. [28]	<ol style="list-style-type: none"> 1. Precast concrete framing, panel and box systems 2. Load bearing block 3. Sandwich panel 4. Steel frame
2003	CIDB [12]	<ol style="list-style-type: none"> 1. Pre-cast concrete framing, panel and box system 2. Formwork system 3. Steel framing system 4. Prefabricated timber framing system 5. Block work system
2010	CIDB [6]	<ol style="list-style-type: none"> 1. Pre-cast concrete system 2. Formwork system 3. Steel framing system 4. Prefabricated timber framing system 5. Block work system 6. Innovative system

CIDB Malaysia has classified IBS to suit the local practice through the years as shown in Table 2.

The future classification of IBS in Malaysian construction industry should be expanded to cater the scope of modular or volumetric construction and hybrid construction. Malaysia is still in the stage of hybridisation construction and in the initial stage to implement modular construction. In the current Malaysian context, CIDB has classified the IBS into six types as depicted in Table 3.

4 Characteristics of IBS

It is plausible to review the essential characteristics of IBS. Each of them is briefly discussed as follow:

4.1 Open System

An open system allows greater flexibility of design and maximum coordination the designer and manufacturer. This system is plausible because it allows the manufacturer to produce a limited number of elements with a predetermined range of product. In addition, it maintains the architectural aesthetic value of the building at the same time [10].

Table 3 Current IBS classifications [12]

Classifications	Descriptions
Pre-cast concrete system	The common IBS used includes precast concrete elements (precast concrete columns, beams, slabs, walls and 3D components), lightweight precast concrete and permanent concrete formworks
Formwork system	Considered as one of the low level or the least prefabricated IBS. The system involves site casting, offer high-quality finishes and fast construction with less labour and materials requirement
Steel framing system	Commonly used with precast concrete slabs, steel framing system has always been a popular choice and used extensively in fast track construction of skyscrapers. Recent development of this IBS includes the usage of light steel trusses consisting of cost effective profiled cold formed channel and steel portal frame system. These are the alternatives to the heavier traditional hot rolled section
Prefabricated timber framing system	This system consists of timber building frames and timber roof trusses. Timber building frame system also has their market and demand, offering attractive designs from simple dwelling units to buildings that required high aesthetical values such as resorts and chalets
Block work system	The construction method of using traditional bricks has been revolutionised by the development of interlocking concrete masonry units and lightweight concrete blocks. The tedious and time-consuming traditional bricklaying tasks is vastly simplified by the usage of these effective solutions
Innovative system	In order to classify new systems introduced in Malaysian construction industry that are not belongs in the five mains IBS in the CIDB's IBS classifications (2003), CIDB introduced innovative system to classified the new and innovative systems in IBS approach

4.2 Closed System

Divided into two categories, which is a production based on the client’s design and manufacturer’s design. The client’s design is design to meet the client’s requirements, such as spaces for various functions and specific architectural design. The production based on the manufacturer’s design includes designing and producing an uniform building (school, low-cost housing and others) [10].

4.3 Modular Coordination

Modular coordination is a coordinated, unified system for dimensioning spaces, fittings, components and others so that all elements fit together without cutting or extending even though the components are produced by different manufacturers [11].

4.4 Standardisation and Tolerances

In order to accomplish the requirement of modular coordination, all the components involved need to be standardised for production. In addition, tolerances at different construction stages such as manufactured, setting out and erection tolerances need to obtain combine tolerances on statistical considerations within the permitted limits [9, 11].

4.5 Mass Produced

The investment in technology, people and factory associated with an industrialisation can be justified economically when mass production volume is achieved by distributing the fixed investment charged over a large number of products without inflating the ultimate cost [9, 10].

4.6 Specialisation

Large production output, standardisation and repetition in industrialisation allow a high degree of specialisation in the production process. The process can be subdivided into a large number of small homogeneous tasks [10]. The adoption of specialised machineries and labours is possible in the industrialisation of construction.

4.7 Integration

In order to complete a project with a good result, proper coordination must exist between various relevant parties involved (consultants, manufacturer, contractor and owner) through an integrated or suitable system [9, 10].

4.8 Production Facility

The initial capital investment for setting up a factory is high and expensive. Plant, equipment, labour and management resources need to be acquired before production can be commenced. Huge investment like this can only breakeven when the demand for the products is continuous [10, 12].

4.9 Transportation

Casting of a large wall panel system can reduce the labour cost up to thirty percent or less. However, these cost savings are partially offset by the transportation cost. In addition, the transportation of large panels is also subject to the country’s road department. These limitations must take into consideration when adopting IBS [9, 10].

4.10 Machineries/Equipment at Site

Suitable machineries or equipments for erecting and assembling IBS is needed such as precast concrete system where mobile crane is required. Therefore, it is necessary to incorporate this additional cost when adopting IBS [10, 12].

5 Concepts of IBS

There are a wide scope of terms and concepts in the field of building industrialisation due to the development of IBS. One of the most significant studies on industrialisation categorisation and concepts in construction was the work by Richard [13]. In his research, he stated that the large numbers of components are sub-assemblies; therefore, construction is still forever site-intense handicraft. As a result, the degree of industrialisation by Roger-Bruno Richard should be an indicator to measure the level of industrialisation adoption in construction [13]. The degree of industrialisation discussed in Richard’s research is in Fig. 1.

It is necessary to provide an exact definition of all concepts and terms for a better understanding on IBS. The selected concepts in IBS are presented in Table 4.

Currently, most of Malaysia’s IBS is at the prefabrication stage in Bruno Richard’s degree of industrialisation. In order for IBS to be mechanised and industrialised, it needs to move up and adopt Bruno Richard’s degree of industrialisation from the early stage that is prefabrication, move up to mechanisation, next is automation, then robotics and lastly reproduction.

Fig. 1 Degree of industrialisation [13]

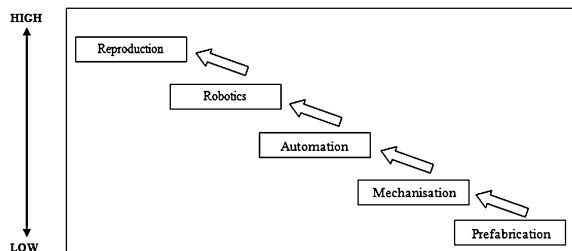


Table 4 Selected concepts in IBS

Terms	Authors	Definitions
Prefabrication	Richard [13]	Prefabrication is a manufacturing process that takes place at a specialised facility or on-site, where different materials are join to form a component part of the final installation
Mechanisation	Richard [13], Abdullah et al. [26]	Mechanisation comes in whenever machinery usage is to ease the workload of the labour (power tools, mobile crane, etc.)
Automation	Richard [13]	Automation is a situation when the tooling (machine) totally takes over the tasks performed by the workers. A supervisor is still around although industrial engineer and programmer are critical participants involved
Robotics	Richard [13]	With robotics, same tools will acquire a multi-axis flexibility to perform by themselves diversified tasks (for example using robotic arms used in the automobile industry). The future of robots is related to Computer Aided Manufacturing (CAM). It generates complex forms that can be different from one unit to the other, opening the way to individualisation within mass production and mass customization. Furthermore, the use of robotics technology such as a robotic arm, ease the activities increase productivity and performance
Reproduction	Richard [13]	The word reproduction is borrowed from printing technology, obviously not from biology. The analogy with printing will serve hereafter to extrapolate a methodology bringing productivity and economy in architecture. The purpose of reproduction is a shortcut of repetitive linear operations which are common in traditional production methods. There are technology producing building components and house using the printing concept with the use of new material (cement + fiber)
Pre-assembly	Abdullah et al. [26]	A process that includes various materials and prefabricated components assemble at an acquire location for subsequent installation as a sub-unit
Standardisation	Thanoon et al. [10]	Standardisation of building elements and components face resistance from the construction industry due economic reason and aesthetic reservation

6 The Way Forward for IBS

A holistic, mechanised, industrialised and sustainable approach needs to be adopted in the current IBS approach in Malaysia.

6.1 Better Understanding of IBS

In order for Malaysian construction industry players (owners, consultants, contractors, manufacturers, etc.) have a better understanding on IBS, the industry requires change management and business engineering to encourage new mindset and increase awareness on the adoption of IBS. Guidance on best practices and success factors to adopt IBS construction is needed. IBS should be handled as a holistic process rather than just a collection of technology solutions [14]. The academicians play a vital role to ensure the new and future construction industry graduates are equipped with IBS knowledge. Skill training center and institute for construction industry need to introduce IBS training programme to increase the availability of the local skill workers in IBS.

6.2 Government Role in IBS

The incentives and promotions by the government for IBS are not sufficient. IBS adoption requires more pull and push factors from the government. Due to small profit margin, the change from conventional to IBS was not feasible, unless more attractive systems and benefits introduced. Any promotions, incentives, policies and development efforts need to focus on the demand and supply of IBS [14]. In addition, government should introduce licence based on IBS classification for the contractors to encourage specialisation rather than one contractor doing all the tasks.

6.3 Sustainability in IBS

IBS contributes to sustainability by producing less waste; less volume of construction materials; increased environmental and construction site cleanliness; better quality control and promote safer and organised construction site [15]. In addition, sustainability involves innovation and the adoption of modern method of construction through industrialisation such as IBS. It is centrally organise, mechanised and automated production operations and focuses on mass production [16]. Using IBS as a platform in pursuing the sustainability agenda can also be immensely rewarding because it can offer organisations and players potential benefits [17]. Local authorities, companies related to environment and sustainability including

government, government agencies and private agencies need to acknowledge IBS contributions toward green, sustainability and sustainable construction in the construction environment.

6.4 Adopting Innovation and Industrialisation in IBS

Problems associated with the construction industry have highlighted the need for an innovative solution within the industry, including a push for further use of industrialisation [18]. Adopting the degree of industrialisation by Roger-Bruno Richard [13] is essential to enhance the industrialisation in IBS. Furthermore, the adoption of modular construction in IBS approachable to solve problems associated with the current IBS and in line with the objectives of Malaysian Construction Industry Master Plan (CIMP 2006–2015) and CIDB Malaysia IBS Roadmap 2011–2015 [19]. Innovation and industrialisation need to be introduced in IBS approach for future development of IBS in Malaysia through material engineering (introduction of new materials to be included in IBS), improvement in construction method and activities (the use of machineries, robots and new technologies) and lastly, production and manufacturing (prefabrication on and offsite).

6.5 Payment and Procurement Mechanism for IBS

The payment and procurement mechanism need to be reviewed. In addition, a new mechanism of payment and procurement needs to be introduced for IBS. The IBS adopters require reliable and safer payment and procurement [14, 20].

6.6 Technical Issues in IBS

Solutions for technical issues in IBS such as joint, standardisation, dimension, certification and other related technical issue are essential to avoid discouragement amongst the Malaysian construction industry players to adopt IBS.

6.7 Supply Chain Management (SCM) and Partnering in IBS

Supply Chain Management (SCM) and partnering concept in IBS has not fully understood by the industry. Currently, the cooperation between contractors, manufacturers and suppliers are weak in many cases. Improving the supply chain is the key to achieving IBS success for contracting companies. Plus, partnering with suppliers and sub-contractors from the earliest project stages is vital to ensure efficient and timely delivery of components and services [14, 21].

6.8 Risk Management in IBS

The construction companies do not well accept IBS because of the failure to deal with risks in the IBS projects. In order to reduce risks, a valid and working risk strategy needs to be developed. Sub-contracting and establishment of IBS subsidiaries can reduce some risk based on contractual 'risk-transfer' solution. The contractor can attempt to own the prefabrication technology by devising a special relationship with one or more prefabrication subcontractor or manufacturer, through project-based joint venture, vertical integration or even internalization [14].

7 Conclusion

The current study has highlighted the definitions, classifications, concepts, characteristics and the way forward for IBS in Malaysia. A holistic, mechanised, industrialised and sustainable approach needs to be adopted in the current IBS approach in Malaysia. Improvement and future research based on the way forward for IBS is essential to achieve a holistic approach in IBS. Finally, the current study is a part of ongoing main research that will further enhance the IBS developments through modular construction and modular building system through the IBS approach in Malaysia. The results of the main research will hopefully provide the basis of a guideline to support and enhance the Malaysian construction industry.

Acknowledgments The Authors wish to thank the Universiti Teknologi MARA, Construction Industry Development Board (CIDB) and a remark of indebtedness to the Acculturation Grant Scheme (RAGS) by the Ministry of Education, Malaysia for its grant award.

References

1. W.A.M. Thanoon, L.W. Peng, M.R.A. Kadir, M.S. Jaafar, M.S. Salit, The experiences of Malaysia and other countries in industrialised building system (IBS), in *International Conference on Industrialised Building Systems* (2003)
2. Z.A. Hamid, K.A.M. Kamar, M.Z.M. Zain, M.K. Ghani, A.H.A. Rahim, Industrialised building system (IBS) in Malaysia: the current state and R and D initiatives. *Malays. Constr. Res. J. (MCRJ)* 2(1), 1–11 (2008)
3. K.A.M. Kamar, M. Alshawi, Z. Hamid, M.N.M. Nawawi, A.T. Haron, M.R. Abdullah, IBS: Revisiting the issues on definition, classification and the degree of industrialisation, in *Industrialised Building System (IBS): Definition, Concept and Issues*, ed. by Z. Hamid et al. (Construction Research Institute of Malaysia: Makmal Kerja Raya Malaysia, Kuala Lumpur, 2011)
4. M.N.M. Nawawi, A. Lee, K.M. Nor, Barriers to implementation of the industrialised building system (IBS) in Malaysia. *Built Human Environ. Rev.* 4, 22–35, (2011)
5. CIMP, *Construction Industry Master Plan 2006–2015 (CIMP 2006–2015)* (Construction Industry Development Board CIDB, Kuala Lumpur, 2007), p. 80

6. CIDB, *IBS Roadmap 2011–2015* (Construction Industry Development Board, Kuala Lumpur, 2010)
7. K.A.M. Kamar, Z. Hamid, The Policies and chronology of industrialised building system (IBS) adoption in Malaysia, in *UIA Press (UIA) in IBS towards Open System in Malaysia*, ed. by A.A. Rahim, Z. Ismail (2011)
8. S.N. Shaari, E. Ismail, *Promoting the usage of Industrialized Building System (IBS) and Modular Coordination (MC) in Malaysia* (Board of Engineer Malaysia: Construction Industry in Engineers, 2003)
9. K.A.M. Kamar, Z. Hamid, M.N.A. Azman, M.S.S. Ahamad, *Industrialized Building System (IBS): Revisiting Issues of Definition and Classification* (2011), p. 13
10. W.A.M. Thanoon, L.W. Peng, M. Razali, A. Kadir, M.S. Jaafar, M.S. Salit, The essential characteristics of industrialised building system (IBS), in *International Conference on Industrialised Building Systems* (Kuala Lumpur, Malaysia, 2003)
11. D.N. Trikha, Industrialised building systems. Prospects in Malaysia, in *World Engineering Congress* (Malaysia, 1999)
12. CIDB, *IBS Roadmap 2003–2010* (Construction Industry Development Board, Kuala Lumpur, 2003)
13. R.B. Richard, Industrialised building systems: reproduction before automation and robotics. *Autom. Constr.* **14**(4), 442–451 (2005)
14. K.A.M. Kamar, Z. Hamid, Z. Ismail, Modernising the Malaysian construction industry through the adoption of industrialised building system, in *Conference on Multi-National Joint Ventures For Construction Works* (Kyoto, Japan, 2010)
15. H. Zabihi, F. Habib, L. Mirsaedie, Definitions, concepts and new directions in industrialized building systems (IBS). *KSCE J. Civil Eng.* **17**(6), 1199–1205 (2013)
16. K.A.M. Kamar, Z.A. Hamis, N. Dzulkalnine, Industrialised Building System (IBS) Construction: Measuring the Perception of Contractors in Malaysia, in *Business Engineering and Industrial Applications Colloquium (BEIAC)*, 2012 IEEE (2012)
17. M.F. Mohammad, Construction Environment: Adopting IBS Construction Approach towards Achieving Sustainable Development, in *AcE-Bs 2013 Hanoi* (Hanoi Architectural University, Hanoi, Elsevier's Procedia Social and Behavioural Sciences, Vietnam, 2013)
18. R. Mahbub, Readiness of a developing nation in implementing automation and robotics technologies in construction: a case study of Malaysia. *J. Civil Eng. Architect.* **6**, 858–866 (2012)
19. M.F. Musa, M.F. Mohammad, R. Mahbub, *Enhancing the quality of life by adopting sustainable modular building system in the malaysian construction industry*. unpublished
20. S.S. Kamaruddin, M.F. Mohammad, R. Mahbub, Enhancing the quality of life by adopting IBS: an economic perspective on mechanisation and automation, in *Quality of Life in the Built Natural Environment 6–7 April 2013*. Procedia-Social and Behavioral Sciences: Langkawi, Malaysia, pp. 71–80, 2013
21. A.S. Abd Shukor, M.F. Mohammad, R. Mahbub, F. Ismail, Supply chain integration in industrialised building system in the malaysian construction industry. *Built Human Environ. Rev.* **4**(1) (2011)
22. R.B. Richard, Industrialised, Flexible and demountable building systems: quality, economy and sustainability, in *International Symposium on Advancement of Construction Management and Real Estate* (2006)
23. K.A.M. Kamar, M. Alshawi, Z.H. Hamid, Barriers to industrialised building system (IBS): the case of Malaysia, in *International Postgraduate Research Conference* (2009)
24. M.R. Abdullah, C. Egbu, Industrialised building system in Malaysia: issues for research in a changing financial and property market, in *BuHu 9th International Prograduate Research Conference (IPGRC)* (Salford, United Kingdom, 2009)
25. S. Hassim, M.S. Jaafar, S. Sazalli, The contractor perception towers industrialised building system risk in construction projects in Malaysia. *Am. J. Appl. Sci.* **6**(5), 937–942 (2009)

26. M.R. Abdullah, K.A.M. Kamar, M.N.M. Nawi, A.T. Haron, M. Arif, Industrialized building system: a definition and concept, in *ARCOM Conference 2009* (Nottingham, United Kingdom, 2009)
27. Y.F. Badir, M.R.A. Kadir, A.H. Hashim, Industrialised building systems construction in Malaysia. *J. Architect. Eng.* **8**(1), 19–23 (2002)
28. Y.F. Badir, M.R.A. Kadir, A.A.A. Ali, *Theory of Classification on Badir-Razali Building System Classification* (Malaysia, 1998)

A Review of the Maintenance Performance Factors for Heritage Buildings

Syed Burhanuddin Hilmi Syed Mohamad, Zainal Abidin Akasah
and Mohammad Ashraf Abdul Rahman

Abstract The building maintenance programme is the important part of the building life cycle. All planned or unplanned maintenance programme are designed to maintain the originality and conditions for the specific building. The comprehensive planning and evaluation processes of building maintenance performance for heritage building is crucial in determining the best practice and procedure in order to meet the prescribed requirements. The awareness programme among involve parties is needed to strengthen their basic understanding about the importance of maintaining the heritage buildings. The lack of maintenance scope and procedure in heritage building is considered as a non-sustainable result to the existing building condition. This lacking situation will be the initial cause of building defect and deterioration problems and have to allocate a lot of money in order to repair and rehabilitate the selected heritage buildings. The aims of this study are to identify and review the related issues of building maintenance performance for heritage buildings. The review will also reveal the identified significant factors which are giving an influence to the building maintenance performance for heritage buildings. The building maintenance performance has considered as one of the major issues in heritage buildings in order to prolong its life expectancy. This paper reviews the previous significant factors in building maintenance performance in heritage building. The relevant significant factors should be considered during planning phase of the maintenance programme.

Keywords Maintenance • Performance factors • Heritage building

S.B.H.S. Mohamad (✉) · Z.A. Akasah
Faculty of Civil and Environmental Engineering, Universiti Tun Hussein Onn Malaysia
(UTHM), Parit Raja, Batu Pahat, Johor, Malaysia
e-mail: burhan@uthm.edu.my

Z.A. Akasah
e-mail: zainal59@uthm.edu.my

M.A.A. Rahman
Faculty of Technology Engineering, Universiti Tun Hussein Onn Malaysia (UTHM),
Parit Raja, Batu Pahat, Johor, Malaysia
e-mail: ashrafr@uthm.edu.my

1 Introduction

Malaysia has been allocated a billion of ringgit for the public and government buildings maintenance especially in repair works, due to the lack of maintenance planning and poor maintenance awareness among public. It is important to have a best maintenance planning programme where the defects development can be detected earlier and repaired. Thus, the government can save a lot of money and prolong the building life span [1]. Nevertheless, the public also need to obtain a clear understanding and explanation on the importance of building maintenance works. This awareness programme needs are subjected to the new buildings and the heritage historical buildings in Malaysia [2]. The awareness programme is perhaps can educate as many as possible the public about the importance of maintaining the heritage historical buildings in Malaysia.

Maintenance of heritage building is becoming important process and task to Malaysia Government in ensuring the nation's heritage buildings and monuments are in good conditions and can be saved for the future generations. Malaysia has its own unique identity with a great social and cultural significance values. Malacca and George Town in Penang have been urbanized more than 5 centuries ago. These two centres for trade and society exchanges between East and West in the Straits of Malacca were recognized by The United Nations Educational, Scientific and Cultural Organization's (UNESCO) as the new listed cultural sites to UNESCO's World Heritage List in July 2008 [3–5].

The given recognition from UNESCO is the key and advantage to Malaysian government in establishing more efforts to conserve the heritage and historical buildings, including the traditional old houses. It is also an approval from UNESCO to prevent the gazetted heritage and historical buildings from being demolished and replaced with new buildings.

Maintenance of heritage buildings and sites in Malaysia are under the Department of National Heritage and prominently known as building conservation. The Department of National Heritage has been established on 1st March 2006. The Department of National Heritage is headed by the Heritage Commissioner which is in charge for the registration of National Heritage and heritage building conservation projects throughout Malaysia [6]. The Department of National Heritage has gazetted 47 buildings/monuments as national heritage sites [7] and 176 buildings/monuments as heritage sites [8].

In maintenance aspect, the essential manifesto that declared the maintenance programme and conservative repair procedure as the fundamental conservation principles was issued by William Morris in 1877 [7, 14].

The conservation and maintenance approaches have been used in maintaining Malaysia's heritage buildings. The heritage building has giving a significant value (beautiful and historical landmark) in initiating the urban and suburban development in Malaysia. It is also plays an important role to generate income through tourism industry [9].

However, the historic preservation technology in building maintenance plays an important role from start to finish for any preservation project. The historic conservation technology criteria includes investigation methods, materials selection, and construction technology methods, which will be implemented in preserving, rehabilitating, restoring or reconstructing techniques of a heritage building [10].

Planning and development processes are always be related to political stability, economy sustainability, social concern and technical issues (knowledge and skills). Although the heritage buildings are considered as the old buildings, but it always need to take into consideration the four mentioned major factors in the maintenance and conservation. The good practice of maintenance management will also be able to increase a building's effective life span, minimize energy usage and optimize the resources consumption.

Recently, the maintenance and refurbishment of old buildings has been emphasized as alternative preservation approaches to redevelopment the heritage building. The approach will able to keep the old buildings fit for modern use. Because of this, the determination of the significant contributing factors of heritage building maintenance performance is essential towards the systematic heritage building maintenance framework [4].

2 Literature Review

2.1 Maintenance

Technically in building maintenance, The British Standard 3811:1993 defined maintenance as the combination of all technical aspects and associated administrative actions which are intended to retain an item or to restore it to require condition in which it can perform its required function [11].

In contrast, the maintenance of heritage building has been recognized as the single most important conservation process in preventing the building from potential defects. The phrase "Prevention is better than cure" is widely used, whether in architectural, mechanical or botanical areas. In addition, Australia ICOMOS is concerned about the lack of clarity on responsibility for maintenance and repair because it is consider as a common cause of deterioration in heritage buildings [12–15].

Researchers have been suggested that maintenance is the important aspect to sustain the heritage building life span as quoted as follows:

1. Maintenance is identified as a system to protect the historic structure building life span [1].
2. Maintenance has been recognized as the most significant technique to ensure the prolongation of the building's life span [16]. The selected solutions should keep the nature and ambience of the building and capable to fulfill the future development requirements with a continuous maintenance programme [15].

3. Maintenance is a comprehensive planning system to extend the life span of the historical structures. The maintenance work also a tool in protecting and preserving the heritage buildings [17].
4. The planned maintenance approach has been adopted in maintenance programme. This is perhaps can sustain the quality of building materials and components [18].
5. The building defect and deterioration problems can be identified in early stages of building maintenance; the preventive maintenance programme can be implemented to avoid any building failure from related defects and deteriorations [18].
6. The general principle in the heritage building maintenance is to maintain the building's original use and appropriate with the place cultural significant. The space reuse of a building shall be attained by inserting a whole new building structure and component within an original space in such a condition that it does not harm the fabric in order to minimize the intervention. The usage of a same quality and properties of materials is important to achieve the originality materials in conservation process of heritage building [12].
7. The importance of maintenance is frequently neglected and still need to have a special attention. The continuous attention shall be made to sustain the originality of the historical heritage building for our future generations [12, 23].
8. The heritage building shall be maintained in practical condition if it is to continue to function satisfactorily without additional expenses to remedy the cost of periods of neglect [12, 15].

The care of fabric is the major care for heritage building maintenance. The proper guidelines in conducting the maintenance especially in repair work, reconstruction work, consolidation work and removal of damaging work shall be justified before commencing the proper processes for renewal of materials or retard the building deterioration (building prevention) [15].

In term of management, detail information of supervision of minor work as well as major work from precautious consideration to safety measures and maintenance works shall be focused in reducing the risk of building deterioration, fire, vandalism and theft [15].

2.2 Heritage Building

Heritage buildings are invaluable asset as remainders to the value of creativity, innovative and hard working achievement of the eldest generations. The values of the country's heritage buildings are essential in empowerment the national identity and the sense of pleasure of surroundings [12]. Therefore, these statements are important in understanding the heritage buildings importance and this definition could be adopted for every heritage building in the world.

National Heritage Act [6], in section 2(1) Act 645 has defined “building” as a building or groups of separate or connected buildings which, because of their architecture, their homogeneity or their place in the landscape, are of outstanding universal value from the point of view of history, art or science. Thus, heritage buildings is recommended to have a specific maintenance programme approach in sustaining its appearance which focused on unique architecture and building materials; and, aesthetic values which focused on heritage and cultural values [19].

2.3 Building Conservation

Building conservation is defined as a technique to preserve heritage historical buildings which are historically and culturally important to the related nation [1]. The building conservation work is executed to conserve the heritage building condition to its original condition with continuously maintenance programme [17].

The principle of conservation stated that all interventions in the fabric shall be handled with effectively and honestly to make clear explanation what is original and what has changed, in order to avoid creating something that is different from what we have in the past [12].

In Malaysia, some of researchers have been reported that the heritage building conservation is considered new. Malaysia has been implemented the conservation works for historical heritage building since approximately 40 years ago [4], started in the 70s and consistently increased in the 80s [20–24].

The conservation of heritage buildings is an approved method by the Department of National Heritage in order to maintain the heritage building through several techniques such as restoration and maintenance works [1]. Heritage conservation has been mentioned as a new practice in maintaining the originality and the uniqueness of Malaysian heritage buildings compared to the developed countries in the world [20, 21]. The Department of National Heritage has gazetted 91 heritage buildings including the traditional buildings from the Malays, Indians, Chinese and Colonials era [4, 20, 21].

The conservation method is involving a group of professionals which are expert in executing and managing the established conservation methods in order to preserve heritage buildings. Therefore, the standard of heritage building conservation can be achieved together with the cultural value embedded in it [15, 25, 26]. The usage of the building and an effective maintenance programme are the major successful factors in preservation of heritage building maintenance [27].

There had been a tendency to focus on the important perspectives such as technical aspects related to the preventive action (daily care and repair) of the heritage building maintenance fabric and the integration of conservation activities into a new comprehensive land development planning [12]. However, the current conservation activity is more emphasized on the critical aspect of effective management especially in strategies and tactics management. On the other hand, this management approach is able to preserve and improve the built cultural heritage [12]. The combination

between technical and management issues will give a best result of sustainable and holistic practice in conservation activity.

The current conservation planning is also concerned about the acceptance and understanding of the heritage building as the cultural significance asset. Then, it can determine a best management decisions to prolong and preserve the existing heritage buildings. The basic concept for protecting something is that we need to go through the identification and articulation processes on why the related heritage building is important and what are the criteria of the related heritage building contribute to that important [12].

2.4 Building Maintenance Management

The key topic and critical issue in development of maintenance culture is the lacking of systematic maintenance work programme. The systematic maintenance programme in the conservation programme is regularly been ignored due to the misinterpretation on both scope of works [1].

Hence, the ignorance of the proper maintenance programme for heritage buildings will deteriorate over time and will reduce the original function. Consequently, this will increase the cost for conservation works [1]. The building deterioration is initiated and propagated when there is a cause of defect due to the lack of maintenance work. Then, it will cause a building failure if no action taken within the life span of the building [16].

Based on BS3811 and practical approach, management is mentioned as a process of controlling and organizing certain situation or thing that involving certain allocation of resources. Maintenance management is the determination of management which is more focusing on the specific organization of maintenance within an agreed policy developed by the company [10].

Building maintenance management approach has been adopted and applied almost decades ago to rectify the building services problems. The maintenance management approach comprises can be categorized under technical and control aspects [12].

For example in maintaining the plant or equipment, the first step is to determine the process of identifying problems and diagnosing causes. Then, monitor the effects, analyze data and prepare a record for the related maintenance process. All of these processes are technically carried out to cope with the current situations and ensure that the selected techniques are achieving the required results [12].

In control aspect, the issues of expenses, labour, spare parts and equipment are been highlighted in order to match the maintenance workload. These are including the location of work, transportation arrangement, setting priorities and coordinating the maintenance activities. It can be extended to budget control, monitoring the cash flow, identify the high maintenance cost plant and collect the relevant information for final decision making [12].

Nevertheless, the level of public awareness of heritage building maintenance importance is gradually increasing [28] but decreasing in terms of maintenance managers knowledge on determine the best maintenance management approach in maintaining the of heritage buildings [3].

From the previous research findings, the most concerning issue in maintenance management is failure to give the priority in maintenance work. If the priority is given at the first place in maintenance programme, it is ideal to use the regular maintenance programme. Through the systematic maintenance programme, the investment performance will be increasing within the building life span and achieving good value for money. On the other hand, maintenance is always given incorrect alleged by public as a low income professional [1].

The certain issues related to maintenance in heritage building will directly determined the significant factors which can influenced the approach of the best maintenance practice. Research theory and practice of maintenance are always improving because of the needs for the best practice in heritage building maintenance management. There is still on-going research that conducted on this particular area and it is a need for research with more specific area in heritage building maintenance prospective. The best maintenance management practice, especially in the perspective of effective management strategy is important and has the potential research gap [20].

However, the fundamental issue is that, we need to identify and determine as many as possible the influence factors which are directly contribute to the heritage building maintenance performance. Then, the effective and comprehensive framework could be proposed for heritage building management system to improve the current practice and to overcome the problem of limited resources in the building maintenance.

2.5 Performance

Performance always relate to how well people or machines do a piece of work or activity. Therefore, the performance of a component became significant because of its ability to satisfy the requirements of the user. A difficulty in defining any general performance requirements in building maintenance lies in the fact that user requirements for the same component may differ widely, and may also change over time [10].

The results of the study in United Kingdom manufacturing industry have indicated the maintenance approach and continuous improvement as the top effective maintenance management approaches. Nevertheless, the continuous concern of the management is also important to give the basic guidelines and directions to the related maintenance management function [29].

Key performance indicators are mainly used to monitor the current and past building performance. It must have a specific method of measurements consisting quantitative and qualitative issues.

Therefore, it is very importance to assess and obtain complete results from building performance in planning the allocation of future budget. Currently, Critical Success Factor (CSF) which is more familiar within management and business sectors having adopted and adapted into building maintenance management system. It was recommended to apply CSF approach to improve the practice for maintenance management system according to organization's goals and objectives. Thus, it performance can be indicated and measured if the aspects conditions, factors and processes are determine as a performance criteria or performance successful variables in the research [9].

The building design itself can be costly and has an interrelationship with the building maintenance work. The benchmarking process is vital in checking and confirming the requirement building's performance up to the standard of quality. It is also to enable the maintenance manager to manage the strengths and weaknesses of their building maintenance management programme. Lastly, there is a request to the government to improve current practices in managing the maintenance of public buildings and identify the significance of the service provided. This will able to help the establishment of building maintenance management performance levels and criteria as useful tools in implementing immediate actions to improve the building maintenance performance [30].

Table 1 Summary of contributing factors to building maintenance performance of heritage building

Contributing factors to building maintenance performance for heritage buildings [4]		References
1	The importance of historical buildings	[1]
2	Human factor	[1, 3, 27, 31, 29, 31]
3	Maintenance policy and organization	[1, 3, 10, 12, 16, 18, 20, 32, 34]
4	Maintenance effectiveness	[1, 3, 11, 16, 27, 31, 34]
5	Task planning and scheduling	[32, 34]
6	Maintenance approach	[1, 3, 16, 18, 20, 32, 34]
7	Financial factor	[1, 3, 10, 16, 27, 31, 32, 35]
8	Risk management	[11, 12, 34]
9	Customer perspective	[32, 35]
10	Information management and computerized maintenance management system (CMMS)	[3, 12, 16, 32, 34]
11	Environment	[3, 11, 18]
12	Technical aspects	[1, 6, 10, 12, 16, 18, 20, 29, 32]
14	Institutional and training facilities	[12, 27, 31, 35]
15	Continuous improvement	[11, 12, 16, 27, 31, 32, 34]
16	Human resources management	[1, 3, 9, 10, 29, 31, 32, 34, 35]
17	Spare part management	[27, 34]
18	Regulations and guidelines	[1, 3, 20, 28, 35]
19	Contracting out maintenance	[1, 12, 27, 32, 34]

Source Summary from literature

3 Factors Contributing to Heritage Building Maintenance Performance

The lists of factors that contribute to the building maintenance performance for heritage buildings from previous literature review are as in Table 1.

4 Conclusion

The interrelationship between significant factors for heritage building maintenance performance shall be analyzed. These significant factors need to be ranked and clarified in order to achieve acceptable result which can give some clues and indicators in developing the comprehensive heritage building maintenance performance framework.

Finally, the critical and significant factors can be identified and a best maintenance framework can be developed for heritage building. This framework is essential in improving the current practice and reducing the high expenses for heritage buildings maintenance and repair works.

Acknowledgments The authors would like to thank Universiti Tun Hussein Onn Malaysia (UTHM) for giving an opportunity and support in conducting this research.

References

1. R.A. Rashid, A.G. Ahmad, Overview of maintenance approaches of historical buildings in Kuala Lumpur—a current practice. *Procedia Eng.* **20**, 425–434 (2011)
2. S.A.H.S. Mustapa, K.S. Kamal, M.Z. Zainul, Rehabilitation of heritage buildings in Malaysia, in international seminar on modern urban and architectural heritage (Museum Bank Mandiri, 2005), pp. 126–133
3. N.F.N. Azhari, E. Mohamed, Public perception: heritage building conservation in Kuala Lumpur. *Procedia-Soc. Behav. Sci.* **50**, 271–279 (2012)
4. S.B.H.S. Mohamad, Z.A. Akasah, M.A.A. Rahman, Factors Contributing to Building Maintenance Performance of Heritage Buildings, eds. by R. Hassan, M. Yusoff, Z. Ismail, N.M. Amin, M.A. Fadzil. in *InCIEC 2013 : Proceedings of the International Civil and Infrastructure Engineering Conference 2013*, (Springer, Singapore, 2014), pp. 851–860
5. UNESCO (2008), Eight new sites, from the Straits of Malacca, to Papua New Guinea and San Marino, added to UNESCO's World Heritage List, 03 Dec 2012. <http://whc.unesco.org/en/news/450>.
6. Act 645. National Heritage Act 2005, 2006
7. Department of National Heritage, Warisan Kebangsaan. Available: <http://www.heritage.gov.my/index.php/ms/daftarwarisan/statistik/warisan-kebangsaan> (2012)
8. Department of National Heritage, Heritage. Warisan. Available: <http://www.heritage.gov.my/index.php/ms/daftarwarisan/senaraiwarisan/tapak/bangunan> (2012)

9. S.H. Zulkarnain, E.M.A. Zawawi, M.Y.A. Rahman et al., A review of critical success factor in building maintenance management practice for university sector. *World Acad. Sci. Eng. Technol.* **59**, 195–199 (2011)
10. P. Wordsworth, *Lee's Building Maintenance Management*, 4th edn. (Blackwell Science Ltd., Oxford, 2001)
11. CIBSE Guide M, *Maintenance Engineering and Management: A Guide for Designers, Maintainers, Building Owners and Operators, and Facilities Managers* (The Chartered Institution of Building Services Engineers London, London, 2008)
12. D. Worthing, S. Bond, *Managing Built Heritage: The Role of Cultural Significance* (Blackwell Publishing Ltd., Oxford, 2008)
13. N. Dann, D. Worthing, Heritage organisations and condition surveys. *Struct. Surv.* **23**(2), 91 (2005)
14. N. Dann, D. Worthing, S. Bond, Conservation maintenance management—establishing a research agenda. *Struct. Surv.* **17**(3), 143–153 (1999)
15. J.S. Kerr, The Seventh Edition Conservation Plan 2013: Guide to the Preparation of Conservation Plans for Places of European Cultural Significance. New South Wales: Australia ICOMOS Inc. Retrieved from <http://australia.icomos.org/wp-content/uploads/The-Conservation-Plan-7th-Edition.pdf> (2013)
16. J.W. Negara, *Garis Panduan Pemuliharaan Bangunan Warisan*. Jabatan Warisan Negara (2012)
17. Y. Robert A, *Historic Preservation Technology* (Wiley, New Jersey, 2008)
18. R. Abdul-Rashid, A.G. Ahmad, The implementation of maintenance works for historical buildings—a review on the current scenario. *Procedia Eng.* **20**, 415–424 (2011)
19. W. Morris, *The SPAB Manifesto* (Society for Protection of Ancient Building (SPAB), London, 1877)
20. A.F. Mohd-Isa, Z. Zainal-Abidin, A.E. Hashim, Built heritage maintenance: a malaysian perspectives. *Procedia Eng.* **20**, 213–221 (2011)
21. A. A Ghafar, *Pemuliharaan Bangunan Warisan di Malaysia Pengalaman dan Cabaran*. Universiti Sains Malaysia Pulau Pinang (2010)
22. A.Z.A. Akasah, B.M. Alias, Analysis and development of the generic maintenance management process modeling for the preservation of heritage school buildings. *Int. J. Integr. Eng. (Issue on Civil and Environmental Engineering)* **1**(2), 43–53 (2009)
23. S.N. Harun, Heritage Building Conservation in Malaysia: Experience and Challenges. *Procedia Engineering* **20**, 41 (2011)
24. UNESCO Bangkok, *Hoi An Protocol for Best Conservation Practice in Asia: Professional Guidelines for Assuring and Preservation the Authenticity of Heritage Sites in the Context of the Cultures of Asia*. UNESCO Bangkok, (2009)
25. B.M. Feilden, *Conservation of Historic Buildings*, 3rd edn. (Butterworth Heinemann, London, 2003)
26. M. Forsyth (ed.), *Structures and Construction Historic Building Conservation* (Blackwell Publishing Ltd, Oxford, 2007)
27. M. Sodangi, A. Bin Idrus, F.M. Khamidi, Examining the maintenance management practices for conservation of heritage buildings in Malaysia, in National Postgraduate Conference (NPC), 19–20 Sept 2011, pp. 1–7
28. N.I. Hashim, M.A.O. Mydin, Maintenance management system of administration heritage buildings in Malaysia. *Ann. Fac. Eng. Hunedoara Int. J. Eng.* **10**(3), 475–478 (2012)
29. C. Cholasuke, R. Bhardwa, J. Antony, The status of maintenance management in UK manufacturing organisations: results from a pilot survey. *J. Qual. Maintenance Eng.* **10**(1), 5–15 (2004)
30. S.E.A. Ali, H.M., Sani, S.I.A., A review of the effect of building design on maintenance management, in *3rd ICBER 2012 Proceedings of the 3rd International Conference on Business and Economic Research* (Bandung, Indonesia, 2012), pp. 648–662

31. M.A.A. Rahman, Z.A. Akasah, M.S. Abdullah et al., Issues and Problems Affecting the Implementation and Effectiveness of Heritage Buildings Maintenance, in *The International Conferences on Civil and Environmental Engineering Sustainability* (Johor Bahru, Malaysia, 2012)
32. B. Chanter, P. Swallow, *Building Maintenance Management*, 2nd edn. (Blackwell Publishing Ltd., Oxford, 2007)
33. B. Wood, *Building Maintenance* (Blackwell Publishing Ltd., Oxford, 2009)
34. C.W. Kuen, S. Zailani, Y. Fernando, Critical factors influencing the project success amongst manufacturing companies in Malaysia. *Afr. J. Bus. Manage.* **3**(1), 16–27 (2009)
35. S.N. Kamaruzzaman, E.A. Zawawi, A. Omar, Preliminary evaluation of problems involved in maintaining heritage buildings in Malaysia. *Prof. J. Inst. Surv. Malaysia* **46**(1), 30–38 (2011)

Strategies in Dealing with Cost Overrun Issues: Perspective of Construction Stakeholders

**Kai Chen Goh, Aaron Boon Kian Yap, Ta Wee Seow,
Md Asrul Nasid Masrom, Hui Hwang Goh and Jia Sin Tey**

Abstract Construction industry in Malaysia is one of the main contributors to economic growth, yet there are still issues related to construction cost overrun. Many factors have triggered the cost overrun issues that might have high possibility to ruin the overall performance of a construction project. To cope with these issues, determination of strategies is essential to ensure effective cost management in construction projects. This study attempts to identify strategies for current construction industry in dealing with cost overrun issues. Literature review and quantitative approach were employed to achieve objectives of the study. Questionnaires were distributed to three key construction stakeholders that are client, contractor and consultant in Penang state, Malaysia. The data obtained from the respondents were analyzed by using Relative Importance Index (RII) method. The findings indicate that the current industry stakeholders have different point of view and opinion in dealing with cost overrun issues. In conclusion, the result of this study serves as a guideline in dealing with the issue of cost overrun.

Keywords Cost overrun · Construction industry · Related important index · Project management

K.C. Goh (✉) · A.B.K. Yap · T.W. Seow · M.A.N. Masrom · J.S. Tey
Department of Construction Management, Universiti Tun Hussein Onn Malaysia,
Parit Raja, Batu Pahat, Johor, Malaysia
e-mail: kaichen@uthm.edu.my

A.B.K. Yap
e-mail: aaronypbk@gmail.com

T.W. Seow
e-mail: tawee@uthm.edu.my

M.A.N. Masrom
e-mail: asruln@uthm.edu.my

J.S. Tey
e-mail: hp120038@siswa.uthm.edu.my

H.H. Goh
Department of Electrical Power Engineering, Universiti Tun Hussein Onn Malaysia,
Parit Raja, Batu Pahat, Johor, Malaysia
e-mail: hhgoh@uthm.edu.my

1 Introduction

Cost overrun becomes a very frequent phenomenon and is almost associated with construction projects in both developed and developing countries, where these overruns sometimes exceeded 100 % of the anticipated cost of the project [1]. Durdyev et al. [2] found that these problems are due to the poor project management system of a construction company and lack of ability to inhibit cost overrunning. As an under development country, Malaysian construction industry is also one of the major industry that contribute to the growth of socio-economic [3]. Nevertheless, Malaysia is still facing huge challenges in achieving a higher level of succession while effectively manage the cost in construction projects. Project expenditures that are always exceeded the budget, followed by the delay in project schedule, building defects and over dependent of foreign workers. In fact, the major issue that is slowing down the progress in the development of the construction industry in Malaysia is cost overrun. This statement was supported by [4–6]. Cost overrun issues occurred when the final cost or expenditure of the project exceeds the budgeted, estimated or target cost [1, 6]. Therefore, it is important to identify the significant factors that contribute the cost over budget, find out the effective way to improve the cost management in the construction industry to minimize the problems. The problem of cost overruns is very critical and it might have a high possibility to further explore to mitigate this problem in future. According to [7], lack of efficient project management by owners or contractors on projects may leads to extra costs for both parties. In addition to the problems that occurred during construction, poor project management can cause failure to meet the quality and suitability of materials, to produce the intended products, or to operate for its intended life. Azis et al. [8] have concluded that one of the major components of project management is cost management; it is also an important tool to control and improve cost performance of projects. This paper reports a research on determining the strategies of current construction industry in dealing with cost overrun issues. The research via extensive literature review and questionnaire survey has determined strategies in dealing with cost overrun issues. The finding represent construction project stakeholders a guideline in order to reach an optimum balance between cost and time which indirectly reduce the issues of cost overrun in construction project.

2 Literature Review

Managing construction cost is one of the important tasks in achieving successful project completion [9–11]. Unfortunately it is very seldom achieving effective cost management and often experiencing significant amount of cost overrun [12].

Rahman et al. [13] showed that frequent design changes were a dominant cause of cost overrun. Hence, it is important to use standardized design on a construction project to avoid changes in design. There are some efforts such as emphasis is given to the coordination of planning pillars, frequent coordination between parties involved, establish Building Information Modeling (BIM) system in design and choosing parties involved among competent personnel and entities can be given to solve the cost overrun issue [14, 15].

Every organisation should make sure there is frequent coordination between parties at planning stage adequately to achieve its benefits. As in any construction project, various parties including consultant, contractors, sub-contractors, Mechanical and Electrical (M&E) organisation, supplier etc. involved. The work of all parties is inter-related and highly depending with the works of other party. Therefore, frequent coordination between the parties is crucial for overcome the cost overrun issue.

Settling financial issue may well settle other issues simultaneously [16]. Hence, contractors are recommended to have enough cash before beginning any project to minimize financial problems [17]. This can be resolved by the selection process of a good-practice contractor i.e. not only on the lowest bidding price, but also the previous working experience and reputation of the contractors and subcontractor [18]. Also, a detailed financial plan for project should be prepared [19] and financial spending be monitored to avoid cost overruns [17].

Ibrahim et al. [20] highlight that improving site management is very critical for reducing cost overrun as it affects on productivity significantly. Based on [9], there are always uncertainties in construction projects which can affect project performance. To improve the performance and resolve the uncertainties faced during execution, it is preferred to arrange regular progress to discuss project related matter in dept and re-plan for further works. Also, every organization has the policy to document the progress of work which can be properly assessed by arranging regular meetings.

Construction works are highly dependent on the machinery and suitable work. However because of unique and complex in nature, construction projects are always subjected to risks which require opting advance technologies at the every construction stage. Further, construction being fragmented and uncertain there are the chances to occur numerous problems during construction execution which may require finding more advanced technique and technology than that being implemented on site as reaction to problems.

There are 43 strategies have been find out based on the previous study. The strategies were categorized into 11 groups in this research (Table 1), namely fluctuation in price of raw material, unstable cost of manufactured material, high cost machineries, lowest bidding procurement method, government policies, length pre-construction phase, cost estimation technique, design related issues, management related issue, poor project (site) management and additional works.

Table 1 Strategies in dealing with cost overrun issues

No.	Strategy	Memon et al. [28]	Memon et al. [29]	Sambasivan and Yau [4]
<i>Fluctuation in price of raw material</i>				
a	Exploration raw material resources from overseas	*		
b	Utilisation of raw material resources from overseas	*		
c	Regulation of raw material price	*	*	
d	Establish effective contract system with raw material suppliers	*		
e	Utilisation of local material			*
<i>Unstable cost of manufactured material</i>				
a	Effective monitoring over manufactured material cost	*		*
b	Effective controls over manufactured material cost	*		*
c	Switching towards industrialization (i.e. IBS)	*	*	
d	Exploring new manufactured material with advanced technology	*	*	
<i>High cost of machineries</i>				
a	Prefer to purchase own machinery	*		
b	Prefer to rent machinery	*		
c	Prefer to contract machinery	*		
d	Systematic control mechanism		*	*
<i>Lowest bidding procurement method</i>				
a	Evaluate bids with lowest possible practical working rates	*		*
b	Consider financial positions of the bidding parties	*		
c	Bidding parties' reputations are major contributing factor	*	*	
d	Bidding parties' bonds cater to satisfaction	*		*
<i>Government policies</i>				
a	Avoid uncertain economic policies	*		
b	Ensure rules of law	*		*
c	Assure authority and autonomy of departments	*		*
d	Projects must not be awarded based on political or other influences but on merit basis	*	*	*
<i>Lengthy pre-construction phase</i>				
a	Perform a pre-construction planning of project tasks and resources needs		*	*
b	Mitigating external influencing factors	*	*	
c	In-time fulfillment of tendering formalities	*		
d	Client dissatisfaction matters	*		

(continued)

Table 1 (continued)

No.	Strategy	Memon et al. [28]	Memon et al. [29]	Sambasivan and Yau [4]
<i>Cost estimation technique</i>				
a	Enhance the coordination between architect, designer, and estimator	*		*
b	Enhance estimator skills	*		
c	Renew estimation techniques	*	*	
d	Omission of manual estimation	*		
<i>Design related issues</i>				
a	Emphasis is given to the coordination of planning pillars	*		*
b	Frequent coordination between parties involved	*	*	*
c	Establish building information modeling (BIM) system in design		*	
d	Choosing parties involved among competent personnel and entities		*	
<i>Management related issue</i>				
a	Strengthen with skilled and qualified management	*	*	
b	Develop human resources management in the construction industry			*
c	Overcome the scarcity of human resources			*
d	Establish training program	*	*	
<i>Poor project (site) management</i>				
a	Employ skilled and efficient management staffs	*	*	*
b	Employ skilled and efficient supervision staffs	*	*	*
c	Standard operating procedures (SOP) are devised	*		
d	Frequent progress meeting		*	
<i>Additional works</i>				
a	Efforts to be taken during planning phase to estimate an additional work	*		*
b	Avoiding undefined goals and scope	*		
c	Comprehensive contract administration		*	

3 Research Methodology

The research methodology for this study was designed to carry out the research work systematically. This study adopted quantitative approach by conducting questionnaire survey. Questionnaire survey is conducted in order to collect the data from the respondents regarding the strategy of current construction industry in dealing with cost overrun issues. The questionnaires were distributed through face-to-face survey and online survey. Sampling of the population was carefully

chosen to have equal participation among the construction stakeholder in Penang state, Malaysia. The data obtained were analyzed by using Relative Important Index (RII) method.

The RII was used to evaluate the ratings of the respondents in the study. This approach was recommended in past studies [21, 22] as the appropriate analytical approach to group ratings of the variables in a given set. The analysis involved the computation of the RII, which is the representative rating point for the collective rating made for each variable in the subset. The five-point Likert scale ranged from 1 (not important) to 5 (very important) was adopted and transformed for each strategy as follows:

$$\text{RII} = \frac{\sum_{i=1}^5 W_i X_i}{A \times N} \quad (1)$$

W_i = Weighting given to each factor by respondents ranging from 1 to 5

X_i = Frequency of the response given from each strategy

A = Highest weight (i.e. 5 in this case)

N = Total number of participants

Based on Eq. 1, the RII for all the attributed were determined first for client, contractor and consultant categories separately, and then for overall samples.

4 Data Analysis

A total of 108 questionnaire sets were distributed randomly amongst the personnel involved in construction industry whereby 48 sets of questionnaire were accomplished through online survey and 60 sets of questionnaire were distributed hand on and collect. Response obtained back were 65 sets of completed questionnaire, while 3 sets of questionnaire were found incomplete and considered as invalid. The rate of responses for the survey is 62.96 % while the rate of valid responses rate for the survey is 60.19 %. The response rate in this study is common and acceptable. Yong and Mustaffa [23] agree that the normal response rate in construction research for postal questionnaire is around 20–30 %.

4.1 Position of Respondents

The positions of the respondents were divided into four categories. The respondents are majorities from technical categories (62 %), middle level management (18 %), top level management (17 %) and low level management (3 %). Technical categories involve civil engineer, site engineer, project engineer, design engineer, contract and technical engineer, architect and quantity surveyor.

4.2 Professional Background

A total of 41 % of the respondents are from civil engineering background, while 29 % from other professional field such as chemical engineering, electrical and electronic engineering, mechanical engineering, marketing, and business management. Respondents with quality surveying and project management professionalism are 15 and 12 % respectively. Only 3 % of the respondents are from architecture professionalism.

5 Results and Findings

Table 2 shows the summary of relative importance index (RII) and ranks (R) of the strategies that were investigated in this research from client, contractor and consultant viewpoints. The ranks are based on relative important index (RII) value.

Based on clients' views, the "exploration raw material resources from overseas" (RII = 0.958) and "utilization of raw material resources from overseas" (RII = 0.958) are the most important strategy. Prefer to rent machinery (RII = 0.667) and establish Building Information Modeling (BIM) system in design (RII = 0.667) was categorised as least important strategy. Based on the study conducted by [24], client's demand for BIM system in local industry is low. One of the reasons is the level of awareness of BIM and the knowledge about BIM is still low [25].

For the contractors' views, frequent coordination between parties involved (RII = 0.831) as the first important strategy and second important strategy was employ skilled and efficient management staffs (RII = 0.826). According to [26], effective staff management can reduce labour costs and thereby increase profit for company. Harty et al. [27] also pointed out that China and India put a significant strain on construction resources and increases the demand for skilled labour. The least important strategy ranked by the contractors was prefer to contract machinery (RII = 0.656).

On the other hand, for the consultants' views, efforts to be taken during planning phase to estimate an additional work (RII = 0.860) considered as first important strategy while exploration raw material resources from overseas (RII = 0.640) was indicated as the least important strategy.

There are some differences in point of view of contractors, clients and consultants regarding the important level of the strategy. Clients ranked "exploration raw material resources from overseas" as the most important strategy while this strategy is contradicted with the point of view of contractors and consultant. Both contractors and consultants ranked the exploration raw material resources from overseas as the least important strategy.

Table 2 Related importance of strategies in dealing with cost overrun issues

No.	Main category	Strategies	Client		Contractor		Consultant	
			RII	R	RII	R	RII	R
1	Fluctuation in price of raw material	Exploration raw material resources from overseas	0.958	1	0.662	43	0.604	44
2	Management related issues	Establish training program	0.767	27	0.749	27	0.780	23
3	Lengthy pre-construction phase	Perform a pre-construction planning of project tasks and resources needs	0.833	14	0.821	3	0.850	2
4	High cost of machineries	Prefer to rent machinery	0.667	4	0.703	3	0.775	3
5	Lowest bidding procurement method	Evaluate bid with lowest possible practical working rates	0.833	1	0.745	3	0.790	1
6	Poor project (site) management	Employ skilled and efficient supervision staffs	0.833	14	0.815	6	0.830	7
7	Government policies	Avoid uncertain economic policies	0.700	40	0.733	33	0.730	40
8	Unstable cost of manufactured material	Effective monitoring over manufactured material cost	0.800	27	0.774	11	0.800	10
9	Cost estimation technique	Enhance the coordination between architect, designer and estimator	0.800	2	0.821	1	0.850	1
10	Design related issues	Emphasis is given to the coordination of planning pillars	0.917	3	0.785	13	0.780	23
11	Poor project (site) management	Standard operating procedures (SOP) are devised	0.917	3	0.774	15	0.780	23

This result shows the similarity in opinions of contractors and consultants. Contractors ranked “avoid uncertain economic policies” as an important strategy while this strategy is vice versa for both consultants and clients. The best interpretation for such differences in that the nature of work for each party is different such as emphasis is given to the coordination of planning pillars and standard operating procedures are devised. Both of the strategies are ranked in different position by clients, contractors and consultants from different point of view. Another example is emphasis is given to the coordination of planning pillars. Client ranked it as third position, contractor ranked it as third-teen position while consultant ranked it as twenty-third position.

6 Conclusion

Financial resources are so limited in developing countries like Malaysia; hence, effective cost management is crucial to create a balance in term of financial viability in construction project. Therefore, carrying out a research in this area will have a paramount importance. In conclusion, this paper, through a variety of data, has demonstrated an increasing awareness of issues that leads to cost overruns in construction projects. On one hand, construction stakeholders namely clients, contractors and consultants do have different strategies in dealing with cost overrun issues. On the other hand, they do agree that the consideration of related issues and with their strategies could significantly improve the overall cost overrun issues.

Acknowledgments The authors express gratefully acknowledgment to the industry stakeholders for their valuable contributions towards the success of this research. This research is fully funded by Ministry of Education (Malaysia) and Universiti Tun Hussein Onn Malaysia (UTHM) under Vot: E043, Exploratory Research Grant Scheme (ERGS) Phase 1/2013.

References

1. N. Azhar, R.U. Farooqui, S.M. Ahmed, in *Cost Overrun Factors in Construction Industry of Pakistan*. Advancing and Integrating Construction Education, Research and Practice (2008), pp. 499–508
2. S. Durdyev, S. Ismail, N.A. Bakar, Factors causing cost overruns in construction of residential projects: case study of Turkey. *Int. J. Sci. Manage.* **3**, 12 (2012)
3. A.H. Memon, I. Abdul Rahman, M.R. Abdullah, A.A. Abdu Azis, Factors affecting construction cost in MARA large construction project: perspective of project management consultant. *Int. J. Sustain. Constr. Eng. Technol.* **1**, 41–54 (2011)
4. M. Sambasivan, W.S. Yau, Causes and effects of delays in Malaysian construction industry. *Int. J. Project Manage.* **25**, 517–526 (2007)
5. I.R. Endut, A. Akintoye, J. Kelly, *Cost and Time Overruns of Projects in Malaysia* (School of Build and Natural Environment, Glasgow Caledonian University, 2009)
6. A.S. Ali, S.N. Kamaruzzaman, Cost performance for building construction projects in Klang valley. *J. Build. Perform.* **1**, 110–118 (2010)
7. P.E. Truman, D. King, Assessment of Problems Associated with Poor Project Management Performance (2013)
8. A.A.A. Azis, A.H. Memon, I.A. Rahman, Q.B.A.I. Latif, S. Nagapan, Cost management of large construction projects in south Malaysia, in *Business, Engineering and Industrial Applications (ISBEIA)* (2012), pp. 625–629
9. K.C. Goh, J. Yang, Importance of sustainability-related cost components in highway infrastructure: perspective of stakeholders in Australia. *J. Infrastruct. Syst.* **20**, 04013002 (2013)
10. A.-D.D. Dominic, S.D. Smith, Rethinking construction cost overruns: cognition, learning and estimation. *J. Financ. Manage. Property Constr.* **19**, 38–54 (2014)
11. K.C. Goh, J. Yang, Managing cost implications for highway infrastructure sustainability. *Int. J. Environ. Sci. Technol.* **18**, 1–10 (2014)
12. A.A.A. Azis, A.H. Memon, I.A. Rahman, A.T.A. Karim, Controlling cost overrun factors in construction projects in Malaysia. *Res. J. Appl. Sci. Eng. Technol.* (2013)

13. I.A. Rahman, A.H. Memon, A.A.A. Azis, N.H. Abdullah, Modeling causes of cost overrun in large construction projects with partial least square-SEM approach: contractor's perspective. *Res. J. Appl. Sci.* **5** (2013)
14. W. Guangbin, Y. Zhang, T. Dan, Research on cost calculation theory and method of construction project based on BIM. *Sci. Technol. Prog. Policy* **21**, 014 (2009)
15. I. Dikmen, M.T. Birgonul, S. Han, Using fuzzy risk assessment to rate cost overrun risk in international construction projects. *Int. J. Project Manage.* **25**(5), 494–505 (2007)
16. A.H. Memon, I. Abdul Rahman, A.A. Abdul Azis, Preliminary study on causative factors leading to construction cost overrun. *Int. J. Sustain. Constr. Eng. Technol.* **2** (2011)
17. A. Enshassi, J. Al-Najjar, M. Kumaraswamy, Delays and cost overruns in the construction projects in the Gaza Strip. *J. Financ. Manage. Property Constr.* **14**, 126–151 (2009)
18. T.Y. Lo, I.W. Fung, K.C. Tung, Construction delays in Hong Kong civil engineering projects. *J. Constr. Eng. Manage.* **132**, 636–649 (2006)
19. L.-H. Long, Y.D. Lee, J.Y. Lee, Delay and cost overruns in Vietnam large construction projects: a comparison with other selected countries. *KSCE J. Civil Eng.* **12**, 367–377 (2008)
20. A.R. Ibrahim, M.H. Roy, Z. Ahmed, G. Imtiaz, An investigation of the status of the Malaysian construction industry. *Benchmark Int. J.* **12**, 294–308 (2010)
21. A. Kazaz, E. Manisali, S. Ulubeyli, Effect of basic motivational factors on construction workforce productivity in Turkey. *J. Civil Eng. Manage.* **14**, 95–106 (2008)
22. A.E. Olusegun, A.O. Michael, Abandonment of construction projects in Nigeria: causes and effects. *J. Emerg. Trends Econ. Manage. Sci. (JETEMS)* **2**, 142–145 (2011)
23. Y.C. Yong, N.E. Mustaffa, Clients, consultants, and contractors' perception of critical success factors for construction projects in Malaysia, in *Proceeding of the 27th Annual ARCOM Conference*, University of West England (2011)
24. X.Q. Teo, A study of building information modelling (BIM) in Malaysia construction industry. Bachelor (Hons.) of Quantity Surveying, Faculty of Engineering and Science, Universiti Tun Abdul Rahman (2012)
25. Z. Zahrizan, N.M. Ali, A.T. Haron, A. Marshall-Ponting, Z. Abd, Exploring the adoption of building information modelling (BIM) in the Malaysian construction industry: a qualitative approach. *Int. J. Res. Eng. Technol.* (2013)
26. I.A. Rahman, A.H. Memon, A.T.A. Karim, Relationship between factors of construction resources affecting project cost. *Mod. Appl. Sci.* **7**, 67 (2012)
27. C. Harty, C.I. Goodier, R. Soetanto, S. Austin, A.R. Dainty, A.D. Price, The futures of construction: a critical review of construction future studies. *Constr. Manage. Econ.* **25**, 477–493 (2007)
28. Z.A. Memon, A.H. Chohan, Q.M. Moin, N.A. Memon, A.I.C. Ani, Issues of cost inflation in construction sector and strategy for its prevention in developing economy, a study of the Pakistan. *Am. J. Sci. Res.* (2012)
29. A.H. Memon, I.A. Rahman, A.A.A. Azis, Time and cost performance in construction projects in southern and central regions of peninsular Malaysia. *Int. J. Adv. Appl. Sci.* **1**, 45–52 (2012)

Risk Level of Factors Contributing to Waste Generation in Construction Phase

Ismail Abdul Rahman, Nor Solehah Md Akhir,
Aftab Hameed Memon and Sasitharan Nagapan

Abstract Construction waste generation is a common problem in the construction industry of Malaysia. This generation of construction waste is occurred due to several factors. Each factor has a different level of risk on the construction performance which is important to determine for effective waste management. Hence, this study is conducted to determine the risk level of various factors contributing to waste generation in the construction phase. A total of 32 factors identified from the literature review were investigated through questionnaire survey. Survey was done using Delphi technique with 2 rounds. Delphi round 1 aimed to determine the risk level of each factor while round 2 focused on confirming the findings of round 1. The panel of expert participating in round one of data collection consisted of 15 experts while, in round two, 11 experts participated. Data collected for probability of occurrence and severity level during round 1, was analyzed with Average Index (AI) formula. Calculated AI values were further analyzed with a risk matrix. Results showed that 14 factors have high risk level while 18 factors have medium risk level. Analysis of round 2 highlighted that the experts agreed with the determined risk level of all the factors except 2 factors i.e. equipment failure and supplier errors. Results also indicate that the factors in the category Human Resource/Manpower are the most severe factors contributing to the generation of construction waste on site. These findings will help the practitioners to prepare an effective strategy to control the waste problem.

Keywords Risk level · Construction waste · Malaysia

I.A. Rahman (✉) · N.S.M. Akhir · A.H. Memon · S. Nagapan
Faculty of Civil and Environmental Engineering, University Tun Hussein Onn Malaysia,
Batu Pahat, Johor, Malaysia
e-mail: ismailar@uthm.edu.my

N.S.M. Akhir
e-mail: solehahakhir@gmail.com

A.H. Memon
e-mail: aftabm78@hotmail.com

S. Nagapan
e-mail: sasi81@yahoo.com

1 Background

Construction industry is very important role player in improving socio-economic condition of any country. It provides the necessary infrastructure, and physical structure for activities such as business, services and utilities [1]. Moreover, it offers several job opportunities, foreign and local investment opportunities [2]. However, the industry is facing the problem of construction waste generation worldwide including Malaysia. Reference [3] stated that wastage level for materials waste in construction projects of Malaysia is up to 10 %. Due to waste generation, one of the major issues faced is increase in the illegal dumpsites nationwide. As reported by Begum and Pereira [4], in Klang Valley only 20 % of C&D waste is disposed at legal landfill while the others are disposed at illegal landfill or private lands.

One of major reasons for these practices of disposing waste into illegal landfills is lack of awareness regarding the construction waste management. Thus, it can be seen commonly, waste disposal is practiced by the practitioners in Malaysia rather than adopting other waste management processes such as reuse, recycle and other [5, 6]. Other than, dumping the waste, a number of contractors eliminate their material waste by practicing open burning (especially timber and packaging waste) and buried (concrete waste especially from piling) [3]. This generation of waste has a negative impact to the environment, cost, productivity, time, social and economy of the industry [6, 7]. In addition, production of waste may weaken the efficiency, effectiveness, value and profitability of construction activities [8].

This waste generation in construction projects is occurred due to several factors which are very important to know for reducing waste at the source as it is the most effective measure in waste management [3]. As each factor causing waste generation have different level of risk, hence, this study is carried out to determine the risk of various factors contributing to waste generation. Knowing risk level of the factors will help the practitioners in preparing an effective strategy to reduce the waste generation.

2 Construction Waste Factor

There are various factors which contribute to the generation of construction waste. Various researchers have highlighted several factors of waste generation worldwide. A study conducted in India revealed that factors of construction waste generation are Design, Operational, Material handling, and Procurement related issues. Reference [9] highlighted that 5 major reasons of construction waste generation in Malaysia include poor site management or supervision, lack of experience, inadequate planning and scheduling, mistakes and errors in design, and mistakes during construction. Reference [10] notified that contractors and consultants agreed that rework, design changes and revision, and waste from uneconomical shapes are major contributors to the material waste generation in Nigeria. Reference [11]

conducted research in Turkish construction projects found that major reasons of material waste include ordering of materials that do not fulfill project requirements defined on design documents, imperfect planning of construction and workers mistakes during operation.

Reference [12] conducted a study to identify the causative factors of waste and found that last minute client requirement was the most significant cause leading to design variation, cost of construction materials. Reference [3] mentioned that overall site management, size of the project and lack of awareness of waste management among construction personnel are common factors of waste generation in construction projects. In order to find the factors causing construction waste in Malaysia and assessing their relative risk, a comprehensive literature review was carried out, and 32 common factors were identified and classified in 7 groups which are Information and Communication (ICT), Equipments, Project and Contract Management, Material, Delivery/Procurement, External/Unpredictable and Human Resources/Manpower as shown in Table 1.

3 Research Methodology and Data Collection

Data was gathered by using questionnaire survey through Delphi Method. Delphi method is a qualitative research method where a panel of experts is asked to provide feedback and answer on particular questions, and it usually involves several iteration or rounds of question [16]. In this study, Delphi method was carried out in 2 rounds where round 1 survey focused on identifying the risk level of each factor. The experts were asked to rank the probability of occurrence and level of severity for each factors using 5 likert point scale as defined in Table 2.

Data analysis was performed statistically to assess the probability of occurrence and level of severity of the factors. It was done with Average Index (AI) method by using Eq. 1 adopted from [30, 34].

$$AI = \frac{\sum(1X_1 + 2X_2 + 3X_3 + 4X_4 + 5X_5)}{\sum(X_1 + X_2 + X_3 + X_4 + X_5)} \quad (1)$$

where;

X_1 Number of respondents for scale 1;

X_2 Number of respondents for scale 2;

X_3 Number of respondents for scale 3;

X_4 Number of respondents for scale 4;

X_5 Number of respondents for scale 5.

Risk matrix technique was adapted from [35] in order to calculate risk level of each factor. Figure 1 shows 5×5 risk matrix used in this study where probability of occurrence ranges from 1 to 5 on the vertical axis and severity level on the horizontal axis. Risk matrix has three different zones where each zone describes

Table 1 Mapping of factors causing construction waste generation

No.	Factors contributing to construction waste	References																									
		[13]	[111]	[114]	[115]	[112]	[116]	[6]	[17]	[18]	[19]	[20]	[21]	[22]	[23]	[24]	[25]	[26]	[27]	[28]	[3]	[29]	[10]	[31]	[32]	[33]	
1	Poor coordination between parties	/	/	/	/	/	/	/	/	/	/	/	/	/	/	/	/	/	/	/	/	/	/	/	/	/	/
2	Poor information quality	/	/	/	/	/	/	/	/	/	/	/	/	/	/	/	/	/	/	/	/	/	/	/	/	/	/
3	Delay information flow among parties	/	/	/	/	/	/	/	/	/	/	/	/	/	/	/	/	/	/	/	/	/	/	/	/	/	/
4	Unsuitable tools used	/	/	/	/	/	/	/	/	/	/	/	/	/	/	/	/	/	/	/	/	/	/	/	/	/	/
5	Shortage of equipment	/	/	/	/	/	/	/	/	/	/	/	/	/	/	/	/	/	/	/	/	/	/	/	/	/	/
6	Equipment failure	/	/	/	/	/	/	/	/	/	/	/	/	/	/	/	/	/	/	/	/	/	/	/	/	/	/
7	Lack of legal enforcement	/	/	/	/	/	/	/	/	/	/	/	/	/	/	/	/	/	/	/	/	/	/	/	/	/	/
8	Error in contract documentation	/	/	/	/	/	/	/	/	/	/	/	/	/	/	/	/	/	/	/	/	/	/	/	/	/	/
9	Last minute client requirements	/	/	/	/	/	/	/	/	/	/	/	/	/	/	/	/	/	/	/	/	/	/	/	/	/	/
10	Lack of waste management plans	/	/	/	/	/	/	/	/	/	/	/	/	/	/	/	/	/	/	/	/	/	/	/	/	/	/
11	Mistakes in quantity surveys	/	/	/	/	/	/	/	/	/	/	/	/	/	/	/	/	/	/	/	/	/	/	/	/	/	/
12	Rework	/	/	/	/	/	/	/	/	/	/	/	/	/	/	/	/	/	/	/	/	/	/	/	/	/	/
13	Vandalism at site	/	/	/	/	/	/	/	/	/	/	/	/	/	/	/	/	/	/	/	/	/	/	/	/	/	/
14	Poor quality of materials	/	/	/	/	/	/	/	/	/	/	/	/	/	/	/	/	/	/	/	/	/	/	/	/	/	/

(continued)

Table 1 (continued)

No.	Factors contributing to construction waste	References																											
		[13]	[11]	[14]	[15]	[12]	[16]	[6]	[17]	[18]	[19]	[20]	[21]	[22]	[23]	[24]	[25]	[26]	[27]	[28]	[3]	[29]	[10]	[31]	[32]	[33]			
15	Ordering errors	/	/	/		/	/	/												/					/				
16	Items not in compliance with specification	/	/	/									/														/		
17	Inventory of materials not well documented				/																						/		
18	Inappropriate use of materials			/																/									
19	Supplier errors																												
20	Wrong material delivery procedures																										/		
21	Damage during transportation	/		/		/							/														/		
22	Wrong material delivery procedure																										/		
23	Effect of weather	/	/	/										/													/		
24	Damages caused by third parties			/																									
25	Unforeseen ground conditions									/																			
26	Poor attitudes of workers	/	/	/		/																				/	/		
27	Damage caused by workers	/	/							/																	/		
28	Insufficient training for workers			/																							/		

(continued)

Table 2 Scale represents the probability of occurrence and level of severity

Scale	Description	
	Probability of occurrence	Level of severity
1	Not occur	No significant
2	Slightly occur	Slightly significant
3	Moderately occur	Moderately significant
4	Often occur	Very significant
5	Very often occur	Extremely significant



Fig. 1 Risk matrix (Adapted from [35])

different level of risk. Green zone indicates that the risk is in low level and can be ignored; yellow zone indicates that risk is in moderate level, and red zone shows that the risk is in high level.

Delphi round 2 focused on confirming the result obtained from the Delphi round 1. Same panel of experts who participated in round 1 were presented the risk level of each factor which obtained from the first round survey and were asked about their agreeability with the findings. The analysis of the data was carried out with frequency analysis.

4 Results and Discussion

4.1 Respondent Demography

In the process of data collection, a panel of expert practitioners from construction industry was selected. In round 1, a total of 15 experts participated. Among the panel, 9 respondents are contractors, 3 consultants, and 3 clients. These respondents are holding different working positions in their organizations which include 1 Senior Project Manager, 3 Project Managers, 2 Assistant Project Managers, 1 Safety and Health Manager, 6 Engineers, 1 Contract Executive and 1 Partner. While, in the second round of data collection, only 11 respondents participated. All the experts participating in data collection process have working experience for more than 10 years.

4.2 Risk Level of the Factors

For assessing risk level of the factors, AI values of probability of occurrence and severity level for each factor were plotted on risk matrix. The results of the occurrence, severity and risk level are presented in Table 3 where red colour shows that the factors have high risk level while yellow colour shows that the risk level of the factors is medium. Table 3 indicates that out of 32 investigated factors, 14 factors have high risk while 18 factors have medium risk. The level of agreeability for determined risk level of the factors was calculated based on frequency and percentage. The results of the agreeability are presented in Table 3.

Table 3, highlights that, among high risk factors, last minute client requirements factor is the most significant as agreed by 10 of 11 experts. This finding coincided with the findings of others research works carried out by Refs. [12, 18, 36] where this factor was found as the most significant factor in contributing to construction waste generation. Last minute client requirements may also contribute to design variation [12, 18, 22, 37, 38]. According to Zhao and Chua [39] frequent changes of design is a common problem occurring in the construction project. On the other

Table 3 Risk level of factors and percentage of agreeability from panels

No	Factors	Category	Delphi Round 1		Delphi Round 2			
			Risk Level		Agree		Disagree	
					Frequency	Percentage (%)	Frequency	Percentage (%)
1	Effect of weather	EXT	3.7	3.7	9	81.8	2	18.2
2	Poor workmanship	HRM	3.5	3.6	9	81.8	2	18.2
3	Poor attitudes of workers	HRM	3.0	3.3	7	63.6	4	36.4
4	Insufficient training for workers	HRM	3.0	3.1	8	72.7	3	27.3
5	Lack of experience	HRM	2.8	3.0	9	81.8	2	18.2
6	Lack of knowledge on construction	HRM	2.7	3.0	7	63.6	4	36.4
7	Poor coordination between parties	ICT	3.0	3.3	7	63.6	4	36.4
8	Delay in information flow among parties	ICT	3.2	3.3	8	72.7	3	27.3
9	Last minute client requirements	PCM	3.5	3.5	10	90.9	1	9.1
10	Ordering errors	MAT	2.7	3.1	8	72.7	3	27.3
11	Items not in compliance with specification	MAT	2.6	3.0	6	54.5	5	45.5
12	Rework	PCM	2.9	3.4	9	81.8	2	18.2
13	Equipment failure	EQP	3.0	3.0	4	36.4	7	63.6
14	Unforeseen ground conditions	EXT	2.7	3.1	9	81.8	2	18.2
15	Effect of accidents at site	EXT	2.6	2.6	8	72.7	3	27.3
16	Damage caused by workers	HRM	2.7	2.9	8	72.7	3	27.3
17	Poor quality of information	ICT	2.4	2.6	10	90.9	1	9.1
18	Poor quality of materials	MAT	2.6	2.9	9	81.8	2	18.2
19	Inappropriate use of materials	MAT	2.5	2.8	8	72.7	3	27.3
20	Lack of enthusiasm among workers	HRM	2.5	2.7	7	63.6	4	36.4
21	Unsuitable tools used	EQP	2.3	2.2	7	63.6	4	36.4
22	Vandalism at site	EXT	2.2	2.3	7	63.6	4	36.4
23	Lack of waste management plan	PCM	3.1	2.9	8	72.7	3	27.3
24	Lack of legal enforcement	PCM	2.6	2.4	8	72.7	3	27.3
25	Shortage of equipment	EQP	2.6	2.2	10	90.9	1	9.1
26	Damage during transportation	DEL	2.3	2.5	9	81.8	2	18.2
27	Inventory of materials not well documented	MAT	2.4	2.1	10	90.9	1	9.1
28	Mistakes in quantity estimations	PCM	2.7	2.9	10	90.9	1	9.1
29	Damages caused by third parties	EXT	2.3	2.7	9	81.8	2	18.2
30	Supplier errors	DEL	2.4	2.4	5	45.5	6	54.5
31	Wrong material delivery procedures	DEL	2.4	2.7	7	63.6	4	36.4
32	Error in contract document	PCM	2.3	2.7	9	81.8	2	18.2

Note Information and communication (ICT), Equipments (EQP), Project and contract management (PCM), Material (MAT), Delivery/Procurement (DEL), External/Unpredictable (EXT) and Human Resources/Manpower (HRM)

hand, for the factor equipment failure, 7 of 11 panels did not agree with the determined risk level. They argued that this factor has a medium level of risk.

Further, it is noted that, among the 14 of high risk factors, five factors are from Human Resource/Manpower (HRM) category of factors, two factors from Information and Communication (ICT) category, two factors in the category of Project and Contract Management (PCM), two factors in the category of Material (MAT), two factors from category External/Unpredictable (EXT), and only one factor in category Equipments (EQP). This shows that Human Resource/Manpower (HRM) category of factors is most critical in causing construction waste generation in construction projects.

5 Conclusion

This study determined the risk level of various factors contributing to construction waste generation. It investigated 32 common factors of waste generated which were identified through literature review. Data collection was carried out with Delphi method consisting of two rounds. Average index and risk analysis of the collected data in the first round of Delphi showed that 14 factors have high risk level while 18 factors have medium risk level. The findings were agreed by the respondents in the second round of Delphi. From the findings, it was highlighted that last minute client requirements is the most significant factor while Human Resource/Manpower (HRM) category of factors is the most critical category in contributing to construction waste generation. These findings are very helpful for the practitioner to prepare effective waste management strategy for overcoming this problem of construction waste generation.

Acknowledgment The authors would like to thank Universiti Tun Hussein Onn Malaysia for supporting this study under FRGS1221. A lot of thanks to construction industry players who gave important information to achieved desired feedback required for this research work.

References

1. R.A. Khan, M.S. Liew, Z. Ghazali, Malaysian construction sector and Malaysia vision : 2020 developed nation status, in *Second World Conference On Business, Economics And Management—WCBE M 2013*, vol. 109 (2014), pp. 507–513
2. M.A. Wibiwo, The contribution of the construction industry to the economy of Indonesia: a systemic approach (2003)
3. A.F. Masudi, C.R.C. Hassan, N.Z. Mahmood, S.N. Mokhtar, N.M. Sulaiman, Construction waste quantification and benchmarking: a study in Klang valley, Malaysia. *J. Chem. Chem. Eng.* **5**(10), 909–916 (2011)
4. R.A. Begum, J.J. Pereira, C&D waste profile of the Malaysian construction industry need a centralized database, in *Sustainable Technologies (WCST) World Congress* (2011), pp. 73–76

5. L.C. Foo, I.A. Rahman, A. Asmi, S. Nagapan, K.I. Khalid, Classification and quantification of construction waste at housing project site. *Int. J. Zero Waste Gener.* **1**(1), 1–4 (2013)
6. J.-Y. Wang, X.-P. Kang, V.W.-Y. Tam, An investigation of construction wastes: an empirical study in Shenzhen. *J. Eng. Design Technol.* **6**(3), 227–236 (2008)
7. M. Marzouk, S. Azab, Environmental and economic impact assessment of construction and demolition waste disposal using system dynamics. *Resour. Conserv. Recycl.* **82**, 41–49 (2014)
8. S. Augustine, Managing waste and cost in the construction industry : a case study of the road construction. Kwame Nkrumah Univ. Sci. Technol. (2011)
9. S. Nagapan, I.A. Rahman, A. Asmi, A. Hameed, R.M. Zin, Identifying causes of construction waste—case of central region of Peninsula Malaysia. *Int. J. Integr. Eng.* **4**(2), 22–28 (2012)
10. T.O. Adeweyu, M. Oтали, Evaluation of causes of construction material waste—case of Rivers State, Nigeria. *Ethiop. J. Environ. Stud. Manage.* **6**(6), 746–753 (2013)
11. G. Polat, G. Ballard, Waste in Turkish construction, in *Proceedings of the 12th Annual Conference of the International Group for Lean Construction IGLC-12*, August, Denmark (2004), pp. 488–501
12. A.B. Wahab, A.F. Lawal, An evaluation of waste control measures in construction industry in Nigeria. *Afr. J. Environ. Sci. Technol.* **5**(3), 246–254 (2011)
13. L.L. Ekanayake, G. Ofori, Building waste assessment score: design-based tool. *Build. Environ.* **39**(7), 851–861 (2004)
14. G.L. Garas, A.R. Anis, A. El Gammal, Materials waste in the Egyptian construction industry (2001), pp. 1–8
15. E.M. Nazez, D. Zaldi, B. Trigunaryyah, Identification of construction waste in road and highway construction projects, in *Proceedings Eleventh East Asia-Pacific Conference on Structural Engineering and Construction (EASEC-11)*, vol. 2008 (2008), pp. 1–7
16. W. Lu, H. Yuan, A framework for understanding waste management studies in construction. *Waste Manage.* **31**(6), 1252–1260 (2011)
17. C.T. Formoso, L. Soboilmen, C. De Cesare, E.L. Isatto, Material waste in building industry main causes and prevention. *J. Constr. Eng. Manage.* **128**(4), 316–325 (2003)
18. C.S. Poon, A.T.W. Yu, L. Jaillon, Reducing building waste at construction sites in Hong Kong. *Constr. Manage. Econ.* **22**(5), 461–470 (2004)
19. V.W.Y. Tam, L.Y. Shen, I.W.H. Fung, J.Y. Wang, Controlling construction waste by implementing governmental ordinances in Hong Kong. *Constr. Innov. Inf. Process Manage.* **7**(2), 149–166 (2007)
20. S.K. Wan, M.M. Kumaraswamy, D.T. Liu, Contributors to construction debris from electrical and mechanical work in Hong Kong infrastructure projects. *J. Constr. Eng. Manage.* **135**(7), 637–646 (2009)
21. H. Yunpeng, Minimization management of construction waste, in *2011 International Symposium on Water Resource and Environmental Protection (ISWREP)*, China (2011), pp. 2769–2772
22. M. Osmani, J. Glass, A.D.F. Price, Architects' perspectives on construction waste reduction by design. *Waste Manage.* **28**(7), 1147–1158 (2008)
23. A.F. Urio, A.C. Brent, Solid waste management strategy in Botswana : the reduction of construction waste. *J. S. Afr. Inst. Civil Eng.* **48**(2), 18–22 (2006)
24. O.F. Kofoworola, S.H. Gheewala, Estimation of construction waste generation and management in Thailand. *Waste Manage.* **29**(2), 731–738 (2009)
25. K. Agyekum, J. Ayarkwa, E. Adinyira, Consultants' perspectives on materials waste reduction in Ghana. *Eng. Manage. Res.* **1**(1), 138–150 (2012)
26. K. Panos, G.I. Danai, Survey regarding control and reduction of construction waste, in *PLEA2012—28th Conference, Opportunities, Limits and Needs Towards an Environmentally Responsible Architecture Lima*, Perú, 7–9 Nov 2012
27. R. Ikau, R. Tawie, C. Joseph, Initial findings on perspectives of local contractors on waste minimization barriers and incentives on construction sites, in *2013 IEEE Business Engineering and Industrial Applications Colloquium (BEIAC)* (2013), pp. 506–509

28. L.Y. Shen, V.W.Y. Tam, C.M. Tam, S. Ho, Material wastage in construction activities—a Hong Kong survey, in *CIB W107: Creating a Sustainable Construction Industry in Developing Countries* (2002), pp. 1–7
29. A. Al-Hajj, K. Hamani, Material waste in the UAE construction industry main causes and minimisation practices. *Archit. Eng. Design Manage.* **7**(4), 221–235 (2011)
30. A.H. Memon, I.A. Rahman, I. Memon, N.I.A. Azman, BIM in Malaysian construction industry: status, advantages, barriers and strategies to enhance the implementation level. *Res. J. Appl Sci. Eng. Technol.* **8**(5), 606–614 (2014)
31. R.B. Surve, S.S. Kulkarni, Construction waste reduction—a case study. *Int. J. Eng. Res. Technol. (IJERT)* **2**(8), 870–875 (2013)
32. N. Domingo, M. Osmani, A.D.F. Price, Reducing construction waste in healthcare facilities: a project lifecycle approach (2008)
33. A.O. John, D.E. Itodo, Professionals’ views of material wastage on construction sites and cost overruns. *Int. J. Organ. Technol. Manage. Constr.* **5**(1), 747–757 (2013)
34. A.H. Memon, I.A. Rahman, A. Asmi, A. Azis, Preliminary study on causative factors leading to construction cost overrun. *Int. J. Sustain. Constr. Eng. Technol.* **2**(1), 57–71 (2011)
35. I. Mahamid, Risk matrix for factors affecting time delay in road construction projects: owners’ perspective. *Eng. Constr. Archit. Manage.* **18**(6), 609–617 (2011)
36. M. Osmani, J. Glass, A. Price, Architect and contractor attitudes to waste minimisation, in *Proceeding of Institution of Civil Engineering, Waste and Resource Management 159 Issue WR2* (2006), pp. 65–72
37. C.S. Poon, Reducing construction waste. *Waste Manage.* **27**(12), 1715–1716 (2007)
38. J. Wang, Z. Li, V.W.Y. Tam, Critical factors in effective construction waste minimization at the design stage: a Shenzhen case study, China. *Res. Conserv. Recycl.* **82**, 1–7 (2014)
39. Y. Zhao, D.K.H. Chua, Relationship between productivity and non value-adding activity, in *Eleventh Annual Conference of the International Group for Lean Construction* (2003)

Building Sustainable Design Performance Through Integrated Value Management Practice

Mohd Nasrun Mohd Nawi, Faizatul Akmar Abdul Nifa
and Siti Halipah Ibrahim

Abstract Maintenance management is a combination of all technical and administrative actions, including supervision actions, intended to retain an item in or restore it to a state in which it can perform a required function. Value management is a proactive, creative, problem-solving service, utilizing a multi-disciplinary team-oriented plan of attack to make explicit the client's value system using functional analysis to discover the relationship between time, cost and quality with the aim of maximizing the overall operation of an establishment. Both of them are interrelated with each other for improving building performance. Alas, lack of a thorough review of design and specification has thus created so many faults and defects during the conception and construction stages in which resulted later in high upkeep costs. For overcoming that issue, this paper will explore the potential of VM approach during the conception phase of bringing on a perfect (fewer defects) design specification of a building. The standard procedure of VM methodology practice which has involved a multidisciplinary project stakeholders in order to avoid the issue over design and unnecessary maintenance costs will be concluded as well.

Keywords Value management (VM) · Building performance · Maintenance management · Integrated team approach · Construction industry

M.N.M. Nawi (✉) · F.A.A. Nifa
School of Technology Management and Logistics, Universiti Utara Malaysia,
Kedah, Malaysia
e-mail: nasrun@uum.edu.my

F.A.A. Nifa
e-mail: faizatul@uum.edu.my

S.H. Ibrahim
Department of Civil Engineering, Faculty of Engineering, Universiti Malaysia Sarawak
(UNIMAS), 94300 Kota Samarahan, Sarawak, Malaysia
e-mail: ihalipah@feng.unimas.my

1 Introduction

Malaysia is a developing nation has a very quick development process in every area including building construction. Both of the sectors either public or private have initiated the need for big and complex construction tasks. Conforming to the high demand of both parties in a short time, it is anticipated that many mistakes and defects have occurred during the conception and construction stages which will ensue later in high upkeep costs. Thus, sustainability in the design process which is considered the element of constructability and maintainability should become a vital requirement in Malaysia construction industry. The primary aim of this paper is to usher in one alternative or proposal for growing a sustainable pattern of building performance such as reducing faulty design in the maintenance aspect of by implementing the concept of value management integrated approach. As highlighted by previous researchers [1–4], with a current situation of low levels of sustainability and maintenance culture in Malaysia, implementation of prevention approach such as including integrated value management is the best strategy practice to reduce design flaws in the construction.

2 Issues and Challenges in Current Design Process

The traditional building design process is one of the primary barriers to produce a sustainable and green construction. The subject of fragmentation in design practice as it is borne out in a sequential fashion, hence contributes to poor communication, conflicts and misunderstanding between designers (or consultants) and contractors [5–9]. The current design process starts with the possessor of the projects briefly explain their requirement of projects to the project director or leader which is the principal consultant (mostly architect). Then the architect will transform the requirement into the architectural design which is then given to the structural engineer to determine the structural integrity by delivering structural analysis and design. The outcome, in a pattern of structural design combined with architectural design and specification are passed to the quantity surveyor to take out building cost estimation and determine the bill of quantity. Afterwards, all these documents are handed to the primary contractor who will then take on the responsibility to raise the building structure and liaise with the manufacturer [1]. In many years, this pattern has been disputed by the industry-led reports [10, 11] because of less performance and accessibility for good care and sustainability. This exercise also creates a significant connection with the issue of wastages, work redundancy, redesign and faulty in design. Among other challenges identified in the literature includes [1, 4, 9];

- The fragmentation of different participants in the construction project;
- Prevalence of costly engineering changes, design iterations, rework and unnecessary liability claims;

- The lack of communication between each of the disciplines involved in the growth process;
- Lack of dependable life-cycle analysis of the task;
- Constructability, supportability and maintainability issue are taken late in the operation;
- Fragmentation of design, construction and maintaining data; and
- Loss of information about design intent

In view of that, the industry follows up reports such as [12–14] have all called on the industry to change from its traditional *modus operandi* and perform better through increased collaboration and integrated plan of action. The reports challenged the building industry to produce a fully integrated service capable of delivering predictable results to clients through operations and team integration. Consequently, this report will talk over the potential of Value Management as a component of integrated team approach to be carried out in this scenario. It is established along the previous studies [1–3, 15–18] in which recommend a value management approach can create a great deal of benefits such as; could bring together various skills and knowledge, and transfers the traditional barriers towards an in force and efficient delivery of the project.

3 Value Management (VM) Definition and Concept

VM is a style of management dedicated to guiding people and promoting innovation with the target of improving overall project performance [19]. It has been applied successfully to increase the numbers of construction tasks to achieve value for money and to fulfill clients' needs [20]. It is a powerful methodology due to its ability to influence thinking, to quickly bring some alteration, to identify the basic offices and to unify a group of strong people into one collective whole [17, 21]. It is a structured approach to establish what value means to a client in filling a perceived need by, clearly defining and agreeing the project targets and showing how they can best be achieved [22]. While [23] defined VM as 'a proactive, creative, problem-solving or problem-seeking service, which maximize the functional value of a project by managing its development from concept to use through structured, team-oriented exercises which make explicit, and appraise subsequent decisions, by reference to the value requirements of the clients.'

The aim of VM is to increase the value of the output, either by enhancing its functionality and eliminating unnecessary costs [17]. As highlighted above, the philosophy of VM is based along the assumption that a certain quantity of unnecessary cost is inevitable in building design due to the inherent complexity of the procedure. Unnecessary cost is the cost that neither provides quality, purpose, life, and appearance nor customer features [24]. According to [25] value management is the term employed to identify the entire philosophy and range of technique.

Thus, value planning, value engineering and value analysis form a subset of value management.

In Value Management, there must always be a Value Outcome. The elements, items, process/system must perform what is intended to behave—it must be able to perform and function accordingly [26]. It is not simplistic “cost reduction” nor “cost cutting”. If by so doing, the component’s needed utility is sacrificed/compromised, the value to the owner has actually minimized. Increasing prices to increase the functional capacity beyond that which is needed also provides little, if at all, actual value to the owner. Anything less than functional capacity: unacceptable. Anything more than the operational capacity: unnecessary and wasteful [27].

As highlighted in the previous section, Value Management approach has been acknowledged as one of the extremely powerful tool because the application of its methodology involves Function Analysis to improve the invention procedure. In addition, Value Management (VM) is a combination of preparation tools and methods to get the optimal proportion of project benefits in relation to project costs and perils. It is the procedure of planning, appraising and producing the project in order to reach the right conclusions about the optimized balance of project benefits, risks and costs. It is like a style of management dedicated to guiding people and promoting innovation with the objective to better overall project performance [3, 28].

This approach has been used successfully to increase the numbers of construction projects to achieve value for money and to satisfy clients’ needs [1, 29]. It is also experienced as a powerful methodology due to its ability to influence thinking, to quickly bring some alteration, to identify the basic functions and to unify a group of strong people into one collective whole [2, 18]. Moreover, VM is a structured approach to establish what value means to a client in filling a perceived need by, clearly defining and agreeing the project targets and showing how they can best be achieved [28]. Fundamentally, VM is defined as ‘a proactive, creative, problem-solving or problem-seeking aid, which maximize the functional value of a task by overseeing its evolution from concept to use through structured, team-oriented exercises which make explicit, and appraise subsequent decisions, by reference to the value requirements of the clients’ [29].

In that respect are various benefits of executing VM such as [18, 30, 31]:

- Value for money by balancing between cost and functional performance
- Optimum solution can be presented
- Participation of all appropriate stakeholders so the demands of the main parties can be held
- Key decisions were rational, explicit, accountable and alternative choices were always taken
- Improve communication, teamwork and shared agreement among the key participants

Established on the advantages and value outcomes for the project, VM has received very encouraging reaction from the Government of Malaysia. The Malaysian government is using the value management in public management and adopted VM methodology in the execution of program project management.

Further to this, the Economic Planning Unit circular dated 29 December 2009 has specified that all government projects worth RM50 million and above must be completed through a value management practice. Granting to the circular, failure to comply with this circular may result in rejection of an application.

4 Approach Towards Sustainable Design Practice

In general, VM process is applied at different levels of a project, however it prefers to be given at an early phase of a task. The steps of the VM job plan can be grouped into five major stages or phases (refer Fig. 1) [1, 3]:

1. Information
2. Speculation
3. Judgement
4. Development
5. Recommendation and Action Plan

Previous section has discussed that to raise a sustainable design of a building by reducing faulty design in a building, it is necessary to integrate and assemble the facility (maintenance) managers, client, designer or any related player at the early phase of the invention procedure. Alas, in the traditional design process (including invention and build procurement), there has no structured or proper methodology towards that plan of attack. In the Value Management workshop, however, it considers the contractors' role early in the invention, thus resulting in more constructible design and bigger measure of cost savings, labor savings and less substance wastage [1, 9]. Through an early interest of construction knowledge and experience approach (during the VM workshop) can minimize the likelihood of producing plans that cannot be efficiently built (faulty design), thereby reducing design rework, improving project schedule, and establishing construction cost saving. As shown in Fig. 2, VM promotes a multi-disciplinary team approach instead of individual or segregation approach in a construction project. Furthermore, in contrast to the traditional construction practice, Value Management team are demanded to work together in concurrently either in making a decision process

Fig. 1 Five steps of the VM job plan [3]

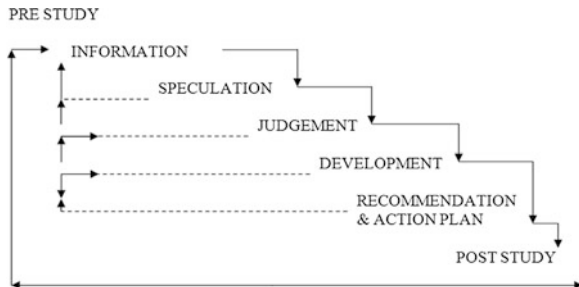
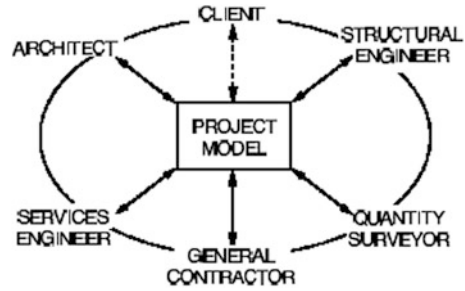


Fig. 2 An integrated project team [1]



or when trouble arises throughout of design, fabrication, and construction phases. On the other hand, the product delivery process has also been integrated to concentrate the number of distinctive parties to a single all-inclusive party [1, 3, 17]. The various separate and phased processes involved have also been combined into a system capable of pitching the same product in a single procedure. This approach indirectly will help the construction stakeholders such as contractors and designers to meet the client needs towards green and sustainable building in the future.

5 Conclusion

The traditional design process in the current practice has been heavily criticized as one of the main hindrances towards an efficient communication and integration between the stakeholders involved during the conception and building process. The building industry, especially Malaysian design practice requires a paradigm shift to produce a fully integrated service capable of delivering predictable results to clients through operations and team integration. This paper recommended that with the use of VM, the goal of a building sustainable design performance is achievable. Withal, the tangible examples of Value Management integration team framework or model in the industry are limited. Even though in that respect are many related studies focused in this arena and attempts to better construction design team integration, all the same, they act not specifically provide any guideline on how to accomplish a successful integrated VM team delivery. Consequently, this paper proposed that research into integrated VM team practice is necessary in order to raise the degree of integration and communication among stakeholders during the design stage if the wide potential of sustainable construction for both the industry and its clients is to be gained.

References

1. M.N.M. Nawi, S.M.F.W.S. Jalaluddin, F. Zulhumadi, J.A. Ibrahim, F. Baharum, Value management: a strategic approach for improving sustainability in the Malaysian government construction projects. Paper presented at joint international conference on nanoscience, engineering and management, Penang Malaysia, 19–22 Aug 2013
2. A. Jaafar, I.R. Endut, N.A.A. Bari, R. Takim, The impact of value management implementation in malaysia. *J. Sustain. Dev.* **2**(2), 210–219 (2009)
3. M.M. Che Mat, *Value Management: Principles and Applications* (Prentice Hall, Petaling Jaya, 2002)
4. F.A.A. Nifa, M.N.M. Nawi, S. Musa, W.N. Osman, Integrated project delivery framework for sustainability in design for campus development: a study on JPP UUM. Paper presented at joint international conference on nanoscience, Engineering and Management, Penang Malaysia, 19–22 Aug 2013
5. N.A. Blacud, S.M. Bogus, E. James, M. Diekmann, K.R. Molenaar, Sensitivity of construction activities under design uncertainty. *J. Constr. Eng. Manage.* **135**(3), 199–206 (2009)
6. P.E.D. Love, A.S. Sohal, Influence of organisational learning practice on reworks costs in projects, in *Proceedings of 8th International Conference On ISO 9000 & TQM (Change Management)*, CMQR at RMIT University, Melbourne, Australia (2002)
7. J.M. Kamara, C.J. Anumba, N.F.O. Evbuomwan, Establishing and processing client requirements—a key aspect of concurrent engineering in Construction. *Eng. Constr. and Archit. Manage.* **7**(1), 15–28 (2000)
8. M.N.M. Nawi, A. Lee, M.N.A. Azman, K.A.M. Kamar, Fragmentation issue in Malaysian Industrialised Building System (IBS) projects. *J. Eng. Sci. Technol. (JESTEC)* **9**(1), 97–106 (2014)
9. M.N.M. Nawi, W.N. Osman, A.I. Che-Ani, Key factors for integrated project team delivery: a proposed study in IBS Malaysian construction projects. *Adv. Environ. Biol.* **8**(5), 1868–1872 (2014)
10. M. Latham, *Constructing the Team, Final Report on Joint Review of Procurement and Contractual Agreements in the UK Construction Industry* (HMSO, London, 1994)
11. J. Egan, *Accelerating Change* (Strategic Forum for Construction, London, 2002)
12. UKCG Report, Construction in the UK Economy, The Benefits of Investment, UK Contractors Group, Construction in the UK economy (2009)
13. Achieving Excellence in Construction, *Procurement Guide 05: The Integrated Project Team: Team Working and Partnering* (Office of Government Commerce, London, 2003)
14. Strategic Forum for Construction, *The Integration Toolkit Guide: Integrated Project Team* (Strategic Forum for Construction, London, 2003)
15. Institute of Value Management, What is value management (2002), <http://www.ivm.org.uk/vmwhatis.htm>
16. Construction Best Practice Programme (CBPP), Fact sheet on value management (1998), <http://www.cbpp.co.uk>
17. N.Z. Abidin, Using value management to improve the consideration of sustainability within construction, unpublished Ph.D. Thesis, Loughborough University, UK (2002)
18. B. Trigunaryyah, Case studies on implementation of constructability improvement by construction project owners in Indonesia, in *Proceedings Clients Driving Innovation: Moving Ideas into Practice*, Gold Coast, Australia, 2006, eds. by K. Brown, K. Hampson, P. Brandon
19. SAVE International, Value methodology standard (2006), http://www.valueeng.org/catalog_monographs.php. US: SAVE International
20. Construction Best Practice Programme (CBPP), *Fact Sheet on Lean Construction* (Construction Best Practice Programme, Garston, 1998)
21. S.D. Green, *A SMART Methodology for Value Management* (Ascot, Chartered Institute of Building, 1992)

22. C.I.B. Cib, *Constructing Success: Code of Practice for Clients of the Construction Industry* (Thomas Telford, London, 1997)
23. S. Male, J.R. Kelly, S. Fernie, M. Gronqvist, G. Bowles, *The Value Management Benchmark: Research Results of an International Benchmarking Study* (Thomas Telford, London, 1998)
24. J.R. Kelly, S. Male, *Value Management in Design and Construction: The Economic Management of Projects* (E & FN Spon, London, 1993)
25. S. Nathaphan, S. Nathaphan, Sustainable value engineering model: a case study in energy cost saving. *International J. Inf. Syst. Logistics Manage. (IJISLM)* **5**(2), 39–46 (2010)
26. A.J. Dell I'sola, *Value Engineering in the Construction Industry*, 3rd edn. (Van Nostrand Reinhold, New York, 1982)
27. M.M. Che Mat, *Perceptions and Implementations of Value Management in Malaysian Construction Industry, Doctoral Dissertation, Faculty of Architecture* (Universiti Teknologi MARA, Shah Alam, Planning & Surveying, 2006)
28. Construction Industry Board, Fact sheet on value management (1997), <http://www.helios.bre.co.uk/valman/intro/cibfactsheet.html>
29. S. Male, J.R. Kelly, S. Fernie, M. Gronqvist, G. Bowles, *The Value Management Benchmark: Research Results of an International Benchmarking Study* (Thomas Telford, London, 1998)
30. R.R. Venkataraman, J.K. Pinto, *Cost and Value Management in Projects* (Wiley, New Jersey, 2010)
31. M.N.M. Nawi, K. Radzuan, N.A. Salleh, S.H. Ibrahim, Value management: a strategic approach for reducing faulty design and maintainability issue in IBS building. *Adv. Environ. Biol.* **8**(5), 1859–1863 (2014)

Homeowner's Prevalence Upkeep Behavior Towards Implementation of Home Maintenance Manual for Residential Building

Ahmad Sharim Abdullah, Nor Rima Mohd Ariff,
Robiah Abdul Rashid, Norsalisma Ismail
and Nur Nabila Mohd Tamim

Abstract Over the decades, Malaysia construction industry is experienced continuous soar growth all over the nation. In retain the property condition, it is essential to understand and well inform in upkeep management. Without a proper upkeep, degradation will gradually develop and directing to unfit property. However, to preserve a property is a tough task as the awareness of upkeep is still premature particularly in adapting upkeep on residential building. This is due to inadequate guidance and regulation for homeowner to execute and perform upkeep. Hence, to provide instructor and assistance for homeowner, a handbook of maintenance manual is needed in order them to practice upkeep accordingly. Thus, in implementing the home maintenance manual for homeowner, this paper establish a study on homeowners prevalence upkeep behaviours to understand factors that influence homeowners upkeep their dwelling.

Keywords Upkeep · Residential building · Maintenance manual

A.S. Abdullah (✉) · N.R.M. Ariff (✉) · R.A. Rashid (✉) · N. Ismail (✉)
N.N.M. Tamim (✉)

Centre of Studies for Building Surveying, Universiti Teknologi MARA (UiTM),
Shah Alam, Selangor, Malaysia
e-mail: ahmadsharim@yahoo.com

N.R.M. Ariff
e-mail: rimaariff@yahoo.com.sg

R.A. Rashid
e-mail: rubyeilza@yahoo.co.uk

N. Ismail
e-mail: salisma999@salam.uitm.edu.my

N.N.M. Tamim
e-mail: nabila6010@gmail.com

1 Introduction

In 2013 Budget tabled by Prime Minister Datuk Seri Najib Tun Razak, Malaysia economy has expanded between 4.5 and 5 % in year 2012 [1]. This was supported by the surge of the construction industry from 4.6 % in year 2011 to 15.5 % in year 2012 [2]. The increased numbers in the Budget 2013 tabled shows that the housing development is one of the prime contributed in Malaysia economic and social development as housing is a part of section in construction development [3]. Therefore, in retaining these developments keep to its top performance, it is necessary to handle scrutiny upkeep for every construction were built. Inadequate of dwelling upkeep may string to unfit dwelling in the future. This was stated by previous report of National House Condition Survey that in United Kingdom there were 14 % were still live in poor housing conditions because of the subsequence lack of upkeep works [4].

Embedded from the previous research, the homeowners' trend shows that many of the homeowners preferred to conduct upkeep after breakdown occur [5]. Even there are certain of the homeowners planned to delay the repairing works due to the thought wanting to save money [6]. This display that the insufficient knowledge have prompt the homeowners conduct upkeep based on their preference. Local authority also have to deal with this obstacle as many homeowner tends to construct upkeep works such as extension and renovation covertly from the authority. These affirm when repair and upkeep works constituted with only 16 % of the total Malaysian construction output and with uncertainty figure cannot be trace of its illegal renovation construction [7]. The uncertainty figure is where upkeep works that involving construction works that might corollary to a faulty because there are no bodies or capable professional guidance to advise them. Thought this might appear of headless act of the homeowners, however in real circumstance this occur due to lack information regarding the regulations that lead to unauthorized new structure works. As an owner of a property, they are obligate have some common knowledge to have impeccable upkeep [5]. This knowledge of upkeep can help homeowners to omit errors in their upkeep and preventing an ad hoc upkeep. As Joseph Rowntree Foundation have endorsed that: "action is needed now to prevent the national repair bill" [5].

2 Aim of Study

To provide information and guidance of implementing home maintenance manual to owner of residential building with the goals on increase living quality.

3 Objective of Study

The objective of the study was to obtain the homeowners' prevalence upkeep behavior towards implementation of home maintenance manual for residential building.

4 Problem Statement

House living in Malaysia showing a great development to be own and become homeowner. Yet still, there is issues arise as the circumstances of Malaysian homeowners' awareness in upkeep are still in learning process. This is point out as the upkeep of house-living in Putrajaya by the Perbadanan Putrajaya Malaysia was only planned when there are signs of wear and tear of the living property [8]. However, when there was fire occurred in 2009 at the Putrajaya has proven the poor maintenance planned in the country [9]. It is marks on the statement given by Former Malaysia Prime Minister, Tun Seri Abdullah Ahmad Badawi, where the country is facing a serious problem in property upkeep [10]. A competent estate agent, Chen King Hoaw, assume this issues arise because of lackadaisical behaviour of homeowner towards upkeep their property [11]. Lackadaisical will lead the homeowner's only maintain their house on basic need of the house. This is result from scarcity of homeowner knowledge in upkeep that lead them upkeep as their desire without concern unfitness the repairing and maintenance works on the building.

5 Literature Review

Homeowner is an individual that has right ownership of a particular dwelling. In conventional economic though, homeowners are acts as both the occupant and householder of their dwelling [12]. They play a large responsibility in upkeep their dwelling to prevent hefty rate of degradation over time. Homeownership offers many benefits, some of them bought due to enhance the quality of life, and some other is to enhance the financial outlook.

Numerous of homeowners are mainly concerns whether dwelling able to work than aware its physical condition. Their anxiety is particularly on the dwelling condition able to carry out the intended functions of homeowners' daily activities needs [13]. In other words, homeowners typically notably of dwelling surface and pay less attention on main structural [13]. This circumstance thought occur because lack of conscious on effect structural degradation to the dwelling. Homeowners lack of upkeep knowledge on the dwelling element and inadequate inspections could result problems in implementing upkeep works [14]. Homeowners' understanding of upkeep is important to show what works needs to be included and excluded. Subjecting in upkeep a house, there are few common upkeep works that are conduct by homeowner which are repairing, inspection, decoration, renovation, extension, housekeeping and landscaping.

5.1 *Repairing*

Repairing is a work after a breakdown had occur and a defect that is clearly on human sight for it to be rectify. To avert the repairing work, homeowners are

obligate to identify the defects before it is appear. Realization of breakdown might occur in the future must come before it is too late to conduct a repair. It is because often the cases that what may appear to be cosmetic defect in a building could be the result of the failure within the building fabric or may have led to serious deterioration within the fabric [4]. In practice, this apparently obvious and simple statement may present a very subtle problem. Even common defect like corrosion of steel is difficult to detect because it occurs, principally at the most inaccessible parts of the structure. The reason is simple, the accessible parts painted, but the inaccessible parts often are neglected.

5.2 Inspection

The inspection based on observation and repairing may conduct under ability of the homeowner's. To conduct inspection, all the elements to inspect needs an upkeep planning. This may restrict some homeowners to structural their planning dual to the hectic life. Lack of forward planning is one of the common self-management of the owners' that lead house remain the same unless it is broken [4]. However, homeowners with high income are usually will consider this aspect. There are still no reasons the situation occur but basically the high income homeowners' intent to do inspection because source of money to upkeep their dwelling [15]. Preference by city of Wichita Homeowner's Maintenance Handbook [16], the preventive upkeep conducted by homeowner where the inspection on the foundation, doors and windows, exterior walls, roof, interior surfaces, floors, electrical system, plumbing system, and etc.

5.3 Decoration

The intentions of decoration are commonly to have a comfort life. A comfortable environment is one of condition where it is freedom from annoyance and distraction, so that working or tasks can be carried out leisurely with unhindered physically or mentally [17]. Thus, many of homeowner attempt to have comfort life by conducting their own decorating in their house. DIY are the common approach by homeowners in conducting upkeep [6]. These are due easy to find information regarding decoration, cheaper, and convenient for unskillful persons to do it. Despite of that, there are some of decoration needs expertise person to perform it [6].

5.4 Renovation and Extentions

In definition of renovations and extension of home is by altering, enlarging or renewing it to accommodate changes in of family needs or lifestyle [18]. It is

challenging yet rewarding undertaking. Within the familiar surroundings of the home, it can personalize by their living environment choice. Homeowner can tailor their rooms into functional, comfortable and aesthetically pleasing settings that fit their lifestyle and taste [18]. Once completed, upkeep can add economic and aesthetic value to home [18]. A renovation project is relatively simple conversion of a room to another use or the consolidation of two rooms into a larger space.

5.5 Housekeeping and Landscaping

Housekeeping is a cleanliness work that needs to be done routinely. Maintaining high standards of cleanliness and housekeeping helps increasing the appearances and value of the place itself [19]. Housekeeping is essential works where for housing are it can be so done by their owned or housemaid or appointed the housekeeping services.

Commonly housekeeping is conducted by the homeowner themselves. Housekeeping is not just cleanliness. It includes keeping work areas neat and orderly, maintaining halls and floors free of slip and trip hazards and removing of waste materials and other fire hazards from work areas. Effective housekeeping is an ongoing operation it is based on schedule times which it need to be done regularly [20].

6 Methodology

This study was based on a questionnaire survey of homeowners in three areas of Shah Alam, Malaysia which are Seksyen U5, Seksyen 17 and Seksyen 7 with total 114 questionnaire were distributed. Questionnaires are distributed with 10 % of amount housing in each of the three areas, as shown in Table 1.

To get sample intended, Judgmental Sampling technique was used by selecting sampling based on the researcher judgment. There were two approaches in selecting the sampler—selecting housing area that has fully developed in past ten years, selecting dwelling that has stand out appearance of upkeep works.

Table 1 Questionnaire distribution on the selected case study area

Case study area	Residential terrace housing units	Percentage distribution (%)	Questionnaire distributed
Seksyen U5	410	10	41
Seksyen 7	379	10	37
Seksyen 17	355	10	36
Total, <i>n</i>			114

7 Result and Discussion

The data collected is based from Mean Score. It is referring from strongly disagree (1), disagree (2), undecided (3), agree (4) and strongly agree (5).

7.1 *Repairing Work*

Table 2 indicates that the responders are agreed (4.27) they conduct repair when only defects are appear repair. This agreement same with Kangwa research where the homeowners intent to have proactive measure when it is breakdown. In approaching the repairing works, homeowners are more likely to used contractors as in Table 2 clarify almost to agree (3.54). Homeowners are more favour of using contractor as they highly trusted the contractor able to handing the jobs. The mean score of using professional advices demonstrate undecided (3.12) because many of the homeowners have not used professional advice. This is due to the thought of high payment of professional advice fees. They assume that the fees usage of professional consult are higher compare with contractor quotation. In safety measure, homeowner are not custom in handling the repairing work by themselves (2.80). The lack of skills and knowledge has lead homeowner to decide use expertise person to handle the problem. Highest trades associated with repairing works are mainly highlighted for plumber and electrician as the several repairing works are outcomes from the building services. The lacks of skills of building services and on behalf of safety, homeowners are sought to use expertise persons to works on it.

7.2 *Inspection*

Table 2 displays homeowner do conduct inspection (3.60), however in measure inspection as preventive upkeep shows that there are numerous of respondent disagree. This is behalf of five of sub-component, only 1 showing agreement. They uncertainty of all others sub-components and almost to disagree display there are quite numbers of homeowners do not conduct proper preventive inspection. Some of disagree respond stated that they conduct inspection by only overview once a while without using any checklist. Several others homeowners also stated that they are not comprehended and informative regarding with the checklist inspection. On the finding, many of the agreement of conducted preventive checklist are mostly have income because many of them are exposed to the important of preventive maintenance.

Table 2 Prevalence upkeep works

Types of upkeep works	Prevalence works	Mean score
Repairing	Conduct repair when only defects are appear	4.27
	Do-it-yourself (DIY) for repairing work using references	2.80
	Used contractor for repairing work	3.54
	Used professional advice for repairing work	3.12
	Overall mean	3.43
Inspection	Conduct inspection to maintain dwelling condition	3.60
	Has upkeep plan preventive checklist	2.84
	Conduct inspection based on plan preventive checklist	2.86
	Research on upkeep planning using references	2.70
	Used professional in advising upkeep plan preventive	2.60
Overall mean	2.91	
Decoration	Has conduct decoration on the dwelling	3.77
	Do-it-yourself (DIY) for decoration work using references	3.36
	Used contractor for decoration work	2.76
	Used professional advice for decoration work	2.24
	Overall mean	3.03
Renovation	Has conduct renovation on the dwelling	3.73
	Do-it-yourself (DIY) for designing dwelling on renovation work using references	3.13
	Used contractor for designing dwelling on renovation work	3.50
	Used professional advice for designing dwelling on renovation work	2.95
	Overall mean	3.33
Extension	Has conduct extension on the dwelling	3.57
	Do-it-yourself (DIY) for designing dwelling on extension work using references	2.96
	Used contractor for designing dwelling on extension work	3.36
	Used professional advice for designing dwelling on extension work	2.63
	Overall mean	3.13
Housekeeping	Conducted housekeeping by their own	4.12
	Used maid for housekeeping	1.88
	Used housekeeping services for housekeeping	2.32
	Has upkeep schedule for housekeeping	3.45
	Overall mean	2.94
Landscaping	Conducted landscaping by their own	3.46
	Used gardener for landscaping	1.46
	Used landscaping services for landscaping	1.88
	Has upkeep schedule for landscaping	2.73
	Overall mean	2.39

7.3 Decoration

Table 2 indicates that the do conduct decoration (3.77) by conducting themselves (3.36). This agreeable with Lather (1997) and Munro (1996) report where the homeowners tend to do themselves as it is cheaper working by their own than using expertise person. Professional advice is the less (2.23) used because of the high expenses fees. On the others hand, DIY will save cost of services fees and only needs to pay on the materials price. Information of decorating they usually search via Internet. This will save lots of money, however it need to be alarm for heavy decorating that needs constructing work. This is for homeowner to be conscious of the quality play out for the decoration based on DIY.

7.4 Renovation and Extension

The mean data of overall renovation shows many of the homeowner had conducted renovation (3.73). In designing their dwelling for renovation, homeowners are completely trusted the contractor in conducting the work (3.50). Regarding to the table, homeowner do not design their dwelling for renovation themselves (3.13) and decline usage professional advice (2.95).

The respondent of extension is resemble as renovation works. They are too dependent with contactor for all the designing work of extension (3.57). There are uncertainty whether to conduct themselves (2.96) and decline of using professional advice.

These imply that many of the homeowner are highly reliance to usage of contractor because there are lack of skill conduct themselves. They are abstain using professional advice as it shows they are more trusted on contractor work. Less fees payment is one more of the reason homeowner choose contractor than professional advice.

7.5 Housekeeping and Landscaping

On the Table 2 shows enormously agree (4.12) of homeowners' conducted housekeeping by themselves. Majority stated of disagree in using maid (1.88) and housekeeping services (2.31). An observed conducted during questionnaire it exhibit that homeowners are usually have scheduling time to do housekeeping. They usually set up in between their free time in performing the housekeeping. Overall of Total Mean Score of housekeeping are 2.94 which imply disagreement but not homeowner disagreement of conducting housekeeping. It indicates the entire housekeeping work of homeowners' response in the questions of questionnaire.

Overall mean it shows that homeowners' undecided (3.46) whether they carry out landscaping by their own. On the other side, it shows that the response of usage gardener and landscaping services are highly disagreement (1.46 and 1.88). Homeowners' stated that they are disagree (2.73) of having a schedule for landscaping works. Overall it is imply that many of the homeowner does not have a heavy landscaping that needs lots of intention and time for upkeep that lead undecided response. The lack of space and time has directed the decision of not wanting a hefty landscape.

7.6 Interpretation of the Results

Compute from the Table 2 and analysis, overall it was found out repairing (4.27) and housekeeping (4.12) are main prevalence activities. Based on the comprehensive results, each of the components that inquiry whether they have conducted the upkeep has clarify the mean reading more than 3.00. Homeowners does perform all elements upkeep probe in the questionnaire. Nonetheless the results, homeowners does still needs guidance in upkeep. This is stated when the repairing is the most consume decision by homeowners. It is uncommon to find homeowners consists routine checklist as they tends to have mentality questioning of the need to fix if it is not broken. They are subtle to find the important of preventive upkeep as the thought to save money for the future breakdown occur. Apart of that, observation find out homeowners lean to neglect preventive maintenance due to the lack of knowledge and guidance to lead them. Although they do not have preventive schedule, the routine works for housekeeping still conducted. These routine works is based on their awareness of cleanliness. However, if they less aware the important of conducting the upkeep, they tend to ignored without taking any advantage to learn.

Works that involved construction and designing, which is out of within homeowners' capability; they are usually assign contractor to in-charge. It is difficult to find respondents' that have awareness and initiative to come across searching information regarding upkeep works conducted. Majority homeowners rarely get professional help as they see it expensive, hedge around with exclusions, informative, and possibly bringing more problems to attention than they can cope with. This is proven as homeowner commonly used contractor services for works involving construction and designing. In term of upkeep which they capable to conduct by their own such as housekeeping and landscaping, they prefer to do it by themselves. DIY is a significant way of getting work done for many, especially those on lower incomes and those with good networks of unpaid help, but standard can be poor. DIY is more likely to contribute to upgrading than to basic essential repair works. Thus, there are some respective upkeep they are capable to conduct by themselves such as decoration work, but work need skills of expertise the will assign contractor.

8 Conclusion

Research regarding homeowner upkeep behaviour is widely known and been studied in the world of education throughout the world by experts. Unfortunately, the benefit application of the research finding in providing policy of household upkeep is yet, not fully applicant in Malaysia. In Malaysia, the upkeep environment demonstrated a beginning interest of improvisation. Notwithstanding of wanting intriguing upkeep matter, the requirements and standard references of house upkeep are still lacking. Based on the finding, the upkeep involving construction or designing, homeowners are favour using contractor advisor. However, upkeep that needs homeowners' supervision still not assists by any enforcement or manual references. Towards improving condition in Malaysia, this study found that homeowners' upkeep behaviour is one of method in understanding homeowners' attitudes, opinions and preferences of their upkeep. Each individual has different perspectives in upkeep his or her dwelling.

Acknowledgments The authors would also like to thank Ministry of Education Malaysia and Universiti Teknologi MARA, UiTM for the Dana Pembudayaan Penyelidikan (RAGS) to carry out this research.

References

1. Propertyguru, Budget 2013: RPGT raised by 5 % (2012). Retrieved Sept 28, 2013, from <http://www.propertyguru.com.my/propertynews/2012/10/6134/budget-2013-rpgt-raised-by-5-/>
2. Moreover, Malaysia budget tablets 2013 (2012). Retrieved Mar 26, 2014, from <http://www.moreover.com/malaysia-news/2012/6010/malaysia-budget-2013/>
3. S. Azlinor, A.R. Rozanah, Quality housing: regulatory and administrative framework in Malaysia. *Int. J. Econ. Manage.* **2**(1), 141–156, (2008)
4. J. Kangwa, F. Olubodun, An investigation into home owner maintenance awareness, management and skill-knowledge enhancing attributes. *Struct. Surv.* **21**(2), 70–78 (2003)
5. J. Kangwa, F. Olubodun, A factor approach to analysis of home maintenance outcomes and attributes of management successes in the owner-occupied sector. *Struct. Surv.* **21**(4) 158–172 (2003)
6. P. Leather, A. Littlewood, M. Munro, *Make Do and Mend: Explaining Home-Owners' Approaches to Repair and Maintenance* (Policy Press, University of Bristol, Bristol, Housing Repair and Maintenance Series, 1998)
7. CIDB (Construction Industry Development Board) *Construction Quarterly by Statistical Bulletin—Fourth Quarter 2006* (CIDB Press, Kuala Lumpur, 2007)
8. Star (The Star Newspaper), Putrajaya to now focus on upkeep (2005, December 14). Retrieved Oct 29, 2013, from <http://blis2.bernama.com/>
9. NST (The New Straits Times Newspaper), Typical case of poor upkeep (2009, Apr 27). Retrieved Oct 29, 2013, from <http://blis2.bernama.com/>
10. Z. Mergawati, N. Leong, Poor Upkeep. *The Star Newspaper*, 24 Sept 2003, p. 1, 3
11. Star (The Star Newspaper), Strata-age time bombs due to poor upkeep (2007, June 18). Retrieved Oct 29, 2013, from <http://blis2.bernama.com/>
12. A.R. Winger, Some internal determinants of upkeep spending by urban homeowners. *Reg. Sci. Urban Econ.* **49**(4), 474–479 (1973)

13. L.O. Abdul, I. Arazi, F.K. Mohd, Investigating building maintenance practices in Malaysia: a case study. *Struct. Surv.* **29**(5) 397–410 (2011). Retrieved Nov 6, 2013, from <http://dx.doi.org/10.1108/02630801111182420>
14. S.A. Azlan, Cost decision making in building maintenance practice in Malaysia. *J. Facil. Manage.* **7**(4) 298–306 (2009). Retrieved Dec 27, 2013, from <http://www.emeraldisight.com/1472-5967.htm>
15. A. Littlewood, M. Munro, Explaining disrepair: examining owner occupiers' repair and maintenance behaviour. *Hous. Stud.* **11**(4), 503–525 (1996)
16. HMH (Homeowner's Maintenance Handbook), Maintenance manual of housing and community services department, city of Wichita (n.d.). Retrieved Dec 9, 2012, from <http://www.wichita.gov/journals-and-magazines/social-policy-journal/spj27/ageing-in-place-the-views-of-older-homeowners-27-pages128-141.html>
17. D.J. Croome, *Noise, Buildings and People* (Pergamon Press, Oxford, New York, Toronto, Sydney, Paris, Frankfurt, 1977)
18. F.D. Ching, D.E. Miller, *Home Renovation* (Van Nostrand Reinhold Company, New York, 1983)
19. Convenience Guru, The importance of maintaining high housekeeping standards (2014). Retrieved Mar 27, 2014, from http://www.convenienceguru.com/newsshow.asp?int_id=4
20. CCOHS (Canadian Centre for Occupational Health and Safety), Why should we pay attention to housekeeping at work? (2008). Retrieved March 27, 2014, from <http://www.ccohs.ca/oshanswers/hsprograms/house.html>

Green Roofs Benefits; Perception by Malaysian Residential Highrise End Users

Wan Zuriea Wan Ismail, Sabarinah Sh. Ahmad, Hikmah Kamarudin and Zarina Ithnin

Abstract The paper aims to identify end users perception towards benefits offered by green roofs at Malaysia high rise residential buildings. The perception is crucial in determining potential of green roofs, as it offers many benefits mainly in providing sustainable residential building. The study was conducted through questionnaire surveys to the end user at selected five case study buildings at Shah Alam and Subang Jaya. Survey results found that end users mostly agree with the benefits offered by green roofs particularly in the aspect of social and aesthetic value benefits. It reveals good potential of green roofs towards providing sustainable highrise residential building in Malaysia.

Keywords Green roofs · Sustainable residential building · Perception

1 Introduction

Rapid development in major urban areas in Malaysia has led to increase in land value, land scarcity and high demand of commercial and residential buildings. With the rate of urbanisation at 73 % [1], vertical urban development, which can save more spaces, is expected to be a preference in major urban areas. Demand for housing in urban areas is increasing and construction of a high rise residential building is an option to meet housing needs for people. Developers have increase construction of sustainable high-rise residential buildings in order to meet rapid decline of green space at urban areas [2].

W.Z.W. Ismail (✉) · S.Sh. Ahmad · H. Kamarudin · Z. Ithnin
Faculty of Architecture, Planning and Surveying, Universiti Teknologi MARA (UiTM),
40450 Shah Alam, Selangor, Malaysia
e-mail: wzuriea@gmail.com

S.Sh. Ahmad
e-mail: sabrin63@yahoo.com

2 Highrise Residential Building

Housing provision is one of Malaysia's national agenda by introducing National Housing Policy [3]. The goal of the National Housing Policy is to provide adequate, comfortable, quality and affordable housing to enhance the quality of life of the people. One of the objectives is to provide adequate and quality housing with comprehensive facilities and a conducive environment [3]. The total number of residential units in Malaysia had increased from 5.55 million in 2000 to 7.34 million in 2010. There was a significant increase recorded in the percentage of multi storey residential from 12.6 % (2000) to 19.9 % (2010) [1]. Due to high demand for residential building, the need for a sustainable built environment should be considered in Malaysian construction industries. One of the preferences is to incorporate the usage of green roofs at high rise residential building. Thus it will provide potential benefits to building users.

3 Green Roofs

Buildings with green roofs are considered as a fairly new phenomenon in the Malaysian Construction Industry although the Green Building Index (GBI) has included green roofs in its assessment criteria for sustainable site planning and management [4]. While green roofs promote greener architecture, reduce urban heat islands effects, they also provide aesthetic value and environmental-friendly outdoor recreational spaces especially to the high rise community. In Malaysia, green roofs can play an important part in the provision of recreational areas in high rise residential buildings especially in high density urban areas. The advantages of green roofs include environmental, economic, amenity and aesthetic benefits [5]. Peck and Kuhn [6], state that green roofs benefits are one of the most valuable features and finding the right benefits for each project is a key to successful of green roofs. According to Taib et al. [7], it is important to conduct a study on the perception as the act of a person depends on their perception. An understanding of how end-users and community perceive the benefits are crucial to determine the potential and future planning of green roofs in Malaysian residential buildings. Lack of appreciation by the community and end-user will hinder the development of green roofs.

3.1 Definition of Green Roofs

A green roof can be defined as a vegetation system that is incorporated into a roof. It consists of components such as growing medium, filter sheet, drainage layer, root barrier and waterproof membrane [8]. Another way to describe green roof is the living vegetation that cover the roof of a building in thin layers. The green roof concept can be found mainly on flat roofs [9]. Green roof systems can be divided

into two types; extensive and intensive and these can be distinguished by the cost, depth of growing medium and the choice of plants [6].

3.2 *Benefits of Green Roofs*

Benefits of green roofs can be classified into three main aspects; (1) Environment benefits, (2) Economic benefits and (3) Amenity and Aesthetic benefits. There are a lot of intersections between all these aspects [10]. The benefits are further discussed as such:

1. *Environment benefits*

- Improve air quality
- Reduce heat absorption and reduce temperature
- Storm water management
- Encourage biodiversity

(a) *Improve air quality/Reduce air pollution*

“The combination of cars, industrial pollutants and building emissions as well as elevated ambient temperatures results in poor air quality in urban area due to increased particulates and air contaminants” [11]. Air pollution or poor air quality in the urban environment is one of major threat to human health. A notable study was done by Yang et al. [12] in Chicago shows that by using green roofs, a large amount of pollutants can be removed. Green roof can be an approach for controlling air pollution that occurs in the country. Bianchini and Hewage [13] also believed that green roofs can be one of air pollution control technology especially at urban area. Plants carry out photosynthesis process by absorbing carbon dioxide (a major automobile emission) and release oxygen to the atmosphere. Therefore, the atmosphere’s composition is being maintained by the plants. Other than that, plant can help in catching and trapping a number of pollute air particles and gases such as smog and dirt that exist in contaminated air, thus ensuring green roofs produce better air quality for urban dweller [14]. Green roof depends on the type of plant grown and the depth of soil used to help improve air quality [15]. For example, the greater the leaf surface area, the more particulate matter can be captured.

(b) *Reduce heat absorption in the building and reducing air temperature in and out of the building*

Development of urban areas nowadays create more and more impervious surface that contributes to higher temperature. Conventional roofs that lack vegetation makes cities or urban area reach high temperature thus lead to greater demand of energy production, global warming and higher pollution [11]. A case study by Teemusk and Mander [16] showed that a green roof offers effective protection against intensive solar radiation by providing a

base roof thus lowering and minimizing urban area temperature. Vegetation at the top of the building offers shading effects that can help to reduce air temperature [14] and reduce indoor and outdoor temperature of the building [16]. According to Wong [14], in Tokyo, Japan, it was noted that a reduction of air temperature between 0.11 and 0.84 °C could be achieved with 50 % vegetation covering the top of the roof. A field test conducted in Singapore also had proved that the use of green roofs can help in reducing surface temperature by as much as 30 °C and lower air temperature by about 4 °C in urban area. According to National Parks Board Singapore [17], a tree evapotranspiration 40 gallons of water in a day, indirectly can reduce heat equivalent to the production of one hundred 100-watt lamps operating 8 h per day. Thus, it is agreed, green roofs may be very helpful in reduce heat. However the percentage of heat reduced depend on the size and type of building either high or low rise building. The greater the size of green roofs, the greater amount of heat will be reduced [18].

(c) *Storm water management*

Clark et al. [19] and Oberndorfer et al. [20] stated that currently, green roofs are mainly valued based on increasing ability to reduce storm water runoff. Green roofs are also ideal for urban storm-water management due to the existing roof space. “Conventional roof merely shed water while green roofs use the most incident water and slowly release the remainder” [21]. In highly developed urban area, flooding generally occurs due to rainwater that tends to flow rapidly from the roof of the building [13]. However with the presence of green roofs, flooding problem can be resolved by retaining and delaying the amount of runoff rainwater that enter the sewage system [13]. Green roofs could assist rainfall water management, however roof greening alone will never fully solve urban runoff problem [22].

(d) *Encourage biodiversity*

Rahman and Ahmad [18] stated that, green roofs at urban area can promote biodiversity by providing habitats for flora and fauna such as beetles, ants, bees and bugs. According to the result obtained by Yuen and Hien [23], green roof should be provided with more plants that would become a spot of insects such as butterfly and caterpillars where children of the residents could observe nature. Cities become more enjoyable with the existing biodiversity [24].

2. *Economic benefits*

- Energy efficient building
- Increase roof life

(a) *Energy efficient building*

Green roofs can affect heating and cooling with moderate transfer of heat and cold in the building [25]. Increase in building energy efficiency can help in reduction of electrical demand at a time, thus reduced electrical

bills. This is due to the green roofs that can handle extreme temperature. For examples, the reduction of heat and temperature will lead to a reduction of air conditioning cost to keep the internal part of the building cooler [18]. Furthermore, according to Rahman and Ahmad [18], green roofs can act as an economical kitchen garden. Other than can save money, it also saves time where residents can only step up to their roof to get some vegetables or fruit. This approach could enhance citizen in utilizing open space and appreciate nature.

(b) *Increase roof life*

Planted roofs can actually protect a roof membrane from intense ultra violet degradation and expansion and contraction from temperature extremes, thereby enhancing their long term performance [26]. USEPA [27], Teemusk and Mander [16] and Bianchini and Hewage [13] agreed that, with green roof at the top of the building, expected lifespan of roof can potentially be extended to 20 more years compared to conventional roofs. Shimmin [24] stated that vegetated roofs last longer than non-vegetated ones. During the day, roof membrane are exposed and absorb solar radiation and make surface temperature increase, while at night, heat is released and temperature of surface decreased. This daily phenomenon assists roof membrane to leak and reduce the longevity of roof. Thus, it can be said that, planted roofs can protect roof membrane from extreme temperature, thereby enhancing their longevity [26].

3. *Social and aesthetic benefits*

- Provide leisure and functional open space
- Health and therapeutic value
- Reduce noise pollution
- Visual amenity value to the building and its surrounding

(a) *Provide leisure and functional open space*

In terms of city planning Tolderlund and Drainage [11] stated the benefits of green roofs that include increasing green space, encouraging community gardens and food production, extending commercial and recreational space, and create space where people can rest and interact [16]. Intensive vegetative roofs also known as park-like roofs provide recreational spaces in urban areas if they are designed for public use [13]. A sense of community can also be fostered [21]. As cited in Rahman and Ahmad [18], Alexander et al. in 1977 found that people will visit urban park only if need to take 3–5 min walk from their office or home. The duration can be achieved when there is a green space available at their roof. In addition, when human views nature, indirectly, there will be benefits for their health.

(b) *Reduce noise/act as sound insulator*

MacDonagh [21] noted that green roofs can act as sound insulator. Medium that involved in the existing green roofs; soil, plants and the air

layer that trapped between the green roofs and buildings provide sound insulation. A test that indicates green roofs can reduce indoor sound by as much as 40–60 dB [11, 15] which is of the great benefit to the building occupants that were affected by airports, industry, trains and traffic [28]. The thickness, plant type, growing medium and plant coverage influence the effectiveness of the green roofs to reduce noise levels [11].

(c) *Visual amenity value to the building and its surrounding*

Aesthetic benefits or visual amenity value also benefit from the existence of green roofs. Vegetation can provide visual contrast and relief from building concrete like asphalt, gravel and tar at urban area. Most landscape architects and developers also believe that green roofs can hide ugly rooftop services and integrate well with the buildings aesthetically. It was supported by Hien and Tan [29] in her article entitled “Effects of Skyrise Greenery on Building Performance”. She stressed that the most attractive benefits of green roof is high aesthetic value that green roof can bring to building and its surrounding environment itself. Indirectly, green roofs can be a medium to soften the urbanised harsh surrounding and offer a tranquil and pleasant view to city dwellers through a living and breathing space. Urban dwellers will have a place to relax and restore [18] while Shimmin [24] perceived green roofs can be seen as a living billboard that gives sense of beauty to a city.

Much research has been written about the benefits of green roofs. Thus, early conclusion can be made that different types of green roofs, will provide its own different benefits for different aspects.

4 Research Methodology

The paper aims to identify perceived benefits of green roofs by the end user of highrise residential building with the presence of green roofs. Five residential buildings at Shah Alam and Subang Jaya have been selected as case studies and a total of 297 respondents were randomly selected to answer the questionnaire based on their general knowledge and perception. A questionnaire was designed in three sections outlining the three main benefits of green roofs outlined earlier. End user responded using a 5-point Likert-type scale with the following responses: “strongly disagree” (1), “disagree” (2), “neutral” (3), “agree” (4), “strongly agree” (5). Data were analyzed using SPSS and mean rating for each set was estimated. For scale of mean refers to the scale as follows; 1.00–1.49 (strongly disagree), 1.50–2.49 (disagree), 2.50–3.49 (neutral), 3.50–4.49 (agree), 4.50–5.00 (strongly agree).

5 Findings and Analysis

The survey obtained information on demographic characteristics of the respondents ($n = 297$). There is a difference of 12 respondents between the randomly picked male and female. The age varies from below 15 years old to 55 years old. Majority of the respondents are between 15 and 25 years old (49.5 %). Malay dominated the number of respondents with 59.3 %, followed by Indian 22.9 %, Chinese 17.2 % and others 0.3 %. Total Malay population for Shah Alam and Subang Jaya district recorded the highest number which is 191,937 [30]. Thus, it can be said that, when the number of population of ethnic increase, the possibility for the type of ethnic is randomly pick to be the respondent in that particular area also increase.

As refer to Table 1, based on average mean score of 3.68, majority of respondents agreed with the benefits of green roofs in environmental aspects. Three potential benefits for environmental aspect with the highest value of mean were; improve air quality (3.90), reduce air temperature (3.77) and reduce heat absorption (3.74). In this case, a few studies have shown that, with the existence of green roofs at the top of a building, can improve air quality in urban environment. This is due to the fact that, the presence of vegetation in the development of green roofs can help a lot in absorbing contaminants and retaining particles suspended in the air and at once act as a bio filters (pollution control technique using living material) [31]. Absorption also can reduce air temperature internal and external of the building. Thus, it also helps to reduce environment temperature. Residential building, parking lots and standards roofs that do not consist of vegetation would lead to temperature rise during hot day and remain warm longer than the surrounding environment [11]. It also prevents natural cooling from wind. Thus, it makes sense that the potential of green roofs can improve air quality was ranked in the first position. Good air quality is needed to promote good health for urban dwellers. The lowest rank for environmental benefits is encouraging biodiversity with mean score 3.29 with 128 (43.1 %) respondents answered neutral in benefits of green roofs. Most of green

Table 1 Environmental benefits

Description		1	2	3	4	5	Mean
Improve air quality	%	0	0.7	28.3	49.8	20.2	3.90
	f	0	2	84	148	60	
Reduce heat absorption in the building	%	0	0.7	32.3	57.6	8.4	3.74
	f	0	2	96	171	25	
Reduce air temperature	%	0.3	0.7	30.0	57.6	10.1	3.77
	f	1	2	89	171	30	
Storm water management	%	0	0.7	40.1	47.1	11.1	3.69
	f	0	2	119	140	33	
Encourage biodiversity	%	3.7	11.4	43.1	33.3	7.1	3.29
	f	11	34	128	99	21	
Average mean							3.68

roofs at highrise residential building are intended for human used. Potential encourage biodiversity can be increased by minimal human interference at green roofs [32].

For economic benefits, average mean score is 3.60; it means that most of respondents agree with the benefits of green roofs in economic benefits. End users choose that green roofs can help in producing an energy efficient building. Thus, it has the highest mean which is 3.70. As mentioned by Shimmin [24], green roofs enhance property values for the building itself, surrounding buildings and help in reducing utility bills. Thermal insulation, shade and evapotranspiration provided by green roofs can lower down the demand of mechanised cooling for example the use of air conditioner in the house. One of the reasons is because; soil that involved in the development of green roofs can act as a natural regulator of temperature. From 297 respondents, 143 (48 %) responded neutral for green roofs can increase the longevity of roof life. This result is in line with research done previously by Zuriea et al. [33] indicating that one of the major problems related with existing green roofs in Malaysia is due to water penetration into the roof structure as a result of the absence of water proofing. This is why respondents tend to choose neutral for green roofs can increase roof life (Table 2).

White and Gatersleben [34] in his paper on ‘Greenery on Residential Building’ has noted that integration of nature in urban area can improve perceptions of that area by providing restorative properties in order to combat stressors like noise pollution and crowding. The result of the study also indicated that houses consist of building-integrated vegetation (green roofs, green walls) were significantly more preferred. They have high visual quality, perceived beauty and had more positive affective quality than those without. It can be concluded that, building-integrated vegetation such as green roofs and green walls would be one of the valuable additions to urban area. Thus, it can be said that, the data above is accepted due to the highest mean of elements in social and aesthetic benefits. Green roofs can provide visual amenity value to the building and surrounding area (mean score 4.22). They can help to improve building appearance and become one of the effective strategies for beautifying the built environment.

The second ranked of potential benefits that been chosen by the residents is green roof can provide leisure and functional open space with mean score of 3.97. Other than Public Park, the residents can choose green roofs that are located at shorter distances from their house. They just need 3–5 min to reach green roofs. Sutic [25] has mentioned that green roofs can provide a pleasing space for people

Table 2 Economic benefits

Description		1	2	3	4	5	Mean
Energy efficient building	%	0	1.0	34.0	57.9	6.1	3.70
	f	0	3	101	172	18	
Increase roof life	%	0.3	3.7	48.1	39.7	6.7	3.50
	f	1	11	143	118	20	
Average mean							3.60

Table 3 Social and aesthetic benefits

Description		1	2	3	4	5	Mean
Provide leisure and functional open space	%	0	0.3	24.9	50.5	22.9	3.97
	f	0	1	74	150	68	
Health and therapeutic value	%	0	0.3	29.0	52.9	16.2	3.86
	f	0	1	86	157	48	
Reduce noise pollution	%	0	1.0	40.4	40.8	41.8	3.70
	f	0	3	120	133	38	
Visual amenity value to the building and its surrounding	%	0.3	0	16.8	42.1	39.4	4.22
	f	1	0	50	125	117	
Average mean							3.94

especially for elderly, handicapped and the young who are more dependent on near-home recreation space. More green roofs can increase the amount of green space and provide more leisure and recreational space for urban residents.

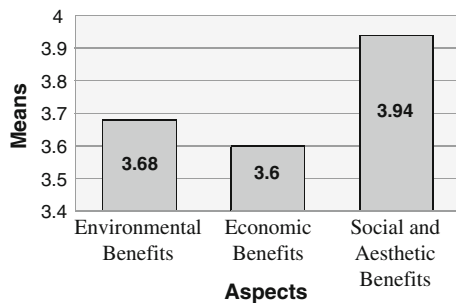
Although the benefits of green roofs for health and therapeutic is ranked third, it is still within the range of highest mean (3.86). According to Ulrich [35], contact with plants either physical or visual can promote direct health benefits. The ability of plants to generate restorative effects help to lower down stress, improve recovery rates of a patient and at once provide higher resistance towards illness. The lowest rank in social and aesthetic benefits is reduce noise pollution with mean score of 3.70. However 38 (41.8 %) respondents choose strongly agree, which the highest percentage for social and aesthetic benefits.

The average mean for the three aspects are slightly different from each other (Fig. 1). Figure 2 shows the illustration graph. Difference for each aspect can be seen clearly. Based on the result, social and aesthetic aspects indicated the highest

Fig. 1 Average mean for each aspect

Aspects	AverageMean
Environmental Benefits	3.68
Economic Benefits	3.60
Social and Aesthetic Benefits	3.94

Fig. 2 Graph that illustrate average mean



mean (3.94), followed by environmental aspects (3.68) and (3.6) for the economic benefits. When there are vegetation at green roofs, covered the harsh building, people can see the attractiveness of the natural view physically. Meanwhile, for environmental benefits, it gives indirect effect for example rooftop garden can improve air quality of urban area. Majority of the respondents agreed with all the benefits of green roofs that have been stated according to each aspect. This is probably due to the fact that majority of the respondents are from students, professional and businessman.

6 Conclusion

This paper describes the result obtained from a questionnaire survey of end users perception on benefits of green roofs at residential building. Majority of the respondents agreed that green roofs will help to improve visual amenity value to residential building and also the surrounding by softening harsh surrounding with a pleasant view to city dwellers. Indirectly it can improve the quality of living for high rise residents. In promoting green roofs as part of sustainable building elements, a study on green roof benefits that are suitable with the local context is necessary. Good perception towards benefits of green roofs will lead to more green roofs application in Malaysian residential buildings

Acknowledgments This research was funded by MoHE under Research Acculturation Grant Scheme (RAGS) grant.

References

1. Department of Statistics Malaysia. Available: www.statistic.gov.my. Accessed 16 May 2014
2. T.L. Ta, *Managing Highrise Building in Malaysia, Where are we?* 2nd NAPREC Conference, INSPEN
3. National Housing Policy. Available: http://www.kpkt.gov.my/kpkt_2013/fileupload/dasar/DRN_BM.pdf. Accessed 14 May 2014
4. Green Building Index. Available: www.greenbuildingindex.org. Accessed 15 May 2014
5. N. Dunnett, N. Kingsbury, *Planting Green Roofs and Living Walls* (Timber Press, London, 2008)
6. S. Peck, M. Kuhn, Design guidelines for green roofs. Available: <http://www.cmhc-schl.gc.ca/en/inpr/bude/himu/coedar/upload/Design-Guidelines-for-Green-Roofs.pdf>. Accessed 14 May 2014
7. N. Taib, A. Abdullah, S.F.S. Fadzil, F.S. Yeok, An assessment of thermal comfort and users' perceptions of landscape gardens in a high-rise office building. *J. Sustain. Dev.* **3**(4), 153 (2010)
8. Greater Manchester Green Roof Guidance (2009). Available: http://www.agma.gov.uk/cms_media/files/green_roofs_guidance_final_draft_04_08_092.pdf?static=1. Accessed 2 June 2014
9. B. Dvorak, A. Volder, Green roof vegetation for North American ecoregions: a literature review. *Landscape Urban Plan* **96**(4), 197–213 (2010)
10. Fausto Miguel, *Green Roof Best Practice Guidelines* (2013)

11. L. Tolderlund, U. Drainage, *Design Guidelines and Maintenance Manual for Green Roofs in the Semi-Arid and Arid West* (Green Roofs for Healthy Cities, USA, 2010)
12. J. Yang, Q. Yu, P. Gong, Quantifying air pollution removal by green roofs in Chicago. *Atmos. Environ.* **42**(31), 7266–7273 (2008)
13. F. Bianchini, K. Hewage, Probabilistic social cost-benefit analysis for green roofs: a lifecycle approach. *Build. Environ.* **58**, 152–162 (2012)
14. M. Wong, *Environmental Benefits Of Green Roofs* (Singapore Environment Institute, 2006). Available: <http://www.nea.gov.sg/cms/sei/PSS23slides.pdf>. Accessed 4 June 2014
15. S.B. Charlie Miller, R.D. Berghage, *The Benefits and Challenges of Green Roofs on Public and Commercial Building* (United States, 2011)
16. A. Teemusk, Ü. Mander, Greenroof potential to reduce temperature fluctuations of a roof membrane: a case study from Estonia. *Build. Environ.* **44**(3), 643–650 (2009)
17. National Parks Board Singapore. Available: <https://www.nparks.gov.sg/cms>. Accessed 5 May 2014
18. S.R.A. Rahman, H. Ahmad, Green roofs as urban antidote: A review on aesthetic, environmental, economic and social benefits. Sixth South East Asian Technical Consortium in King Mongkut University of Technology Thonbur, Bangkok, Thailand (2012)
19. C. Clark, P. Adriaens, F.B. Talbot, Green roof valuation: a probabilistic economic analysis of environmental benefits. *Environ. Sci. Technol.* **42**(6), 2155–2161 (2008)
20. E. Oberndorfer, J. Lundholm, B. Bass, R.R. Coffman, H. Doshi, N. Dunnett, B. Rowe, Green roofs as urban ecosystems: ecological structures, functions, and services. *Bioscience* **57**(10), 823–833 (2007)
21. L.P. MacDonagh, Benefits of Green Roofs, 2005 in www.informedesign.org. Available: http://www.informedesign.org/_news/aug_v04r-p.pdf. Accessed 2 May 2014
22. J. Mentens, D. Raes, M. Hermy, Green roofs as a tool for solving the rainwater runoff problem in the urbanized 21st century? *Landscape Urban Plann.* **77**(3), 217–226 (2006)
23. B. Yuen, W.N. Hien, Resident perception and expectation of rooftop gardens in Singapore. *Landscape Urban Plann.* **73**, 263–276 (2005)
24. H. Shimmin, The vertical garden city and the transformate power of roof gardens. Main historical and sustainable architecture thesis: 59, 2012
25. N. Sutic, How green roofs can improve the urban environment in uptown Waterloo, 2003
26. J. Voelz, J. Loux, *Sustainability and Built Environment* (2006). Available https://extension.ucdavis.edu/sites/default/files/green_roof_02.pdf. Accessed 16 May 2014
27. United States Environmental Protection Agency, Vegetated Roof Cover: Philadelphia, Pennsylvania. (Low-Impact Development Center, 2010). Available: www.lowimpactdevelopment.org/pubs/Roof_cover_Factsheet.pdf. Accessed 16 May 2014
28. V. Nurmi, A. Votsis, A. Perrels, S. Lehvavirta, Cost- benefit analysis of green roofs in urban areas: case study in Helsinki (Ilmatieteen laitos, 2013). Available <https://www.cuge.com.sg/research/images/cugeresearch/CG2/CG6/202.pdf>. Accessed 5 May 2014
29. W.N. Hien, A.Y.K. Tan, Effects of Skyrise Greenery on Building Performance (Ecology and Urban, 2013)
30. Demographic Statistics Division, Malaysia, 2010. Available: <http://www.statistics.gov.my/>. Accessed 16 May 2014
31. R. Fernandez-Cañero, T. Emilsson, C. Fernandez-Barba, M.A. Herrera Machuca, Green roof systems: a study of public attitudes and preferences in southern Spain. *J. Environ. Manage.* **128**, 106–115 (2013)
32. Habitat Action Plan. Available: http://www.greenroofguide.co.uk/downloads/HAP-doc_v2.pdf. Accessed 3 June 2014
33. W.I. Zuriea, S.A. Sabarinah, E.H. Ahmad, I. Zarina, M.A. Irwan, Perception towards Green Roof in Malaysia, MICRA2010 Conference, UiTM Shah Alam
34. E.V. White, B. Gatersleben, Greenery on residential buildings: does it affect preferences and perceptions of beauty? *J Environ Psychol* **31**(1), 89–98 (2011)
35. R.S. Ulrich, in *Effects of Gardens on Health Outcomes: Theory and Research* Healing Garden. ed. by C. Cooper-Marcus, M. Barnes (Wiley, New York, 1999), p 27

Critical Review on the Theoretical Framework and Critical Success Factors in Green Construction

Afzan Ahmad Zaini and Intan Rohani Endut

Abstract Construction activities must conserve energy, land, water and material to successfully implement green construction, while planning and managing the work regarding the minimisation of environmental impacts related to the construction process. Notwithstanding this, many arguments and discrepancies between the ideal form of green construction and existing construction due to the practical difficulties in realizing the concept of green construction. This paper critically reviews the existing green building assessment tools, theoretical framework and the critical success factors based on literature review search. Investigating the existing green building assessment tools, theoretical framework and critical success factors are fundamental in determining the successful implementation of green construction in the Malaysian construction environment.

Keywords Critical success factors • Green building assessment tools • Theoretical framework • Green construction • Malaysian construction environment

1 Introduction

Construction industry in Malaysia is considered the fastest developing country in Asia and has contributed 3–7 % to the Gross Development Product (GDP). The current GDP has contributed to 6.2 % in the first quarter of 2014. For five consecutive quarters, the construction sector continued to register impressive growth with

A.A. Zaini (✉)

Department of Quantity Surveying, Faculty of Architecture Planning and Surveying,
Universiti Teknologi MARA, Shah Alam, Sarawak, Malaysia
e-mail: afzanahmadzaini@gmail.com

I.R. Endut

Faculty of Civil Engineering, Universiti Teknologi MARA, Shah Alam, Sarawak, Malaysia
e-mail: z_intan@yahoo.com

expansion of 18.9 % in the first quarter of 2014 as a result from the geared up performance of residential and mixed housing development [6].

Many different inconsistent definitions of green construction exist from the planning to the execution stage. Among the conflicting definition, [8] defines green construction as the planning and managing a construction project, meeting the requirement in a contract while minimising the impact on the environment while [18] describes green construction as a modernised construction or improvement of traditional construction [15] with comprehensive resources and energy consumption. In addition to that, [12, 15, 18, 22] define green construction as reduce energy, resources and environmental pollution through scientific management and technological progress [10, 15, 21, 23, 31] without compromising quality and health and safety [18, 21, 22, 31]. Subsequently, [29] observe that, green construction requires contractors to plan and manage the construction projects with regards to the minimisation of energy, resources and the amount of waste. These strategies may improve the project's budget and schedule and therefore reduce costs, increase productivity and protect the environment.

2 Overview of Green Building Assessment Tools and Green Construction

Different types green building assessment tools are available worldwide for instance, Green Building Index (GBI) in Malaysia, LEED in United States, BRE-EAM in United Kingdom, CASBEE in Japan, Green Mark in Singapore and Green Star in Australia.

Table 1 demonstrates the comparison between green assessment tools for various countries. From this table, the areas that are more crucial in assessing green building worldwide are energy, site, water and indoor quality optimisation, the use of environmentally preferable product or material and maintenance.

These assessment tools are aim at improving occupant well-being, environmental performance and economic returns of buildings.

Green building rating tool system in Malaysia is known as Green Building Index (GBI). In 2008, the green building rating tool system has become mandatory for all new buildings [25].

The criteria under GBI are:

1. Energy efficiency
2. Indoor Environmental Quality
3. Sustainable site planning and management
4. Material and resources
5. Water efficiency
6. Innovation

Table 1 Comparison of green building rating tools

	Optimize site potential	Optimize energy use	Protect and conserve water	Use environmentally preferable product	Enhance indoor quality	Maintenance practice	Others
GBI (Malaysia)	✓	✓	✓	✓	✓	-	✓
LEEDS (U.S)	✓	✓	✓	✓	✓	-	✓
BREEAM (U.K)	✓	✓	✓	✓	✓	✓	✓
CASBEE (Japan)	✓	✓	✓	✓	✓	✓	✓
GREENSTAR (Australia)	✓	✓	✓	✓	✓	✓	✓
GREENMARK (Singapore)	-	✓	✓	-	✓	✓	✓

The area of green construction partly derived from green building index (GBI) in which “sustainable site planning and management” and “material and resources” are the main criteria [1]. It has been suggested that, the current practices in green construction are OSHAS 18001, ISO 14001, material saving plan, water saving plan, energy saving plan and natural resources to mention but a few [1].

The finding from this study indicates the ISO 18001 practices are high among the current practices in green construction, followed by the rest of the practices which marked as moderate.

3 Investigating the Theoretical Framework

Having defined the term green construction, it is important to discuss the concept and theoretical framework of green construction. Shi et al. [21] describe the concept of green construction as the reflection of sustainable development with the comprehensive application of technology.

Brundtland [3] defines the sustainable development as a development that meets the needs of the present and future generations. The sustainable development in the construction industry is a long term task and the green construction plays a key role in green building [22].

Tam and Tsui [28] observe that, the management and operational performance is an indicator for a successful implementation of green construction. Qi et al. [29] suggest the theoretical framework of green construction include environmental regulations, managerial concern and project stakeholder pressure. Figures 1 and 2 illustrate the concept and theoretical framework of green construction based on initial literature search.

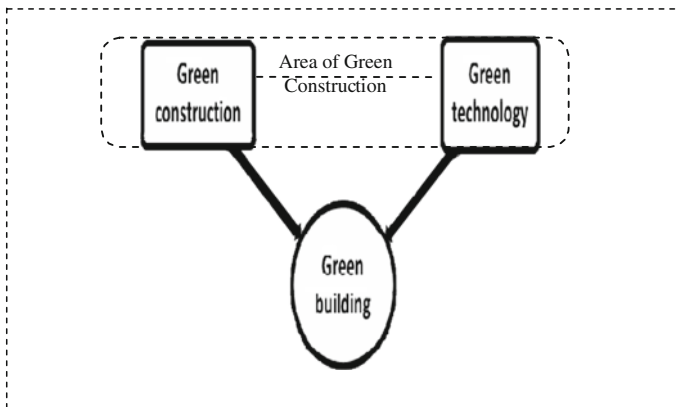
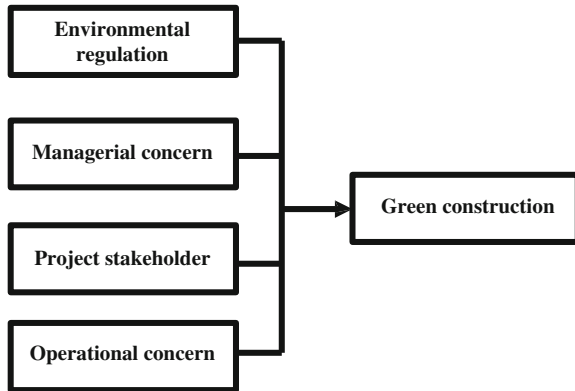


Fig. 1 Concept of sustainable development (Adapted from [21, 22])

Fig. 2 Theoretical framework of green construction (Adapted from [28, 29])



From this theoretical framework, all factors that lead to the successful implementation of green construction are further discussed as below.

3.1 Environmental Regulation

1. Specifying the technologies that must be used
2. Stipulating specific environmental targets that must be achieved
3. Introducing economic measures through distributing environmental costs and benefits
4. Fines and penalties for non compliance with regulations have led to a more respectful attitude towards the environment
5. More regulated industries will tend to include more environmental concerns

3.2 Managerial Concern

1. Commitment of top level management
2. Team effort on site, which includes involvement and support from main contractors, subcontractors and head offices
3. Adapt an environmental innovation strategy
4. Place high value and concern on the environment and its protection
5. Raising environmental awareness is an important role for implementing ISO 14000 and EMS in construction industry
6. Scope and speed of firm's responses to environmental issues
7. Appropriate training to ensure companies implementing the environmental concepts and eliminate confusion on environmental issues.
8. Investment on environmental associated facilities and equipment and setting up related management structures for long term benefits

9. Investment for Research and Development (R&D) in order to maintain a privilege over other competitor
10. Comprehensive environmental planning

3.3 Project Stakeholder

1. Client

- The importance of clients can be reflected by the various ways for instance the clients can influence the adoption of innovation strategy and identify specific requirements for contractors
- Pressure on project participants to improve buildings' lifecycle performance Client strongly shapes the products and processes from the very beginning of construction projects
- Failure to meet the requirements on environmental protection may lead to the removal from the tender lists

2. Community

- Public opinion on firm's environmental performance represents an important factor affecting the way firms do business
- Failing to meet a good environmental performance may lead to a bad image for all companies involved

3. NGO

- Demand of occupational health and safety from the employees lead to positive measures in obtaining OHSAS 18001 and ISO 14001 certifications

3.4 Operational Concern

1. Maintenance and equipment

- Regular maintenance is required to ensure the equipment is functioning properly and to maintain its quality.
- Plants should be properly maintained to avoid creating disturbance to the environment

2. Air pollution control

- Water spray and screening (covering) to minimise flying dusts

3. Noise pollution control

- Avoiding site operations beyond allowable time limits

4. Water pollution control
 - Manage water quality properly on site. Prevent anything that has potential to pollute such as muddy water from entering surface water drainage
 - Monitor water usage and promotion of water conservation, waste water collection and treatment and water reuse and recycle system
5. Waste pollution control
 - Purchasing management to reduce excessive orders
 - Waste reuse and recycling scheme
 - Use of green construction technology such as chemical waste treatment
6. Ecological impact
 - Degree of efforts in reducing ecological impact such as topsoil, trees and vegetation and living habitats
7. Energy Consumption
 - Monitor the energy consumptions in both the construction process and the finished building

4 Investigating the Critical Success Factors

Success factor is a set of facts or influences that contribute to the success or failure of a project [24]. Cooke-Davies [4] distinguishes success factors as inputs to the management systems that lead directly or indirectly to the success of the project or business. McCabe [16] identifies critical success factors as those input factors for the project which will most significantly influence project performance. The choice of critical success factors (CSFs) is important for any project development and should be established at the beginning of the project phase.

The review of literature search highlights the main areas of critical success factors for the successful implementation of green construction. Analysis from literature culminates the awareness and understanding is crucial to ensure a successful implementation of green construction [9, 11, 13, 14, 17, 27, 29, 30].

In addition, the other critical success factors for a successful implantation of green construction established in the literature review includes a proper waste management system [13, 14, 17, 26, 27, 29, 30].

A few suggestions and strategies for the successful implementation of green construction were developed from [2, 5, 7, 20]. Among the strategies are listed below:

1. Standardization of design
2. Stock control to minimize over-ordering
3. Environmental education for the workforce
4. Recycling and waste disposal companies as part of the supply chain

5. Practicing just-in-time delivery approaches
6. Penalties for poor waste management
7. Incentives and tender premiums for waste minimisation
8. Waste auditing
9. Increased use of off-site techniques
10. Use of on-site compactors
11. Suppliers required to provide materials and products in small batch sizes
12. Reverse logistics
13. Imposition of stricter regulations
14. Establishment of longer customer-supplier relationship
15. Increased awareness of environmental
16. Social and economic impact
17. Implementation of environmental management system
18. Support and push from top management
19. Implementation of ISO 14000 certifications
20. Regular audits on green environmental standards
21. Customer's willingness to pay extra for green construction and engagement by government bodies during the formulation of the regulations
22. Setting up energy saving objectives at operational levels
23. Consideration of energy objectives at the strategic planning level
24. Value management of energy plans
25. Lifecycle costing accuracy
26. Proved education/awareness of designers about energy efficient materials and techniques use of cost and environmental assessment tools

In addition, factors that are considered as critical to the successful implementation of green construction based on literature analysis are listed as below:

1. High return on investment
2. Role and responsibilities of stakeholders
3. Effective labour and material management
4. Financial well being and capital intensity of organisation
5. Environmental policies and procedure
6. Clear client's specification design and production.
7. Strict environmental regulations
8. Manager's concern on the environment and its protection
9. Commitment of top level management
10. Education and training
11. Internal and external audit
12. Technology processes and development
13. Site environmental assessment
14. Requirement on green equipment and machineries
15. Financial investment in green technology

5 Conclusion

It has been established that there are many different themes and definition of green construction, but they all aim at improving the existing way of constructing buildings.

Green construction requires people who intend to implement it to spend more time to fully understand the benefits and major critical success factors of green construction. These factors should be treated as significant in the process of implementing and practicing green construction with the aim of improving the environment, health and safety, quality and long term investment.

Acknowledgments This paper is supported by FRGS research grant (project no. 600 RMI/FRGS 5/3(37/2012). The authors also would like to thank Universiti Teknologi MARA for supporting this paper.

References

1. A. Ahmad Zaini, R.E. Endut, A.A. Ahmad Zaini, Creating awareness and understanding in implementing green construction, in Symposium on Business Engineering and Industrial Application, IEEE, Kuching, 22–25 Sept 2013
2. M. Arif, C. Egbu, A. Halem, D. Kulonda, M. Khalfan, State of green construction in India: drivers and challenges. *J. Eng. Des. Technol.* **7**(2), 223–234 (2009) (Highly Commended Award Winner at the Literati Network Awards for Excellence 2010)
3. G. Bruntland, *Our Common Future: The World Commission on Environment and Development* (Oxford University Press, Oxford, 1987)
4. T. Cooke-Davies, The “real” success factors on projects. *Int. J. Project Manag.* **20**, 185–190 (2002)
5. A.R.J. Dainty, R.J. Brooke, Towards improved construction waste minimisation: a need for improved supply chain integration? *Struct. Surv.* **22**(1), 20–29 (2004)
6. Department of Statistics Malaysia. Retrived on 31 May 2014
7. P.C. Egbu, Corporate sustainability and investment on green development, in: *Putrajaya Experiential for Sustainable Development*, Pullman Lakeside Putrajaya (2011)
8. T.E. Glavinich, *Contractors Guide to Green Building Construction: Management, Project Delivery, Documentation, and Risk Reduction* (Wiley, New York, 2008), p. 262
9. A.S. Hijjaz, *Sustainable Architecture and Urban Development: Green Design, Architecture and Materials. Putrajaya Experiential Learning for Sustainable Development* (Pullman Lakeside, Malaysia, 2011)
10. L. Huiling, L. Xige, T. Si, Green Construction Bid Evaluation System Based on Comprehensive Evaluation Method (IEEE, New Jersey, 2011)
11. M.S.M. Idris, *Facility Management Contribution in Green Building Initiatives. Putrajaya Experiential for Sustainable Development* (Pullman Lakeside Putrajaya, Malaysia, 2011)
12. R. Jin, S. Wu, Y. Liu, W. Jiang, X. Liu, *Application of Visual FoxPro on Green Construction Assessment* (IEEE, New Jersey, 2010)
13. B. Jonathan, Can ISO 14000 and eco-labelling turn the construction industry green? *Build. Environ.* **37**(4), 421–428 (2002). doi:[10.1016/s0360-1323\(01\)00031-2](https://doi.org/10.1016/s0360-1323(01)00031-2)
14. P.T.I. Lam, E.H.W. Chan et al., Environmental management system vs green specifications: how do they complement each other in the construction industry? *J. Environ. Manage.* **92**(3), 788–795 (2011)

15. X. Liu *Green construction management system for construction project*. (IEEE, New Jersey, 2011)
16. S. McCabe, *Benchmarking in Construction* (Blackwell Science Ltd, London, 2001)
17. G. Ofori, Greening the construction supply chain in Singapore. *Eur. J. Purchasing Supply Manag.* **6**(3–4), 195–206 (2000)
18. R. Pan, in *Proceeding 2010: IEEE 17th International Conference on Industrial Engineering and Engineering Management IE and EM 2010. Study on Green Construction and Index System of Green Construction Assessment (2010)* ISBN: 9781424464814
19. J. Sarkis, Evaluating environmentally conscious business practices. *Eur. J. Oper. Res.* **107**(2), 159–174 (1998)
20. Q. Shi, Y. Xu, S. Chen, *Green Construction Alternatives Evaluation Using GA-BP Hybrid Algorithm* (IEEE, New Jersey, 2009), pp. 1–5
21. Q. Shi, X. Xie, *A Fuzzy-QFD Approach to the Assessment of Green Construction Alternatives Based on Value Engineering* (IEEE, New Jersey, 2009), pp. 1–6
22. Q. Shi, Y. Xu, *The Selection of Green Building Materials Using GA-BP Hybrid Algorithm*, vol. 3 (IEEE, New Jersey, 2009), pp. 40–45
23. R. Takim, *A framework for successful construction performance*, Ph.D. thesis submitted to Glasgow Caledonian University, 2005
24. L.M. Tan, The Development of GBI Malaysia (GBI). *The Launch of GBI* (Kuala Lumpur, 2009)
25. Y. Tan, L. Shen, H. Yao, Sustainable construction practice and contractors' competitiveness: a preliminary study. *Habitat Int.* **35**(2), 225–230 (2011). doi:[10.1016/j.habitatint.2010.09.008](https://doi.org/10.1016/j.habitatint.2010.09.008)
26. O. Tatari, M. Kucukvar, Cost premium prediction of certified green buildings: a neural network approach. *Build. Environ.* **46**(5), 1081–1086 (2011). doi:[10.1016/j.buildenv.2010.11.009](https://doi.org/10.1016/j.buildenv.2010.11.009)
27. C.M. Tam, V.W.Y. Tam, W.S. Tsui, Green construction assessment for environmental management in the construction industry of Hong Kong. *Int. J. Project Manag.* **22**(7), 563–571 (2004)
28. G.Y. Qi, L.Y. Shen, S.X. Zeng, O.J. Jorge, The drivers for contractors' green innovation: an industry perspective. *J. Clean. Prod.* **18**(14), 1358–1365 (2010). doi:[10.1016/j.jclepro.2010.04.017](https://doi.org/10.1016/j.jclepro.2010.04.017)
29. A. Varnas, B. Balfors, C. Faith-Ell, Environmental consideration in procurement of construction contracts: current practice, problems and opportunities in green procurement in the Swedish construction industry. *J. Clean. Prod.* **17**(13), 1214–1222 (2009). doi:[10.1016/j.jclepro.2009.04.001](https://doi.org/10.1016/j.jclepro.2009.04.001)
30. M. Zhu, F. He, R. Tang, T. Liu, L. Wang, *Primary Practice of Green Mine Construction in Limestone Mine* (IEEE, New Jersey, 2010), pp. 1–4

A Review in Developing a High Rise Building Construction Safety and Health Risk Model

Afzan Binti Ahmad Zaini, Intan Rohani Endut
and Nurzawani Binti Md Sofwan

Abstract The construction industry is starting to gain momentum as Malaysia is becoming a fully industrialised country by the year 2020. Due to the complexity and dynamic nature of a construction project, specifically on high rise building, various hazards and risks are already in place at any stage of a project lifecycle. Safety and health risk assessment is the core of any safety practices in any industry. Risk at the construction site should be assessed prior to manage or mitigate it. Therefore, this paper intends to recognize the theoretical aspects of the likelihood and severity of the hazards in the high rise building construction project and to recognize a theoretical aspects in formulating a high rise building construction safety and health risk model. The methodology employed for this paper includes the secondary data collection from journals, articles and government statistics. The successful investigations will lead to the development of safety and health risk model in the construction industry particularly for high rise building construction. This model has prospect to be commercialized through the intellectual property (IP). The health and safety risk model will promote safety climate in the construction site and hence, enhancing the performance of human capital.

Keywords Hazards • Risk • Safety and health risk model • High rise building construction

A.B.A. Zaini (✉)

Department of Quantity Surveying, Faculty of Architecture Planning and Surveying,
Universiti Teknologi MARA, Kota Samarahan, Sarawak, Malaysia
e-mail: afzanahmadzaini@gmail.com

I.R. Endut

Faculty of Civil Engineering, Universiti Teknologi MARA, Shah Alam, Malaysia

N.B.M. Sofwan

Faculty of Health Science, Universiti Teknologi MARA, Kota Samarahan,
Sarawak, Malaysia

1 Introduction

The construction is the most dangerous industry in terms of occupational safety and health as reported by European Agency for Safety and Health at Work [7]. In Malaysia, construction industry is the third leading cause of occupational accidents from ten occupational sectors after manufacturing and agriculture industries [5]. Occupational accidents are commonly occurred in the construction industry including falling of materials or person from height, stepping on objects and injured by hand tools. Occupational accidents become a great burden for employee and employer. It resulted in absenteeism, loss of productivity, ergonomic disabilities, higher incidence rates of health problems and fatalities. In addition, high cost incurred associated with work injuries and bad reputation to the company turn out to be a troublesome [8, 20].

2 Literature Review

High rise buildings are the recent trend in construction industry these days because of its convenience, advantages, architectural design, grade and luxury. High rise construction is a complex project which poses numerous latent hazards and risks. It is characterized by continual changes, use of many different resources, poor working conditions, no steady employment, tough environments such as noise, vibration, dust, handling of cargo and expose to stochastic elements such as weather conditions, soil characteristics and road accidents [24]. Accident causes from machineries and tools always being a major percentage, but acute effect such as permanent disabilities or deaths are frequently happen in high rise building construction site for instance fall from height.

The nature of construction industry is derived from several fragmentations of the involved parties throughout the various phases of construction projects [24]. It requires harmonization of different interdependent contractors, sub-contractors and operations that may result in increased risk of injury [20]. The project management personnel such as construction managers, project managers, site managers, engineers and supervisors have important roles in the art of safety management and for coordinating other project stakeholders, who have different backgrounds and expectation to uphold safety [6, 27]. Therefore, it is imperative for construction companies to be aware to the issue of managing uncertainty and risk in the construction work.

2.1 Accident Causation

Construction work is acknowledged as a high risk occupational area in modern society [15, 19]. Workers safety can be endangered on events through negligence or

unforeseen circumstances. Human error is believed as the main reason for construction industry accidents and it is stem from carelessness or lack of awareness [1, 22]. From system perspectives, errors are deviations in performance which may result from disturbances in the system where the work is being carried out [24]. On the other hand, low education level of construction workers associated with high risk characteristic of construction works also found to be as one of the accident causes [8].

Constant rotations throughout the project lifecycle could increase the possibility of accidents occurring and distract workers from completing their tasks efficiently. Different culture together with language barriers are some of the most relevant worker culture that may contribute for the accident occurrence [24]. Large numbers of construction workers in Malaysia originated from foreign countries such as Bangladesh, Indonesia and Myanmar. Communication deficiencies among the workers as well as the project management personnel become one of the drawbacks for successful implementation of safety management at the site.

2.2 Hazards and Risks

Accidents are derived from arising hazards and risks in the construction project. Hazard is a source or a situation with a potential harm while risk is the combination of the likelihood and severity of a specified hazardous event occurring. The same hazard does not always present the same risk because it depends on the circumstances and the control in place. Each site has different characteristics due to its condition, location, number of workers and work types. Thus, the risk on a new site can differ from that on past projects. A site-specific management tool that considers the characteristics and changeable conditions of the currently managed construction site is necessary to accurately assess risk. Risks are often associated with the negative impact arises within the organization's environment. The process of identifying risks is derived from hazard recognition in each work activity for entire project lifecycle. The risk quantification method has been used as an analytical technique in a number of studies [4].

Studies by Ahmad Zaini et al. [2] found that 59 probable risks in haulage industry could give adverse effects to the industry had been identified and listed down through the risk identification process. Subsequently, all 59 risks were hierarchically categorized into five different groups of general risk issues denoted as environmental risk, financial risk, political risk, social risk, and technical risk. The technical risk is highest risks amounting to 15 risks, followed by environmental risk with 14 risks, social risk with 13 risks, 9 financial risks and 8 political risks as listed below [2].

1. Environmental Risk

- 1(E)-Traffic congestion
- 2(E)-Accidents

- 3(E)-Bad terrain (road condition)
- 4(E)-Natural disaster (flood, land slide, etc.)
- 5(E)-Inclement Weather (rain, storm, drought)
- 6(E)-Theft
- 7(E)-Hijacking
- 8(E)-Terrorism
- 9(E)-Rising fuel cost
- 10(E)-Disintegrated supply chain
- 11(E)-Supplier failure
- 12(E)-Loss of market share
- 13(E)-Increase in customer demand
- 14(E)-Decrease in customer demand

2. *Financial Risk*

- 15(F)-Economic recession
- 16(F)-Increase in rental cost
- 17(F)-Increase in maintenance cost
- 18(F)-Increase in Local taxes
- 19(F)-Uncontrolled inventory cost
- 20(F)-Workers wage
- 21(F)-Late payment by client
- 22(F)-Late payment to subcontractor
- 23(F)-Lacks of financial support (subsidies)

3. *Political Risk*

- 24(P)-Change in government policies
- 25(P)-Corruptions
- 26(P)-Policies on local workers
- 27(P)-Policies on foreign workers
- 28(P)-Relationship with government
- 29(P)-Political demonstration
- 30(P)-Direct intervention by the government
- 31(P)-Unfair project allocation

4. *Social Risk*

- 32(S)-Safety of workers
- 33(S)-Crisis in partnership
- 34(S)-Problems in outsourcing services
- 35(S)-Complain from vendors and customers
- 36(S)-Dispute with vendors and agents
- 37(S)-Workers absence
- 38(S)-Workers demand salary increment
- 39(S)-Workers strike
- 40(S)-Insufficient workforce
- 41(S)-Ineffective communication

- 42(S)-Bad track record/reputation
- 43(P)-Differences in culture
- 44(P)-Differences in religion

5. *Technical Risk*

- 45(T)-Vehicle (truck) breakdown
- 46(T)-Lacks of worker’s training
- 47(T)-Carelessness
- 48(T)-Lacks of vehicle maintenance
- 49(T)-Goods damage
- 50(T)-Delivering hazardous material
- 51(T)-Delivering precious material
- 52(T)-Miss or Wrong pick up and drop off points
- 53(T)-Time waste; long waiting time of goods
- 54(T)-Limited storage capacity
- 55(T)-Delay in delivery
- 56(T)-Adopting new technology
- 57(T)-Using old technology
- 58(T)-Malfunction of IT system (internet, GPS)
- 59(T)-Data loss.

Study carried out by Hallowell and Gambatese [9] focused on severity level and its relative impact score as shown in Table 1.

2.3 Safety and Health Risk Model

Risk need to be managed in order to control it dangers. Risk in construction projects should be characterized by using a model in order to assist the decision of safety professionals. Risk assessment is developed from identifying the risks which

Table 1 Subjective severity level and relative impact score

Subjective severity level	Severity Score	Relative impact score
Temporary discomfort	1	2
Persistent discomfort	2	4
Temporary pain	3	8
Persistent pain	4	16
Minor first aid	5	32
Major first aid	6	64
Medical case	7	128
Lost work-time	8	256
Permanent disablement	9	1024
Fatality	10	26,214

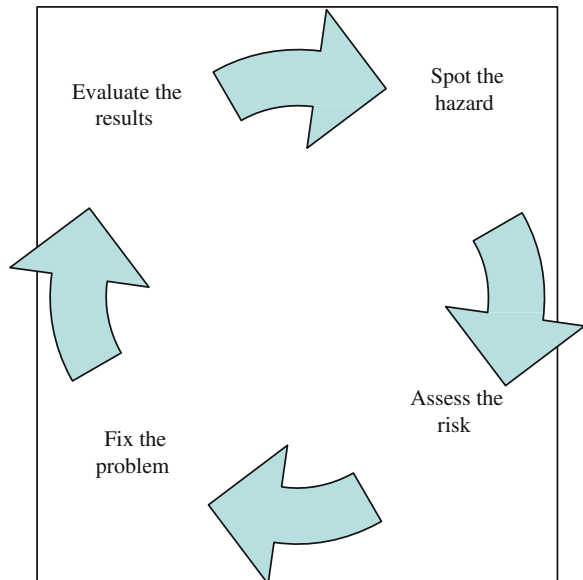
requires a continual and systematic approach. Collecting data on frequency and severity of accidents is also helpful in identifying risks. Nevertheless, the ability of recognizing hazards are varied among different construction personnel. A well-designed safety management system can contribute to the successful implementation of a safety management system in the workplace [13]. Risk assessment is inherently related to risk modeling.

A number of studies on safety and health have generated analytic models that portrayed on the relationship of various factors that lead to construction accidents [11]. Hinze [11] illustrated accidents in terms of a distraction theory. Mitropoulos et al. [16] on the other hand created a system model that showed a complex network of accident contributing factors. The Probability–Impact (P–I) risk model is prevailing and risk is usually assessed through assessing its probability of occurrence and impact. However, the P–I risk model was subject to criticism from researchers who discussed potential improvements in it. Moreover, researchers have investigated different theories and tools [25].

WHSRisk Management Guidelines [26], found that, the SAFE risk management model is a simple and easy to remember process for undertaking risk management. The SAFE risk management model enhances health and safety in the workplace and incorporates a simple four step process. The steps are;

- S Spot the hazard
- A Assess the risk
- F Fix the problem
- E Evaluate the results (Fig. 1).

Fig. 1 SAFE model
(Adopted from WHSRisk Management Guidelines [26])



This model should be undertaken:

- Following a workplace accident, injury or near miss
- Before moving to a new or renovated premises
- Before any new equipment or chemicals are purchased
- When introducing new work tasks and procedures or training programs
- When any previous risk assessment is now likely to be out of date
- When no previous risk assessment has been conducted.

In addition, several models were developed for the integration of risk and occupational safety and health management within the management of the organizations in particular starting from the planning and scheduling tasks of construction projects as addressed by Cagno et al. [3], Kartam [14]. Hadikusumo and Rowlinson [10] developed a tool to visualize construction process and identify the hazards during the design stage. A model integrating occupational safety and health management in the design stage with control in the execution stage is designed by Saurin et al. [22].

Many authors use Fuzzy Set Theory (FST) to produce more realistic representations and solutions. FST offers a natural way of modeling the intrinsic vagueness and imprecision of daily concepts by generating a very precise approach for dealing with uncertainty which grows out of the complexity of human behavior [21].

When conducting risk assessment at construction sites, there are inadequate data or inaccurate information available and safety practices implemented at construction sites are site oriented. However, most of the prevalence risk assessment models are generalized and not depend on which context risk is undertaken [21]. Delimiting the scope of occupational safety and health risk model to the high rise building construction will attribute to specific situation and applicable in similar scopes.

3 Problem Statement

Investigation on the current status of accidents and injuries among construction project participants is crucial because high rise building construction is one of the most risky workplace [12]. High rise buildings remain predominant for high accident rates due to diverse hazards associated with working at heights and with the vertical transportation of materials [8]. The use of quantitative occupational safety risk assessment models based on probabilistic techniques, using data collected at different construction sites and in diverse types of construction projects can lead to imprecise results and do not reflect the reality of the site under analysis [21]. There is a clear gap between the theory and practice of risk modeling and assessment. Occupational safety and health risk model for high rise building construction is developed with the intention of suppressing the gap.

4 Research Aim and Objectives

The aim of this study is to develop a high rise building construction risk modeling for the Malaysian construction industry. This study intends (1) to recognize the likelihood and severity of the hazard and risk at the high rise building construction project and (2) to formulate a high rise building construction safety and health risk model.

However, this paper only focusing on the theoretical aspect of the research objectives.

5 Research Methodology and Process

Secondary data in the form of government statistics, journal and articles are obtained to achieve the first objective and second objective of this paper. However, the study intends paradigm of triangulation methodology which combines both the quantitative (questionnaire) and qualitative (interview) research techniques will be implemented. Secondary data in the form of government statistics will be obtained to achieve the first objective of the research. For the second objective, questionnaire and semi structured interview are primarily preferred due to its ability to gather data from a relatively large number of respondents within a limited time frame.

Furthermore, survey is more often than not concerned with a generalised result when data is abstracted from a particular sample or population [17]. This type of collection data deals with perception and attitudes of people. The targeted sample of this research is 150 personnel including construction workers, project manager and supervisors. Quantitative studies include a substantial amount of literature to provide direction for the research questions or hypotheses. In planning a quantitative study, the literature and theory are used to direct the study deductively as a framework for the research questions or hypotheses. To a certain extent, in quantitative studies, one uses a theory deductively and places it towards the beginning of the plan for a study with the objective to test or verify a theory, rather than develop it [17, 18].

A pilot questionnaire will be designed and pretested amongst the construction workers prior collecting the actual data. Semi structured interview will be conducted to underpin the questionnaires survey. The results obtained from the secondary data, questionnaire survey and semi structured interview will be analysed by using the statistical and content analysis method. This result will help in the formulation of construction of safety and health risk model. Partial Least Square (PLS) regression will be adopted in formulating the safety and health risk model.

The last stage is the validation process within the Malaysian construction project stakeholders. The validation process of the model will be conducted by distributing questionnaires to fifteen (15) selected respondents from the interview survey to support the requirement and action required by the companies. In addition,

validation process is to achieve the continuity of information in relation to the completeness, ease of understanding the model, practical and valid to fit-for-purpose of the construction industry in Malaysia [23].

Finally, conclusions will be drawn for the high rise building construction modeling and recommendations are made for further research.

6 Scope and Limitation of Study

This paper is trying to recognize the theoretical aspect on the likelihood and severity of the hazards in the high rise building construction project and recognize the theoretical aspect on a high rise building construction safety and health risk modeling. The study only focuses on high rise building construction whereas in Malaysia there are many types of building such as educational, administrative and health and welfare buildings to name a few.

7 Significance of the Study

This study assists the construction management personnel to make decision making on managing the occupational risk at the construction site particularly high rise building project. The developed model is found to be benefit in characterizing the high risk construction activities and thus promoting safety climate at the workplace.

Acknowledgments The authors also would like to thank Universiti Teknologi MARA for supporting this paper.

References

1. T. Abdelhamid, J.G. Everett, Identifying root causes of construction accidents. *J. Constr. Eng. Manage.* **126**(1), 52–60 (2000)
2. A.A. Ahmad Zaini, I. Endut, A. Ahmad Zaini, A study of the likelihood and impact of risks in the land cargo transportation, in *IEEE Symposium on Humanities Science and Engineering 2013* (2013)
3. E. Cagno, A.D. Giulio, P. Trucco, An algorithm for the implementation of safety improvement programs. *J. Saf. Sci.* **37**, 59–75 (2001)
4. K.S. Dewlaney, M.R. Hallowel, B.R. Fortunato, Safety risk quantification for high performance sustainable building construction. *J. Constr. Eng. Manage.* **138**, 964–971 (2012)
5. Department of Safety and Health (DOSH). Occupational accidents statistics by sector until June 2014. Retrieved on 28 Feb 2014
6. D.P. Dingsdag, H.C. Biggs, V.L. Sheahan, D.J. Cipolla, *A Construction Safety Competency Framework: Improving OH&S Performance by Creating and Maintaining a Safety Culture* (Cooperative Research Centre, Brisbane, 2006)

7. EASHW, *Facts: Accident Prevention in the Construction Sector*, European Agency for Safety and Health at Work (EASHW) (European Commission Senior Labour Inspectors' Committee, Belgium, 2003)
8. I.W.H. Fung, V.W.Y. Tam, T.Y. Lo, L.L.H. Lu, Developing a risk assessment model for a construction industry. *Int. J. Project Manage.* **28**, 593–600 (2010)
9. M.R. Hallowell, J.A. Gambatese, Population and initial validation of a formal model for construction safety risk management. *J. Constr. Eng. Manage.* **136**, 981–990 (2010)
10. B.H.W. Hadikusumo, S. Rowlinson, Integration of virtually reality construction model and design for a safety-process database. *J. Autom. Constr.* **11**, 501–509 (2012)
11. J.W. Hinze, *Construction Safety* (Prentice Hall, Englewood Cliffs, 1997)
12. D.J. Hsu, Y.M. Sun, K.H. Chuang, Y.J. Juang, F.L. Chang, Effect of elevation change on work fatigue and physiological symptoms for high-rise building construction workers. *J. Saf. Sci.* **46**, 833–843 (2008)
13. Z. Ismail, S. Doostdar, Z. Harun, Factors influencing the implementation of safety management system for construction sites. *J. Saf. Sci.* **50**, 418–423 (2012)
14. N.A. Kartam, Integrating safety and health performance into construction CPM. *J. Constr. Eng. Manage.* **123**(2), 121–126 (1997)
15. C.W. Liao, Y.H. Perng, Data mining for occupational injuries in the Taiwan construction industry. *J. Saf. Sci.* **46**(7), 1091–1102 (2008)
16. P. Mitropoulos, T.S. Abdelhamid, G.A. Howell, Systems model of construction accident causation. *J. Constr. Manage.* **131**(7), 816–825 (2005)
17. S.G. Naoum, *Dissertation Research and Writing for Construction Students* (Butterworth-Heinemann, Oxford, 1998)
18. W.L. Newman, *Social Research Methods: Qualitative and quantitative Approaches*, 3rd edn. (Allyn and Bacon, Boston, 1997)
19. C. Niza, S. Silva, M.L. Lima, Occupational accident experience, association with worker's accident explanation and definition. *J. Saf. Sci.* **46**(4), 959–971 (2008)
20. A. Pinto, I.L. Nunes, R.A. Ribeiro, Occupational risk assessment in construction industry—overview and reflection. *J. Saf. Sci.* **49**, 616–624 (2011)
21. A. Pinto, QRAM a qualitative occupational safety risk assessment model for the construction industry that incorporate uncertainties by the use of fuzzy sets. *J. Saf. Sci.* **63**, 57–76 (2014)
22. T.A. Saurin, C.T. Formoso, L.B.M. Guimares, Safety and production: an integrated planning and control model. *J. Constr. Manage. Econ.* **22**(2), 159–169 (2004)
23. Z. Shehu, The framework for effective adoption and implementation of programme management within the U.K construction industry, in *School of The Built and Natural Environment Glasgow Caledonian University*, Caledonian University, U.K
24. V. Sousa, N.M. Almeida, L.A. Dias, Risk based management of occupational safety and health in the construction industry—part I: background knowledge. *J. Saf. Sci.* **66**, 75–86 (2014)
25. A. Taroun, Towards a better modeling and assessment of construction risk: insights from a literature review. *Int. J. Project Manage.* **32**, 101–115 (2014)
26. WHSRisk Management Guideline, University of Canberra Document, *Document Custodian: Manager Health and Safety*. Date Review: Jan 2013 (2013)
27. P.X.W. Zou, R.Y. Sunindijo, Skills for managing safety risk, implementing safety task and developing positive safety climate in construction project. *J. Autom. Constr.* **34**, 92–100 (2013)

Evaluating Importance Level of Buildability Factors in Cambodian Construction Projects

Heng Ly, Tanit Tongthong and Vachara Peansupap

Abstract Buildability refers to the integration of construction knowledge during the design stage to enhance the ease of construction while meeting all requirements of the owner/client. Insufficient buildability in design could result in design rework, low site productivity, increased cost, and changes in the contract. Many previous studies have explored the buildability factors. However, these buildability factors might vary across the countries due to the differences in site conditions, current construction technologies, and availability of materials, equipment and experiences. This research aims to evaluate the importance level of buildability factors of building construction projects in Cambodia. The questionnaires with five-point Likert scale were distributed to project managers and engineers of building contractors in Cambodia. The analysis of one-sample *t* test showed that there are twelve significant buildability factors. The top five important factors to evaluate buildability were: (1) standardization; (2) completion of design documents; (3) clear specifications; (4) labour skills and (5) design to suit with site conditions. The ranking of the factors and factor categories provides useful information for designers to improve buildability of their designs. The important factors of this research were used for the development of buildability assessment model for building construction projects in Cambodia.

Keywords Buildability factors · Building design · Building construction projects · Cambodia

H. Ly (✉) · T. Tongthong · V. Peansupap
Department of Civil Engineering, Faculty of Engineering,
Chulalongkorn University, Bangkok 10330, Thailand
e-mail: ly.heng@live.com

T. Tongthong
e-mail: tanit.t@chula.ac.th

V. Peansupap
e-mail: pvachara@chula.ac.th

1 Introduction

As the design and construction of projects become increasingly complex, more attention is given to the exchanges of knowledge during the preconstruction stage to develop the best design solution [1]. Buildability is a concept of integrating the construction knowledge into the design [2], therefore the potential construction problems caused by the design could be eliminated. Insufficient buildability in designs could result in design reworks, changes in contract, schedule and cost overruns, claims and disputes during construction [3].

Most building construction projects in Cambodia are still using the traditional construction method. Thus the productivity of the construction industry is low and needed to be improved. The evaluation of buildability of current building projects is very important for buildability improvement. The buildability factors were studied in various advanced construction industries from different perspectives of stakeholders. However, due to the differences in site conditions, current construction technologies, and availability of materials, equipment, and experiences, the buildability factors vary from countries to countries. Therefore, it is necessary to study the buildability factors in the Cambodian construction industry. This paper aims to identify the important factors to evaluate the buildability of medium- and high-rise building designs in Cambodia from the viewpoint of contractors since the designers are usually lack of construction experience and knowledge of construction technologies [1]. This research would benefit the designers to understand the buildability concepts the buildability concepts from the perspective of contractors so that buildability improvement could be made to their designs.

2 Literature Review on Buildability Factors

The report of Construction Industry Research and Information Association (CIRIA) [4] represented seven categories of buildability principles which were to carry out thorough investigation and design, plan for essential site production requirements, plan for a practical sequence of operations and early disclosure, plan for simplicity of assembly and logical trade sequences, detail for maximum repetition and standardization, detail for achievable tolerance, and specify robust and suitable material. The study of CIRIA raised the awareness of the concepts and principles of buildability.

In the U.S., Construction Industry Institute (CII) [5] published 14 concepts in Constructability Concepts File as Constructability guidelines: six for consideration during conceptual planning; seven for design, engineering and procurement stages; and one for site operation. The guidelines were updated in 1997 to cover seventeen concepts: eight for conceptual planning; eight for design and procurement; and one for field operation [6]. The implementation of these constructability guidelines exerts greater emphasis on overall optimization of schedule and cost at the early

phase of a project. Constructability has gained acceptance throughout the industry in the U.S., but the constructability techniques were varied [7]. Under the collaboration of CII Australia and CII U.S. (1993), a Constructability Principles File customized for the Australian context was developed and 12 overriding principles were presented to apply in the project [8]. The concepts of constructability were extended to include operation and maintenance issues to improve effectiveness and efficiency of infrastructure projects [9]. In addition, Arditi et al. [3] concluded that faulty working drawings, incomplete specifications, and adversarial relationships between parties were the main causes of constructability problems from the perspective of design firms.

In the Code of Practice on Buildability of Building and Construction Authority of Singapore [2], a buildable design is achieved by the principles of standardization, simplicity and single integrated elements. Standardization means repetition of design details; simplicity refers to the ease of installing building system; single integrated elements are the prefabricated combined components ready to be installed on site. The Building Design Appraisal System was developed based on these principles to assess the site labour requirement of a design. Poh and Chen [10] supported that the higher score from the appraisal system will result in more efficient labour usage and higher productivity on site.

Wong [11] consolidated the buildability attributes into nine buildability factors to evaluate the buildability of building designs in Hong Kong. These factors covered economic use of contractor's resources, visualization and coordination of design requirements by site staff, adoption of construction detail by contractors, overcoming restrictive site conditions, standardization and repetition, choice between prefabrication and on-site work, simplification of construction details, flexible construction program to minimize impact of adverse weather, and safe construction sequence on the site. A buildability assessment model was developed based on these nine factors. Lam et al. [12] suggested that simplicity, working space to enable safe construction, minimizing water ingress and geotechnical difficulties were the most important buildability factors affecting buildability in Hong Kong.

The buildability factors of in situ reinforced concrete building components were studied by Jarkas. In a series of his study on reinforced concrete column, beam, slab and wall, he identified the buildability factors of these building components and quantified the relationship between these buildability factors and actual productivity [13–15]. The main buildability factors were variability of size of building components, rebar diameter, reinforcement quantity, geometry, dimension, and grid pattern. These studies provide detailed calculations of buildability in the design of reinforced concrete components and also showed the consequences of the design on labour productivity.

Weinstein et al. [16] suggested that design could improve construction safety and they also categorised the design changes affecting the construction plans into access, material handling, fall protection, material substitution, and construction process. Behm [17] reported that 42 % of fatalities studied were linked to design concepts and proposed the consideration of construction site safety in the design of a project to reduce or eliminate potential risks before executing the work on site.

3 Research Methodology

After reviewing the buildability factors from literature, the factors related to design outputs were summarized and grouped into (1) design documents; (2) resources; (3) flexibility to change; and (4) site layout and construction safety. To ensure that the wording of the factors were comprehensible and that the others important factors were not overlooked, a pilot survey with ten experienced engineers were conducted. In total, 20 factors were identified. Table 1 shows the 20 factors under the four categories.

The 20 factors were used to develop the questionnaire to gather the opinions of project managers and engineers of building contractors. The purpose of the study, the definition of buildability and the description of each buildability factor were written on the questionnaires to improve the comprehensibility and assure a common understanding of each respondent. The importance level of each buildability factor was evaluated by 5-point Likert Scale of which the value of 5 denotes very

Table 1 Factor label, factor category and factor name

Factor label	Factor category	Factor name
F1	Design document	Standardization
F2	Design document	Simplicity
F3	Design document	Coordination between design documents
F4	Design document	Completion of design documents
F5	Design document	Clear specification
F6	Design document	Underground construction
F7	Design document	Specify tolerance
F8	Resource	Availability of material
F9	Resource	Availability of machine and equipment
F10	Resource	Requirement of manpower
F11	Resource	Requirement of labour skill
F12	Flexibility	Alternative construction detail
F13	Flexibility	Wide alternative of material
F14	Flexibility	Allowing innovative construction method/technique
F15	Flexibility	Allowing flexible construction sequencing
F16	Safety and site layout	Design to suit with site conditions
F17	Safety and site layout	Design to support transportation of labour and material
F18	Safety and site layout	Safe approach to work
F19	Safety and site layout	Design support safety
F20	Safety and site layout	Allowing safe construction sequence

high importance and the value of 1 indicates very low importance. The respondents were asked to assign the importance of each factor from 1 to 5 and to cross out the inapplicable factors. They were encouraged to provide their comments and suggestions at the end of the questionnaire.

The respondents are contractors, project managers and engineers of mid- and high-rise buildings in Phnom Penh city. The city was selected because it is the capital city of Cambodia, the centre of politics and commerce where the headquarters of many construction companies are located. The questionnaires were distributed through personal contacts.

Thirty-five (35) valid responses were collected back for analysis. All of the respondents have worked in mid- and high-rise building construction and have 8.9 years of experience on average. The respondents were considered to possess adequate knowledge to answer the questionnaire.

4 Method of Data Analysis

The score assigned by the respondents indicated the extent of their agreement on the importance level of each buildability factor. The data collected were analysed with the assistance of the Statistical Package for Social Sciences (SPSS).

First, the overall internal consistency of the questionnaire was tested by Cronbach's alpha. Cronbach's alpha is one of the most commonly used indicators of intercorrelations among test items. The value of Cronbach's alpha varies between 0 and 1 where a higher value implies higher consistency. However, too high value of alpha may suggest that some items in the questionnaires are redundant and should be removed [18]. The Cronbach's alpha of 0.753 in this research suggests that the scale scores have good internal consistency. The minimum recommended level of Cronbach's alpha is 0.7 [19].

The second step in the analysis was to test if the factors could be prioritized. Kendall coefficient of concordance (W) was used to test the null hypothesis (H_0) that the 35 sets of ranking are independent or unrelated at 95 % level of confidence. This coefficient was used by Aibinu and Odeyinka [20] to rank the construction delay factors of project in Nigeria, and by Nkado [21] to rank the construction time-influencing factors of building in the U.K. When the factors are more than 7, the significance of testing can be approximated by chi-square distribution with $(N - 1)$ degree of freedom [22]. The formula is given as:

$$\chi^2 = m(N - 1)W$$

where m is the number of respondents, N is the number of factors.

Finally, the importance level of each buildability factor was determined by using one-tailed one-sample t test of 95 % confidence interval with a statistical significance mean score of 3.5 as cut-off point. This value is the minimum value of the means of all the factors studied.

5 Results

The value of Kendall coefficient of concordance in this study is 0.084. The low value of W enables the rejection of the null hypothesis that the respondents' ratings were unanimous. Therefore, we could conclude with confidence that there was a lack of concordance among the 35 respondents which implied that the responses collected could be regarded as essentially random and that the factors could be prioritized. The top five factors contribute to a buildable design are standardization (F01), completion of design documents (F04), clear specification (F05), requirement of labour skill (F11), and design to suit with site conditions (F16). These factors indicate the top concerns of the contractors about buildability of a building design.

Table 2 indicates the result of one-sample t test. Among the 20 buildability factors, 12 of them pass the test and could be classified with 95 % confidence that they are important factors of design influencing the construction process. The top three factors are related to design documents and all four factors related to resources are important. In contrast, all four factors related to flexibility and the other three factors related to construction safety fail the test. The only factor of design documents that perceived as unimportant is specify tolerance.

Table 2 Result of one-sample t test of mean score of 20 buildability factors

Factor label	Total score	Mean	Relative importance index	Factor rank	Weight (%)	Cumulative weight	t -test (p-value)	Inference
F01	158	4.51	0.90	1	5.64	5.64	0.000	Important
F04	155	4.43	0.89	2	5.53	11.17	0.000	Important
F05	155	4.43	0.89	3	5.53	16.71	0.000	Important
F11	150	4.29	0.86	4	5.36	22.06	0.000	Important
F16	150	4.29	0.86	5	5.36	27.42	0.000	Important
F02	147	4.20	0.84	6	5.25	32.67	0.000	Important
F08	144	4.11	0.82	7	5.14	37.81	0.000	Important
F17	144	4.11	0.82	8	5.14	42.95	0.000	Important
F10	143	4.09	0.82	9	5.11	48.05	0.002	Important
F03	142	4.06	0.81	10	5.07	53.12	0.001	Important
F09	139	3.97	0.79	11	4.96	58.09	0.005	Important
F06	137	3.91	0.78	12	4.89	62.98	0.009	Important
F18	134	3.83	0.77	13	4.78	67.76	0.064	Not important
F19	133	3.80	0.76	14	4.75	72.51	0.067	Not important
F12	132	3.77	0.75	15	4.71	77.22	0.089	Not important
F20	132	3.77	0.75	16	4.71	81.94	0.079	Not important
F13	128	3.66	0.73	17	4.57	86.50	0.233	Not important
F14	128	3.66	0.73	18	4.57	91.07	0.198	Not important
F15	128	3.66	0.73	19	4.57	95.64	0.244	Not important
F07	122	3.49	0.70	20	4.36	100.00	0.475	Not important

6 Implications and Conclusion

This study assessed the importance level of buildability factors from the perspectives of building contractors. The results show that the factors related to design documents are considered as the most important contributors influencing the construction process. This reflects the fact that the contractors encounter many problems during construction caused by design documents. It also implies that some designers in Cambodia are lack of awareness of the influence of their designs on construction process and lack of construction knowledge to improve their designs.

Standardization refers to the use of design standard, repetition of design details and floor layouts. Lack of standardization in design could result in waste of formwork, increased worker supervisions, increased chance of errors, reduced productivity, and increased difficulty in making shop drawings and as-built drawings. Due to the absence of applicable national design standard in Cambodia, the designers are allowed to use any widely recognized design code. Therefore, some projects might not have clear design standard while others use the design standard that the contractors have never encountered before. The contractors need to spend more time to study the requirements of the design standard or to clarify many times with the designers and consultants about the implied details in these projects.

Complete design documents from the designers for the whole project should include architectural drawings, structural drawings, MEP drawings, technical specifications for these drawings, and the calculation notes. Complete design documents from the beginning of the project are very important to ensure that the construction process will not be interrupted by the delay of designs. The drawings should also have good coordination of design details so that the design and construction reworks could be minimized.

Specifications are very important for contractors to estimate the bidding price and to make the method statement for construction. It is a tool of coordination between consultant, designer and contractor about the inspection and acceptance of the works. Conflicts could occur during construction on requirements of the materials used, method to use the materials, and quality of the finished works due to unclear specifications. Tolerance, general notes and typical drawings should follow specific standard, be clear and included in the specifications.

Unlike manufacturing job, construction is a laborious job requiring skilled labours. The traditional cast-in-place construction technique that most Cambodian contractors use consumes numerous manpower to complete a building. Unfortunately, there are very few technical training schools in Cambodia and none of them teaches about the basic and practical skills such as installing scaffolding and formwork, or operating heavy machines. Therefore, skilful workers are very difficult to find and even skilful workers are not acquainted with the modern construction techniques.

Construction site layout affects the efficiency and safety of construction process as a whole. Design to suit with site conditions refers to investigating the site and soil conditions thoroughly and designing the building to suit the given conditions.

Thorough site investigation is not only important to design the foundation but also to eliminate the unexpected encounters of underground objects such as existing foundation, pipeline, electricity line, sewage, and septic tank during construction. A poor soil investigation can result in change in foundation design during the construction and will affect the whole construction process.

Simplicity of design concerns about the geometry of building components, the layout and shape of the building. Since most of the construction works in Cambodia are in situ concrete work, the contractors could 'hand-tailor' the shape of the building according to design, and thus simplicity is not the main concern of the designers as well as the contractors. However, more complicated design will require higher skill and more labour to complete.

Most of the construction materials in Cambodia are imported from neighbouring countries in ASEAN and China. Although the contractors could purchase most of the common construction materials related to reinforced concrete structure from local suppliers, some materials related to prestressed, steel and composite structure require special order or import. In the latter case, the contractors need to consider about the availability and lead time of the materials. Delay in supply of materials could jeopardize the whole construction process.

Similarly, all construction machines and equipment used in Cambodia are also imported. Construction equipment for reinforced concrete structure, bored pile and driven pile are widely available in Cambodia. Other equipment for prestressed, steel and composite structure such as jacking machine, steel stud welding machine are more difficult to find. Designs that require special machines or equipment will preclude the contractors with limited resource or willingness.

Free space on construction site directly affects the selection of construction techniques, the storage of materials, and the usage of construction equipment. The construction difficulties increase as the proximity to the surrounding buildings increases. Construction in confined area limits the number of labour and equipment used, increases the difficulty of transportation within the site, and also increases the potential of accidents on site.

Coordination between designs is poor in Cambodia because the design process is usually divided into several phases responsible by different professionals from different companies. The normal process is that, first, the architect develops the conceptual design according to the requirements of the owner. Then the structural engineer designs the structure of the building based on architectural design. Finally, the MEP engineer designs mechanical devices, wiring of electricity and plumbing system based on architectural and structural design. Normally in Cambodia, MEP is in a separate company from architecture and structure. The change in one drawing will affect the others and lead to inconsistency between design drawings. The fragmented nature of design process results in uncoordinated and conflicting design documents. These conflicts will lead to construction errors or redesigns in the construction phase.

Construction of the basement will increase the difficulty of construction. The difficulty increases as the site get smaller. The contractors need to carefully monitor and reduce the effects of construction on surrounding buildings. The process of basement construction is greatly affected by the weather. Cambodia has a clear

raining and dry season, all the underground works have to be finished within the dry season or the rain will fill the excavated area and delay construction schedule. Moreover, the commonly encountered high water level and soft soil condition also increase the difficulty of excavation.

Factors related to flexibility to change are regarded as minor issues because the contractors will generally follow the drawings and instructions of the designers and consultants without much suggestions since any significant change after the bidding could be claimed as variation order. Moreover, some contractors in Cambodia are lack of knowledge in proposing new construction technique and sequence, and in using modern materials and equipment. The commonly used traditional project procurement method and construction technique also limit the flexibility of design and construction process.

In Cambodia, the contractors consider safety as their management problem and agree to solely assume the responsibility. Since there is no regulation about construction safety in design, designers do not have to consider about the installation of temporary equipment to support safety as well as the erection process in their designs. Moreover, the accidents on site are usually concealed from the public and not reported to the authorities. The emphasis upon safety varies depending on consultants, contractors and project managers. Foreign and standardized companies would concern more about safe approach to work than small local companies. Some local companies even claim that they do not have enough budget to enforce safety on site and that the construction cost would increase if they are too strict in safety implementation.

The ranking of the factors and factor categories provides useful information for designers to improve buildability of their designs. The important factors of this research can be used for the development of buildability evaluation model for building construction in Cambodia.

Acknowledgments The writers would like to appreciate the financial aid of ASEAN University Network Southeast Asia Engineering Education Development Network (AUN/SEED-Net) program throughout the research period and all the respondents of this study for their valuable answers, comments and suggestions.

References

1. F.T. Uhlik, G.V. Lores, Assessment of constructability practices among general contractors. *J. Archit. Eng.* **4**(3), 113–123 (1998)
2. BCA, Code of Practice on Buildability, Building and Construction Authority, Singapore (2013)
3. D. Arditi, A. Elhassan, Y.C. Toklu, Constructability analysis in the design firm. *J. Constr. Eng. Manage.* **128**(2), 117–126 (2002)
4. CIRIA, *Buildability: An Assessment*. Construction Industry Research and Information Association, London (1983)
5. CII USA, *Constructability Concepts File*. Construction Industry Institute, Austin (1987)
6. CII USA, *Constructability Guidelines*. Construction Industry Institute, Austin (1997)

7. J.B. Pocock, S.T. Kuennen, J. Gambatese, J. Rauschkolb, Constructability state of practice report. *J. Constr. Eng. Manage.* **132**(4), 373–383 (2006)
8. A. Griffith, A.C. Sidwell, Development of constructability concepts, principles and practices. *Eng. Constr. Arch. Manage.* **4**(4), 295–310 (1997)
9. E. Saghatforoush, B. Trigunarysyah, E. Too, A. Heravitorbati, Effectiveness of constructability concept in the provision of infrastructure assets, in *Proceeding of the First International Postgraduate Conference on Engineering, Design and Developing the Built Environment for Sustainable Wellbeing (EDBE2011)*, Queensland University Technology, Brisbane, 7–10 Feb 2011, pp. 175–180
10. P.S.H. Poh, J. Chen, The Singapore buildable design appraisal system: a preliminary review of the relationship between buildability, site productivity and cost. *Constr. Manage. Econ.* **16**, 681–692 (1998)
11. W.H. Wong, Developing and implementing an empirical system for scoring buildability of design in the Hong Kong construction industry, Doctoral dissertation, The Hong Kong Polytechnic University, 2007
12. P.T.I. Lam, F.K.W. Wong, F.W.H. Wong, Building features and site specific factors affecting buildability in Hong Kong. *J. Eng. Design Technol.* **5**(2), 129–147 (2007)
13. A.M. Jarkas, The impacts of buildability factors on formwork labour productivity of columns. *J. Civil Eng. Manage.* **16**(4), 471–483 (2010)
14. A.M. Jarkas, The influence of buildability factors on rebar fixing labour productivity of beams. *Constr. Manage. Econ.* **28**(5), 527–543 (2010)
15. A.M. Jarkas, Buildability analysis and measurement of buildability factors influencing rebar installation labor productivity of in situ reinforced concrete walls. *J. Arch. Eng.* **18**(1), 52–60 (2012)
16. M. Weinstein, J. Gambatese, S. Hecker, Can design improve construction safety?: Assessing the impact of a collaborative safety-in-design process. *J. Constr. Eng. Manage.* **131**(10), 1125–1134 (2005)
17. M. Behm, Linking construction fatalities to the design for construction safety concept. *Saf. Sci.* **43**, 589–611 (2005)
18. M. Tavakol, R. Dennick, making sense of Cronbach’s alpha. *Int. J. Med. Educ.* **2**, 53–55 (2011)
19. J.C. Nunnally, *Psychometric Theory* (McGraw Hill, New York, 1978)
20. A.A. Aibinu, H.A. Odeyinka, Construction delays and their causative factors in Nigeria. *J. Constr. Eng. Manage.* **132**(7), 667–677 (2006)
21. R.N. Nkado, Construction time-influencing factors: the contractor’s perspective. *Constr. Manage. Econ.* **13**, 81–89 (1995)
22. S. Siegel, N.J. Castellan, *Nonparametric Statistics* (McGraw Hill, New York, 1988), pp. 235–244

Developing an Accident Causation Model for Accident Prevention at Building Construction Sites

Amran Asan and Zainal Abidin Akasah

Abstract Undoubtedly Malaysian construction industry contributes enormously towards Malaysia's nation economic growth. Despite the significant role of the construction industry plays in the country's development and its heavy contribution towards economic growth and employment, the statistics show a high prevalence of accidents and injuries in the industry, resulting in non-permanent or permanent disabilities, fatalities and damage or loss of property. Past research suggests that on-site construction accidents can be prevented by identifying the root causes, thereby making such predictions based on knowledge and resources on accident causation possible. The aim of this study is to develop an Accident Causation for Accident Prevention (ACfAP) model for key management parties at Malaysia building construction sites. At this stage, this paper will present the initial stage of study (the information gathering phase) by presents the significant groups of accident causations factors for accident prevention. In overall, this ongoing research will be divided into three phases; (i) the information gathering phase;; (ii) the model development phase; and (iii) the model analysis phase. First, previous studies on safety, accident causation and prevention of accidents at construction sites are briefly reviewed from books, theses and journal articles in order to provide a global perspective on the subject. Second, a comprehensive ACfAP will be developed based on the attributes of accident causation obtained from expert surveys. Third, the hypothesised relationships are tested using partial least squares (PLS) path modelling approach. Finally the ACfAP Model for key management at building construction sites will be developed.

Keywords Construction · Accident · Causation · Prevention · Management

A. Asan (✉) · Z.A. Akasah (✉)
Faculty of Civil and Environmental Engineering, Universiti Tun Hussein Onn
Malaysia (UTHM), Batu Pahat, Malaysia
e-mail: amran_asan13@yahoo.com

Z.A. Akasah
e-mail: zainal59@uthm.edu.my

1 Introduction

Malaysia has moved fast to keep pace with the changes of times as the country aspires to achieve strong economic growth and to chart its course as a developed nation by year 2010. In fact, the construction industry is one of the most important and significant sector and has registered positive on the economic and social by yearly employment growth [1] with more than 1,000,000 employed person since 2020 [2]. However, also of significance is the number of construction accidents taking place in the country over the years, leading to a high accident rate with even higher incidence of injuries and fatalities [3]. The fact is working in construction sites is still considered as an extremely dangerous, dirty and difficult job and exposes workers to a lot of occupational hazards and risks [4]. Construction accidents are costly, leading to delays in project completion, increased costs and loss of constructors' reputation [5]. For the workers, accidents cause a loss of ability to work, long-term absenteeism, risk of exclusion from the labour market and even of death due to sickness and injury [6].

Today, the protection of safety and health of construction workers seems challenging because of the diverse and dynamic nature of the industry [7]. Issues of safety and accidents on sites are becoming main areas of concern at every construction projects [8], as the construction industry accounts for the highest percentage of occupational accidents in the country. In fact, numerous of dialogues were held between the government and the key players in the construction sector to improve safety awareness, work procedures and also to look deeply into the strengths and weaknesses of the existing procedure practices [9]. The government has urged both the employers and employees in the construction industry to ensure that workplaces are safe and accident-free and not to take matters of safety lightly [10]. In fact, Construction Industry Development Board (CIDB) Malaysia Act 1994 (Act 520) has been amended accordingly to increase the level of safety at construction sites as a response to the general lack of safety awareness, with the aim of reducing accidents at construction sites [11]. However, in spite of the amendments, there is still room for improvement [12].

At present, many new safety and accident prevention models have been developed, improved and implemented, but as the nature of the construction industry and the processes in the construction works grow in complexity, the potential for serious accidents has also sharply increased [13]. It is predicted that future accident causation and prevention models will become more complicated to keep up with the increase in the usage of high technology tools on site, types of construction procurement and height of building [14]. In this regard, management support is crucial in providing the best solution for safety-related problems and in improving the overall safety level in the construction industry [15, 53, 56]. In short, there is an urgently need to coordinate the development of a new model of safety and health awareness for accident prevention in order to deal with current and future challenges of accidents in the construction industry. Thus, the purpose of this paper is to provide a comprehensive model of accident prevention for key management parties which directly involved in

the building construction projects and to demonstrate the usefulness of this model to reduce accidents in Malaysian building construction sites.

2 Background of Study

The construction industry is well known as one that involves the most hazardous activities. Site accidents are one of the significant and key problems that are common in construction sites [16]. Thousands of people are either killed or disabled during construction industrial accidents every year [17]. Construction industrial accidents also cause huge injuries and loss of human lives, immense environmental damage and deep financial loss [13]. Studies done in many countries such as USA, Finland, Turkey, China and Korea revealed that a high rate of accidents in the construction industry is largely due to poor performance in safety and health provisions [18]. In South Africa, many recent workplace accidents involving loss of limbs and lives have occurred on construction sites [19], which not only can be very devastating but also can lead to major adverse impact to the firm’s daily production [20].

This situation is similar in Malaysia, where the construction industry has also been considered as one of the most hazardous industry [21]. According to official statistics by the Malaysian Ministry of Human Resources, the number of mortality and disability cases involving construction workers in Malaysia is the highest compared to other sectors [3]. In fact, the actual number could be much higher [22], due to unreported accidents, News reports suggest that this figure could go as high as 80 per cent of Malaysian construction workers, as most construction workers are foreign workers, many of them working with expired or without any work permits. According to the Department of Safety & Health Malaysia (DOSH), an average of more than 60 deaths is recorded annually. Between 2007 and 2012, the average number of cases of death, non-permanent disablement and permanent disablement in the construction industry amounted to 70, 50 and 7 cases respectively. These, respectively, made up 53, 40 and 5 % of all occupational accidents across all industries. Figure 1, shows the total number of fatalities in the construction industry



Fig. 1 Number of construction fatalities 2007–2012. Source DOSH Annual Report

for the same period compared to other industries is at an average of 70 cases per year or 53 % out of the average of 133 cases in all sectors [23]. This figures support the assertion that the construction sector is the most dangerous sector in the country, measured in terms of workplace hazards, risk of accidents and workers' safety.

In fact, according to an analysis from a root cause of accidents in construction projects, reveal that many of construction accidents can be attributed to the professional or managerial failures [24]. Contractors, designers, architects and structural engineers are important people who make crucial decisions that affect safety and health of construction workers [25, 55]. Achieving sufficient levels of occupational safety in construction projects can therefore only be achieved through cooperation between all the project stakeholders—the client, the designer, the contractors (and sub-contractors) and suppliers [26]. The management of construction projects can prevent or mitigate accidents by identifying and implementing appropriate control measures that would help to prevent errors or failures that could lead to an accident [22]. An analysis of some 500 accidents records provided by the UK HSE pointed out that the most frequent cause of accidents is inappropriate construction operation, occurring in 88 % of all accidents, which are mainly attributed to poor site management during construction [27]. In Europe, it has been reported that nearly half of senior managers and company directors do not have an up-to-date understanding of their duties and responsibility in ensuring of safety and health at the workplace [28].

In order to prevent construction site accidents, the root causes of accidents must be investigated. Only by understanding and identifying the root causes of accidents, effective and appropriate preventive actions against accidents can be taken [7, 27, 29]. Most accidents are preventable and most if not all construction accidents on sites should be regarded as a failure of the management [19, 54]. Therefore, the knowledge on accident causation will facilitate the creation of a safer, healthier and more conducive working condition and environment at construction sites. However in Malaysia, very few studies have been done for safety awareness and accident prevention based on accident causations in building construction sites. This study seeks to develop and generate a model based on actual needs to prevent accidents at building construction sites.

3 Research Aim and Objectives

The aim of this ongoing research is to develop the accidents prevention model for key management at Malaysian building construction sites. The research objectives of this study are:

- To identify the existence and availability legislation of safety and accident prevention at construction sites.
- To determine the significant factors that causes accidents at building construction sites.

- To assess the hieratically factors of accident causation for accident prevention at building construction sites.
- To develop and validate the Accident Causation Model for Accident Prevention at building construction sites by using Partial Least Squares—Structural Equation Model (PLS-SEM).

4 Literature Review

4.1 Concept of Safety and Accident Prevention

Safety at construction sites is associated with an absence of danger and a low-risk condition [30]. Safety is freedom from danger, harm, and injury to the persons [31]. In this study, safety is achieved when recognized hazards are controlled such that it is lowered to an acceptable level of risk that would create a working environment that is free from danger, harm and injury to the people and the organizations involved directly and indirectly in construction activities. Safety issues at construction sites are essential issues that cannot be taken lightly, as a minor accident may end up serious and may bring huge effects to the workers and the organizations [20]. The purpose of accident prevention is to stop or to avoid accidents from happening. Accident prevention is an integrated program—a series of coordinated activities to reduce unsafe practices and working conditions—based on certain knowledge, attitudes and abilities [32]. By preventing accidents from occurring, contractors gain as major injuries, ill health and fatalities in the construction project are reduced [33]. These benefits also have direct and indirect spillover effects to all players in the construction industry. Because of this, raising awareness on the benefits of accident prevention may encourage these players to invest more on safety and health measures [34].

4.2 Concept of Accident Causation

Many researches has been defined the meaning of an accidents in the construction industry, an accident can be as undesired event which commonly results in physical harm and/or property damage, and it's is usually caused by contact with a source of energy more than a body or a structure can withstand [30]. Accident also can be defined as an unplanned and uncontrolled event in which the action or reaction of an object, substance, person or radiation results in personal injury on the probability thereof [32]. In this stage, in order to prevent an accident the preventive measures must be taken by first knowing the causes of the accidents [35]. Accident prevention requires knowledge of accident causal factors [36], whereas accident investigations techniques should be firmly based on theories of accident causation.

Indeed, a sufficient knowledge would result in a better understanding and prevention efforts could be directed at the root causes of accidents, not at the symptoms, which would result in more effective accident prevention programs [37]. Understanding the causes of accidents would also prevent future accidents from occurring and therefore would reduce injury and ill health and this benefits would also be materialized in the form of a lower cost of projects [20]. However, we can only understand the causes of project accidents by investigating those that have already occurred in the past, such that the appropriate preventive measures can be taken to reduce the risk of accidents happening again in the future. Many accidents at construction sites are caused by a combination of factors, e.g. by one or more unsafe acts and conditions, and in order to improve the overall safety performance, the investigation of the root causes of construction accidents is needed to effect permanent improvement [22].

88 % of construction accidents are due to unsafe acts of workers, 10 % due to unsafe conditions and 2 % are associated with the act of God [32]. Construction accident don't just happen, they are caused by human factors, where 99 % of accidents are caused by either unsafe acts, or unsafe conditions, or both [38]. The fact is construction accidents can be prevented by identifying the roots cause of accidents, which is possible by accident investigation technique such as theories of accident causation and accident prevention which provide explanations of why construction accidents happen [39]. Although it is crucial to identify the causes of accidents, it is not always the case that all hazards in construction workplaces can be identified and eliminated. In such cases, effective accident investigation programs are essential so that critical data to prevent on-site accidents can be collected.

4.3 Legislation and Authorities Applicable to the Malaysian Construction Industry

There are several authorities and laws related to the construction industry in Malaysia. Before the Occupational Safety and health Act, 1994 (OSHA 1994) came into force, the Factories and Machinery Act, 1967 (FMA 1967) has been the fundamental legislation which regulates construction activities in the Malaysian construction industry. FMA 1967 provides regulations on the safety, health and welfare aspects of the operation of factories. The Act defines 'factory' to include 'any premises, place or space' that carries out 'building operation' and 'works of engineering construction'. Therefore, all operations at and safety requirements of building and works engineering construction must comply with the FMA 1967 and the Regulations made thereunder.

OSHA 1994 came into effect in 1994 and become the specific Act to ensure the safety and health of workers in the Malaysian industries. It imposes general duties on the employer to ensure the safety, health and welfare off all his employees. The Act also outlines the duties of employees in maintaining a safe and healthy working

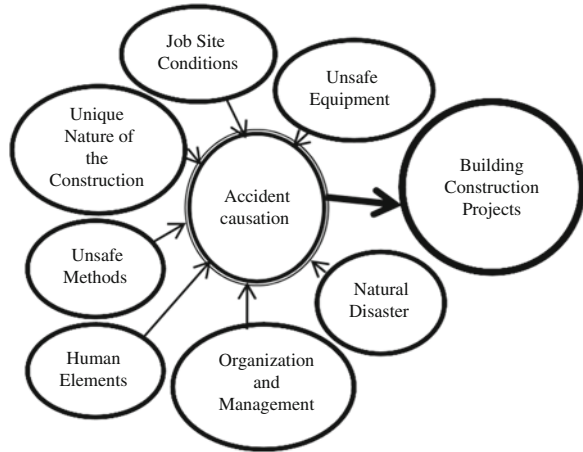
environment. Both FMA 1967 and OSHA 1994 are the current fundamental legislation which regulate activities in the Malaysian construction industry. The Department of Occupational Safety and Health (DOSH) is entrusted with the responsibility to ensure that the management of all construction projects comply with the workplace safety and health regulations, based on OSHA 1994, whereas the enforcement of FMA 1967 is carried out by the Factories and Machinery Department. The government has also set up a specific agency namely National Institute of Occupational Safety and health (NIOSH)—mainly to provide training courses and seminars in the area of occupational safety and health (OSH) and to enhance research in the same. It also assists DOSH in its work to improve the implementation of OSHA.

4.4 Grouping the Causes of Accidents

In preventing construction accidents, root causes of accidents must be understood, as only by understanding and identifying the root causes of accidents can fully effective and appropriate preventive actions of accidents can be taken [27].

Studies done in several countries have identified factors that cause construction accidents which are often grouped into several categories. Ching et al. [40] did a study in the Taiwanese construction industry and found that accidents were caused by the inherently hazardous nature of construction projects, apart from personnel, environment and equipment, project management, and time factors. Kanchanaet al. [41] did a similar study in Sri Lanka and argued that accidents are influenced by safety management from a managerial perspective, and classified the factors causing accidents into six categories: management commitment, implementation, management measures, project nature, individual involvement, and economic investment. Hashem [42] conducted a study in Kuwaiti construction sites and blamed accidents on management, human and project factors. In the United States, Seokho et al. [43] classified that the major causes of accidents in the construction industry were mainly due to three factors; environmental (physical), human (unsafe acts), and injury source (mechanical). Jantanees's [29] study in Australia attributed accidents to work activities, worker characteristics, work environment, mechanisms of accident and location of injury. Manu et al. [18] also conducted a study in the United Kingdom and attributed accidents to the nature of project, methods of construction, site restriction, project duration, design complexity, subcontracting, procurement system and levels of construction. Chan et al. [4] in their study in Hong Kong blamed unsafe working conditions, working process and working behaviors as causes of accidents. Adel et al. [16] conducted a comprehensive study on project risk evaluation in Canada and categorized the causes of accidents into mechanical, electrical, human and physical ambience factors. Himadri and Partha's [44] study in India suggested that the main causes of accidents were height, scaffolding, housekeeping, machinery and personnel factors. Aksorn and Hadi's [45] study in Thai construction sites classified causes of accidents as personal, job,

Fig. 2 Groups of accident causation factors in building construction



management, and workgroup factors. Kamal's [21] study in Malaysia's construction sites attributed accidents to construction hazards, safety culture, work physiology and characteristics of workers. Lilis [46] also conducted her study in Malaysia and attributed accidents to (a lack of) occupational safety and health (OSH) implementation, management commitment, legislation and external support. According to Abdelnaser et al. [47] conducted their study in Libyan construction sites, accidents are attributed to a lack of budget, awareness, training, equipment and attitude.

For this study, 93 accident causation factors were identified and were categorized under 7 groups at this preliminary stage of study. These are unsafe equipment; job site conditions; unique nature of the construction industry; unsafe methods; human elements; organization and management; and natural disaster. This seven categories are then further divided into between three (3) to eighteen (19) factors of accident causation. Figure 2 shows the categories of accident causation factors.

5 Research Methodology

In this ongoing study, quantitative method research is used. A quantitative approach is used to specify numerical assignment to the phenomena under study and to study relationship between facts [48]. The methodology for this research is divided into three phases as shown below.

- Stage I—Information Gathering
- Stage II—Model Development
- Stage III—Model Analysis

5.1 Information Gathering

The first stage is focused on selecting the area of research study and topic, identifying the problem, and setting the aims of the study. The research objectives are formulated based on the identified problems, aims, objectives and scope of study. Literature review is conducted briefly from journals, thesis, articles and books in order to understand ACfAP model from a global perspective. In understanding the problem to be addressed, the mapping study will identify the causal factors affecting accidents in the construction industry. The hierarchical structure of accidents causal factors gives a preliminary idea on what are the factors that past researchers have discovered as contributing to accident causation awareness, which can be used to develop strategies of accidents preventions in the building construction sites. Quantitative methodologies based on the safety and accident causation attributes are then screened by an expert panel made up of representatives of developers, contractors, consultants, professional institutes, academic institutions and government departments.

5.2 Model Development

Phase two consists of actual data collection. It involves various steps including designing the questionnaire and conducting a pilot study and the main survey. The pilot testing will assess content validity by measuring the consistency of the measurement items against extant literature [49]. This pilot test will be conducted on construction practitioners and experts with more than 10 years of experience (engineers, contractors, consultants, developers and researchers) in the construction and property development industry. After pilot- testing the instrument and passing the validity and reliability tests, the main survey will be carried out in building construction practitioners (developers, government departments, consultants, contractors) throughout peninsular Malaysia using three approaches, namely via postal mail, electronic mail and direct visits to construction firms. The second phase also presents the research model and develops the research hypotheses characterizing the relationships depicted in the model. The research hypotheses will be examined using partial least squares (PLS).

5.3 Model Analysis

In phase three, data will be analyzed using appropriate statistical tools. PLS-SEM technique [50] is used as it allows latent constructs to be modelled either as formative or reflective indicators. Hair et al. [51] encourages the use of PLS-SEM as the appropriate method for prediction and theory development because it provides

more robust estimations of the structural model. In the two-stage analytical procedures as employed in the study by Hock et al. [52], confirmatory factor analysis is first conducted to assess the measurement model, after which the structural relationships will be examined. This finding then can be used to predict and understand the role and formation of individual variables and their inter-relationships. The model and the results obtained from the analysis then will be statistically validated. Experts in the construction industry will also be interviewed.

6 Discussion And Expected Outcomes

It is expected that the causal factors of accidents at the building construction sites can be identified and determined. Existing safety practices by management will be examined. ACfAP model will be developed as a framework and guideline for key management to improve safety and to prevent accidents at buildings construction sites.

7 Conclusion

It is hoped that, at the end of this completed study, the ACfAP model will be used as a safety awareness and prevention accidents at building construction sites. The data in this study can be used as a guideline, an assessment framework, process and benchmarking tool by key management parties for developing proper safety strategies and accident prevention for building construction sites and ultimately contribute towards an improved quality of the finished products in the Malaysian construction industry.

Acknowledgments The authors would like to greatly thank Assoc. Prof. Dr. Hj. Zainal Abidin bin Hj. Akasah as the supervisor and UTHM for supporting this study.

References

1. R.Ab. Rahman, K.H. Hassan, Regulating high risk activities in construction industry in Malaysia: the need for legal protection. *Jurnal Undang-Undang dan Masyarakat*, UKM, 246–258 (2008)
2. Department of Statistics Malaysia (2012, 2013)
3. A. Omran, A. Hassan A. Bakar, T.H. Sen, The implementation of OSHAS 18001 in construction industry in Malaysia, *J. Eng. Ann. Faculty Eng. Hunedoara*, Tome VI, Fascicule 3 (2008), (ISSN 1584-2673)
4. K.C. Chan, H. Li, M. Skitmore, The use of virtual prototyping for hazard identification in the Aerly design stage. *Constr. Innov.* **12**(1), 29–42 (2012)

5. W. Wang, J. Liu, S. Chou, Simulation based safety evaluation model integrated with network schedule. *J. Autom. Constr.* **15**(3), 34341–34354 (2006)
6. S. Spangenberg, Large construction projects and injury prevention. Doctoral dissertation, Faculty of Engineering, Science and Medicine, Aalborg University, Denmark (2010)
7. Z.J. Torghabeh, S.S. Hosseinian, Designing for construction workers' safety. *Int. J. Adv. Eng. Technol.* (2012), ©IJAET ISSN:2231-1963
8. Master Builders Association Malaysia, <http://www.mbam.org.my/mbam/> Annual Safety Conference 2012; Malaysia Master Builders Association (MBAM), June 2012
9. New Straits Times (NST), <http://www.nst.com.my>. (27 Sept 2013)
10. New Straits Times (NST), <http://www.nst.com.my>. (25 July 2013)
11. New Straits Times (NST), <http://www.nst.com.my>. (02 May 2012)
12. Business Times, Malaysia (2014) <http://www.nst.com.my/business>
13. B. Knegeting, *Safety Lifecycle Management in The Process Industries: The Development of a Qualitative Safety Related Information Analysis Technique*, ISBN 90-386-1747-X (University Press Facilities, Eindhoven, 2002)
14. R.Y.M. Li, S.W. Poon, Why do accidents happen? A critical review on the evolution of the construction accident causation models; CIB Congress, 10–14 May 2010, Manchester, ISBN 978-3-642-35045-0
15. A. Charehzehi, A. Ahankoob, Enhancement of safety performance at construction site. *Int. J. Adv. Eng. Technol.* (2012), @ IJAET ISSN:2231-1963
16. A. Badria, S. Nadeau, A. Gbodossoub, Proposal of a risk factors based analytical approach for integrating occupational health and safety into project risk evaluation. *Accid. Anal. Prev.* **48**(2012), 223–234 (2012)
17. P.G.P. Sabet, H. Aadal, M.H.M. Jamshidi, K.G. Rad, Application of Domino theory to justify and prevent accident occurrence in construction sites. *IOSR J. Mech. Civil Eng. (IOSR-JMCE)*, p-ISSN: 2320-334X, **6**(2) (Mar–Apr 2013)
18. P. Manu et al., An approach for determining the extent of contribution of construction project features to accident causation. *Safety Sci.* **48**, 687–692 (2010)
19. K. Seevaparsaid-Mansingh, T. Haupt, *Construction Accident Causation: An Exploratory Analysis*, Cape Peninsula University of Technology (2007)
20. N.H. Zakaria, N. Mansor, Z. Abdullah, Workplace accident in Malaysia: Most common causes and solutions, *Bus. Manage. Rev.* **2**(5), 75–88 (2012), ISSN: 2047-0398
21. A. Kamal, M.I.N. Ma'arof, Review on accidents related to human factors at construction site. *Adv. Eng. Forum* **10**(2013), 154–159 (2013)
22. M. Zaimi, A.R.A. Hamid, B. Singh, Causes of accidents at construction sites. *Malays. J. Civil Eng* **20**(2), 242–259 (2008)
23. Department of Occupational Safety and Health Malaysia (DOSH), Annual Report. Summary of Accident Cases, http://www.dosh.gov.my/doshV2/index.php?option=com_wrapper&view=wrapper&Itemid=142&lang=en (2007–2012)
24. Bomel, Contract Research Report 387/2001 Improving health and Safety in construction: Phase 1: Data Collection, Review and Structuring, Health and Safety Executive, London (2011)
25. R. Ghaderi, K. Kasirossafar, Construction safety in design process. *ASCE Conf. Proc.* doi:[10.1061/41168\(399\)54](https://doi.org/10.1061/41168(399)54). AEI 2011: Building Integrated Solutions, Proceeding of the AEI 2011 Conference
26. H. Lingard, N. Blismas, T. Cooke, H. Cooper (2008), The model client framework: resources to help Australian Government agencies to promote safe construction. *Int. J. Managing Projects Bus.* **2**(1), pp. 131–140 (2009)
27. A. Suraji, A.R. Duff, S.J. Peckitt, Development of causal model of construction accident causation. *J. Constr. Eng. Manage.* **127**:337–344 (2001)
28. N. Paton, Senior managers fail to show competence in health and safety. *Occup. Health* **60**(3), 6 (2008)

29. J. Dumrak, S. Mostafa, I. Kamardeen, R. Rameezdeen, Factors associated with the severity of construction accidents: the case of South Australia. *Austr. J. Constr. Econ. Build.* **13**(4), 32–49 (2013)
30. A.S.J. Holt, *Principles of Health and Safety at Work*, (1st Edition Publishing), Technology & Engineering. (2001)
31. S. Phoya, *Health and Safety Risk Management in Building Construction Sites in Tanzania: The Practice of Risk Assessment, Communication and Control* (Chalmers University of Technology, Gothenburg, Sweden, 2012)
32. H.W. Heinrich, D. Petersen, N. Ross, *Industrial Accident Prevention*, 5th edn. (McGraw-Hill, New York, 1980)
33. I. Ellias, H. Felix, O. David, Cost-benefit analysis for accident prevention in construction projects. *J. Constr. Eng. Manage, ASCE.* **138**(8), 991 (2012)
34. E.D. Ferrat, P. Hughes, *Introduction in Health and Safety in Construction*, 2nd edn. (Elsevier, Oxford, 2007)
35. A. Rahim, A. Hamid, M. Zaimi, A. Majid, B. Singh, *An Overview of Construction Accidents in Malaysia*, (Issues in Construction Industry, Univision Press, Malaysian Book Publishers Associate (9101), Faculty of Civil Engineering, UTM, 2008) ISBN 978-983-52-0568-2.
36. P. Manu, N. Ankrah, D. Proverbs, S. Suresh, An approach determining the extent of contribution of construction project features to accident causation. *Safety Sci.* **48**, 687–692 (2010)
37. I.D. Brown, *Accident Reporting and Analysis, Evaluation of Human Work*, J.R. Wilson and E. N Corlett eds., Taylor and Francis, London. (1995)
38. J. Ridley, *Safety at Work*, 2nd edn. (Butterworth Ltd., London, 1986)
39. S.S. Hosseinian, Z. Torghabeh, Major theories of construction accident causation models: a literature review. *Int. J. Adv. Eng. Technol.* (2012), ©IJAET ISSN: 2231-1963
40. C.W. Cheng, S.S. Leu, C.C. Lin, C. Fan, Characteristic analysis of occupational accidents at a small construction enterprises. *Safety Sci.* **48**, 698–707 (2010)
41. K. Priyadarshani, G. Karunasena, S. Jayasuriya, Construction safety assessment framework for developing countries: a case study of Sri Lanka. *J Constr. Dev. Countries* **18**(1), 33–51 (2013)
42. H.M. Al-Tabtabai, Analyzing construction site accidents in Kuwait. *Kuwait J. Sci. Eng.* **29**(2), 2002 (2002)
43. S. Chi, H. Zhang, S. Han, S. Kwon, *Theory Analyzing Safety Risks and Their Impacts on Injury Severity in the U.S. Construction Industry* (2012)
44. H. Guha, P.P. Biswas, Measuring construction site safety in Kolkata, India. *Int. J. Sci. Eng. Res.* **4**(5), 2138–2143 (2013), ISSN 2229-5518
45. T. Aksorn, B.H.W. Hadikusumo, The unsafe acts and decision to err factors of Thai construction workers. *J. Constr. Dev. countries* **12**(1), 2007 (2007)
46. L. Surlenty, *Management Practices and OSH Implementation in SME in Malaysia*, School of Management, USM Minden, Pulau Pinang, (2012)
47. A. Omran, M. Muftah, I. Said, A.A. Hussin, Implementation of safety requirements by contractors in the construction industry in Libya: case studies. *J. Eng. Ann. Tome VI, Fascicule 2* (2008) (ISSN 1584– 2665)
48. S.W. Vanderstoep, D.D. Johnston, *Research Methods for Eeryday Life*, (John Willey & Sons, USA 2009)
49. G.W. Bock, R.W. Zmud, Y.G. Kim, J.N. Lee, Behavioral intention formation in knowledge sharing: examining the roles of extinsic motivators, social psycholological fores, and organizational climate. *MIS Quartery* **29**(1), 87–111 (2005)
50. W.W. Chin, Issues and opinion on structural equation modeling. *MIS Quarterly*, **22**(1), pp vii–xvi (1998)
51. J.F. Hair, C.M. Ringle, M. Sarstedt, PLS-SEM: indeed a silver bullet. *J. Mark. Theory Pract.* **19**(2), 139–151 (2011)
52. C. Hock, C.M. Ringle, M. Sarstedt, Management of multi purpose stadiums: important and performance measurement of service interfaces. *Servi. Technol. Manage.* **14**(2/3), 188–206 (2010)

53. A. Ramli, Z.A. Akasah, M. Idrus, M. Masirin, Safety and health factors influencing performance of malaysia low cost housing: structural equation modeling (SEM) Approach, in *International Conference on Innovation, Management and Technology Research, Malaysia, 22–23 Sept 2013, Procedia—Social and Behavioral Sciences 00* (2013)
54. A.Z. Abidin, M. Idrus, A review of building factors contributing to building safety performance, in *International Conference on Innovation and Technology for Sustainable Built Environment. UiTM Perak, (pp. 437–443), Perak* (2012)
55. A.Z. Abidin, M. Idrus, A preliminary study on building design factors contributing to building safety and health performance apartment in Malaysia, in *International Conference and Culture, Society, Technology and Urban Development in Nusantara, Universiti Pembangunan Panca Budi, Medan, October 2012, (pp.1–20), Medan, Indonesia*
56. A.Z. Abidin, M. Idrus, Factors contributing to safety and health performance of apartments in Malaysia: A Preliminary study. Seminar Penyelidikan dan Inovasi (PePIN), Politeknik Merlimau, Melaka. (2012)

Identification of Malaysian Contractors with Sustained International Operations (CSIO)

Che Maznah Mat Isa, Nur Izzati Abd. Rani, Christopher Nigel Preece and Hamidah Mohd Saman

Abstract Competitive positioning and sustaining the gained international operations are difficult challenges that international construction firms commonly face. The aim of this study is to assess the level of Malaysian contractors' sustained international operations (CSIO). The measurement scales for the CSIO were developed from secondary data provided by Construction Industry Development Board (CDIB) Malaysia on seventeen construction firms that have been operating in international market until 2013 together with the awarded project values, completed projects, countries of operation and diversity of projects. In this paper, a set of dimensions of CSIO were identified and the measures for each dimension were also established using a five-point scale. The findings reveal that the elements in the order of importance to determine the level of CSIO are the consecutive year sustained international operation, value of projects awarded, number of countries, diversity of projects undertaken, international experience and number of projects completed. The measurement tool developed in this study has enabled the identification and ranking of the most experienced and sustained international contractors in Malaysia. Further, the CSIO dimensions will be considered as independent variables as part of future research.

Keywords International construction · Malaysian contractors · Performance · Strategies · Sustainability

C.M.M. Isa (✉) · H.M. Saman
Faculty of Civil Engineering, Universiti Teknologi MARA, Shah Alam, Selangor, Malaysia
e-mail: chema982@salam.uitm.edu.my

N.I.A. Rani · C.N. Preece
RAZAK School of Engineering and Advanced Technology, Universiti Teknologi Malaysia,
Kuala Lumpur Campus, Kuala Lumpur, Malaysia

1 Introduction

Guler and Guillén [1] reported that there has been an increasing interest by venture capital firms to turn into foreign countries in searching for investment opportunities brought by globalization and liberalization. Hence, despite various challenges faced by the contractors domestically, no market is ever safe from foreign competition. Even if the firms stay at home, they eventually have to face foreign competitors in the domestic market. Saturated or stagnant domestic market has pushed many Malaysian contractors to penetrate international markets ([2, 3]). In addition, Ahmad and Kitchen [4] found that the Malaysian construction firms' main motives to expand internationally were to develop new markets, to access cheaper resources, to take advantage of globalization and liberalization of the industry, business opportunities and to minimize competition in domestic markets. These firms have been undertaking various construction projects, ranging from infrastructure, building to other construction related projects since 1986 (CIDB 2013). However, a review on the Engineering News Record (2013) revealed none of Malaysian construction firm was listed in the top 250 international contractors. Despite the government encouragement through various plans such as the 10th Malaysian Plan (10 MP), 3rd Industrial Malaysia Plan (IMP) and Construction Industry Malaysian Plan (CIMP), only 115 firms (or about 2.2 %) of the total Malaysian construction firms registered under Grade 7 and Class A have been operating abroad. This situation may be due the firms' lacking in resources, unsound business plan for working overseas, insufficient information on opportunities abroad and lack of competitive position [5]. Therefore, it is necessary to develop a means to assist contractors to assess the level of sustained international operation within foreign markets. By measuring contractors' sustained international operation (CSIO) with such an assessment tool, the contractors' international activities can be continuously monitored and managed at an earlier stage.

This paper firstly focuses on establishing the CSIO measurement to assess the level of Malaysian CSIO over the period from 1986 until 2013. It describes the identification and justification of the selected elements used to assess the level of CSIO. By means of the secondary data provided by CIDB, the types of data used include the identification of the Malaysian construction firms that have been operating in international markets, value of projects awarded, number of countries of operation, the number of projects completed and the diversity of projects undertaken. The paper details the definition of sustained international operations and experience in relation to international contracting firms through a literature review. Based on the definitions a mechanism or tool has been developed which has enabled the identification and ranking of the most experienced and sustained international contractors in Malaysia.

2 Literature Review

Competitive positioning in international markets and sustaining the gained international positions are difficult challenges that international construction firms commonly face [6]. Most of the previous studies focus on the factors contributing to firms' sustained competitiveness and growth in the global market such as ability to understand the risks involved with international projects [7], having tacit knowledge that other companies find difficult to copy when it spreads internally [8], ability to rapidly develop new knowledge [9], having unique, firm-specific resources that are valuable, rare, inimitable, non-substitutable, and non-tradable [10], and being as first-mover to gain an extremely high market share ([11, 12]). In addition, firms' growth was sustained from inception due to their positioning in emerging high growth lead countries with low competition [8]. Han et al. [13] analyzes the common strategies and lessons obtained from the cases of leading global contractors that have sustained their growth in the competitive global. Those firms were found to be proactive and responsive to changing markets by increasing their overseas revenues and enhancing their competency through more diversified products in order to stabilize their revenue structure.

The sustained international competitive positioning further reflects the sustained firms' performance [14]. Hence, international markets continuous learning, knowledge sharing and efficient transfer of knowledge in a structured and systematic manner is vital for a sustained and profitable firms' business performance [15]. Other key drivers for sustained business success that the construction firms should capitalize are effective project planning, contract management, and project financial ability in order to explore the huge market opportunities with the encouragement from the home government [16]. Jin et al. [17] found that the satisfied customers and stakeholders has resulted in a higher market performance and a more competitive role in the international construction market to reap the financial benefits needed to maintain long-term sustained success.

Very few researchers have comprehensively defined the meaning of CSIO. However, a long term contracts and continuity of projects awarded was found very important to sustain international operation. Zhao et al. [18] revealed that the Chinese firms' in Singapore have sustained international operations after project completion, while some dissolved their operations. It was identified that technical support programme is required for sustained and continuing exporting of services of firms in international markets [19]. Having international experience allows firms to develop organizational capabilities and overcome obstacles to a foreign market entry and further utilize prior experience of a host country to further expand operations in that country to achieve scale economies in their activities [20]. Hence, the firms with less experience in managing international projects were found lacking in knowledge of dealing with host country economic and environmental conditions [21].

Previous researchers have developed various models to assess sustained performance of firms in international markets. Deng and Smyth [22] recommended a

broad approach to address and measure the construct of what constitutes the sustained firms' international operations. Morgan et al. [23] developed a theoretical model for an export venture's performance which is sustained over time by reinvestment, the creation of market-based assets, and learning effects that build and enhance the resources and capabilities available to the export venture. In his empirical study, Flanagan [24] has proposed measurements on contractors' sustained competitiveness. The research undertaken uses a 'standard' procedure by identifying competitiveness indicators, collecting data for the indicators and calculating a competitiveness index. Ibrahim et al. [25] have developed a model to measure team integration performance index for construction firms which takes the form of linear additive weighting model.

Based on the above review, the dimensions of sustained international operations selected are based on the international experience which is defined in terms of number of years the firms have been active in international markets, number of different countries of operations and number and diversity of overseas projects. In addition, a sustained international operation is defined in terms of the number of years of consecutive overseas activities and values of awarded projects. Hence, six (6) dimensions or measures has been identified from previous studies which are number of international experience (y), consecutive years sustained international operations (cy), values of awarded projects (v), number of projects completed (p), number of countries of operations (c) and diversity of project undertaken (d). As a result, a conceptual contractors' sustained international operation (CSIO) model will be developed based on the identified measures and their relative significance. By adopting Ibrahim et al. [25] model the CSIO takes the form of a linear additive weighting model, consisting of a measure for each of the identified measures with a corresponding weighting coefficient identified as part of this research. A linear additive weighting model is considered appropriate based on reviews on previous studies and will be considered as independent variables in the CSIO as part of future research.

3 Methodology

The target population is from the cross-section of Malaysian construction firms those undertaken and completed projects in the international market. The sampling frame is based on the Construction Industry Development Board (CIDB 2013) record with 115 firms registered as global players operating in more than 50 countries. Their involvements in international projects includes various sectors such as buildings, infrastructures, branches of engineering, mechanical and electrical, power transmission and plant, and oil and gas. However, out of 115 firms, only 17 firms were found to still actively operating in international market in 2013. Hence, the secondary data obtained from CIDB Malaysia record was used to assess the level of CSIO of all shortlisted 17 firms.

A review of the available literature identified some potential dimensions for measuring the level of CSIO. The preliminary analysis on the secondary data provided by CIDB has identified six (6) dimensions namely; (1) international experience (years); (2) sustained consecutive years of international operations; (3) value of projects awarded (MYR bil.); (4) number of countries of operations; (5) number of projects completed and (6) diverse projects undertaken as shown in Table 1.

The ratings for each measure are based on a five-point scale, as shown in Table 2. The construction firms were then ranked based on the weightage score given by six (6) dimensions namely; years of experience (Wy), sustained consecutive years of experience (Wcy), value of projects awarded (Wv), number of projects completed (Wp), number of countries operations (Wc) and number of project diversity (Wd).

The range of the scale of each measure was based on the secondary data and the weightage of the measurement is given through series of discussions with experts. Other descriptive statistical analysis techniques such as the mean values and standard deviation were also calculated based on the level of scale allocated for each measure.

4 Analysis and Discussions

4.1 Measurement of Level of CSIO Until 2013

Based on Table 2, the CSIO score for each company is calculated using the 5 point scale for each dimension and the results are shown in Table 4. The formula adopted to determine the CSIO score is as follows:

$$CSIO = Wy + 6Wcy + 5Wv + 4Wp + Wc + 3Wd$$

where:

CSIO CSIO Score

Wy weighted measure for years of international experience

Wcy weighted measure for years sustained consecutive international operations

Wv weighted measure for value of projects awarded

Wp weighted measure for number of projects completed

Wc weighted measure for number of countries of operation

Wd weighted measures for number of diverse projects undertaken

The CSIO score is the summation of the weighted dimensions, where the coefficients are the individual weightings calculated identified from literature reviews.

Table 1 Active construction firms in 2013 (CIDB 2014)

No	Construction firms	International experience (years)	Sustained consecutive years of operations	Value of projects awarded (MYR bil.)	Number of operating countries	Number of completed projects	Number of diverse project
1	Bina Puri Construction Sdn. Bhd.	18	18	3.83	10	52	7
2	Chase Perdana Sdn. Bhd.	8	8	0.26	3	4	2
3	HG Power Transmission Sdn. Bhd.	14	14	0.48	5	19	2
4	HO hup Construction Company Berhad	4	3	0.48	2	2	2
5	Hong giap Sdn. Bhd.	19	19	0.16	2	13	1
6	IJM Construction Sdn. Bhd.	23	23	10.42	8	48	8
7	Jetson Construction Sdn. Bhd.	2	2	0.18	2	2	2
8	Johawaki Sdn. Bhd.	2	2	1.30	1	1	1
9	Malaysian Maritime & Dredging Corp.	2	2	0.09	1	1	1
10	MBI Ventures Sdn. Bhd.	15	15	1.91	1	7	3
11	MTD Construction Sdn. Bhd.	10	10	4.05	6	12	6
12	Muhibbah Engineering (m) bhd.	24	24	4.40	7	74	10
13	Ranhill Berhad	7	6	5.99	3	3	2
14	S.Kian seng Sdn. Bhd.	4	4	2.00	1	1	1
15	Shimeversendat Engineering (M) Berhad	17	17	4.17	8	75	1
16	UEM Builders Berhad	15	11	4.46	6	17	5
17	WCT Berhad	11	11	6.00	4	13	5

Table 2 Measures and scale for each dimension

Dimensions	Weightage	Scale for each measure				
		1	2	3	4	5
1. Number of international experience (years)	Wy	<2	2-4	5-7	8-10	>10
2. Sustained consecutive international operations (years)	6Wcy	<2	2-4	5-7	8-10	>10
3. Value of projects awarded (MYR bil.)	5Wv	0-2.5	2.6-5.0	5.1-7.5	7.6-10.0	>10
4. Number of countries of operations	4Wc	<5	5-9	10-19	20-29	≥30
5. Number of projects completed	Wp	0-15	16-30	31-45	46-60	61-75
6. Diversity of project undertaken	3Wd	<5	5-7	8-10	11-15	>15
CSIO Score	$CSIO = Wy + 6Wcy + 5Wv + 4Wc + Wp + 3Wd$					

An example of the CSIO Score for Firm A (IJM Construction) is as follows:

$$\begin{aligned}
 CSIO \text{ (Firm A)} &= Wy + 6Wcy + 5Wv + 4Wp + Wc + 3Wd \\
 &= 5 + 6(5) + 5(5) + 4(2) + 4 + 3(3) = 81
 \end{aligned}$$

Table 3 shows the ranking of all 17 firms based on the CSIO scores calculated using the formula based on the weightage scale. It also shows the descriptive statistics presented by the mean values (M) and the associated standard deviation (SD) for each indicator contributing to the CSIO score for 17 construction firms (N = 17). The significance of the CSIO score by identifying the key player of international Malaysian contractors is to improve other contractor’s performance. Hence, top contractors’ position can be determined based on the set criteria in order to improve performance.

The table depicts only seven (7) firms have scored more than 50 % which are IJM Construction Sdn Bhd (81 %), Bina Puri Construction Sdn Bhd (70 %), Muhibbah Engineering (M) Sdn Bhd (67 %), Shin Eversendai Engineering (M) Bhd (61 %), UEM Builders Bhd (61 %), HG Power Transmission Sdn Bhd (53 %) and MTD Construction Sdn Bhd (53 %). The average score for all firms is 47.7 % which indicates poor sustained international operations of Malaysian construction firms in the overseas markets.

4.2 Mean Ranking of Dimensions Used to Measure CSIO Scores

Based on Table 4, the rank order of the six dimensions which are considered important in the CSIO measurement is: (1) consecutive year sustained international operations (22.56); (2) value of projects awarded (8.80); (3) number of countries

Table 3 Ranking of contractors based on CSIO scores for year 2013 ($N = 17$) with mean and standard deviation

Firms		Weightage for each sustainability indicator						CSIO score (%)	
		W_y		W_{cy}	W_v	W_c	W_p		W_d
A	IJM. const	5		5	5	2	4	3	81
B	Bina Puri	5		5	2	3	4	3	70
C	Muhibbah Eng.	5		5	2	2	5	3	67
D	Shineversend.	5		5	2	2	5	1	61
E	UEM Builders	5		5	2	2	2	2	61
F	HG Power	5		5	1	2	2	1	53
G	MTD Cons. Sb.	4		4	2	2	1	2	53
H	WCT Berhad	5		3	3	1	1	2	49
I	Hong Giap Sb.	5		5	1	1	1	1	48
J	MBI Ventures	5		5	1	1	1	1	48
K	Ranhill B	3		3	3	1	1	1	44
L	Chase Perd. Sb.	4		4	1	1	1	1	41
M	S.Kian Seng	2		2	1	1	1	1	27
N	HO Hup Const.	2		2	1	1	1	1	27
O	Johawaki Sb.	2		2	1	1	1	1	27
P	Jetson Cons.	2		2	1	1	1	1	27
Q	M'sian Marit.	2		2	1	1	1	1	27
Mean		3.88		3.76	1.76	1.47	1.94	1.53	Ave 47.7
Weighted Mean		3.88		22.56	8.80	5.88	1.94	4.49	
SD		1.36		1.35	1.09	0.62	1.52	0.80	

(5.88); (4) diversity of projects undertaken (4.49); (5) international experience (3.88) and (5) number of projects completed (1.94). The following sections further discuss on the trend of each dimension. The histogram was presented in such that the top contractors are plotted first, followed by others based on the ranking of CSIO scores calculated from Table 4.

Table 4 Ranking of weighted mean for each dimension

Dimension	Mean for each dimension	Coefficient (corresponding weighting)	Weightage mean score	Ranking
W_y	3.88	1	3.88	5
W_{cy}	3.76	6	22.56	1
W_v	1.76	5	8.80	2
W_c	1.47	4	5.88	3
W_p	1.94	1	1.94	6
W_d	1.53	3	4.49	4

1. *International Experience*

The number of international experience of the contractors was determined based on their starting year operated until 2013. For example Firm A, IJM has started their international operation since 1987. Hence, they have accumulated about 23 years of international experience. Figure 1 shows the trend of the firms' international experience for all 17 firms.

It was found that generally, the top ranked contractors have acquired more than 15 years of international experience than the lower ranked contractors.

2. *Years Sustained in International Markets*

Figure 2 shows the trend of firms based on the years sustained in international market. Consecutive years sustained in international markets is more important than the number of international experience. There are some contractors that have been operating earlier but stopped their international operation at some point and started back at a later time. Hence, being able to sustain consecutive contribute strongly to the sustained international operation score in this study. It shows that the top ranked contractors have sustained consecutively more than 15 years of experience. For example, IJM Construction Sdn Bhd has sustained for 23 years, Bina Puri Construction Sdn Bhd for 18 years and Muhibbah Engineering has sustained 24 years in international markets. These firms were



Fig. 1 Firms' international experience



Fig. 2 Consecutive years sustained in international operations

found to have sustained consecutively in international market with no dormant operation.

3. *Value of Projects*

In total there in 2013 there was more than MYR50 billion worth of projects that have been awarded to all 17 firms. The top contractor, Firm A (IJM Construction) has secured more than 20 % of the total value (Fig. 3).

However, the next two ranked contractors (Bina Puri and Muhibbah Engineering) only managed to secure about 8 and 8.7 % of the total value, respectively.

4. *Number of Countries*

In total, there are thirty three (33) countries chosen by the top sustained Malaysian contractors, namely; Argentina, Australia, Bahrain, Bangladesh, Bosnia, Botswana, Brunei, Cambodia, China, Hong Kong, India, Iran, Iraq, Indonesia, Libya, Maldives, Mongolia, Myanmar, Nepal, Oman, Pakistan, Philippines, Qatar, Saudi Arabia, Singapore, Sri Lanka, Sudan, Syria, Thailand, UAE, United Kingdom, Vietnam and Yemen which includes eight (8) ASEAN countries (Fig. 4).

It was found that the majority of the top contractors have chosen both ASEAN and non-ASEAN countries, however, the non-ASEAN countries were found to be the most preferred locations. Firm A (IJM Construction Sdn Bhd)

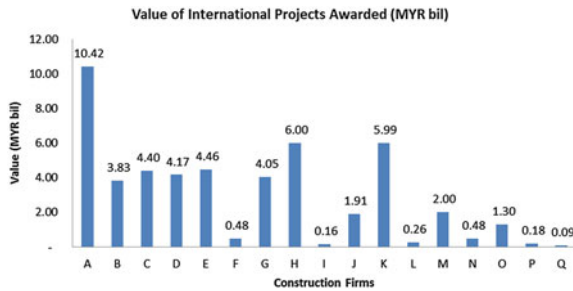


Fig. 3 Value of projects undertaken in international markets



Fig. 4 Number of countries penetrated by firms in international markets F

has penetrated 8 countries (India, Vietnam, Myanmar, UAE, Bahrain, China, Argentina and Australia), Firm B (Bina Puri Construction Sdn Bhd) with 10 countries (Nepal, Pakistan, India, Indonesia, Cambodia, Brunei, Thailand, UAE, China and Mongolia) and Firm C (Muhibbah Engineering) has penetrated 7 countries (Singapore, Cambodia, Qatar, Yemen, Syria, Sudan and Australia).

5. *Number of Project*

Figure 5 shows the number of projects undertaken by the contractors. In general, the results show that the top four ranked contractors have undertaken a high number of projects. Firm A (IJM Construction) has completed 48 projects, Bina Puri with 52 projects and Muhibbah Engineering with 74 projects.

Even though, the highest number of projects (75) has been undertaken by Firm D (Shin Eversendai), however Firm D only have experience in doing one type of project which is structural frame (refer to Fig. 6).

In total there are 18 different project types undertaken by the contractors; piping (water), road, building, highway, mix development, residential, power plant, water treatment, jetty/port, tunnel, bridge, oil and gas, mechanical and electrical, railway, airport, structural frame, telecommunication and power transmission.

The top contractor from Firm A (IJM Construction) has undertaken 8 types of projects under road, mechanical and electrical, railway, building, highway, airport, mix development and residential. Second ranked contractor, Firm B (Bina Puri) has undertaken 7 types of projects namely; piping (water), road,



Fig. 5 Number of projects undertaken

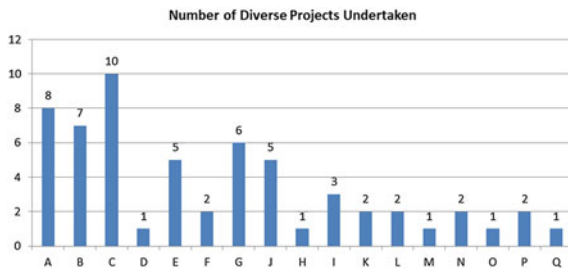


Fig. 6 Number of diverse projects undertaken

building, highway, mix development, residential and power plant. Third ranked contractor, Firm C (Muhibbah Engineering) has undertaken the 10 diverse projects namely; piping (water), bridge, oil and gas, road, mechanical and electrical, railway, jetty/port, building, airport and highway.

By assessing all measures, it was found that the contractor with sustained international operations has received the highest score (81 %), which is Firm A (IJM Construction) has more than 20 years of sustained operations with value of projects awarded of more than MYR 10 bil has penetrated 8 countries and completed 48 number of projects under 8 different types of work in international market.

5 Conclusions

This study has established a range of measurement scales to assess the CSIO in international markets by conducting analysis on the secondary data provided by CIDB Malaysia. The measurement tool has provided a simple and practical way of defining sustained international operations levels using six measures namely international experience, sustained consecutive international experience, project values, project numbers, countries of operation and project diversities. The tool developed has also enabled the identification and ranking of the most experienced and sustained international contractors in Malaysia. Hence, the establishment of the measurement scales will help the contractors and CIDB to assess the level of contractors' sustained operations and improve performance in international markets. Further, the CSIO dimensions will be considered and validated as independent variables as part of future research.

Acknowledgments The authors would like to thank the Faculty of Civil Engineering, UiTM and for providing technical support needed and also to the Research Management Institute, UiTM, Malaysia and Ministry of Science, Technology and Innovation (MOSTI) for granting the financial support (E-science fund: 100-RMI/SF 16/6/2 (33/2012)) for this research. We are also grateful to the professionals and managers from Malaysian construction firms, Malaysian CIDB and other institutions that have participated in this research.

References

1. I. Guler, M.F. Guillén, Institutions and the internationalization of US venture capital firms. *J. Int. Bus. Stud.* **41**(2), 185–205 (2009)
2. A.A. Usman, A.A. Aziz, International markets: Malaysian construction contractors and the stage theory. *Aust. J. Constr. Econ. Build.* **2**(1), 94–106 (2001)
3. C.M. Mat Isa, H. Adnan, I.R. Endut, Malaysian contractors' opinions towards international market expansion, in *International Conference in the Built Environment in the 21st Century (ICiBE2006)*, vol. 1, pp. 287–298 (2006)

4. S.Z. Ahmad, P.J. Kitchen, International expansion strategies of Malaysian construction firms: entry mode choice and motives for investment. *Probl. Perspect. Manag.* **6**(3), 15–23 (2008)
5. S.H. Han, J.E. Diekmann, J.H. Ock, Contractor's risk attitudes in the selection of international construction projects. *J. Const.* **131**(March), 283–292 (2005)
6. S. Korkmaz, J.I. Messner, Competitive positioning and continuity of construction firms in international markets. *J. Manage. Eng.* **24**(4), 207–217 (2008)
7. J. Walewski, *International Project Risk Assessment: Methods, Procedures, and Critical Factors* (Austin, Texas, 2003)
8. M. Spence, D. Crick, An exploratory study of Canadian international new venture firms' development in overseas markets. *Qual. Mark. Res. An Int. J.* **12**(2), 208–233 (2009)
9. S. Chelliah, M. Sulaiman, S. Pandian, The determinants of internationalization of small and medium enterprises (SMES): a case in Malaysia. *Appl. Sci.* **10**(10), 1202–1215 (2010)
10. S. Tallman, John Dunning's eclectic model and the beginnings of global strategy. *Adv. Int. Mark.* **15**(03), 43–55 (1993)
11. A. Green, K. Sedef, R. Bjorn, *Factors Indicating First-mover Advantages And Second-mover Advantages* (Kristianstad University College 2004)
12. B.G. Kalyanaram, R. Gurumurthy, Market entry strategies: pioneers versus late arrivals. *Best Pract.* **12**, 1–10 (1998)
13. S.H. Han, D.Y. Kim, H.S. Jang, S. Choi, Strategies for contractors to sustain growth in the global construction market. *Habitat Int.* **34**(1), 1–10 (2010)
14. F. Deng, G. Liu, Z. Jin, Factors formulating the competitiveness of the chinese construction industry: empirical investigation. *J. Manage. Eng.* **29**(4), 435–445 (2013)
15. T. Ballal, T. Elhag, in *2nd Specialty Conference on Leadership and Management in Construction*, pp. 83–91 (2006)
16. Y. Tan, L. Shen, C. Langston, Contractors' Competition Strategies in Bidding: Hong Kong Study. *J. Constr. Eng. Manage.* **136**(10), 1069–1077 (2010)
17. Z. Jin, F. Deng, H. Li, M. Skitmore, Practical framework for measuring performance of international construction firms. *J. Constr. Eng. Manage.* **139**(9), 1154–1167 (2013)
18. X. Zhao, B.-G. Hwang, G.S. Yu, Identifying the critical risks in underground rail international construction joint ventures: case study of Singapore. *Int. J. Proj. Manag.* **31**(4), 554–566 (2013)
19. W.W. Wong, The internationalization of Malaysian engineering consulting services firms. DBA Thesis, Southern Cross University, Lismore, NSW (2012)
20. J. Lu, X. Liu, M. Wright, I. Filatotchev, International experience and FDI location choices of Chinese firms: the moderating effects of home country government support and host country institutions. *J. Int. Bus. Stud.* **1**(1), 1–22 (2014)
21. M.-Y. Chen, J.-Y. Chang, The choice of foreign market entry mode: an analysis of the dynamic probit model. *Econ. Model.* **28**(1–2), 439–450 (2011)
22. F. Deng, H. Smyth, Nature of firm performance in construction. *J. Constr. Eng. Manage.* **140**(2), 1–4 (2014)
23. N.A. Morgan, A. Kaleka, C.S. Katsikeas, Antecedents of export venture performance: a theoretical model. *J. Mark.* **68**(1), 90–108 (2004)
24. R. Flanagan, W. Lu, L. Shen, C. Jewell, Construction management and economics competitiveness in construction: a critical review of research. *Constr. Manag. Econ.* **25**, 37–41 (2007)
25. C.K.I. Che Ibrahim, S.B. Costello, S. Wilkinson, Development of a conceptual team integration performance index for alliance projects. *Constr. Manag. Econ.* **31**(11), 1128–1143 (2013)

Problems Associated with Delay Analysis Methodology in Malaysian Construction Delay Practice

Nurul Huda Muhamad, Mohammad Fadhil Mohammad,
Asmalia Che Ahmad and Edelin Hussein

Abstract Delay to progress of a construction project is a major source of claims and disputes in the construction industry. At the heart of the matter in dispute often the subject of the degree of each contracting party's responsibility for the delayed project completion. Therefore, various delay analysis methodologies have been developed over the years as aids to answering this question. However, to date lack of research on the extent of use of these methodologies in practice to have been done in Malaysia although it has many studies done in this subject area. This paper is an attempt to fill that gap. The aim of this paper is to identify the problems affecting the use of these methodologies in practice. A survey approach using questionnaire as an instrument was employed to achieve the aim of this study. An extensive of the literature review was conducted. The study only involves the contractors and the clients' consultants. The findings from the survey revealed that "poorly updated programmes", "lack of familiarity with the techniques", "lack of skills in using technique", "unrealistic baseline programme", and "baseline programme without CPM network" were the top five (5) problems on the use of delay analysis methodologies. This seems to suggest that the sophisticated methodologies are not widely used mainly due to a number of problems related to improper programming and lack of skills and familiarity in using the methodologies.

Keywords Delay analysis methodology · Delay · Contract management · Contractors · Consultants · Construction disputes · Construction industry

A remark of indebtedness is also owed to the Research Acculturation Grant Scheme (RAGS) by the Ministry of Higher Education of Malaysia, for its grant award.

N.H. Muhamad (✉) · A.C. Ahmad · E. Hussein
Faculty of Architecture, Planning and Surveying, Universiti Teknologi MARA (Perak),
32610 Bandar Baru Seri Iskandar, Perak, Malaysia
e-mail: nurul885@perak.uitm.edu.my

M.F. Mohammad
Faculty of Architecture, Planning and Surveying, Universiti Teknologi MARA (UiTM),
40450 Shah Alam, Selangor, Malaysia

1 Introduction

Numerous studies have been conducted to identifying and categorizing the principal factors that commonly contribute to delays. However, disagreements on the responsibilities and liabilities for such delays continue to trigger hotly contested EOT claims [1]. This is in line with Yusuwan and Adnan [2] concurrent delays, eligibility of a time extension claim, and non-compliance to contractual requirements, were the top three (3) disputed issues in EOT claims in private funding projects.

According to them no specific explanation with regards to the assessment of the claim is given, and this is left to the professionals involved in the project. In addition, Chong and Leong [3] highlighted that the standard form of contracts should provide a more comprehensive contractual provision regarding the delay analysis and EOT claims. They stated that most standard forms of contract in Malaysia with regards to EOT assessment do not require the contractor to produce delay claims by any delay analysis methodology and the courts and arbitration tribunals have not generally gone into great depths for EOT assessment and delay analysis methodology.

The rankings of findings on the use of delay analysis methodologies in countries ranging from the UK, US, Hong Kong and Malaysia have been identified from the literature review as shown in Table 1. The most well-known and widely used methodologies for the assessment of delay are the s-curve and as-planned versus as-built especially for the contractors and the consultants in Malaysia although these are known to have major flaws. Conversely, methodologies perceived as the most accurate, window analysis, is not widely used. Therefore, this comparison revealed that the simplistic method is more commonly used in practice than sophisticated method by the contractors and the consultants. Possible reasons responsible for its popularity is that it: is simple to use and understand; do not require complete project records and require fewer resources to use [4–6].

According to Ahmad et al. [7], the application of the right delay analysis methodologies within the Malaysian construction industry need to improve due to lack of knowledge and competency in some application of the right delay analysis methodology among the parties involved in determining EOTs. This is in line with Yusuwan and Adnan [2] who found that the choice of method for evaluating the delay as the third most frequently disputed issue associated with EOT claims by contractors. Therefore, there is a need to employ the reliable delay analysis methodologies to perform a detailed programme analysis to reduce the disputes on EOT claims.

Table 1 Comparison the rankings of findings on the use of delay analysis methodologies in countries ranging from the UK, US, Hong Kong and Malaysia

Methodology	Contractor				Consultant			
	Author	A	B	C	D	A	C	D
Country	UK	US	Mal	HK	UK	Mal	HK	
Simplistic								
<i>Non-CPM</i>								
S-curve	8	-	3	-	7	1	-	
Global impact	3	-	8	1	8	7	5	
Net impact	4	-	5	2	6	5	2	
<i>CPM</i>								
As-planned vs as-built	1	1	2	3	2	2	1	
Sophisticated								
<i>CPM</i>								
Impacted as-planned	2	6	4	-	3	4	-	
Collapsed as-built	5	4	7	6	1	8	4	
Window analysis	7	-	6	5	5	6	6	
Time impact analysis	6	2	1	4	4	3	3	

Notes : Author (s)

A Braimah [5], UK

B Arditi and Pattanakitchamroon [21], US

C Muhamad [28], Malaysia

D Kumaraswamy and Yogeswaran [1], Hong Kong

2 Overview of Existing Delay Analysis Methodologies

The delay analysis involves detailed investigation of project records, programmes and their updates, often on retrospective basis, and with the aid of a number of different approaches commonly termed “delay analysis methodologies” (DAMs) [8]. The various delay analysis methodologies, known by a multitude of different named methodologies among practitioners, have been reported in the literature based on the review provided in the article entitled “*Delay Analysis within Construction Contracting Organizations*” by Ndekugri et al. [9]. Ndekugri et al. [9] considers the common aim of all delay analysis methodologies has been to investigate how delays experienced by the various project activities affect others and the project completion date and then to determined how much of the overall project delay is attributable to each party.

An ideal delay analysis methodology should contribute to a fair and accurate delay analysis result that can be accepted by contract participants and professional programme analysts [10]. The delay analysis methodologies can be grouped into two levels of sophistication are the simplistic, which includes the global impact, net

Table 2 Comparison of delay analysis methodology attributes

Delay analysis methodologies	Main issues in delay analysis		
	<i>Delay types</i>	<i>Concurrent delay</i>	<i>Real time analysis</i>
Global impact	X	X	X
Net impact	X	√	X
As-planned versus as-built	X	√	X
Impacted as-planned	X	X	X
Collapsed as-built	√	√	X
Time impact analysis	X	√	√
Window analysis	X	√	√

impact, and as-planned versus as-built and another is detailed, which includes the impacted as-planned, collapsed as-built, time impact analysis, and window analysis [4, 5, 11]. The sophistication methods tend to give more accurate results than the simplistic methods but the former requires more expense, time, skills, resources and project records to operate than the later [5, 12, 13]. Table 2 shows a comparison of the attributes of the delay analysis methodologies identified from the literature.

The above comparisons reveal that none of the delay analysis methodologies consider all three main issues at the same time. The definitions of concurrent delays most commented upon in the literature are; (1) delays, which are on different chains or path of activities, occur on the same time period (2) two or more delays that occur at the same time by one or more of the parties [2, 5, 14–16]. Furthermore, the critical paths may change as the programme changes and therefore, delays which are deemed critical on the as-planned CPM programme might not have been critical when the delay actually occurred [4].

The limitations with the simplistic approach of the global impact, net impact and as-planned versus as-built methodologies are that they do not scrutinize delay types and not operating real-time critical path analysis because these methodologies are only applied once, to the baseline programme, which assumes the critical path(s) were constant throughout the project. These lead to wrong judgement for entitlement of delays and delays potentially being deemed as critical, when in fact they were not [4, 11]. The global impact technique, unlike the net impact and as-planned versus as-built methodologies, has one more limitation that it does not even consider concurrency in delays.

The detailed approach of the collapsed as-built, time impact analysis and window analysis methodologies provides sound methods for performing a delay analysis except for impacted as-planned methodology. The main problems with the impacted as-planned methodology are that it does not scrutinize delay types, not addresses concurrent delays and not operating real-time critical path analysis. The collapsed as-built methodology scrutinizes delay types and addresses concurrent delays, however, the limitation of this methodology is that it does not operating real-time critical path analysis. As a result, it does not account for any changes in the critical path(s) during the project because it freezes the critical path based on the

as-built critical path [17, 18]. Of all the methodologies, the time impact analysis and window analysis methodologies both provide the most systematic and objective methods of quantifying the effect of delays on a project since they both consider the effect of delays in real time analysis and addresses concurrent delays. The court preferred the methodologies that consider what actually happened on project site based on factual evidence [19]. The limitation with both of them is that they do not scrutinize delay type during the analysis; therefore the results obtained need further analysis based on project records to apportion the entitlement [4, 10].

3 Methodology

3.1 Questionnaire Design

A questionnaire was designed based on a comprehensive review of previous related researches, specifically in the area of construction delays, construction contract management, and construction disputes. To support the findings of a literature review, exploratory interviews were conducted with industry practitioners to identify current construction delay practices in the Malaysian construction industry. Following an extensive review of previous related research, consolidated by interviews with industry experts, a set of questionnaires containing three (3) sections were prepared to deal with several issues regarding EOT assessment and delay analysis methodology. However, this paper only presents the analysis results of those problems to the use of the methodologies in practice. A total of ten (10) problems were identified as the most commented upon in the literature. To elicit the frequency of problems to the use of the delay analysis methodologies, respondents were asked to rate against a five-point Likert scale as follows, 1 = strongly disagree, 2 = disagree, 3 = neither agree nor disagree, 4 = agree, and 5 = strongly agree.

3.2 Population and Sampling Size

The two principal targeted groups were: contractor and consultants (architects, civil and structural engineers and quantity surveyors) within the Malaysian construction industry, focusing in the Klang Valley (Kuala Lumpur and Selangor States). To start with, the lists of contractor and clients' consultants were compiled from the Malaysian Construction Industry Directory (MCID) 2008–2009. The target population for contractors was based on companies that are registered with the Construction Industry Development Board (CIDB) of Malaysia under the Class G7 (projects value greater than Ringgit Malaysia 10 Million) categories and were identified from the CIDB directory.

A total of 330 questionnaires were sent to the different target groups in the Malaysian construction organisations. After several attempts to get respondents to respond to the survey, including follow-up calls and a reminder through email, only 80 responses were received, considered satisfactorily completed, giving a response rate of 24 %.

3.3 Data Analysis

Analysis of the raw data was performed with the aid of the Statistical Package for Social Sciences (SPSS) version 20.00. As the data was in terms of ratings measured on a 5-point Likert scale, it was considered ordinal in nature. Therefore, a descriptive analysis by means of identifying the mean score of each problem was found to be the most appropriate analysis to analyse the data. Table 3 show the mean scores of the frequencies of problems to the use of delay analysis methodologies.

Table 3 Problems on the use of delay analysis methodologies

Barriers	Contractors		Clients' consultants		Overall	
	Mean	R	Mean	R	Mean	R
Poorly updated programmes	3.81	2	3.88	2	3.85	1
Lack of familiarity with the techniques	3.68	4	3.93	1	3.81	2
Lack of skills in using technique	3.71	3	3.84	3	3.78	3
Unrealistic baseline programme	3.91	1	3.47	8	3.69	4
Baseline programme without CPM network	3.45	5	3.60	4	3.53	5
Lack of adequate project information	3.41	6	3.58	5	3.50	6
High time consumption in using technique	3.16	7	3.28	9	3.23	7
Difficulty in using the technique	2.94	8 ^b	3.49	6 ^b	3.22	8
Lack of suitable programming software	2.94	8 ^b	3.49	6 ^b	3.22	8
High cost involved in its use	2.87	10	3.19	10	3.03	10

R Ranking

^b For items with equal mean scores, sharing the same ranking order due to the number of respondents scoring 4 or more for the respective items was similar

4 Results and Discussion

4.1 *Problems Associated with Delay Analysis Methodology Usage*

The respondents were asked to rate the frequency of occurrence of ten most contentious problems associated with delay analysis methodologies usage, as drawn from literature and exploratory interviews. In addition, respondents were asked to mention other problems that they perceived as being the most critical problems to the use of the delay analysis methodologies. Table 3 shows the ranking of the problems based on each party's perspective, and also the overall ranking for each of these problems.

Following the interpretation of the five (5) point Likert scales, overall data analysis indicates the top five problems associated with delay analysis methodologies usage, with the mean scores ranging from 3.53 to 3.85 (see Table 3). The five problems, namely poorly updated programmes, lack of familiarity with the techniques, lack of skills in using technique, unrealistic baseline programme and baseline programme without CPM network.

In contrast to these top five problems, respondents contended that "difficulty in using the technique" (mean = 3.22), "lack of suitable programming software" (mean = 3.22), and "high cost involved in its use" (mean = 3.03) were the top three least problems to the use of delay analysis methodologies.

4.2 *Discussion of Identified Problems*

4.2.1 *Poorly Updated Programmes*

The highest rank given to this factor by the respondents corroborates previous findings made by Braimah and Ndekugri [20] in their research into deficiencies in contractor's programmes in UK construction projects. They found that typical of the deficiencies in contractors' programmes that will impair the use of programmes for delay analysis includes: poor baseline programmes, failure to update programmes, and inadequately updated programme. For instance, Arditi and Pattanakitchamroon [21] in a review of factors that affect the selection of a delay analysis methodology noted that analysts were able to use sophisticated delay analysis methodology, such as time impact analysis, in projects that keep up-to-date project programmes but, however, projects with no updated programmes were limited to only simple method, such as as-planned versus as-built methodology. Accurate analysis of delay requires programmes to be up-to-dated, capturing actual progress to date and the plan for performing the remaining activities [14, 19, 22]. This requirement is particularly important for the implementation of the sophisticated methods. The high ranking of this factor further explains the low use of these methodologies.

4.2.2 Lack of Familiarity with the Techniques

This factor was ranked 1st by clients' consultants group and 4th by contractors group. This finding corroborates with previous findings (see Table 1) that the sophisticated methods are more popular with the contractors. However, the ranking from other countries shows that the sophisticated methods are more popular with the consultants (see Table 1). A possible explanation for this unexpected result may be due to lack of awareness among consultants for the sophisticated methods. In addition, most construction contracts in Malaysia do not require the contractor to produce programmes using CPM or to produce delay claims by any particular method [3, 23]. Likewise, the private nature of the methods for resolving disputes from delay claims do not encourage development of awareness of the value of these methodologies because of the difficulty especially for laymen (judges and even technical arbitrators) and that is crucial [3]. The high ranking of this factor suggests a need for remedial review of the curricula of the institutions that provide construction management education. In this respect, the industry appears to be taking the lead, as industry-based providers of continuing professional development are increasingly offering high quality courses on delay analysis.

4.2.3 Lack of Skills in Using Technique

It should be clear from the discussion so far that the preparation and negotiation of EOT claims requires high levels of multidisciplinary skills, particularly in the areas of scheduling, work methods, costing and information technology. The high ranking on the lack of skills in using the techniques by the respondents was to be expected. Also, such ranking may be inferred from the high ranking accorded to unfamiliarity with the techniques. In the research reported by Arditi and Pattanakitchamroon [21] in the US, the majority of contractors (72 %) did not hesitate to conduct full delay analysis by engaging the services of a programming expert who made use of sophisticated work programmes, while in the remaining 28 % of the cases, the contractor provided an elementary analysis conducted by in-house staff using existing programmes and did not provide any formal analysis. The sophisticated methods require more skills to operate than the simplistic methods [5, 21]. Therefore, the high ranking of this factor is likely to result in lacking of emphasis among the contractor respondents and the clients' consultant respondents of Malaysia in their rating of extent of use of the sophisticated methods (see Table 1).

4.2.4 Unrealistic Baseline Programme

The highest rank given to this factor by contractors group although it was ranked 8th by clients' consultants corroborates with previous findings that was made by Danial [24] that the programme of works as prepared by the contractor in Malaysia is usually not detailed, not realistic or do not have the activities properly linked to show the

critical path. In addition, the programme is usually used for ‘show’ only more than anything else which is the cause of many incidents where EOT was not granted [25]. However, the responses from the clients’ consultants indicate that this factor is least important problems on the use of delay analysis methodologies. Therefore, the responses suggest that the low level of involvement of consultants in preparing the baseline programme. This result requires further research attention for the involvement of consultants in delay analysis. The research reported by Chong and Leong [3], the experts, delivered a unanimous opinion that two case studies in Malaysia were weak in terms of the entitlement for EOT due to the lack of accuracy of the work programme such as the programme logical links and in the estimated duration of construction activities. According to Idris [23] there is no specific recommendation by any standard form of contracts in Malaysia in preparing the work programme.

Furthermore, the sophisticated methodology such as time impact analysis requires a detailed and fully functional baseline programme and set of updates to work properly [19]. In the absence of a valid and reliable baseline programme, it causes the failed analysis and defeats the accuracy of programme analysis and becomes difficult to measure variations (impact) from it [19, 26, 27]. Moreover, a revised baseline programmes is necessary when: the critical path changes; delays have consumed the total float on non-critical activities; and the project schedule does not accurately reflect the actual planned execution [14]. Therefore, it is not enough for a baseline to be just available; the programme would have to be valid and reliable in terms of its completeness (i.e. showing all project activities), activity durations, details and relationships [20].

4.2.5 Baseline Programme Without CPM Network

The high ranking of this factor corroborates with previous findings that S-curve was the most well-known and widely used methodology of the contractors and consultants in Malaysia (see Table 1). However, s-curve does not identify and track the activities on the critical path.

5 Conclusions

This paper has successfully achieved its objective. The commonly problems on the use of delay analysis methodologies have been explored. A response rate of 24 % disclosed that poorly updated programmes, lack of familiarity with the techniques, lack of skills in using technique, unrealistic baseline programme, and baseline programme without CPM network, were the top five (5) problems on the use of delay analysis methodologies. These results suggest that the sophisticated methodologies are not widely used mainly due to a number of problems related to improper programming and lack of skills and familiarity in using the methodologies. Improvement in this practice is therefore an essential requirement in

determining what framework might be appropriate for promoting better delay analysis practice toward reducing disputes. Such improvement is likely to involve further studies. Therefore, the findings from this research offer a significant contribution to the industry players, construction organisations, researchers and also academicians.

Acknowledgments The Author is appreciative of the expertise of the supervisory committee and to industry collaborators for their practical and applied evaluations.

References

1. M.M. Kumaraswamy, K. Yogeswaran, Substantiation and assessment of claims for extensions of time. *Int. J. Project Manage.* **21**, 27–38 (2003)
2. N.M. Yusuwan, H. Adnan, Issues associated with extension of time (EOT) claim in Malaysian construction industry. *Procedia Technol.* **9**, 740–749 (2013)
3. H.Y. Chong, Y.W. Leong, Legal approach on assessment of contractors' entitlement to extension of time. *Afr. J. Bus. Manage.* **6**(14), 4815–4823 (2012)
4. S. Alkass, M. Mazerolle, F. Harris, Construction delay analysis techniques. *J. Constr. Manage. Econ.* **14**, 375–394 (1996)
5. N. Braimah, An investigation into the use of construction delay and disruption analysis methodologies. Doctoral thesis, University of Wolverhampton, UK 2008
6. V.A. Lovejoy, Claims schedule development and analysis: collapsed as-built scheduling for beginners. *J. Cost Eng.* **46**(1), 27–30 (2004)
7. S.A. Ahmad, F. Hassan, S. Hassan, M.C. Mat, N.M. Nasir, Z.A. Samad, A study on the practise of delay analysis techniques in the Malaysian construction industry. Paper presented at the 13th pacific association of quantity surveyors congress, Kuala Lumpur, Malaysia, August 2009
8. N. Braimah, I. Ndekugri, Consultants' perceptions on construction delay analysis methodologies. *J. Constr. Eng. Manage.* **135**(12), 1279–1288 (2009)
9. I. Ndekugri, N. Braimah, R. Gameson, Delay analysis within construction contracting organizations. *J. Constr. Eng. Manage.* **134**(9), 692–700 (2008)
10. J.B. Yang, C.K. Kao, Review of delay analysis methods: a process-based comparison. *Open Constr. Build. Technol. J.* **3**, 81–89 (2009)
11. M. Battikha, S. Alkass, A cost-effective delay analysis technique. *AACE Trans. DCL.4.1–DCL.4.7* (1994)
12. K. Pickavance, *Delay and Disruption in Construction Contracts*, 3rd edn. (LLP Reference Publishing, London, 2005)
13. Society of Construction Law (2002) Delay and disruption protocol. Printmost (Southern) Ltd, England. See <http://www.eotprotocol.com>
14. J.J. Ciccarelli, Additional practical applications of the window analysis. *AACE Int. Trans. CDR.06.1–CDR.06.8* (2007)
15. J.S. Lee, Delay analysis using linear schedule in construction. *AACE Int. Trans. CDR.18.1–CDR.18.6* (2007)
16. J.L. Ottesen, Concentrated window analysis results. *AACE Int. Trans. CDR.11.1–CDR.11.13* (2006)
17. W. Menesi, Construction delay analysis under multiple baseline updates. Master's thesis, University of Waterloo, Ontario 2007
18. Z.Q. Zafar, Construction project delay analysis. *J. Cost Eng.* **38**(3), 23–28 (1996)

19. J.C. Livengood, Retrospective TIAs: time to lay them to rest. *AACE Int. Trans. CDR.08.1–CDR.08.9* (2007)
20. N. Braimah, I. Ndekugri, The link between planning and programming practice and the analysis of delay and disruption claims. *AACE Int. Trans. CDR.19.1–CDR.19.7* (2006)
21. D. Arditi, T. Pattanakitchamroon, Analysis methods in time-based claims. *J. Constr. Eng. Manage.* **134**(4), 242–252 (2008)
22. B.E. Hallock, P.M. Mehta, The great debate—TIA versus WINDOWS a better path for retrospective delay analysis?. *AACE Int. Trans. CDR.04.1–CDR.04.25* (2007)
23. N.J. Idris, Effect of work programme in extension of time entitlement. Master's thesis. University Technology Malaysia, Skudai 2006
24. N. Danial, Contractor's application for an extension of time. Master's thesis, University of Technology Malaysia, Skudai 2007
25. Entrusty Group, Is the contractor still entitled to extension of time when there is concurrent delay? *Master Builders J.* **3**, 101–103 (2006)
26. R.B. McCullough, CPM schedules in construction claims. *J. Cost Eng.* **31**(5), 18–21 (1989)
27. R.B. McCullough, CPM schedules in construction claims from the contractor's perspective. *AACE Int. Trans. CDR.02.1–CDR.02.4* (1999)
28. N.H. Muhamad, Delay analysis methodology framework for construction delay practice in Malaysia. Master thesis, University Technology MARA (2013)

An Overview on the Issue of Delay in the Construction Industry

Sunitha V. Doraisamy, Zainal Abidin Akasah and Riduan Yunus

Abstract Construction delay is a common problem in the construction industry. It is important to study this problem by investigating the overview of previous study on the issue of project delays and potential solutions to overcome it. Review of literatures shows the causes and necessary suggestions in project delays which is plaguing the construction industry in different nations. Various causes have been identified and suggestions have been poured out to minimize the problem as much as possible. Delay in projects is something that couldn't be avoided looking at the situation of the construction industry especially in developing countries. Delay in projects happen somewhere during the construction process, and some even at the point of completion of a construction project. The delivery of a construction project on time and according to the expected budget is very much needed. The unsuccessfulness on doing so, has invited many research on this issue to determine and investigate the causes and as well the effect of project delays in the construction industry. There are sectors in Malaysia that contributes to the country's economy, and the construction industry is one of it. This paper is an overview of the issue of a project delay, where the seriousness of this issue could be understood and may help to invite some researchers to proffer solution to this situation in the coming future.

Keywords Overview • Project delay • Cost overrun • Completion

S.V. Doraisamy (✉) · Z.A. Akasah · R. Yunus
Faculty of Civil and Environmental Engineering, Universiti Tun Hussein Onn Malaysia,
86400 Parit Raja, Batu Pahat, Malaysia
e-mail: suni7624@yahoo.com

Z.A. Akasah
e-mail: zainal59@uthm.edu.my

R. Yunus
e-mail: riduan@uthm.edu.my

1 Introduction

Rum and Akasah [1] stated that an improvement on the economic growth in a country will increase the growth of the construction industry. At the same time, there will be an increasing demand on the construction of facilities and buildings. It is also stated that there are more than 50 % of projects that are going through time overrun which is ultimately comes to construction project delay. The situation of construction delay is a definite downfall on the development of a country. Desai and Bhatt [2] explained that the construction delay could be defined as the time overrun where the time of completion is beyond the specified date in a contract or takes more time to complete than the actual date that the parties agreed to deliver a project. When a project is taking more time than the planned schedule, this is taken as a common problem in the construction industry. The meaning of owner delay is when a revenue is lost due to the lack of production facilities and rentable spaces, or not able to have dependence on present facilities.

The problem of project delays in the construction industry is known to be a global phenomenon. In Vietnam, Long et al. [3] found that many problems occurs during the implementation of a construction project, which the two main concerns are time and cost overruns. Along with time and cost overruns, together comes other consequences such as project failure, reduction of profit margin, and the society's disbelief especially on government funded projects, etc. In the study of Sambasivam and Soon [4], they have explained that the delay of construction projects causes a lot of dissatisfaction to all the parties involved and the main role of the project manager is to make sure that the projects are completed within the budgeted time and cost. They further elaborated that in South-East Asia, although Malaysia is known to be a fast developing country but yet still do face the problem of project delays as well. In 2005, about 17.3 % from the 417 government projects in Malaysia were considered to be sick, meaning it has been delayed for more than 3 months or abandoned. The construction sector is indeed one of the sectors that has significant contribution towards the Malaysia's economic growth. However, some of the causes and effects of delays in the construction projects can be categorized as country-specific.

According to Long et al. [3], many factors relate to delay and it differs along with the types of projects, locations, sizes and scopes. The delay of large construction projects which has a complex features and design that requires high in capital, have invited the interest of many researchers to study the related characteristics with the delay of construction projects.

Therefore, delays in construction projects causes distress and anxiety to all the parties in terms of contract, and the project manager plays a vital role in making sure that the projects are completed within the budgeted time and cost, as specified in the contract.

2 Types of Construction Delays

Delay in projects is bound to happen. Some delay will take place at a particular time in the progress and completion of a certain work or activity and some will have the freedom to be completed in which it has its' effects. Scott [5] has mentioned delay caused by employer; delay caused by contractor and "neither" party responsible delay, as types of existing delays in the construction area. According to him, failure in providing site information is considered to be the fault of the employer. When it comes to time and cost overrun Ezeokonkwo [6], says it happens accordance with other situations such as delays in the payment of interim certificates, the client or his representatives are not capable in making decisions quickly, handover of construction sites are done rather late, materials are supplied late and inadequate planning. He further elaborated that when a contractor is not capable to proceed with a work relating to the project diligently and efficiently, which might be caused to reason such as inadequate labour/plant deliverance, the inability to solve this by the contractor makes it as to be the fault of the contractor himself. He also identifies that the cause of delay which is not caused by either the client or the contractor, but caused by reasons which in all ways are immortal, as "Neither" party responsible delay (Extraneous conditions). This sort of delay happens usually for reasons like strikes, riot, harmful weather, force majeure and acts of God, loss and damages due to fire and storm. The inability of the contractor to overcome these sort of matters which show it is reasonably out of his control, is categorized as not the contractor's fault. At the same time, delays caused by nominated subcontractors or suppliers which the contractor has taken all possible steps to avoid or reduce any sort of delay by them, is also could be taken as not his fault either. In the opinion of Ahmed et al. [7], delays could be non-excusable; excusable (with or without compensation) and concurrent delays, where delays that are caused by the contractor, sub-contractor or other party but are within the control of the contractor, is known to be non-excusable delays. These type of delay is due to problems such as breakdown of equipment, improper scheduling or improper management, productivity which are not properly estimated, improper project planning, management of site which are poorly handled and poor supervision, undependable subcontractors or suppliers and problems in general staffing.

Delays caused by factors that are not able to be detected earlier by the contractor or any other party for that matter, are not subjected to their negligence or faults, but is considered to be an excusable delays where at this part, time extension is given in this matter, but not in the case of extension of cost. As elaborated by Ashworth [8], concurrent delays occur when both the owner and the contractor are responsible for the delay. Generally, if the delays can't be disentangled, the contractor can be held responsible for the delay where he will be forced to speed up the works, or be responsible for the ascertained damages, but not allowed to claim the delay damages from the owner.

Knowing and understanding the types of construction delays helps to identify and as well understand the risk that comes along with it. The importance in

identifying and understanding the types of delay can help to process the damages from the consequences of delay as well. Therefore, the types of delay should be referred into properly without misinterpreting it.

3 Studies on Causes of Delays

Apart from others who say delays to be a global phenomenon, Desai and Bhatt [2] says delays on construction projects are a universal phenomenon. They are almost always accompanied by cost and time overruns. Construction project delays have an unfavourable effect on parties such as the developer, contractor and consultant, to a contract which leads to conflict in a relationship, not able to trust, litigation, arbitration, cash-flow problems, and having anxiety or unpleasant feeling towards each other. So, it is important to define the actual causes of delay in order to minimise and avoid any unwanted delays in construction projects in the future. Sambasivam and Soon [4], has rated the causes of delay in their study from the most significant to the least, they are (1) contractor's improper planning, (2) contractor's poor site management, (3) contractor's lack of experience, (4) client's finance and payments for completed work are inadequate, (5) problems with sub-contractors, (6) shortage in material (7) shortage in labour supply, (8) unavailability in equipment and its' failure, (9) communication barrier between parties, (10) mistakes during the construction is in work. These causes does not differ much from the causes identified by Odeh and Battaineh [9] in their survey, which are owner interference, contractor's lack of experience, financing and payments, labourer's lacking in productivity, poor and slow decision making, improper planning, material shortage and problem with subcontractors. Alwi and Hampsom [10], have ranked three causes as the most highest in the construction industry of Indonesia, which are poor professional management, having low skills in design works and documentation, and shortage of materials.

From an analysis from his study, Memon [11] has identified changes that are often made in designs, changing the scope of project, owners who are facing financial difficulties, decisions are made late and ground conditions which were not able to be predicted earlier. From the survey conducted by Frimpong et al. [12], to know the important factors contributing to delay and cost overruns in Ghana groundwater construction projects, it shows that the main causes are shortage in monthly payments from agencies, poor management by contractor, material procurement, lacking in technical performance, and rapid increase of material prices. Delay in the delivery of materials and equipment to construction sites in Nepal is a major contribution towards the delay and cost overruns of the construction projects, as elaborated by Manavazhia and Adhikarib [13] in their survey. Other than contractor, labour and material related causes, Chan and Kumaraswamy [14] linked the consultant-related and client-related causes to the probable time overruns in construction projects in Hong Kong. It is the same in the case of Mansfield [15] and

Frimpong et al. [12], except they have added material-related also as one of the probable causes in cost and time overruns.

Delays can be minimised only when their causes are identified. Knowing the cause of any particular delay in a project would help avoiding it, especially if it identified in the earlier stage itself.

4 Suggestions on Overcoming Project Delays

Long et al. [3] elaborates that human resource training for the need in construction industry is an immense demand. This is a task that not only requires quantity but quality also in its' training scheme. In Vietnam, training future engineer are more focused on structural design, leaving a void on the planning, managing and accessing of knowledge. There must be an importance given to project feasibility study and must be conducted as carefully as possible; especially, with projects that are funded by the government. Long et al. [3], further added that there should be a system which is closely related to the feasibility study, selection of contractors, and financing, etc.

Akinsiku and Akinsulire [16], have suggested that proper budgetary planning must be designed to ensure proper funding for a specific project or have an alternative source in funding or project arrangement such as BOOT and BOT which allows contractors to participate in the design and financing of new projects from the beginning stage of the project itself. Other than that, they have also suggested sufficient planning and the establishment of sufficient quality control system to be put in place to avoid design changes, plus an appropriate time should be allocated so that designs are done carefully, and complete tender documents, to improve the quality of contract documents with minimum errors and avoid lack of compatibility which reduces delay during the construction stages. Issues that are related to design such as changes in drawings, specifications that are incomplete and has faults, client's interference in changes and general change order have detrimental effect on the project deliverance which ultimately contributes time and cost overruns. These are issues that can be controlled by proper design process management and on time decision making.

Jeni and Akasah [17] have even suggested the lean construction [17] concept where this concept enhances the management process in a project where it is able to implement the activities in the project in a more systematic, organized and effective way. This might help in delivering a project on time. Kikwasi [18], have recommended that a construction budget with proper adequacy, on time information conveying, finalisation of design and proper management skills should be the main criteria for the parties in project procurement process. Olusegun and Michael [19], are in opinion that in the effort to reduce the effects of project delay and project abandonment, clients should provide an adequate planning for the project at the starting point itself and have a proper estimation of enough budget availability by the Quantity Surveyor, who controls the funding of the project work throughout the

construction process. The clients should also engage services of competent construction professionals; such as the Architect, who is responsible in producing design which is within the planned budgetary design. The government should issue on taking only competent contractors with strong financial background in executing any contract.

All the recommendations and suggestions that has been laid out by various researches who have studied this issue in various countries, should be taken into consideration and viewed carefully. This might lead to solutions that is either could minimize the problem of project delay or overcome it totally. If all the important and necessary solutions that are proffered in overcoming project delays are put into as a guideline, this might help the specific parties involved in a construction project in completing it accordingly to the time and budget as specified in the contract.

5 Conclusion

Planning is vital to ensure construction projects can be completed within the time allocated, not exceed the budgets and meeting the standards and requirements that have been set by the clients. Failure to have an adequate planning, including financial and physical planning, will cause construction delay, which will have negative impacts such as cost overruns, extension of time and disputes. The cost of materials and machines' operations will be increased due to inflation and inaccurate estimation.

There are various causes that have been identified by different researches on the issue of project delay. Accordingly, appropriate recommendations were proposed to overcome and eliminate problems that hindered the successful of the construction projects. There should be a proper extended study on this issue to proffer solutions to eliminate construction delay, by identifying possible solutions and measuring the level of effectiveness towards the proffered solution.

Acknowledgements The author would like to convey her gratitude to Associate Prof. Dr.Hj. Zainal Abidin Akasah and Dr. Riduan Yunus from UTHM for supporting this paper.

References

1. N.A. Rum, Z.A. Akasah, Implementing life cycle costing in malaysia construction industry: a review, in *Proceedings of International Building and Infrastructure Technology Conference* (Penang, 7–8 June 2011)
2. M. Desai, R. Bhatt, Critical causes of delay in residential construction projects: case study of central Gujarat region of India. *Int. J. Eng. Trends Technol. (IJETT)* **4**(4), 762–768 (2013)
3. L.H. Long, D.L. Young, Y.L. Jun, Delay and cost overruns in vietnam large construction projects: a comparison with other selected countries. *KSCE J. Civil Eng.* **12**(6), 367–377 (2008)

4. M. Sambasivam, Y.W. Soon, Causes and effects of delays in Malaysian construction industry. *Int. J. Project Manage.* **25**(5), 517–526 (2007)
5. S. Scott, The nature and effects of construction delays. *Constr. Manage. Econ.* **11**(5), 358–369 (1993)
6. J.U. Ezeokonkwo, Disruption in construction project: effects on project cost and quality, in *Workshop on the Effective Building Procurement and Delivery in the Nigerian Construction Industry*, eds. by M.E. Obiegbo, J.U. Ezemerihe, S.Akabogu (1995)
7. S.M. Ahmed, S. Azhar, M. Castillo, P. Kappagantula, *Construction Delays in Florida: An Empirical Study* (Department of Community Affairs, Florida, 2000)
8. M. Ashworth, *Construction Delays in Florida: An Empirical Study* (Department of Community Affairs, Florida, 2000)
9. A.M. Odeh, H.T. Battaineh, Causes of construction delay: traditional contracts. *Int. J. Project Manage.* **20**, 67–73 (2002)
10. S. Alwi, K. Hampson, Identifying the important causes of delays in building construction projects, in *Proceedings the 9th East Asia-Pacific Conference on Structural Engineering and Construction* (Bali, Indonesia, 2003)
11. A.H. Memom, Contractor perspective on time overrun factors in Malaysian construction projects. *Int. J. Sci. Environ. Technol.* **3**(3), 1184–1192 (2014)
12. Y. Frimpong, J. Oluwoye, L. Crawford, Causes of delay and cost overruns in construction of groundwater projects in a developing countries; Ghana as a case study. *Int. J. Project Manage.* **21**, 321–326 (2003)
13. M.R. Manavazhia, D.K. Adhikarib, Material and equipment procurement delays in highway projects in Nepal. *Int. J. Project Manage.* **20**, 627–632 (2002)
14. D.M. Chan, M.M. Kumaraswamy, A comparative study of causes of time overruns in Hong Kong construction projects. *Int. J. Project Manage.* **15**(1), 55–63 (1997)
15. N.R. Mansfield, Causes of delay and cost overruns in Nigerian construction projects. *Int. J. Project Manage.* **12**(4), 254–260 (1994)
16. O.E. Akinsiku, A. Akinsulire, Stakeholders' perception of the causes and effects of construction delays on project delivery. *J. Constr. Eng. Project Manage.* **2**(4), 25–31 (Dec 2012)
17. M.L. Jeni, Z.A Akasah, Implementation of lean construction concept among contractors in Malaysia, in *The International Conference on Engineering and Built Environment* (2013), pp. 1–6
18. G.J. Kikwasi, Causes and effects of delays and disruptions in construction projects in Tanzania. *Australas. J. Constr. Econ. Building Conf. Ser. 1* **2**, 52–59 (2012)
19. A.E. Olusegun, A.O. Michael, Abandonment of construction projects in Nigeria: causes and effects, *J. Emerg. Trends Econ. Manage. Sci. (JETEMS)* **2**(2), 142–145 (2011)

Propelling Site Safety Through Accident Causation Models

Noor Aisyah Asyikin Mahat, Faridah Ismail
and Sharifah Nur Aina Syed Alwee

Abstract The function of safety is to locate and define an operational error that allows accident to occur. Previous research suggested that this function could essentially be achieved in two ways—by studying both the causes of accidents and the effectiveness of known controls being utilized. This research draws from the successful experiences of accident prevention key elements worldwide. There are many available theories on the accident accusation. The earliest models of accident causation were simple where subsequence event from the initiation of the chain to its conclusion in the accident. Lack of study was found in Malaysian environment. Thus, this research aims to create proactive measure for accident prevention in construction sites through the adaptive of accident causation theories, which signifies the identification on how hazard in construction sites causes losses. The objectives of the research are to investigate the essential elements from the available theories of the accident causation and to generate adaptive theories for accident prevention. The reviewed on accident accusation theories revealed that the shift in emphasis on the role of the management, and considered the causes of accidents are provoked among others, by actions of contractors. Thus the constraint includes the influence of management, the organisational and the environment factors that demand to be addressed to reduce the causes of an accident. The findings will contribute to the ongoing research for the development of an adaptive prevention theory for construction workplace environment. This is also directly matched to the Strategic Trust No. 3 Construction Industry Master Plan (CIMP 2006–2015), strive for the highest standard of quality, occupational safety and health and environmental practices.

Keywords Safety • Safety performance • Construction site • Accident • Accident causation models

N.A.A. Mahat (✉) · F. Ismail · S.N.A.S. Alwee
Faculty of Architecture, Planning and Surveying, Universiti Teknologi MARA,
Shah Alam, Malaysia
e-mail: nooraisyah@salam.uitm.edu.my

F. Ismail
e-mail: farid346@salam.uitm.edu.my

S.N.A.S. Alwee
e-mail: aina_alwee@yahoo.com.my

1 Introduction

The statistical reported by the Department of Occupational Safety and Health (DOSH), Social Security Organization (SOCSO) as well as the Construction Industry Development Board (CIDB), show an incrementing number of accident fatalities in recent years. A recent investigation related to occupational accidents by sectors, carried out by DOSH, it is that from 164 accident cases reported, there were 69 cases that involving death, 83 case associated with non-permanent disability, and the rest of cases reported were suffering permanent disability. With such a high figures reported, accidents in this industry have captured the attention and concern from both government and non-government organization. According to [1], no one is supposed to be injured or die at work. In a rational-humanist perspective, managers and directors are assumed to have the best interest of workers at heart, and workers are supposed to be about their own safety and that of others. However, in recent years the Malaysian construction industry shows the grim reality for rapidly increasing of injuries and death. Accident that happened in the construction industry reputedly stemmed from construction failure is linked to the shortcoming or failure of safety implementation carried out at the construction site [2]. Malaysia government, through the Human Resources Ministry, targets to reduce a workplace-related accident to three in 1,000 workers by year 2015, as compared to 3.31 in every 1,000 workers in year 2012.

In order to minimise an accident rate from the construction industries, identifying the root causes of accidents by analysing theories of accident causation is essential before proceeding to strategies manuals to implement it. There is a variety of theory of accident causation that can help to understand the occurrence of an accident, analysing the causes and adapting the theories to reality. Accident causation models present factors and processes involved in accidents in order to develop strategies for accident prevention. Major theories of accident causation commonly used are Heinrich Domino Theory, Management-Based Theories, Human Error Model, The Swiss 'Cheese' Model and Accident Root Cause Tracing Model (ARCTM) [3]. According to [4], the different models are based on the different perception of the accident process. From the above mentioned theories, the adaptive accident prevention theories will be created to prevent an accident from occurs in the construction site.

It is important to know the causes of the accident before the accident prevention may take place [1]. According to [3], construction accidents can be prevented just by identifying the root causes of accidents. Accident investigation techniques can be done through the theories of accident causation also a human error. These theories provide explanations of why accidents happen. There are many available theories on the accident accusation. The various theories are based on perceptions of the accident process. This paper attempt to enhance the understanding of the existing accident causation theories and develop practical strategies to overcome the scarcity of safety performance in a construction site. With the understanding on

the existing theories, this research aims to create proactive measure for accident prevention in construction sites through the adaptive of accident causation theories, which signifies the identification on how hazard in construction sites causes losses.

2 Safety and Accident Prevention

Construction industry plays a vital role in developing of countries’ economic growth. Despite the contributions to economic growth, construction industry has always been blamed for the high rates of accidents and fatalities. This issue has placed the construction industry among the industries with unreasonable rates of accidents, permanent and non-permanent disabilities and even fatalities [3]. This is by the statically fatality rate reported by DOSH. Figure 1 shows the occupational accidents by sector reported by DOSH until December 2013. From the figure, construction industry has reported for highest fatality rate compared to other sector. Fatality reported proved that the safety at construction sites still remain one of the leading causes of death in the workplace. As more and more people joined the industry, it is incumbent on the construction companies, project owners, and design professionals to ensure emphasis placed on safety continues to grow.

Improving safety in construction remains a priority in almost every country around the world, because the construction industry stands out among all other industries as the principal contributor to severe and fatal accidents [5]. Safety is concerned with the prevention of accidents, but it is also concerned with the prevention of disease, property damage and anything else that may adversely affect either the organisation or its employees [6]. According to [7], construction accidents lead to delay in project completion, increase the expenses and ruined the reputation and reliability of contractors. Research efforts have focused on developing accident causation models to reveal root causes of construction accidents. Though various

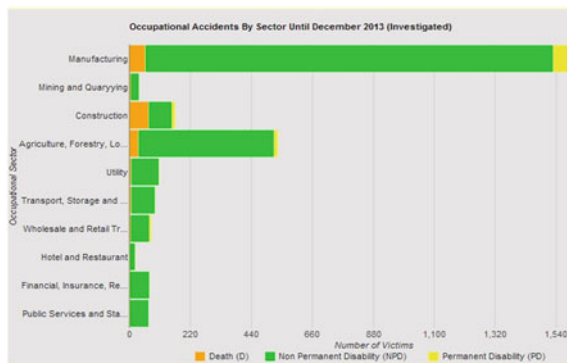


Fig. 1 Occupational accidents by sectors until December 2013. *Source* Department of safety and health Malaysia statistic by sectors

Table 1 Root cause of accident

Author	Root cause of accidents
Hinze and Parker (1978)	Job pressures and crew competition
McClay (1989)	Hazards, human actions, and functional limitations
Raymond (1995)	Lack of supervision by the line managers, Custom and practice in the industry, Lack of coordination
Abdelhamid and Everett (2000)	Management deficiencies, training, and workers attitude
Suraji et al. (2001)	The nature of project, the method of construction, site restriction, project duration, procurement system, design complexity, level of construction and subcontracting contributing to accident causation
Toole (2002)	Lack of proper training, lack of safety equipment, deficient enforcement of safety, unsafe equipment, unsafe method, unsafe condition, poor safety attitude, and the isolated deviation from prescribed behaviour

causes of accidents are acknowledged, the primary factors that bring about accidents are not up till now well implicit. Data existing is insufficient in explaining the principal factors in accident causation on construction sites.

Accident causation is a complex issue, as there are usually several contributing factors that are the root causes of accidents on sites [6]. Accounting for the inter-relationship between these factors and their effects on accidents, it is a critical for an effective accident prevention strategy. A review of the literature on construction safety reveals that much research effort has been heading for at probing accident records to categorize the most common types of accidents also the root cause on how these accidents happen. Table 1 summarizes limited numbers of literatures that highlighted the root cause of construction accidents.

3 Accident Causation Models

There are many theories associated with the cause of an accident, ranging from simple to complex. In general, the objective of these models is to provide tools for enhanced industrial accident prevention programs. Accident prevention has been defined by Heinrich et al. (1980) as “An integrated program, a series of coordinated activities, directed to the control of unsafe personal performance and unsafe mechanical conditions, and based on certain knowledge, attitudes, and abilities” [1]. Other terms that are synonymous with accident prevention such as loss prevention, loss control, total loss control, safety management, and incidence loss control, among many others [5]. Theories and models of construction accidents are evolved based on the enlightenment of how construction accidents occur. Some of the most influential accident accusations models are Domino Theory, Multiple Causation Model, Behavioral Model, Accident Root Causes Tracing Model (ARCTM), also

The ‘Swiss Cheese’ Model. While there are many method and models for examining safety and health occurrence, this research is only discussed three of the accident causation theories which are Domino Theory, Multiple Causation Model and The ‘Swiss Cheese’ Model. These well-known models are highlighted in this paper because of their recognition and application to the construction industry.

3.1 Domino Theory

There are several domino theories of accident causation such as *Heinrich’s Domino Theory* (1930s), *Bird and Loftus’s Domino Theory* (1976) and *Marcum’s Domino Theory* (1978). While each of the domino theory presents a different explanation for the cause of accidents, they all have one thing in common. Domino theories represent accidents as predictable chronological sequences of events or causal factors. Each causal factors builds on the affects the others. If allowed to exist without any form of intervention, these hazards will interact to produce the accident [8].

H.W. Heinrich developed the original domino theory of accident causation in 1930s. Although written decades ago, his works in accident causation is still the basis for several contemporary theories. Heinrich had five dominoes in his model: ancestry and social environment, fault of a person, unsafe act and/or mechanical or physical hazard, accidents, and injury. Figure 2 shows the illustration of Heinrich Dominos Theory. This five-domino model suggested that through inherited or acquired undesirable traits, people may commit unsafe acts or cause the existence of mechanical or physical hazards, which in turn cause injurious accidents [5]. The two key point in Heinrich’s Domino Theory are that (1) injuries are by the action of preceding factors, and (2) removal of the events leading up to the incident, especial employee unsafe acts or hazardous workplaces conditions, prevent accidents and injuries. Heinrich believed that the unsafe act caused more accidents than unsafe conditions. Therefore, his philosophy of accident prevention focused on elimination unsafe acts and people-related factor that lead to injuries [9].

Bird and Loftus [10] rationalized the “Domino theory” in order to replicate the role of management system or management relationship in the sequence of the

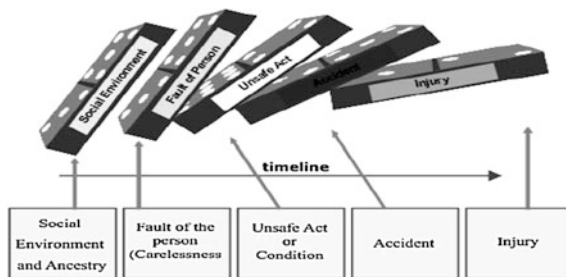


Fig. 2 Domino theory of accident causation

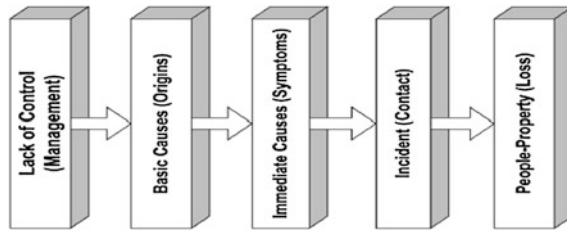


Fig. 3 Updated domino sequence of accident causation theory (Bird [16])

accident causes defined by Heinrich (Domino-based model) (see Fig. 3). The main point in this theory is that management is responsible for the safety and health of the employees. The theory also emphasizes the contact incidents can be if unsafe act and condition are prevented. The updated and modified sequence of events is [3, 11]:

1. Lack of control/management
2. Basic causes/origins (personal or job factors)
3. Immediate causes/symptoms
4. Incident (contact with energy and substance)
5. Loss (property, people, process)

The update domino sequence can be used for accident prevention also in loss control management.

Marcum’s theory focuses on management responsibility for protecting employee safety as well as preventing the downgrading for an organization. The theory attempts to examine the management accidents response protocols to ensure that sustained losses and the subsequently incurred cost were minimized. Marcus theory focus on the human element of misact. The term of *misactsidents* in Marcus theory emphasizes the fundamental aspect of his accident causation theory.

Figure 4 show the Marcum’s Domino Theory of Accident. Misactsidents is an identifiable sequence of misacts associated with *inadequate task preparation* which could lead to *substandard performance* and *miscompensated risks*. Marcum also includes the cost aspect of a loss.

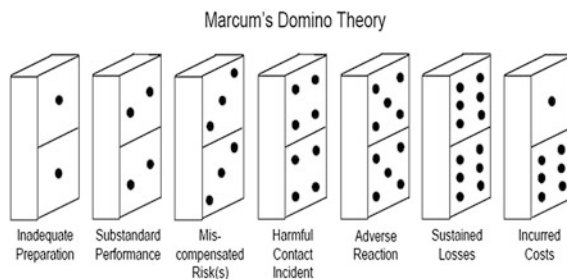


Fig. 4 Marcum’s domino theory of accident causation

According to the revised model of Domino theory that signifies the role of management, the process of incidents begins by the lack of control by management. Planning, controlling, organizing, and leading by management are the factors that can prevent incidents to happen [12].

3.2 Multiple Causation Model

Heinrich’s theory is very much a theory of a single causation. However, very rarely an accident occur due to single causation. Multiple causation theory promotes the idea that accidents result from various hazards or factors interacting manner. Accident happens due to multiple and sometimes complex causal factors. Causal factor seldom contributes equally in their ability to trigger an event or contribute to accident severity.

(i) *Multiple Factor Theory*

Vernon L. Gorse’s multiple factor theory uses four M’s (4 M) to represent the factor causing an accident: machine, media, man, management [9]. Table 2 explain the factor of an accident due to this theory also the characteristic for each feature.

(ii) *System Theory of Causation*

Another variation of multiple causation theories is R.J Firenzie’s Theory of Accident Causation. Theory is based on interaction of three components: person, machine and environment. When human behaviour combine with machine hazard and environment factors, this will affect the probability of mishap [13].

Table 2 Gorse’s accident causation theory

Factor	Description	Characteristic
Machine	Tools, equipment, or vehicles that may contribute to an accident	Design, shape, size, particular type of energy used to operate the equipment
Media	Environmental conditions surrounding an accident; weather, walking surface	Snow or water on a roadway, temperature (outdoor and indoor)
Man	People and human factors that could contribute to an accident	Gender, age, height, weight, condition, memory, recall, knowledge level
Management	Method used to select equipment, train personnel, or ensure relatively hazard free environment	Safety rules, organization, structure, policy and procedures

3.3 The 'Swiss Cheese' Model

The Swiss Cheese model was developed by James Ramon, who uses slices of Swiss Cheese as an analogy to barriers. The theory is currently widely used since it simply suggests that the organization tries to thwart accidents by defenses in order not to allow the risks and hazards become loss [3] (See Fig. 4). The principle idea of the model basically like cheese slice have holes of or latent condition [13]. The Swiss Cheese model shows the development of an accident from latent conditions to active failures that both penetrate a series of safety barriers and eventually lead to accidents. This barrier is varying in size over time [11] (Fig. 5).

The main element of the Swiss Cheese Models is [11]:

- (i) *Decision-makers*
This typical includes corporate management and regulatory authorities. The management is in charge to ensure the vacant resources to achieve and balance two distinct goals; safety, time and cost. This will influence the infallible decisions.
- (ii) *Line management*
Responsible for implementing decisions made by decision makers. They adopt and implement everyday activities in operations.
- (iii) *Pre-conditions*
The decision made by decision makers and action implemented by line management create many of the precondition in which the workforce attempts to carry out their responsibilities safely and effectively.
- (iv) *Unsafe acts*
Unsafe acts carried out by the worker's/operators.
- (v) *Last barriers*
These are the defense or safeguard that are in place to prevent injury, damage or cost interruptions in the event of an unsafe act.

The Swiss cheese model is a good instance for explaining the unpredictability of incidents. They are impossible to foresee and so it is difficult to prevent them. Past chain of accident causation may not always lead to the similar incident on the future

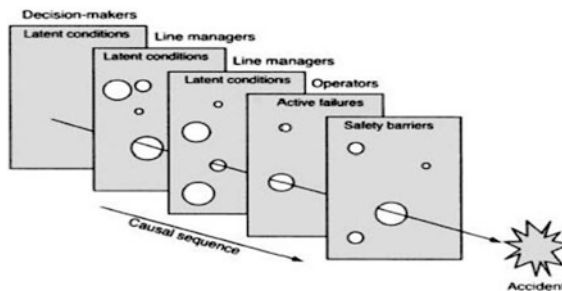


Fig. 5 Swiss cheese accident causation model

occasion. The theory is currently widely used since it simply suggests that the organizations try to prevent accidents by defenses in order not to allow the risks and hazards become loss [14].

4 Findings and Discussion

Models and theories of construction accidents causation are on the basis of explaining how construction accidents occur. Several accident causation models have been presented in this paper. The theories focus on people variables, management aspects, and physical characteristic of hazard. The benefit of understanding accident causation is in recognizing how hazards in the workplace result in losses. Eliminating hazards before they result in losses is the proactive responsibility of everyone in the organization. Accident may still occur despite proactive safety program. It is at that point that an effective accident investigation program is of vital importance for a collection of critical data.

The domino theory described a simple model based on a singular concept of risk. Domino theories describe accidents as predictable chronological sequences of events or causal factors. Each causal factors builds on the affects the others. If allowed to exist without any form of intervention, these hazards will interact to produce an accident. Dominos theory was the starting point for the field of safety, for being well-known throughout the world. The theory emphasis on management as a primary cause of the accidents. Subsequent theories and models of accident causation represented a higher level of complexity and extensiveness [3, 15]. Multiples Causation Models identify involvement of various hazards or factors interacting manner. Accident happens due to multiple and sometimes complex causal factors. Causal factor seldom contributes equally in their ability to trigger an event or contribute to the accident. The Swiss Cheese Theories, which states that, the accumulation of human errors (active failure), result in active and latent failures. The active failures can be notices immediately most of the time, while the latent failures are noticeable just when they are with the supplement causes to violate the systems' defensive actions [3]. The Swiss Cheese theory of accident causation challenges the inappropriate belief of managers that assume that systems are safe and to search for underlying variables.

5 Conclusion

Accident can occur because of failure in one or more factors. Nevertheless, the development of accident causation models over the years from 1960s, is getting more and more complicated. Accident causation models previously were lot simpler than the later complicated models. Theories and models provide an explanation of why incident and accident occurs. These theories and models have considerably

increased the understanding of accidents and how they happen. As much as management tried to avoid them, they still occur because there is always some lingering risk. The task of the safety professionals is to identify the risk, advise management to reduce or eliminate as much as possible, and continue to monitor help assure that the assets of the company, especially its employees, are from those hazards. The shift in emphasis on the role of the management, and considered the causes of accidents are provoked among others, by actions of contractors. Thus the constraint includes the influence of management, the organisational and the environment factors that demand to be addressed to reduce the causes of an accident. Although the safety improvement are on the construction site (safety working environment, safety guidelines and safety program); the crucial area is to targets are the working organization, especially for the employees to understand and take the responsibility to ensure the presence of the hazard can tremendously evade on site.

Acknowledgments The financial support provided by the Ministry of Higher Learning Education (MOHE) and Research Management Institute (RMI) UiTM under research grant no. 600-RMI/RAGS 5/3 (172/2013) is acknowledged. The author would like to acknowledge the government agency, the consultants and the contractors for their kind responses and making available the data needed. This research would not be possible without the valuable advices, guidance and support of all the personal involved.

References

1. A.R. Abdel Hamid, W.Z.W. Yusuf, B. Singh, Hazards at construction sites, in *Proceedings of the 5th Asia-Pacific Structural Engineering and Construction Conference (APSEC 2003)*, Johor Bahru, Malaysia, 26–28 Aug 2003
2. E.W.L. Cheng, H. Li, D.P. Fang, F. Xie, Construction Safety management: an exploratory study from China. *Constr. Innovation* **4**, 229–241 (2004)
3. S.H. Seyyed, J.T. Zahra, Major theories of construction accident models: literature review. *Int. J. Adv. Eng. Technol.* (2012) ISSN: 2231-1963
4. T.P. Mitropoulos, A.G. Howell, S.A. Tariq, Accident prevention strategies. *J. Constr. Eng. Manag.* **135**(5), 407–415 (2012)
5. T.S. Abdel Hamid, J.G. Everett, Identifying root causes of construction accidents. *J. Constr. Eng. Manag.* **126**(1), 52–60 (2000)
6. R. Powell, The measurement of safety performance, Government of Western Australia Department of Commerce (2009)
7. W. Wang, J. Liu, S. Chou, Simulation-based safety evaluation model integrated with network schedule. *J. Autom. Constr.* **15**(3), 341–354 (2006)
8. M.A. Friend, J.P. Khon, *Fundamentals of Occupational Safety and Health*, 5th edn. (The Scarecrow Press, Government Institute, 2010)
9. R.L. Brauer, *Safety and Health for Engineers*, 2nd edn. (Van Nostrand Reinhold, New York, 1994)
10. Bird, F.E., Loftus, R.G. (Eds) *Loss Control Management*. Institute Press (Division of International Loss Control Institute), Loganville, Georgia (1976)
11. M. Rausand, *Accident Models in Risk Assessment* (Wiley, Hoboken, New Jersey, 2011)
12. P. Katsakiori, G. Sakellariopoulos, E. Manatakis, Towards an evaluation of accident investigation methods in terms of their alignment with accident causation models. *Saf. Sci.* **47**(7), 1007–1015 (2009)

13. J.T. Reason, *The Human Contribution: Unsafe Acts, Accidents and Heroic Recoveries*, (Ashgate Publishing Ltd., UK, 2008)
14. B.G. Kanki, R.L. Helmreich, J.M. Anca, *Crew Resource Management* (Elsevier, Amsterdam, 2010)
15. P.G.P Sabet et.al., Application of domino theory to justify and prevent accident occurrence in constructionsite. *IOSR J. Mech. Civil Eng.* 6(2), 72–76 (2013)
16. Bird, F.E. (Ed) *Management Guide to Loss Control*. Institute Press (Division of International Loss Control Institute), Atlanta (1974)

Ventilation Performance Assessment of an Educational Building in a Hot and Humid Climate

Maisarah Ali, Majeed Oladokun, Samsul Baharin Osman,
Niza Samsuddin, Hairul Aini Hamzah and Md Noor Salleh

Abstract Air Handling Units in mechanical ventilation system possess a high degree of potential to circulate contaminants within occupied spaces of a building which often results in sick building syndrome (SBS), building related illness (BRI) and other indoor air quality (IAQ) related issues. This happens despite the expected role of ventilation systems to create a balance of thermal comfort and indoor air quality to the building occupants as well as the stored components. In the hot and humid climate mechanical ventilation systems play an important role of controlling the indoor hygrothermal conditions. Inadequate performance of the mechanical ventilation systems result in several issues ranging from human occupants discomfort, mechanical damages to archival materials and mould problem amongst others. This study presents the measurement and analysis of the mechanical ventilation systems' performance and its effect on various indoor spaces in an academic building in Malaysia. Measurement of airflow, thermal and hygric conditions of the facility together with the aero-biological sampling were executed. The ventilation performance assessment revealed that the AHU fails in its cooling and dehumidification

M. Ali (✉) · S.B. Osman

Department of Manufacturing and Material Engineering, International Islamic University, Malaysia (IIUM), P. O. Box 10, 50728 Kuala Lumpur, Malaysia
e-mail: maisarah@iium.edu.my

M. Oladokun

Department of Architecture, Building Services Engineering, IIUM, Kuala Lumpur, Malaysia
e-mail: majeed.olaide@live.iium.edu.my

N. Samsuddin

Department of Community Medicine, IIUM, Kuantan, Malaysia
e-mail: niza_shamsuddin@iium.edu.my

H.A. Hamzah

Department of Basic Medical Sciences, IIUM, Kuantan, Malaysia
e-mail: hairulaini@iium.edu.my

M.N. Salleh

Department of Biotechnology Engineering, IIUM, Kuala Lumpur, Malaysia
e-mail: mdnoor@iium.edu.my

capacities as most of the occupied zones witnessed elevated humidity and low temperature and hence poor hygrothermal performance. On the other hand, results of bio-aerosol assessment indicates that the AHU performs well in its decontamination capacities by reducing the microbial level between the AHU and the occupied zones. The dominant species of mould in the assessed spaces are *Penicillium* sp., *Yeast*, *Cladosporium* sp., and *Chaetomium* sp. with 100 % occurrence in all the assessed space. On the other hand, Black Mold, *Syntalidium* sp., and zygomycetes are the least species in spaces with 25 % occurrence. The presence of black mould portends a great danger to the occupants' health and therefore requires urgent attention.

Keywords Ventilation performance · Bio-aerosol assessment · Indoor air quality · Building related illness · Hygrothermal performance · Cooling and dehumidification

1 Introduction

The ventilation systems create a balance of thermal comfort and indoor air quality to the occupants as well as the stored components of an indoor environment [3]. Nevertheless, the system contributes on the contrary [4] most especially the Air Handling Units (AHU) which in its distribution of the conditioned air to the downstream possess a high degree of potential to circulate contaminants (bio-aerosol, particulate matters, dust etc.) within and between the indoor space of a building. This often results in sick building syndrome (SBS), building related illness (BRI) and other indoor air quality (IAQ) related issues to the building occupants. On the other hand, inadequate performance of the system can result in elevated hygric profile in the building which in the long run may damage the stored components as well as building fabrics' composition. Such risks appears to be lower in naturally ventilated buildings in comparison to those ventilated through mechanical means. For instance, in an earlier study conducted by Borrego and Perdomo [5], fungal contamination was reported to be reduced in buoyancy driven ventilated building than the forced ventilated counterparts. The reason, according to the study, is not unconnected with the natural ventilation that facilitate movement of particles in the air thereby making spores deposition difficult.

In the hot and humid climate, to which Malaysia belongs, mechanical ventilation systems play an important role in maintaining an indoor hygrothermal condition. This becomes necessary as the climate conditions in this location are characterized by high temperature and humidity. In the report of Tang [6], the maximum/minimum values of both thermal and hygric conditions in Malaysia are given as 35.6 °C/20.6 °C and 100 %/40 % for temperature (T) and relative humidity (RH) respectively. T and RH remain important factors for microbial proliferations as well as human thermal comfort determinant [7]. It therefore becomes more important to design, install and operate mechanical ventilation system in Malaysia to maintain

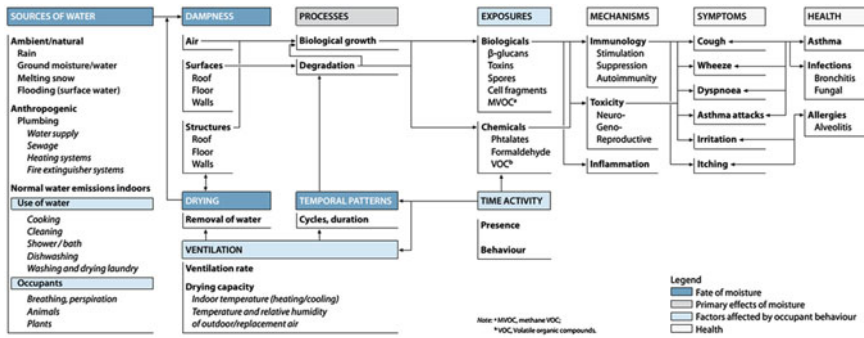


Fig. 1 Pathways linking sources of dampness with health [2]

the hygrothermal conditions as indoor hygrothermal abnormality generates several issues ranging from human occupants discomfort, mechanical damages to archival materials, mould problem, etc. The world health organization guidelines on IAQ [2] revealed (Fig. 1) that ventilation systems is part of the contributing factors to indoor moisture problems together with the associated problems. Cases of microbial infestation of mechanically ventilated buildings have been reported in Malaysia public buildings [8, 9]. The reasons for the problems are not far-fetched from elevated thermal and hygric profiles in the infected buildings. Therefore, adequate consideration is required to be given to mechanical ventilation system in maintaining the hygrothermal gradients in a way to keep a lid on the microbial proliferations.

The need for environmental sustainability in energy consumption has resulted in energy conservation measures within the past few decades. In Malaysia, about 50 % of the energy consumption in the public buildings goes to the heating ventilation and air conditioning (HVAC) systems [6]. Consequentially, in a way to be sustainable in energy usage, there is the need to cut the usage on HVAC system. This notwithstanding, evidence exists in the literature of increase in IAQ problems from energy efficiency improvements [10, 11]. As a result, combining energy efficiency with IAQ requirements in mechanical ventilation system becomes an issue that require careful attention.

1.1 Air Side of Mechanical Ventilation System

In carrying out the dual role of thermal and IAQ control, the air side of mechanical ventilation system decontaminate the air and maintain the air at a suitable comfort level for thermal and hygric conditions. The schematic of a typical air side device (AHU) is as represented in Fig. 2. The hot, humid and contaminated air (location 1) is a mixture of fresh-air (outdoor air) and return air from the conditioned space.

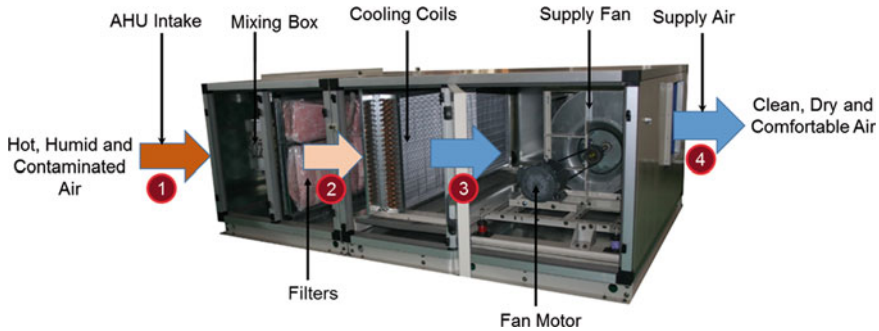


Fig. 2 Scheme of the air handling unit adapted from [1]

The mixing can be done outside or inside the AHU compartment based on ventilation design requirements. After mixing, the air enters the filtration compartment where it passes through a series of filters where the particulate matters and other aerosol contaminations are removed. The air (at location 2) passes over the cooling coils which are maintained at a temperature lower than the dew-point temperature of the incoming air. On moving over the coils, the air is cooled down to a temperature below its dew-point thereby resulting in dehumidification in addition to cooling. The fan with its motor pressurise the air after the cooling coils (location 3) thereby exiting the air at higher speed into the occupied zones of the building. The supply air (location 4) leaving the AHU is expected to be clean, less humid and comfortable under efficient operating performance of the AHU. A good knowledge of the various components of the AHU thus provide better understanding at diagnosing performance related issues on the air side of the mechanical ventilation system.

1.2 Performance Assessment and Verification

Environmental performance of buildings remains an utmost goal for the present day sustainable designs in a way to give the required level of comfort to the users without being detrimental to the environment. In executing building performance assessment, multiple measurement at different time-steps are common to obtain time-series of building performance variables. This become more necessary for mechanically ventilated buildings as the installation of HVAC systems responsible for microclimate control often resulted in antithetical performances to the initial design intent [12]. Performance assessment and verification are carried out in four levels [13]. The options ranges from simple walkthrough inspections and assumptions of various parameters (A) to detailed calibrated computer simulation (D). In option D, detailed measurement is required to provide necessary inputs that represent the operating condition of the facility. Such time-series measurements result in huge amount of

data which according to [14] pose difficulty in interpretation and presentation. As data are useless, until they undergo appreciable refinements for relevant results [15], good data analytics becomes more important in performance assessment. In a recent study, Ali et al. [16] present an improved methodology of data evaluation for IAQ performance appraisal.

1.3 Study Aim and Objectives

This study, using microbial contaminant level and hygrothermal parameters, presents the measurement and analysis of the performance of the ventilation systems and its effect on various indoor spaces in an academic building in Malaysia. The aim is to investigate the performance of the HVAC system in providing the required level of thermal comfort together with air decontamination. The objective of the study is to audit the operative conditions of the air-side of mechanical ventilation systems together with the effects on various parts of the occupied zone. Results of this performance assessment will lead to measures that can be applied to existing building stocks in Malaysia for sustainable operations.

2 Methodology

2.1 Walkthrough Inspection

The work involve walkthrough inspection, measurement of airflow, thermal and hygric conditions of the facility together with the aero-biological sampling of the ambient air. In this inspection, a total of nine (9) spaces were assessed. The spaces include record slides block room, chemical glassware store, temporary store room, equipment store, histopathology lab, immuno histo-chemistry lab, histo-chemistry lab, general cytology and teaching laboratory. In order to relate the effect of external conditions with the indoor operative ambient, the series of measurements were made to include the AHU room and the outdoor space. The measurement involves the time series of hygrothermal parameters in various locations (middle of the occupied zone at 1.5 m above floor level, supply diffusers and return grille) of the selected spaces. In aero-biological sampling, the chemical glassware store, histopathology lab, AHU room and an outdoor space were selected based on the presence of either surface condensation and/or mould growth. Setting up the instrumentation for the performance assessments were carried out under the normal operative conditions of the building.

2.2 Instrumentation and Measurement

The airflow, thermal and hygric variables were measured with ALNOR AVM440 Airflow Instrument while the microbial sampling protocol with SAS SUPER ISO 100. SAS SUPER ISO 100 operates on the principle whereby air-borne microbes are collected on suitable grow media (agar) by impaction [17] produced by aspiration. The Sampling time set-up are 30 s and 1 min for 50 and 100 l of air respectively in accordance with the manufacturer specifications [18]. Table 1 gives detail specifications of the instrumentation. In the microbial sampling, the culture media were of two types: potato dextrose agar (PDA-potato starch 4.0 g; Dextrose 20.0 g; and Agar 15.0 g) and sabouraud dextrose agar (SDA-mycological peptone 10.0 g; glucose 40.0 g; and Agar 15.0 g). The agar were placed in the sampling equipment and during operation, air is impacted over the media at a pre-set volume flow rate of 50 and 100 l suggested in [17] for the kind of investigation. The choice of flow rate is due to level of contamination of the inspected area.

At each of the measuring point, samples were taken in quadruplicate with duplicate each of PDA and SDA for 50 and 100 l of air sample respectively. In addition, at the location with feasible mould growth, additional surface swabs were taken each for PDA and SDA. It is often required that while transporting the impaction device from one measuring point to the other, a field blank needs to be inserted in the measuring device. According to ISO standard [17], the dish should contain the same culture media used for the other sampling points. As a results, two samples were taken as field blank each for PDA and SDA. The duo were taken while the impaction device was being moved between the indoor and outdoor environment. The petri dish holding agar were quickly sealed with paraffin tape immediately after the sampling to prevent secondary contaminations. All the agar plates were sealed in plastic bags to protect the samples during transport for subsequent laboratory analysis. In the laboratory, the agar plates were incubated for 7 days at 25 ± 2 °C. The microbes were counted and identified to their specific

Table 1 Specification of measurement equipment

Equipment	Variable	Accuracy	Resolution	Range	Manufacturer
ALNOR AVM440 Airflow instrument	Relative humidity	± 3 %	0.1 %	5–95 %	TSI Incorp.
	Temperature	± 0.3 °C	0.1 °C	–10 to 60 °C	
	Velocity	± 3 % of reading or ± 0.015 m/s	0.01 m/s	0–30 m/s	
SAS SUPER ISO 100	Bio-aerosols	Nominal air flow rate: 100 l/min;			PBI Intl
		Sampling efficiency: 100 % over 4 microns aerosol size			

genus by macroscopic and microscopic examinations. The colony forming units (CFU) per cubic meters of air (CFU/m³) was estimated accordance with the formula suggested in [19].

3 Results and Discussion

3.1 Outdoor Conditions

The indoor hygrothermal conditions track the amount present in outdoor environment [20]. Therefore, it essential to take note of the outdoor condition in ventilation performance assessment. Mean annual hourly weather (hygrothermal) conditions for Indera Mahkota, Kuantan, Malaysia (obtained from the nearby weather station) where the case study building is located revealed that the hottest and coldest months in the location is May and August with T value 34.1 and 21.8 °C respectively. In terms of humidity, the condition is highly humid year round with peak value of 100 % and least humid condition in July with RH of 55 %. In a bid to ensure a representative conditions of the conditions in the building in relation to weather, the measurement protocol was carried out in May 2014.

3.2 Indoor Conditions

Tables 2 and 3 summarize the AHU room that served the various occupied zones (type I ventilation class) together with measured data from the occupied zones (types I and II ventilation class). The mixing of air in the AHU room is revealed (Table 2) where return air (T = 21.6 °C, RH = 78.4 %) and fresh air intake (T = 27.7 °C, RH = 75.6 %) combined to give the air intake of (T = 23.2 °C, RH = 77.8 %). On getting to the occupied zones (Table 3), the humidity conditions at the supply (column 6) revealed values (>80 %) above the conditions with which the air enters the AHU. These variations suggest a malfunction in the dehumidification efficiency of the AHU.

In addition, for type I ventilation class, the temperature at the supply outlets (column 5) show values ranging between 15.3 and 20.5 °C. These operative conditions is far below that which is specified in Malaysian Standard on energy efficiency [21] as 23–26 °C. A further observation of Table 3 shows the conditions at the supply and return outlets (columns 5, 6, 8 and 9). For the thermal conditions (columns 5 and 8), the difference between supply and return temperature is more than the accuracy of the measuring equipment (± 0.3 °C). The increment in return air temperature over the supply suggest the heat extraction from the occupied zones. As for the hygric conditions (columns 6 and 9), the difference between the supply and return air is less than the measuring equipment accuracy (± 3 %). This points out that the moisture generation in occupied zones are of less significance.

Table 2 Summary of indoor microclimatic conditions of the AHU room

Location	Insp. ID	AHU return			Fresh-air intake			AHU intake			Int. ambient		
		Vel.	T	RH	Vel.	T	RH	Vel.	T	RH	Vel.	T	RH
K	009	4.23	21.6	78.4	3.66	27.7	75.6	1.94	23.2	77.8	0.41	23.1	78.2

Consider the type II ventilation class, which involve ventilation only with supply and extraction fan, the two spaces (locations D and J) show a high level of indoor temperature and humidity (Table 3). This suggests a reason why care should be taken in the use of such system of ventilation in a hot and humid climate environment. The mass balance (balance of air volume between supply and return) into the occupied zones is investigated and presented in Table 4. It is revealed that in nearly all the spaces, the supply flow rate surpasses that of return flow rate. This suggest that the excess of supply over return escapes through other openings. Therefore it can be concluded that the spaces are not air-tight as required by the guidelines on energy efficiency.

From the foregoing, the observed conditions of the AHU performance reveals a poor performance of the ventilation system to maintain the thermal and hygric conditions in the occupied zones. This may lead to moisture problem in form of condensation and its associated mould proliferations as good air distribution is a good way of preventing microbial infestation [22].

3.3 Bio-aerosol Assessment

The results of bio-aerosol investigations is presented in Tables 5 and 6. In general, the findings revealed a great deal of variation between the mould growth on SDA and PDA. This results relates to the submission of [23, 24] that a direct relationship exists between the type of culture media and the species composition of microbes isolated from air. It is further evidenced that the outdoor environment is charged with higher microbial loadings as expected with values of 8.93×10^2 and 8.33×10^2 CFU/m³ for SDA and PDA media respectively. The contaminant level in the AHU room is reduced (3.87×10^2 and 2.87×10^2 CFU/m³) compare to that of the outdoor due to the proportion of outdoor (fresh) air allowed into the AHU room. In the locations B and E (Chemical Glassware Store and Histopathology) the values are below the contaminant level of the AHU with values of 4.67×10^2 and 2.93×10^2 CFU/m³ (location B) and 2.60×10^2 and 9.3×10^1 CFU/m³ (location E). This reduction in the levels between the AHU room and the occupied zone suggests an effective filtration in the AHU.

Further comparison between locations B and E revealed a higher contamination in B over E. This is an indication of a more contaminated zone in B than E. The results of the species identifications (Table 6) revealed additional mould in B other than E. The presence of black mould (*Stachybotrys chartarum*) in B portends

Table 3 Summary of indoor microclimatic conditions of the assessed spaces

(1) Location ^b	(2) Insp. ID	(3) Vent. Class ^a	Supply			Return			Int. Ambient			Ext. Ambient		
			(4) Vel.	(5) T	(6) RH	(7) Vel.	(8) T	(9) RH	(10) Vel.	(11) T	(12) RH	(13) Vel.	(14) T	(15) RH
A	001	Type I	2.54	15.8	83.8	0.48	16.6	83.1	0.11	17.1	79.9	0.15	27.1	82.4
B	002	Type I	1.71	15.5	85.1	0.62	16.4	84.9	0.16	17.9	76.4	0.15	27.1	82.4
C	003	Type I	1.64	15.3	84.8	0.16	16.0	84.4	0.10	17.2	78.4	0.30	26.9	85.7
D	004	Type II	0.39	22.1	99.1	3.58	19.7	79.4	0.08	19.3	74.9	0.12	26.7	82.9
E	005	Type I	1.02	19.8	81.4	0.64	21.1	77.1	0.22	21.7	74.5	0.15	27.1	82.4
F	006	Type I	1.07	19.9	80.2	0.54	20.2	79.5	0.09	22.1	72.7	0.15	27.1	82.4
G	007	Type I	1.22	19.3	82.6	0.59	21.1	77.3	0.17	21.5	73.3	0.15	27.1	82.4
H	008	Type I	1.20	20.5	78.7	0.60	20.7	78.1	0.15	21.9	73.0	0.15	27.1	82.4
J	010	Type II	1.55	30.0	67.8	1.46	27.5	76.4	0.20	28.8	71.6	0.30	25.3	89.8

^a Ventilation Class; *Type I* Constant air volume air-conditioning and ventilation systems; *Type II* Ventilation only system

^b Location IDs: *A* Record slides block room; *B* Chemical glassware store; *C* Temporary store room; *D* Equipment store; *E* Histopathology lab
F Immuno histo-chemistry lab; *G* Histo-chemistry lab; *H* General cytology; *J* Laboratory; *K* AHU room
L Outdoor space

Table 4 Rate of air inflow and outflow into and out of the measured spaces

Location	Vent. class	Supply flowrate	Return flowrate
A	Type I	0.91	0.09
B	Type I	0.61	0.11
C	Type I	0.59	0.03
D	Type II	0.07	0.64
E	Type I	0.37	0.23
F	Type I	0.38	0.10
G	Type I	0.44	0.11
H	Type I	0.43	0.11
J	Type II	0.56	0.53

Table 5 Microbial prevalence in the air at the measured locations

Locations	Fungi (CFU/m ³)	
	SDA	PDA
B	4.67×10^2	2.93×10^2
E	2.60×10^2	9.3×10^1
K	3.87×10^2	2.87×10^2
L	8.93×10^2	8.33×10^2

Table 6 Type of fungi/moulds isolated from the different locations

Type of fungi/mould	Sampling locations				Occurrence (%)
	B	E	K	L	
<i>Penicillium</i> sp.	+	+	+	+	100
<i>Yeast</i>	+	+	+	+	100
<i>Rhodotorula</i> sp. (yellow yeast)	+	+	-	+	75
<i>Cladosporium</i> sp.	+	+	+	+	100
<i>Fonsecaea</i> sp.	+	-	+	+	75
<i>Chaetomium</i> sp.	+	+	+	+	100
<i>Aspergillus</i> sp.	-	+	-	+	50
<i>Black Mold</i>	+	-	-	-	25
<i>Syntalidium</i> sp.	-	-	+	-	25
<i>zygomycetes</i>	-	-	+	-	25
<i>Other species</i>	+	-	-	-	25

B Chemical glassware store; E Histopathology; K AHU room; L Outdoor space

grave health risk to human occupants in that environment. As shown in Table 6, the dominant species of mould are *Penicillium* sp., *Yeast*, *Cladosporium* sp., and *Chaetomium* sp. with 100 % occurrence in all the assessed space. On the other hand, *Black Mold*, *Syntalidium* sp., and *zygomycetes* are the least species in spaces with 25 % occurrence.

4 Conclusions

The ventilation performance assessment revealed that the AHU fails in its cooling and dehumidification capacities as most of the occupied zones witnessed elevated humidity and low temperature and hence poor hygrothermal performance. On the other hand, results of bio-aerosol assessment shows that the AHU performs well in its filtration efficiencies by reducing the microbial contaminant level between the AHU and the occupied zones. The dominant species of mould in the assessed spaces are *Penicillium* sp., *Yeast*, *Cladosporium* sp., and *Chaetomium* sp. with 100 % occurrence in all the assessed space. On the other hand, *Black Mold*, *Syntalidium* sp., and *zygomycetes* are the least species in spaces with 25 % occurrence. The presence of black mould portends a great danger to the occupants' health and therefore requires urgent attention. The study also pointed why mould growth intensities differ in indoor environment by the different substrates they found themselves. The knowledge accrued from this findings can serve as a good start to determine which of the building material compositions support more growth than the other in Malaysia as this can assist in material selections for various design considerations. It is therefore recommended that the AHU system tuning be implemented to correct the deficiencies in its ability to maintain the required thermal and hygric profiles in the occupied zones. On the locations with higher viable mould colony and presence of black mould, an urgent remediation is needed to abate possible health related issues associated with mycotoxin and microbial volatile organic compound from the toxigenic mould.

Acknowledgments The results presented in this study is part of a multidisciplinary research project (FRGS12-067-0126) engineered towards indoor mould growth prediction using thermal characteristics in the tropical climate buildings by the Ministry of Higher Education (MOHE) Malaysia. The financial supports is gratefully acknowledged.

References

1. Dunham-Bush, in *Modular Central Station Air-Handling Units: CS3 Series*. Available http://www.dbamericas.com/pdf/installation_manuals/CS3.pdf
2. World Health Organization, WHO guidelines for indoor air quality: dampness and mould, WHO Regional Office for Europe, Copenhagen, Denmark 978 92 890 4168 3, (2009)
3. J. Hensen, R. Lamberts, *Building performance simulation for design and operation*. (Taylor & Francis, London, 2011)
4. S.C. Wilson, R.N. Palmatier, L.A. Andriychuk, J.M. Martin, C.A. Jumper, H.W. Holder et al., Mold contamination and air handling units. *J. Occup. Environ. Hyg.* **4**, 483–491 (2007)
5. S. Borrego, I. Perdomo, Aerobiological investigations inside repositories of the National Archive of the Republic of Cuba. *Aerobiologia* **28**, 303–316 (2011)
6. C.K. Tang, N. Chin, *Building energy efficiency technical guideline for passive design* (Building Sector Energy Efficiency Project (BSEEP), Malaysia, 2013)
7. J.A. Clarke, *Energy Simulation in Building Design* (Butterworth-Heinem, Oxford, 2001)

8. A.F. Cruetz, Keeping a lid on superbugs, in *New Straits Times* (2013). Available <http://blis2.bernama.com.ezproxy.psz.utm.my/getArticle.do?id=147876&tid=79&cid=3>
9. A.F. Cruetz, 'Sick' hospital ready to serve. *New Straight Times* (2013). Available <http://blis2.bernama.com.ezproxy.psz.utm.my/getArticle.do?id=21492&tid=49&cid=3>
10. H. Hens, IEA annex 14: condensation and energy. *J. Build. Phys.* **15**, 261–273 (1992)
11. E. Di Giuseppe, in *Nearly Zero Energy Buildings and Proliferation of Microorganisms: A Current Issue for Highly Insulated and Airtight Building Envelopes* (2013). Available <http://link.springer.com/book/10.1007/978-3-319-02356-4>
12. P. Baggio, C. Bonacina, P. Romagnoni, A.G. Stevan, Microclimate analysis of the Scrovegni Chapel in Padua—Measurements and simulations. *Stud. Conserv.* **49**, 161–176 (2004)
13. EVO, International performance measurement and verification protocol, in *Energy Project Financing: Resources and Strategies for Success*, ed. by EVO, vol. 1 (2009), p. 277
14. P. Horan, M.B. Luther, Using psychrometric chart in building measurements, in *44th Annual Conference of the Architectural Science Association, ANZAScA2010*, Auckland, New Zealand, 2010, pp. 1–8
15. S.P. Corgnati, V. Fabi, M. Filippi, A methodology for microclimatic quality evaluation in museums: application to a temporary exhibit. *Build. Environ.* **44**, 1253–1260 (2009)
16. M. Ali, M.O. Oladokun, S. Osman, An improved method to evaluate indoor microclimatic data: case study of a book archive in a hot and humid climate, in *13th International Conference on Indoor Air Quality and Climate, Indoor Air 2014*, Hong Kong, (2014)
17. British Standard Institution, BS ISO 16000-18:2011 Indoor air—Part 18: Detection and enumeration of moulds—Sampling by impaction, ed. by BSI (2011)
18. PBI International, in *SAS Spec Book*. Available www.massetrecovery.com/pictures12/sasmanual.pdf
19. British Standards Institution, BS ISO 16000-17:2008 Indoor air—Part 17: Detection and enumeration of moulds—Culture-based method, ed. by BSI (2008)
20. M. Steeman, M. De Paepe, A. Janssens, Impact of whole-building hygrothermal modelling on the assessment of indoor climate in a library building. *Build. Environ.* **45**, 1641–1652 (2010)
21. MS 1525, Code of practice on energy efficiency and use of renewable energy for non-residential buildings, ed. by Putrajaya (Department of Standards Malaysia, Malaysia, 2007)
22. S. Borrego, P. Lavin, I. Perdomo, S. Gomez de Saravia, P. Guiamet, Determination of indoor air quality in archives and biodeterioration of the documentary heritage, *ISRN Microbiol.*, vol. 2012, p. 680598 (2012)
23. R. Ogórek, A. Lejman, K. Matkowski, Influence of the external environment on airborne fungi isolated from a cave. *Pol. J. Environ. Stud.* **23**, 435–440 (2014)
24. M. Ali, M.O. Oladokun, S. Osman, S. Niza, H. Hairul Aini, Influence of indoor microclimate distribution on mould infestation in a university library, in *InCIEC 2014: International Civil Engineering and Infrastructure Engineering Conference*, Kota Kinabalu, Sabah, Malaysia (in press)

Part III
Fluvial and River Engineering Dynamic

Nutrient Uptake and Growth of Bovine Rectal Bacteria in Application of Textile Wastewater Bioremediation

N.M. Sunar, A.S.M. Kassim and N.M. Noor

Abstract Textile industry produces wastewater that has been adversely affected in quality. The anthropogenic influence of this industry has inevitably caused negative impact to the environment. It consumes considerably high amount of processed water that eventually yield highly polluted wastewater. The bovine rectal bacterium (BRB) is used in this study as an alternative for green technology method for treating the textile wastewater without causing any serious unacceptable damage to the natural environment and human health. This paper presents the BRB that consumed selected nutrients in the textile wastewater. The chosen nutrients used to study the optimum growth of BRB are magnesium sulphate ($MgSO_4$), ferric chloride ($FeCl_3$), calcium chloride ($CaCl_2$) and phosphate buffer. The BRB growth rate in textile wastewater in different types of nutrients and incubation time were evaluated in both; aerobic and anaerobic conditions. Consequently, this study provides the knowledge of suitable nutrient for the growth of BRB. These BRB can be further employed at large scale of effluent textile wastewater treatment systems for effective green remediation.

Keywords Bovine rectal bacteria · Nutrients · Textile wastewater

1 Introduction

Textile wastewater treatment remains a complicated problem due to high total of dissolved solids, presence of toxic heavy metals, non biodegradable nature of organic and presence of free chlorine and silica. Thus, any adopted treatment systems should be able to address these issues to ensure the textile wastewater must be treated before it was discharged to the open water to reduce the potential

N.M. Sunar (✉) · A.S.M. Kassim · N.M. Noor
Department of Chemical Engineering Technology, Faculty of Engineering Technology,
University Tun Hussien Onn Malaysia, 86400 Parit Raja, Batu Pahat, Johor, Malaysia
e-mail: shuhaila@uthm.edu.my

environmental hazards. The textile industry can be classified into three categories, cotton, woolen, and synthetic fibers depending on the raw materials used [1]. The important events in textile chemical processes that involved interactions of surfaces include wetting, dispersing, emulsification, chemical or dye adsorption on fibers, adhesion, vaporization, sublimation, melting, heat transfer, catalysis, foaming and defoaming [2]. It contains various waste chemical pollutants such as sizing agents, wetting agents, complex agents, dyes, pigments, softening agents, stiffening agents, fluorocarbon, surfactants, oils, wax and many other additives which are used throughout the processes [3]. The major sources of waste from textile operations can be contributed by the following activities, raw wool scouring, yarn and fabric manufacture, wool finishing, woven fabric finishing, and knitted fabric finishing.

Textile industries consume large volumes of water and chemicals for the wetting process of textiles. The chemical reagents used are very diverse in chemical compositions, ranging from inorganic compounds to polymers and organic products. In general, the wastewater from textile industries is characterized by high value of BOD, COD, pH, and color [4, 5].

The conventional wastewater treatments are used efficiently but the effluent still contains nutrients, heavy metals and organic matter [6]. The process for treating wastewater requires a tremendous cost by the use of mechanical systems. Pollutants in wastewater from textile factories vary greatly and the final effluents depend on the chemicals and treatment processes used. Pollutants that are likely to be present include suspended solids, biodegradable organic matter, toxic organic compounds and heavy metals [7]. Most of the treatment methods involved toxic chemicals. By using chemicals in wastewater treatment, it might cause a serious pollution and environmental impact on organisms. Soluble organics that come from the manufacturer in textile industries will cause the depletion of dissolved oxygen. The untreated textile wastewater with high level of BOD and COD values are highly toxic to biological life [5]. The deposition of solids into a quiescent stretch of a stream will impair its normal aquatic life. The sludge that come from the surface of the active agents in the processing of the textiles from the industries will undergo progressive decomposition resulting oxygen depletions and can produce noxious gases [8]. If wastewater contains the amount of contaminants that are higher than the approved water standard, the costs of treatment will be increased in order to achieve the standard. It will also involve higher costs due to the complex systems which need higher power usage during aeration stage and also the maintenance cost of the treatment plant. These processes require the input of a wide range of chemicals and dyestuffs, which generally are organic compounds of complex structures. This practice has in adversely imparts negative impacts towards the environment due to the chemical byproducts and high amount of carbon dioxide emissions [9].

Nowadays, biological wastewater treatment plants are used to remove the dissolved and the particles of organic matter in wastewater. Some of the suspended organics will occur in a natural process of flocculation and settling. The decomposition of organic matter will naturally decay as a result of microorganism presence in water body. Biological treatment was constructed to accelerate the natural

decaying process and neutralized the waste before it is finally discharged into the receiving water. It is an alternative technology that was designed to reduce the chemicals used to protect the environment and decrease substantially in the cost of aeration. It is also flexible technology operating in a wide range of flow and characteristics with energy saving consumption. The wastewater treatment method such as using bacteria is more widely used to degrade more contaminants [10].

Bovine rectal bacterium (BRB) is an alternative source in biological process that able to treat the wastewater by removing its contaminants. According to Othman et al. [11], the BRB used on restaurant kitchen-sink wastewater was found to be adequately coupled with the aerobic heterotrophic bacteria, sulphate reducers and sulphide oxidizers for acetate COD removal as well as the wastewater carbon. The oxidation process of reaction by BRB as microbes donated electrons and reduction reactions accept electrons. The BRB served as biocatalyst to drive the reaction by consuming the electron donors, acceptor and carbon sources. Bacterial colonization and persistence at the bovine mucosa is a dynamic process that is likely depending on the ability of bacteria to attach to the epithelial cells or use potentially limited nutrient. The number of cultured bacteria reported increases between day 1 and 4 post application and then the bacterial growth decreased slowly [12]. The content of bovine sewer is based on the food that was provided to the bovine. Basically, the characteristics of local bovine sewer can be simplified as in Table 1.

Previously, many researchers have been focused on the persistency of *E. coli* harboring the bovine terminal rectal mucosa [12]. The use of BRB was recently reported by Othman et al. [11] for restaurant kitchen-sink wastewater treatment. However, to our knowledge no work has been reported that has employed BRB for textile wastewater treatment. The growth of microorganisms is affected by nutritional factors. Nutrients that are needed by microorganisms include carbon, nitrogen, sulfur, phosphorus and vitamin. The nutrient in bacteria is important to enhance the bacterial growth where it can be functional as food to the microorganisms [13]. Therefore, this paper presents the BRB that consumed selected nutrients to treat the textile wastewater. The BRB growth rate in textile wastewater in different types of nutrients and incubation time were discussed.

In the concept of sustainable development based on environmental problems of excessive chemicals usage and operational cost, it is critical to recommend alternative ways to treat the potential pollutions. Therefore, this paper suggests the potential of using BRB in bioremediation of textile wastewater.

Table 1 Characteristics of bovine sewer [11]

Parameter	Percentage (%)
Total solids	3–6
Total volatile solids	80–90
Total Kjeldahl nitrogen	2–4
Cellulose	15–20
Lignin	5–10
Hemicelluloses	20–25

2 Materials and Methods

2.1 Textile Wastewater

The wastewater samples were collected from local textile factory located at Sri Gading Industrial Area, Batu Pahat, Johore Malaysia. The samples were prepared for incubation with BRB solution on the same day. The samples were stored at 4 °C prior to the preservation procedure.

2.2 Sample Preparation

The BRB is obtained from a healthy cow's rectum at a local feedlot situated at Institute of Kluang Veterinary Johore, South Malaysia. The cow's tail was jacked up to decrease sudden side to side movements or flicking, both of which may caused injury. The disposable plastic sleeves that covered the hands and arms were well coated with a non-irritating, water soluble lubricant. These disposable plastic sleeves were worn inside out as to keep the sleeve seams from getting contact with the rectal. The fecal was carried out by cupping the hand and gently raking feces caudally towards the anus, by allowing them to pass out of the anus beside the arm without removing hand [14]. The BRB samples were added to de-ionized water at 1:5 ratios to form bacterial slurry. This bacterial slurry was kept between 2 and 4 °C after settlement at about 24 h to obtain the supernatant. The supernatant was filtered and solid captured were analyzed for total suspended solid (TSS) and volatile suspended solids (VSS). The supernatant obtained from bacterial slurry was transfer into stock bottle as biological seed solution. The six shakes for aerobic and anaerobic treatment were each filled with different types of nutrients. Each shake contained nutrient, textile wastewater, BRB seed solution and de-ionized water (DW). These samples were shaken for 24 h at room temperature to form mixed liquor [11]. The total mixed liquor was maintained at volume of 180 mL after the addition of nutrient and textile liquor.

2.3 Nutrients Preparation

The nutrients used are ferric chloride (FeCl_3), calcium chloride (CaCl_2), magnesium sulfate (MgSO_4) and phosphate buffer. All nutrients solutions were prepared according to the Standard Methods for Examination of Water and Wastewater [15]. The flask from the reactor was prepared by mixing 20 mL of BRB, 30 mL textile wastewater and 130 mL dilution water. The mass of this substance contains about 3,575 mg in 130 mL CaCl_2 with the concentration 19.86 g/L of substance in 180 mL of total volume sample in the reactor. The concentration of ion phosphate in the stock solution of phosphate buffer was presented in Table 2.

Table 2 Concentration of ion phosphate in phosphate buffer stock solution

Substance	Amount (g)	Concentration of stock solution(mg/L)	Conc. of phosphate (mg/L)
KH_2PO_4	8.5	8,500	1,398
K_2HPO_4	21.75	21,750	2,793
$\text{Na}_2\text{HPO}_4 \cdot 7\text{H}_2\text{O}$	33.4	33,400	2,787
NH_4Cl	1.7	1,700	711

The pH was maintained at pH 7.2. The MgSO_4 solution was prepared by dissolving 22.5 g $\text{MgSO}_4 \cdot 7\text{H}_2\text{O}$ in distilled water to 1 L. The CaCl_2 solution was prepared by dissolving 27.5 g of CaCl_2 diluted to 1 L in distilled water. Meanwhile, the FeCl_3 solution was prepared by dissolving 0.25 g $\text{FeCl}_3 \cdot 6\text{H}_2\text{O}$ in distilled water to 1 L. These different nutrients were then tested for fixed interval time at 0, 3, 5 and 7 days of incubation period.

2.4 Biofilm Formation

The anaerobic experimentation was prepared differently from the aerobic, which was using the biofilm bacterial developed from the BRB samples. The biofilm technique was selected for bacterial enrichment as it was reported having the ability to increase the biomass concentration, facilitate the separation between liquid and solid and improved the overall productivity [16]. Initially, the sample of 150 g BRB was diluted into 1 L of de-ionized water with added 2 g of sulfate. The slurry was poured into sterilized conical flasks. Then, a 50 cm of net was immersed into the sample. The growth of biofilm was observed for about one week to ensure the microbial had attached into the net. The attached microbial slime on the net was considered as biofilm of BRB that contains active microbial activity.

2.5 BRB Growth

The study of BRB growth is typically represented by the amount of organic suspended material in the mixed liquor of a reactor or known as mixed liquor volatile suspended solids (MLVSS). The loading on reactor is typically defined as the mass of substrate applied on unit mass MLVSS over a defined period of time. By considering treatment processes the loading is commonly referred to as the food to microbial mass ratio. The MLVSS is therefore an important parameter to be monitored for the bioprocess wastewater treatment to ensure an adequate population of bacterial growth [17]. In this study the method of volatile suspended solids concentration are used to estimate the size or mass of bacterial population. The bacteria were organic in composition thus they volatilized in a muffle furnace at

550 °C. The mixed liquor volatile suspended solids (MLVSS) concentration is used in activated sludge process to estimate the bacterial population [18]. The growth of microorganisms contributed to the increase in the number of microbial population that also measured as an increase in microbial mass. The volatile suspended solid (VSS) and nonvolatile suspended solid (NVSS) procedures were followed accordingly to the Standard Method Examination for Water and Wastewater [15].

3 Results and Discussion

3.1 Textile Wastewater

The characteristic of textile wastewater was examined and summarized in Table 3. The results indicated that the textile wastewater does not comply with the standard limit of Environmental Quality (Industrial Effluent) Regulation 2009 [19] for textile industries. Encouraged by the characteristic results obtained from the textile wastewater, this study was then progressed in aerobic and anaerobic conditions. The BRB growth was subjected to the different nutrients for both conditions.

3.2 Nutrient Consumed in Aerobic Condition

Figure 1 represents the cumulative bacterial concentration for nutrients that was incubated for 7 days. The results of all nutrients for aerobic condition showed declined trends of BRB concentration during all incubation days. The graph for FeCl_3 shown the BRB concentration was high during the initial of this experiment which was 1,867 mg/L. The bacterial concentration was decreased to 1,100 mg/L after 2 days and continued decreasing until 233 mg/L at the reaction of 7 days detention time. The results of bacterial concentration by using FeCl_3 were in line with previous research, stated that adding FeCl_3 was able to enhance the redox potential and to lower pH [20]. The BRB concentration by using CaCl_2 was also

Table 3 The characteristics of textile wastewater sample

Parameter	Value
Chemical oxygen demand (COD)	581 mg/L
Oxidation reduction potential	169.5 mV
Total organic carbon (TOC)	245 mg/L
Alkalinity	150 mg/L as CaCO_3
pH	10.34
Total nitrogen	25.3 mg/L
Nitrite nitrogen, $\text{NO}_2\text{-N}$	0.141 L

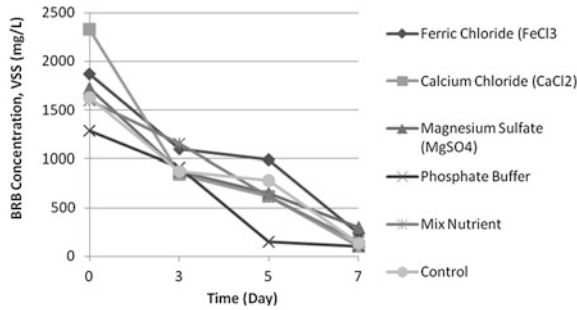


Fig. 1 BRB concentrations using different nutrients (mg/L) over a period of time (day) for aerobic treatment of textile wastewater

decreased starting at day '0' onwards. Before day 4 the value of bacterial concentration was at 840 mg/L. Then, the bacterial concentration was further decreased to 100 mg/L at day 7. From this analysis the results obtained were parallel with Li et al. [21] that had investigated the possibility of CaCl_2 level in the medium might influence plasmid stability. They had observed in earlier experiments that higher percentages of bacterial colonies were found after growth at an elevated calcium levels. A dramatic improvement was observed by screening the colonies and found in plasmid retention time with calcium concentrations started to lose plasmid at day 4. This finding recommends future study as the interruption on plasmid by level of CaCl_2 possibly decreasing the growth of BRB in samples.

The BRB concentration in MgSO_4 was observed at 1,723 mg/L at the initial day of the experiment. The value of BRB population was decreasing slowly to 300 mg/L at day 7. Previously, Tabei et al. [22] reported in their study that the relationship was investigated between MgSO_4 and luminescence in *Vibrio fischeri* under nutrient-starved conditions. At under MgSO_4 starved condition; luminescence was not fully induced at 14 h, and decreased at 24 h. In this study, the result of adding MgSO_4 as nutrient was in line with Tabei et al. [22] for the mechanisms is decreasing but slightly contrast according to the specified length of time. The value of BRB concentration in phosphate buffer was also decreasing from 915 mg/L at day 3 to 100 mg/L at day 7 of the experiment. This result was in agreement with the previous study by previous research. Qazi et al. [23] reported that the performance of first growth microbial activity cycled indicated almost 88.8 % reduction of VSS until 12 days of hydraulic detention time. The samples were inoculated with 5 % culture broth that was prepared in low phosphate buffer medium containing mixed population of methanogens isolated from cow dung.

This concluded that the BRB used exhibited high tolerance in bacterial concentration especially for aerobic conditions. Several mechanisms such as bacterial antagonism and predatorism phenomenon would possibly occur when using the same source of nutrients as food.

After having determined the BRB concentration for every type of nutrients and the control sample, the analysis was further integrated to identify the optimum

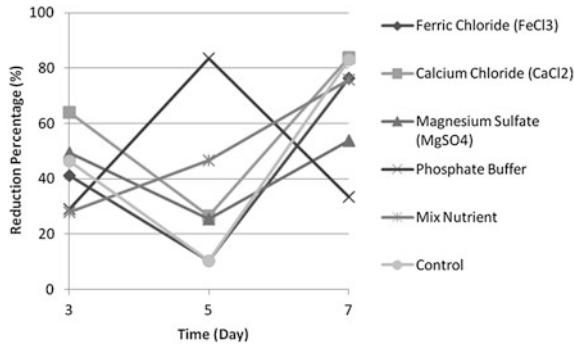


Fig. 2 The reduction percentage of BRB concentration by using different nutrient (mg/L) against time (day) in aerobic condition of textile wastewater

nutrient for BRB concentration. Based on the analysis from this study it was found that all the graphs showed similar trends where all of the samples of the bacterial concentration were decreasing with the increased of incubation time until 7 days of the experiment. It was due to the insufficient of the food supply during the experiment. The bacterial community in this scenario is forced to metabolize their own protoplasm without any replacement because the concentration of the available food is at a minimum condition. During this phase the scenario was known as lysis can occur in which the nutrient remaining in the dead cells diffuse out to furnish the remaining cells with food.

Followed by observing the reaction of nutrients for 3 days, the increasing of BRB concentration belongs to the mixed nutrients with 28 % while the highest decreasing BRB concentration is CaCl₂ with 64 % (Fig. 2). After 5 days, the nutrient of phosphate buffer had the highest value of BRB concentration loss which is about 84 %. However, the BRB concentration in phosphate buffer was tremendously reduced to 33 % on day 7. This gives the lowest loss percentage among other nutrients. From this analysis it can be concluded that using phosphate buffer as nutrient is the optimum condition of BRB population growth by looking at the reactions for 3 to 7 days. The phosphate buffer gave the lowest nutrient percentage value due to the maintaining of BRB concentration that sustained it from decreasing and give sufficient, long lasting of food supply. Thus, for the longest aerobic reaction the use of phosphate buffer was suitable to maintain the BRB survival.

3.3 Nutrient Consumed by Biofilm of BRB in Anaerobic Condition

The biofilm from BRB was prepared for anaerobic conditions of textile wastewater. The performance of the BRB biofilm bacterial concentration was represented in Fig. 3. The samples were tested without any addition of nutrient which was acting

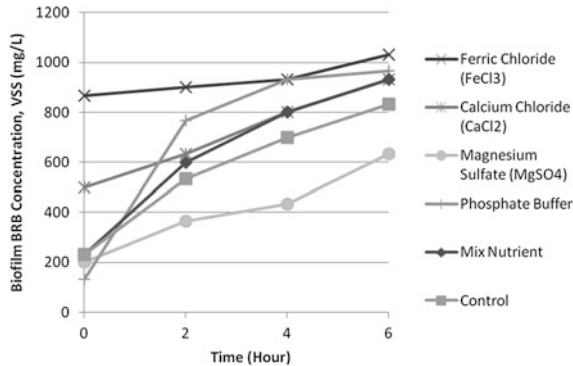


Fig. 3 The BRB biofilm concentration by using different nutrient (mg/L) against time (day) for anaerobic condition of textile wastewater

as a control sample. The control sample was designed to observe the BRB biofilm bacterial concentration. The BRB biofilm concentrations in the control sample had shown the increased in value up to 833 mg/L at the final hours of the experiment.

The graph shown the BRB biofilm concentration in FeCl_3 was relatively high during 0 h which is 867 mg/L. The BRB biofilm concentration was increased to 900 mg/L at day 2. Then, the BRB biofilm concentration continued to increase at an average about 933 mg/L. Finally, it was increased to 1,033 mg/L at the reaction of 6 h detention time. According to Apenzeller et al. [20], the same trends that is the number of total *E. coli* would increase with time in the presence of FeCl_3 which was used as nutrient and electron acceptor under aerobic condition. Thus, the results approved that potentially the same mechanisms occurred in this study; however the textile wastewater was used in this study.

Meanwhile for CaCl_2 nutrient, the BRB biofilm concentration was also increased by the increasing of incubation time. According to Martinez [24], increased of salinity in the media consequences the increased of bacterial growth. There was marked decline of culture growth after 24 h, observed for both *S. maltophilia* and *P. aeruginosa*. Therefore, this study was in line with other researchers, however this result was provided for BRB biofilm concentrations. The BRB biofilm concentrations in MgSO_4 had shown the optimum bacterial concentration which is 633 mg/L at the 6 h of the experiment. Stated by Russel and Thomas [25] the results showed that MgSO_4 is able to reverse the antibiotic activity such as vancomycin on bacterial such as *E. coli*. The influence of magnesium salts was most marked at the highest concentrations but had a slight initial effect on the antimicrobial activity of 1 mg/mL of *Vancomycin* on further incubation. However, growth occurred and increased until 6 h interval times with 0.25 % concentration of Mg salt. The finding in this study possibly was affected by the antimicrobial and antibiotic activity effect influences by Mg that was provided as a nutrient. Typically, in the condition when considering the contents of ion sulfate, it can reduce biologically to sulfide under anaerobic conditions which can then combine with hydrogen to form hydrogen

sulfide (H_2S). The bacterial concentration decreased with the increasing value of ion sulfate [26].

Based on the graphs of BRB biofilm concentration (Fig. 3), by using phosphate buffer, the value of biofilm bacterial concentration was increased starting at hour 0 onwards. According to Kushner and Lisson [27] and Eason et al. [28] in their studies had identified the bacteria growing on the alkaline agar exhibited marked morphological changes by using nutrient broth with phosphate buffer. Thus, from this condition it was convinced that the result obtained from this analysis provide the same mechanisms and trend of BRB growth. Figure 3 shows that the phenomenon of bacterial concentration by mixing all types of nutrient as a nutrient in BRB biofilm in aerobic textile wastewater shows the same trend with other nutrients. The BRB biofilm showed the growth phase results thus concluded that excessive amount of food was available surrounding the microorganisms. The rate of metabolisms and growth is assumed functioning depending on the ability of the microorganism to process the substrate.

The analysis was then integrated to identify the optimum nutrient for anaerobic condition for every type of nutrients. The overall patterns of the BRB biofilm concentration versus time is shown in Fig. 4. According to BRB biofilm growth phase results it can be concluded that an excessive amount of food was available surrounding the microorganisms. Therefore, rate of metabolisms and growth is possibly functioning depending on the ability of the BRB to process the substrate.

Figure 4 shows the percentage of BRB biofilm concentration and the effects of nutrients were observed by the detention time in hour. In interval time for 0 to 3 h in $FeCl_3$ was observed to be able to increase the BRB biofilm concentration. After 6 h of incubation time in anaerobic treatment, the $FeCl_3$ had shown the lowest percentage of bacterial growth. However, among all nutrients the $FeCl_3$ was at the highest number of concentration that is at 1,033 mg/L after 6 h of incubation period (Fig. 3). The analyses concluded that $FeCl_3$ was selected as the nutrient that gives

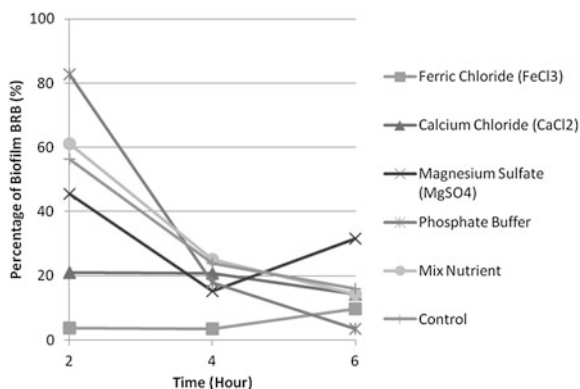


Fig. 4 The percentage of BRB biofilm concentration by using different nutrient (mg/L) against time (day) for anaerobic condition of textile wastewater

optimum growth of BRB biofilm. This is because FeCl_3 was sufficient to maintain and increase the BRB biofilm concentration. The anaerobic results by using biofilm bacteria had shown the synthesis phenomenon that normally occurred in the duration of one to two days. However, it was recommended that this anaerobic condition should be utilized in more length of time to prove the reduction or known as endogenous metabolism state of bacteria. The increased interval time will obtain the maximum BRB concentration until its start to degrade. The test to identify the effects of heavy metals in textile wastewater should also be investigated to ensure high concentration of ion heavy metals did not interfere with the BRB growth. In this study, to maintain the anaerobic condition the reactor contents were avoided from having contact with dissolved oxygen and were free from inhibitory concentrations of such heavy metals and sulfides.

4 Conclusion

The BRB exhibited high tolerance of BRB concentration especially in aerobic condition. The phosphate buffer was observed as the optimum nutrient for BRB that able to sustain the food supply in aerobic condition for textile wastewater. Meanwhile FeCl_3 was examined as the optimum nutrient for BRB biofilm growth in anaerobic condition of textile wastewater. The FeCl_3 able to maintained the BRB biofilm concentration that sustains the BRB biofilm growth. It is concluded that the anaerobic results by using BRB biofilm had shown the synthesis phenomenon with these positive growths. In summary, this study provides new potential for textile wastewater biotreatment. Hence, it should be further employed at large scale of effluent textile wastewater treatment systems for in bioremediation that enhances the use of green technology for sustainable treatment.

Acknowledgments The authors gratefully acknowledge Short Term Grant (STG) UTHM for the financial support. Special thanks to research team members of DWEE, Faculty of Civil and Environmental Engineering (FKAAS), Universiti Tun Hussien Onn Malaysia.

References

1. N.M. Rosli, Development of biological treatment system for reduction of COD from textile wastewater, Master's thesis, Universiti Teknologi Malaysia, (2006)
2. S.W. Perkin, Surfactants a primer (1998), <http://infohouse.p2ric.org/ref/03/02960.pdf>. Assessed on 20 Jan 2012
3. J. Paul, Removal COD and colour from textile wastewater using limestone and activated carbon, Master's thesis, Universiti Sains Malaysia, (2008)
4. B.V. Babu, H.T. Rana, V.R. Krishna, M. Sharma, COD reduction of reactive dyeing effluent from cotton textile industry (2000), <http://discovery.bits-pilani.ac.in/~bvbabu/CODphe.pdf>. Assessed on 12 Dec 2012

5. S. Palamthodi, D. Patil, Y. Patil, Microbial degradation of textile industrial effluents. *J. Biotechnol.* **10**(59), 12687–12691 (2011)
6. M. Samsudin, Treatment of slaughter house wastewater using fruit enzyme, Degree thesis, Universiti Teknologi Malaysia, (2010)
7. N. Tufekci, N. Sivri, I. Toroz, Pollutants of textile industry wastewater and assessment of its discharge limits by water quality standards. *J. Fish. Aquat. Sci.* **7**, 97–103 (2007)
8. W.W. Eckenfelder, D.L. Ford, A.J. Engle, *Industrial Water Quality* (McGraw-Hill, New York, 2009)
9. M.K. Burhanuddin, Investigation of factors enhancing the efficiency of wastewater treatment by anammox bacteria, Degree thesis, Universiti Tun Hussein Onn Malaysia, (2011)
10. T.E. Schultz, Biological wastewater treatment (2005), <http://www.environmental-expert.com/articles/biological-wastewater-treatment-6573/view-comments>. Assessed on 2 Sep 2012
11. A.R. Othman, R. Seswoya, R. Hamdan, N.A. Zakaria, Bovine rectal bacteria can solve COD problems with acetate liquor and restaurant kitchen-sink wastewater. International conference on environmental and computer science (IACSIT Press, Singapore, 2011), pp. 124–127
12. H. Sheng, J.Y. Lim, M.J. Knecht, C.J. Hovde, Role of *Escherichia coli* O157:H7 virulence factors in colonization at the bovine terminal rectal mucosa. *J. Infect. Immun.* **74**(8), 4685–4693 (2012)
13. J.G. Black, *Microbiology: Principles and Exploration*, 5th edn. (Wiley, New York, 2002)
14. Penn Veterinary Medicine, Preparing for the rectal palpation (2012), <http://cal.vet.upenn.edu/projects/fieldservice/dairy/perepro.htm>. Assessed on 20 Feb 2012
15. APHA (American Public Health Association), AWWA (American Water Works Association), and WEF (Water Environment Federation), *Standard methods for the examination of water and wastewater*, 20th edn. (Washington DC, 1999)
16. C.T. Huang, Fundamentals and applications of biofilms microbial attachment and biofilm formation (2000), <http://cthuang.bst.ntu.edu.tw/biofilms/biofilms-2-ppt.pdf>. Assessed on 9 Mar 2012
17. J.M. Willey, L.M. Sherwood, C.J. Woolverton, *Prescott's Microbiology*, 8th edn. (McGraw Hill, New York, 2008)
18. M.H. Gerardi, *Wastewater Bacteria* (Wiley-Interscience, Hoboken, 2006)
19. DOE (Department of Environment of Malaysia), Environmental Quality (Industrial Effluent) Regulation 2009, www.apps.doe.gov.my/regulation/view.php/Regulation/Environment. Assessed on 2 Jan 2013
20. B.M.R. Apenzeller, Y. Carolina, F. Jorand, J.C. Block, Advantage provided by iron for *Escherichia coli* growth and cultivability in drinking water. *Appl. Environ. Microbiol.* **71**(9), 5621–5623 (2005)
21. H. Li, S. Bhaduri, W.E. Magee, Maximizing plasmid stability and production of released proteins in *Yersinia enterocolitica*. *Appl. Environ. Microbiol.* **64**(5), 1812–1815 (1998)
22. Y.M.E. Tabei, A. Ogawa, H. Morita, Requirements for sulfur in cell density-independent induction of luminescence in *Vibrio fischeri* under nutrient-starved conditions. *J. Basic Microbiol.* **52**(2), 216–223 (2011)
23. J.I. Qazi, M. Nadeem, S.S. Baaig, S. Baig, Q. Syed, Anaerobic fixed film biotreatment of dairy wastewater. *J. Sci. Res.* **8**(3), 590–593 (2011)
24. R.F. Martinez, Effect of iron and sodium chloride on biofilm development of *Stenotrophomonas maltophilia*. Master's thesis, DePaul University Chicago, (2011)
25. A.D. Russel, I.L. Thomas, Effect of Mg^{++} on the activity of vancomycin against *Escherichia coli*. *J. Microbiol.* **14**(6), 902–904 (1996)
26. E. Metcalf, G. Tchobanoglous, F.L. Burton, *Wastewater Engineering: Treatment Disposal Reuse*, 3rd edn. (McGraw-Hill, New York, 1991)
27. D.J. Kushner, T.A. Lisson, Alkali resistance in a strain of *Bacillus cereus* pathogenic for the larch sawfly *Pristiphora erichsonii*. *J. Microbiol.* **21**, 96–108 (1959)
28. G. Eason, B. Noble, I.N. Sneddon, On certain integrals of Lipschitz-Hankel type involving products of Bessel functions. *Phil. Trans. Roy. Soc. London* **A247**, 529–551 (1955)

Neural Network Hydrological Modeling for Kemaman Catchment

Tuan Asmaa Tuan Resdi and Wei-Koon Lee

Abstract This paper reports on the evaluation of feed forward back-propagation (FFBP) network, radial basis function network (RBFN), and generalized regression neural network (GRNN) for hydrological modeling of Kemaman watershed in Terengganu. Thirteen (13) meteorological parameters are considered in the input, which includes rainfall, temperature, mean relative humidity and evaporation. The outputs are water levels at four river gauging station. The models were developed and the training results compared in terms of the correlation coefficient and normalized root mean square error. It is shown that the RBFN model is superior over the FFBP and GRNN models, and the performance is sensitive to the various input parameters considered.

Keywords Hydrological modeling · River stage · FFBP · GRNN · RBF

1 Introduction

Hydrologic models are simplifications of reality and based on knowledge and understanding of hydrological processes [1]. The mathematical representation of hydrological processes involves the transformation of meteorological inputs such as precipitation, temperature, and solar radiation, to outputs in the forms of river flow, reservoir storage and groundwater table through surface and subsurface movement of water and energy [2]. Popular hydrological models include conceptual models and physical-based models. A conceptual model is a lumped model which uses spatially averaged parameters and thus do not take into considerations the complex features of the hydrological system. On the other hand, physical-based models are

T.A. Tuan Resdi
Faculty of Civil Engineering, UiTM, Shah Alam, Malaysia

W.-K. Lee (✉)
FloodMIND, IIESM, Faculty of Civil Engineering, UiTM, Shah Alam, Malaysia
e-mail: Leewei994@salam.uitm.edu.my

typically more complex and require expensive computing time to solve partial differential equations (PDEs) which approximate the heterogeneous characteristic of a catchment [3].

As an alternative, Artificial Neural Network (ANN) models, which are treated as universal approximators, are very much suited to the dynamic and nonlinear modeling of hydrological system. The main advantage of this approach over traditional methods is that it does not require detailed understanding of the complex nature of the underlying processes to be explicitly described in mathematical form.

ANN models which are properly trained using historical data are reported to function well in diverse applications such as prediction of hydrological parameters of interest [4], flood forecasting [5, 6], rainfall-runoff modeling [7–9], tidal forecasting [10–12], and water quality modeling [13].

In this paper, we investigate the performance of ANN in hydrological modeling of Kemaman catchment in the east coast state of Terengganu using hourly data of rainfall, evaporation, temperature and humidity. Section 2 gives an overall description of the study area; Section 3 details the features of feed forward back-propagation (FFBP) network, radial basis function (RBF) neural network, and generalized regression neural network (GRNN) used in the present study; Section 4 describes the network architecture design; Section 5 describes the network training and the input data sensitivity study. Conclusions and recommendations are made in Sect. 6.

2 Description of Study Area

In Terengganu, flood occurs primary due to monsoon rainfall, coupled with backwater phenomenon during high tides. In addition, low water current in river regime, as well as velocity and direction of wind that opposes the direction of river flow usually aggravates the situation [14]. Kemaman is located between latitude $3^{\circ} 50'N$ – $4^{\circ} 35'N$ and longitude $102^{\circ} 50'E$ – $103^{\circ} 40'E$ [15]. The total area of the Kemaman district is 8,000 square miles (254,000 ha). The mean maximum and minimum annual temperatures are 31 and 21 °C, respectively, while the average annual rainfall is 2,500 mm. Every year, Kemaman is almost always flooded. For example, during the infamous flood in December 2013 recently, which was the worst in past 50 years, the river stage was recorded to be above the danger level condition over an extended duration. The water level in Sungai Kemaman was above the danger stage of 20.08 m (Jambatan Ban Ho), 15.27 m at Jambatan Air Putih and 19.37 m at Jambatan Tebak [16]. The combined effect of heavy rains and high tides has drowned nearly 80 % of the district.

Hydrological network is widely established in Kemaman. There are ten (10) rainfall stations, four (4) river stage stations, one (1) station on evaporation, and one (1) station on mean relative humidity and temperatures. In addition, there are two (2) tidal stations within the vicinity which may be taken into consideration to assess the impact of tidal water level to the observed river stage. However, we have chosen



Fig. 1 Distribution of the hydrological network of stations in Kemaman

to pursue this consideration in a later work. The distribution of these stations is given in Fig. 1 and their respective detailed locations and station ID provided in Table 1. For the purpose of this study, the corresponding hydrological data were obtained from the relevant departments responsible for their respective stations, namely Department of Irrigation and Drainage (DID), Malaysian Meteorological Department (MMD), and Department Of Survey and National Mapping (JUPEM).

3 Artificial Neural Network Model

A feed forward neural network is an artificial neural network where connections between the units do not form a directed cycle. On the other hand, FFBP is a representative learning model where the network repeatedly adjusts the weights and biases in the network so as to minimize the error function. Figure 2 shows the typical structure of a FFBP network which can be described in the form of $I_p H_q O_r$, where I is the input layer, H is the hidden layer, O is the output layer, and p, q, r are the number of neuron in the respective layer. FFBP algorithm is very sensitive to the selected initial weight values, and may suffer from local minima issue [17, 18].

The basic structure of RBF is similar to a traditional feed-forward neural network which is shown in the Fig. 3 [19]. It was developed by Powell [20], with 3 layers, namely the input layer, hidden layer and output layer [21]. The input layer is a set of N sensory units, and the number of this element of N -dimensional is equal

Table 1 Description of the hydrological network of stations in Kemaman

Station	Station number	Location	Latitude longitude
Rainfall	4333096	Klinik Bidanat Kg. Ibok	04° 19' 40"N 103° 22' 05"E
Rainfall	4434093	Sek. Men. Keb. Badrul Alam Shah	04° 25' 40"N 103° 27' 05"E
Rainfall	4232104	Sek. Keb. Pasir Gajah	04° 14' 20"N 103° 17' 50"E
Rainfall	4334094	Sek. Keb. Kijal	04° 19' 55"N 103° 29' 15"E
Rainfall	4332001	Jambatan Tebak	04° 22' 40"N 103° 15' 45"E
Rainfall	4232002	Jambatan Air Putih	04° 16' 15"N 103° 11' 55"E
Rainfall	4131001	Kg. Ban Ho	04° 08' 00"N 103° 10' 30"E
Rainfall	4234109	Jps. Kemaman	04° 13' 55"N 103° 25' 20"E
Rainfall	3933001	Hutu Jabor	03° 55' 05"N 103° 18' 30"E
Rainfall	4534092	Sek. Keb. Kerteh	04° 30' 30"N 103° 26' 40"E
Evaporation	4333301	Bandar Di Ketengah	04° 21' 45"N 103° 20' 50"E
Temperature	49465	Hospital Kemaman	04° 14' 00"N 103° 25' 00"E
Mean relative humidity	49465	Hospital Kemaman	04° 14' 00"N 103° 25' 00"E
Water level (station 1)	4232452	Sg. Kemaman at Rantau Panjang	04° 16' 50"N 103° 15' 45"E
Water level (station 2)	4232401	Sg. Kemaman at Jam. Air Putih	04° 16' 15"N 103° 11' 55"E
Water level (station 3)	4131453	Sg. Cherul at Ban Ho	04° 08' 00"N 103° 10' 30"E
Water level (station 4)	4332401	Sg. Tebak at Jam. Tebak	04° 22' 40"N 103° 15' 45"E
Tidal water level	48507	Kompleks LKIM, Cendering	05° 15' 54"N 103° 11' 12"E
Tidal water level	48485	Pelabuhan Kuantan, Tanjung Gelang	03° 58' 30"N 103° 25' 48"E

to input features vector u . The input units are fully or directly connected to the hidden layer with hidden units. The goal of the hidden layer is to cluster the data and reduce its dimensionality. The hidden layer is named the RBF units. These RBF units are also fully connected to the output layer. The output layer supplies the

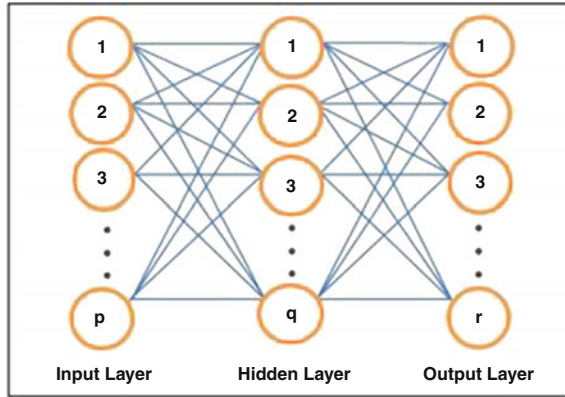


Fig. 2 Typical structure of a feed forward back-propagation FFBP neural network

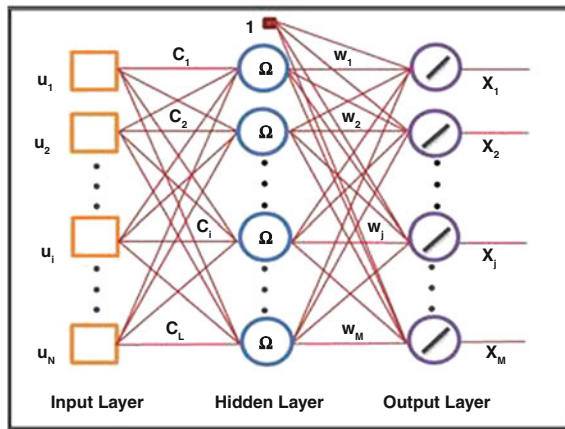


Fig. 3 Typical structure of a radial basis function neural network (RBF)

response of neural network to the activation pattern applied to the input layer. The transformation from the input space to the RBF unit space is governed by nonlinear Gaussian function [22], whereas the transformation from the RBF unit space to the output space is linear. The network training for RBFN is divided into two stages: the weights from the input to hidden layer are determined, then the weights from the hidden to output layer.

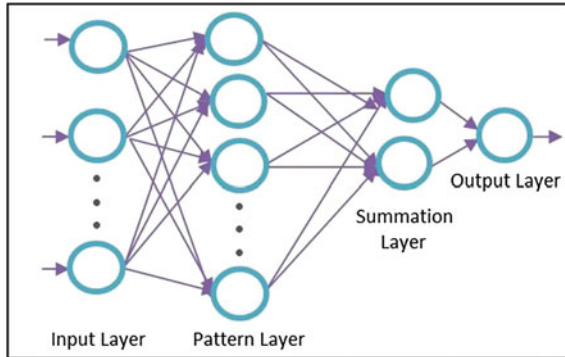


Fig. 4 Typical structure of a general regression neural network (GRNN)

GRNN is a variant of RBF neural network, and is often used for function approximation and the estimation of continuous variables [23]. Figure 4 shows the typical structure of GRNN. The advantages of GRNN are fast learning and convergence to the optimal regression surface as the number of sample becomes very large. Successful implementation depends heavily on the spread factor to obtain a smooth approximation. In the training procedure, GRNN does not frequently encounter local minima problem as in FFBP applications and it also does not generate physically unreasonable estimates.

4 Model Development

For FFBP model, network training is performed using Levenberg-Marquardt optimization, a standard virtual in nonlinear optimization technique, which approaches second order training speed and eliminates the need to tune learning rate and momentum coefficient. The network training performance function is the mean square error, MSE, given by the averaged squared error between the network output and the target output [18]. The Levenberg-Marquardt algorithm is given by the Newton like method by using the formula of

$$x_{k+1} = x_k - (H + \mu I)_K^{-1} g_k, \quad (1)$$

where x_k is a vector of the current weights and biases, H_k is the Hessian matrix for the second derivatives of the performance index at the current values of the weights and biases and g_k is the current gradient.

The nonlinear unconstrained optimization problem in the training of a RBFN can be calculated by using the formula

$$J(w, c) = \sum_{k=1}^K \|y^k - f(u^k)\|^2, \tag{2}$$

where the input and output training patterns (u, y) , $k = 1, 2, \dots, K$. The training problem will become quadratic once the radial basis function centers c_{ν} s are known.

The probability density function $Y(X)$ in GRNN is the normal distribution [23]. Each training sample, X_i , is used as the mean of a normal distribution.

$$Y(X) = \frac{\sum_{i=1}^n Y_i \exp(-D_i^2/2\sigma^2)}{\sum_{i=1}^n \exp(-D_i^2/2\sigma^2)}, \tag{3}$$

$$D_i^2 = (X - X_i)^T \cdot (X - X_i), \tag{4}$$

where σ is the standard deviation. The distance D_i , between the training sample and the point of prediction, is used as a measure of how well each training sample can represent the position of prediction, X . If the distance, D_i , between the training sample and the point of prediction is small, the term $\exp(-D_i^2/2\sigma^2)$ increases. For $D_i = 0$, $\exp(-D_i^2/2\sigma^2)$ equals unity and the point of evaluation is represented best by this training sample. The term $Y_i^* \exp(-D_i^2/2\sigma^2)$ for the i th training sample is the biggest and it contributes very much to the prediction.

In the design of network architecture, a number of factors to be considered include the number of hidden layers, number of neurons in each layer, learning factor for the FFBP model, spread factor for the GRNN model, and spread constant for the RBF model. For the purpose of comparing the performance of the three network models, the trained network performances are evaluated using the normalized root mean square error, RMS and the correlation coefficient, R [10, 11]:

$$RMS = \sqrt{\frac{\sum_{j=1}^M (Y_j - O_j)^2}{\sum_{j=1}^M O_j^2}}, \tag{5}$$

$$R = \frac{\sum_{j=1}^M (Y_j - \bar{Y})(O_j - \bar{O})}{\sqrt{\sum_{j=1}^M (Y_j - \bar{Y})^2 (O_j - \bar{O})^2}}, \tag{6}$$

where M is the total number of sample, Y_j and O_j are the value of predictions and observations, \bar{Y} and \bar{O} are the arithmetic mean.

5 Network Training

We consider 13 sets of hydrological inputs, which comprise relative humidity, evaporation, temperature, and rainfall data from 10 stations as detailed in Table 1. The output comprises 4 river stage outputs for water level at Stn. 1–4 (station ID: 4232452, 4232401, 4131453 and 4332401, respectively) (Table 1). We use 30-day hourly observation from 1st to 30th January 2009 for the purpose of network training. Three distinct ANNs are considered and compared, namely the FFBP, GRNN and RBF neural network. The models are designed using MATLAB Neural Network Toolbox.

For the FFBP model, the initial trials examine the training performance as a function of the number of layer and the number of neuron in the layers. Table 2 shows the representative FFBP network structures tested. Network structure 1 has a single hidden layer ($I_{13}H_9O_4$), network structure 2 ($I_{13}H_{4,5}O_4$) and 3 ($I_{13}H_{11,12}O_4$) have 2 hidden layers, and network structure 4 ($I_{13}H_{11,12,2}O_4$) has 3 hidden layers. Training results in terms of the normalized root mean square error RMS, and correlation coefficient R, for all the four river stage stations are shown in Fig. 5. Overall, the correlation coefficients are well below 0.75, and the normalized root mean square errors are in the order of 0.1 or higher. Highest R values are obtained

Table 2 FFBP network structures considered

Network Structure	Network
Network structure 1	$I_{13}H_9O_4$
Network structure 2	$I_{13}H_{4,5}O_4$
Network structure 3	$I_{13}H_{11,12}O_4$
Network structure 4	$I_{13}H_{11,12,2}O_4$

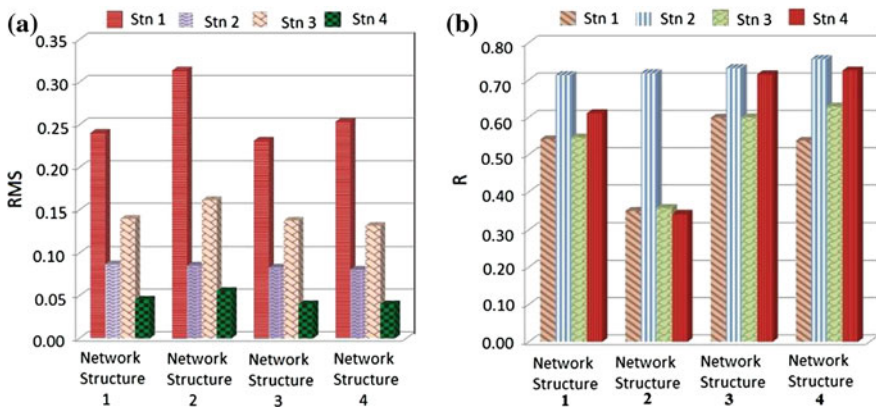
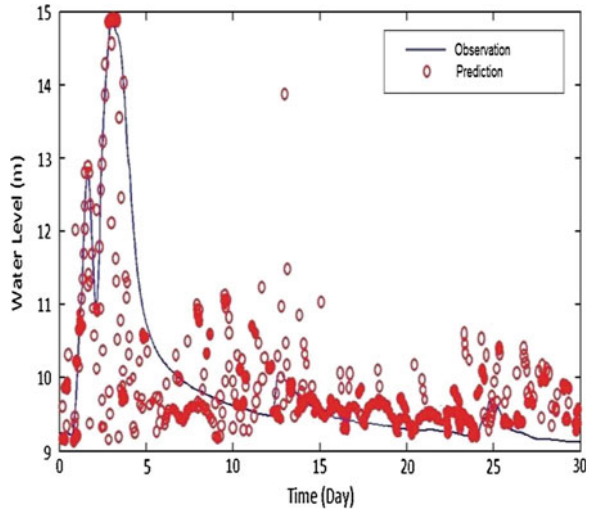


Fig. 5 FFBP model: effect of number of neuron on normalized root mean square error (RMS) and correlation coefficient (R). **a** Normalized root mean square error (RMS). **b** Correlation coefficient (R)

Fig. 6 FFBP model: 30-days water level training for Stn. 2. RMS = 0.0807, R = 0.7558



for Stn. 2, whereas Stn. 1 gives the lowest RMS values. The best performance is obtained from network structure 4, where RMS = 0.2537, R = 0.5370 for Stn. 1, RMS = 0.0807, R = 0.7558 for Stn. 2, RMS = 0.1321, R = 0.6288 for Stn. 3, and RMS = 0.0397, R = 0.7248 for Stn. 4. Figure 6 plots the exemplarily training data fit for Stn. 2. Based on visual inspection, rising limb up to the peak water level is well fitted but deteriorates considerably along the recession curve.

Figure 7 shows the RMS and R values for the RBF model as a function of the spread constant. The best performance is observed at the optimum value of 0.2,

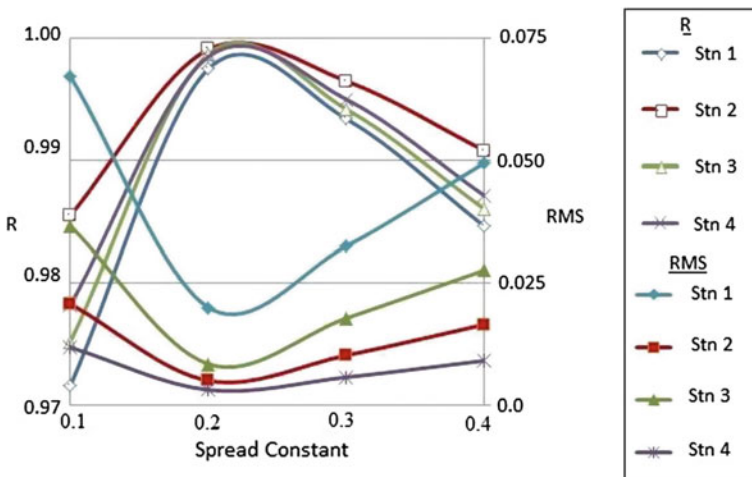
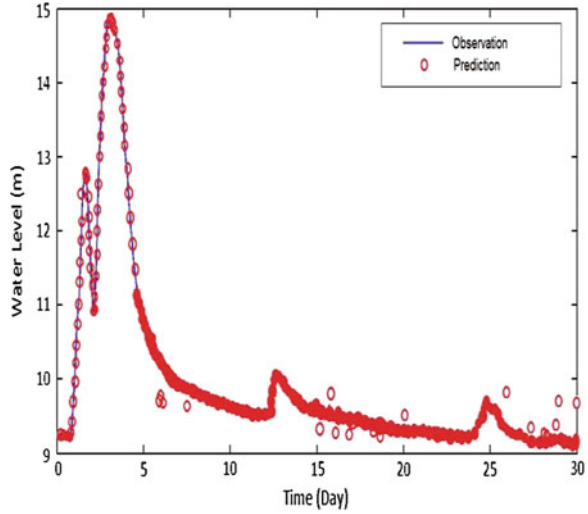


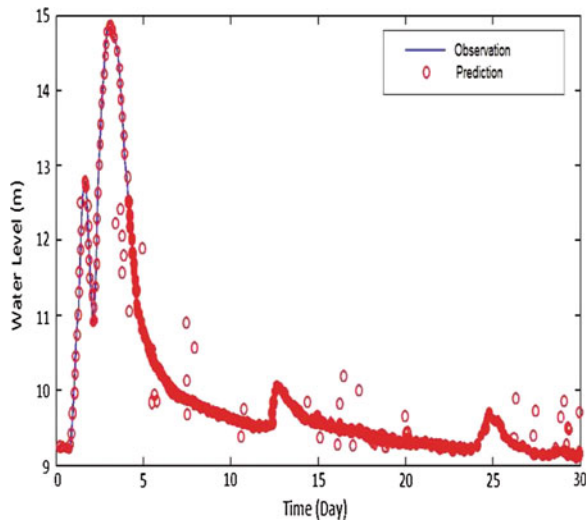
Fig. 7 RBF model: effect of spread constant on normalized root mean square error (RMS) and correlation coefficient (R)

Fig. 8 RBF model: 30-days water level training for Stn. 2. RMS = 0.0050, R = 0.9991



where RMS is well below 0.0200, and R is well above 0.9987 for all stations. The training data fit for Stn. 2 (Fig. 8) is found to improve over that produced by the GRNN model (Fig. 9), with excellent agreement at both rising and falling limb except a few scatter. The RMS and R values for Stn 1–4 are 0.0200, 0.9975 for Stn. 1, 0.0050, 0.9991 for Stn. 2, 0.0084, 0.9987 for Stn. 3 and 0.0031, 0.9985 for Stn. 4. Note that Stn. 1 has the poorest results in comparison. This may be attributed to the fact that the station is the farthest downstream and additional influence from tidal water level could be important.

Fig. 9 GRNN model: 30-days water level training for Stn. 2. RMS = 0.0130, R = 0.9940



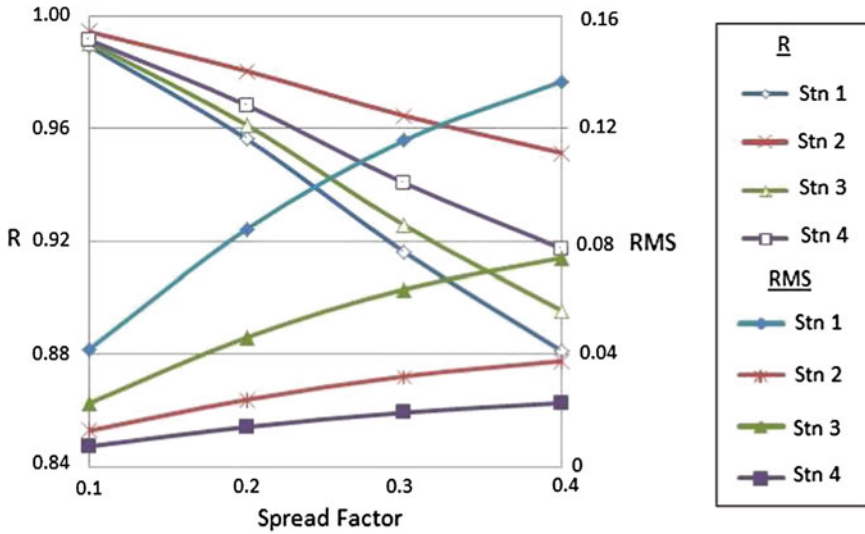


Fig. 10 GRNN model: effect of spread factor on normalized root mean square error (RMS) and correlation coefficient (R)

Figure 10 shows the RMS and R values for the GRNN model as a function of the spread factor. Results shows that as the value of spread factor increases, the training performance worsen. Overall, training performance is the best for Stn. 2. For the representative optimum spread factor value of 0.1, the R values for Stn. 1–4 are 0.9892, 0.9940, 0.9906 and 0.9915 respectively, with the corresponding RMS values being 0.0420, 0.0130, 0.0228 and 0.0074. Figure 8 shows that the overall training data fit of the GRNN model for Stn. 2 is much better than those produced by the FFBP models (Fig. 6), where only some minor scatters are observed on the recession curve.

Based on the preceding results, it is concluded that the RBF model produced the best trained network in the present investigation. Using the RBF model, we proceed to examine the sensitivity of the results when different combinations of the inputs are considered. Table 3 summarizes the RMS and R values for all four river stage stations (Stn. 1–4) with different input data set. It is observed that the best training result is obtained for case 1, i.e. where the maximum 13 sets of data are utilized. Results deteriorate if only the rainfall data is considered, suggesting that accurate prediction of the river stage is sensitive to hydrological variables such as temperature, humidity and evaporation.

Table 3 Sensitivity of different combination of input data

Case	R	e	H	E	RMS				R			
					Stn. 1	Stn. 2	Stn. 3	Stn. 4	Stn. 1	Stn. 2	Stn. 3	Stn. 4
1	√	√	√	√	0.0200	0.0050	0.0084	0.0031	0.9975	0.9991	0.9987	0.9985
2	√				0.1759	0.0499	0.0890	0.0297	0.7909	0.9128	0.8438	0.8522
3	√			√	0.1636	0.0468	0.0828	0.0278	0.8214	0.9235	0.8661	0.8722
4	√		√		0.1523	0.0450	0.0796	0.0265	0.8467	0.9294	0.8770	0.8847
5	√	√			0.4144	0.0467	0.0827	0.0274	0.7676	0.9240	0.8664	0.8764
6	√		√	√	0.1210	0.0350	0.0637	0.0205	0.9055	0.9580	0.9230	0.9325
7	√	√	√		0.0701	0.0203	0.0368	0.0119	0.9690	0.9860	0.9749	0.9780

6 Conclusion

In the present study, FFBP, RBF and GRNN network models were developed and trained using up to 13 hydrological input data sets to produce river stage predictions at four locations in Kemaman catchment, Terengganu. Network training uses 30-day hourly observations from 1st to 30th January 2009 and the performances are compared based on normalized root mean square errors RMS and correlation coefficient R. Results show that the RBF model performs the best, whereas the FFBP model is the most inferior. Using the optimum spread constant of 0.2, the RBF model gives excellent prediction for all 4 water level stations with $RMS < 0.0200$, and $R > 0.9987$. Sensitivity study also shows that all 13 hydrological inputs are crucial to produce the best results.

For future works, the functionality of the network models will be further examined for their ability to produce good forecast. In addition, the sensitivity of adjacent tidal water level to the predictions can also be assessed to evaluate the importance of tidal influence to the water level in these river stage observation points.

Acknowledgments The authors acknowledge the financial support from Institute of Postgraduate Study (IPsIs) and Research Management Institute (RMI), UiTM. We also thank DID, MMD and JUPEM for the data provided in the present study.

References

1. V.P. Singh, *Computer Models of Watershed Hydrology* (Water Res. Pub., Colorado, 1995), pp. 1–22
2. D.A. Hughes, Three decades of hydrological modelling research in South Africa. *S. Afr. J. Sci.* **100**, 638–642 (2004)
3. Z. Yu, Chapter 172: Hydrology: modeling and prediction. *Encyclopedia of Atmosphere Science*, vol. 3 (Academic Press, London, 2002), pp. 980–986. doi:[10.1006/rwas.2002.0172](https://doi.org/10.1006/rwas.2002.0172)

4. ASCE Task Committee on Application of Artificial Neural Networks in hydrology. Artificial neural networks in hydrology-II: hydrologic applications. *J. Hydrol. Eng.* **5**(2), 124–137 (2000)
5. G.R. Rakhshandehroo, M. Vaghefi, M.M. Shafiee, Flood forecasting in similar catchments using neural networks. *Turk. J. Eng. Env. Sci.* **34**, 57–65 (2010). doi:[10.3906/muh-0908-7](https://doi.org/10.3906/muh-0908-7)
6. T.A. Mohammed, S. Al-Hassoun, A.H. Ghazali, Prediction of flood levels along a stretch of the Langat river with insufficient hydrological data. *Pertanika J. Sci. Technol.* **19**(2), 237–248 (2011)
7. A.S. Tokar, P.A. Johnson, Rainfall runoff modeling using artificial neural networks. *J. Hydrol. Eng.* **4**(3), 232–239 (1999)
8. G.F. Lin, L.H. Chen, A non-linear rainfall-runoff model using radial basis function network. *J. Hydrol.* **289**, 1–8 (2004)
9. N.J. de Vos, T.H.M. Rienjes, Constraints of artificial neural networks for rainfall runoff modelling: trade-offs in hydrological state representation and model evaluation. *Hydrol. Earth Syst. Sci. Discuss.* **2**, 365–415 (2005)
10. W.K. Lee, Long term tidal forecasting and hindcasting using QuickTIDE tidal simulation package. *J. Inst. Eng. Malays.* **68**(2), 59–64 (2007)
11. W.K. Lee, Long term tidal forecasting using back-propagation neural network, in *Proceedings of Malaysian Science and Technology Congress (MSTC)*, COSTAM, 19–21 Nov 2012
12. W.K. Lee, T.A. Tuan Resdi, Neural network approach to coastal high and low water level prediction, in *Proceedings of the International. Civil & Infrastructure Engineering Conference (InCIEC 2013)* (2014), pp. 275–279
13. H.R. Maier, G.C. Dandy, The use of artificial neural networks for the prediction of water quality parameters. *Water Res.* **32**(4), 1013–1022 (1996)
14. M.B. Gasim, J.H. Adam, M.E. Toriman, S.A. Rahim, H. Juahir, Coastal flood phenomenon in Terengganu, Malaysia: special reference to dungun. *Res. J. Env. Sci.* **1**(3), 102–109 (2007)
15. I. Sulong, H. Mohd-Lokman, K. Mohd Tarmizi, A. Ismail, Mangrove mapping using landsat imagery and aerial photographs: Kemaman District, Terengganu, Malaysia. *Environ. Dev. Sustain.* **4**(2), 135–152 (2002)
16. Kosmo (4 Dis 2013). Banjir: 1,443 lagi mangsa dipindah di Terengganu, http://www.kosmo.com.my/kosmo/content.asp?y=2013&dt=1204&pub=Kosmo&sec=Terkini&pg=bt_20.htm#ixzz2xq0tUFUF
17. J. Joshi, V.M. Patel, Rainfall-runoff modelling using artificial neural network (a literature review), in *National Conference on Recent Trends in Engineering & Technology*, May 2011
18. S. Solanki, H.B. Jethva, A review on back-propagation algorithms for feedforward networks. *Int. Res. Anal.* **2**(1), 73–75 (2013)
19. A.R. Senthil Kumar, K.P. Sudheer, S.K. Jain, P.K. Agarwal, *Hydrol. Process.* **19**, 1277–1291 (2005). doi:[10.1002/hyp.5581](https://doi.org/10.1002/hyp.5581)
20. M.J.D. Powell, Radial basis functions for multivariable interpolation: a review. *Proceedings of IMA Conference Algorithms for Approximation* (1987), pp. 143–167
21. F. Schwenker, H.A. Kestler, G. Palm, Three learning phases for radial-basis-function networks. *Neural Netw.* **14**, 439–458 (2001)
22. E. Mutlu, I. Chaubey, H. Hexmoor, S.G. Bajwa, Comparison of artificial neural network models for hydrologic predictions at multiple gauging stations in an agricultural watershed. *J. Hydrol. Process.* (2008). doi:[10.1002/hyp.7136](https://doi.org/10.1002/hyp.7136)
23. D.F. Specht, A general regression neural network. *IEEE Trans. Neural Netw.* **2**(6), 568–576 (1991)

Hydrodynamic Model for the Investigation of Environmental Flow in Johor River Estuary

Wei-Koon Lee and NurHidayah Aqilla binti Zaharuddin

Abstract Large-scale coastal reclamation at Pulau Tekong Singapore, which is situated at the confluence of Johor River estuary and Straits of Johor, inevitably alters the local hydrodynamics. Meanwhile, in order to prevent saline intrusion from reaching the Johor River Waterworks (JRWW) operated by PUB Singapore, the government of Malaysia has recently proposed to build a tidal barrage at Kota Tinggi across Johor River. The scheme is expected to reduce the need of salinity flushing from the Linggiu Dam further upstream, thus lowering the average riverine discharge into Johor River estuary. The coupled effect of the above is likely to affect the advection and diffusion of pollutants in Johor River estuary. In the present study, we simulate the flow field in Johor River estuary using a set of hyperbolic shallow water equations on an adaptive quadtree grid system. Our objective is to understand the environmental flow in the study area after the completion of the above-proposed developments.

Keywords Johor River estuary • Pulau Tekong reclamation • Hydrodynamic model • Tebrau Strait • Water quality profile

1 Introduction

Johor is located at south of Peninsular Malaysia, neighboring Singapore, which is separated by Tebrau Strait (also known as Johor Strait) (Fig. 1). It is one of the most developed states in the country, and our only southern gateway. Tebrau Strait is divided into the east and west channels which are disjointed since the completion of

W.-K. Lee (✉)

Fluvial and River Engineering Dynamics Group (FRiEnD) IIESM,
Faculty of Civil Engineering, UiTM, Shah Alam, Malaysia
e-mail: Leewei994@salam.uitm.edu.my

N.A.b. Zaharuddin

Faculty of Civil Engineering, Universiti Teknologi MARA, Shah Alam, Malaysia

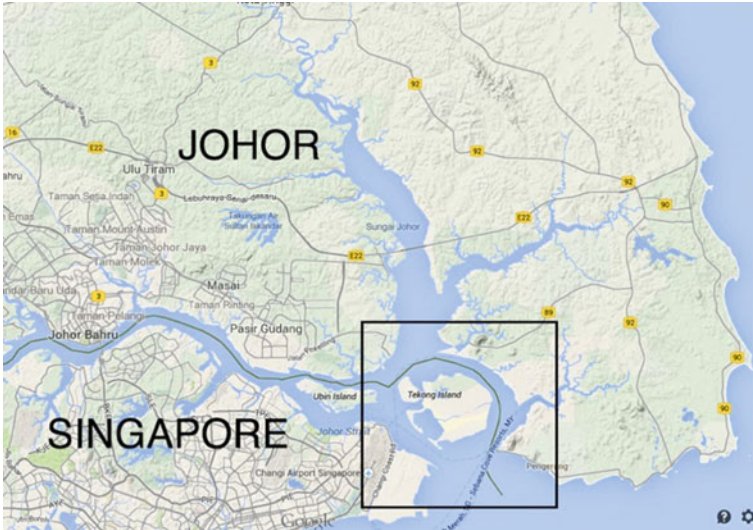


Fig. 1 Location of study. *Inset* highlighting location of Pulau Tekong which is under reclamation. (Source Google map)

the Johor Causeway in year 1923. Over the decades, the water quality of the narrow strait has deteriorated owing to the lack of vigorous mixing and hydrodynamic trapping. At present, water quality of the strait is quoted as amongst the most polluted in Malaysia, in particular East Tebrau Strait [1]. Meanwhile, port and navigation activities in Pasir Gudang continue to exert increasing stress on the ecological health of the water especially the east channel where the port is located [2].

Since late 1970s, Singapore has been carrying out coastal reclamation works at the confluence of Johor River Estuary and East Tebrau Strait. Essentially, a group of islands at the north-east of Singapore, notably Tekong Besar and Tekong Kecil, are reclaimed into a much larger land mass in stages and the work has continued to present day (Fig. 2). Back in year 2002, Malaysia had expressed concern over the development. A number of studies have since been carried out to investigate the environmental impact of the scheme [e.g. 3, 4]. However, the case was subsequently dropped after independent investigation showed that the proposed reclamation work has negligible impact on Malaysian water [5].

More recently, the government of Malaysia has proposed to build a tidal barrage across Johor River at Kota Tinggi in order to prevent saline intrusion from reaching the Johor River Waterworks (JRWW) [6]. JRWW extracts water from the Johor River upstream of Kota Tinggi and is currently the largest source of potable water supply to Singapore. It is operated by Public Utilities Board (PUB) Singapore and has a total output of 250 mgd (UK gallons) [7]. The proposed tidal barrage is expected to reduce the need of salinity flushing from Linggiu Dam further upstream, thus lowering the average riverine discharge into Johor River estuary.

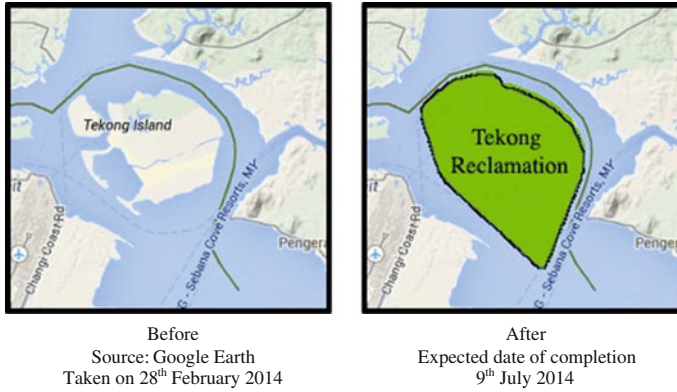


Fig. 2 Pulau Tekong: before and after reclamation

The coupled effect of reduced riverine discharge and increased constriction in the vicinity of Pulau Tekong will inevitably alter the local hydrodynamics to differ from the previous studies. It is likely that the advection and diffusion of pollutants in Johor River estuary will be affected, with potential negative impact.

In the present study, we present the water quality profiles along Tebrau Strait and Johor River obtained from in situ measurement and laboratory tests to characterize the present state of the water quality. A hydrodynamic model of the area is presented using a set of hyperbolic shallow water equations on quadtree grid system. The simulated flow field is validated against the observed water level fluctuation and velocity distribution in and around the estuary. The present work laid the foundation for the subsequent step to simulate the advection of pollutants in the area. Our eventual objective is to understand the compound impact of the proposed reclamation scheme in Pulau Tekong and the proposed tidal barrage across Johor River at Kota Tinggi on the environmental flow and pollutant mixing in East Tebrau Straits and Johor River Estuary.

2 Shallow Water Equations

We consider two-dimensional depth-averaged shallow water equations in the form of a non-homogenous hyperbolic system [8]:

$$\mathbf{W}_t + \mathbf{A}_F(\mathbf{W})\mathbf{W}_x + \mathbf{A}_G(\mathbf{W})\mathbf{W}_y = \mathbf{S}. \tag{1}$$

where that the subscripts x , y and t denote partial derivatives with respect to the x -direction, y -direction, and time respectively. The vector of unknowns, \mathbf{W} , the flux function vectors, \mathbf{F} and \mathbf{G} , and the source term vectors, \mathbf{S} are defined as:

$$\mathbf{W} = \mathbf{W}(x, y, t) = [h, q_x, q_y]^T, \quad (2)$$

$$\mathbf{F} = \mathbf{F}(x, y, t) = \begin{bmatrix} q_x \\ q_x^2/h + gh^2/2 \\ q_x q_y/h \end{bmatrix}, \quad (3)$$

$$\mathbf{G} = \mathbf{G}(x, y, t) = \begin{bmatrix} q_y \\ q_x q_y/h \\ q_y^2/h + gh^2/2 \end{bmatrix}, \quad (4)$$

$$\mathbf{S} = \mathbf{S}(x, y, \mathbf{W}) = \left[0, gh \frac{dz}{dx}, gh \frac{dz}{dy} \right]^T. \quad (5)$$

Here, h is the water depth, $q_x(x, y, t)$ and $q_y(x, y, t)$ are the flow rate components, g is the gravity acceleration 9.81 m/s^2 , and z is the bed elevation measured from a fixed datum.

The system matrix of the quasilinear Eq. 1 takes the form of:

$$\mathbf{A}(\mathbf{W}) = \begin{bmatrix} \mathbf{A}_F(\mathbf{W})n_x & 0 \\ 0 & \mathbf{A}_G(\mathbf{W})n_y \end{bmatrix}, \quad (6)$$

where $\mathbf{n} = (n_x, n_y)$ is the unit vector, and the Jacobian matrices \mathbf{A}_F and \mathbf{A}_G are given by:

$$\mathbf{A}_F(\mathbf{W}) = \frac{\delta \mathbf{F}}{\delta \mathbf{W}} \begin{bmatrix} 0 & 1 & 0 \\ c^2 - u_x^2 & 2u_x & 0 \\ -u_x u_y & u_y & u_x \end{bmatrix}, \quad (7)$$

$$\mathbf{A}_G(\mathbf{W}) = \frac{\delta \mathbf{F}}{\delta \mathbf{W}} \begin{bmatrix} 0 & 0 & 1 \\ -u_x u_y & u_y & u_x \\ c^2 - u_y^2 & 0 & 2u_y \end{bmatrix}, \quad (8)$$

where $c^2 = gh$.

Solution of the system of equation requires the system matrix to be non-singular. We follow the method of [9, 10]: a viscous correction term is added to Eq. 1 to balance the diffusion term in the system. The equivalent system produced can then be tuned in such a way that any centered approximation (in space) will solve up to second order all equilibria solutions, and thus of the original system.

3 Description of Location of Study

Johor River (N $1^\circ 27' - 1^\circ 49'$, E $103^\circ 42' - 104^\circ 01'$) originates from the central part of the state of Johor, and it flows southwards with a total length of approximately 122.7 km (Fig. 1). Our study area is the Johor River Estuary (JRE) and the

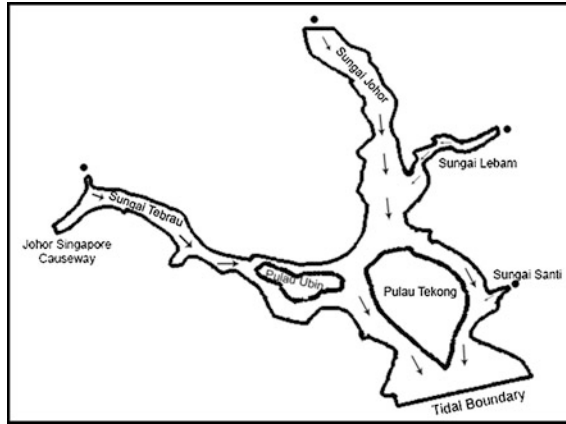


Fig. 3 Computational domain, showing tidal open boundaries, locations of river inlet (*)

adjoining East Tebrau Strait (ETS) (Fig. 3), with a total combined catchment area of up to 2,636 km². Natural forest and low land swamps are the dominant features in the northern and central catchment; oil palm and rubber plantations with swamps occupy most of the southern part of the basin. Urbanized land use spreads out primarily along the coastline from Johor Bahru to Pasir Gudang. Kota Tinggi, which is located about 40 km north of the confluence, is a much smaller urban landscape where Johor River traverses.

The bathymetry of the location as shown in Fig. 4 is discretized from [17]. The water depth in JRE and ETS varies between 1.0 m up to 16.9 m deep under mean sea condition, with an average depth of 6.5 m [11]. The deepest sections lie along the well-maintained navigational channel from Pasir Gudang Port to Singapore Strait southward of Pulau Tekong.

The flow field in JRE is dominated by the interaction between riverine discharge and astronomical tides. There is a tidal station (No. 48484) located at Jeti Kastam Johor Bharu (1° 27' 42"N, 103° 47' 30"E) which is maintained and operated by Department of Survey and Mapping Malaysia (JUPEM). The tide is mixed semi-diurnal dominant [12], with spring tidal range between 1.59 and 4.21 m, and neap tidal range between 2.34 and 3.5 m.

Basin-wide mean annual rainfall of the study area is 2,470 mm [13]. The average discharge of Johor river is 37.5 m³/s [11] but the discharge from other smaller rivers are generally not available. Considering similar meteorological factor, we estimated the combined average total inflow entering ETS and JRE to be 69.0 m³/s under regular flow condition. These are mainly contributed by Sungai Johor (54 %), followed by Sungai Lebam (34 %), Sungai Tebrau (7 %) and Sungai Santi (5 %) (Fig. 3), based on their relative catchment size [11].

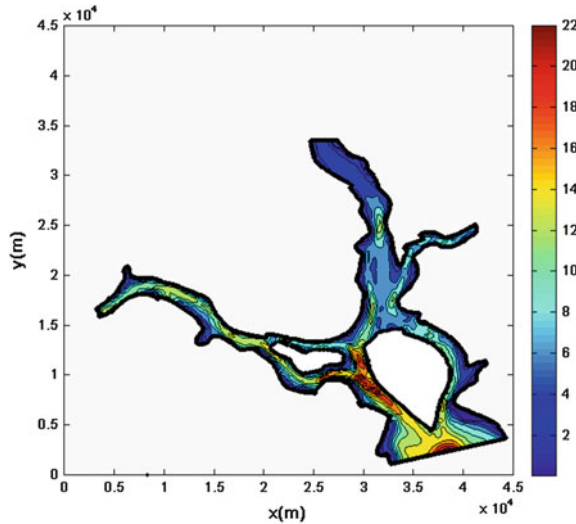


Fig. 4 Bathymetry of Johor River estuary within the computational domain

4 Water Quality Profile

Eight (8) strategic locations, denoted stations B–L (Table 1), were chosen along the coast of ETS and JRE (see Fig. 5) to obtain the general water quality profile of the area under the present state. An additional location, West Tebrau Strait (WTS) (station A), is included to compare the water quality on either side of Johor causeway.

Stations B–F in ETS are located in the highly industrialized area. The water appears to be dark and polluted in this region, in particular, oil slick and foam can be observed in station D during the site visit. Pasir Gudang Port is located between station D and E. Navigational activities are observed to be prevalent between stations D and F. Despite the narrow and busy strait, fish and mussel farming thrive between station C and E, and more fishing villages dot the coast line along Sungai Johor (e.g. station G and H). The water appears to be cleaner in stations F–H, and J–L where Johor River widens to meet the sea. Meanwhile, station I at the upstream of Johor River, appear to yellowish likely due to higher sediment concentration.

Table 2 gives the in situ water quality measured using *Horiba U-50 Series* water quality meter with multiple-sensors and automatic calibration function. The readings are taken during day time (9 a.m.–5 p.m.) with temperature ranging between 28 °C to just above 36 °C, and water depth of up to 0.95 m.

Specific gravity (SG), salinity, total dissolved solids are measured using the principle of conductivity conversions. Given $\sigma_t = (SG - 1) \times 1,000$, the SG obtained is observed to range from fresh water at station I (SG = 1.000) to SG = 1.018 at station L. Both the values of salinity and total dissolved solids (TDS) follow the

Table 1 Water quality sampling stations

Stn.	Location	Site description
A	East Tebrau Strait	Near old Johor Bahru checkpoint
B	West Tebrau Strait	Near JUPEM tidal station 48484
C	Permas Jaya	Fishing village
D	Pasir Gudang	Near Pasir Gudang Port; adjacent to Sultan Iskandar Power Station
E	Kampung Pasir Puteh	Fishing village
F	Sarang Buaya	Near Tanjung Langsat Industrial Complex
G	Tanjung Langsat	Fishing village
H	Kong Kong	Fishing village
I	Jalan Jemaluang	Next to west abutment of bridge crossing Johor River
J	Teluk Sengat	Near jetty (low tide condition)
K	Jambatan Senai-Desaru Highway	Below east abutment
L	Sungai Belungkor	Near Tanjung Belungkor Ferry Terminal

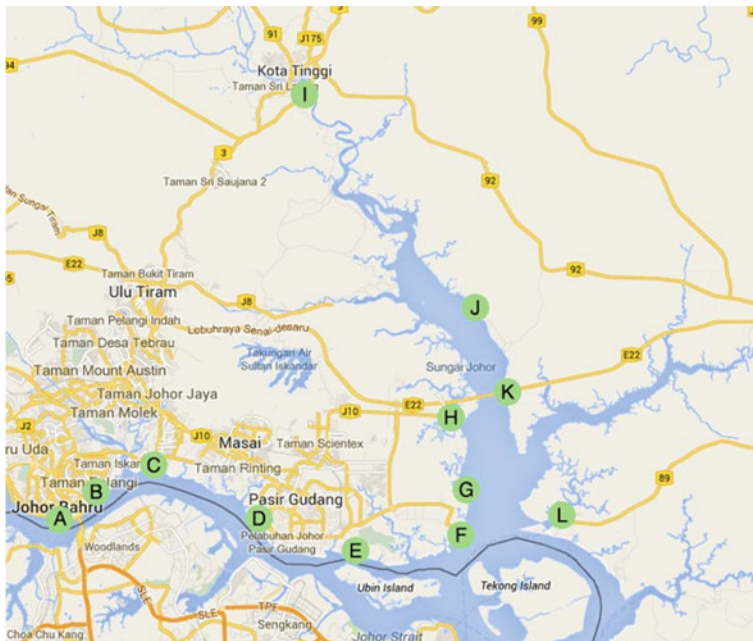


Fig. 5 Location of water quality sampling stations

trend of the σ_t (or SG) value of the station. Station I has the lowest values for both salinity and TDS, followed by station D. The value of SG, salinity, and TDS at stations D is relative low, possibly due to high fresh water discharge from the cooling

Table 2 In-situ water quality measurement for sampling stations, A–L

Station	Temp (°C)	Specific gravity (σ_t)	Salinity (PPT)	TDS (g/L)	TURB (NTU)	COND (mS/cm)	pH	ORP (mV)	DO (mg/L)
A	28.73	11.4	20.4	18.4	41.7	32.3	6.67	216	8.13
B	35.34	11.9	24.1	23.2	407.0	38.1	5.27	295	21.86
C	36.25	13.9	27.3	26.0	0.0	42.6	5.70	276	16.78
D	32.72	1.3	8.4	8.9	339.0	15.3	5.65	264	15.14
E	32.29	16.8	29.2	27.5	160.0	45.2	6.00	265	16.23
F	35.54	16.8	30.8	28.9	561.0	47.4	4.96	331	14.69
G	31.96	5.1	13.3	12.9	317.0	23.1	4.40	360	10.79
H	30.48	17.5	29.4	27.7	20.0	45.4	5.96	262	19.76
I	31.02	0.0	0.3	0.4	804.0	0.6	4.82	413	17.17
J	31.60	17.2	29.4	27.7	22.9	45.4	5.49	293	17.94
K	30.36	17.5	29.3	27.7	14.2	45.4	5.20	327	18.14
L	30.66	18.2	30.4	28.6	21.2	46.7	5.39	309	18.70

system of Tenaga Nasional Berhad (TNB) Sultan Iskandar power plant. With the exception of station G and I, all stations have salinity $>2.4\%$ (2% at station A), and TDS >9 g/L.

Horiba U-50 Series measures in situ turbidity using light scattering method. From the results, it is found that turbidity in ETS (stations B, D–G) at >160 NTU, with the exception of station C, which gives a nil reading curiously. Meanwhile, turbidity of JRE (stations H, J–L) is much lower comparatively (<42 NTU). The highest turbidity is recorded at the upstream of Johor River, i.e. station I at 804 NTU. It is worth noting that the turbidity at station A (~ 42 NTU) on the other side of the causeway is much lower than station B (407 NTU) in ETS, which is almost 10 times higher.

The values of conductivity, pH and oxidation reduction potential (ORP) are measured using electrode methods. Conductivity in ETS is generally >38 mS/cm, except station D (15 mS/cm) near the outlet of the power station discharge. Moving eastward, the conductivity increases with values exceeding 45 mS/cm near the confluence and in JRE, with the only exception of station G (23.1 mS/cm). The conductivity on either side of Johor causeway is found to be of the same order; station I at the upstream of Johor River has near zero conductivity.

The water is generally acidic in both ETS and JRE, but close to neutral at station A in WTS (pH 6.67). The lowest pH values are recorded at station G (pH 4.40), followed by station I (pH 4.82). We note that station G is found to be unique compared to the other stations, with relatively low values of salinity, TDS, conductivity, and pH.

Oxidation reduction potential (ORP) is a measurement that indicates the degree to which a substance is capable of oxidizing or reducing another substance. Large, positive ORP readings are obtained for all stations (highest at station I, at 413 mV),

Table 3 Water quality test for stations A, B, F, and H

Station	BOD (mg/L)	COD (mg/L)	Ammonium NH ₃ -N (mg/L)	Phosphorus P (mg/L)	Nitrite NO ₂ - (mg/L)	Nitrate NO ₃ - (mg/L)	Suspended solid, TSS (mg/L)
A	4.49	1,180	0.8	0.54	0.016	0.04	102
B	2.04	1,960	0.7	0.77	0.040	0.00	447
F	0.96	1,260	0.1	0.20	0.013	0.02	37
H	2.87	110	0.1	0.36	0.121	0.23	60

indicating that the water in ETS and JRE is a strong oxidizing agent. The dissolved oxygen (DO) measured using polarographic method shows that all stations have low percent saturation of DO at <12 %.

Water samples were collected from station A, B, F and H, and tested in the laboratory for additional water quality parameters (Table 3). The biological oxygen demand (BOD), is found to be low, but the chemical oxygen demand (COD) extremely high >1,180 mg/L, except station H (110 mg/L) which is farthest from ETS.

Following the Malaysia Marine Water Quality Criteria and Standard [14], the ammonium levels adjacent to the causeway (stations A and B) is extremely high (Class 3), but improve to Class 2/E at stations F and H. The similar trend applies to phosphorous levels. Meanwhile, the nitrite and nitrate values are the highest at station H (Class 3), and lowest at station F.

The suspended solid (SS) tests show that station A and B falls into Class 3, that is, typical of marine water in ports, or oil and gas field, but station B on the ETS is over 4 times higher than station A, attributed to the proximity to Pasir Gudang Port. Stations F may be classified as Class 2 which is suitable for marine life; station H, however, is higher slightly higher, characteristic of mangroves estuarine and river mouth water.

5 Flow Field Simulation

The computational mesh is generated using an adaptive quadtree grid system (Fig. 6). Quadtree grid has a tree-like indexing system suitable for solving partial differential equations discretised in Cartesian coordinates. The mesh is produced by recursively subdividing the domain into quadrants using a quadtree to store and manipulate the mesh information. The level of subdivision is user prescribed and maximum subdivision can be adopted to better approximate complex boundary and to allocate computational resources on specific area of interest within the domain. For a full description of the quadtree grid generator, the readers are referred to [15, 16].

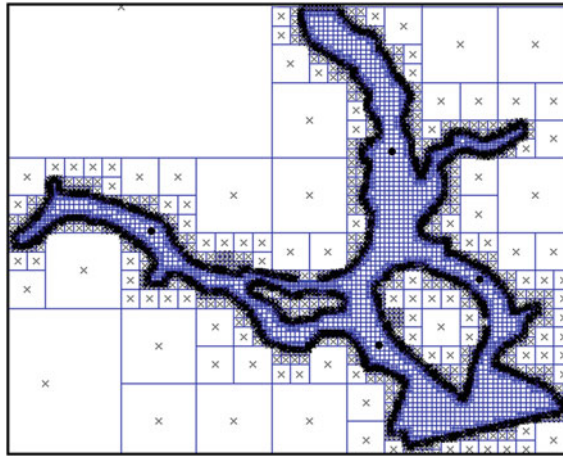


Fig. 6 Computational grid, showing refined mesh along domain boundary, and non-computational cell marked ‘x’. Also showing locations of velocity sampling points ‘•’: P, Q, R and S, clockwise from top

For flow field simulation, the river inflow and tidal forcing are superposed while maintaining mass conservation in the domain. Figure 7 shows the simulated water level fluctuation agrees well with the observed tidal water level fluctuation at JUPEM tidal station 48484 at Jeti Kastam, Johor Bahru. Four (4) representative locations have been chosen to sample the velocity variation: Johor River (P), Tekong East (Q), Tekong West (R), and Tebrau Strait (S), where their respective locations are as shown in Fig. 6. Figure 8 plots the observed depth-averaged velocities at these locations.

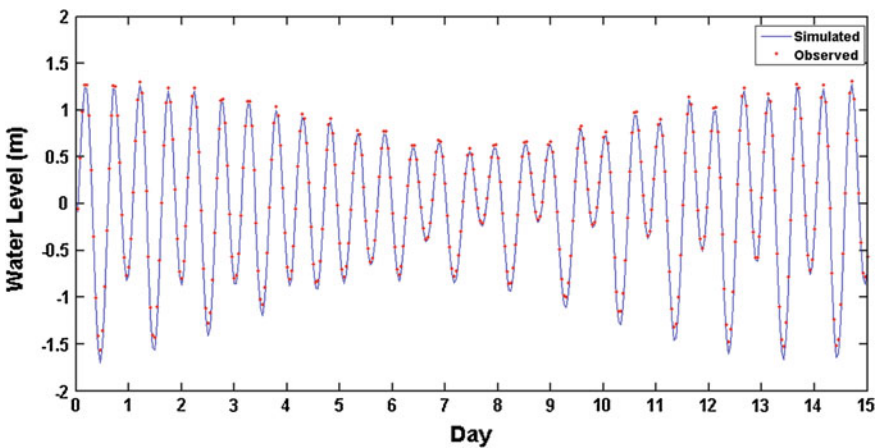


Fig. 7 Simulated and observed water level fluctuation at JUPEM tidal station 48484

The average velocity in Johor River is in the order of 2.0 m/s which agree well with [11, 17]. The values range from 1.75 m/s during neap tide, and a maximum of 2.6 m/s during spring tide. Flow velocity increases as it bifurcates at the confluence into the narrow Tekong East which maintains a minimum velocity of 2.05 m/s during the neap cycle, and reaching 2.93 m/s during the spring cycle. Meanwhile, flow in Tekong West, which is wider in comparison, slows to the range of 1.13–1.52 m/s.

Flow in ETS is much slower compared to the aforementioned locations. Maximum velocity during spring tide may reach 0.77 m/s, but falls to 0.23 m/s during neap tide. This results in overall poor flushing effect and long residence time. Under extreme condition, transport of pollutants or tracers can be severely hindered such as report in [18] and thus calls for further investigation.

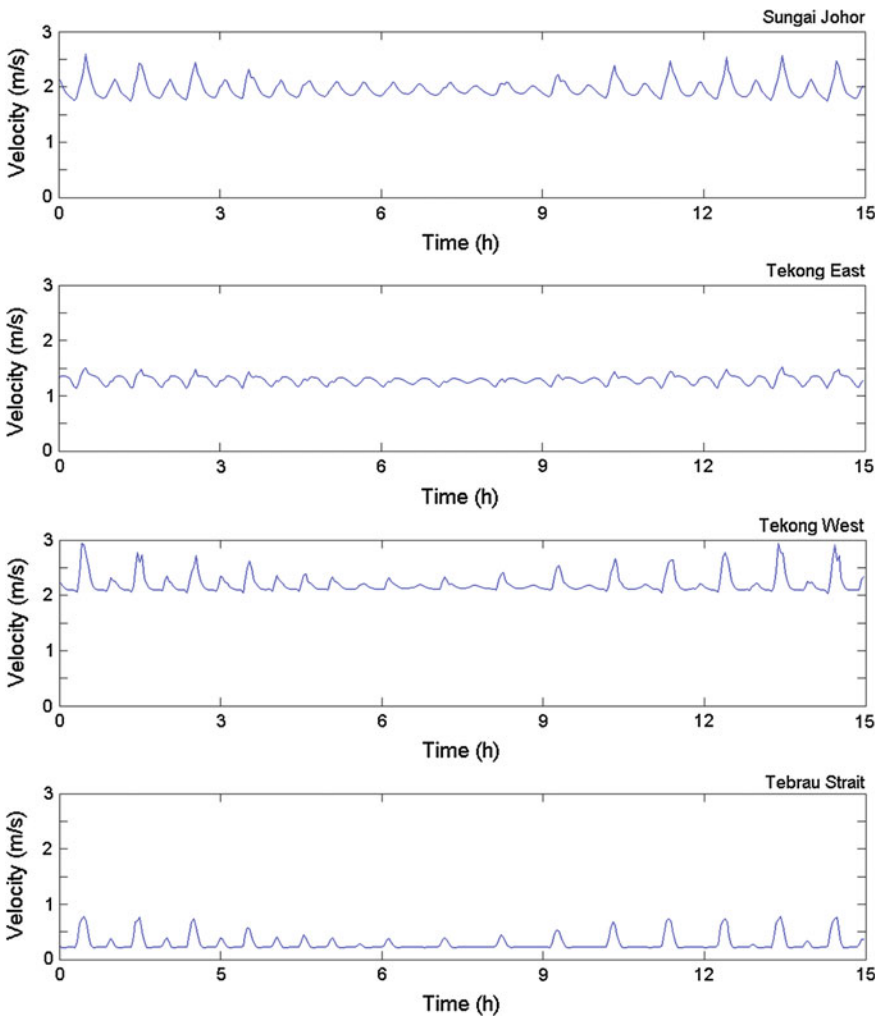


Fig. 8 Temporal velocity variation at four locations in the domain

6 Summary and Future Work

We presented the field and laboratory measurement of water quality profile for JRE and ETS. The poor marine water quality in ETS can be attributed to the lack of hydrodynamic flushing in the strait, as verified in our numerical model based on shallow water equations, considering tidal fluctuation and riverine discharge in the domain. Next, we will investigate the fate of pollutants in ETS and JRE by performing particle tracking using the flow field produced. In addition, changes to JRE flushing after the construction of the tidal barrage at Kota Tinggi will be evaluated to determine the environmental impact of the proposed development.

Acknowledgments The authors gratefully acknowledge the support provided by the Ministry of Education Malaysia and Research Management Institute (RMI) of Universiti Teknologi Mara (UiTM), Malaysia under the FRGS Grant FRGS/1/2012/ TK03/UITM/03/6.

References

1. Z. Zainudin, N.A. Rahman, N. Abdullah, N.F. Mazlan, Development of water quality model for Sungai Tebrau using QUAL2K. *J. Appl. Sci.* **10**, 2748–2750 (2010)
2. Malaysian Coastal Resources Study Team, Ministry of Science, Technology and the Environment, The coastal resources management plan for South Johore, Malaysia. ICLARM Tech. Rep. Coast. Area Manage. **33**, 144 (1992)
3. Syamsidik, H.L Koh, Impact assessment modeling on coastal reclamation at Pulau Tekong, in *Integrating Technology in the Mathematical Science* (2003)
4. Syamsidik, *Singapore Coastal Reclamation: History and Problems* (Academic Seminar of Indonesian Students Association, 2003)
5. T. Koh, J. Lin, The land reclamation case: thoughts and reflections, in *Singapore Year Book International Law Contributors*, vol. **X** (2006)
6. H. Mohamad Salleh, Construction of Sungai Johor barrage Kota Tinggi, Johor. Water Supply Department, Ministry of Energy, Green Technology and Water. Available from: <http://www.jba.gov.my/index.php/en/rujukan/technical-papers/537-construction-of-sungai-johor-barrage-kota-tinggi-johor>. Accessed 1 Apr 2014
7. A-control & i, Johor River waterworks. Available from: <http://www.a-control.com.sg/index.php/showcase-project/johor-river-water-works>. Accessed 1 Apr 2014
8. W.K. Lee, Chaotic mixing in wavy-type channel and two-layer shallow flows. D.Phil. thesis, Engineering Science, University of Oxford, 2011
9. W.K. Lee, A.G.L. Borthwick, P.H. Taylor, A fast adaptive quadtree scheme for a two-layer shallow water model. *J. Comput. Phys.* **230**, 4848–4870 (2011)
10. T. Chacon-Rebollo, A.D. Delgado, E.D. Fernández-Nieto, An entropy-correction free solver for non-homogeneous shallow water equations. *Math. Modell. Numer. Anal.* **37**, 755–772 (2003)
11. Deltares, Imares & Boskalis, Project SI 4.1—phase 2: a quick-scan of literature and available numerical models. Report, prepared for EcoShape, Dec 2010
12. W.K. Lee, Long-term tidal forecasting and hindcasting using QuickTIDE tidal simulation package. *IEM J.* **68**(2), 58–64 (2007)
13. A. Shafie, Extreme flood event: a case study on floods of 2006 and 2007 in Johor, Malaysia. M.Sc. thesis, Colorado State University, 2009

14. Department of Environment, Malaysia marine water quality criteria and standard. Ministry of natural resources and environment. Available from: <http://www.doe.gov.my/webportal/en/info-umum/piawaian-dan-kriteria-kualiti-air-marin-malaysia/>. Accessed 20 Apr 2014
15. B.D. Rogers, M. Fujihara, A.G.L. Borthwick, Adaptive q-tree Godunov-type scheme for shallow water equations. *Int. J. Numer. Meth. Fluids* **35**, 247–280 (2001)
16. Q. Liang, A.G.L. Borthwick, G. Stelling, Simulation of dam- and dyke-break hydrodynamics on dynamically adaptive quadtree grids. *Int. J. Numer. Meth. Fluids* **46**, 127–162 (2004)
17. E. Simoons, Hydrodynamic analysis of the Johor River Estuary. Master thesis, Hydraulic Engineering, TUDelft, 2010
18. W.K. Lee, A.G.L. Borthwick, P.H. Taylor, Tracer Dynamics in two-layer density-stratified estuarine flow. *J. Eng. Comput. Mech.* ICE, UK, 2014. doi:[10.1680/eacm.13.00008](https://doi.org/10.1680/eacm.13.00008)

A Conceptual Review of Tsunami Models Based on Sumatera-Andaman Tsunami Event

N.H. Mardi, M.A. Malek, M.S. Liew and H.E. Lee

Abstract Sumatra-Andaman tsunami was categorized as the third worst tsunami by the United State Geology Survey (USGS). The tsunami was triggered at 00:58:53 UTC by a massive earthquake with recorded moment magnitude of 9.1 at the west coast of North Sumatera. Malaysia is one of the countries affected by the 26th December 2004 tsunami. Others countries also affected by this event include Indonesia, Sri Lanka, Thailand, India, Maldives, Myanmar, Bangladesh, Somalia, Tanzania, Kenya and Yemen. The earthquake epicenter is located where the Indian Plate subducted under the Burma Plate. This tsunami event has raised the awareness of many people. Today, several tsunami numerical models have been developed to model and forecast tsunami events in the future. This paper reviews five tsunami numerical models namely TUNA, TUNAMI, COMCOT, MOST and ANN Tsunami Forecast. Most of these models have been used by other researchers to perform tsunami simulation based on Sumatera-Andaman tsunami event. Each model have their own similarities, differences and limitations. A non-mathematically intensive approach is employed to choose a suitable tsunami numerical model for the case study in Malaysian offshore areas. Future studies will be conducted using one of the tsunami numerical models.

Keywords Tsunami · Tsunami Numerical Model · Sumatera-Andaman

N.H. Mardi (✉) · M.A. Malek
Department of Civil Engineering, College of Engineering,
Universiti Tenaga Nasional, Kajang, Malaysia
e-mail: nurulhanimardi@gmail.com

M.A. Malek
e-mail: Marlinda@uniten.edu.my

M.S. Liew
Faculty of Geoscience and Petroleum Engineering,
Universiti Teknologi Petronas, Tronoh, Malaysia
e-mail: shahir_liew@petronas.com.my

H.E. Lee
Offshore Engineering Centre, Universiti Teknologi Petronas, Tronoh, Malaysia
e-mail: aaronlhe@gmail.com

1 Introduction

The term ‘tsunami’ originates from a Japanese word defined as a wave that undergoes height and velocity amplification as the wave enters a harbour [1]. It has a short wave period and long wavelength characteristics [2]. Therefore it can travel very fast towards coastal shoreline with massive energy to devastating effects. Tsunami is considered as a major coastal catastrophe, it has the potential to desolate the surrounding coasts within the tsunami source point. Tsunami waves can be generated by seaquakes, submarine landslide, and impact of large objects such as asteroids to the sea surface [1]. There are three stages of tsunami processes which are tsunami generation, tsunami propagation and tsunami run-up and inundation.

The tsunami event starts with the tsunami generation. A seaquake in the deep ocean will create a sudden movement on the tectonic plate. The energy that is released from the hypocenter will be transferred to the surrounding waters. It should be noted that tsunamis gather their energies mainly from vertical plate movement in a seaquake event, although horizontal submarine landslides may also contribute to the mix. This excitation as evident from the 2004 Indian Ocean Tsunami, can amount to that of comparable with 32,000 atomic bombs of Hiroshima size [3]. The sudden release of such enormous energy will cause a considerable initial water disturbance on the water–air interface.

This initial process is called the initial condition or tsunami initial vertical displacement. Upon tsunami generation, the tsunami wave will then propagate across the sea in all directions. Usually tsunami occurrences in the open sea are difficult to be detected in large water depths where the tsunami travels unnoticed to many owing to its small height, large wavelength and hence, low steepness as compared to the existing stochastic wind waves. As this tsunami wave approach the shore line, the tsunami wave height and turbulence will increase rapidly. The height increment in shallow water can be approximately described by Green’s Law shown in Eq. 1.

$$\frac{h_c}{h_o} = \left(\frac{d_o}{d_c}\right)^{1/2} \quad (1)$$

where h_o and h_c are tsunami height at offshore area and coastal area, d_o and d_c are the corresponding water depth at the offshore area and coastal area.

Malaysia is a country located in South East Asia. It is situated on the Eurasian plate where there are many daily seismic activities. They occur due to instability of respective plates. On certain unfortunate occasions, this instability could lead to the occurrences of earthquakes. When an earthquake occurs, it has the possibility of causing a tsunami event. Most of the countries surrounding the source point will be affected, although the extent of effect will vary from different locations. Malaysia has experienced the tsunami due to Sumatera-Andaman earthquake in 2004. Figure 1 shows the location of Sumatera-Andaman tsunami. The tsunami event has recorded 800 km fault length and 85 km fault width with 11 m vertical displacement. Malaysia recorded a total of 68 deaths at the coastal areas of north Malaysia during that event [1].



Fig. 1 Location of Sumatra-Andaman tsunami

2 Tsunami Numerical Model

This conceptual review aims to choose a suitable tsunami numerical model for use in Malaysian offshore areas. Currently, there are several tsunami numerical models available. All of these models include tsunami generation, propagation, run-up and inundation. The study will focus on reviewing the various numerical models from a non-mathematically intensive perspective rather than commercial tsunami models like that of COOLWAVE, FUNWAVE and MIKE21. Numerical models are preferred since the algorithm used can be viewed in its entirety, studied and tailored to various case studies in Malaysia. In this paper five tsunami numerical models will be reviewed. Most of these models have been employed by others researcher in the studies of Sumatra-Andaman tsunami. Result produced between these models have been compared for benchmarking purposes. The numerical models are as discussed in the following sub sections.

2.1 Method of Splitting Tsunami (MOST)

This model was developed by Titov from Pacific Marine Environmental Laboratory (PMEL) and Synolakis from the University of Southern California. This is a

standard model used by NOAA Centre Tsunami Research (NCTR), which is part of the National Oceanic and Atmospheric Administration (NOAA) organisation. In a past study, Titov and Gonzalez [4] was used MOST for tsunami simulation in the Pacific Ocean. This tsunami event is generated from a source near Alaska. The tsunami run-up ends at the Hawaiian shoreline. Results from this model are used to develop tsunami hazard mitigation tools for the Pacific Disaster Center (PDC) [4]. MOST can be used to simulate three processes of tsunami which are the generation, transoceanic propagation and inundation of dry land. The MOST model is capable of generating tsunami caused by earthquake.

Elastic deformation theory had been used to generate the tsunami wave. During the deformation phase, MOST is used to calculate the contribution of dislocation of a given region at the sea floor. This will generate an initial tsunami wave front [5]. In the propagation phase, MOST uses numerical dispersion scheme and non-linear shallow (NSW) equation in spherical coordinates taking into account the Coriolis effect. The output for the propagation phase are wave height, zonal and meridional velocities. All the outputs will be used during as the initial and boundary conditions for inundation phase [5]. The inundation phase will characterize the tsunami behavior at the shoreline including the tsunami run-up. At this phase, there will be a depth-integrated of NSW wave equations on a set of nested Digital Elevation Model (DEM) grids, and a run-up algorithm. This is performed to predict onshore flooding. The outputs of inundation phase are the respective wave height, zonal velocity, and meridional velocity alongside associated run up values [5].

2.2 Cornell Multi-Grid Couple Tsunami Model (COMCOT)

COMCOT was developed by Professor P.L.-F. Liu at Cornell University, USA. COMCOT is able to study the process of tsunami, including its generation, propagation, run-up and inundation. Compared with other models, COMCOT has implemented multiple tsunami generation sources; for example, transient faulting, landslides, water surface disturbances or wave maker [6]. All these sources can generate tsunami propagation in different ways. During tsunami generation, COMCOT used elastic dislocation theory by Maninsha and Smylie and Okada. For tsunami propagation, run-up and inundation, this model employs the linear and nonlinear Shallow Water Equation theory. Both theories can be used in Spherical or Cartesian coordinate systems [6]. To solve the Shallow Water Equation theory, COMCOT adopts the Leap-Frog finite difference schemes.

COMCOT is considered as one of the establish tsunami numerical model. It has been used in many regional studies such as in Singapore [7, 8], Taiwan [9], Brunei [10] and China [11]. In 2006, Wang and Liu [12] has conducted an analysis of 2004 Sumatra earthquake fault plane mechanism and Indian Ocean tsunami. The study objective is to compare the satellite data with numerical simulation using different fault plane model. There were two fault planes proposed namely, transient fault plane and impulsive fault plane. A series of numerical simulations for tsunami

generation and propagation was performed using COMCOT at the Bay of Bengal. The satellite data is obtained from two satellites located at the Bay of Bengal during the 2004 tsunami event. Results comparison revealed that, the transient fault plane shows very good correlation with the satellite measurement. The output from the impulsive fault plane model also showed good correlation with satellite measurements, however, only after an additional fine tuning step which involves an inverse method to minimize the errors incurred in the sea surface elevation.

2.3 TUNA model

Teh. S.Y. and Koh. H.L. from Universiti Sains Malaysia (USM) developed TUNA model in 2005. TUNA is an in-house tsunami model developed in Malaysia. It can simulate all processes in a tsunami event, which include generation, propagation, run-up and inundation. The TUNA model consists of two parts: (1) generation and propagation (TUNA-M2); (2) run-up; and inundation (TUNA-RP). TUNA model utilizes the Okada equation for tsunami sources generation due to an earthquake. Linear Shallow Water Equation (SWE) is applied at tsunami wave propagation process as recommended by the Intergovernmental Oceanography Commission [13]. The linear SWE is discretized by employing the explicit finite difference method and staggered scheme [1]. However, for tsunami run-up and inundation, a non-linear SWE is used.

In 2009, Koh et al. [14] conducted a study entitled ‘Simulation of Andaman 2004 tsunami for assessing impact on Malaysia’. The purpose of study is to simulate the 26 December 2004 Andaman tsunami using TUNA. The tsunami simulated include all of the tsunami process (generation, propagation and inundation). The result produced by TUNA was compared with the result produce by COMCOT model and on-site survey result. At the end it showed that the TUNA model shows good correlation and performance, when benchmarked against COMCOT. TUNA also has been used to successfully perform tsunami simulations in waters such as the Indian Ocean [15], Straits of Malacca [16], Andaman Sea [2, 14] and South China Sea [1, 17].

2.4 Tohoku University Numerical Analysis Model for Investigation of Nearfield Tsunami No.2 (TUNAMI-N2)

Professor Dr Fimihiko Imamura from Disaster Control Research Centre at Tohoku University, Japan developed TUNAMI-N2 source code beginning from year 1995. TUNAMI-N2 is known as one of the TUNAMI models. TUNAMI used the linear theory for deep sea, the shallow water theory in shallow area and run-up on land with constant grids [18]. The model uses staggered Leap-Frog scheme to solve the

Shallow Water Equations in shallow and deep sea. In Malaysia, TUNAMI is well known since this model had been used by Malaysian Metrological Department (MMD). There are many studies performed using the TUNAMI model such as studies in Sabah waters [19, 20], South China Sea [21], Sulu Sea [22, 23], Celebes Sea [22] and Gulf of Thailand [24].

Shaari et al. [25] has performed tsunami simulation using the TUNAMI model generated by the Sumatra-Andaman earthquake. A nonlinear SWE had been applied in the TUNAMI model. The tsunami simulation was performed according to three different source models. During tsunami propagation, it was found that tsunami wave height resulting from Model 1 have similar to the one reported by Koh et al. [14]. The result of this simulation was also compared with tidal gauge data collected from Langkawi and Penang tidal stations. It is was found that the simulated wave-forms and observed data generally follow the same pattern for Model 1.

2.5 Artificial Neural Network (ANN)

Artificial Neural Network (ANN) is one of the branches in the Artificial Intelligence (AI) method that can be used to solve various problems. Several researches were conducted on tsunami forecasting and prediction using ANN. Basically ANN model is an enhanced tsunami model developed for special purposes. The advantage of using ANN is its effectiveness when capturing the so called system identity and mapping the input and output relationship. Moreover, ANN has the ability to represent both linear and nonlinear relationships and learn, through corrective iterations, the relationship from raw data.

Romano et al. [26] used ANN to conduct a study about tsunami forecasting. The purpose of this study is to forecast tsunami time arrival and maximum tsunami wave height. The input data include the size of earthquake and historical locations. There were two study areas, first area covers the Indian Ocean, Andaman Sea and Singapore waters where the earthquake is generated from Sunda Arc. The second area covers South China Sea and Singapore waters where the tsunami is generated from Manila trench. ANN is able to resemble data produced by another model, which is TUNAMI-N2-NUS. As a result, TUNAMI-N2-NUS and ANN similar wave height and time arrival.

3 Discussion

Five models have been reviewed in this paper. Table 1 shows the summary of five tsunami numerical models used in Sumatra-Andaman tsunami case study. All the numerical models are summarised in terms of model type, techniques and outcomes. It is found that, all models are capable to perform tsunami simulation at all the three main stages (tsunami generation, propagation, runup and inundation). It is

Table 1 Summary of tsunami numerical models

Tsunami numerical model	Techniques		Outcome
	Tsunami generation	Tsunami and run-up	
Method of splitting tsunami (MOST)	Elastic deformation theory	Non-linear shallow water equation discretized using: Spitting Method	<ul style="list-style-type: none"> – Wave height – Wave velocity – Time of arrival
Cornell multi-grid couple tsunami model (COMCOT)	Linear elastic dislocation theory and Okada equation	Shallow water equation discretized using: Leap-Frog scheme	<ul style="list-style-type: none"> – Wave height – Wave velocity – Time of arrival
TUNA model (i) TUNA-M2 (ii) TUNA-RP	Okada equation	Shallow water equation discretized using: explicit finite difference method and staggered scheme	<ul style="list-style-type: none"> – Wave height – Wave velocity – Time of arrival
Tohoku University numerical analysis model for investigation of nearfield tsunami (TUNAMI)	Okada equation	Shallow water equation discretized using: Leap-Frog scheme	<ul style="list-style-type: none"> – Wave height – Wave velocity – Time of arrival
Artificial neural network (ANN)	<ul style="list-style-type: none"> – Multilayer back propagation – Feed forward back propagation – Generalized regression neural networks 		<ul style="list-style-type: none"> – Tsunami travel time – Max. wave height – Tsunami run-up

noted too, that all these tsunami numerical models were capable to simulate tsunami due to earthquake. Nevertheless, COMCOT stands out to be more advanced due to its ability to perform advance tsunami source generation such as transient faulting, landslides, water surface disturbances or wave maker.

In terms of tsunami generation technique, most of these models utilized the Okada equation except for MOST. MOST utilizes elastic-plastic model at its generation process. COMCOT utilizes a linear-elastic dislocation theory alongside the Okada equation. Such techniques are widely used to simulate ground deformation produced by tectonic faults (earthquakes). The various theories discussed share rather similar input requirements like that of fault parameters in order to simulate tsunami source generation due to an earthquake event. Such parameters include but are not limited to fault length, fault width, fault displacement, focal depth, dip angle, strike angle and rake angle.

Most of models in this review has utilized Shallow Water Equation (SWE). The SWE are derived from Navier-Stoke equation. The equation has been applied as recommended by the Intergovernmental Oceanography Commission (IOC). Equations 2, 3 and 4 show the governing equations of SWE.

$$\frac{\partial h}{\partial t} + \frac{\partial(uh)}{\partial x} + \frac{\partial(vh)}{\partial y} = 0 \quad (2)$$

$$\frac{\partial(uh)}{\partial t} + \frac{\partial(u^2h + \frac{1}{2}gh^2)}{\partial x} + \frac{\partial(uvh)}{\partial y} = 0 \quad (3)$$

$$\frac{\partial(uh)}{\partial t} + \frac{\partial(uvh)}{\partial x} + \frac{\partial(v^2h + \frac{1}{2}gh^2)}{\partial y} = 0 \quad (4)$$

where x , y and t are independent variable. Height h is dependent variable respect to water displacement and velocities u and v in x - and y -directions [27]. SWE can be divided into linear Shallow Water Equation and non linear Shallow Water Equations. Linear Shallow Water Equation is largely used for tsunami propagation and non linear Shallow Water Equation is used for tsunami wave run-up. Generally, all model utilized non linear SWE in tsunami wave propagation and run-up process.

To solve the SWE, TUNA utilizes explicit finite difference method with staggered scheme. Meanwhile, TUNAMI and COMCOT used Leap-Frog Scheme and MOST used the spitting method. In term of outcome, all of these five model would generate a similar output which are, tsunami wave height, wave velocity and time arrival. From the review, the author found that TUNAMI and COMCOT could be considered as an establish model, since it is one of the earliest model developed in this field. Besides, these model has been use widely by others researcher to performed tsunami simulation.

Meanwhile, the author found that ANN tsunami forecasting model is an enhanced model. It has applied the multilayer back propagation, feed forward back propagation and generalized regression neural networks technique for various learning processes to simulate and forecast tsunamis. The limitation of ANN model is that it requires long term and somewhat reliable data in order to perform data training, testing and validating. Studies have shown that the data-driven approach using ANN is effective and efficient. This model to date also produces outputs in terms of tsunami wave height and time of arrival.

Another important factor in numerical model is the computational period. TUNA would have less computational time requirements as compared to other models since the model is somewhat optimized for a single cause of tsunami generation which is earthquake. It also utilizes linear Shallow Water Equations in propagation which significantly reduces computational effort therein as compared to a nonlinear model. The author infers that a modularized algorithm would have better efficiency that which is evident in TUNA which is divided into two part namely, TUNA-M2 (tsunami generation and propagation) and TUNA-RP (tsunami run-up and inundation). Other tsunami simulation models require longer computational time since the overall tsunami process is not simulation separately as compared to TUNA model. It is with these consensus and discussion that it is inferred that TUNA is most well suited to simulate tsunamis affecting Malaysian offshore areas.

4 Conclusion

This paper described and compared five tsunami numerical models namely MOST, COMCOT, TUNA, TUNAMI and ANN Tsunami Forecast. These models have been widely used by many researchers to perform tsunami numerical simulation. Having done some comparison between these five models, the author discussed their respective pros and cons. TUNA is a tsunami model developed in Malaysia utilizing both linear and nonlinear SWE discretized using a staggered finite difference scheme with Okada's generation equations. It has the ability to generate tsunami waves due to seaquakes. The author chose the TUNA model for use in further studies to perform tsunami simulation in the vicinity Malaysian offshore areas, flanking the South China Sea and Sulu Sea. This is regards to TUNA's computational efficiency with acceptable accuracy based on sound theory and the fact that the model is developed in house Malaysia which suggests ease of availability to the author. TUNA has also been proven to be comparably consistent with the other models. This future study will investigate the tsunami occurrences due to earthquakes from Manila Trench and Sulu Trench and their impact on the Malaysian offshore areas. The expected outcome would be maximum tsunami wave height, tsunami wave velocity and tsunami time arrival and is anticipated to heighten the knowledge and awareness of tsunami hazards for Malaysian offshore and coastline areas.

Acknowledgments The authors wish to express acknowledgement and sincere gratitude to Universiti Teknologi Petronas and Yayasan Universiti Teknologi Petronas (YUTP) and Petronas Carigali Sdn Bhd for the collaboration and financial support.

References

1. S.Y. Teh, H.L. Koh, Tsunami simulation for capacity development, in Proceedings of the International Multi Conference of Engineers and Computer Scientists 2011, IMECS 2011, vol II, Hong Kong, 16–18 March 2011
2. S.Y. Teh, H.L. Koh, A.I. Md Ismail, Modeling tsunami runup and inundation due to the Andaman Tsunami along beaches in Malaysia and Thailand, in Proceeding of the 2nd IMT-GT 2006 Regional Conference on Mathematics, Statistics and Applications, Malaysia, 2006
3. G. Tom, *Oceanography—An Invitation to Marine Science*, 7th edn. (Cengage Learning, Canada, 2009)
4. V.V. Titov, F.I. Gonzalez, Implementation and testing of the Method of Splitting Tsunami (MOST) model, US Department of Commerce, National Oceanic and Atmospheric Administration, Environmental Research Laboratories (Pacific Marine Environmental Laboratory, Seattle, 1997)
5. Method of Splitting Tsunami (MOST) Software Manual, USA: The National Oceanic and Atmospheric Administration (NOAA), 2006
6. X.M. Wang, User Manual for COMCOT Version 1.7 (First Draft), Ithaca (Cornell University, NY, 2009)
7. K. Megawati, F. Shaw, K. Sieh, Z. Huang, T.-R. Wu, Y. Lin, S.K. Tan, T.-C. Pan, Tsunami hazard from the subduction megathrust of the South China Sea: Part I. Source characterization and the resulting tsunami. *J. Asian Earth Sci.*, **36**, 13–20 (2009)

8. Z. Huang, T.-R. Wu, S.K. Tan, K. Megawati, F. Shaw, X. Liu, T.-C. Pan, Tsunami hazard from the subduction Megathrust of the South China Sea: Part II. Hydrodynamic modeling and possible impact on Singapore. *J. Asian Earth Sci.*, **36**, 93–97 (2009)
9. T.-R. Wu, H.-C. Huang, Modeling tsunami hazard from Manila trench to Taiwan. *J. Asian Earth Sci.*, **36**, 21–28 (2009)
10. M.F. Chai, T.L. Lau, T.A. Majid, Potential impacts of the Brunei Slide tsunami over East Malaysia and Brunei Darussalam. *Ocean Eng.* **81**, 69–76 (2014)
11. Y. Liu, A. Santos, S.M. Wang, Y. Shi, H. Liu, D.A. Yuen, Tsunami hazards along Chinese coast from potential earthquake in South China Sea. *Phys. Earth Planet Inter.* **163**, 233–244 (2007)
12. X. Wang, P.L.-F. Liu, An analysis of 2004 Sumatra earthquake fault plane mechanisms and Indian Ocean tsunami. *J. Hydraul. Res.* **00**, 1–8 (2006)
13. Numerical Method of Tsunami Simulation with the Leap Frog Scheme, 1, Shallow Water Theory and Its Difference Scheme in Intergovernmental Oceanographic Commission (IOC), Intergovernmental Oceanographic Commission, UNESCO, Paris 1997, pp. 12–19
14. H.L. Koh, S.Y. Teh, P.L.-F. Liu, A.I. Md. Ismail, H.L. Lee, Simulation of Andaman 2004 tsunami for assessing impact on Malaysia. *J. Asian Earth Sci.*, **36**, 74–83 (2009)
15. K.L. Cham, S.Y. Teh, H.L. Koh, A.I. Md Ismail, Numerical simulation of the Indian Ocean tsunami by TUNA-M2, in *Proceeding of the 2nd IMT-GT 2006 Regional Conference on Mathematics, Statistic and Application*, Malaysia (2006)
16. H.L. Koh, S.Y. Teh, L.M. Kew, N.A. Zakaria, Simulation of future Andaman tsunami into Straits of Malacca by TUNA. *J. Earthq. Tsunami* **3**(02), 89–100 (2009)
17. S.Y. Teh, H.L. Koh, Simulation of tsunami due to the Megathrust in South China Sea, in *Proceedings of the 2013 3rd International Conference on Environmental and Computer Science (ICES 2010)*, Kunming, China, 18–19 Oct 2010
18. F. Imamura, A.C. Yalciner, G. Ozyurt, *Tsunami modelling manual*, UNESCO IOC International Training Course on Tsunami Numerical Modelling (2006)
19. Z. A. Mokhtar, F. Imamura, S. Koshimura, Study on appropriate modeling of tsunami in Malaysia for risk evaluation. *Bulletin of the International Institute of Seismology and Earthquake Engineering* (2007)
20. S.N. Basri, Y. Fujii, B. Shibazaki, H. Yanagisawa, Study on tsunami inundation simulation in the northwestern coastal of Sabah, Malaysia. *Bulletin of the International Institute of Seismology and Earthquake Engineering* (2012)
21. F.Z. Saleh, Y. Fujii, B. Shibazaki, Updating Numerical Simulation for Tsunami Forecasting Database considering sources along the Manila Trench. *Bulletin of the International Institute of Seismology and Earthquake Engineering* (2011)
22. M. Aziz, B. Shibazaki, Y. Fujii, Tsunami Numerical Simulation Around Sulu Sea and Celebes Sea. *Bulletin of the International Institute of Seismology and Earthquake Engineering* (2011), pp. 1–50
23. N. I. Nurashid, S. Bunichiro, F. Yushiro, Y. Hideaki, Tsunami Inundation Modeling along the East Coast of Sabah, Malaysia for Potential Earthquakes in Sulu Sea. *Bulletin of the International Institute of Seismology and Earthquake Engineering* (2013), pp. 127–132
24. A. Ruangrassamee, N. Saelem, Effect of tsunami generated in the Manila trench on the Gulf of Thailand. *J. Asian Earth Sci.*, **36**, 56–66 (2009)
25. N.A. Shaari, Y. Fujii, H. Yanagisawa, Validation of tsunami inundation modeling for the 2004 Sumatra-Andaman earthquake for making hazard maps in Penang and Langkawi, Malaysia. *Bullet. IISEE* **47**, 121–126 (2013)
26. M. Romano, S.-Y. Liang, M.T. Vu, P. Zemskey, C.D. Doan, M.H. Dao, P. Tkalich, Artificial neural network for tsunami forecasting. *J. Asian Earth Sci.* **36**(1), 29–37 (2009)
27. C. Moler, Chapter 18: shallow water equations. *Experiments with MATLAB, math works [Online]*. Available: <http://www.mathworks.com/moler/exm1/chapters.html>. Accessed 12 Sept 2014

Heavy Metal Removal Using *Cabomba Caroliniana* as Submerged Vegetation Species in Constructed Wetland

A.K. Nur Fadzeelah, J. Lynna Juliana
and A. Muhammad Habibuddin

Abstract Recently, Constructed Wetlands (CWs) has become an option of low-cost and alternative treatment for removing heavy metal such as lead, copper and cadmium in wastewater. In this study, the aim was to determine the feasibility of *Cabomba Caroliniana* as a submerged vegetation species used in the CWs system in removing of copper from this kind of wastewater. A laboratory scale of Subsurface Flow System (SSF) as one of CWs types was set up outdoor and all the experiments had been run for consecutive 40 days. An artificial pollutant used was copper sulphate aqueous ($\text{CuSO}_4 \cdot 5\text{H}_2\text{O}$) with the concentration of 5 ppm. Meanwhile, five parameters had been studied which were pH, biological oxygen demand (BOD), chemical oxygen demand (COD), total solids and copper ion concentration. The results showed that the *Cabomba Caroliniana* in SSF of CWs system had a great potential in heavy metal removal from the decrease pattern shown in BOD, COD, total solid and copper ion concentrations (Cu^{2+}).

Keywords *Cabomba Caroliniana* · Constructed Wetlands · Subsurface Flow System · Copper ions

1 Introduction

The increasing use of metals and chemicals in process industries has resulted in generation of large quantities of effluent that contain high level of toxic heavy metals and their presence poses environmental-disposal problems as they are not

A.K. Nur Fadzeelah (✉)
Faculty of Chemical Engineering, UiTM Kampus Pasir Gudang,
81750 Masai, Johor, Malaysia
e-mail: nurfadzeelah122@ppinang.uitm.edu.my

J. Lynna Juliana · A. Muhammad Habibuddin
Faculty of Chemical Engineering, Universiti Teknologi MARA,
40450 Shah Alam, Selangor, Malaysia

non-degradable and tends to accumulate in living organisms [1]. Besides they are toxic and carcinogenic. The common toxic heavy metals found in industrial wastewater include zinc, copper, nickel, mercury, cadmium, lead and chromium [1–2]. Conventional treatment technologies for removal of heavy metal from wastewater such as precipitation, membrane filtration, ion exchange, and adsorption are very non economical. It is due to all these methods are non-destructive which only generates secondary secondary wastes such as toxic chemical sludge [2]. Hence, more efficient and low-cost of treatment process need to be identified which could overcome such drawbacks.

Constructed wetlands (CWs) have been widely proposed as it offers an efficient treatment technology with minimum inputs, low investment costs, low operating costs and no external energy input [3]. Besides, they are used not only to degrade organic substances and nutrients from municipal sewage, storm water, and agricultural runoff but also to remove metals from mining effluent and special industrial wastewater [4].

Other than the selection of plant species, various factors such as geographical distribution, climate and habitat conditions, wastewater composition, availability of the plants in nurseries, long term maintenance and agronomic management costs, and project aims, are considered as important criteria that need to take into consideration while designing a CW [5]. Previous studies have noted that plants enhance treatment efficiency, not only by taking up nitrogen and heavy metals as nutrient from wastewater but also constituting a favorable environment for the development of a microbial population [6–7]. Nevertheless, the vegetation species need to survive the potentially toxic effects of the effluent and its variability. Therefore the choice of vegetation species is important issue in CWs [8]. In this study, *Cabomba Caroliniana* has been introduced as a vegetation species in the Subsurface Flow (SSF) System of CWs. The aim was to determine the feasibility of *Cabomba Caroliniana* as a submerged vegetation species used in the CWs system in removing of copper from heavy metal wastewater.

2 Materials and Methods

2.1 Chemicals and Materials

The vegetation species used in this study was *Cabomba Caroliniana* which also known as *Carolina Fanwort*. The plant has an average of stem length of 15 cm each. Prior to the experiment, the plant was nurtured for three weeks with supplement of liquid fertilizer as the source of nutrient and approximately 400 g of this plant was used for two units of CWs.

In addition, natural and pebble rocks were used in every unit of CWs. The natural rock was acting as a supporting medium for the soft-stemmed of *Cabomba Caroliniana* while the pebble rock was used to increase the stabilization of this

vegetation species. In this study, copper sulphate aqueous ($\text{CuSO}_4 \cdot 5\text{H}_2\text{O}$) was chosen as the artificial pollutant for heavy metal wastewater with the initial concentration of 5 ppm.

2.2 Experimental Set Up

A laboratory scale of SSF as one of CWs types was set up in this study. Treatment tank, which served as the cell of CWs are made from Perspex material with the dimension of 30 cm \times 40 cm \times 50 cm (w \times l \times h). Besides treatment tank, this system comprised the following components: (a) circulation tank (b) pump; to recycle the water sample from outlet to inlet treatment tank (c) aerator; to supply the sufficient oxygen for the vegetation species and (d) water conduit; to connect and circulate the water sample from one component to another component.

Ten points of vegetation coordinate with 10 cm distance between two points had been set up in the treatment tank. In order to investigate the feasibility of *Cabomba Caroliniana* in treating the artificial pollutant, blank unit; the unit without the artificial pollutant, were studied as a reference for polluted unit.

2.3 Experimental Procedure

The experiment was conducted from 24th January until 4th March of 2013 and it had been performed outdoor with the units were placed under shady conditions. All the units were run continuously for consecutive 40 days where the influents were circulated throughout the experiment. A volume of 500 to 600 mL of samples volume was withdrawn from both units at approximately 2.00 p.m.–2.30 p.m. with a sampling interval of every five days. The samples then were preserved in a freezer at 4 °C prior to the analysis.

2.4 Analytical Methods

All the collected samples were analyzed for biochemical oxygen demand (BOD), chemical oxygen demand (COD), total solid (TS) and copper ion concentration. For pH parameter, the value was determined in situ with portable pH meter of Mettler Toledo sevenGo.

BOD was measured using Dilution Method which referred to Method 8043 of HACH method number (adapted from Klein and Gibbs [9]). Meanwhile, COD was measured using Dichromate Reactor Digestion Method test. This method had been

simplified over the Dichromate Reflux method. The Dichromate Reflux method is based on the requirement of two main official sources for chemical analysis in water and wastewater; Clesceri et al. [10] and EPA Methods and Guidance for Analysis of Water, version 2.0. The reference method number for Clesceri et al. [10] and EPA were 5220D and 410.4, respectively. While for the analysis procedure, the Colorimetric method for specific range of 0–1,500 mg/L were applied using spectrophotometer (HACH, DR2800).

For total solid analysis, Gravimetric Method (2540B) which was adapted from Clesceri et al. [10] had been applied in this study. Meanwhile for determining of trace copper ion (Cu^{2+}) concentration, Inductively Couple Plasma-Optical Emission Spectrometry (ICP-OES) (Thermo Scientific, iCAP 6000) had been used.

3 Results and Discussion

3.1 pH Analysis

Figure 1 displays the pH profile for polluted and blank units versus days. The average pH of both polluted and blank units showed the same range which was from 7.50 to 8.24. The small differences values for maximum and minimum pH show that the pH was consistent throughout the experiment. This result was supported by Díaz et al. [11], which the average pH of CWs was from 7.50 to 8.60.

3.2 BOD Analysis

Figure 2 and Table 1 show the pattern of BOD concentrations for both units versus days and the percentage of BOD and COD removal at day 40, respectively. This figure shows the highest and the lowest of BOD concentrations are 3.66, 0.63 and

Fig. 1 pH profile for polluted and blank units versus days

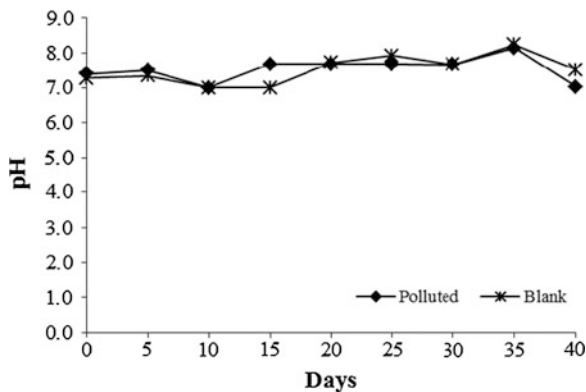


Fig. 2 BOD concentration pattern for polluted and blank units versus days

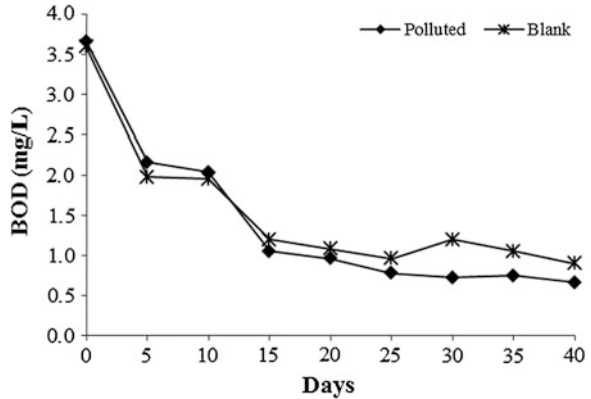


Table 1 The percentage of BOD and COD removals after 40 days

Parameter	Polluted unit			Blank unit		
	Day 0 (mg/L)	Day 40		Day 0 (mg/L)	Day 40	
		(mg/L)	(%)		(mg/L)	(%)
BOD	3.66	0.66	81.9	3.59	0.90	74.9
COD	64	18	71.9	23	10	56.5

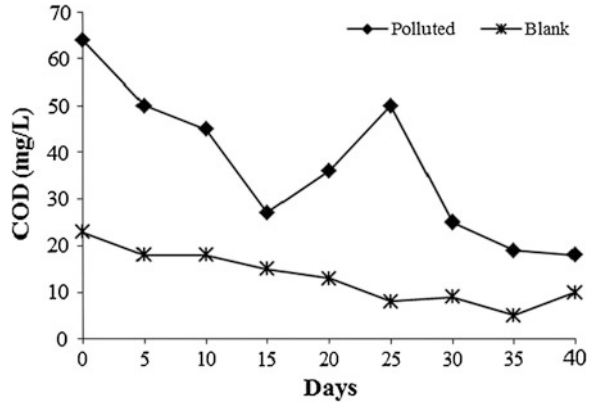
3.59, 0.90 mg/L for polluted unit and blank unit, respectively. From these values, the initial BOD concentrations for both units exhibited a close value although the blank unit was not contained any pollutant compound. This result was similar with Headley et al. [12], which reported that a smaller amount of BOD removal in CWs might be due to the slow of decomposition of organic solids accumulated within the substrate interstices. Meanwhile, the removal efficiency of BOD in polluted unit (81.9 %) was higher than in the blank unit (74.9 %) as shown in Table 1.

Meanwhile for the graph pattern, the BOD concentration for both units decreased gradually for the first 15 days and became slightly decreased until day 25. Then, the BOD concentrations showed a constant pattern until day 40. This finding was supported by Ayaz [13] which mentioned that the extended detention time can decrease in the BOD removal performances in the CWs system.

3.3 COD Analysis

Figure 3 illustrates the pattern of COD concentrations for both units versus days. For the polluted unit, this figure has a similar pattern with BOD concentration pattern where the gradual decrement can be seen from day 1 until day 15. However, this pattern was started to increase from day 15 for 10 days and was decreased until

Fig. 3 COD concentration pattern for polluted and blank units versus days



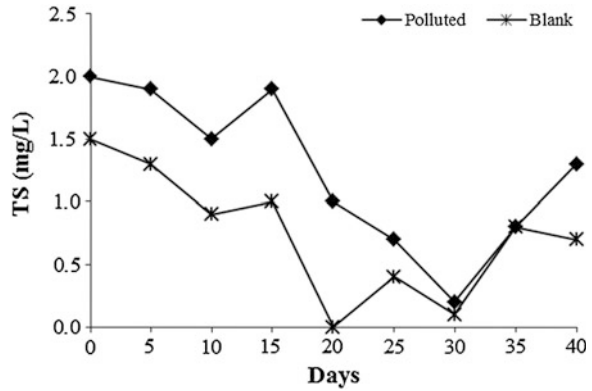
day 40. In contrast with the blank unit, the figure demonstrates the consistent decrement pattern throughout the experiment.

In general, this figure shows that the patterns of COD concentration for both units were reduced until day 40 to 74.9 and 56.5 % for polluted and blank units, respectively as shown in Table 1. The result was supported by Maine et al. [8] which the COD largely decreased in the wetland effluent. Meanwhile, fluctuate behavior for polluted unit was due to the wide fluctuation in the influent concentration might be attributed to marked variation observed in the substrate removal efficiency [14].

3.4 Total Solid Analysis

Figure 4 illustrates the amount of total solids for both units versus days. The total solid pattern for both units showed the same behavior throughout the experiment, which gradually decreased from day 1 until day 30. It can be shown that the concentration of total solid were reduced significantly due to the removal of total solid for polluted and blank units which were 90.0 and 93.3 %, respectively. It might be due to the leaves feature of *Cabomba Caroliniana* for which the sediments are trapped through the vegetation. Besides, the gravity sedimentation also causes the total suspended solids separation with the benefit of gravel's existence which filters most of the suspended solids [15]. However, the graph patterns for both units were radically increased after day 30. This might be due to the rate of the decaying of the plant tissue in the water sample after day 30 since the roots of submerged plant will trap the solid in the sedimentation process [16].

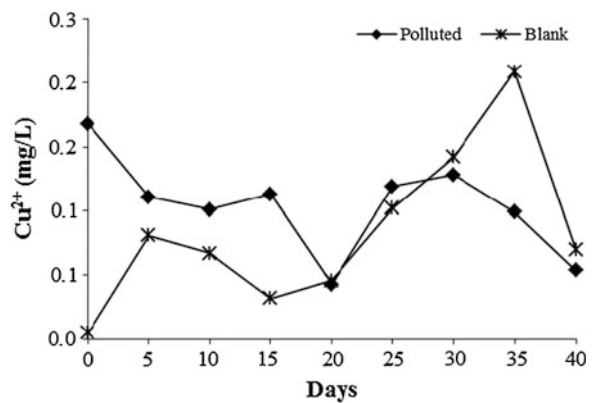
Fig. 4 Total solid concentration pattern for polluted and blank units versus days



3.5 Copper Ion Analysis

The concentration of copper ions is shown in Fig. 5 which both units exhibited the same trend of graph pattern. The pattern was gradually decreased from day 1 until day 20 which demonstrated that the ability of the used of submerged plant in removing heavy metals may be due to their uptake with water absorption and accumulation in plants tissues or through metal precipitation [17]. However, after day 20, both units demonstrated a wide fluctuating behavior of copper ion concentration in the CWs system. In an article by Zhang et al. [18], they reported that the fluctuation occurs in might be due to the evaporation of water and the present of other contaminant in the wastewater sample.

Fig. 5 Copper ions (Cu^{2+}) concentration profile for polluted and blank units versus days



4 Conclusion

Form this study, it can be summarized that *Cabomba Caroliniana* in SFF of CWs system had a great potential in heavy metal removal from the decrease pattern of BOD, COD and total solids concentrations. However, for overall performance this summary can only be made for the treatment duration from day 1 until day 20 due to the decaying process of vegetation species.

Acknowledgments The authors wish to thank Universiti Teknologi MARA (UiTM) for funding this project under Dana Kecemerlangan Research Fund.

References

1. S. Ahluwalia, D. Goyal, Microbial and plant derived biomass for removal of heavy metals from wastewater. *Bioresour. Technol.* **98**(12), 2243–2257 (2007)
2. F. Fu, Q. Wang, Removal of heavy metal ions from wastewaters: a review. *J. Environ. Manage.* **92**(3), 407–418 (2011)
3. A.S. Sheoran, V. Sheoran, Heavy metal removal mechanism of acid mine drainage in wetlands: a critical review. *Miner. Eng.* **19**(2), 105–116 (2006)
4. S. Cheng, W. Grosse, F. Karrenbrock, M. Thoennesen, Efficiency of constructed wetlands in decontamination of water polluted by heavy metals. *Ecol. Eng.* **18**, 317–325 (2002)
5. C. Leto, T. Tuttolomondo, S. La Bella, R. Leone, M. Licata, Effects of plant species in a horizontal subsurface flow constructed wetland—phytoremediation of treated urban wastewater with *Cyperus alternifolius* L. and *Typha latifolia* L. in the West of Sicily (Italy). *Ecol. Eng.* **61**, part A(0), 282–291 (2013)
6. D. Zhu, C. Sun, H. Zhang, Z. Wu, B. Jia, Y. Zhang, Roles of vegetation, flow type and filled depth on livestock wastewater treatment through multi-level mineralized refuse-based constructed wetlands. *Ecol. Eng.* **39**, 7–15 (2012)
7. A.M. Ray, R.S. Inouye, Development of vegetation in a constructed wetland receiving irrigation return flows. *Agric. Ecosyst. Environ.* **121**(4), 401–406 (2007)
8. M.A. Maine, N. Suñe, H. Hadad, G. Sañchez, C. Bonetto, Influence of vegetation on the removal of heavy metals and nutrients in a constructed wetland. *J. Environ. Manage.* **90**, 355–363 (2009)
9. R.L. Klein, C. Gibss, Standard method for examinations of water and wastewater. *J. Water Pollut. Control Fed.* **51**(9), 2257 (1979)
10. L.S. Cleseri, A.E. Greenberg, A.D. Eaton, *Standard Methods for the Examination of Water and Wastewater*, 20th edn. APHA (American Public Health Association), AWWA (American Water Works Association), WEF (Water Environment Federation) (1998)
11. F.J. Díaz, A.T. ÓGeen, R.A. Dahlgren, Agricultural pollutant removal by constructed wetlands: Implications for water management and design. *Agric. Water Manag.* **104**, 171–183 (2012)
12. T.R. Headley, E. Harity, L. Davinson, Treatment at different depths and vertical mixing within a 1-m deep horizontal subsurface flow wetland. *Ecol. Eng.* **25**, 567–582 (2005)
13. S.C. Ayaz, Post treatment and reuse of tertiary treated wastewater by constructed wetlands. *Desalination* **226**, 249–255 (2008)
14. V.S. Mohan, G. Mohanakrishna, P. Chiranjeevi, D. Peri, P.N. Sarma, Ecological engineered system (EES) designed to integrate floating, emergent and submerged macrophytes for the treatment of domestic sewage and acid rich fermented-distillery wastewater: evaluation of long term performance. *Bioresour. Technol.* **101**(10), 3363–3370 (2010)

15. N. Anis, Treatment of industrial wastewater using constructed wetlands: Removal of chemical oxygen demand and total suspended solid. F.o.C.a.N.R. Engineering, Trans. Pahang: University Malaysia Pahang (2009)
16. F.E. Dieberg, J.J. Juston, T.A. DeBusk, K. Pietro, B. Gu, Relationship between hydraulic efficiency and phosphorus removal in a submerged aquatic vegetation-dominated treatment wetland. *Ecol. Eng.* **25**(1), 9–25 (2005)
17. P.-Y. Xue, G.-X. Li, W.-J. Liu, C.-Z. Yan, Copper uptake and translocation in a submerged aquatic plant *Hydrilla verticillata* (L.f.) Royle. *Chemosphere* **81**(9), 1098–1103 (2010)
18. D.Q. Zhang, S.K. Tan, R.M. Gersberg, J. Zhu, S. Sadreddini, Y. Li, Nutrient removal in tropical subsurface flow constructed wetlands under batch and continuous flow conditions. *Environ. Manage.* **96**, 1–6 (2012)

Effect of Vibration on Hydraulic Conductivity of Clogged Soil

Fauzi Baharudin, Mohd Shafee Harun and Nur Syafiqah Roslee

Abstract Riverbank Filtration System (RBF) is regarded as the pre-treatment technology to treat surface water and ground water resources. RBF technology is used for pre-treatment existing raw surface water supplies but also develop sustainable water supplies for demand. However, riverbank filtration system needs to be maintained regularly because filter media is being clogged as the solids are trapped. When the solid particles are trapped, the water will not be able to flow easily. The clogging may decrease the sustainability of ground water abstraction. The results of this effect, it will charge of additional costs of monitoring, replacement and rehabilitation of wells. The location of this study is located at Damansara River, Seksyen 13, Shah Alam. The river are primarily comes from Klang River which most of its water comes from the industrial activities that discharged into the river. The objective of this study is to assess the effect of hydraulic conductivity (K) due soil clogging. Besides that, the study also intended to identify whether the vibration method is an effective method for clogging dispersion in soil. Throughout the study, tests that have been conducted are Falling Head test and vibration method by using sieve shaker. The average of hydraulic conductivity before vibration is 0.000319 cm/s while after vibration is 0.000201 cm/s. The frequency of vibration for soil sample is 50 Hz for 10 min. The duration of study was conducted within 2 months.

Keywords Hydraulic conductivity · Riverbank filtration · Soil clogging · Vibration

F. Baharudin (✉) · N.S. Roslee
Faculty of Civil Engineering, Department of Water Resources and Environment,
Universiti Teknologi MARA, Shah Alam, Selangor, Malaysia
e-mail: fauzi1956@salam.uitm.edu.my

M.S. Harun
Institute for Infrastructure Engineering and Sustainable Management (IIESM),
Universiti Teknologi MARA, Shah Alam, Selangor, Malaysia

1 Introduction

Riverbank filtration (RBF) systems consist of well fields that draw water from an aquifer that is hydraulically connected to surface waters. The concept of RBF is associated with filtration which is the process where fluid that contains solids can be removed by pass through porous medium. Particles can be in form of coarse, medium and fine depending on the requirement that needed. There are multiple benefit of RBF include a reduction of organic contaminants [1], natural organic matter, micro pollutants, pathogens and suspended solids [1, 2]. Kuehn and Mueller [3] found that the process of riverbank filtration system such as coagulation and flocculation, sedimentation can be eliminated and also the filtration compared the process of conventional water treatment that needed the three processes as to complete the system to achieve good quality of water. The development of riverbank filtration system is believed to have the ability to produce clean potable water [4]. According to Zhang et al. [4], operation of riverbank filtration is lower capital cost investment and operating because of lower energy needed and usage of chemicals are reduced compared to conventional water treatment which uses a lot of energy consumptions. It is also pre-treat surface water with poor quality and also reduced their cost of conventional process [4].

Riverbed clogging has been identified as a definite problem of riverbank filtration system [4]. Clogging of the riverbed is considered inevitable during RBF process because river water containing particulate matter infiltrates the riverbed during flow of water towards the well [5]. There are four types of clogging. They are mechanical, physical, chemical and biological clogging. Jaramillo [6] have stated that mechanical clogging may happen when the flow is blocking through porous media. It is due to the gas entrapment where dissolved or released into the porous media. Then, the permeability of media can be change and directly prevent the water from pass through the aquifer. Suspended solids are deposited and removed in the upper layer of the aquifer and are not able to infiltrate the aquifer. Sediment that suspended at the surface water and ground water interface, the deposition of fine grains and growth and deposition of microorganism may lead to physical clogging [6]. According to Caldwell [7], compound's precipitation into the pores of aquifer may cause chemical clogging. Iron, nitrate concentrations, ammonia and hardness of water influences factors of chemical clogging [7].

Clogging is both desirable and unsavory processes. The efficiency of clogging may increase natural filtration process since its characteristic similar to the "Schmutzdecke" in slow-sand filter: rich in organic matter, with high concentrations of microbes. However, riverbank filtration system needs to be maintained regularly because it may be harmful because it leads to a decrease on hydraulic conductivity of riverbed sediments [8]. The RBF system is able to be clogged as the solids are trapped [5], which is a problem for sustainability of groundwater abstraction and drinking water supply [1, 9].

Mayer et al. [10] have discovered that the appropriate parameter to conduct dispersion of soil by using vibration amplitude. Absorbed ultrasonic energy per unit volume and the ultrasonic vibration amplitude are correlated for soil particle distribution in dispersion experiments. Reviews of ultrasonic vibration as a method of soil dispersion indicate that no standard method is as use. Edward and Bremner [11] also conducted a research on ultrasonic vibration as a method of soil dispersion. Their discovery have shown that the factors like power output, treatment period, soil water ratio and specification of the ultrasonic equipment may affect the efficiency of dispersion [11]. The ultrasonic vibration amplitude is determined from Mayer et al. [10] findings. It is difficult as to measure the vibration amplitude at the lower end of the ultrasonic probe as to vibrate at the soil water solution. So, it is needed a cylindrical shape of probe. The result will be expressed based on the influence of solution volume, influence of insertion depth and influence of absorbed energy and vibration amplitude on dispersion. In this research, there is no influence of solution volume on the absorbed power found. Besides that, the absorbed power also increases with increasing of inserting depth [10].



Fig. 1 Location of Damansara river, Selangor

Therefore, this research was carried out to assess the effect of hydraulic conductivity due to soil clogging and to investigate whether vibration method is an effective method to disperse soil clogging. This was accomplished by using a combination of laboratory testing and analyses which are Falling Head test and vibration method. The study provides useful insight into the implementation of vibration method as to recognize the most effective method to disperse clogging in soil. Figure 1 shows the location of the soil sample taken which is located at Seksyen 13, Shah Alam, Selangor.

2 Methodology

Two laboratory experiments were chosen for this study, which are Falling Head test and vibration method. These experiments were chosen because the tests are specific on determination of soil properties.

2.1 Falling Head Test

This test was used to determine the K of fine soils such as fine sands, silts and clay. The K is a measure of how easily a particular fluid will pass through a soil. It is suitable for soils having coefficients of hydraulic conductivity less than 10^{-4} m/s. Figure 2 shows the disturbed soil sample was put into the prefabricated steel mould and compacted before being set up for testing. The soil sample was fit with the end cap as shown in Fig. 3. The end cap was equipped with inflow tube as to allow water flow from upper water tank. Then, the prefabricated steel mould was put into falling head tank as shown in Fig. 4. The reading for the test was taken when the water start to flow out from the falling head tank. From the experiment, the duration of water flow out was about a half-month because the size of tank was big.

Fig. 2 The disturbed sample was put into the mould



Fig. 3 The prefabricated steel mould fitted with end cap



Fig. 4 Set up of prefabricated steel mould into falling head tank



In this study, the falling head test commenced by connecting the soil sample contained in the prefabricated steel mould to standpipe tubes. The time of water dropping within a specified distance along the standpipe tube was recorded. These procedures were done in triplicates and the average saturated hydraulic conductivity of soil was calculated. The falling head test was setup in accordance to the standard laboratory procedure. Equation 1 is used for estimating the hydraulic conductivity, K of the sample where L = the height of soil sample column, A = sample cross section, a = the cross section of the standpipe, Δt = the recorded time for the water column to flow through the sample, and h_1 and h_2 = the upper and lower water level in the standpipe measured using the same water head reference.

$$K = \frac{aL \ln(h_1/h_2)}{A(\Delta t)} \quad (1)$$

2.2 *Vibration Method*

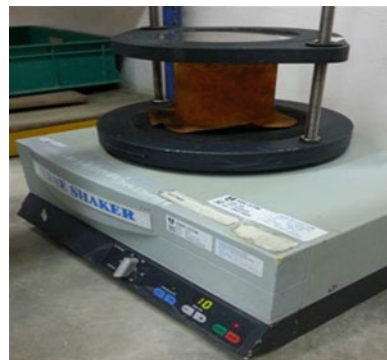
The soil sample was air dried before vibration method was conducted. The condition of place should be clean, warm and dry area in the process of drying soil. Besides that, the soil was left to dry about 2–3 days. It is not recommended to use heat or oven because it may affect the soil properties.

Figure 5 shows the condition of soil after 3 days. Assumption has been made that the soil specimens will become loosen after vibration method was applied. Sieve shaker is actually an apparatus that being used for sieve analysis of aggregates. For this study, sieve shaker was applied as to investigate whether this apparatus could provide necessary vibration to consider it as an effective method for dispersion of soil clogging as shown in Fig. 6. The permeability describes of how easily water is able to move through soil. Permeability is related to the connect-edness of the void spaces and to the grain size of the soil. The time taken was set about 10 min to vibrate with frequency of 50 Hz. During vibration, the particles of soil can be seen and constant moving through the soil, setting particles in motion

Fig. 5 Air-dried soil sample



Fig. 6 Sieve shaker used for vibration method



and moving them closer together for the highest density possible. After using the sieve shaker, the permeability test was repeated as to identify the value of permeability, K of soil specimens either increase or decreasing within the time period.

3 Results and Discussions

3.1 Condition of Soil Before Vibration

Figure 7 shows the average coefficient of permeability, K , of soil sample within the time period of 10 days. From the result, it may show that the value of k become decreasing after through the experiment of permeability. It can say that the soil already to form clogging around the soil and make water not easier to flow and penetrate through soil sample.

Before conducted with vibration method, the soil sample was air dried or taken to test laboratory as soon as possible. To dry the soil sample, the condition of place should clean, warm and dry area. Besides that, the soil was left to dry about 2–3 days. It is not recommended to use heat or dry the soil sample with oven because it can affect the soil properties.

3.2 Condition of Soil After Vibration

Figure 8 shows the permeability of soil sample after apply vibration of 50 Hz. It showed that the value of K increase within the time.

In Fig. 8, the soil sample with vibration of 50 Hz frequency slightly increases with time. Based on the sample, it showed that the sample becomes loose which also contained of soil, water and air. Loose soil allows water to drain freely, preventing waterlogged soil, while supplying the air and nutrients plant roots need

Fig. 7 The hydraulic conductivity gradually decreasing over the time

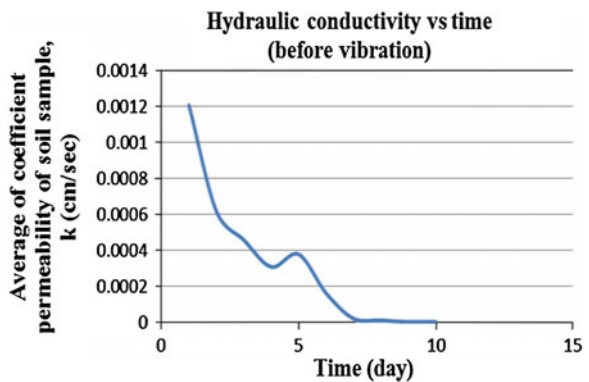
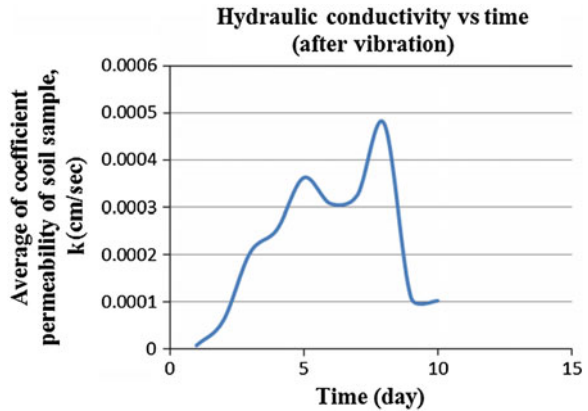


Fig. 8 Hydraulic conductivity versus time after vibration of 50 Hz



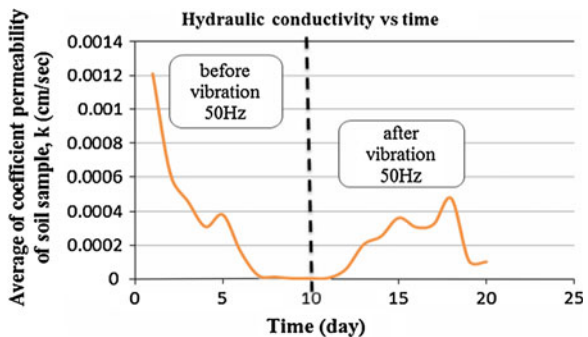
to thrive. It also allows roots to penetrate the soil easily to reach for moisture and nutrients and build a strong support system for the plant. Soil that is compacted or heavy with clay and silt particles often needs amending to loosen the soil and prepare it for planting.

The graph showed that the permeability increased within time period. From day 1 until day 7, the value of permeability of soil sample increasing and show the improvement of soil permeability after applied vibration method by using sieve shaker. After day 8, the value of permeability, K , slightly dropped from 0.000477 to 0.000132 cm/s. It can be said that, the soil sample began to form clogging again after through second testing of permeability.

3.3 The Condition of Soil Before and After Vibration

From Fig. 9, the average of hydraulic conductivity before vibration was higher than after vibration; 0.000319 and 0.000201 cm/s respectively. Based on graph, the result showed that the vibration method can be an effective method on clogging dispersion in soil.

Fig. 9 Relationship before vibration and after vibration of hydraulic conductivity



From day 1, the soils are in permeable condition where the water can still flow through them. It is because they consist not only of solid particles, but also have interconnected network of pores [12]. The degree which soils are permeable depends on some factors such as type of soil, grain size distribution, water content, degree of compaction and history of soil. After 5 days, the water content in soil is less than the porosity. It is because some of the void space has already filled with soil gas or it can be called as air. In saturated porous media, water can moved through the cross sectional area of the pore space. Somehow, when the water is replaced with air, it could only moves through area that occupied with remaining water. From that, it can effect on hydraulic conductivity become lower. Based on the soil sample, it can show that the soil sample was already clogged.

The sieve shaker was used because the equipment may produce vibration which can help to make the soil sample become loose and increased the permeability of soil and able to achieve the objective of this study. Even though there are many types of vibration equipment, but the most preferable method is by using sieve shaker because of the availability of equipment in laboratory. The concept of vibration was applied as for sieve analysis test for soil, but this study only use the sieve shaker as a medium to shake or vibrate the soil sample. In the bulk soil consistency, very loose soil was highly with void ratio, e , which is low strength and compressible. Most soils have some water in the voids where voids filled then soil is 100 percent saturated. Besides that, the portion of void filled then soil is partially saturated.

4 Conclusion

Based on the overall assessment, it can be considered that vibration method can be considered as an effective method for soil dispersion but such study still needs further investigation. First objective is achieved in determining the hydraulic conductivity due soil clogging. From the result of hydraulic conductivity, the graph shows that the average values of permeability of soil sample, 0.000319 and 0.000201 cm/s where is slightly decreasing within the time period which indicates that the soil clogging happen during that time. So, the objective is achieved. For second objective, is to identify whether the vibration method as the effective method of clogging dispersion in soil. After testing the clogging soil sample with sieve shaker, frequency of 50 Hz and vibration within 10 min is produced, it can be concluded that, the value of permeability, K , is also increased.

Inevitably, some recommendations are required as to improve the quality of this study. Based on the study, some errors might have occurred during the testing of soil sample, such as trapped air in a sample or the sample is not fully saturated. Besides that, the stopwatch used in this experiment may not accurately used. Errors can also be considered if the sample already settles during that test and disturbed by flowing water at inlet.

Besides that, numbers of the soil sample should be more than 3 samples with larger volumes of soil. With numbers of different samples, they can be applied with different frequency of vibration. So, the study will give some variation of results after vibration using sieve shaker. This study only covered with one sample which has become a limitation to make comparison of soil samples. Not only that, the soil samples should be equipped with proper physical laboratory modeling where the samples are easier to be monitored from time to time to get accurate result. The best way to achieve the objectives for this study is that the experiment time should be extended and long test period is required as to define the quality of permeability result after through vibration method and maybe the dropped values of permeability will increase again.

Acknowledgments The authors would like to express special thanks to Faculty of Civil Engineering and Research Management Institute (RMI), UiTM for all support rendered. All valuable comments from referees are very much appreciated. This research is supported by Ministry of Higher Education (MOHE) under RAGS Fund with reference no. 600-RMI/RAGS 5/3 (198/2012).

References

1. N. Tufenkji, J.N. Ryan, M. Elimelech, The promise of bank filtration. *Environ. Sci. Technol. Am. Chem. Soc.* **36**(21), 423A–428A (2002)
2. W.W.J.M. de Vet, C.C.A. van Genuchten, M.C.M. van Loosdrecht, J.C. van Dijk, Water quality and treatment of river bank filtrate. *Drinking Water Eng. Sci.* **3**, 79–90 (2010)
3. W. Kuehn, U. Mueller, Riverbank filtration: an overview. *J. Am. Water Works Assoc. (AWWA)* **92**(12), 60–69 (2000)
4. Y. Zhang, S. Hubbard, S. Finsterle, Factors governing sustainable groundwater pumping near a river. *Groundwater* **49**(3), 432–444 (2011)
5. C. Ray, J. Schubert, R.B. Linsky, G. Melin, *Riverbank Filtration: Improving Source of Water Quality* (Kluwer Academic Publishers, The Netherlands, 2002), pp. 1–15
6. M. Jaramillo, Riverbank filtration: an efficient and economical drinking water treatment technology. *Dyna Columbia* **79**, 148–157 (2012)
7. T.G. Caldwell, Presentation of data for factors significant to yield from several riverbank filtration systems in the U.S. and Europe, in *Riverbank Filtration Hydrology—Impacts on System Capacity and Water Quality*, ed. by S.A. Hubbs (Springer, Dordrecht, 2006), pp. 299–344
8. A.A. Goldschneider, K.A. Haralampides, K.A.K. MacQuarrie, River sediment and flow characteristics near a bank filtration water supply: implications for riverbed clogging. *J. Hydrol.* **344**(1–2), 55–69 (2007)
9. J. Schubert, *Riverbank Filtration Hydrology: Significance of Hydrologic Aspects on RBF Performance*, in NATO Advanced Research Workshop, Samorin, Slovakia, vol. 60 (Springer, The Netherlands, 2004), pp. 1–20
10. H. Mayer, A. Mentler, M. Papakyriacou, N. Rampazzo, Y. Marxer, W.E. Blum, Influence of vibration amplitude on the ultrasonic dispersion of soils. *Int. Agrophysics* **16**, 53–60 (2002)
11. A.P. Edwards, J.M. Bremner, Dispersion of soil particles by sonic vibrations. *J. Soil Sci.* **18**(1), 47–63 (1967)
12. *Permeability Testing in Unconsolidated Materials* (2003), Retrieved from Robertson GeoConsultants Inc. http://www.robertsongeoconsultants.com/hydromine/topics/Permeability_Testing/Permeability%20Testing.pdf. Access on 10 Apr 2014

Investigation of pH Impacts on Mineralization of CO₂ in Conditions Representative of the Malay Basin

Erfan Mohammadian, Hossien Hamidi, Amin Azdarpour and Radzuan Junin

Abstract This paper discussed effects of temperature, pressure salinity and presence of rock and pH behavior of the system and formation of carbonates. Experiments are conducted in a high pressure high temperature reactor and effluents were collected, weighed and photographed using SEM. The aim of this research was to enhance the knowledge about mineralization mechanisms of CO₂ sequestration in saline aquifers.

Keywords Carbonates · pH changes · Deep saline aquifers · CO₂ sequestration

1 Introduction

Since the industrial revolution, consumption of fossil fuels has been increased drastically which resulted in the considerable increase in the concentration of carbon dioxide in the atmosphere. The rise in the greenhouse effect and therefore global warming is the main outcome of the latter (IPCC) [1]. To date several options have been proposed to mitigate the amount of CO₂ in the atmosphere. Of all the proposed methods, CO₂ sequestration in saline aquifers is known as one the most promising solutions to carbon dioxide mitigation. Simply putting, subsurface sequestration is injection of large quantities of CO₂ deep into the subsurface formation where it can be stored permanently [2].

Due to large occurrence and large theoretical storage volumes, saline aquifers are considered the best options among other geological formation such as hydrocarbon

E. Mohammadian (✉) · H. Hamidi · A. Azdarpour · R. Junin
Faculty of Chemical Engineering, Universiti Teknologi MARA, 40450 UiTM Shah Alam,
Selangor, Malaysia
e-mail: erfana@salam.uitm.edu.my

E. Mohammadian
Faculty of Petroleum and Renewable Resources, Universiti Teknologi Malaysia, Skudai,
Johor Bahru, Malaysia

reservoirs, CBM and ocean storage. It has been estimated that world aquifers could provide a storage capacity of up to $11 \times 1,012$ tonnes of CO_2 which is enough to store several hundred years of the world's CO_2 emission [6].

2 Mechanisms of Sequestration

There are four main mechanisms of sequestration which contribute in rendering the injected carbon dioxide immobile: structural trapping (particular to H/C reservoirs), residual phase trapping mineralization and dissolution of and carbon dioxide in formation brine. Mineral trapping is reaction of CO_2 with minerals existed in rock to form stable components i.e. carbonates and almino-silicate. The carbon dioxide secured by mineralization mechanism is proven to be the safest in terms of releasing back to atmosphere [4]. However the time scales of the reaction is known to be very long. Therefore the attempt has been undertaken to accelerate the mineralization reactions. It has been showed in earlier researches that pH of the system along with pressure, temperature and brine chemistry plays a major role in efficiency of mineralization mechanism and eventually in sequestration efficiency [3, 5]. One of the methods to do so is adding the buffer solutions to the system in order to keep the brine in conditions favorable for precipitation of carbonates in thus increasing the efficiency of the sequestration process.

Aforementioned parameters need to be investigated further as they determine the economic and technical viability of CO_2 sequestration as a promising technology to mitigate Carbon dioxide in the atmosphere. The aim of this study is to experimentally investigate variations of pH of the system comprises of brine, sand and supercritical CO_2 under various conditions of pressure, temperature and brine composition. The purpose to do so is gaining a better insight on the effect of brine's salinity towards the reaction and to analyze the chemical reaction in the formation.

3 Experimental

A fabricated high pressure high temperature stainless steel, autoclave reactor was fabricated (see Fig. 1) and utilized in this research. The reactor could withstand pressures as high as 210 atm and temperatures as high as 100 °C thanks to an adjustable electric furnace surrounded it. Pure CO_2 (99.998 % pure) was used in all the experiment. The synthetic brine was prepared in a manner to mimic brines in Malay basin with total salt concentration of 10,000 and 15,000 ppm (see Table 1). The sand was collected at Pantai Kelanang, Selangor, Malaysia. The composition of the sand is shown in Fig. 2. It is apparent from the figure that the major constituent

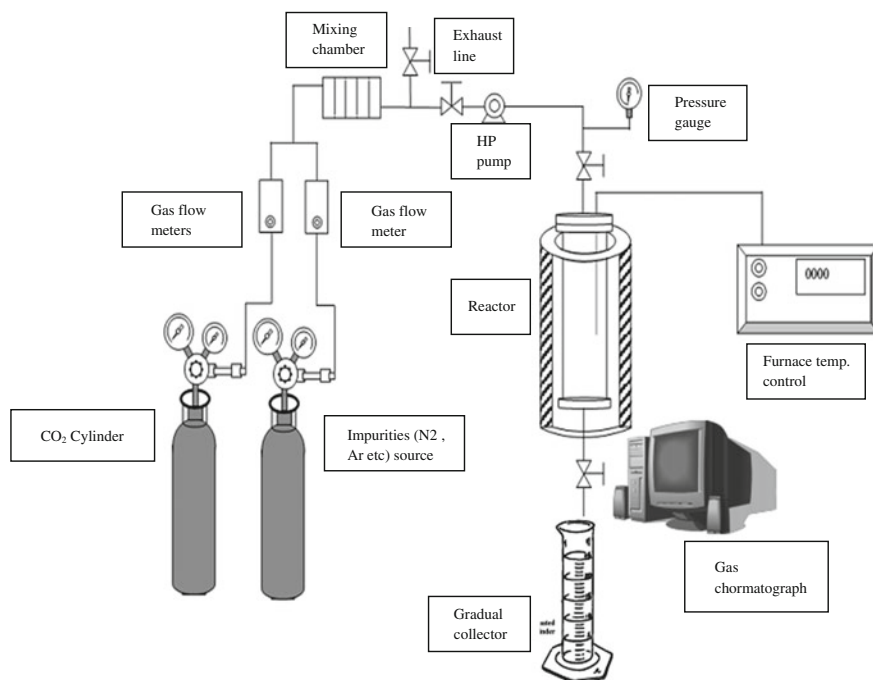


Fig. 1 Experimental setup

Table 1 Brine composition

Component	Sample 1	Sample 2
Mgcl ₂	2,000	2,000
CaCl ₂	500	1,500
KCL	1,000	–
Fe ²⁺	1,000	3,000
Nacl	5,000	7,000
HCO ₃	500	1,500
TDS	10,000 ppm	15,000

of the sand is SiO₂, CaO, MgO₂ and Fe₂O₃ with mass fractions of 63, 8, 7 and 6 % respectively. The Sand was washed, sieved to particles not bigger than 150 μm and dried in the oven. The brine composition is mimicked in a manner to represent that of brine in Malay basin as shown in Table 1.

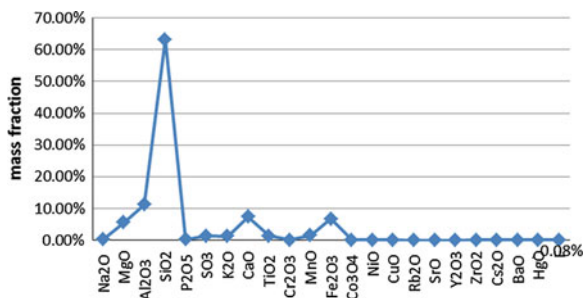


Fig. 2 XFR analysis of the sand

4 Experimental Procedures

pH of the system comprised of sand and brine was measured in ambient conditions initially. The sample then placed in the reactor and was injected with supercritical CO_2 and after the reaction the pH of the system was measured.

High pressure CO_2 is injected to the reactor preheated to the desired temperatures filled with the brine and sand. The ratio of the brine to sand is 1–5 respectively and in the experiments no more than 5 g of sand. The reaction was given 2 h and the effluents were collected and pH measurement was conducted right afterward. After the experiments the solid from the reactor was weighed and the compared to the pre-reacted sand to investigate formation of carbonates. The solid were also photographed using SEM to verify formation of carbonates.

5 Results and Discussion

Figures 3 and 4 illustrate the pH variations of a system comprised of brine and supercritical CO_2 in a system comprised of brine and CO_2 at pressure of 90 and 120 atm and temperature range of 60–100 °C.

Generally, the pH of the system is reduced as CO_2 is introduced to the system. This is of course due to solubility of CO_2 in brine and formation of carbonates. Moreover, the increase in the temperature, increases pH of the system. This is due to enhancing of the rate of the reaction at higher temperatures. The initial pH of 15,000 ppm brine is slightly higher than that of for 10,000 ppm which due to the existence of higher concentrations of minerals such as magnesium and iron in the rock. However after reaction pH of 10,000 ppm will be higher as lower concentrations of the same minerals is available for supercritical CO_2 to form carbonates. From Figs. 1 and 2 it can be inferred that increasing the pressure results in the decrease in the pH as well.

Fig. 3 pH changes of a system comprised of 10,000 and 15,000 ppm brine, before and after reaction with CO₂ at 90 atm

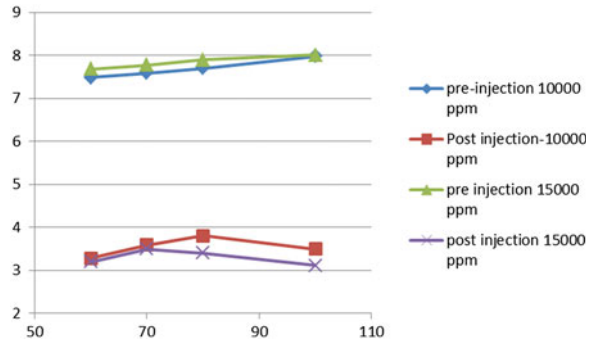
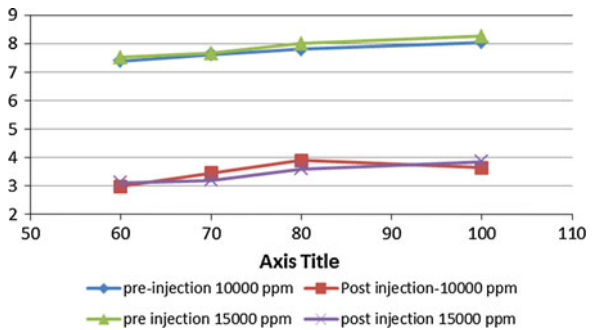


Fig. 4 pH changes of a system comprised of 10,000 and 15,000 ppm brine, before and after reaction with CO₂ at 120 atm



The result from Fig. 5 and 6 are very similar to those of Figs. 1 and 2 in terms effects of pressure, temperature and salinity on the pH. The curious point is that at the two pressure series, it can be observed that end point (final) pH values for the system including the sand is considerably higher those of without brine. It therefore could be concluded that the sand acts as a buffer solution and increases the pH of the system. The latter is due to the chemical composition of the sand used in this research and need to be verified for other sands as well.

A post-reaction sample of the rock was imaged with SEM (400×) as can be seen in Fig. 7. The big dark particles were rich in Si. Ca was major in the medium light pieces, and the brightest spots were rich in Fe.

After each experiment the amount of solid gathered from the reactor is weighed and also was photographed using SEM. The SEM results confirmed the formation of carbonates as well. The amount of solid pre- and post-reaction is shown in Table 2. It can be seen from the table that the amount of solid content increased in conditions that favor higher pH. Therefore it can be concluded that increasing pH enhances formation of carbonates. Table 2 summarizes the results of carbonate formation in various conditions.

Fig. 5 pH changes of a system comprised of 10,000 and 15,000 ppm brine and sand, before and after reaction with CO₂ at 90 atm

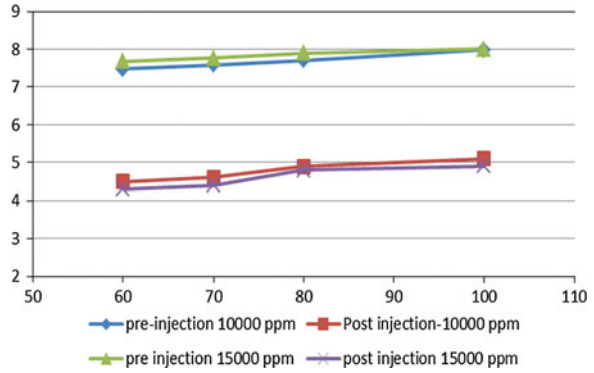


Fig. 6 pH changes of a system comprised of 10,000 and 15,000 ppm brine and sand, before and after reaction with CO₂ at 120 atm

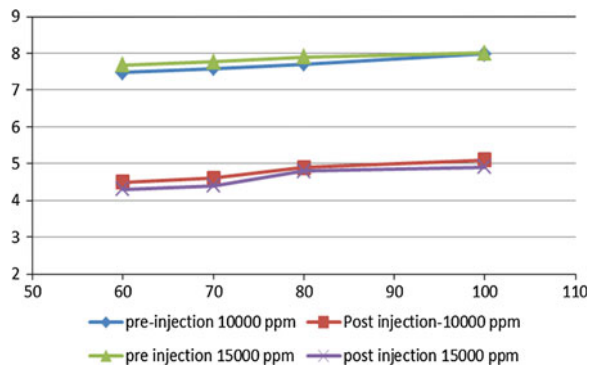


Fig. 7 SEM image of a 300 μm portion of the sample (rock)

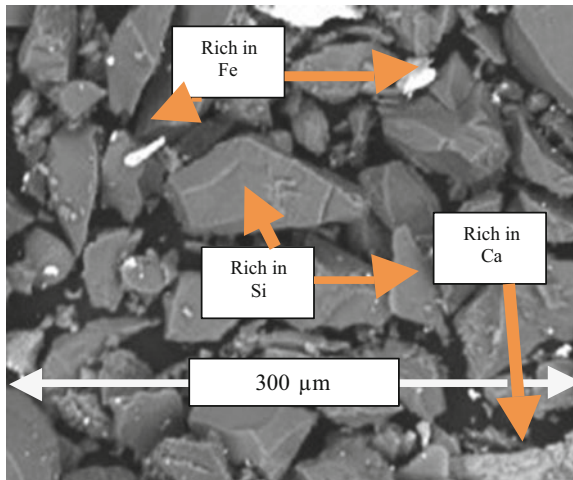


Table 2 Formation of solids as CO₂ dissolves in 15,000 brine

Pressure (atm)	Temperature (°C)	Initial pH	Final pH	W1 ^a	W2 ^b
90	60	7.68	4.3	5	5.04
90	70	7.77	4.4	5	5.06
90	80	7.9	4.8	5	5.10
90	100	8.01	4.91	5	5.13
120	60	7.51	4.33	5	5.08
120	70	7.66	4.52	5	5.12
120	80	8	4.7	5	5.20
120	100	8.25	4.9	5	5.26

^a W1 weight of sand used before the reaction

^b W2 weight of sand used before the reaction

It can be seen from Table 2 that the increase in the pressure and temperature leads to the increase in formation of more solids. Moreover, at higher salinities of the brine, assuming more amounts of carbonate generating ions such as Fe, Ca and Si are available in the rock.

6 Conclusions

Several experiments have been conducted and following conclusions can be made:

The injection of carbon dioxide into saline aquifers lowers the pH of the system substantially.

The reduction in the pH is controlled by pressure, temperature and salinity of brine as well as rock composition. In the current experiments the presence of the sand acted as buffer solution and increased the pH and as a result formation of carbonates is enhanced. Moreover, higher salinity of brine led to higher initial pH and lower final pH in contrast with lower salinity brine.

Acknowledgment This research was funded by a UiTM Research Excellence Fund (Grant No. 600-RMI/DANA 5/3/RIF 547/2012). We gratefully acknowledge these supports. The authors also wish to thank the Faculty of Chemical Engineering at Universiti Teknologi MARA in Shah Alam, Malaysia for providing the laboratory facilities in completing this work.

References

1. IPCC, Carbon dioxide capture and storage, special report, Intergovernmental Panel on Climate Change (2007)
2. S.S. Bachu, Special report on carbon dioxide capture and storage. IPCC (2005)

3. R. Qui, T. LaForce, M.J. Blunt, Design of carbon dioxide storage in aquifers. *J. Green House Gas Control* (2008) (Department of Earth Science and Engineering, Imperial College London, London SW7 2AZ, UK) **3**(2), 195–205
4. A. Shariat, R. Moore, S.A. Mehta, Laboratory measurements of CO₂–H₂O interfacial tension at HP/HT. Carbon Management Technology conference, CMTC (2012)
5. M.L. Druckenmiller, M.M. Maroto-Valer, Carbon sequestration using brine of adjusted pH to form mineral carbonates. *Fuel Process. Technol.* **86**(14–15), 1599–1614 (2005)
6. R.C. Fuller, J.H. Prevost, M. Piri, Three-phase equilibrium and partitioning calculations for CO₂ sequestration in saline aquifers. *J. Geophys. Res.* **111**, B06207 (2006)

Part IV
Geotechnical Engineering

The Engineering Properties of Dredged Marine Soil Solidified with Activated Steel Slag

Chee-Ming Chan and Nor Hanisah Hamzah

Abstract Dredging is the operation of removing material from one part of the water environment and relocating it to another. Generally, the purpose of dredging is to relocate underwater sediments and soils for the offshore construction, maintenance of waterways and reclamation. Dredging produces a very large amount of dislodged materials known as dredged soils, which are commonly considered a waste. Generally, dredged soil is dumped into open sea and causes environmental problems. On the other hand, steel slag is an industrial waste resulting from the process of steel-making. However, for the last 3 decades, almost 35 % of the steel slag produced was dumped in landfills. As such, this study is about the mixing of a dredged marine soil with activated steel slag, with the aim of determining the effectiveness of the slag in solidifying the soil. The dredged soil was collected from Marina Melaka and categorized as a high plasticity silt (MH). It has a natural moisture content of 130.7 %, specific gravity 2.53, liquid limit 66 % and plastic limit 51.6 %. The steel slag was first ground to particles smaller than 2 mm for mixing with the soil. It was activated with 4, 6, 8, 10 and 12 mol of sodium hydroxide (NaOH), with only the optimum molarity resulting in maximum improvement of the soil being used throughout the study. 3 predetermined ratios of clay: activated steel slag were examined, i.e. 3:7, 5:5 and 7:3, and the soil-slag specimens were left to cure for 3, 7, 14 and 28 days. The solidified specimens were subjected to the unconfined compressive strength (UCS) test, the vane shear test as well as the bender element test at the respective ages. It was found that greater strength and stiffness improvement were produced by higher steel slag content. Longer curing periods resulted in more significant improvement of the engineering properties too. The steel slag addition also helped reduce moisture in the originally wet soil. Overall it can be concluded that activated steel slag from Malaysian steel-making industry can be potentially used to solidify the otherwise waste dredged marine soils for reuse as a sound geomaterial.

Keywords Activated steel slag · Solidification · Dredged soil · Unconfined compressive strength · Bender element

C.-M. Chan (✉) · N.H. Hamzah
Universiti Tun Hussein Onn Malaysia, Batu Pahat, Johor, Malaysia
e-mail: chan@uthm.edu.my

1 Introduction

Dredging is the operation of removing material from one part of the water environment and relocating it to another. Dredging was carried out in many different locations and for many different purposes, but the main objectives are usually to recover materials which have some values to use, or to create a greater depth of water. Dredging of ports and harbours is the most common form of dredging. For example, during the large scale construction of Busan New Mega Port in Korea, a large amount of soft soils has been dredged from the construction site in order to remove siltation in the navigation channel and to restore a viable marine environment [1].

Technically, dredging tends to relocate underwater sediments and soils for offshore construction, maintenance of waterways, reclamation and soil improvement. Dredging produces a very large amount of dredged materials. It was reported that between tens of millions of tonnes of materials were dredged from the English and Welsh ports, harbours and their approach channels every year, where in 1994 alone the amount of dredged material was estimated at some 40 million tonnes [2].

Dredged soils were considered as waste. Commonly, they are dumped into open sea, or disposed of in special landfills. Dredging is recognized as having the potential for major environmental impact. Whether in the extraction operation or in the relocation stage, precaution actions must be taken to minimize disturbance to the marine life.

Although the normal dredged material is not heavily contaminated, some can be subjected to high-risk contaminants. There is a variety of harmful substances, including heavy metals, oil, tributyltin (TBT), polychlorinated biphenyls (PCBs) and pesticides, which can be easily found on the seabed sediments in ports and harbours. The dredging and disposal processes can release these contaminants into the water column, making them available to be taken up by animals and plants, with the potential to cause contamination and poisoning over a larger area.

According to Shi [3], steel slag is a byproduct from either the conversion of iron to steel in a basic oxygen furnace (BOF) or the melting of scrap to make steel in an electric arc furnace (EAF). Today, most metallurgical slags are used as aggregates for different applications, and only the ground granulated blast furnace slag is used for a partial Portland cement replacement [4]. Kourounis et al. [4] also reported that the main types of metallurgical slags are properly fast cooled iron blast furnace slag, steel slag, phosphorus slag, copper slag and lead slag.

In Germany and most other industrial country, used blast furnace and steel slags are used as an aggregate for civil engineering [5]. According to Kourounis et al. [4], 50 million tons of steel slag was produced worldwide every year. Europe produced 12 million tons of steel slag per year. For the last 30 years, intensive research work have established about 65 % of steel slag reused today in qualified fields of applications. The remaining 35 % of steel slag were dumped.

On the other hand, steel slag is known to have cementitious and/or pozzolanic properties [6]. Due to this unique property of steel slag, it has the potential to be used as an alternative cementitious or binding material. This is a desirable feature

for additives to solidify poor quality soils with low bearing capacity and high compressibility, such as dredged marine soils. If the materials could be mixed and transformed into a uniform mixture, the steel slag’s cementitious property could effectively bind the soil particles into a stronger and stiffer form for reuse as a good soil.

The present study attempts to determine the potential of steel slag in solidifying dredged marine soils. A soil sample was collected from a dredging site for the trial, with steel slag sourced from a local steel-making plant. Different mix ratios were examined and the test specimens were allowed to mature for up to a month. The relevant laboratory tests were performed to measure the improved engineering properties at the predetermined curing periods.

2 Materials and Methods

2.1 Raw Materials

The soil sample was retrieved from Marina Melaka, in the state of Melaka in Peninsular Malaysia. Dredging was necessary to deepen the marina waters for docking of speed boats and private yachts, primarily for marine tourism purposes. A backhoe dredger mounted on a barge was mobilized for the project. Bulk, disturbed samples were obtained at depths of 3–6.5 m below the water level, depending on the tidal conditions (Figs. 1 and 2). The dredged marine soil was in a slurry form, dark grey in colour and contained some shell fragments and other debris commonly found in nearshore deposits. Figure 3 shows the shell fragments extracted from the soil. As they were relatively large and visually discernible with naked eyes, they were manually removed from the soil sample prior to mixing in the laboratory. Such large pieces of debris would have been detrimental to the uniformity of mixing with the steel slag if left in the soil, leading to segregation and non-uniform distribution of the cementation matrix. The marine soil was oven-dried for 24 h,

Fig. 1 Dredging works at Marina Melaka, Melaka

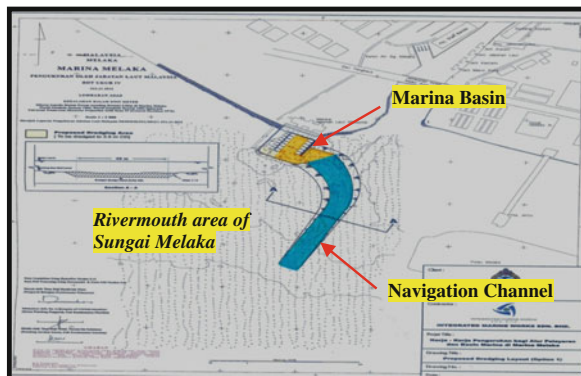


Fig. 2 Backhoe dredger at work in the Marina Melaka, Melaka



then crushed and ground into its original fine particles ($<425 \mu\text{m}$) before been used in this study. The key properties are as follows: natural water content 130.7 %, specific gravity 2.53, liquid limit 66 % and plastic limit 56.1 %. The mixing water content was fixed at 0.75 times the liquid limit, i.e. approximately 50 %.

The arc electric furnace (EAF) steel slag was supplied by a steel manufacturer from Terengganu, a state on the eastern coast of Peninsular Malaysia. As received, the steel slag were in chunks of 20–60 mm, clearly unsuitable for mixing with the soil and producing test specimens of relatively small dimensions, i.e. 38 mm diameter and 76 mm height. The steel slag was therefore broken up and ground with an industrial grinder into finer particles. The ground slag was next put through a sieve with 2 mm aperture, where only those passing the sieve were used in the specimen preparation (i.e. particles which are $<2 \text{ mm}$). The ground slag was stored in airtight containers at room temperature of 20 °C. This was to avoid oxidation of the ground slag if exposed to moisture in the air.

Fig. 3 Shell fragments extracted from the dredged soil sample



The grinding process has a significant implication on the subsequent mixing and solidifying exercises due to 3 factors. Firstly, the steel slag was physically reduced to smaller fractions for ease of mixing with the soil. Secondly, the size reduction process actually helped increase the exposed surface of the steel slag for reaction in the soil mass. Thirdly, and perhaps most importantly, the finer slag particles with the 'unreacted' inner surfaces enabled greater chemical reaction and hence solidification of the wet soil.

NaOH was used as the steel slag activator in the present study. The NaOH dilution was prepared by mixing NaOH pallets with distilled water to form solutions of 2, 4, 6, 8 and 10 mol. A mixture of soil and steel slag at the ratio of 1:1 was added to the solutions respectively. This procedure was carried out to determine the suitable molarity of NaOH for solidifying the dredged soil. From the generally declining trend obtained between the strength and molarity of the NaOH solution from 4 mol onwards, it was decided that 4 mol was to be used throughout the study for preparing the soil-slag mixtures. Note too that the mixing water content was taken as the volume of NaOH solution added to the soil-slag mixture, which was prefixed at about 50 %, corresponding to 0.75 times the liquid limit of the soil. This was essential to ensure ease of achieving uniformity in mixing, yet not producing a mixture which is too wet to be formed into cylindrical specimens for storage and subsequent tests.

2.2 Test Specimen Preparation

As mentioned earlier, the soil and slag were used in their dry, ground forms in order for the mixing water content to be known and controlled. They were first manually mixed in the mixing bowl of a conventional kitchen mixer, before the addition of the 4 mol NaOH solution. As the dry materials' mass (soil + slag) was always kept at 200 g, with the soil:slag ratio (dry weight) varying between 3:7, 5:5 and 7:3, the constant amount of NaOH solution added was 97 ml. It ensues that the mixtures, regardless of the clay:slag ratios, always had the same mixing water content of 48.5 %, which is equivalent to 0.75 times the liquid limit of the soil.

The mechanical mixing was maintained for 10 min to ensure even mixing of the materials. The homogeneous mixture was then transferred into a cylindrical steel mould (38 mm diameter, 76 mm height) and the mould was tapped to remove any entrapped air. 70 times of tapping was adopted for each layer of mixture placed in the mould, where 4 sequential placement and tapping of the layers were found to produce a satisfactorily compacted, homogenised specimen. Extruded from the mould, the specimens were carefully wrapped and sealed tightly using plastic food wrapper to prevent loss of moisture due to evaporation. The specimens were left to cure up to a month in a storage box with raised platforms. A bleach and water solution was introduced beneath the raised platform to prevent fungal growth on the specimens during the extended curing period. A pair of specimens for each mix ratio and curing

period was prepared for the tests. Considering that the bender element test is non-destructive, it was first conducted on the specimens before the unconfined compressive strength (UCS) test, which loads the specimen to failure and destruction.

2.3 Strength Measurements

Laboratory vane shear and unconfined compressive strength (UCS) test were performed to determine the undrained shear strength of the untreated and treated dredged marine soil. The vane shear test was mainly used for the natural soil sample as it was not possible to make a free-standing cylindrical specimen from the soil in slurry form. The test was conducted in accordance with the procedure given in BS 1937:7:1990 (Clause 3) [7]. Random samples were taken from the stored bulk samples retrieved from site and subjected to the vane shear test. At a natural water content of almost twice the liquid limit, the liquefied soil registered zero strength on the scale of the apparatus.

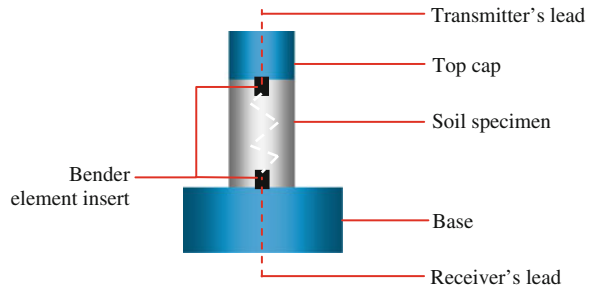
The UCS test is arguably the most popular method for soil's shear strength measurement, as it is one of the fastest and cheapest methods to measure shear strength. The method is used primarily for saturated, cohesive soils recovered from thin-walled sampling tubes, and generally inappropriate for dry sands or crumbly clays because the materials would fall apart. The remoulded dredged soil with water content 15 % short of the liquid limit made the test feasible as specimens could be formed into cylinders, not dissimilar to those extruded from the samplers. The test procedure was as prescribed in BS 1377:7:1990, Clause 7 [7].

2.4 P-Wave Velocity Measurements

P-wave velocity is determined by using the bender element (BE) test setup by GDS UK, as shown in Fig. 4. Bender elements are made from strips of piezoelectric material wired in such a way that the application of an electrical voltage causes the element to extend or bend in one direction or the other. The extension-contraction movement (forward-backward) produces P- or compression waves in the medium of propagation, whereas a bending movement (side-to-side) results in S- or shear waves travelling through the medium.

Referring to Fig. 4, the transmitter is first activated with a voltage to initiate vibration of the bender element. The vibration is then transferred to the soil medium and P- or S- waves (depending on the excitation mode of the transmitter bender element) will propagate through the specimen. On the opposite end, the initially at-rest receiver bender element picks up the vibration sent through the specimen and begins to vibrate itself. The vibration of the receiver, albeit small, would generate a small voltage which can be captured as a waveform on an oscilloscope or its manifestation via a computer programme on screen. This is attributed to the

Fig. 4 Bender element test setup



piezoelectric properties of the bender element, which could convert an electrical energy into kinetic form and vice versa. A sinusoidal waveform is usually used in these tests. Examples of the transmitted and received P-waves are shown in Fig. 8.

The bender element test is essentially a non-destructive measurement of the small strain stiffness (i.e. shear strain <0.001) of the specimen. If the P-wave velocity of the specimen is known, the small strain bulk modulus (K) can be determined. This follows that the P-wave velocity (v_p) is determined by simply taking the tip-to-tip travel distance between the transmitter and receiver bender elements (L) divided by the travel time (t). Assuming that the soil medium is homogeneous, isotropic and elastic, a multiplication of the bulk density of the medium's material (ρ) and the square of v_p would give the bulk modulus (K), i.e. $K = \rho v_p^2 = \rho (L/t)^2$.

The bender element test was conducted according to the procedure in the Bender Element Test System Manual by GDS Instruments Ltd. [8]. The specimen's mass, height and diameter were measured and recorded before performing the test in order to determine the moisture content and the density of the specimen. As shown in Fig. 4, the specimen was then carefully placed on the base, with the receiver bender element inserted in the middle of the bottom end of the specimen. The transmitter element, readily installed in the top cap, was placed at the top end of the specimen. A single sinusoidal wave (10 kHz frequency, ± 10 V amplitude) was used to trigger the transmitter bender element into generating P-waves. The rate at which readings were taken per channel was 100,000 samples per second within 10 ms of sampling time.

3 Results and Discussions

At the end of the unconfined compressive strength test, the stress-strain relationship was recorded along with the moisture content for each specimen. The moisture content of the soil-slag specimens at different ratios was found to decrease with curing time (Fig. 5). It can be observed that more moisture reduction was recorded with higher percentage of slag in the mixture. The seemingly parallel trend lines for specimens 5:5 and 7:3 indicate similar rate of moisture reduction, though 5:5 was consistently below that of 7:3. This suggests greater moisture loss with higher slag

content. The trend line for 3:7 confirms this hypothesis where the water reduction rate over the 28 days was more pronounced. The moisture loss can be accounted for by the hydration and cementation mechanisms resulting from the chemical reaction of the steel slag in contact with pore water of the soil. Besides, it is possible that the porous steel slag provided greater surface area for entrapment and absorption of the moisture, hence resulting in a drop in the moisture content.

Figure 6 shows the stress-strain relationship from the unconfined compressive strength tests for specimens 3:7. This set of data was presented as they represent the general results from the tests, and that the 3:7 specimens gave the highest strength and stiffness improvement. It is apparent that 14 days of curing is inadequate to produce meaningful solidification, i.e. see the almost overlapping curves of specimens 3, 7 and 14 days. Compared to the curve for the 28-day specimens, the unconfined compressive strength (q_u , defined as the highest stress attainable, corresponding with the peak of the curve) almost doubled. Note too that the 3- and 7-day curves depict the typical behaviour of a soft material under compression with barely discernible peaks. The initial rise of the curves is steep, indicating uniaxial compression of a stiff material. This sheds light on the improved stiffness of the

Fig. 5 Moisture loss with curing time

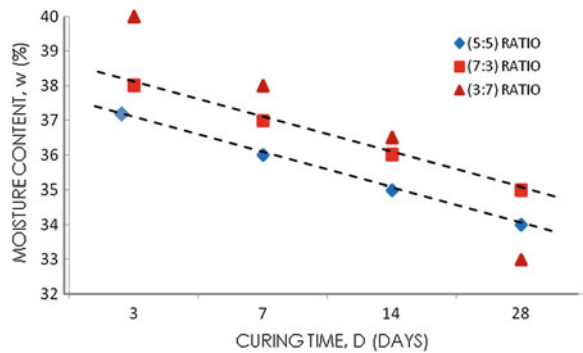
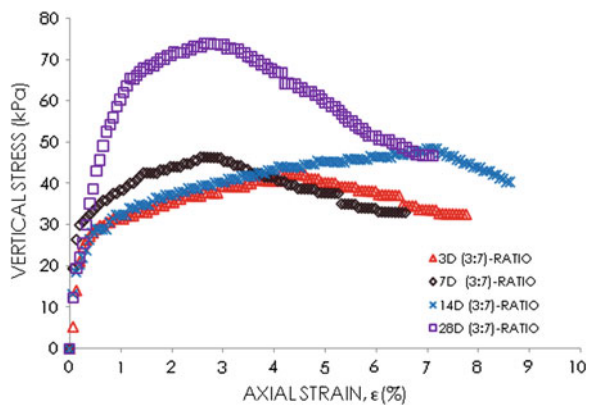


Fig. 6 Stress-strain curves from UCS test



soil-slag mixture, where the slag contributed somehow to the originally soft and the bender element test results.

Figure 7 summarizes the unconfined compressive strength (q_u) for all the specimens. Clearly the higher percentage of slag in the mixture induced greater strength improvement, i.e. comparing the 3:7 plot with those of 7:3 and 5:5. Interestingly, in the final two weeks of curing, the 7:3 and 5:5 specimens showed marked increase of strength to within the same range as the 3:7 specimens. As such, it can be expected that 50 % addition of activated steel slag was sufficient to achieve approximately the same strength as 70 % addition of activated steel slag, though with longer time. Overall the strength increment rate seems to have not reached its maximum in all cases, suggesting higher strength levels achievable with prolonged curing. This is different to soil solidification with cement where the strength usually reached 90–95 % of its maximum by 28 days of age.

The P-waves captured from the bender element tests for specimen 5:5 are shown in Fig. 8. From the plot, the P-wave arrival time (t) is taken as the time lapse from time zero to the first major deflection point in the received signal. Logically speaking, the P-wave velocity (v_p) would increase with time as stiffness increased with progress of the solidification mechanism, i.e. shorter travel time where the received signal moves closer to the transmitted one. However, as can be seen from the plots over the 28-day curing period, this is not always true. The discrepancy can be explained by the ability of the bender element test in detecting (and be affected by) anomalies within the specimen, such as localized weak zones or voids. These inherent weaknesses could be caused by improper mixing and preparation of the specimens. They were invisible and not discernible in the unconfined compressive strength test, because of the large strain loading mode and measurements adopted. It can therefore be said that the bender element test, being an indirect small strain stiffness monitoring tool, has high sensitivity in identifying non-uniformity in soil specimens.

Anomalies aside, v_p generally increased with curing time, as illustrated in Fig. 9. V_p for specimens 5:5 rose dramatically from about 970–1,300 m/s in a month.

Fig. 7 Unconfined compressive strength (q_u)—curing period

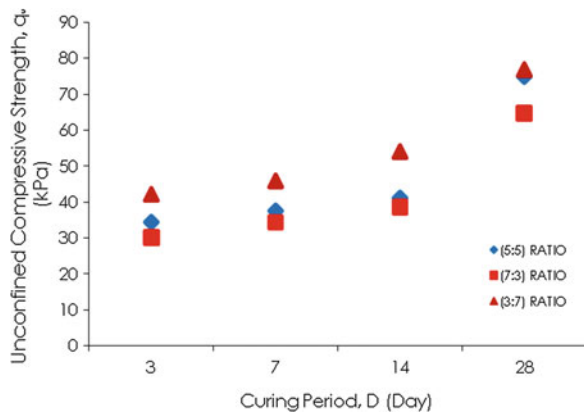
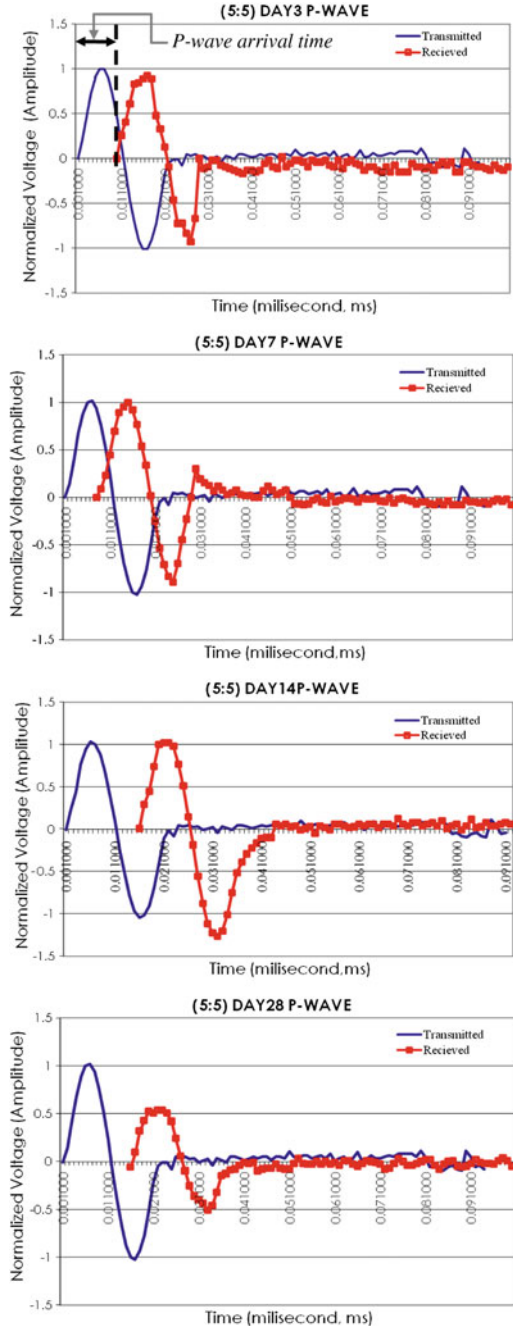


Fig. 8 Waveforms (P-wave) from the bender element tests



The same anomalies in the other specimens could have caused the 5:5 specimens to have the highest v_p despite not admixed with the highest dosage of slag. Indeed, the 3:7 specimens showed a slight dip on day 7 before rising in the following intervals of 14 and 28 days. The overall bender element test results (i.e. stiffness) corroborated with those from the unconfined compressive strength test, with indication of an on-going solidification process beyond 28 days. It would be of interest to ascertain the long term improvement of the solidified material in future studies.

Considering that the strength and stiffness of the solidified specimens share a common rising trend with time, it follows that a correlation can be established between the 2 parameters. Figure 10 relates q_u with K , with apparent distinction of the correlation according to the slag content. This is albeit the appreciable scatter of the data point, especially for specimens 5:5.

Fig. 9 P-wave velocity changes with curing time

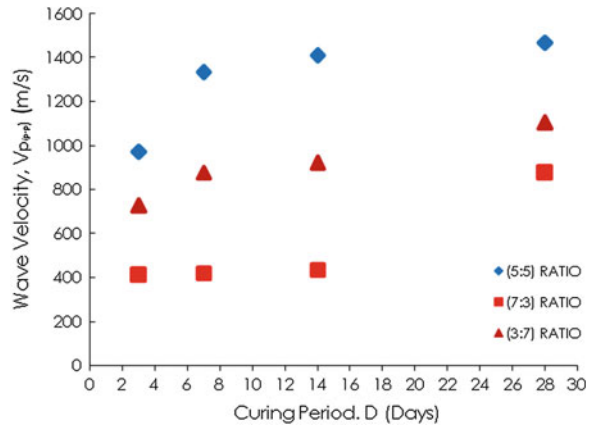
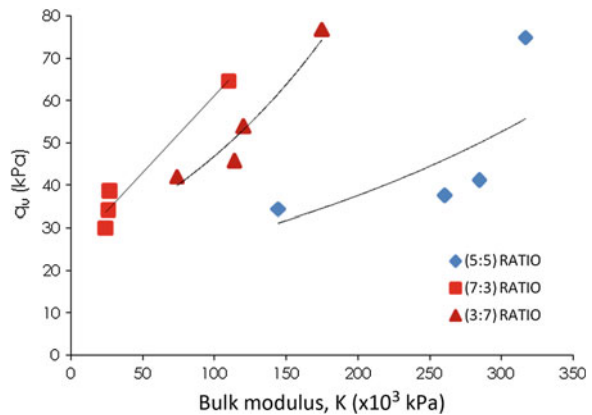


Fig. 10 q_u — K



4 Conclusions

Steel slag activated with 4 mol NaOH solution was found to be effective in solidifying a dredged marine soil from Malaysian waters. In general, the slag addition reduced the moisture content of the soil, increased the strength as well as stiffness. As can be concluded from the current study, the engineering properties of the solidified soil could attain greater improvement beyond 28 days. As for the tests and measurement systems used, the bender element test was found to have high sensitivity towards inherent anomalies in the specimens, which are not usually observed in the conventional strength test results. It is proposed that further work should include longer curing periods and a wider spectrum of mix ratios of soil and slag, as well as trials with different dredge marine soils from the surrounding waters. Only with a comprehensive database can the solidified material be applicable with confidence for assured long term performance.

Acknowledgments This study was supported by Research Grant RACE Vote 1115 from the Ministry of Education, Malaysia. Appreciation is also due to N.H. Hashim and R. Hamdan for their technical input, and the relevant laboratories for their technical support.

References

1. Y.T. Kim, J. Ahn, W.J. Han, M.A. Gabr, Experimental evaluation of strength characteristic of stabilized dredged soil. *J. Mater. Civ. Eng.* **22**, 539–544 (2010)
2. J.S. Lee, J.C. Santamarina, Bender elements: performance and signal interpretation. *J. Geotech. Geoenvironmental Eng.* **131**, 1063–1070 (2005)
3. C. Shi, Steel slag: its production, processing, characteristics and cementitious properties. *J. Mater. Civ. Eng.* **16**, 230–236 (2005)
4. S. Kourounis, S. Tsvivilis, P.E. Tsakiridis, G.D. Papadimitriou, Z. Tsibouki, Properties and hydration of blended cements with steelmaking slag. *Cem. Concr. Res.* **37**, 815–822 (2007)
5. X. Wu, H. Zhu, X. Hou, H. Li, Study on steel slag and fly ash composite Portland cement. *Cem. Concr. Res.* **29**, 1103–1106 (2009)
6. H. Motz, J. Geiseler, Product of steel slags an opportunity to save natural resources. *Waste Manage.* **21**, 286–295 (2001)
7. British Standards Institution (BSI), BS1377: Methods of test for soils for civil engineering purposes (1990)
8. GDS Instruments UK, Manual: GDS bender elements system (2005)

SOFT Soil Subgrade Stabilization Using Waste Paper Sludge Ash (WPSA) Mixtures

Norazlan Khalid, Mazidah Mukri, Faizah Kamarudin,
Abdul Halim Abdul Ghani, Mohd Fadzil Arshad
and Fauzi Baharudin

Abstract This paper presents findings on the soft soil stabilization using waste paper sludge ash (WPSA). A laboratories testing was conducted to determine the compressive strength, total shear strength and effective shear strength on soft soil subgrade stabilized using WPSA mixtures. Instead, the microstructure of soft soil and stabilized soft soil was investigated to evaluate the role of WPSA to the strength of stabilized soft soil. The soft soil subgrade sample, categorized as slightly sandy CLAY of intermediate plasticity used in this study was stabilized using Class-C of WPSA. The first objective is to determine the maximum compressive strength and optimum percentages of WPSA mixtures. The second objective is to determine the total shear strength and effective shear strength of soft soil stabilized with optimum percentage of WPSA. The third objective is to investigate the effect of WPSA to the strength of stabilized soft soil by microstructure testing by scanning electron microscopic test (SEM). This study involved three main testing. First testing was unconfined compression test to determine the compressive strength. Second testing was consolidated undrained test to determine the total shear strength and third testing was consolidated drained test to determine the effective shear strength. Third testing was microstructure testing by scanning electron microscopic test (SEM). The result shows, the addition of 10 % WPSA were giving the highest compressive strength about 737 kPa and improved the total strength and effective strength to stabilize the soft soil due to the crystal formation from the pozzolanic reaction.

Keywords Soil stabilization · Soft soil · Subgrade · Waste paper sludge ash

N. Khalid (✉) · M. Mukri · F. Kamarudin · A.H.A. Ghani · M.F. Arshad · F. Baharudin
Faculty of Civil Engineering, Universiti Teknologi MARA, Shah Alam, Malaysia
e-mail: aln_kh82@yahoo.com

1 Introduction

Soft soil usually found in coastal or river area with a different thickness can be categorized as problematical and complex soil with the unpredictable behavior. Soft soils formed by weathering process, sediment deposits or hydrothermal activities. Basically, in natural condition the strength of soft soil less than 25 kPa and possess up 85 % moisture content and very high compressibility with undesirable engineering properties [1, 10, 12].

The soil improvement can be classified and group into the soil modification, stabilization, or both. The treatment process to improve the features of the texture, increase strength and increase CBR value classified as soil stabilization and soil modification. This process of soil stabilization is totally suitable for a long term of periods [7]. Soil stabilization or soil improvement is a most economical techniques to enhance the soil density increase its cohesion, friction resistance and reduction of plasticity index was established and introduced many years ago by many researchers are using lime and/or cement to stabilized/treat the soft soil [4, 13]. Nowadays, fly ash stabilization offered another material for soil improvement for soft subgrade. The potential of fly ash in soil stabilization was increased the compressive strength, increased the CBR values, improve swelling, shrinkage and modulus of elasticity of stabilized soil [6, 11].

This study aims to shows the potential use of waste paper sludge ash (WPSA) as an additive and to show the optimum percentage of WPSA to stabilize soft soil. Instead, this study aims to obtain basic information and data for the utilization of WPSA to stabilize soft soil. Several testing has been performed such as compressive strength and shear strength on stabilized soft soil.

2 Methodology

2.1 Soft Soil Sample

The soft soil sample was collected in disturbed and undisturbed from Kampung Sijangkang, Banting, Selangor, Malaysia at 1–2 m depth from ground level. The physical and engineering properties based on the BS 1377: Part 2: 1990 [3] was conducted on the soft soil sample. Meanwhile the chemical composition for soft soil samples was obtained from X-Ray Fluorescence test (XRF test).

2.2 Waste Paper Sludge Ash (WPSA)

The wastepaper sludge ash (WPSA) is a main additive to stabilize the soft soil was used in this study. This white WPSA was in a powder form is a waste product from

the combustion of waste paper in paper recycling factories was obtained from Malaysia Newsprint Industries in Pahang, Malaysia. The WPSA has been tested for the physical properties accordance to BS 1377 [3] and the constituent of chemical compositions of sample from X-Ray Fluorescence test (XRF test).

2.3 Sample preparation and testing

In this study, the optimum percentage of WPSA was determined based on the compressive strength of soft soil mixed with several percentages (2, 4, 6, 8, 10, 12, 14 and 16 %) of WPSA. The optimum percentages of WPSA resulted to the maximum of compressive strength was used to mix with soft soil to determine the total shear strength, effective shear strength and microstructure testing. Meanwhile the scanning electron microscope (SEM) testing was performed on the samples mixed with optimum WPSA. Instead, the samples mixed with optimum WPSA were prepared for chemical composition by XRF test.

The strength testing based on BS 1377:1990 [3] was conducted on soft soil stabilized with optimum percentage of WPSA were unconfined compressive test (UCT), consolidated drained test (CU) test and consolidated drained test (CD). The entire samples at 38 mm × 76 mm were mixed and compacted at maximum dry density and at optimum moisture content.

3 Materials Properties

3.1 Soft Soil Properties

Based on the properties result of soft soil sample shown in Table 1, it shows that the soft soils sample considered as fine soil with covered about 9.78 % sand size, 79.19 % of fine or silt size and 11.03 % clay size. Instead soft soil sample had specific gravity about 2.65 and natural water content about 100.87 % with plastic index is about 22.79. The soft soil samples categorized as slightly sandy CLAY of intermediate plasticity.

Table 2 presents the chemical composition of soft soil sample. It shows that, the soft soil containing high proportion composition for three main components of silicon dioxide, alumina oxide and iron oxide. Based on the three main components, the soft soil sample has pozzolanic properties.

Table 1 The physical properties of soft soil sample

Properties	Values
Natural moisture content, w, (%)	100.87
Specific gravity, (Gs)	2.60
Plastic limit (%)	15
Liquid limit (%)	44
Plastic index (%)	29
Optimum moisture content (%)	28
Maximum dry density (Mg/m ³)	1.47
<i>Particle size distribution</i>	
Gravel (%)	0
Sand (%)	9.78
Fine/Silt (%)	79.19
Clay (%)	11.03
Classification	Slightly sandy CLAY of intermediate plasticity

Table 2 The chemical composition of soft soil sample

Element	Concentration (%)
SiO ₂	63.54
Al ₂ O ₃	23.79
Fe ₂ O ₃	6.41
CaO	0.46
K ₂ O	1.52
Na ₂ O	0.22
MgO	0.26
SO ₃	0.67
P ₂ O ₅	3.13
L.O.I	–

3.2 Waste Paper Sludge Ash (WPSA) Properties

The physical properties result for WPSA shown in Table 3 showed that WPSA classified as light materials due to the lower specific gravity value about 1.66. Instead WPSA considered as fine waste materials due to the 99 % containing of fine sizes. Table 4 showed the chemical composition result for WPSA. It can be seen; WPSA classified as Class-C fly ash due to high calcium oxide (CaO) content (more than 10 %) [2]. According to ASTM C618, this Class-C WPSA describes as pozzolanic properties and has cementitious properties. However, this Class-C fly ash classified as self-cementing features and capable to modify the soil properties without activator material in stabilization process [5, 6].

Table 3 The physical properties of WPSA

Properties	Values
Specific gravity, (Gs)	1.65
<i>Particle size distribution</i>	
Sand (%)	0.08
Fine/Silt (%)	99.92
Clay (%)	0
Classification (ASTM C618)	Class-C fly ash

Table 4 The chemical composition of waste paper sludge ash (WPSA)

Element	Concentration (%)
CaO	71.75
SiO ₂	15.08
Al ₂ O ₃	7.26
MgO	2.41
SO ₃	1.22
Fe ₂ O ₃	0.91
K ₂ O	0.54
Na ₂ O	0.19
L.O.I	–

4 Results and Discussion

Figure 1 present the graph pattern of compressive strength for soft soil stabilized with addition of series percentages WPSA mixtures. It can be seen from the graph, the trends and pattern of the compressive strength of soft soil stabilized with different percentage of WPSA. The result showed that, the strength of soft soil stabilized with WPSA was improved from 392 to 737 kPa with the increment mixed of WPSA from 2 to 10 % of WPSA respectively. However, after addition of

Fig. 1 Graph of different percentage of WPSA on loess compressive strength

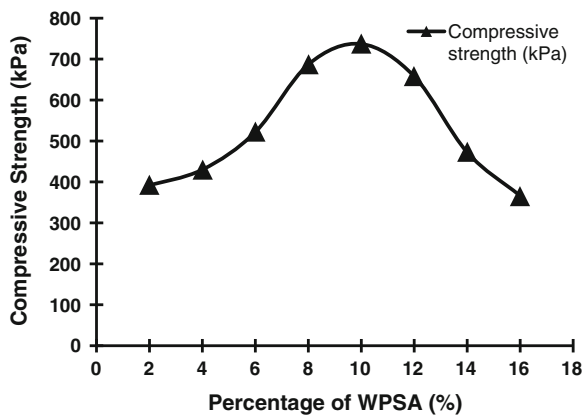


Table 5 The compressive strength result of soft soil and soft soil stabilized with 10 % WPSA

Samples	Compressive strength (kPa)
Soft soil (control)	327
Soft clay + 10 % WPSA	737

10–16 % WPSA, the pattern of graph showed the decrement in compressive strength from 737 to 366 kPa respectively. Therefore, the optimum percentage of WPSA was determined about 10 % to stabilize the soft soil with the highest of compressive strength about 737 kPa.

Table 5 shows the summarized result for compressive strength among unstabilized soft soil and soft soil stabilized with of 10 % WPSA at maximum compressive strength. The result showed an increment about 2.25 times for soft soil stabilized with addition of 10 % WPSA from soft soil (control).

Figure 2 shows the three dimensional view for particle with fabric arrangement between soft soil and stabilized soft soil with 10 % WPSA using scanning electron microscope (SEM) at 2,500–5,000 \times magnifications. It can be seen from Fig. 2a, in original state condition the soft soil particle with open spacing between particles were formed in flaky and angular shape together. Meanwhile, Fig. 2b show the

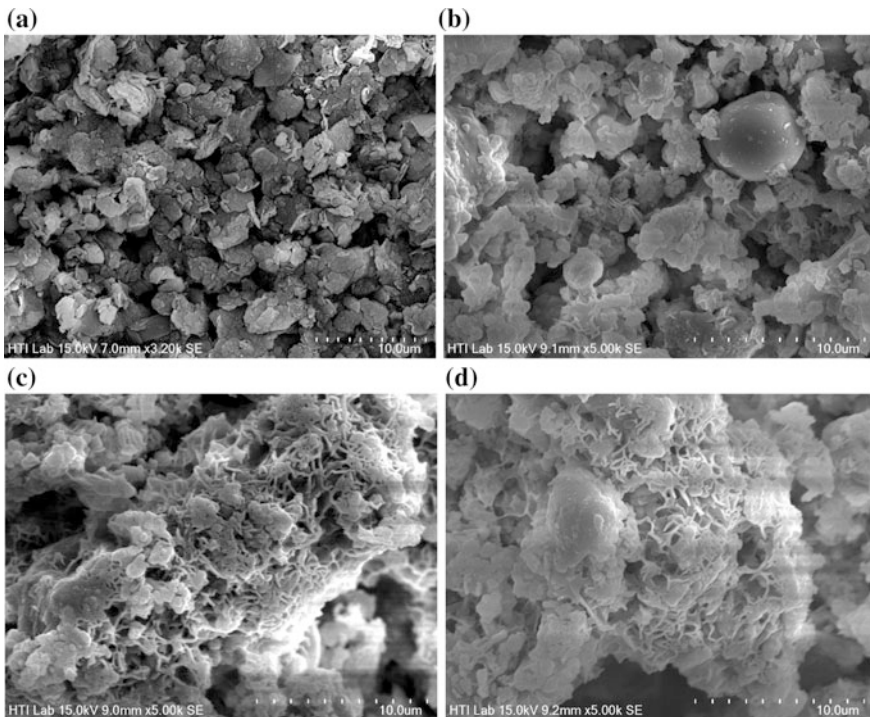


Fig. 2 Microstructure of natural soft soil and soft soil stabilized with 10 % WPSA. **a** Unstabilized soft soil at magnification 3,200 \times . **b** Bonding process of soft soil stabilized with 10 % WPSA at magnification at 5,000 \times . **c** and **d** Formation of ettringite needle-like for soft soil stabilized with 20 % WPSA at Magnification at 5,000 \times

Table 6 The shear strength result of soft soil and soft soil stabilized with 10 % WPSA

Samples	Consolidated undrained test		Consolidated drained test	
	Total strength		Effective strength	
	Cohesion c_u (kPa)	Friction ϕ_u (degree)	Cohesion c' (kPa)	Drained friction ϕ' (degree)
Soft soil (control)	29	5	0	26
Soft soil + 10 % WPSA	40	5	0	35

changes of microstructure due to the pozzolanic material reaction of soft soil after mixed with 10 % WPSA at magnification of 5,000 \times . It can be seen clearly that the existing cementing product bind the group of particle together and the decrement of spacing between particles. Figure 2c, d shows the there are a crucial changing in microstructure formation of the stabilized soft soil with 10 % WPSA. It was found the crystal formation known as ettringite (crystal formation) created on stabilized soft soil with 10 % WPSA. More ettringite formation is observed due to the 10 % WPSA was added to stabilize sample. The formation of cementitious product react form pozzolanic activity clearly observed. These cementitious products known as calcium silicate hydrate (CSH), calcium aluminate hydrate (CAH) and ettringite formation not only enhance the bonding strength among cluster together but also reduce the volume of the pore space. The ettringite needle-like are abundantly formed act as a bound bridge to the clusters and describe the improvement in the strength of stabilized clay contribute from the amount of ettringite formation [8, 9].

Table 6 presents the result of total shear strength and effective shear strength from consolidated undrained test and consolidated drained test respectively between soft soil and soft soil stabilized with 10 % WPSA. It shows an increments about 35 % for effective shear strength with increment in drained friction (ϕ') from 26 $^\circ$ to 35 $^\circ$ for soft soil stabilized with 10 % WPSA compared to unstabilized soft soil. The soft soil stabilized with 10 % WPSA shows the best result in term of effective strength due to the high of internal locking of friction between the particles. Meanwhile, in saturated soil the total shear strength increases about 38 % with the increment value of undrained cohesion (c_u) from 29 to 40 kPa for soft soil stabilized with 10 % WPSA compared to soft soil due to the cohesion between particles of WPSA and soft soil as glued and electrostatic attraction between soft soil ions and WPSA ions.

5 Conclusions

From the laboratories study, the following conclusions can be drawn:

- i. The 10 % of Class-C WPSA is the optimum percentage to stabilize the soft soil for sandy CLAY of high plasticity at the maximum compressive strength about 720 kPa.

- ii. The soft soil stabilized with addition 10 % WPSA was improved the compressive strength about 2.2 times increment compared to unstabilized soft soil (control). The soft soil stabilized with 10 % WPSA improved the effective shear strength with the increment about 35 % of internal friction (ϕ') from 26° to 35° compared to soft soil only. Meanwhile it was improved the total shear strength with increment 38 % of cohesion (c_u) from 29° to 40° compared to soft soil only.
- iii. The small amount addition of 10 % WPSA to stabilize soft soil was improved the total strength and effective strength due to the crystal formation from the pozzolanic reaction. These were giving significant to stabilized soft soil.

Acknowledgments The authors are thankful to the research management institute, UiTM Shah Alam for providing research acculturation grant scheme (RAGS) for completing this study and also to faculty of civil engineering, UiTM Shah Alam, Malaysia for providing the facilities.

References

1. A.I.M. Abdullah, P. Chandra, Engineering properties for coastal subsoils in Peninsula Malaysia, in *Proceedings of the 9th South East Asia Geotechnical Conference*, vol. 1., Bangkok, Thailand, pp. 127–138 (1987)
2. American Society for Testing and Materials, ASTM C618. Specification for coal fly ash and raw or calcined natural pozzolanic for use as a mineral admixture in portland cement concrete, in *Annual Book of ASTM Standards* (ASTM, Philadelphia, USA, 2008)
3. British Standard Institution, in *British Standard Method of Test for Soils for Civil Engineering Purposes* (BS 1377, London, 1990)
4. S. Koliass, R.V. Kasselouri, A. Karahalios, Stabilisation of clayey soils with high calcium fly ash and cement. *Cem. Concr. Compos.* **27**, 301–313 (2005)
5. A. Misra, D. Biswas, S. Upadhyaya, Physico-mechanical behavior of self-cementing class C fly ash–clay mixtures. *J. Fuel* **84**, 1410–1422 (2005)
6. Z. Nalbantoglu, Effectiveness of Class C fly ash as an expansive soil stabilizer. *Construct. Build. Mater.* **18**, 377–381 (2004)
7. A.J. Olaweraju, Soil stabilization, in *M. Eng Seminar on Course Title : Advance Soil Mechanics (CVE 821)*, Civil Engineering Department, Federal University of Technology, Akure, Ondo State, Nigeria (2004)
8. K. Onitsuka, C. Modmoltin, M. Kouno, in *Investigation on Microstructure and Strength of Lime and Cement Stabilization Ariake Clay*, vol. 30, No. 1. Report of Faculty Science and Engineering, Saga University (2001)
9. G. Rajasekaran, Sulphate attack and ettringite formation in the lime and cement stabilized marine clays. *Ocean Eng.* **32**(2005), 1133–1159 (2005)
10. J.M. Said, S.N.L. Taib, Peat stabilization with carbide lime. *UNIMAS E. J. civ. Eng.* **1**, 1–6 (2009)
11. A. Senol, T.B. Edil, C.H. Benson, Md.S. Bin-Shafique, Use of class C fly ash for stabilization of soft subgrade, in *Fifth International Congress on Advances in Civil Engineering*, Istanbul Technical University, Istanbul, Turkey, 25–27 Sept 2002
12. M.R. Taha, Geotechnical properties of soil-ball milled soil Mixtures, in *Proceedings of 3rd Symposium on Nanotechnology in Construction* (Springer, Berlin), pp. 377–382
13. I. Yilmiz, B. Civelekoglu, Gypsum: an additive for stabilization of swelling clay soils. *Appl. Clay Sci.* **44**(1–2), 166–172 (2009)

Prediction of Inundation Settlement Using Rotational Multiple Yield Surface Framework in Unsaturated Granite Residual Soil

M.J. Md. Noor, I.B. Mohamed Jais and Y. Ashaari

Abstract Inundation settlement is triggered due to the rise of the groundwater table. In designs, it is usually ignored since the analysis assumes that the foundation soil is fully saturated at the base of shallow foundations. The problem that arises from this scenario is that when the construction was done in dry season, and when wet season comes, the groundwater table rises causing the partially saturated soil to be fully saturated, hence causing a reduction to the shear strength of the soil and followed by wetting collapse. The concept of effective stress and shear strength interaction demonstrates the soil behaviour to resist settlement in two conditions, which are due to loading and wetting. The latter is simulated in a modified Rowe cell to measure settlements due to suction loss under lateral pressures exerted to the wall of the cell at k_0 condition. The complexity of this behaviour will be explained applying the Rotational Multiple Yield Surface Framework and verified by the test data observed. The ability of the framework to predict inundation settlement will be presented.

1 Introduction

Wetting collapse or inundation settlement is triggered when there is a shear strength decrease due to the loss of suction as the soil becomes fully saturated. Pereira and Fredlund [22] commonly refer collapsible soil as a metastable structured soil

M.J. Md. Noor (✉) · I.B. Mohamed Jais · Y. Ashaari
Faculty of Civil Engineering, Institute for Infrastructure Engineering
and Sustainable Management, Universiti Teknologi MARA,
Shah Alam, Malaysia
e-mail: mohdjamaludinmdnoor@yahoo.com

I.B. Mohamed Jais
e-mail: ismac821@salam.uitm.edu.my

Y. Ashaari
e-mail: yasminashaari@yahoo.com

where an increase in pore water pressure will result in a volume decrease for a metastable-structured soil. As specified by Dudley [9], Barden et al. [4] and Mitchell [21], there are four (4) factors required to produce collapse in the soil structure:

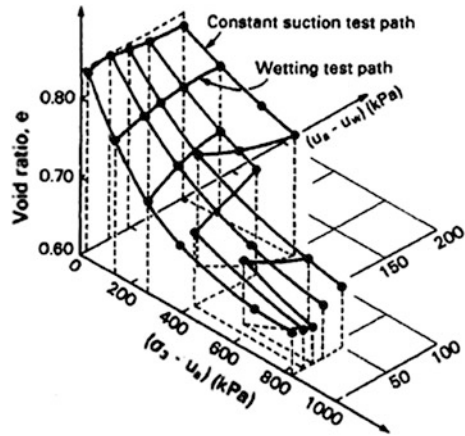
1. an open, partially unstable, unsaturated fabric.
2. a high enough net total stress that can cause the structure to become metastable.
3. a bonding or cementing agent that stabilizes the soil in the unsaturated condition.
4. the addition of water to the soil causing the bonding or cementing agent to be reduced and the intergranular contacts to fail in shear, resulting in a reduction in the total volume of the soil mass.

Pereira and Fredlund [22] noted based on studies conducted by Jennings and Burland [15], Barden et al. [4] and Hodek and Lovell [14] that collapsible behaviour of compacted soils depend on the percentage of fines (especially clay fractions), initial water content, initial dry densities and the process of compaction applied. In fact, Tadepalli et al. [24] confirms that collapsible soils are always unsaturated and the reduction of matric suction is one of the major causes for the occurrence of collapse. Therefore, the objective of this study is to evaluate this complex settlement behaviour using the theoretical non-linear shear strength model based on Rotational Multiple Yield Surface Framework of Md. Noor and Anderson [20].

Biot [5] presented a three-dimensional consolidation theory based on the assumption that the soil is isotropic and linear elastic. Two constitutive relationships were proposed in order to describe the deformation state of unsaturated soil, which are in relations to the soil structure and water phase. Fredlund and Rahardjo [11] reported two independent stress variables used in the formulations and in total, four (4) volumetric deformation coefficients were required to link the stress and deformation states. Bishop [6] attempted to link the deformation behaviour of unsaturated soils with single valued effective stress equation, however, resulted in limited success [15]. It is reported by Fredlund and Rahardjo [11] that there is no unique relationship between volume change and effective stress for most soils.

Matyas and Radhakrishna [17] introduced the concept of state parameters for an unsaturated soil consisting of stress variables; $\sigma_m = (\sigma_1 + 2\sigma_3)/3 - u_a$, $(\sigma_1 - \sigma_3)$, and $(u_a - u_w)$ for triaxial compression, along with the initial void ratio and degree of saturation. For isotropic compression, the stress parameters reduced to $(\sigma_3 - u_a)$ and $(u_a - u_w)$ and the void ratio and degree of saturation were used to represent the deformation state of the soil. Three-dimensional state surfaces were formed with void ratio and degree of saturation plotted against the independent state parameters, $(\sigma - u_a)$ and $(u_a - u_w)$. The void ratio results [17] produced a single warped surface, with the soil structure always decreasing in volume as the $(u_a - u_w)$ stress is decreased or as the $(\sigma - u_a)$ stress is increased as shown in Fig. 1. The graph demonstrates significant volume reduction as suction approaches zero.

Fig. 1 Void ratio constitutive surface under isotropic loading from Matyas and Radhakrishna [17]



1.1 Wetting Collapse Behaviour for Partially Saturated Soil

Tadepalli et al. [24] found that Matyas and Radhakrishna [17], Escario and Saez [10] and Cox [8] presented volume change behaviour of collapsible soil based on step wise inundation and the inundation was conducted by controlling the pore air and pore water pressures in a closed system. Matyas and Radhakrishna [17] found that the soil structure behave more rigid or less compressible at high matric suction. Escario and Saez [10] then reported that there was a reduction in total volume as a result of matric suction decrease and the volume change became most significant at low suction values.

Pereira and Fredlund [22] found that collapsing soil shows three distinct phases of deformations during the wetting process. The first occurs at high matric suction and is characterised based on small volumetric deformations of the soil in response to relatively large decrease of suction and this is known as “precollapse” phase.

The second phase occurs at intermediate values of matric suction and it is characterised based on significant volumetric deformations in the collapsing soil due to reduction of suction. This behaviour can be explained in terms of combination of structural rearrangements and the occurrence of local shearing of both, connecting bonds and the clay particles. The rearrangement of the soil structure involves both micro and macrostructure of the soil mass, which is termed as “collapse” phase.

The third phase occurs at low suctions and requires no additional volumetric deformations as it responds to further reduction in suction and this small deformations observed can be attributed to secondary compression of the soil skeleton herein termed as “postcollapse” phase. This contradicts the occurrence of massive settlement near saturation as reported by Alonso et al. [1], Escario and Saez [10], Matyas and Radhakrishna [17] and Bishop and Blight [7].

1.2 Characterizing Collapse Behaviour of Unsaturated Soil According to Rotational Multiple Yield Surface Framework

Md. Noor [18] developed a hypothetical volume change framework to explain the volume change behaviour of coarse grained soils due to inundation and load increase. Based on studies conducted by Alonso et al. [1, 2], Sharma [23], Wheeler et al. [25] and Gallipoli et al. [13], there are limitations to the elasto-plastic critical state framework, which lead to the development of the Rotational Multiple Yield Surface Framework (RMYSF). This framework works from the standpoint of soil stress strain behaviour. The magnitude of deviator stress in the stress-strain response determines the major principal net stress while the net confining pressure determines the minor principal net stress and the axial strain is taken as the yield parameter. Yielding or soil compression is considered based on the combined effects of the principal stresses and suction through the concept of Mohr circle stress diagram in the extended Mohr-Coulomb space.

Md. Noor [18] suggested applying the Mohr stress diagram, since it represents graphically the state of stress at any point in a soil mass by considering the combined effect of principal stresses and suction. The soil compression which governs the volume change behaviour of soils can be simulated based on the interaction of the stress state and the mobilized shear strength state. The mobilized shear strength increases with mobilized friction angle, therefore the curvilinear shape of the mobilized shear strength envelope rotates about the suction axis towards the soil shear strength envelope at failure as soil structure is compressed.

This framework is unique since the mobilized shear strength envelope acts as the yield locus since the axial strain along the locus is constant irrespective of the net stress or effective stress. Soil compression occurs when the state of stress exceeds the mobilized shear strength; henceforth the stress state exceeds the yield surface.

Md. Noor [18] revealed that the characteristics of volume change behaviour for coarse-grained unsaturated soils are:

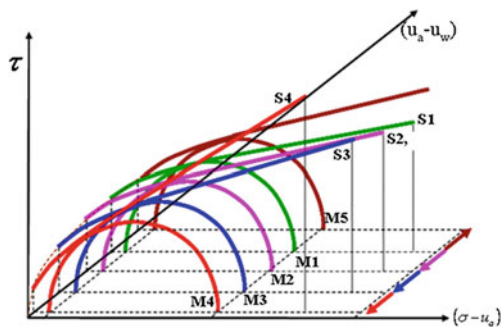
1. The soil compression due to particle rearrangement is irrecoverable.
2. The changes in the applied stress are driving the stress state to the yield limit or the mobilized shear strength envelope.
3. Collapse failure does not occur at critical state since it occurs under stress changes. Moreover, the collapse occurs due to the availability of the space for the particles to rearrange themselves [3] causing reduction in the overall volume, and it is not straining under constant volume.
4. The framework involves multiple yield surfaces since under a specific constant loading condition the soil compression ceases at one point, and changes to the loading condition produces further compression, which also ceases at another point [12]. It is suspected that the soil compression ceases when stress equilibrium is achieved between the state of stress in the soil and the mobilized shear strength.

5. Soil compression due to inundation must exhibit massive volume decrease near saturation, and the compression stops when 100 % saturation is achieved [24].
6. Soil compression in a coarse-grained soil is immediate and the compression in fine grained soil is a slow process before stress equilibrium is reached due to the slow rate of dissipation of pore air and pore water pressure.
7. Collapse can occur under drying or suction increase conditions.

Consider the initial equilibrium stress where the Mohr circle at M1 is about to touch the soil mobilized shear strength envelope represented by the envelope S1 shown in Fig. 2. When suction is reduced due to inundation the Mohr circle is shifted from M1 to M2 moving in a direction parallel to the suction axis without affecting its diameter since the major and minor principal net stresses remained constant. During this retreat it extends beyond the shear surface envelope S1 and hereby triggers soil compression known as wetting collapse. This has caused the shear strength envelope to rotate about the suction axis, marking the increase in mobilized friction angle, ϕ'_{mob} , to the yield envelope S2 where a state of stress equilibrium is reinstated.

Md. Noor [18] illustrated that as suction is further reduced, the Mohr circle advances to positions M3 and M4 and the corresponding rotated yield surface envelopes at equilibrium are at S3 and S4, respectively. As the curves become steeper, closed to saturation, the yield envelope gets steeper as it approaches the frontal plane (τ against $(\sigma - u_a)$), representing steep reduction in mobilized shear strength. This large turning of the yield envelope represents significant vertical compression which signifies the massive volume reduction when suction approaches zero as reported by Alonso et al. [1], Escario and Saez [10], Matyas and Radhakrishna [17] and Bishop and Blight [7].

Fig. 2 Proportionate rotation of the *curvilinear lines* representing the yield envelopes when Mohr circles retreat towards lower suction [18]



2 Soil Sample and Tests Results

The soil sample was taken from Kuala Kubu Baharu yielded the following physical properties tabulated in Table 1. The particle size distribution shows that approximately 30 % of fines exist within the granite residual soil and about 13 % consist of clay. This shows that the sand dominates the soil, hence will influence the minimum internal angle of friction at failure, for the CSESSSM model. The soil is described as well graded very silty gravelly SAND which conforms to findings by Marto and Kasim [16] for some of the residual soil located almost the same locality within the central region.

2.1 Simulation of Wetting Collapse Behaviour Using Modified Rowe's Cell Apparatus

Laboratory test using the modified Rowe's cell apparatus which accommodates specimen of 300 mm diameter and 150 mm height was executed at different variations of constant applied stress i.e. 150 and 300 kPa. This simulation in the laboratory is conducted to validate the RMYSF of Md. Noor and Anderson [19] since this model can explain the wetting collapse behaviour due to loss of suction in terms of shear strength and net stress for saturated and unsaturated soils.

The first stage of wetting at constant net stress of 150 kPa showed small settlement value during loading. During wetting at suction changes from 100 to 60 kPa, small settlement values were recorded. However, when suction dropped to 20 kPa and finally at full saturation, massive collapse was recorded. Due to the rotation of the mobilized shear strength envelope, the soil is regaining its stiffness to achieve equilibrium since there is a loss of suction. This behaviour is illustrated in Fig. 3 and the visualization of rotating mobilised shear strength envelope due to loss of suction is shown in Figs. 4, 5 and 6.

The results from the simulation using RMYSF of Md. Noor and Anderson [19] showed good agreements with the laboratory modelling. An interesting debate

Table 1 Physical characteristics of Kuala Kubu Baharu granite residual soil

Soil physical properties	Description
Gravel content	19.7 %
Sand content	51.3 %
Silt content	16 %
Clay content	13 %
Average specific gravity	2.66
Average in situ moisture content	19.34 %
Average maximum dry density, ρ_{dry}	1.93 Mg/m ³
Average optimum moisture content, OMC	13.85

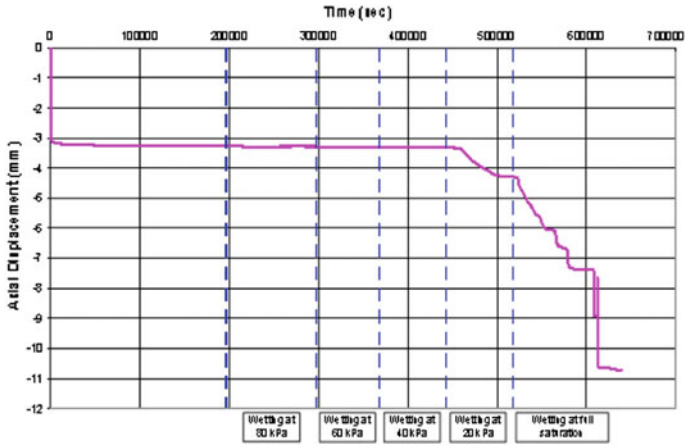


Fig. 3 Wetting collapse settlement at constant applied stress of 150 kPa

Fig. 4 Simulation of loading collapse settlement based on the RMYSF

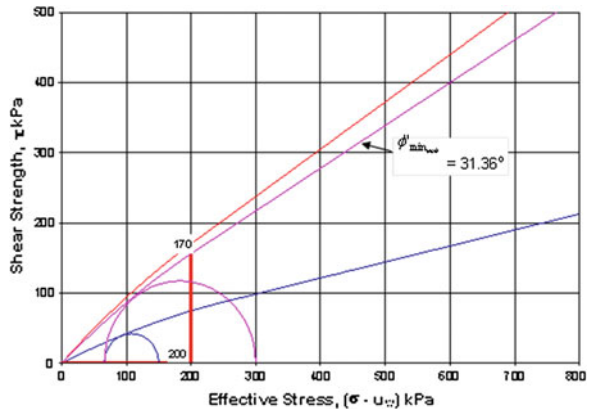


Fig. 5 Simulation of wetting collapse settlement after the soil is loaded at constant applied stress of 150 kPa

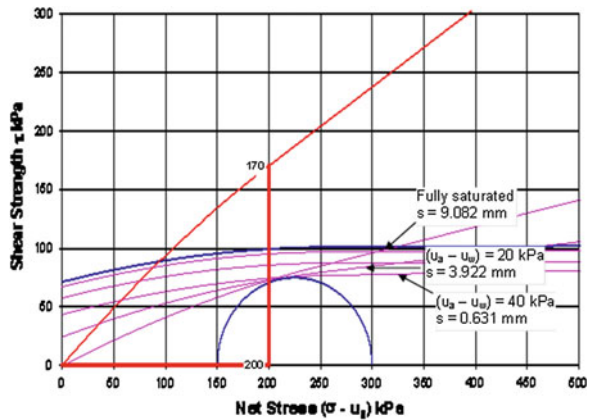
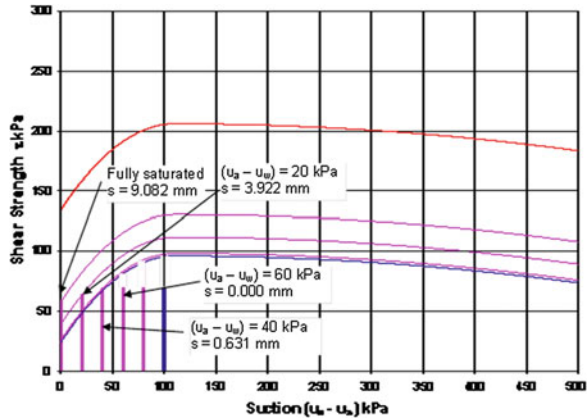


Fig. 6 Suction decreases to saturation causing massive rotation of the shear strength envelope resulting in wetting collapse settlement at 150 kPa



arises when the soil was loaded up to the initial stress of 150 kPa at constant suction of 100 kPa, settlement occurred abruptly where the soil is at its initial stress state and the particles were still uncompressed. But after the soil is allowed to regain its stiffness, it was then inundated i.e. the suction was reduced to 80 and 60 kPa, but the Mohr circle at an applied stress of 150 kPa was not in contact with the minimum mobilised shear strength envelope since the apparent cohesion, c_s was closed to the apparent cohesion at residual suction, c_s^{max} . These behaviours exhibit no change in strains when it was wetted and these were proven from the laboratory modelling.

However, as the Mohr circle was in contact with the minimum mobilized shear strength envelope i.e. at reduced suction of 40 kPa, wetting settlement started to occur until massive settlement was obtained due to full saturation of the soil i.e. zero suction. When the strength envelope was generated from the shear strength against suction axes, it is clearly seen that the lines representing the Mohr circles is not in contact with the minimum mobilized shear strength envelope at reduced suctions of 80 and 60 kPa. However as the Mohr circle was in contact with shear strength envelope at suctions of 40, 20 and 0 kPa, the Mohr circle lines are moving towards saturation, rotating the shear strength envelope to the specified axial strain causing wetting collapse settlement as effective stress decreases shown in Figs. 5 and 6.

The second stage at constant net stress of 300 kPa showed massive loading settlement. However, when the soil was inundated up to full saturation, small amounts of settlement were recorded which signified that the soil has experienced packing during compression. Md. Noor [18] explained that minimal settlement occurred during wetting for higher applied stress since the soil has experience particle rearrangement and compression; hence the void ratio or room for settlement of the soil has become less and this has been proven and validated in the laboratory modelling as shown in Fig. 7. Although, there was massive settlement observed after the soil has achieved full saturation, the value was rather small and this supported and agreed with the explanation by Md. Noor [18].

The result from the simulation showed that as the soil was loaded at an applied stress of 300 kPa, massive loading collapse settlement occurred as the soil was

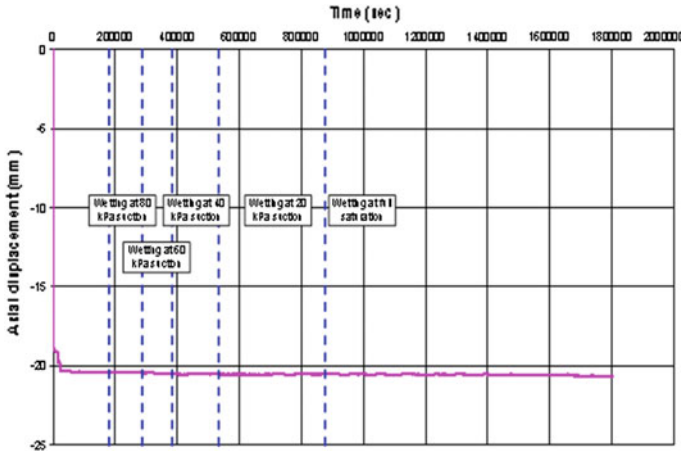


Fig. 7 Wetting collapse settlement at constant applied stress of 300 kPa

compressed where the particles were compacted together and the void spaces were less than the previous loading stage. Therefore, when the soil was inundated, the reduced void spaces were filled with water but the particles have difficulty in arranging themselves since the void spaces are small resulting in less wetting collapse settlement as explained by Md. Noor [18].

Figure 8 exhibits the soil settlement behaviour at constant net stress of 300 kPa represented by the Mohr circle and the suction is reduced until the soil is fully saturated causing rotation of the mobilised shear strength envelope. Figures 9 and 10 illustrate the rotation of the mobilised shear strength envelopes when load is applied and during wetting. When the Mohr circle is in contact with the mobilised shear strength envelope, every increase of the Mohr circle will rotate the shear strength envelope causing settlement during wetting. However, since the soil is compressed at constant net stress of 300 kPa, the particles have experience packing

Fig. 8 Loading collapse behaviour of the soil at applied stress of 300 kPa

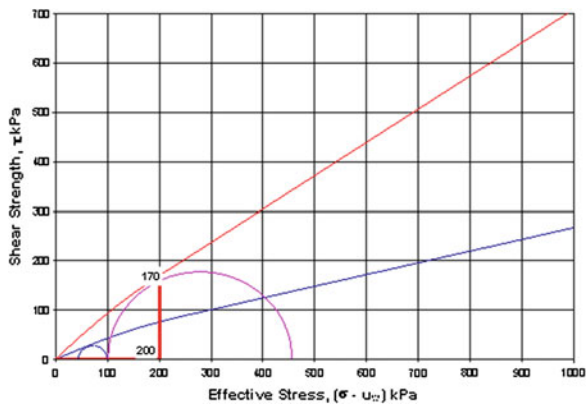


Fig. 9 Simulation of wetting collapse settlement after the soil is loaded at constant applied stress of 300 kPa

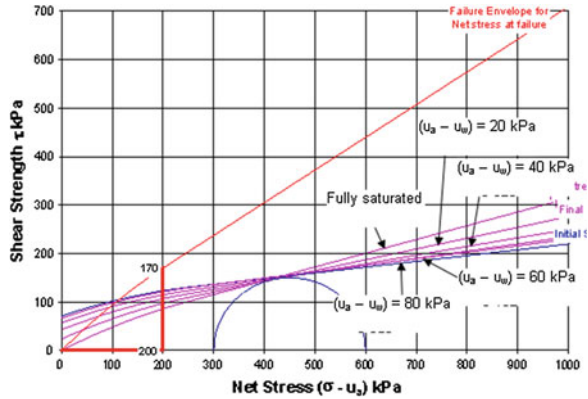
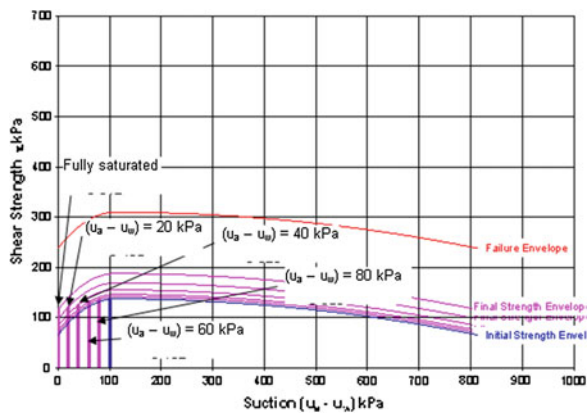


Fig. 10 Suction decreases to saturation causing massive rotation of the shear strength envelope resulting in wetting collapse settlement at 300 kPa



during the rearrangement; hence wetting collapse settlement is small. If the Mohr circles are visualised in terms of shear strength against suction axis as shown in Fig. 10, it is seen again that when the suction is closed to zero, there is massive rotation to the envelope causing more settlement at saturation. This simulation supported Md. Noor [18] statement and verified from the laboratory model that as the effective stress increases, wetting collapse settlement decreases.

3 Conclusions

Based on the validation and findings obtained, it can be concluded that:

- Collapse settlement physical modelling using the modified Rowe’s cell apparatus verified the simulation using RMYSF and proved that the RMYSF of Md. Noor and Anderson [19] is valid and could simulate the wetting collapse behaviour of the soil under effective stress decrease.

- Based on the simulation of collapse settlement using RMYSF against the physical model, RMYSF yielded almost similar results and good agreements to the experimental modelling compared considering different types of soil based on the unique relationship of minimum mobilised friction angle, $\phi_{\min_{mob}}$ against axial strain, ϵ_a established from stress strain response of different soil types. The RMYSF mapped the true stress strain response to establish the unique relationship curves for different soils.

Acknowledgments This research was conducted with the financial support from the Fundamental Research Grant provided by the Ministry of Higher Education of Malaysia and managed by Research Management Institute, University Technology MARA, Shah Alam, Malaysia.

References

1. E.E. Alonso, A. Gens, A. Josa, A constitutive model for partially saturated soil. *Geotechnique* **40**(3), 405–430 (1990)
2. E.E. Alonso, A. Lloret, A. Gens, D.Q. Yang, Experimental behaviour of highly expansive double-structure clay, in *Proceedings of 1st International Conference on Unsaturated Soils*, Paris, pp. 11–16 (1995)
3. L. Barden, A.O. Mador, G.R. Sides, Volume change characteristics of unsaturated clays. *J. Soil Mech. Fdn. Eng. Am. Soc. Civ. Eng.* **95**, 33–51 (1969)
4. L. Barden, A. McGowan, K. Collins, The collapse mechanism in partly saturated soil. *Eng. Geol.* **7**(1), 49–60 (1973)
5. M.A. Biot, General theory of three-dimensional consolidation. *J. Appl. Phys.* **12**(2), 155–164 (1941)
6. A.W. Bishop, The principle of effective stress. *Teknisk Ukeblad* **106**(39), 859–863 (1959)
7. A.W. Bishop, G.E. Blight, Some aspects of effective stress in saturated and unsaturated soils. *Geotechnique* **13**(3), 177–197 (1963)
8. D.W. Cox, Volume change of compacted clay till, in *Institution of Civil Engineers Conference on Clay Fills*, London. pp. 79–86 (1978)
9. J.H. Dudley, Review of collapsing soils. *J. Soil Mech. Fdn. Eng. Am. Soc. Civ. Eng.* **96**, 925–947 (1970)
10. V. Escario, J. Saez, Measurements of the properties of swelling and collapsing soils under controlled suctions, in *Proceedings of the 3rd International Conference on Expansive Soils*, Haifa, Israel, pp. 195–200 (1973)
11. D.G. Fredlund, H. Rahardjo, *Soil Mechanics for Unsaturated Soil* (Wiley, Canada, 1993)
12. D.G. Fredlund, H. Rahardjo, Ko-volume change characteristics of an unsaturated soil with respect to various loading paths. *Geotechn. Test. J.* **26**(1), 79–91 (2003)
13. D. Gallipoli, A. Gens, R. Sharma, J. Vaunat, An elasto-plastic model for unsaturated soil incorporating the effects of suction and degree of saturation on mechanical behaviour. *Geotechnique* **53**(1), 123–136 (2003)
14. R.J. Hodek, C.W. Lovell, A new look at compaction processes in fills. *Bull. Assoc. Eng. Geol.* **16**(4), 487–499 (1979)
15. J.E. Jennings, J.B. Burland, Limitations to the use of effective stresses in partly saturated soils. *Geotechnique* **12**(2), 125–144 (1962)
16. A. Marto, F. Kasim, *Characterisation of Malaysian Residual Soil for Geotechnical and Construction Engineering*. Department of Geotechnics and Transportation, Universiti Teknologi Malaysia. Research report (Unpublished) (2003)

17. E.L. Matyas, H.S. Radhakrishna, Volume change characteristics of partially saturated soils. *Geotechnique* **18**(4), 432–448 (1968)
18. M.J. Md. Noor, Shear strength and volume change behaviour of unsaturated soils. Ph.D. thesis, University of Sheffield, UK (Unpublished) (2006)
19. M.J. Md. Noor, W.F. Anderson, A qualitative framework for loading and wetting collapses in saturated and unsaturated soils, in *Proceedings of 16th South East Asian Geotechnical Conference*, Kuala Lumpur, Malaysia (2007)
20. M.J. Md. Noor, W.F. Anderson, A comprehensive shear strength model for saturated and unsaturated soils, in *Proceedings of the 4th International Conference on Unsaturated Soils*, ASCE Geotechnical Publication No. 147, Carefree, Arizona, USA, pp. 1992–2003 (2006)
21. J.K. Mitchell, *Fundamentals of Soil Behaviour* (Wiley, New York, 1976)
22. J.H.F. Pereira, D.G. Fredlund, Volume change behaviour of compacted gneiss soil. *J. Geotech. Geoenviron. Eng.* **126**(10), 907–916 (2000)
23. R.S. Sharma, Mechanical behaviour of unsaturated highly expansive clays. Ph.D. thesis. University of Oxford, UK (Unpublished) (1998)
24. R. Tadepalli, H. Rahardjo, D.G. Fredlund, Measurement of matric suction and volume change during inundation of collapsible soil. *ASTM Geotechn. Test. J.* **15**(2), 115–122 (1992)
25. S.J. Wheeler, R.S. Sharma, M.S.R. Buisson, Coupling of hydraulic hysteresis and stress-strain behaviour in unsaturated soils. *Geotechnique* **53**(1), 41–54 (2003)

Enhancement in Electrical Resistivity Tomography Resolution for Environmental and Engineering Geophysical Study

Andy Anderson Bery and Rosli Saad

Abstract The Geophysical surveys, including electrical resistivity tomography, are an ideal for many environmental and engineering geophysical studies about the Earth's subsurface characterizations. This paper present application of electrical resistivity tomography method in two different sites condition and sites investigation purpose. The first investigation site is located in Penang Island and the second investigation site in Perak, Malaysia. There are two different optimized arrays used in our data acquisition, which are wenner-schlumberger array and pole-dipole array. In this study, we are using single channel for the wenner-schlumberger array and multi-channel system for the pole-dipole array. Interestingly, we have used merge data level technique for these two arrays in order to aim for better improvement in electrical resistivity tomography resolution results known as inverse modeling models. As we are considering electrical resistivity tomography results with the geological reference such as borehole record, it shows that the technique is applicable and has their technical merit. The accuracy and their technical viability can be assured by the electrical resistivity tomography result models and thus it is applicable in environmental and engineering geophysical studies.

Keywords Electrical resistivity tomography · Modeling · Borehole · Technical merit · Geophysics

1 Introduction

The Earth's subsurface structure is a hidden structure which is unseen by naked human eyes. The subsurface structure information is needed for engineers and developers for site construction for development purpose. Thus, imaging subsurface is conditions would assist in determining the different characterizations of the

A.A. Bery (✉) · R. Saad

Geophysics Section, School of Physics, Universiti Sains Malaysia, 11800 Penang, Malaysia
e-mail: aab12_phy025@student.usm.my

Earth's subsurface material. In this study, we are deciding to use electrical resistivity tomography for imaging the Earth's subsurface conditions. Different properties of the subsurface material which is based on their resistivity values enables for geophysicists and engineers to interpret the Earth's subsurface condition. Many researchers such as [1–5] have used this electrical resistivity method to investigate the subsurface characterizations and conditions. Beside that, other geophysical methods such as induced polarization is used in environmental study to differentiate soil's properties and subsurface water (low zone) by [6], seismic refraction tomography for subsurface layering investigation as described by [7, 8] and salt water intrusion mapping by [9]. In this paper, we are representing two different investigation sites which related to environmental and engineering geophysics study with the application of electrical resistivity tomography method.

2 Study Objectives and Geology Sitting

The first objective of this study is to develop and enhance in electrical resistivity tomography resolution by using two different arrays and second is to verify its technical merit in environmental and engineering geophysical study.

2.1 Universiti Sains Malaysia, Penang Island

The first investigation site is situated at Universiti Sains Malaysia main campus. The objective is to determine the dimension of the man-made buried bunker. This buried man-made bunker was built during second world war by the British Army to store their artilleries and weapons. The igneous rocks are the major portion of this site investigation. All the igneous rocks are granites. These granites can be classified on the basis of proportion of alkali feldspar to total feldspars. The view from the investigation site is shown in Fig. 1.

2.2 Bukit Bunuh, Lenggong, Perak

The second site investigation is situated at Bukit Bunuh, Kota Tampan, Lenggong, Perak. The objective of the study is to identify the Earth's subsurface structure. The electrical resistivity tomography model is then correlated with the borehole record which to assist in interpretation. The geology of the site investigation was dominated by granitic rock from end Jurassic to Carbonaceous low period. The origins of these rocks are suspected from Bintang Range which is located at West of Lenggong by [10]. This area consists of few lithology which are granitic rock, tefra dust and alluvium. The view from the investigation site is in Fig. 2.

Fig. 1 The view of survey setting at first study site



Fig. 2 The view of survey setting at second study site

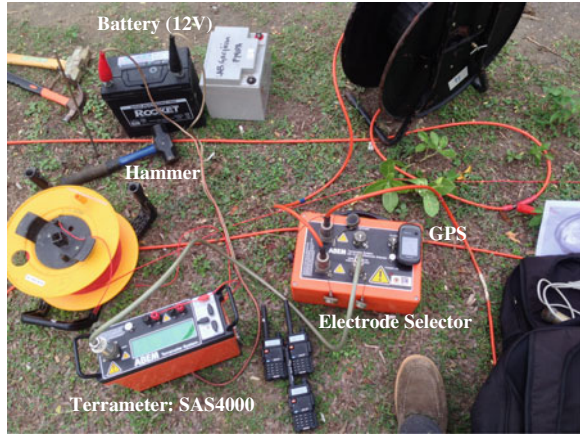


3 Methodology

The electrical resistivity tomography survey was conducted using 1 set of Terrameter: ABEM SAS4000, 1 set of Electrode Selector: ES10-64, 2 sets of ABEM Multi electrode LUND cables, 41 pieces of stainless steel electrodes, 42 pieces of ABEM Jumper cable (clip to clip), 1 piece of 50 m measuring tape, 1 unit of 12 V battery pack, 1 piece of hammer, 1 piece of electrode and jumper cable for remote (C2), 1 set of global positioning system and a log book for record. Some of the scientific equipments used in this study are shown in Fig. 3.

The minimum electrode distance used for first site investigation in Penang Island is 1.5 m meanwhile, for the second investigation site in Lenggong, Perak, minimum electrode distance is 5.0 m apart each. The minimum electrode spacing is decided based on the study objective and also accessibility along the survey line. The total length of survey line for the first investigation site is 60.0 m and the second site is 200.0 m.

Fig. 3 Some of the scientific equipments used in this study which consisted of ABEM SAS4000 terrameter, electrode selector, resistivity cables, hammer and GPS



A general definition of electrical resistivity for the fact that if there is electric field exist inside a material (as its medium), it will cause an electric current to flow through the material. In this study, the material is the Earth's subsurface. Thus, the electrical resistivity given as (Greek: rho) is defined as:

$$\rho = E/J \quad (1)$$

where ρ is the material conductor resistivity, E is the electric field magnitude (V/m) and J is the current density magnitude (A/m^2). Equation (1) is applied to a condition which E and J are inside the material conductor (the Earth's subsurface).

The resistivity raw data sets obtained from the infield is gathered for processing purposes. In the electrical resistivity processing, it used the resistivity inverse method which is the regularized of least squares optimization method by [11]. The objective function in the optimization scheme aims to minimize the difference between the measured apparent resistivity with the modelled apparent resistivity. In this study, we used the inversion of electrical resistivity data with the L2 norm smoothness constrained least squares method. This inversion scheme aims to minimize the misfit square between the measured and modelled data. Then, the data sets were modelled into two-dimensional pseudo-sections. The resistivity inversion implementation was applied through RES2DINV software, which is a two-dimensional inverse modelling code.

In this study, we are deploying the merge data level technique that aims to enhance the electrical resistivity tomography resolution. Figure 4 shows the development of the merging data level technique used in this study. For understanding, we showed the development of this technique with minimum electrode distance of 1.5 m. Thus, the total length of pseudo-section line is 60.0 m. The above section (red in colour) is the datum point's location for the pole-dipole array used in building up a pseudo-section of the electrical resistivity tomography. The total of datum point for the pole-dipole array is 1,387. The middle section (blue in colour) is the datum point's location

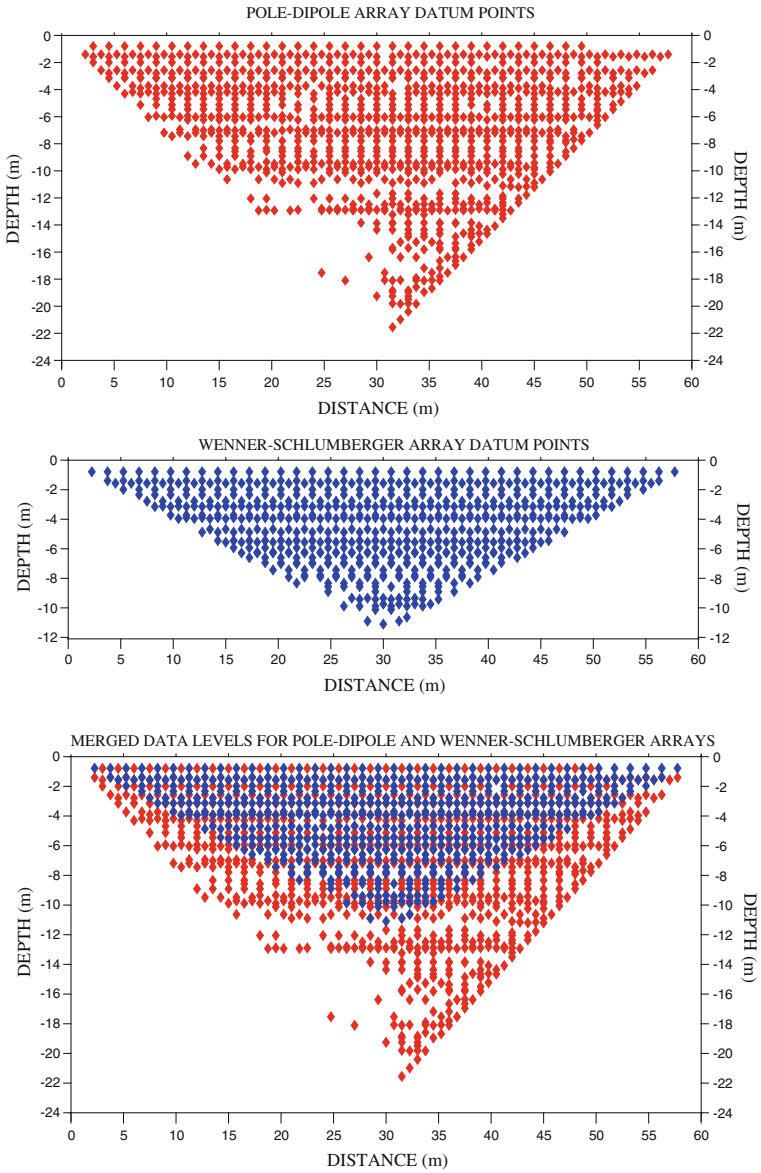


Fig. 4 Development for enhancing the vertical and horizontal resolution in electrical resistivity pseudo-section

for the wenner-schlumberger array used in building up a pseudo-section. The total of datum point for the wenner-schlumberger array is 665. Meanwhile, the bottom one is the development for enhancing the resolution in electrical resistivity tomography. The location of the datum points is located in different portions of the pseudo-section. The maximum of datum points (data) for this merging is the summation of both arrays that is 2,052 (1,387 + 665).

4 Results

Figure 5 shows a resistivity model of the first site investigation in Universiti Sains Malaysia campus. The information as in Fig. 5 shows the resistivity value distribution below the survey line. It shows that there is strong lateral and vertical variability in resistivity distribution. This is caused by the properties of the both two different arrays. The resistivity values approximately 200–1,000 Ω m is given by the mixes of soil (clayey sand) in compacted form. The low resistivity value distribution from 1.0 to 50.0 Ω m is due to the buried man-made bunker structure which is shown by the black thick line. The buried man-made structure is rectangular in shape and the dimension is approximately 13.0 m length and 7.0 m height. The robust constrain is used in modeling inversion which is less sensitive to noisy data points. In addition, there are sharp boundaries at subsurface resistivity changes. Thus, it's shown that the

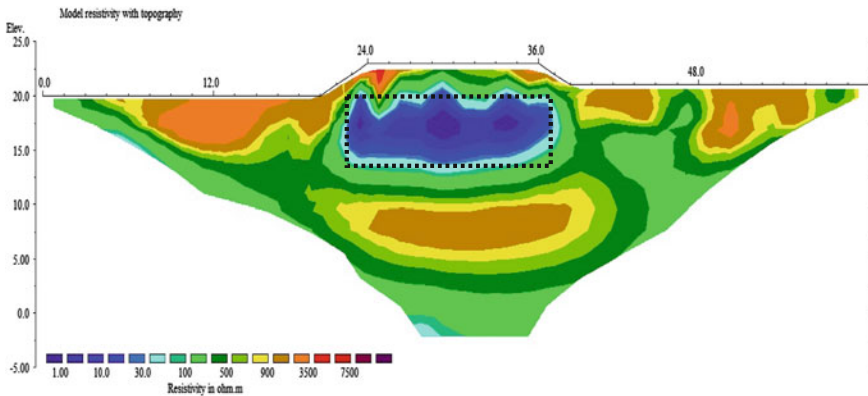


Fig. 5 The electrical resistivity tomography result for determining the dimension of the buried man-made bunker



Fig. 6 The *inside view* of the buried man-made bunker

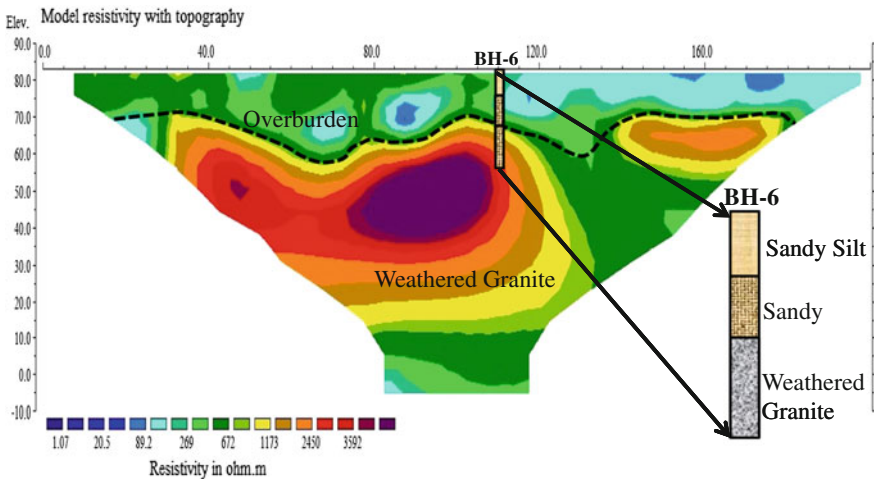


Fig. 7 The electrical resistivity tomography result for subsurface characterization along with geological information from borehole (BH-6)

geophysical method is suitable in locating and determining dimension of the buried man-made bunker. For the confirmation of this resistivity tomography result, we show the inside view of the buried man-made bunker as in Fig. 6.

Figure 7 shows a resistivity model of the second site investigation in Bukit Bunuh, Lenggong, Perak. The information as in Fig. 7 shows the resistivity value distribution below the survey line. There appears to be strong lateral and vertical variability in resistivity distribution. The standard least-squares constrain is used for modeling inversion which attempts to minimize the difference between the observed and calculated apparent resistivity values. From the resistivity value

distribution, it shows significant boundary between the overburden (sandy silt to sandy soil) and weathered granite bedrock. This boundary is shown by thick black dash line in the resistivity inversion model as in Fig. 7.

Interestingly, it appears to be reliable in geology-specific qualitative when there are correlation made by all the relevant information such as from borehole record as geological references. Thus, to highlight this good correlation of geotechnical borehole record with electrical resistivity tomography model, we also show the lithologies of the subsurface material as in Fig. 6.

5 Conclusions

This electrical resistivity tomography method is a good tool in imaging the Earth's subsurface characterization. In this study, we are only showing the application of this electrical resistivity method related to environmental and engineering studies. Moreover, we have successfully applied the merged data levels technique for both wenner-schlumberger and pole-dipole arrays datum points. This technique is successful in merge not only two, but more suitable arrays depending on the objective of the investigation or study. Even though, the time taken used in this are twice than normal electrical resistivity survey, this technique is applicable and has their technical merit especially in enhancing the resolution. Thus, both the study objectives are successfully achieved in this study. The accuracy and their technical viability can be assured by the final results of electrical resistivity tomography models from both investigation sites.

Acknowledgments Andy A. Bery would like to thank geophysics postgraduate students and laboratory assistant, Mr. Yaakub Othman for their assistance in data acquisition. In addition, thanks to the Centre for Global Archaeological Research Malaysia (CGAR), USM for sponsoring engineering drilling works at the second study site. The author also wants to give appreciation to Jeff Steven and Eva Diana for their support. Lastly, the author would like to express profound appreciation to anonymous reviewers for insight comments for this research article.

References

1. A. Sirhan, M. Hamidi, Detection of soil and groundwater domestic pollution by the electrical resistivity method in the West Bank, Palestine. *Near Surface Geophys.* **11**, 371–380 (2013)
2. A. Derahman, H. Awang, N.M. Osman, in *Groundwater Level Detection by Using a Two-Dimensional Electrical Resistivity Imaging*, ed. by R. Hassan, M. Yusoff, Z. Ismail, N.M. Amin, M.A. Fadzil. Proceedings of the International Civil and Infrastructure Engineering Conference 2013, XXVII, p. 907 (2014)
3. L. Mejus, R. Yaccup, Survei potensi air tanah dengan menggunakan kaedah keberintangan geoelektrik di projek cadangan pembangunan tapak RAMSAR, Tasek Bera, Pahang Darul Makmur. *Geol. Soc. Malaysia, Bull.* **52**, 97–101 (2006)

4. A.A. Bery, R. Saad, Merging data levels using two different arrays for high resolution resistivity tomography. *Electron. J. Geotech. Eng.* **18V**, 5507–5514 (2013)
5. A.A. Bery, R. Saad, Y.C. Kiu, N.A. Kamaruddin, High resolution time-lapse resistivity tomography with merging data levels by two different optimized resistivity arrays for slope monitoring study. *Electron. J. Geotech. Eng.* **19C**, 503–509 (2014)
6. A.A. Bery, R. Saad, High resolution time-domain induced polarization tomography with merging data levels by two different optimized arrays for slope monitoring study. *Electron. J. Geotech. Eng.* **18Z**, 5921–5928 (2013)
7. A.A. Bery, Synthetic modelling application in high resolution seismic refraction tomography. *World Appl. Sci. J.* **28**(5), 625–628 (2013)
8. A.A. Bery, R. Saad, Seismic refraction velocities and engineering parameters analysis for environmental study. *Electron. J. Geotech. Eng.* **18Q**, 3719–3730 (2013)
9. S.S. Abdul Nassir, M.H. Loke, C.Y. Lee, M.N.M. Nawawi, Salt-water intrusion mapping by geoelectrical imaging survey. *Geophys. Prospect.* **48**, 647–661 (2000)
10. S. Mokhtar, Paleolithic site comparison study of Kota Tampan with Temelong village and its contribution to the cultural end of Pleistosein age in Southeast Asia. *Malaysia Museum J.* **32** (1993)
11. Y. Sasaki, Two-dimensional joint inversion of magnetotelluric and dipole-dipole resistivity data. *Geophysics* **54**, 254–262 (1989)

Geophysical Characterisation of Road Subsurface

Haryati Awang and Alicia David

Abstract Road makes a very huge contribution for the development of economic and also to the social benefits. Poorly maintenance of the roads may reduce the efficiency of the business and trading. There are few non-destructive methods have been introduced and developed to measure the strength and deformation properties of layer that made up the pavement structure. The properties are either used to design new pavement structures or to diagnose the causes of existing problem so that appropriate rehabilitation strategies can be chosen. This study is about determining the ground profile of defect and non-defect pavement using electrical resistivity method. The purpose of this study is to investigate subsurface condition under the defect and non-defect of road pavement using electrical resistivity on actual field. Since the testing was conducted on pavement, the actual electrodes of one and half (1.5) foot steel were changed to 4 inches nails. The resistivity was measured by injecting current to the ground through electrodes and the resultant voltage difference was measured at two potential electrodes. In this study, 3 locations with different damages were selected and the resistivity value of defect and non-defect pavement were measured and profiled. Three types of defects which are crocodile cracking at the parking bay for busses, rutting and potholes at access road and transverse cracking located at car park area were investigated. The finding of this study shows that the value of electrical resistivity varies from one defect to another. This is because of influence of few factors during the early construction and the types of defect on the pavement. The advantage of using electrical resistivity method in determining the defect and non-defect pavement is its one of the non-destructive method that can be applied without making and leave major damage to the pavement surface.

Keywords Electrical resistivity · Road · Pavement · Defect · Subsurface

H. Awang (✉) · A. David
Faculty of Civil Engineering, Universiti Teknologi MARA, Shah Alam, Malaysia
e-mail: harya406@salam.uitm.edu.my

1 Introduction

Roads and means of transport make a crucial contribution to economic development and growth; and bring important social benefits. Poorly maintained roads constraint mobility, significantly raise vehicle operating costs, increase accident rates and their associated human and property costs, and aggravate isolation, poverty, poor health, and illiteracy in rural communities. Postponing road maintenance results in high direct and indirect costs. If road defects are repaired promptly, the cost is usually modest. If defects are neglected, an entire road section may fail completely, requiring full reconstruction at three times or more the cost, on average, of maintenance costs.

Problems such as undulating pavement, severe potholes or even sinkholes were common. The usual practice was to discard and replace the original soft soil with suitable material prior to construction. However, before maintenance work is carried out, investigation should be conducted in detail to obtain information together with the pavement sub surface profile. There are few testing that can be conducted to measure the strength and deformation properties of the layers that make up the pavement structure. Method of testing that is commonly used either destructive or non-destructive is such as coring, ground-penetrating radar, dynamic cone penetrometer, capacitance sounding and many others. One of the most invasive and less destructive is electrical resistivity method where it could result an image profile for the underneath pavement which is also new in market.

This paper presents the finding of characterizing the defect of road pavement using geophysical method. The objectives are to determine the subsurface profile of the road and to compare the profile of defect and non-defect road by resistivity images.

1.1 Previous Study

There are few methods of testing that were conducted for the pavement investigation. The test methods can be destructive in nature such dynamic cone penetration test or coring for laboratory assessment. In order to limit the damage of road surface non-destructive test is become a popular method of investigations. Geophysical methods nowadays become a popular non-destructive method in civil engineering industries including roads and highways.

In general, geophysical prospecting involves a number of different techniques that help identify anomalies in the physical and chemical properties of the subsoil, including the propagation of electromagnetic [e.g.; ground penetration radar (GPR)], gravity, acoustic, electrical, or magnetic signals. For road investigation [1, 2] used electromagnetic concept in assessing the value of GPR imaging of flexible pavements. It transmitted an electromagnetic signal into the medium of interest (pavement) and partially reflected on encountering changes in the electrical properties.

The reflected signal is recorded at a receiver. The series of reflections recorded at a receiver allow an image of the interior structure to build up. The depth of a layer of material is determined from the time it takes to reflected wave to be detected. Evaluation of the actual thickness and dielectric permittivity of asphalt pavement using a set of capacitance values versus sensing electrode positions which considered as sounding curve was developed a decade ago [3]. Detection to the presence of internal damage such as voids or cracks under road structure used a Colibri prototype that mounted behind a vehicle [4]. A shock applied on the road surface and creates vibrations to the pavement structure. Compression wave velocities are estimated when the impact echo method is applied. With an intermediate solicitation, surface road vibrations can be measured and the Frequency Response Function (FRF) can be evaluated.

2 Materials and Methods

The idea of choosing electrical resistivity method to investigate the road pavement is because it is inexpensive, easy to handle and the important part is that, this method is a non-destructive method. It is also practically used for shallow depth investigation. Unlike other geophysical method such as seismic method which is very sensitive to vibration, electrical resistivity is easy to handle and to conduct as it implements current distribution to the ground. Due to the electrical resistivity technology has recently evolved with the increased sophistication of electrical hardware and software so that the high technology equipment used can measure the electrical resistive properties of earthen materials. As resistance is the ability of the material to inhibit an electrical current; therefore it is the opposite or reciprocal of electrical conductivity. The main equipment used in this study for the electrical resistivity measurement was ABEM Terrameter SAS 4000 with multi electrodes system. It consists of 41 nail electrodes that were pinned into the ground along a survey line with 0.5 m spacing. Field measurements followed a practiced scheme [5]. Two cables were laid and connected to each electrodes starting from electrode number one (E1) and end up with electrode number 41 (E41). Each of the cables has 21 take outs where E1 and E21 were connected to first and last take out of cable number one respectively. The first takeout of cable number two was also connected to E21 and the last takeout to E41. Both cable number one and cable number two were connected by electrode selector (switching unit) at the center of the survey line. The main unit of Terrameter SAS 4000 was also connected to the switching unit. The schematic layout of the resistivity line is shown in Fig. 1. The electrical tomography profiles were interpreted using the RES2DINV resistivity and induced-polarization interpretation software. This calculation program is based on least-square method. This inversion method constructs the sub surface images using rectangular prisms and determines the resistivity values for each of resistivity contours [6, 7].

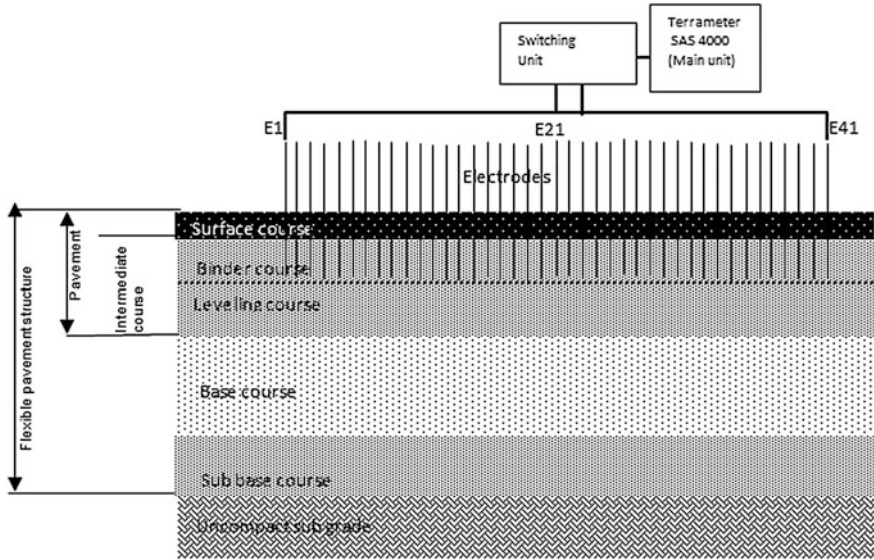


Fig. 1 Schematic diagram of electrical resistivity alignment

This study was conducted at the parking lot in university vicinity where three (3) types of defect were identified at different locations. The first defect was crocodile cracking at the parking bay for busses (Fig. 2), second defect was rutting and potholes at access road and the third defect was transverse cracking located at car park area (Fig. 3).

Fig. 2 Recording resistivity line at defect of cracks area (crocodile cracking)

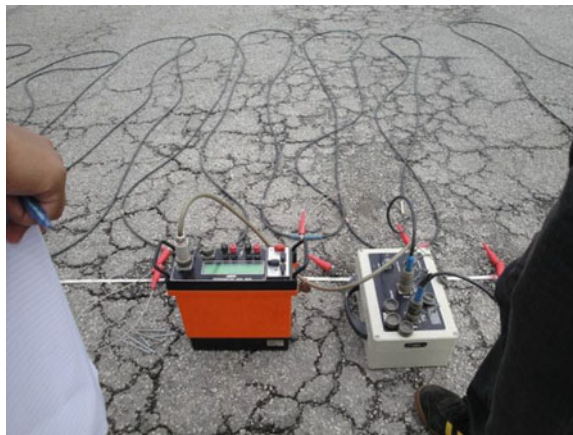


Fig. 3 Recording resistivity line at defect of transverse cracking



3 Result and Discussion

Results from field measurements of the three different defects are presented and discussed here. Figure 4 is the trapezoidal image obtained from pavement that having crocodile cracking at the middle of the whole length. The total length of this line was 20 m and the defect was located at the middle of the line. The crocodile crack was located from distance 9 to 15 m, making the cracking 6 m long. The image shows that the defect area is quite large where resistivity values under the defect pavement range from 40.1 to 65.7 Ω m indicated by green colour. The resistivity for non-defect pavement shows higher values, range from 108 to 176 Ω m indicated by reddish colour.

This pavement receives heavy load every day because it is one of parking bay for the busses. From the on-site observation and the result above, it is clearly seen that the defect occurred only at certain location and not the entire parking bay. It is suspected that the defect might be due to improper constructions practices that resulted to pavement distress. The improper practices can be claimed as the location of defect area was not well compacted and the temperature of bitumen mixed was less than 100 °C. The blue colour on the left side shows low resistivity value of less

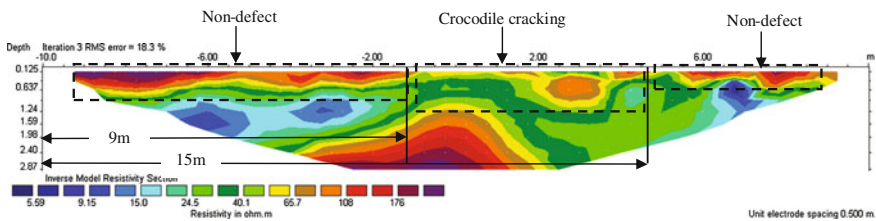


Fig. 4 Resistivity image of pavement having crack (crocodile cracking)

than 24 Ω m indicated the present of high conductive material probably saturated soil. The wet condition is arising from surface water that infiltrates through the pavement crack and seep under high resistive layer, the non-defect pavement.

Figure 5 shows the trapezoidal image that obtained from pavement that having rutting surface and pothole. The length of this test is 20 m long and the defect approximately from 0 to 9 m. The rutting at 1.5 m until 8 m, it's about 6.5 m in length and the pothole located at 9 m. The resistivity values for non-defect pavement range from 331 to 446 Ω m and the defect pavement range from 182 to 246 Ω m. This testing were conducted at access road to *Kolej Teratai*, UiTM. This road also experience heavy load because it is the route for busses and cars. Figure 4 in Chapter [Enhancement in Electrical Resistivity Tomography Resolution for Environmental and Engineering Geophysical Study](#) shows the arrangement of the defect on the pavement. From the picture taken, rutting and pothole happened to occur on the wheel path. Pavement distress can occur if the pavement or the structure is poorly designed. For example, if an inadequate geotechnical exploration was done to come up with the faulty pavement design parameters, the paving was designed using underestimated traffic loads, the recommendation procedures were not followed or inappropriate pavement design procedures were followed. Therefore, insufficient thickness may become the reason of this defect to occur.

Figure 6 shows the result in trapezoidal image of pavement having transverse crack. The length of testing has been fixed at 20 m length. The defect were

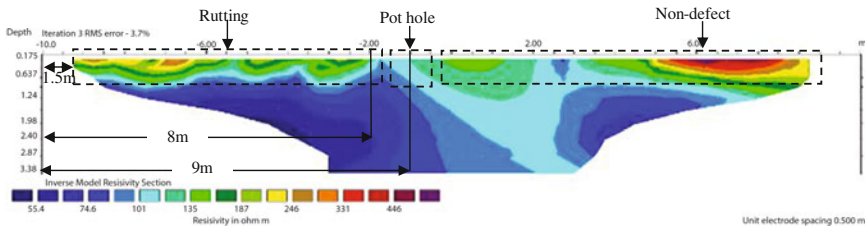


Fig. 5 Resistivity image of pavement having deformation of rutting and pothole

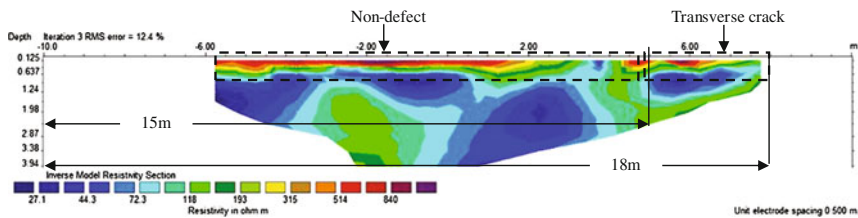


Fig. 6 Resistivity image of pavement having transverse crack

identified occur at 15–18 m. The resistivity values for non-defect pavement range from 514 to 840 Ω m and resistivity value range from 315 to 514 Ω m. Figure 6 in chapter [Enhancement in Electrical Resistivity Tomography Resolution for Environmental and Engineering Geophysical Study](#) shows the area of having the transverse crack. This area having very light load because it is a parking space for cars and very few cars parks at this area every day. From the result, it clearly shows that the pavement has high resistivity value and it is difficult to differentiate the defect and non-defect area. According to the observation, this parking area has been resurfaced and the layer is quite thick. Furthermore, it is only a line of cracking so it is difficult to see the obvious result. This crack may due to the roots of the tree that grow bigger near to the parking area. This location situated at parking space at *Kolej Delima*, UiTM.

The advantage of using electrical resistivity method in determining the defect and non-defect pavement is its one of the non-destructive method that can be applied without making and leave major damage to the pavement surface. Moreover, one-, two- or three-dimensional prospecting can be done. Compared to other techniques applied in pavement assessment which can destroy the surface area. Classical techniques have restricted measurement scales that are usually incompatible with the subsurface variability. Electrical prospecting can be applied within a large range of scales by adjusting the inter-electrode spacing. It means that we can investigate the soil structure below the pavement that might be the cause of the defect.

The improvement of computer controlled multi electrodes arrays has led to an important development of electrical imaging. As a consequence of these improvements, electrical surveys can provide spatially dense and detailed measurements over large areas at low cost. Even though there are many advantage of using electrical resistivity, however this method can be affected by many different factors and they can act as the same time that leads the measurements more difficult to interpret. From the point of view of the technical aspect, the contact between the pavement and the electrodes can be one of the problems.

Systematic errors due to poor electrodes contact. Field prospecting using electrical resistivity can be associated with laboratory studies. For example is coring. The purpose of this preliminary study is to compare the findings from electrical resistivity with the actual sample under controlled conditions. The non-uniqueness of the solution in the inversion scheme can lead to ambiguity or misinterpretation. Thus, a basic knowledge of the medium under study is recommended before inversion. The inversion procedure cannot be precise due to several factors. To reduce the inversion ambiguity and so improve the quality of the interpretation, data from several different prospecting methods should be integrated.

The value of electrical resistivity may be varying for each defect. This is because of influence of few factors during the early construction and the types of defect occur on the pavement. Table 1 shows the summary of resistivity values for defect and non-defect according to the type of pavement failure mode.

Table 1 Summary of resistivity values for defect and non-defect according to the type of pavement failure mode

Type of defects	Resistivity (Ω m)	
	Defect area	Non-defect area
Cracking (crocodile crack)	40.1–65.7	108–176
Deformation (rutting) and pothole	182–246	331–446
Cracking (transverse crack)	315–514	514–840

4 Conclusion

As a conclusion, the value of resistivity of the defect and non-defect pavement are varies as shown in Table 1. This is because it depends on few factors such as voids and degree of water saturation. Each pavement may have varieties of voids distributions and connectivity of the crushers. It is due to degree of compaction during the road construction. Degree of water saturation commonly relates to the voids distribution. The greater the void distribution, the higher the degree of water saturation is. Thus, the electrical current in the pavement depends on the amount of water in the pores and on its quality. The opening from the defect also allows the water to infiltrates into the pavement. From this study, it can conclude that the value of resistivity of defect pavement is lower that non-defect pavement but varies for every pavement. It is because we could not predict the degree of compaction of every pavement during its earlier construction.

Acknowledgments We would like to thank the Institute of Infrastructure and Sustainability Management (IISEM), Faculty of Civil Engineering, UiTM, for giving support and to the Research Management Institute, UiTM for providing the financial support (Dana Kecermelangan).

References

1. M.O. Gordon, K. Broughton, M.S.A. Hardy, The Assessment of the Value of GPR Imaging of Flexible Pavements, *NDT&E International* **31**(6), 429–438 (1998)
2. J. Clerk Maxwell, *A Treatise on Electricity and Magnetism*, vol. 2, 3rd edn. (Clarendon, Oxford, 1892), pp. 68–73
3. Y.A. Dashevsky, O.Y. Dashevsky, M.I. Filkovsky, V.S. Synakh, Capacitance sounding: a new geophysical method for asphalt pavement quality evaluation. *J. Appl. Geophys.* **57**, 95–106 (2005)
4. J.M. Simonin, J.C. Dargenton, C. Heinkele, Structural roadway assessment using the frequency response function, non-destructive testing in civil engineering Nantes, France, June 30th–July 3rd, 2009
5. M.H. Loke, *A Practical Guide to 2-D and 3-D Surveys*. *Electr. Imaging Surveys Environ. Eng. Stud.* (1997, 1999)
6. M.H. Loke, R.D. Barker, Rapid least-squares inversion of apparent resistivity pseudosections by a quasi-Newton method. *Geophys. Prospect.* **44**, 131–152 (1996)
7. M.H. Loke, T. Dahlin, A comparison of the Gauss-Newton and quasi-Newton methods in resistivity imaging inversion. *J. Appl. Geophys.* **49**, 149–162 (2002)

Data Acquisition Challenges on Peat Soil Using Seismic Refraction

Mohd Jazlan Mad Said, Adnan Zainorabidin
and Aziman Madun

Abstract This paper was briefed about difficulty in seismic refraction during data acquisition on peat soils. Seismic refraction is commonly used for subsurface characterization. This method can determine the subsoil profile by differentiate its soil velocity. Peat is known with high compressibility and more 75 % of organic content that give challenges is seismic refraction. Challenges of seismic refraction such as attenuation of seismic wave, poor signal to noise ratio (S/N) and seismic source energy explained in this paper. This problem is common for geophysicist but technical purposes for engineering community is good to have better data acquisition. The purpose of this paper is to shown proper data acquisition for seismic refraction on peat soil. The raw data of seismic wave taken from seismograph for takeout spacing of 1, 3 and 5 m are shown in results and discussion for comparison of seismic data quality.

Keywords Peat · Attenuation · Signal to noise ratio (S/N) · Seismic refraction

Fundamental Research Grants Scheme: Vot 1224 Undrained Dynamic of Malaysian Peat Soil, Universiti Tun Hussein Onn Malaysia (UTHM).

M.J.M. Said (✉)

Universiti Tun Hussein Onn Malaysia, Batu Pahat, Johor, Malaysia
e-mail: mohdjazlan18@gmail.com

A. Zainorabidin · A. Madun
Faculty of Civil and Environmental Engineering, Universiti
Tun Hussein Onn Malaysia, Batu Pahat, Johor, Malaysia
e-mail: adnanz@uthm.edu.my

A. Madun
e-mail: aziman@uthm.edu.my

1 Introduction

Subsurface characterization is very important to the engineers to obtain information of soil structure underneath of earth surface. This characterization is an critical stage in the analysis and design of proposed structures to identified all relevant information about the sub-soil conditions in particular, type of soil or rock, its extent or thickness and its properties are generally obtained through sampling and testing or by in situ testing [1]. Seismic refraction is one of the geophysical methods often used in subsurface characterization. Seismic refraction method is widely used in site investigation to determine the elastic properties of the subsurface materials [2] and was used to determine the soil profiles by using seismic wave travel through subsurface soil. Subsurface characterization on peat poses difficulties to the engineers due to its complex characteristics. Peat soil is known as organic soils and very challenging soil for civil engineers due to its unique characteristics [3]. Attenuation in peat soil is very high which cause difficulty in data acquisition by using seismic refraction technique since peat soil is very high with organic content and high void ratio. This problem is common for geophysicist but technical purposes for engineering community is good to have better data acquisition. The purpose of this paper is to shown proper data acquisition for seismic refraction on peat soil. This paper explained about challenges of seismic refraction on peat and the methods to improve the field acquisition and data quality.

2 Peat Soil

Peat soil is an organic with content more than 75 % which caused a lot of problem for construction due to unpredictable behaviour of its properties. Peat soil is very unstable soil which contain organic materials, have high water content (more than 100 %), high compressibility (0.9–1.5) and low strength (typically 5–20 kPa) [4]. It's in the category of problematic soil because has low shear strength and high compressibility [5]. Peats has very high in situ void ratio because of the very compressible and bendable hollow cellular fibres form an open entangled network of particles and the high initial water content [6].

3 Seismic Refraction Theory

Seismic refraction survey is often used in subsurface characterization due to its uncomplicated method, cost-effective and non-destructive to the ground surface. This method characterize geologic structure using seismic body waves and application in studying of the dynamic characteristics of subsurface materials of underlying layers e.g. the distributions and variations of thickness and velocity

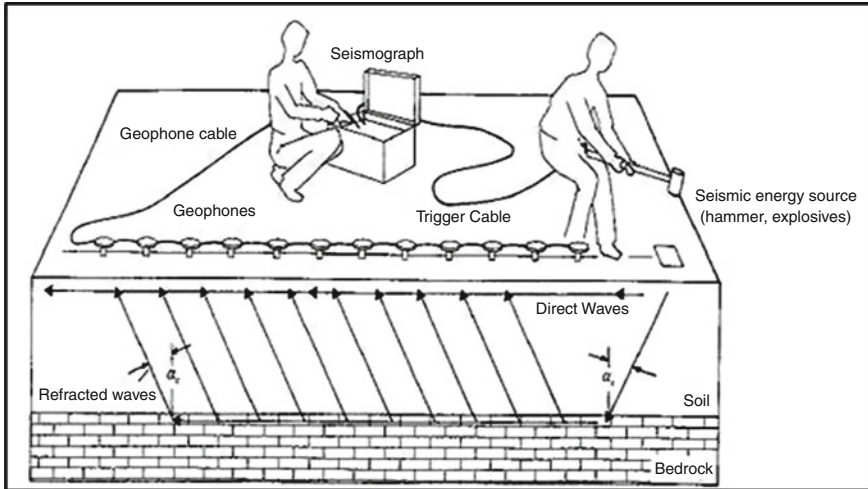


Fig. 1 Seismic refraction method [8]

value in the ground [7]. By measuring the travel times of the seismic body waves, the nature and depth of the surface can be computed which shown the velocity of soil layers. The velocity of seismic wave that travelling through the subsurface varies with material composition and stiffness. Figure 1 show the seismic refraction technique used in determining soil profile of subsurface.

4 Seismic Challenges on Peat Soil

4.1 Attenuation of Seismic Wave

Attenuation is very important factor in seismic research for good quality data of seismic. As seismic wave travel in the ground, the energy of the wave will be dissipated through distance from the seismic source but doesn't affect the frequency of medium (soil). This dissipation is the consequence of wave energy losses in the subsoil and it is named as "attenuation" [9]. Seismic wave attenuation is affected by soil material damping. Peat soil is recognized with high void ratio and high organic content where these properties will affect the seismic wave propagation. The wave attenuation of peats is greater than clays or sands. Thus this will decrease the signal to noise ratio that need to observe in the seismograph during data acquisition.

4.2 Poor Signal to Noise Ratio(S/N)

Signal to noise ratio is a measure used in science and engineering that compares the level of a desired signal to the level of background noise. In data acquisition, it's require to gain high quality raw data where have high S/N and reduced noise. In seismic refraction method, it's important to identify between the signal of wave propagation on subsurface and noise or disturbance from unwanted source such as walking people and moving traffics. Since wave attenuation is very high in peat soil, the signal to noise ratio of wave is very difficult to observe. To increase the S/N in seismic refraction, the operator needs to create seismic source using heavy sledgehammer impact into the steel plate on the ground for 20–30 successful blows for data stacking. Staking of data usually performed during data acquisition to improve data quality. This will give difficulty to the operator during data acquisition because need extra man power to create desire seismic source.

4.3 Seismic Source Energy

Steel plate often used as base plate in seismic refraction to generate seismic waves and this plate is very heavy. Peat soil has very high compressibility and can easily penetrate by the steel plate after blow for only few times. Peat also very soft that when hitting the steel plate, the energy wave seismic is absorbed and reduce the energy needed for wave to propagate through seismic array line. If the seismic wave energy is absorbed, it's required more seismic wave energy thus need to increase the effort of man power. Figure 2 show the penetration of impact plate on peat soil during data acquisition.

Fig. 2 Penetration of impact plate on peat soil during data acquisition



5 Methodology

In seismic refraction, the equipment consists of three main components which are source, detector and recorder. The source of seismic survey is 7 kg of sledge hammer where strike on an impact plate. For detectors, use a 24 unit of vertical geophone and ABEM Terraloc MK-8 seismograph was used for recorder Fig. 3 shows the equipment of seismic refraction survey.

For data acquisition, there are two reels of geophone cable and each reel consists of 12 geophones connector point. During setup the geophone cable, the cable was in linear or straight line to have optimum result during recording. There are three separate tests with different geophone spacing: 1, 3 and 5 m. The geophones should be placed on clear area and approximately level with the ground. For the seismograph, it placed at the center of geophone array line. Figure 4 shows the seismic refraction equipment arrangement of geophone array lines. The offset distance are different between three tests depend on the critical distance of soil layer on site viewed in seismograph. Table 1 show the offset distance for acquisition of different geophone takeout spacing for Test 1, Test 2 and Test 3.

Fig. 3 Equipment of seismic refraction survey



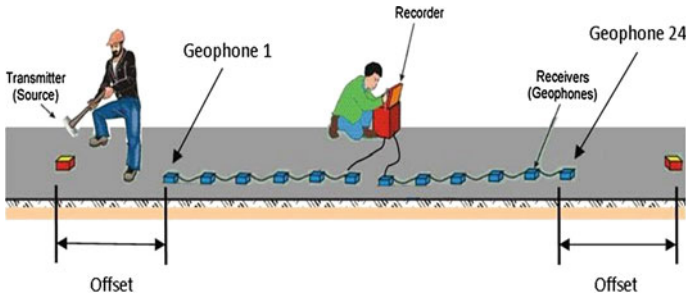


Fig. 4 Seismic refraction equipment arrangement

Table 1 Offset distance and geophone takeout spacing for Test 1, Test 2 and Test 3

Test	Geophone takeout spacing (m)	Offset distance (m)
1	1	10
2	3	15
3	5	25

6 Results and Discussion

Seismic raw data is compared between Test 1, Test 2 and Test 3 for data quality of S/N. There are three shot point location to compare the critical S/N quality such as Shot 1 and Shot 7 are offset distance at both end of array seismic line while Shot 4 at the centre of array seismic line.

From raw seismic data, it does show distinctly the differences between data quality of different geophone takeout spacing. In Fig. 5 show the seismic raw data from first offset distance (Shot 1). From the figure, Test 1 with geophone takeout spacing of 1 m show very clear seismic data compare with Test 2 and Test 3. It show seismic wave for every traces clear without major poor S/N. While for seismic raw data Test 2 is less clear and at the last 8 traces the seismic wave have attenuated where there S/N quality is poor. In Test 3, the S/N quality is very poor even have been stacked for more than 10 times. Seismic wave for every 24 traces could not show actual wave in soil layer since it have attenuated by peat soils. For Fig. 7 which shot taken from the other end of seismic array line for offset distance has shown similar pattern of S/N quality with the Shot 1. Figure 6 show seismic raw data taken from the centre of array line where the S/N quality for every test is slightly different compare data from offset distance. Test 1 still show data quality greater than Test 2 and Test 3 where seismic wave attenuation reduced in peat soils.

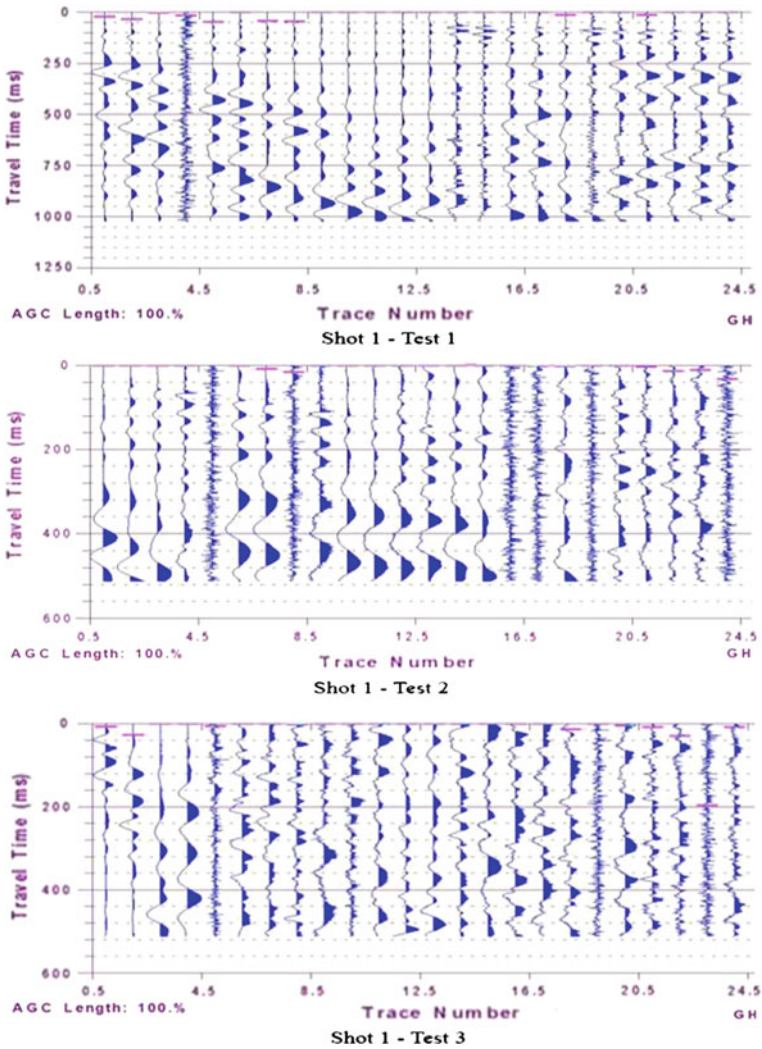


Fig. 5 Shot 1 at offset distance

From the results of all test, it's clearly show that the geophone takeout spacing gives better seismic raw data quality and can be helpful for the operator to interpret the first arrival of seismic wave for data processing and analysis. Shorter geophone takeout spacing with short offset distance is much more appropriate for data

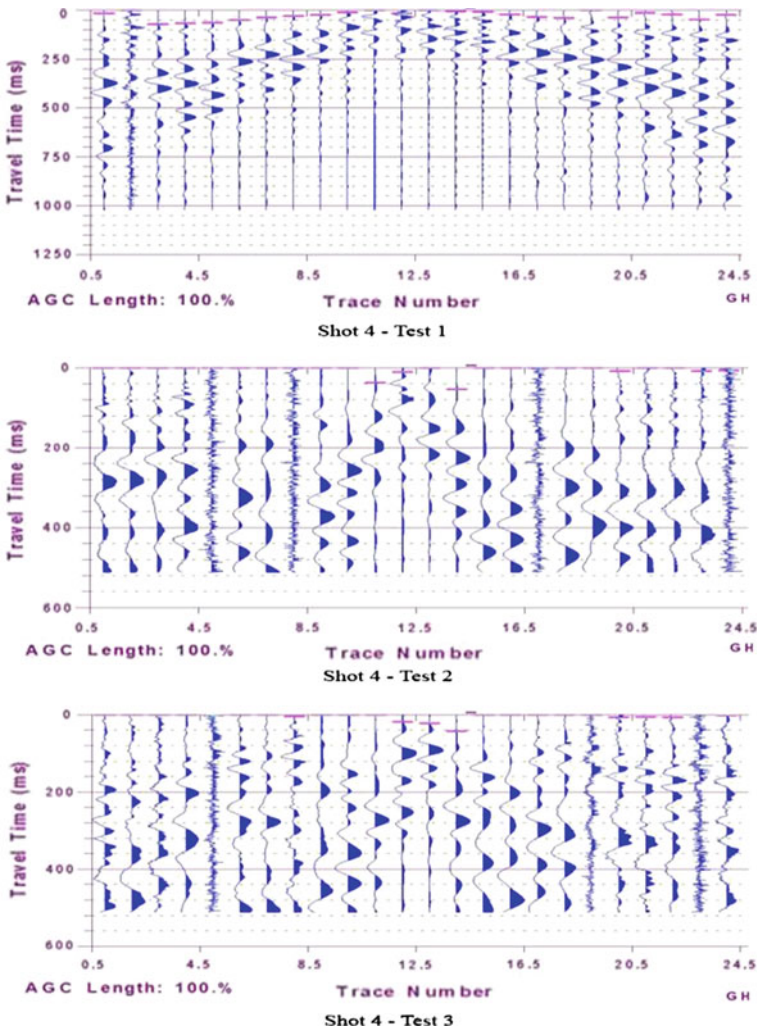


Fig. 6 Shot 4 at centre of array line

acquisition on peat soils since peat have very high seismic attenuation. As for seismic source, the seismic energy can be increased by preventing impact plate penetrate deeper into the peat soil. Impact plate should be having larger surface area and light enough to prevent penetration of impact plate.

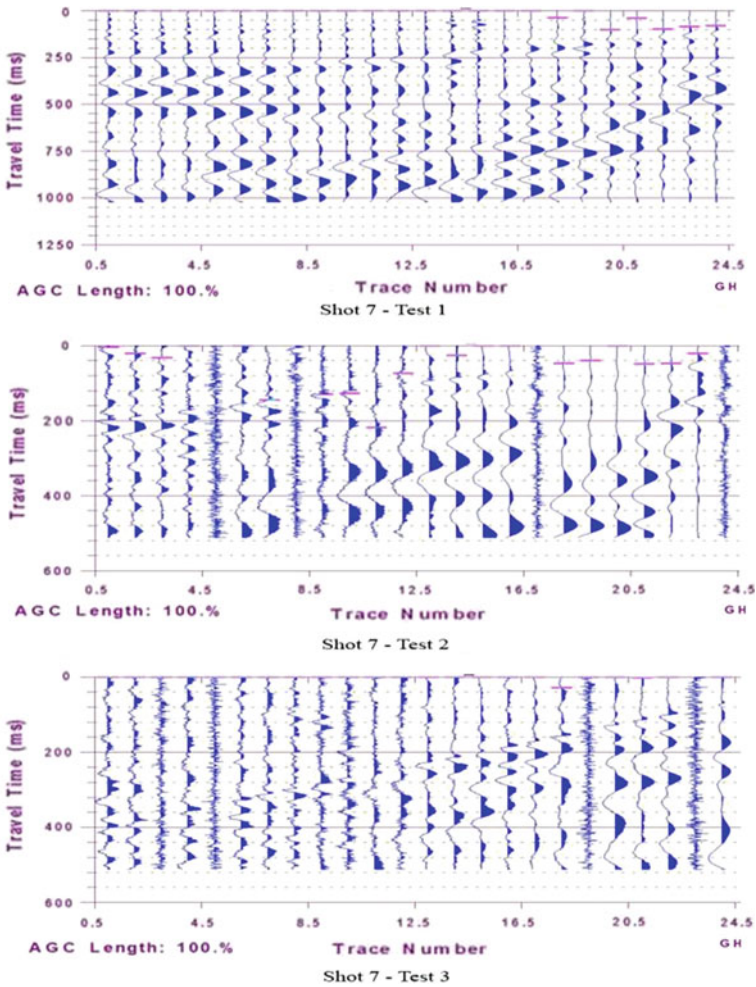


Fig. 7 Shot 7 at offset distance

7 Conclusion

Peat soil is very challenging to the geophysicist's especially involving seismic wave for subsurface characterization due to its complex characteristics. High attenuation in peat soil gives difficulty for the data interpretation and processing. Short geophone takeout spacing and short offset distance gives better S/N data quality in seismic refraction method. Impact plate need to be modified to have larger surface area and light to prevent impact plate penetration and give good source energy into the peat soil. As conclusion, this paper can give good technical information for the engineers to perform subsurface characterization on peat at shallow depth.

Acknowledgment Gratitude is expressed to Assoc. Prof. Dr. Adnan Zainorabidin for funding and supervises this research through Fundamental Research Grant Scheme (vot 1224 “Undrained Dynamic Behaviour of Malaysian Peat Soil”) and Dr. Aziman Madun for guidance to conduct this research.

References

1. A. Boominathan, Seismic site characterization for nuclear structures and power plants. Special section: geotechnics and earthquake hazards. *Curr. Sci.* 87(10) (2004)
2. E.A. Ayolabi, L. Adeoti, N.A. Oshinlaja, I.O. Adeosun, O.I. Idowu, Seismic refraction and resistivity studies of part of Igbogbo Township, South-West Nigeria. *J. Sci. Res. Dev.* 11, 42–61 (2008)
3. A. Zainorabidin, D.C. Wijeyesekera, Geotechnical challenges with malaysian peat. In: *Proceedings of the AC&T* (2007), pp. 252–261
4. S.N. Razali, in *Behaviour of Peat Soil in Instrumented Physical Model Studies*. Malaysian Technical Universities Conference on Engineering and Technology 2012. *Procedia Engineering*, vol. 53 (2013), pp. 145–155
5. J.M. Said, Peat stabilization with carbide lime. *Unimas E-J. Civil Eng.* 1(1) (2009)
6. S. Kazemian, B.K.H. Bujang, A. Prasad, M. Barghchi, A state of art review of peat: geotechnical engineering perspective. *Int. J. Phys. Sci.* 6(8), 1974–1981 (2011)
7. M.A. Riahi, S.H. Tabatabaei, A. Beytollahi, A. Ghalandarzadeh, M. Talebian, M. Fattahi, M. Seismic, Refraction and downhole survey for characterization of shallow depth materials of bam city, southeast of iran. *J. Earth Space Phys.* 37(4), 41–58 (2012)
8. American Society for Testing and Materials. D5777 - Standard Guide for Using the Seismic Refraction Method for Subsurface Investigation. 2000
9. Ü. Dikmen, Modeling of seismic wave attenuation in soil structures using fractional derivative scheme. *J. Balkan Geophys. Soc.* 8(4), 175–188 (2005)
10. L.V. Socco, C. Strobbia, Surface-wave method for near-surface characterization: a tutorial. *Near Surf. Geophys.* 2, 165–181 (2004) (European Association of Geoscientists & Engineers)

The Characteristics of Pontian Peat Under Dynamic Loading

Siti Nurul Aini Zolkefle, Adnan Zainorabidin
and Habib Musa Mohamad

Abstract Peat soils impose special problems in Geotechnical Engineering design as well as Civil Engineering and constructions. Most of researchers conducted investigations on the dynamic loading of soft soils such as sand and clay, but only a few had discovered the behaviour of peat in terms of static and dynamic loadings. Hence, this paper presents the behaviour of peat soil located in Pontian, Johor as well as to obtain the dynamic parameters of peat soil such as shear modulus and damping ratio by using different frequencies. The index properties test, static test and cyclic test have been performed to determine the characteristics and also the parameters required by using stress-controlled cyclic triaxial test of 1 and 2 Hz loading frequencies. All tests were conducted in RECESS, UTHM. The findings explained that Pontian peat behaves differently during the frequencies of 1 and 2 Hz. The shear modulus behaviour on the Pontian peat increase as the loading frequency and effective stresses increased. The results show that the maximum shear modulus of Pontian peat was 1.19 MPa for the frequency of 1 Hz and 1.4 MPa for 2 Hz. Both at effective stress of 100 kPa. Meanwhile, damping ratios show a reduction in the increasing of effective stress and loading frequency applied. The maximum damping ratio in 1 Hz frequency was noted at 44 % and the

Fundamental Research Grants Scheme: Vot 1224 “Undrained Dynamic of Malaysian Peat Soil”, Universiti Tun Hussein Onn Malaysia (UTHM).

S.N.A. Zolkefle (✉) · A. Zainorabidin · H.M. Mohamad
Faculty of Civil and Environmental Engineering, Universiti Tun Hussein Onn Malaysia,
Batu Pahat, Johor, Malaysia
e-mail: putri_aizlin@yahoo.com

A. Zainorabidin
e-mail: adnanz@uthm.edu.my

H.M. Mohamad
e-mail: habibmusa_mohamad@yahoo.com

maximum value for 2 Hz was 35 %. Both at effective stress of 13 kPa. For further research, the cyclic loading can be conducted with different frequencies to show clearly the behaviour of peat in terms of dynamic loading and the cause of frequency influences should also be stated as it would affect the results pattern.

Keywords Cyclic loading · Peat soil · Damping ratio · Shear modulus · Frequency · Cyclic triaxial

1 Introduction

Currently, the industrial and urban development increases the demanding of new land areas, mainly for industrial purposes. The rules of economic very often decided about the localization where it mostly would be at nearby roads and waterways [1]. Ascribable, the most popular locations are placed on the weak soils such as peat. These soft soil deposits are widespread in the world, mainly in Malaysia. Malaysia consists of three million hectares covered with peat which approximately about 8 % of the land area of the country [2]. Peat soils were observed to be predominantly along the coastal area with the annual rate intensities of peaty soil predicted as 2 cm per year [3].

Peat soil is described differently at a time for their qualitative and quantitative measurement [4]. Besides, they impose special problems in Geotechnical Engineering design as well as Civil Engineering and constructions. High surface loading or frequencies imposed on such soils necessarily resulted in large settlements, which must be accommodated in the design consideration and it will take long-term maintenance on such soils [5].

Past researcher had come out with different varied approach towards the solutions for these types of soft soil. However, there is still lack knowledge of the engineers in long term designation. Although peat is a critical soil, which have a low bearing capacity and high moisture content with the fibrous organic matter and that it is unsuitable for use as foundation materials for any construction works [6]. It has been agreed that the significant parameters in Geotechnical Engineering controlling the response of soil towards the cyclic loading are shear modulus and damping ratio [7]. These parameters must be determined to accurately measure their expected and required response towards earthquake shaking [8] and also for the design of Geotechnical engineering problems [9].

The cyclic properties of peat that have been most substantially investigated in prior work are the variations of shear modulus and damping ratio with cyclic shear strain. Previous work identified in the literature on the performance of peat cyclic was associated with [10, 11]. Mercer Slough peat in Washington, [8, 12] peat in Sherman Island, California, [13] Montezuma Slough and Clifton Court peat, [14] California Bay Delta, [15] Bogota's Subsoil Peat and [16] West Johor Peat.

2 Study Area

Pontian was one of the problematic peat land located in the state of Johor. The study area located in the Museum Nanas, MARDI station, Pontian, Johor with the latitude and longitude of $N1^{\circ} 30' 1.824''$ and $E103^{\circ} 27' 36.931''$. The distance was approximately 94 km from UTHM to the study area, thus takes about 1 h and 35 min. Besides, this station was located at 1.2 m above the sea level and 12 m from the nearest mountain and the depth of peat soil was about 1–10 m [16]. Figure 1 shows the road condition near the study area.

As seen in Fig. 1, road in Pontian experienced damages and patches along the ways which mainly caused by the ground settlement since heavy traffic frequently passing the road. Since the road was developed on the peaty ground, it should be noted that peat would behave differently compared to the other soft soil. The characteristics of peat are often noted as highly compressible and the settlement is immediate due to its high water absorption and decomposition characteristics. Extra consideration must be taken into account to develop the long term effect. Figure 2 shows the location of the study area in Pontian site.

It shows that the study area was surrounded by palm oil plantation and some fruit trees. Since the area was located in the museum, then there are hectares of pineapple field around the site. The soil conditions are quietly different because mostly it contains roots and branches and very difficult to sampling.

Most research has been devoted to the cyclic response of inorganic soils such as sand, clay, silt and gravel with significant organic content. However, there were increasing interests in cyclic response of highly organic deposits such as peat have been developed.

Fig. 1 Patches along Pontian road, Johor



Fig. 2 Location of the study area



3 Method Approach

As mentioned, peat characteristically has the low bearing capacity, high moisture content and highly compressible type of soil which requires knowledge and considerations in order to work with peat soil. Thus, this paper will evaluate the characteristics and behaviour of peat soil under dynamic loading for the frequencies of 1 and 2 Hz. Approximately 12 numbers of undisturbed Pontian peat (POpt) specimens are collected. The index properties test, static test and cyclic test have been performed to determine the characteristics and also the parameters required. All tests are conducted in the laboratory at the Research Centre of Soft Soil (RECESS) at Universiti Tun Hussein Onn Malaysia. Firstly, the index properties test such as listed in the Table 1 was done to determine the physical properties of peat soil in Pontian. All tests were done using the guide references shown in Table 1 [17, 18]. The effective stresses used in both static and dynamic tests are 13, 25, 50 and 100 kPa. The proposed value of effective stresses and frequencies applied are based on the previous research whereby mostly in Malaysia, the continuous loading is affected by the change of water level, traffic loading and minor causing by an earthquake. Consolidated isotropic undrained triaxial test is conducted to implement the static test and cyclic triaxial test for the accomplishment of the dynamic test.

Conventional stages used in monotonic triaxial testing, which are saturation stage, consolidation stage and shearing stage for all effective stresses. Then, cyclic

Table 1 Test carried out

	Test	Guide references	Remarks
Index properties test	Degree of humidification	Von post scale	To determine the degree of decomposition of peat sample on site
	Specific gravity	BS 1377: Part 2:1990: 8.3	To determine the specific gravity of peat
	Moisture content	BS 1377: Part 2: 1990: 3.2	To evaluate the effect of temperature on drying process of peat
	Organic content	BS 1377: Part 3: 1990: 4	To evaluate the loss of ignition of peat
	Liquid limit	BS 1377: Part 2: 1990: 4.3/4.4	Determine the consistency limit of peat
	Fiber content	ASTM D1997-91 (2001)	To determine the quantity of fibers in a peat sample
	pH test	BS 1377: Part 3: 1990: 9	Determine the salinity value of peat sample
Static test	Monotonic triaxial	BS 1377: Part 7: 1990: 9	To determine the cyclic amplitude from the stress-strain curve
Dynamic test	Cyclic triaxial	ASTM D5311-92 (1996)	To evaluate the parameters of dynamic loading

triaxial, is followed to obtain dynamic parameters such as damping ratio and shear modulus of peat soil. All effective stresses are applied in the testing of cyclic triaxial using two different loading frequencies. Same stages as monotonic triaxial are applied and additional stage called ‘cyclic’ is used after shearing stage.

Sampling soil location was done at MARDI Station, Pontian, Johor. Ground water table was found at the depth of less than 1 m during the sampling. The soil was excavated to a depth of 0.3 m and then a tube sampler with the size of 50 mm diameter and 100 mm height were pushed slowly into the soil. The quality of samples was maintained by ensuring the sharpness of the tube. The undisturbed peat soils were waxed at both the ends of the tubes and sealing with the aluminums and plastics sealed to prevent the loss or gain of moisture. Jolting during transport was avoided. The samples were kept in the laboratory under constant temperature in the air conditioned room.

When conducting laboratory tests, great care has been taken during the sample preparation. Top and bottom of the specimen was trimmed and the trimming process was carried out carefully since peat soil containing fibers which can be easily disturbed. Besides, the process also done as quickly as possible to minimize the disturbance and also the moisture content of the specimen [19].

4 Cyclic Triaxial Equipment and Procedure

The machine used to perform results in the cyclic behaviour of Pontian peat was a cyclic triaxial machine. Sample preparation for the cyclic triaxial test is similar to that of the monotonic test. A specimen sized of 50 mm diameter and 100 mm height was mounted on the base of the pedestal sealed with a rubber membrane and ends with filter paper and porous stone at each end. Figure 3 illustrated the specimen setup for cyclic triaxial test.

Same as the monotonic triaxial test, two rubber o-rings were equipped around the drainage lead of the top cap and another two around the triaxial base to ensure that it is an airtight. At the first stage, specimens are saturated by the increments of 50 kPa for cell pressure and back pressure applied according to the specification.

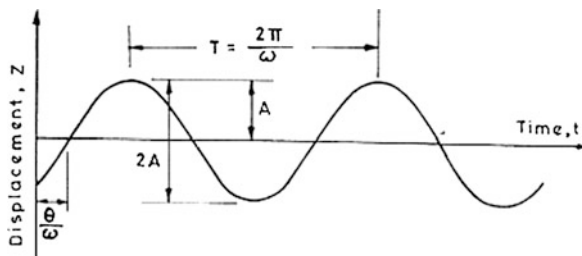
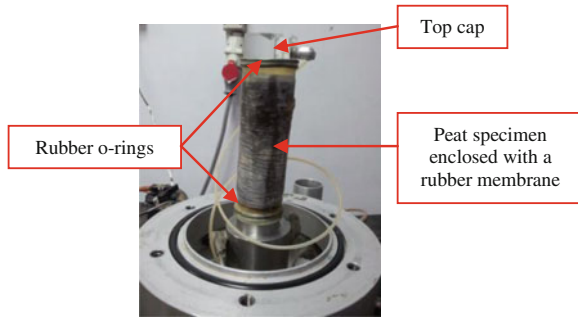


Fig. 3 Specimen setup of GDS instrument for cyclic triaxial test

Fig. 4 Particle displacement as a function of time [20]



Then, all specimens were subjected to 24 h consolidation based on the standard based on each effective stresses (13, 25, 50 and 100 kPa) respectively. During the shearing process, specimens were first isotropically consolidated by applying an axial load to at least half of its maximum monotonic deviator stress in order to limit the amplitude during the cyclic stage. The specimen was continued to a cyclic loading by the means of internal load cell with the condition of anisotropic and systematically controlled by the GDSLAB software.

In cyclic triaxial tests, vibration was produced in the form of different pattern that caused by dynamic loading. The simplest form of dynamic loading is illustrated in Fig. 4.

The vibration motion during dynamic loading will produce an equation as in (1) expressed below [20].

$$Z = A \sin(\omega t - \theta) \quad (1)$$

where:

Z displacement of the rotating mass at any time

θ phase angle

A displacement amplitude from the mean position or single amplitude

ω circular frequency in radians per unit time

During the cyclic stage, specimens used were dynamically loaded up to 100 cycles and specifically used only one-way loading with a stress-controlled conditions at 1 and 2 Hz loading frequency.

5 Index Properties

The physical properties of the soil samples were shown in Table 2. The preliminary identification of the soil was made based on the index properties tests conducted on the peat soil sample. Peat was classified based on the degree of humification known as von post scale and the organic and fiber content in the soil sample. The degree of

Table 2 Index properties of POPT

Parameters	Results
Moisture content	898.91 %
Organic content	76.55 %
Fiber content	43.65 %
Liquid limit	255 %
Specific gravity	1.28
Soil pH	3.72
Degree of humidification	Hemic (H5)

humidification test was done by based on the appearance of soil waster that is extruded when a sample of soil is squeezed in the hand.

Loss on ignition test has been conducted on the samples collected to obtain the organic content of the samples. From Table 2, it can be observed that the peat soil in Pontian was identified as a Hemic-type (H5) with an organic content of 76.55 %. This peat soil has very high value of liquid limit (255 %). This is due to the sample contains lots of fiber which results in high water absorption capacity [21]. Since the sampling location was located in the pineapple field, there are possibilities of the soil to have high fiber content. However, compared to [19], fiber content of peat soil in West Malaysia was in the range of 31 and 77 %.

6 Static Test Results

Consolidated isotropic undrained (CIU) triaxial test has been performed to observe the maximum values of deviator stress (σ_{dmax}) during the shearing stage. Each σ_{dmax} of the specimen was very significant in the determination of the amplitude data for cyclic stage. After implementing repetitive monotonic triaxial test in each specimen, the σ_{dmax} for all effective stresses were determined. The volumes of each specimen before testing were maintained in order to achieve better results for the stress-strain curves. Figure 5 expressed the results of stress-strain curves from monotonic triaxial test.

As seen in the Fig. 5, maximum deviator stress at failure are obtained and the results pointed that the σ_{dmax} increases as when σ' increased. All tests have been done until the strain limit of 20 % based on the standard used. All the σ_{dmax} for each effective stresses are recorded and tabulated in the Table 3.

Table 3 indicates the values of half of the maximum deviator stress ($0.5 \sigma_{dmax}$). These values are considered as cyclic amplitude values and used during the input data for cyclic stage. The amplitude for every cycle should be within the range unless failure will occur. The amplitude values in Table 3 pointed increasing with the increased in σ' . This result agreed with [16, 22] which mentioned that the results were influenced by the origin and characteristics of the soil specimen that may have undergone by agricultural activities or machineries. Besides, [23] added that the

Fig. 5 POpt graph of deviator stress (σ_d) versus axial strain (ϵ_a) with different effective stress (σ')

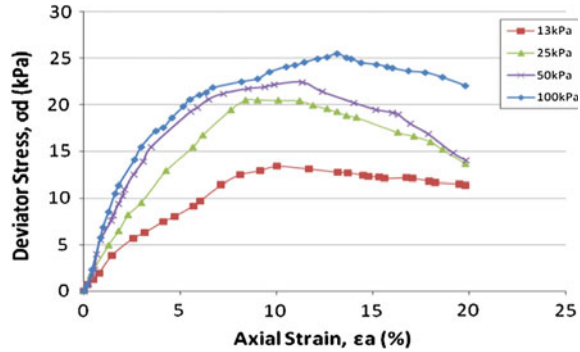


Table 3 Cyclic amplitude values for POpt

σ' (kPa)	E_{amax} (%)	σ_{dmax} (kPa)	$0.5 \sigma_{dmax}$ (kN)
13	10	13.41	0.013
25	12.9	20.53	0.020
50	11.33	22.4	0.022
100	13.12	25.49	0.025

relationships between deviator stresses by the means of axial strain for peat soil are increasing with the increased of effective shear stress.

7 Cyclic Triaxial Test Results

7.1 Shear Modulus (G) Behaviour

Shear modulus (G) of peat soil plays a vital role mainly in Geotechnical engineering design in terms of dynamic loading. Figures 6 and 7 indicated the results of cyclic G at the loading frequency of 1 and 2 Hz. Meanwhile, Table 4 indicates the average values of cyclic G for POpt both at the frequency of 1 and 2 Hz.

From the findings obtained, the cyclic G of Pontian peat increases as the σ' increased within 5 % shear strain. Besides, $\sigma' = 100$ kPa pointed the highest value of G in Pontian peat with below than 2.5 % shear strain in both frequencies. Table 4 indicates that the maximum G was pointed at 1.19 MPa for the frequency of 1 Hz and 1.4 MPa for 2 Hz frequency. From the results, the value of G pointed increased when frequency increased from 1 to 2 Hz. This result agreed with [12] whereby they had observed the effect of loading frequency on the secant modulus of Sherman Island peat for the frequency of 1 and 0.01 Hz. The results indicated that the loading frequency of 0.01 Hz having a smaller secant modulus (8 MPa) compared to 1 Hz (10 MPa) in shear strain of 0.003 %. This is followed by [11] which had performed the strain-controlled cyclic triaxial test for shear modulus of

Fig. 6 G with different σ' at 1 Hz

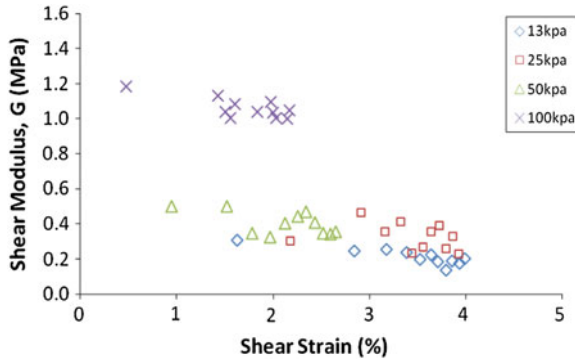


Fig. 7 G with different σ' at 2 Hz

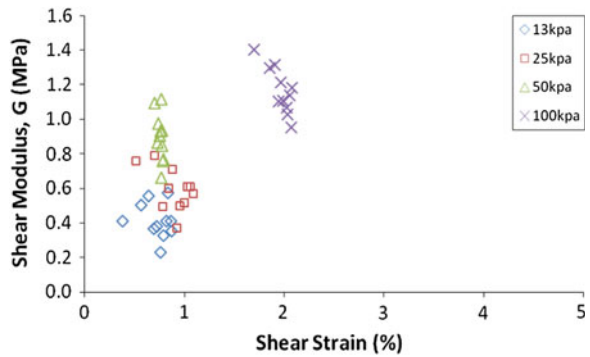


Table 4 Range values of G (Mpa) for POpt

σ' (kPa)	1 Hz	2 Hz
13	0.13–0.3	0.22–0.56
25	0.22–0.47	0.37–0.8
50	0.34–0.5	0.66–1.1
100	1–1.19	0.95–1.4

Mercer slough peat. He showed that the result was increased from the loading frequency of 0.1–10 Hz, which approximately 0.15–0.24 MPa. This is proved that the cyclic G behaviour of Pontian peat indicate between the range of peat soil in other places. Besides, the results of the Pontian pet show that the cyclic G at both frequencies having the medium stiffness level of soil compared to other peat soil.

7.2 Damping Ratio (D) Behaviour

Cyclic D was defined as the damping coefficient divided by the critical damping coefficient. Besides, D usually represents as the ability of a material to dissipate the dynamic load or dampen the system such as by the soil friction, heat or plastic yielding [24].

Findings explained that the results of cyclic D expressed the vise versa. The variations of cyclic D over shear strain with different σ' for Pontian peat are shown in Figs. 8 and 9. Both figures represent 1 and 2 Hz frequencies. These figures show reductions in the increasing of σ' . Cyclic D at 1 and 2 Hz indicate different shear strain at less than 5 % with a varied percentage of cyclic D. However, $\sigma' = 13$ kPa pointed the highest value of cyclic D instead of $\sigma' = 100$ kPa. Table 5 shows the range values of cyclic of cyclic D for Pontian peat at both frequencies.

It shows that the behaviour of cyclic D for Pontian peat decreases as σ' and frequency increased. The maximum cyclic D in 1 Hz loading frequency was noted at 44 %. Meanwhile, 35 % was the maximum value for 2 Hz.

Previous researcher, [12] proved that the damping ratio of Sherman Island peat decreased as the loading frequencies imposed are increased. They had indicated that the frequency of 1 Hz is much lower damping than 0.01 Hz frequency in shear strain of 0.003 %, which is about 4 and 6 % respectively. They also stated that the difference between D at 1 and 0.01 Hz were increased as the cyclic shear strain was increased. Same goes to [11] which pointed that the damping ratio of Mercer Slough peat was increased from approximately 14 to 15 % at 0.1–10 Hz. The values of D of Pontian peat are quite different compared to both Sherman Island and Mercer Slough peat. This result proved that Pontian peat having higher energy dissipation than other types of peat since its fiber content and organic content of the natural peat may be differ.

Fig. 8 D with different σ' at 1 Hz

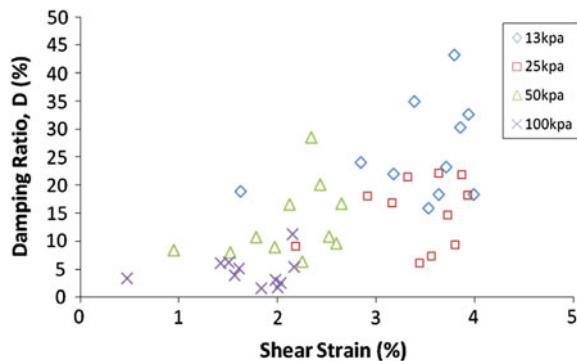


Fig. 9 D with different σ' at 2 Hz

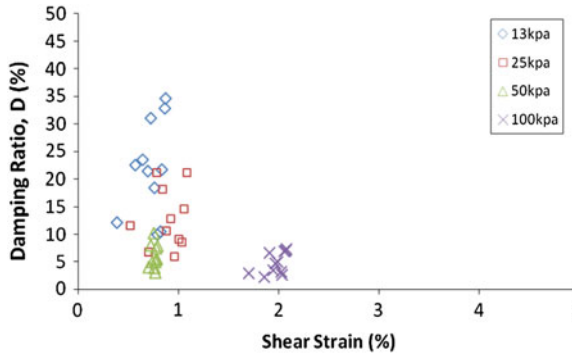


Table 5 Range values of D (%) for POpt

σ' (kPa)	1 Hz	2 Hz
13	15–44	9–35
25	6–23	5–22
50	6–29	3–11
100	1–12	2–8

8 Conclusions and Recommendations

A series of conventional monotonic triaxial tests were conducted to obtain the σ_{dmax} at failure during static loading. Cyclic triaxial tests were implemented after the static test to in order to obtain cyclic parameters for the dynamic behaviour of Pontian peat soil. After analyzing those cyclic parameters, conclusions have been made as follows:

- Pontian peat characterizes as a Hemic-type (H5) with 76.55 % organic content, 255 % liquid limit and 898.91 % water content.
- The σ_{dmax} of Pontian peat increased as the σ' increased during the monotonic triaxial test.
- The G behaviour of Pontian peat increased as the loading frequency and σ' increased.
- Results indicate that the maximum G was 1.19 MPa for the frequency of 1 Hz and 1.4 MPa for 2 Hz.
- Pontian peat show that the G at both frequencies having the medium stiffness level of soil compared to other peat soil.
- The results of D for Pontian peat show a reduction in the increasing of σ' and loading frequency applied.
- The maximum damping ratio in 1 Hz frequency was noted at 44 % and the maximum value for 2 Hz was 35 %. Both at effective stress of 13 kPa.
- Pontian peat having higher energy dissipation than other types of peat.

The analysis describes in this paper observed the values of D and G for cyclic response of peat soil in Pontian, Johor within two different frequencies and σ' applied. For a better comprehension of the subject, further investigations on dynamic loading of peat soil required to critically identify the consequences on dynamic parameters. As suggested, the cyclic loading can be conducted with various numbers of frequencies to show the effect of it towards the peat soil. The cause of frequency influences should also be stated as it would affect the results pattern.

Acknowledgments The special acknowledgment to beloved supervisor, Assoc. Prof. Dr. Adnan bin Zainorabidin for his support and supervision during research and accomplishment of this paper. Also, special thanks to Fundamental Research Grant Scheme (Vot No. 1224 “Undrained Dynamic Behaviour of Malaysian Peat Soil”) in supporting this paper.

References

1. Z. Meyer, T. Kozłowski, Organic soil with elasto-plastic properties settlement under periodic load. 11th Baltic Sea geotechnical conference, Gdansk, pp. 285–292 (2008)
2. J.M. Said, S.N.L. Taib, Peat stabilization with carbide lime. UNIMAS E-J. Civ. Eng. **1** (1) (2009)
3. H. Al-Ani, E. Oh, G. Chai, Characteristics of embedded peat in coastal environments. Int. J. Geomate **5**(1), 610–619 (2013)
4. A. Zainorabidin, Static and dynamic characteristics of peat with macro and micro structure perspective, Ph.D. thesis in civil engineering, University of East London (2011)
5. M.S. Islam, E. Hoque, M.M.K. Munshi, Geotechnical characteristics of peaty soil in Bangladesh. 2nd international conference on advances in soft soil engineering and technology, Putrajaya, pp. 67–78 (2003)
6. P.K. Kolay, H.Y. Sii, S.N.L. Taib, Tropical peat soil stabilization using class F pond ash from coal fired power plant. Int. J. Civ. Eng. **3**, 2 (2011)
7. P. Kallioglou, T. Tika, G. Koninis, S. Papadopoulos, K. Ptilakis, Shear modulus and damping ratio of organic soil. Geotech. Geol. Eng. **27**, 217–235 (2009)
8. T.M. Wehling, R.W. Boulanger, L.F. Harder Jr., M.W. Driller, Confinement and disturbance effects on dynamic properties of fibrous organic soil. XV ICSMGE satellite conference on lessons learned from recent strong earthquakes, pp. 211–217 (2001)
9. T.G. Sitharam, L. Govindaraju, A. Sridharan, Dynamic properties and liquefaction potential of soil. Curr. Sci. **87**(10), 1370–1378 (2004)
10. S.L. Kramer dynamic response of peat, final research report, research project T9233, Task 28 (1996)
11. S.L. Kramer, Dynamic response of Mercer slough peat. J. Geotech. Geoenviron. Eng. **126**(6), 504–510 (2000)
12. R.W. Boulanger, R. Arulnathan, F.H.J. Leslie, R.A. Torres, M.W. Driller, Dynamic properties of Sherman Island peat. J. Geotech. Geoenviron. Eng. **124**(1), 12–20 (1998)
13. T. Kishida, T.M. Wehling, R.W. Boulanger, M.W. Driller, K.H. Stokoe II, Dynamic properties of highly organic soils from Montezuma Slough and Clifton Court. J. Geotech. Geoenviron. Eng. **135**(4), 525–532 (2009)
14. R.E.S. Moss, J. Hollenback, Seismic response of peaty organic soils as a levee foundation material. Geo-frontiers conference proceedings, Dallas (2011)
15. C.A. Moreno, E.E. Rodriguez, Dynamic behaviour of Bogota’s subsoil peat and its effect in seismic, wave propagation. 13th world conference on earthquake engineering, Canada (2004)

16. A. Zainorabidin, I. Bakar, Engineering properties of in situ and modified hemic peat soil in western Johor. 2nd international conference on advances in soft soil engineering and technology, Putrajaya, pp. 173–181 (2003)
17. British Standards, Soils for civil engineering purposes, BS1377 (1990)
18. ASTM Standards, Annual Book of ASTM Standards, Section 4: Construction, Soil and Rock (I), vol. 04:08, pp. 1147–1156 (2007)
19. Y. Duraisamy, B.K. Huat, A.A. Aziz, Engineering properties and compressibility behaviour of tropical peat soil. *Am. J. Appl. Sci.* **4**, 768–773 (2007)
20. S. Saran, Soil Dynamics and Machine Foundations (Suneel Galgotia for Galgotia Publications (P) Ltd., New Delhi, 1999)
21. P.K. Kolay, M.P. Pui, Peat stabilization using gypsum and fly ash. *UNIMAS E-J. Civ. Eng.* **1** (2), 1–5 (2010)
22. S.G. Paikowsky, A.A. Elsayed, P.U. Kurup, Engineering properties of Cranberry Bog Peat. 2nd international conference on advances in soft soil engineering and technology, Putrajaya, pp. 153–171 (2003)
23. S. Cola, G. Cortellazo, The shear strength behaviour of two peaty soils. *Geotech. Geol. Eng.* **23**, 679–695 (2003)
24. R. Luna and H. Jadi, *Determination of dynamic soil properties using geophysical methods*. Proceedings of the first international conference on the application of geophysical and NDT methodologies to transportation facilities and infrastructure, St. Louis (2000)

Assessment of Riverbank Soil Properties at Sg. Damansara

Fauzi Baharudin, Mohd Shafee Harun, Norazlan Khalid
and Zulina Mohd Yusof

Abstract Riverbank failure is a common issue whereby almost every year riverbanks are prone with problems, such as erosion, breaching or retirements. Among the major causes are due to the use of geotechnical unstable materials, seepage and sliding of soil. Therefore, the main issue to be tackled is to evaluate riverbank soil properties. Soil properties evaluation is significant for riverbank assessment and this paper gives better justification for problem arise. This study focuses on the characterization of soil properties and the identification of the physical and mechanical soil properties of undisturbed soil sample. This is seen as an opportunity to overcome any issues related to the riverbank failure. The location of this study is located at Damansara River, Seksyen 13, Shah Alam, Selangor. Laboratory experiments that have been conducted are Moisture Content Test, Specific Gravity Test, Atterberg Limit Test, Particle Distribution Test, Compaction Test, Permeability Test and also Shear Strength Test. The soil at Damansara River riverbank is classified as well graded silty sand. Moisture content for both samples is 33 and 39 %. The specific gravity for both samples recorded as 2.27 and 2.61. Furthermore, plastic limit for each sample is 31 and 35 % while liquid limit is 42 and 50 %. Dry density for Sample 1 is 1.85 Mg/m^3 while Sample 2 is 1.70 Mg/m^3 . The permeability of the soil is range of 10^{-3} to 10^{-5} . The strength of riverbank soil is low due to the condition of soil properties which is sand where the value of cohesion, c' , recorded is 8 kPa while internal friction, ϕ , value is 20.4° .

Keywords Riverbank soil · Soil testing · Physical properties of soil · Mechanical properties of soil

F. Baharudin (✉) · N. Khalid · Z.M. Yusof
Faculty of Civil Engineering, Universiti Teknologi MARA, Shah Alam, Selangor, Malaysia
e-mail: fauzi1956@salam.uitm.edu.my

M.S. Harun
Institute for Infrastructure Engineering and Sustainable Management (IIESM),
Universiti Teknologi MARA, Shah Alam, Selangor, Malaysia

1 Introduction

Riverbank failure is a common problem which this failure often occurs along the riverbank likes settlement and erosion. The study of soil properties at riverbank results from a geotechnical point of view on soil stability [1]. Soil is one of the natural resources. Soil is a complex system consists of soil organic matter (SOM), water, minerals and air [2, 3]. Usually, organic matters are comes from the plant or animal that remains in the soil is considered pollutant. Besides, water is also has greater effect on soil engineering properties because water can flow through the soil particle causing seepage and sliding to the soil. Soil quality includes mutually interactive attributes of physical, chemical and biological properties, which affect many processes in the soil that make it suitable for agricultural practices and other purpose [4]. Soils are divided into two major groups which are coarse soils and fine soils. Coarse soils are classified for the particle that having greater size such as sand and gravel. Meanwhile, for fine soils are classified for the particle that having finer particle size such as silt and clay.

The properties of soil are divided into two which are physical and mechanical properties. Physical properties are identified in order to get the result of plasticity, compression, permeability and the classification of the soil. The parameters of physical properties are including particle density, liquid limit, plastic limit, particle size, permeability and compaction [1]. The three phase of soil; solid, liquid and gas are mixed naturally, causing difficulties in visualizing the relative proportion. Thus, the physical properties of soil can be identified by laboratory test [5]. Meanwhile, mechanical properties are identified to investigate the problem of shear failure due to the shear strength of the soil. Mechanical properties are concern on applied forces or stress and strains such as settlement problem [5]. Many researches on soil properties have been conducted [6–8] but information on the physical and mechanical properties of soil along the bank of Damansara River are still unknown. The objective of this study are to characterize the riverbank soil properties and to identify the physical and mechanical properties of undisturbed soil samples collected from Damansara River which is located at Seksyen 13, Shah Alam, Selangor near to the Management and Science University. The sample of soil is obtained from Fig. 1 shows the location of the soil sample taken.

2 Methodology

This study is focusing on identifying the soil sample at riverbank. The soil sample from the riverbank can be categorized into two types which are disturbed and undisturbed samples. The soil sample would be undisturbed when the condition of soil structure in the sample is close enough to the condition of soil in situ to allow tests of structural properties of the soil to be used to approximate the properties of the soil in situ and it is usually obtained by coring method. While disturbed sample

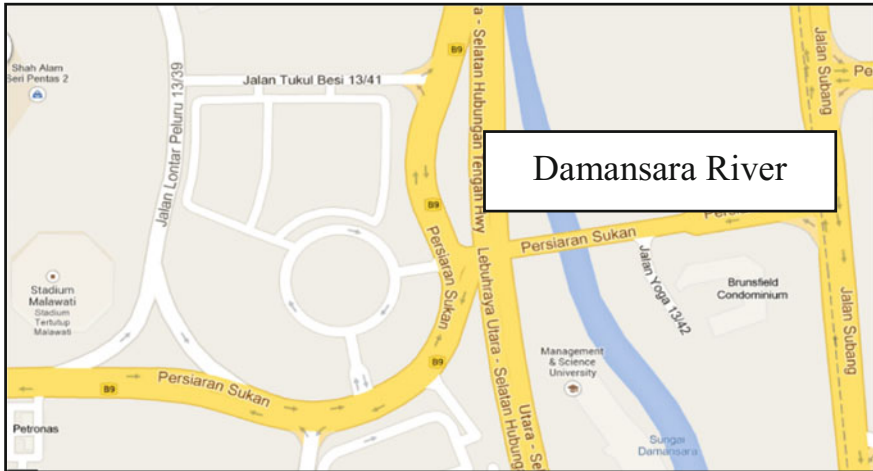


Fig. 1 Location of Damansara River, Selangor

is one in which the structure of the soil has been changed sufficiently that tests of structural properties of the soil will not be representative of in-situ conditions. This equipment used to get the soil sample was hand auger as shown in Fig. 2. There were two samples taken from the riverbank; Sample 1 and 2 which are distance 5 m from the river and the other one is 1 m far away from the sample one. Then, for both samples were removed about 0.4 m deep of topsoil with 2 m depth. Laboratory tests have been conducted on moisture content, plasticity, particle size distribution analysis, specific gravity, permeability, compaction, and shear strength. These laboratory experiments were evaluated in accordance with ASTM standards. The choice of the laboratory experiments are made based on determination of soil properties.

Fig. 2 Hand Auger soil sampling



2.1 Moisture Content

This test is used to determine the ratio of the weight of water to the weight of the soil. The mass of the water can be removed from the soil by heating at 105 °C within 24 h using oven drying method, expresses as a percentage of dry mass [7]. Moisture content is required as a guide to classification of natural soils. The water mass is determined by measured the difference between the weight of wet and oven dry samples using analytical weight balance.

2.2 Atterberg Limit

This cone penetration test is performed to determine the Plastic Limit (*PL*) and Liquid Limit (*LL*) of a riverbank soil. The Atterberg Limit defines the ranges of moisture content that a soil behaves as a solid, plastic and liquid. *PL* of the soil is defined as the moisture content above which the soil will behaves as plastic. Where *LL* is defined as the moisture content above which the soil behaves as a liquid. The term plasticity is applied to silt and clay indicated an ability of the soil to be rolled and molded without breaking apart. Figure 3 shows the cone penetration test used to determine the *PL* and *LL*.

2.3 Particle Size Distribution

The particle size of soil can be characterized by sieve analysis test. Sieve analysis is the method of classify the soil by using nest of standard test sieves as shown in Fig. 4. The method employs sieving and sedimentation of soil suspension as indicated in Fig. 5 to separate the particles. At the end of this test, the weight of soil retained on each sieve is measured and the cumulative percentage of soil retained is calculated and tabulated on particle size distribution curve. The Unified Soil

Fig. 3 Cone penetration test



Fig. 4 Sieve analysis of particle size distribution



Fig. 5 Hydrometer analysis of particle size analysis



Classification System (*USCS*) is a method used to classify soil used in engineering and geology to describe the texture and grain size of a soil.

2.4 Specific Gravity

Specific gravity of the soil is defines the proportional weight of soil to the weight of water at equal volume. The specific gravity of soil is determined using density bottle or pycnometer as shown in Fig. 6.

Fig. 6 Pycnometer

2.5 Permeability

Permeability is the rate of water flow through one unit area of soil face due to the different in hydraulic gradient. The hydraulic gradient is determined by using Darcy's law. The permeability of the soil can be identified by using falling head test. This test is carried out to determine the permeability of the soil. Permeability test is very important to identify the ability of soil in allowing the flowing of water. Figure 7 shows the falling head test was setup in accordance with publication manual produced by Head (1982).

Equation 1 is used for estimating the hydraulic conductivity, K of the sample where L = the height of soil sample column, A = sample cross section, a = the cross section of the standpipe, Δt = the recorded time for the water column to flow through the sample, and h_1 and h_2 = the upper and lower water level in the standpipe measured using the same water head reference.

$$K = \frac{aL \ln(h_1/h_2)}{A(\Delta t)} \quad (1)$$

Fig. 7 Falling head test

Fig. 8 Standard proctor test of soil



2.6 Compaction

Compaction is physical process of improving the strength and physical properties of the soil which is achieving the maximum dry density within the limit of optimum water content at the same time. Compaction is defined as the process of packing the particle of soil become close together by mechanical manipulation to reduce void ratio of the soil, which results in increase in its dry density. Proctor standard test as shown in Fig. 8 is used to demonstrate for a specific amount compaction energy applied on the soil equip on water content where at same time the soil attains maximum density. The water content corresponding to the maximum density achieved is called optimum moisture content.

2.7 Shear Strength

The strength of soil is measure to determine the maximum stress that soil can induce without causing any failure. The strength will depend on whether the soil deformation occurs under fully drained condition (no build up pore water pressure during deformation) or undrained condition (full build up pore water pressure during deformation). In triaxial compression test, a specimen of soil is subjected to three principal compressive stresses at right angle to each other. The specimen failed by changing one of the stresses.

3 Results and Discussions

3.1 Moisture Content Analysis

Table 1 shows the geotechnical of soil on physical properties for Sample 1 and 2. The soil samples were taken from the riverbank of Damansara River. From the analysis, it can be seen that the soil Sample 2 contained higher moisture content than Sample 1. The moisture content for both sample is low due to the type of soil which is sand. Sand is a group of soil categorized as cohesionless soil whereby the particles of soil have low of moisture content.

3.2 Atterberg Limit Analysis

Table 2 shows the PL and LL of the soil. The soil particle size can bring changes in water content which is soil properties. The relationship between PI and LL is used to establish the subgroup of fine soil. The importance of these LL and PL is that it represents the upper and lower bounds of plastic state. The ranges of different plastic states are called PI. Thus, the PI for Sample 1 is 11 % while Sample 2 is 15 %.

3.3 Particle Size Distribution Analysis

Figure 9 shows the size distribution of soil for Sample 1. From the sieve analysis, the classification of soil can be obtained by grading curve. The graph shows the correlation of soil particle size to the percentage of sample weigh passing through that obtained during sieve analysis. Based on the grading curve available, the engineering criteria of the soil can be briefly determined. Thus, the type of soil for Sample 1 was identified as well graded silty sand. These results are due to the

Table 1 Moisture content of soil

Number of sample	Moisture content (%)
Sample 1	33.12
Sample 2	39.74

Table 2 Plastic limit and liquid limit of the soil

Number of sample	Plastic limit (%)	Liquid limit (%)
Sample 1	31.21	42
Sample 2	35.27	50

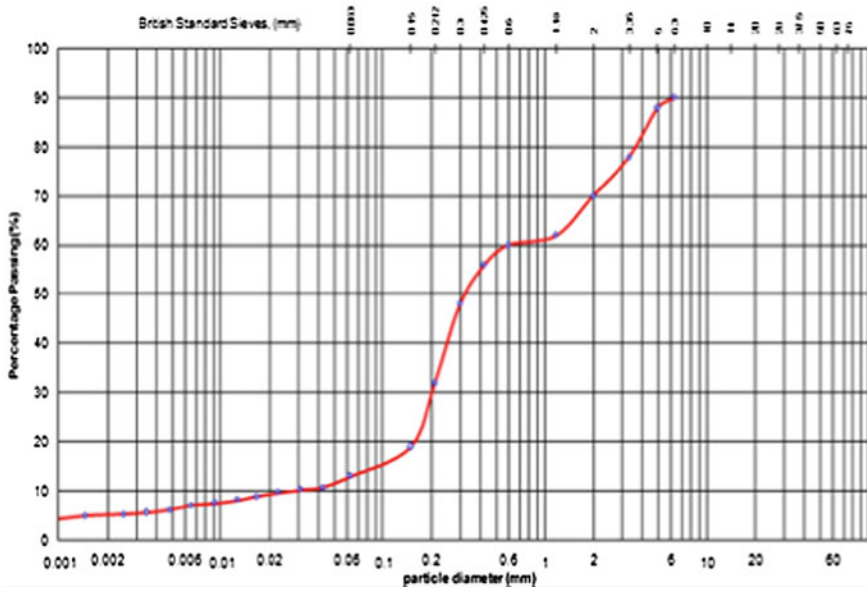


Fig. 9 Graph of particle size of soil for Sample 1

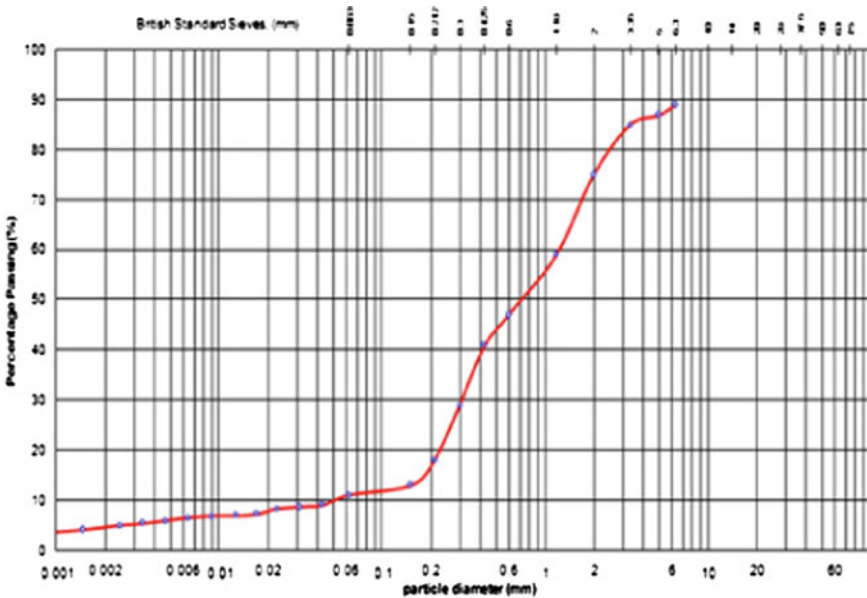


Fig. 10 Graph of particle size of soil for Sample 2

particle size of soil fraction for gravel is 30 %, sand is 57 %, silt is 7.96 % and clay is 5.07 %. The d60, d50, d30 and d10 are 0.6, 0.331, 0.202, and 0.027.

The uniformity coefficient (C_u) is a measure of the particle size range whereas coefficient of gradation (C_g) is a measure of the shape of the particle size curve. The C_u and C_g for Sample 1 is 21.98 and 2.5. Both C_u and C_g will unify for single sizes soil. Range for C_u is between 2.5 and 3.0 is indicates well graded soil. From Figs. 9 and 10 the particle size distribution for the soil is plotted as a semi logarithmic curve known as grading curve. Result of Sample 2 is shown in Fig. 10 which is indicating same type of soil Sample 1 which is well graded silty sand. The particle size fractions of Sample 2 were consists of gravel 25 %, sand 64 %, silt is 6.47 and clay 4.53 %. The fraction of soil is depends on the d60, d50, d30 and d10 are 1.231, 0.745, 0.310 and 0.058.

3.4 Specific Gravity Analysis

Table 3 shows the particle density both of the soil Sample 1 and 2. The results indicated that specific gravity of Sample 1 is 2.27 while Sample 2 is 2.61. Sample 1 is a little bit low rather than Sample 2. These results were obtained by carried out laboratory test which is by using density bottle or called small pycnometer.

3.5 Compaction Analysis

Table 4 shows the compaction for both sample which are Sample 1 and 2. Reducing the amount of void ratio and permeability of the soil, with that the porosity of the soil also reduced. Under the small void ratio the dry density start approaching specific gravity of soil become very dense.

The value dry density and saturated density reach equal whereby the soil become less settlement. The average of both sample are achieved maximum dry density is 1.77 Mg/m³.

Table 3 Specific gravity of Sample 1 and Sample 2

Number of sample	Specific gravity (ρ_s)
Sample 1	2.27
Sample 2	2.61

Table 4 Optimum moisture content and maximum dry density of soil

Number of sample	Optimum moisture content (%)	Maximum dry density (%)
Sample 1	17.49	1.855
Sample 2	21.90	1.695

While the percent optimum moisture content of Sample 2 is higher than Sample 1 which is Sample 1 is 17.49 % and Sample 2 is 21.90 %.

3.6 Permeability Analysis

Permeability test in this study are conducted in laboratory by using falling head test. Figure 11 shows that the hydraulic conductivity become decrease as the time is longer. The longer the time of conducting the experiment, the soil will start to clogs at certain times. Thus, the results were decrease as the soil was clogging. The time of conducting the experiment was start 10 days; however the reading is taken five times which is day 2, 4, 6, 8 and 10 as shown in Table 5. The range of value k (m/s) for sand is indicates the soil is good drainage.

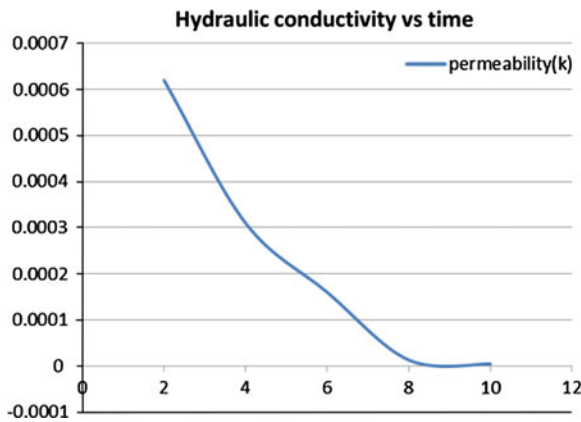


Fig. 11 Hydraulic conductivity versus time

Table 5 Hydraulic conductivity of soil

Day	Average hydraulic conductivity, K (m/s)
2	6.2×10^{-6}
4	3.7×10^{-6}
6	1.6×10^{-6}
8	1.7×10^{-7}
10	4.7×10^{-8}

3.7 Shear Strength Analysis

Figures 12 and 13 shows the Mohr circle for total stress and effective stress for both sample. For total stress has the phi, ϕ of 18.4° and the shear stress, c is 15 kPa. Whereas the effective stress has the phi, ϕ' of 20.4° and the shear stress, c' is 8 kPa. The data of shear strength is important for further design analysis of soil stability purposes.

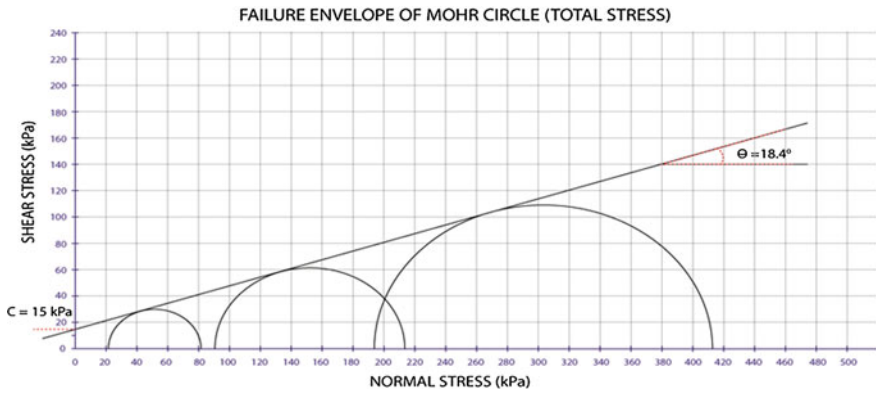


Fig. 12 Mohr Coulomb strength envelope total stress

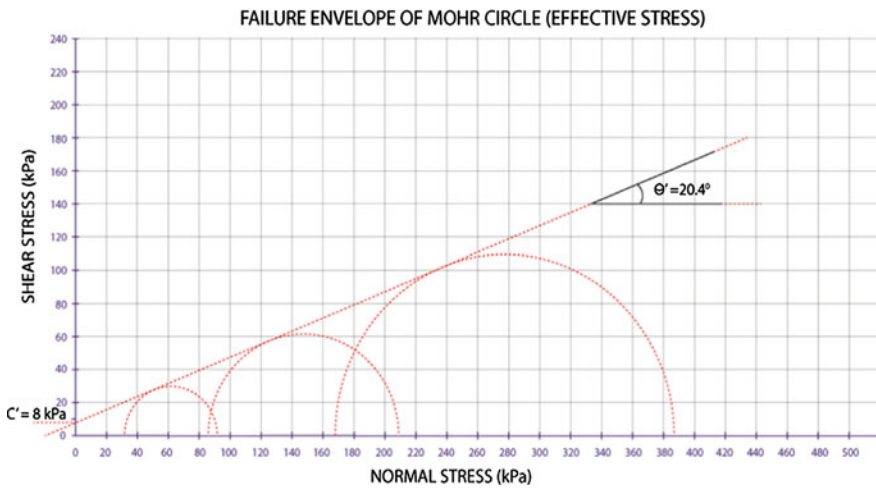


Fig. 13 Mohr Coulomb strength envelope effective stress

4 Conclusion

Soil classification is a part of geotechnical study. From the results, it shows that the type of soil at riverbank of Damansara River is well graded silty sand (SWM). The type of soil is identified based on particle size distribution test analysis. Essentially, determining the grain size distribution of soil tells whether the soil is sustainable or usable for its intended use. This type of soil is categorized as sandy soil due to the low moisture content and high permeability. However, the result also indicates that this soil has lower strength due to possibility of interaction between ground water at ground surface with the soil. Therefore, mitigation measure is compulsory in order to prevent soil erosion and settlement. The slope stability of the riverbank needs to be considered as one of the priority factor of bank failure.

The identification of soil properties is also important to classify the soil material. The soil sampling plays critical role because starting from the time of soil sampling, type of sampling and location of sampling can affect the results of the study. The best sampling time is during the sunny day because the soils have optimum water content compared to rainy day. Meanwhile, the water content of the soil at the riverbank can be excessive during rainy day. Other than that, types of sampling are important role because undisturbed sample usually give the actual results compared to disturbed sample. The coring method is the best method to get the undisturbed sample rather than used digging. The geotechnical properties of soil also need to give more attention in improving the soil structure by using additives or reinforcing material such as natural or geosynthetic fiber. This material plays important role in preventing settlement or erosion of the soil especially at the riverbank.

Acknowledgments The authors would like to express special thanks to the Faculty of Civil Engineering and RMI UiTM for all support rendered. Last but not least, valuable comments from colleagues and referees are very much appreciated. This research is supported by Ministry of Higher Learning (MOHE) under RAGS Fund with reference no. 600-RMI/RAGS 5/3 (198/2012).

References

1. M.D. Hossain, T. Sakai, M.Z. Hossain, River embankment and bank failure: a study on geotechnical characteristics and stability analysis. *Am. J. Environ. Sci.* **7**(2), 102–107 (2011)
2. D.J. Vishal, N.P. Narahari, R.R. Punit, Physico chemical properties of four farm site soils in area surrounding Rajkot, Gujarat, India. *Int. J. ChemTech Res.* **1**(3), 709–713 (2009)
3. F. Hector, R.M. Oscar, M. Enrique, O.M.D. Carmen, L.B. Ana, Heavy metals in agricultural soils and irrigation wastewater of Mixquiahuala, Hidalgo, Mexico, *African. J. Agric. Res.* **6**(24), 5505–5511 (2011)
4. K. Rakesh, K.U. Rakesh, S. Kishan, Y. Brijesh, Vertical distribution of physico-chemical properties under different topo-sequence in soils of Jharkhand. *J. Agric. Phys.* **12**(1), 63–69 (2012)
5. R. Whitlow, *Basic Soil Mechanics* (Prentice Hall, Singapore, 2004)

6. L. Pietola, R. Horn, M. Yli-Halla, Effect of trampling by cattle on the hydraulic and mechanical properties of soil. *J. Soil Tillage Res.* **82**, 99–108 (2005)
7. M.D. Soriano-Soto, A. Calvo-Cases, C. Boix-Fayos, A.C. Imeson, Effect of climate on some soil properties and related thresholds the erosion response of soils in a limestone area. *J. Phys. Chem. Earth* **20**(3–4), 281–286 (1995)
8. A. Banin, A. Amiel, A correlative study of the chemical and physical properties of a group of natural soils of Israel. *Geoderma* **3**, 185–198 (1969)

Stress-Strain Behavior of Parit Nipah Peat

Siti Hajar Binti Mansor and Adnan Bin Zainorabidin

Abstract Stress can produce a deformation because real material is not rigid, the deformation will measure the strain. Stress-strain is important in determining peat behaviour. Peat cannot support too much load on it because of peat have very low strength, high compressibility and long-term settlement. The objective of this study is to determine the behaviour of stress-strain characteristic using different test. The undisturbed samples were collected at Parit Nipah, Batu Pahat, Johore, Malaysia. The tests are direct simple shear and direct shear box. These methods cover the determination of the stress-strain relationship of peat and to investigate the behaviour of peat. Normal stresses are 12.5, 25, 50 and 100 kPa with 0.1 mm/min rate of shear. This study is to know the stress-strain between direct simple shear test and direct shear test based on peat specimens of hemic. The test results will contribute and establish the drained shear characteristic of testing peat. It shows that direct simple shear test stress-strain is increasing clearly than direct shear test. Besides that, direct simple shear is suitable to use on peat soil rather than direct shear box. This research can help the geotechnical engineers and can be used in the development of foundation and as well as constructions.

Keywords Hemic • Direct simple shear • Direct shear box • Stress-strain

Postgraduate Intensive Grantt (Vot 1348) and Fundamental Research Grantt Scheme: Vot 1224, Universiti Tun Hussein Onn Malaysia (UTHM).

S.H.B. Mansor (✉)

Universiti Tun Hussein Onn Malaysia, Parit Raja, 86400 Batu Pahat, Johore, Malaysia
e-mail: gf130037@siswa.uthm.edu.my

A.B. Zainorabidin

Faculty of Civil and Environmental Engineering, Universiti Tun Hussein Onn Malaysia, Parit Raja, 86400 Batu Pahat, Johore, Malaysia
e-mail: adnanz@uthm.edu.my

1 Introduction

Peat soil is a problematic soil. Peat soil usually has low shear strength and the determination of stress strength of peat soil is difficult in geotechnical engineering because of high water content and organic matter. Peat contains 100 % of pure organic material which has 65 % organic matter or less than 35 % mineral content [3]. That is why engineer tendency to avoid any construction and building on the soil. Lack of research has been focused on the stress-strain strength behaviour of peat. Laboratory testing has become an important part in soil investigation. This research is focused at Parit Nipah, Batu Pahat, Johore. Stress-strain strength is the most important thing to know the behaviour of peat.

The direct shear test is an old development. The direct simple shear test is a new improvement of direct shear box. Both devices will be applied shear directly to the soil specimen, but the direct shear test has inhomogeneity of the resultant strains and applied stress compare to direct simple shear test that can minimize them [2]. The shearing condition of direct simple shear and direct shear box are shown in Fig. 1a, b. This research will focus on the challenging of Malaysian peat soil in construction for infrastructure due to the stress-strain relationship. The stability of the structure that build on peat soil is depending on the change of peat soil with time unless the load structure transferred to the foundation.

2 Hemic Peat

There are three types of peat soil, such as fibrous, hemic and amorphous. The following description of peat characteristics can be understood on the water content, fiber content, degree of humification, color, organic content and Atterberg limit. Hemic peat is different from fibrous and amorphous. Hemic contain less fiber than fibrous. Hemic has fiber content from 33 to 67 %. It is based on the degree of decomposition of peat that can be shown in Table 1.

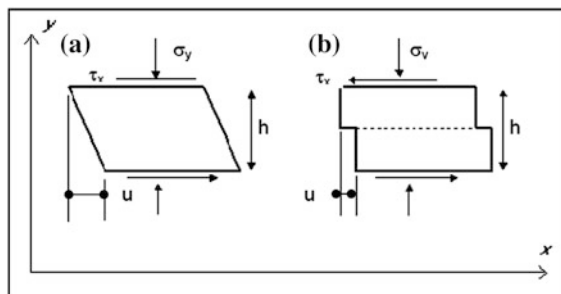


Fig. 1 Conditions of (a) direct simple shear and (b) direct shear box [2]

Table 1 Malaysian soil classification system (MSCS) for organic soil and peat [4]

Soil group	Organic content	Group symbol	Degree of humidification	Subgroup name	Field identification
Peat	>75 %	Pt	H1–H3	Fibric or fibrous peat	Dark brown to black in colour. Material has low density so seems light. Majority of mass is organic so if fibrous the whole mass will be recognized plant remains. More likely to smell strongly of highly humidified
			H4–H6	Hemic or moderately decomposed peat	
			H7–H10	Sapric or amorphous peat	

3 Direct Simple Shear

Direct simple shear test is more accurate than direct shear test and triaxial test [1]. Simple shear is in cylindrical shape. It obtained more homogenous distribution to shear and normal stresses, and resulting strains. Besides that, it purposed is to apply the specimen with a simple shear strain deformation [3]. Direct simple shear test can shear a soil to unlimited displacement without creating a substantial non-uniformities in stress and strain distributions. The major advantage of this test is, it can observe the rotation of principal stress direction [3].

4 Direct Shear Box

After the text edit has been completed, the paper is ready Direct shear box is the simplest, straightforward and the oldest procedure to determine the shear strength of soils. Specimen inside the direct shear box is sheared along the horizontal plane and shows that the failure plane is horizontal. The specimen is in square shape. There's been a criticized on direct shear box that relate to the non-uniformity of stress-strain throughout the specimen because of rigid platens that used to confine the specimen as stated from Saada and Townsend, 1981 [2].

5 Soil Sampling

The undisturbed peat sampling of Parit Nipah, Johore was performed to a depth of 0.5 m. The sample tubes were PV C tube, with a wall thickness of 1.5 mm, an inside diameter of 100 and 75 mm in length of 100 mm. On extraction, the undisturbed samples were carefully sealed with plastic film and aluminium foil that placed inside the curing chamber. Besides that, paraffin wax was used to protect the

samples from losing moisture. Next, the extruded sample is trimmed with a palate knife carefully. The sample for direct simple shear test was trimmed with circular mould that has 63 mm diameter and 30 mm height. The direct shear box is trimmed in a square mould with a size of 60 mm × 60 mm × 25 mm. Parit Nipah peat carried out 4 direct simple shear tests and 8 direct shear box test. The specimen must be cut properly so that the disturbance is small.

6 Experimental Investigation

In the investigation of direct simple shear test, normal stresses that have been carried out on undisturbed specimens are 12.5, 25, 50 and 100 kPa. Normal stress was imposed on top of the specimen properly. The shear rate is 0.1 mm/min. The direct simple shear apparatus used in this research is shown in Fig. 2a, b.

Another test was also performed that is direct shear box. Direct shear box also carried out using the undisturbed specimens with the same normal stresses and imposed on top of the specimen as a direct simple shear test. The testing also involved with the same rate of shear, 0.1 mm/min. Testing procedures and the result data are as follows. The specimens for both methods are in the same condition. They are naturally consolidated.

6.1 Peat Soil Sample

Some soil properties test has been done to prove the specimen is peat soil. Peat specimens were collected at Parit Nipah, Batu Pahat, Johore. It is hemic peat. Hemic peat has 520.47 % of natural water content, organic content of the specimen was 88 %, liquid limit was 170 % and specific gravity of hemic peat was 1.58.

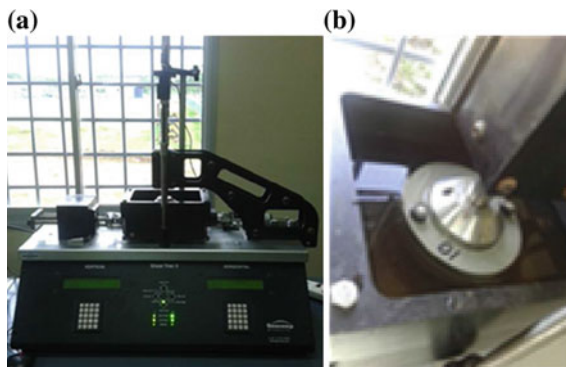


Fig. 2 a Simple shear test. b Specimen in simple shear

6.2 Direct Simple Shear Testing Procedure

It was conducted on a cylindrical specimen that retained inside a series of thin rings based on ASTM D6284-00. A soil specimen surrounded by a stack of rings. The size of the specimen is 63 mm in diameter with 30 mm height. The specimen was thoroughly saturated with water bath for 24 h before run the test. The specimen is consolidated anisotropically under a vertical stress and deformation by application of shear stress. The specimen was then put into the ring shear with normal stress applied were 12.5, 25, 50 and 100 kPa with 0.1 mm/min rate of shear. The specimen is then sheared from top platen with constant normal stress.

6.3 Direct Shear Box Testing Procedure

The peat specimen was prepared properly based on BS standard 1377:1990 (Part 7). As shown in Fig. 3a and b, the specimen was in a square with the size of $60 \times 60 \times 25$ mm. It was thoroughly saturated with water bath for 24 h before run the test. The test equipment consists of a metal box which a soil specimen is placed. Porous stones were placed at the bottom and the top of the specimen. Normal stress is applied through a metal plate. The box is split horizontally into two halves. Then, the specimen was put into the shear box with normal stresses between 12.5, 25, 50 and 100 kPa. The shear rate was 0.1 mm/min.

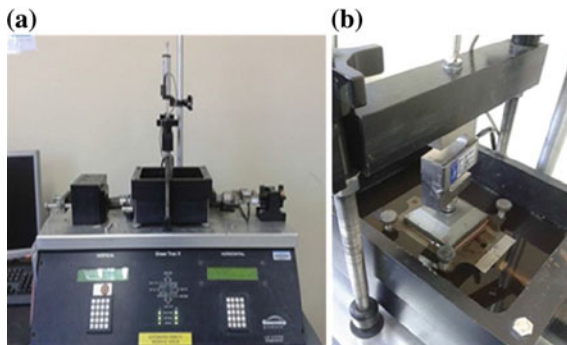


Fig. 3 a Direct shear box test. b Specimen in direct shear box

7 Results and Discussion

In Fig. 4, there are different shear parameter between direct simple shear and direct shear box. It shows that direct shear box has higher shear stress than direct simple shear because of the different shearing mechanism from each test.

The relationship between the shear stress and shear strain obtained from direct simple shear test are shown in Fig. 5. The different curves are based on different normal stress (kPa) that applied. Normal stresses are 12.5, 25, 50 and 100. As can be seen in this figure, shear stress increase with shear strain and show the peak stress until the soil is failing to shear. Peak stress can be found in the constant load test. As illustrated in this figure, when normal stress increased the stress-strain also increased, probably because of the peat fiber and normal stress that respond on the tested peat. Figure 5 shows the stress-strain relationship graph at different normal stresses.

The Fig. 6 shows a specimen that was taken out after direct simple shear test. The zone failure can be seen in the figure, proved the applicability of direct simple

Fig. 4 Shear parameter of direct simple shear and direct shear box

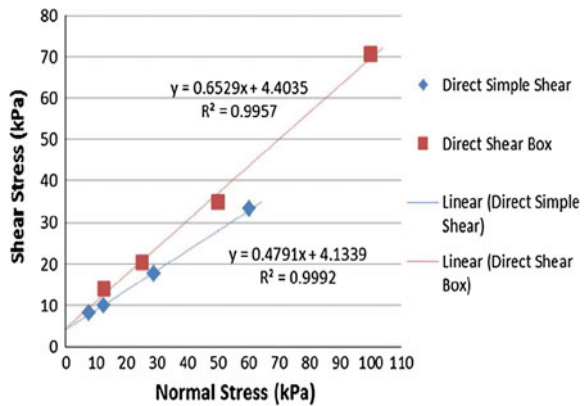


Fig. 5 Stress strain relationship of peat with different normal stress of 12.5, 25, 50 and 100 kPa after simple shear

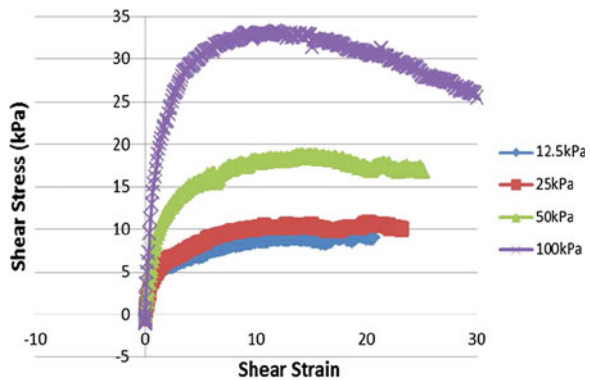
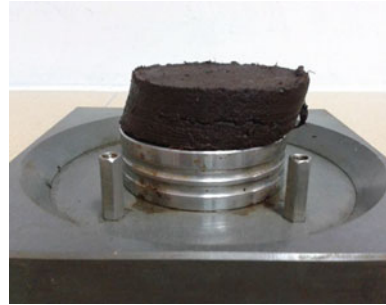


Fig. 6 Peat soil taken out from the stack of rings after test



shear test. Usually cohesive soil has the connection with shear failure. The complete soil failure can happen along one zone or sliding surface and create soil displacement.

The test involved a change of normal stress to define the stress obtained from the shear box and are presented in Fig. 7. It shows that the shear stress is increasing continuously based on the increment of the normal stresses. But, there are small differences of strains from each stress. It is because the plane failure of direct shear is at horizontal plane and at the center of the specimen. The fiber in the middle of the specimen will be affected more than the other area of the specimen.

Figure 8 shows a peat specimen that is done after the direct shear box test. As can be seen below, the strain was occurring at the center of the specimen at horizontal plane. This is because of the relative displacement of the two halves of the box.

Fig. 7 The shear stress of peat with different normal stress of 12.5, 25, 50 and 100 kPa after direct shear box

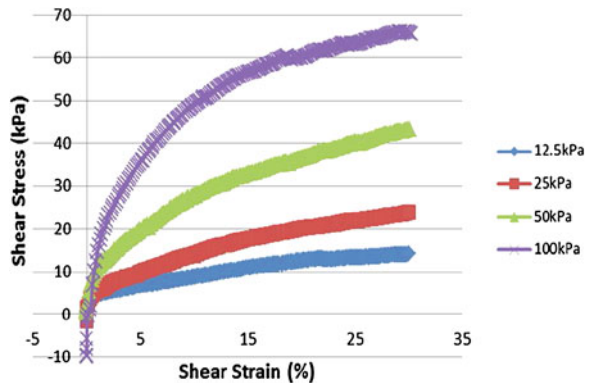
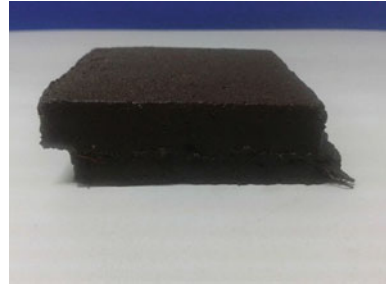


Fig. 8 Peat soil taken out from shear box test



8 Conclusion

The comparative study between direct simple shear test and direct shear box test are based on the following conclusion:

1. The behavior of peat is largely based on its fibrosity and anisotropic. Both tests are increasing continuously in shear stress. There are differences of shear stresses between direct simple shear test and direct shear box test but shows clear differences in strains. This is because the shear strain homogeneity is increased inside the direct simple shear specimen.
2. The vertical load applied might have been different in these cases considered and influence the strain homogeneity during shearing.
3. Based on the results, direct shear box test gives higher estimates of strengths than direct simple shear. This is because of the different shearing mechanism that imposed to specimen or due to the size of the specimen and the specimen handling manner.
4. The graph of direct shear box is increasing continuously because of the shearing process that only acting at the center of specimen and not spread entire surface of the specimen to the weakest point. A direct simple shear graph shows the peak stress of the specimen and finally decrease because simple shear sheared around the entire specimen.

Acknowledgments The special gratitude to my supervisor for the guidance, encouragement and valuable support and to members of the staff of the Civil and Environmental Engineering Department (UTHM), Research, Innovation, Commercialization and Consultancy Office (ORICC) and Research Centre of Soft Soils (RECESS) who helped me in many ways. I also acknowledge my sincere indebtedness and gratitude to for their love, dream, courage and sacrifice throughout my life.

References

1. A.W. Bishop, G.E. Green, V.K. Garga, A. Anderson, J.D. Brown, A new ring shear apparatus and its application to the measurement of residual strength. *Géotechnique* **21**(4), 273–328 (1971)
2. H. Hanazawa, N. Nutt, T. Lunne, Y.X. Tang, M. Long, A comparative study between the NGI direct simple shear apparatus and the Mikasa direct shear apparatus. *Soils Found.* **47**(1), 47–58 (2007)
3. B.B.K. Huat, S. Kazemian, A. Prasad, M. Barghchi, State of an art review of peat: general perspective. *Int. J. Phys. Sci.* **6**(8), 1988–1996 (2011)
4. A. Zainorabidin, D.C. Wijeyesekera, Geotechnical challenges with Malaysian peat. Paper presented at the 2nd annual conference on the advances in computing and technology, The School of Computing and Technology (2007)

Effect of Fines Content on Liquefaction Susceptibility of Sand-Kaolin Mixtures

Aminaton Marto, Choy Soon Tan, Ahmad Mahir Makhtar,
Lim Mei Yen and Ung Shu Wen

Abstract Recent empirical observations reveal that not only the clean sand is susceptible to liquefaction hazard, both silty sand and clayed sand are also liquefiable. This paper presents the cyclic behaviour of sand-fines mixtures at various fines content. The sand-fines specimens were reconstituted by mixing clean sand with different percentages of plastic fines (kaolin) by weight to a constant relative density of 20 % using dry tamping method. The specimen had been tested with stress controlled cyclic triaxial test under consolidated undrained condition with effective confining pressure of 100 kPa, cyclic load of 0.1 kN and cyclic frequency of 0.5 Hz. The results show that the liquefaction resistance of sand matrix soils increased as fines content increased from 0 to 25 %, whereas this trend was reversed for value of fines content greater than 25 %. In fact, the 25 % of kaolin by weight is also the threshold fines content of sand-kaolin mixtures. Hence this finding justifies that the concept of fines threshold content could be used to significantly explain the influence of fines content on the liquefaction susceptibility of sand-fines mixtures.

Keywords Threshold fines content · Cyclic triaxial test · Sand matrix soils

1 Introduction

Soil liquefaction is an earthquake hazard where the granular material is transformed from a solid state into a liquefied state. The significant increasing of pore water pressure initiates liquefaction process when the effective stress reaches to zero. This phenomenon causes the soil to act like a liquid. Early researchers described that the

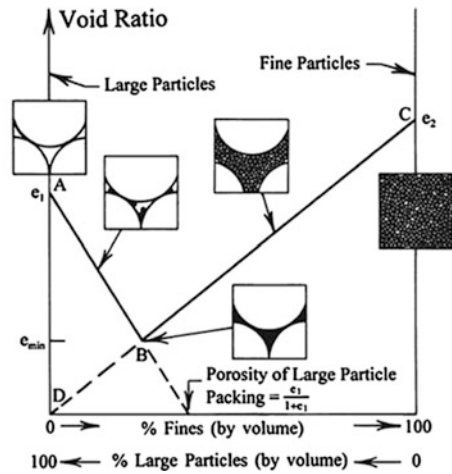
A. Marto · C.S. Tan · A.M. Makhtar · L.M. Yen (✉) · U.S. Wen
Faculty of Civil Engineering, Construction Research Alliance, Universiti Teknologi Malaysia (UTM), 81310 Johor Bahru, Johor, Malaysia
e-mail: limmie-yen@yahoo.com

C.S. Tan
e-mail: cstan8@live.utm.my

Table 1 List of earthquake events [1]

Year	Earthquake	Characteristics of liquefied soils
1964	Niigata	70 % fines and 10 % clay fraction
1968	Tokachi	90 % fines and 18 % clay fraction
1983	Idaho	70 % fines and 20 % clay fraction
1999	ChiChi	Fines content as high as 36–53 %
1999	Adapazari	70 % fines with plasticity 0–25
2009	Olanche	Fines content as high as 15 ± 8 %
2010	Christchurch	Grey fine silty sands

Fig. 1 Composition characteristic of sand matrix soils [9]



most susceptible soil type is loose to moderately dense granular soils. However, several past earthquake events give a contradictory observation that sand matrix soils also exhibit liquefaction behaviour as described in Table 1.

Since then, numerous researches have been carried out globally to study on the roles of fines within the matrix of sand. However, the research breakthroughs are in contradiction. The present of fines within the matrix of sand could either increase [2–4] or decrease [5–7] the liquefaction susceptibility of particular soils.

In general, specimens with higher fines content tend to have more pack in terms of the density. Thevayanagam and Martin [8] had developed a more complete soil classification system to define the microstructure of sand matrix soils. The addition of fines particles will primarily infill the intergranular voids between sand grains and then secondly to form metastable grain contacts which will loosen the sand skeleton. There are three different phases which are: (i) filling-of-voids; (ii) transition zone and (iii) replacement-of-solid. The limiting value of fines content on the transition zone from the sand dominant to the fine dominant (transition zone) is

known as the threshold fines content (f_{th}), which normally is located within 20–40 % of fines content. The schematic diagram of the composition characteristic of sand matrix soils is shown in Fig. 1. Therefore, the aims of this paper are to first compare the cyclic behaviour of sand-fines mixtures at various fines content and secondly to justify whether the concept of fines content could be used to explain the contradictory results obtained from previous research.

2 Laboratory Testing

2.1 Soil Classification Test

The soil classification test that was carried out in this study were particle size test (wet sieving method and hydrometer test), specific gravity test (small pycnometer method), and limiting density test. All tests were carried in accordance with BS 1377: 1990 Part 2 except for the limiting density test. The reason was that the standard methods described in BS procedure limits only to a maximum fines content of 15 % while the sand matrix soils tested in this study exceeded this limitation; having the percentages of plastic fines (kaolin) by weight at 10, 20, 25, 30 and 40 %. Therefore, techniques recommended by other researcher [10] were used to determine the limiting void ratio.

2.2 Cyclic Triaxial Test

Cyclic triaxial test under consolidated undrained condition was conducted on sand with various percentages of fines content to determine their engineering properties. All the tested samples were prepared at 20 % relative density and with the height of 100 mm and diameter of 50 mm of cylindrical size. Prior to saturation process, carbon dioxide gases and de-aired water was flushed through the specimens from the bottom drainage line to the top until an amount equal to the void volume specimen was collected. Saturation process was carried out with a linear increase of cell and back pressure with constant differences of 10 kPa effective stress. This process was stopped until minimum B-value of 0.96 was achieved. With back pressure of 200 kPa, the samples were then isotropically consolidated to an effective stress of 100 kPa prior to cyclic loading. The cyclic loading was imposed in the form of sine form with amplitude of 0.1 kN and frequency of 0.5 Hz.

3 Results and Discussion

3.1 Soil Classification Test

The clean sand used in this study was a poorly graded medium sand (SP) with a particle density (G_s) of 2.63. It was obtained from a river in Johor Bahru, Malaysia. The plastic fines used in this study was the White Kaolin manufactured by Kaolin (Malaysia) Sdn Bhd, with a G_s of 2.62, plastic limit of 38 and liquid limit of 25. The white kaolin was added into the sand to create sand matrix soils with various fines percentages, in particular at 10, 20, 25, 30 and 40 % by weight. The physical properties of the reconstituted sand matrix soils including the coefficient of curvature (C_C) and the coefficient of uniformity (C_U) are presented in Table 2 while the grain size distribution is shown in Fig. 2.

By plotting the limiting void ratio of sand-kaolin mixtures against percentages of kaolin by weight as shown in Fig. 3, the positive hyperbolic curve was obtained. The addition of kaolin from 0 to 25 % will primarily infill the voids between sand grains, hence the void ratio is decreasing. On the other hand, when the addition of kaolin exceeded the threshold fines content (at 25 % of kaolin by weight) the fines became abundant and formed the metastable grain contacts between sand grains. This condition loosened the sand skeleton while the kaolin itself started to act as the dominant grain in holding the bearing capacity.

Table 2 Physical properties of sand-kaolin mixtures

Weight (%)		Label	G_s	Density (Mg/m^3)		Grading		USCS
Sand	Kaolin			Min.	Max.	C_U	C_C	
100	0	SA1	2.63	1.37	1.59	1	1	SP
90	10	SK1	2.63	1.41	1.70	4	2	SP
80	20	SK2	2.63	1.45	1.80	13	7	SW
75	25	SK3	2.63	1.47	1.87	16	8	SW
70	30	SK4	2.63	1.39	1.76	39	3	SW
60	40	SK5	2.63	1.28	1.63	61	2	SW

Fig. 2 Particle size distribution of sand-kaolin mixtures

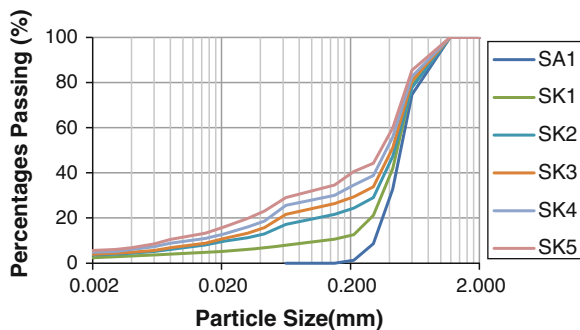
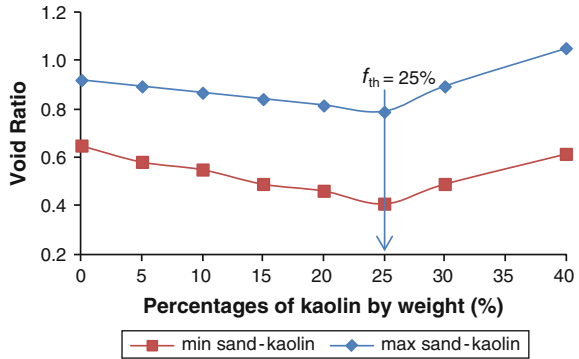


Fig. 3 Threshold fines content of sand-kaolin mixtures



3.2 Cyclic Triaxial Test

Cyclic triaxial test under consolidated undrained condition was conducted on six types of specimen at constant relative density. All specimens were isotropically consolidated to an initial effective pressure of 100 kPa prior to cyclic loading. A total number of 50 cycles in the form of sine wave with a frequency of 0.5 Hz and amplitude of 0.1 kN was imposed on the specimen. The soil specimens were considered liquefied when the value of pore pressure was equivalent to the initial cell pressure, resulting with zero effective stress in soil specimen. The typical test results of undrained cyclic triaxial loading tests were plotted in Fig. 4, particularly the deviator stress and the pore pressure development for the clean sand specimen. Figure 5 shows the number of cycles required to cause the liquefaction for sand-kaolin mixtures at various percentages of kaolin by weight.

In overall, the results showed that the number of cycles required by sand-fines mixtures to achieve liquefaction increased as fines content increased. This trend continues from 0 to 25 % of kaolin added in the parent sand. This is because the addition of kaolin (in small amount), which relatively smaller than sand particles,

Fig. 4 Typical data for cyclic triaxial test

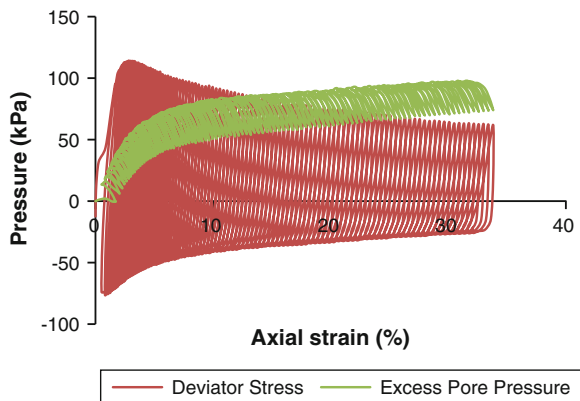


Fig. 5 Number of cycles for liquefaction initiation of sand-kaolin mixtures

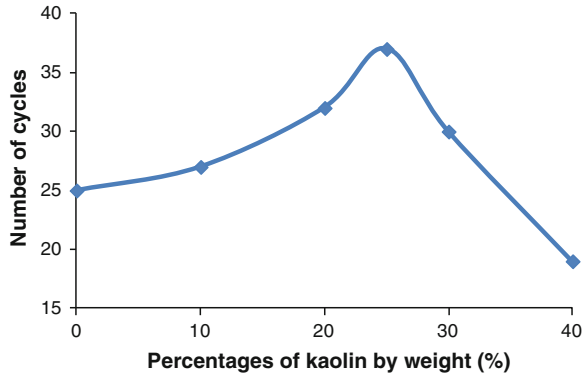
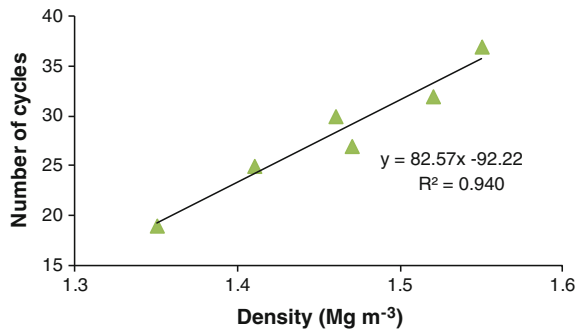


Fig. 6 Number of cycles for liquefaction initiation at relative density of 20 %



infill the voids within the matrix of parent sand. This filling-of-voids phase, making the sand matrix soils less compressible, which also increase the liquefaction resistance. On the other hand, the number of cycles required to achieve liquefaction behaviour decreased when fines content exceeded 25 %. At this condition the volume of fines was larger than the volume of available void within the sand matrix soils causing the separation of sand grains. This is known as replacement-of-solid phase. Therefore, the fines would start to dominate the parent sands and held the responsibility in the soil bearing skeleton. This is the reason why the trend line in Fig. 4 is similar to the void ratio curve in Fig. 3.

Figure 6 shows the number of cycles required for liquefaction initiation corresponded to relative density of 20 %. It shows that the relationship between density and liquefaction susceptibility is directly proportional. In fact, the highest density in this figure corresponded to the specimen for sand-kaolin mixture of 25 % kaolin by weight. The density state at threshold fines content is the densest because it is the transition zone of filling-of-voids phase and replacement-of-solid phase. The sand grain and the fine grain are having the closest packing configuration. The liquefaction is more susceptible in looser state soils. Therefore, liquefaction resistance is at the highest at threshold fines content, and hence, requires more cycles to initiate

the liquefaction. This findings justifies the concept of fines threshold content which is vital and must be considered to explain the influence of fines content on the liquefaction susceptibility of sand-fines mixtures.

4 Conclusion

An experimental study of undrained cyclic triaxial loading tests on sand-kaolin mixture indicates that the liquefaction resistance of the sand-fines mixtures increased as fines content increased, and the trend is reversed beyond the threshold fines content. This finding justifies the concept of fines threshold content which could be used to significantly explain the influence of fines content on the liquefaction susceptibility of sand-fines mixtures.

Acknowledgment The authors gratefully acknowledged the financial supports by the Ministry of Education (MOE) under the Fundamental Research Grant Scheme (Vot 4F316) and also the Universiti Teknologi Malaysia (UTM) through Zamalah program, in undertaking the research to publish the results. The support of the Construction Research Centre and Construction Research Alliance, UTM is also acknowledged.

References

1. C.S. Tan, A. Marto, The role of fines in liquefaction susceptibility of sand matrix soils. *Electron. J. Geotech. Eng.* **18**, 2355–2368 (2013)
2. N.Y. Chang, S.T. Yeh, L.P. Kaufman, Liquefaction Potential of Clean and Silty Sands. in *Proceeding of 3rd International Earthquake Microzonation Conference*, vol. 2 (1982), pp. 1017–1032
3. C.P. Polito, J.R. Martin, Effects of nonplastic fines on the liquefaction resistance of sands. *J. Geotech. Geo. Environ. Eng.* **5**, 408–415 (2001)
4. M. Derakhshandi, E.M. Rathje, K. Hazirbaba, S.M. Mirhosseini, The effect of plastic fines on the pore pressure generation characteristics of saturated sands. *Soil Dyn. Earthq. Eng.* **5**, 376–386 (2008)
5. J.H. Troncosco, R. Verdugo, Silt Content and Dynamic Behavior of Tailing Sands. in *Proceeding of 12th International Conference on Soil Mechanics and Foundation Engineering* (1985), pp. 1311–1314
6. J.P. Koester, *The Influence of Fine Type and Content on Cyclic Resistance* (ASCE, New York, 1994), pp. 17–33
7. J.A. Sladen, R.D. D'Hollander, J. Krahn, Back analysis of the Nerlek Berm liquefaction slides. *Can. Geotech. J.* **22**, 579–588 (1985)
8. S. Thevanayagam, G.R. Martin, Liquefaction in silty soils—screening and remediation issues. *Soil Dyn. Earthq. Eng.* **22**, 1035–1042 (2002)
9. P.V. Lade, Reply to the discussion by Jefferies, Been, and Olivera on “Evaluation of static liquefaction potential of silty sand slopes”. *Can. Geotech. J.* **49**, 751–752 (2012)
10. P.V. Lade, C.D. Liggio, J.A. Yamamuro, Effects of nonplastic fines on minimum and maximum void ratios of sand. *Geotech. Test. J.* **4**, 336–347 (1998)

An Evaluation of Shrinkage Measurement on Undisturbed Peat Soil Using Modified Techniques

Nursyahidah Binti Saedon, Adnan Bin Zainorabidin
and Ismail Bin Bakar

Abstract Peat soils occur in many countries and naturally formed by the decomposition of plant matter. It will give rise to an extreme of challenging ground conditions and peat soils also are known as a very problematic soft soil. For peat soil condition, shrinkage effect is one of the factors that can affect the strength and moisture content of soils. The aim of the study is to evaluate the shrinkage measurement of peat soils with modified techniques to compare with the British Standard method. Peat samples were collected from Parit Nipah (PPN) and Pontian (PP). Linear shrinkage of undisturbed peat soil is observed every hour until there are no volume changes. Linear measurement for modified method that using undisturbed sample is extremely different and higher than British standard method which is using reconstituted soil sample that had been sieve passing 425 μm . Sieve process will disrupt the composition of actual peat soil because it will remove any decomposed plants. The shrinkage measurements during the drying process influenced the volume of peat soils as the volume decreases when the soil is shrunk.

Keywords Undisturbed peat · Linear shrinkage · Modified technique

This research was funded by Malaysian Technical University Network (MTUN), Centre of Excellence (CoE) Grant Vot C012 with title 'Soft Soil Engineering and its Challenging Ground', Universiti Tun Hussein Onn Malaysia.

N.B. Saedon (✉) · A.B. Zainorabidin · I.B. Bakar
Faculty of Civil and Environmental Engineering,
Universiti Tun Hussein Onn Malaysia, Batu Pahat, Johor, Malaysia
e-mail: nursyahidah.saedon@yahoo.com

A.B. Zainorabidin
e-mail: adnanz@uthm.edu.my

I.B. Bakar
e-mail: bismail@uthm.edu.my

1 Introduction

Peat is found in all parts of the world except in deserts and the arctic regions that is estimated that have about 1 billion acres of peat land in the world or about 4.5 % of total land areas [1]. Distribution of peat soil was predominantly in a tropical area. Peat also has been identified as one of the major types of soil that found in Malaysia. According to Zainorabidin and Bakar [2], almost 13 % or 16,500 km² of areas in Sarawak was covered by peat and it is the most extensive peat lands in Malaysia. 90 % of the area has more than 1 m thickness of peat. They also mentioned that in Peninsular Malaysia, peat soils are found in the coastal areas especially in the west area which are Pontian, Batu Pahat, Kuantan and Pekan districts, West Selangor and Perak. Before any construction works will begin, the study of properties of peat soil, including shrinkage must be conducted in order to avoid any failure in future development.

That expansiveness is the most important geotechnical problems due to their volume and moisture content changes to a process of swelling and shrinkage of soils [3]. Shrinkage limit of a soil is defined that water content at which a reduction in water content will not cause a decrease in the volume of the soil mass, but an increase in water content will cause an increase in the volume of soil mass [4]. In terms of linear shrinkage, it appears have been introduced by the Texas Highway Department in 1932 [5] and it is currently described as a standard test procedure as bar linear shrinkage test in British Standard BS 1377:1990 [6]. The linear shrinkage test is used to calculate one-dimensional shrinkage, although the volumetric shrinkage may be calculated. The linear shrinkage is a measure of the average oven dry length of the sample after shrinkage of the original length, which occurs at initial water content at or above the liquid limit.

Haines [7] and Stirk [8] also defined soil shrinkage as the specific volume change of soil relative to its water content and mainly due to clay swelling properties. This process is reversible with changes in water content and the reverse to shrinkage is swelling. Cerato and Lutenegger [9] was performed linear shrinkage test by conducting liquid limit test with Casagrande cup. A third of the soil was placed in a greased brass mold approximately 140 mm long and 25 mm in diameter. The soil was placed in the mould in three layers and tapped against a flat surface in between the layering to remove air bubbles from the soil. The sample was allowed to air dry for 4 h. Then the soil sample was placed in an oven at 105 °C for 18 h. After the soil was dry, the mould was removed from the oven and allowed to cool. The length of the soil sample was measured three times with digital calipers and the average was used to calculate linear shrinkage using the equation:

$$LS = \left(1 - \frac{L_{avg}}{L_0} \right) \times 100 \quad (1)$$

where:

LS Linear Shrinkage (%)

L_{avg} Average Length (mm)

L_0 Original Length of Brass mold (mm)

In 2006, Waikato Regional Council [10] had published an article which entitled 'For Peat's Sake: Good Management Practises for Waikato peat farmers'. They had mentioned that peat is a highly productive growing medium in term of environment. It needs drainage and cultivation to establish productive pastures and crops. Peat shrinkage is estimated to occur at about 20 cm per year after the initial cultivation, reducing to 2 cm per year as the peat becomes more compact and resilient. They investigate that too much drainage of peatlands can cause shrinkage or loss of wetlands and it will reduce water levels in neighbouring wetlands and peat lakes.

2 Problem Statement

The aim of study is to review behaviour of peat under undisturbed sample by observing on shrinkage effect with modified techniques in order to make it compatible with real phenomenon. As known, peat soil was formed by decomposition of plant matter and the composition and behaviour of peat soil is variable. Ho For peat, shrinkage effect, including some important part in determining the strength and moisture content. It is a common cause of foundation problems, especially in road construction. It is also in contributed to the cause of settlement of soil. The changes of moisture content may also be due to periods of unusual rain, changes in humidity or unusual drought. By referring British Standard, oven dried temperature for a soil is 105 ± 5 °C. However, it will be problem to peat soil because of their composition with high fibre content which consists of root and wood decayed.

3 Preparing of Undisturbed Sample

Undisturbed sample must be taken with extreme care to maintain the properties of in situ soil and minimize the degree of disturbance. Landva et al. [11] also agreed with the difficulty in obtaining undisturbed samples of soft soil. Undisturbed sample were used in laboratory investigation such as moisture content, organic content, triaxial testing and any related testing that involved undisturbed sample. For peat samples, Hillis and Brawner [12] and Zainorabidin [13] mentioned that the sample will be different from in situ soil by the duration until the testing was conducted due to high moisture content of peat soil that is more than 100 %.

Previously, undisturbed sample was collected from 100 mm diameter of PVC tube have been pushed manually by rotating the tube into the ground that had been

excavated about 1 m depth from the ground surface. After the whole tube was planted in the ground, the tube with soil sample was taken out by using champ. Then, the tube sampler with soil was sealed with wax on top and bottom of the soil in order to maintain the natural moisture content and properties of soil. Lastly, the samples was covered with aluminium foil and wrapping with plastic. It is similar to disturbed soil, which the sample is placed into a container and stored in the controlled humidity room to prevent any loss moisture and growth of fungus. Some of testing such as moisture content and bulk density, the samples should be tested as soon as they were transported to prevent the samples from the effects of deteriorating due to the long-term storage.

However, in this study, the sample was collected by using the diameter of PVC tube samplers which is 50 mm with sharp cutting edge angle (5° – 10°) on the base of the PVC tube. Clayton and Siddique [14], Siddique et al. [15], and Rahman and Siddique [16] agreed that tube sampler must sharpen the edge angle less than 5° in order to obtain good quality sampling and minimize the degree of disturbance of the

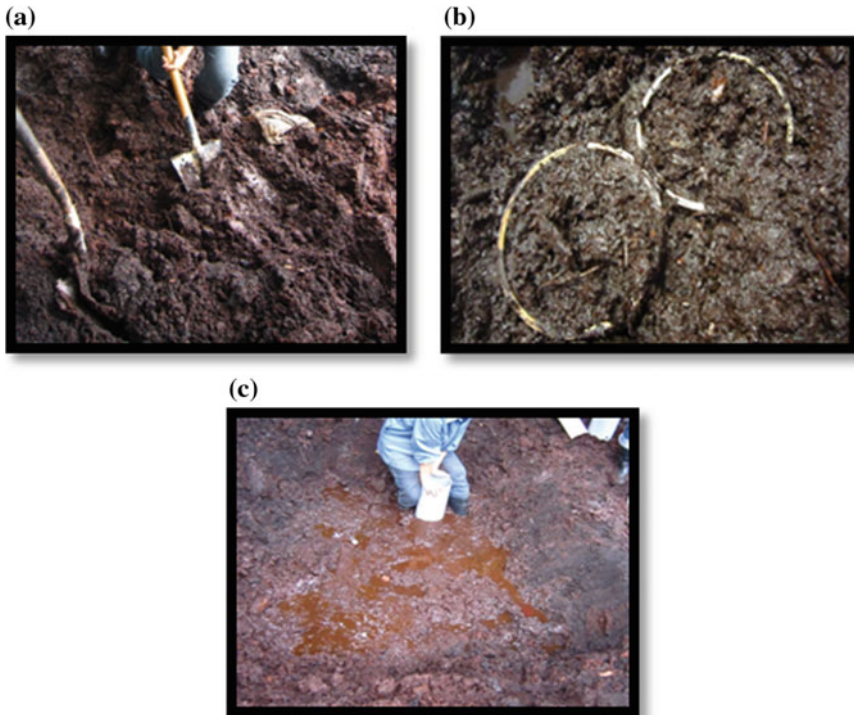


Fig. 1 (a) Area of samplers 3 m width \times 3 m breadth \times 1 m height was excavated in order to obtain a peat soil sample without any visible root and branches; (b) PVC tube sampler with 50 mm diameter with sharp cutting edge at base of tube is inserted manually by rotating the tube into the ground; and (c) groundwater level is high while collecting the sample is one of the problems in sampling method of soil

sample. It also can cut any fibre and visible root and branches surrounding the base of tube sample that disrupt the process of inserting a tube on field site. Method of collecting sample was similar to the previous procedure that begins with removing top soil in order to avoid any visible root and branches. It is also important to minimize the disturbance of soil and to avoid any problem during collecting sample (Fig. 1).

4 Materials and Methods

This study was conducted by developing modified techniques; however, it was compared with past literature that referred to British Standard Institution (BS 1377-2:1990). Peat soils were collected from the same locations and depth as past literature. Undisturbed peat soil is obtained from Parit Nipah (PPN) and Pontian (PP). Some direct testing was observed by extrude on squeezing the peat soil in accordance to Von Post classification system due to humidification and colour of peat. Then, sample of undisturbed soil is collected in order to conduct testing that related in this study. Topsoil of pertaining area needed to remove for about 0.4 m in order to avoid sample from visible litter or branches and roots. Meanwhile, for undisturbed sample, due to difficulties in accessing the area with heavy machinery, sample is collected manually by using PVC tubes with 50 mm diameter sizes.

In this study, it is divided by two types of testing, which are basic properties of soil and shrinkage measurement. For index test, the sample is conducted in order to determine moisture content, fibre content, specific gravity and organic content. Shrinkage effect is main tests in this study. Undisturbed sample is prepared to conduct this testing. From past literature that conducted by Seth [17], the shrinkage behaviour of peat soil was determined by British Standard BS 1377-2:1990 bar linear shrinkage method using the reconstituted sample that passing through 425 μm wet sieving. The bar shrinkage mould with wet soil that had been sieved with the length measurement of 139 mm was first placed open-aired until the soil shrunk away from the walls of the moulds. Then, it is placed in the oven at temperature 60 °C until shrinkage has largely ceased, and lastly at 105 °C oven-dried to complete the drying process. However, the modified shrinkage method was used an undisturbed sample with approximately 50 mm diameter and 20 mm height. The undisturbed sample was collected manually by using PVC tubes with 50 mm diameter sizes. The sample was extruded from the PVC tube and it was trimmed in 20 mm height of specimen before it was placed into the container. The undisturbed soil sample was placed into 105 °C and observed every hour until 24 h. The changes of shrinkage behaviour were observed by three points that are point x, y and z to take an average value. The data obtained were analysed and compared with previous data.

5 Results and Discussions

From the past literature that studied by Seth [17], it was mentioned some result of basic properties of peat soils in Parit Nipah (PPN) and Pontian (PP). Peat sample was collected at the depth of 0.5 m from the top of the soil. The value of moisture content (MC), fibre content (FC), organic content (OC) and specific gravity (SG) of peat soils were obtained as 668.4, 33.23, 89.87 and 1.43 % for Parit Nipah (PPN). Meanwhile, similar basic properties of Pontian (PP) areas are 508.09, 22.59, 75.45 and 1.62 %.

In this study, the basic properties of peat soil also had been conducted. Moisture content of peat soil in Parit Nipah (PPN) and Pontian (PP) was measured at 701 and 658 % respectively. While, the fibre content of Parit Nipah (PPN) is 40.97 % and Pontian (PP) is 38.65 %. Organic content and specific gravity for Parit Nipah (PPN) were obtained as 78.77 and 1.43 % respectively. The value of organic content and specific gravity for Pontian (PP) were 76.55 and 1.28 %.

(a) Bar Linear Shrinkage

Based on past literature, bar linear shrinkage of soil was tested according to BS 1377-2:1990. This method was conducted for the determination of the linear shrinkage of the fraction of soil sample passing a 425 mm test sieve from linear measurements on a bar of soil. The percentages of linear shrinkage obtained from linear method according to British Standard are 34.77 and 33.09 % for Parit Nipah (PPN) and Pontian (PP) respectively. According to the previous study, these values are in the range of shrinkage for West Malaysia peat which is 20–40 % [18].

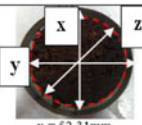
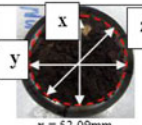


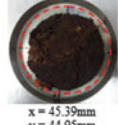

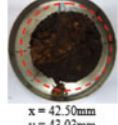
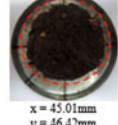
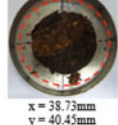
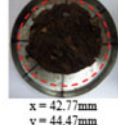
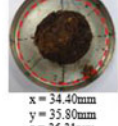

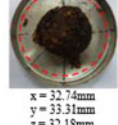
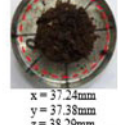
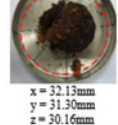
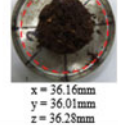
(b) Modified Linear Shrinkage

A modified linear shrinkage test was conducted to show that the behaviour of peat soil is variable due to decomposition plant and fibre content. The sample with high fibre content and voids will give higher value of linear shrinkage instead of peat sample that had been sieved into required size. As mentioned before, undisturbed samples with 50 mm diameter were used in order to compare it with real phenomenon. The changes of diameter were measured by three points which are point x, y and z and it was recorded every hour until 24 h as mentioned by British Standard of moisture content using oven-dry testing. The changes of diameter and volume for two different locations which are Parit Nipah (PPN) and Pontian (PP) peat sample were observed as Table 1.

As shown in Fig. 2, the changes of diameter for Parit Nipah (PPN) sample give a constant value after 10 h oven drying process. The sample was measured by three points in order to have precise value and maintaining the point of measurement. Difference reading diameter before and after oven dried within 24 h was measured as 22.173 mm of diameter (Fig. 3).

The reading of diameter changes for Pontian (PP) peat sample begins with constant after 12 h oven-dried sample. Loss of diameter sizes during oven-dried process within 24 h is 18.913 mm of diameter. The loss of diameter after 24 h of

Table 1 Diameter changes in 50 mm sample size with two different locations

Time (hrs)	Parit Nipah (PPN)	Pontian (PP)
1	 x = 52.31mm y = 51.53mm z = 51.75mm	 x = 52.09mm y = 51.22mm z = 51.30mm
2	 x = 48.77mm y = 48.74mm z = 48.36mm	 x = 48.72mm y = 49.55mm z = 49.63mm
3	 x = 45.39mm y = 44.95mm z = 45.54mm	 x = 47.03mm y = 47.23mm z = 46.71mm
4	 x = 42.50mm y = 43.03mm z = 43.11mm	 x = 45.01mm y = 46.42mm z = 45.68mm
5	 x = 38.73mm y = 40.45mm z = 40.28mm	 x = 42.77mm y = 44.47mm z = 43.76mm
6	 x = 34.40mm y = 35.80mm z = 36.31mm	 x = 40.76mm y = 41.64mm z = 41.99mm
7	 x = 32.74mm y = 33.31mm z = 32.18mm	 x = 37.24mm y = 37.38mm z = 38.29mm
8	 x = 32.13mm y = 31.30mm z = 30.16mm	 x = 36.16mm y = 36.01mm z = 36.28mm

(continued)

Table 1 (continued)

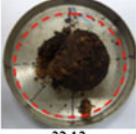



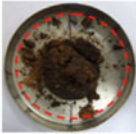









8	 <p>x = 32.13mm y = 31.30mm z = 30.16mm</p>	 <p>x = 36.16mm y = 36.01mm z = 36.28mm</p>
9	 <p>x = 31.84mm y = 31.23mm z = 29.88mm</p>	 <p>x = 36.02mm y = 35.88mm z = 35.75mm</p>
10	 <p>x = 31.79mm y = 31.02mm z = 29.81mm</p>	 <p>x = 35.62mm y = 35.78mm z = 35.53mm</p>
11	 <p>x = 31.69mm y = 30.08mm z = 29.36mm</p>	 <p>x = 35.56mm y = 35.56mm z = 35.18mm</p>
12	 <p>x = 31.63mm y = 29.13mm z = 28.89mm</p>	 <p>x = 33.50mm y = 32.33mm z = 32.89mm</p>
24	 <p>x = 31.61mm y = 29.02mm z = 28.56mm</p>	 <p>x = 33.09mm y = 32.21mm z = 32.71mm</p>
25	 <p>x = 31.59mm y = 28.99mm z = 28.49mm</p>	 <p>x = 33.00mm y = 32.19mm z = 32.68mm</p>

Fig. 2 Changes in diameter against duration of Parit Nipah peat soil (PPN)

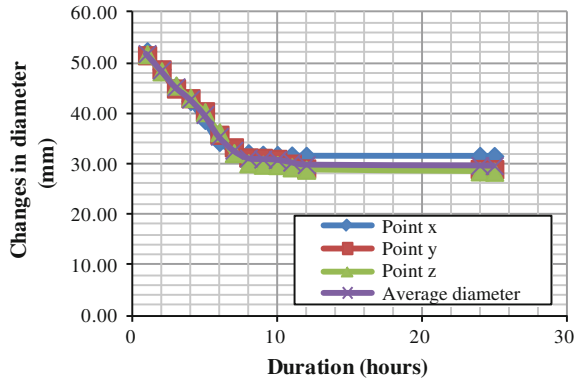
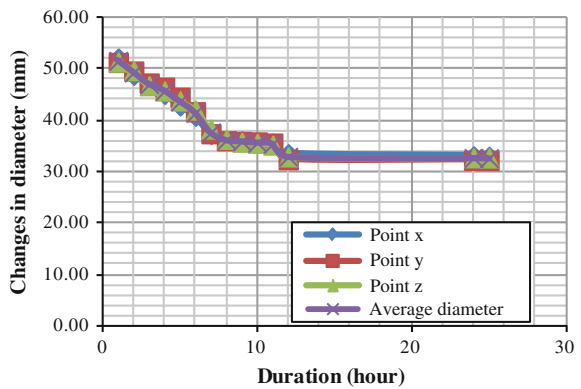


Fig. 3 Changes in diameter against duration for Pontian peat soil (PP)



Pontian (PP) peat sample is less than Parit Nipah (PPN) peat sample. However, Parit Nipah (PPN) peat sample was given a constant reading 2 h earlier than Pontian (PP) peat sample.

Based on Fig. 4, range of volume changes for Parit Nipah (PPN) peat is 43218.56 mm³ decreased to 8385.59 mm³. While Pontian (PP) peat sample give a range of volume changes between 46792.46 mm³ and 11110.66 mm³. Figure 4 was shown the changes in volume of Parit Nipah peat sample (PPN) slightly similar to the Pontian peat sample (PP) with different changes of volume during oven-dry process are 34832.98 mm³ and 35681.80 mm³ respectively. It shows that Pontian (PP) peat soil gives higher volume changes than Parit Nipah (PPN) peat soil.

Figure 5 shows that Pontian (PP) peat sample has the smallest linear shrinkage compared to Parit Nipah (PPN) peat sample as it was measured 42.753 % for Parit Nipah (PPN) peat sample and 36.699 % for Pontian (PP) peat sample after being let stood in oven dried for 24 h with 105 °C of temperature. It shows that the optimum linear shrinkage occurred at 12 h because after the period, there are no changes to the diameter of the peat soil specimen.

Fig. 4 Changes in volume due to duration for two different locations

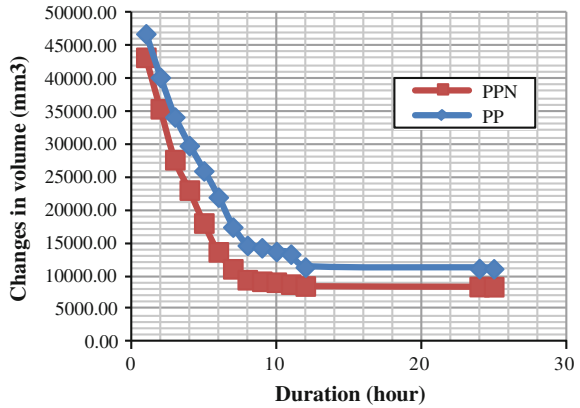
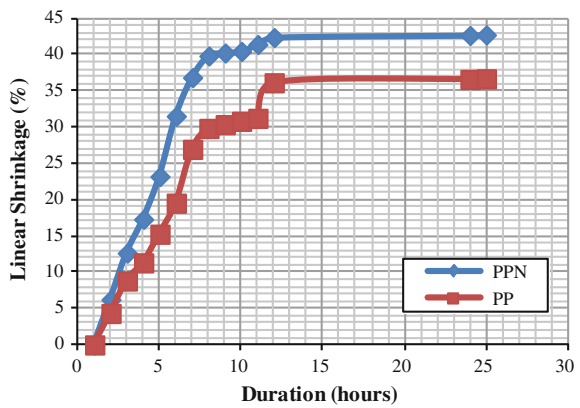


Fig. 5 Linear shrinkage measurement for two different locations



It can be concluded that the decreasing value of diameter also affecting the volume of the peat soil. It is also can be related to the fibre content which is the fibre content of Pontian (PP) peat sample is less contained than Parit Nipah (PPN) peat sample. Higher fibre content will resulting higher void within the sample and it will increase the value of linear shrinkage of the sample. Table 2 shows the summary of data for all tests that have been conducted.

Table 2 Summary of data

Laboratory test		MC(%)	FC (%)	OC (%)	SG (%)	LS (%)
Bar linear shrinkage [17]	PPN	668.40	33.23	89.87	1.43	34.77
	PP	508.09	22.89	75.45	1.62	33.09
Modified method	PPN	701.00	40.97	78.77	1.43	42.75
	PP	658.00	38.65	76.55	1.28	36.70

6 Conclusions

The conclusion of this study can be drawn as follows:

- (a) The study of peat soils behaviour from two different locations has been obtained from its physical properties and shrinkage measurement of peat soils.
- (b) The fibre content of peat sample will give high effect to the volume changes and shrinkage measurement. Different locations and different conditions of peat soil will give variable behaviour due to non-homogeneity.
- (c) Linear measurement for a modified method that using an undisturbed sample is extremely different and higher than the British standard method which is using a reconstituted soil sample that had been sieve passing 425 μm . Sieve process will disrupt the composition of actual peat soil because it will remove any decomposed plants.
- (d) The shrinkage measurements during the drying process influenced the volume of peat soils as the volume decreases when the soil is shrunk.

Acknowledgments The special acknowledgement to beloved supervisor, Assoc. Prof. Dr. Adnan bin Zainorabidin for big support and supervision during my study and completion of this paper. Not forgotten to Prof. Dato' Dr. Ismail Bakar who had guiding me and this research was funded by Malaysian Technical University Network (MTUN), Centre of Excellence (CoE) Grant Vot C012 with title 'Soft Soil Engineering and its Challenging Ground', Universiti Tun Hussein Onn Malaysia. Heartfelt acknowledgements are expressed to my beloved family. Also, thanks to the Research Centre of Soft Soils (RECESS), UTHM staff in guiding and providing laboratory facilities.

References

1. S. Deboucha, R. Hashim, A. Alwi, Engineering properties of stabilized tropical peat soil. *EJGE* **13**, Bund. E, (2008)
2. A. Zainorabidin, I. Bakar, Engineering Properties of In-Situ and Modified Hemic Peat Soil in Western Johor, ed. by Huat et al. in *Proceedings of 2nd International Conference on Advances in Soft Soil Engineering and Technology* (2003), pp. 173–182
3. M.I. Dorota, W. Emilia, Testing shrinkage factors: comparison of methods and correlation with index properties of soils, *Bull. Eng. Geol. Environ.* **72**, 15–24 (2013)
4. McGraw-Hill Science and Technology Dictionary, Shrinkage Limit (2003)
5. P.B. Heidema, The Bar-shrinkage Test and the Practical Importance of Bar-linear Shrinkage as an Identifier of Soils. in *Proceedings of the 4th International Conference on Soil Mechanics and Foundation Engineering*, vol. 1 (1957), pp. 44–48
6. BS 1377:1990, Method of Testing Soils for Civil Engineering Purposes. British Standard Institute, London
7. W.B. Haines, The volume-changes associated with variations of water content in soil. *J. Agric. Sci.* **13**(3), 296–310 (1923)
8. G. Stirk, Some aspects of soil shrinkage and the effect of cracking upon water entry into the soil. *Aust. J. Agric. Res.* **5**(2), 279–296 (1954)
9. A.B. Cerato, J. Lutenegeger, Shrinkage of Clays. in *Proceedings of the 4th International Conference on Unsaturated Soils, ASCE*, vol. 1 (2006), pp. 1097–1108

10. Waikato Peat Management Council, For peat's sake: good management practises for Waikato peat farmers, 2006
11. A.O. Landva, P.E. Pheeney, D.E. Mersereau, Undisturbed sampling of peat. Test. Peat Org. Soils, ASTM STP **820**, 141–156 (1983)
12. S.F. Hillis, C.O. Brawner, The Compressibility of Peat with Reference to Major Highway Construction in British Columbia. in *Proceedings 7th Muskeg Research Conference* (1961) pp. 204–227
13. A. Zainorabidin, Static and dynamic characteristics of peat with macro and micro structure perspective, PhD thesis, University of East London, 2010
14. C.R.I. Clayton, A. Siddique, Tube Sampling Disturbance-forgotten Truths and New Respective. in *Proceedings of the Institution of Civil Engineers, Geotechnical Engineering*, vol. 149, Issue 3 (2001), pp. 195–200
15. A. Siddique, S.M. Farooq, C.R.I. Clayton, Disturbances due to tube sampling in coastal soils. *J. Geotech. Eng.* **2000**(126), 568–575 (2000)
16. M.M. Rahman, A. Siddique, Effects of sampling disturbance and its minimization in reconstituted over-consolidated Dhaka clays. *Dhaka Univ. Eng. Tech. J.* **1**(1), 18–26 (2010)
17. N.M. Seth, *The shrinkage behaviour of peat soil in Parit Nipah and Pontian* (Final Year Project Faculty of Civil and Environmental Engineering, UTHM, Batu Pahat, 2013)
18. R. Hashim, S. Islam, Engineering properties of peat soils in Peninsular. Malaysia, *J. Appl. Sci.* **8**, 4215–4219 (2008)

Rainfall Infiltration into Unsaturated Soil

Aniza Ibrahim, Muhammad Mukhlisin and Othman Jaafar

Abstract As a tropical country, Malaysia is in the region of residual unsaturated soil. The prolonged and high intensity of rainfall will affect the parameters such as pore water pressure and moisture content of soil. This paper presents the experimental test result of rain water infiltration into soil column for unsaturated soil. The main objectives were to study the effect of rainfall intensity and duration to water infiltration into the soil. In this study, two types of soils were used; gravelly sand and kaolin. Rainfall with designated intensities and durations were applied to the soil column apparatus. The soil column apparatus system involved three components; water supply system, soil column and instrumentation, and effluent system. The result showed that during wetting process, the value of pore water pressure was gradually increased until the rainfall stopped and drying process took place. The top section of soil column responds earlier than middle and bottom for both during wetting and drying process. The changes from high to low intensity give smaller value of pore water pressure for intensity type 2 for both soils. The result also shows that different length of tensiometer affect to small changes for both type of soil. Result of volumetric water content for both soil have a good agreement with the responds to pore water pressure. These shows that the middle section of soil column has the ponding condition where water infiltrates and stay longer at this section before its continue to infiltrate to bottom section.

Keywords Infiltration • Soil column • Pore water pressure • Volumetric water content

A. Ibrahim (✉)

Department of Civil Engineering, Universiti Pertahanan Nasional Malaysia,
Kuala Lumpur, Malaysia
e-mail: aniza@upnm.edu.my

M. Mukhlisin

Department of Civil Engineering, Polytechnic Negeri Semarang, Negeri,
Semarang, Indonesia

O. Jaafar

Department of Civil and Structural Engineering, Universiti Kebangsaan Malaysia,
Selangor, Malaysia

1 Introduction

As a tropical country, Malaysia is in the region of unsaturated residual soil, which composed with the negative pore water pressure (pwp) above the groundwater table. With high seasonal rainfall, the changes of parameter such as pwp and moisture content of the soil will lead to the instability of soil especially slope [1]. These rainfall-induced slope failure are mostly due to the loss of matric suction by rainwater [1, 2].

During and after a rainfall event, partly of the rainwater that reaches the slope surface infiltrate into the soil while others become the surface runoff. As water infiltrates the slope, matric suction is decreasing as the soil moisture is increasing, subsequently change the structure of soils, and lessen the frictional and cohesive strength between [3]. Consequently, negative pwp between the soil particles and shear strength is decreasing, hence affects the slope stability [4, 5]. This can be concluded that the higher the rainfall intensity, the higher infiltration rate through the soil and hence lower the slopes' factor of safety [1].

The mechanism of rain water infiltration into the soil event is complex due to its high nonlinearity of soil water characteristic and soil permeability [6]. The complexity is concerning by the parameters such as soil initial moisture condition, soil water retention ability, soil porosity, evaporation rate and others [7] and [2]. Therefore, the needs to study the infiltration mechanisms are crucial with the intention of understanding the behavior of soil under various rainfall intensity and duration.

Soil column apparatus is normally used to perform simulated water infiltration into soil. This apparatus has been used widely to enhance the understanding of rainfall infiltration mechanism. Yang et al. [8] and [9] examined the effect of rainfall intensity and duration, and provides the verification of soil water redistribution and hysteresis phenomenon. [3] also used soil column to investigate the mechanism of rainfall and provide evidence on transient pwp distribution and redistribution of rainfalls.

Even though many researchers have been conducted using soil column for various purposes, the pwps that measured were at the same place or using the same length of tensiometers. In this study, the introduction of difference length of tensiometers inserted into the soil column will measure difference points of pwp. Therefore, behavior of soil of can be further investigated.

2 Material Properties

There were two types of soils used for the experiment; gravelly sand and kaolin. Both of the soils were commercially obtained, and two types of properties were investigated; basic and hydraulic soil properties. Basic soil properties are including soil moisture content, bulk density, and porosity. Meanwhile, hydraulic properties of soil are soil saturated hydraulic conductivity and soil-water characteristic curves

(SWCC). The experiment for both types of soil properties were conducted in the laboratory. For hydraulic properties, results obtained from the experiment were then fitted using Van Genuchten [10] numerical equation.

3 Experiment Setup

The soil column apparatus system consists of water supply system, soil column apparatus and instrumentation, and effluent system as shown in illustration of Fig. 1.

3.1 Water Supply System

For the experiment, water supply for the infiltration is using flow pump and regulator as shown in Fig. 2b. The flow regulator used in this study was Masterflex L/S economy, which attached to the pump driver that has speed indicating 1–10.

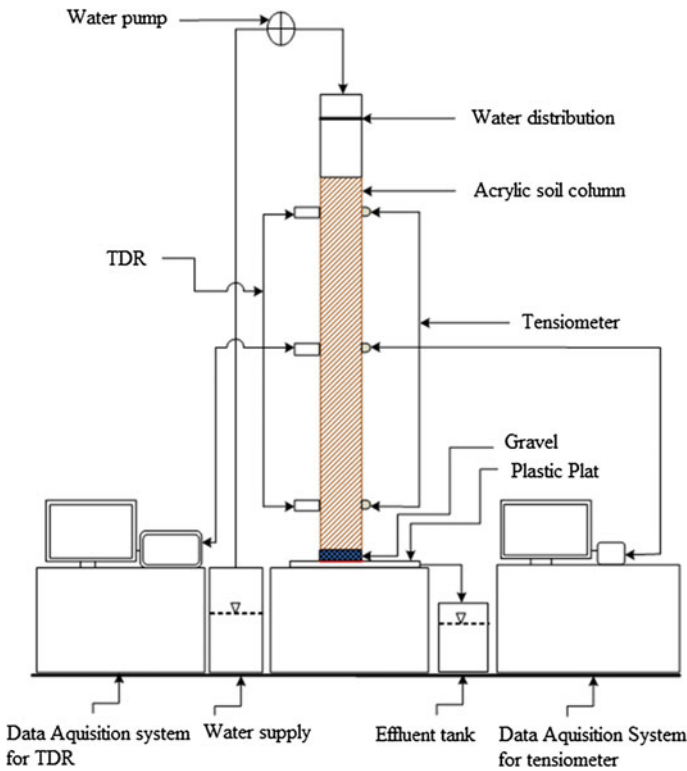


Fig. 1 Schematic diagram of soil column model

The water was flow through 1.6 mm internal diameter tube that attached to the pump. The simulated rainfall from the system will flow through into the rainfall distributor, and to the top of the soil.

3.2 Soil Column and Instrumentations

Soil column apparatus in this study was using transparent acrylic cylinder Fig. 2a. The size of the cylinder is 1,500 mm high and 203 mm diameter. The sample for each soil for the the experiment is 1,000 mm height which placed on the 20 mm gravel



Fig. 2 Soil column apparatus **a** Soil column cylinder **b** flow regulator **c** tensiometer **d** TDR **e** data logger for TDR **f** data logger for tensiometer **g** effluent rain gauge

at the bottom of the column. The gravel was used to prevent any soil substance from entering the effluent system.

There were two instruments attached to the soil column. Threaded holes were drilled at the sides of the acrylic cylinder for installation of Time Domain Reflectometry (TDR) and tensiometer.

3.3 Time Domain Reflectometry (TDR)

In this experiment, TDR is used to measure volumetric water content (vwc). Three (3) units of TRIME-IT TDR by IMKO Micro modultechnik GmbH were attached to the soil column as shown in Fig. 2a. This type of TDR consists of two metal rods inserted into the soil through the threaded holes, and sealed before rainfall is applied to the top of column. Data can be collected through data logger from IMKO Micro modultechnik GmbH (Fig. 2e). Three TDR were located at three different location at the soil column. The locations were at 0.9, 0.6, and 0.3 m from the bottom of the column which identified as top, middle, and bottom respectively.

3.4 Tensiometer

Tensiometer is used to measure pwp of soil. In this study, mini tensiometer type T5 from UMS GmbH product was inserted to the soil. The tensiometer is assembled with several components such as 5 mm high grade porous ceramic tip, acrylic glass shaft, and sensor body. The tensiometer is needed to calibrate for at least two hours each in order to provide bubble free which prevent any error in data collecting. Two types of tensiometer shaft length were used in the experiment; 5 (type A) and 10 cm (type B) in order to detect pwp at several places. Data can be collected through data logger from AT Delta-T Devices Ltd as shown in Fig. 2f. Three (3) unit for each type of tensiometers were located at three different location at the soil column. The locations were at 0.9, 0.6, and 0.3 m from the bottom of the column which identified as top, middle, and bottom respectively.

3.5 Effluent

Effluent from the infiltration was measured by rain gauge placed at the bottom of the soil column (Fig. 2g). The rain gauge, Rainlog Datalogger by Rainwise is an eight inches tipping bucket that collects 0.01 and 0.5 inch/tip minimum and maximum respectively. For this experiment, the rain gauge is set for 0.01 inch/tip and logged every 10 min.

Table 1 Experiment rainfall duration and intensities

No	Experiment	Type of soil	Rainfall duration (hour)	Rainfall intensity (mm/hour)
1	RG11	Gravelly sand	3	18.54
2	RG12	Gravelly sand	6	18.54
3	RG13	Gravelly sand	12	18.54
4	RG14	Gravelly sand	24	18.54
5	RG21	Gravelly sand	3	3.480
6	RG22	Gravelly sand	6	3.480
7	RG23	Gravelly sand	12	3.480
8	RG24	Gravelly sand	24	3.480
9	RK11	kaolin	3	18.54
10	RK12	kaolin	6	18.54
11	RK13	kaolin	12	18.54
12	RK14	kaolin	24	18.54
13	RK21	kaolin	3	3.480
14	RK22	kaolin	6	3.480
15	RK23	kaolin	12	3.480

3.6 Infiltration Experiments

A series of infiltration tests were designed and conducted in the laboratory as shown in Table 1. Two types of rainfall intensities were applied to the experiment; 18.54 and 3.48 mm/h for type 1 and 2 respectively. The designated simulated rainfall duration was 3, 6, 12, and 24 h. Unfortunately, the 24 h duration of rainfall for kaolin was not performed due to the water ponding condition occurred at the top of the soil column.

4 Results and Discussion

4.1 Soil Properties

Basic properties for both types of soils are shown as in Table 2. While the result of soil saturated hydraulic conductivity (K_s) and SWCC are as shown in Figs. 3 and 4.

4.2 Pore Water Pressure (P_{wp})

The result of pwp for gravelly sand are as shown in Fig. 5b, c for 5 and 10 cm tensiometer length respectively. Results show that the initial value of pwp is high

Table 2 Basic properties of soils

Parameter	Unit	Gravelly sand	Kaolin
<i>Atterburg limit</i>			
Plastic limit	%	–	31.9
Liquid limit	%	–	56
Plasticity index	%	–	24
<i>Soil composition</i>			
Gravel	%	8.5	0
Sand	%	88.7	4.3
Silt	%	2.6	40
Clay	%	0.2	55.7
<i>Soil classification</i>			
	Kg/m^2	SP	MH
		Poorly graded sand	Sandy classic silt
Bulk density (ρ_b)		1,572	1,106
Porosity (e)		0.41	0.58
Moisture content	%	0.13	0.37

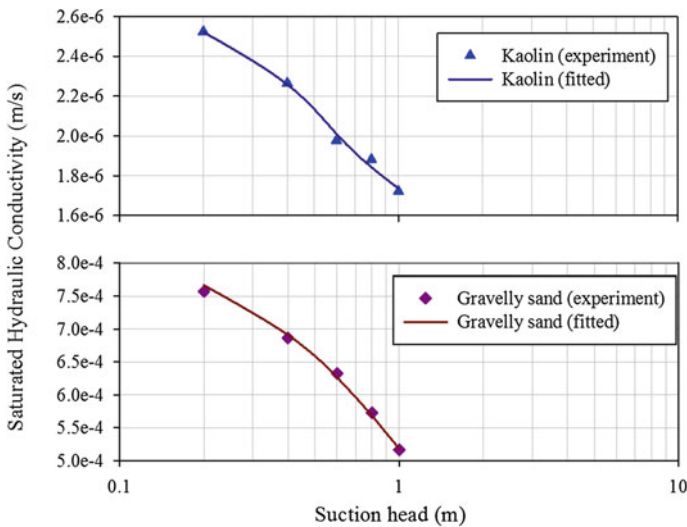
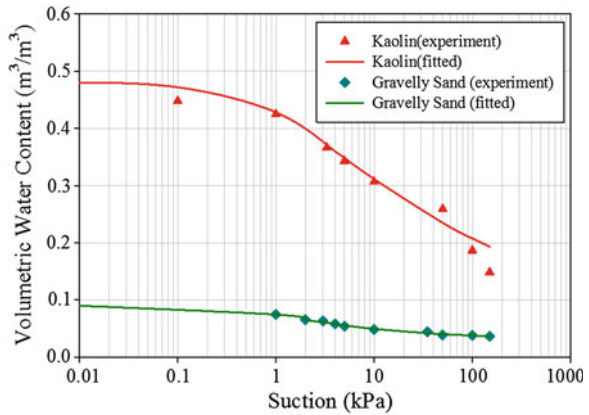


Fig. 3 Saturated hydraulic conductivity

due to the original condition of the soil which has very low moisture content. The results indicated that during the wetting or rainfall process, pwp at the top section of the column increase rapidly compare to the middle and bottom. Meanwhile, during the drying process, the value of pwp at the top is increased, then by the middle and bottom section. But, there are no significant changes when RG21 is applied for middle and bottom section. For RG23, the changes are detected at the top middle

Fig. 4 SWCC for soils



section but not at the bottom section. The value of pwp is changes at RG23 and RG24. Other than that, based on the result, there are no significant changes between type A and b tensiometers. Maximum value for pwp for at top, middle, and bottom section is at the experiment RG12, RG14, and RG15 respectively. The minimum value of pwp for top, middle and bottom section are at experiment of RG24, RG11, and RG23 respectively.

Meanwhile, Fig. 6b, c shows the result of kaolin. Similar to gravelly sand, kaolin experience the increasing value of pwp while rainfall is applied and decreasing while in drying process. The initial value of pwp is very high due to the very low moisture content. The value starts to increases as tensiometer detect the present of water infiltration. Result shows that at intensity 1, the top section experience highest value of pwp compare to middle and bottom section during wetting process. At drying process, the value of pwp at top section decreased and become the lowest value, while the bottom is the highest. At intensity 2, the same pattern of pwp are shown for all experiment, but the value of pwp are higher compare to intensity 1 due to the fact that intensity 1 is higher than intensity 2. The maximum value of pwp for kaolin is at RK22 for top and middle section, and the bottom section is at RK24. While the result shows that minimum value for all section are at RK11. Similar to gravelly sand, there is no significant changes for type A and B tensiometer for kaolin.

4.3 Volumetric Water Content (Vwc)

When rainfall is applied to the soil column, the value of vwc is gradually increased. When rainfall is stopped and during drying process, the value of vwc is gradually decreased. For gravelly sand, the changes of vwc value started at RG12 for top and middle section, and bottom section started at RG22. The value of vwc for the top section is the fastest to respond to the rainfall, but the highest value is detected at

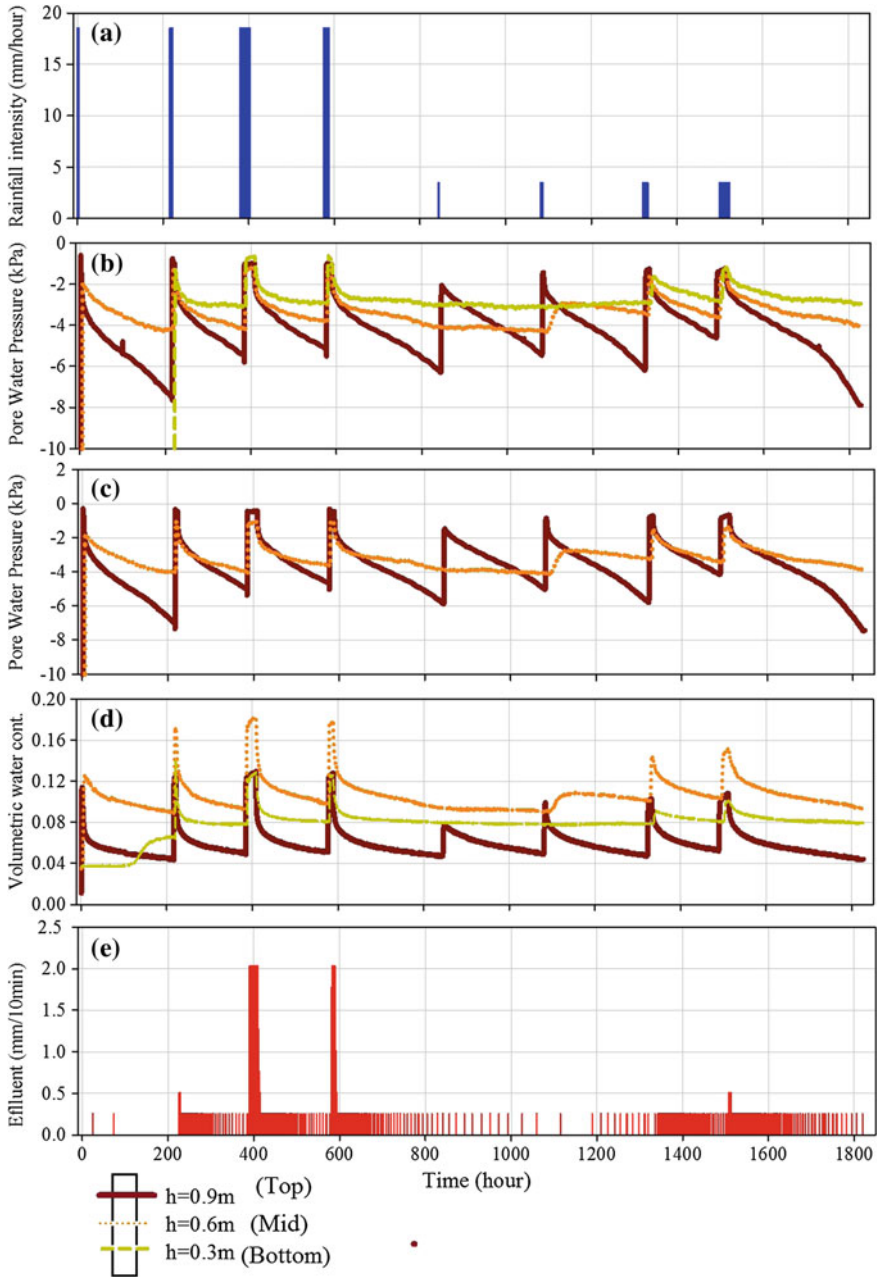


Fig. 5 Soil column results for Gravelly sand **a** Rainfall intensity **b** Pwp for 5 cm tensiometer **c** Pwp for 10 cm tensiometer **d** Vwc **e** Effluent

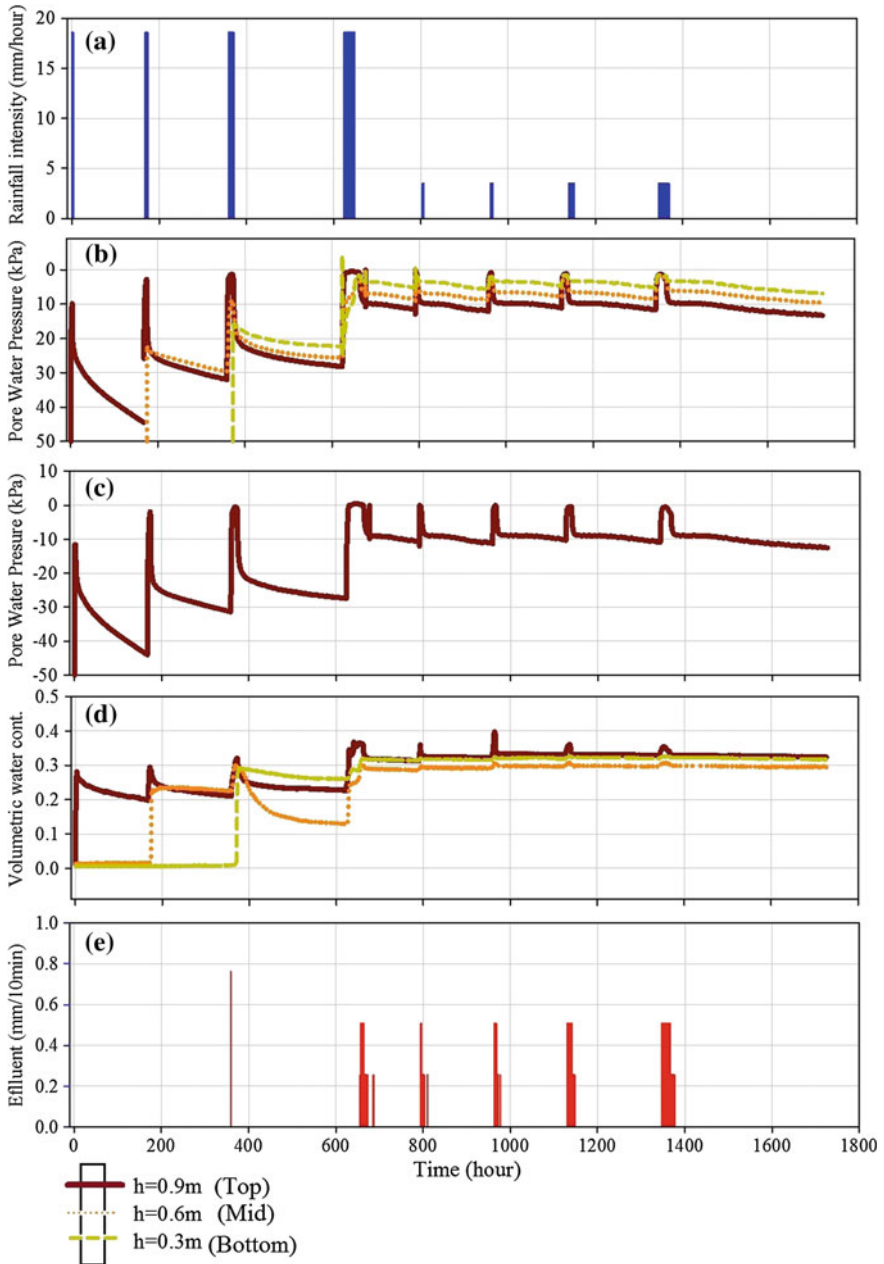


Fig. 6 Soil column results for kaolin **a** Rainfall intensity **b** Pore waterpressure for 5 cm tensiometer **c** Pwp for 10 cm tensiometer **d** Vwc **e** Effluent

the middle section. Top section also is the lowest value during the drying process and by bottom and middle section subsequently. During RG21 and RG22, there are no significant changes of vwc value for middle and bottom section due to the lower rainfall intensity applied. The value is started to change in RG23 and RG24. Result shows that the maximum value of vwc for top section is at RG14, while RG13 for both middle and bottom section. Other than that, minimum value for vwc is at RG11 for all sections.

For kaolin, Fig. 6d shows that for intensity 1, the increasing value of vwc is started at the top section, middle and bottom at RK12, RK13, and RK14 respectively. It is clearly shows that the top section responds earlier than middle and bottom section. The results show that after RK13, the lowest value of vwc is at the middle section, and the highest is at bottom section. The pattern of value has changed starting RK21 with top and middle section having the highest and lowest value of vwc respectively. The maximum value of vwc is at RK22 for top and middle section, while bottom section is at RK24. The minimum value for all sections is at RK11.

4.4 Effluent

The result of effluent for gravelly sand and kaolin are as in Fig. 5e and Fig. 6e respectively. For gravelly sand, result shows that the effluent is started after 225.5 h of RG12 for 0.51 mm. Then the effluent is decreased to 0.254 mm at 389 h (RG13), and 2.03 mm at 582 h (RG14). Meanwhile, for kaolin, the effluent is detected at 359 h after RK13 was applied with 0.762 mm. Then there are no effluent detected until after RK14 for 0.508 mm. Then, the effluent started to decreased to 0.254 mm at 663.8 h (RK14).

5 Conclusion

A series of infiltration experiments were conducted to study the pattern of pwp and vwc. The simulated rainfall is applied to the top of soil column with the designated duration and intensity, and the effluent is collected at the end of infiltration process. The result shows that the initial pwp for both type of soil were very high due to the low moisture content. Then, the value of pwp started to increased when rainfall is applied. During wetting process, the value was gradually increased until the rainfall stopped and drying process took place. The top section of soil column responds earlier than middle and bottom for both during wetting and drying process. The changes from high to low intensity give smaller value of pwp for intensity 2 for both soils. The result also shows that different length of tensiometer only lead to small changes for both type of soil. Result of vwc for both soil have a good agreement with the responds to pwp. At the beginning of experiment, top section

achieved highest value during rainfall was applied. For gravelly sand, the results indicated that the middle section achieved highest value after RG1 for both during drying and wetting process and the lowest is the top section. These indicating that the middle section has the ponding condition where water infiltrates and stay longer at this section before its continue to infiltrate to bottom section. Contra with gravelly sand, for kaolin, the top section is dominating the highest value while bottom section is the lowest. The result also shows that the infiltration rate of kaolin is lower than gravelly sand. This is supported by the soil basic properties which the kaolin has greater porosity compare to gravelly sand. Other than that, the saturated hydraulic conductivity shows that kaolin is lower permeability than gravelly sand.

References

1. B.B.K. Huat, F. H. Ali, T. H. Low, Water infiltration characteristics of unsaturated soil slope and its effect on suction and stability. *Geotech. Geol. Eng.* **24**, 1293–1306 (2006)
2. M. Mukhlisin, K. Kosugi, Y. Satofuka, T. Mizuyama, Effects of soil porosity on slope stability and debris flow runout at a weathered granitic hillslope. *Vadose Zone J.* **5**, 283–295 (2006)
3. N. Gofar, L.M. Lee, A. Kassim, Instrumented soil column model for rainfall infiltration study, presented at the GEOTROPIKA (2008)
4. J.M. Gasmu, H. Rahardjo, E.C. Leong, Infiltration effects on stability of a residual soil slope. *Comput. Geotech.* **26**, 145–165 (2000)
5. M. Mukhlisin, A. Saputra, A. El-Shafie, M.R. Taha, Measurement of dynamic soil water content based on electrochemical capacitance tomography. *Int. J. Electrochem. Sci.* **7**, 5457–5466 (2012)
6. R.A. Willians, M.S. Beck, *Introduction to Process Tomography, Process Tomography: Principles, Techniques and Applications*, 1 ed. (Butterworth-Heinemann, 1995), pp. 3–10
7. L.M. Lee, A. Kassim, N. Gofar, Performance of two instrumented laboratory models for the study of rainfall infiltration into unsaturated soils. *Eng. Geol.* **117**, 78–89 (2011)
8. H. Yang, H. Rahardjo, E.C. Leong, Behavior of unsaturated layered soil columns during infiltration. *J. Hydrol. Eng.* (2006)
9. I.G.B. Indrawan, H. Rahardjo, E.C. Leong, Drying and wetting characteristics of a two-layer soil column. *Can. Geotech. J.* **44**, 20–32 (2007)
10. M.T. Van Genuchten, A closed-form equation for predicting the hydraulic conductivity of unsaturated soils. *Soil Sci. Soc. Am. J.* **44**(5), 892–898 (1980)

Predicting Uniaxial Compression Strength (UCS) Using Bulk Density for Kuala Lumpur Granite and Limestone

Haryati Awang and Noor Akma Mohd Naru

Abstract In engineering practice particularly in measuring strength properties of rock, uniaxial compressive strength (UCS) is considered as one of the key in characterizing rock material. However, sometime it is quite difficult or impossible to full fill the test requirement especially when dealing with rock that consists of discontinuities or fractures. Samples that were sent to laboratory for UCS test sometime have not enough length due to breakage during coring process in drilling activities or during transportation. In order to overcome this problem, a study was carried out to use simple method of testing as an alternative to predict the strength. Bulk density test of rock sample is one of the simple measurements that can be used to predict the UCS. The values of UCS can be correlated with the corresponding bulk density of the rock. In this study a total of 73 samples consisted of 29 granite and 44 limestone were used for UCS and bulk density test. The significant of the bulk density as variable in the correlation was evaluated in the T-test responding by P-value. Both P-value and least squares regression (R^2) showed the strong relation between UCS and bulk density of granite and limestone sample. The finding from experimental works and statistical analysis showed that, this study preceded a reliable method to predict the UCS of rock using bulk density.

Keywords Uniaxial compressive strength · Bulk density · Limestone · Granite · Kuala Lumpur

1 Introduction

Rapid development in Malaysia particularly around Kuala Lumpur city generates a huge number of construction activities since 90's. The highway and railway projects for instant are Stormwater Management And Road Tunnel (SMART tunnel),

H. Awang (✉) · N.A.M. Naru
Faculty of Civil Engineering, Universiti Teknologi MARA, 40450 Selangor, Malaysia
e-mail: harya406@salam.uitm.edu.my

highways and most recently is the Mass Rapid Transit (MRT) project that will cross and loop the city. This project triggered to the construction of surface and underground structures which involve geotechnical investigations of ground material i.e. soil and rocks. One of the properties that are not less important to measure is compression strength of the granite and limestone rocks that are dominantly founded the Kuala Lumpur area [1].

As strength is very important factor to be considered before designing any engineering structure so there are many methods that can be used to determine the strength parameter of rock. One of them is uniaxial compressive strength (UCS). The UCS of rock is a property that is very often measured and used by engineers to design surface and underground structures, and also to drill wells for mineral exploration and exploitation [2]. According to [3], UCS is considered as one of the key properties in characterization of rock materials in engineering practice. As the standard laboratory test to determine UCS is tedious works that involve heavy machinery such as coring, cutting and trimming, correlations between UCS and other indirect methods are often required for the purpose of estimating the UCS [4–7]. Therefore, a correlation with an easily measured physical property are preferred to predict the UCS. Bulk density is one of physical properties that is always being measured in the UCS test procedures. According to [8], predicting UCS strength by using bulk density is one of simple method that can be applied on the field directly without laboratory testing. By correlating with strength, this method prepares a preliminary value of rock strength parameter which is important for preliminary design. Regression analysis and a statistical method of T-test were used to determine the reliability of using bulk density, a simple measured physical property, in predicting the strength of rock.

2 Materials and Methods

2.1 Samples Collection and Preparation

The rock samples for this study were collected from the Kuala Lumpur area. A total of 29 number of granite and 44 numbers of limestone were collected during site investigation works at Sungai Besi and Ampang sites using borehole drilling method. Figures 1 and 2 show the core samples taken from the sites.

The rock cores were brought to Rock Mechanic Laboratory in Universiti Teknologi MARA for sample preparation and testing.

The cylindrical rock samples were trimmed by cutting and lapping on both ends. A trimming process was performed to obtained samples with better flatness and straightness. The samples were prepared for average diameter (D) and average length (L) in ratio of $L = 2D$. The diameter, length and mass of specimen were measured correctly using vernier caliper.

Fig. 1 Parts of granite core samples from Ampang site in Kuala Lumpur

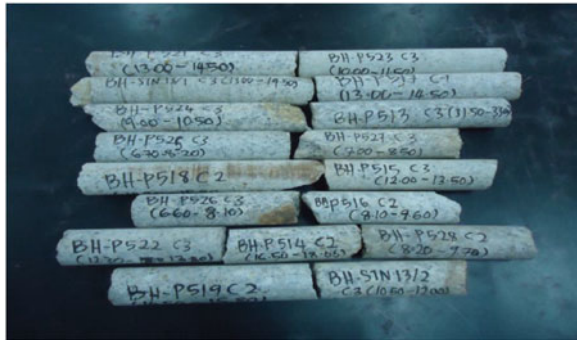
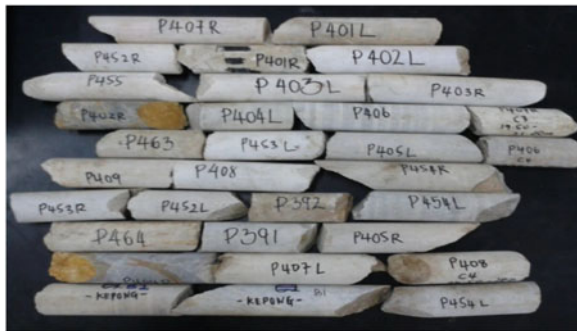


Fig. 2 Parts of limestone core samples from Sungai Besi site in Kuala Lumpur



2.2 Test Procedures

The testing procedures of UCS and sample preparation are accordance to standard procedures as recommended by ISRM [9], guidelines. Another physical dimension measured during sample preparation was volume and weight of the sample where bulk density was calculated by weight over volume. The volume and density of the rock sample was measured in accordance with the ISRM guidelines.

2.3 Statistical Analysis

Statistical method was used in this study to analyse the results of the uniaxial compression test and bulk density test. The statistical analysis method used is least squares regression analysis and T-test where the equations of the best fit of the correlation coefficients (R^2) and T-test analysis for each case were determined. These determined equations will be used to predict the uniaxial compressive strength from the results of the bulk density measured.

Method of comparison between measured and predicted UCS was also used in this study to check the capability and reliability of the prediction. This method is according to [10].

3 Result and Analysis

The result for bulk density and UCS test for granite and limestone are listed in Tables 1 and 2. The bulk density value range from as low as 2.46 g/cm³ to a high of 2.59 g/cm³ for granite and between 2.48 to 2.68 g/cm³ for limestone as summarised

Table 1 Test results of Kuala Lumpur granite (Ampang site)

Sample No.	Sample name	Diameter (mm)	Height (mm)	Weight (g)	Volume (10 ⁻⁴ m ³)	Bulk density (g/cm ³)	Max load (kN)	UCS (MPa)
1	P467	52.13	104.26	545.00	2.23	2.45	62.01	29.05
2	P474	51.74	103.48	554.40	2.18	2.55	98.40	46.80
3	P475	51.66	103.32	515.60	2.17	2.38	55.99	26.71
4	P476	47.41	94.82	416.70	1.67	2.49	65.91	37.33
5	P478	52.05	104.10	552.90	2.22	2.50	80.63	37.89
6	P479	52.07	104.14	566.10	2.22	2.55	104.14	48.90
7	P481	51.93	103.86	544.90	2.20	2.48	73.18	34.55
8	P483	52.24	104.48	588.30	2.24	2.63	135.78	63.34
9	P485	51.75	103.50	551.20	2.18	2.53	111.76	53.13
10	P486	52.20	104.40	545.80	2.23	2.44	67.12	31.38
11	P492	51.92	103.84	533.00	2.20	2.42	64.76	30.58
12	P494	51.99	103.98	559.00	2.21	2.53	104.07	49.02
13	P495	51.55	103.10	502.00	2.15	2.33	55.31	26.50
14	P496	51.20	102.40	552.00	2.11	2.62	125.69	61.04
15	P497	51.72	103.44	574.00	2.17	2.64	134.83	64.17
16	P498	51.16	102.32	528.00	2.10	2.51	82.94	40.34
17	P499	52.26	104.52	574.00	2.24	2.56	87.82	40.93
19	P502	51.88	103.76	508.50	2.19	2.32	51.91	24.55
20	P503	51.64	103.28	558.30	2.16	2.58	127.62	60.92
21	P506	52.00	104.00	548.00	2.21	2.48	86.40	40.68
22	P515	51.59	103.18	557.00	2.16	2.58	106.15	50.77
23	P516	51.75	103.50	566.90	2.18	2.60	134.85	64.10
24	P517	51.25	102.50	565.20	2.11	2.67	120.95	58.62
25	P519	51.83	103.66	555.80	2.19	2.54	89.98	42.64
26	P521	51.60	103.20	571.70	2.16	2.65	137.64	65.23
27	P522	51.11	102.22	557.90	2.10	2.66	131.78	61.78
28	P526	52.08	104.16	579.40	2.22	2.61	93.56	43.91
29	SN13/2	51.89	103.78	566.50	2.19	2.58	89.36	42.33

Table 2 Test results of Kuala Lumpur limestone (Sungai Besi site)

Sample No.	Sample name	Diameter (mm)	Height (mm)	Weight (g)	Volume (10^{-4} m^3)	Bulk density (g/cm^3)	Max load (kN)	UCS (MPa)
1	P415L	51.62	103.24	524.80	2.16	2.43	8.72	4.17
2	P411	51.74	103.48	529.10	2.18	2.43	8.80	4.19
3	P437	51.65	103.30	524.40	2.16	2.42	8.85	4.21
4	P412	52.07	104.14	541.50	2.22	2.44	10.50	4.93
5	P402R	52.25	104.50	547.00	2.24	2.44	11.35	5.29
6	P385	51.77	103.54	557.00	2.18	2.56	12.26	5.83
7	P426	53.40	106.80	601.20	2.39	2.51	13.37	5.97
8	P431	51.74	103.48	555.30	2.18	2.55	13.55	6.45
9	P402L	52.34	104.68	547.70	2.25	2.43	16.04	7.45
10	P410	51.95	103.90	557.30	2.20	2.53	17.08	8.06
11	P404R	52.01	104.02	539.40	2.21	2.44	17.60	8.28
12	P394	51.82	103.64	552.80	2.19	2.53	29.66	14.06
13	BI KPG	52.40	104.80	558.50	2.26	2.47	37.01	17.16
14	P401L	52.70	105.40	559.60	2.30	2.43	37.82	17.34
15	P392	51.93	103.86	540.30	2.20	2.46	37.10	17.52
16	P396	51.95	103.90	558.00	2.20	2.53	39.38	18.58
17	P423R	52.43	104.86	578.00	2.26	2.55	42.91	19.89
18	P414L	51.28	102.56	551.20	2.12	2.60	42.08	20.37
19	P452 R	52.44	104.88	569.30	2.27	2.51	44.59	20.64
20	SN 11/1	51.53	103.06	565.90	2.15	2.63	47.63	22.83
21	P449	52.16	104.32	585.70	2.23	2.63	49.47	23.15
22	P453 R	52.58	105.16	598.20	2.28	2.62	54.53	25.11
23	P384	51.81	103.62	576.00	2.18	2.64	55.28	26.22
24	P454 R	51.88	103.76	567.10	2.19	2.59	61.66	29.16
25	P430	52.20	104.40	576.90	2.23	2.58	62.88	29.38
26	P415R	51.64	103.28	583.90	2.16	2.70	62.04	29.62
27	P442	51.77	103.54	584.60	2.18	2.68	73.11	34.73
28	P421	51.88	103.76	578.00	2.19	2.63	63.15	29.87
29	P406	51.81	103.62	590.00	2.18	2.70	77.39	36.71
30	P390	51.92	103.84	580.80	2.20	2.64	80.70	38.11
31	P418	51.71	103.42	577.70	2.17	2.66	88.34	42.06
32	P433	52.78	105.56	612.90	2.31	2.65	98.17	44.86
33	P441	52.90	105.80	618.10	2.33	2.66	103.99	47.31
34	P404 L	51.87	103.74	597.00	2.19	2.72	101.28	47.93
35	P438	52.86	105.72	623.15	2.32	2.69	111.65	50.87
36	P443	51.75	103.50	582.20	2.18	2.67	110.01	52.29
37	P436	52.94	105.88	627.10	2.33	2.69	116.19	52.78
38	P 454 L	51.87	103.74	591.50	2.19	2.70	119.48	56.53

(continued)

Table 2 (continued)

Sample No.	Sample name	Diameter (mm)	Height (mm)	Weight (g)	Volume (10 ⁻⁴ m ³)	Bulk density (g/cm ³)	Max load (kN)	UCS (MPa)
39	SN 11/2	51.88	103.76	593.20	2.19	2.70	120.91	57.19
40	P428	51.73	103.46	588.45	2.17	2.71	120.50	57.32
41	P435	51.58	103.16	589.00	2.16	2.73	148.69	70.41
42	B2 KPG	52.00	104.00	598.90	2.21	2.71	152.62	71.16
43	P440	51.60	103.20	609.10	2.16	2.82	183.80	87.88
44	P429	52.04	104.08	615.50	2.21	2.78	195.25	91.78

Table 3 Range value of UCS and bulk density for Kuala Lumpur granite and limestone

	Granite	Limestone
UCS (MPa)	24.55–65.23	4.17–91.78
Bulk density (g/cm ³)	2.46–2.59	2.48–2.68

in Table 3. The UCS value ranges from 35.97 to 59.77 MPa for granite and from 9.41 to 42.06 MPa for limestone. The wide range of UCS value for limestone is due to the present of discontinuity features in limestone samples such as lamination and bedding. The discontinuities caused an early failure during UCS test that resulted low compressive strength.

3.1 Analysis of UCS and Bulk Density

The UCS of two rock groups are plotted against bulk density. Figure 3 shows the scatter plot of UCS against bulk density of granite rock. The best fit line for this plot

Fig. 3 Scatter plot for UCS against bulk density for granite

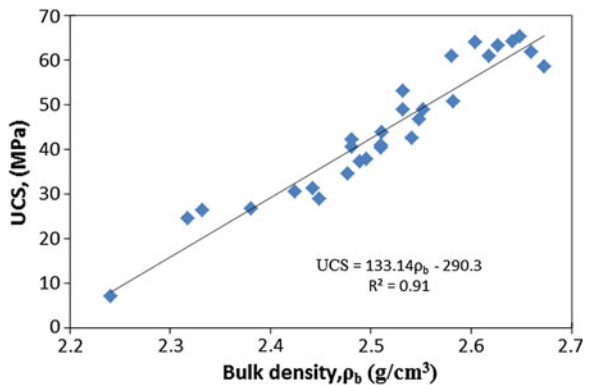
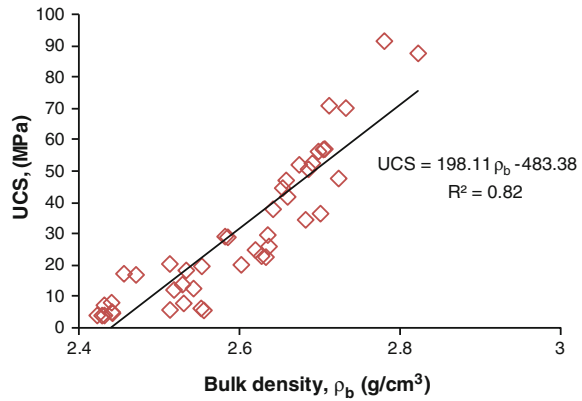


Fig. 4 Scatter plot for UCS against bulk density for limestone



is a linear line as determined by regression analysis with regression coefficient of $R^2 = 0.91$. The equation of UCS for granite is as Eq. 1 where

$$UCS_{gr} = 133.14\rho_b - 290.3 \tag{1}$$

Scatter plot of UCS against bulk density for limestone is shown in Fig. 4. A linear line with regression coefficient of $R^2 = 0.82$. The equation of UCS for limestone is as Eq. 2 where

$$UCS_{lst} = 198.11\rho_b - 483.38 \tag{2}$$

Both of rock samples which are granite and limestone showed the best fit line with linear trend line. However of limestone plot was lower than granite as the correlation of limestone and has lower regression coefficient, $R^2 = 0.82$. The comparison between both type of rocks with regard to correlation between UCS and bulk density can be seen in Fig. 5. The lower the density the lesser strength of the rocks.

3.2 Statistical Analysis Using T-Test

In order to obtain a meaningful data, a statistical test was carried out to determine the most significant physical properties of rock such as bulk density (ρ_b) to predict the UCS test. Simple regression analysis using statistical test (t-test) was selected to analyse the most significant parameter that influenced the UCS. In the T-test it was important to observe the P-value. The p-value is a probability value that is used in determining the level of significance from the data obtained. The range of P-value in relation with significance was described in [11] where P-value less than 0.01 is described as very significance and P-value more than 0.10 is described as not statistically significance (Table 4).

Fig. 5 Comparison between the plot of granite and limestone in relation to UCS and bulk density

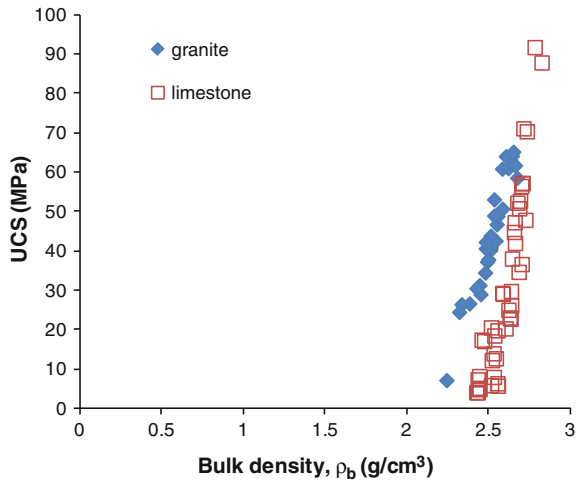


Table 4 Summary of statistical analysis

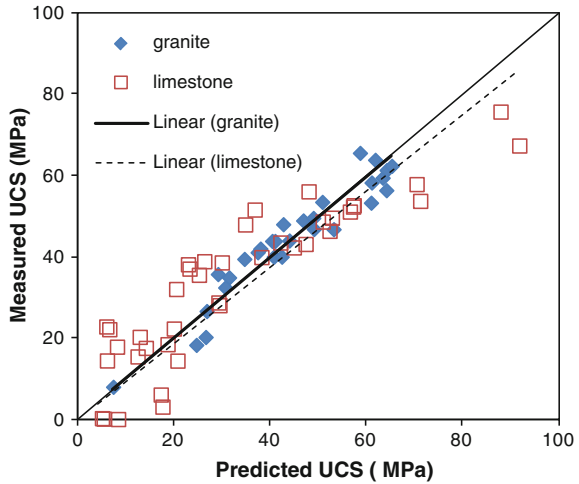
Rock type	P-value	R-Sq (%)	Correlation equation
Granite	0.000	91.0	$UCS_{gr} = -290 + 133 \rho_b$
Limestone	0.000	82.0	$UCS_{lst} = -483 + 198 \rho_b$

From the Statistical Analysis using T-Test effect of the bulk density to the UCS, it was found that the UCS is influenced by bulk density as shown in Table 3. It was proven by the P-value of granite and limestone is 0.000 and $R^2 = 91\%$ for granite and 82% for limestone. The R-squared values means how much the data fitted to the correlation line or curve between two variables, such as UCS versus bulk density. $R^2 = 1$ shows the significant relationship between the bulk density (ρ_b) and UCS. This means that the bulk density (ρ_b) value is significant as a variable to predict UCS. So, bulk density can be a predictor value to estimate the UCS.

3.3 Comparison Between Predicted and Measured UCS

To check the prediction capability of the derived equation, data of bulk density from the test were used in the obtained empirical equations to calculate the predicted UCS for both types of rocks. The predicted values of UCS were then plotted against the measured values of UCS as in Fig. 6. The error of the predicted value is represented by the distance that each data point plot from 1:1 diagonal line. A point lying on the line indicates an exact prediction. For the granite, the data points fall closer to the diagonal line compared to limestone. This suggests that the ability to predict the UCS of rocks using physical property of bulk density is the best for granite rock.

Fig. 6 Comparison between the plot of granite and limestone in relation to UCS and bulk density



4 Conclusions

The physical and mechanical properties of Kuala Lumpur granite and limestone were successfully determined. The range of bulk density of granite is 2.46–2.59 g/cm³ and for limestone sample which is 2.48 until 2.68 g/cm³ respectively. The range of UCS value of granite is 24.55–65.23 MPa and for limestone samples is about 4.17–91.78 MPa. This study proved that a correlation with an easily measured physical property such as bulk density is preferred to predict the UCS. The derived equations resulted from empirical test validated by regression and statistical analysis (t-test) suggested that predicting UCS strength by using bulk density, a simple measured physical property, is one of simple method that can be applied on the field directly. The t-test analysis suggested that bulk density is the significant predictor for UCS of both types of rocks. However, the capability and reliability of using bulk density as a predictor for UCS is more significance for Kuala Lumpur granite as shown by the regression coefficients of 91 % and 82 % for granite and limestone respectively. The wide range of UCS of limestone is may be one of the factors that affect the significance of regression analysis. These coefficients were also validated by the graph of comparison between the experimental and predicted UCS of limestone and granite where the best fit line suggested that Kuala Lumpur granite is more reliable in predicting UCS of the rocks.

Acknowledgments We would like to thank the Institute of Infrastructure and Sustainability Management (IISEM), Faculty of Civil Engineering, UiTM, for giving support and to the Research Management Institute, UiTM for providing the financial support (Dana Kecermelangan).

References

1. C.S. Hutchison, D.N.K. Tan (eds.), *Geology of Peninsular Malaysia* (University of Malaya/ Geological Society of Malaysia, Kuala Lumpur, 2009)
2. V.C. Kelessidis, *Need better knowledge of in-situ unconfined compressive strength of rock (UCS) to improve rock drillability prediction* (Department of Mineral Resources Engineering, Technical University of Crete, Hania, Greece, 2009), pp. 763–794
3. A. Basu et al., Predicting uniaxial compressive strength by point load test: significance of cone penetration. *Rock Mech. Rock Eng.* **39**(5), 483–490 (2006)
4. E. Broch, J. Franklin, J. *Rock Mech. Min. Sci.* **9**(6), 669–697 (1972)
5. M. Fener, S. Kahraman, A. Bilgil, O. Gunaydin, A Comparative Evaluation of Indirect Method to Estimate the Compressive Strength of Rock. *Rock Mech. Rock Eng.* **38**, 329–343 (2005)
6. P.J.N. Pells, *Aust. Geomech.* **G5**(N1), 54–56 (1975)
7. M. Akram, M.Z.A Bakar, Correlation between uniaxial compressive strength and point load index for salt-range rocks. *Pak. J. Eng. Appl. Sci.* **1** (2007)
8. K.R. Vincent, A.C. Oliver, Synthesizing bulk density for soils with abundant rock fragments. *Soil Sci. Soc. Am. J.* **58**(2), 455 (1994)
9. E.T. Brown (ed.), *Rock Characterization, Testing and Monitoring, ISRM Suggested Methods* (Pergamon, Oxford, 1985), pp. 111–116
10. S. Kahraman, *Int. J. Rock Mech. Min. Sci.* **38**, 981–994 (2001)
11. A. Jeromy, *Correlation, Multiple Regression & Logistic Regression. Research Methods*, pp. 325–711 (2007)

Laboratory Test Methods for Shear Strength Behavior of Unsaturated Soils Under Suction Control, Using Triaxial Apparatus

Pooya Saffari, Mohd Jamaludin Md Noor, Basharudin Abdul Hadi and Shervin Motamedi

Abstract The shear strength of an unsaturated soil is controlled by two variables; net stress and suction. The conventional triaxial machine which is used for obtaining the shear strength of saturated soils cannot be used for unsaturated soil conditions due to weakness in suction control during the consolidation and shearing stages. In the view of this, the standard triaxial apparatus needs to modify and develop for unsaturated conditions. The main aim of this paper is devoted to give a description of current methods and techniques using triaxial apparatus for obtaining data to interpret the accurate shear strength behavior of unsaturated soils. In additional some of the key aspects related to air diffusion and volume change measurement are highlighted.

Keywords Unsaturated soils • Triaxial machine • Flushing system • Suction control

P. Saffari (✉) · M.J.M. Noor
Department of Civil Engineering, Universiti Teknologi MARA, Shah Alam, Malaysia
e-mail: pooya_sa2002@yahoo.com

M.J.M. Noor
e-mail: mohdjamaludinmdnoor@yahoo.com

B.A. Hadi
Department of Civil Engineering, Universiti Teknologi MARA, Penang, Malaysia
e-mail: basha_uitma@yahoo.co.uk

S. Motamedi
Department of Civil Engineering, University of Malaya, Kuala Lumpur, Malaysia
e-mail: shervin@um.edu.my

1 Introduction

Nowadays, several branches of knowledge, such as petroleum, soil science, agricultural and especially geotechnical engineering relate to the understanding of unsaturated soil mechanics. In the last two decades, some efficient efforts were made in furtherance of the numerical technique, theoretical framework and experimental methods related to unsaturated soil mechanics [1].

One of the main parameters in soil mechanics which plays a main role in a large number of geotechnical problems such as slope stability, bearing capacity and lateral earth pressure is shear strength. The shear strength of an unsaturated soil is controlled by two variables; net stress and suction. The most widely laboratory methods used for the investigating of shear strength of a soil is the triaxial test. The triaxial test is multipurpose and can be used for the determining of many soil parameters such as shear strength, permeability and consolidation characteristics of soils. This procedure includes facilities which are able to control and measure the magnitude of stresses, pore pressures, axial forces, axial strain and volume change. These abilities are key to improving our understanding of soil behavior [2]. The conventional triaxial method which is used for obtaining the shear strength of saturated soils cannot be used for unsaturated soil conditions due to weakness of quantification and controlling of soil suction with respect to an increase in shear strength during the consolidation and shearing stages. In the view of this, practical and cost effective modifications for determining the shear strength of unsaturated soils must be developed [3]. Several researchers such as [2, 4–9] proposed and developed some triaxial testing devices for unsaturated soils.

The main aim of this paper is devoted to give a description of current methods and techniques using triaxial apparatus for obtaining data to interpret the accurate shear strength behavior of unsaturated soils. Cylindrical triaxial system and its considerations base of Axis translation suction control are discussed. In additional some of the key aspects related to air diffusion and volume change measurement are highlighted.

2 Cylindrical Triaxial Apparatus

Since the pioneering work of [10], the triaxial test has been widely used for that laboratory measurement involving measurement of stress-strain and strength characteristics of soils. The actual triaxial test is usually carried out on a cylindrical soil specimen subjected to an all round confining pressure. In saturated specimens, the confining pressure generally applied by water pressure inside a cell. A loading rod, which is typically in contact with the top of the soil specimen, applies axial stress. The soil specimen is usually enclosed in a rubber membrane. Two porous caps are positioned along the top and underside of the specimen to allow movement of water from the sample. The volume change of the sample is measured by the volume of water released from the sample.

In the modified triaxial testing, which used for unsaturated soils, measurement and control of pore-air, pore-water pressures, volume changes and matric suction is accommodated independently. Some of the methods and modifications to the processes applied during the testing of unsaturated soils are highlighted below. A schematic diagram of a modified triaxial apparatus by [9] is given in Fig. 1.

2.1 Pore Water Pressure Control

Pore-water pressure (u_w) in unsaturated soils is negative ($u_w < 0$) and typically measured or controlled through an HAE (high-air-entry) ceramic disk [11–14]. HAE is placed underneath the specimen and connected to the measuring system water compartment. The ceramic disk allows the slow flow of water while resists the passage of free air onto the base pedestal. The matric suction in the specimen ($u_a - u_w$) must not exceed the air entry value of the disk to prevent air flow into the water compartment, otherwise it makes a discontinuity between pure water and the water in the measurement system [15].

In recent years, some of the researchers used double drainage system for triaxial testing on low permeability soils. In this method at each end of soil specimen a peripheral annular coarse stone and an internal high-air-entry are placed. As a

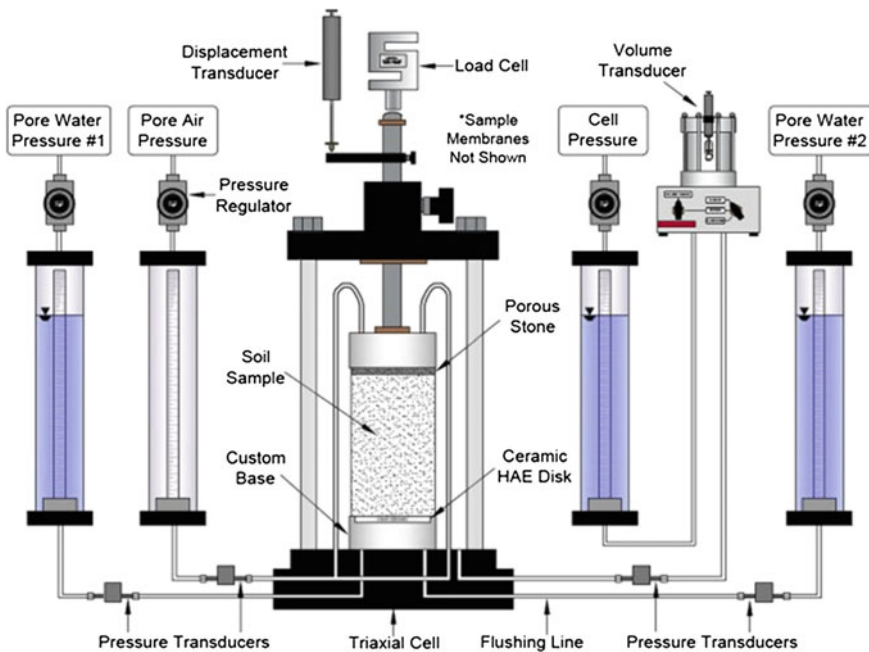


Fig. 1 A schematic diagram of a modified triaxial apparatus [9]

result, u_w can be applied at both ends [16, 17]. This technique reduced equalization time significantly; however, increase the chance of trapped air bubbles in the center of the soil specimen [12].

2.2 Pore Air Pressure Control

To control and measure the pore-air pressure a controlled pore-air line is essential. This line is connected to a coarse porous stone at the top cap of the soil specimen which is used as a drainage element for air. The coarse porous stone provides continuity between the air voids and the pressure control system. It has low air entry value and prevents the flow of water to the measuring and controlling system [2]. Air pressure is applied from the top of the specimen and the difference between air pressure and cell pressure is taken as the net stress applied; $(\sigma - u_a)$ [18]. Matric suction also is controlled by pore-air line and measured as the difference between air pressure and pore-water pressure; $(u_a - u_w)$.

2.3 Axis-Translation Technique

As mentioned above, applied matric suction cannot exceed the air entry value of HAE. Moreover, if negative pore water approaches -110 kPa, air bubbles will accrue under the disk [2]. These limitations to the applying matric suction can be overcome using axis-translation technique.

In an unsaturated soil, pore air pressure typically is atmospheric ($u_a = 0$). As a result, pore water pressure become negative due to atmospheric pressure. During the axis-translation procedure, pore air pressure is raised up above atmospheric pressure. With respect to that, pore water pressure becomes positive without any problems associated with cavitation. The principle associated with this technique is shown in Fig. 2 [19].

It should be noted that there is still some possibility of air to diffuse into the water under the disk. This is normal for a small amount of diffused air [2]. However, over a long period of time, this could become problematic if much air flow under the disk and causes it to lose saturation. To cope with this problem a flushing system should be used.

2.4 Flushing System

Any diffused air must be removed from under the HAE. In order to achieve this, a circular grooved compartment under the disc can be used. In this compartment water can flow from one of the pure pressure lines connected to the bottom base to

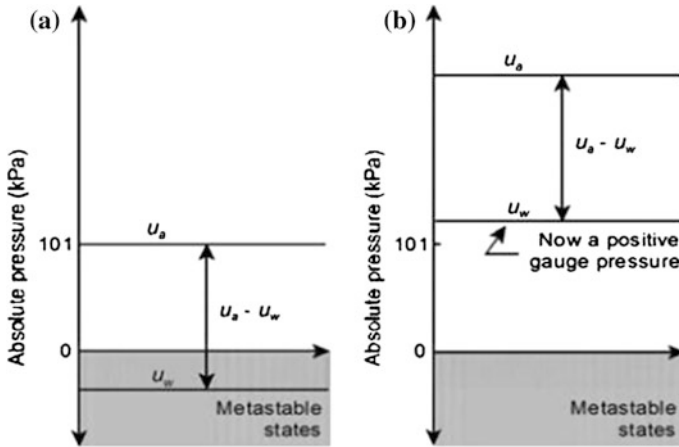
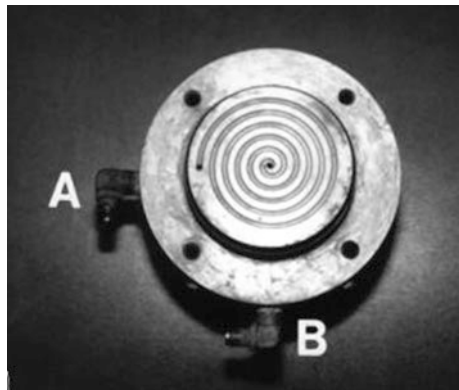


Fig. 2 Axis translation procedure to avoid cavitation. **a** Atmospheric conditions. **b** Axis-translation [18]

the other pore pressure line. The flow of water is applied by creating a differential pressure between two lines [2, 4]. The flow of water flushes out any diffused water from under the disk (Fig. 3).

The volume of removing bubbles should be evaluated in a burette connected to the pure pressure lines to prevent mistakes in the measurement of pore water. The specimen water volume change also must be adjusted. The pressure in flushing line should set equal to the pore water pressure to avoid water from entering or leaving soil sample. The flow of water inside flushing line is applied by the difference in pressure head between collector and storage tanks. However, sometimes the trapped air bubbles do not mobilize by flushing in one direction only. As a result a flow

Fig. 3 Plan view showing grooved channels for flushing porous disk above water compartment, and pore-water ports (A, B) [2]



reversal unit in the flushing system is needed to reverse the water flow under the HAE disc [20]. Figure 4a, b is a schematic diagram of the flushing system with a unsaturated triaxial apparatus in two different directions.

2.5 Volume Change Measurements

Measuring of volume change in unsaturated soil testing has been always one of the main challenges for the researchers. Volume change in unsaturated soil testing can be governed from three different cases: stresses, drainage and air phase compression. These soil volume changes cannot measure directly from variation in water

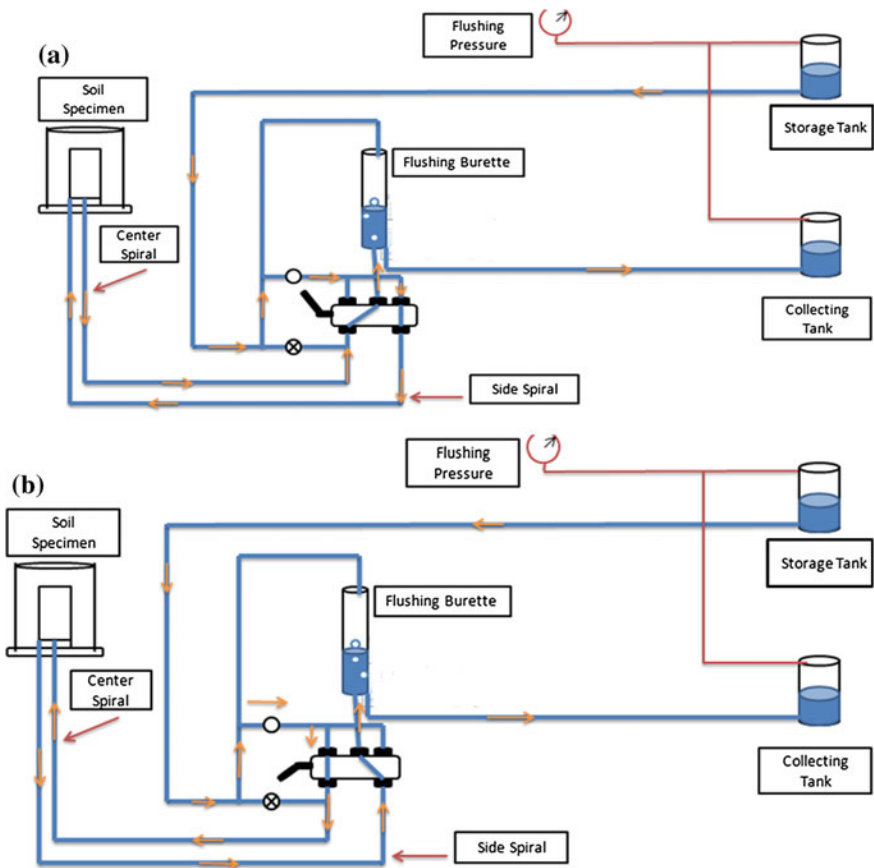


Fig. 4 Schematic diagram of the flushing system in a unsaturated triaxial apparatus in two different directions (a, b)

volume as same as the techniques practiced in conventional saturated soil triaxial testing. Lately a number of measurements have been demonstrated which can be separated into three general categories [21].

1. *Cell Liquid Measurement*

In this method, volume changes of the specimen are measured by volume changes in confining cell liquid. The cell should be filled completely with the water. The effect of piston intrusion and volume changes of the whole cell should be considered and corrections should be applied. The method is simplicity, however, using that may cause some problems such as Plexiglas creep due to stress, water leakage or sudden expansion of cell wall during a pressure increase.

To reduce the possibility of errors, [11] suggested the addition of an inner cell placed in the outer cell base. This method is known as double wall triaxial test. They used mercury as a liquid in the inner cell and deducted overall volume change by measuring the fall and rise of the mercury vertical level surrounded the specimen. There are two disadvantages of using this method. First the specimen is invisible inside the cell and second, the hazard of using mercury. The method has been developed in subsequent years by [13, 22] however the hazard problem still was not eliminated. Later on [23, 24] replaced mercury with water inside the inner cell and measured water volume by a high-precision cathetometer. Recently the method has been improved by some modifications on inner cell and also water volume change reading [14, 25–27].

2. *Direct Air-Volume and Water-Volume Measurements*

In this technique, soil volume change is obtained from measuring the air and water volume changes. Pore air and pore water are separated via porous stones and HAE ceramics and then the volume of them, entering and leaving the pore spaces are recorded by pressure-volume controllers. Small temperature and atmospheric pressure changes and also undetectable air leakage must be taken into the account. The method helps to implement a large number of test paths due to monitoring air volume/pressure separately [28–30].

3. *Direct Measurements on the Specimen*

In this approach soil volume change is obtained directly from the measurement of axial and radial soil sample displacements. This method can be done in three different categories. In the first category, which is suitable for samples by small deformations, local displacement sensors are placed directly onto the specimen and axial/radial deformation is recorded during the test [31]. This method is most commonly used and several technologies have been tried such as Hall Effect transducers [32] and miniature LVDTs [33]. Radial displacements are recorded at one to three points and help to assess the volumetric strain by making some assumptions to the shape of the specimen. An initial rigid soil specimen is required for such direct measurement.

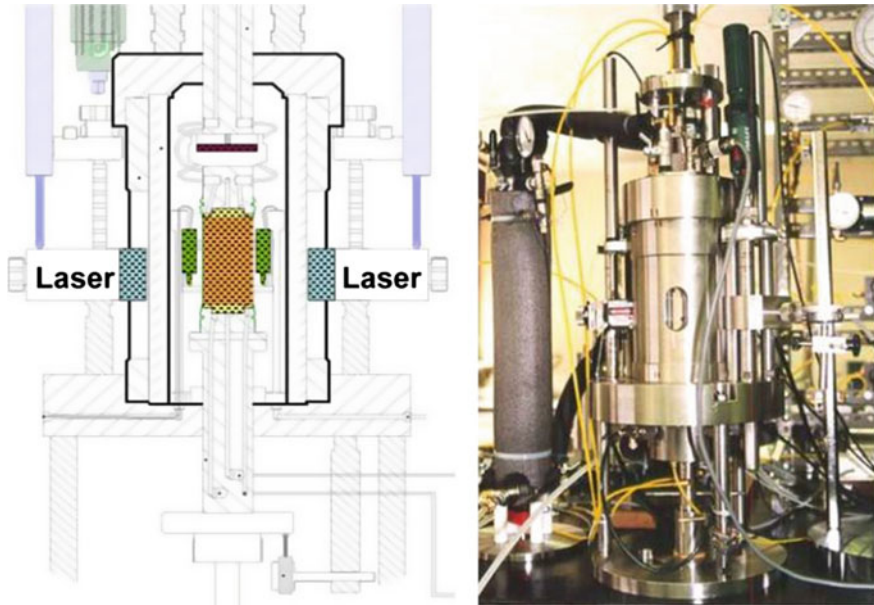


Fig. 5 Volume change measurement by electrooptical lasers [34]

Second category includes some non-contacting methods such as lasers. Figure 5 shows volume change measurement by electrooptical lasers used by [34]. In this method two long-range, electro-optical lasers are placed on two diametrically opposite sides of soil specimen to measure radial deformations. Another laser is mounted over the entire specimen high to assess more accurately deformation. The method allows observation of small and non-uniformities deformations. However, using laser is costly and requires sophisticated installation procedures.

The last category is obtaining soil volume changes and specimen deformation base on image processing. Several pictures are taken during the test and then by analysing the images, specimen profile and volume changes are obtained. In this method the magnification effect and the different reflection should be considered. Similar to laser, soil deformations are measured from the entire height of the specimen and direct contact is not needed [35, 36].

3 Conclusion

Triaxial apparatus is one of the most common methods to assess the soil properties. The conventional triaxial testing used for saturated soils is not accurate for unsaturated conditions and some modifications are essential. The following concluding remarks some modifications is needed to take place into the cylindrical triaxial apparatus:

- Pore water pressure and pore air pressure must be controlled and measured independently by using HAE (high-air-entry) ceramic disc and coarse porous stone respectively.
- To reduce the risk of air bubbles under the HAE disk and increasing the chance of applying higher pore water pressure, axis-translation technique is suggested.
- A flushing system underneath the HAE disk is required to remove diffused air bubbles and reduce the errors of measuring pore water pressure and soil volume change.
- The volume change of unsaturated soil is governed from three different approaches: cell liquid measurement, direct air-volume and water-volume measurement and direct measurement of the specimen.

Acknowledgments This research was funded by a UiTM E-Science fund (Grant No. 100-RMI/SF 16/6/2 (1/2013)). We admirably acknowledge these supports. The authors also wish to thank the faculty of Civil Engineering at Universiti Teknologi MARA for its support.

References

1. S.K. Vanapalli, M.V. Nicotera, R.S. Sharma, Axis translation and negative water column techniques for suction control. *Geotech. Geol. Eng.* **26**, 645–660 (2008)
2. D. Wulfsohn, B.A. Adams, D.G. Fredlund, Triaxial testing of unsaturated agricultural soils. *J. Agric. Eng. Res.* **69**, 317–330 (1998)
3. D.G. Fredlund, Stress state variables for unsaturated soils. *J. Geotech. Eng.* **103**, 447–464 (2006)
4. J.M. Padilla, et al., An automated triaxial testing device for unsaturated soils. *Geotech. Spec. Publ.* **147**, 1775–1786 (2006) (Unsaturated Soils 2006, ASCE GSP, 2006)
5. Z. Cabarkapa, T. Cuccovillo, Automated triaxial apparatus for testing unsaturated soils. *Geotech. Test. J.* **29**(1), 21–29 (2006)
6. R. Sivakumar et al., Twin-cell stress path apparatus for testing unsaturated soils. *Geotech. Test. J.* **29**(2), 175–179 (2006)
7. A. Jotisankasa, M. Coop, A. Ridley, The development of a suction control system for a triaxial apparatus. *Geotech. Test. J.* **30**(1), 69–75 (2007)
8. Y.J. Cui et al., Use of a differential pressure transducer for the monitoring of soil volume change in cyclic triaxial test on unsaturated soils. *Geotech. Test. J.* **30**(3), 227–233 (2007)
9. R.E. Burrage, et al., A cost effective triaxial test method for unsaturated soils. *Geotech. Test. J.* **35**(1) (2011)
10. A. Casagrande, Characteristics of cohesionless soils affecting stability of slopes and earth fills. *J. Boston Soc. Civ. Eng.* **23**(1), 13–32 (1936)
11. A. Bishop, I. Donald, The experimental study of partly saturated soil in the triaxial apparatus. In: *5th International Conference Soil Mechanics and Foundation Engineering*, Paris (1961)
12. L.R. Hoyos, L. Laloui, R. Vassallo, Mechanical testing in unsaturated soils. *Geotech. Geol. Eng.* **26**(6), 675–689 (2008)
13. A. Josa, et al., Stress–strain behaviour of partially saturated soils. In: *9th European Conference on Soil Mechanics and Foundation Engineering*, Dublin (1987)
14. C. Rampino, C. Mancuso, F. Vinale, Laboratory testing on an unsaturated soil: equipment, procedures, and first experimental results. *Can. Geotech. J.* **36**(1), 1–12 (1999)
15. D.G. Fredlund, H. Rahardjo, *Soil Mechanics for Unsaturated Soils* (Wiley, New York, 1993)

16. Barrera, M., *Estudio experimental del comportamiento hidro-mecanico de suelos colapsables*. Universitat Politècnica de Catalunya, Barcelona (2002)
17. Romero, E., Characterization and thermo-hydro-mechanical behaviour of unsaturated Boom clay: an experimental study. Thesis, Universitat Politècnica De Catalunya, Barcelona, Spain. Universitat Politècnica de Catalunya, Barcelona (1999)
18. D.Y.F. Ho, D.G. Fredlund, A multistage triaxial test for unsaturated soils. *Geotech. Test. J.* **5** (1/2), 18–25 (1982)
19. F. Marinho, W. Take, A. Tarantino, Measurement of matric suction using tensiometric and axis translation techniques. *Geotech. Geol. Eng.* (2008)
20. T.H. Salman, *Triaxial Behaviour of Partially Saturated Granular Soils at Low Stress Levels* (University of Sheffield, Sheffield, 1995)
21. L. Laloui et al., Advances in volume measurement in unsaturated triaxial tests. *Soils Found.* **46** (3), 341–349 (2006)
22. P. Delage, S.D. Silva, E.D. Laure, Un nouvel appareil triaxial pour les sols non-satures. In: *9th European Conference on Soil Mechanics and Foundation Engineering*, Dublin, pp. 25–28 (1987)
23. Y. Cui, *Etude du comportement d'un limon compacte non saturé et de sa modélisation dans un cadre elastoplastique*. Ecole Nationale des Ponts et Chaussées, Paris (1993)
24. Y. Cui, P. Delage, Yielding and plastic behaviour of an unsaturated compacted silt. *Geotechnique* **46**(2), 291–311 (1996)
25. S. Aversa, M. Nicotera, A triaxial apparatus for testing unsaturated soils. *Geotech. Test. J.* **25** (1), 3–15 (2002)
26. C. Ng, L. Zhan, Y. Cui, A new simple system for measuring volume changes in unsaturated soils. *Can. Geotech. J.* **39**, 757–764 (2002)
27. H. Toyota, N. Sakai, T. Nishimura, Effects of stress history due to unsaturation and drainage conditions on shear properties of unsaturated cohesive soil. *Soils Found.* **41**(1), 13–24 (2001)
28. B. Adams, D. Wulfschön, D. Fredlund, Air volume change measurement in unsaturated soil testing using a digital pressure–volume controller. *Geotech. Test. J.* **19**(1), 12–21 (1996)
29. F. Geiser, *Comportement mécanique dun limon non saturé: étude expérimentale et modélisation constitutive* (Ecole Polytechnique Fédérale de Lausanne (EPFL), Switzerland, 1999)
30. A. Laudahn, K. Sosna, J. Bohac, A simple method for air volume change measurement in triaxial tests. *Geotech. Test. J.* **28**(3), 313–318 (2005)
31. C. Clayton et al., The use of Hall effect semiconductors in geotechnical instrumentation. *Geotech. Test. J.* **12**(1), 69–76 (1989)
32. C. Clayton, S. Khattrush, A new device for measuring local axial strains on triaxial specimens. *Geotechnique* **36**(4), 593–597 (1986)
33. E. Klotz, M. Coop, On the identification of critical state lines for sands. *Geotech. Test. J.* **25** (3), 288–301 (2002)
34. E. Romero, et al., A new suction and temperature controlled triaxial apparatus. In: *14th International Conference on Soil Mechanics and Foundation Engineering*, Hambourg (1997)
35. P. Gachet et al., Interfacial behaviour of unsaturated soil with small-scale models and use of image processing techniques. *Geotech. Test. J.* **26**(1), 12–21 (2003)
36. A. Rifai, L. Laloui, L. Vulliet, Volume measurement in unsaturated triaxial test using liquid variation and image. In: *3rd International Conference on Unsaturated Soils*, Recife, Brazil (2002)

The Study of Interface Shear Strength Between Geotextile and Soil Liner Containing Different Percentage of Sodium Bentonite

M. Mukri, A. Azmi, S. Hashim, S. Aziz, F.H. Ahmad and N. Khalid

Abstract The purpose of this research is to focus on the interface shear strength between geotextiles and soil with different percentage of sodium bentonite. Firstly, the physical properties of the soil samples must be identified in order to determine the soil classification. The laboratory tests include atterberg limit test, shrinkage limit test, specific gravity test, pH test, sieve analysis test and hydrometer test. The soil samples are natural soil sample, soil added with 0 % of sodium bentonite, soil added with 2.5 % of sodium bentonite, soil added with 5.0 % of sodium bentonite, soil added with 7.5 % of sodium bentonite and soil added with 10 % of sodium bentonite. Based on the test results, the added percentages of sodium bentonite did not appear to have any effect on the properties of the soil samples such as the liquid limit, plastic limit and specific gravity. This is because the values obtained were approximately the same and no apparent changes were detected. However, the shrinkage limit and pH test results shows an increasing trend with the increase of sodium bentonite percentage. The natural soil can be classified as Sandy SILT of Intermediate Plasticity (*MI*). After classifying the soil samples, compaction tests were performed to get the values of optimum moisture content required during direct shear box test. As with liquid limit plastic limit and specific gravity tests, the results for compaction and direct shear test also did not give good results, as the values of optimum moisture content, cohesion and friction angle were also quite similar to each other. Thus, it can be clearly said that, as an admixture, sodium bentonite did not affect the soil samples, therefore not suitable for this type of soil.

M. Mukri (✉) · A. Azmi · S. Hashim · S. Aziz · F.H. Ahmad · N. Khalid
Faculty of Civil Engineering, University Teknologi MARA, Shah Alam, Malaysia
e-mail: ce_mazidah@yahoo.com

N. Khalid
e-mail: aln_kh82@yahoo.com

1 Introduction

Urbanization and population growth not only increased the standard of living in Malaysia, it also increases the waste generation. Municipal solid waste consists of waste generated from residential, commercial, institution and public parks [1]. Landfills for municipal and hazardous waste are constructed for the purpose of containing the waste in a concentrated unit with low mobility. In order to accomplish this, it is necessary to restrict the flow of water through the upper and lower boundaries of the landfill, referred to as the cover and the base liner of the landfill [2].

Landfills or dumping sites, has long been used as the final destination of collected waste produced by humans. As stated by Masirin et al. [3], a total of 230 landfills which contained about 7.34 million tones of solid wastes were generated in Malaysia. This solid waste volume is still increasing at the rate of 1.5 % per year due to increase in urbanizations, change in living standards and consumption patterns.

Modern landfill is highly engineered containment systems that are located, designed, operated, and monitored to fulfil the requirements of the federal system. It is intended to minimise the impact of solid waste to the environment such as air pollution, water pollution, global warming and also to human's safety. In the modern landfill construction, the liner system is used. The main purpose of using liner system is to protect the soil and ground water pollution originating in the landfill.

Geosynthetic Clay Liners (GCLs) are prefabricated alternative to compacted clay liners that may be used for cover and base liner systems at lower costs and equivalent hydraulic performance [2]. A unique characteristic of sodium bentonite is that it can draw water from adjacent soils, possibly reaching water contents in excess of 100 % [4]. The liner system consists of compacted low permeability soil and geosynthetic material. The stability of this system is controlled by the shear strength of each component of the system. The geomembrane and geosynthetic interface shear resistance can be low and usually lower than soil interface shear resistance [5].

2 Scope of Study

The main focus in this study is to determine the interface shear strength between geotextiles and soil liner containing different percentages of sodium bentonite. This research is based on the laboratory testing. There were five samples of soil tested in the laboratory in order to determine the physical properties of soil. The basic physical property tests of soil samples performed in the laboratory were such as plastic limit and liquid limit tests, shrinkage limit test, specific gravity test, pH test, sieve analysis test and hydrometer test. After all the tests have been conducted, the soil samples were moulded and compacted at the optimum moisture content condition as a preparation for direct shear test. These samples were tested in the 60 mm × 60 mm direct shear box to determine the interface shear strength between geotextile and soil liner containing different percentages of sodium bentonite.

3 Material Used for the Experiment

A modern landfill was designed and constructed to contain liquid leachate, segregated the areas for hazardous waste and monitoring the pollution. However, a poorly designed or operated landfill may cause many problems. Over the past several years, different geosynthetics manufacturers have proposed several unique GCL products that attempt to minimize hydraulic conductivity while maximizing shear strength [6]. Throughout the years, geosynthetic clay liners (GCLs) has been increasingly selected to replace compacted clay liners (CCLs) in composite liner and cover systems for waste containment facilities [7].

In this study, sodium bentonite is used in order to determine the reaction between soil and sodium bentonite. Sodium bentonite will expand when wet and will absorb water as much as several times its volume because of its excellent colloidal properties [8]. Sodium bentonite is a naturally occurring, mined clay mineral that is extremely hydrophilic because of its small size clay particles and the electrical imbalance on the surface of the clay particles. When placed in the vicinity of water or water vapor, the matric suction of dry sodium bentonite clay attracts water molecules into its well developed diffuse double layer leaving little free-water in the voids and resulting in a low saturated hydraulic conductivity [9]. In addition, sodium bentonite is capable of self-healing. That is, if the soil is punctured or dried to the point of desiccation, the soil is able to swell when it comes into contact with water to regain its previous hydraulic properties (McCartney 2002).

Geotextile is made of permeable fabrics, which depending on the methods used, combine the filaments or tapes into the planar textile structure. The vast majority of geotextiles are either woven or nonwoven. For this research, the geotextiles that were used to shear with soil added with sodium bentonite is non-woven type of geotextile.

4 Sample Preparation and Testing Method

The soil samples were tested based on British Standard for physical properties and engineering properties. In this study, the physical properties of the soil which are natural soil and soil with different percentage of sodium bentonite were determined through the various tests such as plastic limit, liquid limit, shrinkage limit test, specific gravity, and pH test. Meanwhile, sieve analysis test and hydrometer test were performed on natural soil only. The aim of these tests is to determine the characteristic of the soil and to classify the types of the soils. Meanwhile for engineering properties test, the tests were compaction test and shear box test. Compaction test were tested with samples of 0, 2.5, 5, 7.5 and 10 % of sodium bentonite for the compaction properties in order to determine the optimum moisture content and maximum dry density. Direct Shear Test was conducted to analyse the effectiveness of interface friction angle between geotextile and natural soil mix with

different percentages of sodium bentonite Shear box is used for the direct shear test to measure the normal and shear stress on the failure surface directly.

The shear box is normally the most preferred method for soil shear testing because it is a fast and economical method of measuring shear strength. A specimen is placed in a shear box which has two stacked halves to hold the sample; the contact between the two halves is at approximately the mid-height of the sample. Soil without admixture at the top, bound by geotextile at the middle and soil with the admixture (sodium bentonite) were be placed at the bottom part of the apparatus. Geotextile and soil with admixture were placed exactly at the failure plane. A normal load was applied to the specimen and the specimen was sheared across the pre-determined horizontal plane between the two halves of the shear box. The size of direct shear box that was used is 60 mm × 60 mm, which can give a more efficient result for soil shear strength as stated by Ingold [10]. Lastly, falling head test was performed to determine the correlation between hydraulic conductivity parameter and shear strength of the soil sample.

5 Test Results and Discussion

This study is laboratory based research which involved fine grained soil subjected to several laboratory testings. All the standard tests were conducted based on British Standard as references.

5.1 Basic Properties Test

Table 1 shows that the soil that were taken at Kampung Kundang, Banting Selangor, can be classified as Sandy SILT of Intermediate Plasticity (*MI*).

Based on the result, it shows the relationship of sodium bentonite percentage with soil physical properties. From the table, it is apparent that the values of liquid limit, plastic limit, plasticity index and specific gravity are quite similar to each other. The percentage of sodium bentonite did not seem to affect or cause any changes to the soil's liquid limit, plastic limit and specific gravity. However, the results of shrinkage limit test and pH test give good relationship as they show an increasing trend when the content of sodium bentonite increased.

Table 1 The summary for soil physical properties

Sample no.	LL	PL	PI	SL	SG	PH
S-0SB	44	38	6	11.67	2.4	3.96
S-2.5SB	63	49	14	13.33	2.46	4.37
S-5.0SB	54	37	17	14	2.44	4.76
S-7.5SB	61	48	12	15.67	2.6	5.15
S-10SB	65	45	20	16	2.62	5.28

5.2 Compaction Test

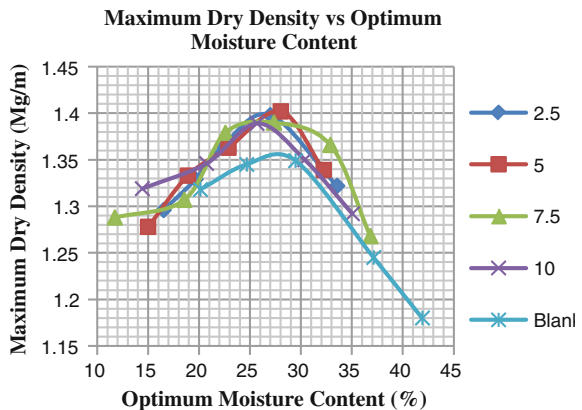
The results of the compaction test show that the values of maximum dry density, ρ_d *MDD* and optimum moisture content, *OMC* for all the samples added with bentonite are not much different from each other. The values for ρ_d *MDD* ranges from 1.35 to 1.40 Mg/m³ and the values for *OMC* ranges from 25.5 to 28.5 %. However, it could be clearly seen that by adding bentonite to the soil samples, the maximum dry density increases. Supposedly, the water content increases with the increase in sodium bentonite content. Chalermyanont and Arrykul [11] stated that the more bentonite was added, the optimum water content increased and maximum dry density decreased. Such occurrence could not be observed in this study, as shown by Fig. 1, which shows the combination graph of maximum dry density against optimum moisture content.

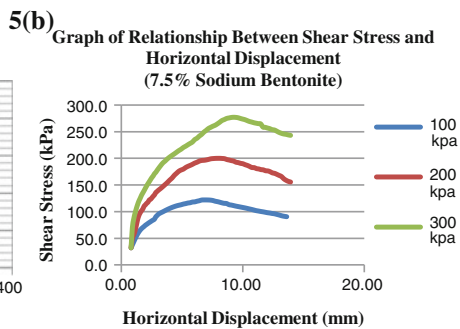
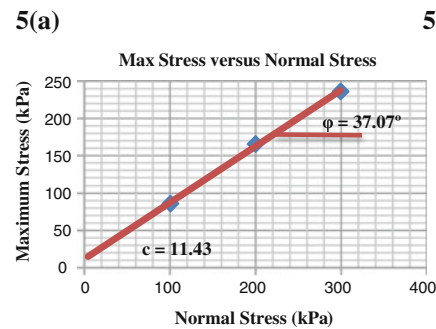
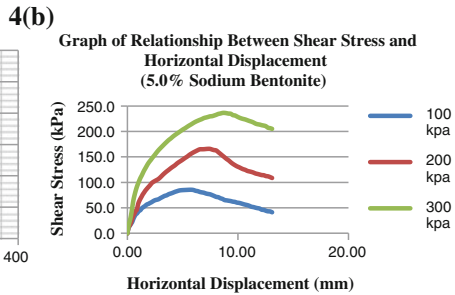
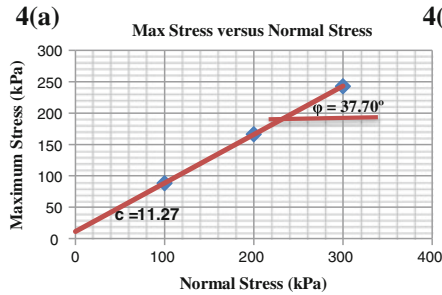
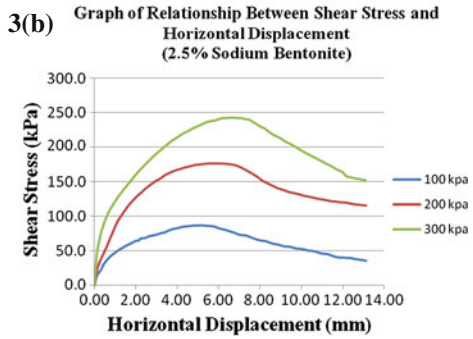
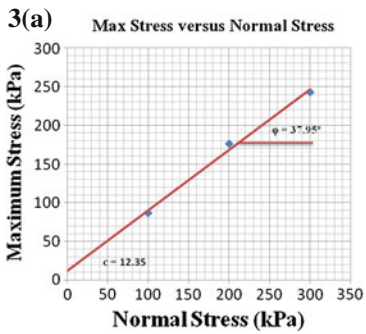
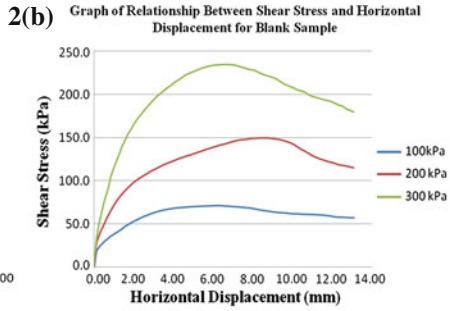
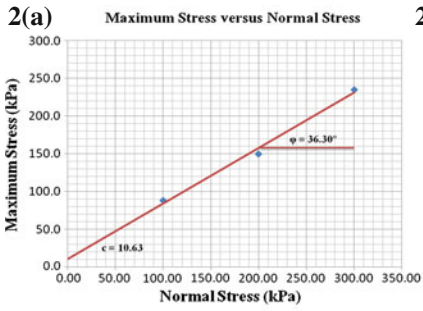
5.3 Direct Shear Test

Direct shear Test was performed with applied normal stress of 100, 200 and 300 kPa. Experimental result of direct shear test from Figs. 2 to 6 shows 5 samples prepared using the optimum moisture content that was obtained from the compaction tests. It can be said that, the value of the maximum shear stress can be determined by plotting the stress-strain data from the shear box test (Figs. 2b, 3b, 4b, 5b, 6b). From the graph in Figs. 2a, 3a, 4a, 5a, 6a, the value of cohesion, *c* and the internal friction angle ϕ were determined.

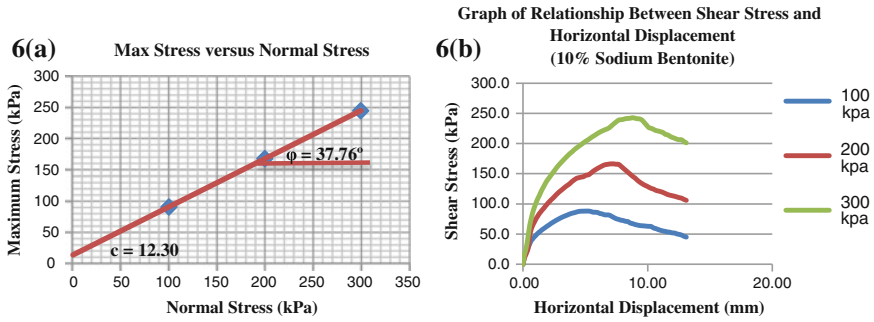
Based on the Table 2, it shows that the higher value for *c* is at soil added with 2.5 % of sodium bentonite, that gives the value of 12.35 kPa and friction of 37.95 %. As for the rest, the soil that was added with 10 % of sodium bentonite is found to produce the lowest value for *c* with 11.27 kPa and friction with 37.70 %. It can be said that the more sodium bentonite were added to the soil, the lower the shear strength tend to be,

Fig. 1 The combination of maximum dry density against optimum moisture content





Figs. 2–6 Graph of relationship between shear stress and horizontal displacement for S-0SB, S-2.5SB, S-5SB, S-7.5SB and S-10SB



Figs. 2–6 (continued)

Table 2 Value for maximum stress and normal stress

Sample	Shear strength parameter			C	Ø
	Max stress @ 100 kPa	Max stress @ 200 kPa	Max stress @ 300 kPa		
S-0SB	88	149.7	234.9	10.63	36.3
S-2.5SB	86.5	176	242.5	12.35	37.95
S-5.0SB	85.4	165.7	236.5	11.43	37.07
S-7.5SB	89.6	167.5	244.5	12.3	37.76
S-10SB	88.3	166.4	242.9	11.27	37.70

due to the swelling of the soil. It can be presumed that the cohesion value from the result is insignificant as the shear between soil and geotextile will affect the movement of the soil particle. Only natural soil sample give lower value of cohesion but the other samples give quite similar value for cohesion. Apart from that, the value for the friction angles did not show any apparent change with the increasing percentage of sodium bentonite, the result is quite similar to each other.

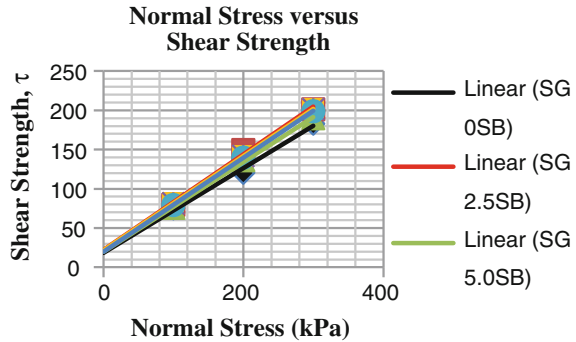
5.4 Interface Shear Strength Between Soil with Different Percentage of Sodium Bentonite and Geotextiles

Based on the Table 3 and Fig. 7, the most higher results shows that soil added with 2.5 % of sodium bentonite, meanwhile soil added with 7.5 % of sodium bentonite also give a value that not much different from SG-2.5SB but then it drop after more percentage of sodium bentonite added in the soil. In comparison to experimental results, it can be stated that the increment percentages of sodium bentonite in soil mixtures decrease the shear strength of the GCLs. However, based on the result that has been conducted in the laboratory, the value of shear strength did not give a good relationship in adding percentage of sodium bentonite. This is because due to the soil type that effect the shear strength of the soil.

Table 3 Value for shear strength

	100 kPa	200 kPa	300 kPa
Sample	τ_1	τ_2	τ_3
SG-0SB	75.27	120.6	183.18
SG-2.5SB	79.82	149.61	201.47
SG-5.0SB	75.94	136.61	190.1
SG-7.5SB	81.70	142.04	201.68
SG-10SB	79.52	139.88	199.00

Fig. 7 Graph of normal stress versus shear strength



5.5 Hydraulic Conductivity

The value of k for the natural soil sample for test 1 in 300 s is 2.341×10^{-7} cm/s and for test 2 in 420 s the value is 1.768×10^{-7} cm/s. The average of the two tests is 2.054×10^{-7} cm/s. The sample is only tested for natural soil sample because the value of soil added with different percentage sodium bentonite give quite similar value to the natural soil. Since the sample is natural soil, the value for the hydraulic conductivity is acceptable as the hydraulic requirement is 1×10^{-7} cm/s. According to Chalermyanont (2004), hydraulic conductivity of sand can be reduced if sand is mixed with a very impervious material such as sodium bentonite.

6 Conclusion

Based on the finding data of physical properties and engineering properties, it is apparent that the value for liquid limit, plastic limit, plasticity index and specific gravity have quite similar value result each of them. The percentage of sodium bentonite added did not affect and cause any changes to the these soil properties. However, the values of shrinkage limit and pH showed a good relationship as it increases when the percentage of sodium bentonite were increased. For compaction test, the sodium bentonite did not give good relationship to the soil as the optimum

moisture content and maximum dry density result are not consistent. Supposedly the sodium bentonite increases with increase of water content. Chalermyanont and Arrykul [11] stated that the more bentonite was added, the optimum water content increased and maximum dry density decreased. On the other hand, the shear box test can be said to produce a more consistent results. It showed that the shear strength decreases with increasing percentage of sodium bentonite added to the soil, due to the swelling of the soil. Only natural soil sample give lower value of cohesion whereas the rest of the samples give quite similar value for cohesion. Apart from that, the value of the friction angle did not show any changes with increasing percentage of sodium bentonite, the result is quite similar to each other. It can be concluded, based on the analysis of the results, that the use of sodium bentonite is not suitable for this type of soil. This is because the values for physical properties and engineering properties did not show significant changes and give almost similar values for each of the sample.

Acknowledgments The authors wish to express their sincere gratitude to the Dana Kecemerlangan RIF, UiTM, Shah Alam, Selangor for providing the financial support. The authors also wish to thank all parties, either involved directly or indirectly in making this research a very great success.

References

1. K.H. Chua, E.J.M. Sahid, Y.P. Leong, Sustainable municipal solid waste management and GHG abatement in Malaysia (2011)
2. J.S. McCartney, J.G. Zomberg, R.H. Swan, Internal and Interface Shear Strength of Geosynthetic Clay Liners (Gcls) (2002)
3. M. Masirin, M. Idrus, M.B. Ridzuan, S. Mustapha, M.D. Rashidah, An overview of landfill management and technologies: a Malaysian case study at Ampar Tenang, *1st National Seminar on Environment, Development and Sustainability (PSISenviro2008)*, 28–29 July 2008, Selangor, Malaysia (2008)
4. D.E. Daniel, H.Y. Shan, J.D. Anderson, Effects of partial wetting on the performance of the bentonite component of geosynthetic clay liners, in *Proceedings Of Geosynthetics '93, IFAI*, March 1993, vol. 3 (1993) pp. 1483–1496
5. T.D. Stark, T.A. Williamson, H.T. Eid, HDPE geomembrane/geotextile interface shear strength. *J. Geotech. Eng. ASCE*. **122**(3), 197–203 (1996)
6. A. Bouazza, Geosynthetic clay liners. *Geotext. Geomembr.* **20**, 3–17 (2002)
7. T.D. Stark, Bentonite migration in geosynthetic clay liners (1998)
8. I.E. Odom, Smectite clay minerals: properties and uses. *Philos. Trans. R. Soc. A: Math. Phys. Eng. Sci.* **311**(1517), 391 (1984). Retrieved October 30, 2012, from http://en.wikipedia.org/wiki/Bentonite#cite_note-Odom-1
9. J.K. Mitchell, Fundamentals of soil behavior (1994)
10. T.S. Ingold, Some observations on the laboratory measurement of soil–geotextile bond. *Geotech. Test. J.* **5**(3), 57–67 (1982)
11. T. Chalermyanont, S. Arrykul, Compacted sand-bentonite mixtures for hydraulic containment liners. *Songklanakarin J. Sci. Technol.* (2005)

Part V
Innovative Construction Materials
and Structures

Experimental Investigation on Shear Strengthening of RC Continuous T-Beams with Different Layer of CFRP Schemes

M.B.S. Alferjani, A.A. Abdul Samad, Blkasem S. Elrawaff,
Omer Elzaroug and N. Mohamad

Abstract Carbon fiber reinforced polymer (CFRP) is a material suitable for strengthening the reinforced concrete (RC) beams. Although many in situ RC beams are of continuous constructions, there has been very limited research on the behavior of such beams with externally applied FRP laminate. In addition, most design guidelines were developed for simply supported beams with external FRP laminates. This paper presents the results of a test program for shear strengthening characteristics of strips bidirectional flexible carbon-fiber polymer sheets bonded to reinforced concrete (RC) continuous beams. A total of three beams with size of $150 \times 320 \times 3650$ mm, flange width = 400 mm and flange thickness = 120 mm concrete beams were tested and various sheet configurations and layouts were studied to determine their effects on the ultimate shear strength and shear capacity of the beams. From the test results, it was found that all schemes were found to be effective in enhancing the shear strength of RC beams. It was observed that the strength increases with the number of sheet layers, which provided the most effective strengthening for RC continuous T-beam. Beam strengthened using this scheme showed a 23.21 % increase in shear capacity as compared to the control beam. Two prediction models available in the literature were used for computing the contribution of CFRP strips and compared with the experimental results.

Keywords CFRP · Continuous T-beam · Shear strengthening

M.B.S. Alferjani (✉) · A.A. Abdul Samad · N. Mohamad
Faculty of Civil and Environmental Engineering, UTHM, Batu Pahat, Malaysia
e-mail: mr84bl@yahoo.com

B.S. Elrawaff · O. Elzaroug
Faculty of Civil Engineering, Omar al Mukhtar University, Bayda, Libya

1 Introduction

The advancement of the new material systems like carbon fiber reinforced polymers (CFRP), utilized for the strengthening and rehabilitation of existing structures, are getting higher requests and extensive variety of uses lately. The most productive system for enhancing the shear strength of disintegrated RC members is to externally bond fiber-strengthened polymer (FRP) plates or sheets [1]. FRP composite materials have encountered a ceaseless build of usage in structural reinforcing and repair applications as far and wide as could reasonably be expected, in the latest decade, [2]. Besides, these materials are promptly accessible in a couple of structures, going from assembling plant made laminates to dry fiber sheets, which might be wrapped to adjust to the geometry of a structure. The most beneficial system for upgrading the shear strength of decayed RC members is to remotely bond fiber-fortified polymer (FRP) plates or sheets [3]. CFRP has attracted researchers' interests worldwide to investigate the feasibility and effectiveness of using CFRP as reinforcements or prestressing tendons in concrete structures [4]. CFRP laminates gained importance over steel plate bonding because they offer superior performance, such as resistance to corrosion, and high stiffness-to-weight ratio. Even though CFRP laminates are produced and utilized in different applications, the most common form is built-up woven fabric that is externally bonded to a structural element by the wet lay-up method. Since the CFRP reinforcing gives additional flexural or shear reinforcement, the resolute quality for this material application depends on upon how well they are sustained and can transfer stress from the bond section to CFRP laminate. Any sort of surface deformity, for instance, void and delamination (disbond) between CFRP overlay and substrate may affect and generally incapacitate the structural uprightness and execution of the system; furthermore, it may restrict the future of the structure [5–8]. Shear failure of RC beams, brought on by their weak nature, has been acknowledged as the most disastrous failure mode, it happened with no advance warning of distress. Shear deficiency may happen in view of various variables, for instance, needing shear fortification or diminishment in steel area due to corrosion, expanded administration burden and development slips. This paper focused on using Carbon Fiber Reinforced Polymer (CFRP) frameworks involving adaptable sheets.

2 Shear Strength of RC Beam Strengthened With FRP Sheet

2.1 ACI 440 Model [5]

The shear strength provided by FRP reinforcement can be determined by calculating the force resulting from the tensile stress in the FRP across the assumed crack. Therefore, The shear contribution of FRP is expressed as follows:

$$V_f = \frac{A_{fi} f_{fe} (\sin \alpha + \cos \alpha) d_{fv}}{S_f} \tag{1}$$

where

$$f_{fe} = \epsilon_{fe} E_f \tag{2}$$

The tensile stress of the FRP is directly proportional to the level of strain that is influenced by the models of failure of the FRP system where the effective strain is the maximum strain that can be achieved in the FRP. The determination of the effective strain is based on the wrapping scheme, whether it is completely wrapped or two and three sided wraps. For completely member, the mode of failure id expected to be loss of aggregate. To preclude this mode of failure, the maximum strain used for design should be limited to 0.4 % for completely wrapped applications.

$$\epsilon_{fe} = 0.004 \leq 0.75 \epsilon_{fu} \tag{3}$$

For three and two sides of FRP wrap, strain is calculated using a bond-reduction coefficient k_v and is expressed as:

$$\epsilon_{fe} = k_v \epsilon_{fu} \leq 0.004 \tag{4}$$

The bond reduction coefficient can be computed as follows:

$$k_v = \frac{k_1 k_2 L_e}{11,900 \epsilon_{fu}} \leq 0.75 \tag{5}$$

The active bond length is the length over which the majority of the bond stress is maintained. This length is given by the following equation:

$$L_e = \frac{23,300}{(n_t E_f)^{0.58}} \tag{6}$$

k_1 is a modification factor for concrete strength while k_2 a modification factor for wrapping scheme for these modifications factors are given as follows:

$$k_1 = \left(\frac{f'_c}{27} \right)^{2/3} \tag{7}$$

$$k_2 = \frac{d_{fv} - L_e}{d_{fv}} \text{ (For U-wraps)} \tag{8}$$

$$k_2 = \frac{d_{fv} - 2L_e}{d_{fv}} \text{ (For two sides bonded)} \quad (9)$$

2.2 Khalifa Model

The contribution of externally bonded FRP sheets to the shear capacity of an RC beam may be calculated from the equation as rewritten in ACI format as follows:

$$V_f = \frac{A_f f_{fe} (\sin \beta + \cos \beta) d_f}{s_f} \leq \left(\frac{2\sqrt{f'_c} b_w d}{3} - V_s \right) \quad (10)$$

Because CFRP linearly elastic until failure, the effective stress may be computed as follows:

$$f_{fe} = R f_{fu} \quad (11)$$

R is a Reduction Coefficient Based on CFRP sheet Fracture Failure. The reduction coefficient was established as a function $\rho_f E_f$ of and expressed in equation:

$$R = 0.5622(\rho_f E_f)^2 - 1.22(\rho_f E_f) + 0.78 \quad (12)$$

Reduction Coefficient Based on CFRP Debonding Failure. The effective width W_{fe} based on the shear crack angle of 45° and the wrapping scheme is expressed in equations:

If the sheet is wrapped around the beam entirely

$$W_{fe} = d_f \quad (13)$$

If the sheet is in the form of a U-wrap

$$W_{fe} = d_f - L_{eff} \quad (14)$$

If the sheet is bonded to only the sides of the beam

$$W_{fe} = d_f - 2L_{eff} \quad (15)$$

The effective bond length, is a function of the thickness of the FRP sheet and the elastic modulus of the FRP. As the stiffness of the sheet increases the effective bond length decreases.

$$L_{eff} = e^{6.134 - 0.5 \ln(t_f E_f)} \quad (16)$$

The final expression for the reduction coefficient R , for the mode of failure controlled by CFRP debonding is expressed in equations:

$$R = \frac{(f'_{cu})^{2/3} W_{fe}}{\varepsilon_{fu} d_f} [199.9 - 6.156(t_f E_f)] \times 10^{-6} \quad (17)$$

3 Experimental Program

3.1 Test Specimens and Materials

The test system involved of testing a fabrication and testing of three reinforced concrete two-span continuous T-beams under four-point loading. All beams were designed according to ACI 318-08 with identical size of 150 width, 320 mm depth and 1825 mm effective length of each span, flange width = 400 mm and flange thickness = 120 mm. reinforcement details including longitudinal reinforcement in the form of 14 mm and stirrups reinforcement of 6 mm size at 200 mm spacing center to center were identical for all beams. Figure 1 shows specimen details and the place of strain gauge on reinforcement.

Tables 1, 2 and 3 showed a mechanical properties of CFRP bi-directional, main reinforcement and epoxy. The concrete was ready mix with a compressive strength of 30 N/mm². On the other hand, the main reinforcement with length of 600 mm was tested under uniaxial tension using Universal Testing Machine (UTM) to determine the yield strength. The adhesive used was Sikadur-330, a two-part epoxy impregnating resin A and B. CFRP bi-directional present in this study.

4 Strengthening Scheme and Test Set-up

The beams were tested as continuous T-beam with a shear span to an effective depth ratio of 2.5. One beam was not strengthened and was considered as a reference beam and two beams were strengthened using externally bonded CFRP strips with different schemes. The test set-up as well as strengthening schemes are shown in Fig. 2. Each specimen has different an where for B2.5-C, it was tested with no wrapping and loaded to failure. For B2.5-UA-V1, it was wrapped with one layer of CFRP at three sides of the beam with orientation of 0/90°. For B2.5-UA-V2, it was wrapped with two layers of CFRP at three sides of the beam with orientation of 0/90°. Table 4 shows the specimens designation.

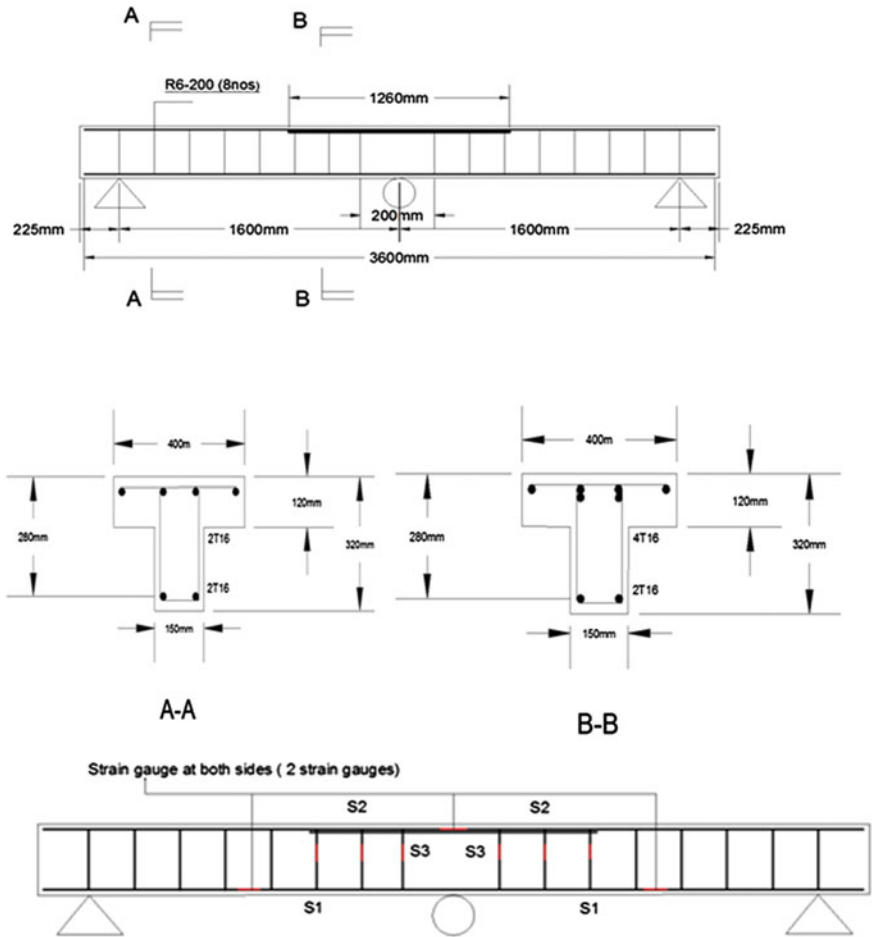


Fig. 1 Reinforcement and cross section details

Table 1 Material properties of main reinforcement

Type	Diameter of bar (mm)	Yield strength (N/mm ²)	Average strength (N/mm ²)
High yield steel	12	546.2	547.033
		544.4	
		550.5	
	14	553.7	554.233
		552.6	
		556.4	
High yield steel	6	273.913	256.209
		265.061	

Table 2 Mechanical properties of CFRP

Density	1.75 g/cm ³
Tensile strength	3,800 N/mm ² (nominal)
Tensile E-modulus	230,000 N/mm ² (nominal)
Elongation at break	1.5 % (nominal)

Table 3 Mechanical properties of Sikadur-330

Density	1.3 ± 0.1 kg/L
Tensile strength	30 N/mm ²
Thermal resistance	Continuous exposure +45 °C
Elongation at break	0.9 %

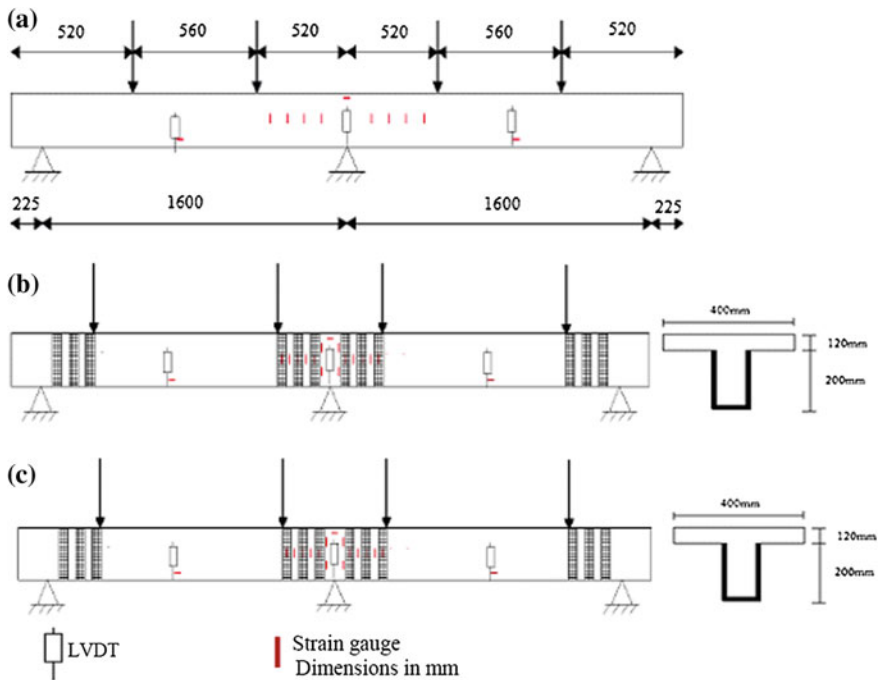


Fig. 2 Test set-up and strengthening schemes. **a** Control beam C2.5-C, **b** Beam B2.5-U-V1 (U-wrap), **c** Beam B2.5-U-V2 (2 layers U-wrap)

Table 4 Specimens designation

No.	Specimen	CFRP orientation (°)	Wrapping schemes	Loading and strengthening condition
1	B2.5-C	–	–	–
2	B2.5-UA-V1	0/90	3 sides	Initially strengthened (1 layer)
3	B2.5-UA-V2	0/90	3 sides	Initially strengthened (2 layer)

5 Experimental Results

5.1 Ultimate Load and Modes of Failure

All specimens failed in shear, as expected. For the control beam, B2.5-C, flexural cracks started to form near the mid span at the bottom of the beam at a load approximately 55 kN. The shear cracks began to appear at a load of approximately 120 kN and as the load increased, the shear crack widened and propagated up to the final failure at a load level of 220.4 kN. The mode of failure was shear crushing of the concrete. For specimens C2.5-U-V1, which wrapped three sides with CFRP, the first crack occurred at 63 kN at the bottom mid span of the beam. This beam exhibited the first crack at a higher load than the control beam C2.5-C due to the presence of the external bond of CFRP system. The diagonal shear cracks were observed at 157 kN and the corresponding failure load occurred at 247.72 kN. The enhancement of the load is 31 % higher than the control beam. On the other hand, a specimen C2.5-U-V2, which wrapped at three sides of the beam, the first crack occurred at 65 kN. The diagonal shear cracks were observed at 175 kN and the failure of the specimen occurred when the total applied load reached 271.65 kN. This was an increase of 46 % in ultimate load capacity compared to the control beam. Table 5 shows the first cracks load, ultimate load, contribution of CFRP and the modes of failure for all beams. Figures 3, 4 and 5 show cracking patterns and failure modes of the beams.

Table 5 Experimental result

Beams	a _v /d	CFRP orientation	First crack	Ultimate load	Shear force	Contribution of CFRP	Shear enhancement	Mode of failure
B2.5-C	2.5	–	55	220.4	73.3	–	–	Diagonal shear failure
B2.5-U-V1		0/90° (U-strips)	63	247.7	82.37	27.32	12.2	Rupture or shear failure
B2.5-U-V2		0/90° (U-strips)	65	271.65	90.32	51.25	23.21	Rupture or shear failure

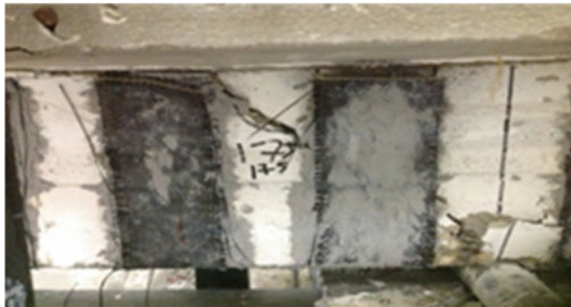
Fig. 3 Cracking and failure pattern of beam B2.5-B



Fig. 4 Cracking and failure pattern of beam C2.5-UA-V1



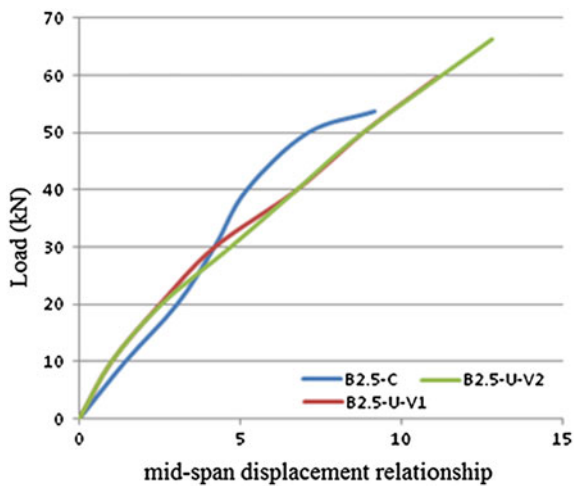
Fig. 5 Cracking and failure pattern of beam C2.5-U-V2



6 Load-Displacement Behavior

Figure 6 shows the total applied load versus mid-span deflection relationship for all tested specimens. All beams showed very similar stiffness trend to each other. The

Fig. 6 Ultimate load versus mid-span displacement relationship



smallest deflection was observed for beam B2.5-C. It was also observed that the stiffness of the beam strengthened with one layer of CFRP (B2.5-U-V1) was less than that of the beam strengthened with two layers of CFRP (B2.5-U-V2).

7 Load-Strain Relationship

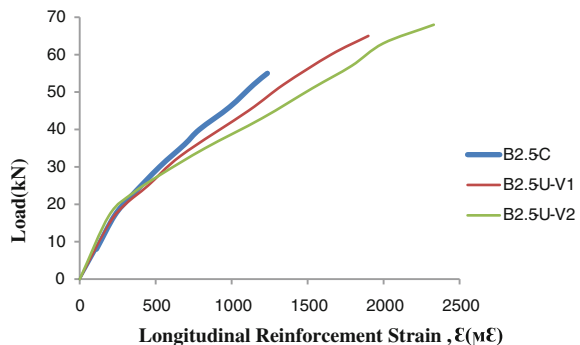
7.1 Longitudinal Steel Strain

The applied load versus strain curve for specimens B2.5-C, B2.5-U-V1 and B2.5-UV2, (initially strengthened) are shown in Fig. 12. The control specimen B2.5-C attained a maximum strain of $1,235 \mu\epsilon$ recorded at the failure. For initially strengthened beams, at ultimate load, specimens B2.5-U-V1 and B2.5-U-V2 (two layer of CFRP) measured a maximum strain of $1,900 \mu\epsilon$ and $2,330 \mu\epsilon$ respectively at mid span. However, for specimen B2.5-UA-V2 (two layer of CFRP), the strain observed higher than the specimen of B2.5-UA-V. Figure 7 illustrates the comparison of the load versus strain curve.

7.2 Strain in Transverse Stirrups Steel Bar

These specimens were reinforced with 6 mm steel stirrups with 200 mm center to center. Figures 8, 9 and 10 illustrate the applied load versus strain in stirrups for specimens B2.5-C, B2.5-U-V1 (initially strengthened) and B2.5-U-V2 (initially strengthened). These strain gauges were placed at the mid height of the steel stirrups. In control specimen B2.5-C, the strain gauge S2 obtained the maximum strain value over S1 and S3 due to the formation of diagonal crack across the stirrup.

Fig. 7 Comparison of load versus strain in tensile steel



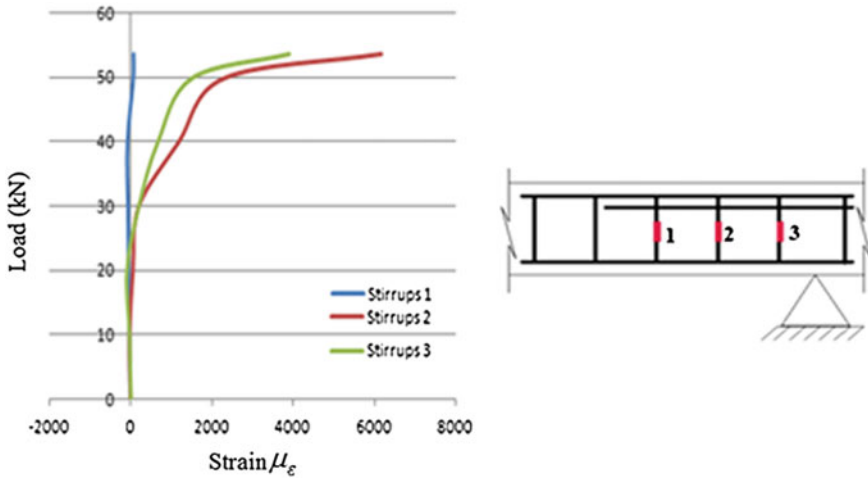


Fig. 8 Load versus strain in steel stirrups for control specimen B2.5-C

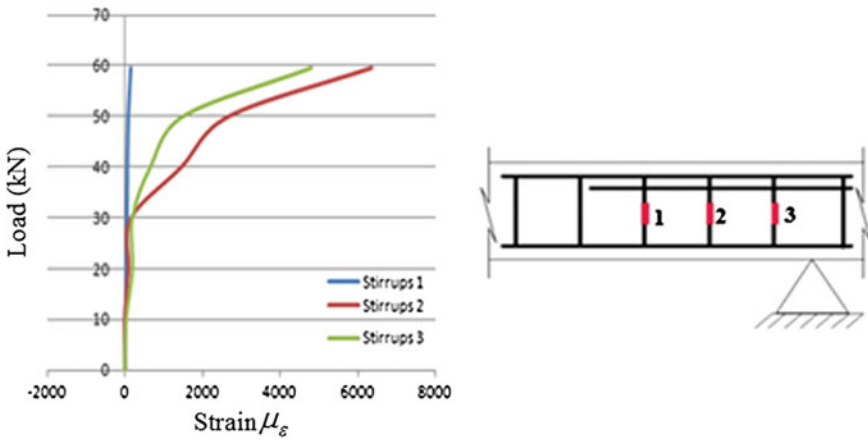


Fig. 9 Load versus strain in steel stirrups for initially strengthened specimen B2.5-UA-V

The maximum stirrup strain observed at strain gauge S2 was 6,144 $\mu\epsilon$. For initially strengthened beams, the specimens C2.5-UA-V and C2.5-UAV2 had attained a maximum stirrup strain of 6,334 $\mu\epsilon$ (S2) and 8,566 $\mu\epsilon$ (S2) respectively. For specimen B2.5-UA-V2 (two layer of CFRP), a break of steel stirrups was observed. For specimen B2.5-U-V2 (two layer of CFRP), it was observed that the stirrups strains was less than B2.5-U-V1 for the same load.

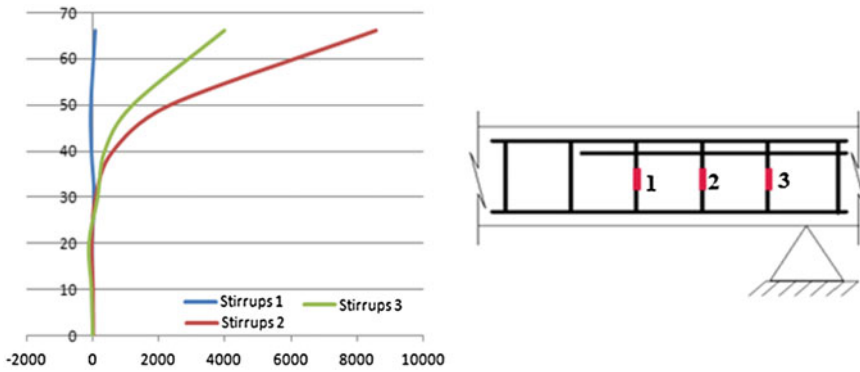


Fig. 10 Load versus strain in steel stirrups for initially strengthened specimen B2.5-UA-V2

7.3 Strain, Strain in CFRP Strips and Concrete Surface

Figures 11, 12 and 13 illustrate graphs of local strain distribution in CFRP and concrete strain for specimens B2.5-C, B2.5-U-V1 and B2.5-U-V2. For control beam B2.5-C, the strain at location C4 increased rapidly beyond the applied load 10 kN by the initiation of crack near the location of the strain gauge. The recorded maximum strain in the concrete surface was 1,109 $\mu\epsilon$. For the initially strengthened

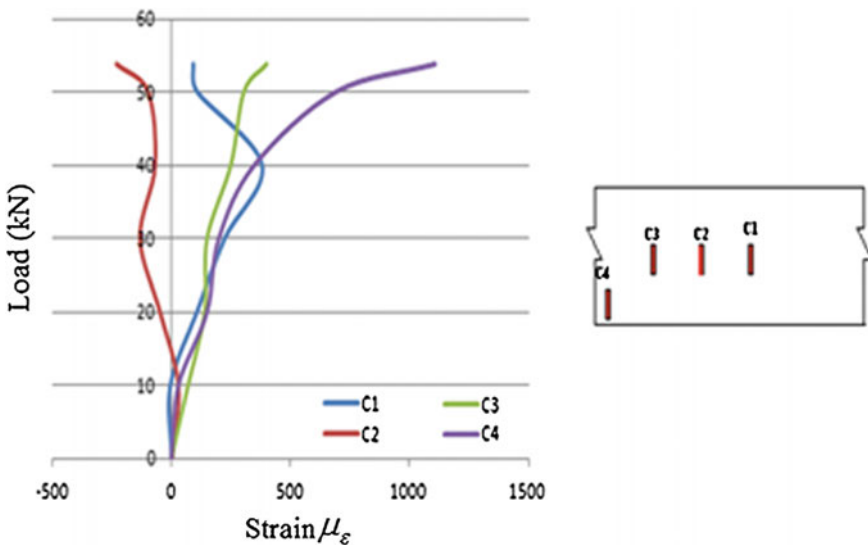


Fig. 11 Load versus strain in the concrete surface for control beam B2.5-C

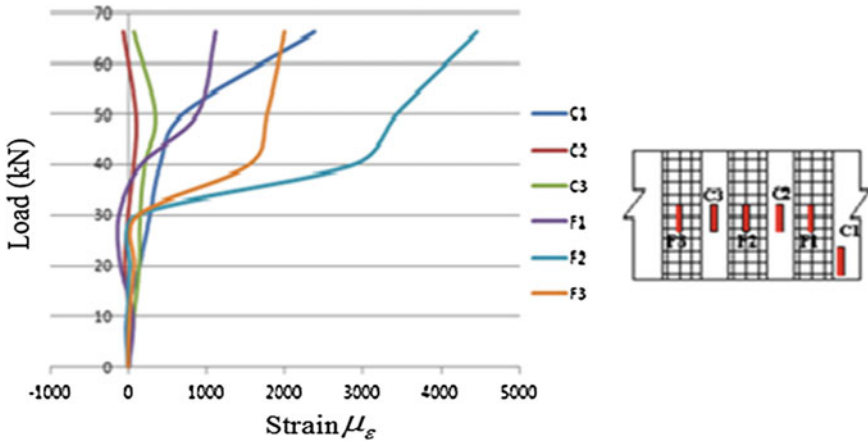


Fig. 12 Load versus strain in CFRP strip and concrete surface for initially strengthened specimen B2.5-UA-V2

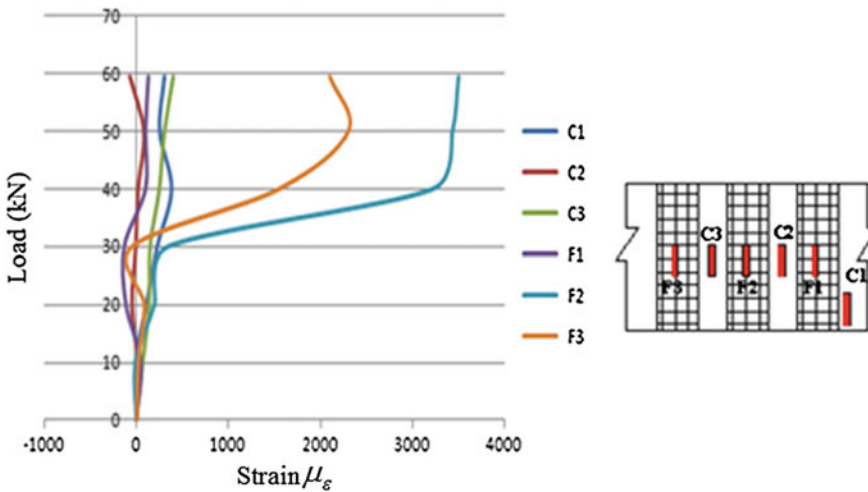


Fig. 13 Load versus strain in CFRP Strip and concrete surface for initially strengthened specimen B2.5-UA-V2

beams, specimen C2.5-U-V1 had recorded a maximum strain in CFRP at 3,500 $\mu\epsilon$ (strain location F2). However in specimen C2.5-U-V1, the strain value F2 increased gradually till the applied load of 60 kN. In specimen C2.5-UA-V2 (two layer of CFRP), the maximum strain recorded in CFRP was 4,456 $\mu\epsilon$ (strain location F2). In this specimen, the strain value at F2 was increased until the applied load of 66 kN

and beyond this load level, the strain had increased rapidly beyond this point, the CFRP fabric strain increased significantly until failure occurred due to the initiation of diagonal shear crack. From observation on comparison between the behavior of stirrups shows that for beams C2.5-UA-V2, the stirrups strain were higher than CFRP strain at the ultimate load except for C2.5-UA-V1 beam which the stirrups strain was lower than CFRP strain at the ultimate load.

8 The Comparison of Experimental and Theoretical Results

The comparison of experimental and theoretical results of the control and initially strengthened beams are shown in Table 6. The shear capacity contributed by the external CFRP reinforcement was estimated by subtracting the shear strength of the reference beam from the CFRP strengthened beam. The strip technique had proved that the shear capacities of the initially strengthened T-beams ranging from 12.2 to 23.21 % over the control beam. The shear capacity of these T-beams was theoretically computed using ACI 440 Format and Khalifa Model. The shear strength of the strengthened beams is computed by adding the contribution of shear strength of external CFRP reinforcement V_f . It can be seen that the experimental values of the strengthened for all beams B2.5-C, B2.3-U-V1 and B2.5-U-V2 were higher than the experimental results. From the overall discussion, it can be concluded that the predicted theoretical results of the T-beams shows reasonable accuracy with the experimental results.

Table 6 Comparison of experimental and theoretical results

Specimens	Theoretical value		Exp. results $V_{f,exp}$ KN	$\frac{V_{f,exp}}{V_{f,theory}}$	
	V_f KN			Khalifa Model	ACI 440 Model
	Khalifa Model	ACI 440 Model			
B2.5-C	–	–		–	–
B2.5-U-V1	13.23	12.9	9.1	0.68	0.7
B2.5-U-V2	26.98	21.93	17.02	0.63	0.77

9 Conclusion

The test results indicated that strengthening of RC continuous beams using externally bonded CFRP strips can be used to enhance the shear capacity of continuous T-beams. For beams tested in the experimental program, the shear capacity increased at a ranged from 12.2 to 22.21 %. An increase in the number of layers of CFRP strips has resulted in stiffer and stronger beams. Beams wrapped with two layers of CFRP strips achieved higher shear capacity. Beams wrapped with double layers of CFRP strips have resulted in a significant increase for about 11.01 % in shear capacity compared with beam with one layer of CFRP strips. However, the two layers of CFRP strips could not prevent yielding of stirrups for the beam provided with only the minimum link in the beam.

Acknowledgments This work has been supported by the first author and tested at Omar Al Mukhtar University Libya, Department of Civil Engineering.

References

1. M.B.S. Alferjani et al., Shear strengthening of reinforced concrete beams using carbon fiber reinforced polymer laminate: A review. *Am. J. Civ. Eng.* **2**(1), 1–7 (2014)
2. O. Buyukozturk, O. Gunes, E. Karaca, Progress on understanding deboning problems in reinforced concrete and steel members strengthened using FRP composites. *Const Building Mater.* **3**, 9–19 (2004)
3. M.B.S. Alferjani et al., Use of carbon fiber reinforced polymer laminate for strengthening reinforced concrete beams in shear: a review. *Int. Refereed J. Eng. Sci. (IRJES)* **2**(2), 45–53 (2013)
4. M.B.S. Alferjani et al., CFRP laminate flexural and shear strengthening technique of reinforced concrete beams: a review. *Int. J. Eng. Res. Dev.* **6**(3), 39–49 (2013)
5. ACI 440.2R-02 and 08, *Guide for Design and Construction of Externally Bonded FRP Systems for Strengthening Concrete Structures* (American Concrete Institute, USA, 2002)
6. J.Y. Kim, F. De Flaviis, L. Jofre, M.Q. Feng, Microwave-based NDE of FRP-jacketed concrete structures, in *International SAMPE Symposium and Exhibition (Proceedings)*, vol. 46, May 2001, pp. 439–450
7. D. Hughes, M. Kazemi, K. Marler, R. Zoughi, J.J. Myers, A. Nanni, in Microwave detection of delaminations between fiber reinforced polymer (FRP) composite and hardened cement paste, in *Proceedings for the 28th Qualitative Nondestructive Evaluation Conference*, Brunswick, Maine, vol. 21, July–August 2001, pp. 512–519
8. J. Newman, C. Zweben, in Nondestructive inspection of composite-strengthened concrete structures, in *47th International SAMPE Symposium*, vol. 47, May 2002

Bending Strength of Pre-tensioned (PRT) Concrete Beam

Nurul Huda binti Suliman, Siti Hawa binti Hamzah,
Afidah binti Abu Bakar and Norliyati Mohd Amin

Abstract This paper presents a preliminary study on bending strength of pre-tensioned (PRT) concrete beam as the experiment result can be used in maintenance planning. The production of beam was according to BS8110, BS4449:2005 and BS5896 for concrete, reinforcement bar and strand, respectively. For the bending test, theoretically and practically was conducted in accordance to BS5400 standard. The result showed cracked beam retrofitted with fiber reinforced polymer (FRP) plate and carbon fiber reinforced polymer (CFRP) sheets are able to increase the bending strength of beam up to 43 and 42 %, respectively.

Keywords Bending strength · Pre-tension concrete beam · Crack · Concrete maintenance · Fiber reinforced polymer

1 Introduction

Concrete girder is a critical superstructure of a bridge, used to resist vertical cyclic load from vehicles and dead loads. The increasing of traffic volume will give distress to girder and leads to form cracks. As the crack is the indication of disintegration in concrete or structure, a proper maintenance should be carried out to avoid repetitive crack occurrence. In Structural Health Monitoring (SHM), it is

N.H.b. Suliman (✉) · S.H.b. Hamzah · A.b.A. Bakar · N.M. Amin
Faculty of Civil Engineering, Universiti Teknologi MARA Malaysia,
Shah Alam, Selangor, Malaysia
e-mail: huda_4606@yahoo.com

S.H.b. Hamzah
e-mail: shh@salam.uitm.edu.my

A.b.A. Bakar
e-mail: afida334@salam.uitm.edu.my

N.M. Amin
e-mail: norli380@salam.uitm.edu.my

significant to identify load capacity of structure to be repaired. Using this information, therefore, the repair action can be planned well in order to preserve the complex safety of bridge users without negligence of the economic issues.

The Public Work Department of Malaysia (*Jabatan Kerja Raya*, JKR) has reported in Annual Bridge Report 2009 that several bridges along the federal routes in Peninsular Malaysia are experiencing durability and structural problems [1]. These are identified by using bridge inspection guide of Road Engineering Association Malaysia, REAM [2]. The major type of damage occurred on highway bridge is concrete crack. Cracks were caused by overloading, poor design, foundation movements, or excessive tension forces applied to the structures [3].

Maintenance work must be carried out when there is an existence of structural damage on the bridge which can contribute to collapse or deterioration. This work is to determine and improve the existing strength of the structural element to its original strength to ensure the bridge has adequate level of safety. The restoration is mainly to conduct the structural maintenance to load bearing elements [2]. The process may involve cutting several segments of the elements and rebuilding them or by applying some additional material to the structure so that the strength of the restored structure increases to its original strength or even higher [4].

Typically, the repair method for disintegrated girder caused by crack is to join the steel pre-stressing strands but this method performs poorly during fatigue and unable to restore the ultimate strength of the girder [5]. The use of Fiber Reinforced Polymer (FRP) plates in retrofitting practice is more applicable at bridge beam as it can restore the ultimate strength of the damaged beam and withstand the repetitive loading. The capability of FRP plate was proved able to increase member's stiffness and load capacity as well as reducing the crack dimensions [5]. Moreover, the deflection of a retrofitted member was also smaller compared to the un-retrofitted member.

Another repair method is using carbon fiber reinforced polymers (CFRP) sheets as it is a cost-effective construction material to the civil engineering industry [6]. According to the findings from a research, by applying CFRP, it can reduce the length of crack and crack spacing [7]. Findings from another research showed the usage of double plies of CFRP sheets increased the load capacity by 70 % compare to single ply application [8].

1.1 Scope of Study

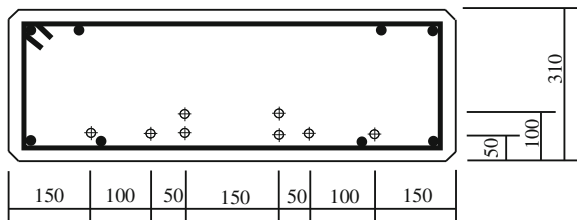
It is impractical to attain the existing bridge girders on site because of the limitation of the laboratory test equipment that only have the ability in testing significant size of samples dimension. The sizes of bridge girders on site are usually more than 15 m long. Moreover, it is also difficult to deal with the actual bridge girders because cutting portions are needed to be carried out and will agitate the traffic users and traffic flows on site. It is more practical to execute the crack measurement on the fresh beam samples rather than using the existing bridge girder.

Therefore, this preliminary study was performed to determine the improvement in bending strength of cracked PRT concrete beam samples after retrofitted with FRP plates and CFRP sheets. There were 3 numbers of PRT concrete beams each of 725 mm (B) × 310 mm (D) and overall length of 4,000 mm were tested in the laboratory of Civil Engineering, Universiti Teknologi MARA. The concrete mix was batched on the same date with a target strength requirement of 50 N/mm² to be achieved in 28 days. Table 1 shows the strength value obtained from concrete cube tests. These concrete beams were pre-tensioned with eight numbers of seven-wire strands of Ø12.9 mm nominal diameter arranged as shown in Fig. 1. The characteristic of strand shows in Table 2. Other materials used are Ø10 mm of longitudinal reinforcement and link bar.

Table 1 Characteristic of concrete through cube test

Characteristics	Sample	Day 1	Day 7	Day 14	Day 28
Maximum load (N)	Sample 1	398	421.8	574.7	684.3
	Sample 2	–	489.4	617.5	654.7
	Sample 3	–	568.3	640.8	710.2
Average		398	498.2	611	683.1
Stress (N/mm ²)	Sample 1	39.8	42.18	57.47	68.43
	Sample 2	–	48.94	61.75	65.47
	Sample 3	–	57.83	64.08	71.02
Average		39.0	49.82	61.10	68.31
Mass (kg)	Sample 1	2.44	2.44	2.38	2.42
	Sample 2	–	2.44	2.48	2.38
	Sample 3	–	2.46	2.44	2.44
		2.44	2.45	2.43	2.41

Fig. 1 Cross-section of PRT beam (dimension in mm)



*Concrete cover= 25mm

Table 2 Characteristic of wire strand through tensile test

Characteristic	Load (kN)	Stress (kPa)	Deformation (mm)	Strain (%)
Maximum	199.43	1525.90	46.14	23.07
Break point	132.74	1015.61	50.36	25.18
0.2 % yield strength	183.73	1405.76	21.85	10.93
Upper yield point	159.53	1220.62	17.87	8.93

2 Experimental Study

The test was conducted using Universal Testing Machine (UTM) in the laboratory of Civil Engineering, Universiti Teknologi MARA.

2.1 Bending Test

There were 3 numbers of beams tested of which 1 beam as a control and the other 2 beams were retrofitted with FRP plates and CFRP sheets after the first crack appeared. The control beam labelled as BC1 while the retrofitted beam with FRP plates and CFRP sheets were labelled as BR1 and BR2 respectively. The bending test was conducted on the specimens under the action of two point loads. The span between the supports was $L = 3,600$ mm and the two point loads were applied at one-third lengths. There were 4 numbers of transducers and 6 numbers of strain gauges used to measure deflections and strains, respectively. The test was conducted using Universal Testing Machine (UTM) with loading capacity of 2,500 kN at a deflection control rate of 0.009 mm/s. The setup of testing is shown in Fig. 2.

For a rectangular beam loaded under four-point bending setup where the loading span is one-third of the support span, the value of yield stress, σ_y are calculated using Eq. (1) which F is the load (force) at the fracture point; L is the length of the support (outer) span; b is breadth; and d is depth.

$$\sigma_y = FL/bd^2 \quad (1)$$

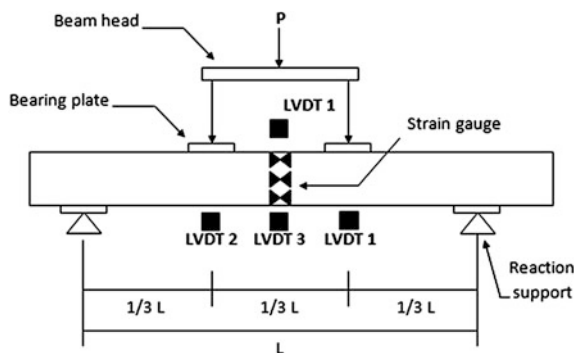


Fig. 2 Experimental setup

From the Eq. (1), a graph of strain versus stress was plotted to find the value of yield load, P_y where the first crack is expected to occur. Theoretically, this P_y conform the value of observation load, P_o as $P_o \approx P_y$.

2.2 Crack Repair

2.2.1 FRP Plate

There were two FRP plates with dimensions 100 mm (B) \times 1.2 mm (T) \times 2,400 mm (L) attached to the tension part of the beam. The plates were placed parallel to the direction of principal stress as shown in Fig. 3.

2.2.2 CFRP Sheet

Two layers of CFRP sheets were used with U-Wrap technique applied to the tension area. The wrapping was each at 800 mm under the 2 loading points. Figure 4 shows the dimensions of CFRP sheets retrofitted scheme. In order to observe crack at the center part of the beam, the middle span of beam about 400 mm was not wrapped with CFRP sheets.

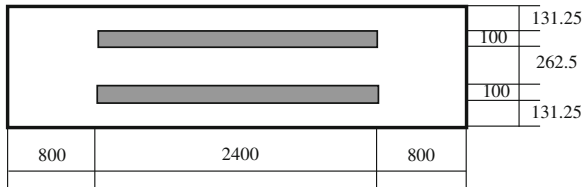


Fig. 3 Setting of FRP PLATES at the soffit of the beam (plan-view, dimension in mm)

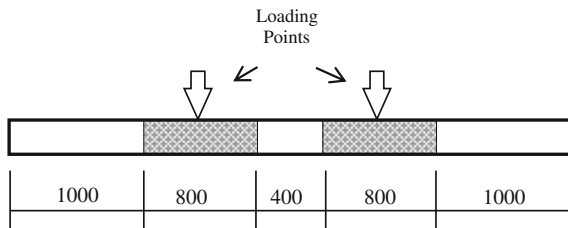


Fig. 4 Setting of CFRP sheets (elevation-view, dimension in mm)

3 Result and Discussion

3.1 Bending Strength of the Control Beam (BC1)

The load and deflection gradually increased until the first crack appeared when the load capacity reached 320 kN as recorded by data logger. Then the progression of load and deflection slowly increased until the load was 530 kN. After that, the load sustained about 10 min, however the deflection regularly increased before the beam completely failed. The graph in Fig. 5 shows the relationship between load and displacement. Therefore, it can be concluded that the crack load, P_{cr} is 320 kN and the maximum load, P_{max} of the beam is 530 kN. Theoretically, the ultimate bending strength of the beam is 27 N/mm². Table 3 shows the results of maximum load and bending strength of BC1.

3.2 Bending Strength of the Retrofitted Beam (BR1 and BR2)

There was significantly increase in maximum load for beam retrofitted using FRP plates (BR1) which is 800 kN, that is 34 % increment compared to control beam (BC1). As well as for beam retrofitted using CFRP sheets (BR2), the maximum load increased about 33 % from BC1 to 791 kN. Therefore, the bending strengths for BR1 (41 N/mm²) and BR2 (40 N/mm²) are higher compare to BC1. This proves that both retrofit methods are able not only to preserve but also increased the load

Fig. 5 The relationship between load and displacement at midpoint of the beam

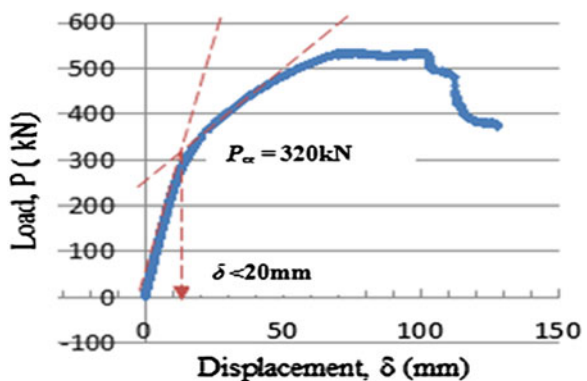


Table 3 Strength of BC1

Specimen	Yield load, P_y (kN)	Maximum load, P_{max} (kN)	Yield strength, σ_y (N/mm ²)	Bending strength, σ_{max} (N/mm ²)
BC1 (control)	320	530	17	27

capacity and bending strength of the cracked beam. Although the performance of both FRP plates and CFRP sheets are slightly similar, the factor of cost and operational procedure should be considered between these two methods in planning for effective maintenance work. Table 4 shows the summary of the overall results.

3.3 Deflection Behaviour

The deflection of symmetrically loaded beam was measured at point of middle span about tension parts of the beam. This significant deflection measured by LVDT 3. The result of this experiment showed that the value of deflection of both retrofitted

Table 4 Summary of beam strength

Specimen	Maximum load, P_{max} (kN)	Bending strength, σ_{max} (N/mm ²)	% of improvement
BC1 (control)	530	27	–
BR1	800	41	34
BR2	791	40	33

Table 5 Summary of deflection

Specimen	BC1 (control)	BR1	BR2
Deflection (mm)	128	80	84
% of reduction	–	37 %	34 %



Fig. 6 The deflection curve of the beams. BC1 (a), BR1 (b) and BR2 (c)

beam were reduced compared to control beam. BR1 had reduced about 37 % (80 mm) and BR2 was 34 % (84 mm) from the control beam, BC1 (128 mm). Table 5 shows the comparative result of deflection between all beams. Figure 6 shows the deflection curve for BC1—(a), BR1—(b) and BR2—(c).

4 Conclusion

The structural characteristics of control beam and retrofitted beams were investigated and concluded as following:

- (a) Retrofitted beam using FRP plates (BR1) increased the bending strength of cracked beam by 34 % and CFRP sheets increased by 33 % as compare to BC1.
- (b) FRP plates and CFRP sheets are effective in controlling the propagation of crack lengths and crack widths.
- (c) The competency of both retrofitting methods is equivalent.

Acknowledgments The experimental process was held with the assistance from laboratory technicians and civil engineering undergraduate students of FCE UiTM Shah Alam, Norzahiah, Amirah and Ahmad Zaid. The authors cordially acknowledge the grant of Research Intensive Faculty from Research Management Institute, UiTM; Reference No.: 659/2012) and grant of ERGS/1/2012/TK03/UITM/03/3.

References

1. JKR, *Annual Bridge Report 2009* (Public Work Department of Malaysia, Kuala Lumpur, 2010)
2. S. Ng, M. Ku, *Bridge Problems in Malaysia* (Evenfit Consult. Sdn. Bhd, Kuala Lumpur, 2009)
3. S. Idris, Z. Ismail, *Appraisal of Concrete Bridges: Some Local Example* (Jurutera, Board of Engineers Malaysia, Kuala Lumpur, 2007)
4. JKR, *Bridge Appraisal, Rehabilitation, and Maintenance* (Public Work Department of Malaysia, Kuala Lumpur, 1996)
5. Y. Obaidat, *Structural Retrofitting of Concrete Beams using FRP-Debonding Issues* (Lund University Publications, Sweden, 2011)
6. Y.-J. Kim, M. Green, G. Fallis, Repair of bridge girder damaged by impact loads with prestressed CFRP sheets. *J. Bridge Eng.* **13**, 15–23 (2008)
7. O. Rosenboom, S.H. Rizkalla, Experimental study of intermediate crack debonding in fiber-reinforced polymer strengthened beams. *ACI Struct. J.* **105**(1), 41–50 (2008)
8. B. Miller, A. Nanni, Bond between CFRP sheets and concrete, in *ASCE 5th Materials Congress*, Proceedings, ASCE, Cincinnati, pp. 240–247, 1999

Chloride Permeability of Nanoclaved Ultra-High Performance Concrete

M.J. Mohd Faizal, M.S. Hamidah, M.S. Muhd Norhasri,
I. Noorli and M.P. Mohamad Ezad Hafez

Abstract It is widely recognized that the ingress of chlorides into concrete can initiate reinforcement corrosion and ultimately result in deterioration of the concrete structure. Chloride permeability of concrete has been recognized as a critical intrinsic property affecting the durability of reinforced concrete. From the previous research, the use of nano clay (NC) in cement mortar due to chloride permeability has been well-documented. In this paper, the ability of ultra-high performance concrete (UHPC) to withstand the action of chloride penetration were investigated. An experimental research was carried out in order to investigate the influence of incorporating NC material as cement replacement into ultra-high performance concrete (UHPC-NC) on chloride-related transport characteristic. The workability, compressive strength and charge passed in rapid chloride permeability test (RCPT) of UHPC-NC were reported. Those parameters were also determined for normal strength concrete (NPC) and plain without nano clay ultra-high performance concrete (UHPC) as comparison. Three (3) series of UHPC-NC mixes were produced incorporating 1 % (UHPC-NC1), 3 % (UHPC-NC3) and 5 % (UHPC-NC5) of NC

M.J. Mohd Faizal (✉)
Faculty of Civil Engineering and Earth Resources, Universiti Malaysia Pahang,
Kuantan, Pahang, Malaysia
e-mail: faizaljaafar@ump.edu.my

M.S. Hamidah · M.S. Muhd Norhasri
Faculty of Civil Engineering, Univeristi Teknologi MARA,
Shah Alam, Selangor, Malaysia
e-mail: hamid929@salam.uitm.edu.my

M.S. Muhd Norhasri
e-mail: norhasri@gmail.com

I. Noorli
Faculty of Civil and Environmental Engineering, Universiti Tun Hussien Onn,
Batu Pahat, Johore, Malaysia
e-mail: noorli@uthm.edu.my

M.P. Mohamad Ezad Hafez
Faculty of Architecture, Planning and Surveying, Universiti Teknologi MARA,
Shah Alam, Selangor, Malaysia

replacing cement (OPC). The results showed that incorporating NC in concrete mixes causes a reduction in the workability. It was also found that replacing of OPC with NC improved the strength of UHPC-NC as compared to those mixes without NC material. The optimum NC replacement level recorded at 3 % (UHPC-NC3) from the total weight of OPC. For the chloride permeability, it is clearly shown that the presence of NC has important benefit in terms of chloride resistance.

Keywords Ultra-high · Performance concrete · Nano clay · Workability · Strength · Chloride permeability

1 Introduction

Currently, the development research on nanotechnology in concrete includes characterization of cement hydration and influence of the addition or replacement of nano-size particles applied to concrete properties [1]. One can claim that concrete utilizes nanotechnology because it contains nano-particles as ingredients including nano-water particles and nano-air voids. However, to claim the use of nanotechnology, it is able to control the amount and the locations of these nano-ingredients inside the concrete. As well documented in [2–4], nano concrete have been defined as a concrete made with Portland cement particles that are less than 500 nm as the cementing agent.

It has been recognized that the main factor influencing the durability of concrete structure is the chloride-ion penetration such as sea water, sea wind and sea moisture. Generally, the durability of structure made by normal concrete is only 20–30 years but some structure is less than 10 years. This is because of the quick diffusion of the chloride ion in concrete structure and reinforcement start to corrode [5–8]. For the durability of concrete, permeability is believed to be the most important characteristic, which is related to its microstructural properties, such as the size, distribution, and interconnection of pores and microcracks [9]. Ideally, the use of nano clay as ultra-filler in concrete can help to reduce the total voids content in concrete thus resist the chloride permeability, hence the present study was initiated.

Since the corrosion of steel reinforcement due to chloride penetration is the major cause of durability problems in concrete. This paper also reviews the incorporation of nano clay (NC) in ultra-high performance concrete (UHPC) and its effect to the chloride penetrability characteristic of the resulted concrete. For the concrete permeability, Lizarazo-Marriaga and López Yépez [10] investigates the influence of the silica fume content on chloride-penetration of high performance concrete (HPC) using RCPT technique. They were found that silica fume gives a benefit to resist high chloride penetration to HPC. Other researcher [11] revealed

that RCPT value of mix containing 40 % of fly ash is higher than 30 % of fly ash. Concrete mix with slag also shows lower chloride permeability as compared to fly ash mixes.

Previous research by [12] noted that the use of GGBS in HPC has greater ability to resist the chloride penetration. As well-documented in [13, 14] have stated that chloride penetration resistance in mortar concrete improved significantly as nano clay was added is dense in microstructure with more stable bonding structures. It is also revealed that the use of NC have been shown to reduce permeability as NC able to strengthen the interfacial transition zone between the cement paste and aggregate. This findings also agreed by [15] found that NC markedly improved the chloride penetration resistance of the cement mortars.

Therefore, it is proved that NC within pore solution affects the permeability of cement paste. In comparison with previous research, this study aimed to evaluate the chloride permeability of ultra-high performance concrete (UHPC) incorporating different levels of NC as cement replacement.

2 Methodology

2.1 Material Properties

In this research, ordinary Portland cement (OPC) was used in all concrete mixes. Meanwhile, the commercially available nano clay (NC) was used to produce the ultra-high cementitious material. The raw NC powder (hydrophilic bentonite) was procured from Sigma Aldrich (M) Sdn. Bhd. The calcination process of raw NC was performed by heating the raw NC using high temperature furnace carbolite type HTF3 ELP at the temperature of 700 °C for 3 h process period [16]. Figure 1 shows the raw NC before and after calcination process. This treatment was carried out in order to crystalline structure. The chemical composition of the OPC and NC are listed in Table 1. To clarify its microstructure, Field Emission Scanning Electron Microscopy (FESEM) analysis were carried out on the neat OPC and NC powder.

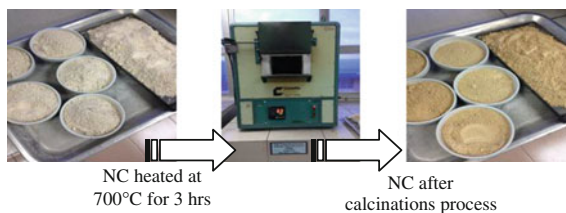


Fig. 1 Calcination process for NC

Table 1 Chemical composition of ordinary portland cement and nano clay (wt%)

Compound (%)	OPC	NC
SiO ₂	11.6	65.9
Al ₂ O ₃	2.2	15.1
CaO	75.17	4.3
TiO ₂	0.4	0.9
Fe ₂ O ₃	5.38	11.4
K ₂ O	0.43	0.24

2.2 Specimens Fabrications

Ultra-high performance concrete (UHPC) mixes were cast incorporating 1, 3 and 5 % (UHPC-NC1, UHPC-NC3 and UHPC-NC5, respectively) of nano-clay (NC) as a cement replacement by weight of ordinary Portland cement (OPC). There are two (2) concrete grades without NC was also prepared as control mixes namely normal strength concrete (NPC) and ultra-high performance concrete (UHPC). Since concrete mixes with a 0.20 water to cement ratio (w/c) were produced, it was necessary to apply a high-range water-reducing commercial chemical admixture (Glenium ACE 389 SURETEC supplied by BASF (M) Sdn. Bhd.) in order improve the workability of the concrete mixes. In this present study, the target slump in range of 70–90 mm has been considered. Table 2 shows the mix designation and a summary of the concrete mix design used. In this present research, the cube samples with dimensions of 100 mm × 100 mm × 100 mm and cylinder samples with 100 mm diameter and 200 mm height were cast for compressive strength and rapid chloride permeability test (RCPT) respectively. After mixing, all test specimens were demoulded at 1 day and then cured in water.

2.3 Testing Procedure

In order to determine the properties of concrete mixes, three (3) tests method namely slump test (workability of fresh concrete), compressive strength (strength

Table 2 Mix designation and a summary of the concrete mix design

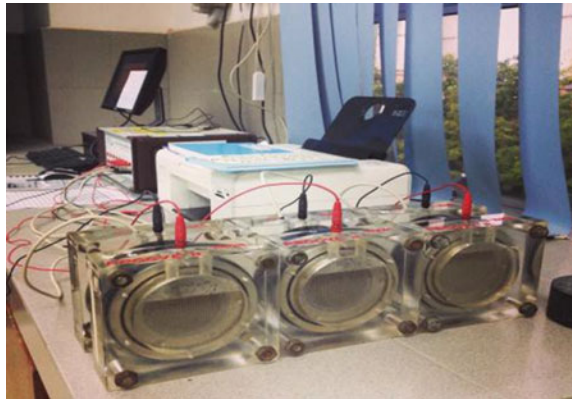
Mix design	Raw materials (kg/m ³)					
	Cement	NC	Agg.	Sand	Water	Glenium
NPC	380	0	995	815	190	2.85
UHPC	800	0	433	800	160	11.55
UHPC-NC1	797	8	433	800	160	6.38
UHPC-NC3	776	24	433	800	160	6.98
UHPC-NC5	760	40	433	800	160	7.60

properties) and chloride transport (Rapid Chloride Permeability Test) were conducted. The slump test procedure is in accordance with BS EN 12350-2:2009. For concrete compressive strength tests, the recommendations of BS EN 196-3:2005 were followed. Compressive strength test at 7 and 28-days were carried out and each result corresponds to the average of three (3) replicates.

ASTM C1202 tests for RCPT standard were conducted at 3, 7 and 28 days with six (6) samples at each age. RCPT was conducted to determine the resistance of concrete to chloride ion penetration. Before the RCP test, the procedure to prepare the samples calls as 2-day specimen preparation. On the first day, the samples were removed from the moist room to be cut using water-cooled diamond saw. The samples were slices to dress the top, middle and bottom edge. The sides of the samples were sealed with silicon. The second day of preparation began with the desiccation process to water-saturate the samples using desiccator chamber connected to a vacuum pump and the pressure was maintained less than 1 mm Hg (133 Pa) for 3 h. Then, the container was then filled with distilled water until the samples totally submerged (the pump was left maintain running) for 2 h. The desiccation chamber was return to atmospheric pressure and the samples were left submerged for 18 ± 2 h.

After complete the preparation, current input analog-to-digital converter (A.D.C.) external voltage of 60 volts was applied to concrete samples of 100 mm diameter and 50 mm thickness. This concrete samples was in contact with a solution of 0.3 N of sodium hydroxide (NaOH) in the anode and 3 % of sodium chloride (NaCl) solution in the cathode. During the test, the main parameter measured was the current flow through the concrete for a period of 6 h. A data logger system recorded the temperature, charge passed and current for every 5 min. The RCP test setup is shown in Fig. 2.

Fig. 2 RCPT arrangement setup (ASTM C1202)



3 Result and Discussion

3.1 Morphology Examination

The particle images of OPC and NC (before and after calcination process) have been observed using FESEM. The image has been magnifying to 6,000 times smaller than a standard microscope to obtain better and quality image. Figure 3 illustrated the microstructure of OPC are granular, angular and non-uniformly (uneven microstructure). Meanwhile, Fig. 4 displays the particle images of uncalcined NC and NC particles after calcined at temperature 700 °C for 3 h is presented in Fig. 5. It can be seen that after the calcination process, the NC particles chemically changes from

Fig. 3 FESEM micrograph of OPC particles

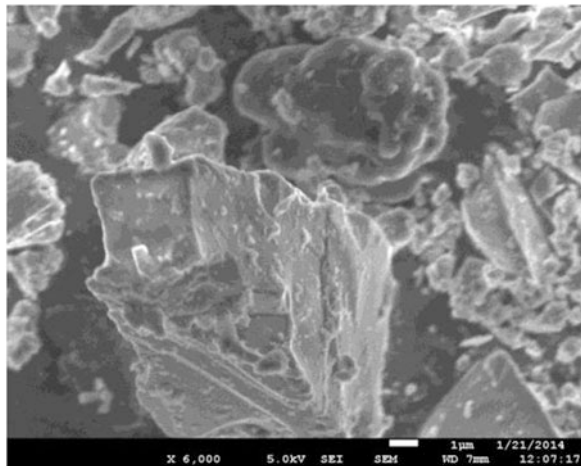


Fig. 4 FESEM micrograph of untreated NC particles

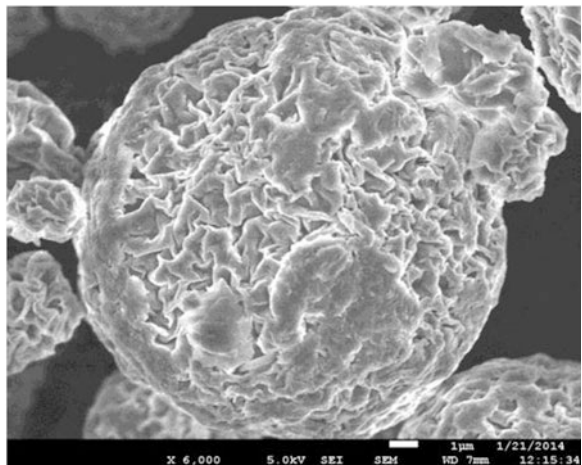
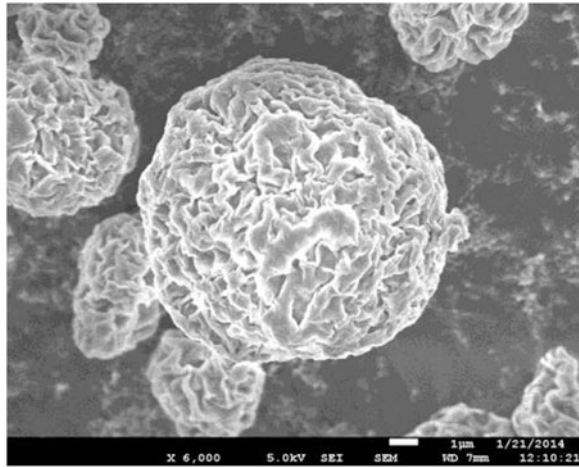


Fig. 5 FESEM micrograph of treated NC particles



crystal to amorphous (dehydrolixation) structure. The microstructure of calcined NC was curly and forms like fibre reinforced structure. It is also clearly shown the surface area of calcined NC much smoother as compared to OPC.

Table 1 displays that the content of silica (SiO_2) for NC was higher as compared to OPC. Almost 66 % of SiO_2 is recorded for NC, content of alumina oxide (Al_2O_3) for NC is also 15 % higher as compared to OPC. On the other hand, the content of calcium oxide (CaO) for NC is lower compared to OPC. This lower content of CaO will reduce the formation of calcium hydroxide in cement paste. It can be concluded that NC is reactive pozzolanic material that contribute to secondary hydration leads to strength increment.

3.2 Workability and Strength

The workability of fresh concrete for NPC, UHPC and UHPC-NC with different levels of NC replacement is presented. The relationship between replacement levels of NC and slump values is shown in Fig. 6. It is revealed that the replacement of NC to OPC can reduce the slump of UHPC-NC and increase the water demand of normal consistency. The higher the NC material replacement level, the greater affecting the water demand thus decrease the slump. It is likely due to the higher water adsorption of NC as a result of finer particles of NC. Due to water absorbed, the NC particles will fill the spaces between the stacked silicates layers. The workability of UHPC incorporating NC is related to the degree of wetness of concrete mixes.

Figure 7 shows the compressive strength of NPC, UHPC and three (3) series nanoclaved UHPC. At 7-days of age, it shows that the optimum strength is recorded by UHPC concrete with no addition of NC as cement replacement. The nanoclaved

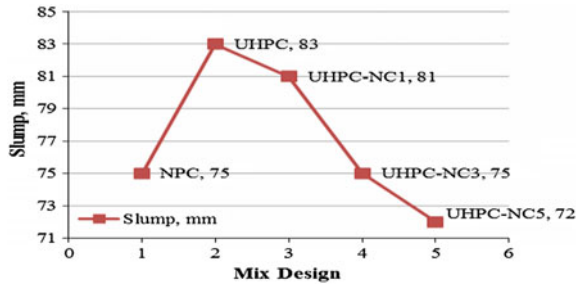
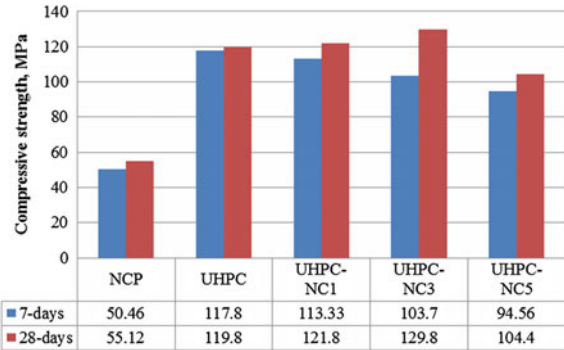


Fig. 6 Slump values for all mixes

Fig. 7 Compressive strength of NPC, UHPC and UHPC-NC



UHPC did not show strength increment corresponding to that UHPC without NC. The finer particles of NC did not improve significantly the nanoclaved UHPC strength at early. It can be that the finer particles of NC only acts as ultra-filler in the concrete due to high content of OPC cement. However, at 28-days of age, it is noticed that the compressive strength of nanoclaved UHPC increase marginally. UHPC made of 3 % NC recorded highest strength which is 129.8 MPa. Among of nanoclaved UHPC samples, UHPC-NC3 recorded highest in terms of compressive strength as compared to those of UHPC-NC1 and UHPC-NC5. The presence of NC will create the nano pozzolanic reaction thus develops more hydration gel.

3.3 Chloride Permeability

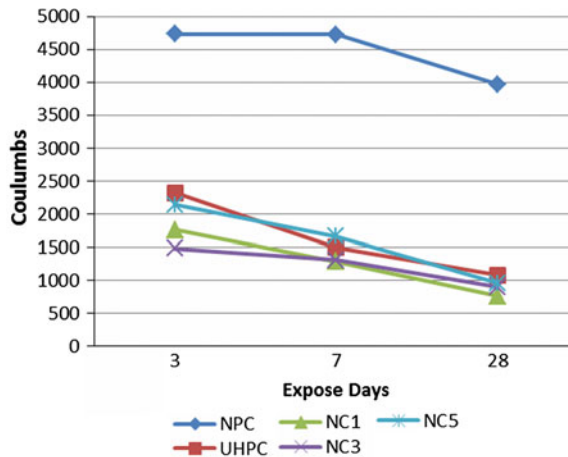
The RCPT results for NPC, UHPC and UHPC-NC concrete mixes are tabulated in Table 3. It is found that charge passed decreases as the ages prolonged and displays in Fig. 8. However, the charge passed were also decreases as the level of NC replacement increases. Almost all UHPC and nanoclaved UHPC samples showed low chloride ion penetrability below 2000 Coulombs at 7-days. On the other hand,

Table 3 Chloride permeability for NPC, UHPC and UHPC-NC samples

Age	Sample designation	Average charge	Maximum temp. (°C)	Class ^a
3	NPC	4,735	50	H
	UHPC	2,324	42	M
	UHPC-NC1	1,762	35	L
	UHPC-NC3	1,478	31	L
	UHPC-NC5	2,139	38	M
7	NPC	4,726	51	H
	UHPC	1,495	35	L
	UHPC-NC1	1,286	32	L
	UHPC-NC3	1,308	31	L
	UHPC-NC5	1,660	38	L
28	NPC	3,967	44	M
	UHPC	1,079	32	L
	UHPC-NC1	765	29	VL
	UHPC-NC3	899	28	VL
	UHPC-NC5	957	30	VL

^a H High, M Moderate, L Low, VL Very Low

Fig. 8 Charge passed measured on NPC, UHPC and UHPC-NC samples



at 28-days all nanoclaved UHPC samples recorded very low chloride ion penetrability (below than 1000 Coulombs) except for NPC and UHPC samples. According to ASTM C1202, the NPC samples show high chloride ion penetration (charge passed >4000 Coulombs) at 3 and 7-days, meanwhile chloride penetration of NPC and 28-days can be classified as moderate (charge passed in range 2000–4000 Coulombs). For UHPC samples, it is observed that the UHPC samples at 3-days can be classified moderate chloride ion penetrability. However, the charge passed for UHPC samples at 7 and 28-days showed low chloride ion penetration.

It can be observed that, the presence of NC has benefit in terms of resisting chloride penetration. NC acts as an ultra-filler material and yields a significant

reduction in the total charge passed. Among the UHPC-NC mixes, UHPC-NC1 samples have proved lowest chloride penetration compared to other nanoclaved UHPC. Previous researchers [13–15] also found that NC improved the chloride penetration into concrete and reduced diffusion coefficients of chloride ion.

The replacement of 1 % NC in UHPC mixes produces an increment on the chloride penetration resistance of about 2.3 times from day-3 to day-28. It is believed that, the good chloride resistance of NC blended concretes is due to the high diffusion in porous and the refinement of the pore structure. Another factors that affect the chloride permeability of samples due to lower water cement ratio less than 0.4 used for producing UHPC and UHPC-NC concretes.

4 Conclusion

From the findings, the conclusions can be drawn as follows:

1. It is demonstrated that increase in NC content decrease the workability of nano claved fresh concrete.
2. It is proved that inclusion of NC material improve the strength of UHPC at 28-days as compare to those mixes without NC material. The optimum NC replacement recorded at 3 % of total weight of OPC cement.
3. It is deduced that the presence of NC material able to resist chloride penetration. UHPC-NC1 has been proved to be very low chloride penetration characterised compared to other UHPC mixes with inclusion of 3 and 5 % NC replacing cement. Replacement of NC material acts as an ultra-filler material thus significantly reduced in the total charge passed.

References

1. U. Faheem, Clays, nanoclays, and montmorillonite minerals. *Metall. Mater. Trans. A*, **39A**, 2804–2814 (2008)
2. P. Balaguru, K. Chong, Nanotechnology and concrete: research opportunities. in *Proceedings of ACI Session on Nanotechnology of Concrete: Recent Developments and Future Perspectives*, Denver, USA, 7 Nov 2006
3. J.H. Monica, T.A. Harris, Nanotechnology innovations for the construction industry. *Prog. Mater Sci.* **58**, 1056–1102 (2013)
4. P. Brightson, G. Baskar, S.B. Gnanappa, Strength and durability analysis of nano clay in concrete, *Life Sci. J.* **10**(7s), 1172–1177, ISSN 1097–8135
5. C. Arya, N.R. Buenfeld, J.B. Newman, Factors influencing chloride-binding in concrete. *Cem. Concr. Res.* **20**, 291–300 (1990)
6. S. Ahmad, Reinforcement corrosion in concrete structures, its monitoring and service life prediction—a review. *Cem. Concr. Compos.* **25**, 459–471 (2003). doi:[10.1016/S0958-9465\(02\)00086-0](https://doi.org/10.1016/S0958-9465(02)00086-0)

7. U.M. Angst, B. Elsener, C.K. Larsen, Ø. Vennesland, Chloride induced reinforcement corrosion: electrochemical monitoring of initiation stage and chloride threshold values. *Corros. Sci.* **53**, 1451–1464 (2011). doi:[10.1016/j.corsci.2011.01.025](https://doi.org/10.1016/j.corsci.2011.01.025)
8. W. Chen, H.H. Mo, Y.B. Yang, S. Liang, Y.W. Chen, B.L. Zhen, J.H. Chen, W.Y. Guo, Technology of chloride-resistant high performance concrete. *Key Eng. Mater.* **405–406**, 296–302 (2009). doi:[10.4028/www.scientific.net/KEM.405-406.296](https://doi.org/10.4028/www.scientific.net/KEM.405-406.296)
9. X. He, X. Shi, Chloride permeability and microstructure of portland cement mortars incorporating nanomaterials, transportation research record. *J. Trans. Res. Board*, No. 2070, (Transportation Research Board of the National Academies, Washington, D.C., 2008), pp. 13–21. doi: [10.3141/2070-03](https://doi.org/10.3141/2070-03)
10. J. Lizarazo-Marriaga, L.G. López Yépez, Effect of Silica Fume Addition on the Chloride-Related Transport Properties of High-Performance Concrete. *Dyna*, year **79**(171), (Medellin, 2012), pp. 105–110. ISSN 0012–7353
11. S.N. Vinay, Y.T. Vikram, Effect of different supplementary cementitious material on the microstructure and its resistance against chloride penetration of concrete, in *Proceedings Advanced Materials for Construction of Bridges, Buildings, and Other Structures III*, Engineering Conferences International Year 2003 (ECI Digital Archives, New York, 2003)
12. K. Patel, The use of nanoclay as a constructional material. *Int. J. Eng. Res. Appl. (IJERA)*, **2** (4), 1382–1386 (2012). ISSN: 2248–9622
13. N. Farzadnia, A.A. Abang Ali, R. Demirboga, Development of nanotechnology in high performance concrete. *Adv. Mater. Res.* **364**, 115–118 (2012). doi:[10.4028/www.scientific.net/AMR.364.115](https://doi.org/10.4028/www.scientific.net/AMR.364.115)
14. L. Song, W. Sun, J. Gao, Y. Zhang, Influence of GGBS on time dependent chloride diffusion coefficient of HPC. *Adv. Mater. Res.* **243–249**, 5703–5710 (2011). doi:[10.4028/www.scientific.net/AMR.243-249.5703](https://doi.org/10.4028/www.scientific.net/AMR.243-249.5703)
15. H. Xiaodong, S. Xianming, Chloride permeability and microstructure of portland cement mortars incorporating nanomaterials, *Journal of the Transportation Research Board*, No. 2070 (Transportation Research Board of the National Academies, Washington, D.C., 2008), pp. 13–21. doi: [10.3141/2070-03](https://doi.org/10.3141/2070-03)
16. M.S. Morsy, S.H. Alsayed, M. Aqel, Effect of nano-clay on mechanical properties and microstructure of ordinary portland cement mortar. *Int. J. Civ. Environ. Eng. IJCEE-IJENS* **10** (1), 21–25 (2010)

2D Multi-scale Simulation and Homogenization of Foamed Concrete Containing Rubber Bars

Zainorizuan Mohd Jaini, Shahrul Niza Mokhatar, Yuantian Feng and Mazlan Abu Seman

Abstract One of new innovation in modified concrete is foamed concrete containing rubber bars. The function of rubber on foamed concrete is to improve the strength and enhance the resistance toward high strain rate loadings. The production of foamed concrete containing rubber bars, therefore, leads to the heterogeneous material condition or so-called composite. Mostly, the investigations of strength and material properties of modified concrete are conducted using experimental approaches with various parametric and proportions. This study, however, intends to numerically analyse the strength and elastic properties of foamed concrete containing rubber bars through multi-scale simulation. The unit cell consists of foamed concrete and rubber bar was modelled using the hybrid finite-discrete element method. The damage model of rotating crack was defined on foamed concrete, while rubber bar remain as elastic. It was revealed that foamed concrete containing 5 mm diameter of rubber bars with proportion below that 3 % produces optimum strength. Results that obtained from multi-scale simulation show a favourable agreement with that obtained from experimental study and rule of mixtures.

Keywords Multi-scale simulation · Rule of mixtures · Foamed concrete · Rubber bar · Hybrid finite-discrete element method

Z.M. Jaini (✉) · S.N. Mokhatar
Jamilus Research Center, Universiti Tun Hussein Onn Malaysia, 86400 Parit Raja
Johor, Malaysia
e-mail: rizuan@uthm.edu.my

S.N. Mokhatar
e-mail: shahruln@uthm.edu.my

Y. Feng
Zienkiewicz Center for Computational Engineering, Swansea University,
Singleton Park, Swansea 86400, Wales, UK
e-mail: y.feng@swansea.ac.uk

M.A. Seman
Faculty of Civil and Earth Resources, Universiti Malaysia Pahang,
26300 Kuantan, Pahang, Malaysia
e-mail: mazlan@hotmail.co.uk

1 Introduction

Foamed concrete is well known of its lightweight where the density is 25–60 % lower than normal concrete. Despite has an advantage in weight due to low density, foamed concrete has major drawback in strength. Many researchers such as Jones and McCarthy [1], Nambiar and Ramamurthy [2], and Puttappa et al. [3] stated that the compressive strength of foamed concrete is around 1–15 MPa, which is approximately 40 % lower than normal concrete. Consequently, fibre reinforcements become the thrive approach to enhance the strength and material properties of foamed concrete. Such investigations have been conducted by using polypropylene [4, 5] and natural fibres [6, 7]. Other types of fibre include steel, carbon, glass and rubber. The use of fibre reinforcement has been identified as enhancing the tensile and flexural strengths of foamed concrete, especially in resisting crack propagation.

Meanwhile, the use of rubber as fibre reinforcement in concrete has been investigated by Kumaran et al. [8], Garrick [9], and Ismail et al. [10]. The fascination toward sustainability materials in construction industry is the main desire for the application of rubber in modified concrete. All these investigations were conducted experimentally using cylinder or cube test to obtain the strength and material properties. Although experimental test is broadly applied and well accepted in the investigation of strength and material properties of concrete, this approach requires lots of preparations and consumes time at least up to 28 days. Therefore, this study intends to use multi-scale simulation using the hybrid finite-discrete element method in order to predict the strength and elastic properties of foamed concrete containing rubber bars. Although a technique known as rule of mixtures can be implemented in predicting the strength and elastic properties of various composite materials, this method has not provide an adequate analysis beyond the elastic range.

2 Rule of Mixtures and Multi-scale Method

Basically, concrete containing fibres or reinforcement bars is always treated as heterogeneous, but in several conditions, can also be adopted as homogeneous. As a result, the strength and material properties are generally known as in condition of effective. In order to possess as a homogenous material, analytical and numerical methods can be employed with consideration that the composite consists of matrix and fibre.

2.1 Rules of Mixtures

Rule of mixtures is an analytical method to approximately estimate composite material properties. This method is upon an assumption that a composite property is

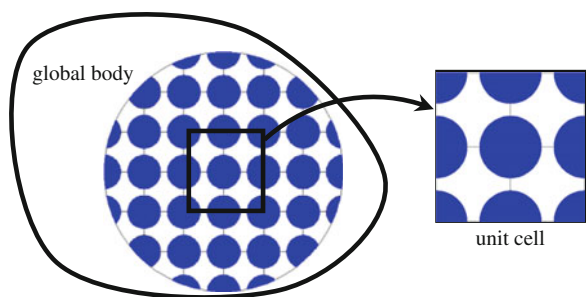
the volume weighed average of the phase of matrix and dispersed phase properties [11]. The rule of mixtures is widely used in composite engineering, regardless, there are also such applications in fibre-reinforced concrete and particle-reinforced concrete. Although this analytical method is simple and easy in predicting the effective elastic properties such as Young's modulus, Poisson' ratio and density, the interaction between phases of matrix and reinforcement is totally ignored. The equations to calculate the effective strength and effective elastic properties using the rule of mixture can be referred in many literatures, for instance Hsieha et al. [12]. On the other hand, Pucharenko and Morozov [13] have used the modified rule of mixtures that considers the influence of contact zone between concrete and fibre reinforcements. In other extensive analysis, Carpinteri and Pugno [14] have introduced the fractal rules of mixture for fragmentation of reinforced concrete with different bar configurations.

2.2 Multi-scale Analysis

Multi-scale analysis refers to a style of modelling in which multiple models at different scales are used simultaneously to describe a system. The different models usually focus on different scales of resolution, e.g. length, shape and volume fraction. Within this context, the most common goal of multi-scale analysis is to predict the macroscopic behaviour of the engineering materials. Multi-scale analysis basically represented in a unit cell or also known as representative volume element [15]. Figure 1 shows the representation volume element that obtained from periodical cells of a global body.

The multi-scale analysis can be conducted using numerical approach where a unit cell is employed with proper boundary conditions and apposite applied loadings. Jaini et al. [16] have employed the linear boundary condition with applied strain displacement in a multi-scale analysis using the hybrid finite-discrete element method. Meanwhile, Zhou and Molinari [17] used the applied velocity in analysis

Fig. 1 The representative volume element from a global body to a unit cell



of brittle materials. By manipulating the linear stress-strain relation and solve simultaneously its simplified form in the two-dimensional plane strain, this yields the following equations:

$$E^* = \frac{(R_x + 2R_y)(R_x - R_y)}{(R_x + R_y)} \quad (1)$$

$$v^* = \frac{R_y}{(R_x + R_y)} \quad (2)$$

where E^* and v^* are the effective Young's modulus and Poisson's ratio respectively, while R_x and R_y are the reaction forces that produced in the boundaries of the unit cell.

3 Experimental Study

The experimental study was conducted to establish the material properties that required during the multi-scale simulation and as verification of numerical results.

3.1 Material Preparation and Specimen

In experimental study, 16 specimens were casting involve four specimens of controlled foamed concrete (Specimen A) and four specimens for each foamed concrete with rubber bar in diameter of 5 mm (Specimen B), 10 mm (Specimen C) and 15 mm (Specimen D). All specimens were casting using $150 \times 150 \times 150$ mm mould with required density of foamed concrete approximately $1,400 \pm 5$ kg/m³. The mix proportion of foamed concrete is based on 1:2 of cement to sand while water to cement ratio is 0.55. During the casting process, rubber bars were carefully arranged on the fresh concrete according to the specific spacing and layer as can be referred in Table 1, Figs. 2 and 3.

Table 1 Specification arrangement of rubber bar

Specimen	Diameter bar (mm)	Spacing (mm)	Volume rubber (%)
A	0	0	0
B	5	25	3.14
C	10	30	8.73
D	15	35	12.57

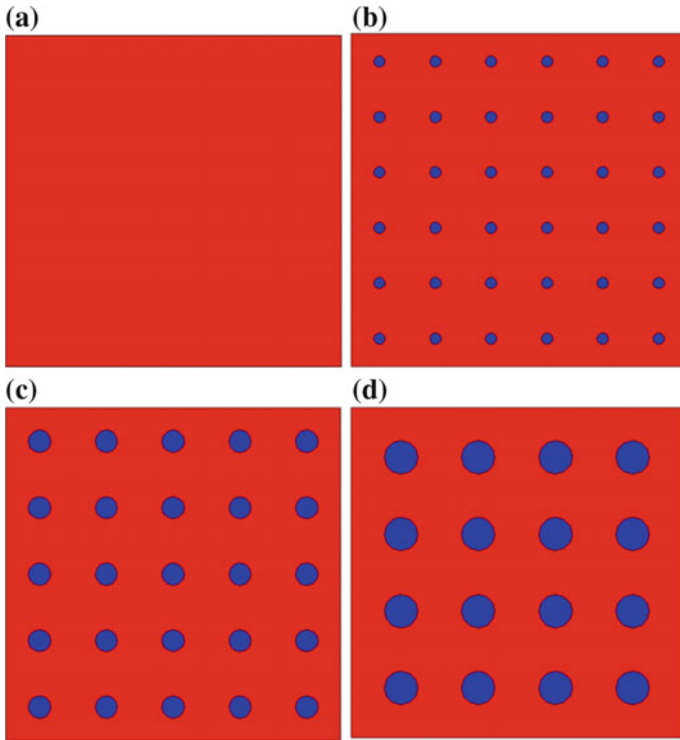
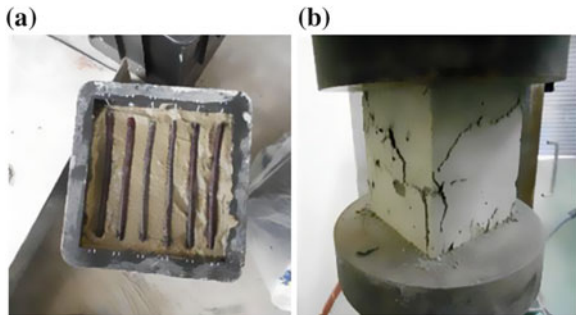


Fig. 2 The arrangement of rubber bars on the foamed concrete. **a** Specimen A. **b** Specimen B. **c** Specimen C. **d** Specimen D

Fig. 3 Preparation of cube specimens and compressive test. **a** Cube preparation. **b** Compression test



3.2 Compressive Strength Test

The compression test for all specimens of foamed concrete and foamed-rubber concrete were conducted after curing process of 7 and 28 days. Figure 4 shows the compressive strength of specimens without rubber bars, and with 5, 10 and 15 mm

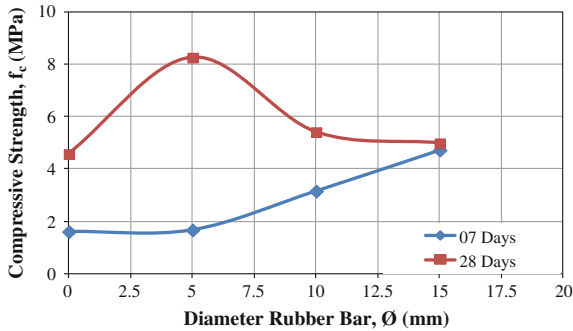


Fig. 4 Compressive strength of foamed-rubber concrete

diameter of rubber bars. It was found that foamed concrete containing rubber bar with diameter 5 mm produces highest yet optimum strength. It is easy to understand in modified concrete, high volume fraction of fibre or particle will significantly reduce the strength of concrete.

3.3 Tensile Strength and Elastic Properties

Since the experimental study only provide compressive strength of foamed concrete. Therefore, it is necessary to further determine the elastic properties and tensile strength of foamed concrete using empirical formula. According to Jones and McCarthy [1], Byun et al. [18], and Ramamurthy and Nambiar [19], the tensile strength and Young's modulus of foamed concrete can be calculated using the following equations:

$$E = 0.42f_c^{1.18} \quad (3)$$

$$f_t = 1.03(f_c)^{0.5} \quad (4)$$

where E is Young's modulus, f_c is compressive strength and f_t is tensile strength. The average Poisson's ratio of foamed concrete, ν is taken as 0.2.

4 Multi-scale Simulation

Multi-scale simulation was conducted to numerically investigate the strength and material properties of foamed concrete containing rubber bars. The modelling and simulation of a unit cell of foamed-rubber concrete were conducted using the hybrid finite-discrete element method.

4.1 Model

In the 2D multi-scale simulation, there are three different models of unit cell. Unit cell of 25 mm × 25 mm, 30 mm × 30 mm and 35 × 35 mm were extracted from Specimen B, Specimen C and Specimen D respectively. The use of different sizes of unit cell is to understand its effect on strength and material properties. In all types of unit cell, the diameter of rubber bar was increased from zero up to unit cell size. Through the hybrid finite-discrete element method, as can be seen in Fig. 5, each unit cell model was discretized using triangular 3-noded elements with partially bonded between rubber and foamed concrete. Three boundaries of the unit cell were constrained, whilst the free boundary was imposed by linear ramp-up of the strain displacement loading.

4.2 Constitutive Law

The rotating crack was used as material model for foamed concrete. This material model only requires Young’s modulus, Poisson’s ratio, density and tensile strength. Crack propagation is also included in the material model. Crack is governed by fracture energy and damage elastic modulus that automatically calculated from stress-strain curve. In the hybrid finite-discrete element method, discrete crack will be inserted in the failed region when the tensile strength in a principal stress reaches zero. Details about insertion process of discrete crack can be found in Jaini et al. [16] and Klerck et al. [20]. Meanwhile, rubber bar was defined as elastic, hence,

Fig. 5 A unit cell model of foamed-rubber concrete with strain displacement loading at free boundary, $\delta = L_x = L_y$

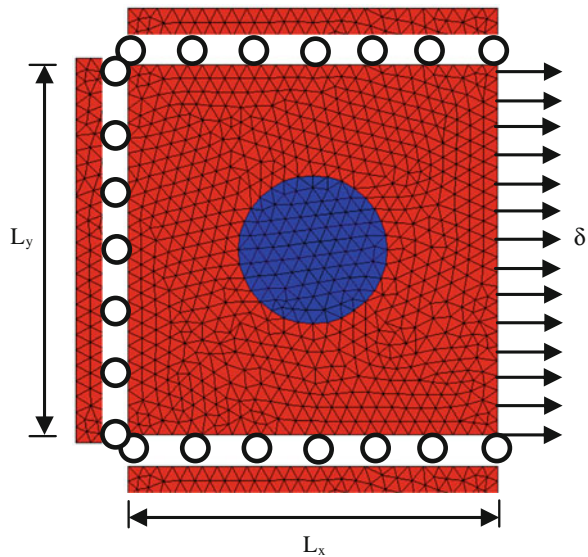


Table 2 Material properties of foamed concrete and rubber

Material	Properties			
	E (GPa)	ν	ρ (kg/m ³)	f_t (MPa)
Foamed concrete	2.523	0.2	1,400	0.689
Rubber bar	0.015	0.5	1,100	–

only entails elastic material properties. The material properties of foamed concrete and rubber bar can be referred in Table 2. It should be emphasized here that the Young's modulus and tensile strength of foamed concrete were directly determined from equations as stated in (3) and (4).

4.3 Tensile Strength

Due to the strain displacement loading, the unit cell of foamed-rubber concrete experiences deformation and later intrinsic cracks when the computed stress exceeded the yield stress defined in the foamed concrete. Therefore, the peak stress is taken as the tensile strength of the specimen. At the softening phase, the discrete cracks propagate and coalesce until the unit cell experiences total failure, basically, can be observed by sudden drop of the stress level. By measuring the reaction forces at the both boundaries of axis- x and y , the Young's modulus and Poisson's ratio can be calculated using the equations in (1) and (2). The Young's modulus can also be confirmed by measuring the gradient of elastic stress-strain curve. Figure 6 shows the stress distribution on the unit cell of foamed-rubber concrete at peak stress and during the propagation of cracks. Meanwhile, the crack condition on the foamed-rubber concrete can be seen in Fig. 7. The cracks occur in directions that attempt to maximize the energy release rate and minimize the strain energy density. In addition, the cracks progressively grow further along the boundaries of the existing mesh elements, mostly in the horizontal and interfacial transition zone of foamed concrete and rubber bar.

Similar like compressive strength that obtained from experimental study, the tensile strength of foamed-rubber concrete from multi-scale simulation disclosed that the optimum strength is occur due to 5 mm diameter of rubber bar. The experimental and numerical results revealed that the present of rubber bar increase the toughness of foamed concrete, but excessive volume fraction create interfacial zone that reduce the strength. A comparison of tensile strength between direct correlation of experimental study, multi-scale simulation and rule of mixtures can be referred in Table 3. The accuracy using multi-scale simulation is more than 90 %, while rule of mixtures totally unable to predict the optimum tensile strength of foamed-rubber concrete. Rule of mixtures is really depends on the strength of rubber bar. As volume fraction of rubber bar keep increase, the tensile strength of foamed-rubber concrete constantly decrease. Therefore, it is difficult to predict the optimum tensile strength in rule of mixture. Figures 8, 9 and 10 display the results

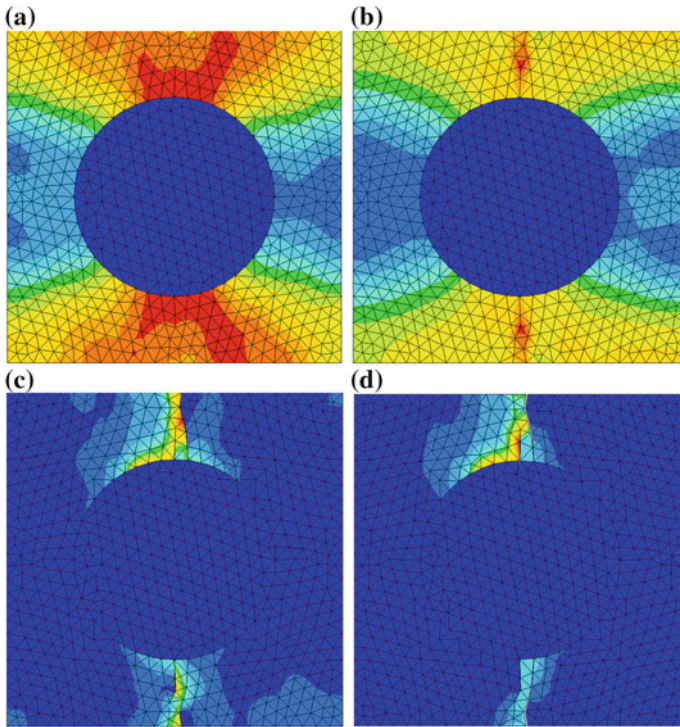


Fig. 6 Stress distribution on the unit cell of foamed-rubber concrete. **a** Peak stress. **b** Before microcrack. **c** Initial crack. **d** Crack initiation

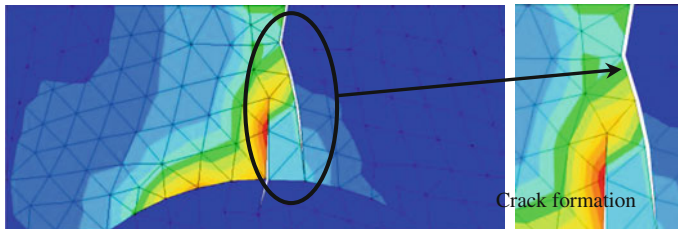


Fig. 7 Stress distribution on the unit cell of foamed-rubber concrete

Table 3 Tensile strength of foamed-rubber concrete, a comparison between experiment, multi-scale and rule of mixture

Diameter bar (mm)	Specimen	Tensile strength (MPa)		
		Experiment	Multi-scale	Rule of mixture
0	A	0.689	0.689	0.689
5	B	0.927	0.843	0.673
10	C	0.750	0.744	0.643
15	D	0.719	0.684	0.612

Fig. 8 Tensile strength of unit cell 25 mm × 25 mm

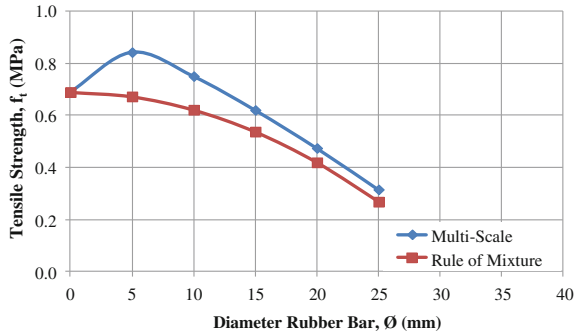


Fig. 9 Tensile strength of unit cell 30 mm × 30 mm

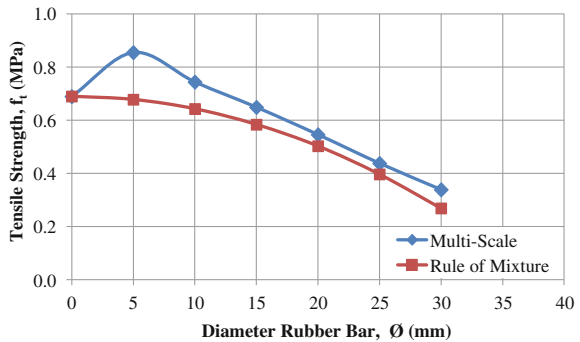
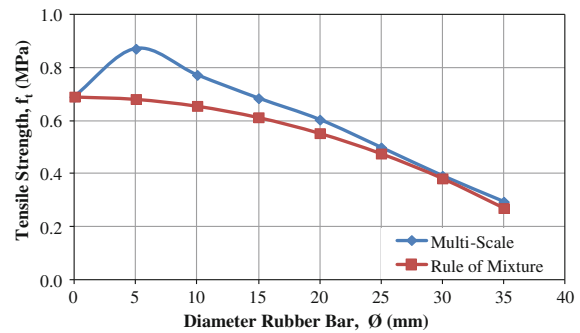


Fig. 10 Tensile strength of unit cell 35 mm × 35 mm



of tensile strength. As favourable results were obtained, this is an evidence that multi-scale simulation through comprehensive material model and appropriate selection of representative volume element can be used to predict tensile strength of modified concrete.

4.4 Young's Modulus

Results of Young's modulus for different unit cells at various diameters of rubber bar are shown in Figs. 11, 12 and 13. The increment in diameter of rubber bar tends to reduce the Young's modulus. This pattern corresponds to the tensile strength and stiffness of foamed-rubber concrete. Despite produces high value in tensile strength, results of Young's modulus from multi-scale simulation always become the lower bound to rule of mixtures. It was also found that the size of unit cell has no

Fig. 11 Young's modulus of unit cell 25 mm × 25 mm

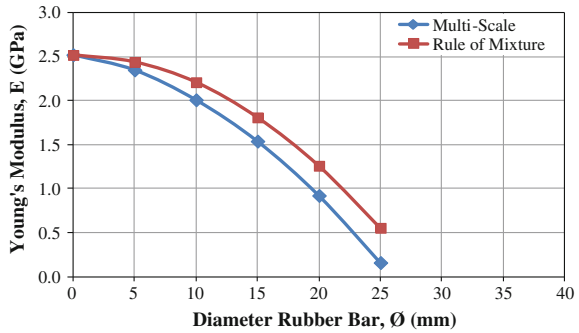


Fig. 12 Young's modulus of unit cell 30 mm × 30 mm

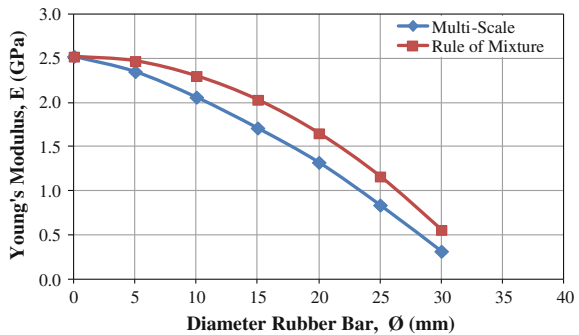
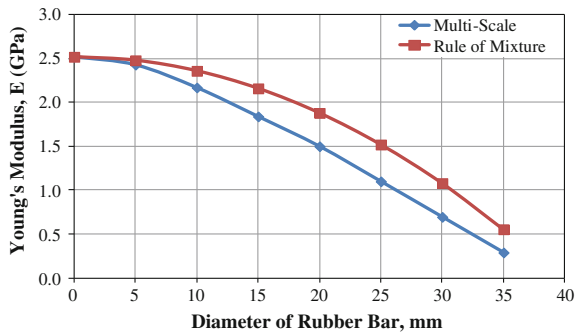


Fig. 13 Young's modulus of unit cell 35 mm × 35 mm



significant effect on Young’s modulus. This can be seen at all unit cells with similar volume fraction of rubber bar, as example 78.54 % volume fraction of rubber bar will produce Young’s modulus approximately 0.554 GPa.

4.5 Poisson’s Ratio

The prediction of Poisson’s ratio for foamed-rubber concrete using multi-scale simulation and rule of mixtures shows a favourable agreement to each other, especially for unit cell with diameter of rubber bar less than 15 mm. Figures 14, 15 and 16 display the results for Poisson’ ratio. As diameter of rubber bar increases, Poisson’s ratio gradually increases. In this case, it was found that the characteristic of rubber has a dominant influence on Poisson’s ratio. For each 5 mm increment of rubber bar, Poisson’s ratio increase almost 10–25 %. Moreover, foamed concrete containing rubber bar with size less than 35 mm still in the stable condition, transform from a quasi-brittle material to ductile.

Fig. 14 Poisson’s ratio of unit cell 25 mm × 25 mm

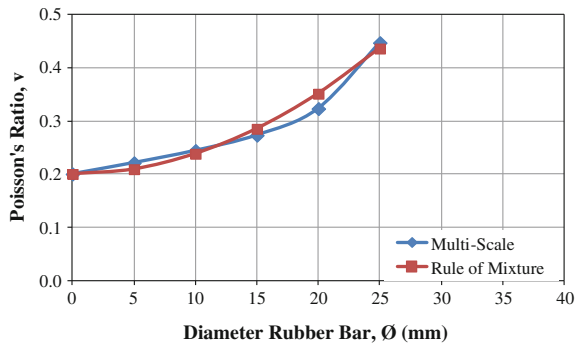


Fig. 15 Poisson’s ratio of unit cell 30 mm × 30 mm

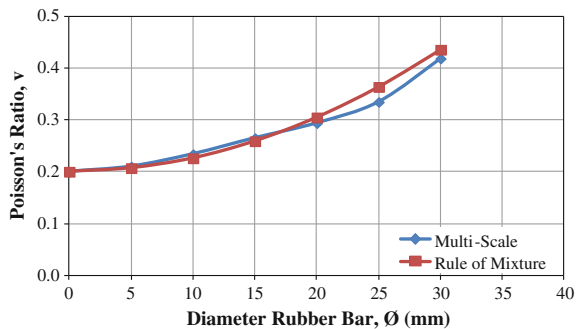
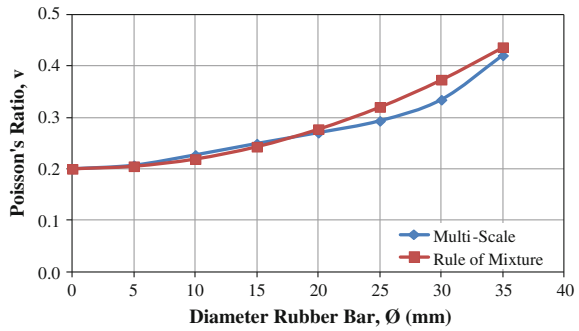


Fig. 16 Poisson's ratio of unit cell 35 mm × 35 mm



5 Conclusion

The prediction of strength, Young's modulus and Poisson's ratio of foamed-rubber concrete has been performed using multi-scale simulation. In a unit cell, the rotating crack model and linear elastic were employed for foamed concrete and rubber bar respectively through the hybrid finite-discrete element method. It was found that the multi-scale simulation can accurately predict the tensile strength. The optimum and highest strength has been observed in foamed concrete containing rubber bars with diameter less than 5 mm while the proportion of rubber bar must not more than 3 %. A comparison of results between multi-scale simulation and experimental study shows a favourable agreement with accuracy more than 90 %. Meanwhile, both multi-scale simulation and rule of mixtures have ability in predicting Young's modulus and Poisson's ratio of foamed-rubber concrete. However, current technique that applied in multi-scale simulation only eligible for the uniform distribution of fibres or bars. It was also found that, the selection of unit cell from periodical cells of a global body play a vital role in predicting the tensile strength. In contrast, size of unit cell has no significant effect on Young's modulus and Poisson's ratio.

Acknowledgments The authors would like to thanks the Ministry of Education, Universiti Tun Hussein Onn Malaysia and Swansea University for funding and facilities support. This study was conducted under grant scheme of STG-UTHM Code 1282.

References

1. M.R. Jones, A. McCarthy, Preliminary views on the potential of foamed concrete as a structural material. *Mag. Concr. Res.* **57**(1), 21–31 (2005)
2. E.K.K. Nambiar, K. Ramamurthy, Models relating mixture composition to the density and strength of foamed concrete using response surface methodology. *Cem. Concr. Compos.* **28**(9), 752–760 (2006)
3. C.G. Puttappa, A. Ibrahim, K.U. Muthu, H.S Raghavendra, Mechanical properties of foamed concrete, in *Proceedings of the International Conference on Construction and Building Technology* (Kuala Lumpur, Malaysia, 2008)

4. J. Hadipramana, A.A.A. Samad, A.M.A. Zaidi, N. Mohammad, N. Ali, Contribution of polypropylene fibre in improving strength of foamed concrete. *Adv. Mater. Res.* **626**, 762–768 (2013)
5. D. Fukang, Mechanical properties and energy-saving effect of polypropylene fiber foamed concrete. *Res. J. Appl. Sci. Eng. Technol.* **6**(11), 2012–2018 (2013)
6. N.M.S. Hasan, H.R. Sobuz, M.S. Sayed, M.S. Islam, The use of coconut fibre in the production of structural lightweight concrete. *J. Appl. Sci.* **12**(9), 831–839 (2012)
7. H. Awang, M.A.O. Mydin, M.H. Ahmad, Mechanical and durability properties of fibre lightweight foamed concrete. *Aust. J. Basic Appl. Sci.* **7**(7), 14–21 (2013)
8. G.S. Kumaran, N. Mushule, M. Lakshmiopathy, A review on construction technologies that enables environmental protection: rubberized concrete. *Am. J. Eng. Appl. Sci.* **1**(1), 40–44 (2008)
9. G.M. Garrick, Analysis and testing of waste tire fiber modified concrete, MRes thesis, Louisiana State University, United States, 2005
10. M. Ismail, P. Forouzani, A.H. Noruzman, Engineering properties of concrete incorporating scrap rubber tire, in *Proceedings of the 13th East Asia-Pacific Conference on Structural Engineering and Construction* (Sapporo, Japan, 2013)
11. V. Suresh, R. Sivasubramanian, R. Maguteeswaran, Study and investigation of analysis of metal matrix composite. *Int. J. Mech. Eng. Technol.* **3**(2), 171–188 (2012)
12. C.L. Hsieha, W.H. Tuan, T.T. Wu, Elastic behaviour of a model two-phase material. *J. Eur. Ceram. Soc.* **24**(15–16), 3789–3793 (2004)
13. J. Pucharenko, V. Morozov, A structural model and strength predicting of fiber-reinforced concrete. *J. World Appl. Sci.* **23**, 1111–1116 (2013)
14. A. Carpinteri, N. Pugno, Fractal rules of mixture for multi-scale fragmentation of heterogeneous materials. *Int. J. Mech. Control* **6**(2), 31–37 (2005)
15. G. Lu, E. Kaxiras, *Handbook of Theoretical and Computational Nanotechnology: An Overview Multiscale Simulation of Material* (American Scientific, Cambridge, 2005)
16. Z.M. Jaini, Y.T. Feng, S.N. Mokhtar, M.A. Seman, Numerical homogenization of protective ceramic composite layers using the hybrid finite-discrete element methods. *Int. J. Integr. Eng.* **5**(2), 15–22 (2013)
17. F. Zhou, J.F. Molinari, Stochastic fracture of ceramics under dynamic tensile loading. *Int. J. Solids Struct.* **41**(22), 6573–6596 (2004)
18. K.J. Byun, H.W. Song, S.S. Park, Development of structural lightweight foamed concrete using polymer foam agent, in *Proceedings of the 9th International Congress on Polymers in Concrete* (Bologna, Italy, 1998)
19. K. Ramamurthy, E.K.K. Nambiar, A classification of studies on properties of foam concrete. *Cem. Concr. Compos.* **31**(6), 388–396 (2009)
20. P.A. Klerck, E.J. Sellers, D.R.J. Owen, Discrete fracture in quasi-brittle materials under compressive and tensile stress states. *Comput. Method Appl. Mech. Eng.* **193**(27), 3035–3056 (2004)

Qualitative Fault Tree and Event Tree Model of Bridge Defect for Reinforced Concrete Highway Bridge

Wan Safizah Wan Salim, Mohd Shahir Liew and A'fza Shafie

Abstract Due to a large number of bridges to monitor which contribute to the issue on the cost of inspection and maintenance that must be given priorities in the future maintenance process, it is important to have a comprehensive system in managing the bridge performance assessment by proposing the framework of structural integrity management system for reinforced concrete highway bridge in Malaysia. This new proposes system is using risk-based approach which may be emulated from SIMS of offshore platform structure. In general, the objectives of this study are to identify the bridge performance indicator in term of cause-consequence scenario in order to develop the framework of risk-based bridge management system and to create the risk matrix for prioritizing the inspection for maintenance. However, this paper only focuses on the evaluation part of the system which concentrates on the development of qualitative bridge defect model by using fault tree and event tree method. Fault tree method is used to identify the possible causes of bridge defect by considering the mechanism of bridge failure with referring to the failure mechanism classification from the existing practiced bridge management system and also based on literature review. While, event tree model is developed to determine what is the consequences of the bridge defect are and based on the developed event tree model, the consequences are divided into five condition of bridge failure known as

W.S.W. Salim (✉)

Department of Civil Engineering, Universiti Teknologi PETRONAS, Tronoh,
Perak, Malaysia

e-mail: wansafizah@perlis.uitm.edu.my

W.S.W. Salim

Faculty of Civil Engineering, Universiti Teknologi MARA, Selangor, Malaysia

M.S. Liew

Faculty Geoscience and Petroleum Engineering, Universiti Teknologi PETRONAS,
Tronoh, Perak, Malaysia

e-mail: shahir_liew@petronas.com.my

A. Shafie

Department of Fundamental and Applied Science, Universiti Teknologi PETRONAS,
Tronoh, Perak, Malaysia

e-mail: afza@petronas.com.my

disastrous, severe, medium, minor and good. Both models are significant for probability quantification and thus to determine the risk of bridge defect.

Keywords Bridge management • Risk assessment • Fault tree method • Event tree method

1 Introduction

Overall, there are about more than 10,000 bridges in Malaysia owned by Public Work Department (JKR), Malayan Railways (KTMB), Kuala Lumpur City Council (DBKL) and Malaysia Highway Authority (LLM) which consists of various types of bridge that are concrete bridge, steel bridge, masonry bridge and wooden bridge [1]. In general, the concrete type bridge constitutes the major portion of bridge type in Malaysia as a record from JKR was shown that more than 80 % of their bridge types are made of concrete [2].

Malaysia have a huge number of bridges to be observed with several issue related to the bridge management due to numbers of ageing bridge, the low fund for maintenance and occurrence of catastrophic bridge failure [3]. Hence, the comprehensive assessment and management system is essential to develop in order to reduce cost related to bridge performance assessment and which bridge should be given the priorities to be maintained first. Furthermore, in current situation of increasing of traffic demands and ageing bridge, it is significant to have an effective method for deciding which bridges need inspection first and which ones can be less observation, thus the need to prioritize.

At present, Malaysia uses a system known as Bridge Management System (BMS) to evaluate the bridge performance for further maintenance action. The system is generally based on condition evaluation and cost optimisation [4, 5]. Moreover, the inspection frequencies of the existing system are generally time-based but some of the bridges maybe required less frequency of inspection compared to the bridge with high potential of failure. Furthermore, the current bridge management system is more concerned on the prediction of probability of failure rather than to consider the consequences if the failure occurred during the decision making stage.

Since repair and maintenance fund is always limited, the other approach of management system is important to be introduced to rank the necessity of inspection for future maintenance by considering both the probability of failure and its consequences during the decision making process. Thus, the cost of inspection of bridges that categorized in a good condition may be reduced by increasing the interval of the next inspection. This approach for the decision making in the asset integrity management system is more recognised as risk-based approach and mainly using risk-based inspection (RBI) as risk assessment tool.

As the risk assessment method has been successfully implemented in structural integrity management of offshore platform structure in order to ensure the fitness of

structure for its purpose with long term reduction in operating and assessment cost [6, 7], it is possible to develop the bridge management system by using the same approach. Thus, the framework of Bridge Integrity Management System (BIMs) for reinforced concrete highway bridge was introduced using RBI as an assessment tool. In order to determine the risk value, a model for causes and outcomes identification of failure should be developed. Thus, the aim of this paper is to propose a fault tree (FT) and event tree (ET) model for bridge defect as a part of analysis process for the structural integrity management system of concrete highway bridge in assessing and managing the bridge performance.

2 Risk Assessment Method

There is several definition of risk that has been defined by many people with referring to the application of risk in numerous fields. Ettouney and Alampalli [8] define the risk as an outcome rating to systems with a degree of uncertainties for an occurrence of uncertain events and technically, risk can be defined as a combination of probability (also known as likelihood) and consequence of failure [9–11]. Both failures can be determined through a tool namely risk-based inspection in order to decide which structure elements have high possibility to fail and which structure should be given the priorities in inspection for future risk reduction or mitigation action. RBI is one of the important tools for risk assessment and management in prioritizing and managing in-service inspection plan and maintenance action. The main objective of using RBI in asset integrity management system is to simplify and standardized the assessment procedures and reduce the managing cost without compromising safety [9]. Normally, RBI is more concern on the elements defect rather than the whole system.

There are many methods and techniques available to be used for the determination of probability and consequence of failure. Fault tree and event tree are among examples of method that have being used in risk assessment. Fault tree are one of the most commonly used technique in probabilistic risk analysis and many research have been reported used FT analysis in many areas especially in risk assessment [12, 13]. However, using ET alone for model and analysis are very few. It is almost impossible to use ET method alone in the whole process of risk evaluation. Normally, modelling and analysis uses logic tree is by combination of both fault tree and event tree method [13, 14] and by combination method probably may produce a better result rather than using FT or ET alone.

2.1 Fault Tree Method (FT)

FT is used to identify the combinations of event which could cause a major accident. The basic concept in FT is the translation of physical system into a structured

logical diagram that shows the relation between system failure and failures of the components of the system which specified causes lead to one specified main event of interest [15, 16]. Fault tree analysis (FTA) is considered as deductive approach of failure analysis starting with a potential undesirable event called TOP event. All the possible way that cause the TOP event occurred is determined using logical gates such as AND/OR gates which is the most widely used to combine the causal event. In general, the fault tree model consists of two basic components, ‘gates’ and ‘event’ where ‘gates’ act as connector to show the relationship between of the main ‘event’ and lower event that contribute to the occurrence of the main event (Top event). Tables 1 and 2 shows some of ‘gates’ and ‘event’ symbols that normally used in the development of fault tree model. An example of fault tree model is shown in Fig. 1.

Table 1 Gate symbols and definition [8]







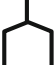

Gate symbol	Gate name	Definition
	AND gate	Output event occurs if all input events occur simultaneously (number of inputs ≥ 2)
	OR gate	Output event occurs if at least one of the input events occurs (number of inputs ≥ 2)
	Exclusive OR gate	Output event occurs if one, but not both, of the two inputs events occurs
	Priority AND gate	Output event occurs if all input events occur in the right order from left to right

Table 2 Event symbols and meaning [8]

Event symbol	Meaning
	TOP event or intermediate event description box. These events are further developed by a logic gate
	Basic event
	House event. Logic event which either occurs or does not occur with certainty (i.e. TRUE of FALSE)
	Transfer symbol

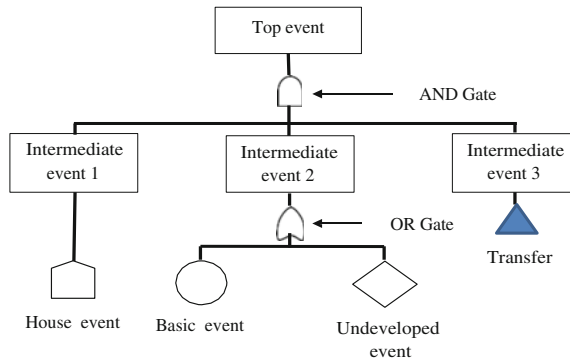


Fig. 1 Fault tree concept

FT method has been widely used especially in risk assessment studies for identifying causes and probability of failure. In risk assessment studies specifically for bridge structures, McDaniel et al. [17] has shown that analysis failure through fault tree model can help in identifying countermeasures to minimize risk failures and the study are based on case study of segmental box girder bridges. Zhu et al. [12] had uses the fault tree analysis to model the probability of existence of major distress mechanism to identify the important risks and their relative severity and to rank the performance trends of bridges. Johnson [18] uses the fault tree analysis to show the interactions of the complex processes of erosion at bridge piers and abutments and to determine the overall probability of bridge failure due to scour and channel instability.

However, the used of fault tree method not only limited to the risk assessment research only. For instance, Sianipar and Adams [19] introduce the use of fault tree method to model bridge element interaction in order to identify, represent and measure interaction phenomena which the fault tree result can be used to access the deterioration rate and improve deterioration prediction of an element. The identifying of the root causes of failure may assist the inspector of structure assessment in the future for choosing the elements for inspection such as a study done by LeBeau and Wadia-Fascetti [20] which used the fault tree analysis to trace the contributed sources of a bridge collapse for future use in identifying critical elements for inspection in bridge system through a case study of Schoharie Creek Bridge Collapse.

2.2 Event Tree Method (ET)

In contrast to the FT, ET is an inductive approach that visually represents the outcome which can arise in a system after a failure has occurred [21]. Event tree starts from possible initiating event (IE) and leading to a series of possible

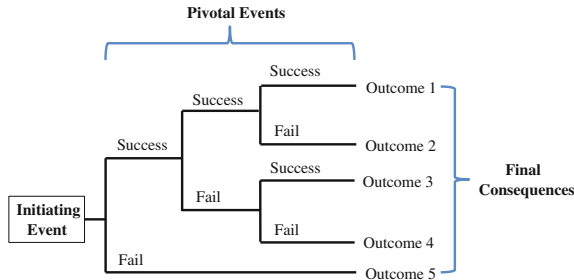


Fig. 2 Event tree concept [21]

undesirable conditions (pivotal events) until reach the definitive consequences of the system failure. Pivotal events also can be defined as an intermediate event in between IE and final consequences of the failure [22]. This basic concept of ET is summarized in Fig. 2.

Compared to FT, It is very rare to see ET applied specifically in bridge related studies. However, as FT, it was widely applied to the risk assessment in various industries such as chemical processing, oil and gas industry and transportation. For example, in the Beim and Hobbs [23] case studies, the event tree were used to model possible paths that lead to closure of Poe Lock and effectively portrayed how a complex system can fail. Hong et al. [24] proven that ET is among the effective technique for probabilistic risk analysis through their study of using ET for analysis of underwater earth pressure balance (EPB) type shield tunneling below the river.

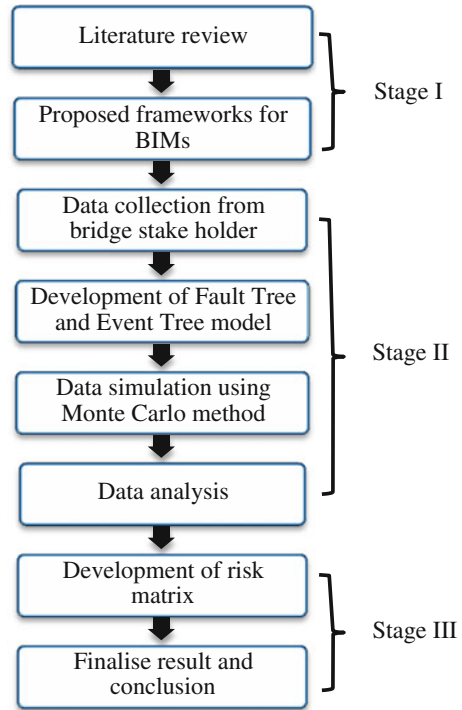
3 Research Methodology

The methodology of this research involve with the development of propose framework for the new bridge management system namely BIMs, Data collection from one of the main bridge stake holder in Malaysia (JKR), qualitative modelling of cause-consequence factor of bridge defect, data simulation and analysis and development of risk matrix for prioritizing the bridge inspection. The study is divided into three stages and the overall flow of the process is illustrated in Fig. 3.

The literature review was initially conducted to identify types and technique used for bridge management that currently practiced in the whole world, generally and specifically practiced in Malaysia and to identify the factors that may affect bridge performance.

The potential causes of bridge defect was identified through FT model based on the literature review and existing bridge performance assessment data which is known as condition rating data. This data is extracted from current practiced system (BMS). While for this study, the ET method is used to model the consequences of bridge defect. Since, there is some missing and non-existing data for both causes

Fig. 3 Research flow



and the consequences of bridge failure, the Monte Carlo Method will be used for data simulation in the purpose of getting more data for statistical calculation. However, this paper only focuses on the development of qualitative model of FT and ET for the bridge defect.

The research concentrates on the reinforced concrete highway bridge types and only focuses on the defect of slab and pier elements. Ten bridges from Penang and Selangor states of Malaysia were selected for the assessment. The selected bridge ranged in age between eleven and seventeen years.

4 Result and Discussion

4.1 Fault Tree Model

In order to develop the fault tree for the bridge defect, the technical knowledge of the bridge and its structural components is required through a compilation of a list of possible causes, failure modes and mechanism that driven to the total bridge defect. This information is gathering from previous related study [12, 17, 19, 20, 25] and also from previous and current damage record of bridge inspection report. In this

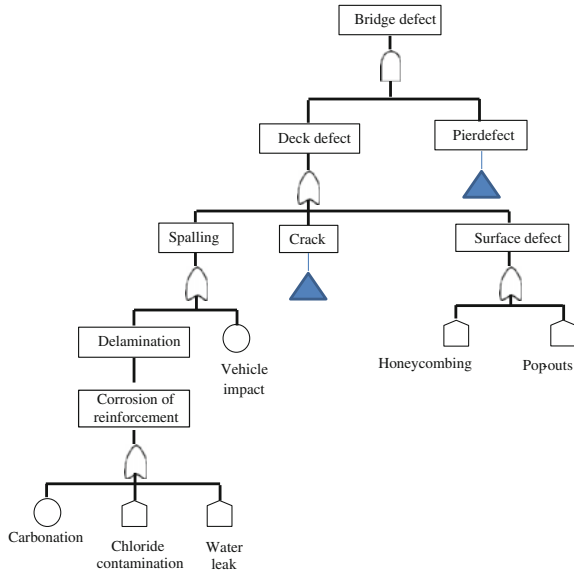


Fig. 4 Fault tree model for bridge defect

study, most of the information for the identification process of the failure causes is collected from JKR BMS database in terms of the condition rating. This condition rating is referring to the rating of the current bridge performance through inspection. Figures 4, 5, 6 and 7 shows the FT model for bridge defect, sub-FT model for crack on deck, sub-FT model of pier defect and sub-FT model for crack on pier, respectively. Generally, concrete bridge is composed of substructure and superstructure and further divided into several members such as deck, pier, girder and abutments. However, in this study only focuses on the defect of deck and pier which contribute to the bridge defect since this two member consider among the major components of

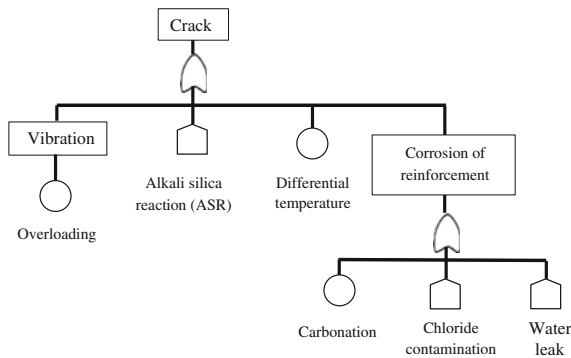


Fig. 5 Sub-fault tree model for crack on deck

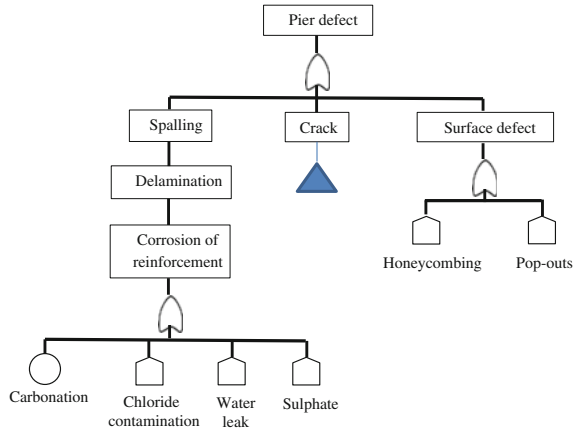


Fig. 6 Sub-fault tree model of pier defect

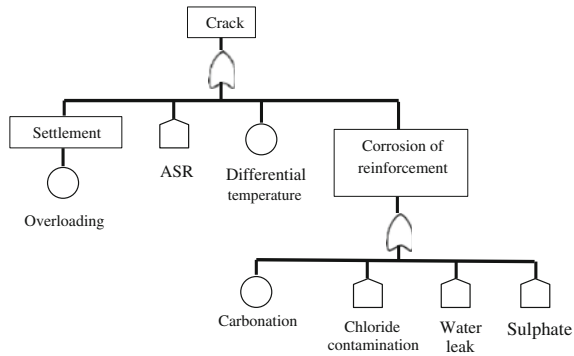


Fig. 7 Sub-fault tree model of crack on pier

bridge. Due to the limited access of existing bridge inspection data, the identification causes of bridge defect only considering on the environmental condition and traffic impact.

The top event of this FT model is defined as bridge defect. The FT model is constructed with consider the mechanism of failure and also a few possible situation that could cause the occurrence of defect to the pier and deck which could lead to the total defect to the bridge. The overall possibility of bridge defect will be determined after examining the individual event probabilities from each level of FT.

4.2 Event Tree Model

In contrast to the FT model, the ET model is developed based on the background reading of the related topic in order to identify factors that may contribute to the consequences of bridge failure. This event tree model is important for the determination of risk value and Monte Carlo simulation also will be used in an attempt to get a data for the future quantitative analysis. The propose ET model for the bridge defect is illustrated in Fig. 8.

The event tree consists of five pivotal events associated with the case of bridge defect as an initiating event that create 22 paths of outcomes and each of tree branch and path probabilities will be calculated. The success or failure of the pivotal events has been identified at the each event tree branch as either ‘Yes’ or ‘No’. The result of consequences path is represented by the level of bridge condition either collapses, partial collapse or no collapse through classification by five levels, namely disastrous, severe, medium, minor and good.

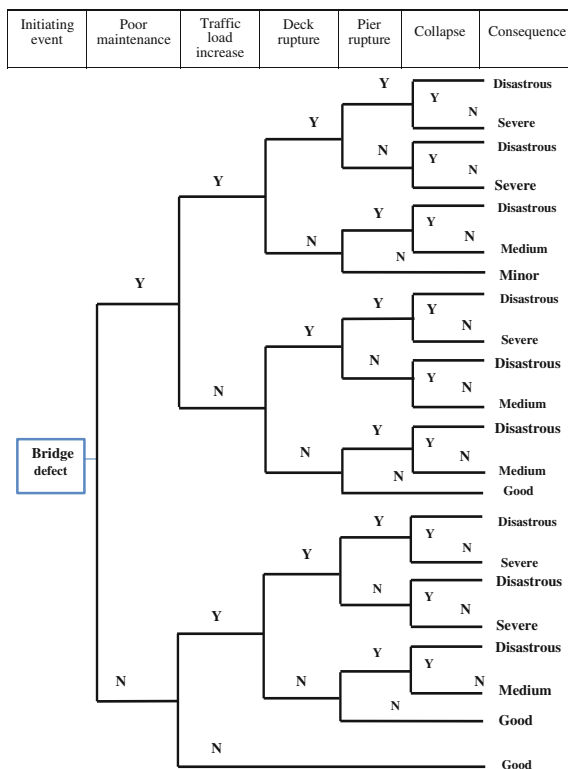


Fig. 8 Event tree model for consequences of bridge defect

5 Conclusion

The framework of BIMs was emulated from SIMS of offshore structure using the risk assessment concept in the analysis process which involving the development of risk matrix for future use in the decision making process of maintenance and repair work of bridge structure. In the purpose of developing the risk matrix which needs of quantification of probability and consequences of failure, the FT and ET method are among the available technique in the risk determination process. In this study, the combination of FT and ET method is used to model the bridge defect and its consequences of reinforced concrete highway bridge and the model is built as a part of risk analysis for the purpose of evaluating the risk of bridge failure. The FT is used to identify the causes and mechanism of bridge defect. The basic causes that may contribute to the bridge defect are carbonation, chloride contamination, traffic load, alkali silica reaction, temperature and sulphate which resulted in the form of failure mechanism such as crack, spalling and corrosion. Whereas, the consequences of bridge defect are identified through ET model. The outcomes of bridge defect is classified based on the how serious the bridge condition if collapse occur. The level of consequences is categorised as disastrous, severe, medium, minor and good.

Acknowledgments The authors are very grateful to the Public Work Department of Malaysia (JKR) for their support in terms of information and bridge data. The authors also would like to thank the Department of Higher Education, Ministry of Education, Malaysia and Universiti Teknologi MARA, Malaysia for sponsoring the post graduate student in this study.

References

1. S.M. Idris, Z. Ismail, *Appraisal of Concrete Bridges: Some Local Examples* (Jurutera, 2007), pp. 36–41
2. N.S. King, Malaysian Bridge—Status and Condition, Lecture Notes for Special Course on Bridge Assessment and Rehabilitation, Civil Engineering Department. Universiti Putra Malaysia, 2–4 Nov 1999
3. N.S. King, Key issues in bridge management. Special Issue of IEM J. Bridge Eng. (2001)
4. T.K. Weng, N.S. King, S.M. Hashim, Z. Jasmani, The JKR bridge management system (JKR BMS). 2nd regional conference on computer applications in civil engineering, Johor Bahru, 12–13 Nov 1991
5. W. Omar, N.S. King, S.M. Hashim, System approach in bridge management. 7th road engineering of Asia and Australasia (REAAA) conference, Singapore, 22–26 June 1992
6. D. Straub, J.D. Sorensen, M.H. Faber, Benefit of risk based inspection planning for offshore structures. OMAE'05 25th international conference on offshore mechanics and arctic engineering, Hamburg, 4–9 June 2006
7. P.E. O'Connor, J.R. Bucknell, S.J. DeFranco, H.S. Westlake, F.J. Puskar, Structural integrity management (SIM) of offshore facilities. 2005 offshore technology conference, Houston, 2–5 May 2005
8. M.M. Ettouney, S. Alampalli, *Infrastructure Health in Civil Engineering Theory and Components* (CRC Press, Taylor and Francis Group, Boca Raton, 2012)

9. J.D. Andrews, T.R. Moss, *Reliability and Risk Assessment* (Professional Engineering Publishing Limited, Bury St Edmunds, 2002)
10. American Petroleum Institute (API), *Risk Based Inspection, API Recommended Practice 580*, 2nd edn. (API Publishing Services, Washington, DC, 2009)
11. Joint Technical Committee, *Risk Management, AS/NZS 4360 Australian/New Zealand Standard*. 3rd ed. (Standard Australia International Ltd, Sydney, NSW and Standards New Zealand, Wellington, 2004)
12. W. Zhu, S. Setunge, R. Gravina, S. Venkatesan, Use of fault tree analysis in risk assessment of reinforced concrete bridges exposed to aggressive environments. *Concr. Aust.* **34**(1), 50–54 (2008)
13. R.A. Pullen, S. Flanagan, J.D. Andrews, Using fault trees to access risk in an operational environment. *J. Syst. Saf.* 1–3 (2001)
14. X. You, F. Tonon, Event tree and fault tree analysis in tunnelling with imprecise probabilities. *GeoCongress*, pp. 2885–2894, (2012)
15. T. Aven, *Risk Analysis Method Risk Analysis: Assessing Uncertainties Beyond Expected Value and Probabilities* (Wiley, New York, 2008)
16. W.S. Lee, D.L. Grosh, F.A. Tillman, C.H. Lie, Fault tree analysis, methods and applications—A review. *IEEE Trans. Reliab.* **R-34**(3), 194–203 (1985)
17. C. D. McDaniel, M. Chowdhury, W. Pang, K. Dey, Fault-tree model for risk assessment of bridge failure: case study for segmental box girder bridges. *J. Infrastruct. Syst.* **19**(3), 326–334 (2013)
18. P.A. Johnson, Fault tree analysis of bridge failure due to scour and channel instability. *J. Infrastruct. Syst.* **5**(1), 35–41 (1999)
19. P.R.M. Sianipar, T.M. Adams, Fault-tree model of bridge element deterioration due to interaction. *J. Infrastruct. Syst.* **3**(3), 103–110 (1997)
20. K.H. LeBeau, S.J. Wadia-Fascetti, Fault tree analysis of Schoharie creek bridge collapse. *J. Perform. Constructed Facil.* **21**(4), 320–326 (2007)
21. J. Susnik, L.V. Lyroudia, Z. Kapalen, D.A. Savic, Major risk categories and associated critical risk event trees to quantify (2011)
22. C.A. Ericson II, *Hazard Analysis Techniques for System Safety* (Wiley, New York, 2005)
23. G.K. Beim, B.F. Hobbs, Event tree analysis of lock closure risks. *J. Water Resour. Plan. Manage.* **123**(3), 169–178 (1997)
24. E.S. Hong, I.M. Lee, H.S. Shin, S.W. Nam, J.S. Kong, Quantitative risk evaluation based on event tree analysis technique: application to the design of shield TBM. *Tunn. Undergr. Space Technol.* **24**, 269–277 (2009)
25. N.S. King, K.M.S. Ku Mahamud, Bridge Problems in Malaysia. Seminar on bridge maintenance and rehabilitation, Kuala Lumpur, 24 Feb 2009

Experimental Investigation of Cold-formed Steel (CFS) Channel Material at Post Elevated Temperature

Fadhluhartini Muftah, Mohd Syahrul Hisyam Mohd Sani,
Ahmad Rasidi Osman, Mohd Azran Razlan and Shahrin Mohammad

Abstract Cold formed steel (CFS) is the popular structural material used in the building nowadays due to a variety of advantages in its manufacturing, fabrication and erection. The main objective of the study is to study the properties of the CFS at post elevated temperature. When this material is exposed to fire the steel material properties are degraded. Therefore, it is important to predict the degradation of material properties of CFS after exposed to elevated temperatures. The micro-structure test was found that after exposing to 1,000 °C temperature compared to normal CFS, the composition of eight elements in CFS has increased as Carbon, C is the highest at 129.7 %, meanwhile, thirteen elements are decreasing as Silicon, Si is the highest at 80.6 %. Results from tensile coupon test of post elevated temperature CFS shows that the cold formed steel that expose to fire may regain its yield strength within 10–60 % for range temperature 400–1,000 °C when compared to the Class 4 steel in EC3-1-2. The pattern of the reduction factor of CFS is similar to the hot rolled steel S460.

Keywords Cold-formed steel channel · Material · Post elevated temperature · Ultimate strength

F. Muftah (✉) · M.S.H. Mohd Sani · A.R. Osman · M.A. Razlan
Faculty of Civil Engineering, Universiti Teknologi Mara Pahang, Bandar Pusat Jengka,
Pahang, Malaysia
e-mail: fadhlu@pahang.uitm.edu.my; fadhluhartini@gmail.com

M.S.H. Mohd Sani
e-mail: msyahrul210@pahang.uitm.edu.my

A.R. Osman
e-mail: rasidi@pahang.uitm.edu.my

M.A. Razlan
e-mail: azran@pahang.uitm.edu.my

S. Mohammad
Faculty of Civil Engineering, Universiti Teknologi Malaysia, Johor Bahru, Johor, Malaysia
e-mail: Shahrin@utm.my

1 Introduction

Material properties of steel either hot-rolled or cold-formed are providing an important role in the performance of steel structural members for the purpose of design. Next, it is significant to discover the mechanical properties of steel structural member after knowing the material properties. The main important to study the material properties of Cold-formed Steel (CFS) under elevated temperature because it has a small value of section factors such as the ratio of heated volume to cross sectional area of the structural member was reduce the resistance of unprotected CFS. The need of post fire study of structural material is to determine the rehabilitation method and repairing strategy on the structure that facing the fire of heating condition. The different stage of temperature should be studied to evaluate the current status of the material after exposing to high temperature. Thus determine the reliability of using the material for steel structure is known as recyclable material. In other hands, the properties of steel after exposed to high temperature could be different at the steel channel section due to stress residual results from the cold forming process. Therefore, in these study four (4) different locations at channel CFS has been identified as samples to determine the mechanical strength after expose to high temperature.

Malaysia is in the transition process in adoption the structural design guideline from British Standard (BS), Malaysian Standard (MS), ISO standards, ASTM, ACI, JIS, AS/NZ as MS to Eurocode. A lot of effort needs to be put to implement it includes in the research work. Hence the verifying the local material sources such as CFS to the current code of practice is important to give safe, reliable design, and rehabilitation work. CFS are usually are made by class 4 cross sections, reduce post-elastic strength consequence reduces ductility. It insufficient plastic rotation capacity for formed plastic hinge, hence the elastic global frame analysis is usually interest [1]. The section also experiences in occurrence of local buckling before reaching the yield strength in one or more part in cross section. Eurocode 3-1-2 [2] has tabulated the reduction factors relative to its ambient, strength for Class 4 cross section hot rolled and welded sections, however CFS is not available.

Previous research on the material properties has been mostly focused on hot-rolled steel, and limited data are available for the mechanical properties of cold-formed steel at elevated temperatures [3]. Chen and Young [4] are studied of steady and transient tensile tests at different temperatures of range 20–1,000 °C for cold-formed steel grade G550 with plate thickness of 1.0 and G450 with plate thickness of 1.9 mm. From the experiment, they established a combined equation at elevated temperature for yield strength, elastic modulus, ultimate strength and ultimate strain of CFS. Wei and Jihong [5] is reported the ductility of the G550 CFS decreases with increasing temperature below 200 °C and showed the ultimate strength at 200 °C is higher than at 100 °C during the steady state test. Kankanamge and Mahendran [6] is determined the mechanical and material properties of cold-formed steel with different grades and thickness on elevated temperature in the range of 20–700 °C. They are found that some improvement of the equation to predict the

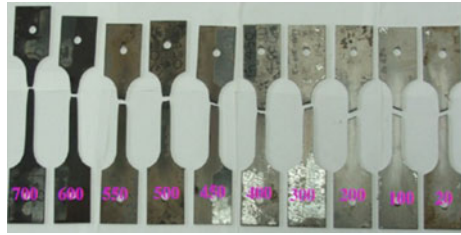


Fig. 1 The failure modes of coupon tensile test specimens at elevated temperature [6]

yield stress, stress strain curves and elastic modulus for difference grades and thickness. Figure 1 is shown the failure modes of tensile specimens at elevated temperatures for CFS thickness 1.90 mm grade 450.

Qiang et al. [7] reported that currently the standard of reuse of steel structure after exposed to fire is still unavailable. They have conducted post fire test on very high strength steel S960. Therefore, it is important to investigate the properties of cold-formed steel material at post elevated temperatures. This paper presents the details of an experimental study of cold-formed steel at post elevated temperatures approximately up from 200 to 1,000 °C.

2 Experimental Investigation

2.1 Test Specimen

Two channel types were used in this study named C75.10 and C75.0.75. The description of the channel section listed in the Table 1.

The specimens of coupon for tensile test are cut from the CFS channel section. It was cut from 4 locations from the cross-section as shown in Fig. 2. FT is denoted for flat top, CT is corner top, FS is flat side, and CB is corner bottom. The specimen size was prepared as per ASTM Standard E21-92 [8] and Australian Standard AS 2291 [9].

Table 1 The dimension of the two CFS channel in the study

Designation	B (mm)	D (mm)	T (mm)
C75.10	38	75	1
C75.0.75	38	75	0.75

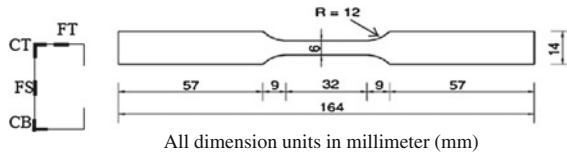


Fig. 2 Coupon test specimen taken location and its dimension

2.2 Process of Testing Procedure

The specimens have been passing through two stages of condition. The first condition is heating condition to simulate the cold formed steel under heating in the furnace. Then the specimens were cooled to ambient condition for a period of time until it achieves ambient temperature. Then, the cooled specimens were tested for tensile until it fails.

2.3 Elevated Temperature Exposure

The specimen is heated under elevated temperature in furnace Carbolite Furnace CFS, 1100 with a maximum temperature up to 1,100 °C. The preselected temperatures in this study were up to 1,000 °C with a range of 200 °C. The test at ambient temperature (25 °C) as a control to compare the post fire material strength of cold formed steel. All specimens have been exposed at preselected temperature for 10 min, which it was cold at ambient temperature [7]. In this study, thermocouple is not located in the furnace since the specimen temperature assumes same as the environment temperature as the high conductivity of steel and thin in thickness [10]. The heating rate of the specimen for 200 and 400 °C is 0.38 °C s⁻¹, 600 and 800 °C is 0.29 °C s⁻¹, and 1,000 °C is 0.21 °C s⁻¹. The observation of the specimens colour was made right after the heating.

2.4 Tensile Coupon Test

The tensile coupon test was done in Universiti Teknologi MARA, Pahang. The cooled specimens at ambient temperature were tested for tensile tests until failure using Universal Tensile Machine (UTM) with maximum load of 50 kN under displacement control rate of 1 mm/min.

2.5 Chemical Test at Post Elevated Temperature

The GDS-Chemical analysis of metal testing services has been used to determine the metal based properties of CFS. The sample was taken randomly in the section that is square in shape at size 20 mm and the thickness is 0.75 and 1.0 mm. The galvanized coating was removed prior the test to get the material base metal. Both CFS at normal temperature and post elevated temperature at 1,000 °C was tested.

3 Result and Discussion

3.1 Chemical Properties Evaluation

The material chemical composition of CFC is consisting of 22 known chemical elements. The first five highest percent of element is found in CFS are Iron, Fe, Nickel, Ni₂, Zirconium, Zr, Carbon, C, and Manganese, Mn as in Table 2. Fe₂ are not found in CFS. All elements are shown a difference when exposing to 1,000 °C temperature except Plumbed, Pb as shown in Fig. 3. Eight elements are increased in composition as Carbon, C is the highest at 129.7 %. Thirteen elements are decrease in composition as Silicon, Si at 80.6 %.

Table 2 The chemical composition of CFS material

Weight (%)	C	Sb	S	P	B ₂	Sn	B	Fe	Pd	Zr	Co
Normal temp.	0.0505	0.0162	0.0085	0.0309	0.0015	0.0506	0.00106	99	0.0112	0.178	0.00753
1,000 °C	0.116	0.0285	0.0138	0.0358	0.00166	0.0539	0.00112	99.2	0.0112	0.149	0.00223
Weight (%)	Sn ₂	Nb	Cr ₂	V	Ti	Mn	Al	Ni ₂	Mo	Cu ₂	Si
Normal temp.	0.0339	0.00615	0.0213	0.0189	0.0274	0.175	0.0182	0.314	0.00753	0.0903	0.0145
1,000 °C	0.0283	0.00508	0.0173	0.0144	0.0194	0.111	0.00966	0.152	0.00351	0.0352	0.00281

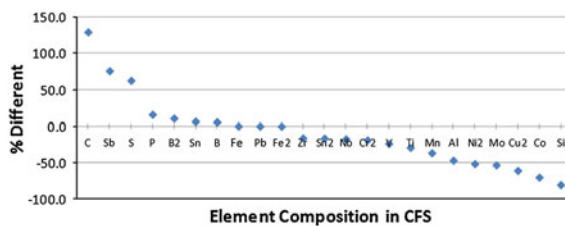


Fig. 3 The different in chemical composition of CFS after expose to 1,000 °C

3.2 Weight Reduction and CFS Observation

The change in colour of the specimens was observed right after it takes out from the furnace as shown in Fig. 4. At 200 and 400 °C the CFS change to light white colour as illustrated in Fig. 5. At 600 °C, CFS change white and yellow on the surface, but black colour was observed at its outline as shown in Fig. 6. At 800 °C the CFS change to yellow colour and the coating was peeling out as presented in Fig. 7. Meanwhile, Fig. 8 showed the specimen at 1,000 °C CFS was changed to dark yellow and the coating was lost and burned. All weights measured the same value for before and after heated for all temperatures. No significant reduction in the weight of sample in this study.

Fig. 4 The specimens at the furnace



Fig. 5 The coupon specimen after expose to 400 °C temperature



Fig. 6 The coupon specimen after expose to 600 °C temperature



Fig. 7 The coupon specimen after expose to 800 °C temperature



Fig. 8 The coupon specimen after expose to 1,000 °C temperature



4 Post Elevated Temperature Test Results

In this study the three important material properties were determined i.e. yield strength, Elastic modulus, and Ultimate strength.

4.1 Yield Strength

According to EC3-1-5 [11], the average yield strength can be calculated using the following equation. The design yield strength of carbon steel is determined at 0.2 % of plastic strain at ambient and higher strain are acceptable for fire conditions at 2 % as illustrated in Fig. 9a, b. However, 0.2 % proof strain is recommended for CFS with Class 4 cross sections. The average yield stress at ambient is 452.75 MPa for C75.10 and 472.75 MPa for C75.075 as it designing as G450 as shown in Fig. 10. The significant consistence reduction of yield strength is observed for steel post heated up to 400 °C. This is because by the strength integrity in the part of the cross section is still strong. Beyond this, the strength is inconstant for various positions in the section due to losing in its integrity. Taking the average value of the yield strength, the reduction in yield strength for both sections are quite similar up to 400 °C. Reduction factor for 200 °C is on average 0.86 and at 400 °C is 0.72 to its ambient strength. Table 3 is detail value of reduction factor relative to its ambient strength regard its location in the cross section.

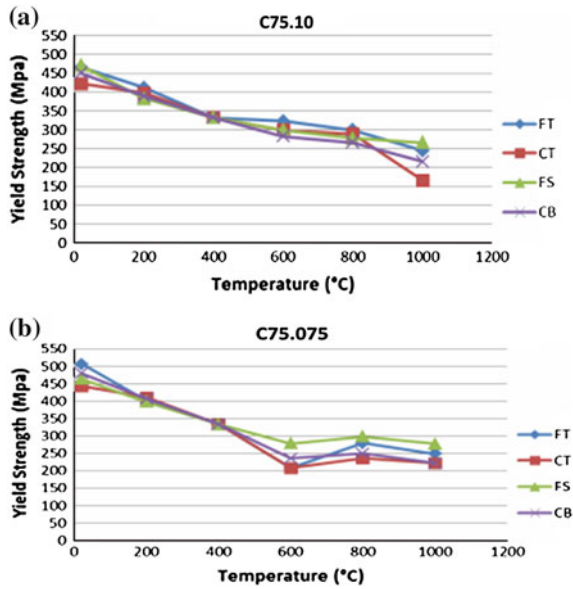


Fig. 9 a and b. Yield strength according to position in section C75.10 and C75.075 respectively

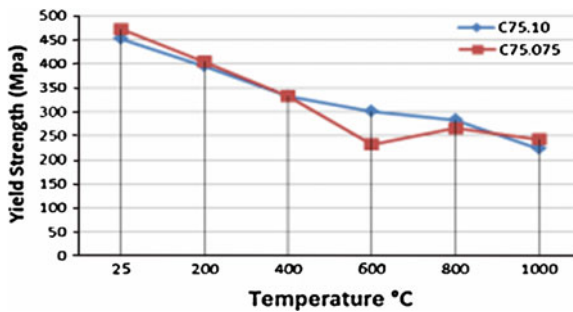


Fig. 10 Average yield strength in the both sections

Table 3 Reduction factors of yield strength

Temperature (°C)/location	Yield strength (MPa)—1 mm				Yield strength (MPa)—0.75 mm			
	FT	CT	FS	CB	FT	CT	FS	CB
25	1.000	1.000	1.000	1.000	1.000	1.000	1.000	1.000
200	0.884	0.941	0.813	0.865	0.794	0.928	0.860	0.850
400	0.715	0.787	0.707	0.738	0.658	0.752	0.719	0.695
600	0.693	0.709	0.637	0.627	0.411	0.470	0.600	0.493
800	0.644	0.683	0.590	0.590	0.551	0.533	0.644	0.522
1,000	0.526	0.394	0.567	0.479	0.492	0.501	0.600	0.463

4.2 Elastic Modulus

The channel sections at normal temperature are resulting in 185 GPa for both sections which can be considered as 200 GPa. After exposing to high temperature, the Elastic Modulus of the CFS is suddenly dropped about 75 % of its original elastic modulus as shown in Fig. 11. It shows that CFS becomes softer and easy to deform under low load after exposing to high temperature. This result was reversed to the study conducted by Qiang et al. [7] on high strength steel S960. They found that after cooled down 600 °C S960, steel can regain its elastic modulus. The steel recovers 70 and 60 % its elastic modulus after cooling up to 800 and 1,000 °C respectively.

4.3 Ultimate Strength

The ultimate strength of CFS is 644 MPa and 650 MPa for C75.10 and C75.075 respectively as shown in Fig. 12a, b. The ultimate strength is generally reduced gradually as the temperature exposure is increasing. As shown in Fig. 13, the reduction in ultimate strength is inconsistent across the cross section. It concluded that, the strength at peak is not integrated into the part of the cross section due to change in material composition as the steel is burned. The results in ultimate strength for both C75.10 and C75.075 are similar. The thickness does not affect the ultimate strength of CFS after exposed to high temperature. The value reduction factor relative to ultimate strength at ambient as tabulated in Table 4.

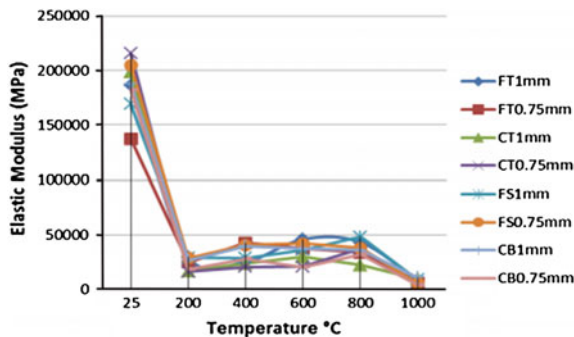


Fig. 11 The elastic modulus of normal and high temperature

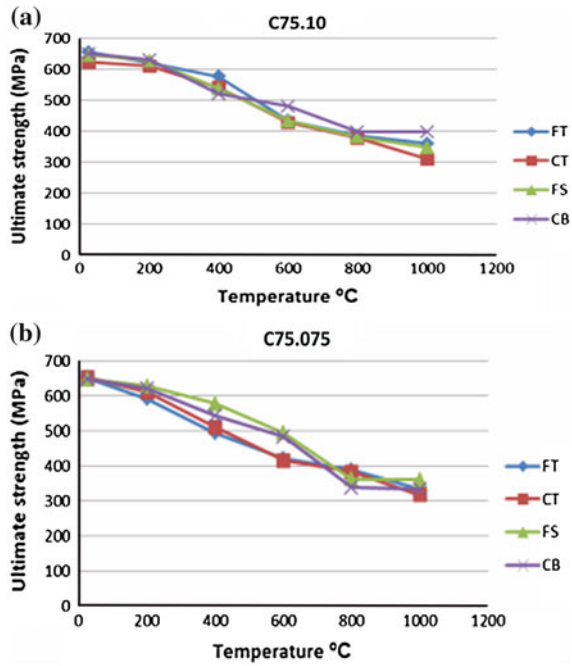


Fig. 12 a and b. The ultimate strength according to position in section C75.10 and C75.075 respectively

Fig. 13 The average ultimate strength in the both sections

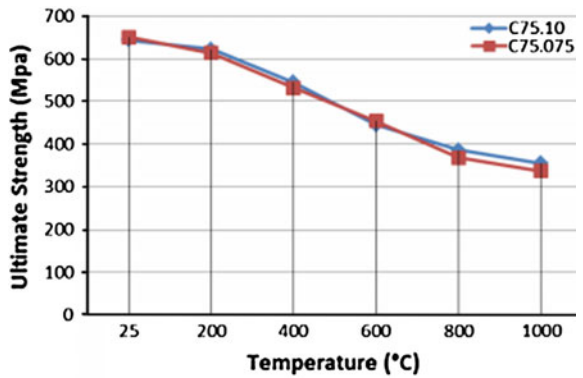


Table 4 The reduction factors of ultimate strength

Temperature (°C)/location	Ultimate strength (MPa)—1 mm				Ultimate strength (MPa)—0.75 mm			
	FT	CT	FS	CB	FT	CT	FS	CB
25	1.000	1.000	1.000	1.000	1.000	1.000	1.000	1.000
200	0.948	0.981	0.972	0.969	0.909	0.936	0.968	0.957
400	0.880	0.870	0.833	0.800	0.759	0.783	0.891	0.837
600	0.663	0.687	0.670	0.739	0.646	0.637	0.763	0.744
800	0.588	0.607	0.591	0.613	0.597	0.588	0.558	0.521
1,000	0.550	0.499	0.540	0.611	0.512	0.485	0.556	0.513

4.4 Comparison of Testing Results to Steel Structure Design Standard of EC3-1-2

The steel structural fire resistance can be assessed using EC3-1-2 for structural that been designed in ambient temperature using EC3-1-1 [12]. EC3-1-2 [2] is meant for steel structure with passive fire protection. It is also covered for cold formed steel members and sheeting within the scopes of EN 1993-1-3 [13]. The steel thermal material properties in EC3-1-2 [2] are only specifying the stainless steel and carbon steel material. Therefore the cold formed steel is parked under carbon steel. The steel material model from EC3 has been used in designing steel structures in Malaysia. The reduction factors for Class 4 steel section in EC3 is used to compare to the post high temperature strength of CFS for both sections as shown in Fig. 14. EC3 has given the reduction factor for steel at elevated temperature. It found that, the reduction factor for post high temperature exposure for both samples are resulting in similar value to the EC3-1-2 [3] for temperature below 300 °C at elevated temperature. It shows that, the yield strength remains same for lower temperature below 300 °C after the CFS been cool. However, the CFS has recovered the yield strength for temperature 300–1,000 °C after it’s been cool.

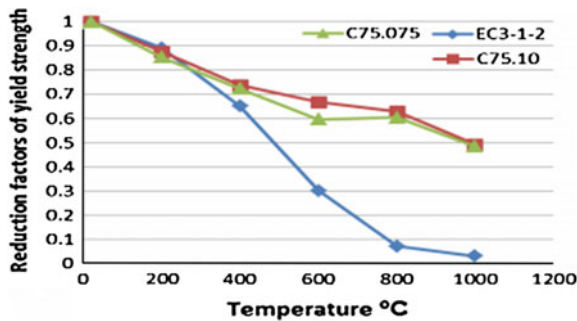


Fig. 14 The reduction factors of yield strength of both sections and compared with EC3

4.5 Comparison of Testing Results to Other Researchers

The comparison of the post fire study of cold formed steel can be compared to the other researches testing result. The study of the cold formed steel at elevated temperature has been conducted by many researches. But the research data of the post fire study that is available are for hot rolled only. Therefore the comparison could be done in the cold-formed steel under elevated temperature for belong to the same grade as shown in Fig. 15.

The yield strength of cold formed steel after exposed to fire are compared to elevated temperature in the form of reduction factor. The yield strength of cold formed steel is significantly dropping when compared to data from Dolamune and Mahendran [14] from the same grade G450 and Ranawaka and Mahendran [15] for G550. However, it well suits to Jihong and Wei [16] for lower grade 345 MPa. This comparison are not really suitable for both samples are in different condition. In other hands, the pattern of post fire of hot rolled steel S960 was conducted by Qiang et al. [7] and was compared to S460 and S960 from research data and mild steel S235 and S275 from British design standard BS 5950 [17] as shown in Fig. 16. It has shown that S460 having same recovering in the yield strength pattern of cold formed steel after expose to fire.

A predictive equation is developed for post fire yield strength reduction factor for C75 of grade 450 MPa as shown in Fig. 17. Due to the abrupt change of reduction factor, two equations are proposed as stated in Eqs. 1 and 2. A good predictive equation to the results with regression value of $R^2 = 0.98$ and 0.9 for Eqs. 1 and 2 respectively. Qiang et al. [7] has also produced a set of yield strength reduction factor that also consists of two equations with a range of temperature 20–600 °C, and 600–1,000 °C.

$$20 \leq \theta \leq 600$$

$$\frac{f_{yP\theta}}{f_y} = 3 \times 10^{-7}\theta - 0.0008\theta + 1.0179 \tag{1}$$

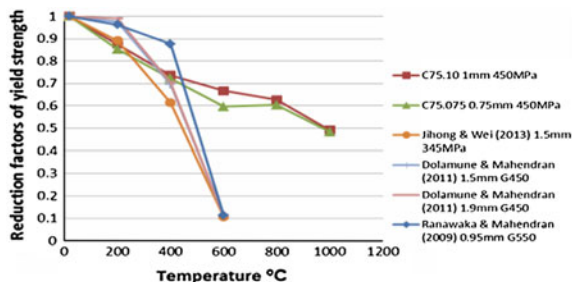


Fig. 15 The comparison of test sample to other steel material at elevated temperature

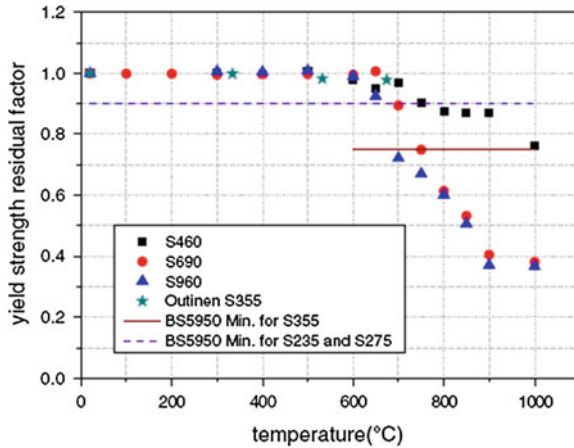


Fig. 16 Residual factor of yield strength by Qiang et al. [7]

$$600 < \theta \leq 1,000$$

$$\frac{f_{yP\theta}}{f_y} = -1 \times 10^{-6}\theta + 0.0019\theta + 0.0095 \tag{2}$$

The study of post fire of cold formed steel is still very limited since the usage is very high. Fire causes can be happened even for small fire case, and the potential to reuse the steel is there. The lack of information on this subject can cause the safety of the structure are not guarantee, beside waste also can happen if the steel still can be used. The discussion and equation is only applicable to predict the yield strength. More accurate data and varieties of steel can be used to confirm the post fire properties of cold formed steel.

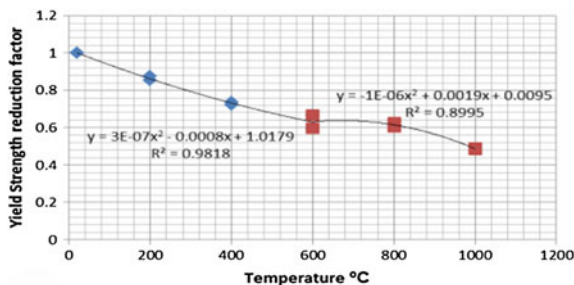


Fig. 17 The yield strength reduction factor for C75 for grade 450 MPa

5 Conclusions

From the chemical composition result, all elements in Cold-formed Steel (CFS) in normal temperature and 1,000 °C temperature are shows a difference. All weights were measured for before and after heated for all temperature specimens and concluded is same. Reduction factor for yield strength for 200 and 400 °C temperature is 0.86 and 0.72 respectively to its ambient strength. The Elastic modulus of the CFS is decreased 75 % of its original elastic modulus when expose to high temperature. In addition, the reduction in ultimate strength is illustrated not consistent across the cross section and also showed the results for both C75.10 and C75.075 of ultimate strength are similar.

Furthermore, the cold formed steel that exposes to fire may regain its yield strength within 10–60 % of range temperature 400–1,000 °C when compared to the Class 4 steel in EC3-1-2 [2]. The pattern of reduction factor is similar to the hot rolled steel S460. Two predictive equations have been produce for range 20–600 °C, and 600–1,000 °C that's also similar to hot rolled steel. Finally, the study of post elevated temperature can be extended to determine the properties of CFS in column or beam structure. With the result, the CFS can be compared with Eurocode or other standard.

Acknowledgments The authors gratefully acknowledge the financial support from the Universiti Teknologi Mara Pahang under Dana Kecemerlangan Grant. Thanks also extend to Faculty of Civil Engineering and Faculty of Wood Technology for providing machinery and equipment. Special thanks are extended to the lecturer and technician of UiTM Pahang and UTM Johor Bharu for their help during the experimental program.

References

1. D. Dubina, V. Ungureanu, R. Landolfo, *Building Framing, in Design of Cold-formed Steel Structures: Eurocode 3: Design of Steel Structures. Part 1–3—Design of Cold-formed Steel Structures*, 1st edn. (Wiley-VCH Verlag GmbH & Co. KGaA, Weinheim, 2012)
2. Eurocode 3 Part 1-2 (EN 1993-1-2), *General Rules—Structural Fire Design* (2005)
3. J.H. Lee, M. Mahendran, P. Makelainen, Prediction of mechanical properties of light gauge steels at elevated temperatures. *J. Constr. Steel Res.* **59**(12), 1517–1532 (2003)
4. J. Chen, B. Young, Experimental investigation of cold-formed steel material at elevated temperatures. *Thin-Walled Struct.* **45**, 96–110 (2007)
5. C. Wei, Y. Jihong, Mechanical properties of G550 Cold-formed steel under transient and steady state conditions. *J. Constr. Steel Res.* **73**, 1–11 (2012)
6. N.D. Kankanamge, M. Mahendran, Mechanical properties of cold-formed steels at elevated temperatures. *Thin-Walled Struct.* **49**(1), 26–44 (2011)
7. X. Qiang, F.S.K. Bijlaard, H. Kolstein, R. Xia, Experimental study on high strength structural steel S460 in fire and after cooling down. *IES J. Part A: Civil Struct. Eng.* **6**(2), 104–111 (2013)
8. ASTM E21-92, *Standard Test Methods for Elevated Temperature Tension Tests of Metallic Materials* (1998)
9. AS 2291-2007, *Metallic Materials—Tensile Testing at Elevated Temperatures* (2007)

10. J.L. Hoon, M. Mahendran, P. Makelainen, Prediction of mechanical properties of light gauge steels at elevated temperatures. *J. Constr. Steel Res.* **59**(12), 1517–1532 (2003)
11. Eurocode 3 Part 1-5 (EN 1993-1-5), *General Rules and Rules for Building* (2005)
12. Eurocode 3 Part 1-1 (EN 1993-1-1), *General Rules—Plated Structural Elements* (2006)
13. Eurocode 3 Part 1-3 (EN 1993-1-3), *General Rules—Supplementary Rules for Cold-formed Members and Sheeting* (2006)
14. K. Dolamune, M. Mahendran, Mechanical properties of cold-formed steels at elevated temperatures. *Thin-Walled Struct.* **49**(1), 26–44 (2011)
15. T. Ranawaka, M. Mahendran, Experimental study of the mechanical properties of light gauge cold-formed steels at elevated temperatures. *Fire Saf. J.* **44**(2), 219–229 (2009)
16. Y. Jihong, C. Wei, Elevated temperature material degradation of cold-formed steels under steady- and transient-state conditions. *J. Mater. Civ. Eng.* **25**, 947–957 (2013)
17. BS 5950-1:2000, *Structural Use of Steelwork in Building Code of Practice for Design. Rolled and Welded Sections* (2000)

The Thermal Stability Property of Bio-composites: A Review

Z.A. Rasid

Abstract Composite material has played important role as an alternative material to metal in many industries. However as the growing of environmental concern throughout the world becomes so high, the interest on the green or bio-composite as to replace fossil based composite has also increased. Bio-composite, a type of composite materials that constitutes of natural fibres and bio-polymers, comes with the environmental advantages of being renewable, biodegradable and sustainable. However green composites also come with several disadvantages such as low in mechanical properties, low in thermal stability and high in water absorption. The level of these disadvantages vary from one bio-composite to another since there are lots of factors that determine these properties. Due to this, a large number of researches have been conducted to improve these properties with the aim of applying bio-composites as structural components. In this paper, a review is made on the thermal stability property of the bio-composites. The review includes the discussion on tests conducted to study the instability behavior of the bio-composites and factors that will improve the thermal stability of bio-composites. It was found that the addition of the high volume fraction of fibres to the bio-composites may not increase the thermal stability of the bio-composite. However, thermal stability can be improved by giving chemical treatments to the bio-composites that improves the compatibility of the fibres and the polymers of the bio-composites.

Keywords Green composite • Bio-composite • Bio-polymers • Natural fibres • Thermal stability

Z.A. Rasid (✉)

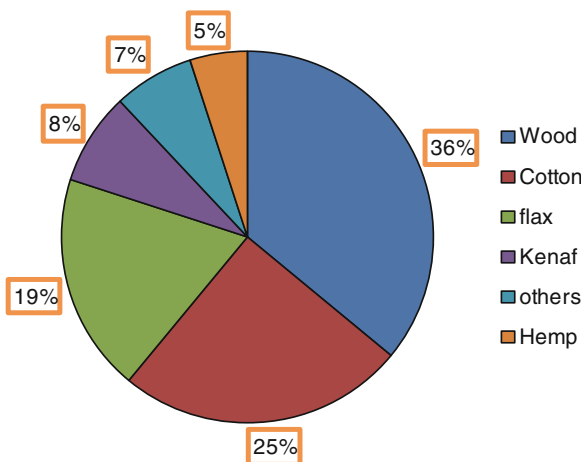
Department of Mechanical Precision Engineering, Malaysia-Japan International Institute of Technology, Universiti Teknologi Malaysia, Kuala Lumpur, Malaysia
e-mail: zainudin@ic.utm.my

1 Introduction

Bio-composites have attracted tremendous attention among researchers of late due to its environmental friendly advantages of being renewable, biodegradable and sustainable. These advantages of the bio-composites provide motivation for researchers that have been looking for a replacement to fossil based composites that pollute the environment. Bio-composite which is also known as green composite [1, 2] is composite that is formed from natural fibre and bio-polymer. Natural fibre can be based on vegetable, animal and mineral and can also be man-made. Compare to other natural fibres, the man-made natural fibre has high quality that guarantees sufficient reproducibility of its mechanical characteristics [3]. Figure 1 shows the use of several natural fibres for composite application as interior parts of automobiles and lorries in Europe [4]. Others in Fig. 1 refers mainly to jute, coir, sisal and abaca.

Polymer can be classified into fossil based, bio-based and partially bio-based such as shown in Fig. 2 [5], where each of these categories can be further grouped into bio-degradable and non-biodegradable. Bio-polymer that constitutes the green composite is bio-based and bio-degradable. Bio-polymers can be classified into thermoplastic natural starch (TPS) such as corn, sago and wheat starches and starch derivatives such as the polylactide acid (PLA), poly-l-Lactide acid (PLLA), polyhydroxyalkanoate (PHA), polyhydroxybutyrate (PHB), polyhydroxybutyrate-co-valerate (PHBV) and cellulose acetate (CA) which can be cellulose acetate butyrates (CAB) and cellulose acetate propionate (CAP). PLA and PLLA due to their better mechanical properties are the most commercialized bio-polymers [6]. The good compatibility between natural fibre and bio-polymer which can result in improved properties of bio-polymers is considered possible because both constituents have chemical similarity [7]. Numerous researches on bio-composites are

Fig. 1 Pie chart on the use of natural fibres for composites in the European automotive industry 2012 [4]



Bio-degradable	PBS PBSL PBSA PCL PBST PBSAT PTMAT PCBS	Starch blends (with biodegradable fossil based) PLA blends (with biodegradable fossil based)	PLA, PLLA PHB, PHBV CA, CAP, CAB
Non-biodegradable	PE PP PET PBT PA6,66 PVC PUR ABS Epoxy Synthetic rubber	Starch blends (with PE) PA610 PTT (From biobased 1,3-PDO) PBT (From biobased succinct acid) PA6,66 (From biobased ethylene) PVC (From biobased ethylene) PEIT (From sorbitol and bioethylene) PUR (From biobased polyol) Epoxy Resin (From biobased glycerol) ABS (From biobased succinct acid) SBR (From biobased succinct acid) Alkyde resin	Biobased PE PA11 Biobased PB
	Fossil based	Partial bio-based	Bio-based

Fig. 2 Classification of polymers [5]

such as on kenaf-PLA [8], jute-PHB [9], hemp-CAB [10], sisal-starch [11], bamboo-PLA [12] and flax-PLLA [13].

Green composite is renewable and sustainable because its' constituents originated from living trees such as kenaf, hemp, sago and corn trees which can always be re-planted. Natural fibre such as kenaf and bio-polymer such as starch come in abundance as contrast to the fossil based composites that are known to have limited and irreplaceable resources. At the same time, by the acts of enzymes, bacteria and fungi, green composite can be biodegraded to biomass or biological by-products. Besides being not degradable, the fossil based polymers will cause the release of a huge amount of gas and will lead to environmental pollution and global warming when they are disposed [14].

Natural fibres come at lower density, weight and price and they are less abrasive to machine as compared to glass fibre. Due to its lower weight, a typical natural fibre has specific mechanical properties comparable to mechanical properties of glass fibre. Furthermore natural fibre is safe if compared to glass fibre that gives health risk to human if inhaled. Certain bio-polymers such as PLA have comparable mechanical properties to properties of fossil based polymers such as poly-propylene. Even though processed bio-polymers such as PLA and PLLA are expensive, combining them with cheaper natural fibres will offset the overall cost of the green composites [14].

The advantages of green composite are so attractive environmentally and economically that numerous researches have been conducted to improve the setbacks that come along with these advantages. The main disadvantages of the green composite are having low mechanical properties, thermal instability and remarkable sensitivity to moisture [15]. The low mechanical properties and thermal instability are due to poor wettability or dispersion of natural fibres within matrix and poor interfacial adhesion between the two constituents of the bio-composites. Natural fibres have strong inter-fibre hydrogen bonding that holds them together [16]. Good dispersion of the fibres within matrix and good interfacial adhesion between the constituents are important to ensure load transfer from polymer to fibre occurs effectively. These two weaknesses are mainly attributed by poor compatibility between the two constituents of the bio-polymer [17]. The incompatibility between constituents occurs because polymers such as PLA are hydrophobic while natural fibres are mostly hydrophilic. Natural fibres are hydrophilic because they allow hydrogen bonding to occur between the free hydroxyl groups of cellulosic molecules with water molecules [18]. Thermal instability of bio-composite includes degradation of crystallinity, mass and organoleptic degradation properties such as odor and colours. It also results in gaseous products upon degradation typically above 200 °C which can create high porosity, low density and reduced mechanical properties [19]. As a consequence to their low mechanical properties, green composites are hardly used in structural applications and they are limited to furniture, packaging, pharmaceutical and non-structural automotive applications. The hydrophilic nature of the natural fibres has also caused the bio-composite to have high moisture absorption that can also result in property reduction of the bio-composites while in service. Another setback of bio-polymers comes from polymers such as PLA. PLA besides having great mechanical properties is a brittle material. To be applied in structural applications, PLA has been modified using plasticizer such as polyethylene glycol (PEG) to improve its elongation and impact properties.

Numerous studies on green composites are devoted to improving mechanical, thermal stability and water absorption properties of the bio-composites. This is done by controlling aspects of the fibre and bio-polymers (the individual factor), improving wettability and surface adhesion between fibres and polymers (the incompatibility factor) and controlling the manufacturing process of the bio-composite. This study is to review these numerous research works on the bio-composites focusing on the improvement of the thermal stability of the bio-composites. Factors that improve the properties of the bio-composites are firstly discussed. The results on several tests conducted on bio-composites to determine the thermal instability such as the differential scanning calorimetry (DSC), the dynamic mechanical analysis (DMA), the thermogravimetric analysis (TGA) and the heat deflection temperature (HDT) are then analyzed.

2 The Improvements on the Bio-composites

2.1 The Individual Factors

It is essential to consider properties of several natural fibres before choosing the best reinforced fibre to be suited for bio-composites. The important fibre properties to be considered include physical, mechanical, thermal sensitivity, moisture absorption capability, wettability and adhesive properties of fibres to polymer matrix [20]. These properties depend on fibres’ characteristics such as geometry, degree of polymerization, fibril angle and most importantly the chemical composition of the fibres [21] that affects the hydrophilic nature of the fibres. Table 1 shows several physical, mechanical and moisture absorption properties of several most commonly used natural fibres along with properties of E-glass for comparison purpose. It shows that some of the natural fibres such as hemp, kenaf and sisal posse specific Young’s modulus (E/d) and elongation at failure properties that are at par to the corresponding properties of the E-glass fibre. It also shows one main advantage of natural fibres where the density of the glass fibre is about 80 % more than most natural fibre.

The chemical composition of a fibre affects the mechanical, thermal, moisture absorption and viscoelastic properties of the fibre [22]. A natural fibre is the lignocellulosic and chemically composed of mainly cellulose, hemicelluloses or pectin, lignin and waxes. Table 2 shows the chemical compositions of several natural fibres but these values may vary from other listing due to different growing and harvesting conditions of the fibres. The hemicelluloses part of the fibre is fully amorphous that it is partially soluble in water and alkaline solutions. The lignin part of a fibre cements together the distinct cells of the fibre while the waxes need to be eliminated for good adhesion of the fibre within bio-polymers [21].

Table 1 Properties of the natural fibres as compared to the petroleum based fibres [5, 34, 35]

	Density (g/cm ³)	Tensile strength (MPa)	E (GPa)	Spec. E (E/d)	Elong at failure (%)	Moisture absorption (%)
E-glass	2.55	2,400	73	29	3	–
Abaca	1.5	885	27–32	18–21	–	–
Bamboo	0.6–1.1	140–230	11–17	10–28	–	8.9
Coir	1.25	220	6	5	15–25	10
Cotton	1.52	400	12	8	3–10	8.5
Flax	1.4	60–80	60–80	24–46	1.2–1.6	7
Hemp	1.48	550–900	70	47	1.6	8
Jute	1.46	400–800	10–30	7–21	1.8	12
Kenaf	1.45	930	53	36.5	1.6	–
Ramie	1.5	500	44	29	2	12–17
Sisal	1.33	600–700	38	29	2–3	11

Table 2 Chemical composition of several fibres [5, 21]

	Cellulose (wt%)	Hemi-cellulose (wt%)	Lignin (wt%)	Waxes (wt%)	Moisture absorption (%)
Bamboo	26–43	30	21–31	–	8.9
Coir	32–43	0.15–0.25	40–45	–	10
Cotton	85–90	5.7		0.6	8.5
Flax	71	18.6–20.6	2.2	1.5	7
Hemp	68	15	10	0.8	8
Jute	61–71	14–20	12–13	0.5	12
Kenaf	72	20.3	9	0.5	14
Ramie	68.6–76.2	13–16	0.6–0.7	0.3	12–17
Sisal	65	12	9.9	2	11

The geometry factors that affect the properties of a bio-composite include the diameter, length, aspect ratio, fibre loading and the cell-wall thickness of a fibre. The diameters of the chopped fibres in the manufacturing of bio-composites are usually varied and an average value is taken for analysis purpose. Low in diameter and high in length of a fibre will result in a high aspect ratio of that fibre. This can promote better adhesiveness and improved mechanical properties of the bio-composite. For good results, fibre aspect ratio must be in the range of 100–200 [23]. The irregular shape and length of the fibres at the same time can improve flexural strength of the bio-composite [19]. Fibres can only contribute to strengthen the composite performance if the fibre length is longer than the critical fibre length [23, 24]. At the same time, very long fibres can cause fibre entanglement such that the properties of the bio-composite can be reduced. The processing of the composite may cause damage to the fibres and reduce the average length of the fibre. This can be due to the high shear stress developed during the processing stage of the composite. Furthermore, the existence of naturally developed microvoids and surface kink bend may also cause the surface degradation [25]. In their study [25], the reduction of 74 % in average length of the fibres during the processing stage may occur. The processing of bio-composite may also align the fibres to be in the flow direction such that the properties of the bio-composite will not be the same in all direction.

2.2 The Incompatibility Factor

Being hydrophilic, natural fibres are incompatible with hydrophobic bio-polymers such as PLA. The poor incompatibility between the two constituents has caused poor dispersion of fibres within matrix and weak adhesion between the two constituents. Polar hydroxyl groups on the fibre surface have difficulty forming a well bonded interface with a non-polar matrix because the hydrogen bonds tends to form

bonds with each other and prevent the wetting of the filler surface [26]. The lack of interfacial interactions leads to internal strains and porosity, low mechanical properties of the bio-composites and environmental degradation of the bio-composites [21]. At the same time, the dispersion of the fibres depends on the viscosity of the polymer and the surface tension of both materials where the surface tension of the polymer must be as low as possible or at least lower than the surface tension of the fiber [21]. Strategy to improve the incompatibility issue is through one of the following ways: fibre surface modification, the use of interface-active additives and matrix modification [7]. The surface modification of the fibres involves grafting functional groups on the fibres or coating fibers with additives that carry suitable functional groups in order to make the fibre surface more compatible with the matrix material [7]. Fibre surface modification can be classified into physical and chemical methods. The physical treatments are to change structural and surface properties of the fibre and thereby influence the mechanical bonding in the matrix [21]. The mechanical properties and the water absorption properties are then improved. The physical treatment includes the electric discharge such as cold plasma and corona treatments. In the corona and cold plasma treatment, surface oxidation is used to improve surface energy of the cellulose fibres. In the chemical treatment, reagents that contain functional groups that are capable of bonding with hydroxyl from the natural fibres are used. Examples of chemical treatments are alkaline treatment (mercerization treatment), silane treatment, isocyanate treatment and acetylation. In the mercerization treatment, fibre surfaces are cleaned or bleached by chemical (commonly NaOH) in order to change the fine structure of the native cellulose through de-polymerization and production of short length crystallite. By controlling mercerisation parameters such as alkali concentration, temperature and time, composite properties can be improved [7]. In the second strategy, a third material known as a coupling agent (CA) is used. These coupling agents work on several strategies such as eliminating weak boundary layers (silane) and producing deformable layers. These treatments along with the surface treatments are well reviewed and their descriptions are summarized in Table 3.

3 Results and Discussions

Thermal properties of bio-composite and its constituents can be analyzed using several tests such as given in Table 4. One of the important purposes of these tests is to determine the thermal stability of bio-composites. Thermal stability is the resistance to permanent change (degradation) in properties caused solely by heat. This is crucial since bio-composite may go through high temperature case in their manufacturing stage and in their service.

Table 3 Surface treatment description

Physical/chemical treatment	CA/chemical	Descriptions
Corona treatment	–	Fibre surface is oxidized and surface energy is increased
Plasma treatment	Ionized gas	Electric current excites a feeding gas into an ionized gas called plasma. As such surface modification such as increasing surface energy and surface cross-linking can be achieved
Alkali treatment/mercerization	NaOH	Alkali is to remove lignin and waxes of the fibre. Due to that hydrogen bonding is disrupted improving surface tension and roughness. Fibre bundles will be reduced into individual fibres
Silane treatment	Silane	Silane coupling agents are chemicals with groups attached to a silicon atom. Some attach to hydrophilic fibre surface and others attach to hydrophobic surfaces, thus coupling the two
Acetylation/esterification	Acetyl group such as acetic anhydride	Fibres are soaked into acetic anhydride to coat the OH groups of the fibre with more hydrophobic molecules, thus making it more hydrophobic
Maleated coupling	Maleic anhydride	Maleic anhydride reacts and removes the hydroxyl groups (OH) of the amorphous part of the fibre. This reduces the hydrophilic tendency while creating covalent carbon-carbon bond
Steric acid treatment	Steric acid	The carboxyl group of the stearic acid reacts with the hydrophilic hydroxyl groups of the fibre and improves water resistance properties. Pectin and waxes are removed from the fibre. Fibre bundles are breaking down

Table 4 Tests for thermal properties of bio-composites

Test	Purpose	Properties
Differential scanning calorimetry (DSC)	Determine absorbed or released heat when a substance undergoes changes or degradation	T_g , T_m , crystallinity, temperature
Dynamic mechanical analysis (DMA)	Determine visco-elastic properties over ranges of temperature	Storage modulus (E'), loss modulus, loss factor, T_g
Thermogravimetric analysis (TGA)	Determine change of mass of a substance with temperature change	Remaining weight (%)
Heat deflection temperature (HDT)	Determine if a material loss its rigidity over a small range of temperature	HDT: temp at which a material with certain load deflect

3.1 DSC

In the DSC analysis, the quantity of heat either absorbed to or released from a substance is detected as the substance undergoes physical or chemical change. The DSC analysis can determine the glass transition temperature, T_g , melting temperature, T_m , crystallization temperature, T_c and % of crystallinity. T_m is taken from the exothermic peak while the endothermic peak represents the T_c . In the study by Lee and Wang [6], the crystallization temperature and the melting temperature for PLA-Bamboo (BF) and PBS-BF with and without treatment of coupling agent lysine-dissocyanate (LDI) are shown in Table 5. It shows that while the addition of BF and LDI has slightly increase the T_c for PLA composite but the significant increase of about 29 % is obtained for PBS/BF/LDI (0.65 %).

The addition of BF and LDI however does not significantly change the value of T_m . The increase in the values of T_c shows that the BF and especially the LDI with its urethane linkage between the BF and polymer matrix have enhanced the nucleation of polymer matrix. It can be said that coupling agent LDI improves thermal stability of bio-composites. An opposite finding can be seen in the DSC study of the kenaf-chitosan bio-composite conducted by Julkapli and Akil [27]. The endothermic peaks that represent the crystallization temperature, T_c occur in the temperature range of 122 and 167 °C depending on the volume fraction of kenaf dust. The higher the kenaf volume fraction is, the lower the endothermic peak is. The endothermic peak in the DSC plot can be associated to the degradation of the polysaccharide structure of chitosan. Increasing the percentage of kenaf in the chitosan polymer decreases the acetylglucosamine group of chitosan and thus decreases the crystallinity level of the chitosan bio-composites. As such the thermal stability of the chitosan biocomposite is decreased with the addition of the kenaf [27].

A DSC study on the PLA-kenaf treated with 3-glycidoxypropyl trimethoxy silane (GPS) [28] has shown that the effect of adding kenaf fibre and GPS is not significant in changing T_g and T_m . However the crystallinity of the PLA-kenaf composite shows an increase to 24.9 % when 5 % GPS is applied. A DSC study on

Table 5 Thermal properties of the bio-composites from DSC test [6]

Bio-composites	T_c (°C)	T_m (°C)
Neat PLA	112.8	165.3
PLA/BF	115.2 (2.13)	162.3 (-1.81)
PLA/BF/LDI (0.11 %)	118.4 (4.96)	162.7 (-1.57)
PLA/BF/LDI (0.33 %)	118.7 (5.23)	161.8 (-2.12)
PLA/BF/LDI (0.65 %)	119.4 (5.85)	162.2 (-1.88)
Neat PBS	68.1	112.1
PBS/BF	74.6 (9.54)	112 (-0.09)
PBS/BF/LDI (0.11 %)	78.0 (14.54)	112.1 (0.00)
PBS/BF/LDI (0.33 %)	80.2 (17.77)	112.3 (0.18)
PBS/BF/LDI (0.65 %)	82.2 (20.70)	112.9 (0.71)

Values in parentheses are % of change

the PHB-bamboo fibre (BF) bio-composite was conducted by Krishnaprasad et al. [29] where the volume fraction of BF was increased from 5 to 39 %. It can be seen that the addition of bamboo microfibrils shows no significant effect on the T_g , T_m and T_c of the PHB.

3.2 DMA

In the study by Kim et al. [30], storage modulus was found to decrease with temperature for treated and non-treated bio-composites with fibre constituents of wood flour and bamboo and matrices of PBS and PLA. The decrease is well known to be due to the increased polymer chain mobility at higher temperature. The treatment of compatibilizing agent of maleic anhydride-grafted polypropylene (MAPE) has slightly improved the storage modulus, the loss factor and the glass transition temperature, T_g of the bio-composites [30] due to the enhanced interfacial adhesion and compatibility between the fibres and the polymer. Cheung et al. [31] shows that the addition of silk fiber into the PLA matrix has shifted the whole TGA curve and thus increasing the storage modulus (E'), the loss modulus (E'') and the glass transition temperature (T_g) of the bio-composite. This is due to the effect of fibre that introduces mechanical limitation to the polymer. In a study by Huda et al. [8] on treated and non-treated PLA-kenaf bio-composites, the treatments of alkali (NaOH) and silane on the bio-composite have improved the thermal stability of the bio-composite compared to the neat PLA such as shown in Table 5.

The combination of alkali and silane treatments gives the highest values of T_g and the storage modulus (E'). The treatment of NaOH to remove the lignin of the kenaf fibre proves to be a crucial step in this study. The treatments of NaOH and silane that improve the interfacial adhesion between the PLA and the kenaf fibres explain the improvement on the T_g and the storage modulus.

3.3 HDT

Studies shows that the reinforcement of fibres has slightly improved the HDT of bamboo-PLA and wood flour-PBS [30], significantly decrease the HDT of the banana fibre-PLA [32] but significantly improves the HDT of the kenaf-PLA such as shown in Table 6 [8]. As previously, the existence of fibers prevents the deformation of kenaf-PLA composites which promotes the crystallization of PLA in the composites [8]. The treatment of maleic anhydride (MA) has improved the surface adhesion of the bio-composite and as such the improvement of the HDT of the bio-composites can be seen [30]. However, Table 6 shows that the combine treatments of NaOH and silane only shows slight improvement of the HDT of the bio-composites as compared to the improvements made by individual treatment.

Table 6 Thermal properties of the bio-composites from DMA [8]

Bio-composite	T _g (°C)	E' at 25 °C (GPa)	E' at 40 °C (GPa)	E' at 60 °C (GPa)	HDT (°C)
Neat PLA	63	3.1	3.1	1.7	64.5
Kenaf-PLA	61	4.4	4.4	2.7	170.3 ± 1
KF-PLA-NaOH	60	5.2	5.2	4.5	172.8 ± 1
KF-PLA-Silane	68	5.8	5.8	5.2	173.4.8 ± 1
KF-PLA-NaOH-Silane	67	8.1	8.1	7.1	173.4 ± 1

3.4 TGA

Exposing to high temperature can result in several changes to physical or chemical composition of bio-composites which can end up with property degradation of the bio-composite. Biocomposite may not be exposed to high temperature while in service but it is exposed to high temperature for example during its manufacturing process. Improving thermal degradation means improving thermal stability of the bio-composite. Among thermal degradation improvements can be observed are lower % of weight loss, higher starting degradation temperature, lower rate of degradation and degradation curve shifting up. In the TGA, the degradation, measured over the increase of temperature can be in terms of the weight, mechanical properties, chemical properties or the organoleptic properties such as odor and color. In the work of Julkifi and Akil [27], the TGA of the kenaf-chitosan bio-composite shows that the increase of the volume fraction of kenaf does not give significant change in thermal stability of the bio-composite. Two stages of degradation were reported: the degradation due to the evaporation of water that occurs at the temperature range of 25 and 140 °C and corresponds to the loss of about 10 % weight loss and the degradation of the polymer itself occurs at the temperature range of 110 and 220 °C and corresponds to about 30 % weight loss. The degradation in the second stage includes the pyrolysis of the chitosan polymer, the decomposition of kenaf fibres and the depolymerization of the chitosan polymer. Studies show that the initial degradation temperature of bio-composite is lowered with the addition of fibers [6, 15, 33]. This may be due to the fact that natural fibres have lesser thermal stabilities that seemed to enhance the deformation of the crystalline structure of PLA at high temperature [33]. However a treatment by the addition of lysine-diisocyanate or silane to the bio-composite has increased the degradation temperature [6, 33]. In contrast the study by Krishnaprasad et al. [29] shows the increase in thermal stability with the addition of bamboo microfibrils to the PHB where the weight loss is reduced by 21.3 %.

4 Conclusion

A review on the thermal stability of bio-composites was conducted. Four tests that give the effect of thermal properties over the change of temperature are discussed. It can be said that thermal properties degrade with temperature at their glass transition temperature. The addition of fibre may improve slightly the thermal stability but at the same time may cause the decrease in thermal stability of bio-composites. However thermal stability can be improved by treating the fibres with coupling agents or alkali.

Acknowledgments This work is supported by the Malaysia-Japan International Institute of Technology, Universiti Teknologi Malaysia. The authors would like to thank the faculty and the University.

References

1. E. Bodros, I. Pilin, N. Montrelay, C. Baley, Could biopolymers reinforced by randomly scattered flax fibre be used in structural applications? *Compos. Sci. Technol.* **67**, 462–470 (2007)
2. B.L. Shah, S.E. Selke, M.B. Walters, P.A. Heiden, Effects of wood flour and chitosan on mechanical, chemical, and thermal properties of polylactide. *Polym. Compos.* **29**(6), 655–663 (2008)
3. A.K. Bledzki, A. Jaszkievicz, Mechanical performance of biocomposites based on PLA and PHBV reinforced with natural fibres—a comparative study to PP. *Compos. Sci. Technol.* **70** (12), 1687–1696 (2010)
4. M. Carus, Biocomposites: 350,000 tons production of wood and natural fibre composites in the European Union in 2012. <http://bio-based.eu/news/biocomposites/> (2013)
5. M.F. Omar, A.K. Bledzki, H.P. Fink, M. Sain, Biocomposites reinforced with natural fibers: 2000–2010. *Prog. Polym. Sci.* **37**(11), 1552–1596 (2012)
6. S.H. Lee and S. Wang, Biodegradable polymers/bamboo fiber biocomposite with bio-based coupling agent. *Compos. Part A.* **37**, 80–9 (2006)
7. D. Puglia, A. Tomsucci, J.M. Kenny, Processing, properties and stability of biodegradable composites based on mater-bi and cellulose fiber. *Polym. Adv. Technol.* **14**, 749–756 (2003)
8. M.S. Huda, L.T. Drzal, A.K. Mohanty, M. Misra, Effect of fiber surface-treatments on the properties of laminated biocomposites from poly (lactic acid) (PLA) and kenaf fibers. *Compos. Sci. Technol.* **68**, 424–432 (2008)
9. R. Belhassen, J.A. Méndez, S. Boufi, J.P. López, J. Puig, A. Pèlach, P. Mutjé, Preparation and properties of biocomposites based on jute fibers and blend of plasticized starch and poly (β -hydroxybutyrate). *J. Appl. Polym. Sci.* **114**(1), 313–321 (2009)
10. A.K. Mohanty, A. Wibowo, M. Misra, L.T. Drzal, Effect of process engineering on the performance of natural fiber reinforced cellulose acetate biocomposites. *Compos. A Appl. Sci. Manuf.* **35**(3), 363–370 (2004)
11. V.P. Cyras, C. Vallo, J.M. Kenny, A. Vázquez, Effect of chemical treatment on the mechanical properties of starch-based blends reinforced with sisal fibre. *J. Compos. Mater.* **38**(16), 1387–1399 (2004)
12. Q.F. Shi, H.Y. Mou, Q.Y. Li, J.K. Wang, W.H. Guo, Influence of heat treatment on the heat distortion temperature of poly (lactic acid)/bamboo fiber/talc hybrid biocomposites. *J. Appl. Polym. Sci.* **123**(5), 2828–2836 (2012)

13. F. Roussi re, C. Baley, G. Godard, D. Burr, Compressive and tensile behaviours of PLLA matrix composites reinforced with randomly dispersed flax fibres. *Appl. Compos. Mater.* **19** (12), 171–188 (2012)
14. S.Y.Z. Zainuddin, I. Ahmad, H. Kargarzadeh, I. Abdullah, A. Dufresne, Potential of using multiscale kenaf fibers as reinforcing filler in cassava starch-kenaf biocomposites. *Carbohydr. Polym.* **92**, 2299–2305 (2013)
15. A.A. Yussuf, I. Massoumi, A. Hassan, Comparison of polylactic acid/kenaf and polylactic acid/rise husk composites: the influence of the natural fibers on the mechanical, thermal and biodegradability properties. *J Polym. Environ.* **18**, 422–429 (2010)
16. D. Nabi Saheb, J.P. Jog, Natural fiber polymer composites: a review. *Adv. Polym. Technol.* **18** (4), 361–363 (1999)
17. R. Moriana, F. Vilaplana, S. Karlsson, A. Ribes-Greus, Improved thermo-mechanical properties by the addition of natural fibres in starch-based sustainable biocomposites. *Compos. A Appl. Sci. Manuf.* **42**(1), 30–40 (2011)
18. K. Okubo, T. Fujii, E.T. Thostenson, Multi-scale hybrid biocomposite: processing and mechanical characterization of bamboo fiber reinforced PLA with microfibrillated cellulose. *Compos. A Appl. Sci. Manuf.* **40**(4), 469–475 (2009)
19. I.S.M.A. Tawakkal, R.A. Talib, K. Abdan, C.N. Ling, Mechanical and physical properties of kenaf-derived cellulose(KDC)—filled polylactic acid (PLLA) composites. *Bioresources.com.* **7**(2), 1643–1655 (2012)
20. H.Y. Cheung, M.P. Ho, K.T. Lau, F. Cardona, D. Hui, Natural fibre-reinforced composites for bioengineering and environmental engineering applications. *Compos. B Eng.* **40**(7), 655–663 (2009)
21. A.K. Bledzki, S. Reihmane, J. Gassan, Properties and modification methods for vegetable fibers for natural fiber composites. *J. Appl. Polym. Sci.* **59**, 1329–1336 (1996)
22. R. Moriana, F. Vilaplana, S. Karlsson, A. Ribes-Greus, Improved thermo-mechanical properties by the addition of natural fibres in starch-based sustainable biocomposites. *Compos. A Appl. Sci. Manuf.* **42**(1), 30–40 (2011)
23. A. Ashori, A. Nourbakhsh, Reinforced polypropylene composites: effects of chemical compositions and particle size. *Bio-resource Technol.* **101**(7), 2515–2519 (2010)
24. S.R. Karmakar, Chemical technology in the pre-treatment processes of textiles. *Tex. Sci. Technol.* **12**, 279–315 (1999)
25. R.M. Taib, S. Ramarad, Z.A. Mohd Ishak, M. Todo, Water absorption and tensile properties of kenaf bast fiber-plasticized poly (lactic acid) biocomposites, in *Proceeding of the Polymers Processing Society 24th Annual Meeting June 15–19* (Salerno Italy, 2008)
26. H.M. Akil, M.F. Omar, A.A.M. Mazuki, S. Safiee, Z.A.M. Ishak, A. Abu Bakar, Kenaf fiber reinforced composites: a review. *Mat. Des.* **32**(8–9), 4107–4121 (2011)
27. N.M. Julkifli, H.M. Akil, Thermal properties of kenaf-filled chitosan bio-composites. *Polym.-Plastics Technol. Eng.* **49**, 147–153 (2010)
28. B.H. Lee, H.S. Kim, S. Lee, H.J. Kim, J.R. Dorgan, Bio-composites of kenaf fibers in polylactide: role of improved interfacial adhesion in the carding process. *Compos. Sci. Technol.* **69**, 2573–2579 (2009)
29. R. Krishnaprasad, N.R. Veena, H.J. Maria, R. Rajan, M. Skrifvars, K. Joseph, Mechanical and thermal properties of bamboo microfibril reinforced polyhydroxybutyrate biocomposites. *J. Polym. Environment* **17**, 109–114 (2009)
30. H.S. Kim, B.H. Lee, S. Lee, H.J. Kim, J.R. Dorgan, Enhanced interfacial adhesion, mechanical, and thermal properties of natural flour-filled biodegradable polymer biocomposites. *J. Therm. Anal. Calorim.* **104**(1), 331–338 (2011)
31. H.Y. Cheung, K.T. Lau, X.M. Tao, D. Hui, A potential material for tissue engineering: Silkworm silk/PLA biocomposite. *Compos. B* **29**, 1026–1033 (2008)
32. P.J. Jandas, S. Mohanty, S.K. Nayak, Thermal properties and cold crystallization kinetics of surface-treated banana fiber (BF)-reinforced PLA nanocomposites. *J. Thermal Calorimeter* **114**, 1265–1278 (2013)

33. S. Mohanty, S.K. Verma, S.K. Nayak, Dynamic mechanical and thermal properties of MAPE treated jute/HDPE composites. *Compos. Sci. Technol.* **2**, 538–547 (2005)
34. P. Wambua, J. Ivens, I. Verpoest, Natural fibres: can they replace glass in fibre reinforced plastics? *Compos. Sci. Technol.* **63**, 1259–1264 (2003)
35. M.P. Westman, L.S. Fifield, K.L. Simmons, S.G. Laddha, T.A. Kafentzis, *Natural Fiber Composites: A Review* (A Report by the Pacific Northwest National Laboratory for US Department of Energy, PNNL-19220, 2010)

Finite Element Analysis of Staggered Micro Couple Resonant Sensor Structure

N.A. Shuib, A.F. Zubair, N.H. Saad, A.A. Bakir,
M.F. Ismail and I.P. Almanar

Abstract Improvement in the design of staggered couple micro resonant structure based on closed loop butterfly shape spring design in fixed beam resonator has been made previously [1]. To further improve its performance in electronic applications especially in sensor design, finite element analysis (FEA) was used to determine the performance of the single resonator used including its natural frequency, mass, and frequency response in terms of the length of its sleeve, L_s , where the performance of the structure of the sensor mainly depends on the displacement of the sensor along its excitation axis. In this work, COMSOL Multiphysics software was used.

1 Introduction

Many applications nowadays used MEMS considering the integration of mechanical elements, sensors, actuators, and electronics on a common silicon substrate with MEMS structure such as an electronic nose [1]. These multiple number of sensors will complicate the sensing system, signal processing, readout and pattern recognition

N.A. Shuib (✉) · A.F. Zubair · N.H. Saad · A.A. Bakir · M.F. Ismail · I.P. Almanar
Faculty of Mechanical Engineering, Universiti Teknologi MARA (UiTM),
Shah Alam, Malaysia
e-mail: norazimahshuib@gmail.com

A.F. Zubair
e-mail: ahmadfaiz@ppinang.uitm.edu.my

N.H. Saad
e-mail: norhayatisaad@salam.uitm.edu.my

A.A. Bakir
e-mail: azmanbakir@ppinang.uitm.edu.my

M.F. Ismail
e-mail: mohdfauzi305@ppinang.uitm.edu

I.P. Almanar
e-mail: my.meinput@yahoo.com

system. Thus, the design of the resonator sensor can be improved by analyzing its performances.

The purpose of this study is to compare 4 design of integrated structure model of staggered couple micro resonant sensors with different sleeve length, L_s . This study was based on the available model structure of micro electro mechanical system (MEMS) structure and properties. All the data from previous research on MEMS design structure will be used in analyzing the model of staggered couple micro resonant sensors which then will be improved.

2 Literature Review

In these recent years, most of MEMS companies will face challenging in MEMS development as mismatch between the technology and the market because the technology is too incremental over the competition and market for MEMS industry too small. Mismatch in this elaboration refers to the relation between technology achievements and market value available in the industry. For MEMS manufacturer, one of the key to success is to develop new enhanced MEMS structure that integrated with human biology to satisfy customer requirements in medical.

Resonator sensors often have a relatively high mechanical quality factor (Q-factor), which leads to a high resolution of frequency and hence high sensitivity [2]. A high Q-factor also implies low energy losses from the resonator and therefore low power requirements to maintain the resonance, which simplifies the operating electronics.

Frequency domain sensors have advantages including that the signal output is essentially digital in contrast to analogue signal output [3]. Therefore, the detected signal can be directly connected to digital circuits, which ensures high accuracy detection and simplicity compared with other type of sensors.

COMSOL Multiphysics COMSOL Multiphysics and its MEMS module have proven to be the right tool for such a problem [4].

There is various shape and dimensions of resonator and each shape have several vibration modes such as transversal, longitudinal, torsional and lateral [5]. Each mode has its own displacement patterns, resonant frequency and Q-factor. The value of resonant frequency of all modes is designed to be manipulated by the change of mass, internal forces and stiffness of resonator. An unbalanced resonator design yields energy losses at the mount due to reaction forces required to maintain the unbalanced resonator vibration which reduces the Q-factor. In order to be perfectly balanced, a vibrating structure must have a fixed centre of gravity and the sum of forces and moments resulting from the vibration should be zero [6].

3 Methodology

The main purpose of this research is to study and develop new design structure of staggered micro couple resonant sensors. Performance of the structure will be determined using finite element analysis that covering eigenfrequency study, and frequency response analysis.

3.1 Design Development Process

Design improvement is one of way to improve the resonator’s performance. The improvement are done by considering the changing of dimensions and structure based on the previous design in [1] using AutoCAD software. This study will focus on making variations on the length of single resonator with fixed beam and the frequency of each length is determined using COMSOL Multiphysics. By analyzing the suitable length, the resonator was then been connected to micro couple spring which was stimulated with butterfly shape structure.

The design is shown in Fig. 1 and Table 1 explain the details of the geometrical design of the fixed beam resonator (Fig. 2).

3.2 Research Instrument

COMSOL Multiphysics software to determine performance of resonator sensor array. COMSOL Multiphysics is practical simulation software that can be used on MEMS structure pattern. In this study, model was imported from CAD file.

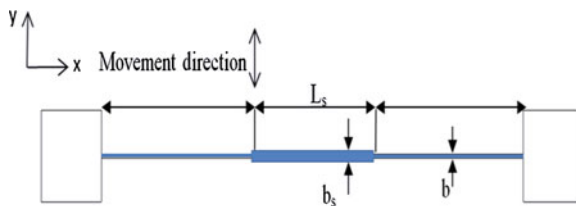
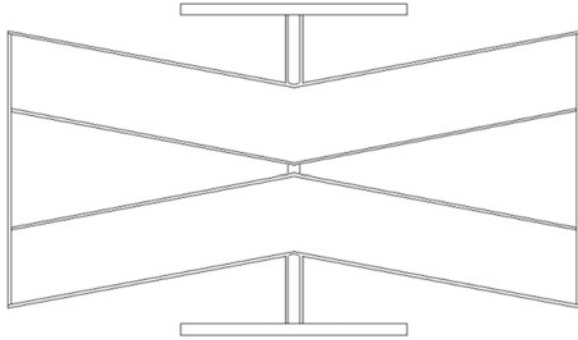


Fig. 1 Schematic of a fixed-fixed beam resonator (top view)

Table 1 Details of the geometrical design parameter of a fixed-fixed beam resonator

Geometrical design parameter	Dimension (μm)
Length of beam, L	500
Width of resonator, b	4
Length of controlled surface area, Ls	100, 200, 300, 400
Width of controlled surface area, bs	10

Fig. 2 Original design of closed loop butterfly spring design



The focused parameter with the model frequency are natural frequency, the effective stiffness and mass, and frequency response on single resonator. All this parameter can be solved by adding physics data on the analysis study. To get the value of six modes of eigenfrequencies, all the model structure were analyzed with appropriate meshing module and parameter solver.

4 Results and Discussion

4.1 Design and Finite Element Analysis of Fixed-Fixed Beam Resonator

Fixed-fixed beam was chose as the resonator element of micro couple resonant structure. The beam has a lateral prime mode vibration that responds more sensitivity to a change of mass. Energy losses can be reduced with the properties of lateral mode vibration due to viscous and acoustic damping. The damping losses can be reduced by facilitating the movement of gas surrounding the vibrating beam. [1] This is accomplished by reducing the effective surface area of the resonator which is perpendicular to the resonator movement. The structure performance was analyzed based on a 5 μm structure thickness.

4.2 Eigenfrequency Analysis of Single Resonator

The result are shown in Table 2 and the displacement study result are shown in Figs. 3, 4, 5 and 6.

From the result, it was observed that shorter length of controlled surface area, the value of eigenfrequency become higher. Higher eigenfrequency value can lead to high quality factor of the resonator. Quality factor describes the number of oscillations of system before the system was damped out.

Table 2 Result of the eigenvalue analysis

Length (μm)	Eigen frequency (Hz)	Deflection distance (μm)	Effective mass, m_{eff} (kg)
100	94,782	2.3939×10^{-6}	1.8145×10^{-11}
200	73,593	2.3812×10^{-6}	2.9801×10^{-11}
300	60,676	2.4140×10^{-6}	3.4935×10^{-11}
400	51,422	2.4935×10^{-6}	4.6580×10^{-11}

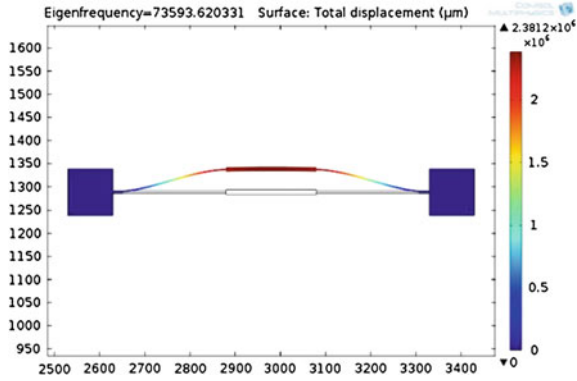


Fig. 3 Eigenfrequency analysis result of fixed-fixed beam resonator for different length of controlled surface area, L_s (a) $L_s = 100 \mu\text{m}$

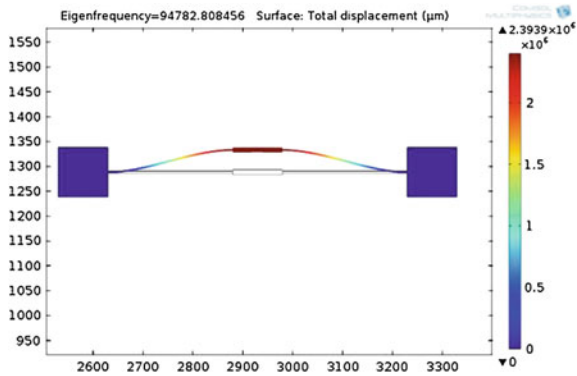


Fig. 4 Eigenfrequency analysis result of fixed-fixed beam resonator for different length of controlled surface area, L_s (b) $L_s = 200 \mu\text{m}$

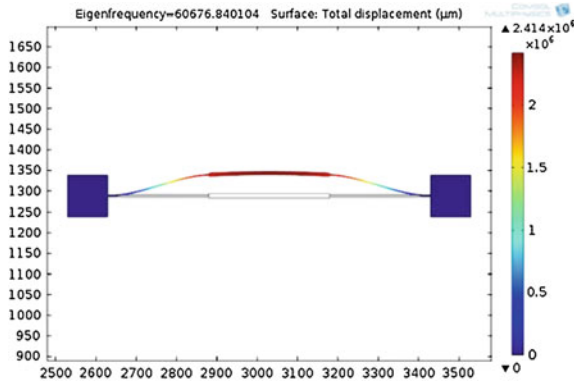


Fig. 5 Eigenfrequency analysis result of fixed-fixed beam resonator for different length of controlled surface area, (c) $L_s = 300 \mu\text{m}$

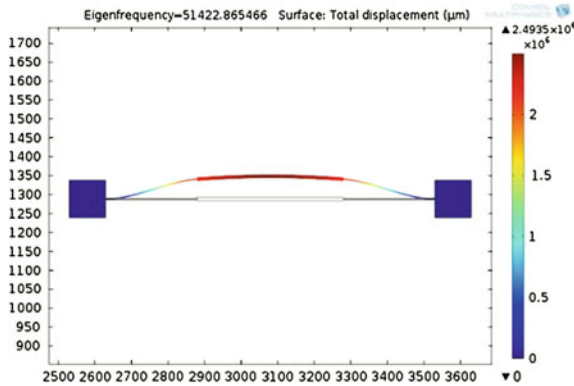


Fig. 6 Eigenfrequency analysis result of fixed-fixed beam resonator for different length of controlled surface area (d) $L_s = 400 \mu\text{m}$

4.3 Mechanical Couple Spring

A new closed loop butterfly shape spring was designed initially [7, 8] to couple the resonator array sensor together. The spring will act as connector agent and designed as butterfly shape in order to control the stiffness by configuring spring design parameter. In this study, butterfly design was made to result in better performance by changing the dimensions and shape of the structure and analysis was made to determine the eigenfrequency values of the structure (Table 3 and Fig. 7).

Table 3 Details of geometrical design parameter of butterfly spring

Geometrical parameter description (μm)	Dimension
Width of spring element 1, S_1	2.5
Width of spring element 2, S_2	7.9
Width of spring element 3, S_3	10
Width of spring element 4, S_4	15
Spring width 1, bsp_1	10
Spring width 2, bsp_2	71
Spring width 3, bsp_3	103
Spring width 4, bsp_4	255
Spring length, L_{sp}	500

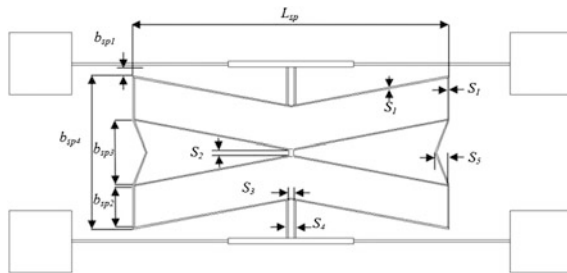


Fig. 7 Schematic of a closed loop butterfly spring design used to couple two fixed-fixed beam resonators

From eigenfrequency analysis, the first six eigenmodes of the structure were observed to examine any unwanted eigenmodes that might be formed by the designed butterfly spring within the modal frequencies of couple structure Fig. 8.

From the analysis result in Table 4, it was observed that the frequency, second mode $f(2) = 67.3$ kHz that almost equivalent to the expected frequency that is 50 kHz. From the analysis, it was observed that at the mode 2, the spring starts to twist but the mid-joint beam reduces displacement of the spring in the x-axis.

From the analysis, it was observed that higher the value of natural frequency, the value of stiffness or spring constant, k had become smaller. In this situation, when spring has greater eigenfrequency, it will be less stiff that can lead to increase in value of the amplitude of the response. Thus, to reduce the amplitude of the response in order to increase the performance of resonator sensor, the deflection of spring vibration should be reduced. In other words, stiffer spring can increase the bandwidth of the frequency response and reduces the amplitude of the response.

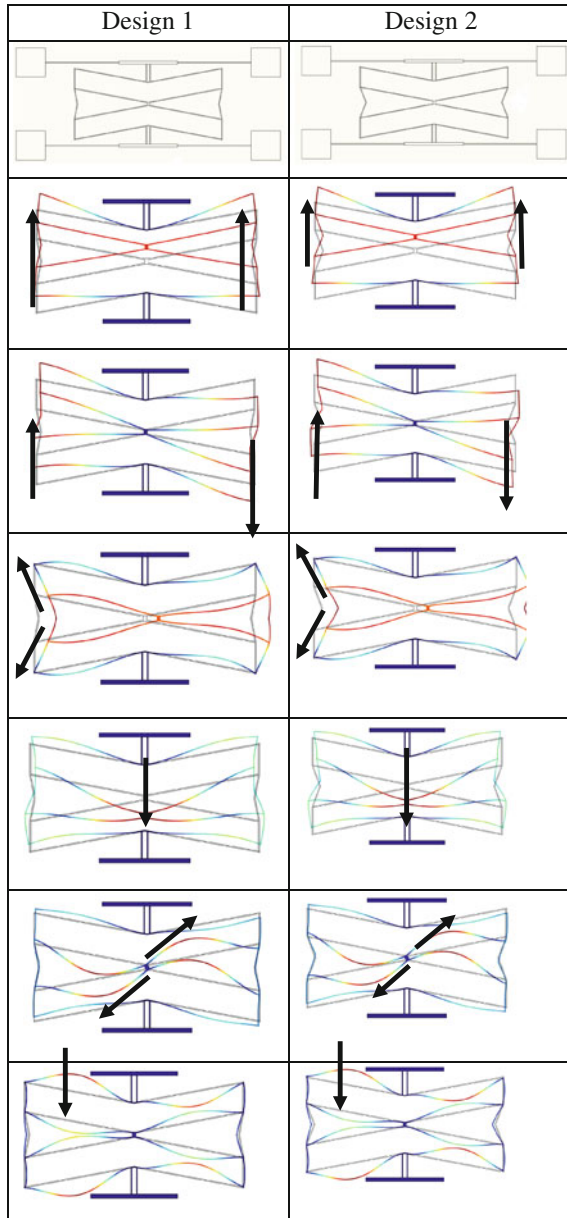


Fig. 8 The six eigenmode of the structure

Table 4 Performance parameter of butterfly spring

Mode	Natural frequency (kHz)		Spring constant k (N/m)	
	Design 1	Design 2	Design 1	Design 2
1	32.146	31.973	0.5055	0.4088
2	67.305	65.781	0.4502	0.4547
3	136.548	132.460	0.4128	0.4088
4	146.608	144.957	0.3433	0.3402
5	248.903	245.768	0.2853	0.2872
6	318.720	315.516	0.2777	0.2821

5 Conclusion

From the analysis, the change of the shape and dimensions of single resonator and closed loop butterfly spring will affect the value of natural frequency and also stiffness of the resonator sensor. In order to increase the value of natural frequency, in the case of single resonator, the length of controlled surface area, L_s need to be reduced.

From the study also shown that mechanical couple spring that applied the shape of butterfly spring as closed loop to join the resonator by giving them fixed twist and controlled the vibration of two resonators, the performance can be improved by increasing the natural frequency of the resonator. This can be done by changing the shape to be more controllable in oscillations and reduced the amplitude of the resonator sensor.

Acknowledgments The authors appreciate the supports of the Faculty of Mechanical Engineering UiTM and RAGS Grant No: RAGS/2012/UITM/TK01/6 via Project Code: 600-RMI/RAGS 5/3(43/2012).

References

1. N.H. Saad, Modelling and performance evaluation of coupled micro resonator array for artificial nose. Phd. thesis, University of Birmingham (2010)
2. E.B. Jones, N.M. White, J.M. Tudor, S.P. Beeby, US patent 7498721—resonant sensor assembly. <http://www.patentstorm.us/patents/7498721/description.html>. Brunel University (2009)
3. Z. Cui, D. Chen, S. Xia, Modelling and experiment of a silicon resonant pressure sensor. *Analog Integr. Circ. Sig. Process* **32**, 29–35 (2002)
4. J.V. Crosby, M.G. Guvench, Experimentally matched finite element modeling of thermally actuated SOI MEMS micro-grippers using COMSOL multiphysics. In: *Proceedings of the COMSOL Conference* (2009)
5. G. Stemme, Resonant silicon sensors. *J. Micromech. Microeng.* **1**(2), 113–125 (1991)
6. V. Kaajakari, T. Mattila, A. Lipsanen, A. Oja, Nonlinear mechanical effects in silicon longitudinal mode beam resonators. *Sens. Actuators A* **120**(1), 64–70 (2005)

7. N. H. Saad, et al., Performance Analysis of A Coupled Micro Resonator Array Sensor, Eurosensors XXII, Dresden, Germany 60–63 (2008)
8. N. H. Saad et al., Analysis of MEMS mechanical spring for coupling multimodal micro resonators sensor: *Microelectronic Engineering* **86**, 1190–1193 (2009)

An Experimental Study of Reinforced Concrete Beams with Artificial Aggregate Concrete Infill Under Impact Loads

Shahrul Niza Mokhatar, Zainorizuan Mohd Jaini,
Mohd Khairy Burhanudin, Mohamad Luthfi Ahmad Jeni
and Mohd Nasrul Naim Ismail

Abstract The aim of this paper is to examine the impact response of reinforced concrete (RC) beam with artificial aggregate concrete block infill (RCAI) through experimental study and to propose the innovations of lightweight reinforced concrete utilizing polyethylene (PE) waste materials as an artificial aggregate. The study consists of the determination of optimum percentage of PE waste material as coarse aggregate replacements in the concrete mix and dynamic testing where an approximately 100 kg of impact weight dropped onto several beam specimens. Four concrete cube mixes with 0, 3, 6 and 9 % PE aggregate for 14 and 28 days respectively were prepared and tested under compression tests. Meanwhile, eight beam specimens categorized as normal reinforced concrete (NRC), RCAI and beam specimen that consists 6 % polyethylene waste material as a coarse aggregate (RC6A) were prepared and tested under low velocity impact loads under 1.54 m drop height of impact weight (5.5 m/s velocity). The behavior of the beam

Short Term Grant Scheme STG1324. (Universiti Tun Hussein Onn Malaysia).

S.N. Mokhatar (✉) · Z.M. Jaini · M.K. Burhanudin
Jamilus Research Center, University Tun Hussein Onn Malaysia, Batu Pahat, Johor, Malaysia
e-mail: shahruln@uthm.edu.my

Z.M. Jaini
e-mail: rizuan@uthm.edu.my

M.K. Burhanudin
e-mail: khairy@uthm.edu.my

M.L.A. Jeni
Faculty of Engineering Technology, University Tun Hussein Onn Malaysia, Batu Pahat,
Johor, Malaysia
e-mail: luthfi@uthm.edu.my

M.N.N. Ismail
Faculty of Civil and Environmental Engineering, University Tun Hussein Onn Malaysia,
Batu Pahat, Johor, Malaysia
e-mail: nasrulnaim@hotmail.com

specimens are studied in terms of crack patterns (shear and flexural), crushing beneath the impact region and residual displacement at the mid-span. As results, it is observed that the 6 % of PE waste material in the concrete mix influence the strength of concrete about 10 %. Based on the failure mode results, all the beams are failed under drop height of 1.54 m. In addition, it is found that the residual displacement of RCAI is significantly lower than those of NRC and RC6A.

Keywords Impact loads · Reinforced concrete beam · Artificial aggregate concrete infill

1 Introduction

Producing an innovative lightweight concrete still becomes most important interest among researchers. Normal concrete has density about $2,400 \text{ kg/m}^3$ that would contribute to weight penalty in large volume structure. Lighter weight of concrete structures is desirable particularly when dealing with large open floor plans and in a high-rise building [1]. Many researchers such as Vimonsatit et al. [1], Mohamad and Mahdi [2], and Jung et al. [3] have studied the performance of infilled or sandwich structures that usually comprise a conventional concrete with foamed concrete and other materials to reduce the weight. However, the applications still have the disadvantage to some points such as an economic issue, achievement to the standard strength and low resistance to dynamic loads.

Meanwhile, each Malaysian generates almost 0.8 kg garbage every day that is mostly containing polyethylene (PE) materials. Inmate urban areas are estimated to produce 1.5 kg garbage every day. The waste plastic bags are one of the major contributions to the increasing number of solid waste production in this country, and only 1 and 3 % are ever recycled. Plastic bags can be a nuisance in the society. It can cause a wastage problem as most plastic bags are not biodegradable if buried. Use of plastic bags is increasing adverse impact on the environment as well as being a big problem in landfills. Therefore, innovative solutions have to be developed to solve this problem. One of the considerable actions is producing the waste plastic bags as artificial aggregates that can be used on concrete. However, the strengths and behaviour of concrete containing PE aggregates should be extensively investigated in order to understand the ability of this concrete as a structural material and to ensure that the concrete structure can carry meaningful load without experience severe failures under impact loads. Al Bakri et al. [4] has been found that the compressive concrete containing PE aggregates are lower than normal concrete, but PE aggregate suitable for coarse aggregate replacement in concrete through their physical analysis; thus, it is can be used as infill block to replace ineffective volume of RC beam. The incorporation of PE aggregate can significantly improve some properties of concrete because this type of artificial aggregate has high toughness,

good abrasion behavior, low thermal conductivity and high heat capacity [5, 6]. The PE aggregate is significantly lighter than natural aggregate, therefore, its incorporation lowers the densities of the resulting concrete. This property can be used to develop lightweight concrete. The use of shredded waste PE aggregate in concrete can reduce the dead weight of concrete, thus lowering the earthquake risk of building, and it could be helpful in the design of earthquake-resistant building [7].

The direct applications of PE-concrete as a concrete structure are still in doubt due to its strength. However, PE-concrete can be used as infill for RC beam. The combination of PE-concrete infill and normal concrete produces so-called composite-based-concrete-structure that has advantage due to lighter weight. RC beam is highly designed to carry compression while steel reinforcements transfer tension stress and loadings. The relationship between transfer tension stress and strain in normal concrete cross-section is almost linear at small value of stress (for stresses less than 40 % of the compressive concrete strength). In this condition, the inner part, under neutral axis, only acts as a passive volume that has a small contribution on the crack and failure resistances. In addition, when an RC structure is subjected to flexural and shear, the concrete volume under neutral axis of the cross-section is considered ineffective when it is in tension at ultimate limit states. Figure 1 shows the typical strain, stress and force diagram of RC section.

One of the important considerations for the effective use of structural materials is impact loading. An impact loading pre dominantly one of the accountability focuses for structural elements both in steel and concrete. In fact, an RC structure under impact loading shows the dissimilar behaviour than statically loaded structures. Thus, this kind of severe loading is one of the dynamic factors that should consider in the analysis and design of structures. The prediction on how high and low velocities impact load will affect normal RC elements has been experimentally investigated in the study of several studies such as Gueraud et al. [8], Fiquet and Dacquet [9], Kishi et al. [10], Saatci and Vecchio [11], Fujikake et al. [12] and Chen and May [13]. However, investigations concerned with dynamic (impact) behaviour of RC beam with PE-concrete infill have not been done so much yet. Thus, the objective of this paper are to presents the results of impact response of RC beam with artificial aggregate concrete block infill (RCAI) through experimental study and to propose the innovations of lightweight reinforced concrete (RC) utilizing waste materials as an artificial aggregate.

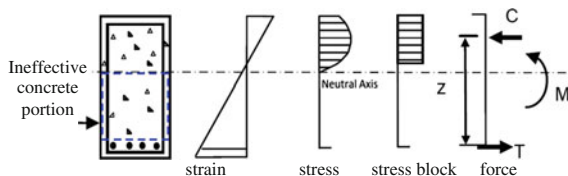


Fig. 1 Strain, stress and force diagram of a reinforced concrete section

2 Materials/Specimen Preparation

2.1 Artificial Polyethylene Coarse Aggregate (APECA)

APECA is made from waste plastic bag and undergone the heating process at about 150 °C for 10 min and the standard sizes used in this study are range in 14–20 mm. Initially, the waste plastic bags are compressed and formed into the round diameter like small ball. The compacted waste plastic bag has a diameter around 30 mm before shrink to the size around 14–20 mm during the heating process as shown in Fig. 2.

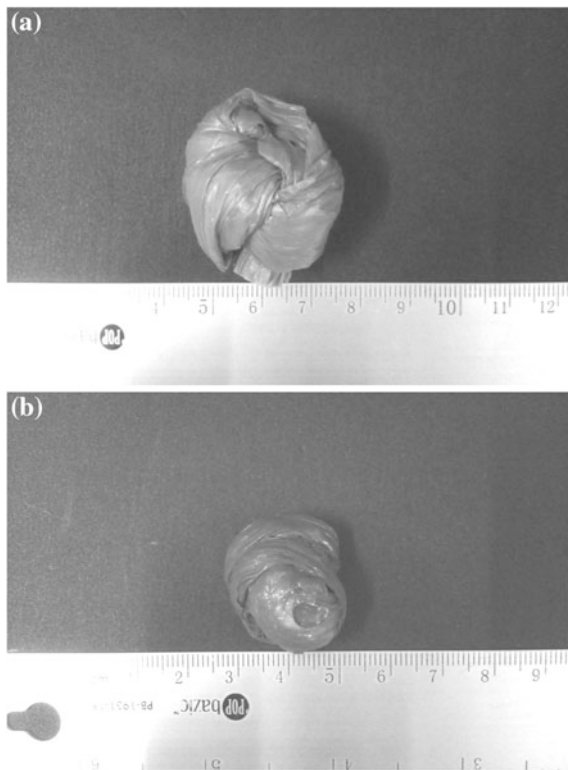


Fig. 2 Condition of APECA before and after heating process. **a** Before, **b** after

Table 1 Specimen size and volume of the sample

Sample	Size	Volume (m ³)
Cube	0.15 m × 0.15 m × 0.15 m	3.375 × 10 ⁻³
Beam	0.12 m × 0.15 m × 0.80 m	0.0144
AAC block	0.05 m × 0.07 m × 0.70 m	0.00245

Table 2 Amount of APECA

Sample	Percentage of APECA (%)	Coarse aggregate (kg)	APECA (kg)
Cube	6	3.68	0.11
Beam	6	15.7	0.48
AAC block	6	2.67	0.08

2.2 Concrete Mix Design

Concrete is designed to achieve a compressive strength of 25 N/mm² on day 28 and based on the design of normal concrete mixes recommended by the Department of Environment (DOE). Concrete mix designs are intended to produce a mixture that is suitable to achieve the objectives. Mix designs are based on the three groups mix concrete. First group is specimen of normal concrete (NRC) as control specimens, the second group is RCAI using 6 % APECA in the artificial aggregate concrete block infill and the third group is beam specimen that consists 6 % PE waste material (RC6A). The volumes of concrete are determined to ensure the ratio between all the materials is suitable for grade 25. Table 1 shows the specimen size and volume for cubes, beams and artificial aggregate concrete (AAC) blocks.

Meanwhile, the amount of APECA that used in this study is shown in Table 2.

A total of eight beam specimens of size 120 mm width, 150 mm high and 800 mm length were prepared for drop weight load test. Four AAC blocks containing 6 % APECA of size 50 mm width, 70 mm high and 700 mm length were also provided for block infill. The beam is reinforced with 8 mm in diameter two steel bars at bottom part. The stirrups of 6 mm is designed on the beam along 80 mm interval. The details of reinforcement arrangement are shown in Fig. 3.

3 Impact Test Setup

Tests for specimen of NRC, RCAI and RC6A were carried out in University Tun Hussein Onn Malaysia in order to investigate the low-velocity impact behavior and failure mechanism of the beams. Several measuring devices and testing items are required for development of impact tests in order to guarantee a reliable method of testing and their ability to produce experiments under real conditions.

The test set-up was individually designed to be able to test beam specimens under impact loading. In this study, approximately 100 kg drop-weight is acted

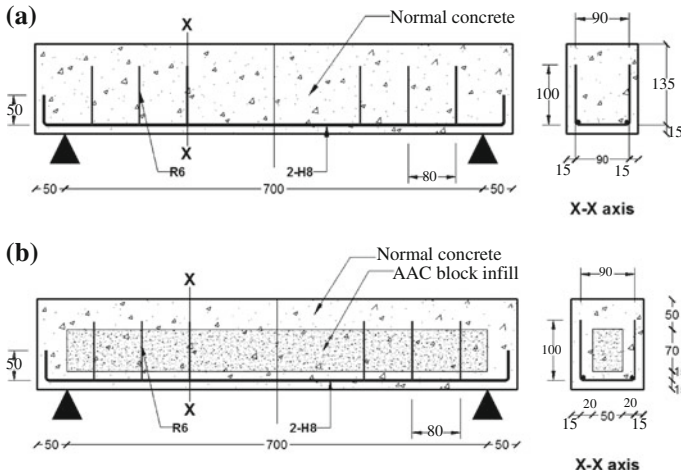


Fig. 3 RC beam and RCAI details. **a** Dimensions of RC beam (specimens of NRC and RC6A). **b** Dimensions of RCAI

vertically from a certain height of 1.54 m. The steel frame and main structure for the falling weight impact tests is shown in Fig. 4.

During the impact tests, the steel frame structures and support conditions should be stiff enough to support the load without significant deformation. The vertical movement of the support conditions during the impact process will affect the displacement and another measurement value. The final displacement and mode of failure for each beam specimens were determined.

To ensure that the test perform correctly, the following checks are carried out:

- Assemble and place the support position in the correct dimension. Set the beam specimen on the support system and align it from the both directions.
- Ensure that the connections between all the components work properly.
- Lift up the drop weight to the desired height and measure the height, finally, set it to fall.

4 Experimental Results and Discussion

4.1 Compressive Strength Test

The compression test for four concrete cube mixes of 0, 3, 6 and 9 % APECA as coarse aggregate were conducted after curing process of 7 and 28 days. Figure 5 shows the compressive strength of specimens for each percentage of APECA for 7

Fig. 4 Main structure of falling weight system. 1 drop weight, 2 steel frame, 3 strain gauge, 4 support, 5 steel plate, 6 beam specimen

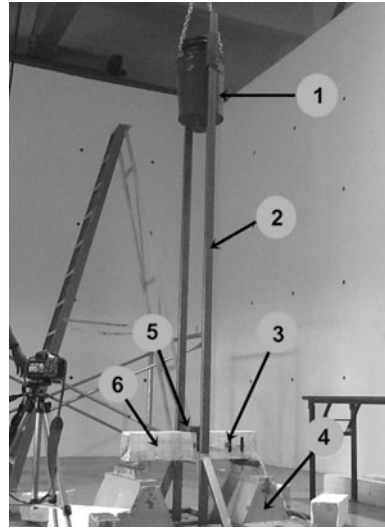
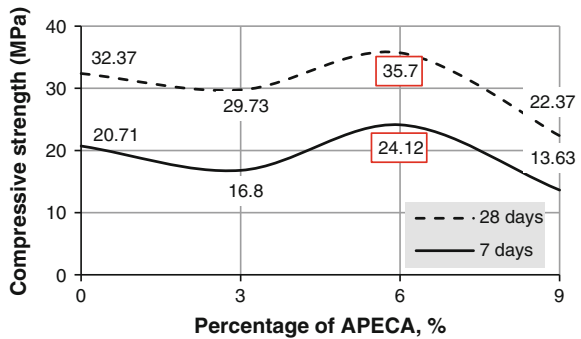


Fig. 5 Compressive strength of different percentage of APECA in concrete mix



and 28 days. It can be seen that the concrete mixes containing 6 % APECA produces highest yet optimum strength about 10 % from normal concrete. Meanwhile, concrete with 9 % APECA will significantly reduce the strength of concrete about 60 %. It is may be due to the bond strength between artificial aggregate and cement paste.

4.2 Impact Test Results

A weight of mass approximately 1 kN (100 kg) is set to drop from a height, h of 1.54 m above the top of the beam and then released. This gives tip velocity, v of 5.5 m/s which is calculated using the following simple equation:

Table 3 Residual displacement of the specimen at mid-span

Beam	No. specimen	Vel. (m/s)	Disp. (mm)	Average disp. (mm)
NRC	1	5.5	14	15.5
	2		17	
RCAI	1	5.5	10	11
	2		12	
RP6A	1	5.5	20	21
	2		22	

Vel. velocity, Disp. displacement

$$v = \sqrt{2gh} \therefore g = 9.81 \text{ m/s} \quad (1)$$

The overall failure modes and residual displacement of the specimen NRC, RCAI and RC6A are recorded using suitable devices and the results are presented herein.

Comparisons of residual displacements for all tested beams under 5.5 m/s velocities are presented in Table 3. The displacement of the beam is recorded at the mid-span of the beam due to the critical point occurs at this zone. The main focus of this investigation was to establish a comparative study between the NRC, RCAI and RP6A. Based on the results, it is observed that the residual displacement of RCAI is 11 mm which displays smaller value than that of NRC at about 15.5 mm, while, RP6A gives significant higher value of displacement about 21 mm as compared to NRC and RCAI. The displacement mainly depends on the stiffness of the beam. Thus, it is obvious that the stiffness of RCAI is higher than that of NRC. In addition, it is also observed that the utilization of 6 % APECA in the concrete mix weakens the specimen under low velocity impact loads. It is due to the poor bonding interaction between APECA and cement matrix.

The crack pattern and failure surfaces of NRC, RCAI and RP6A were successfully recorded. The results are presented in Fig. 6 and Table 4. It is observed that all specimens are failed under 5.5 m/s velocity. The vertical and shear crack predominantly occurred near the mid-span started from the bottom surface of these three specimens. There is some crushing and wide diagonal cracks approximately 5 mm width were generated from an impact point to the bottom region for NRC specimen as shown in Fig. 6a. Observations made from the development of crack pattern and damage for RCAI in Fig. 6b revealed that the failure modes are determined to some crush beneath the impact zone and severe shear cracks that started from supports propagating towards loading point. It shows that the RCAI beam experienced shear crack at an angle of approximately 45° due to the location of AAC block infill parallel to the support direction (refer Fig. 3b). This suggests that the length of AAC block should be provided until the end of the RC beam surface in order to avoid large shear crack orientation. Overall, the crack pattern at

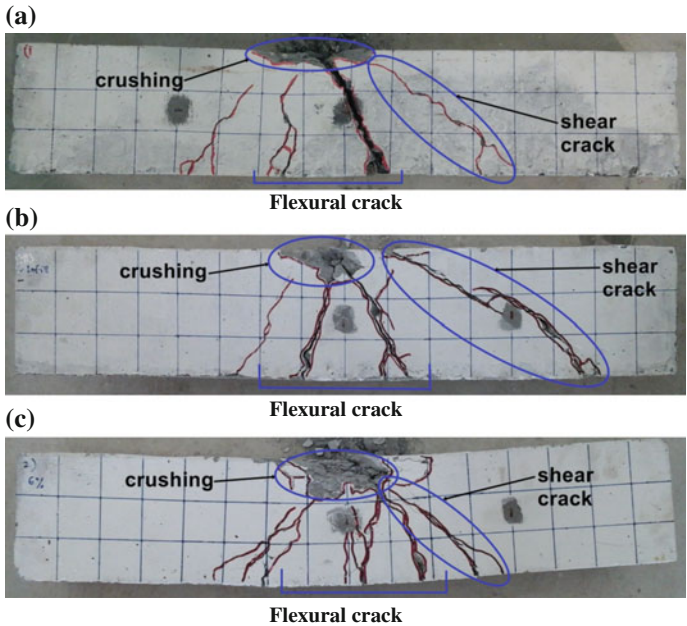


Fig. 6 Failure and crack pattern of tested beam. **a** NRC, **b** RCAI, **c** RP6A

Table 4 Failure mode of specimen

Specimen	Shear-span (mm)	Vel. (m/s)	Failure characteristics
NRC	700	5.5	Flexure and diagonal cracking
RCAI			Crushing, flexure and shear crack
RP6A			Severe crushing, more flexure and shear crack

Vel. velocity

the mid-span is comparatively similar to NRC beam. In addition, only fine diagonal cracks are observed that can be related to the small value of residual displacement at mid-span. From Fig. 6c, the specimen RP6A developed more cracking from the bottom of the beam to the top. Several fine vertical cracks were observed localized near the mid-span, which started from the bottom edge of the beam. Besides, it is also seen that the extensive crushing generated cratering phenomenon in the collision region. This may be due to the brittleness of the material. Further, the nonexistence of top reinforcement on the beam significantly affected the local failure in the compressed area and generating impact cratering.

5 Conclusion

An experimental investigation into compressive strength made with 0, 3, 6 and 9 % as well as behavior of RCAI under 1.54 m drop height of impact weight has been described. Based on the experimental results, the following conclusions were drawn:

- Concrete mixes containing 6 % APECA produced highest yet optimum strength about 10 % from normal concrete and achieved the characteristic strength of concrete grade 25.
- The stiffness of RCAI is higher than that of NRC due to the smaller value of residual displacement of RCAI.
- The crack pattern of RCAI specimen near mid-span is in reasonable agreement with NRC. Fewer cracks width was generated by RCAI near mid-span as compared to NRC that can be related to a small value of residual displacement. However, length of AAC block should be provided until the end of the RC beam surface in order to avoid large shear crack orientation.
- Some improvement in term of providing appropriate rebound prevention jigs is necessary to avoid significant movement of specimen during impact tests.
- Lightweight RC utilizing PE waste materials as an artificial aggregate can be proposed, and further study should be conducted numerously.

Acknowledgments The authors would like to acknowledge financial and facilities support provided by University Tun Hussein Onn Malaysia under short term grant scheme STG 1324.

References

1. V. Vimonsatit, A.S. Wahyuni, H. Nikraz, Reinforced concrete beams with lightweight concrete infill. *J. Sci. Res. Essay* **7**(27), 2370–2379 (2012)
2. N. Mohamad, M.H. Mahdi, Testing of precast lightweight foamed concrete sandwich panel with single and double symmetrical shear truss connectors under eccentric loading. *J. Adv. Mater. Res.* **335–336**, 1107–1116 (2011)
3. W.Y. Jung, M.C. Matt, A.J. Aref, Analytical and numerical studies of polymer matrix composite sandwich infill panels. *Compos. Struct.* **68**, 359–370 (2010)
4. A.M.M. Al Bakri, G.C.M. Ruzaidi, M.N. Norazian, H. Kamarudin, S.M. Tarmizi, Effects of HDPE plastic waste aggregate on the properties of concrete. *J. Asian Sci. Res.* **1**(7), 340–345 (2011)
5. N. Saikia, J.D. Brito, Use of plastic waste aggregate in concrete. *Constr. Build. Mater.* **34**, 385–401 (2012)
6. N. Saikia, J.D. Brito, Waste polyethylene terephthalate as an aggregate in concrete. *Mater. Res.* **16**(2), 341–350 (2013)
7. S. Akcaozoglu, C.D. Atis, K. Akcaozoglu, An investigation on the use of shredded waste PET bottles as aggregate in lightweight concrete. *Waste Manage.* **32**(2), 285–290 (2010)
8. R. Gueraud, A. Sokolovsky, M. Kavyrchine, M. Astruc, Study of the perforation of reinforced concrete slabs by rigid missiles—general introduction and experimental study, part I. *Nucl. Eng. Des.* **41**, 91–102 (1977)

9. G. Fiquet, J. Dacquet, Study of the perforation of reinforced concrete slabs by rigid missiles—experimental study Part II. *Nucl. Eng. Des.* **41**, 103–120 (1977)
10. N. Kishi, T. Ohno, H. Mikami, T. Ando, Effects of boundaries conditions on impact behaviors of reinforced concrete beams subjected to falling-weight impact loads. *J. Struct. Eng. Japan Soc. Civ. Eng.* **731/I-63**, 299–316 (2002) (Japanese)
11. S. Saatci, F.J. Vecchio, Nonlinear finite element modeling of reinforced concrete structures under impact loads. *ACI Struct. J.* **106**, 717–725 (2009)
12. K. Fujikake, B. Li, S. Soeun, Impact response of reinforced concrete beam and its analytical evaluation. *J. Struct. Eng. Am. Soc. Civ. Eng.* **135**(8), 938–950 (2009)
13. Y. Chen, I.M. May, Reinforced concrete members under drop-weight impacts. *Proc. Inst. Civ. Eng.* **162**(1), 45–56 (2009)

Factors Effecting the Thermal and Microstructures of Recycled Glass Concrete

Renga Rao Krishnamoorthy and Ridzuan Mohd Ali

Abstract This paper researches a measurement of thermal conductivity of crushed recycled glass concrete using Unitherm™ Model 6000 Guarded Hot Plate Thermal Conductivity Instrument. Thirty six (36) samples of recycled glass concrete was produced with two types of water to cement ratio (0.4 and 0.5). Recycled glass was used to replace fine aggregate in proportions of 0, 10, 20, 30, 40, and 50 %. In addition, the microstructure behavior of recycled glass concrete was observed using the scanning electron microscopy (SEM) and energy-dispersive X-ray (EDX). According to experimental results water cement ratio, moisture condition and percentage of crushed recycled glass of the specimen revealed as affecting factors on the conductivity of concrete.

Keywords Concrete · Recycle glass · Thermal properties · Microstructures · ASR

1 Introduction

Waste is generated incessantly from time to time owing to the overwhelming industrialization and the growth of the human population. Nevertheless, the construction industry has realized that material prices soar sky-rocketing due to global economic demand and thus paving way for a holistic approach encompassing the use of waste material. This holistic approach reduces the green house effect, minimizes the landfill space and reduces the demand for extraction of natural raw material for construction activity. Recycling of waste materials has become a critical and challenging issue not only in Malaysia but also worldwide. There is an open debate about how the wastage is now converted into carbon foot print by the

R.R. Krishnamoorthy (✉) · R.M. Ali
Faculty of Civil Engineering, University Technology Mara, Shah Alam, Malaysia
e-mail: rao@salam.uitm.edu.my

R.M. Ali
e-mail: ridzuan1995@salam.uitm.edu.my

developed countries and developing countries. In the context of glass, it is noticeably clear that this material was not the prime choice for construction industry to be incorporated into their dwellings or structures. Lack of findings about the advantages of using recycled glass in concrete could be an added factor and the question raised is about the return on investment if this recycled product is to be incorporated together with concrete. Currently glass is one of the least recycled materials in a majority of countries and requires relatively large amounts of energy to be consumed in order to process the raw constituents [1].

Recycling of glass has many benefits in the construction industry; however, its usage has been scarce. In Malaysia, there are largely three glass bottle manufacturers and they produce approximately 600 tonnes of fresh bottles each day. Unfortunately, only a mere 10 % of these used bottles will eventually head back to the factories to be recycled to make new ones. Glass, astoundingly, may well be the least recycled discard.

Glass and cement are chemically incompatible. As a siliceous material, the use of recycled glass as a sand replacement in concrete possesses a high risk of alkali-silica reaction (ASR) expansion. Therefore, cracks were observed when recycle glass was used as a sand replacement in concrete without any precautions to minimize this risk. The potential risk of ASR in concrete with the presence of recycled glass as an aggregate replacement was first investigated by Schmidt and Asia (1963) [2]. ASR is considered as a major obstacle that restrains the use of recycled glass in concrete [3]. Different materials were used as ASR suppressors to mitigate the potential risk of ASR, such as ground granulated blast furnace slag, metakaolin, PGP and lithium nitrate (LiNO_3) [4]. The test results confirmed that LiNO_3 and PGP have significantly reduced the ASR expansion.

Concrete is very much used compared to steel owing to its economics. It is the commonly used construction material. Concrete on its own portrays a good fire resistance because it has low thermal conductivity compared to steel. Understanding the overall thermal property of concrete and recycled glass concrete materials draws importance. It involves the understanding of heat transfer process and heat sink which is very essential in predicting the temperature profile and heat flow through the material itself. An analysis of conduction heat transfer through structure is of great importance in civil engineering problems such as heat flow into a building in energy efficient building design, planning and design of building for thermal comfort, design of a radiation shield in nuclear power stations, analysis of bridge deck and other exposed structures for solar thermal loading and etc. [5, 6]. The use of structures with high thermal resistance has become of great importance in hot weather countries where temperature can reach high levels, especially in summer [7]. The low value of the thermal conductivity is desirable due to the associated ability to provide thermal insulation [6].

This research investigates the effect of recycled glass as a sand replacement in concrete on thermal conductivity performance and microstructure of concrete contain crushed recycled glass.

2 Specimen Preparation

The research on the effects of the water cement ratio and percentage of glass on thermal properties, were designed accordingly and shown in Tables 1 and 2. The control mix was designed to achieve the required design strength of 30 MPa. The cement, coarse aggregate, water/binder ratio and the dosage of the lithium nitrate were kept constant for each water cement ratio of mixed which is 0.4, and 0.5 to show the effect of percentage of the recycled glass on the thermal conductivity of concrete.

In this research, the sand (fine aggregate) will be replaced by a certain percentage of recycle crushed glass (fine aggregate). The percentage will be 10, 20, 30, 40 to 50 % of recycled glass aggregate and one sample is normal mixed concrete (100 % of sand) which will be used as a control sample. The specimen will keep dry for 24 h before curing. All the specimens were placed in a water tank until the time of the test which is 28 days after casting.

2.1 Test Method

The amount of heat flow depends on the thermal conductivity and thickness of the specimen, and on the magnitude of the temperature difference. Under thermal

Table 1 Recycled glass concrete mixture designs with W/C = 0.4

Mixtures	Sand (%)	Recycle glass (%)	Cement (Kg)	Water (Kg/L)	Fine aggregate (Kg)		Coarse aggregate (Kg)	Lithium nitrate (G)
					Sand	Recycle glass		
WC40-0	100	0	8.9	3.6	8.8	0	16.3	0
WC40-10	90	10	8.9	3.6	7.92	0.88	16.3	44.5
WC40-20	80	20	8.9	3.6	7.04	1.76	16.3	44.5
WC40-30	70	30	8.9	3.6	6.16	2.64	16.3	44.5
WC40-40	60	40	8.9	3.6	5.28	3.52	16.3	44.5
WC40-50	50	50	8.9	3.6	4.4	4.4	16.3	44.5

Table 2 Recycled glass concrete mixture designs with W/C = 0.5

Mixtures	Sand (%)	Recycle glass (%)	Cement (Kg)	Water (Kg/L)	Fine aggregate (Kg)		Coarse aggregate (Kg)	Lithium nitrate (G)
					Sand	Recycle glass		
WC50-0	100	0	7.1	3.6	10.2	0	16.6	0
WC50-10	90	10	7.1	3.6	9.18	1.02	16.6	35.5
WC50-20	80	20	7.1	3.6	8.16	2.04	16.6	35.5
WC50-30	70	30	7.1	3.6	7.14	3.06	16.6	35.5
WC50-40	60	40	7.1	3.6	6.12	4.08	16.6	35.5
WC50-50	50	50	7.1	3.6	5.1	5.1	16.6	35.5

Table 3 Test parameters

Parameter	Variables for test	Mixture type
W/C ratio (%)	40, 50	Concrete
Moisture condition	Wet, dry	Concrete
Percentage of recycle glass	0, 10, 20, 30, 40, 50	Concrete

equilibrium conditions; when all the temperatures are steady, the thermal conductivity of specimen can be determined from the Fourier linear heat flow equation.

$$\lambda = (W/A) * (d_1/dT_1) \quad (1)$$

where; λ is Thermal conductivity of the test specimen, W is electric power input to the center heater, A is main heater surface area, d_1 is specimen 1 thickness, dT_1 is temperature gradient from hot plate to cold plate 1.

2.2 Test Variables and Mix Proportions

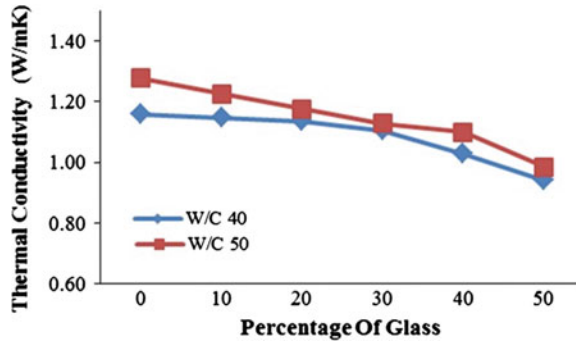
Thermal conductivity measurements were performed with particular reference to their dependence on some other interacted factors such as water–cement (W/C) ratio and percentage of recycle glass as a replacement of fine aggregate. To determine the thermal conductivity coefficient in concrete specimens a test for each parameter was selected as shown in Table 3.

3 Result and Discussion

3.1 Dependence of Thermal Conductivity on W.C Ratio

To determine a change in the thermal conductivity affected by the W/C ratio, tests were conducted from concrete specimen rather than the neat cement paste specimen like that research done before [8, 9] with water cement content of 0.4 and 0.5. Using concrete specimen will represent the thermal conductivity as in real situation compare to only using plain concrete. The concrete specimens, were adopted to show the dependence of thermal conductivity on the W/C ratio when the amount of aggregates in concrete changed according to a change in the amount of cement. Test results in Fig. 1 show that the coefficient of thermal conductivity of the cement is increased when the w/c increased. This showed that the thermal conductivity coefficient is easily influenced by the components of concrete. This result gave a different result compared with the result done before by other researchers [8, 9] which using plain concrete. The research done before claimed that with the addition of the amount of cement for a lower W/C ratio the thermal conductivity of paste specimens increases

Fig. 1 Thermal conductivity of different water cement ratio

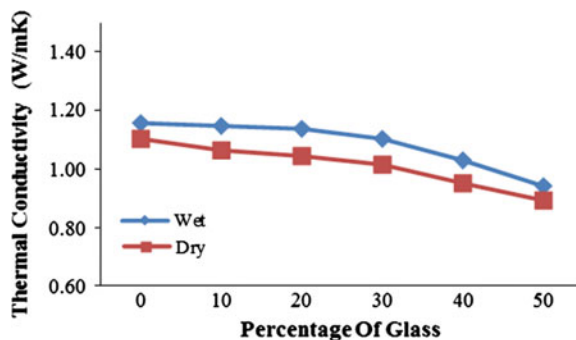


since cement has a higher thermal conductivity value than water. But in reality other constituents of concrete specimen need to be considered too.

3.2 Dependence of Thermal Conductivity on Moisture Condition

Among all the material parameters involved, moisture condition is known to be a key influencing factor. As shown in Fig. 2, thermal conductivity increasing with the sample stated from wet to dry. The status of concrete specimen changes from dried to saturated thermal conductivity is dramatically increasing [8]. Other research done before the thermal conductivity of the screeds is increased significantly by the presence of moisture [9]. This is attributed to changes in air voids filled with water, whose thermal conductivity is superior compare to air. The thermal conductivity of concrete increases with increasing moisture content and since water has a conductivity about 25 times that of air, when the air in the pores has been partially displaced by water or moisture, the concrete must have greater conductivity [10]. Moisture which was the water inside the void in concrete microstructure became the natural medium to transfer the heat from one side to another.

Fig. 2 Thermal conductivity of different moisture condition



3.3 Dependence of Thermal Conductivity on Percentage of Glass as a Fine Replacement

As shown in Figs. 3 and 4 thermal conductivity coefficient positively decreased proportionally with the increased of glass percentage as fine replacement. The thermal conductivity coefficient decreased gradually with the increased of recycle glass content in specimen. Research done before found that mixes with a high fine aggregate proportion had a higher thermal conductivity compared to a high portion of course aggregates [9, 11]. Sand as a fine aggregate has a good thermal conductivity, with replacing the fine aggregate with recycle glass will reduce the ability of sand to transfer heat. The recycled glass then will be function as sand in term aggregates are uniformly distributed in the mix but in same time reduce the ability of concrete to transfer heat.

The addition of LiNO_3 in the concrete mix is seen as a precaution to minimize the ASR risk, but during the concrete casting, severe bleeding and segregation were observed. This resulted from the inherent smooth surface and very low water absorption of the recycle glass sand, which leads to lack in adhesive bond between the components of concrete mix [2, 12]. Additional percentage of recycle glass in the concrete mix shows an obvious effect, that the thermal conductivity decreases.

Fig. 3 Thermal conductivity of different percentage of glass with same WC different moisture condition

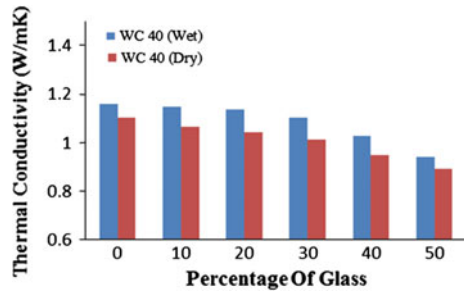
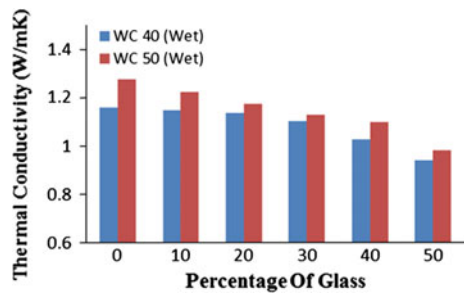


Fig. 4 Thermal conductivity of different percentage of glass with different WC



4 Microstructural Examination of Concrete Cores

Scanning electron microscopy (SEM) and energy- dispersive X-ray (EDX) analysis were used to examine the nature of the hydrated binder and the binder-aggregate interfacial zones. The locations of the EDX analyses are marked on each SEM image. Note that the peak height in the EDX spectra is proportional to the amount of element present. A brief summary of SEM/EDX analysis is given below.

Figure 5 shows the typical composition of the hydrated paste in Mix WC40-0 (reference) and its interface with an aggregate. It can be seen that in the concrete specimen there are fine needle-shaped crystals in the paste are probably ettringite which connecting the paste in the concrete. This was one of the reason why the concrete without glass have a good thermal conductivity compared with the concrete with some percentage of glass because the heat can be transferred through the fine needle-shaped crystal.

The composition of the paste in Mix WC40-10, which contained 10 % crushed recycle glass was found to have been enriched with silica, as predicted (Fig. 6).

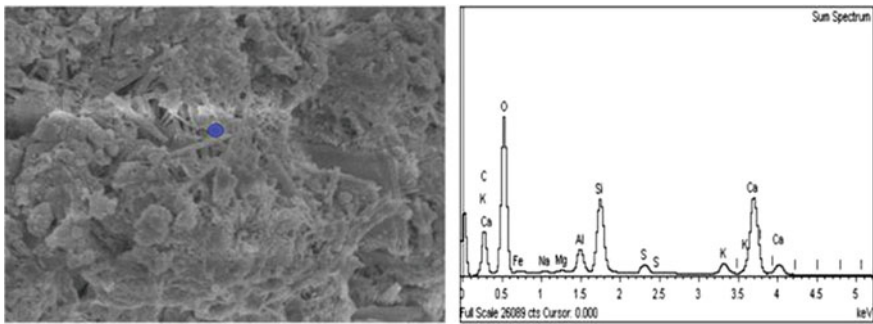


Fig. 5 SEM view of cement paste near a glass particle in Mix WC40-0 (reference), and its EDX spectrum

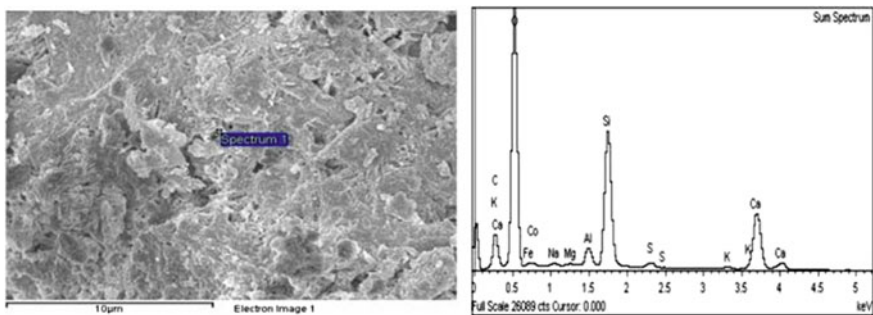


Fig. 6 SEM view and EDX composition of paste in Mix WC40-10 which contained 10 % crushed recycle glass

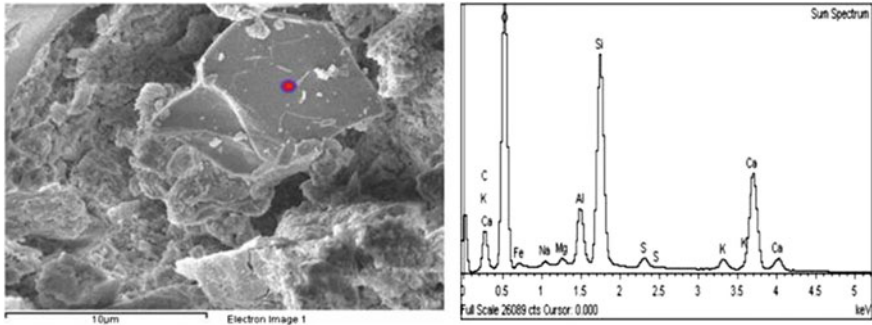


Fig. 7 SEM view and EDX composition of paste near a reacted glass particle in Mix WC40-30

While composition showed in Fig. 7 above showed that of unreacted or partially reacted glass [13]. The composition of the paste in Mix WC40-30 (30 % crushed recycle glass) also showed enrichment in silica. This maybe one of the reason why the thermal conductivity coefficient reduce when the crushed recycle glass added. When the particle of glass embedded in the concrete paste it can be seen that there are spaces between the glass and concrete paste which will be obstacle for the heat to transfer smoothly. The smooth and plane surface of the recycled glass particles also gave a significantly effects weakened the bond between the cement paste and the glass particle as a good heat conductor.

5 Conclusion

An experimental research was conducted to conclude the influencing factors on the thermal conductivity of concrete when the crushed recycle glass replaces the fine aggregate using the Unitherm™ Model 6000 Guarded Hot Plate Thermal Conductivity Instrument which the principle of steady stated is adopted. The following conclusions may be made based upon the systematic investigation of the thermal properties of the different concrete samples tested:

1. The water cement ratio affects the thermal conductivity of recycled glass concrete. According to the test result, with an increase in the water cement ratio, then the thermal conductivity will also increase since there is an increase in the aggregate content. Overall this influences the thermal conductivity of the specimen.
2. The thermal conductivity of the concrete is increased significantly by the presence of moisture.
3. The thermal conductivity coefficient decrease with the increase in percentage of crushed recycle glass.

4. Crushed recycle glass has a good and excellent potential in construction industry not only in reducing energy costs and effects of global warming, it also provide good insulation in concrete to be utilized in tropical countries.

Acknowledgments The authors would like to express their sincere gratitude to Research Management Institute (RMI, UiTM) for providing financial support for this research. It was funded under Research Intensive Faculty (RIF) Fund, UiTM.

References

1. K.H. Poutos, A.M. Alani, P.J. Walden, C.M. Sangha, Relative temperature changes within concrete made with recycled glass aggregate. *Constr. Build. Mat.* **22**, 557–565 (2008)
2. A. Schmidt, W.H.F. Asia, Alkali-aggregate reaction tests on glass used for exposed aggregate wall panel work. *J. Am. Concr. Inst.* **60**, 1235–1236 (1963)
3. R.K. Dhir, T.D. Dyer, M.C. Tang, Expansion due to alkali-silica reaction ASR of glass cullet used in concrete, in *ProcIntSymp on Recycling and Reuse of Waste Materials* (Dundee University, UK, 2003), pp. 751–761
4. B. Taha, G. Nounu, Using lithium nitrate and pozzolanic glass powder in concrete as ASR suppressors. *Cement Concr. Compos.* **30**, 497–505 (2008)
5. M.I. Khan, Factors affecting the thermal properties of concrete and applicability of its prediction models. *Build. Env.* **37**, 607–614 (2002)
6. Y. Xu, D.D.L. Chung, Effect of sand addition on the specific heat and thermal conductivity of cement. *Cem. Concr. Res.* **30**, 59–61 (2000)
7. K.S. Al-Jabri, A.W. Hago, A.S. Al-Nuaimi, A.H. Al-Saidy, Concrete blocks for thermal insulation in hot climate. *Cem. Concr. Res.* **35**, 1472–1479 (2005)
8. K.H. Kim, S.E. Jeon, J.K. Kim, S. Yang, An experimental research on thermal conductivity of concrete. *Cem. Concr. Res.* **33**, 363–371 (2003)
9. A. Alani, J. MacMullen, O. Telik, Z. Zhang, Investigation into the thermal performance of recycled glass screed for construction purposes. *Constr. Build. Mat.* **29**, 527–532 (2012)
10. R. Demirboga (2002), Influence of mineral admixtures on thermal conductivity and compressive strength of mortar, *Energy Build* **35**, 189–192 (2003)
11. A.H.C. Shin, U. Kodide, Thermal conductivity of ternary mixtures for concrete pavements. *Cem. Concr. Compos.* **34**, 575–582 (2012)
12. B. Taha, G. Nounu, Properties of concrete contains mixed colour waste recycled glass as sand and cement replacement. *Constr. Build. Mat.* **22**, 713–720 (2008)
13. A. Shayan, A. Xu, Performance of glass powder as a pozzolanic material in concrete: a field trial on concrete slabs. *Cem. Concr. Res.* **36**, 457–468 (2006)

Determination of Rayleigh Damping Coefficient for Natural Damping Rubber Plate Using Finite Element Modal Analysis

Ahmad Idzwan Yusuf and Norliyati Mohd Amin

Abstract The consideration of Rayleigh damping coefficients of α and β are an important aspect to determine damping matrix in dynamic analysis. In this paper, finite element modal analysis is used on square natural damping rubber plate with various boundary conditions to determine its dynamic properties and damping coefficients α and β . Based on the finding, Rayleigh damping coefficient can be computed and different boundary conditions show different value of Rayleigh damping coefficient.

Keywords Damping · Rayleigh damping · Modal analysis · Finite element · Rubber plate

1 Introduction

In engineering, damping is one of the most important aspects in order to make sure the system remains stable and undamaged. Talbot and Woodhouse [1] on their research paper said that damping is important in structural engineering since it controls the amplitude of resonant vibration response. When a structure is excited with force vibration near its natural frequency, a small force will cause a high stress to the structure which can thus lead to failure of the structure. However, with sufficient amount of damping, the stress can be reduced [2]. Damping is a dissipation

A.I. Yusuf (✉)

Faculty of Civil Engineering, University Technology MARA,
Shah Alam, Selangor, Malaysia
e-mail: idz_wan89@yahoo.com

N.M. Amin

Institute for Infrastructure Engineering and Sustainable Management (IIESM),
University Technology MARA, Shah Alam, Selangor, Malaysia
e-mail: norli830@salam.uitm.edu.my

of energy or energy loss in a vibration system. Based on Stevenson [3], damping can be defined as reduction of response motion of a structure in term of energy loss.

Since damping is important to a structure, many researchers have tried to understand this damping mechanism. There are several types of damping mechanism assumption that can be used in both single degree of freedom systems and multi degree of freedom systems which are viscous damping, Coulomb damping and hysteretic damping. In viscous damping assumption, a dash port constant C is introduced in the system and the damping force is assumed to be proportional to its velocity. Rayleigh damping is one of the viscous damping mechanism. On the other hand, Coulomb damping is an assumption of damping force that is caused by the motion of surface sliding against each other. It is also called as friction damping. Moreover, Hysteretic damping is a damping force related to displacement of the structure and it is also called as structure damping. Amongst all of these assumptions of damping, viscous damping and hysteretic (structural) damping mechanism are the most commonly used in dynamic analysis in order to determine damping in structures [4].

Dynamic responses of vibration in a structure are mainly controlled by damping. The understanding of damping mechanism in vibration analysis is still an issue although there are a number of literature available related to this mechanism [5]. Those are the determination of damping matrix, C in the equation of motion that contains mass, M and stiffness, K is still less comprehensive compared to determination of mass and stiffness matrix. It is because predicting vibration parameters with respect to damping is difficult in practice [4, 6]. Also, Woodhouse [7] stated that the main reason for this problem is because there is no universal mathematical model to represent damping forces because it is unclear which state variable force depends on.

Modal analysis is a technique to determine dynamic properties of a system in a form of natural frequency, mode shape and damping factor. These properties are also called as modal data or modal parameters. Mathematical model for systems dynamic behavior can be developed by using these properties. The formulated mathematical model is known as the modal model. There are two types of modal analysis which are experimental modal analysis and analytical modal analysis. Experimental modal analysis is a determination of dynamic properties by using real structure whereas analytical modal analysis is using finite element software. Therefore, modal analysis can be used as an indicator of structural dynamic response and determination of damping.

So, it is important to select a proper type and value of damping for dynamic analysis because it has a great influence on structural dynamic response. The main objective of this paper is to determine Rayleigh damping coefficients α and β of natural damping rubber plate by using finite element modal analysis with various boundary conditions. One natural damping rubber plate with the thickness of 5 mm and 500 mm x 500 mm in dimension is used in this research. ANSYS 14.0 finite element software is used to analyze the dynamic properties of the rubber plate and Rayleigh damping mechanism assumption is used.

2 Rayleigh Damping

The concept of Rayleigh damping had been introduced by Lord Rayleigh in order to solve numerically on the damping problem in a vibrating system and the concept is commonly used in solving finite element problem [6]. Rayleigh damping is the simplest and convenient way to determine numerically damping matrix [C] under the following form:

$$[C] = \alpha M + \beta K \tag{1}$$

where M and K are the mass and stiffness respectively while α and β are the coefficients related to mass and stiffness of the system. Rayleigh damping is also called as classical damping or proportional damping [8].

In the formulation of Rayleigh damping, it is considered that mass proportional damping effect is dominant in the lower frequencies and the stiffness proportional damping is dominant at the higher frequencies. Therefore α and β are the attributes of the lower and higher resonant frequencies, respectively. Figure 1 shows the general graphical representation of Rayleigh damping [5].

Previously, there are a number of studies that had been made to improve the formulation of Rayleigh damping in vibration analysis in order to get an accurate value of damping matrix. Liu and Corman [4] have studied analytically regarding the extension formulation in Rayleigh damping which is in term of double series. Two forms are established. Hence, with this extension, it will provide more choices in formulating damping matrix in the equation of motion of dynamic analysis. The extension formulations are then compared with experimental modal analysis and thus show that the data is fitted.

Mohammad et al. [6] had done experimental work and finite element study to determine Rayleigh damping coefficient α and β to be used in modal superposition technique in order to determine the damping ratio of other modes by using

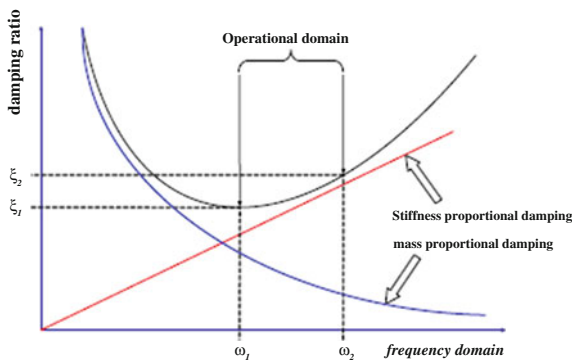


Fig. 1 Graphical representation of Rayleigh damping formulation [5]

numerically finite element and validating the result from experiment works. This method has been found very effective in the estimation of the transient response.

The introduction of finite element software has lead the researchers to study more about Rayleigh damping to get more accurately on the value of damping matric in dynamic analysis of the system. Jie and Yuanfeng [9] did a study to comprehend the influence of Concrete-Filled Steel Tubular (CFST) Bridge in dynamic analysis with different types and different values of damping coefficients by using finite element ANSYS software. Three types of damping were used in ANSYS which are material damping, Rayleigh damping and constant damping. The value of damping used are 0.03, 0.05 and 0.08. Vertical and horizontal forces are applied to the bridge and the responses were measured. This study shows that different types and values of damping have greatly influenced the dynamic response in the CFST Bridge.

Kyriazoglou and Guild [5] had done a hybrid study to determine the damping properties of laminated plated by using experimental works and the finite element method. Finite element ABAQUS Standard version 6.2 software was used in this research. Rayleigh damping and mass proportional damping were used in the software while in experimental analysis specific damping capacity (SDC) was used to measuring damping during the first mode of resonance.

From Eq. 1, Rayleigh damping matrix is proportional to mass and stiffness of a system. Based on this equation, Trombetti and Silvestri [10] had done an analytical study to determine the “optimal” damper system in structures based on Rayleigh damping matrix considering a new way to insert viscous dampers in the structures. Damping analysis was done by separating the mass proportional damping (MPD) and stiffness proportional damping (SPD) in the 6th story of a structure. They showed that the system with MPD system, when excited at base, will have higher damping efficiency compared to SPD.

Alipour and Zareian [11] had done an experimental and numerical study to determine the uncertainties effect of using Rayleigh damping in vibration analysis of inelastic structure and a treatment that can improve the result of the analysis by using this Rayleigh damping formulation. This study showed that by using the stiffness proportional damping part, it will develop ambiguous force which may result to overestimate the design when the structure is non-linear. They suggested that other types of damping are used in vibration analysis such as hysteresis and coulomb damping. As for this finding, Zareian and Medina [12] proposed a more appropriate and easy mode to apply the numerical modeling approach for implementing Rayleigh type damping in structures. This approach eliminates the presence of unrealistic damping forces in inelastic time history responses. As a result, the implication is that the proposed approach will provide improved inelastic dynamic response predictions.

Table 1 Properties of rubber plate

Density (kg/m ³)	Young's Modulus (pa)	Poisson's ratio	Bulk modulus (pa)	Shear modulus (pa)
1,130	1.6499e + 006	0.49989	2.5e + 009	5.5e + 005

Table 2 Dimension of rubber plate

Material	Size (mm)	Thickness (mm)	Boundary condition
Rubber plate	500 × 500	5	1 fixed, 2 fixed, 3 fixed, all fixed

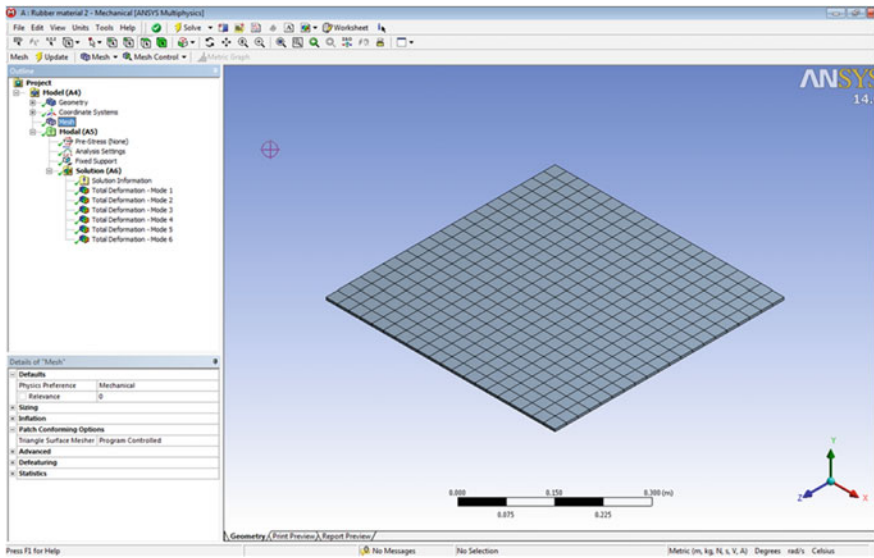


Fig. 2 Finite element model discretization of a rubber plate

Fig. 3 Variation of damping ratio for one fixed end rubber plate

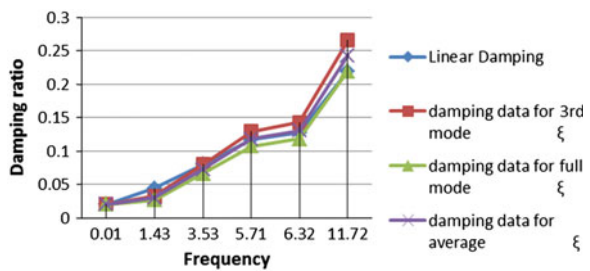
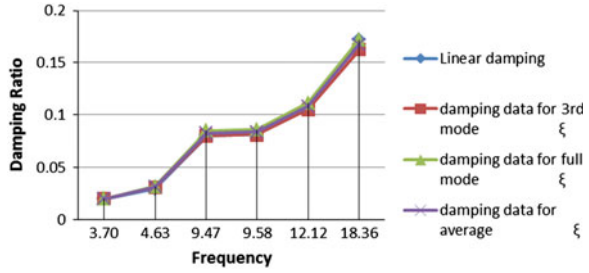


Table 3 Interpolated damping ratio for one fixed end rubber plate

No of modes	Natural frequency (Hz)	Natural frequency (rad/sec) ω	Linear damping ξ	α (3rd mode)	β (3rd mode)	damping data for 3rd mode ξ	α (full mode)	β (full mode)	Damping data for full mode ξ	α (average)	β (average)	Damping data for average ξ
1	0.00157	0.009864624	0.02	0.000390177	0.04529895	0.02	0.000390938	0.037475302	0.02	0.000390558	0.041387126	0.02
2	0.22801	1.432632432	0.0442532	0.000390177	0.04529895	0.032584547	0.000390938	0.037475302	0.026980607	0.000390558	0.041387126	0.029782577
3	0.56176	3.529650432	0.08	0.000390177	0.04529895	0.08	0.000390938	0.037475302	0.066192737	0.000390558	0.041387126	0.073096368
4	0.90854	5.708538528	0.117142398	0.000390177	0.04529895	0.129329575	0.000390938	0.037475302	0.106998843	0.000390558	0.041387126	0.118164209
5	1.0054	6.31712928	0.127516735	0.000390177	0.04529895	0.143110543	0.000390938	0.037475302	0.118399105	0.000390558	0.041387126	0.130754824
6	1.8648	11.71691136	0.219564076	0.000390177	0.04529895	0.265398539	0.000390938	0.037475302	0.219564076	0.000390558	0.041387126	0.242481308

Fig. 4 Variation of damping ratio for two fixed end rubber plate



3 Basic Formulation of Rayleigh Damping

The equation of motion of a system under external dynamic loading given;

$$[M]\{\ddot{u}\} + [C]\{\dot{u}\} + [K]\{u\} = \{F(t)\} \tag{2}$$

where $[M]$, $[C]$ and $[K]$ are mass, damping and stiffness matrix, \ddot{u} , \dot{u} , u are acceleration, velocity and displacement vector and $F(t)$ is external dynamic loading vector. If $\{u\}$, the displacement vector is expressed as

$$\{x\} = [X]\{p\} \tag{3}$$

where $[X]$ is a matrix of size $(n \times m)$ of the first m eigenvector and $\{p\}$ is the generalized displacement vector of size $(m \times 1)$, substituting in Eq. (2) become

$$[M][X]\{\ddot{p}\} + [C][X]\{\dot{p}\} + [K][X]\{p\} = \{F(t)\} \tag{4}$$

Multiplying Eq. (4) by $[X]^T$ yields

$$[X]^T[M][X]\{\ddot{p}\} + [X]^T[C][X]\{\dot{p}\} + [X]^T[K][X]\{p\} = [X]^T F(t) \tag{5}$$

It is known that

$$[X]^T[M][X] = [I], \quad [X]^T[K][X] = [\Omega^2] \tag{6}$$

where $[I]$ is a unity matrix of size $(m \times m)$ and $[\Omega^2]$ is a diagonal matrix of the first m natural frequencies. Since the square matrices associated with the first and last term of Eqs. (5) are diagonal, the second term square matrix is expressed as

Table 4 Interpolated damping ratio for one fixed end rubber plate

Natural frequency (Hz)	Natural frequency (rad/sec) ω	Linear damping ξ	α (3rd mode)	β (3rd mode)	Damping data for 3rd mode ξ	α (full mode)	β (full mode)	Damping data for full mode ξ	α (average)	β (average)	Damping data for average ξ
0.58816	3.695526912	0.02	-0.0977927	0.017984567	0.02	-0.113170163	0.01911055	0.02	-0.10548143	0.018547559	0.02
0.73664	4.628456448	0.029692539	-0.0977927	0.017984567	0.031056104	-0.113170163	0.01911055	0.032000699	-0.10548143	0.018547559	0.031528401
1.5073	9.47066736	0.08	-0.0977927	0.017984567	0.08	-0.113170163	0.01911055	0.08452006	-0.10548143	0.018547559	0.08226003
1.5251	9.58250832	0.081161956	-0.0977927	0.017984567	0.081065964	-0.113170163	0.01911055	0.085658465	-0.10548143	0.018547559	0.083362214
1.9293	12.12217776	0.10754749	-0.0977927	0.017984567	0.104972431	-0.113170163	0.01911055	0.111162846	-0.10548143	0.018547559	0.108067639
2.9217	18.35762544	0.172329787	-0.0977927	0.017984567	0.162413427	-0.113170163	0.01911055	0.172329787	-0.10548143	0.018547559	0.167371607

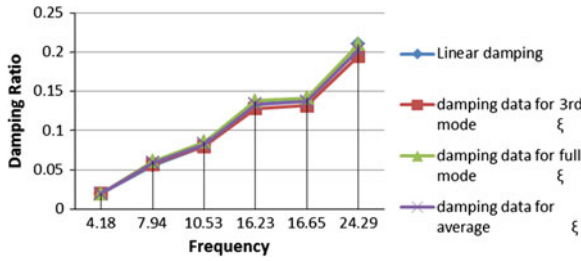


Fig. 5 Variation of damping ratio for three fixed end rubber plate

$$[X]^T[C][X] = 2 \begin{bmatrix} \zeta_1 \omega_1 & 0 & 0 \\ 0 & \zeta_2 \omega_2 & 0 \\ 0 & 0 & \zeta_1 \omega_1 \end{bmatrix} \tag{7}$$

If

$$[C] = \alpha[M] + \beta[K] \tag{8}$$

Then

$$[X]^T[C][X] = \alpha + \beta[\Omega^2] \tag{9}$$

from Eq. (7) and (9),

$$2\zeta_1 \omega_1 = \alpha + \beta \omega_1^2, 2\zeta_2 \omega_2 = \alpha + \beta \omega_2^2, 2\zeta_i \omega_i = \alpha + \beta \omega_i^2 \tag{10}$$

This equation is not valid if ζ exceed 1. α and β are needed to generate ζ_i for given ω_i .

4 Methodology

Finite element modal analysis software which is ANSYS 14.0 is used to determine the natural frequency and mode shape of the rubber plate. The rubber plate is modeled by using specific dimension and properties. Tables 1 and 2 show the dimension and the properties used in modeling the rubber plate. Hexahedral shell elements were used to model the behavior of the plate. Figure 2 shows the discretisation of the rubber plate elements. There are 400 numbers of element and 3,003 numbers of nodes. The meshing size is 25 mm.

Table 5 Interpolated damping ratio for three fixed end rubber plate

Natural frequency (Hz)	Natural frequency (rad/sec) ω	Linear damping ξ	α (3rd mode)	β (3rd mode)	Damping data for 3rd mode ξ	α (full mode)	β (full mode)	Damping data for full mode ξ	α (average)	β (average)	Damping data for average ξ
0.66519	4.179521808	0.02	-0.116703349	0.016251298	0.02	-0.139099035	0.017533367	0.02	-0.12790119	0.016892333	0.02
1.2644	7.94447808	0.055585711	-0.116703349	0.016251298	0.057209107	-0.139099035	0.017533367	0.060892276	-0.12790119	0.016892333	0.059050691
1.6755	10.5275016	0.08	-0.116703349	0.016251298	0.08	-0.139099035	0.017533367	0.085684813	-0.12790119	0.016892333	0.082842406
2.5831	16.23013392	0.133900288	-0.116703349	0.016251298	0.128285107	-0.139099035	0.017533367	0.137999236	-0.12790119	0.016892333	0.133142171
2.6496	16.64796672	0.137849571	-0.116703349	0.016251298	0.131770504	-0.139099035	0.017533367	0.141769794	-0.12790119	0.016892333	0.136770149
3.8655	24.2877096	0.210059091	-0.116703349	0.016251298	0.194950889	-0.139099035	0.017533367	0.210059091	-0.12790119	0.016892333	0.20250499

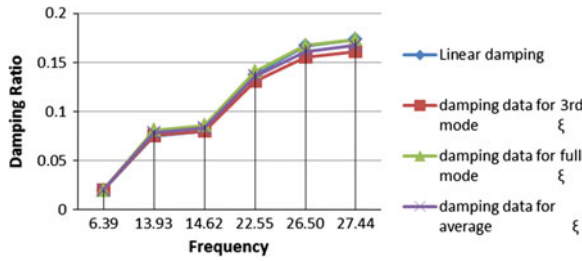


Fig. 6 Variation of damping ratio for all fixed end rubber plate

5 Result and Discussion

Finite element modal analysis gives the result of mode shape and natural frequency for natural damping rubber plate with various boundary conditions. From the result of natural frequency, linear interpolation is used to determine the damping ratio of the rubber plate. From the value of natural frequency and damping ratio, the coefficient α and β are determined.

Figure 3 and Table 3 show the result for rubber plate with one fixed end boundary condition. From the graph, it can be observed that damping with full mode approximation matched the best with the datum value based on linear interpolation. Hence the Rayleigh damping coefficient are $\alpha = 0.000390938$ and $\beta = 0.037475302$.

Figure 4 and Table 4 show the result for rubber plate with two fixed end boundary conditions. From the graph, it can be observed that damping with full mode approximation matched the best with the datum value based on linear interpolation. Hence the Rayleigh damping coefficient are $\alpha = -0.113170163$ and $\beta = 0.01911055$.

Figure 5 and Table 5 show the result of rubber plate with three fixed end boundary conditions. From the graph, it can be observed that damping with full mode approximation matched the best with the datum value based on linear interpolation. Hence the Rayleigh damping coefficient are $\alpha = -0.139099035$ and $\beta = 0.017533367$.

Figure 6 and Table 6 show the result of rubber plate with all fixed end. From the graph, it can be observed that damping with full mode approximation matched the best with the datum value based on linear interpolation. Hence the Rayleigh damping coefficient are $\alpha = -0.275070914$ and $\beta = 0.013008022$.

Table 6 Interpolated damping ratio for all fixed end rubber plate

Natural frequency (Hz)	Natural frequency (rad/sec) ω	Linear damping ξ	α (3rd mode)	β (3rd mode)	Damping data for 3rd mode ξ	α (full mode)	β (full mode)	Damping data for full mode ξ	α (average)	β (average)	Damping data for average ξ
1.0164	6.38624448	0.02	-0.235996364	0.012049939	0.02	-0.275070914	0.013008022	0.02	-0.25553364	0.01252898	0.02
2.2174	13.93236768	0.075003435	-0.235996364	0.012049939	0.075472735	-0.275070914	0.013008022	0.08074462	-0.25553364	0.01252898	0.078108677
2.3265	14.6178648	0.08	-0.235996364	0.012049939	0.08	-0.275070914	0.013008022	0.085666026	-0.25553364	0.01252898	0.082833013
3.5896	22.55417472	0.137847493	-0.235996364	0.012049939	0.130656449	-0.275070914	0.013008022	0.140594591	-0.25553364	0.01252898	0.13562552
4.2178	26.50128096	0.166617815	-0.235996364	0.012049939	0.155216864	-0.275070914	0.013008022	0.167174851	-0.25553364	0.01252898	0.161195857
4.3666	27.43622112	0.173432562	-0.235996364	0.012049939	0.161001579	-0.275070914	0.013008022	0.173432562	-0.25553364	0.01252898	0.167217071

6 Conclusion

Based on the result, Rayleigh damping coefficient α and β can be determined by using finite element modal analysis. The results also show that different boundary conditions will give different value of coefficient α and β . In this model proposed, it is assumed that the dissipation energy is only through material damping. Damping from external sources is not included. As an extension of this work, one can verify this result by using experimental modal analysis. One can also determine Rayleigh damping coefficient using other materials such as steel, iron and etc. and compare the value of α and β .

References

1. J.P. Talbot, J. Woodhouse, The vibration damping of laminated plates. *Compos. A Appl. Sci. Manuf.* **28**(12), 1007–1012 (1997)
2. G.D. Gounaris, N.K. Anifantis, Structural damping determination by finite element approach. *Comput. Struct* **73**, 445–452 (1999)
3. J.D. Stevenson, Structural damping values as a function of dynamic response stress and deformation levels. *Nucl. Eng. Des.* **60**, 211–237 (1980)
4. M. Liu, D.G. Corman, Formulation of Rayleigh damping and its extensions. *Comput. Struct.* **57**(2), 277–285 (1995)
5. C. Kyriazoglou, F. Guild, Finite element prediction of damping of composite GFRP and CFRP laminates—a hybrid formulation—vibration damping experiments and Rayleigh damping. *Compos. Sci. Technol.* **66**(3–4), 487–498 (2006)
6. D.R.A. Mohammad, N.U. Khan, V. Ramamurti, On the role of Rayleigh damping. *J. Sound Vib.* **185**(2), 207–218 (1995)
7. J. Woodhouse, Linear damping models for structural vibration. *J. Sound Vib.* **215**(3), 69–547 (1998)
8. J.F. Semblat, Rheological interpretation of Rayleigh damping. *J. Sound Vib.* **206**(5), 741–744 (1997)
9. W. Jie, W. Yuanfeng, Influence of damping change on dynamic response of concrete-filled steel tubular arch bridges. *Adv. Steel Struct.* **II**, 1675–1680 (2005)
10. T. Trombetti, S. Silvestri, On the modal damping ratios of shear-type structures equipped with Rayleigh damping systems. *J. Sound Vib.* **292**(1–2), 21–58 (2006)
11. A. Alipour, F. Zareian, Study Rayleigh damping in structures . uncertainties and treatments, in *The 14 World Conference on Earthquake Engineering* , (Beijing, China, 2008), October 12–17, 2008
12. F. Zareian, R.A. Medina, A practical method for proper modeling of structural damping in inelastic plane structural systems. *Comput. Struct.* **88**(1–2), 45–53 (2010)

Construction of Roller Compacted Concrete Dam in Malaysia: A Case Study at Batu Hampar Dam

Assrul Reedza Zulkifli, Abdul Rahim Abdul Hamid,
Mohd Fadhil Arshad and Juhaizad Ahmad

Abstract Rapid and economical construction are among numerous advantages of the construction of roller compacted concrete (RCC) dam compared to conventional dam. However, the complex process of RCC dam construction is facing difficulties due to lack of understanding and involvement from the local construction industry player since this type of construction in Malaysia is still new. Therefore, this paper presents the process of RCC dam construction in Malaysia. Site observation and the review on literature of RCC dam construction was conducted to get the real view on the construction process of such project. The expert panel interview was conducted to get the view on RCC dam construction. Panel interview result was analysed and supported with the literature to gather the process of RCC dam construction. From the result analysis, the construction processes which consist of determination of mix design, RCC production and RCC placement is presented.

Keywords Roller compacted concrete (RCC) · Dam · Process · Construction

A.R. Zulkifli · J. Ahmad (✉)

Faculty of Civil Engineering, Universiti Teknologi MARA, Shah Alam, Selangor, Malaysia
e-mail: juhaizad@salam.uitm.edu.my

A.R. Zulkifli

e-mail: reedza03@gmail.com

A.R.A. Hamid (✉)

Faculty of Civil Engineering, Universiti Teknologi Malaysia, Johor Bahru, Malaysia
e-mail: rahimfka@gmail.com

M.F. Arshad (✉)

Institute Infrastructure Engineering and Sustainable Management (IIESM),
Universiti Teknologi MARA, Shah Alam, Selangor, Malaysia
e-mail: fadiil2013@yahoo.com

1 Introduction

The new technology is adopted for the construction of gravity dam and the technology is known as roller compacted concrete (RCC). Reference [1] stated that RCC has been rapidly developing over the past 40 years and now is commonly used for gravity dam application. Recently, Malaysia started adopting RCC technology to the gravity dam construction. With the fact that the construction of RCC dam is still new in Malaysia, the understanding on such construction is very limited among local construction industry player. The first RCC dam in Malaysia is Kinta dam which is situated in Ipoh and constructed by Japanese contractor (Hazama Corporation). It was completed in 2007. In 2008, the construction of Batu Hampar dam is started which is the second RCC dam project in Malaysia. *Dekon Sdn. Bhd.*, the local contractor who had no previous experience of RCC dams was selected to construct the dam. The government intention to develop local knowledge or expertise of RCC instead of recourse to international contractor is the main reason why Dekon was selected [2].

The understanding and involvement from the local construction player is still at the early stage. Therefore, the construction personnel such as engineer, the supervisor, the technician, until the general workers has very limited knowledge on the RCC dam project that leads to difficulties. Hence, there is a need to capture the knowledge of RCC dam construction.

This study will serve as an avenue for further understanding the construction of RCC dam among the local construction industries player.

This paper presents the process of the construction of Roller Compacted Concrete Dam in Malaysia with Batu Hampar dam in Rembau, Negeri Sembilan as the case study since Malaysia has just started to adopt the RCC dam technology in the construction of the Dam project. The scope of this study is focused on construction stage of RCC dam project. This study involves interview sessions with the professional and semi-professional construction personnel who were involved in RCC dam project in Malaysia.

Concrete in general are defined as a composite construction material composed primarily of aggregates, cement and water. According to America Concrete Institute (ACI), Roller compacted concrete (RCC) is defines as concrete compacted by roller compaction [3]. RCC is considered for application where no slump concrete that can be transported, placed and compacted by using the normal construction equipment that being used in earthfill and rockfill works [3]. Parallel to this, [4] defines RCC as no slump consistency concrete that is placed in a thin horizontal lifts and compacted by vibratory rollers. The application of RCC is considered when it is economical competitive with other construction method and in this case is the application of RCC method for construction of a gravity type of dam [4].

RCC dam construction requires four basic component which includes ingredient for the concrete, production of the concrete, transportation and placement of the concrete to the dam [5].

1.1 RCC Mix Design

The typical RCC mix design contains approximately 5–6 % water, 5–10 % cement and flyash, 30–35 % fine aggregates and 60–65 % coarse aggregates. This design possesses the characteristic required by the gravity dam which is strength and permeability properties [4]. RCC mixture proportioning procedure is very similar to conventional concrete. According to [6] the general methodology of RCC mixes proportion by used soils approach is:

1. Selection of suitable aggregate.
2. Select range of trial mixes which consist of various cement and fly ash content.
3. Determine desirable moisture content.
4. Prepare RCC cylinder and specimen for strength testing and durability testing.
5. Select mix proportion based on laboratory result.

1.2 RCC Placement

According to [7] the machineries used to construct RCC dam are similar to the construction of earth embankment which is dozer, dump truck and roller compactor. Dump truck used to transport the RCC mixture to the dam site, and dozer used to spread the RCC material at certain thickness, then the roller compactor required to compact the RCC material [7].

According to [3] RCC lift minimum thickness is ranging from 150 mm to 1 m but in normal practice in United State is rarely exceeded 0.6 m and the thickness is depending on mixture proportions, plant and transport capability, placement rates, spreading and compacting procedure, and the size of placement area.

2 Methodology

The overall view of the RCC dam construction was captured from site observation and literature review. Then, interview questions were drafted. Interview sessions were conducted and the statement given by the respondent was recorded. The respondent (5 person) are the site personnel who are involved in the construction of Batu Hampar dam. The interview was recorded using a digital recorder to record statement given by the interviewee and were converted into a written form. Furthermore, content analysis was done on the answer and statement given by every respondent.

3 Result and Discussion

From the analysis, the processes of RCC construction works as shown in Fig. 1 are listed below:

1. Determination of RCC mix (RCC design mix)
2. Aggregates production
3. Foundation preparation and treatment
4. Diversion culvert and river diversion works
5. RCC mix production
6. RCC placement works
7. Instrumentation works

3.1 Determination of RCC Mix

Three combined mix aggregates grading namely T1(63-25)mm size, T2(25-5)mm size and T3(5-0.75)mm size which is coarse, medium and fine size of aggregates are adopted. This mix aggregates grading meets the specified grading envelope as in specification. Cement with low heat of hydration is the ideal cement to prevent temperature rise in concrete. To lower the heat of hydration of RCC, less amount of cement is used and type F Flyash is used to replace the quantity of cement. It was finalized and approved by RCC dam specialist as follows:

1. T1-28, T2-34, and T3-38 %
2. Cement- 65 kg/m³ and Flyash-105 kg/m³
3. Moisture content between 4.5 and 5.4 %
4. Vebe time with a 12.5 kg surcharge was 15–30 s
5. Retarder is used to increase the initial setting time, thereby maintaining fresh lift joint
6. Bedding mortar used to treat the cold joint for RCC lift

3.2 Aggregates Production

Three types of aggregates produced based on specification namely T1 (63-25)mm, T2 (25-5)mm and T3 (5-0.75)mm which is coarse, medium and fine size of aggregates. Before RCC placement take place, the aggregates needs to be stockpiled at least 80 % of total amount of aggregates required to complete the project.

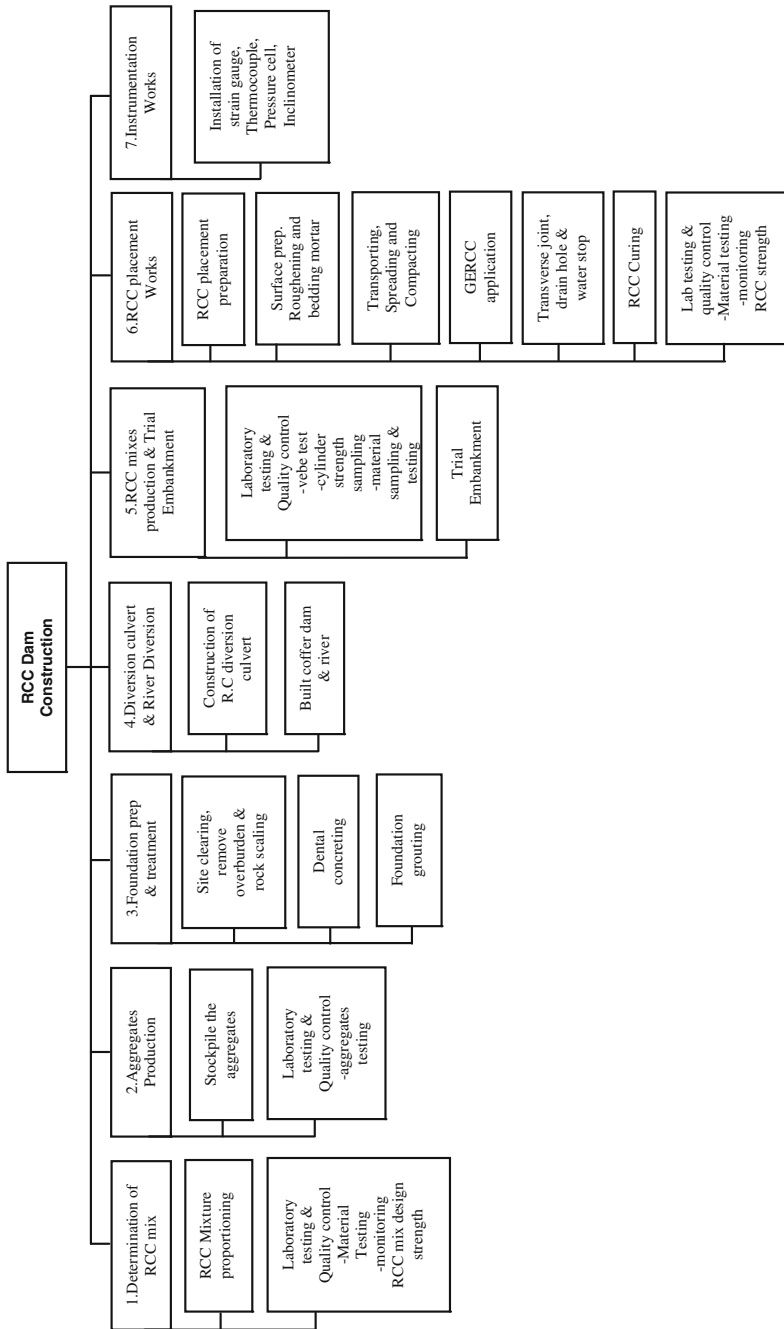


Fig. 1 Works breakdown structure of RCC dam construction

3.3 Foundation Preparation and Treatment

Site clearing and removing overburden are the first step in preparing the RCC dam foundation. After site clearing and removing the soil or overburden was done, rock scaling works are the next step that to be done. Rock scaling works are to determine the type of rock where the specification state that, dam are to be sit on grade 2 or better rock. Foundation grouting are carried out is to strengthen the foundation and to ensure permeability of the foundation is high. The concept is to seal of the void, crack and fracture inside the rock that will strengthen the foundation for the dam to sit. The granite rock is permeable and as a result, fewer amounts (volume) of grouting are needed.

3.4 Diversion Culvert and River Diversion

Diversion culvert is a reinforced concrete structure with 15 m diameter \times 60 m long, complement with upstream and a downstream cofferdam. This is to allow the river flow trough cofferdam into the diversion tunnel and flow to downstream of the river.

3.5 RCC Mix Production

Continuous pugmill type of production plant is used for RCC production which is able to produce maximum capacity of 400 m³/h [2]. This plant control proportion of aggregates component by volumetric, and cement and flyash by weight control. Due to weather condition in Malaysia, chill water is used to lower the temperature of RCC mix.

3.6 RCC Placement Works

At the beginning stage of RCC placement, RCC is to be placed at a series of 15 m wide strips from downstream to upstream in 6 m section. The thickness of placement is 300 mm and compacted by vibratory roller compacter. The time allowed from mixing of RCC, transport, spreading and compaction is 45 min. Immediately after RCC has compacted, the field density test (FDT) was carried out using nuclear density meter to measure the density of RCC. Then, if the compaction achieved 98 % above, the next layer is continued with the same method and routine. Figure 2 shows the routine of RCC placement works.

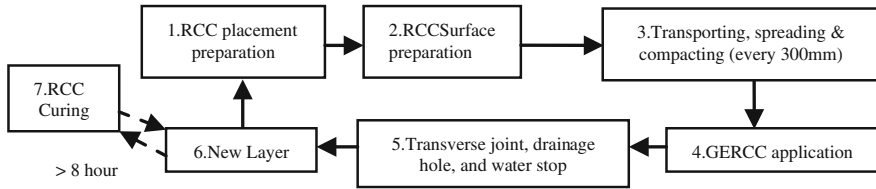


Fig. 2 RCC placement routine



Fig. 3 Carpenter fixing the formworks at upstream of the dam

3.6.1 RCC Placement Preparation

System formworks were used to form 65 m vertical wall of upstream RCC dam where the erection of formworks was made as the level of RCC increases. Every increasing level of RCC, system formworks is lifted up using a mobile crane and carpenters tied bolt and nut of the formwork. Figure 3 shows the formworks at upstream of Batu Hampar dam. The precast concrete blocks embedded with steel plate are arranged by using mobile crane along the area where RCC is to be placed that form a downstream step as shown in Fig. 4 which is the same method used in China 131 m high Jiangya Dam, precast concrete block were used to form the step in downstream face of the dam [8].

3.6.2 RCC Surface Preparation

When the RCC surface are left more than 8 h, normally due to plant breakdown or other issues that RCC placement are needed to be stopped, lift joint treatment needs to be performed before continuing a new layer of RCC. On the surface of old RCC



Fig. 4 Concrete block are arrange to form a 600 m downstream step

layer, roughening was performed by using high pressure water jet blasting and the time to implement it is determined by hardening time which is 8 h after compaction. Immediately after green cutting was done, bedding mortar is spread and the new layer of RCC placement is continued. This method was carried out to ensure the good bonding between joint lift which is between the layers of RCC.

3.6.3 Transporting, Spreading and Compacting

In the early stage of RCC placement works, RCC was transported by dump truck directly from the RCC mixing plant. The usage of dump truck was recognized as inefficient due to the site was at narrow steep side that lead to frequent needs to change and erect the temporary access for placement works. Therefore, the conveyor system is essential to transport RCC directly to dam site.

Conveyor system is required to transport RCC. However, due to the unavailability of technology in Malaysia, cost and other management issues, the conveyor system was not applied at the beginning of the placement works. The conveyor system was used only when the RCC reached level 95 m (lowest level was RL 75 m). Figure 5 shows conveyor system that has been apply at Batu Hampar dam.

RCC that was deposited from dump truck at the dam site was spread with 300 mm thickness by tracked dozer. Single drum vibratory roller compacter was used to compact the RCC. Single Vibratory rollers compacter makes one round trip over the concrete without vibration and continued with at least three round trips with vibration. Practically five (5) to seven (7) passes with vibration is enough to achieve the 98 % compaction density. This method is fast and sufficiently accurate which contributes to uniformly compacted RCC [9]. Immediately after compaction was sufficiently carried out, density of the RCC or field density test was tested using



Fig. 5 Conveyor system apply at Batu Hampar dam when the RCC level reach higher level



Fig. 6 RCC transporting, spreading, and compacting, nuclear density meter used to check the density every layer of RCC placement completed

nuclear density meter. Figure 6 shows RCC Transporting and spreading and compacting process.

3.6.4 GERCC Application

Grout enriched RCC (GERCC) is produced by adding 3:1 or 4:1 water-cement ratio grout to the uncompacted RCC and then concrete vibrator used to compact the concrete. Grout was mixed using mixer and spread manually using bucket that as shown in Fig. 8. The concept of using GERCC in RCC dam is to be applied at location of RCC placement where difficult to access by vibratory roller compacter. By applying GERCC it fills the void in RCC and create the smooth surface especially for upstream and downstream portion where it can be seen clearly after formworks have been dismantled. According to [10] at Kinta dam, GERCC are applied at the entire upstream and downstream faces (including the stepped spillway), the transition zone between RCC and rock abutments, drainage gallery walls, as well as encasement of waterstops, drains, and reinforcing steel.

3.6.5 Transverse Joint, Drainage Hole and Water Stop

At the upstream and downstream edges of the dam, galvanized steel plates were installed in advance as a contraction joint at 15 m spacing. Then, water-stop and drainage holes were set in the upstream face of the dam. The drainage hole and water stop were set at the upstream face of the dam prior the increase of RCC. Drainage hole function is to collect and convey the water that seep thru the dam and the water are drain out from drainage gallery to downstream river.

Transverse joints are installed to prevent temperature cracks in the concrete [11]. The installation took place after the completion of RCC placement layer and before it hardens, and prior to the placement of the next layer. Transverse joint were cut by a vibratory blade machine and galvanized thin plates were installed in the cutting plane to prevent closing that has shown in Fig. 7. Figure 8 shows the location of water stop, drainage hole and transverse joint.

3.6.6 RCC Curing

After placement, if the commencement of next layer of RCC is more than 24 h, the concrete is cured by water ponding.

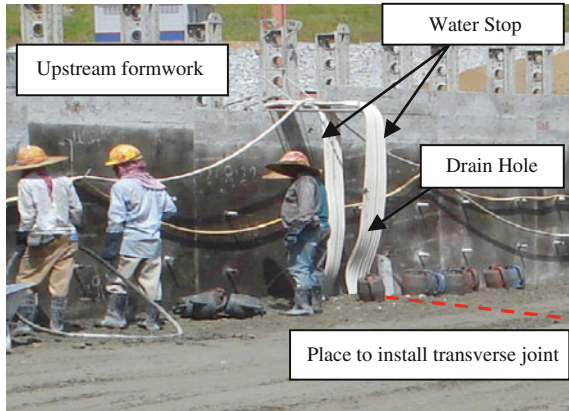
3.6.7 Laboratory Testing and Quality Control of the RCC Dam

Various quality control measures were executed at RCC dams so that the quality of materials is monitored carefully. Quality control methods that were applied at Batu Hampar dam is as in Figs. 5, 6, 7 and 8.

Fig. 7 Transverse joint were cut and installed a galvanize thin plate at Batu Hampar dam



Fig. 8 Water stop, drainage hole and transverse joint location, from left, workers apply GERCC at upstream face of the dam



3.7 Concrete Strength

Concrete strength is being monitored according to date the cylinder sample was taken and compressive strength test is conducted 7, 14, 28, 56, 96 and 180 day. It was carried out from the determination of RCC mix process until RCC placement works are completed. To monitor the compressive strength of RCC, compressive strength test and indirect tensile strength test is carried out at the stated days.

3.8 Density of RCC

Nuclear density meter is used to check the density of the RCC after compaction is carried out. The number of passes of the vibratory roller is manually counted to ensure the adequate compaction of RCC layer.

3.9 Vebe Consistency Test of RCC Mix

RCC concrete is dry and lean, the slump test cannot be used to measure its consistency [12]. The Vebe test with the standard container is conducted to monitor the consistency and workability of RCC mix. The test is conducted once every batch of RCC production. Optimum Vebe time is between 15 and 25 s, where it is the optimum in workability of RCC.

3.10 RCC Material Testing

RCC material testing is carried out in the early stage of RCC construction until the end of RCC construction works. The RCC material are tested to ensure the consistency of the RCC material. Table 1 shows the major material testing for Batu Hampar dam project.

3.11 Instrumentation

According to [11], the instrumentations installed in dams are for the purpose of:

1. Monitoring overall performance of the dam structure to ensure dam safety.
2. Monitoring the behaviour of the RCC dam.

Different instrumentation, monitors different character or behavior of the dam. The instrument that has been installed at Batu Hampar dam are as stated in Table 2.

Every 10 m height of RCC dam, the instrumentation was installed by slotting the instrument in the RCC lift and the cable was laid inside the RCC by trenching it to cable riser pipe, before continuing RCC placement as usual.

Table 1 Material testing at batu hampar dam

Material	Test	Frequency
Cement	Chemical composition, moisture content, specific gravity, finess, temperature	Every delivery to site
Flyash	Same with cement testing	Every delivery to site
Aggregates	Flakiness test, sieve analysis, specific gravity, soundness, and others testing that related to aggregates. Instructed by engineer	1 per day and every new production of aggregates stockpile

Table 2 Instrument installed at batu hampar dam

	Instrument type	Application
1	Vibrating wire piezometer	Measure the pore water pressure
2	Combine biaxial inclinometer/magnetic extensometer	Ground lateral movement and settlement
3	Thermocouple	Temperature of the dam
4	Vibrating wire strain gauge	Measuring strain in mass of RCC dam
5	Vibrating wire pressure cell	Measure the internal stress of RCC
6	Surface settlement/deflection point	Vertical and horizontal displacement of the dam

4 Conclusions

The process of RCC dam construction in Malaysia started from determination of RCC mix until RCC placement works. Before RCC placement started, it requires the preparation process which involves the preparation of RCC mix, foundation preparation, and diversion works. Preparation of RCC mix includes finalizing the RCC mix and production of RCC. Further to RCC placement works, it requires the complex of construction method in order to place a large amount of mass concrete to form a gravity type of dam. The instrumentation is installed at the dam during construction stage to monitor overall performance of the dam structure to ensure dam safety.

References

1. T. Warren, A. Denoyer, A. Ulas, Taking advantage of RCC: Ted Warren discusses the history of roller compacted concrete (RCC) dam construction and its various applications and advantages to gravity dam design and construction. *Int. Water Power Dam Constr.* **63**(7), 20–23 (2011)
2. C. Wagner, Batu Hampar dam—design and construction of an RCC dam. *Dams Reservoirs* **21**(2), 77–90 (2011)
3. Department of The Army, US A. C. o. E. W., DC, Engineer manual—engineering and design roller-compacted concrete [Engineer Manual]. EM 1110-2-2006 (2000)
4. R.P. Bass, Alternative dam construction techniques. *Proceedings of the 1991 Georgia Water Resources Conference*, Athens, Georgia, 19–20 Mar 1991
5. L. Uribe, D. Bosshart, Challenging RCC dam construction for the Ralco project in Chile. *Int. J. Hydropower Dams* **9**(4), 95–99 (2002)
6. Y. Choi, J. Groom, RCC mix design—soils approach. *J. Mater. Civil Eng.* **13**(1), 71–76 (2001)
7. R.P. Bass, *Rehabilitating Dams with Roller Compacted Concrete Bridging the Gap* (2003), pp. 1–9
8. B.A. Forbes, Using sloped layers to improve RCC dam construction. *Civil Struct. Hydro Rev. Worldwide (HRW)* **11**(3) (2003)
9. E.G. Nawy, Roller compacted concrete, in *Concrete Construction Engineering Handbook*, 2nd edn. (CRC LLC, USA, 2008), pp. 1–72
10. B.A. Forbes, D. Hansen Kenneth, J. Kitzgerald Thomas, State of the practice—grout enriched RCC in dams, in *United States Society on Dams Annual Conference*, Portland Oregon, (April/ May 2008), pp. 1–17
11. Q.H.W. Shaw, Chapter 2: RCC construction, RCC mixes, RCC instrumentation and RCC dams study. Ph.D. thesis, University of Pretoria, (2011)
12. S. Nagataki, T. Fujisawa, H. Kawasaki, State of art of RCD dams in Japan. Paper presented at the 50^o Congresso brasileiro do concreto, Salvador (1st Brazilian RCC symposium, Sept 2008)

Partial Replacement of Glass Fiber with Kenaf Waste in Cement Board Production

Zakiah Ahmad, Mohd Fadzil Arshad and Affah Azrae

Abstract Waste plantation can be utilized as a raw material in the production of construction materials such as bricks and cement board in order to achieve sustainable technologies. This study investigated the potential of waste kenaf bast fiber from decortications extraction method as the glass fibre replacement in the manufacturing of cement board. These boards were made from waste kenaf bast fiber, cement and water at a cement:fibre:water ratio of 2:1:2. Six (6) series of mixtures with different kenaf replacement; Series 1 (100 % kenaf), Series 2 (80 % kenaf fiber and 20 % glass fiber), Series 3 (60 % kenaf fiber and 40 % glass fiber), Series 4 (40 % kenaf fiber and 60 % glass fiber), Series 5 (20 % kenaf fiber and 80 % glass fiber) and Series 6 (100 % glass fiber) were prepared and and 460 mm × 460 mm size of boards were cast. The target board density was 650 kg/m³. The effects of using different percentages replacement of kenaf waste on internal bond and bending strength of the resulted cement boards were investigated after 28 days curing process. The mechanical and physical properties of the boards were evaluated based on MS 934 (1986). The results showed that boards Series 4 achieved the highest bending strength and internal bond (IB) strength compared to other boards and satisfied the requirement for lightweight board as stipulated in Malaysian Standard MS 934.

Keywords Bending strength · Cement board · Kenaf bast fiber · Glass fiber · Internal bond

Z. Ahmad · M.F. Arshad (✉)
Institute for Infrastructure Engineering and Sustainable Management,
Universiti Teknologi MARA, Shah Alam, Selangor, Malaysia
e-mail: fadil2013@yahoo.com

Z. Ahmad
e-mail: zakiah@salam.uitm.edu.my

A. Azrae
Faculty of Civil Engineering, Universiti Teknologi MARA, Shah Alam,
Selangor, Malaysia

1 Introduction

Natural fibers have been used in building and transportation industry for various types of application such as in the production of hardboard, particleboard, wall panels, ceiling finishes and roof sheeting and also as interior and exterior parts of cars and boats. Natural fibers have been proven to offer an advantages such as low cost and low density compared to glass fibres [1]. Natural fibers are also renewable resources.

In recent years, there have been rapid growths in research of using natural fiber in cement composites by using different natural fibers mostly from cellulosic materials such as coconut coir [2], kenaf fibre [3, 4, 5] wood fiber, i.e. Acacia Mangium [6] and etc. From these researches, they showed that the production of cement board using natural fiber is promising. Furthermore, the result showed that significant improvement in increase strength, stiffness and fracture toughness [2, 4, 7].

Kenaf is a crop newly planted in Malaysia to replace tobacco. This crop has an advantage of short period for harvesting and can be used to produce cement or polymer based composite [5]. In Malaysia, there are a lot of initiatives by government to promote kenaf plantation in order to replace tobacco. During the process of extracting kenaf to obtain kenaf core and bast fibre for various uses, some of them will be left unused for more than two weeks which has low in quality and usually brown in colour. These fibers are considered as waste.

Since ceiling board is considered as non-structural element which needs less strength compared to other structural elements therefore, the utilizing of kenaf waste which has low quality is possible as a supplement to the existing raw materials. Studies have shown that natural fibers have the potential in replacing glass fibre and asbestos in ceiling board. Glass fibre in ceiling production is well known to have bad affect to human health [3, 4]. Furthermore, literature indicated that glass fiber does not degrade and can cause cancer if exposed for long term [8]. The waste generation from kenaf process keeps increasing as kenaf has been planted widely in Malaysia and the market for kenaf fiber is still limited which cause waste management problem in the future. Hence, this study investigated the suitability of using waste kenaf fiber as a raw material in cement board manufacturing to replace glass fiber. The mechanical properties such as tensile and bending properties were investigated.

2 Materials and Methods

2.1 Material Preparation

Kenaf waste used was taken from Lembaga Kenaf Malaysia which located in Kuala Rompin, Pahang. This 'waste kenaf' used in this study is defined as the kenaf (combination of bast fiber and core) that has been processed and left unused for

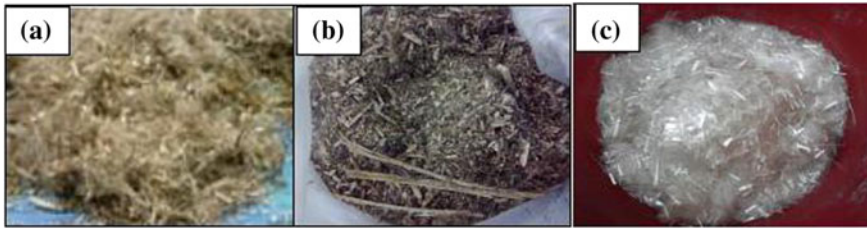


Fig. 1 Fiber used in this study; **a** kenaf waste at after 2 weeks, **b** kenaf waste after 1 month and **c** glass fiber

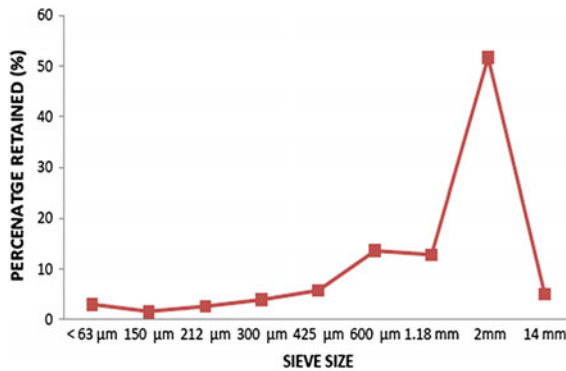


Fig. 2 Particle size distribution of kenaf waste

more than a month. Figure 1 shows the difference between kenaf particles at less than 2 weeks period and after one month period.

The collected kenaf waste came with random size after being grinded by decorticator machine. The waste kenaf when observed closely contained different sizes of kenaf bast fibre and core. This is the kenaf waste being used in this study and denoted as kenaf particles.

The kenaf waste particles were sundried for at least 24 h to reduce the moisture content. In order to get some information on the particle size of the randomly collected kenaf waste, the kenaf waste was sieved.

The dried waste was classified by its particle sizes using sieve analysis ranging from 63 μm to 2 mm. According to the sieve analysis, about 57 % of the waste passed through 2 mm screen and these particles were discarded (Fig. 2). The retained particles were further sieved by using 14 mm sieve. Only the particle that passed 14 mm sieve were used in the manufacturing of cement board. It was found that about only 5 % particles retained which have size up to 30 mm and these particles were not used in this study. Based on the previous research, the size of the particles can effect on the strength of cement board [9]. The larger particle size gave higher strength compared to finer particles [5] because higher content of particles sizes can reduced the compressive strength of composites due to filler effect in the

cement composites provide by the finer particles. Glass fiber coated with polypropylene resin was used is as shown in Fig. 1c. The length of the fiber was 10 mm.

2.2 Determination of Physical and Chemical Properties of Kenaf Waste Particles

The moisture content of the kenaf waste was determined by oven dry method. The weight of kenaf was measured before and after placing in the oven for 24 h at the temperature of 60 °C. The percentage of moisture content was determined.

The apparent bulk density of the kenaf waste was determined by using the Archimedes principle. It was calculated by weighing a bundle of kenaf waste and recorded as M_{fa} . The bundle was then immersed in canola oil which has density of 920 kg/m³ until wetted. The weight of kenaf waste fiber bundles in canola oil was recorded as M_{fs} . The apparent bulk density of kenaf waste fibre bundle was then calculated by using formula (1):

$$\rho_b = \rho_s \frac{M_{fa}}{M_{fa} - M_{fs}} \quad (1)$$

where

- ρ_b is the bulk density of kenaf waste fibre
- ρ_s is the density of the solvent (canola oil)
- M_{fa} is the weight of the fibre in air
- M_{fs} is the weight of the fibre in solvent.

Chemical analysis was conducted in order to determine the sugar content in kenaf waste and the test was conducted in Forest Research Institute Malaysia (FRIM), Kepong.

2.3 Manufacture of Cement Board

2.3.1 Mix Design

Six (6) series of cement board with various percentages of kenaf waste replacements; 0, 20, 40, 60, 80 and 100 % were manufactured under laboratory conditions. Each series have a target density of 650 kg/m³ with ratio of cement to fiber to water; 2:1:2 as shown in Table 1).

Table 1 Mix design

Ratio by weight	2:1:2 (cement:fiber:water)			
Target density	650 kg/m ³			
Mix proportion	Cement (kg)	Fibre		Water (kg)
		Kenaf waste (kg)	Glass fibre (kg)	
Series 1 (100 % kenaf waste)	1.1	0.55	0	1.1
Series 2 (80 % kenaf waste)	1.1	0.44	0.11	1.1
Series 3 (60 % kenaf waste)	1.1	0.33	0.22	1.1
Series 4 (40 % kenaf waste)	1.1	0.22	0.33	1.1
Series 5 (20 % kenaf waste)	1.1	0.11	0.44	1.1
Series 6 (0 % kenaf waste)	1.1	0	0.55	1.1

2.3.2 Casting and Batching

To manufacture cement board, firstly, the dry materials; cement, kenaf waste and glass fiber were mixed by using the Particleboard Mixer and then water was added until uniformity was obtained. Then the mixture was placed into mattress mould. The boards were pressed by using Hydraulic Cold Press machine and were clamped for 24 h to allow initial cement curing. The boards were left to cure at room temperature for 28 days. Figure 3 shows the prepared board. Then the specimen were trimmed and cut into three specimens for each type of testing; density, moisture content, bending strength and tensile or internal bond strength in accordance with MS 934 (1986) [10].

2.4 Determination of Physical and Mechanical Properties of Board

All the tests conducted were based on MS 934 (1986) [10].

Fig. 3 Cement board with kenaf waste



2.4.1 Moisture Content

The moisture content of the boards was determined by oven dry method. The samples were taken at random and the dimension of the specimen was 100 mm × 100 mm × 20 mm. The specimen was taken from bending specimens just after the test was conducted.

2.4.2 Density

Density of the cement board was determined by preparing the specimen with size; 100 mm × 100 mm × 20 mm. The length, thickness and width of each specimen were measured. The density was computed from the dimension and weight of specimen taken from the bending specimen at the time of test.

2.4.3 Bending Test

A static three-point bending tests were conducted. The beam of size; 400 mm × 100 mm × 20 mm was used. Three (3) replicates for each series of board mixture were prepared.

2.4.4 Tensile or Internal Bond Test

The tensile strength tests or also called internal bond (IB) tests were carried out perpendicular to the surface of the board. Each test specimen was cut to the size of 50 mm × 50 mm × 20 mm which suitable to be gripped on the testing machine. The timber holder was glued to each face of the board by using Sikadur resin (Fig. 4). The rate of applications of force until failure was applied for not less than 30 s and not more than 120 s. The totals of eighteen (18) specimens were prepared with three

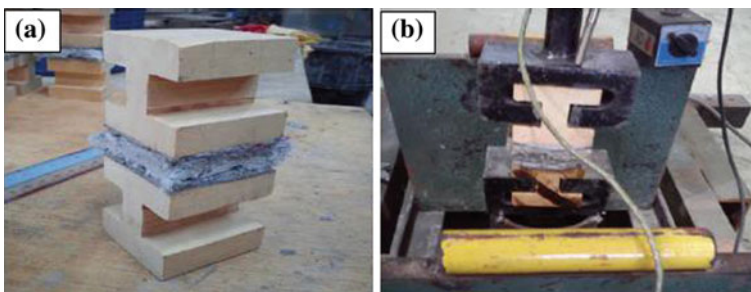


Fig. 4 Tensile test of cement board: **a** board specimen was mounted onto the timber holder and **b** test set-up

(3) specimens from each cement board series. Figure 6 shows the sample for tensile test as specified in MS 934 (1986) [10].

3 Results and Discussion

This section discusses the results obtained from all the tests conducted in Sect. 2.

3.1 Bulk Density

Based on the result of bulk density of kenaf waste, it possessed low density (0.677 kg/cm^3) compared to other wood based fibre such as *Leucaenaleucocephala* ($1.037\text{--}1.541 \text{ kg/cm}^3$) [9], oil palm trunk fibre (OPTF) (1.0 kg/m^3) [11] and has much lower density compared to glass fibre ($2.5\text{--}2.6 \text{ g/cm}^3$) [12, 1]. The low density of kenaf waste fibre indicates that kenaf waste fibre can be one of the potential as raw material in producing lightweight non-structural application such as ceiling board.

Based on Marzuki et al. [9], the value of bulk density in wood is an important factor to explain the compaction ratios of different wood to cement ratios. The lower density will allow better compaction. However, the compaction ratio is also influenced by wood to cement ratio. Furthermore, it is well known from practice that the lower density of the particles produces stronger and excellent mechanical and physical properties.

3.2 Moisture Content

The moisture content of kenaf waste was determine for 3 consecutive days and it was found that the moisture content was 3.2 % and is considered low since the kenaf waste was sundried.

3.3 Sugar Content of Kenaf Waste

Based on sugar content analysis conducted at FRIM, Kepong, kenaf waste contained about 5.6 % sugar content. But this result is much lower compared to coconut coir (6 %), oil palm trunk (11 %) and sugar cane (16 %) [13]. Sugar content in the fiber is one of the important factors that need to be determined if involved with cement because it could affect or retard the cement setting and also the strength of resulted boards [6, 9, 14]. In general, this level of sugar content is considered

allowable in cement board if the sugar content is less than 0.5 % of the dry mass of the particles used [15].

3.4 Properties of Cement Boards

Table 2 summarizes all the results i.e., moisture content, density, bending strength and tensile strength or internal bond (IB) strength of cement board made from different percentages of kenaf waste and glass fiber. The minimum requirements of MS 943 are given in the last row of the table. Each value presented is the average of three (3) specimens. A total of seventy two (72) samples were tested.

3.4.1 Moisture Content and Density of the Cement Board

Figure 5 shows the result of moisture content for all types of specimen from Series 1 to Series 6. As expected, results show that kenaf cement board made from kenaf fibre replacement of Series 1 to Series 5 (100 to 20 % replacement of kenaf waste) have higher moisture content than cement board made from only glass fibre (Series 6). It also surprise to see that as the percentage of kenaf reduces, the moisture content increases.

The trend for moisture content is similar to the trend for density as shown in Fig. 6 where the density increases as the kenaf fibre decreases up to 40 % and then decreases as the glass fibre content increases. This can be due to kenaf as cellulose

Table 2 Summary properties of kenaf cement board

Series of ceiling board	Moisture content (%)	Density (kg/m ³)	Bending		Tensile	
			Failure load (N)	MOR (MPa)	Failure load (N)	Tensile strength (MPa)
Series 1 100 % kenaf	4.55	490	79.73	1.20	744	0.30
Series 2 80 % kenaf	4.83	540	158.2	2.37	620	0.25
Series 3 60 % kenaf	5.22	600	243.3	3.64	1,797	0.72
Series 4 40 % kenaf	5.58	720	526.35	7.89	1,980	0.79
Series 5 20 % kenaf	3.49	650	224.74	3.37	2,454	0.98
Series 6 0 % kenaf	3.04	540	712.55	10.68	4,218	2.14
MS 934		>1,000		9.00		0.5

Fig. 5 Effect of percentage of kenaf waste replacement to moisture content of board

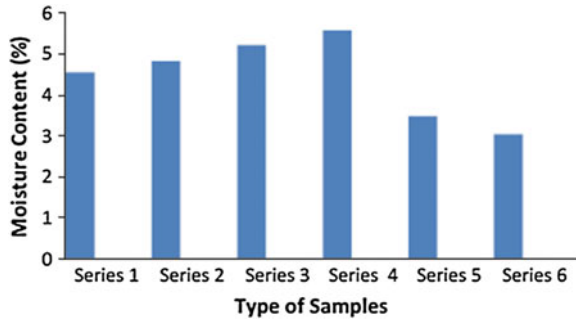
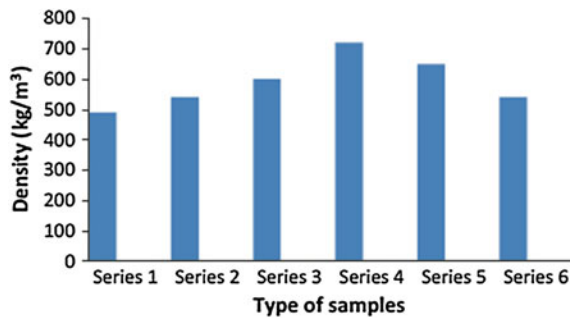


Fig. 6 Effect of percentage of kenaf waste replacement to density of board



fibres are hydrophilic and have pores in their structure which result in high moisture content and produce boards with low density.

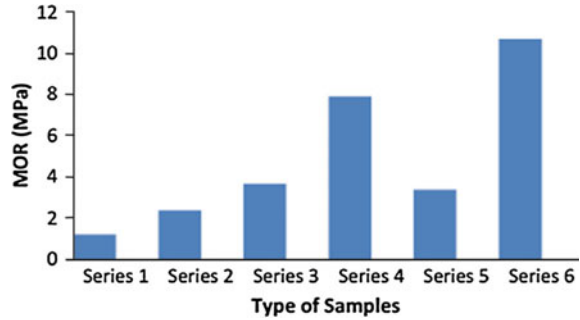
The highest moisture content was found on Series 4 (40% kenaf and 60% glass fibre) samples which are 5.58% which is similar with the density. The lowest moisture content was found on Series 6 (100% glass fibre) which is only 3.04% and for this series; the density is also the lowest. Therefore, the moisture content of the composite depends on the density of the composites. This is due to the fact that glass fibre has higher density compared to kenaf. This resulted in more voids in board and produced a cement board with low density.

However, the result of moisture content for the composite prepared in this study was much lower than moisture content for composite board made from coconut coir fiber investigated by Asasutjarit et al. [2] which is 9.13%. Lower density of kenaf waste composite board also made the composite board suitable as application for non-structural purposes such as ceiling board.

3.4.2 Bending Strength Properties

Figure 7 shows the result for bending strength (MOR) of kenaf cement board made from different percentages replacement of kenaf waste and glass fiber. MOR ranged from 1.20 to 10.68 MPa. The addition of kenaf waste has significantly affected the

Fig. 7 Bending strength (MOR) for all type of specimens



bending strength of the composites. The MOR of boards for Series 1 (100 % Kenaf waste) to Series 5 (20 % Kenaf waste) were less than control specimens; Series 6 (100 % Glass fibre).

Here it can be seen the effect of sugar content in the kenaf waste has significant effect on the strength of the cement board. The presence of sugar may have retardation effect on the setting and strength development of the Portland cement matrix.

This is reflected in the strength value of the board. From Fig. 7, it can be seen that as the percentage of kenaf waste decreases, the strength increases except for Series 5. For composite Series 4, it can be seen that the density and moisture content were the highest and the bending strength was also the highest excluding sample of Series 6.

The high moisture content may have allowed the Portland cement to further hydrate which enhanced the strength of the composite. This is in agreement with earlier studies by Eusebio et al. [16] and Zhou and Kamdem [17]. Wang and Sun [18] and Papadopoulos et al. [19] also observed that density of particleboards and wood components significantly influenced the particleboard strength properties.

The optimal percentage replacement of kenaf waste content in order to obtain the highest bending strength for the composites was 40 % for this study. The bending strength of composite Series 4 (40 % kenaf fibre and 60 % glass fibre) is about 26 % lower than the composite Series 6 (100 % glass fibre).

In the beginning of this project, it has been hypothesised that the kenaf waste cement composite will be very low and the glass fiber cement composite is high. That's why this study investigated the effect of replacing the kenaf waste with the glass fiber at certain percentages in order to improve the properties of the cement board and it has been proven that with the replacement of 60 % glass fiber the strength of the composite improved by more than 550 % compared to composite with 100 % kenaf waste. As shown in Table 2, cement board Series 4 (40 % kenaf waste: 60 % glass fiber) can be considered to produce an acceptable board that satisfied the strength properties of the Malaysian Standard MS 934 (1986). In MS 934 for board of density more than $1,000 \text{ kg/m}^3$, the minimum bending strength is 9 MPa. However, this board has density (650 kg/m^3) which is less than $1,000 \text{ kg/m}^3$ but the bending strength is approximately 8 MPa very close to 9 MPa.

The bending strength of 100 % glass fiber cement board found in this study is more than 9 MPa which definitely satisfied the requirement of the MS 934.

3.4.3 Tensile Strength Properties

To see the effect of kenaf to glass fiber ratio on the tensile strength of the cement board, the histogram was plotted as shown in Fig. 8.

This tensile strength measures the internal bond (IB) strength of cement and the fibers. Cement board of Series 1(100 % kenaf waste) had an average IB strength of 0.30 MPa which was lower than control composite in Series 6 (100 % glass fibers) (IB strength, 2.14 MPa) (Table 2).

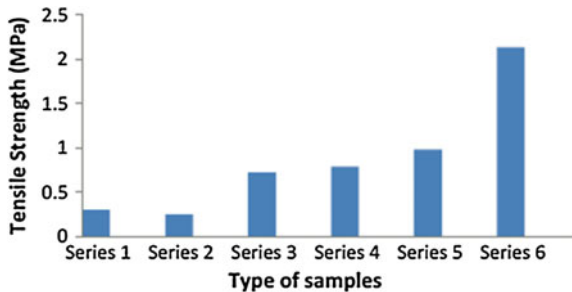
Here again the same trend can be seen which is as the percentage kenaf waste decreases, the IB strength increases but optimum at Series 5 (20 % kenaf waste: 80 % glass fiber) with the IB strength of 0.98 MPa. The IB strength for composite Series 5 is 69 % higher than the IB strength for composite Series 1 (100 % kenaf waste). This indicates that glass fiber has better bonding with cement compared with kenaf waste that contained sugar.

3.4.4 Modes of Failure

Figure 9 shows the example of failure modes from the bending test conducted on composite cement board. Almost all the specimens were failed in diagonal and at the center.

However, it can be observed that, for the specimen in Series 4 (60 % Glass fibre) and Series 6 (100 % Glass fibre) achieved the highest failure load, the specimens were not broken into pieces. It can be the results from the bridges effect provides by the glass fibre which hold one another and not collapsed as shown in Fig. 9b as compared with the Fig. 9a for Series 1 (100 % Kenaf waste) specimen, which was easier to break and very brittle.

Fig. 8 Tensile strength for all type of specimen



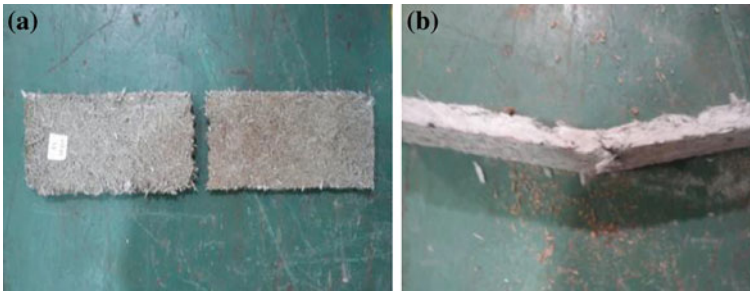


Fig. 9 Mode of failure in bending strength specimen: **a** Series 1 and **b** Series 6

3.4.5 Comparison with Other Boards

Table 3 shows the comparison of the physical and mechanical properties of manufactured cement board from kenaf waste with commercial cement boards and boards made from other type of cellulosic materials. It can be seen that the properties of the cement board from kenaf waste prepared in this study is within the range of properties of commercialized ceiling board and comparable to boards made from other cellulose materials. It can be concluded that cement board from kenaf waste which has low density can be used as non structural application such as ceiling board or panels.

Table 3 Comparison between boards made from kenaf waste with others board

Type of board		Thickness (mm)	Density (kg/m ³)	Moisture content (%)	MOR (MPa)	IB (MPa)
Board from kenaf waste (current study)	Series 4 (40 % kenaf)	20	720	5.58	7.89	0.79
	Series 5 (20 % kenaf)	20	650	3.49	3.37	0.98
Commercial ceiling board	Aqua panel ceiling board (cement with fibre glass) ^a	12.5	1,150	–	7	0.49
	Nutec ceiling board (cement, cellulose fibre and silica) ^b	6	1,260	6.25	7.4	1.02
Others cellulose fibre board	Kenaf core ^c	12	300	5–7	2	0.17
	Kenaf stalks ^d	10	600–700	–	12–17	0.3–0.5
	Rice-hull and sawdust ^e	10	400–700	3–5	1.5–9.3	–
	Narrow leaved cattail fibre ^f	10	200–400	4–13	0.7–3.7	0.07–0.17

Source ^a[20], ^b[21], ^c[22], ^d[23], ^e[24] and ^f[8]

4 Conclusion

The aim of this study is to utilize the kenaf waste in the production of low density cement board especially for the application in ceiling board for house applications and also as building industries.

The physical and mechanical properties of cement board produced from kenaf waste and glass fibre at different ratios were evaluated. This was done using six (6) series of mixture; Series 1 (100 % kenaf waste), Series 2 (80 % kenaf waste and 20 % glass fiber), Series 3 (60 % kenaf waste and 40 % glass fiber), Series 4 (40 % kenaf waste and 60 % glass fiber), Series 5 (20 % kenaf waste and 80 % glass fiber) and Series 6 (100 % glass fiber). At the end of the investigation, the following conclusions are drawn.

- Cement board made from kenaf fibre replacement of Series 1 to Series 5 (100 to 20 % replacement of kenaf waste) have higher moisture content than cement board made from only glass fibre (Series 6).
- The trend for the density of the board is similar to the trend for moisture content where the density increases as the kenaf waste decreases up to 40 % and then the density decreases as the kenaf waste decreasing further.
- The bending strength or Modulus of Rupture (MOR) of cement board of Series 1 (100 % of Kenaf waste) to Series 5 (20 % of Kenaf waste) are less than control specimens Series 6 (100 % Glass fibre).
- The optimal percentage replacement of Kenaf waste content in order to obtain the highest bending strength for the composites was 40 % for this study. The bending strength of composite Series 4 is about 26 % lower than the composite Series 6 with 100 % Glass fibre.
- Cement board Series 4 (40 % kenaf waste: 60 % glass fiber) can be considered to be an acceptable board that satisfied the strength properties of the Malaysian Standard MS 934. In MS 934 for board of density more than $1,000 \text{ kg/m}^3$, the minimum bending strength is 9 MPa. However, this board has density (720 kg/m^3) which is less than $1,000 \text{ kg/m}^3$ but the bending strength is approximately 8 MPa very close to 9 MPa. The bending strength of 100 % glass fibre cement board found in this study is more than 9 MPa which definitely satisfied the requirement of the MS 934.
- The same trend can be seen which is as the percentage kenaf waste decreases, the internal bond (IB) strength increases and optimum at Series 5 with the IB strength of 0.98 MPa. This indicates that the higher the bond strength of the composite, the higher the bending strength.
- It can be concluded that kenaf waste has the potential to be used as natural materials in composite industry to produce ceiling board in the future.

Acknowledgments This research was financially supported by the Malaysia Kenaf and Tobacco Board (Grant: 100-RMI/GOV 16/6/2 (5/2012)) is greatly acknowledged.

References

1. M.P. Westman, L.S. Fifield, K.L. Simmons, S.G. Laddha, T.A. Kafentzis, *Natural Fiber Composites: A Review*. (U.S. Department of Energy, Pacific Northwest National Laboratory, 2010)
2. C. Asasutjarit, J. Hirunlabh, J. Khedari, S. Charoenvai, B. Zeghmati, U.C. Shin, Development of coconut coir-based lightweight cement board. *Constr. Build. Mater.* **21**, 277–288 (2007)
3. M.R. Ishak, A comparison of mechanical properties between kenaf core fiber and kenaf bast fiber reinforced polyester composites. Unpublished Bachelor Degree Thesis, Universiti Teknikal Malaysia, 2007
4. F.F. Udoeyo, A. Adetifa, Characteristics of kenaf fibre-reinforced mortar composites. *IJRRAS* **12**(1), 18–26 (2012)
5. L.F. Ma, H. Yamauchi, O.R. Pulido, Y. Tamura, H. Sasaki, S. Kawai, Manufacture of cement-bonded boards from wood and other lignocellulosic materials: relationships between cement hydration and mechanical properties of cement bonded boards, in *Proceeding of Wood-cement Composites in the Asia-Pacific Region*, Rydges Hotel, Canberra, Australia, 10 Dec 2000, pp. 13–23
6. R. Sudin, W.A. Ibrahim, Cement bonded particleboard from acacia mangium—a preliminary study. *J. Trop. For. Sci.* **2**(4), 267–273 (1990)
7. P.E.G. Warden, H. Savastano Jr., R.S.P. Coutts, Fibre-cement composites from brazilian agricultural and industrial waste materials, in *Australian Centre for International Agriculture Research Proceedings*, No. 107 (2000), pp. 165
8. T. Luamkanchanaphan, S. Chotikaprakhan, S. Jarusombati, A study of physical mechanical and thermal properties for thermal insulation from narrow-leaved cattail fibers. *Asia Pac. Chem. Biol. Environ. Eng. Soc.* **1**, 46–52 (2012)
9. A.R. Marzuki, S. Rahim, M. Hamidah, R.A. Ruslan, Effects of woods: cement ratio on mechanical and physical properties of three-layered cement-bonded particleboards from *Leucena leucocephala*. *J. Trop. For. Sci.* **23**(1), 67–72 (2011)
10. MS 934, *Malaysian Standard-Specification for Wood Cement Board*. (Standard and Industrial Research Institute of Malaysia (SIRIM), Malaysia 1986)
11. Z. Ahmad, H.M. Saman, P.M. Tahir, Oil palm trunk fiber as a bio-waste resource for concrete reinforcement. *Int. J. Mech. Mater. Eng. (IJMME)* **5**(2), 199–207 (2010)
12. N. Abilash, M. Sivapragash, Environmental benefits of eco-friendly natural fiber reinforced polymeric composite materials. *Int. J. Appl. Innovation. Eng. Manage. (Ijaiem)* **2**(1), 53–59 (2013)
13. N.I. Wan Azelee, J.M. Jahim, A. Rabu, A.M.A. Murad, F.D.A. Bakar, R.M. Ilias, Efficient removal of lignin with the maintenance of hemicellulose from kenaf by two-stage pretreatment process. *Carbohydr. Polym.* **99**, 447–453 (2014)
14. M. Aro, Wood strand cement board, in *International Inorganic-Bonded Fiber Composites Conference*, No. 11 (2008), pp. 169–179
15. H.G. Schwarz, M.H. Simatupang, Suitability of beach for use in the manufacture of wood cement. *Holz Roh Werkst.* **42**, 265–270 (1984)
16. D.A. Eusebio, F.P. Soriano, R.J. Cabangon, P.G. Warden, R.S.P. Coutts, Wood fiber reinforced cement composites from eucalyptus pellita and acacia mangium kraft pulp. *For. Prod. Res. Dev. Inst. J.* **24**(1), 57–65 (1998)
17. Y. Zhou, D.P. Kamdem, Effect of cement/wood ratio on the properties of cement-bonded particleboard using CCA-treated wood removed from service. *For. Prod. J.* **52**, 77–81 (2002)
18. D. Wang, X.S. Sun, Low density particleboard from wheat straw and corn pith. *Ind. Crops Prod.* **15**, 43–50 (2002)
19. A.N. Papadopoulos, G.A. Ntalos, I. Kakaras, Mechanical and physical properties of cement-bonded OSB. *Holz Roh Werkst.* **64**, 517–518 (2006)
20. Aquapanel, Cement Board Outdoor Climate Shield, <http://www.aquapanel.com>. 6 June 2014

21. Information Service to Architectural, Engineering and Construction Industries, <http://www.specifile.co.za>. 6 June 2014
22. J. Xu, R. Sugawara, R. Widyorini, G. Han, S. Kawai, Manufacture and properties of low-density binderless particleboard from kenaf core. *J. Wood Sci.* **50**, 62–67 (2004)
23. H. Kalaycioglu, G. Nemli, Producing composite particleboard from kenaf (*Hibiscus cannabinus* L.) stalks. *Ind. Crops Prod.* **24**, 177–180 (2006)
24. S.W. Kang, Y.S. Park, J.S. Lee, S.I. Hong, S.W. Kim, Production of cellulases and hemicellulases by *Aspergillus niger* KK2 from lignocellulosic biomass. *Bioresour. Technol.* **91**, 153–156 (2004)

A New Method to Treat Oily Water Using Rice Husk Ash Onboard Vessel

M.R. Zoolfakar and M.S.M. Shukor

Abstract All vessels must have bilge water. The bilge is referred as water come from rough seas, rain, leaks in the hull or other interior spillage. The water that collects in the bilge must be pumped out to prevent the bilge from becoming too full and threatening to sink the ship. Depending on the design of the ship and function, bilge water may contain water, oil, urine, detergents, solvents, chemicals, particles, and other materials. Absorption process is widely being used by various treatment plants, either for treating water or wastewater. The main function of absorption is to remove any contaminants such as heavy metals, organic and inorganic chemicals from it. One of the components of absorption is rice husk ash. The aim of this study is to investigate the suitability of rice husk ash as an absorbent, specifically to absorb oil in bilge water. Zinc chloride was added to the rice husk ash since an activated carbon enhanced absorption capacity. It was found that oil was removed from the water and clear water was produced after the absorption process. Thus, the use of rice husk ash water has proven to be one of the best options for ship-owner in oily water treatment.

Keywords Oily water · Rice husk · Oil absorbent · Bilge

1 Introduction

Nowadays everyone is concerned regarding environmental pollution. We want to life in healthy life, thus any issue towards pollution will attract peoples' attention. These include sea. Since seas are connected with each other without boundary,

M.R. Zoolfakar (✉) · M.S.M. Shukor
Marine Engineering Technology Section, University Kuala Lumpur,
Kuala Lumpur, Malaysia
e-mail: redzuan@unikl.edu.my

M.S.M. Shukor
e-mail: syazanyshukor@gmail.com

pollution from one end of the corner can easily separate and polluted other. One source of the pollution comes from sea transportation, which well known as vessel.

Knowing this threat, the International Maritime Organization under United Nation has produced a guideline and law known as Marine Pollution (MARPOL). One of the rule mention that, any mixture oily water (bilge) discharge overboard must be treated. Figure 1 illustrated the typical system of treating oily water on board of the vessel.

Many methods of treating oily water had been introduced to treat the contaminated water, i.e. centrifugal force and filtration. For a big vessel, space and energy (electricity) is not an issue, however, for a small boat it does. Hence, a complicated system similar to Fig. 1 can not be addressed to all vessels. An alternative system which much simple, i.e. using filter will be an option. Interesting, latest research indicates some of organic material, have a possibility to absorb oil and can be used as parts of the filter in separating oil water. One of organic material is rice husk.

Rice husk is referred as a waste product produced from rice production. It happens when the husk is removed from the grain in the first stage of the milling process. The product will then be heated at certain temperature before it can be used as part of the oily water filter. The heating process is important as carbonization of the product, makes the contaminant absorption ability high [1].

From the literature, rice husk ash holds a potential to be used in water treatment process, for removing physical, chemical or biological impurities in water. Rice milling generates a product known as husk which surrounds the paddy grain as shown in Fig. 2. About 78 % of weight is perceived as rice, broken rice and bran. The remaining 22 % weight of paddy is perceived as husk. Commonly, this husk is used as a fuel to generate steam for parboiling process.

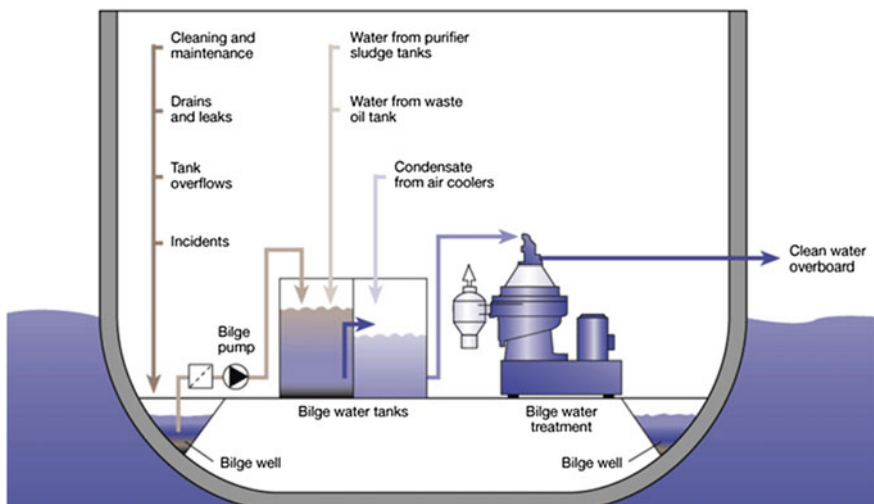


Fig. 1 Bilge water system in vessel

Fig. 2 Rice husk obtained from the rice mill after husking stage



This husk contains about 75 % of the organic volatile matter and another 25 % of the weight of this husk is converted into ash during the firing process (refer Fig. 3). Which is known as rice husk ash (RHA) [2].

Malaysia produces a couple of million tons of RHA annually. RHA is a great environmental threat that can damage the land and the surrounding area. Thus, there are lots of measures suggested to dispose them by promoting the commercial use of RHA. Rice husk contains approximately 20 % silica that is a good absorbent for the removal of heavy metals, phenols, pesticides, and dyes [2]. These ashes have a potential as a source of activated carbon that can be used as absorbent in water

Fig. 3 Rice husk ash (RHA) formed after burning process



treatment. The physical characteristics of rice husk ash such as its ash content and moisture content, as well as its chemical characteristics which is chemical composition and the presence of functional groups affect its absorption capabilities [3].

Rice husk ash has a potential to be used in water treatment process, for removing physical, chemical or biological impurities in water. There are previous researches in the application of rice husk ash as an absorbent for different type of contaminants [4]. The research done according to the absorption capacity of rice husk ash in various types of substance, which has proven that rice husk ash is a good absorbent.

Carbon that is initially prepared by carbonization has insufficient porosities to be used for most applications. Thus, some enhancements need to be done in order to create further porosity, widen existing porosity, modify the surface porosities and modify the carbonization process. This can be achieved through processes called Physical Activation and Chemical Activation [5].

Physical Activation: Physical activation is a modification to a carbon by making use of two gasifying agents which are carbon dioxide and water vapour, where these agents precipitate the carbon atoms from the structure of the porous carbon high temperature which is over than 800 °C, thus creating more pores and enlarging the existing pores. However, this process is a bit complex with the gaseous reaction that can bring no result to enhancement [6].

Chemical Activation: Chemical activation is where RHA product mixed with dehydrating agent (Zinc Chloride or Phosphoric Acid or Potassium Hydroxide or Potassium Carbonate) at a certain amount of time and is heated up to 800 °C. It is a suitable process for product enhancement where the activated carbon can be impregnated with a range of chemicals or altered the surface functionalities to enhance the chemisorption capacity for selected absorbents [7]. A typical physical characteristic of rice husk ash is illustrated in Table 1.

Table 1 Physical characteristics of rice husk ash

Parameter	Value
Average particle size	412 μm
Bulk density	175.3 kg/m^3
Moisture content	1.1 %
Volatile matter content	7.36 %
Ash content	80.58 %
Fixed carbon content	10.96 %
Heating value	21.76 MJ/kg
BET surface area	65.36 m^2/g
BJH adsorption surface area of pores	52.35 m^2/g
BJH desorption surface area of pores	26.62 m^2/g
Cumulative pore volume	0.039 cm^3/g
BET pore diameter	34.66 \AA
BJH adsorption average pore diameter	43.27 \AA
BJH desorption average pore diameter	58.34 \AA

2 Methodology

The first step is to design a model of a filter for the experiment. The model consists 3 layers of compartment which are gravel, sand course and rice husk ash, as illustrated in Fig. 4. The design consisted with fixed bed of filter media and the water flows downward through the media.

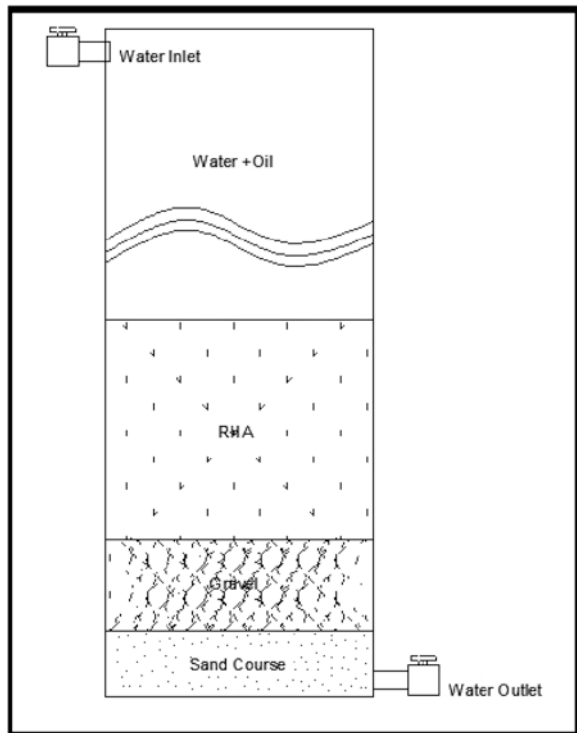
The next step is to perform experiments. Two experiments had been conducted:

1. to identify the absorbent of rice husk ash filter for oil contaminated water (crude oil and water), and
2. to examine the amount of crude oil could be absorbed by RHA.

The process of the first experiment is as follows (refer Fig. 5):

- 100 ml of water was poured into a small transparent container,
- 5 ml amount of crude oil being drips gently inside the container,
- 10 g of rice husk was put inside the transparent container,
- The water are then been stirred and the result be taken after 30 and 60 min.

Fig. 4 Filter model



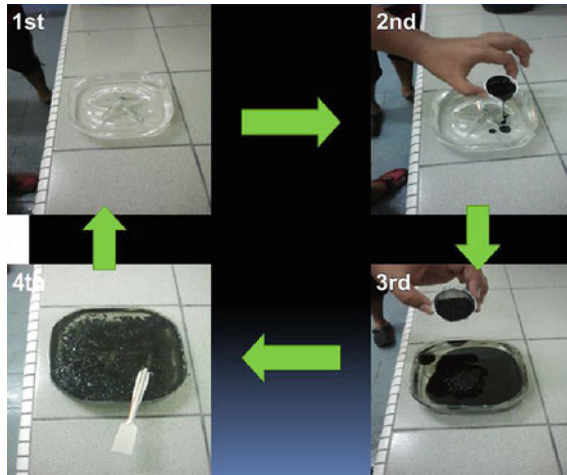


Fig. 5 Procedure for absorption test

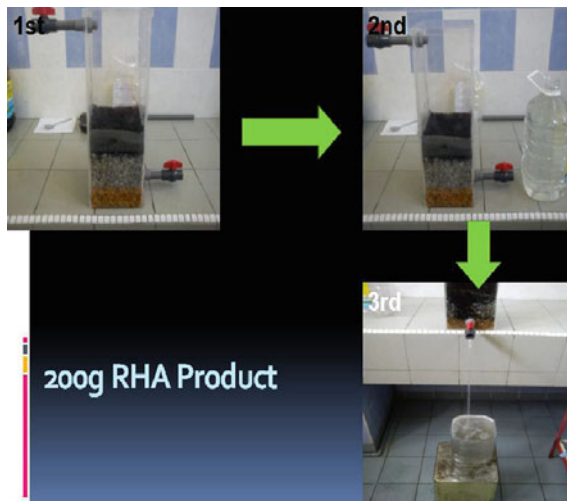


Fig. 6 Filtration experiment uses model filter

The process of Second experiment as follows (refer Fig. 6):

- 3 l water was poured inside the model from top water inlet while closing the outlet valve,
- 100 ml amount of crude oil was poured inside the model,
- Open the outlet valve,
- Time was taken until no more water outlet from the model,
- The above step were repeated until oil is present.

3 Result and Discussion

Filtration experiment was conducted to compare the quality of water by using rice husk ash to determine the amount of crude oil that can be filtered by using 200 g of rice husk ash with activated carbon product. Filtration experiments were performed in the prepared filter model. Fresh water sample (3,000 ml) was poured into the filter and 100 ml of crude oil was poured right after. The water then was collected at the filter outlet and was determined through visualization of the crude oil in the water. The process continued with adding another 3,000 ml of fresh water into the filter and 100 ml of crude oil. The process was then repeated until the water outlet sample surface showed oily substance through a filtering process as illustrated in Table 2.

Absorption experiment was conducted to compare the efficiency of oil removal between fresh water and sea water. The experiment was performed in 5.5 l water container that had been cut and can be loaded with 100 ml of water for visual inspection. After loading 100 ml of fresh water sample at room temperature, 5 ml of crude oil was added into the fresh water.

10 g of rice husk ash was added into the fresh water and the absorption started. The same absorption experiment was also performed by using sea water since the bilge water also contains sea water. The absorption was conducted in two different containers for 30 and 60 min to allow the rice husk ash to absorb the crude oil. After the pre-determined time, the slurry was filtered through a piece of cloth and the water sample was then inspected for visualization through the colour and oil content as indicated in Table 3.

Table 2 Filtration experiment

Stage	Amount of water in L	Amount of crude oil in ml	Time	Water condition
1	3	100	3 m 45 Sec	Clear
2	3	100	3 m 42 Sec	Clear
3	3	100	3 m 40 Sec	A bit ash leaked through water outlet
4	3	100	3 m 35 Sec	Another bit of ash leaked through water outlet and water become feculent
5	3	100	3 m 28 Sec	Water surface showed a bit of oil substance and the water become feculent
6	3	100	3 m 09 Sec	The oil started to leak and the surface of the water showed the oily content and the smell of crude oil determined. The water becomes feculent

Table 3 Absorption experiment

Water type	Quantity in ml	Amount of crude oil (ml)	RHA product (g)	Condition after 30 min	Condition after 60 min
Fresh water	100	5	10	No crude oil form on water surface	No crude oil form on water surface
Sea water	100	5	10	No crude oil form on water surface	No crude oil form on water surface

Based on the result obtained from the experiments, the water sample was determined as clear water without crude oil content at first. After the rice husk ash reached the certain time of limitation for absorbent, it did not perform the absorbing process. This is similar to the experiment through filtration model. The absorbent of 200 g rice husk ash was limited to 500 ml of crude oil. Then the rice husk ash must be replaced with new rice husk ash product in order to perform the absorption process. The water inlet also plays an important role in rice husk ash first phase before it becomes into a very small particle and drains out with water.

4 Conclusion

From the study, it is shown that rice husk can be used as a potential low cost absorbent material for crude oil from water either fresh water or sea water. It is in line with the aim of this study to investigate the suitability of rice husk ash as an absorbent. The study will be continued by performing more experiment, including using digital oily water monitoring device for accurate results with prototype rig. Despite limitations at the preliminary stage of study, these promising results will be a sparking point for a better outcome in the future.

Acknowledgments One would like to thank MARA for awarding a grant (SGPIM) for carry out this research.

References

1. S.N. Islam, Removal of contaminants in water by using rice husk ash (RHA) as absorbent (2012)
2. M. Ahmaruzzaman, V.K. Gupta, Rice husk and its ash as low-cost absorbents in water and wastewater treatment. *Ind. Eng. Chem. Res.* **50**, 13589–13613 (2011)
3. K. Srinivasan, N. Balasubramaniam, T. Ramakrishna, Studies on chromium removal by rice husk carbon. *Indian J. Environ. Health* **30**, 376–387 (1998)
4. A. Imyim, E. Prapalimrungsi, Humic acids removal from water by aminopropyl functionalized rice husk ash. *J. Hazard. Mater.* **184**, 775–781 (2010)

5. H. Marsh, F.R. Reinoso, *Activated Carbon* (Elsevier Science Ltd, UK, 2006)
6. V. Inglezakis, S. Pouloupoulos, *Adsorption, Ion Exchange and Catalysis* (Elsevier, UK, 2006)
7. C. Saka, BET, TG–DTG, FT-IR, SEM, Iodine number analysis and preparation of activated carbon from acorn shell by chemical activation with ZnCl₂. *J. Anal. Appl. Pyrol.* **95**, 21–24 (2012)

Influence of Different Fillers on the Tensile Properties of 50/50 NR/NBR Blend

Nurul Husna Rajhan, Rozaina Ismail, Hanizah Ab. Hamid
and Azmi Ibrahim

Abstract This paper reviews the relationship of the effect of different fillers used in the natural and nitrile rubber compounds on the tensile properties. The use of fillers in the rubber compounds is well known in order to modify and improve their properties. Thus, four different grades of carbon black and non-carbon black fillers were used to achieve the aim of the study. A comparison between carbon black and calcium carbonate system leads to further scientific findings for the understanding of the tensile properties of filled rubber compounds. The tensile properties of the five samples were investigated by using a Tensile Instron Machine. Five test pieces were tested for every sample at a stretching rate of 500 mm/min at standard laboratory temperature. Then, median values of the five test pieces of each sample were calculated. As the conclusion, different types of fillers results to different properties of the elastomers. Carbon black fillers can be proved to have better tensile properties compared to non-carbon black fillers. The best filler with the highest tensile properties was N220 with 23.63 MPa and elongation at break at 638.63 %.

Keywords Carbon black · Calcium carbonate · Fillers · Tensile test

N.H. Rajhan (✉) · R. Ismail · H.Ab. Hamid · A. Ibrahim
Department of Structure and Materials, Universiti Teknologi Mara (UiTM),
Selangor, Malaysia
e-mail: nunurajhan@yahoo.com

R. Ismail
e-mail: rozaina_fka_uitm@yahoo.com

H.Ab. Hamid
e-mail: hanizah696@salam.uitm.edu.my

A. Ibrahim
e-mail: azmi716@salam.uitm.edu.my

1 Introduction

Reinforcing fillers have been used in rubber compounds over the years. Before, the main purpose of using fillers is to lower the cost of the end products. Somehow, nowadays the uses of fillers are focusing on modifying and improving the mechanical, electrical and/or optical properties of rubber compounds [1]. Fillers can be categorized into two groups; non-reinforcing fillers and reinforcing fillers. In some cases, semi-reinforcing fillers are also mentioned.

As stated above, the purpose of the reinforcing fillers nowadays is to improve the physical properties of rubber compounds. The semi-reinforcing fillers also enhance the physical properties, but the effect is not too high. The non-reinforcing fillers are made up of cheap and easily available materials. They have been used to reduce the cost and give colour to the final product [2]. The most common reinforcing fillers are carbon blacks and non-black fillers. Carbon black is the major reinforcing filler for tires and many other rubber and plastic products. However, carbon black imposes a restriction of the colour of the vulcanized products. On the other hand, non-carbon black fillers offer the possibility that any colour can be mixed in and be seen in the products. Non-carbon black fillers can be used to impart a number of desirable properties to rubber compounds, i.e. improvement in tear strength and increment in compound adhesion in multi component products [3]. Calcium carbonate (CaCO_3), kaolin clay, precipitated silica, talc, barite, amorphous silica, diatomite are examples of non-black fillers.

Characteristics of the fillers are also important in determining the properties of rubber compounds such as particle sizes, particle shapes, and surface area. This is because fillers play an important role in order to make contact with rubber chain to reinforce the rubber compounds. Smaller particle sizes of fillers have a large contact surface area to the rubber compounds. Thus the reinforce potential also increases. Other than that, the shape also influences the surface contact to the rubber compounds. A planar particle has more surface available for contacting the elastomer matrix than spherical particles with similar particle size [1].

Many works [4–8] have been performed to study the relationship of the effect of fillers to the rubber compounds. Wang [4] exploited the role of filler networking in dynamic properties of filled rubber. Sobhy et al. [5] had explored the cure characteristics and physicomechanical properties of calcium carbonate reinforcement rubber composites. They found that the optimum concentrations of CaCO_3 are 20 pphr (parts per hundred rubber) and 40 pphr for natural rubber (NR) and nitrile rubber (NBR) respectively. At higher filler contents, all the measured properties are decreased, resulting in a poor dispersion of the filler on the rubber matrix.

Mostafa et al. [6] investigated the effect of reinforcing fillers on the mechanical behavior of elastomer. For filled rubber, tensile strength increases sharply with filler content. Improvement of these strength properties depends on the type of addition of filler and its adhesion characteristic with the rubber matrix. Saad et al. [7] studied

the effects of carbon black content on cure characteristics, mechanical properties and swelling behavior of 80/20 NBR/CIIR blend. They proved that the scorch time and cure time decreased with increasing carbon black loading while the cure rate index increased.

Sirin et al. [8] also studied the influence of CaCO_3 component on mechanical properties and thermal analysis of low density polyethylene's composites. With addition of CaCO_3 , mechanical properties of the composites were decreasing while hardness values showed increment. However, only a little research has been carried out on relationship between fillers to the mix of rubber blends of natural and nitrile rubber. Thus, this work is performed to study the influence of different fillers on the tensile properties of natural/nitrile rubber blend. Five kinds of compounds were fabricated by different types of fillers. The tensile properties of the five compounds were investigated by using a Tensile Instron Machine.

2 Literature Review

2.1 Carbon Black Fillers

Carbon black is one of the most stable chemical products which most widely used as a nanomaterial and its dimension ranges from 10 to 500 nm [9]. Figure 1 shows the carbon black pellets [10]. The small sizes of the carbon black particles will result a large advantages of rubber properties such tensile strength, resistance and hysteresis. However, the smaller particle sizes will increase the cost of production. Other than that, smaller fillers require more energy for their dispersion, thus the mixing process will be difficult [3].

Fig. 1 Carbon black pellets [10]



Table 1 Particle sizes of various types of carbon black fillers [3]

Type name	Type code	Average particle diameter (nm)
Super abrasion furnace	SAF	20 (oil furnace)
Intermediate super abrasion furnace	ISAF	23 (oil furnace)
High abrasion furnace	HAF	23 (oil furnace)
Fast extrusion furnace	FEF	40 (oil furnace)
General purpose furnace	GPF	50 (oil furnace)
Semi-reinforcing furnace	SRF	60 (oil furnace) 80 (gas furnace)
High modulus furnace	HMF	60 (gas furnace)
Fine thermal	FT	180
Medium thermal	MT	470

Carbon black is a product of incomplete combustion. It is a dark component of smoke and its production process starts with “smoke.” Most of carbon blacks used today are made by oil furnace process. FEF (Fast Extrusion Furnace), HAF (High Abrasion Furnace), SAF (Super Abrasion Furnace) and ISAF (Intermediate Super Abrasion Furnace) blacks are the main types of carbon black. The particle sizes of various types of carbon blacks are shown in Table 1. There are five important properties of carbon black; particle size, structure, physical nature of the surface, chemical nature of surface and particle porosity [3].

Also, carbon blacks are graded with respect to a four-character code, N_{xyz} where N is referring to “normal curing” which means that the filler does not interfere much with vulcanization chemistry and xyz describes the reinforcing character. Table 2 shows the particle range of rubber-grade carbon blacks by American Standard Test Method (ASTM) classification.

Table 2 Carbon black classification by ASTM [11]

Classification N_{xyz} x	ASTM D1765-86 Average (elementary) particle size (nm)	ASTM D1765-96 N_2 average specific area (m^2/g)
0	1–10	>150
1	11–19	121–150
2	20–25	100–120
3	26–30	70–99
4	31–39	50–69
5	40–48	40–49
6	49–60	33–39
7	61–100	21–32
8	101–200	11–20
9	201–500	0–10

2.2 Non-carbon Black Fillers

Two types of calcium carbonates that have been used in rubber industries are ground natural limestone and precipitated calcium carbonate. The ground natural limestones have particles sizes of 700–500 nm with low aspect ratio, low surface area, and poor polymer-filler adhesion. Meanwhile, precipitated calcium carbonates have a much higher surface area because their particle sizes are about to 40 nm [1]. However, ground natural calcium carbonates are widely used in rubber compound because of their low cost and able to resist to very high loadings.

3 Experimental

3.1 Materials

Natural rubber SMR L and nitrile rubber medium ACN (Acrylonitrile) were supplied by Lembaga Getah Malaysia (LGM). Five types of different fillers, N220 (ISAF black), N330 (HAF black), N550 (FEF black), N660 (GPF black), and CaCO₃ (calcium carbonate) were used. Other material such as zinc oxide, stearic acid and sulphur are required as the basic ingredients of compounding unfilled rubber or filled rubber. Antioxidant, tetramethylthiuram disulphide (TMTD) and N-cyclohexyl-2-benzothiazole sulphenamide (CBS) are additives that have been selected in order to increase the properties of r Moreover, each of them has specific function. However, they are capable to function in more than one manner.

All compounds have the same composition, except for the fillers (N220, N330, N550, N660 and CaCO₃) which are varied to prepare the rubber compounds with different fillers. Therefore, the total amount of fillers in each formulation was kept constant at 25 pphr. The samples of rubber compounds were named as N1, N2, N3, N4, and C1. The “N” indicates the sample of carbon black fillers, meanwhile “C” indicates calcium carbonates. All the ingredients in the rubber compounds are in pphr as shown in Table 3.

3.2 Mixing and Compounding

Mixing of rubber compound was performed by using a laboratory open two-roll mill (400 mm diameter and 600 mm working length). The mixing process was conducted carefully and the right sequence was followed in order to get the finest rubber compounding. It was assuredly essential to break the molecular of the crude rubber before adding in other ingredients. All the ingredients were added and carried out by following the same manner and conditions of mixing. The rubber compound obtained was in a sheet left. For all purposes, the minimum time

Table 3 Formulation of rubber compounds

Ingredients	Compound number (pphr)				
	N1	N2	N3	N4	C1
Natural rubber (SMR L)	50	50	50	50	50
Nitrile rubber (NBR medium ACN) (Krynac 833)	50	50	50	50	50
N220 (ISAF black)	25	–	–	–	–
N330 (HAF black)	–	25	–	–	–
N550 (FEF black)	–	–	25	–	–
N660 (GPF black)	–	–	–	25	–
Calcium Carbonate (CaCO ₃)	–	–	–	–	25
Zinc Oxide (ZnO)	5	5	5	5	5
Stearic acid (St.Acid)	2	2	2	2	2
TMQ	2	2	2	2	2
Sulphur	1.5	1.5	1.5	1.5	1.5
CBS	0.5	0.5	0.5	0.5	0.5
TMTD	0.5	0.5	0.5	0.5	0.5

between vulcanization and testing should be 16 h. The samples should be protected from all external influences which might cause damage during the interval between curing and testing.

3.3 Preparation for Tensile Samples

Tensile test is one of the important tests and mostly applied in order to determine the mechanical properties of rubber based-material. Tensile test provides the tensile stress-strain properties include tensile strength, tensile modulus, and elongation at break. The standard method for determining these properties is accordance to ISO 37 [12].

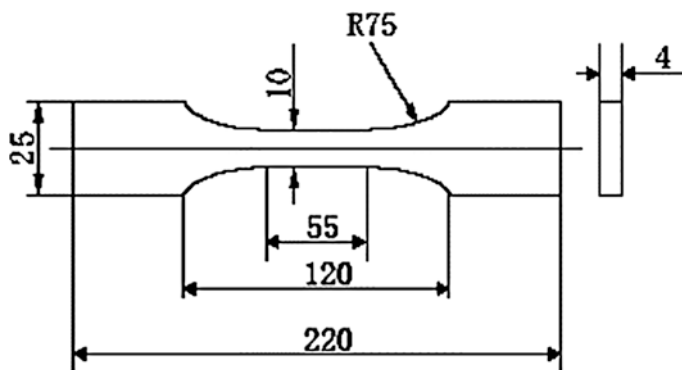
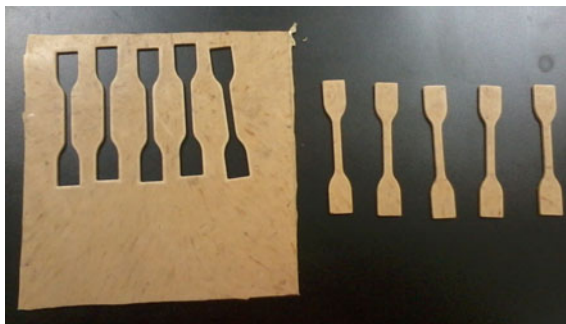
**Fig. 2** Dumbbell shape of tensile test specimen [13]

Fig. 3 Example of tensile specimens



The samples were cut to the dumb-bell shape or ‘dog bone’ shape as shown in Fig. 2 and [13]. The thickness at the centre and at each end of the test length of each specimen was measured with thickness gauge. Each specimen was placed on the grip of the tensile machine at a certain gauge length. It is strongly recommended that the load cell be reset to zero before each test. Five test pieces (refer Fig. 3) were tested for every sample at a stretching rate of 500 mm/min at standard laboratory temperature. A Tensile Instron Machine (refer Fig. 4) was used to conduct this experiment. Then, median values of the five test pieces of each sample were calculated.

Fig. 4 A tensile instron machine



4 Results and Discussion

The results of the tensile test including tensile strength, elongation at break, and tensile modulus of the five different fillers are recorded as in Table 4. The results obtained indicate the influence of different fillers on tensile properties of the rubber compounds. Figure 5 shows the effects of different fillers on tensile strength. CaCO_3 has the lowest value of tensile strength which is 7.54 MPa, compared to the other four types of fillers, which are carbon black fillers. The highest value of tensile strength of these compounds is N220 with 23.63 MPa. Then, it is followed by N330, and N550 with values of 20.04 and 16.47 MPa respectively.

However, there is some error for N660. There are a lot of possibilities of incorrect value for N660. It might be due to the error during mixing process. It is possible that the N660 compound was not properly cooked, either undercooked or overcooked. Other than that, incorrect weighing could be one of the factors. Theoretically, the value of tensile strength of N660 should be lesser than N550, N330 and N220. This is because of these four types of carbon blacks, the particle sizes of carbon black N660 are much larger compared to N220, N330 and N550. Therefore, the contact area of N660 to the rubber compound is smaller. Thus, the reinforcing potential also decreases.

Nagdi [14] claimed that the elongation at break means the elongation at the time of rupture of a rubber compound. From Fig. 6, the best elongation at break of these five fillers loading is N220 with value of 638.63 %. The decreasing trend is 638.63 % for N220 followed by N330 and N500 with values of 601.88 and 535.27 % respectively. However, sudden increasing of N660 with value of 602.01 % is due to the error that had been discussed before. The value of CaCO_3 is higher compared to other carbon blacks except N220 which is 628.85 %. This is because, CaCO_3 is quite sticky compared to carbon black. Thus, CaCO_3 needs high loads to break their specimens.

Figure 7 shows filled rubber compounds of the five different fillers are strongly increased modulus at 100, 300 and 500 % elongation. Tensile modulus, as applied to the elastomers is defined as the force required to produce a certain elongation. In addition, tensile modulus measure the stiffness and vulcanization degree of rubber compounds [14]. There is a steady increment in tensile modulus for the five

Table 4 Results of different types of fillers on the tensile properties

Types of fillers	Load at break (N)	Tensile strength (MPa)	Elongation at break (%)	Tensile modulus		
				M100	M300	M500
N220	235.471	23.63	638.63	2.01	5.88	13.44
N330	197.98	20.04	601.88	2.03	6.12	14.12
N550	160.113	16.47	535.27	2.21	6.67	14.59
N660	211.814	21.15	602.01	2.25	6.71	14.60
CaCO_3	67.494	7.54	628.85	0.99	1.69	3.82

Fig. 5 Effect of different fillers on tensile strength

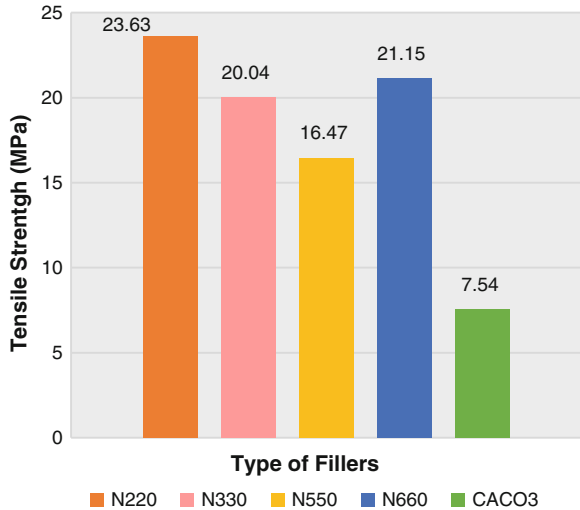
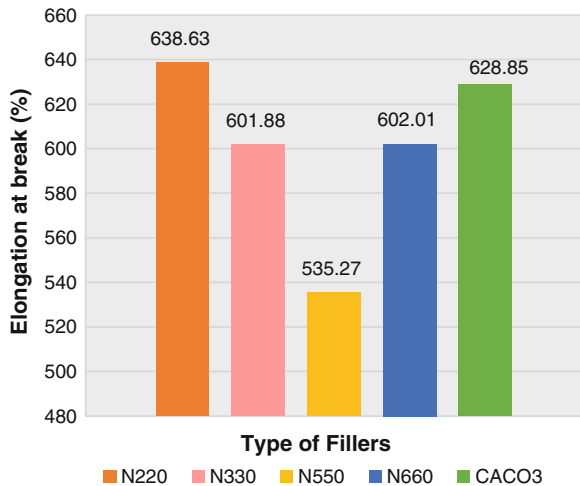
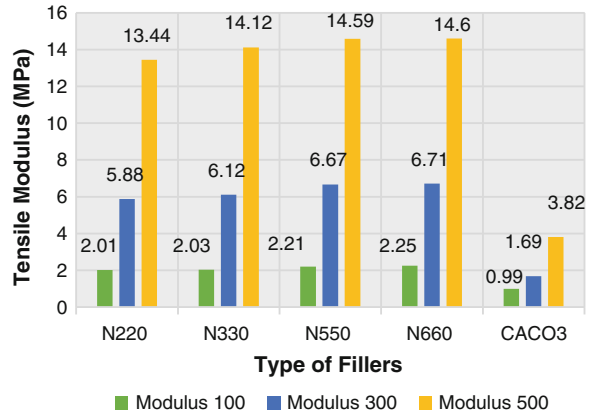


Fig. 6 Effect of different fillers on elongation at break



different filler loadings for tensile modulus at 100, 300 and 500 %. It can be seen that N660 with value of 14.60 MPa is the highest tensile modulus at 500 %, followed by N500, N330 and N220 which are 14.59, 14.12, and 13.44 MPa respectively. CaCO₃ is the lowest value of 3.82 MPa for 500 %. The same trend discovered for tensile modulus at 300 and 100 %. The graph shows the increasing values in 300 % modulus, starting from N220, N330, N550, and N660 fillers which are 5.88, 6.12, 6.67, and 6.71 MPa. CaCO₃ is also the lowest value for 300 % which is 1.69 MPa. Same trend discovered for 100 % modulus starting from CaCO₃, N220, N330, N550, and N660.

Fig. 7 Effect of different fillers on tensile modulus



5 Conclusion

Based on this study, it can be concluded that different filler loadings give different values of tensile results to the rubber compounds because different materials have different properties. Rubber-filled compound are depending on the chemical nature of the elastomer, the sizes and structure of the fillers, the mixing conditions and curing time. Tensile strength increases when the surface contact between rubber and fillers are increase. Thus, smaller particle sizes of fillers has better tensile strength. Carbon black fillers can be proved to have better tensile properties compared to non-carbon black fillers. From this study, the tensile strength of N220 is the highest, followed by N330, N550 and CaCO₃. The error of results of N660 can be avoided by properly inspecting the rate of curing.

Acknowledgments The author would like to acknowledge that this research has been carried out as a part of RAGS project funded by Ministry of Education (MOE) and support from Research Management Institute (RMI), Universiti Teknologi Mara (UiTM).

References

1. A. Mujkanovi, L. Vasiljevi, G. Ostoji, Non-black fillers for elastomers, in *13th International Research/Expert Conference Trends in the Development of Machinery and Associated Technology*, (2009), pp. 865–868
2. A. Aruniit, J. Kers, K. Tall, Influence of filler proportion on mechanical and physical properties of particulate composite. *Agron. Res. Biosyst. Eng.* **5**(1), 23–29 (2011)
3. U.K. Niyogi, *Polymer Science*. Delhi (2007)
4. M.-J. Wang, *The Role of Filler Networking in Indianapolis*. Indiana (1998)
5. M.S. Sobhy, D.E. El-Nashar, N.A. Maziad, Cure characteristics and physicomechanical properties of calcium carbonate reinforcement rubber composites. *Egypt. J. Sol.* **26**(2), 241–257 (2003)

6. A. Mostafa, A. Abouel-Kasem, M.R. Bayoumi, M. G. El-Sebaie, Rubber-filler interactions and its effect in rheological and mechanical properties of filled compounds. *J. Test. Eval.* **38** (3), 1–13 (2013)
7. I.S. Saad, M.S. Fayed, E. M. Abdel-Bary, Effects of carbon black content on cure characteristics, mechanical properties and swelling behaviour of 80/20 NBR/CIIR blend, in *13th International Conference on Aerospace Sciences & Aviation Technology, ASAT-13*, 2009, pp. 1–9
8. K. Sirin, M. Balcan, F. Doğan, The influence of filler component on mechanical properties and thermal analysis of PP-LDPE and PP-LDPE/DAP ternary composites, in *Polypropylene*, ed. by D. Fatih (InTech, Croatia, 2012), p. 500
9. D.T. Norman, *Rubber Grade Carbon Blacks*, 13th edn. (Vanderbilt Rubber Handbook, 1990)
10. F. Cinaralp, L. Zullo, Reinforcing filler in the rubber industry: assessment as potential nanomaterials with a focus on tyres, *European Tyre & Rubber*, 2012. Available Online: www.etrma.org. Accessed 26 May 2014
11. J.L. Leblanc, Rubber-filler interactions and rheological properties in filled compounds, vol. 27 (2002)
12. BS ISO 37 Rubber, Vulcanized or Thermoplastic—Determination of Tensile Stress-Strain properties, , 2011
13. A. Samsuri, *An Introduction to Polymer Science and Rubber Technology* (Pusat Penerbitan Universiti, Universiti Teknologi MARA, Shah Alam, 2009), p. 270
14. K. Nagdi, *Rubber as an Engineering Material: Guideline for Users* (Carl Hanser Verlag, Munich, 1993)

The Effect of Rolling Direction to the Tensile Properties of AA5083 Specimen

Latifah Mohd Najib, Anizahyati Alisibramulisi,
Norliyati Mohd Amin, Ilyani Akmar Abu Bakar and Sulaiman Hasim

Abstract Tensile tests are commonly used to provide information on the tensile properties of materials. However, limited tests have been done on the orientation angles of material for the same properties. Thus, the present paper discusses the effect of three different angles to the tensile properties of aluminium alloy AA5083 dog-bone specimens based on the original rolling direction. For this purpose, the angles chosen and tested were 0° , 45° and 90° . It is found that, as the orientation angle increases, the ultimate tensile strength also increases. In contrast, the Young's Modulus decreases as the angle increases. It is also observed that the material is much more ductile when the work hardening increases. Thus, the rolling directions give a significant effect on the tensile properties of AA5083 specimens tested.

Keywords Rolling direction · Tensile properties · AA5083 · Angle orientation

L.M. Najib (✉) · A. Alisibramulisi · N.M. Amin · I.A.A. Bakar · S. Hasim
Faculty of Civil Engineering, Universiti Teknologi MARA (UiTM),
40450 Shah Alam, Selangor, Malaysia
e-mail: efa90_green@yahoo.com.my

A. Alisibramulisi
e-mail: aniza659@salam.uitm.edu.my

N.M. Amin
e-mail: norli830@salam.uitm.edu.my

I.A.A. Bakar
e-mail: dyeyanie@yahoo.com

S. Hasim
e-mail: sulaimanhasim@yahoo.com

A. Alisibramulisi · N.M. Amin
Institute for Infrastructure Engineering and Sustainable Management (IIESM),
Universiti Teknologi MARA (UiTM), 40450 Shah Alam, Selangor, Malaysia

1 Introduction

Aluminium 5083 is a strong magnesium-manganese-chromium-aluminium alloy. It can be hardened by cold work but it cannot be heat treated for higher strength. Its ductility is better than most other 5,000 series alloys [1]. The AA5083 can be used as plate alloy in marine application or structural component in transportation application.

During the rolling process to produce metals in plate or sheet form, there are several factors that can be considered in the rolling direction, such as the subsequent annealing and the grains of microstructure and macrostructure, as it becomes elongated when it rolls. Based on the rolling direction, a preferred crystallographic (texture) of orientation can be developed which causes variation of properties due to its direction [2]. However, limited tests have been done on the orientation angles of material. Thus, this study investigates the effect of rolling direction to the tensile properties of AA5083 plate specimen.

2 Experimental Program

The tensile specimens used in this study are an aluminium alloy series of AA5083-H321 and the standard test methods for tension testing of metallic materials—ASTM E8 [3] is referred.

2.1 Specimen Preparation

AA5083 rectangular plate with dimensions of 3.0 mm × 610 mm × 915 mm was cut to 0°, 45° and 90° angles from the rolling direction and each angle has three specimens. Therefore, there were nine specimens in total. The tensile samples were rectangular, with 200.0 mm total length, 20.0 mm width of grip section, 12.5 mm width, 50.0 mm gauge length, 12.5 mm radius of fillet, 57.0 mm length of reduced section, 50.0 mm length of grip section and 3.0 mm thickness. At first, the rectangular specimens were machined by using Hydraulic Swing Beam Shearing Machine, and then followed with dog-bone specimens that were machined by using CNC milling machine (DMC 635 V). Nine (9) tensile specimens of the respective angles are illustrated in Fig. 1. Details of AA5083 chemical composition are tabulated in Table 1 and the respective processes are illustrated in Figs. 2, 3 and 4.

Fig. 1 Plan view of cutting specimens from the AA5083 plate

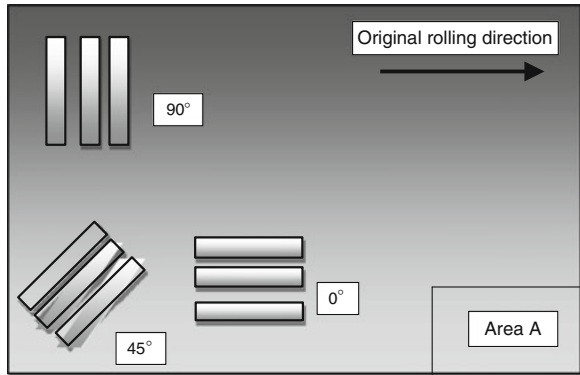


Table 1 Chemical composition of AA5083

Element	Percentage (%)
Aluminium (Al)	Balance
Magnesium (Mg)	4.0–4.9
Manganese (Mn)	0.40–1.0
Chromium (Cr)	0.05–0.25
Silicon (Si)	0.40 max
Iron (Fe)	0.40 max
Copper (Cu)	0.10 max
Zinc (Zn)	0.25 max
Titanium (Ti)	0.15 max
Others, each	0.05 max
Others, total	0.15 max

Fig. 2 Half depth hole drilling at the specimen's grip section



Fig. 3 Full holes drilling assisted by large g-clamp



Fig. 4 CNC milling machine that was used to cut the specimens into dog-bone shape



Microstructures were analyzed by using optical microscopy (Olympus BX-51) as illustrated in Figs. 5, 6 and 7. The scanning shows a homogeneous elongated grain. It is proven that the grain orientation is in accordance to the angle oriented from the rolling direction of the cut plate AA5083.

Fig. 5 Tensile specimen of 0° to the rolling direction

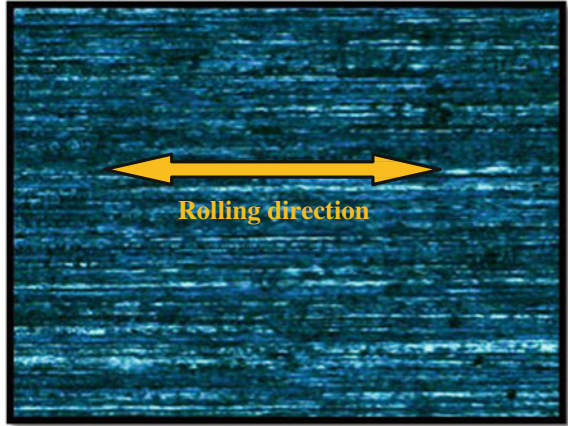


Fig. 6 Tensile specimen of 45° to the rolling direction

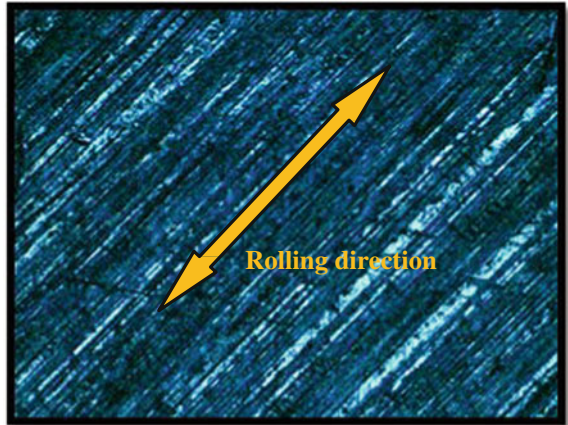


Fig. 7 Tensile specimen of 90° to the rolling direction

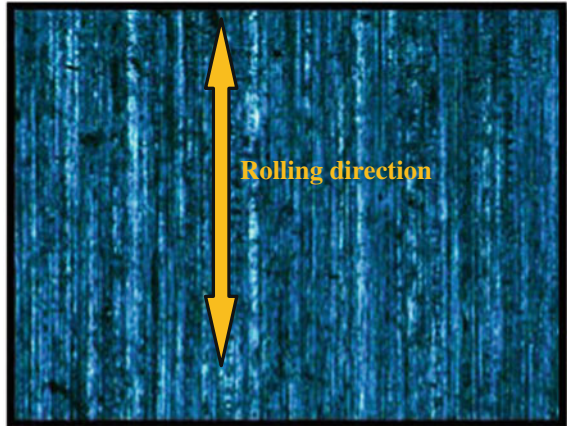


Fig. 8 Universal Testing Machine, UTM-1000



2.2 Tensile Tests

The UTM-1000 machine (Fig. 8) is used to determine the strength of AA5083 plate specimen and extracting other parameters such as deformation, strain, modulus of elasticity, and work hardening.

3 Results and Discussions

In this section, rolling direction effects to the tensile properties of AA5083 specimen will be discussed.

3.1 Tensile Properties

The tensile behaviors of the AA5083 specimen tested based on the respective orientation angles are shown in Fig. 9. Its corresponding tensile properties are tabulated in Table 2.

Fig. 9 The relationship between engineering stress and engineering strain for three different angles

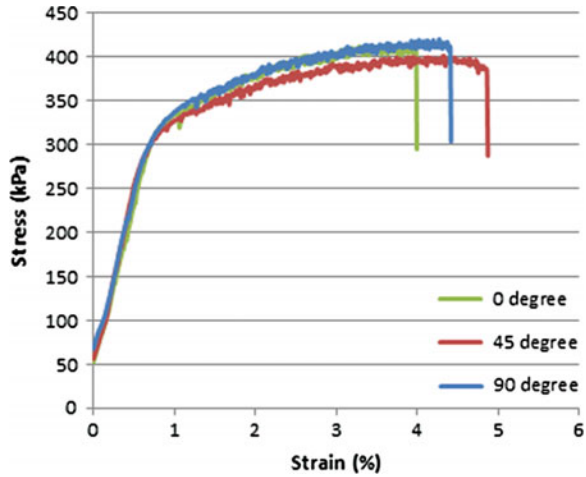


Table 2 Tensile test result

Degree to rolling direction	Maximum force, F_{max} (kN)	Ultimate tensile strength, UTS (MPa)	Fracture stress (MPa)	Modulus of elasticity, E (GPa)	Work hardening, w
0°	15.63	416.90	384.76	52.77	1.19
45°	15.16	404.23	610.33	49.17	1.25
90°	15.83	422.17	422.88	47.92	1.22

It is found that the maximum force and stress are resulted from the 90° orientation. This is in accordance to the result of Said et al. [4] for Al-Cu-Li specimen. It is expected that 0° orientations will give higher strength if it is properly heat treated and aged. It appears that the force and tensile stress increase as the orientation angle increases. In contrast, the Young’s Modulus decreases as the orientation angle increases. In other words, the grain that is elongated 0° to the tensile force gives higher Young’s Modulus. Liu et al. [5] and Askeland et al. [6] also found that, there was also a correlation between the grain orientation and the deformation structure. The 45° orientation gives the highest strain and work hardening result. This is due to the increasing stress level is directionally proportional to the change of plastic deformation. However, the effect of work or strain hardening only occur in the early stages of plastic deformation. Thus, once the structure deforms and breaks down, the influence of work hardening will also disappear. It is also evident that the specimen is much more ductile when the work hardening increases as stated by Dieter et al. [7]. Thus, the highest elongation to fracture and fracture stress are obtained from the same angle orientation. Nevertheless, it can be summarized that the tensile specimens’ response curves change as the rolling directions change.

3.2 Tensile Fracture Surfaces of AA5083

The overall tensile fracture images as well as its cross section surfaces of the rectangular shape specimen were captured to determine the deformation behavior of the chosen alloy as depicted in Figs. 10 and 11 respectively. The applied tensile stress on the specimen will result in separation of the solid body into two which is denoted as fracture. From the images snapped, ductile fracture was observed. This is due to its appearances of cup-and-cone fracture showing gross plastic deformation on both of the fracture surfaces. It is also worth noting that the specimens' modes of failures are in accordance to the response curves shown in Fig. 9 and tabulated data in Table 2.



Fig. 10 The tensile fracture of AA5083 specimens



Fig. 11 Closer view of the fracture (cross section)

4 Conclusions

Based on the above investigation, it was observed that as the orientation angles increases, the ultimate tensile stress also increases (maximum value was obtained from the 90° orientation). In contrast, the Young's Modulus decreases as the angle increases. In other words, the grain that is elongated 0° to the tensile force gives higher Young's Modulus. It was also observed that the 45° orientations give the highest strain and work hardening result. It is evident that, the material is much more ductile when the work hardening increases. The tensile fracture surfaces show that it fails under ductile manner. Thus, it can be concluded that the rolling direction does has a significant effect on the tensile properties of the AA5083 specimen tested.

Acknowledgment The authors would like to thank Faculty of Civil Engineering and Reseach Management Institute (RMI), Universiti Teknologi MARA, Malaysia for all supports in establishing this research.

References

1. Austral Wright Metals, Aluminium Grade 5083, UNS A95083 Product Data Sheet (2005)
2. J.R. Davis, *Tensile Testing*, 2nd edn. (ASM International, United States of America, 2004)
3. American Society for Testing and Materials—ASTM, *Standard Test Methods for Tension Testing of Metallic Materials* (E8/E8M-11, United States of America, 2012)
4. O.S. Es-Said, C.J. Parrish, C.A. Bradberry, J.Y. Hassoun, R.A. Parish, A. Nash, N.C. Smythe, K.N. Tran, T. Ruperto, E.W. Lee, D. Mitchell, C. Vinquist, Effect of stretch orientation and rolling orientation on the mechanical properties of 2195 Al-Cu-Li Alloy, *J. Mater. Eng. Perform.* **20**(7), 1171–1179 (2011)
5. Q. Liu, D. Juul Jensen, N. Hansen, Effect of grain orientation on deformation structure in cold-rolled polycrystalline aluminium. *Acta Mater.* **46**, 5819–5838 (1998)
6. D.R. Askeland, P.P. Fulay, *Essentials of Materials Science and Engineering* (Cengage Learning, Canada, 2009)
7. G.E. Dieter, H.A. Kuhn, S.L. Semiatin, *Handbook of Workability and Process Design* (ASM International, United States of America, 2003)

Multicriteria Assessment of Ageing Civil and Structure Facilities in Onshore Process Plants

Dabo Baba Hammad, Nasir Shafiq and Muhd Fadhil Nuruddin

Abstract The main objective of this study was to prioritize the criteria for the inspection of civil and structure facilities in onshore process plants based on asset integrity management theory framework. A pairwise comparison of criteria against the alternatives was done using Delphi Technique. Analytic Hierarchy Process (AHP) was used to rank the criteria. The judgment was acceptable with a consistency Index of (CI) of 0.01. Impact on safety was ranked the most important criteria in the inspection of civil and structure facilities based on the experts' judgment. While impact on asset and impact on production are of equal importance. Finally, impact on reputation is less important to all the criteria studied. The ranking technique may be used in making maintenance decision for any type of structure if the design and maintenance data cannot be reached. However, it is recommended to add sub criteria in future study.

Keywords Maintenance criteria · Facilities structure · Onshore plants

1 Introduction

Civil and Structure facilities popularly known as C&S are designed to withstand load, stress etc. However, damage due to extreme event is always possible during their life cycle. Most often, C&S facilities are designed for the period of 30 years and above [1]. But sometimes undetected and unrepaired damage may lead to early

D.B. Hammad (✉) · N. Shafiq · M.F. Nuruddin
Civil Engineering Department, Universiti Teknologi PETRONAS,
Bandar Seri Iskandar, 31750 Tronoh, Perak, Malaysia
e-mail: Dbhammad_g01661@utp.edu.my

N. Shafiq
e-mail: nasirshafiq@petronas.com.my

M.F. Nuruddin
e-mail: fadhilnuruddin@ptronas.com.my

failure to loss of properties and or even live(s). This may consequently lead to costly repair or replacement. Most often, civil engineering structure serve as a base to support the load and vibration of equipment resting on them. The loading and vibration stresses imposed by the equipment due to extreme operating condition may likely lead to early deterioration of the equipment's foundation and supports. This necessitates constant monitoring and inspection in order to ensure safe and reliable working condition. Any failure on the foundation or support of such system may pose threat not only to technical function of the plant, but also may lead to safety, reputation and environment consequences [2]. Therefore, identifying and ranking of criteria for inspection of civil and structures facilities is sine qua non in the integrity management of onshore process plant. Due to the reasons discussed above, various inspection and maintenance strategies are being used for the maintenance of such a system to increase the availability of the plant in one hand and to reduce the operating and maintenance cost of the plant in another hand. According to Khan and Haddara [3], industries worldwide spend a huge amount of money on maintenance of production system in an effort to maintain optimal production. For instance, each year US industries spend a well over \$300 billion on plant maintenance and operation [4]. Apparently, the cost of designing and building structures are much smaller than the cost of operating a building or other structures over the course of its lifecycle [5]. Similarly, Arunraj and Maiti [6], confirmed that, the cost of maintenance itself is still rising in absolute terms and as a proportion of total expenditure. In some industries it is the second highest or even the highest element of operating costs. Hence, it is clear that much efforts is needed to enhance production, optimize maintenance cost, improve safety and remain relevant in the current competitive market. In view of the fact, the purpose of maintenance is to maximize availability and efficiency of structures and control rate of deterioration of facilities at a minimized cost [7]. In addition, with increase in global awareness and competitiveness, more emphasis is placed on safety, environment, human and social issues and not just on minimizing the maintenance cost. In contrast, Tummala et al. [8] observed that, failures and effects on equipment as well as the corresponding preventive actions are not presented well between different departments in the company. He further asserted that, maintenance is becoming complex due to many factors such as increase demands for tighter regulatory requirement, shorter allowable maintenance time and lower maintenance budgets etc.; and this has significantly intensify the difficulty in maintenance operations. Shen et al. [9] concluded that, taking in cognizance of the current economic climate, budget for maintenance of civil structures are unlikely to meet the ever increasing maintenance need. The process of making inspection and maintenance decision for civil and structure facilities, involved many interdependencies, which mostly are identifiable yet difficult to model. According to Xenidis and Angelides [10], the interdependencies may include; physical, functional, economic and legal interdependencies. In other words, there is need for the careful selection of inspection criteria for

maintenance decision. This implies that, maintenance planning is a multi-criteria task that involved objective and subjective source of data. Therefore, it is required to have defined criteria that can be used as a guide in the inspection and maintenance of civil and structural facilities. This will help in realizing optimal decision in maintenance of civil structures based on priority. Hence, this study intends to rank the inspection criteria based the importance of the civil and structures facilities in onshore process plant.

2 Civil Structures in Onshore Plants

There are various types of civil structures in onshore process plants serving various functions ranging from support, protection to means of movement within the plant. Table 1 shows classes of civil structures, their types and function that are commonly available in onshore plants.

Table 1 List of civil and structures in onshore plants

Structure class	Structure type		Structure functions
Foundation	Equipment foundation	A1	Foundation is the link between the structure and its eventual support, which is the soil itself. With respect to onshore plants, it provides supports for pumps
	Tank foundation	A2	Foundation is the link between the structure and its eventual support, which is the soil itself. It a heavy concrete structure that support tank in place
Structures	Pipe rack	A3	Pipe rack might be the most important artery of any plant. It conveys the pipes and cable containers (raceways) from one equipment to another
	Pipe bridge	A4	For elevating pipes above ground level
Infrastructures	Access road	A5	A large plant must have access road to serves a link between all the units
	Separation pit	A6	A pit usually constructed of reinforced concrete to house the oil and oil separation system
	Open drainage	A7	Drainage systems (oil water sewer—manhole and surface water), effluent treatment system, basin, Road and paving
	Tank bundwall	A8	A dike wall surrounding a storage tank to serve a protection against flooding as well as spill in case the tank leaks

3 Multicriteria Decision Analysis

There are many multi criteria decision making techniques such as multi-attribute value theory (MAVT), multi attribute utility theory (MAUT), multi group hierarchical discrimination (MHDIS), neural network (NN) and fuzzy set theory (FS). However, a study done by Yu and Shing [11], has indicated that, there is not much difference between MADT and Analytic Hierarchy Process (AHP). Similarly a study by Tang et al. [12], confirmed that, AHP is easy to use, this make it the most widely used MCDA tool in both academic research and real life applications. Ishizaka and Nemery [13] opined that, AHP can be applied is solving problems that involved; choice selection, ranking problem and sorting problems. Based on its flexibility, [14] affirmed that, AHP allows the decision makers to model a problem in a hierarchical structure showing the relationship of the goal, objectives (criteria), and alternatives. By definition, Analytic Hierarchy Process, popularly known as AHP is a multi-criteria decision making tool, Saaty [15]. It is a mathematically simple tool that can be described more effectively by using matrix in the linear algebra. This technique is capable of handling a large number decision factors and provide a systematic procedure of ranking many decision variables. AHP was composed departing from several previously existing but non-associated techniques and concepts such as hierarchical structuring of complexity, pairwise comparisons, redundant judgments, and the eigenvector method for deriving weights and consistency. The three major reasons behind the adoption and use of analytic hierarchy process (AHP) are highlighted as follows; As a mathematical and logical decision making tool, it helps in analysing the decision problem on a logical manner and aids in converting decision makers intuition's and subjective judgement and feelings into numbers which can be questioned by others and can be explained by other as well. It is a good tool for reducing complex problem into sub-problem to be tackled once at a time. This is the fundamental way that human decision makers works. Study has suggested that, human being can compare 7 ± 2 things at a time. Therefore to deal with a large and complex decision making problems, it is essential to break it down to a simple hierarchy.

Decision, particularly group decision making requires process that that will includes that decision makers inputs, revisions and learning and communicate them to others so as to reach a collective decision. Hence, AHP is created to formalize the process, place it on a scientific footing and also help in aiding natural decision making process. Bevilacqua and Braglia [16] listed three steps that serves as a guide in the application of AHP in decision analysis

First of all, definition of the decision criteria to form a hierarchy of objectives as shown on Fig. 1. Second stage is the pair wise comparison and the third stage is the development of normalized eigenvector of the matrix which can be obtained by calculating priority vector and deriving weight of the elements.

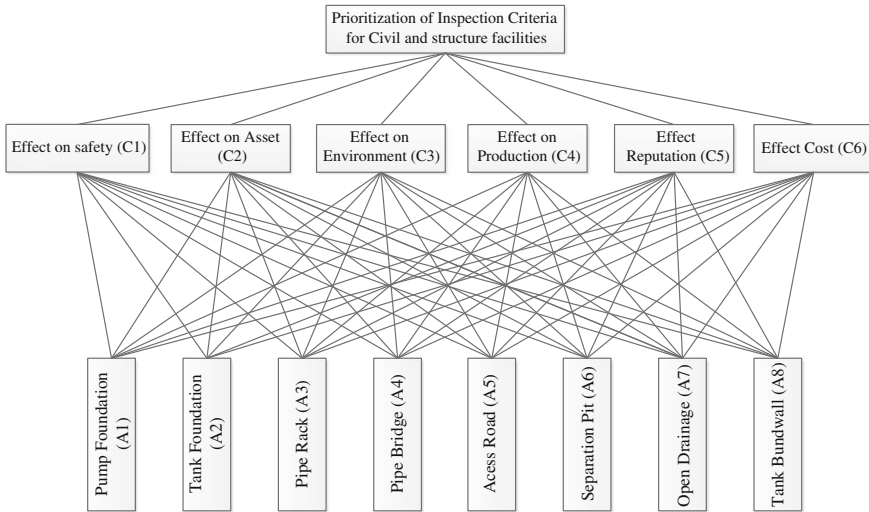


Fig. 1 Composition of the inspection for criteria and civil and structures facilities

4 The Proposed Inspection Criteria

Criteria for the inspection of any engineering facilities largely depends on the purpose for which the inspection was intended. The criteria for transfer of ownership may be different from criteria to be observed in assessing facilities for maintenance reasons. Similarly, inspection for insurance may be different from inspection for performance and sustainability. Therefore, with regards to this work, the criteria selected were intended for maintenance reasons only. It is generally believed that, criteria for inspection and maintenance nowadays are beyond the earlier perception of maintenance for performance reasons only. Maser [17] opined that, less dramatic but for more serious, are the social and economic consequences of making day-to-day decision regarding the health and future of any infrastructure without adequate tools and information. In line with Maser’s observation, Tan et al. [5] upholds that, there are many criteria for inspection and maintenance, but most of them overlapped. However, he cautioned that large criteria does not guaranteed accuracy of the selection decision model. However, Flores-Colen et al. [18] proposed a methodology for service performance of rendering facades in current buildings, based on several inspections with visual appraisals and onsite testing. He classified the criteria for the inspection of facades in buildings into technical or physical performance perspective, risk perspective and cost perspective for maintenance decision making. However, it was concluded that the decision criteria for prioritization of actions needed a detailed investigation. According to Arangio et al. [19], relevant attribute such as reliability, safety, maintainability and integrity are considered essential properties to guarantee, with reference to the whole life-cycle, the survivability of the system under the relevant accidental or exceptional hazard

scenarios, security issues, system robustness, serviceability and durability. On this note, various literatures have concluded that, criteria for inspection and maintenance are not exhaustible and depends on the types of inspector and his perception on in-service performance and maintenance needs, Flores-Colen et al. [18]. Hence, this studies tried to prioritize some few attributes that a generally critical to the inspection of engineering systems as discussed below;

- (i) *Impact on safety*: Generally safety is a fundamental principle in any engineering design. It is primarily concerned with sudden catastrophic incident that could result in serious injury or death [20]. A case of Bhopal incident lead to the death of Thousands people in the local community. It is generally believed that, the time in which safety event take place is often short. Hence impact that a defective structure may have on users is considered very critical and therefore requires adequate attention. Therefore in considering any maintenance planning, the criticality of the structure with regards to safety is considered very important in assessing any defect.
- (ii) *Impact on asset*: According to Ratnayake and Markeset [21], an asset is defined as any physical core, acquired (i.e. the organization has either the possession or the custody of the asset) elements of significant value to the organization, which provides and request service for the organization. Hence, an asset form the basis of entity of any organization. It is important to note that, a defects that will have an adverse effect on the asset may have a direct impact on the entire objective of the organization.
- (iii) *Impact on the environment*: Of recent, many events have occurred that solicited for environmental concern. One example of such an event is Macandor well blowout in in the Gulf of Mexico. This event has cost BP a huge sum of dollars as a result of environmental impact the event has caused [21]. It is therefore not arguable that, the impact industrial organization has on the quality of social and ecological environment of the future generations. Environmental and social concern are expressed as health, safety and environment (HSE) in industrial asset operation. Many holds the notion that, defects or failure of civil structures in process plants may have negligible or no serious impact on the environment. Nevertheless, there are instance where the structures carries critical equipment such as tank, column, vessel etc. In this case, if the supporting structure failed, there is every tendency for the equipment to be affected and this may eventually leak of containment that may litter the environment.
- (iv) *Impact on production*: Companies nowadays are face with challenges of increasing demands in terms of quality and quantity of products and services, responsiveness and costs reducing. To deal with these demands, company must have a reliable production system, well maintained by an efficient and inexpensive maintenance system. A performance and well-organized maintenance service contributes to the production system consistency, it will extend the life of industrial equipment and thus the best overall performance of the plant.

- (v) *Impact Reputation*: This is public information regarding a player's trustworthiness. A player reputation reflects the information that third parties have on how trustworthy his behaviour has been in the past. It thus be seen as a rating in which a stakeholder state if the entity meets the expectations of the stakeholder.
- (vi) *Impact on cost*: The main objective of any business entity is to generate revenue that can be used to sustain its function and services. Therefore cost is an essential criteria that derives any decision in business management. Factors such as the cost of inspection, either internally or outsourced, the cost of maintenance material, maintenance labour cost etc. cannot be ignored. Therefore any effort to optimise the cost of inspection and maintenance of the facilities remained essentially important.

Common structures and their usage in onshore oil and gas process facilities have been identified and briefly discussed. This has formed the basis for this study. Furthermore, AHP has been identified as the simplest multi criteria decision analysis tool. It is observed that, AHP is popularly used in selection, prioritising and ranking of element or cases with multiple attributes. Since, engineering system is considered complex with many elements serving different functions, many criteria must be considered for the inspection or maintenance of such facilities.

5 Methodology

Delphi survey technique was used to collect relevant data for the study. According to Bertolini et al. [22], the Delphi technique is a structured process which investigates a complex or ill-defined issue by means of a panel of experts. This methodology considered appropriate research design for this type of study. This is due to the fact that, it allow individual opinions to be obtained from group experts using a communicative process. Therefore, eleven (11) member panel of experts was set up. The experts were selected based on their area of expertise and working experience. The experts include, 5 site engineers with experience of 5–10 years, and 6 faculty staff specialists in construction materials and structures. The working experience of the faculty staff is between the ranges of 10–30 years. The panel worked for the period of 1 year, that is from September, 2011 till August, 2012. Various meeting sessions were organized among which two were basically for the Delphi session. In the first meeting, a number of maintenance criteria were generated individually and anonymously by the experts. The generated criteria were collected and organized into Analytic Hierarchy Process (AHP) questionnaire. The questionnaires were distributed to the experts in the second meeting. However, in the second meeting only Nine (9) experts participated. Therefore, the findings in this study is based on consensus of Nine (9) experts. The experts ranked the criteria based on importance. Analytic hierarch process was used in the analysis of the experts responses using Microsoft excel 2010. According to Shafiq and Silvianita

[23], AHP application system is described in three steps; decomposition of a complex decision problem as hierarchy, the pairwise comparison and the procedure and the analysis of results.

5.1 Decomposition

The hierarchy of this problem is decomposed into three (3) levels. As shown on Fig. 1, Level 1 represents the alternatives, which is classes of civil structures and facilities, level 2 is the criteria selected for investigation, while the uppermost level represents the main objective of the analysis, which is prioritization of criteria for inspection and maintenance of the civil and structures facilities (Tables 2 and 3).

5.2 Pairwise Comparison

Based on the hierarchy, a questionnaire was developed and distributed to experts in the plants maintenance. 30 questionnaires were distributed and 9 were completed and duly returned. However, one of the questionnaires was not properly filled therefore discarded. Thus, 8 questionnaires were considered in this paper. The questionnaires were structured to elicit experts' judgment on how importance a

Table 2 Definition of inspection criteria

Definition of criteria	Code
Impact on safety	C1
Impact on asset	C2
Impact on environment	C3
Impact on production	C4
Impact on reputation	C5
Impact on cost	C6

Table 3 Definition of alternatives

Definition of alternative	Acronym	Code
Pump foundation	PF	A1
Tank foundation	TF	A2
Pipe rack	PR	A3
Pipe bridge	PB	A4
Access road	AR	A5
Separation pit	SP	A6
Open drainage	OP	A7
Tank bundwall	TB	A8

Table 4 AHP scale [24]

Scale	Definition	Explanation
1	Equal importance	Two alternatives contribute equally to the objectives
3	Moderate importance of one over another	Experience and judgment slightly favored one alternative over another
5	Essential or strong importance	Experience and judgment strongly favored one alternative over another
7	Demonstrated importance	An alternative is strongly favored and its dominance is demonstrated in practice
9	Extreme importance	The evidence favoring one alternative over another is of the highest possible order of affirmation
2, 4, 6, 8	Intermediate values between the two adjacent judgments	When compromised is needed

Table 5 Pairwise comparisons of criteria

	C1	C2	C3	C4	C5	C6
C1	1	1.36	1.85	1.26	3.43	1.08
C2	0.73	1	2.16	0.86	2.52	1
C3	0.54	0.46	1	0.4	1.59	0.5
C4	0.79	1.17	2.52	1	3.7	1.17
C5	0.29	0.4	0.63	0.27	1	0.4
C6	0.93	1	2	0.86	2.52	1

criteria is compared to its pair. The judgment was made on a scale of 1–9 as opined by Satty [15] and described in (Tables 4 and 5).

$$A = \begin{bmatrix} a_{11} & \dots & a_{1n} \\ \vdots & \vdots & \vdots \\ a_{n1} & \dots & a_{nn} \end{bmatrix} = \begin{bmatrix} w_1/w_1 & \dots & w_1/w_n \\ \vdots & \vdots & \vdots \\ w_n/w_1 & \dots & w_n/w_n \end{bmatrix} \tag{1}$$

5.3 Calculation of Consistency Ratio

Consistency in pairwise comparison matrix means that, when basic data is available, all other data can be logically deduced from them. In this study, after obtaining the local weight as shown on Table 6, then the consistency ratio was obtained based on the comparative of weighs of the criteria using matrix (2). While the consistency index is describe in Eq. (3).

Table 6 Matrix for the relative importance of criteria

	C1	C2	C3	C4	C5	C6	Rank
C1	0.23	0.25	0.18	0.27	0.23	0.21	0.23
C2	0.17	0.19	0.21	0.18	0.17	0.19	0.19
C3	0.13	0.09	0.10	0.09	0.11	0.10	0.10
C4	0.18	0.22	0.25	0.22	0.25	0.23	0.22
C5	0.07	0.07	0.06	0.06	0.07	0.08	0.07
C6	0.22	0.19	0.20	0.18	0.17	0.19	0.19

Table 7 Random index from [24]

n	3.00	4.00	5.00	6.00	7.00	8.00	9.00	10.00
RI	0.58	0.90	1.12	1.24	1.32	1.41	1.45	1.49

$$A = \begin{bmatrix} w_1/w_1 & \dots & w_1/w_n \\ \vdots & \ddots & \vdots \\ w_n/w_1 & \dots & w_n/w_n \end{bmatrix} X \begin{bmatrix} w_1 \\ \vdots \\ w_n \end{bmatrix} = n \begin{bmatrix} w_1 \\ \vdots \\ w_n \end{bmatrix} \tag{2}$$

$$\text{where: } CI = \frac{\lambda_{max} - n}{n - 1} \tag{3}$$

Random Index of Analytic Hierarchy Process is shown is Table 7

$$\text{Therefore: } CR = \frac{CI}{RI}$$

$$CR = 0.01$$

A consistency rating of 0.10 or less is considered acceptable. However, if an inconsistency has been encountered, the process of evaluation of the judgment matrix should be repeated. Perhaps, the judgment in this study proved to be consistent and therefore acceptable.

6 Result and Discussion

The result of the experts’ judgment in this study has shown that, impact on safety (C1) is assessed to be the most important criteria in the inspection of civil and structure facilities in onshore process plants. This has indicated that, safety is considered the most important factor to be considered in any engineering system which agrees with the globally accepted engineering best practices. Similarly, impact on production (C4) which remain a core objective of any plant has been judged to be second in importance. Factors such as frequency of production, quality of Units production and volume of production are important indicators in the plants

performance. Hence, defect on any civil or structure system that may alter these core indicators may require frequent and urgent attention for inspection and maintenance. The study has also indicated that, there is relationship between effect on asset (C2) and effect on cost (C6). On this note, it is quite believable that, reliable and available civil and structure facilities helps in optimizing the general maintenance cost of the plant. Although, the impact on environment (C3) is of critical importance, however, is rated second to the last in terms of importance. While, the lowest rated criteria is impact of reputation (C5). Despite the fact that, reputation remain an important factor in marketing of a product, but is considered less importance if compared to the remaining criteria as found in this study. This may not be unconnected with the characteristics of the experts most of whom are from engineering background.

7 Conclusion

The principal objective of this study was to prioritize the criteria for the inspection and maintenance of civil and structure facilities in onshore process plant. On this note, a hierarchy of inspection criteria for civil structures and facilities was developed. Pair wise comparison of the criteria against the main objective was successfully obtained using Analytic Hierarchy Process (AHP). The effect of structural defects on safety is considered the most critical as indicated by this study. This is consistent with the global engineering standard of practice which considered safety as the most vital criteria in the development of any engineering system. The finding is highly consisted with a consistency index of 0.01 and consistency ratio of 0.01, this has indicated a sharp consensus among the participating experts. Therefore, the judgment is consistent with engineering and business value of the cases under study. Although, sourcing of the experts for this type of study proved to be challenging, it is recommended to have more experts' involvement so that, the finding may be generalized.

References

1. R.T. Ratay, *Structural Condition Assessment* (Wiley, USA, 2005)
2. N. Smith, O.I. BuTuwaibeh, I.C. Cruz, M.S. Gahtani, Risk-based assessment (RBA) of a gas/oil separation plant, in *SPE International Conference on Health, Safety and Environment in Oil and Gas Exploration and Production* (2002)
3. F.I. Khan, M.M. Haddara, Risk-based maintenance (RBM): a quantitative approach for maintenance/inspection scheduling and planning. *J. Loss Prev. Process Ind.* **16**, 561–573 (2003)
4. D. Frangopol, M. Liu, Multiobjective optimization for risk-based maintenance and life-cycle cost of civil infrastructure systems, in *System Modeling and Optimization*, ed. by F. Ceragioli, A. Dontchev, H. Futura, K. Marti, L. Pandolfi (Springer, Boston, 2006), pp. 123–137

5. Z. Tan, J. Li, Z. Wu, J. Zheng, W. He, An evaluation of maintenance strategy using risk based inspection. *Saf. Sci.* **49**, 852–860 (2011)
6. N.S. Arunraj, J. Maiti, Risk-based maintenance—techniques and applications. *J. Hazard. Mater.* **142**, 653–661 (2007)
7. N.S. Arunraj, J. Maiti, Risk-based maintenance policy selection using AHP and goal programming. *Saf. Sci.* **48**, 238–247 (2010)
8. M.F. Ng, V.M.R. Tummala, R.C.M. Yam, A Risk-based maintenance management model for toll road/tunnel operations. *Constr. Manage. Econ.* **21**, 495–510 (2003)
9. Q. Shen, K. Lo, Q. Wang, Priority setting in maintenance management: a modified multi-attribute approach using analytic hierarchy process. *Constr. Manage. Econ.* **16**, 693–702 (1998)
10. Y. Xenidis, D.C. Angelides, A risk-based decision making methodology for planning and operating safe infrastructure systems against various hazards, in *Computational Methods in Earthquake Engineering*, ed. by M. Papadrakakis, M. Fragiadakis, V. Plevris (Springer, The Netherlands, 2013), pp. 591–609
11. J.R. Yu, W. Shing, Fuzzy analytic hierarchy process and analytic network process: an integrated fuzzy logarithmic preference programming. *Appl. Soft Comput.* **13**, 1792–1799 (2013)
12. S.L. Tang, I.U. Ahmad, S.M. Ahmed, M. Lu, *Qualitative Techniques for Decision Making in Construction* (Hong Kong University Press, China, 2004)
13. A. Ishizaka, P. Nemery, *Multi-Criteria Decision Analysis: Methods and Software* (Wiley, United Kingdom, 2013)
14. A.C. Márquez, *Criticality Analysis for Asset Priority Setting*, (Springer, London, 2007), pp. 107–126
15. T. L. Saaty, *Decision Making with Analytic Network Process: Economic, Political, Social and Technological Applications with Benefits, Opportunities, Costs and Risks* (Springer Science +Business Media, LLC, USA, 2006)
16. M. Bevilacqua, M. Braglia, The analytic hierarchy process applied to maintenance strategy selection. *Reliab. Eng. Syst. Saf.* **70**, 71–83 (2000)
17. K.R. Maser, Inventory, condition and performance assessment in infrastructure facilities management. *J. Prof. Issues Eng.* **114**, 271–280 (1988)
18. I. Flores-Colen, J. de Brito, V. Freitas, Discussion of criteria for prioritization of predictive maintenance of building facades: survey of 30 experts. *J. Perform. Constr. Facil.* **24**, 337–344 (2010)
19. S. Arangio, M. Ciampoli and F. Bontempi, *Structural integrity monitoring for dependability* (Anonymous CRC Press, 2008), pp. 11–19
20. I. Sutton, *Process Risk and Reliability Management—Operational Integrity Management* (Elsevier, USA, 2010)
21. R.M. Chandima Ratnayake, T. Markeset, Asset integrity management for sustainable industrial operations: measuring the performance. *Int. J. Sustain. Engineering* **5**, 145–158 (2012)
22. M. Bertolini, M. Bevilacqua, F.E. Ciarapica, G. Giacchetta, Development of risk-based inspection and maintenance procedures for an oil refinery. *J. Loss Prev. Process Ind.* **22**, 244–253 (2009)
23. N. Shafiq, Silvanita, Prioritizing the pipeline maintenance approach using analytic hierarchy process. *Int. Rev. Mech. Eng. (IREME)* **4**, 346–352 (2010)
24. T.L. Saaty, *Fundamentals of Decision Making and Priority Setting Theory with the Analytic Hierarchy Process* (RWS Publication, Pittsburgh, 1994)

Comments on Structural Reliability for Design and Construction as Per Eurocode

K.A. Al Sanjery and J.Y. Sia

Abstract The replacement of the British standards by the Eurocode, and the Malaysian decision to adopt this change has raised some concerns with regards to the effects it may have on design and construction. Among these effects are the aspects of the structural reliability management introduced in EN 1990 and the respective Malaysian National Annex. In this respect the code introduced measures and procedures to enable engineers to assess the probability of failure of a particular structure and to estimate the partial factors for actions and materials. As such it will be mandatory for engineers, designing in accordance with Eurocodes, to follow the recommendations stipulated in these codes. Furthermore the code introduces specific measures, depending on the class of the building, to be considered for quality management. This will minimize human errors and enhance safety and quality of the structure. Applying all these measures should produce structures with high level of safety, durability and economy. The objectives of the paper are to study the aspects related to structural reliability with respect to probability of failure and quality management measures proposed by the Eurocode. It is also intended to highlight the limitations of the procedure and values given in the code. Accordingly comments have been given on the validity of the partial factors introduced in the code, and new values of probability of failure for reference periods 25, 75 and 100 years have been calculated. Furthermore the procedure to calculate the reliability index β illustrated. It is concluded that in order to produce durable structure with reasonable level of probability of failure, and considering economical aspects, all requirements of the Eurocode must be considered. In addition, Engineers should assess carefully the class of building to be designed and to estimate the probability of failure for that particular building. This should be carried out in agreement with the

K.A. Al Sanjery (✉)

Department of Civil Engineering, SEGI University,
Kota Damansarah, 47810 Petaling Jaya, Selangor, Malaysia
e-mail: kousay@segi.edu.my

J.Y. Sia

Department of Business Administration, SEGI University,
Kota Damansarah, 47810 Petaling Jaya, Selangor, Malaysia
e-mail: jyingsia@gmail.com

client. It is proposed that steps towards building a national reliability model, takes into consideration local conditions, should be considered. It is also hoped that this study will open up further investigation and research in this area.

Keywords Reliability · Design · Construction · Eurocode · Quality management

1 Introduction

It has been long established that uncertainties in anticipated loads and load carrying capacity of a structure are inherent in structural design. The source of these uncertainties, which can cause failure, are:

- (a) Human causes; this includes approximation, calculation errors, communication problems, lack of knowledge, and greed. Uncertainties can also arise, during construction, due to the use of inadequate materials, method of construction, misuse, and inadequate maintenance.
- (b) Natural causes; this result from unpredictability of design loads and uncertainty attributed to the mechanical behaviour of the materials used in construction.

Due to these inherent problems [1], indicated that a complete structure may never be absolutely safe but always with a finite probability of failure. To minimize this probability, the Eurocode 1990 introduces two main approaches:

1. Structural reliability and quality management system (Annex B of Eurocode 1990)

In this approach certain preventive measures and numerical values for reliability index and partial safety factors have been suggested to be used.

These are intended to reduce both human errors and natural causes of failure. The main tools selected in this annex are:

- differentiation by values of β factors
- alteration of partial factors
- design supervision differentiation
- measures aimed to reduce errors in design and execution of the structure, and gross human errors
- adequate inspection and maintenance according to procedures specified in the project documentation.

It should be noted that some of these parameters (β and partial factors) may need to be verified and/or new values need to be calculated.

2. Reliability—based design criteria/Basis of analysis (Annex C of Eurocode 1990)

The code presents methods of analysis based on probabilistic approach which can be used by engineers for any type of building or when a certain level of reliability is required.

Both approaches are discussed in the following paragraphs, and more emphasis are placed on approach 1 with regards to quality management system and verification of the reliability index β .

It would be essential that engineers, professional organisations, contractors, and clients should refer to EN 1990 Eurocode, annexes B and C to determine the required level of reliability for any particular structure.

2 Structural Reliability and Quality Management Systems

Reliability is defined as “Ability of a structure or a structural member to fulfill the specified requirements during the design working life for which it has been designed”. Also quoted as “equal to the probability that a structure will not fail to perform its intended function” [1, 2].

Different level of reliability may be adopted for structural resistance and serviceability. The choice of the level of reliability for a particular structure should take account of the relevant factors, which include the following:

The possible cause and/or mode attaining a limit state;

The possible consequences of failure in terms of risk to life, injury, potential economic losses, frequency of use and public aversion to failure, the expense and procedure necessary to reduce the risk of failure.

The purpose of reliability differentiation, introduced in EN 1990 Eurocode, is the socio-economic optimisation of the resources to be used to build construction works, taking into account all the expected consequences of failure and the cost of construction.

This can be achieved by:

- (a) Preventive and protective measures with regard to quality management system
- (b) Measures relating to design calculation which cover representative values of actions and the choice of partial factors.

2.1 Consequences Classes

Consequences classes are introduced based on the assumed consequences of failure and the exposure of the construction works to hazard. These are given in Table 1. It can be seen, however, that the table do not cover all types of buildings, which could have a larger impact compared with the buildings listed in the table, such as hospitals, nuclear buildings, overhead transmission lines, shelters, bridges etc.

Table 1 Definition of consequences classes

Consequences classes	Description	Examples of buildings and civil engineering works
CC3	High consequence for loss	Grandstands, public buildings
CC2	Medium consequence for loss	Residential and office buildings, public buildings
CC1	Low consequence for loss	Agricultural buildings

2.2 Differentiation by Reliability Index (β) Values

Reliability classes (RC) have been introduced in the code and defined in accordance with reliability index β . These are RC1, RC2, and RC3 associated with respective consequent classes CC1, CC2, and CC3. The code presented minimum values of β for the various types of buildings to be achieved in design. The reliability index β is a function of the probability of failure P_f . The code recommended minimum values for β for reference periods 1 and 50 years. These recommended values for (1 and 50 years) are given in Table 2, these are marked with ^a. Further values for reference periods of 25, 75 and 100 years for the three classification classes RC3, RC2 and RC3 have been calculated and given in the same table.

The general form of the equation used in the calculation, as presented in the code is:

$$[\Phi(\beta_n) = \Phi(\beta_1)]^n$$

where:

n number of years

β_1 reliability index for 1 year

Table 2 Recommended minimum values for reliability index β (ultimate limit states)

Reliability class	Minimum values of reliability index β and probability of failure P_f				
	1 year reference period	25 years reference period	50 years reference period	75 years reference period	100 years reference periods
RC3	5.2 ^a	4.57	4.42 ^a	4.33	4.27
	9.96×10^{-8}	2.49×10^{-6}	4.99×10^{-6}	7.47×10^{-6}	9.96×10^{-6}
RC2	9.96 ^a	2.49×10^{-6}	4.99×10^{-6}	7.47×10^{-6}	9.96×10^{-6}
	4.7 ^a	3.99	3.83 ^a	3.72	3.65
RC1	1.3×10^{-6}	3.25×10^{-5}	6.49×10^{-5}	9.75×10^{-5}	1.3×10^{-4}
	4.2 ^a	3.41	3.21 ^a	3.09	3.01
	1.33×10^{-5}	3.32×10^{-4}	6.65×10^{-4}	9.97×10^{-4}	1.33×10^{-3}

^a values of β given in Eurocode EN1990 Annex B

It should be pointed out that using the recommended partial factors given in the Eurocode generally lead to a structure with a value greater than 3.8 for a 50 year reference period. This indicates that the code quite safe with reliability class RC2, but need to be verified when reliability class RC3 are to be considered.

Furthermore the use of expressions (6.10a) or (6.10b) instead of the classical fundamental equation for combinations of actions (6.10) [3], as given Eurocode 1990 applicable to ultimate limit states of resistance can further reduce the reliability index [4].

However, these values are considered only notional values that do not necessary represent actual failure rates which depend mainly on human error. They are used as operational values for code calibration purposes and comparison of reliability levels of structure. Therefore the Eurocode left the door open for engineers to verify the probability of failure, at the same time indicating that human error is more important.

2.3 Differentiation by Measures Relating to the Partial Factors

An alternative way of achieving reliability differentiation is by distinguishing classes by γ_F (partial factor for action) to be used in fundamental combinations for loading. For example, for the same design supervision and execution inspection levels, a multiplication factor K_{FI} , may be applied to the partial factors as given in Table 3.

2.4 Design Supervision Differentiation

Three possible design supervision levels (DSL) have been identified as shown in Table 4.

These measures can be extended to include classification of designers and/or design inspectors (checkers, controlling authorities, etc.), depending on their competence and experience, for the relevant type of construction works being designed.

Table 3 K_{FI} factor for actions

K_{FI} factor for actions	Reliability class		
	RC1	RC2	RC3
K_{FI}	0.9	1.0	1.1

Table 4 Design supervision and inspection levels (DSL and IL)

Reliability class	Design supervision levels	Inspection level	Characteristics	Requirements
RC3	DSL3	IL3	Extended supervision and inspection	Third party checking and inspection
RC2	DSL2	IL2	Normal supervision and inspection	Checking by different persons than those originally responsible for design and inspection
RC1	DSL1	IL1	Normal supervision and inspection	Self-checking and inspection

2.5 Inspection During Execution

Referring to the same table, three inspection levels (IL) for products and construction works have been introduced, these are given in the Table 4.

3 Basis for Partial Factor Design and Reliability Analysis

Annex C of the code EN 1990 provides information and Theoretical background to calculate partial factors and ψ values to be used in design. These can be determined in either of two ways:

- (a) On the basis of calibration to a long experience of buildings tradition.
- (b) On the basis of statistical evaluation of experimental data and field observations, adopting probabilistic reliability theories such as:
 - First order reliability method (FORM) Level II
 - Full probabilistic Level III

The partial factors and ψ values proposed in the current Eurocode were based on method (a) above. However, the code recommends that, irrespective of the method used, the reliability levels should be as close as possible to the target reliability index β given in the code. Therefore the reliability index must be first calculated in order to calculate the other factors. The code also recommends that because of lack of a long experience of buildings tradition and scare of statistical data a combination of both methods (a) and (b) above for the calculation of β and ψ may be used.

Table 5 Relation between β and P_f

P_f	10^{-1}	10^{-2}	10^{-3}	10^{-4}	10^{-5}	10^{-6}	10^{-7}
β	1.8	2.32	3.09	3.72	4.27	4.75	5.20

3.1 Determination of Reliability Index B and Probability of Failure P_f

The reliability index β should be first calculated in order to calculate the probability of failure P_f , the partial safety factors for loads, and ψ factor.

An estimate of the reliability index β , can be obtained by adopting the procedure in accordance with Level II (semi probabilistic method) introduced in Annex C of Eurocode 1990. In this method β is a quantity fully equivalent to the probability of failure P_f which is represented by the formula given in the code as:

$P_f = \Phi(-\beta)$, where Φ is cumulative distribution function of the standardised normal distribution. This relationship, as given in the code, is shown in Table 5.

The failure probability P_f can be expressed through a performance function g , such that the structure will fail if $g \leq 0$; such as: $P_f = \text{Prob.}(g \leq 0)$, where:

$$\begin{array}{l}
 g = R - E \\
 \left. \begin{array}{l}
 R: \text{ is the resistance} \\
 E: \text{ is the effect of action} \\
 g: \text{ the performance function}
 \end{array} \right\} \begin{array}{l}
 \text{all are random} \\
 \text{variables with normal} \\
 \text{distribution}
 \end{array}
 \end{array}$$

$$\text{and } \beta = \mu_g / \sigma_g; \mu_g = \mu_R - \mu_E; \sigma_g = (\sigma_R^2 + \sigma_E^2)^{1/2}$$

where:

- μ_g mean value of g
- σ_g standard deviation = coefficient of variation in statistic distribution $\times \mu_g$
- μ_R is the mean characteristic resistance based on long-term experience
- σ_R standard deviation = coefficient of variation in statistic distribution $\times \mu_R$
- μ_E is the mean characteristic value of action
- σ_E standard deviation = coefficient of variation in statistic distribution $\times \mu_E$

Detailed procedure and examples to calculate β can be referred to Haig et al. [4].

3.2 Effect of Reliability Index B on Partial Factors and Ψ Values

The targeted values of reliability index, given in Table 2, represent minimum values. It should be noted that these values are associated with certain reference periods. These reference periods are not necessary represent the life span of a

building. Therefore when a life span for a building is required, a certain reference period should be assigned. This, however, may require further study and clarification.

It must be remembered that the reliability index values are only notional values, actual failure depend mainly on human error and this has not been considered in the derivation of these factors. As mentioned earlier, class RC 3 buildings have not been rigorous considered in the Eurocode, and therefore values of β , partial factors and Ψ must be calculated.

It has also been noticed that using a definite value of a reliability index β for the calculation of Ψ factor as per table C4 of the Eurocode (Annex C of Eurocode 1990), where various methods are proposed, can give deferent values [4]. This need further investigation.

4 Conclusion

The reliability approach of the Eurocode to estimate the partial factors was based on a semi statistical method. In this approach the human factor has not been included, and therefore to asses a more accurate probability of failure, human error must be considered. It is therefore suggested that the model presented for reliability management by the Eurocode, including all measures for quality management recommended by the code must be fully implemented without exclusion.

The partial factors presented in the code ensure certain level of probability of failure, therefor it is recommended that when important and special types of buildings to be designed values of β and respective partial factors need to be established.

Further study considering local environment, and establishment of reliability index and consequent development of partial factors and Ψ factor should be carried out for all classes of buildings including those which are not mentioned in the code.

Acknowledgments The author appreciate the work done by Soon Kim Hioh, thesis submitted as partial fulfilment of the requirements for BSc (Honour) degree in civil engineering University Infrastrucure Kuala Lumpur. October 2011

References

1. S. Andrzej, K. Nowak, R. Collins, *Reliability of Structures*, Mcgraw-hill-International editions Civil Engineering Series (2000)
2. J. Schneider, *Introduction to Safety and Reliability of Structures*. International Association for Bridge & Structural Engineering. ISBN 3-85748-093-9 (1997)
3. Draft Malaysian Standard, 09D004RO Eurocode: Basis of Structural Design, ICS: 91.010.30, 2nd edn. Department of Standards Malaysia (2009)
4. H. Gulvanessian, J.A. Calgaro, M. Holicky, *Designers' Guide to Eurocode: Basis of Structural Design*, (Institution of Civil Engineers Thomas Telford, London, 2012)

Part VI
Micro and Nano Technology in
Constructions and Civil Engineering

Influence of Ionic Substitution on the Mechanical Properties of Nanosized Biphasic Calcium Phosphates

Mohamad Firdaus Abdul Wahid, Koay Mei Hyie,
Mardziah Che Murad and N.R. Nik Roselina

Abstract Synthetic hydroxyapatite ceramics have been used for bone repair, implants coating and as fillers. However, hydroxyapatite ceramics have low resorption rate. In order to increase resorption rate, researchers suggested that adding another calcium phosphates phase would overcome this problem. Combining β -tricalcium phosphates (β -TCP) with hydroxyapatite (HA) would increase resorption rate without compromising other properties. The mixture containing β -TCP with HA is known as biphasic calcium phosphates (BCP) ceramics and existed at various ratios depending on processing conditions. BCP is obtained by heating calcium apatite at temperature above 750 °C. Calcium apatite is influenced by preparation synthesis particularly on reaction temperature and reaction pH. The ratio of HA/ β -TCP is depending on calcium phosphates ratio of synthesized apatite and heat treatment temperature. Biphasic calcium phosphate ceramic have been used as biomaterial in bone defects reconstruction applications. Furthermore, recent advancements in nanotechnology have increase investigation on nanosized BCP. By producing nanosized BCP, the material properties could be improved particularly in mechanical properties. It is known that micrometer sized calcium phosphates have poor mechanical properties. Thus cannot be used in load bearing applications. It is suggested that by reducing particles size into nanometer, better properties of calcium phosphates can be obtained particularly in sinterability, biocompatibility and mechanical properties. Furthermore, these properties can be altered by substituting various ions. In this review, the synthesis methods and characteristics of calcium phosphates were studied. Numerous properties of calcium

M.F.A. Wahid (✉) · K.M. Hyie (✉) · M.C. Murad (✉) · N.R. Nik Roselina (✉)
Faculty of Mechanical Engineering, Universiti Teknologi MARA,
40450 Shah Alam, Selangor, Malaysia
e-mail: mfaw1504@gmail.com

K.M. Hyie
e-mail: hyie1105@yahoo.com

M.C. Murad
e-mail: mardziahcm@yahoo.com

N.R. Nik Roselina
e-mail: roseline_roseley@uitm.salam.edu.my

phosphates are improved compared to micro meter sized structured by doping with various ions. Moreover, mechanical properties and phase stability of ion doped calcium phosphates after heat treatment should be investigated in more detail.

Keywords Biphasic calcium phosphate · Ionic substitution · Sintering · Mechanical properties

1 Introduction

Calcium phosphates are very important and significance for humans as they exist in the bones and teeth. Numerous medical applications have shown interest in calcium phosphates because they display excellent properties. Because of chemical compositions similarity to biological bone and teeth, most of artificially prepared calcium phosphates retain remarkable biocompatibility. Researchers use this property to create synthetic bone grafts that are used as surface coated or fully made of [1]. Yet, calcium phosphates are not mechanically strong due to brittleness and poor fatigue behavior. The most common calcium phosphates group is shown in Table 1.

Bone is made of organic-inorganic ceramic composite with collagen fibrils comprising well-arrayed, surrounded, nanocrystalline, needle-like inorganic particles with length of 25–50 nm [3]. Bone structural order can be divided into several hierarchical levels and reveals the component materials. The bone mineral part is composed of natural calcium phosphates comprising various elements such as carbonate, magnesium, zinc, strontium and fluoride, absorbed onto the crystal surface or incorporated into crystal lattice [4].

Synthetic hydroxyapatite (HA) with chemical formula of $\text{Ca}_{10}(\text{PO}_4)_6(\text{OH})_2$ has similar chemical compound to the inorganic component of bone matrix. This has led to numerous research efforts to use synthetic HA as bone substitute [5, 6]. However the resorption rate of HA was too low and thus provoke complications due to the mechanical mismatch between bone and HA [7]. Therefore, researchers have focused towards the use of more soluble calcium phosphates by introducing TCP. As a result biphasic calcium phosphates term was used. LeGeros et al. [8] reported that the word biphasic calcium phosphate was first used by Nery et al.

Table 1 Common calcium phosphates group and their formula [2]

Compound	Abbreviation	Formula	Molar ratio
α -tricalcium phosphate	α -TCP	$\alpha\text{-Ca}_3(\text{PO}_4)_2$	1.5
β -tricalcium phosphate	β -TCP	$\beta\text{-Ca}_3(\text{PO}_4)_2$	1.5
Amorphous calcium phosphates	ACP	$\text{Ca}_x\text{H}_y(\text{PO}_4)_z \cdot n\text{H}_2\text{O}$, $n = 3\text{--}4.5, 15\text{--}20 \%$ H_2O	1.2–2.2
Calcium deficient hydroxyapatite (metastable form)	CDHA or Ca-def HA	$\text{Ca}_{10-x}(\text{HPO}_4)_x(\text{PO}_4)_{6-x}(\text{OH})_{2-x}$ ($0 < x < 1$)	1.5–1.67
Hydroxyapatite	HA or Hap	$\text{Ca}_{10}(\text{PO}_4)_6(\text{OH})_2$	1.67

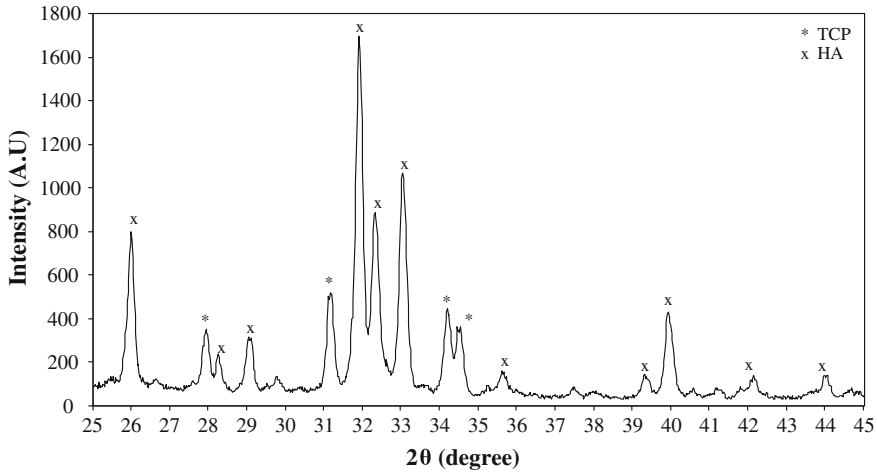


Fig. 1 XRD pattern of biphasic calcium phosphates consisting of HA and β -TCP

They used it to describe bioceramic that contained a mixture of HA and β -TCP based on analysis of the X-ray diffraction which showed that their mixture consisted of 20 % HA and 80 % β -TCP. Dorozkhin [2] mentioned that in year 1986, LeGeros in the USA and later Daculsi in France started basic studies on this ceramic. They also observed BCP *in vitro* properties. The properties of biphasic are depending on the ratio of more stable (hydroxyapatite) and more soluble (tricalcium phosphate). By changing the ratio, it is possible to prepare biphasic with adjustable properties. This bioceramics can be applied to bone defects, in non-load or load bearing areas and as modified pieces which will sustain their shape over long periods of time [9].

The phases of biphasic calcium phosphates are homogeneously mixed at the micro or nano level and thus strongly combined with each other. However, the presence for each individual phase can be easily detected by X-ray diffraction (XRD) which shows that they remain unaffected (Fig. 1).

The concept of using biphasic calcium phosphate is to achieve proper balance between more stable phases and more soluble phases [10]. The major biomedical properties are maintained without comprising artificial bone strength. This paper reviews the knowledge on biphasic calcium phosphates concerning about preparation techniques, heat treatment process, mechanical properties and lastly with ionic substitution.

2 Synthesis

Various methods have been developed for the past decade to produce calcium phosphates. For instance, precipitation method [11], sol-gel method [12], hydrothermal method [13], solid state mixing [14], hydrolysis method [15], and emulsion method [16].

Sol-gel method synthesis method for calcium phosphates is quite easy. Compared to other method, this process can be done at lower temperatures [12]. Calcium and phosphorus molecular level mixing can be achieved by using this method. In addition, chemical homogeneity can be improved. Sol-gel method can be used to obtain biphasic calcium phosphates but difficult to produce pure hydroxyapatite. Many different solvent can be used in this method such as ethanol, phosphorus, gels and alkoxides [4].

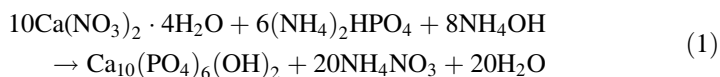
Solid state synthesis is a dry synthesis method. The procedure is relatively simple and can be used for mass production of calcium phosphates powder. In a typical process, a mixture of inorganic components such as CaO and $\text{CaHPO}_4 \cdot 2\text{H}_2\text{O}$ are prepared with the use of water and acetone. Then, the mixture is milled, dried and calcined at high temperature (1,000 °C). Milling is an important factor in this method. This parameter affects the product powder size. The shape of powder obtained from this method was irregular with micron sized particles [14].

The hydrolysis method usually involve dissolution and precipitation processes. Calcium phosphates apatite with 20 nm grain size has been formed by this method. Temperature, pH value and other ions are the main factors that affect phase transformation [15]. This synthesis receives low preparation of calcium phosphates.

Hydrothermal method required high temperature and pressure during synthesis. This method is able to produce nano sized particles. Besides, powder produce from hydrothermal method is well crystallized, uniform, and homogeneous. But, the amounts that can be produced in laboratory are insufficient [13]. This method has limited commercial use and is quite expensive.

In emulsion method, agglomeration of calcium phosphates can be reduced. This method requires low temperature during synthesis. Moreover, this technique is able to control the particles morphology and microstructure. For example, calcium phosphates powders are produced by using calcium nitrate and phosphoric acid as precursors in liquid medium and cyclohexane, hexane and isooctane were used as surfactants [16]. The type of surfactants used and the surfactants concentration are the main factors in emulsion method. This method can be considered as an advantage in producing nanosized calcium phosphates.

Among various methods, precipitation method is the simplest method to synthesize nanosized calcium phosphates. Usually this method is prepared by using calcium nitrate and diammonium hydrogen phosphates as the starting materials [11]. The precipitation reaction is conducted at pH value above 7 with the use of ammonia solution as a pH correction. Ammonia solution is added after two mixtures are combined. Also, it is conducted at various temperatures ranging from room temperature to the boiling point of water. One of the chemical reactions to produce hydroxyapatite can be explained by the following reaction.



It was found that the grain size is increasing with increasing synthesis reaction temperature. It is advised to precise control over the parameters in order to gain nanosized grain. Precipitation method is favorable for the synthesis of biphasic calcium

phosphates due to straightforward synthesis and cost effective. In order to produce excellent properties of ceramics, it is important to control ceramic synthesis and understand what factors may affect its physical, chemical and biological properties.

3 Sintering of BCP

Biphasic calcium phosphates ceramics are a mixture of HA and β -TCP. These ceramics have been used as bone substitute materials for two decades. Thus various products of HA/TCP phase ratios have been commercially available [8]. They are produced by sintering a mixture of HA and TCP powders or from thermal decomposition of calcium phosphates apatite. Sintering single phase is more preferable than a mixture of HA and TCP as it produces high strength mechanical properties.

For instance, BCP is produced by sintering non-stoichiometric calcium phosphates apatite such as HA at temperature above 600 °C [17]. Usually sintering temperature is done at above 1,000 °C [18]. Further explanation regarding solid-state mechanism for this conversion is available in this journal [19]. Moreover, the condition of synthesis was found to effect resulting BCP by altering the HA/TCP ratio [20]. Preparation and heat treatment interconnected each other for BCP fabrication. Figure 2 shows micrograph of BCP ceramics obtained after sintering at 1100 °C HA and β -TCP phases cannot be distinguished from this micrograph

Densification of biphasic calcium phosphates occurs at high temperature. Compare to pure HA and TCP, BCP sintering ability is much lower. Currently, there is no prove for any mutual sintering between HA and TCP. In order to obtain a product that is fully densified BCP ceramics, high temperature at least 1,250 °C is required. However, very high temperature would favor β to α TCP phase transformation. To counter this problem, substituting ion (e.g magnesium) would increase sintering ability of β -TCP at much higher temperatures without transformation to α -TCP phase.

Another method to fully densifying beta TCP without α phase formation is using assisted sintering such as two steps sintering (TSS) and hot pressing (HP). The advantage of using these techniques would prevent grain growth. If BCP ceramics are sintered at low temperatures, microporous ceramic are produced. Porous BCP ceramics have superior biological properties compared to dense BCP. It is due to micropores that able to stimulate bone formation. The resulting porosity happens due to incomplete sintering process. Thus porous BCP mechanical properties are not very reliable for load bearing applications.

4 Mechanical Properties

Strength and elastic modulus are usual used as the properties to characterize mechanical behavior of synthetic bone. The target properties should fall within range of natural bone. For instance, compressive strength of natural cortical bone is

Table 2 Summary for other strength and porosity of human bone [16]

Type of bone	Flexural strength (MPa)	Tensile strength (MPa)	Modulus (GPa)	Porosity (%)
Cortical bone	135–193	50–151	12–18	5–13
Cancellous bone	NA	1–5	0.1–0.5	30–90

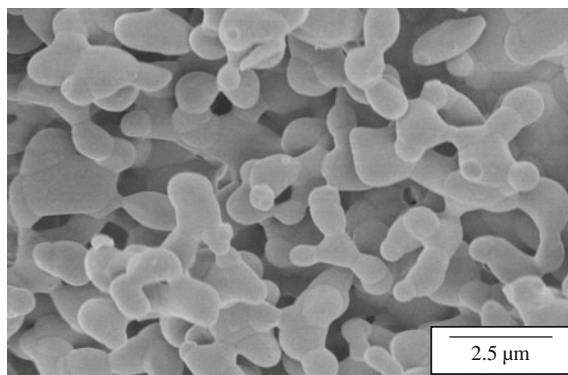
between 130 and 180 MPa while the compressive strength of cancellous bone is between 4 and 12 MPa [16]. It is essential that synthetic bone should match to human natural bone and do not collapse after bone replacement. Table 2 summarizes the other strength and porosity of human cortical and cancellous bone for reference.

The use of calcium phosphates in loading applications is limited due to low mechanical support. It is because calcium phosphates are somewhat low in tensile strength and also brittle. Generally, the brittleness of tricalcium phosphate is less compared to hydroxyapatite. However, TCP degradation is quicker compared to HA resulting in faster loss in mechanical strength over time [21].

Mechanical properties of calcium phosphates are influenced by several characteristics such as porosity, composition and microstructure. Porosity distribution, fraction, pore size and architecture have a strong effect on the mechanical properties of calcium phosphates. Increasing pore size would enhance bone formation. However, this will lead to a decreased in strength. For instance, mechanical strength is decrease to factor of four when total porous volume is increased from 10 to 20 % [21].

Besides, mechanical behavior is also affected by grain size and crystallinity. The more noticeable crystalline phase and smaller grain size would increase overall strength of calcium phosphates. Moreover, ceramic strength is proportional to the reciprocal square root of the grain size and the microstructures of calcium phosphates are often a result of the way they were processed [17]. The phases existent in the calcium phosphates are determined by the composition and the heat treatment. Thus, affect the mechanical properties of calcium phosphates ceramic. Nevertheless, the trend of characteristic and mechanism are not well understood [16].

Fig. 2 FESEM of biphasic calcium phosphates consisting of HA and β -TCP



5 Ionic Substitution

There are various components exist such as F^- , Mg^{2+} , Zn^{2+} and CO_3^{2-} in natural bone. Therefore, numerous ions have been added to calcium phosphates ceramics in order to improve biological and mechanical properties of synthetic calcium phosphates ceramics. In general, doping with several ions will affect the microstructural properties of calcium phosphates such as change in the thermal stability of calcium phosphates, decomposition of single phase into other phase and also grain size.

Kalita and Bhatt [22] have conducted an experiment regarding nanocrystalline HA doping with Mg^{2+} and Zn^{2+} ions. The aim of this experiment was to study the effects of metal ions on powder morphology and sintering characteristics. It was observed that 1 wt% Mg^{2+} doped into HA produced smaller grain size than pure HA. On the contrary, same amount of Zn^{2+} doped into HA produced larger grain size than pure HA. After sintering at 1,300 °C, 1 wt% metal ions showed higher compression strength and hardness compared to undoped HA. Compression tests showed that Mg^{2+} and Zn^{2+} doped HA produced compression strength of 281 and 223 MPa compared to undoped HA with strength of 211 MPa. Vickers hardness of 1 wt% Mg^{2+} and 1 wt% Zn^{2+} doped HA were 380 and 350 HV than undoped HA was 325 HV.

In term of biological effect, granules of 5.7 at.% Mg doped HA were implanted into rabbit femoral bone defects. It was observed that osteoconductivity (new bone growth on synthetic bone) was enhance compared to commercial HA granulate [23]. Using precipitation method, magnesium substitution was found to reduce crystal size, prevent crystallization and greater solubility material was produced [24]. For Zn doped HA, Zn^{2+} ion was found to enhance the osteoblast response [25]. Furthermore, experiment done by Stanic et al. [26] produced Zn doped HA that was able to reduce the presence of bacteria such as *E. coli* and *Staphylococcus aureus*.

6 Conclusion

Biphasic calcium phosphates ceramics can be synthesized by several methods and advances in nanotechnology will benefit to the development of BCP ceramics. Biphasic calcium phosphates ceramics are made of a mixture of HA and β -TCP. It is achieved by sintering calcium apatites. By controlling HA and β -TCP ratio, a better potential in biological and mechanical properties can be obtained. Furthermore, addition of ions into ceramics could improve calcium phosphates properties. Numerous works need to be done to study final composition of calcium phosphates ceramics after heat treatment process. Heat treatment or sintering is a unique process because the proportions, nature and distribution of calcium phosphates are to some extent uncontrolled. Nevertheless, the calcium phosphates powder preparation method and shaping process are also significance for the improvement of calcium phosphates.

Acknowledgment The authors would like to thank Research Management Institute (RMI) UiTM and Ministry of Higher Education Malaysia for financial supports. The research is conducted at Faculty of Mechanical Engineering, Universiti Teknologi MARA (UiTM), Malaysia under support Grant 600-RMI/RAGS 5/3 (57/2012).

References

1. Z. Evis, T.J. Webster, Nanosize hydroxyapatite: doping with various ions. *Adv. Appl. Ceram.* **110**(5), 311–321 (2011)
2. S.V. Dorozhkin, Biphasic, triphasic and multiphasic calcium orthophosphates. *Acta Biomater.* **8**(3), 963–977 (2012)
3. H. Zhou, J. Lee, Nanoscale hydroxyapatite particles for bone tissue engineering. *Acta Biomater.* **7**(7), 2769–2781 (2011)
4. N.I. Ponomareva, T.D. Poprygina, S.I. Karpov, M.V. Lesovoi, B.L. Agapov, Microemulsion method for producing hydroxyapatite. *Russ. J. Gen. Chem.* **80**(5), 905–908 (2010)
5. M. Sadat-Shojai, M.-T. Khorasani, E. Dinpanah-Khoshdargi, A. Jamshidi, Synthesis methods for nanosized hydroxyapatite with diverse structures. *Acta Biomater.* **9**(8), 7591–7621 (2013)
6. G.S. Kumar, A. Thamizhavel, Y. Yokogawa, S.N. Kalkura, E.K. Girija, Synthesis, characterization and in vitro studies of zinc and carbonate co-substituted nano-hydroxyapatite for biomedical applications. *Mater. Chem. Phys.* **134**(2–3), 1127–1135 (2012)
7. S. Pramanik, A.K. Agarwal, K.N. Rai, A. Garg, Development of high strength hydroxyapatite by solid-state-sintering process. *Ceram. Int.* **33**(3), 419–426 (2007)
8. R.Z. LeGeros, S. Lin, R. Rohanizadeh, D. Mijares, J.P. LeGeros, Biphasic calcium phosphate bioceramics: preparation, properties and applications. *J. Mater. Sci. Mater. Med.* **14**(3), 201–209 (2003)
9. G. Daculsi, S. Baroth, R. LeGeros, *20 years of Biphasic Calcium Phosphate Bioceramics Development and Applications, in Advances in Bioceramics and Porous Ceramics II* (Wiley, New York, 2010), pp. 45–58
10. S.E. Lobo, T. Livingston Arinze, Biphasic calcium phosphate ceramics for bone regeneration and tissue engineering applications. *Materials* **3**(2), 815–826 (2010)
11. M. Descamps, L. Boilet, G. Moreau, A. Tricoteaux, J. Lu, A. Leriche, V. Lardot, F. Cambier, Processing and properties of biphasic calcium phosphates bioceramics obtained by pressureless sintering and hot isostatic pressing. *J. Eur. Ceram. Soc.* **33**(7), 1263–1270 (2013)
12. I.S. Gunawan, A. Naqshbandi, S. Ramesh, Synthesis of zinc doped-biphasic calcium phosphate nanopowder via sol-gel method. *Key Eng. Mater.* **531–532**, 614–617 (2013)
13. F. Ren, R. Xin, X. Ge, Y. Leng, Characterization and structural analysis of zinc-substituted hydroxyapatites. *Acta Biomater.* **5**(8), 3141–3149 (2009)
14. W.-J. Shih, Y.-F. Chen, M.-C. Wang, M.-H. Hon, Crystal growth and morphology of the nano-sized hydroxyapatite powders synthesized from $\text{CaHPO}_4 \cdot 2\text{H}_2\text{O}$ and CaCO_3 by hydrolysis method. *J. Cryst. Growth* **270**(1–2), 211–218 (2004)
15. S. Gomes, J.-M. Nedelec, G. Renaudin, On the effect of temperature on the insertion of zinc into hydroxyapatite. *Acta Biomater.* **8**(3), 1180–1189 (2012)
16. A.J. Wagoner Johnson, B.A. Herschler, A review of the mechanical behavior of CaP and CaP/polymer composites for applications in bone replacement and repair. *Acta Biomater.* **7**(1), 16–30 (2011)
17. C.B. Carter, M.G. Norton, *Ceramic Materials* (Springer, New York, 2013)
18. M. Lukić, Z. Stojanović, S.D. Škapin, M. Maček-Kržmanc, M. Mitrić, S. Marković, D. Uskoković, Dense fine-grained biphasic calcium phosphate (BCP) bioceramics designed by two-step sintering. *J. Eur. Ceram. Soc.* **31**(1–2), 19–27 (2011)
19. S.V. Dorozhkin, Mechanism of solid-state conversion of non-stoichiometric hydroxyapatite to diphasic calcium phosphate. *Russ. Chem. Bull.* **52**(11), 2369–2375 (2003)

20. J. Marchi, P. Greil, J.C. Bressiani, A. Bressiani, F. Müller, Influence of synthesis conditions on the characteristics of biphasic calcium phosphate powders. *Int. J. Appl. Ceram. Technol.* **6**(1), 60–71 (2009)
21. G. Hannink, J.J.C. Arts, Bioresorbability, porosity and mechanical strength of bone substitutes: what is optimal for bone regeneration? *Injury* **42**, S22–S25 (2011)
22. S.J. Kalita, H.A. Bhatt, Nanocrystalline hydroxyapatite doped with magnesium and zinc: synthesis and characterization. *Mater. Sci. Eng. C* **27**(4), 837–848 (2007)
23. E. Landi, G. Logroscino, L. Proietti, A. Tampieri, M. Sandri, S. Sprio, Biomimetic Mg-substituted hydroxyapatite: from synthesis to in vivo behaviour. *J. Mater. Sci. Mater. Med.* **19**(1), 239–247 (2008)
24. A. Bigi, G. Falini, E. Foresti, A. Ripamonti, M. Gazzano, N. Roveri, Magnesium influence on hydroxyapatite crystallization. *J. Inorg. Biochem.* **49**(1), 69–78 (1993)
25. T.J. Webster, E.A. Massa-Schlueter, J.L. Smith, E.B. Slamovich, Osteoblast response to hydroxyapatite doped with divalent and trivalent cations. *Biomaterials* **25**(11), 2111–2121 (2004)
26. V. Stanić, S. Dimitrijević, J. Antić-Stanković, M. Mitrić, B. Jokić, I.B. Plečaš, S. Raičević, Synthesis, characterization and antimicrobial activity of copper and zinc-doped hydroxyapatite nanopowders. *Appl. Surf. Sci.* **256**(20), 6083–6089 (2010)

Performance of Carbon Nanotubes (CNT) Based Natural Rubber Composites: A Review

Rozaina Ismail, Azmi Ibrahim, Hanizah Ab. Hamid,
Mohamad Rusop Mahmood and Azlan Adnan

Abstract Carbon nanotubes (CNTs) are hollow cylinders of molecular-scale tubes of graphitic carbon with outstanding properties. They are possessed high strength, high stiffness and good electrical conductivity depending on their structure and diameter. This review outlines the performance of carbon nanotubes based on results of the author's research, essentially composites and describes the properties of carbon nanotube elastomeric composites. The Functionalization of CNTs and the applications of these materials are also discussed. The capability of carbon nanotubes to impart the conductivity to insulating elastomeric matrices has been clearly shown. Most markedly, this work has illustrated the performance encountered with the properties of CNT based Natural Rubber.

Keywords Performance · Multiwall carbon nanotubes (CNT) · Natural rubber (NR) · Elastomer · Composites

R. Ismail (✉) · A. Ibrahim · H.Ab. Hamid
Faculty of Civil Engineering, Universiti Teknologi MARA (UiTM),
Shah Alam, Selangor, Malaysia
e-mail: rozaina_fka_uitm@yahoo.com

A. Ibrahim
e-mail: azmii716@yahoo.com

H.Ab. Hamid
e-mail: hanizah_ah@yahoo.com

M.R. Mahmood
Faculty of Electrical Engineering, Universiti Teknologi MARA (UiTM),
Shah Alam, Selangor, Malaysia
e-mail: rusop@salam.uitm.edu.my

A. Adnan
Faculty of Civil Engineering, Universiti Teknologi Malaysia (UTM),
Skudai, Johor, Malaysia
e-mail: azelan_fka_utm@yahoo.com

1 Introduction

Basically, a carbon nanotube is a graphite sheet rolled into a cylinder of nanometer ($1 \text{ nm} = 10^{-6} \text{ m}$) diameter and up to several millimeters long. Carbon nanotubes (CNT) are hollow cylinders of carbon atoms. The armchair, zigzag, and chiral are three types of nanotubes which can be either a metal or a semi-conductor. They can be varied in the function due to the way they “roll up” and there are not in symmetrically position. The diameter of a carbon nanotube can be thinner than a human hair by 50,000 times. Compared to steel per unit weight, nanotube is stronger [1].

2 Structure of Carbon Nanotubes

The structure of CNTs affect the properties as well as electrical, mechanical, thermal, and optical conductivity.

There are many different types of nanotubes. The most common distinction is on the number of layers, so called walls. The term “carbon nanotubes” is used herein to denote nano-sized particulate forms of carbon, especially carbon nanotubes (CNTs), graphite nanofibers (GNFs) and/or carbon nanofibers (CNFs). The carbon nanotubes can be in a form of single-walled, double-walled and multi-walled nanotubes as shown in Fig. 1 [1].

3 Properties of Carbon Nanotubes

The properties of polymers with regards to their response to externally applied cyclical stresses, both are temperature and also time dependent. The Young’s modulus, elastic and viscous moduli, and glass transition temperature are the mechanical properties of the nanocomposites. The function of the magnetic field strengths is used to align the carbon nanotubes, are dependent on the epoxy system

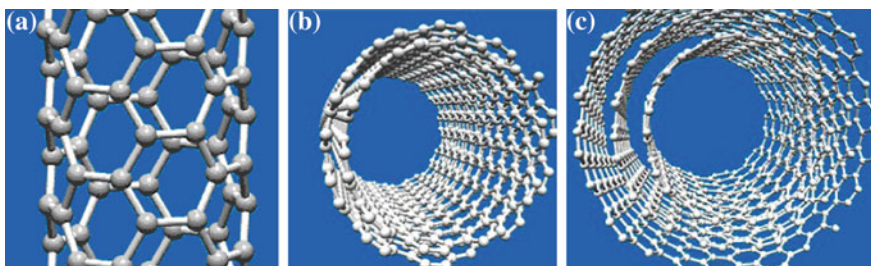


Fig. 1 Structure of **a** single-walled, **b** double-walled and **c** multi-walled nanotubes [1]

used. The properties of the resulting composites are superior to those that were not exposed to a magnetic field [2]. The imitated of the appearance of the CNTs properties would be used for energy storage demand as well for transmission of electrical energy. Though it is known that CNT's have high aspect ratio, Young's modulus over one terra pascal, Tensile strength of 200 GPa, these properties never remain the same for all the CNT'S [1].

3.1 Performance Properties of CNT Elastomer Composites

Incorporation of CNTs in polymer matrix changes the performance properties such as tensile strength, tensile modulus, elongation at break, toughness, dynamic mechanical thermal analysis (DMTA), etc. The phase morphology of the composite materials throws light on the properties of CNTs based polymer nanocomposite [3]. The reinforcement of elastomeric materials by addition of mineral fillers represents one of the most important aspects in the field of rubber science and technology. The true stress versus strain curves for unfilled natural rubber matrix and up to 8.3 wt% carbon nanotubes NR composites at 20 °C are represented in Fig. 2 [4].

The use of hybrid fillers (carbon nanotubes in addition to carbon black or silica, for example) has been shown to give promising results by promoting an enhancement of mechanical and electrical properties with regard to each single filler [5]. Bhattacharyya et al. [4] examined both experimentally and analytically, as shown in Figs. 3 and 4 by made use of the damping characteristics of the specimens with 0.5 and 1 wt% nanotube contents are. The damping ratio increases with strain to a certain value, and then decreases for further increases in the strain with the specimens with CNTs. It is found that the clear peaks in damping ratio

Fig. 2 Stress–strain curves for pure latex films and composites [4]

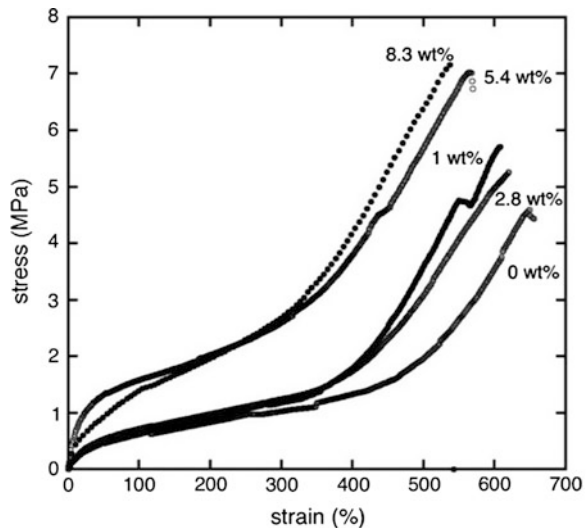


Fig. 3 Damping ratio of 0.5 wt% CNT specimen [4]

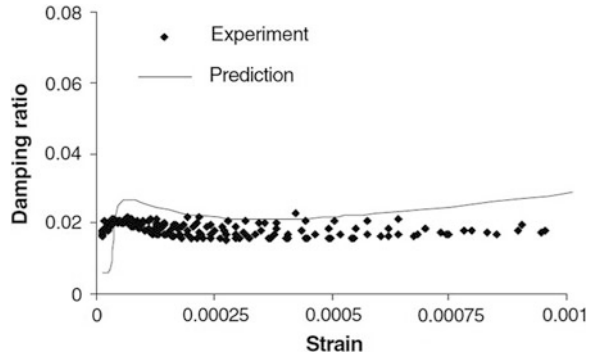
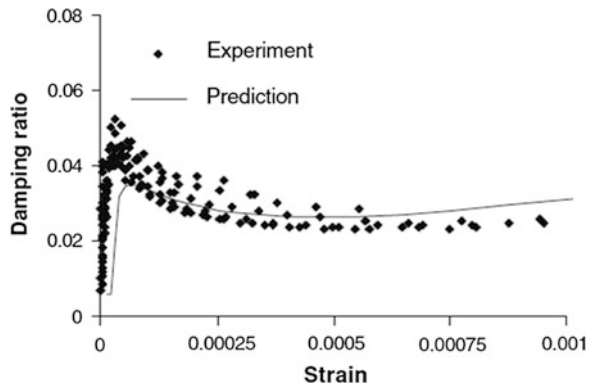


Fig. 4 Damping ratio of 1 wt % CNT specimen [6]



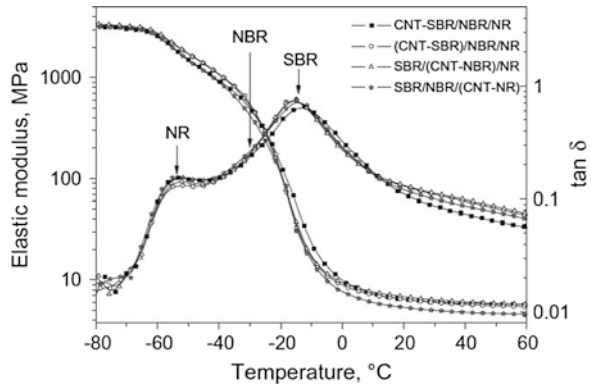
supporting the existence of a “stick-slip” motion between the resin and nanotubes. It can be seen that the nanotube weight ratio affects the damping ratio. The specimen with 1 wt% gives the higher maximum damping ratio compared to others specimen which contained the 0.5 wt%-specimen and the neat specimen [6].

3.2 Dynamic Properties of CNT Composites

Lee [8] introduced and improved the dynamic properties of laminated MWCNTA new concept for the optimization of dynamic behavior of laminated nanocomposites. The orientation of fiber in continuous fiber-reinforced composites was affected by replaced different wt% of carbon nanotubes (CNTs) in each layer [7]. The dynamic-mechanical behavior of the investigated blends does not differ from each other [8] (Fig. 5).

The dynamic mechanical properties of rubber composites filled with carbon nanotubes (CNTs) and various particle- sized carbon blacks (CB) was beneficial to improve performance of elastomer such as tire [9]. Arash et al. [11] was performed

Fig. 5 Dynamic-mechanical properties of four investigated blends [8]



the dynamic mechanical analysis in order to get information on the polymer–filler interface [10]. The dynamic mechanical thermal analysis (DMTA) test was conducted by evaluating the viscoelastic properties of composites multi walled carbon nanotube/epoxy at different weight fractions (0.1, 0.5 and 1 wt%). It is found that the composite has shown a good behavior [11].

3.3 Mechanical Properties of CNT Composites

Harris [12] has been driven a desire work on the preparation of nanotube/polymer composites to exploit the tubes' stiffness and strength. His study has also been focused on other properties, the ability of nanotubes to improve the mechanical characteristics of a polymer has often been a valuable added benefit [12]. It can be concluded that CNTs have shown a great reinforcement effect [13–16].

In the past decade, nano as a filler composites have attracted intense attention and study, involved the unique properties of nanostructures and potential to create new materials with great properties. The goal of nano-filler composite is to adjust and apply a matrix with nano sized particles. In order to make a new functional materials, this nano sized particles need a modification to the matrix texture by interaction with nano fillers during processing, especially with improved mechanical properties [1].

3.4 Resistance Properties of a Carbon Nanotube Network

Waris and Liu [17] stated that there are two types of resistances for the strain sensing phenomenon in a carbon nanotube network. There are the intrinsic resistance, R_{CNT} , and the intertube resistances. He review a CNTs-based piezoresistive strain sensors. The intertube resistances are divided into two types: the contact

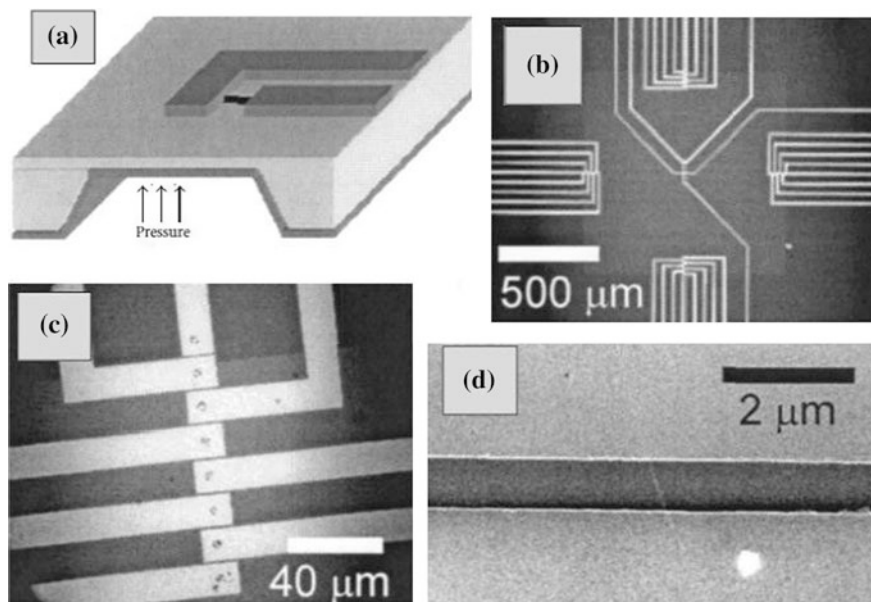


Fig. 6 **a** A single-walled carbon nanotube device on a membrane. **b** An optical image of the membrane with electrodes. **c** The devices are zoomed near the edge of the membrane, **d** SEM image [17]

resistance, R_C , (resistance between tubes that are physically in contact) and the tunneling resistance, R_T , (resistance between tubes that are separated by small gap) as shown in Fig. 6. The piezoresistive effects of a carbon nanotube network are primarily due to the modification in intrinsic resistance and intertube resistance [17].

4 Functionalization of CNTS

There are several comprehensive review papers that describe the chemistry of functionalized CNTs and the reaction mechanisms between the CNTs and functional groups. The dispersion of CNTs in the matrix and interfacial interactions between the CNTs and polymer will affect the performance of a CNTs nanocomposite. However, the aromatic nature of the bond caused the carbon atoms on CNTs walls chemically stable [18–23]. Peng [24] has reviewed the dispersion and the functionalization of CNTs for polymer-based nanocomposites. The current understanding of CNTs and CNT/polymer nanocomposites with two particular topics: (i) the principles and methods for CNTs dispersion and functionalization and (ii) the effects of CNTs due to dispersion and functionalization on the properties of CNTs/polymer nanocomposites.

5 Application of CNTS Composites

The advancement of the applied and basic science used to create innovative applications, performing biological safety evaluation that will encourage the social acceptance of CNTs, and the development of safe-controlled CNT structures are highly anticipated in the near future [25–27]. Battacharya et al. [28] carried out damping experiments which to validate the work which satisfactory correlations are found to exist between the theory and experiments in modeling and characterization of multiwall carbon nanotube reinforced polymer composites for damping applications. The sol-gel-derived multi-wall carbon nanotube/hydroxyapatite nanocomposite powders for bone substitution developed by [29] shows homogenous dispersion of nanotube in well-crystallized hydroxyapatite ceramic matrix [29].

6 Summary

This paper describes the review performance of carbon nanotubes based on results of the author's research, essentially elastomeric composites and describes the properties of carbon nanotube elastomeric composites. It describes about the advantage of and applications of CNT and finally some of the properties of CNT being mentioned and simulated the structure according to the structure. The capability of carbon nanotubes to impart conductivity to insulating elastomeric matrices has been clearly shown. In conclusion, this preliminary review in carbon nanotube-based elastomeric composites has demonstrated the potential of this new form of carbon as a reinforcing filler of rubber materials.

Acknowledgments The authors would like to acknowledge that this research has been carried out as part of a project RAGS funded by Ministry of Education (MOE) and support from Research Management Institute (RMI), Universiti Teknologi MARA (UiTM).

References

1. E.N. Ganesh, Single walled and multi walled carbon nanotube structure, synthesis and applications. *Int. J. Innovative Technol. Exploring Eng. (IJITEE)* **2**(4) (2013). ISSN: 2278-3075
2. E. Camponeschi, R. Vance, M. Al-Haik, H. Garmestani, R. Tannenbaum, Properties of carbon nanotube—polymer composites aligned in a magnetic field. *Carbon* **45**, 2037–2046 (2007)
3. B.F. Jogi, M. Sawant, M. Kulkarni, P.K. Brahmankar, Dispersion and performance properties of carbon nanotubes (CNTs) based polymer composites: a review. *J. Encapsul. Adsorpt. Sci.* **2**, 69–78 (2012)
4. S. Bhattacharyya, C. Sinturel, O. Bahloul, M.L. Saboungi, S. Thomas, J.P. Salvetat, Improving reinforcement of natural rubber by networking of activated carbon nanotubes. *Carbon* **46**, 1037–1045 (2008)

5. Liliane Bokobza, Elastomeric composites based on nanospherical particles and carbon nanotubes: a comparative study. *Rubber Chem. Technol.* **86**(3), 423–448 (2013)
6. X. Zhou, E. Shin, K.W. Wang, C.E. Bakis, Interfacial damping characteristics of carbon nanotube-based composites. *Compos. Sci. Technol.* **64**, 2425–2437 (2004)
7. H. Rokni, A.S. Milani, R.J. Seethaler, K. Stoeffler, Improvement in dynamic properties of laminated MWCNT-polystyrene composite beams via an integrated numerical–experimental approach. *Compos. Struct.* **94**, 2538–2547 (2012)
8. H.H. Le, M.N. Sriharish, S. Henning, J. Klehm, M. Menzel, W. Frank, S. Wießner, A. Das, K.-W. Stöckelhuber, G. Heinrich, H.-J. Radsch, Dispersion and distribution of carbon nanotubes in ternary rubber blends. *Compos. Sci. Technol.* **90**, 180–186 (2014)
9. W. Zepeng, Experimental study on property of rubber composites filled with carbon nanotubes. *Adv. Mater. Res.* **87–88**, 110–115 (2010)
10. M. Kolodziej, L. Bokobza, J.L. Bruneel. Investigations on natural rubber filled with multiwall carbon nanotubes. *Compos. Interfaces* **14**(3), 215–228 (2007)
11. A. Montazeri, A. Khavandi, J. Javadpour, A. Tcharkhtchi, Viscoelastic properties of multi walled carbon nanotube/epoxy composites at the different nanotube content. *J. Nano Res.* **13**, 33–39 (2011)
12. P.J.F. Harris, Carbon nanotube composites. *Int. Mater. Rev.* **49**(1), 31–43 (2004)
13. D. Yue, Y. Liu, Z. Shen, Study on preparation and properties of carbon nanotubes/rubber composites. *J. Mater. Sci.* **41**, 2541–2544 (2006)
14. I.T. Kim, A. Tannenbaum, R. Tannenbaum, Anisotropic conductivity of magnetic carbon nanotubes embedded in epoxy matrices. *Carbon* **49**, 54–61 (2011)
15. G. Sui, W.H. Zhong, X.P. Yang, Y.H. Yu, S.H. Zhao. Preparation and properties of natural rubber composites reinforced with pretreated carbon nanotubes. *Polym. Adv. Technol.* **19**, 1543–1549 (2008)
16. S.H. Ahmad, M.A. Tarawneh, S.Y. Yahya, R. Rasid. Reinforced thermoplastic natural rubber (tpnr) composites with different types of carbon nanotubes (MWNTS), Chapter 21, in *Nanotechnology and Nanomaterials* (2011). ISBN 978-953-307-497-9
17. W. Obitayo, T. Liu. A review: carbon nanotube-based piezoresistive strain sensors. *J. Sens.* **2012**, 15 (2012) (Article ID 652438)
18. C.A. Mitchell, J.L. Bahr, Sivaram Arepalli, J.M. Tour, R. Krishnamoorti, Dispersion of functionalized carbon nanotubes in polystyrene. *Macromolecules* **35**, 8825–8830 (2002)
19. X.L. Xie, Y.W. Mai, X.P. Zhou, Dispersion and alignment of carbon nanotubes in polymer matrix: a review. *Mater. Sci. Eng. R* **49**, 89–112 (2005)
20. S. Xin, Y. Shuai, Z. Guo, Y. Feng, Functionalization of multi-walled carbon nanotubes with thermo-responsive azide- terminated poly(N-isopropylacrylamide) via click reactions. *Molecules* **2013**(18), 4599–4612 (2013)
21. G. Clave, G. Delpont, C. Roquelet, J.S. Lauret, E. Deleporte, F. Vialla, B. Langlois, R. Parret, C. Voisin, P. Roussignol, B. Jousselman, A. Gloter, O. Stephan, A. Filoramo, V. Derycke, S. Campidelli, Functionalization of carbon nanotubes through polymerization in micelles: a bridge between the covalent and noncovalent methods. *Chem. Mater.* **25**, 2700–2707 (2013)
22. M. Assali, M.P. Leal, I. Fernandez, N. Khier. Synthesis and non-covalent functionalization of carbon nanotubes rings: new nanomaterials with lectin affinity. *Nanotechnology* **24**, 085604 (12 pp) (2013)
23. D. Wang, Y. Huang, W. Cai, M. Tian, P. Liu, Y. Zhang, Functionalized multi-wall carbon nanotubes/silicone rubber composite as capacitive humidity sensor. *J. Appl. Polym. Sci.* **131**, 40342 (2014)
24. P.C. Ma, N.A. Siddiqui, G. Marom, J.K. Kim, Dispersion and functionalization of carbon nanotubes for polymer-based nanocomposites: a review. *Composites: Part A* **41**, 1345–1367 (2010)
25. K. Takeuchi, T. Hayashi, Y.A. Kim, K. Fujisawa, M. Endo, The State-of-the-art science and applications of carbon nanotubes. *Nanosyst. Phys. Chem. Math.* **5**(1), 15–24 (2014)
26. L. Bokobza, Multiwall carbon nanotube elastomeric composites: a review. *Polymer* **48**, 4907–4920 (2007)

27. S. Pande, A. Chaudhary, D. Patel, B.P. Singh, R.B. Mathur. Mechanical and electrical properties of multiwall carbon nanotube/polycarbonate composites for electrostatic discharge and electromagnetic interference shielding applications. *RSC Adv.* **2014**(4), 13839 (2014)
28. S. Bhattacharya, A. Alva, S. Raja, (2014). Modeling and characterization of multiwall carbon nanotube reinforced polymer composites for damping applications. *Int. J. Comput. Methods Eng. Sci. Mech.* **15**(3), 258–264 (2014)
29. T. Hooshmand, A. Abrishamchian, F. Najafi, M. Mohammadi, H. Najafi, M. Tahriri, Development of sol-gel-derived multi-wall carbon nanotube/hydroxyapatite nanocomposite powders for bone substitution. *J. Compos. Mater.* **48**(4), 483–489 (2014)

Nano Filler Reinforced Intumescent Fire Retardant Coating for Protection of Structural Steel

Hammad Aziz, Faiz Ahmad and M. Zia-ul-Mustafa

Abstract This paper described the effect of reinforcement of an inorganic nano filler in intumescent fire retardant coating (IFRC). In this study, intumescent coating contained phosphorous, nitrogen and boron based compounds. Four formulations were developed in order to determine the thermal protective performance of coating. Furnace test was conducted to find out the intumescent factor. Bunsen burner test was conducted according to ASTM E-119 for thermal insulation of the coating. Further, char morphology and microstructure of char was examined by using field emission scanning electron microscopy. Fourier transform infrared spectroscopy was performed to confirm the chemical functional groups present in the char. Thermogravimetric analysis was carried out to determine the residual weight/thermal stability of coating. Tests revealed that coating containing 1.0 wt% of nano alumina as an inorganic filler provides better fire protection, char morphology and anti-oxidation property as compared to coating without containing nano alumina.

Keywords Nano filler · Fire protection · Char morphology · Chemical functional groups

1 Introduction

Structural steel is extensively used in construction sector like buildings, bridges, offshore and onshore structures, maritime applications etc. Indeed, it is an important part of any construction industry. The integrity and load bearing ability of structural

H. Aziz (✉) · F. Ahmad · M. Zia-ul-Mustafa
Department of Mechanical Engineering, Universiti Teknologi PETRONAS,
Bandar Seri Iskandar, 31750 Tronoh, Perak, Malaysia
e-mail: engr.hammad.aziz03@gmail.com

F. Ahmad
e-mail: faizahmad@petronas.com.my

steel starts to decline when the temperature reaches to its critical temperature (500–550 °C) [1–3]. This is because of high thermal expansion of steel that leads to thermal movement in other parts of the structure.

Two types of fire protection system are used such as active and passive fire protection system. Intumescent fire retardant coating (IFRC) being passive fire protection system has gained extensive recognition in the world. It is one of the easiest ways of protecting structural steel from fire. Besides protecting structural steel [4], it offered more than a few advantages like it does not change the intrinsic properties of the material [5], can be easily applied on various materials like metals, wood, textiles, polymers [6–8] etc. In case of fire, safe evacuation of the workers from the site is the major requirement set by the building regulations in most of the countries like UK, USA and Europe.

Intumescent stems from the word “intumescence” signify swelling of the substance in case of fire. IFRC forms on heating an expanded multi-cellular char layer with thickness superior then the original thickness of the coating [9, 10]. Conventional fire retardant coatings were based upon ammonium polyphosphate as an acid source, pentaerythritol as a carbon source and melamine as a blowing agent. Their fire performance and anti-oxidation property was poor at high temperature leading to the underlying material unprotected [11]. Expandable graphite was used as synergistic agent in order to enhance the anti-oxidation property of the conventional fire retardant coating [11, 12]. Various types of flame retardant fillers such as aluminum trihydroxide and magnesium hydroxide were used that gives off water vapors upon heating. These fillers were used in very high amount that ultimately destroy properties of polymers [13].

Mohamad et al. [14] had used alumina as mineral filler in an epoxy based formulation. Bigger cell size was achieved with residual weight 31.6 % by using 3 wt% of filler.

Recently, nano filler based coating has gained a lot of attention due to its simplicity, cost effectiveness and used in very small amount. Nano-coatings reveals excellent properties as compared to conventional fire retardant coating with micron size filler [15].

The flame retardancy was enhanced by using 2 wt% of halloysite nano tube (HNT) in the polymer. Higher wt% of HNT will lead to negative effect with decreased flame retardancy [16].

In this work, an epoxy based nano intumescent coating was developed by reinforcing with nano alumina as inorganic filler with expandable graphite as carbon source. Their effect on thermal insulation, char expansion, char morphology and anti-oxidation property was investigated.

2 Research Methodology

2.1 Materials

Ammonium polyphosphate (APP-acid source) containing 20 % phosphorus was purchased from Clariant Malaysia Sdn. Bhd. Expandable graphite (EG-carbon source) was purchased from Kaiyu Industrial (Hong Kong) Lts, China. Melamine (MEL-blowing agent) was purchased from SABIC KSA. Boric acid (BA-flame retardant additive) was purchased from Merck Malaysia Sdn. Bhd. Alumina having particle size 20–30 nm (Al_2O_3 -inorganic filler) was purchased from Dong Yang (HK) Int'l Group Ltd. Bisphenol A BE-188 (BPA-epoxy binder) with tetraethylene tetramine H-4014 (curing agent) was purchased from ACR tech. Taiwan.

2.2 Preparation of IFRC

First of all APP, MEL and BA were ground together using ROCKLAB grinder for 1 min. Nano alumina was placed in an oven at 60 °C for 2 h to remove any moisture contents present in filler. Adding epoxy resin with all ground material, EG and nano alumina were mixed using shear mixture at 40–45 rpm for 15–20 min. Further, curing agent was added and mixed for another 10–15 min at 40–45 rpm until uniform dispersion achieved. Finally, the coating was then applied on steel substrate of dimensions (100 mm × 100 mm × 1.25 mm) and (50 mm × 50 mm × 1.25 mm) for bunsen burner and furnace test respectively. The thickness of coating was measured using PosiTector 6,000 coating thickness measuring gauge and it was 1.5–2.0 mm. Table 1 showed the chemical composition of different formulations studied.

Table 1 Intumescent coating formulations

Intumescent formulations	Ingredients (wt%)
IF1 (control)	APP = 11.14, EG = 5.57, MEL = 5.57, BA = 11.14, epoxy resin = 66.58
IF2	IF1 + 0.5 nano alumina
IF3	IF1 + 1.0 nano alumina
IF4	IF1 + 1.5 nano alumina

2.3 Preparation of Substrate

The steel substrate of required dimensions was cut using shear cutting machine. After cutting, samples were subjected to sand blasting to remove any dust particles and to clean the surface in order to provide better adhesion of the coating with structural steel substrate.

3 Characterization Techniques

3.1 Furnace Test

Furnace test was conducted using Carbolite CWF laboratory furnace having chamber volume 13 l to investigate the char expansion. The heating rate was 20 °C/min. Furnace test was divided into three segments. During first segment samples were heated to 500 °C at respective heating rate. After that dwell time was 60 min in order to ensure complete burning of coating. In third and final segment samples were quenched to room temperature. The resultant char was then analyzed physically.

3.2 Bunsen Burner Test

Small scale bunsen burner test was conducted using portable burner QPlus manufactured in Korea having gas flow rate 105 g/h. The temperature of flame used was mimicking to ASTM E-119 fire curve to determine the fire performance. Three K-type thermocouples were attached to unexposed face of the steel substrate while other end of thermocouples was attached to ANARITSU AM8000 data logger. The distance between the burner head and coated surface was 7 cm. The temperature recorded on the unexposed side of the steel substrate after every min using thermocouples known as backside temperature. Temperature of flame was also recorded by using K-type thermocouple. The schematic diagram for bunsen burner test is shown in Fig. 1.

3.3 Field Emission Scanning Electron Microscopy (FESEM)

The char morphology and microstructure of char obtained after fire test was examined using variable pressure FESEM SUPRA 55VP, manufactured by Carl Zeiss A.G., Germany. The working voltage was 4–5 kV. The system vacuum varied from 3.00e-005 to 2.00e-005 mbar.

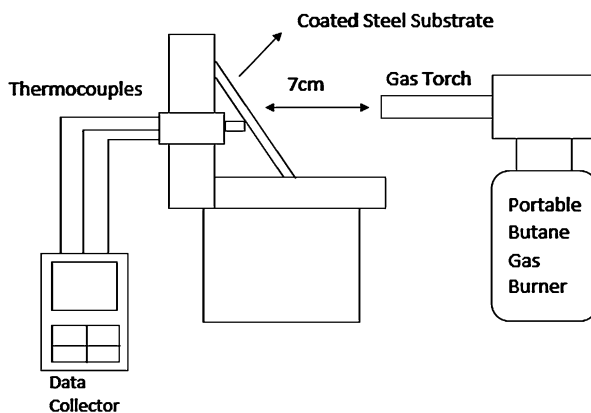


Fig. 1 Schematic diagram for thermal insulation test

3.4 Thermogravimetric Analysis (TGA)

TGA analysis was carried out at heating rate of 10 °C/min under N₂ over 30–800 °C by using Perkin-Elmer TGA Q50 and data was recorded with the help of pyris data analyzer.

3.5 Fourier Transform Infrared Spectroscopy (FTIR)

The chemical functional groups presents in the char was analyzed by using a spectrum one manufactured by Perkin Elmer Inc. in the range of 4000–400 cm⁻¹.

4 Results and Discussions

4.1 Furnace Test

Furnace test was conducted for 2 h to investigate the physical structure and intumescent factor. After 2 h the samples were taken out from furnace. Intumescent coating was converted into expanded multi-cellular char with thickness better than the original coating thickness. Physical structure of IF1 was poor while some part of char was detached from the substrate with cracks were observed on the outer surface of the char. After modification of IF1 with nano alumina, physical structure of char was improved and optimized for IF3 i.e. 1 wt% of nano alumina. Above optimum level of nano size alumina, bigger cracks were observed. Intumescent factor (I) [17] defined in (1), where d_0 is the thickness of the substrate, d_1 is the total

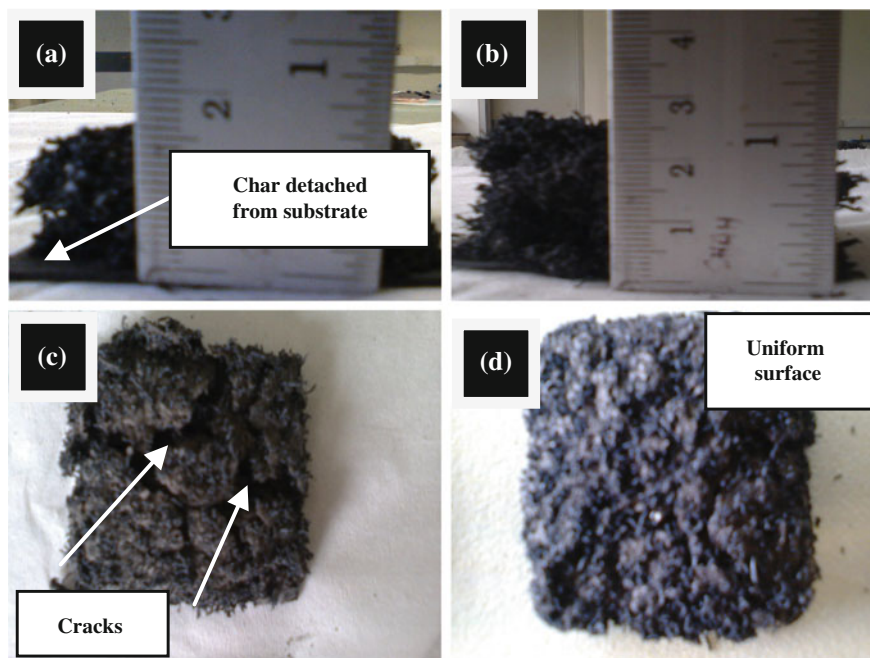


Fig. 2 Char after furnace test, a IF1, b IF3, c IF1 and d IF3

thickness of coating including substrate and d_2 is the final thickness after furnace test. Figure 2 shows the char obtained after furnace test for IF1 and IF3 with scale and their outer surface. IF1 had less expansion compared to IF3.

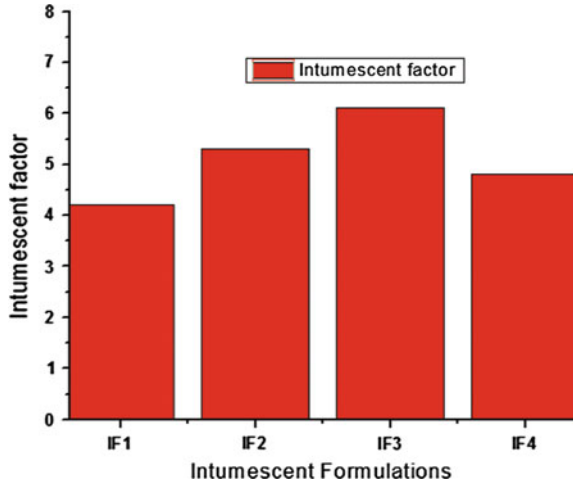
$$I = (d_2 - d_0) / (d_1 - d_0) \quad (1)$$

Figure 3 shows the intumescent factor for different formulations studied. By adding nano size filler the intumescent factor was increased and optimize at 1.0 wt% of nano alumina. Above this value “I” was decreased as for IF4.

4.2 Bunsen Burner Test

Bunsen burner test was conducted using portable gas burner. Mean backside substrate temperature for IF1 after 1 h was 265.4 °C. Initially the temperature of coating was started to rise but after the intumescence takes place temperature remained constant for approximately 20 min. The integrity of char obtained from IF1 was poor and it did not conserve the thermal insulation for longer time possibly due to absence of nano filler. Char was easily oxidized at the point where the flame was stagnant with a small hole formed at that area. When the coating was modified

Fig. 3 Intumescent factor of formulations



by nano size alumina, the insulation time was increased while only small area of char oxidized. It is possible that nano size filler was migrated on to the top surface of coating due to its large surface area and formed non-deformable ceramic layer that protects the substrate for longer time. Figure 4 showed the char obtained after bunsen burner test for IF1 and IF3. The final backside temperature for IF2, IF3 and IF4 was 153.7, 102.5 and 310.4 °C as shown in Fig. 5. High amount of nano filler hindered the expansion to take place provides negative effect on the protective performance of the coating. Inorganic nano filler limits the diffusion of oxygen to the structural steel substrate. But too high content of inorganic filler obstructs the fused carbonaceous material from swelling through “lamp wick” effect (high wt% of nano particles forms intense cross-linking network that prevents amine and carbon dioxide gases from swelling), hinders the melt flowing leading to negative effect on fire protective performance and it may even exceed to the positive effect of fire protection [18].

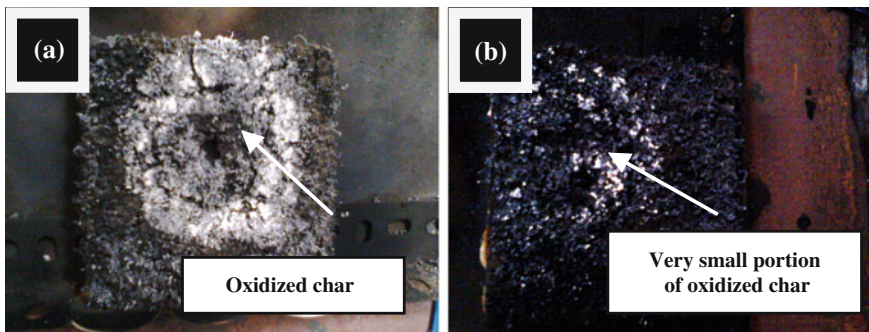
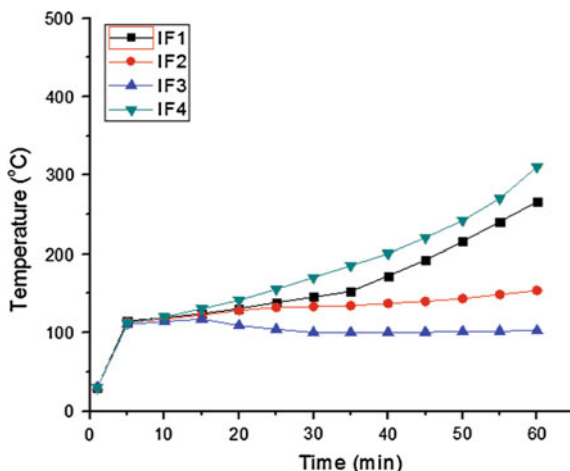


Fig. 4 Char obtained after 1 h of fire test, **a** IF1, **b** IF3

Fig. 5 Backside substrate temperature versus time



4.3 Field Emission Scanning Electron Microscopy (FESEM)

The char morphology was an important factor in order to investigate the thermal efficiency of char. Uneven, non-uniform and loose microstructure of char was observed for IF1 with cracks. These cracks helped in penetrating the heat of flame inside to the underlying material. IF3 containing 1.0 wt% of nano size filler had worm like outer surface due to expansion of EG. This was helpful because it provide thermal resistance of char. The inner surface of char had dense, continuous, and uniform honey comb like structure with an average cell size diameter 11 μm . Large cracks were observed for IF4 with cell size about 200 μm . These cracks reduced the thermal efficiency or integrity of char by allowing the heat of flame to penetrate inside to underlying material [17]. IF3 had good microstructure apart from thermal insulation and it was optimized at 1.0 wt% of nano alumina filler as shown in Fig. 6.

4.4 Thermogravimetric Analysis (TGA)

In the intumescent materials, there are four different degradation stages despite of the composition of the coating. Different degradation stages are named as melting, intumescence, char formation and char degradation [19] and these occurred at temperature ranges from (0 to 200°C), (200 to 300°C), (300 to 450°C) and (450 to 800°C) respectively. During first stage 10–15 % of weight loss was occurred due to melting and degradation of the polymer matrix. Unvolatilized solvent and small molecules of the polymer were responsible for weight loss at this stage [20]. Boric acid had two steps thermal degradation. During the first step 100–140 °C, it was dehydrated into metaboric acid. During the second step 140–180 °C, metaboric acid

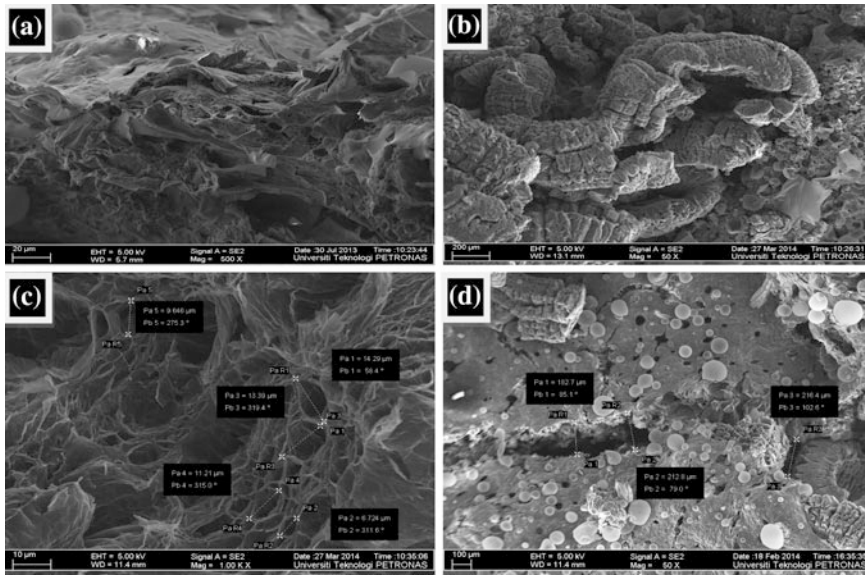


Fig. 6 Microstructure of char, a IF1, b, c IF3 and d IF4

was dehydrated into boron oxide [5]. Huang et al. [21] introduced the term onset temperature “ T_{onset} ”, temperature at which 5 % of weight loss occurred. Formulation without containing nano size filler had low T_{onset} i.e. 99 °C while for formulation containing 1.0 wt% nano alumina had high T_{onset} i.e. 120 °C. It illustrates that by addition of nano size filler; T_{onset} increased and it delays the thermal degradation of coating. During second stage 5–10 % of weight loss was occurred. APP began to degrade above 210 °C by releasing amine gases such as ammonia and converted into phosphoric acid. EG began to decompose above 200 °C by liberating carbon dioxide and sulfur dioxide gas. Melamine began to decompose in this stage by releasing non-flammable gases like ammonia and carbon dioxide. During third stage 25–35 % of weight loss was taken place due to further degradation of intumescent material to form char. Melamine was degraded at 280–370 °C by forming a carbon like foamed layer onto the substrate [20]. Boron phosphate was formed in this stage due to reaction between the phosphoric acid and boron oxide [5]. In the final stage, char layer was degraded with only inorganic material remained. Final residual weight at 800 °C for IF1, IF2, IF3 and IF4 was 29.008, 38.302, 42.034 and 23.622 % respectively as shown in Fig. 7. It was noted that the coating without containing nano alumina has higher weight loss in this stage i.e. 21 % which starts decreasing by adding nano size filler while for formulation containing 1.0 wt% nano alumina has 15 %. It was concluded that nano size filler increases the onset temperature and also enhanced the residual weight. Higher residual weight means higher thermal stability of coating at higher temperature or higher anti-oxidation degree [11, 22]. Char was stable at higher temperature compared to formulation

Fig. 7 TGA curves for formulations studied

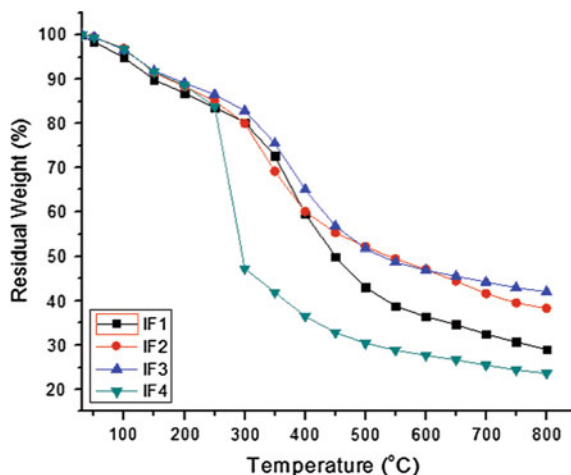


Table 2 Residual weight at different temperature

Formulations	Residual weight (wt%)		
	500 °C	650 °C	800 °C
IF1 (control)	43.062	34.958	29.008
IF2 (0.5 %)	52.131	44.459	38.302
IF3 (1.0 %)	53.121	46.783	42.034
IF4 (1.5 %)	30.447	26.641	23.622

without containing nano alumina. Table 2 showed the residual weight of formulations at different temperatures.

4.5 Fourier Transform Infrared Spectroscopy (FTIR)

FTIR spectrum was performed to investigate the chemical functional groups present in the char. Due to high thermal insulation of IF3, it was only considered for comparison with control formulation i.e. IF1 for FTIR spectra. The bending peak at 3435.07 cm^{-1} was assigned to O-H hydroxyl group due to the decomposition of epoxy resin. The weak bending peak at 2260.80 cm^{-1} represented the (-CH₃-CH₂-) of cured epoxy resin [23]. Two bending peaks at 1607.56 and 1403.50 cm^{-1} represented (C=O) and (C=C) due to amorphous carbon which is the microcrystal of graphite and amino groups due to (APP and MEL) respectively [20, 24]. (P-O-P) region was present from $1400\text{--}800\text{ cm}^{-1}$ [25]. The absorption peak at 1191.51 cm^{-1} was assigned to P=O bond in the APP [17]. The bending peaks at 1085.61 and 932.81 cm^{-1} were representing the (P-O-P) group. Two bending peaks at 623.67 and 548.19 cm^{-1} represented the (B-O-P) group due to the formation of boron

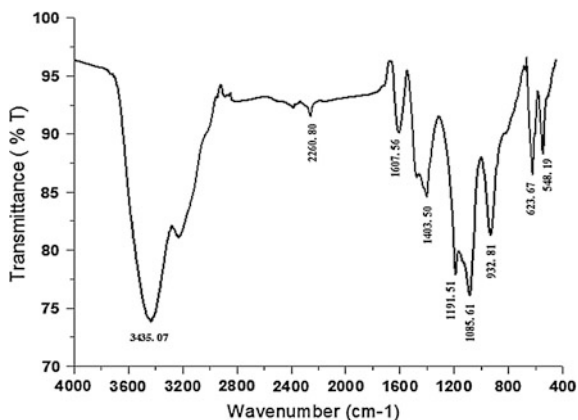


Fig. 8 IR spectra for IF1

phosphate. It can be seen that the intumescent char was mainly composed of phosphate based compounds as shown in Fig. 8.

The peaks for IF3 were identical with the IF1 due to presence of common ingredients like acid source, carbon source, blowing agent and flame retardant additive as shown in Fig. 9. The bending peak at 3215.37 cm^{-1} corresponded to the hydroxyl group (O-H) due to decomposition of an epoxy resin. The T_{onset} for IF3 was higher as compared to control formulation. The weak bending peak at 2261.30 cm^{-1} represented the (-CH₃-CH₂-) of cured epoxy resin [23]. Two bending peaks at 1620.80 and 1454.98 cm^{-1} represented (C=C) due to amorphous carbon which is the microcrystal of graphite and amino groups due to (APP and MEL) respectively [20, 24]. The bending peak at 1620.84 cm^{-1} was represented the C=O bond. It can be seen that the intensity of C=O bond was lowered than the control formulation. High intensity of C=O signifies the oxidation degree of intumescent char layer [26]. But after reinforcement with nano alumina as inorganic filler, the anti-oxidation degree was enhanced implies that the intumescent char can sustain at higher temperature. But for control formulation, intumescent char was not sustained at higher temperature instead it being converted into gases and escape out. (P-O-P) region was present from 1400 to 800 cm^{-1} [25]. The absorption peak at 1198 cm^{-1} was assigned to P=O bond present in APP [17]. The bending peaks at 1090.85 and at 933.48 cm^{-1} were representing the (P-O-P) group. The bending peak at 624.97 cm^{-1} represented the (B-O-P) group due to the formation of boron phosphate. The peak at 550.65 cm^{-1} represented the Al-O group due to the presence of nano alumina. The char containing C=C, P=O and P-O-P was more stable and have high decomposition temperature [27].

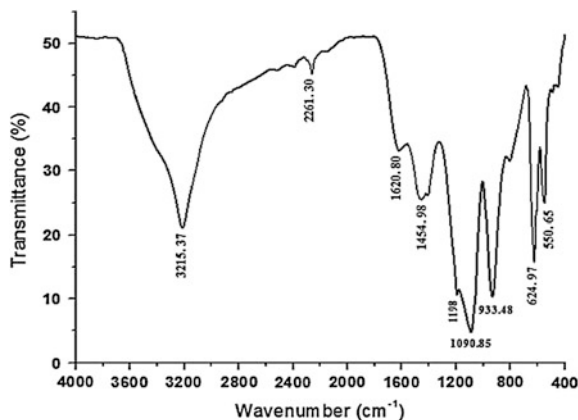


Fig. 9 IR spectra for IF3

5 Conclusion

The research work described the thermal performance of halogen free intumescent fire retardant coating with and without containing nano size alumina in order to protect the structural steel from fire. Furnace test showed that by increasing the wt% of nano alumina, intumescent factor was increased up to certain limit i.e. 1.0 wt% but after that it started to decline due to lamp wick effect. Thermal insulation test showed that coating without any nano alumina filler had mean backside temperature of steel substrate 265.4 °C while for IF3 was only 102.5 °C after 1 h. FESEM results described that the IF1 had uneven and non-uniform char structure with bigger cell size diameter while for IF3 worm like outer surface, honey comb like inner structure which was continuous and multi-porous preventing the heat of flame to penetrate inside to the underlying material. TGA results showed that by increasing the wt% of nano alumina, the residual weight was enhanced up to 1.0 wt% of nano alumina. Residual weight was enhanced up to 45 % compared with coating without nano-size filler which improves the anti-oxidation property of the char at high temperature. FTIR results showed that the intensity of C=O was decreased by reinforcing nano alumina in the control formulation. Thermal performance, microstructure and anti-oxidation degree of char was enhanced by modification with nano alumina and it was optimized at 1 wt% of nano alumina.

Acknowledgments The author acknowledges the facilities and materials provided by Universiti Teknologi PETRONAS, Malaysia in order to carry out this research work.

References

1. M. Jimenez, S. Duquesne, S. Bourbigot, Characterization of the performance of an intumescent fire protective coating. *Surf. Coat. Technol.* **201**, 979–987 (2006)
2. M.C. Yew, N. Ramli Sulong, Fire-resistive performance of intumescent flame-retardant coatings for steel. *Mater. Des.* **34**, 719–724 (2012)
3. H. Aziz, F. Ahmad, M. Zia-ul-Mustafa, Effect of titanium oxide on fire performance of intumescent fire retardant coating. *Adv. Mater. Res.* **935**, 224–228 (2014)
4. S. Duquesne, P. Bachelet, S. Bellayer, S. Bourbigot, W. Mertens, Influence of inorganic fillers on the fire protection of intumescent coatings. *J. Fire Sci.* **31**, 258–275 (2013)
5. M. Jimenez, S. Duquesne, S. Bourbigot, Intumescent fire protective coating: toward a better understanding of their mechanism of action. *Thermochim. Acta* **449**, 16–26 (2006)
6. L. Yang, F. Liu, E. Han, Effects of P/B on the properties of anticorrosive coatings with different particle size. *Prog. Org. Coat.* **53**, 91–98 (2005)
7. X. Almeras, M. Le Bras, P. Hornsby, S. Bourbigot, G. Marosi, S. Keszei, F. Poutch, Effect of fillers on the fire retardancy of intumescent polypropylene compounds. *Polym. Degrad. Stab.* **82**, 325–331 (2003)
8. F. Wang, Z. Zhang, Q. Wang, J. Tang, Fire-retardant and smoke-suppressant performance of an intumescent waterborne amino-resin fire-retardant coating for wood. *Front. Forestry China* **3**, 487–492 (2008)
9. S.V. Levchik, E.D. Weil, A review of recent progress in phosphorus-based flame retardants. *J. Fire Sci.* **24**, 345–364 (2006)
10. H. Aziz, P.S.M. Binti Megat Yusoff, M. Zia-ul-Mustafa, Effect of kaolin clay and alumina on thermal performance and char morphology of intumescent fire retardant coating. *MATEC Web of Conferences*, vol. 13 (2014), p. 04013
11. G. Li, G. Liang, T. He, Q. Yang, X. Song, Effects of EG and MoSi₂ on thermal degradation of intumescent coating. *Polym. Degrad. Stab.* **92**, 569–579 (2007)
12. G. Li, J. Yang, T. He, Y. Wu, G. Liang, An investigation of the thermal degradation of the intumescent coating containing MoO₃ and Fe₂O₃. *Surf. Coat. Technol.* **202**, 3121–3128 (2008)
13. C.A. Wilkie, A.B. Morgan, *Fire Retardancy of Polymeric Materials* (CRC Press, Boca Raton, 2012)
14. W.F. Mohamad, F. Ahmad, S. Ullah, Effect of inorganic fillers on thermal performance and char morphology of intumescent fire retardant coating. *Asian J. Sci. Res.* **6**, 263–271 (2013)
15. Z. Wang, E. Han, W. Ke, An investigation into fire protection and water resistance of intumescent nano-coatings. *Surf. Coat. Technol.* **201**, 1528–1535 (2006)
16. J. Zhao, C.L. Deng, S.L. Du, L. Chen, C. Deng, Y.Z. Wang, Synergistic flame-retardant effect of halloysite nanotubes on intumescent flame retardant in LDPE. *J. Appl. Polymer Sci.* **131** (2014)
17. G. Wang, J. Yang, Influences of glass flakes on fire protection and water resistance of waterborne intumescent fire resistive coating for steel structure. *Prog. Org. Coat.* **70**, 150–156 (2011)
18. Z. Wang, E. Han, W. Ke, Fire-resistant effect of nanoclay on intumescent nanocomposite coatings. *J. Appl. Polymer Sci.* **103**, 1681–1689 (2007)
19. G.J. Griffin, A.D. Bicknell, T.J. Brown, Studies on the effect of atmospheric oxygen content on the thermal resistance of intumescent, fire-retardant coatings. *J. Fire Sci.* **23**, 303–328 (2005)
20. Z. Wang, E. Han, W. Ke, Influence of nano-LDHs on char formation and fire-resistant properties of flame-retardant coating. *Prog. Org. Coat.* **53**, 29–37 (2005)
21. G. Huang, S. Wang, Pa Song, C. Wu, S. Chen, X. Wang, Combination effect of carbon nanotubes with graphene on intumescent flame-retardant polypropylene nanocomposites. *Compos. Part A Appl. Sci. Manuf.* **59**, 18–25 (2014)
22. G. Wang, Y. Wang, J. Yang, Influences of polymerization degree of ammonium polyphosphate on fire protection of waterborne intumescent fire resistive coating. *Surf. Coat. Technol.* **206**, 2275–2280 (2012)

23. S. Ullah, F. Ahmad, P. Megat-Yusoff, Effect of boric acid and melamine on the intumescent fire-retardant coating composition for the fire protection of structural steel substrates. *J. Appl. Polym. Sci.* **128**, 2983–2993 (2013)
24. S. Ullah, F. Ahmad, Effects of zirconium silicate reinforcement on expandable graphite based intumescent fire retardant coating. *Polym. Degrad. Stab.* **103**, 49–62 (2014)
25. S. Bourbigot, M. Le Bras, R. Delobel, J.-M. Trémillon, Synergistic effect of zeolite in an intumescence process. Study of the interactions between the polymer and the additives. *J. Chem. Soc. Faraday Trans.* **92**, 3435–3444 (1996)
26. Y. Dong, G. Wang Influence of nano-boron nitride on fire protection of waterborne fire-resistive coatings. *J. Coat. Technol. Res.*, 1–8
27. F. Fan, Z. Xia, Q. Li, Z. Li, H. Chen, Thermal stability of phosphorus-containing styrene-acrylic copolymer and its fire retardant performance in waterborne intumescent coatings. *J. Therm. Anal. Calorim.* **114**, 937–946 (2013)

Deposition Behavior of Titanium Dioxide Nanoparticles During Electrophoretic Deposition: Effect on Particle Size

Norain Ramli and Noorsuhana Mohd Yusof

Abstract The purpose of this research are to investigate the deposition behavior of different sized nanoparticle using pulse DC in EPD and to study the effect of particle size reduction on crack formation of TiO₂ deposited layer. EPD is one of the electrokinetics phenomenons acted as the motion of charged particles in a liquid medium under the influence of an electric field and the deposition on the surface of a substrate with an opposite charge (Naim et al. in *Colloids Surf A* 360:13–19, 2010 [1]). EPD can be prepared in aqueous or non-aqueous solutions. Four different sizes of TiO₂ nanoparticle suspension were used in order to observe the effect of particles size on deposition. The zeta potential was measured with Zetasizer-NanoSeries, Malvern. Increasing the suspensions concentration influence the zeta potential values to change as well. The deposited layer upon drying was observed by FESEM.

Keywords Titanium dioxide nanoparticle • Particles size • Colloidal stability

1 Introduction

Titanium is a metal element of group IVB that has a melting point of 1,675 °C and an atomic weight of 47.90 g/mole. It has high strength to density ratio and inertness to many corrosive environments. Its principle use is as TiO₂ as paint filler in paint and pigments. The whiteness and high refractive index of TiO₂ are unequaled for whitening paints, paper, rubber, plastics and other materials. A small amount of mineral grade TiO₂ is used in fluxes and ceramics.

N. Ramli (✉) · N. Mohd Yusof
Faculty of Chemical Engineering, Universiti Teknologi MARA (UiTM),
Shah Alam, Malaysia
e-mail: norainramli@yahoo.com

N. Mohd Yusof
e-mail: noorsuhana@salam.uitm.edu.my

Recently, electrophoretic deposition (EPD) technique has been used for the fabrication of thin films and coatings. EPD technique offers many processing advantages for the deposition of TiO₂ films, such as high deposition rate, low cost of equipment and possibility of uniform deposition on substrates of complex shape [2]. The increasing interest in EPD is attributed to many successful applications of this method in nanotechnology.

Research by Vandeperre and Van Der Biest [3] indicate that there are parameters need to be considered to control the morphology and microstructure of the deposited layer electrophoretically (i) physical factors included of the applied voltage, deposition time, suspension concentration and substrate specifications and (ii) chemical parameters including zeta potential, liquid-phase dielectric constant, raw materials morphology and their particle size included conductivity, viscosity and stability of the suspension.

Besides, another parameter related to the suspension stability is particle size. For larger particles, the main problem is that they tend to settle due to gravity and difficult to get uniform deposition from suspension that sediment. Basically, the mobility of particles due to electrophoresis must be higher due to gravity so that smooth deposit layer can be observed.

2 Experimental

2.1 Materials

The high purity solid powder of titanium dioxide with undefined size (higher than 99.9 %), ethanol liquid, acetone liquid and acetyl acetone liquid supplied by Merck Chemicals was used along the experiments. Iodine powder also supplied by Merck Chemicals. The titanium dioxide suspension prepared is too concentrated and could accelerate suspension into the precipitate. To avoid suspension from easily precipitate, the titanium dioxide suspension is going to dilute with deionised water.

Deionised water is used as homogeneous suspension for dilution process in this experiment because it is considered more environments friendly. The titanium dioxide suspension then will be dilute into standard solution 0.1 wt% concentration using deionised water as aqueous mediums. Dilution process will be carried out by applying series dilution steps. Other than that, the pre-treatment of the EPD cells (ceramic filter electrode) is done by using the acetone solution. The initial pH value of suspension is 5.4, which is at acidic base. The pH of suspension is constant along the experiment.

2.2 Apparatus

A ceramic filter with dimension (5 mm × 25 mm × 1.5 mm) is used as EPD cell for both electrode anode and cathode with the same dimension. Glass beaker of 50,

100, 250 ml and volumetric flask of 50 ml is used in preparing suspension and also for dilution process. A centrifugal machine (SIGMA 3.18 K) is used to studies the effect of distribution time to particles size. Pulsed DC power supply model 8082A from HEWLETT PACKARD is used to supply current during EPD experiment. Zeta Potential meter with Particle Sizer (Zetasizer-NanoSeries, Malvern) is used to analysis zeta potential and average diameter size of titanium dioxide particles in suspension. These analyses are used to characterize the suspension before conducting EPD experiment. Lastly, the characteristic on deposited layer at the electrode cathode is evaluating using FESEM.

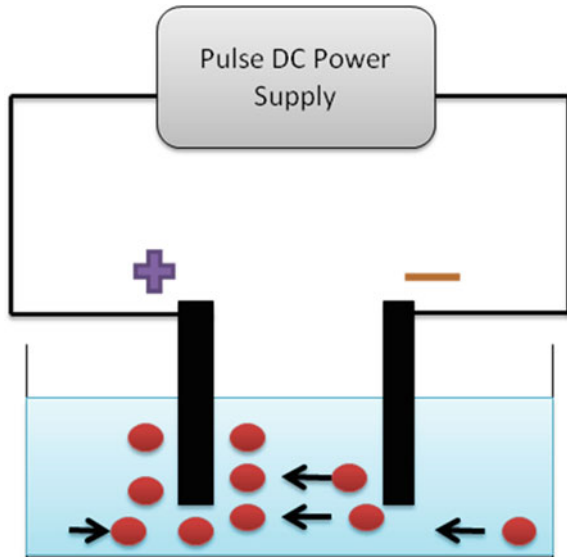
2.3 TiO₂ Suspension Preparation

The method chooses for preparation of TiO₂ suspension is referring to [4]. The 0.2 g of TiO₂ powder was mixed with 150 ml organic solvent of ethanol and 0.4 ml of acetylacetone to prepare the suspensions. The suspensions then were covered with parafilm or aluminum foil to prevent evaporation and stirred for 15 h with a magnetic stirrer before the suspension was added with charging solution of 4 ml acetone, 2 ml de-ionized water and 27 mg iodine powder dissolved in 100 ml of solvent ethanol.

2.4 EPD System and Process

After preparing the EPD cells, the EPD experiment can be started by measure 40 ml of TiO₂ suspension and pour into the beaker. Both of EPD cells are connected to the pulsed DC power supply. Separation distance between EPD cells is set to 20 mm and specified supply voltage is 5 V and at constant frequency of 500 Hz. Based on voltage supply over the surface of EPD cells, current densities is recorded in the data logger that connected to the pulsed DC supply. At the same time identify and justify which one is electrode anode and electrode cathode. The submerged area of EPD cells is not considered as long as the alligator clip not submerged in the suspension. This is because it going to disturb the current supplies to the EPD cells. The deposition time is fixed at 10 min for each experiment. After EPD experiment is done, the EPD cell is removed from the suspension and dry for 24 h at 60 °C in the drier.

The parameter that needs to be varied is particle size. In this case, the particle size is assumed to vary based on distribution time of suspension by centrifuge process. Others parameter such as voltage supply, frequency, distance between EPD cells and deposition time are setting constant. The current densities are depending on the voltage supply and the surface of EPD cells that immersed. From these variations of distribution time, the optimum distribution time or size of particle during EPD can be determined by measuring the highest deposited of particle on

Fig. 1 EPD experiment setup

EPD cells. The negatively charged particles in suspension migrating towards the positive electrode and will deposit on the electrode cathode and vice versa. Figure 1 below shows the diagram for EPD experiment setup.

3 Results and Discussion

3.1 Characterization of TiO_2 Suspension Before EPD

The characterization of TiO_2 suspension is including zeta-potential analysis and particle size distribution. The analysis is done by Zeta-Potential and Nanosizer Analysis Equipment.

3.1.1 Zeta-Potential of TiO_2 Suspension

Zeta potential-nanosizer analysis will represent in two parameters of results which are zeta potential and the size distribution for 10, 20, 30 and 40 min of TiO_2 suspension samples. Nanosizer depending on its number, volume and intensity of the particles can be known by using Dynamic Light Scattering (DLS) with measuring Brownian motion. Basically this is related to the size of the particles. While, the zeta potential can be analyzed by determining the electrophoretic mobility using Henry's equation (Malvern Zetasizer 2012).

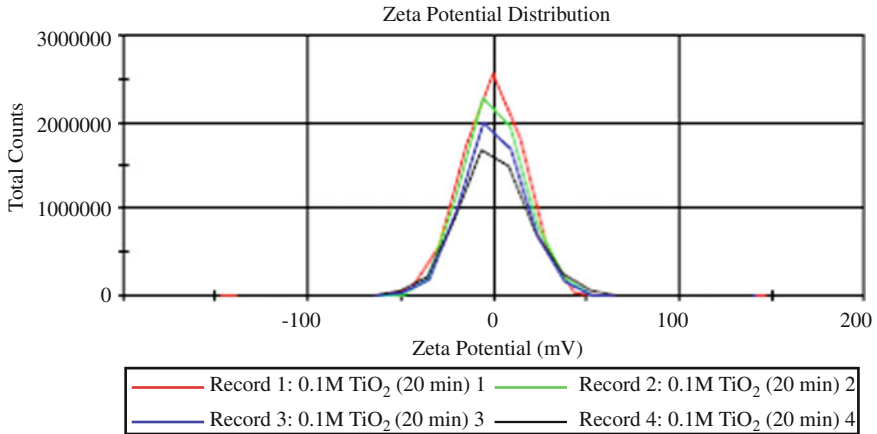


Fig. 2 Zeta potential distribution graph for 10 min

The purpose of zeta potential analysis is to determine the condition of the samples before the EPD analysis. Based on results observed from this analysis is the tendency of location of deposition of TiO₂ particles will take place (anode or cathode) during EPD experiment. More than that, the acidity or base of the sample also can be identifying.

For 30 min sample, the zeta potential is 0.289 mV. The positive value represent that the sample is tends to acidic, but still in lower number. This is proved by pH meter that used to check the pH of TiO₂ suspension at pH 5.4 and result to the deposition of particles at the cathode cell. This attributed to the adsorption of the H⁺ ions onto the particle surfaces which improves the electrostatic repulsion force [5]. If pH value decreases from 4.5 to 2.0, the large amount of positive ions will results to the reduction of the double layer thickness and the repulsive force between the particles. Thus, will promote particle to agglomerate and rises poorer deposition results [5]. Besides that, based on result quality it shows that the TiO₂ suspension sample may be aggregating or in other words the suspension is not stable. This may affect the experimental result.

While for 10, 20 and 40 min samples, the zeta potential value are -0.0317, -0.0340 and -0.151 mV respectively. The negative values are too slightly and cause any possibility to the location of deposition of TiO₂ particles. In this case the samples for 10, 20 and 40 min are assume to deposit at cathode cell due to the same pH of TiO₂ suspension. Figures 2, 3, 4 and 5 shows the zeta potential distribution graph for 10, 20, 30 and 40 min.

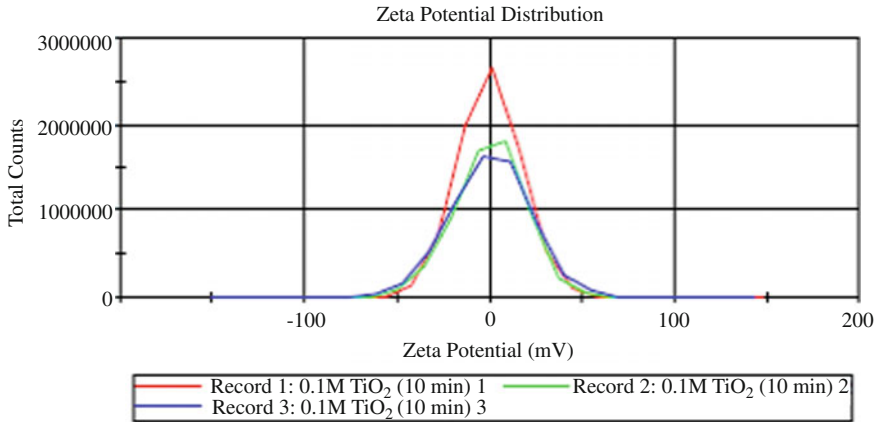


Fig. 3 Zeta potential distribution graph for 20 min

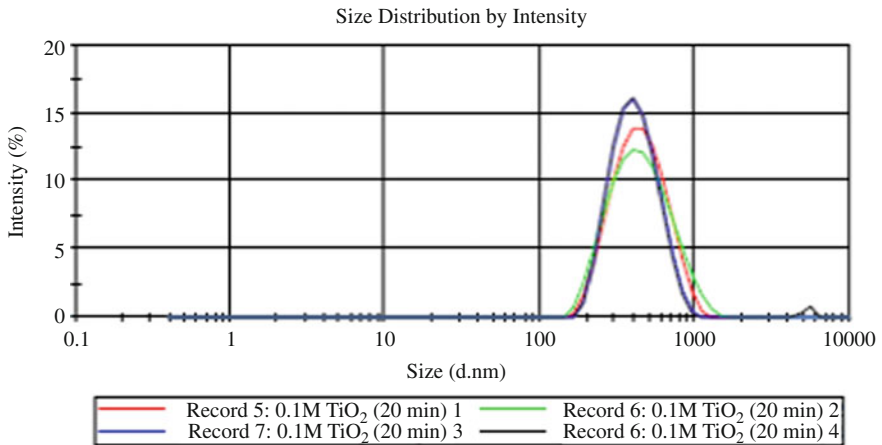


Fig. 4 Zeta potential distribution graph for 30 min

3.1.2 Particle Size Distribution of TiO₂ Suspension

The same sample used for zeta potential analysis will be used for zeta-nanosizer. The purpose of analyzing the particle size distribution of TiO₂ suspension before the EPD experiment is to determine the TiO₂ particle size in the samples of 10, 20, 30 and 40 min. The particle size data can be obtained by using zeta-nanosizer, Malvern equipment. The average of particle size values is taken based on size distribution by intensity graph. The average particle size for 10 min sample is 420 nm, while average particle size for 20 min sample is 405 nm and for the 30 min sample the average particle size is 309 nm. Finally for 40 min sample the average

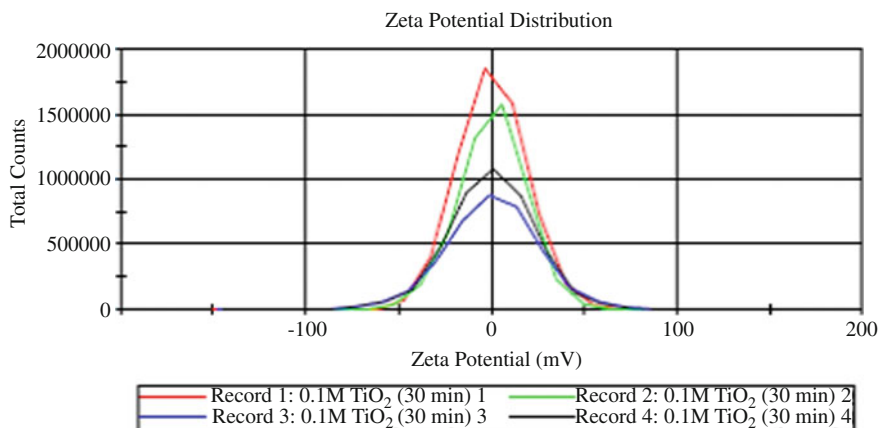


Fig. 5 Zeta potential distribution graph for 40 min

particle size is 305 nm. Based on particle size distribution from 10 to 40 min, it shows that the longer centrifuge times, the smaller size of particle is obtained. This is logic because the heavier or large particle is precipitated at the bottom of Felcol bottle. For centrifuge time of 10 min, the large particle is precipitate at bottom will be take out by syringe. Steps is continues until for 40 min and the only small particle is remaining at the bottom of Felcol bottle.

3.1.3 Characterization of Deposited TiO_2 Particles on the EPD Cells

Figure 6 shows the image of 20 K magnificant of deposited layer on surface of electrode cathode for 1.0 M TiO_2 suspension. This is actually the trial sample to identify either TiO_2 suspension can be deposited on ceramic filter electrode or not. Based on this image, it is proved that the TiO_2 suspension can be deposit at ceramic filter electrode. The image shows that the TiO_2 particles are likely stable and constant along the surface of electrode.

Figures 7, 8, 9 and 10 shows the image of deposited layer on the surface of electrode cathode for 10, 20, 30 and 40 min distribution time at 10 K magnificant. It shows that the images are not clear. It is because the presence of charging on surface of electrodes that affects the analysis. Even though the electrodes were coated before, there is still charged exist at the surface of electrodes. Other reason is that the TiO_2 suspension used is diluted to 0.1 M concentration because initial concentration of TiO_2 suspension is too thick. Other than that, this could occur because of instability of suspension during the EPD experiment.

Fig. 6 Image from FESEM

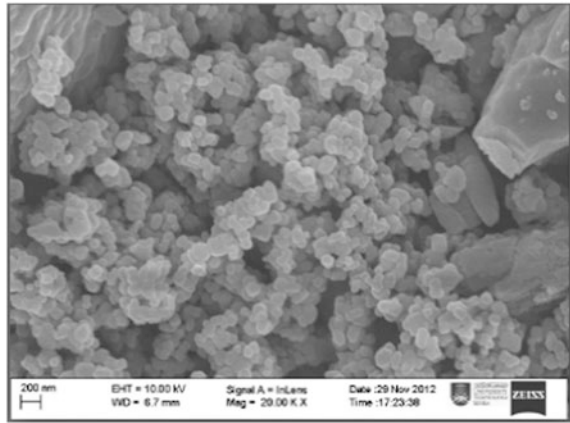


Fig. 7 Image for 10 min distribution time

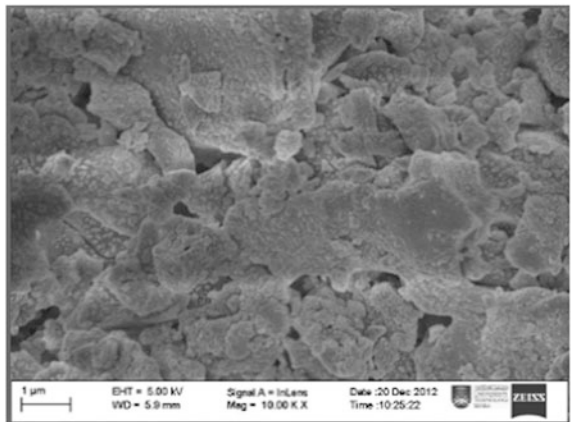


Fig. 8 Image for 20 min distribution time

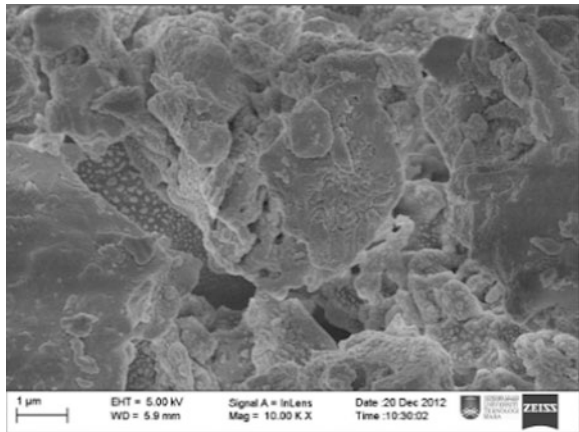


Fig. 9 Image for 30 min distribution time

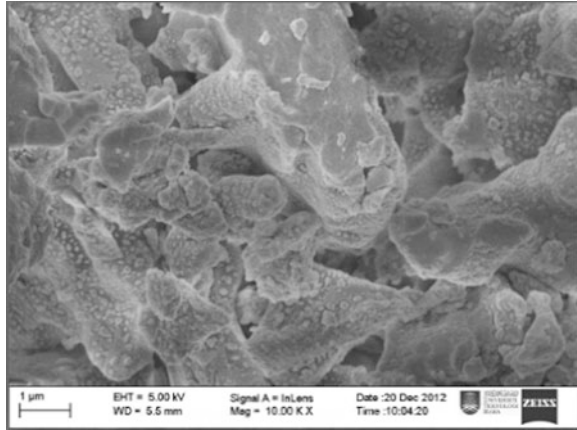
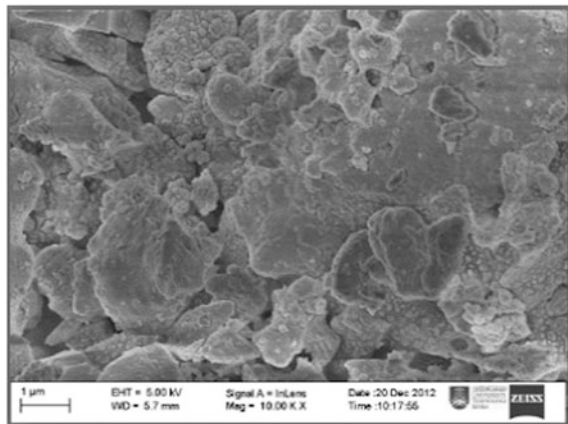


Fig. 10 Image for 40 min distribution time



4 Conclusion

The purpose of zeta potential analysis is to determine the condition of the samples before the EPD analysis. For 30 min sample, the zeta potential is 0.289 mV. The positive value represent that the sample tend to be acidic, but still in lower number. This is proved by pH meter that is used to check the pH of TiO_2 suspension at pH 5.4 and results to the deposition of particles at the cathode cell. While for 10, 20 and 40 min samples, the zeta potential value are -0.0317 , -0.0340 and -0.151 mV respectively. In this case the samples for 10, 20 and 40 min are all deposited at cathode cell due to the same pH of TiO_2 suspension. The centrifuge method used to differentiate the size of particles is not too effective. This is because based on zeta-nanosizer analysis it shows that the particle size distribution for different time of centrifuge give the result of size that very slightly difference. The average particle

size for 10 min sample is 420 nm, while average particle size for 20 min sample is 405 nm and for the 30 min sample the average particle size is 309 nm. Finally for 40 min sample the average particle size is 305 nm. Based on particle size distribution from 10 to 40 min, it shows that the longer centrifuges time, the smaller size of particle can be obtained.

5 Recommendation

The experiments need to be done by properly scheduled because as the suspension has been prepared, the EPD analysis must be done as soon as possible. So that any of contamination can be eliminated. Furthermore, the sample cannot be stored for long period because of the TiO₂ suspensions can easily sediment due to it high density. That is why the suspension is need to sonicated (homogenizer) prior EPD experiment. Since the TiO₂ suspensions can easily sediment, it is recommended that to add the adsorption of poly(acrylic acid) (PAA) in the aqueous suspension onto the surface of TiO₂ nanoparticles. This is because the PAA can provide the colloidal stability of aqueous suspension. But, further study need to be done about the use of PAA.

In order to obtain a good image in determining the deposition on the EPD cells using FESEM, it is recommended that for EPD cells to coating. This result to the reduction of surface charging by the TiO₂ deposited particles.

Acknowledgments The authors would like to acknowledge Universiti Teknologi MARA for Research Intensive Faculty (RIF) Project number 600-RMI/DANA 5/3/RIF (317/2012) for the financial support to carry out this research and also to the staff of Faculty of Pharmacy, Universiti Teknologi MARA, Puncak Alam for their help in FESEM-EDS and TEM analysis.

References

1. M.N. Naim, M. Iijima, H. Kamiya, I.W. Lenggono, Electrophoretic packing structure from aqueous nanoparticle suspension in pulse DC charging. *Colloids Surf. A* **360**, 13–19 (2010)
2. A.R. Boccaccini, J. Cho, T. Subhani, C. Kaya, F. Kaya, Electrophoretic deposition of carbon nanotube–ceramic nanocomposites. *J. Eur. Ceram. Soc.* **30**, 1115–1129 (2010)
3. L. Vandeperre, O. Van Der Biest, Electrophoretic forming of laminated ceramic composite tubes. *Key Eng. Mater.* **132–133**, 2013–2016 (1997)
4. S. Dor, S. Rühle, A. Ofir, M. Adler, L. Grinis, A. Zaban, The influence of suspension composition and deposition mode on the electrophoretic deposition of TiO₂ nanoparticle agglomerates. *Colloids Surf. A* **342**, 70–75 (2009)
5. J. Ma, W. Cheng, Deposition and packing study of sub-micron PZT ceramics using electrophoretic deposition. *Mater. Lett.* **56**, 721–727 (2002)

Preparation and Characterization of Corn Starch Nanocrystal Reinforced Natural Rubber Nanocomposites via Co-coagulation Process

K.R. Rajisha, L.A. Pothan, S. Thomas and Z. Ahmad

Abstract Corn starch nanocrystals were found to serve as an effective reinforcing agent for natural rubber (NR). Starch nanocrystals were obtained by the sulfuric acid hydrolysis of starch granules. After mixing the latex and the starch nanocrystals, the resulting aqueous suspension was made into coagulum and then it is mixed with the dry NR and cross linking agents, in two roll mill followed by compression molding. The composite samples were prepared by varying filler loadings, using a colloidal suspension of starch nanocrystals and NR latex and dry rubber. The morphology of the nanocomposites prepared was analyzed by Field Emission Scanning Electron Microscopy (FESEM) and FESEM analysis revealed the size and shape of the crystal and their homogeneity dispersion in the composites. The crystallinity of the nanocomposites was studied using XRD analysis which indicated an overall increase in crystallinity with increased in filler content. The mechanical properties of the nanocomposites such as stress-strain behaviour, tensile strength, tensile modulus and elongation at break were measured according to ASTM standards. The tensile strength and modulus of the composites were found to improve tremendously with increasing nanocrystal content. This dramatic increase observed in the modulus and the tensile strength can be attributed to the formation of starch nanocrystal network. This network immobilizes the polymer

K.R. Rajisha

Department of Chemistry, CMS College, Kottayam, Kerala, India
e-mail: ncst2013@gmail.com

L.A. Pothan

Department of Chemistry, Bishop Moore College, Mavelikara, Kerala, India
e-mail: lalyaley@yahoo.co.uk

S. Thomas

Centre for Nanoscience and Nanotechnology, Mahatma Gandhi University,
Kottayam, Kerala, India
e-mail: sabumacromol@gmail.com

Z. Ahmad (✉)

Institute of Infrastructure Engineering and Sustainable Management,
Universiti Teknologi MARA, Shah Alam, Malaysia
e-mail: zakiah@salam.uitm.edu.my

chains leading to an increase in the modulus and other mechanical properties. The DMA studies of the composites were carried out and it reveals the effective reinforcing mechanism of starch nanocrystal on NR matrix.

Keywords Corn starch · Nanocrystals · Natural rubber matrix · FESEM · XRD

1 Introduction

Starch is an abundant biopolymer, which is totally biodegradable. Starch nanocrystals obtained from starch have been used as fillers in polymeric matrices leading to desired reinforcing effect [1–3]. During the last decade, nano-material derived from natural polymers has been used as reinforcement in polymers and have been named as “green” bionanocomposites [4]. Many research works published in the area of starch based bionanocomposites show the relevance on this topic in the current scenario of polymer research [5–8]. Chitin, cellulose and starch are the crystalline residue that can be obtained from different natural polysaccharides with a uniform structure after acidic or alkaline hydrolysis. These nanoparticles from different sources have different geometrical characteristics. For example, the nanocrystals obtained from cellulose and chitin have a rod shaped structure while that of starch have a platelet shaped structure [9].

This study investigated the natural rubber composite by incorporating corn starch nanocrystals to replace conventionally used carbon black (manufactured by burning oil or natural gas in controlled conditions), hence making the composite a completely biodegradable. Many studies have been done to replace carbon black in rubber compounds. Novamont (Novara, Italy) is currently working in partnership with Goodyear Tire and Rubber, to produce tires using silica and nanoparticles derived from corn starch, partially replacing the conventional carbon black. This patented innovation, called Biotred, not only presents environmental advantages but also reduces the rolling resistance of tires [10]. Many attempts have been reported to blend polysaccharide nanocrystals with polymeric matrices. The resulting nanocomposite materials display outstanding mechanical properties and thermal stability. For example, starch nanocrystals consist of crystalline nanoplatelets about 6–8 nm thick with a length of 20–40 nm and a width of 15–30 nm [11]. They have been used as a new kind of fillers, showing interesting reinforcing and barrier properties in natural rubber [12]. In this approach, corn starch nanocrystals constitute possible filler for natural rubber which can have an admirable contribution in developing new environmental friendly strong composites.

Starch nanocrystals, the nanoscale biofiller derived from native starch granules, have been compounded with many different kinds of polymer matrices. The intrinsic rigidity of starch nanocrystals, special platelet-like morphology, strong interfacial interactions, and the percolation network organized by nanocrystals,

contribute to the mechanical performance, thermal properties, solvent absorption, and barrier properties of the composites.

In the present work, a new nanocomposite based on natural rubber filled with corn starch nanocrystals was prepared. The nanocrystals were characterized by FESEM and XRD. By varying the weight percentage of starch nanocrystals in the NR matrix the surface morphology, swelling behavior, and crystallinity of the various composites were investigated. The mechanical properties of the composites were also analyzed.

2 Experimental

2.1 Materials

Natural rubber latex was kindly supplied by Rubber Research Institute of India (RRI, Kottayam, India). It contained spherical particles of natural rubber with an average diameter around 1 μm , and the dry rubber content determined was about 61 wt%. The density of dry NR, was 1.4 g cm^{-3} , and it contained $\sim 98\%$ of *cis*-1,4-polyisoprene. Corn starch powder was purchased from Luba chemicals, Mumbai. Other chemicals like 36 N H_2SO_4 , BaCl_2 , sodium azoture (protectant against microorganisms) etc. needed for the preparation of starch nanocrystals were obtained from local sources.

2.2 Preparation of Corn Starch Nanocrystals

Corn starch nanocrystals were prepared by sulfuric acid hydrolysis of native corn starch powder. About 36 g of corn starch granules were mixed with 250 ml of 36 N H_2SO_4 for 5 days at 40 $^\circ\text{C}$, with a stirring speed of 100 rpm. The aqueous suspension was washed by successive centrifugation with distilled water until neutrality (confirmed by litmus paper testing). At this stage, starch suspension can be believed to be broken into nanocrystals, which changes the refractive index of the solution which is evident from the opaque nature of the suspension. The dispersion was completed by a further 10 min ultrasonic treatment in a B12 Branson sonifier. The resultant aqueous suspension constituted of starch fragments with a homogeneous distribution in size. The solid fraction of this aqueous suspension had a weight concentration of about 3.4 wt%.

2.3 Nanocomposite Processing

Nanocomposites of starch nanocrystal with natural rubber as a matrix were prepared via a two-step process involving:

Table 1 Formulations for the prepared nr composites

Sample code	NR latex (g)	SNC	Dry NR	Zno (g)	Stearic acid (g)	TMTD (g)	CBS (g)	Sulphur (g)
NRC	5	0	95	2.5	1.25	0.2	1.3	2.25
NRC1	5	1	95	2.5	1.25	0.2	1.3	2.25
NRC2.5	5	2.5	95	2.5	1.25	0.2	1.3	2.25
NRC5	5	5	95	2.5	1.25	0.2	1.3	2.25
NRC7.5	5	7.5	95	2.5	1.25	0.2	1.3	2.25

- i. *Master-batch preparation in NR latex with filler.*
- ii. Compounding of the master batch with solid NR and vulcanizing agents using a two-roll mill followed by subsequent curing.

Master batch preparation: In the master batch processing step, NR latex and SNC (starch nanocrystal) in aqueous medium were mixed together well to obtain a uniform dispersion of SNCs in NR latex. The concentration of the latex and SNCs was adjusted to have a final SNC concentration of 20 wt%. This dispersion is then coagulated using 1 % formic acid. The coagulated mass is separated out by dried in an oven. This master batch is then powdered and used for the next processing step. NR latex without SNCs was also prepared by the same method and was used as the control master-batch for comparison.

Compounding: In this step, the compounding of the master batch with solid natural rubber and vulcanizing agents in a two-roll mixing-mill with different weight percentages of nanowhiskers was carried out. The formulations used are given in Table 1. The resulting films were conditioned at room temperature in desiccators containing P₂O₅.

2.4 Characterization Techniques

- i. *Field Emission Scanning Electron Microscopy (FESEM)*

Morphology of the composites was studied using field emission scanning electron microscopy. A FESEM, CARC-ZEISS, SUPRA40 UP was used to observe the morphology of starch nanocrystal and different starch nanocomposite. The films were sputter coated with platinum to ensure conduction observed with an accelerating voltage of 5 kV.

- ii. *X-ray diffraction (XRD)*

X-ray diffraction patterns were taken by using Ni-filtered Cu-K α radiation ($\lambda = 0.154$ nm) by Bruker D8 Advanced X-Ray Diffractometer. The latex nanocomposite samples were scanned in step mode by 1.5 % min scan rate in the range of $2\theta < 12^\circ$. The specimens of 1×1 cm films were used for the analysis.

iii. *Dynamic Mechanical analysis*

Dynamic mechanical properties of the nanocomposites prepared after curing were investigated by dynamic mechanical analyzer (DMA, GABO EPLOXOR 500 N). For the measurements, rectangular specimens of 50 mm in length, 5 mm in width and 2 mm in thickness were sectioned from larger samples. The tests were performed in tensile mode at a frequency of 10 Hz with a static strain of 0.6 % and dynamic strain of 0.1 %, in a temperature range between -100 and 150 °C with a heating rate of 3 °C/min.

iv. *Mechanical measurement (Tensile test)*

The non linear mechanical properties of the samples were studied using Universal Testing Machine in accordance with ASTM D 412-2002. Dumbbell shaped specimens 5 mm wide, 8 mm long and about 1 mm thick were used for tensile measurements. The tensile curves obtained were analyzed for strain at break and modulus. The tests were conducted at a crosshead speed of 500 mm/min at ambient temperature. The mechanical properties of nano filled latex composites were studied at ambient temperature.

3 Results and Discussions

The morphology of the NR/starch nanocrystal materials were determined from field emission scanning electron microscopy and XRD analysis.

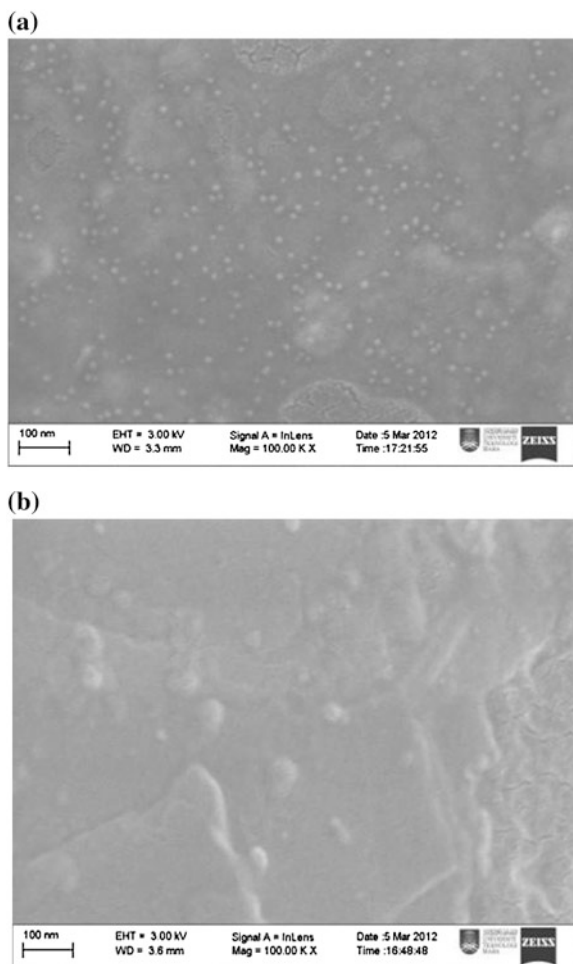
3.1 Morphology Analysis of Nanocomposites

The distribution level of the filler within the matrix was evaluated by observing the FESEM image of the surface fractured films. Figure 1a, b show the nanocomposite films of NR nanocomposite with 2.5 and 7.5 wt% of nanocrystals respectively.

In the FE-SEM micrograph a homogenous dispersion of starch nanocrystals which appears like white dots can be observed. A uniform distribution of the nanocrystal in the matrix is clearly seen for the compositions. Such an even and uniform distribution of the filler in the matrix is essential for obtaining optimum properties. As the filler loading is increased the nanocrystals showed a tendency to agglomerate which can be observed in Fig. 1b.

The particle size of the nanocrystal was observed to be in the range 12 nm and it is in agreement with some earlier work in this area.

Fig. 1 FESEM micrograph of nanocomposites with different wt% of nanocrystals (NRC); **a** 2.5 and **b** 7.5



3.2 Morphology Analysis of Starch Nanocrystals

The morphological analysis of starch nanocrystal was done using x-ray diffraction analysis. The XRD pattern displayed two weak peaks at $2\theta = 11.0^\circ$, double peak at $2\theta = 14.16^\circ$ and $2\theta = 19.5^\circ$ and a strong peak at $2\theta = 22.19^\circ$ and $2\theta = 25.88^\circ$ (Fig. 2).

From the XRD data, it was observed that the diffraction patterns recorded for the lyophilized sample of pure corn starch nanocrystal displayed a typical A-type amylose with X-ray diffraction patterns at 2θ with the first peak around 15° , the second peak near 18° , and the third main reflection around 23° .

A comparative study of the XRD peaks of native starch with prepared starch nanocrystals was also conducted. From the diffractograms, both the native corn starch and hydrolysed corn starch showed the characteristic peak at 18° and 23° .

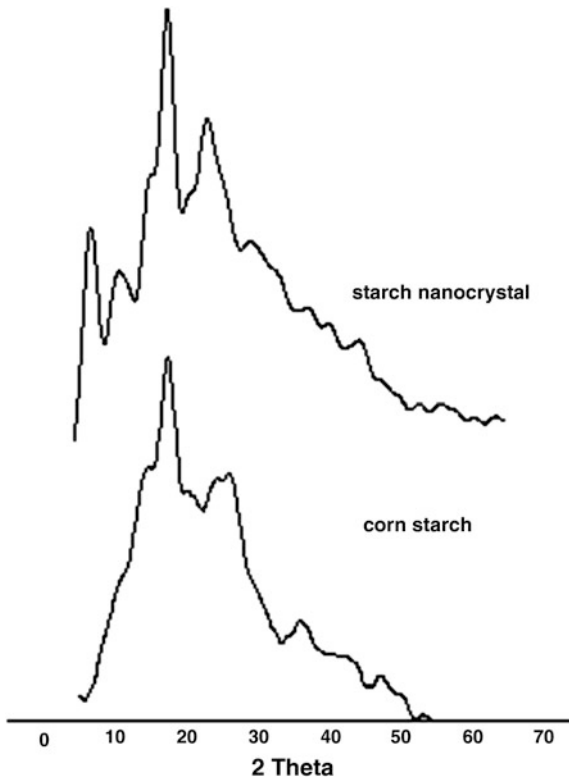


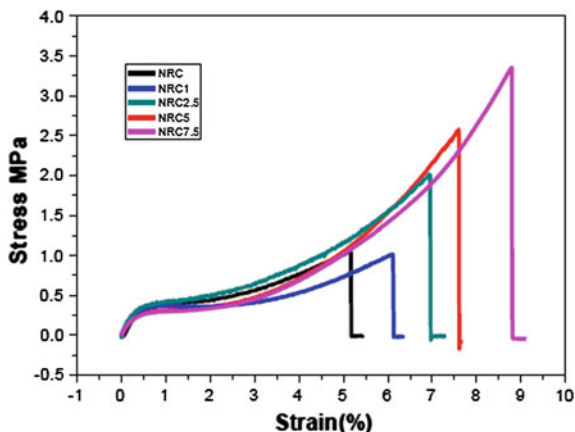
Fig. 2 X-ray diffraction patterns of starch nanocrystals and corn starch powder

But these two peaks are more prominent in the diffractogram of corn starch nanocrystal and this indicates a very high extent of crystallinity in starch nanocrystals.

3.3 Mechanical Properties of Nanocomposites

The starch nanocrystal obtained from sulfuric acid hydrolysis was very promising reinforcing material for polymer nanocomposites because of their high stiffness and strength. Studies on the reinforcing effect of starch nanocrystals with other fillers like clays, organoclays, carbon black, fly ash, and chitin whiskers in natural rubber matrix reports that starch nanocrystal is a good substitute for carbon black, as it can induce a reinforcing effect in terms of stiffness, strength and elastic behavior. These nanocomposites from renewable resources have the added advantages such as, low cost, easy availability, good biocompatibility, and ease of modification chemically and mechanically.

Fig. 3 Stress-strain curves of starch nanocrystal/NR nanocomposites



The tensile behavior of the corn starch nanocrystal reinforced with NR latex nanocomposite films was analyzed at room temperature. Figure 3 shows the stress-strain curves of starch-natural rubber composite with increasing starch content. It is found that stress increases regularly with strain till the sample breaks. As the filler loading is increased the tensile strength as well the modulus increases remarkably. The sharp increase in the tensile strength of the NR nanocomposites with addition of the filler shows the reinforcing effect of starch nanocrystal.

The reinforcing effect of the starch nanocrystals strongly depended on their ability to form a rigid three-dimensional network, resulting in strong interactions such as hydrogen bonds between the filler. Tensile test experiments give clear evidence for the presence of a three-dimensional network within the nanocomposites samples. In higher concentration, there is more number of possible polymer-filler interactions which enhances the reinforcement.

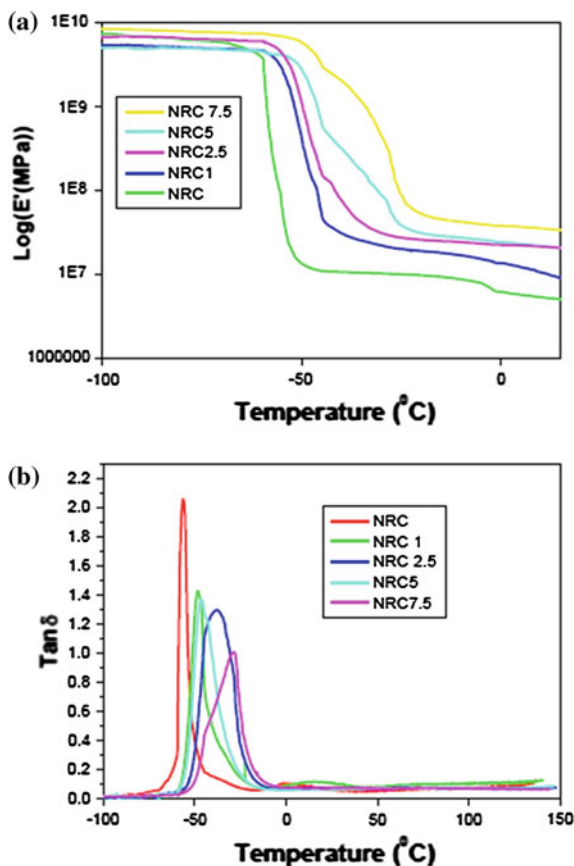
3.4 Dynamic Mechanical Properties by DMTA

Dynamic mechanical measurements were performed for NR films filled with different starch contents. The plot of the logarithm of the storage modulus, $\log(E')$, and the tangent of the loss angle, $\tan \delta$ versus temperature at 1 Hz are displayed in Fig. 4.

The curve of $\log(E')$ corresponding to the unfilled matrix is typical of a fully amorphous high molecular weight thermoplastic behavior. For temperatures below the glass transition temperature, NR is in the glassy state: the storage modulus slightly decreases with temperature but remains roughly constant above 1 GPa.

Then, a sharp decrease over 3 decades is observed around -60°C , corresponding to the primary relaxation process associated with the glass-rubber transition. This modulus drop corresponds to an energy dissipation phenomenon displayed in the concomitant relaxation process where $\tan \delta$ passes through a

Fig. 4 Graphs of DMTA for corn starch nanocrystals/NR nanocomposite films;
a Logarithm of the storage tensile modulus E' versus temperature at 1 Hz and
b tangent of the loss angle $\tan \delta$ versus temperature at 1 Hz



maximum. Then, the modulus reaches a plateau around 1 MPa, corresponding to the rubbery state. The broad temperature ranging from -40 to 180 $^{\circ}\text{C}$ of the rubbery state is ascribed to the high molecular weight of the polymer, resulting in a highly entangled state of the macromolecules. The evolution of $\tan \delta$ with temperature displays a peak located in the temperature range of the glass transition of the NR matrix. This relaxation process, is associated with the anelastic manifestation of the glass-rubber transition of the polymer. This mechanism involves cooperative motions of long chain sequences.

4 Conclusion

Potato starch nanocrystals appeared to be an effective reinforcing agent for natural rubber. Starch nanocrystals were obtained after sulfuric acid hydrolysis of potato starch granules (filler). The homogenous dispersion of the filler into the polymer

matrix is one of the key parameters for obtaining excellent mechanical properties. Wide-angle X-ray analysis showed that the processing by casting and evaporation at 40 °C did not affect the crystallinity of starch nanocrystal. The mechanical properties of the prepared composite materials were studied through tensile testing. The reinforcing effect of the prepared nanocrystals thus appears to be an excellent nanofiller for NR latex and have the potential for replacing conventional polymer composite and nanocomposite which are a real threat to the environment. The overall improvement in property was expected to be due to the possible formation of a three-dimensional network of starch nanocrystals within the nanocomposites network.

Acknowledgments This research was financially supported by the Malaysia Kenaf and Tobacco Board (Grant: 100-RMI/GOV 16/6/2 (5/2012)) is greatly acknowledged. The authors wish to thank the technical staff in the Composite Laboratory, Faculty of Applied Science and Faculty of Pharmacy, UiTM for their assistance and support.

References

1. A. Dufresne, Polysaccharide nano crystal reinforced nanocomposites. *Can. J. Chem.* **86**, 484–494 (2008)
2. A. Helene, P. Jean-Luc, M. Sonia, D. Danielle, D. Alain, Starch nanocrystal fillers in an acrylic polymer matrix. *Macromol. Symp.* **221**, 95–104 (2005)
3. A. Helene, M. Sonia, D. Danielle, A. Dufresne, Waxy maize starch nanocrystals as filler in natural rubber. *Macromol. Symp.* **233**, 132–136 (2006)
4. M. Darder, P. Aranda, E. Ruiz-Hitzky, Bionanocomposites: a new concept of ecological, bioinspired, and functional hybrid materials. *Adv. Mater.* **19**, 1309–1319 (2007)
5. H.Y. Kim, D.J. Park, J.Y. Kim, S.T. Lim, Preparation of crystalline starch nanoparticles using cold acid hydrolysis and ultrasonication. *Carbohydr. Polym.* **98**, 295–301 (2013)
6. D. LeCorre, J. Brass, A. Dufresne, Influence of native starch's properties on starch nanocrystals thermal properties. *Carbohydr. Polym.* **87**, 658–666 (2012)
7. D. Chen, D. Lawtona, M.R. Thompson, Q. Liub, Biocomposites reinforced with cellulose nanocrystals derived from potato peel waste. *Carbohydr. Polym.* **90**, 709–716 (2012)
8. H.Y. Kim, J.A. Hanb, D.K. Kweonc, J.D. Parkd, S.T. Lima, Effect of ultrasonic treatments on nanoparticle preparation of acid-hydrolyzed waxy maize starch. *Carbohydr. Polym.* **93**, 582–588 (2013)
9. P.J. Jenkins, A.M. Donald, The effect of acid hydrolysis on native starch granule structure. *Starch—Stärke*, **49**, 262–267 (1997)
10. H. Angellier, S. Molina-Boisseau, L. Lebrun, A. Dufresne, Processing and structural properties of waxy maize starch nanocrystals reinforced natural rubber. *Macromolecules* **38**, 3783–3792 (2005)
11. O. van den Berg, M. Schroeter, J.R. Capadona, C. Weder, Nanocomposites based on cellulose whiskers and (semi)conducting conjugated polymers. *J. Mater. Chem.* **17**, 2746–2753 (2007)
12. M. Labet, W. Thielemans, A. Dufresne, Polymer grafting onto starch nanocrystals. *Biomacromolecules* **8**, 2916–2927 (2007)

Low Dense CNT for Ultra-Sensitive Chemoresistive Gas Sensor Development

Amirul Abd Rashid, Nor Hayati Saad, Daniel Bien Chia Sheng, Teh Aun Shih, Muhammad Aniq Shazni, Mohammad Haniff and Mai Woon Lee

Abstract This work was aimed to develop chemoresistive base sensor on silicon platform. Carbon nanotube (CNT) with low density was grown on passive interdigitated (IDE) based sensor which later can be functionalized with other material for the selectivity of the targeted goals. Low dense CNT will provide a bigger area of the functionalities element adhered to the wall hence increase the sensitivity of the sensor. In situ CNT growth was achieved using a PECVD machine with the time parameter was varied targeting for low dense CNT grow in-between the IDE fingers. SEM analysis reveals that low dense CNT was evidence for growth time as short as 30 s and as the time increase, the density was also increasing. Resistive probing of the grown CNT samples shows a drop in resistance compared to non-grown CNT which confirmed that the CNT successfully conducting the electron. CO₂ gas testing shows that the low dense sensor shows better detection performance compared to high dense sensor. However, further study needs to be conducted to measure the level of amorphous carbon which determine the purity of the such CNT nanostructure.

Keywords Low dense CNT · Chemoresistive · Gas sensor · Passive IDE

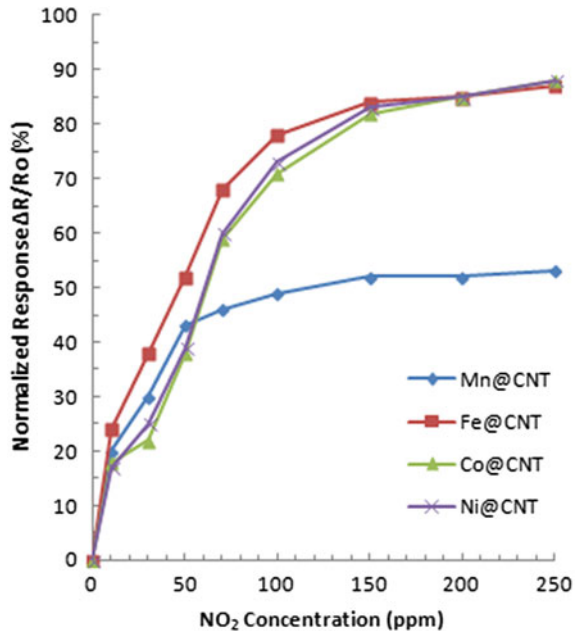
1 Introduction

Carbon nanotube (CNT) had drawn a big attention of research and studies since it was discovered by Iijima in 1991 [1]. The application of CNT can be seen in almost all fields including nanotechnology, electronics, optics, material science,

A.A. Rashid (✉) · D.B.C. Sheng · T.A. Shih · M.A. Shazni · M. Haniff · M.W. Lee
Nanoelectronics Lab, MIMOS Berhad, Technology Park Malaysia,
57000 Kuala Lumpur, Malaysia
e-mail: amirul2550@salam.uitm.edu.my

A.A. Rashid · N.H. Saad
Micro-nano Electromechanical System Laboratory (MINEMS), Faculty of Mechanical Engineering, Universiti Teknologi MARA, 40450 Shah Alam, Selangor, Malaysia

Fig. 1 The response of different CNT doped with different metal to detect NO_2 gas at different concentration [8]



bio-engineering and even in architecture [2, 3]. The sensor is one of the areas which deeply penetrated by CNT advancement due to its unique electrical properties, heat conduction efficiency and extraordinary mechanical strength [4–6]. Nevertheless, in order for CNT works efficiently as sensor particularly to detect various gas types, various metal needs to be doped to the surface of CNT [7, 9]. Depending on the target gas, the selectivity of the sensor can be achieved by functionalities this CNT by electro-deposition or sputtering process with materials such as Tungsten or Tin Oxide [10, 11]. The sensing mechanism is the change of electrical conductivity of the material of the sensor surface [12]. Figure 1 exhibit the capability of CNT for response NO_2 gas at different concentration after doped with various metals. For next generation gas sensor that able to detect sub-ppm. concentration, the sensitivity of the sensor must be improved [13]. Despite of improved the CNT properties by growing single wall CNT [14], another is to reduce the density of the multi wall CNT. Bigger open area between CNTs will allow more metal dopant attached to the surface of CNT wall, hence the sensitivity of the sensor can be increased significantly.

In the current state of this study, the density level was controlled by manipulating the PECVD parameters. The performance of the different level of density was carried out by growing the CNT on silicon base IDE to prove that the low density CNT indeed give a better electrical response performance compared to the dense CNT device.

2 Experimental Details

Low dense CNTs were synthesized on Tungsten IDE by PECVD process. For high dense CNT growth, a barrier layer of Nitrate with thickness of 10 nm were deposited on the overall IDE surface. Subsequently, 5 nm of Cobalt catalyst was deposited using radio frequency-magnetron sputtering at a base pressure of $\sim 10e^{-3}$ mbar. The samples then load into PECVD chamber for the CNT growth process. A critical parameter for PECVD includes gas flow rate (Acetylene 100 sccm), chamber temperature (700 °C), chamber pressure (2,000 mTorr) and RF power (150 W) was used.

In order to produce less dense CNT, the same procedure was used except the step for Nitrate barrier was omitted. The growth time was also varied between 30 s and 5 min in order to investigate correlation between time to growth rate of low dense CNT's. The morphology of the grown CNTs was characterized using a JEOL field emission scanning electron microscopy system. Raman spectra were obtained on the nanotube samples with NT-MDT Raman spectroscopy system using a 473 nm air-cooled blue laser as an excitation for analysis. Emission intensities from the samples were measured from the peak height.

For the electrical properties, the grown CNT on IDE been packaged on the customized interconnected PCB (Harwin). The packaged sensor then placed inside a chamber and connected to the typical LCR meter. The initial resistance of the samples was measured at room temperature before the chamber filled up with the specific ppm level of CO₂ begin with 500 up to 2,000 ppm During each interval ppm, the chamber was allowed to stabilize with CO₂ for a while before the gas level increased. The commercial CO₂ sensor was also placed inside the chamber to measure the specific CO₂ ppm level required. By supplying 1 V power at certain ampere, the changes of resistance data were collected so the changes over ppm level can be analyzed. The same procedure was done on both low density and high density CNT sensor.

3 Result and Discussion

Figure 2a illustrates the typical growing mechanism of the dense CNT on the IDE. Because of the availability of Nitrate barrier layers, the whole IDE surface will grow with CNT's after going through the PECVD process. In contrast, samples without the nitrate barrier will cause the catalyst layer to diffuse on the metal surface of the IDE.

With that, CNT's will not able to grow. In contrast, the catalyst which lies on SiO₂ of the IDE still manage to nucleate even though at lower rate and this will produce lower dense CNT in between the IDE electrodes as shown in Fig. 2b.

Figure 3a–d show SEM images of CNTs grown on Co catalyst layer without a Nitrate layer at different growth duration from 30 s to 5 min. It was revealed that the

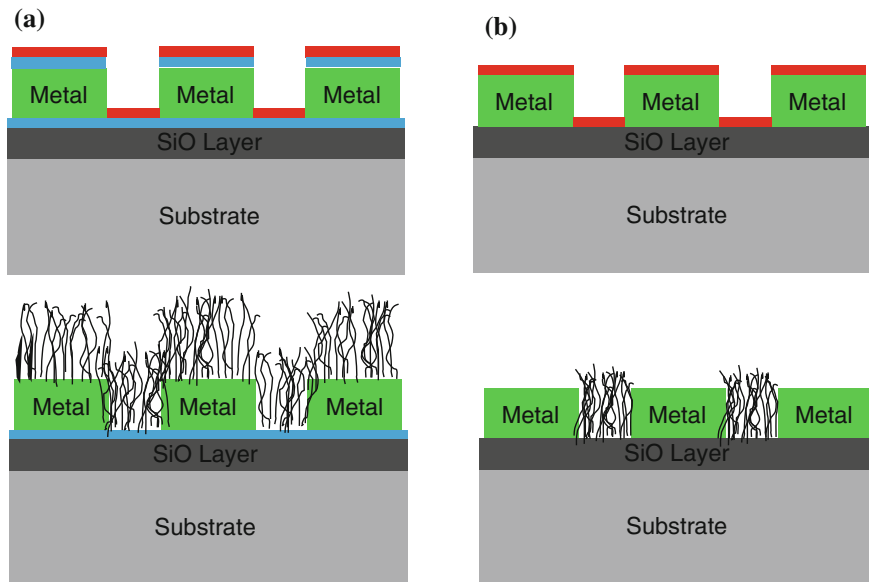


Fig. 2 Typical CNT growth process (a) and selective growth by excluding nitrate diffusion barrier layer (b)

randomly-oriented CNTs with the low density formation were selectively grown on the catalyst surface in-between the IDE where the deposition of nanotubes only occurred on the SiO_2 layer, while no growth was observed on the Tungsten IDE. It was also found that the density of nanotubes increases proportionally with increasing the growth duration, indicating a constant growth rate during the synthesis process.

Based on the results, it is expected that the formation of Co seeds layer on SiO_2 was formed during the nucleation step to allow diffusion and dissolution of carbon feedstocks into them during the growth process. In contrast, it is possible to assume that the Co catalyst was diffused into the tungsten layer at high annealing temperature of $700\text{ }^\circ\text{C}$, thus forming a cobalt-tungsten mixture at the top of IDE structure. Therefore, this mixture formation is likely to suppress the nanotube growth, and eventually formed an amorphous carbon layer on tungsten IDE instead of nanotube formation. Figure 3e illustrates the SEM images of CNTs growth on Co catalyst supported by the TiN layer. It was observed that the highly dense CNTs were successfully grown on the entire area of IDE structure. Additionally, the TiN layer also tends to improve the growth rate of nanotube by preventing any possible diffusion of Co catalyst into it. In comparison, the growth rate of Co catalyst on the TiN layer is about 70 % higher than to that of Co catalyst on the SiO_2 layer. The schematic of the proposed growth mechanism of low density and high density CNTs growth is shown in Fig. 2.

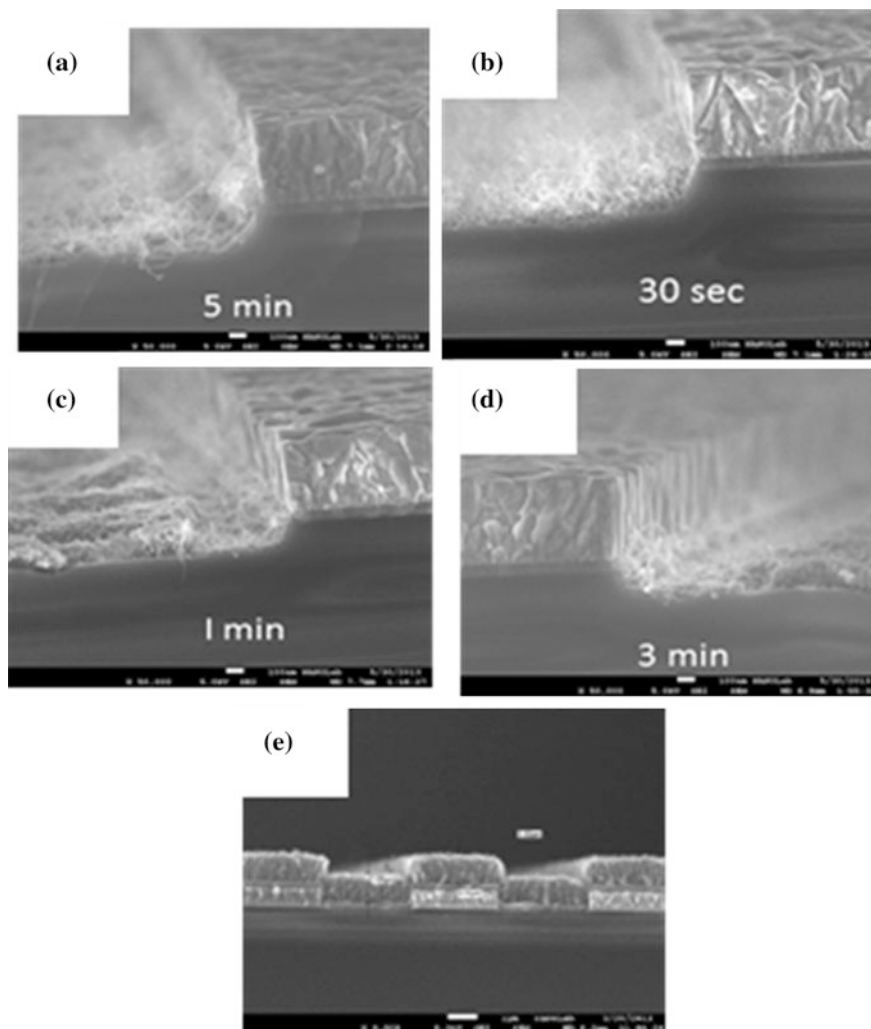
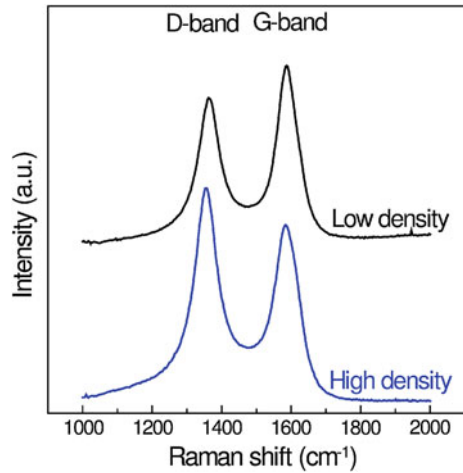


Fig. 3 Cross section images of low dense CNT grown at different growth duration (a–d) and typical high dense CNT (e)

Raman spectra of CMTs with low density and high density formation are shown in Fig. 4. From the results, two major peaks were found, a G-band at around $\sim 1,587 \text{ cm}^{-1}$ and D-band around $\sim 1,356\text{--}1362 \text{ cm}^{-1}$. The G-band represents the ordered graphite corresponding to the stretching mode of the C–C bonds in the graphite plane, whereas the D-band represents the disordered graphite structure associated with defects. The quality of nanotubes was evaluated based on the peaks intensity ratio, I_G/I_D . The calculated I_G/I_D ratio for both low density and high density of CNTs is about 1.22 and 0.82, respectively. It was noted that the I_G/I_D ratio of

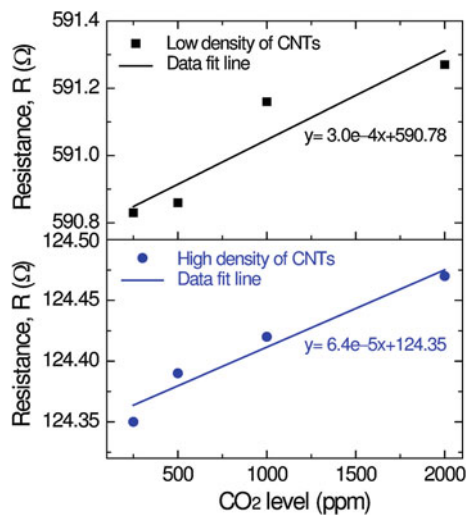
Fig. 4 Raman spectra of MWCNTs grown with low and high density formation



CNTs for low density formation is about ~ 1.45 orders of magnitude than that of high density formation, indicating lower degree of defects. It was also observed that the I_G/I_D ratio increases with increasing the growth time. Hence, it is expected that the larger structural defect was appeared in denser CNTs.

In order to investigate the influence of CNTs density on gas sensing performance, a response of resistance changes was investigated by exposing the sensor in CO₂ level, having a range of 250–2,000 ppm. Figure 5 shows the change in resistance as a function of CO₂ level for low and high dense CNTs. It is expected that the low density formation of CNTs has least connected-channels of the IDE, thus resulting in higher initial resistance. Meanwhile, for high density formation,

Fig. 5 Resistance changes as a function of CO₂ level for low and high dense CNTs



the larger intersection among the neighboring CNTs and also to the IDE leads to behave as good electrical contact. From the results, it was observed that the sensor with low density formation exhibits larger resistance changes by about ~ 4.6 orders of magnitude than that of high density formation, with a sensitivity of 22 m Ω /100 ppm. This increased sensitivity could be attributed to the larger portion of isolated nanotubes with thin bundles in the low density CNTs. This leads to enhance the absorption probability of CO₂ per nanotube, thereby resulting in larger resistance changes.

4 Conclusion

This study shows that low, dense CNT was successfully grown in-between IDE electrode at minimum 30 s duration. However, further study needs to be conducted to investigate the level of amorphous carbon exist on each group to determine the purity of the CNT nanostructure. At the same time, sensitivity and selectivity comparison among the groups upon CNT functionalization will determine acceptable growth time to produce high sensitive low dense CNT gas sensor.

Acknowledgments The authors wish to thank MIMOS Berhad for facility accessibility to perform this experiment, Universiti Teknologi MARA (UiTM) and Ministry of Higher Education Malaysia (MOHE) for the financial support under the Exploratory Research Grant Scheme (File No: 600-RMI/ERGS5/3(18/2013)).

References

1. Y.D. Zhao, W.D. Zhang, H. Chen, Q.M. Luo, Direct electron transfer of glucose oxidase molecules adsorbed onto carbon nanotube powder microelectrode. *Anal. Sci.* **18**(8), 939–941 (2002)
2. T.K. Fukui, K. Tanaka, *The Science and Technology of Carbon Nanotubes*. (Elsevier Science, Amsterdam, 1999)
3. J. Wang, Carbon-nanotube based electrochemical biosensors: a review. *Electroanalysis* **17**(1), 7–14 (2005)
4. M. Meyyappan, L. Delzeit, A. Cassell, D. Hash, Carbon nanotube growth by PECVD: a review. *Plasma Sources Sci. Technol.* **12**(2), 205 (2003)
5. V. Raffa, O. Vittorio, C. Riggio, G. Ciofani, A. Cuschieri, *Physical Properties of Carbon Nanotubes For Therapeutic Applications Carbon Nanotubes for Biomedical Applications* (Springer, Berlin Heidelberg, 2011), pp. 3–26
6. C. Cantalini, L. Valentini, J.M. Kenny, L. Lozzi, S. Santucci, Carbon nanotube gas sensors: current status and future prospects, in *Sensors, Proceedings of IEEE, IEEE* (2004)
7. Z. Zanolli, R. Leghrib, A. Felten, J.J. Pireaux, E. Llobet, J.C. Charlier, Gas sensing with Au-decorated carbon nanotubes. *ACS Nano* **5**(6), 4592–4599 (2011)
8. Information on http://www.ytca.com/gas_sensor_technology
9. A.A. Rashid, et al. Nanostructure integration in MEMS sensor: fabrication and development process, in *Proceedings of the 4th International Conference on Nanostructures (ICNS4)*, Kish Island, Iran (2012)

10. A. Dieguez, A. Romano-Rodríguez, J.R. Morante, J. Kappler, N. Barsan, W. Göpel, Nanoparticle engineering for gas sensor optimisation: improved sol-gel fabricated nanocrystalline SnO₂ thick film gas sensor for NO₂ detection by calcination, catalytic metal introduction and grinding treatments. *Sens. Actuators B: Chem.* **60**(2), 125–137 (1999)
11. M. Trojanowicz, Analytical applications of carbon nanotubes: a review. *TrAC Trends Anal. Chem.* **25**(5), 480–489 (2006)
12. Ting, et al. Recent progress in carbon nanotube-based gas sensors. *Nanotechnology* **19**(33), 332001 (2008)
13. P. Qi, et al. Toward large arrays of multiplex functionalized carbon nanotube sensors for highly sensitive and selective molecular detection. *Nano Lett.* **3**(3), 347–351 (2003)
14. Y. Chen, L. Yu, D. Feng, M. Zhuo, M. Zhang, E. Zhang, T. Wang, Superior ethanol-sensing properties based on Ni-doped SnO₂ p–n heterojunction hollow spheres. *Sens. Actuators B: Chem.* **166**, 61–67 (2012)

Stripping Performance and Volumetric Properties Evaluation of Hot Mix Asphalt (HMA) Mix Design Using Natural Rubber Latex Polymer Modified Binder (NRMB)

E. Shaffie, J. Ahmad, A.K. Arshad, D. Kamarun and F. Kamaruddin

Abstract Stripping one of the most common pavement failure usually occurs in pavement structures. This failure reduced the service life of the pavement, reduced driver safety and increase cost of maintenance. Polymer modified binder has been conducted previously to find an alternative material in pavement construction that can be used as new improvement for asphalt mix design. This paper presents the stripping potential benefits of natural rubber (NR) for the asphalt mixtures used on pavement. This research evaluates the physical properties and stripping performance of dense graded Superpave-designed HMA mix. Two different types of dense graded Superpave HMA mix were developed consists of unmodified binder asphalt mix (UMB) and natural rubber polymer modified binder asphalt mix (NRMB). Natural rubber polymer modified binder was prepared from addition of 8 % of NR into asphalt binder. Stripping results from Modified Lottman test and Boiling Water test were determined to evaluate the performance of these mixtures. Results showed that all the mixes passed the Superpave volumetric properties criteria which indicate that these mixtures were good with respect to durability and flexibility. The Stripping result of NPMB demonstrates better resistance to stripping than those prepared using UMB mix. Addition of NR to the binder has certainly improved the binder properties significantly and hence increase the resistant to stripping of the asphalt mixture. The results also shows that the optimum NR obtained is 8 % by weight of asphalt binder is the most effective proportion that having potential to improve physical properties and the performance of polymer modified asphalt binder. Therefore, it can be concluded that the NR polymer is suitable to be used as a modifier to modified binder in order to enhance the properties of the binder and thus improves the performance of asphalt mixes.

Keywords Modified binder · Natural rubber · Physical properties · Stripping · Superpave mix design

E. Shaffie (✉) · J. Ahmad · A.K. Arshad · F. Kamaruddin
Faculty of Civil Engineering, Universiti Teknologi MARA, 40450 Shah Alam, Malaysia
e-mail: eka@salam.uitm.edu.my

D. Kamarun
Faculty of Applied Science, Universiti Teknologi MARA, 40450 Shah Alam, Malaysia

1 Introduction

Stripping is defined as the physical separation of the asphalt cement from the aggregate produced by the loss of adhesion between the asphalt cement and the aggregate which is primarily due to the action of water or water vapour [1]. It is a distress in the asphalt pavement which happens due to moisture susceptibility of the HMA mixture [2]. This process occurs when the water gets in between the aggregate surface and it replaces the asphalt coating. Stripping initiates at the bottom asphalt layer for the most part and works its way upward, weakening the entire structure through its progression. This influences the crack to form and may cause the pavement structure to completely disintegrate. As a result, the performance of asphalt pavement reduced and the maintenance costs increased. Therefore, in order to alleviate this problem, there are many approaches to improve the performance of asphaltic pavement. Previously, unmodified asphalts binders were able to encounter the traffic volumes and loads exerted on them. However, nowadays, due to the rapid development, the increasing of road usage by heavy vehicles with high tyre pressure and high axle load has caused serious distress to the pavement such as rutting, shoving and bulging. This defect reduced the service life of the pavement and increases the cost of maintenance. Therefore, the asphalt properties of existing pavement should be improved by asphalt binder modifications to obtain better pavement performance.

Currently, there are many types of additives and modifier like rubber, polymer, mineral fiber etc. have been added into asphalt pavement mixes to increase the performance of asphaltic pavement. One of the approach can be considered to improve the performance of asphaltic pavement was by modification of the bituminous binder. Polymer additives to asphalt materials are being advocated as having high potential for improving long-term pavement performance through their ability to improve the properties of the asphalt binder and the resulting asphalt concrete mix. Several additives and modifier such as NR (natural rubber latex), SBS (Styrene Butadiene Styrene Block Copolymer), SBR (Styrene Butadiene Rubber Latex), and EVA (Ethyl Vinyl Acetate) have been studied by previous researchers to improve the asphalt binder properties, but only few types are suitable and compatible with binder for modification [3].

Fernando et al. [4] had carried out investigation to improve asphalt properties by using various kind of natural rubber latex such as field latex, concentrated latex and skim latex. They found that the penetration value had been reduced whilst the softening point was increased. In addition, Nopparat et al. [5] studied the potential of modification of binder using natural rubber on the asphalt binder properties. It was found that the roads paving with natural rubber-modified asphalt shall have more strength and durability than using non- modified asphalt. Study conducted by Nrachai et al. [6] found that the natural rubber latex is the best alternative for road making due to flexibility and stability improvement in asphalt pavement and extend service life of the road pavement.

Some previous studies on natural rubber polymer were made to mix the polymers in the essential amounts manually at different mixing condition. However, this result could not produce a consistent asphalt binder properties results. Study by Airey et al. [7] found that the addition of polymer is intended to improve asphalt binder properties. However, this improvement is likely depends on the asphalt binder mixing conditioned which is consider to be somewhat unclear due to various interaction, percentage of polymer and mixing blending condition. Hence, there is a need to investigate the properties and performance of the natural rubber (NR) polymer modified binder at selected mixing variables.

The application of natural rubber by mixing with asphalt materials in roadwork is an alternative material that may help increase domestic consumption of natural rubber. Furthermore, these mixes has the potential to enhance further the mechanical properties of asphalt mixes and thus improve the quality of road pavement, extend service life of the road, and reduce expenditures in maintaining road pavement. Hence, in this study, a new asphalt binder based on natural rubber (NR) polymer was conducted. The application of NR in modified asphalt binder is expected to improve engineering properties of asphalt binder.

2 Materials and Method

The study focused on the evaluation volumetric properties and stripping performance of Natural Rubber Polymer modified Binder (NRMB) of Hot Mix Asphalt (HMA) using Superpave methods. The Superpave mix design procedure involves careful material selection and volumetric proportioning as a first approach in producing a mix that will perform successfully. All the design procedures were according to AASHTO and ASTM as guides to ensure the laboratory works and materials were fulfilled specifications. Figure 1 show the experimental procedure followed in this research.

2.1 Aggregate Preparation

Granite aggregates, natural rubber latex polymer and penetration grade 80/100 of binder are the main materials to use in this research. Granite aggregates were obtained from Blacktop Quarry, Rawang located in Klang Valley. All materials were undergoing several tests of materials physical properties to ensure the quality of HMA mixture.

The aggregates were processed by washing, oven drying and sieving. All the aggregates were sieved to the appropriate size using sieving machine and then stored in individual bins according to the size of aggregates. This method was used to determine the grading of aggregates including coarse and fine fractions. Washed-

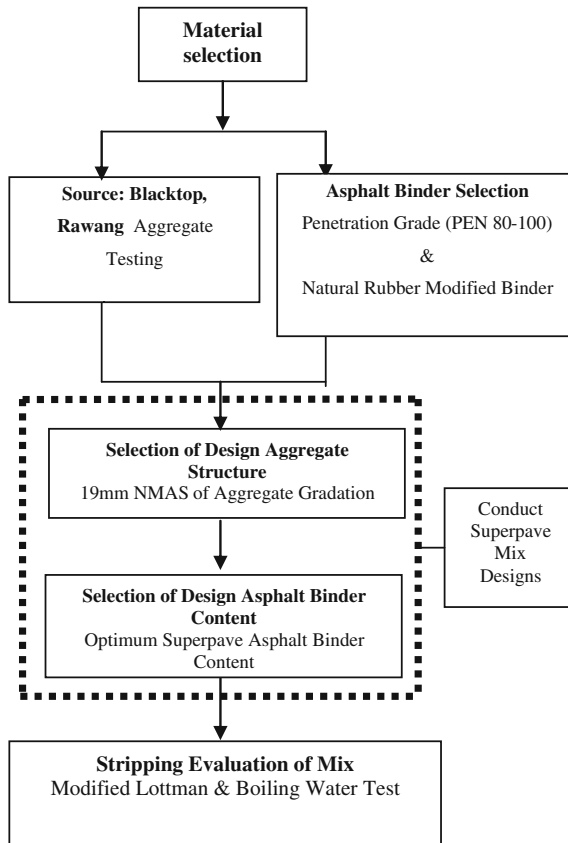


Fig. 1 Flow chart of the experimental procedure

sieve (ASTM C117) was then conducted to determine the proportion of mineral filler required in the aggregate gradation. The specific gravity of the coarse aggregate (ASTM C127) and fine aggregate (ASTM C128) tests was then conducted to evaluate the absorption rate of the aggregate and the volume of water in the aggregate. It was expressed as bulk specific gravity, saturated-surface-dry (SSD) specific gravity and apparent specific gravity. The specific gravity of aggregate was useful in making weight-volume conversions and in calculating the volumetric properties of compacted hot mix asphalt specimens.

Physical properties test were then conducted on the aggregates which conforms to the consensus and source properties as required in the Superpave system. The tests included Flat and Elongated particles (ASTM D4791), Abrasion Test (AASHTO T96) and Aggregate Impact Value (AASHTO T96).

2.2 Asphalt Binder Preparation

Two different asphalt binders were used (a) Unmodified binder (UMB) and (b) natural rubber polymer modified binder (NRMB). Natural Rubber (NR) was used in this study, which was provided by the ACP-DMT company from Port Klang. NR is an elastomeric hydrocarbon polymer that exists as a natural milky sap produced by several species of plants. Compared to the unmodified binder, all these have been used in the mixing with other road materials and have shown improvement in the modified version of bitumen. Table 1 shows the properties of the natural rubber latex (NR).

The NRMB was produced by modifying binder of penetration grade 80/100 with addition of 8 % natural rubber polymer by weight of asphalt. For the preparation of a sample, 500 g of base asphalt binder was melted at 110 °C and poured into a 500 ml container. Then, the asphalt binder was heated in the oven at 150 °C until it became liquid. The NR was added slowly into the liquid asphalt binder and was sheared with a high shear mixer with mechanical stirrer at selected mixing conditioned. The optimum percentage of NR was obtained from previous research done by Shaffie et al. [8]. Figure 2 shows the equipment and sample preparation process.

Table 1 The properties of the natural rubber polymer

Property	Value	Unit
Total solid content	65.5 %	%
PH	4.5	
Brookfield viscosity	600 max	Cps
MST	1,800 min	Seconds

Fig. 2 Mixing process of polymer modified asphalt binder



2.3 Superpave Mix Design

Superpave mix design was performed in order to prepare HMA Superpave mixtures for the mix design of SP 19 mm. Superpave mix design procedure was used a test sample of 100 mm in diameter and 64 mm in height. 30 samples were prepared in order to determine the optimum binder content (OBC) for each mixture. The binder content was ranged from 5 to 7 % with 0.5 % increment. The major steps involved in volumetric testing and analysis process are selection of materials, selection of design asphalt content and evaluation of performance of the design mixture [9]. The design traffic level selected for this study was medium to high traffic of 3 to ≤ 30 million equivalent single axle loads (ESALs). For Superpave-designed mix, the acceptable volumetric properties at 4 % air void are based on the established Superpave criteria at design number of gyrations. The traffic load for medium to high roadway application in this study requires compaction parameters at initial compaction ($N_{\text{initial}} = 8$ gyrations), design compaction ($N_{\text{design}} = 100$ gyrations) and maximum compaction ($N_{\text{maximum}} = 160$ gyrations). The purpose of Superpave mix design is to determine the estimated asphalt content, $P_{b,\text{est}}$ to achieve 4 % air voids (96 % G_{mm}) at N_{design} . Selection of the design optimum binder content *consists* of varying the amount of asphalt binder in the design aggregate structure to obtain acceptable volumetric properties when compared to the established mixture criteria based on the SGC specimens with 4 % air voids. Each specimens was compacted to N_{design} gyrations and the volumetric properties, optimum binder content (OBC), voids in mineral aggregate (VMA), voids filled with aggregate (VFA), air voids (AV) and dust proportion (DP) of the mixtures were determined. Two different mixes were developed in this study; unmodified binder (UMB) mix and natural rubber polymer modified binder (NRMB) mix. The Superpave gradation developed for the mixtures is shown in Fig. 3.

2.4 Testing Procedure

Superpave volumetric design process requires the determination of the moisture susceptibility of the mix. Modified Lottman Test (AASHTO T283) and Boiling water test (ASTM D3625) were used to verify that the design trial mix formulated is susceptible to damage by moisture in the pavement. Moisture susceptibility test procedures measures the loss of strength or stiffness of an asphalt mix due to moisture induce damage.

The Modified Lottman test (AASHTO T283) is performed by compacting samples to an air void level of $7\% \pm 0.5\%$. Three samples are selected as a control and tested without moisture conditioning; and another three samples were selected to be conditioned by saturating with water at 70–80 % followed by immersing in water for 24 h at 60 °C in a water bath. The samples were then tested for indirect tensile strength (ITS) by loading the samples at constant head rate (50 mm/min vertical deformation at 25 °C) and maximum compressive force required to break the

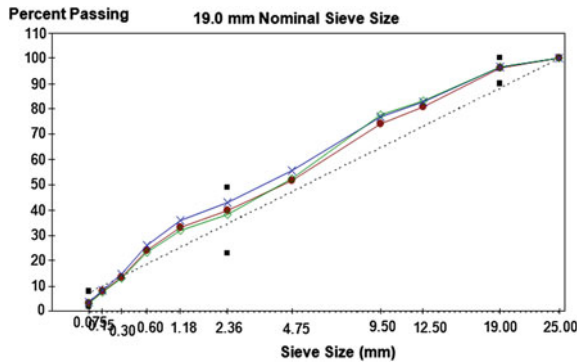


Fig. 3 Aggregate structure gradation

specimens were recorded. Tensile Strength Ratio (TSR) results were determined by comparing the indirect tensile strength (ITS) of unconditioned samples with the control samples. The Tensile Strength ratio (TSR) values in the test are an indication of the potential for moisture damage. Higher TSR value indicates greater resistance of the mix to moisture damage. Retained tensile strength ratio (TSR) was used with 80 % as the boundary between mixtures resistant and sensitive to moisture [10].

The boiling water test is one of the tests required to test for the stripping performance which is a subjective test for the effects that moisture has on a particular HMA mix. The test used primarily as an initial screening test of a HMA mix. Hence, this test also use for qualifying the polymer modifier to be incorporated into the asphalt cement to be used in asphalt mixtures. A loose mixture (passing a 9.5 mm sieve and retained on a 4.75 mm sieve) was placed in boiling water and was allowed to remain in the boiling water for 10 min. By observing the loose HMA in the water, the moisture damage was measured. The percentage rated as either above or below 95 % for the total visible area of the aggregate that retained its original coating of asphalt cement.

3 Results and Discussion

3.1 Determination of Aggregate Physical Properties

The aggregates were tested in terms of the sources of aggregate properties testing. In Superpave mix design, the aggregate source properties are critical in achieving high performance of HMA. Table 2 shows the results of the source aggregate properties testing. Results showed that the aggregate source properties are acceptable and fulfilled the Superpave mix design criteria. The flakiness and elongation index result is 3.1 and 16.6 % which meet the requirement of need to be lesser than criteria of 20 % based on ASTM D4791. While for the Aggregate Impact Value (AIV) and Abrasion test the result is 21.75 and 25.35 % which is the criteria is

Table 2 Summarizes of aggregate testing

Test method	Results (%)	Criteria (%)
Flakiness (ASTM D4791)	3.1	<20
Elongatio (ASTM D4791)	16.6	<20
Aggregate Impact Value (AASHTO T96)	21.75	<45
LA Abrassion (AASHTO T96)	25.35	<45

need for not more than 45 % required in ASHTO T 96. Thus, the aggregate from Blacktop quarry, Rawang can be used in Superpave mix design and also suitable for used in the road work. When all of the aggregate criteria are met, the materials selection process is considered completed.

3.2 Determination of the Volumetric Properties of HMA Mix Design

As mentioned earlier, Superpave mix designs were conducted to determine design binder content. Superpave specimens were prepared and tested according to AASHTO TP4 requirement and specification. Traffic level was selected based on common traffic level operating on most Malaysia highways. In this study, the traffic will be limited to medium to high roadway application. In Superpave system, medium to high traffic loadings is equivalent to between 3 and 30 million design equivalent single axle loads (ESALs) with 20 years design life. The design number of gyrations, $N_{\text{initial}} = 8$; $N_{\text{design}} = 100$; and $N_{\text{max}} = 160$ was used to vary the compactive effort of the design mixture and was a function of traffic level. Selection of design asphalt binder content was obtained based on 4 % air voids specimens. All other mixture properties were checked at the design binder content to verify that they meet the criteria. The volumetric properties of all mixtures were present in Table 3. Based on this result, it can be concluded that all the mixture properties meet the Superpave Criteria. The design binder content obtained for UMB is 5.7 and 5.1 % for NRMB.

The results show that the modification binder with natural rubber polymer give more accurate result for the %VMA and %VFA which is 15.1 and 73.5 which is lesser than control sample. For the dust proportion the modified binder result is 0.9 which followed the criterion which is between 0.6 and 1.2. While for percentage of theoretical maximum density (Gmm) is 85.9 % lesser than 89 % which is fulfill the requirement. The compaction of the mixtures to maximum number of gyrations, N_{max} which represents traffic greater than the design traffic is one of the important verification of the design asphalt binder content obtained. It is important for verification under the Superpave system to avoid and prevent mixture that will compact excessively under traffic become plastic and produce permanent deformation.

Table 3 Design mixture properties at asphalt binder content

Superpave mix design properties	UMB	NRMB	Criterion
Asphalt content (%)	5.7	5.1	–
Air voids (%)	4.0	4.0	4.0 %
VMA (%)	15.8	15.1	Min 13
VFA (%)	74.5	73.5	65–76
Dust Proportion	0.8	0.9	0.6–1.2
Gmm@Nini (%)	85.5	85.9	≤89

Figure 4 show the densification curves at the design binder content for both mixes. All mix types satisfy the Superpave criteria that shown from the densification curves that obviously indicated.

3.3 Determination of Moisture Susceptibility

Moisture susceptibility test procedures measures the loss of strength of an asphalt mix due to moisture induce damage. Results of the Modified Lottman test conducted on both mixtures are as shown in Table 4 and Fig. 5. Results showed that the average tensile strength values for all unconditioned samples were higher compared to conditioned specimens. At conditioned samples, the tensile strengths were 912 kPa for unmodified binder mix and 1,076 kPa for natural rubber polymer modified binder mixes. The results of indirect tensile strength of unconditioned samples showed a similar trend with the conditioned samples which showed the natural rubber modified binder has the highest indirect tensile strength values. From the TSR values, it clearly shows that the ratio unconditioned and conditioned samples for all mixes were greater than 80 % (AASHTO T283) and can be concluded that all mixes have resistance to moisture damage which could sustain the load from vehicles and exposed to severe condition without large degradation of the structure. NRMB mix which has TSR of 88 % showed the most significant effect to reduce stripping potential with 7 % higher TSR value compared UMB mix which has TSR of 81 %. This can be explained by incorporation of natural rubber (NR) polymer modified binder to bituminous mixes increase the strength. This was true because natural rubber polymer absorbs the binder that needed to coat the aggregate thus improving the stripping resistance.

Test results from ASTM D3625 testing procedure (Boiling water test) are shown in Table 5. This table indicates that all mixes tested showed less than 5 % coating loss, which showed greater than 95 % coating retained or in other words all mixes were resistance to moisture damage. However, the difference in percent of coated areas was small which is for NPMB is 98 % while for the UMB is 97 %. This result can show that NPMB mix has the highest value which indicates that the addition natural rubber polymer into the mix has significantly improved the pavement

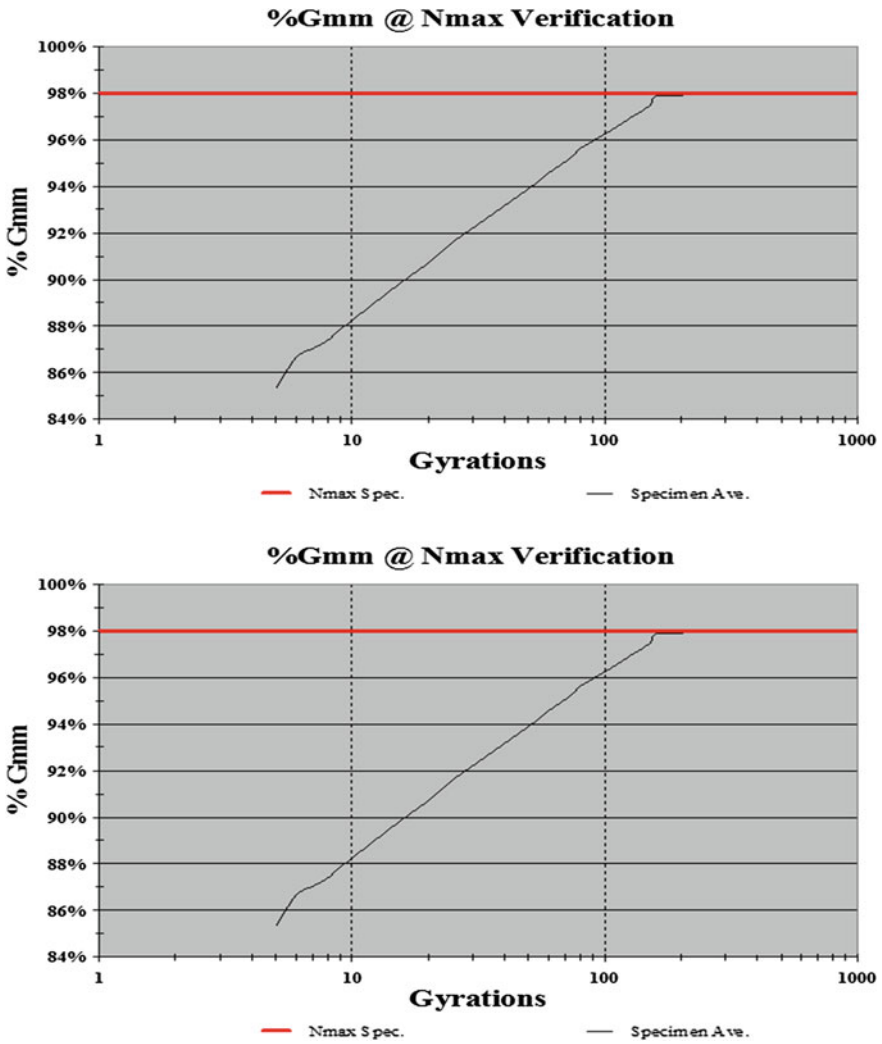


Fig. 4 The densification curves at the design binder content for both mixes

Table 4 Modified lottman test result

Superpave mixture design		UMB	NRMB
Unconditioned	Average air voids (%)	7.0	7.1
	Average tensile strength (KPa)	1,127	1,223
Conditioned	Average air voids (%)	7.0	6.9
	Saturation level (%)	72.7	74.3
	Average tensile strength (KPa)	912	1,076
	TSR	81.0	88.0

Fig. 5 Indirect tensile strength of conditioned and unconditioned samples for UMB and NRMB

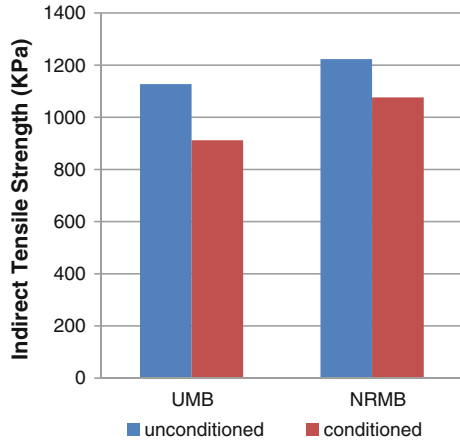


Table 5 Boiling water test results

Aggregate type	Mix type	Percentage retained coating (%)	Retained coating greater than 95 % (Yes/No)
Granite	UMB	97	Yes
	NPMB	98	Yes

performance. This test is very subjective and known to provide inconsistent results in terms of identifying moisture susceptibility mixtures. This is due to the test procedure which only needs observation and personal interpretation.

4 Conclusions

Based on the results obtained from this study, the following conclusions have been reached:

1. Local aggregates meet both Superpave consensus aggregate and sources aggregate requirement. It can be concluded that Blacktop quarry, Rawang has a good quality aggregate. Thus, the aggregates are acceptable and suitable for used in road works.
2. Locally aggregate gradations are suitable for Superpave mix design, since all mix design in accordance to Superpave system meet the Superpave requirements.
3. The TSR values are higher for NRMB mix compared to UMB mix, which somehow indicates that NR binder demonstrates better resistance to stripping than those prepared using Unmodified binder due to natural rubber polymer that were added to the binder coat the aggregate thus improving the stripping resistance.

4. The Boiling water test (ASTM D3625) method is a subjective test, however the results has shown to be consistent in term of identifying stripping quality of HMA mixes.

Thus, with addition of natural rubber polymer to the binder has significantly improved the cohesion as well as adhesion properties of the binder, and hence the performance to stripping.

Acknowledgments Special thanks to the Research Management Institute (RMI) of Universiti Teknologi MARA for providing the financial support under Excellent fund. The authors would like to thank the Faculty of Civil Engineering, Universiti Teknologi MARA Malaysia for providing the experimental facilities and to all technicians at Highway and Traffic Engineering Laboratory.

References

1. T. Kennedy, F. Roberts, K. Lee, in *Evaluating Moisture Susceptibility of Asphalt Mixtures Using the Texas Boiling Test*, Transportation Research Record 968, TRB, National Research Council, Washington, D.C., pp. 45–54, (1984)
2. F. Roberts, P. Kandhal, E. Brown, D. Lee, T. Kennedy, in *Hot Mix Asphalt Materials Mixture Design and Construction*, 2nd edn. (NAPA Education Foundation, Lanham, Maryland, 1996)
3. G. Polacco, Rheological properties of asphalt/SBS/clay blends. *Eur. Polymer J.* **44**(11), 3512–3521 (2008)
4. M.J. Fernando, M. Nadarajah, in *Use of Natural Rubber Latex in Road Construction, Polymer Modified Asphalt Binders*, ASTM STP 1108, ed by. K. R. Wardlaw, S. Shuler (American Society for Testing and Material, Philadelphia, 1992)
5. V. Nopparat, P. Jaratsri, N. Nuchanat, Modification of asphalt cement by natural rubber for pavement construction, *Rubber Thai J.* **1**, 32–39, (2012). Journal home page: www.rubberthai.com
6. T. Nrachai, P. Chayatan, L. Direk, The modification of asphalt with natural rubber latex. *Proc. Eastern Asia Soc. Transp. Stud.* **5**, 679–694 (2005)
7. G.D. Airey, Rheological evaluation of ethylene vinyl acetate polymer modified bitumen. *J. Constr. Build. Mater.* **16**, 473–487 (2002)
8. E. Shaffie, J. Ahmad, K. Arshad, D. Kamarun, A. Shafie, Effect of blending interaction on physical properties of natural rubber latex (NRL) modified asphalt binder, National Postgraduate Seminar, (2013)
9. R.B. McGennis, R.M. Anderson, T.W. Kennedy, M. Solaimanian, in Background of SUPERPAVE asphalt mixture design and analysis. Publication No. FHWA-SA-1995-003
10. R.P. Lottman, in *Predicting Moisture-Induced Damage to Asphaltic Concrete*. TRB, National Research Council, Washington, D.C, NCHRP Report 192: (1978)

Effect of Sintering Temperature on V₂O₅ Doped Barium Zinc Tantalate (BZT) Dielectric Properties

H. Jaafar

Abstract The structure and dielectric properties of Barium Zinc Tantalate (BZT) doped by vanadium pentoxide (V₂O₅) with a variety of values of mol% doping from 0, 0.1, 0.25, 1.0, 1.5 and 2.5 were prepared using a solid state method. The addition of V₂O₅ did not disturb the 1:2 ordering structure of the BZT ceramic. The grain size increased when the addition of doping increased. A small amount of doping elements increased the relative density. The dielectric constant (ϵ_r) value of the BZT significantly improved with the addition of the V₂O₅ for the specimens sintered at 1,300 °C and it could be explained by the increase of the relative density. The $\tan \delta$ of the V₂O₅ doped with BZT ceramics is lower than pure BZT ceramics, and decreases as the V₂O₅ content increases. Meanwhile, for the minimum return loss (dB), it is shown that the best result is produced when it is doped with 0.5 mol % V₂O₅ and sintered at 1,250 °C. The best microwave dielectric properties obtained are $\epsilon_r = 66.81$, $\tan \delta = 0.035$, minimum return loss = -50.23 which occur for the 0.5 mol% doped V₂O₅ and when sintered at 1,300 °C/4 h.

Keywords Barium zinc tantalite • Vanadium pentoxide • Phase formation • Surface morphology • Dielectric properties

1 Introduction

The formation of BZT materials into dense ceramic resonators with excellent dielectric properties requires very careful and demanding processing procedures because BZT is difficult to optimize on a commercial scale. This problem, which is related to the BZT production cost, is significant. The atomic scale structure of BZT depends on the processing conditions since they control the extent to which the

H. Jaafar (✉)

Faculty of Earth Science, Universiti Malaysia Kelantan, Jeli Campus, 17600 Jeli, Kelantan, Malaysia

e-mail: hidayani@umk.edu.my

octahedral B-sites of the parent of simple perovskite are occupied in an orderly manner by the Zn and Ta cations [1]. The most common method that is always used to produce complex perovskites is the solid state method. This method is the easiest method to produce BZT but it still has to deal with high sintering temperature (1,500–1,550 °C) and long soaking time (120 h) to produce very excellent dielectric properties [2]. Several researches have reported that by adding the dopants such as BaZrO₃ [3], Al₂O₃ [4], ZrO [5], TiO₂ [6], SnO₂ [7], BaWO₄ [8] into the BZT the sintering temperature can be reduced and the dielectric properties improved.

Kawashima et al. [9] further report that to achieve a perfect hexagonal structure at 1,350 °C it takes at least 120 h. However, Desu and O'Bryan [10] point out that there is another factor at work during these long sintering times, where weight loss tends to occur due to the loss of volatile ZnO. They note that the c^*/a^* ratio and ordering do not occur simultaneously in the data of Kawashima et al. [9] as would be expected if the only factor was ordering. They have suggested that the continuous c^*/a^* ratio after ordering is complete due to the loss of the ZnO. The loss of ZnO is greater on the surface compared with the bulk because of the slow diffusion rate of Zn through the dense ceramic.

The microwave dielectric properties of BZT are affected by their structure. The ordering of B site cations has influenced the Q values of BZT ceramics [11]. For pure BZT, high temperature for sintering is needed to achieve high Q values but sintering at temperatures above 1,500 °C leads to the volatilization of ZnO and also increases the cost of manufacturing. The escape of ZnO leads to poor densification and decreases the dielectric properties of BZT [2].

However, the effects of V₂O₅ doped BZT have yet to be reported before. Therefore, in this research, the microstructure and dielectric properties of V₂O₅ doped BZT ceramics are investigated.

2 Experimental

Pure BZT ceramics were doped with 0.1–2.5 mol% of V₂O₅, and prepared using the conventional solid state reaction method. High purity of raw materials BaCO₃ (>99 %, Merck, Darmstadt, Germany), ZnO (>99 %, Merck, Darmstadt, Germany) and Ta₂O₅ (>99 % Aldrich Chemical Co.) were weighted and mixed stoichiometrically with a zirconia ball for 3 h and calcined at 1,150 °C for 1 h. The calcination temperature was optimized based on the XRD analysis and surface morphology [12]. After refilling with V₂O₅ additive, the powder was dried and pressed into disc-shaped pellets with a diameter of 15 and 1 mm thickness at 125 Mpa and sintered at 1,200–1,350 °C for 4 h.

The crystal structure of the sintered pellets was studied by using an X-ray diffraction (XRD) using the Bruker D8 Advance with CuK α radiation (40 kV, 30 mA) a diffracted beam monochromator and a step scan mode with the step size of 0.1° and scan in the range of 10°–90° of 2 θ . The density was measured based on the Archimedes method. For the dielectric properties, the analysis was conducted

by using the HP4219B RF Impedance Analyzer (1 MHz–1 GHz). The selected samples will be measured for the actual antenna application using HP8720D Network Analyzer (50 MHz–20 GHz) to find the resonance frequency.

3 Results and Discussion

Generally, to determine the lowest sintering temperature, the temperature should be satisfied with some requirements such as the pellet should be in very good condition. Figure 1 shows the visual observation for sintering temperatures, which are at 1,200, 1,250, 1,300 and 1,350 °C doped with 0.1 mol% of V_2O_5 with 4 h of soaking. Figure 1 shows that the sintering temperature at 1,350 °C gives the poorest performance due to the broken pellets caused by the unsuitable temperature for these materials. Thus, the temperature 1,350 °C is not acceptable to be applied in this research. At the sintering temperature of 1,200 °C, the pellets formed a big crack on the surface and were not fully sintered due to the insufficient temperature to develop the desired structure and properties. Therefore, the sintering temperatures, which are at 1,250 and 1,300 °C are the most suitable to be applied in this research. The reason as to why these temperatures are acceptable is due to the fully sintered surface for every amount of dopant. Hence, 1,250 and 1,300 °C were applied in order to determine the effect of V_2O_5 dopants to BZT.

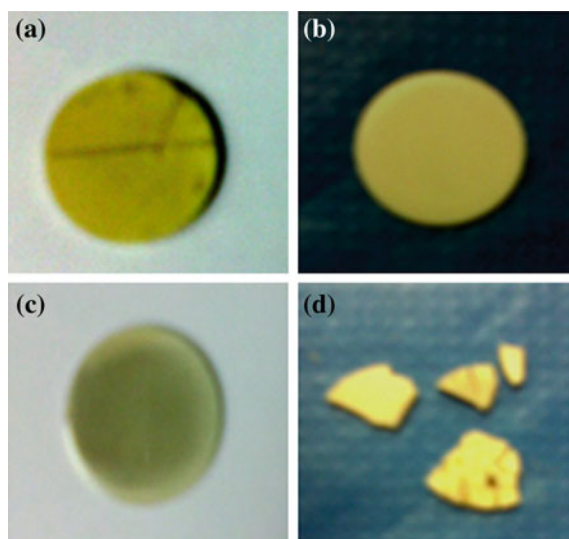


Fig. 1 BZT doped with V_2O_5 and sintered at **a** 1,200 °C **b** 1,250 °C **c** 1,300 °C **d** 1,350 °C

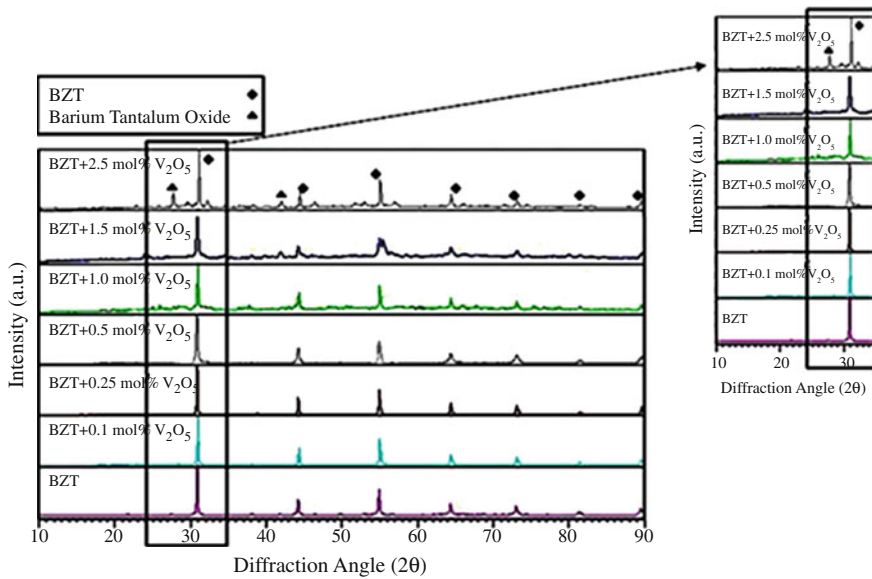
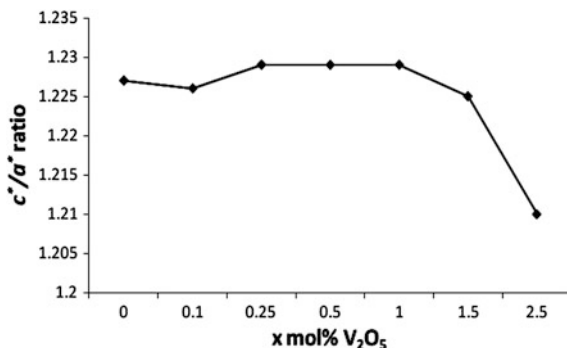


Fig. 2 XRD pattern for BZT with V_2O_5 dopant of 0, 0.1, 0.25, 0.5, 1.0, 1.5, and 2.5 mol%. Insert shows peaks at 24° – 42° of $2\theta^{\circ}$ for BZT, and V_2O_5

Figure 2 shows the XRD patterns of BZT + $x V_2O_5$ ceramics with $0 \text{ mol}\% \leq x \leq 2.5 \text{ mol}\%$ sintered at $1,300^{\circ}\text{C}$ for 4 h. In Fig. 2, the XRD analysis shows that the BZT was doped from 0.1 until 1.0 mol% with V_2O_5 , which formed a single phase of BZT and which causes the structure of this phase to be hexagonal. On the other hand, the BZT doped from 1.0 to 2.5 mol% V_2O_5 , had formed the second phase which is Barium Tantalum Oxide which might be formed due to the evaporation of ZnO during sintering. Although there is a second phase in 1.5–2.5 mol%, the hexagonal structure is maintained. This indicates that the doped V^{5+} ions occupied the B sites of the BZT lattice structure without changing the original structure of the BZT. The ionic radius of V^{5+} (0.054 nm) is smaller than that of Ta^{5+} (0.064 nm) and Zn^{2+} (0.074 nm). Therefore, since V^{5+} ion could enter either the Ta^{5+} and Zn^{2+} vacant site, the hexagonal structure and Barium Tantalum Oxide second phase were maintained.

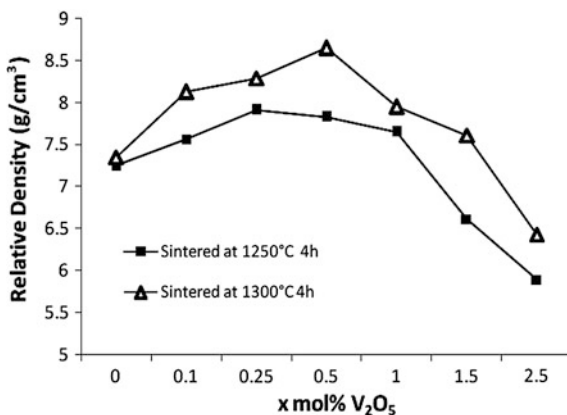
Figure 3 shows the change of the c^*/a^* ratio for doped BZT with V_2O_5 in every mol%. For the BZT doped V_2O_5 , the structure was hexagonal. Initially, when the mol% of V_2O_5 increased from 0 to 1.5 mol%, the lattice constant was constant with 1.229 and this was similar to the theoretical value of pure BZT [13]. Result shows that the arrangement of atom is in a hexagonal structure and indicates that V^{5+} ions had entered the unit cell and substituted either Zn^{2+} or Ta^{5+} ions without changing the structure of BZT. However, the lattice constant dropped from 1.229 to 1.21 at 1.5 mol% to 2.5 mol% V_2O_5 due to the formation of the second phase but the hexagonal structure still remained the same.

Fig. 3 Lattice constant for BZT + $x\text{V}_2\text{O}_5$ sintered at 1,300 °C for 4 h



The relative densities of the BZT + $x\text{V}_2\text{O}_5$ ceramics with $0.0 \text{ mol}\% \leq x \leq 2.5 \text{ mol}\%$ as a function of V_2O_5 are illustrated in Fig. 4. Relative density sintered at 1,300 °C was higher than that at 1,250 °C. BZT + $x\text{V}_2\text{O}_5$ that sintered at 1,300 °C increased with the increasing V_2O_5 content. After reaching a maximum value of 0.5 mol% V_2O_5 , the densities of ceramic decreased with the amount of V_2O_5 increasing from 1.0 to 2.5 mol% V_2O_5 at 1,300 °C. The density when doped with 0.1 until 0.5 mol% V_2O_5 and sintered at 1,300 °C was higher than the theoretical density (theoretical density of BZT is 7.92 g/cm^3). The density that increased with the addition of small amount of dopants is attributed to the growth of grains at lower sintering temperature and improves the densification of doped BZT. The decrease in density at high amount of dopants may be attributed to the existence of the secondary phase of the doped BZT. For the specimens sintered at 1,250 °C, the relative density slightly increased with the addition of V_2O_5 but significantly decreased when V_2O_5 content increased. However, the value of BZT + $x\text{V}_2\text{O}_5$ that sintered at 1,250 °C was lower than the theoretical density. Generally, the effectiveness of the sintering aids depended on several factors such as the sintering temperature, viscosity and solubility [14].

Fig. 4 The variation of the relative density with V_2O_5 for BZT ceramics sintered at various sintering temperatures for 4 h



The SEM micrographs of the specimens using V_2O_5 -doped BZT ceramics at different mol% of V_2O_5 sintered at $1,300\text{ }^\circ\text{C}$ and with 4 h soaking time are illustrated in Fig. 5. 0 mol% of BZT + xV_2O_5 had produced the grain size with an average of approximately $1.43\text{ }\mu\text{m}$. The level of porosity for the doped BZT, then became lower when the V_2O_5 , was added and the grain size was denser and this gives a compacted microstructure. This observation in the porosity and level of sintering from the FESEM seems to be parallel with the observation from the density analysis. By doping with 0.1 mol%, the structures became denser with fewer pores, compared to the pure BZT. The grain sizes also decreased to $0.4\text{ }\mu\text{m}$ for (BZT + 0.1 mol% V_2O_5). The results further reveal that a small amount of V_2O_5 gives an effect on the size reduction, acts as a good grain growth inhibitor and leads to the grains being well-formed. The size distribution of the doped BZT ceramics was predominantly determined by the amount of the V_2O_5 addition. The increasing

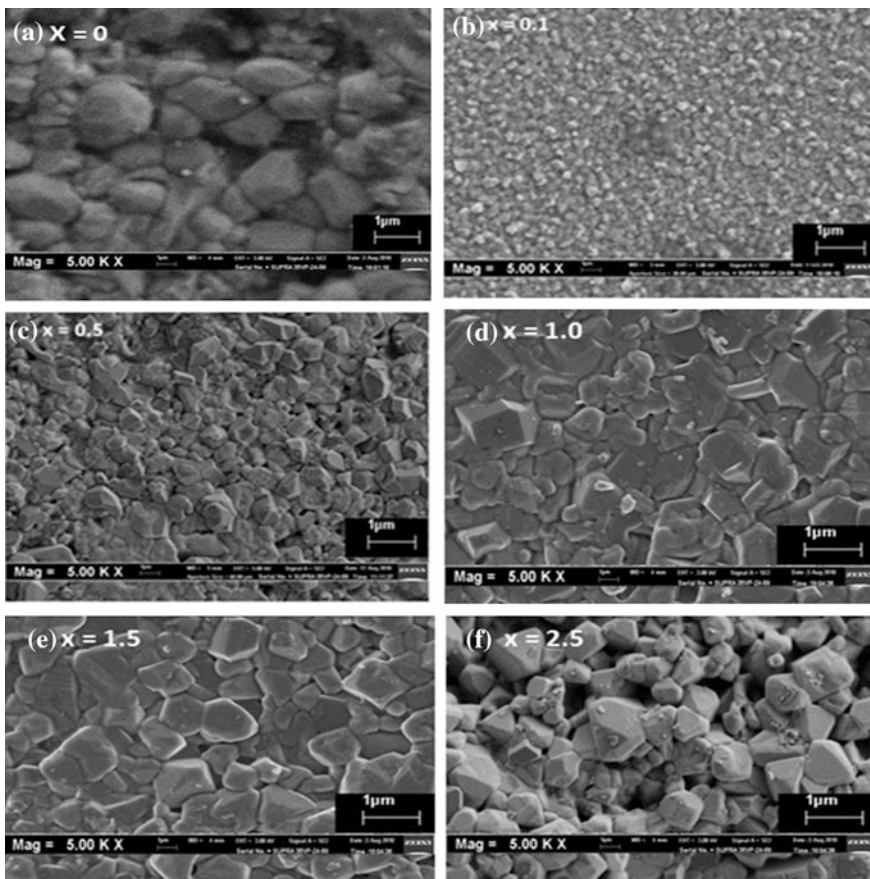


Fig. 5 The SEM micrograph of BZT + xV_2O_5 for different mol%. **a** $x = 0$, **b** $x = 0.1$, **c** $x = 0.5$, **d** $x = 1.0$, **e** $x = 1.5$, **f** $x = 2.5$ sintered at $1,300\text{ }^\circ\text{C}$ for 4 h

amount of mol% of V_2O_5 caused the grains to turn from circle to rod-like grains and the grain size grew larger. The growth formation of the rod-like grains indicates that the grains grew with the help of the liquid phase sintering temperature [15]. It was also caused by the agglomeration of the grain in order to minimize the surface area during sintering. Even though the coarse grain materials generally give the result in porous bodies, grain materials that are too fine are also expected to show a similar result. If a distribution of grain size is considered, the ideal densification of the system might be reached through an optimal mixture of coarse and fine grains. The doping element with ionic radius close to the B-site ions leads to the increased grain growth and improves the microwave dielectric properties of the sintered $BZT + xV_2O_5$ ceramic. The influence of the microstructures has been visualized by means of monitoring the dielectric properties of various V-doped BZT ceramics.

The dielectric constant (ϵ_r) for undoped and V-doped BZT ceramics at room temperature is shown in Fig. 6. The relationship between ϵ_r values of $BZT + xV_2O_5$ and sintering temperatures presents a trend similar to that between the densities and SEM micrographs, since a higher density means a lower porosity. The ϵ_r increased slightly with the increasing mol% V_2O_5 . The increase in the ϵ_r value could be explained by the higher densities. Further addition of mol% V_2O_5 , decreased the dielectric constant due to the formation of second phases and resulted in density reduction.

Figure 7 shows the variation of $\tan \delta$ with pure BZT and BZT doped with 0.1 to 2.5 mol% of V_2O_5 . For the BZT sintered at 1,300 °C, the $\tan \delta$ value was about 0.05 and decreased with the addition of V_2O_5 , and it illustrated a minimum value when $x = 0.5$ mol%. This trend is also similar to $BZT + xV_2O_5$ that sintered at 1,250 °C. The $\tan \delta$ value increased when the mol% of V_2O_5 increased from 1.0 to 2.5 mol% for both temperatures. The $\tan \delta$ increased until 0.5 mol% and decreased with the addition of V_2O_5 because of the formation of secondary phases as shown in Fig. 2, even though the hexagonal structure did not change. The

Fig. 6 Variation of the ϵ_r with V_2O_5 for BZT ceramics sintered at various sintering temperatures for 4 h

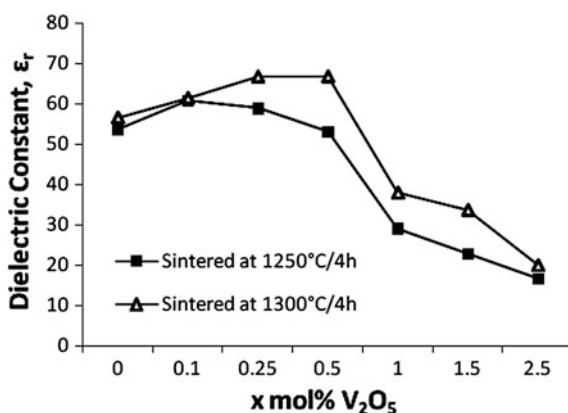
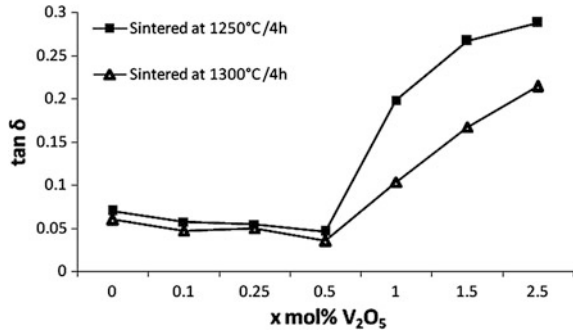


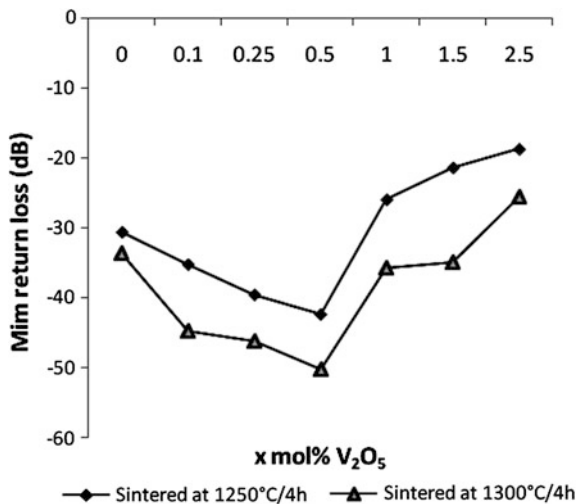
Fig. 7 Variation of the $\tan \delta$ with V_2O_5 for BZT ceramics sintered at various sintering temperatures for 4 h



enhancement of the $\tan \delta$ value could be explained by the increased relative density. The specimen exhibited the highest $\tan \delta$ value when the grain growth was completed. Therefore, the increased grain size was also very important for the improvement of the $\tan \delta$ value.

The function of minimum return loss is to determine the effectiveness of the resonator function to receive and transmit effective signal. The minimum return loss value of BZT + xV_2O_5 ceramics with $0.0 \text{ mol}\% \leq x \leq 2.5 \text{ mol}\%$ is illustrated in Fig. 8. It appears that, the minimum return loss for the sample that sintered at 1,250 °C was higher compared to that at 1,300 °C. The sample with $x = 0.5 \text{ mol}\%$ that sintered at 1,300 °C showed the lowest minimum return loss value, -50.23 dB. However, based on the result, it shows that the reduction of the minimum return loss values indicates that these doped BZTs can minimize the return loss during the operation. This suggests that (BZT + V_2O_5) materials would have a very high level of efficiency in a telecommunication system.

Fig. 8 Variation of the minimum return loss with V_2O_5 for BZT ceramics sintered at various sintering temperatures for 4 h



4 Conclusion

Microstructure and microwave dielectric properties of BZT + $x\text{V}_2\text{O}_5$ ceramics with $0.0 \text{ mol}\% \leq x \leq 2.5 \text{ mol}\%$ were investigated. BZT has a 1.229 lattice constant which is in the form of a hexagonal structure. The addition of V_2O_5 did not change the hexagonal structure despite the existence of the secondary phase. The signature of the V_2O_5 doping was also observed in the grain size lowering of the BZT ceramics, which is one of the factors in the variation of dielectric properties. On the other hand, the relative density increased and grain growth occurred when a small amount of V_2O_5 was added. Therefore, the increased relative density and grain size could be responsible for the improvement of the dielectric properties. The ϵ_r value of the BZT had significantly increased with the addition of V_2O_5 . The increased ϵ_r value could be related to the increased relative density and grain size. Meanwhile, the $\tan \delta$ of the V_2O_5 -doped BZT ceramics was observed to be lower than that of pure BZT ceramics and decreased as the V_2O_5 content increased. Minimum return loss also decreased when V_2O_5 was doped into BZT. As a conclusion, by doping the BZT with V_2O_5 respectively, the multiphase DR ceramics fabricated in this research can be manufactured with high dielectric properties, as compared to the pure BZT.

References

1. M. Bieringer, M. Sandra, D. Liam, Cation ordering, domain growth, and zinc loss in the microwave dielectric oxide $\text{Ba}(\text{Zn}_{1/3}\text{Ta}_{2/3})\text{O}_3$. *Chem. Mater.* **15**, 586–597 (2003)
2. M.T. Sebastian, *Dielectric Materials for Wireless Communication*. (Elsevier Ltd., Amsterdam, 2008)
3. P.K. Davies, J. Tong, T. Nega, Effect of ordering induced domain boundaries on low loss $\text{Ba}(\text{Zn}_{1/3}\text{Ta}_{2/3})\text{O}_3$ — BaZrO_3 perovskite microwave dielectrics. *J. Am. Ceram. Soc.* **80**, 1727–1740 (1997)
4. M.H. Kim, S. Nahm, W.S. Lee, M.J. Yoo, J.C. Park, H.J. Lee, Effect of microstructure on microwave dielectric properties of Al_2O_3 added $\text{Ba}(\text{Zn}_{1/3}\text{Ta}_{2/3})\text{O}_3$ ceramics. *Jpn. J. Appl. Phys.* **43**, 1438–1441 (2004)
5. J.I. Yang, S. Nahm, C.H. Choi, H.J. Lee, H.M. Park, Microstructure and microwave dielectric properties of $\text{Ba}(\text{Zn}_{1/3}\text{Ta}_{2/3})\text{O}_3$ with ZrO_2 addition. *J. Am. Ceram. Soc.* **85**, 165–168 (2002)
6. M.H. Kim, S. Nahm, W.S. Lee, M.J. Yoo, N.G. Gang, H.J. Lee, Structural variation and microwave dielectric properties of TiO_2 added $\text{Ba}(\text{Zn}_{1/3}\text{Ta}_{2/3})\text{O}_3$. *J. Eur. Ceram. Soc.* **24**, 3547–3552 (2004)
7. H.K. Kim, B.J. Kim, S. Nahm, W.S. Lee, M.J. Yoo, N.K. Kang, H.J. Lee, Y.S. Kim, S.Y. Ryon, Microstructure and microwave dielectric properties of SnO_2 added $\text{Ba}(\text{Zn}_{1/3}\text{Ta}_{2/3})\text{O}_3$ ceramics. *Jpn. J. Appl. Phys.* **43**, 4259–4262 (2004)
8. J.S. Kim, J.W. Kim, C.I. Cheon, Y.S. Kim, S. Nahm, J.D. Byun, Effect of chemical element doping and sintering atmosphere on the microwave dielectric properties of barium zinc tantalates. *J. Eur. Ceram. Soc.* **21**, 2599–2604 (2001)
9. I. Kawashima, H. Ozawa, M. Kotani, M. Suzuki, T. Kawano, M. Gomibuchi, T. Tai, Characterization of ganglioside expression in human melanoma cells: immunological and biochemical analysis. *J. Biochem* **114**, 186–193 (1993)

10. S. Desu, H. O'Bryan, Microwave loss quality of $\text{Ba}(\text{Zn}_{1/3}\text{Ta}_{2/3})\text{O}_3$ ceramics. *J. Ameri Ceram. Soc.* **68**(10), 546–551 (1985)
11. M.R. Varma, S. Biju, M.T. Sebastian, Preparation of phase pure $\text{Ba}(\text{Zn}_{1/3}\text{Ta}_{2/3})\text{O}_3$ nanopowders for microwave dielectric resonator applications. *J. Eur. Ceram. Soc.* **26**, 1903–1907 (2006)
12. H. Jaafar, Z.A. Ahmad, F. Ain, Effects of calcination temperature on the phase formation and microstructure of barium zinc tantalate. *Adv. Mater. Res.* **173**, 61–66 (2011)
13. M. Lufasso, Crystal structures, modeling and dielectric property relationship of 2:1 ordered $\text{Ba}_3\text{MM}'_2\text{O}_9$ (M= Mg, Zn, Ni; M0= Nb, Ta) perovskites. *Chem. Mater.* **16**, 2148–2156 (2004)
14. X. Lin, L. Zhao, M. Zhao, Effects of V_2O_5 addition on the phase-structure and dielectric properties of zinc titanate ceramics. *J. Electroceram.* **18**, 103–109 (2007)
15. J. Wang, Z. Yue, J. Yan, Z. Gui, Effects of $\text{ZnO}-x\text{V}_2\text{O}_5$ substitution on the microstructure and microwave dielectric properties of ZnNb_2O_6 ceramics. *J. Electroceramics* **21**, 116–119 (2008)

Fabrication of a-C:B/n-Si Solar Cells with Low Positive Bias by Using Palm Oil Precursor

A. Ishak, K. Dayana, I. Saurdi and M. Rusop

Abstract Boron doped amorphous carbon (a-C:B) film for heterojunction carbon-based photovoltaic solar cells were successfully fabricated on n-type silicon using palm oil precursor by the influenced of low positive bias voltage in the range of 0–50 V. The rectifying curve were found for all samples under dark measurement revealed that those samples were p-type semiconductor. The +30 V was found the optimized of the electronic properties with the open circuit voltage, current density, fill factor and efficiency were approximately 0.259034 V, 1.299456 mA/cm², 0.240011 and 0.080788 %, respectively. The conversion efficiency of a-C:B has been improved under the influenced of low positive bias.

Keywords Amorphous carbon · Palm-oil · Positive bias · Boron · Pyrolysis-CVD · Carbon solar cell

1 Introduction

Renewable precursors such as camphor powder, turpentine oil, coconut oil have been used for synthesise many diversity of carbon instead of non-renewable precursor [1–3]. Beside of those precursors, palm oil the other abundantly promising

A. Ishak (✉) · K. Dayana · I. Saurdi · M. Rusop
NANO-ElecTronic Centre (NET), Faculty of Electrical Engineering,
Universiti Teknologi MARA (UiTM), Shah Alam, Selangor, Malaysia
e-mail: ishak@sarawak.uitm.edu.my

A. Ishak · I. Saurdi
Faculty of Electrical Engineering, UiTM Sarawak Kampus, Kota Samarahan,
Jalan Meranek, Sarawak, Malaysia

M. Rusop
NANO-SciTech Centre (NST), Institute of Science, Universiti Teknologi MARA (UiTM),
Shah Alam, Selangor, Malaysia
e-mail: rusop@salam.uitm.edu.my

'green' source was successfully synthesized the carbon nanotube (CNT) [1–3]. Palm oil is scientifically known as hexadecanoic acid which was derived from fibrous exocarp and mesocarp of the fruits of palm tree [2–4]. The palm oil is contained carbon (67), hydrogen (127) and oxygen (8) to form the chemical binding of $C_{67}H_{127}O_8$ (3). If optimize energy were used for break down the binding, high number of carbon (67) will be released. Dc bias either positive or negative were reported by others groups in helping to accelerate particles through bombarding process [5, 6]. The DC bias tried to attract the opposite charge atom and repel the equalize charge being reach on the substrate [7, 8]. As a result, the chamber under deposition will be dominated by negative charge of carbon and boron atoms rather than unwanted particles thereby could minimize the other particles from being deposited on the surface of substrate.

The present of amorphous carbon (a-C) in CNT has brought the negative effect of CNT production, it has benefited to the other area in semiconductor industry especially for fabricated carbon-based photovoltaic solar cell by the ability to be a semiconductive material [9, 10]. However, undoped a-C was reported as a weakly p-type [10, 11] in nature despite of complex structure, high density of defect which restricted to dope efficiently and those factors were the main barrier for its application in various electronic devices. As such, it was hypothesis that by properly control the doping the existing of defect could be reduced and at the same time could be modified the electronic properties.

In this paper, the carbon-based solar cell of boron doped amorphous carbon (Au/a-C:B/n-Si/Au) were fabricated on the n-type silicon using low positive bias from 0 to +50 V. There are less study on low positive bias for fabricated Au/a-C:B/n-Si/Au solar cell using palm oil precursor. To the best of our knowledge, none of the report on the use of 'green' source from palm oil fabricated by low positive bias for Au/a-C:B/n-Si/Au carbon-based photovoltaic solar cell.

2 Experimental Details

The influenced of low positive bias on boron doped (a-C:B) a-C solar cells were deposited by using bias-assisted pyrolysis-CVD onto the corning glass substrates (thickness: 1 mm) and n-Si (100) (thickness $325 \pm 25 \mu\text{m}$, resistivity 1–10 $\Omega \text{ cm}$). Substrates (glass and n-silicon) were together cleaned with acetone (C_5H_6O) followed by methanol (CH_3OH) for 15 min in Ultrasonic Cleaner (power Sonic 405), respectively and the glass substrates were then rinse with DI water for 15 min. However, excess oxide layers of n-type silicon substrates were continued by the etching process with diluted hydrofluoric acid (10 %) solution for about 2 min before rinsing in DI water. Substrates were then blown with nitrogen gas. The cleaned of glass and silicon substrate was finally attached inside the chamber as shown Fig. 1.

The deposition temperature was set at 325 °C for 1 h deposition. A liquid palm oil precursor was heated outside the chamber at 150 °C by using hot platter (Stuart

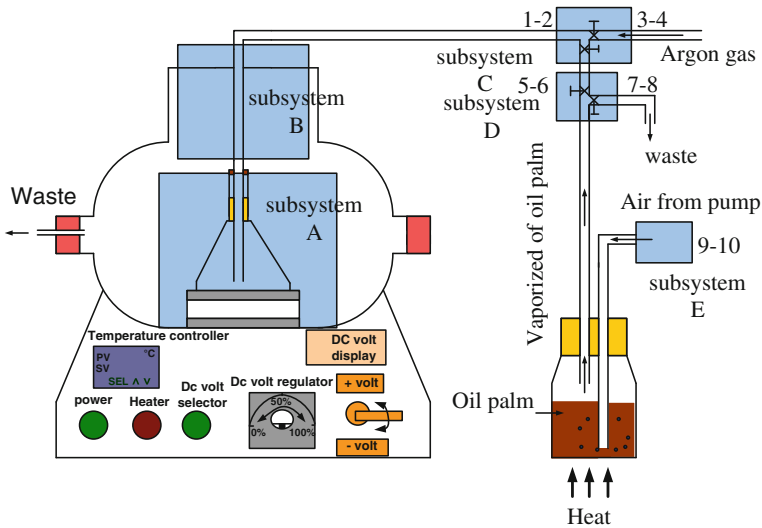


Fig. 1 The schematic diagram of bias assisted pyrolysis-CVD

CB162). The vaporized of palm oil was then pressured into the chamber by using aquarium air pumps (GA8000). The amount of vaporized palm oil, carrier gas argon used into were set to be constant at 114, 200 mL/min, respectively. For doping process, 160 mg of boron was placed on the heater metal plate by using aluminium foil. The positive bias is varied in the range of +10 to +50 V. The zero bias is also fabricated and used as a reference.

In the measurement of solar cell device, both sided of silicon (bottom and top) is deposited with approximately 60 and 12 nm of gold, respectively. The gold contact of 60 nm were sputtered at the top of 12 nm gold for conform the point of probe is properly contacted on the gold metal contact. The light closure is attached at the top of the device as shown in Fig. 2 to ensure light strike only the area of 2 cm². The other probe is connected to the conductive metal holder as shown in Fig. 2.

Solar simulator (Bukuh Keiki EP200), surface profiler (Veeco Dektak 150), JASCO UV-VIS/NIR Spectrophotometer (V-670 EX) and Park system XE-100 atomic force microscope (AFM) to characterize the electronic and optical properties.

3 Result and Discussion

3.1 Current Density-Voltage Characteristic Under Dark

Figure 3 shows the current density voltage (J-V) characteristics of the solar cell under dark at 100 mW/cm² using AM 1.5 solar simulator fabricated by low positive

Fig. 2 The measurement technique of Au/a-C:B/n-Si/Au solar cell

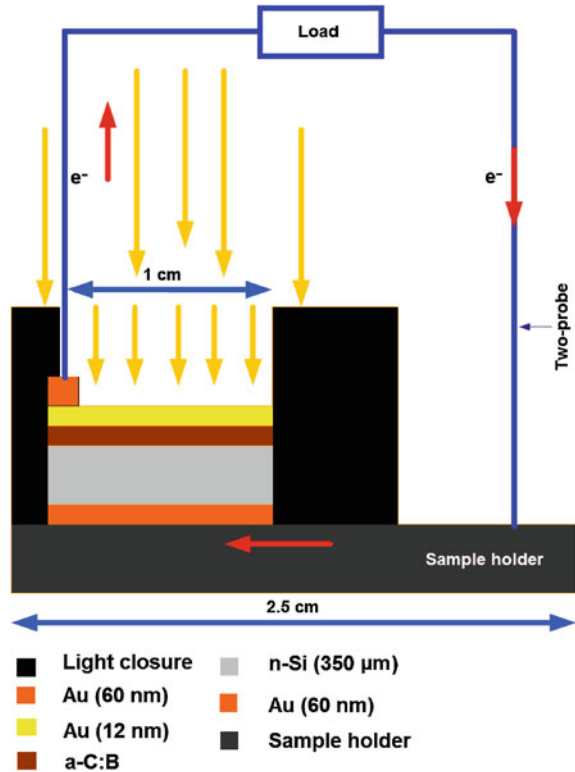
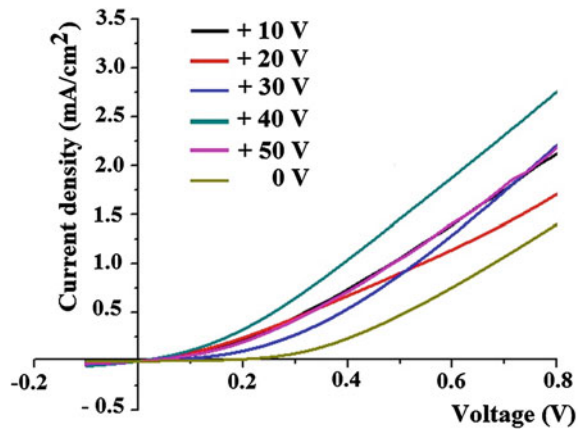
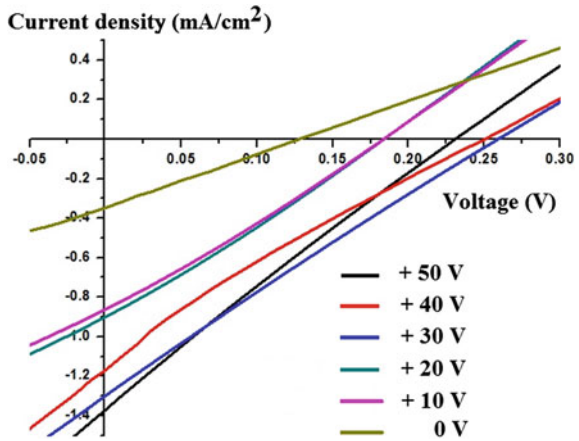


Fig. 3 The current-voltage characteristics under of Au/a-C:B/n-Si/Au under dark at different positive bias voltage



bias voltage. The rectifying curve are found for J-V characteristics for all samples of heterojunction carbon-based solar cell. We predicted, the diode formation is came from the different layer of n-type Si and p-type a-C:B. The a-C:B layer acted as a

Fig. 4 The current density-voltage characteristics of the working curve of the Au/a-C: B/n-Si/Au solar cell fabricated with positive bias voltage



p-type while silicon substrate acted as an n-type which formed the rectifying behaviour. The same trend behaviour of heterojunction carbon solar cell were obtained by others but fabricated using different method and precursor [12–14]. Beside forming of diode behaviour, precursor of palm oil has a good potential in fabricated photovoltaic carbon solar cell in the near future as proved in Fig. 4 where various level of working curve are present.

3.2 Current Density-Voltage Characteristic Under Illumination

The light illuminated J-V characteristics of heterojunction carbon solar cell fabricated by low positive bias voltage using palm oil precursor is shown in Fig. 4. The photo current and open circuit voltage are found varied under the influenced of low positive bias voltage as depicted in Fig. 4. The curves of all solar cell devices by our configuration is less broaden and more to a straight line curve compared with ideal solar cell. This phenomena is attributed from the series and shunt resistance from the material and metal contact configuration which significantly affect the solar cell devices. The high series resistance gives rise to the voltage drop and therefore minimize the full photovoltaic voltage across the load. The shunt resistance on the otherhand, deviate some part of the current from generated carriers and therefore deteriorate the photo current density J_{sc} .

The electronic properties are summarized in Table 1. The efficiency of boron doped fabricated without the used of low positive bias has found lower as compared with low positive bias where its open-circuit voltage (V_{OC}), current density (J_{SC}), fill factor (FF) and efficiency (%) are 0.127516 V, 0.346546 mA/cm², 0.254029 and 0.011225 %, respectively. The electronic properties of boron doped fabricated by low positive bias in the range of +10 to +50 V are shown in Table 1. The optimize

Table 1 The electronic properties of boron-doped a-c solar cell fabricated with low positive bias voltage

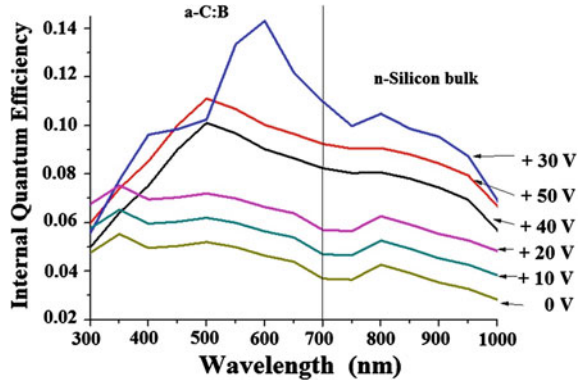
Positive bias (V)	Open circuit voltage (V_{OC})	Current density (mA/cm^2)	Fill-factor (FF)	Conversion efficiency (%)
0	0.127516	0.346546	0.254029	0.011225
+10	0.183422	0.861707	0.270101	0.042691
+20	0.184036	0.946730	0.273165	0.047594
+30	0.259034	1.299456	0.240011	0.080788
+40	0.250352	1.169343	0.217392	0.063641
+50	0.231440	1.321446	0.238328	0.078289

efficiency is found at +30 V where its V_{OC} , J_{SC} , FF, % is 0.259034 V, 1.299456 mA/cm^2 , 0.240011, and 0.080788 %. We found, convention efficiency has been improved under the influenced of low negative bias. Low values of V_{OC} , and J_{SC} are believed from low built-in voltage which caused by defects in a-C:B thin film and thus influenced the shorter lifetime and diffusion length and movement of drift carriers. The drift of carriers by built-in electric field plays an important role in cells [12–14]. Less of drift carriers might be due to the smaller built in voltage and therefore electron-hole pairs generated are recombined near surface. The shorter lifetime of excess carriers and diffusion length are responsible for the low photocurrent [13–15]. The existing of weakly pi (π) [15–17] bond are easy to be broken and therefore, form high density of intrinsic defect. Furthermore, boron will induce high concentration boron defect [15, 16]. All these defect will introduce deep state in the gap, and as a result, the lifetime of minority carriers and diffusion length will be reduced, which in turn reduce the photocurrent density.

3.3 External Quantum Efficiency

Figure 5 shows spectral response of boron doped a-C solar cell fabricated from 0 to +50 V using palm oil precursor. The highest spectral response is at sample of +30 V while the lowest is at sample of 0 V. The highest spectral response is supported by the highest convention efficiency as shown in Table 1 and Fig. 4. We found all samples fabricated with low negative bias has higher spectral response compared without low negative bias. Although solar cell properties are low, our objective is to clarify the function of boron and successfully vaporized of palm oil used as a precursor. The spectral response indicates two broad bands at the peak wavelength approximately 550 and 720 nm. It was reported that the wavelength above 700 nm is negligible since the photocurrent is mostly generated in the silicon substrate [15, 16, 18]. In the region below 700 nm, we predicted the boron doped layers act as carbon photon absorber, and quantum efficiency has a peak in short wavelength region. The photo current peak at approximately 550 nm is good agreement with the

Fig. 5 Spectral response of a-C:B solar cell fabricated with low positive bias voltage

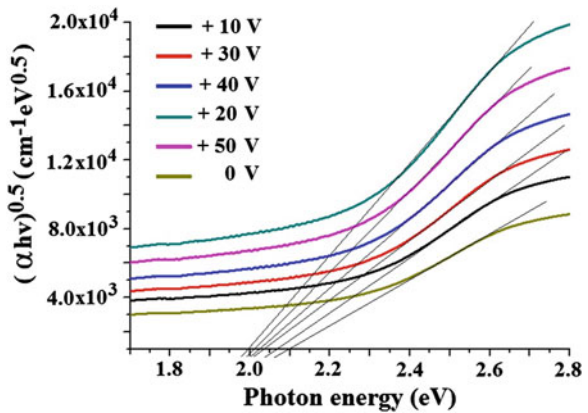


optical band gap measurement of boron doped thin film. We conclude the observed responses in the wavelength range from 300 to 700 nm are characteristics of the a-C:B cells.

3.4 Optical Properties

The optical properties of thin films are investigated by UV-visible spectroscopy measurements using the films deposited on glass substrates in the wavelength in the range of 200–1200 nm, to derive the Tauc optical band gap (E_g) for amorphous semiconductors [18, 19]. The E_g of the thin films is obtained from the extrapolation of the linear part of the curve at the $\alpha = 0$, using the Tauc relation, $(\alpha h\nu)^{1/2} = B_2(E_g - h\nu)$, where B_2 is the Tauc parameter. The estimated E_g of a-C:B is approximately in the

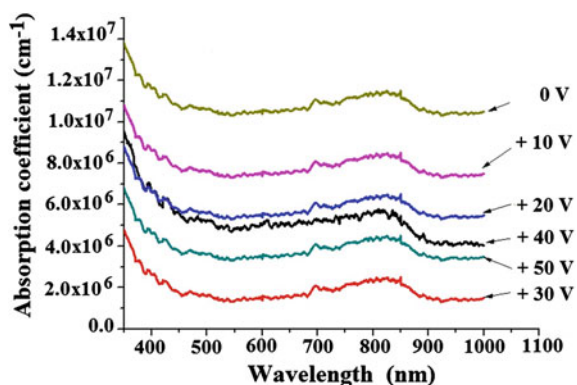
Fig. 6 The optical band gap of a-C:B thin film deposited with low positive bias voltage



range of 1.8 to 2.1 eV as shown in Fig. 6. The boron doped a-C thin film deposited by low positive bias decreased gradually the E_g from 2.1 to 1.8 eV. The interstitial doping of boron (B) in a-C films through modification of C-B bonding configurations might caused the changing of E_g . The declined in E_g by low positive bias voltage may be indicated an increase of tetrahedral (sp^3) fraction due to graphitization of the a-C:B film which is probably induced by B content in the film similar to the high nitrogen content in the film induce graphitization in nitrogen doped thin films [6, 20]. The values of these E_g were a good agreement why the spectral response and efficiency of boron doped with low positive bias have higher than without the use of low negative bias. The E_g of carbon solar cell by low positive bias are in the range of optimum E_g of solar cell (1 to 2 eV). None of the report of E_g by using this method and precursor have been found in the literature. However, the decreasing of E_g due to other parameters such as the percentage of dopants, (nitrogen and phosphorous), and deposition temperatures have been reported by others [19, 20].

The absorption coefficient of a-C:B thin film deposited with low positive bias voltage in the range of 0 to +50 V is shown in Fig. 7. The results show all a-C:B films are responded with the photon energy at difference absorption distance for generating of minority carriers when reach the depletion region. The Aurum (Au) electrode films was high absorption coefficient (α) of about 2.4×10^5 to $5.3 \times 10^5 \text{ cm}^{-1}$ in the lower wavelength region [12, 13]. All a-C:B thin films have high α from 2.0×10^6 to 1.2×10^7 compared with Au and therefore, photon incident on the front surface of a-C:B thin films might be strongly absorbed by the Au electrode rather than a-C:B. As a result, most part of the generated electron-hole pairs are recombined in the surface and only a few of them can arrive at depletion region. The low external quantum efficiency and high α in lower wavelength region of the Au electrode, a-C:B are taught to be responsible for low external quantum efficiency and conversion efficiency of a-C:b/n-Si solar cells.

Fig. 7 The absorption coefficient of a-C:B thin film deposited with low positive bias voltage



4 Conclusion

The a-C:B heterojunction carbon solar cell has been successfully fabricated using palm oil as precursor under the influenced of low positive bias. Although the conversion efficiency is still low, it has shown that there is the possibility of the improvement of the efficiency of the a-C:B/n-Si heterojunction photovoltaic solar cells by optimizing the deposition conditions. The electronic properties of a-C:B heterojunction carbon solar cell were improved when deposited with low positive bias. The optimum a-C:B/n-Si was found at +30 V where the V_{OC} , J_{SC} , FF, and η were 0.259034 V, 1.299456 mA/cm², 0.240011, and 0.080788 %, respectively. The optical band gap of a-C:B at 0 V is approximately 2.1 eV and slightly drop to be 1.85 eV under negative bias deposition. Deposition with low negative bias were improved the electronic properties of a-C:B as well as optical band gap of a-C:B thin film. The results would encourage the future prospects of clean, low-cost and reasonably high efficiency carbon solar cells. Further studies on the junction properties of a-C:B/n-Si structure is still under progress.

Acknowledgments Authors are grateful for Ministry of Higher Education Malaysia and faculty of electrical engineering UiTM sarawak for the scholarships and study leave. The authors are also thankful to the staffs of NANO-ElecTronic Center (NET) and NANO-SciTech Centre of Universiti Teknologi MARA, UiTM for equipment and facilities.

References

1. K. Ghosh, M. Kumar, T. Maruyama, Y. Ando, Micro-structural electron-spectroscopic and field-emission studies of carbon nitride nanotubes grown from cage-like and linear carbon sources. *Carbon* **47**, 1565–1575 (2009)
2. A.B. Suriani, A.A. Azira, S.F. Nik, R.M. Nor, M. Rusop, Synthesis of vertically aligned carbon nanotubes using natural palm oil as carbon precursor. *Mat. Lett.* **63**, 2704–2706 (2009)
3. P. Ghosh, T. Soga, R.A. Afre, T. Jimbo, Simplified synthesis of single-walled carbon nanotubes from a botanical hydrocarbon: turpentine oil. *J. Alloy. Compd.* **462**, 289–293 (2008)
4. S. Paul, S.K. Samdarshi, A green precursor for carbon nanotube synthesis. *New Carbon Mater.* **26**, 85–88 (2011)
5. A. Ishak, K. Dayana, M. Rusop, Surface morphology and compositional analysis of undoped amorphous carbon thin films via bias assisted pyrolysis-CVD. *Adv. Mat. Res.* **667**, 468–476 (2013)
6. M. Rusop, S.M. Mominuzzaman, T. Soga, T. Jimbu, M. Umeno, Nitrogen doping in champletic carbon films and its application to photovoltaic cell. *Surf. Rev. Lett.* **12**, 35–39 (2005)
7. H. Zhu, J. Wei, K. Wang, W. Dehai, Applications of carbon materials in photovoltaic solar cells. *Sol. Energy Mater. Sol. Cells* **93**, 1461–1470 (2009)
8. M.H. Mamat, Z. Khusaimi, M.Z. Musa, M.F. Malek, M. Rusop, Fabrication of ultraviolet photoconductive sensor using a novel aluminium-doped zinc oxide nanorod–nanoflake network thin film prepared via ultrasonic-assisted sol–gel and immersion methods. *Sens. Actuators* **171**, 241–247 (2011)
9. S.S. Shariffudin, M.H. Mamat, M. Rusop, Electrical and optical properties of nanostructured zinc oxide thin films influenced by annealing temperature. *J. Nanosci. Nanotechnol.* **12**, 8165–8168 (2012)

10. X.M. Tian, M. Rusop, Y. Hayashi, T. Soga, T. Jimbo, M. Umeno, A photovoltaic cell from p-type boron-doped amorphous carbon film. *Sol. Energy Mater. Sol. Cells* **77**, 105–112 (2003)
11. Y. Hayashi, S. Ishikawa, T. Soga, M. Umeno, T. Jimbo, Photovoltaic characteristics of boron-doped hydrogenated amorphous carbon on n-Si substrate prepared by rf plasma-enhanced CVD using trimethylboron. *Diam. Relat. Mater.* **12**, 687–690 (2003)
12. M. Rusop, X.M. Tian, S.M. Mominuzzaman, T. Soga, T. Jimbo, M. Umeno, Photoelectrical properties of pulsedlaser deposited boron doped p-carbon/n-silicon and phosphorous doped n-carbon/p-silicon heterojunction solar cells. *Sol. Energy* **78**, 406–415 (2005)
13. H.A. Yu, T. Kaneko, T. Yoshimura, S. Suhng, S. Sasaki, The spectro-photovoltaic characteristics of a carbonaceous film/n-type silicon (C/n-Si) photovoltaic cell. *Appl. Phys. Lett.* **69**, 4078–4080 (1996)
14. Z.Q. Ma, B.X. Liu, Boron-doped diamond-like amorphous carbon as photovoltaic films in solar cell. *Sol. Energy Mat.* **69**, 339–334 (2001)
15. M. Rusop, X.M. Tian, S.M. Mominuzzaman, T. Soga, T. Jimbo, M. Umeno, Photoelectrical properties of pulsedlaser deposited boron doped p-carbon/n-silicon and phosphorous doped n-carbon/p-silicon heterojunction solar cells. *Sol. Energy* **78**, 406–415 (2005)
16. K.M. Krishna, Y. Nukaya, T. Soga, T. Jimbo, M. Umeno, Solar cells based on carbon thin films. *Sol. Energy Mater. Sol. Cells* **65**, 163–170 (2001)
17. K.L. Narayanan, O. Geotzberger, A. Khan, N. Kojima, M. Yamaguchi, Boron ion implantation effect in C₆₀ films. *Sol. Energy Mater. Sol. Cells* **65**, 329–335 (2001)
18. S. Bhattacharyya, C. Vallee, C. Cardinaud, O. Chauvet, G. Turban, Studies on structural properties of amorphous nitrogenated carbon films from electron energy loss, ellipsometry, auger electron spectroscopy, and electron-spin resonance. *J. Appl. Phys.* **85**, 2162–2169 (1999)
19. Hiroki Akasaka, Takatoshi Yamada, Naoto Ohtake, Effect of film structure on field emission properties of nitrogen doped hydrogenated amorphous carbon films. *J. Diam. Relat. Mat.* **18**, 423–425 (2009)
20. M. Rusop, S.M. Mominuzzaman, T. Soga, T. Jimbo, M. Umeno, Effect of substrate temperature on growth of nitrogen incorporated camphoric carbon films by pulsed laser ablation. *Int. J. Mod. Phys. B* **16**, 866–870 (2002)

Effect of Nanoclay in Soft Soil Stabilization

Norazlan Khalid, Mazidah Mukri, Faizah Kamarudin,
Abdul Halim Abdul Ghani, Mohd Fadzil Arshad, Norbaya Sidek,
Ahmad Zulfaris Ahmad Jalani and Benard Bilong

Abstract The effectiveness of using nanoclay in soft soil stabilization was investigated by mean of laboratory testing to evaluate the compressive strength, effective shear strength and Atterberg limit test parameters. The soft soil sample, classified as slightly sandy CLAY of intermediate plasticity was used in this studies. The nanoclay was produced from pulverizing soft soil sample into nano sized using ball milling process. From the scanning electron microscopic (SEM) test and nano size analysis, it was found that the nanoclay particles were obtained from the milling process. However, only 3 % nanoclay was used in this study due to the limited samples produced from milling process. The first objective of this study was to determine the compressive strength of 3 % nanoclay mixed with soft soil and the second objective was to determine the effective shear strength of 3 % nanoclay mixed with soft soil. Meanwhile, the third objective of this study was to determine the Atterberg limit parameter: liquid limit (LL), plastic limit (PL) and plastic index (PI) of 3 % nanoclay mixed with soft soil. This study involved three main testing such as unconfined compression strength to determine the compressive strength and consolidated drained test to determine the effective shear strength. Meanwhile, the Atterberg limit test were conduct to determine the liquid limit (LL) and plastic limit (PL). The result showed that the mixing of 3 % nanoclay with soft soil was improved the soil strength and effectiveness of the shear strength.

Keywords Nanoclay · Nanoparticle · Soil stabilization · Soft soil

N. Khalid (✉) · M. Mukri · F. Kamarudin · A.H. Abdul Ghani · M.F. Arshad · N. Sidek ·
A.Z. Ahmad Jalani · B. Bilong
Faculty of Civil Engineering, Universiti Teknologi MARA, Shah Alam, Malaysia
e-mail: aln_kh82@yahoo.com

1 Introduction

Soft soil behavior is unpredictable and considered as a problematic soil to the geotechnical engineer's due to the undesirable engineering properties. Soft soil has the smallest particle sizes usually less than 2 μm produced from weathering processes, hydrothermal activities, or sediment deposits [1]. The Unified Soil Classification System (USCS) classified soft soil as a small-particle soil of which 50 % passes through Sieve No. 200 (US Specification, 0.075 mm). Soft soil has very high compressibility with possess up 85 % for moisture content sensitivity due to be easily activities on its surface [2, 3]. Soft soil usually found in coastal area or river area and the thickness is different depending on that area. The soft soil in Malaysia is usually found in coastal area at west coast of Peninsular Malaysia. The thickness of soft clay soil strata in West Coast of Peninsular Malaysia is (5–35 m) and (3–20 m) thick at East Coast of Peninsular Malaysia [1].

Soil stabilization is the process by which the engineering properties of soil layers can be improved or treated by addition of other soil types, mineral materials or by mixing the appropriate chemical additive into the pulverized soil and the carry out compaction [4]. The aim of soil stabilization is to improve the soil density, increase its cohesion, friction resistance and reduction of plasticity index [5].

Nanoparticles are often crystalline and are referred as nanocrystals. The transition from micro particles to nano particles can lead to a number of changes in physical properties. This is because of the increase in ratio of surface area and changes in volume. The large surface area of nanoparticles will increase a lot of interactions between intermixed materials such as nanocomposites which leading to special properties such as increase in strength of the materials [6]. Nano size is more reactive than its original size, and act as a good catalyst. Nanoparticle size becomes more reactive and able to produce materials with new applications due to increase in the total size of the surface over large and therefore it becomes more reactive [3]. There are increments of research and development in nanoparticles that have been used as a filler or additives for various desired effect [7].

A study has been performed to show the effectiveness use of nanoclay on compressive strength, effective shear strength, liquid limit and plastic limit to stabilized soft soil. The results showed that the application of nanoclay particle was improved the geotechnical properties of soft soil in soil strength and effectiveness of shear strength.

2 Methodology

2.1 Soft Soil Sample

The soft soil samples in grey colour collected from Kampung Sijangkang, Selangor, Malaysia in disturbed and undisturbed sample at 2 m from ground level. The samples were tightly sealed and wrapped with plastic after collection to maintain

the original moisture contents and stored at room temperature in the laboratory. The samples were tested for physical and engineering properties in accordance to BS 1377: Part 2: 1990 [8]. The chemical composition of soft soil was obtained by X-Ray Fluorescence test (XRF test).

2.2 Nanoclay Sample

The powder of nanoclay sample produced from pulverizing of natural soft soil sample that collected from Sijangkang, Selangor, Malaysia into nano sizes ranging (1–100 nm) using ball milling process. The 30 balls of zirconium oxide with 5 mm diameter and 2.98 g in weight for each were used in 80 ml bowl volume. A minimum 10 g soil samples with 24 h of milling process with speed of 400 rpm. The nanoclay size was analyzed using Zeta Potential Particle Analyzer after milling process. The chemical composition for nanoclay was obtained by XRF test.

2.3 Sample Preparation and Testing

Two samples, as shown in Table 1 were prepared out of which the first sample of soft soil considered as control. Whereas the second samples was prepared by mixing 3 % nanoclay with the soft soil. The 3 % of nanoclay was used due to the very limited amount of nanoclay samples produced from the pulverization of soft soil from milling process. The samples of 3 % nanoclay mixed with soft soil based on optimum moisture content at maximum dry density of soft soil.

The samples shown in Table 1 were prepared and analyzed for a scanning electron microscope (SEM) for soil particle and fabric arrangement and XRF test for chemical composition. The main testing was conducted were unconfined compressive test (UCT), consolidated drained test (CU) test and Atterberg limit test. The entire testing based on BS 1377:1990 [8]. The compression test and consolidated drained test were conducted by compacting into mould 38 mm × 76 mm. The specimen samples for UCT and CU test wrapped and placed at room temperature condition to protect from loss of moisture content before tested allow the reaction between soil and 3 % nanoclays.

Table 1 Details of sample

Specimens	Nanoclay (%)
Soft soil	–
Soft soil + 3 nanoclay	3

3 Experimental Results

3.1 Soft Soil Properties

The result for physical properties of soft soil samples are shown in Table 2. Based on the soft soil properties result, it shows in the natural state, the natural water content of soft soil was much higher about 128 % and the specific gravity of 2.65. Based on the size distribution result, the soft soil sample covered about 8.18 % sand size, 80.60 % of fine or silt size and 11.22 % clay size. The plastic limit and liquid limit are 24.96 and 48.77 % respectively. Meanwhile the plastic index is about 22.79 %. Based on the results properties, the soft soil samples classified as slightly sandy CLAY of intermediate plasticity.

The chemical composition results for soft soil determined by XRF test presented in Table 3. It shows that, the soft soil samples having pozzolanic properties due to

Table 2 The physical properties of soft soil sample

Properties	Values
Natural moisture content, w (%)	128
Specific gravity (Gs)	2.65
Plastic limit (%)	22.91
Liquid limit (%)	45.70
Plastic index (%)	22.79
Optimum moisture content (%)	24
Maximum dry density (Mg/m ³)	1.43
Particle size distribution:	
Gravel (%)	0
Sand (%)	8.18
Fine/Silt (%)	80.60
Clay (%)	11.22
Soil classification	Slightly sandy CLAY of intermediate plasticity

Table 3 The chemical composition of soft soil sample

Element	Concentration (%)
SiO ₂	63.02
Al ₂ O ₃	17.27
Fe ₂ O ₃	3.59
CaO	0.15
K ₂ O	2.05
Na ₂ O	0.21
MgO	1.03
SO ₃	0.67
L.O.I	–

the containing high percentage composition for major constituent components such as silicon dioxide (SiO₂), alumina oxide (Al₂O₃) and iron oxide (Fe₂O₃).

3.2 Nanoclay Soil Properties

The nanoclay samples in the powder form were collected after pulverization by milling process and tested for nanosize distribution as shown in Table 4. A particle of samples classified as nanosize when the diameter size is within range of 1–100 nm [2, 3]. From the size distribution graph for nanoclays shown in Fig. 1, it indicate there are about 90 % of nano diameter particle within range of 1–100 nm in 1 g of soft soil after undergo milling process. That proportion is sufficient to be classified as nanoclay and fully used to modified soil.

The chemical composition result for nanoclay presented in Table 5. It indicates that the chemical composition of nanoclay samples and natural soft soil samples are

Table 4 The size statistic by volume

Size (d.nm)	Mean Volume (%)
32.67	0.2
37.84	3.0
43.82	10.1
50.75	17.2
58.77	19.8
68.06	17.9
78.82	13.7
91.82	9.0
105.7	5.2
122.4	2.6
141.8	1.0
164.2	0.3

Fig. 1 Graph of size distribution for nanoclays

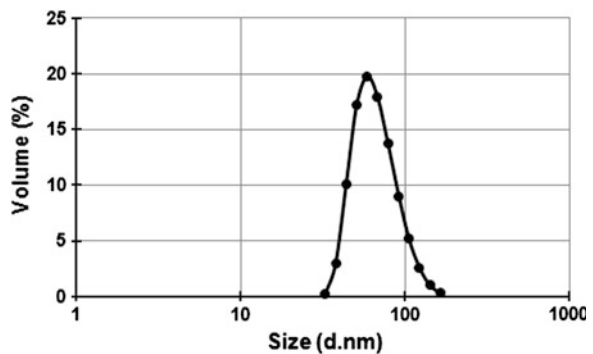


Table 5 The chemical composition of nanoclay soil

Element	Concentration (%)
SiO ₂	70.27
Al ₂ O ₃	12.07
Fe ₂ O ₃	8.13
CaO	0.28
K ₂ O	0.92
Na ₂ O	0.37
MgO	0.14
SO ₃	0.94

almost similar. The nanoclay samples have pozzolanic properties due to the percentage composition for major constituent components such as silicon dioxide (SiO₂), alumina oxide (Al₂O₃) and iron oxide (Fe₂O₃).

4 Results and Discussion

The three dimensional view for soil particles arrangement and fabric of soft soil was measured using scanning electron microscope (SEM) test due to its higher resolution capacity together with large depth of focus. Figure 2 shows the microstructure of natural clay soil at magnification 2500x and 6000x. It can be seen that the natural soft soil shows a flaky shapes and dispersion of fabric with a particle arrangement has an irregular shape with more open arrangement and spacing between the particles.

Figure 3 shows the microstructure of 3 % nanoclay mixed with soft soil at magnification 6000x and 10,000x. It shows that the soft soil particles formed as

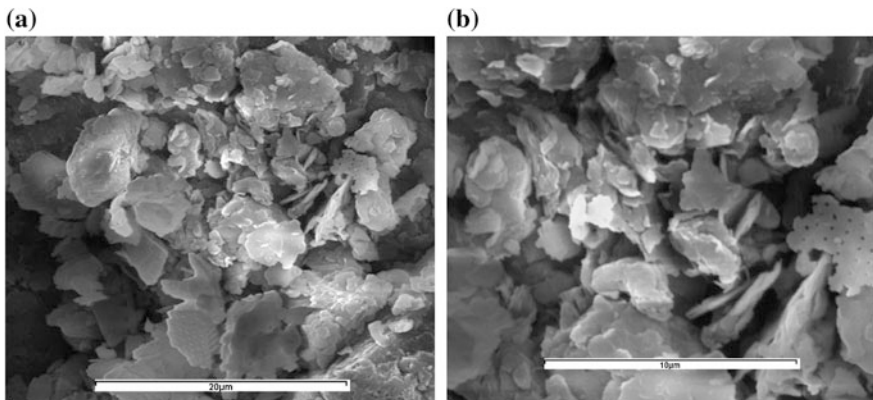


Fig. 2 Microstructure of natural soft soil. **a** Magnification at 2500x. **B** Magnification at 6000x

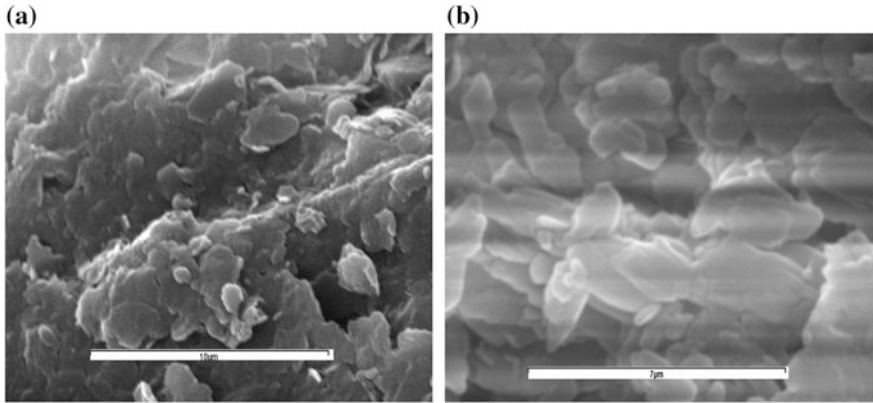


Fig. 3 Microstructure of 3 % nanoclay mixed with soft soil. **a** Magnification at 6000x. **b** Magnification at 10,000x

more coherent mass due to the interaction with 3 % nanoclay. The nanoclay was increased in surface area of for the reaction with clay soil. Thus, this desired improvement in the engineering properties of the soil due to the reaction with nanoclay and the formation was more uniform and giving the smooth surface.

Figure 4 shows the graph of axial strain versus deviator stress between soft soils and 3 % nanoclay mixed with soft soil. It shows that the maximum shear strength increased together with the decrement of axial strain for 3 % nanoclay mixed with soft soil sample compared to soft soil (control) sample only.

Table 6 presents the maximum result or compressive strength of 3 % nanoclay mixed with soft soil accordingly to the graph shown in Fig. 4. From the results, it shows that the influence of 3 % nanoclay mixed to soft soil shows significant

Fig. 4 Graph stress strain curve of unconfined compression test

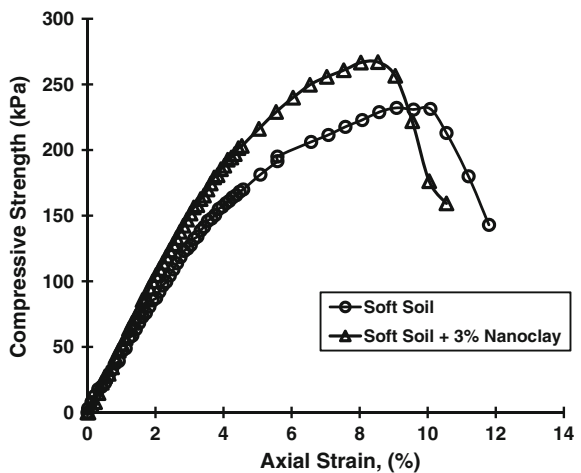
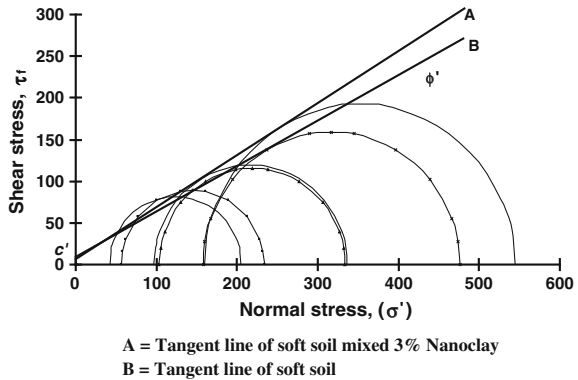


Table 6 The result of compressive strength soft soil mixed with 3 % nanoclay

	Compressive strength (kPa)
Soft soil	231.4
Soft soil + 3 % nanoclay	267.0

Fig. 5 Mohr-Coulomb failure envelope for soft soil and 3 % nanoclay stabilize soft soil



improvement and increment of compressive strength over original soft soil albeit the small percentage amount of nanoclay were used. It indicates that, the using of 3 % nanoclay was resulting the compressive strength result due to the interaction and bonding developed between of nanoparticles with soft soil matrix.

Instead, the Mohr circles of effective stress for soft soil (Line B) and 3 % nanoclay stabilized soft soil (Line A) shown in Fig. 5. The failure envelope of soft soil and 3 % nanoclay mixed with soft soil was drawn based on the best fit tangent line. Table 7 shows the values of effective cohesion (c') and effective friction angle (ϕ') getting from the Mohr-Circle. The 3 % nanoclay mixed with soft soil displayed higher internal friction angle compared with unstabilized soft soil. The soft soil mixed with 3 % nanoclay showed the best result of effective strength and hence having the high internal particle bonding between the soil particles and produced the greater of effective shear strength.

Table 7 The effective shear strength parameters of soft soil mixed with 3 % nanoclay based on mohr-coulomb failure criteria

	c' (kPa)	ϕ'
Soft soil	8	29
Soft soil + 3 % nanoclay	6	32

Table 8 The result of compressive strength soft soil mixed with 3 % nanoclay

	Liquid limit (LL)	Plastic limit (PL)	Plastic index (PI)
Soft soil	45.7	22.9	22.8
Soft soil + 3 % nanoclay	51.8	33.0	18.8

Table 8 show the changes result for Atterberg limit parameter (Plastic Limit, Liquid Limit and Plastic Index). It can be seen, the liquid limit (LL) and plastic limit (PL) value increase about 13 and 44 % respectively upon the mixing of 3 % nanoclay to the soft soils. Meanwhile the plastic index (PI) reduced about 17 % upon the mixing of 3 % nanoclay indicating of soil improvement and that nanoclay particles is good for geotechnical structure for soil liner and fill cap [2, 3].

5 Conclusions

Based on the study the following conclusions are made:

- (i) The soft soil classified as slightly sandy CLAY of intermediate plasticity soils can be stabilized using 3 % of nanoclay.
- (ii) The soft soil stabilized with addition 3 % nanoclay was improved the compressive strength about 15 % increment compared to unstabilized soft soil.
- (iii) The soft soil stabilized with 3 % nanoclay improved the effective shear strength with the increment about 10 % of internal friction (ϕ') compared to soft soil only.
- (iv) The liquid limit (LL) and plastic limit (PL) of soft soil stabilized with 3 % nanoclay slightly higher about 13 and 44 % respectively compared to soft soil. Instead the plastic index (PI) decrease about 17 % compared to soft soil.
- (v) The small amount of 3 % nanoclay, were giving significant to stabilized soft soil. It is, therefore, suitable to improve the geotechnical properties of soft soil for applications.

Acknowledgments The author would like to express an acknowledgement to the Research Management Institute, UiTM Shah Alam for providing Research Acculturation Grant Scheme (RAGS) to complete this study and also to Faculty of Civil Engineering, UiTM Shah Alam, Malaysia, and for providing the facilities such as the geotechnical laboratory and advanced geotechnical laboratory to accomplish this study. The author also wishes to acknowledge cooperation given by laboratory technician and the undergraduate student from Faculty of Civil engineering, UiTM Shah Alam for this study.

References

1. A.I.M.B. Abdullah, P. Chandra, Engineering properties for coastal subsoils in Peninsula Malaysia, in *Proceedings of the 9th South East Asia Geotechnical Conference*, vol. 1 (Bangkok, Thailand, 1987), pp. 127–138
2. M.R. Taha , S.Y. Lim, Z. Chik, Ciri-Ciri Asas Beberapa Tanah Dikisar. *Jurnal Kejuruteraan* **21**, 1–10 (2009)
3. M.R. Taha, Geotechnical properties of soil-ball milled soil mixtures, in *Proceedings of 3rd Symposium on Nanotechnology in Construction* (Springer, 2009), pp. 377–382

4. A.L. Olaweraju, Soil stabilization. Mechanical Engineering Seminar on Course Title: Advance Soil Mechanics (CVE 821) (Civil Engineering Department, Federal University of Technology, Akure, Ondo State, Nigeria, 2004)
5. S. Dartvelle, Numerical and granulometric approaches to geophysical granular flows. Ph.D. thesis, Department of Geological and Mining Engineering, Michigan Technology University, Houghton, Michigan, 2003
6. P. Holister, J. Weener, C.R.Vas, T. Harper, Nanoparticles, technology white papers nr. 3. Cientifica Ltd (2003)
7. U. Faheem, Clays, nanoclays, and montmorillonite minerals. Metall. Mat. Trans. A **39A**, 2084–2814 (2008)
8. British Standard Institution, *British Standard Method of Test for Soils for Civil Engineering Purposes* (BS 1377, London, 1990)

Compatibility of Plastomeric Modified Bituminous Blends: Its Effect on the Performance Behavior of Modified Bituminous Mixture

Noor Zainab Habib, Ibrahim Kamaruddin and Madzalan Napiah

Abstract This paper present a part of research study conducted to investigate the effect of compatibility of polymer bitumen blend on the performance behavior of the well graded bituminous concrete mixture. Bituminous mixture was prepared by using 80/100 Pen bitumen for control mix, while polyethylene modified mixture was prepared by blending linear low density polyethylene (LLDPE) with 80/100 Pen bitumen. The concentration of polymer in the blend was kept at 1, 2 and 3 % by weight of bitumen content. The compatibility of polymer bitumen blend as revealed by morphological analysis using transmission electron microscopy (TEM) shows that as the concentration of polymer in bitumen increases the formation of polymer network was observed. It was found that at higher polymer concentration formation of polymer bitumen network considered responsible for improved performance which was also confirmed by dynamic creep results of the modified bituminous samples.

Keywords Morphology · Compatibility · Linear low density polyethylene · Rutting · Polymer modified bitumen

1 Introduction

Compatibility which is defined as state of dispersion between two dissimilar components [1] has significant effect on the performance behavior of the modified binder. Compatibility of the polymer modified binder does not only depend on

N.Z. Habib (✉)

Environmental Engineering Department, Universiti Tunku Abdul Rahman,
Jalan Universiti Bandar Barat, 31900 Kampar, Perak, Malaysia
e-mail: nzainab@utar.edu.my

I. Kamaruddin · M. Napiah

Civil Engineering Department, Universiti Teknologi PETRONAS, Bandar Seri Iskandar,
31750 Tronoh, Malaysia
e-mail: ibrakam@petronas.com.my

polymer characteristic but on the mixing process, temperature and bitumen characteristics. Thermoplastic plastomers, whenever blended with bitumen always shows little compatibility, whether blended at higher temperature or at high shear rate. Difference in densities between the two also considered as one of the vital factor responsible for immiscible blend which ultimately ends up with the phase segregation [2].

For modified bituminous blend compatibility which is regarded as more physical rather than chemical phenomenon, resulted in the formation of phase segregated layer in the polymer bitumen blend. The resulted phase segregation which occurs at macro scale caused the polymer to float at the top of bitumen [3]. The network formation occurred due to polymer modification was considered as only due to entanglement of polymer chain that were formed due to physical crosslink as observed by scanned images taken by transmission electron microscopy (TEM) or by fluorescence microscopy. Polyethylene (PE) due to their non-polar nature is also immiscible to certain extent because of its higher molecular weight [4] but it absorbs the aromatic components of the base bitumen and do swell up [5]. The swelling of the polymer is thus considered due to absorption of oily component from bitumen which eventually build physical network during blending of polymer with bitumen at higher temperature [4].

To know the extent of compatibility of polymer with bitumen, morphological analysis is widely used using highly sophisticated tools which provide an insight about prevailing bitumen structure, composed of multiphase system [6]. It is reported that the bi phase structure which is observed during scanning is composed of swollen polymer within bitumen matrix while the chemically reacted polymer showing even distribution among bitumen matrix is considered as governing factor affecting the workability and mechanical properties of the polymer modified bituminous blend (PMB) [7].

Rutting which commonly occurs in top 50–100 mm layer of flexible pavement due to accumulation of permanent deformation significantly reduces both structural and functional performance of the pavement. In order to overcome this problem of consolidation of the pavement layer due to repeated loading polymer modified bitumen is commonly used. Among thermoplastic polymers polyethylene because of its cheap cost is widely used in order to increase the pavement life [8]. It is also known that the use of synthetic polymer either by chemical or physical blending improves the properties of elasticity, strength and adhesion which ultimately increases the pavement life [9]. Thus the compatibility of polymer bitumen blend is considered as an important affecting parameter defining the properties of the ultimate polymer bitumen blend.

In this paper the performance behavior of Linear low density polyethylene modified bituminous mixture is evaluated. Dynamic creep samples prepared with virgin and LLDPE modified binders were evaluated for resistance against permanent deformation. Morphological analysis of the PMB using TEM was used to understand the formation of polymer bitumen network which is considered responsible for strength enhancing factor of the modified bituminous mixture.

2 Methodology

2.1 Material used

Materials used in this study includes

- 80/100 penetration grade base bitumen obtained from the PETRONAS Refinery, Malaysia.
- The polymer linear low density polyethylene resin (LLDPE) used for modification was supplied by Polyethylene Malaysia, with a melt flow index 0.9 g/10 min and density of 0.8958 g/cm³.
- Crushed aggregates used in this study include crushed granite obtained from quarry located at outskirts of Ipoh Malaysia, while river sand was used as fine aggregate. Ordinary Portland cement was used as filler. Physical properties of material used are shown in Table 1.

2.2 Sample Preparation

1. *Polymer Modified Bituminous Blend (PMB)*: PMB blend was prepared by mixing about 400 gm of bitumen with polymer in shear mixer at 120 rpm, while the temperature was kept at 160 °C. The concentration of LLDPE was kept as 1–3 % by weight of the bitumen. The modified bitumen was then sealed in containers covered with aluminum foil and stored for further testing and Marshall Sample preparation. Virgin bitumen was also subjected to same shearing action in order to have uniformity in testing conditions. Empirical test such as penetration (ASTM D-5), softening point (ASTM D-36) and viscosity ASTM (D-4402) were then conducted on the prepared samples. Test results are presented in Table 2.

Table 1 Physical properties of material used

Material	C.A	F.A	Polymer LLDPE	Bitumen	Filler
Specific gravity	2.63	2.64	0.895	1.01	3.26

Table 2 Properties of virgin and polymer modified bitumen

	Penetration (mm)	Softening Pt. (°C)	Viscosity (Pa. s)	P.I
80/100 pen bitumen	84	53	0.44	0.5
1 % LLDPE	35	53	0.63	-1.5
2 % LLDPE	30	53	0.76	-1.85
3 % LLDPE	25	60	1.43	-0.7

2. *Morphological Testing*: Morphological testing was performed by using TEM model ZEISS LIBRA 200 FE. All slides for TEM were prepared by dissolving virgin bitumen and polymer modified bitumen in toluene of reagent grade and then sonacating the sample for 1.15 h. The sonicated samples were then transferred on copper grid. The copper grid was then coated with Formvar. Before scanning the solvent was evaporated.
3. *Marshall Samples*: All Marshall Samples were prepared according to ASTM D1559. Standard size 101.6 mm (4 in.) diameters and 60–65 mm (2½ in.) high samples were prepared by using Gyrotory compactor. Gyrotory compactor was adjusted at an angle of gyration of 1.25° and normal pressure of 600 kPa. The number of gyration was kept at 200 according to ASSHTO 2001 specification. For Marshall Sample preparation, well graded aggregate according to JKR specification, Malaysia for ACW–14 (asphalt concrete wearing course, as shown in Table 4) was blended with bitumen at varying bitumen percentage between 4–6.5 %, in order to get the optimum bitumen content for a mix. Two different types of Marshall Samples namely control mix prepared with virgin bitumen and LLDPE polymer modified Marshall Samples using polymer modified bitumen with polymer concentration varying between 1 and 3 % by weight of bitumen. The optimum bitumen content (OBC) obtained for control mix and polymer modified bituminous mixture samples are presented in Table 3. All creep samples were prepared at these OBC values.
4. *Experimental Set up for Dynamic Creep Test*: The dynamic creep test was performed according to British Standard DD 226. The creep deformation of standard Marshall Specimens prepared at optimum bitumen content for control and LLDPE modified mix was measured as a function of pulse counts. The load

Table 3 Optimum binder content (OBC)

Mix type	Optimum binder content (OBC) (%)
Control mix	5.0
1 % LLDPE	5.2
2 % LLDPE	5.4
3 % LLDPE	4.7

Table 4 JKR gradation for ACW 14

Sieve size	Gradation limits	Gradation used
20 mm	100	–
14 mm	80–95	87
10 mm	68–90	77
5 mm	52–72	60
3.35 mm	45–62	51
1.18 mm	30–45	34
425 µm	17–30	19
150 µm	7–16	12
75 µm	4–10	6

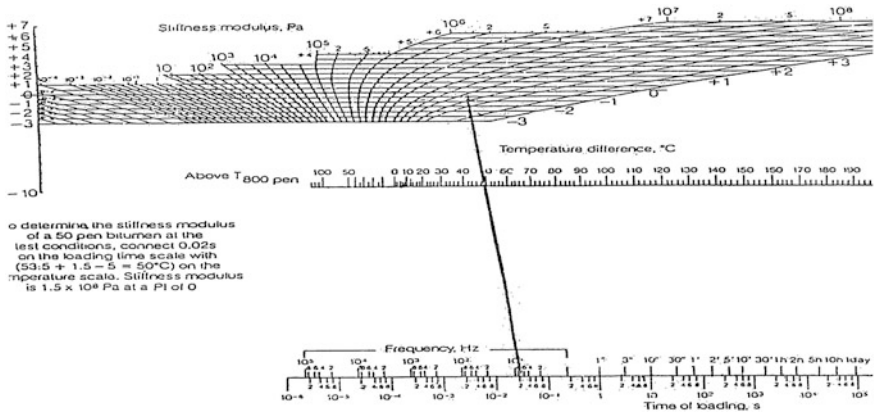


Fig. 1 Van der Pool nomograph for S_{bit} determination

used represents the repeated application of axle loads on the pavement structure. The specimen was preloaded with 12 kPa stress for two minutes before being subjected to 100 kPa stress for 1 h. The results obtained were used to develop the relationship between mixture stiffness to the binder stiffness as obtained by Van der Poel nomograph (refer Fig. 1) to predict mechanical performance of mix.

3 Analysis of Results

3.1 Empirical Test Results

Polymer modification significantly alters the rheological behavior of the bitumen as observed by the penetration and viscosity test results. At 1 % polymer concentration a sharp decrease in penetration value to 35 from 84 dmm value of base bitumen indicates the hardening effect induced by the modification. The changes in bitumen physical and chemical properties are considered responsible for this behavior. The use of the high molecular weight polymer LLDPE having melt flow index of 0.9 g/10 min also increases the viscosity of the PMB. Thus it became obvious from the result that thermoplastics influence more on the penetration with an increase in the viscosity of the bitumen [10]. The same trend with the decrease in the value of penetration with the increase in concentration of polymer was observed for other polymer concentrations as shown in Table 2.

Although LLDPE has melting temperature around 122 °C but doesn't get completely dissolved into bitumen even blending for one hour but it sufficiently increases the hardness of the PMB. The increase in the viscosity and thus the hardness of PMB was considered due to absorption of some oily component of

bitumen and release of low molecular weight fraction into the bitumen which increases the viscosity of the PMB [11]. This release of lower molecular weight fraction sufficiently increase the viscosity till the end of mixing process, and by the time it cools harden mixture was formed. The hardening of the bitumen can be beneficial as it increases the stiffness of the material, thus the load spreading capabilities of the structure but also can lead to cracking [10].

The results obtained by the softening point test shows that modification does not alters the softening temperature till 2 % polymer concentration in bitumen. At 3 % polymer concentration the segregation of the polymer and bitumen in the brass ring used for softening test was observed due to phase segregation. The lower layer which constitute majority of bitumen soften almost at the same temperature as of bitumen and get deformed upon heating, while the top phase segregated polymer bitumen layer remains as it is. As the polymer concentration increase the effect of polymer modification became more obvious as observed by increase in softening temperature for 3 % LLDPE modified binder. The softening test results for 3 % LLDPE PMB concentration indicates that the higher softening temperature was due to discharge of lower molecular weight polymer chain in bitumen which increases the softening temperature of the blend. At this concentration the higher softening temperature makes the binder more creep resistant.

3.2 Viscosity Test Results

Viscosity of the modified binder, representing the flow behavior of the material has considerable influence on internal friction and thus on shearing behavior of bituminous mixture. Binder with sufficient viscosity gives better aggregates interlocking offering higher internal frictional angle among aggregates when modified binder is used in the bituminous mixture [10]. The viscoelastic properties of the bituminous mixture which are mainly dependent on the temperature and loading also get affected by the viscosity behavior of the material. The internal structure of the base bitumen also plays an important role deciding the viscosity behavior [5] which changes from *sol* to *gel* or to *gel-sol* upon modification with polymer. The compatibility of the blend also depends on the difference in molecular weight of the polymer and bitumen. Irrespective of type of mixing used either by mechanical or chemical method, the structure of the polymer and base bitumen does affect the viscosity of the final blend [12]. From the Table 2 increase in bitumen viscosity from 0.44 to 1.43 Pa. s at 135 °C shows increment in bitumen's viscosity after polymer modification. The trend observed for enhancement in modified binder viscosity was quite linear with an increase in polymer concentration. All the viscosity test results shows that the viscosity of the blend for all polymer concentration are well below 3 Pa. s, as mentioned by ASSHTO specification ASSHTO MP1 [11] for a workable mix.

Thus improved viscous property of modified binder is considered as one of additional factor increasing the cohesion and internal friction angle of mixture offering higher shear strength thereby reducing the chances of rutting.

3.3 Morphological Analysis

Extent of the compatibility of the polymer bitumen can be well understood by the scanned images. The TEM analyzed samples describes the existence of polymer network among continuous polymer bitumen phase. It was observed from the scanned images as shown in Figs. 2, 3 and 4, that the LLDPE because of low miscibility in bitumen appeared as distinct polymer domains among dispersed polymer bitumen blend.

For polymer modified bituminous blend the difference in densities of polymer and bitumen leads to the formation of phase segregation. Thus the network formed due to this was considered due to the entanglement of polymer chain which occurs as result of physical cross link [2]. Thus from the scanned TEM images the presence of helical chain in dispersed polymer bitumen blend confirms the presence of phase segregation.

This phase segregation which is considered as typical representative of polyethylene modified blend was observed at all concentration of the polymer. For 1 % LLDPE modified blends it appeared as distinct separate domain which in fact reflects the absence of well-connected polymer network. For 2 % LLDPE, slight formation of network was observed. In other words it can be comprehended that although the blending temperature, time and shearing rate was kept constant for all bituminous blend but the addition of 1 and 2 % LLDPE in bitumen failed to form

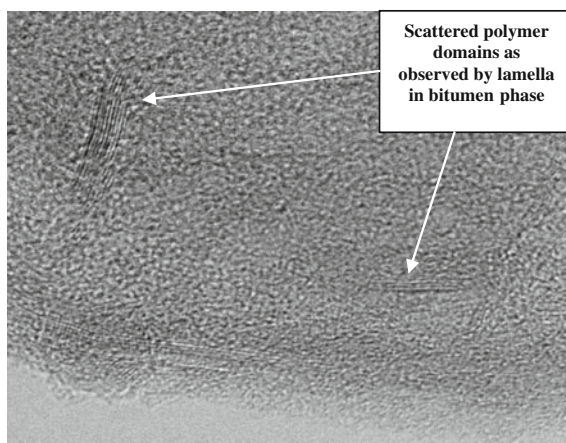


Fig. 2 TEM image of 1 % LLDPE

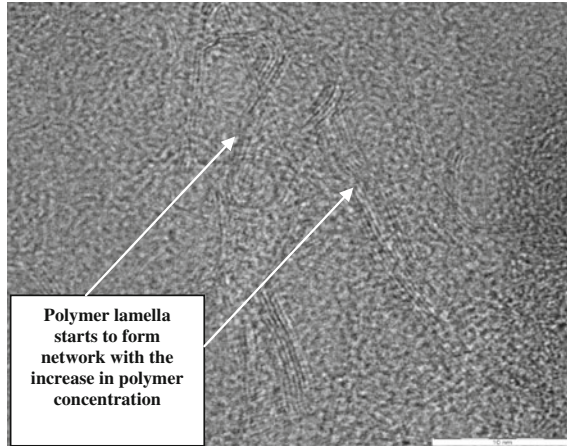


Fig. 3 TEM image of 2 % LLDPE

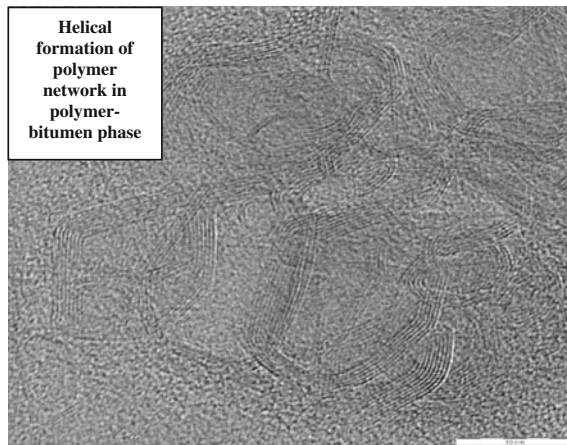


Fig. 4 TEM image of 3 % LLDPE

complete physical cross linked polymer network. At 3 % LLDPE concentration the formation of polymer network was observed. Thus formation of this network in the form of helical chain in dispersed polymer bitumen layer was considered mainly responsible for viscoelastic characteristic of the bituminous blend.

As these helical chains are well connected thus by the sliding past of these chain under stress it would allow to accommodate more stresses by realigning themselves once the strain was being removed. It can be concluded safely that the presence of these helical chains would thus make the blend more creep resistant and thus the bituminous mixture.

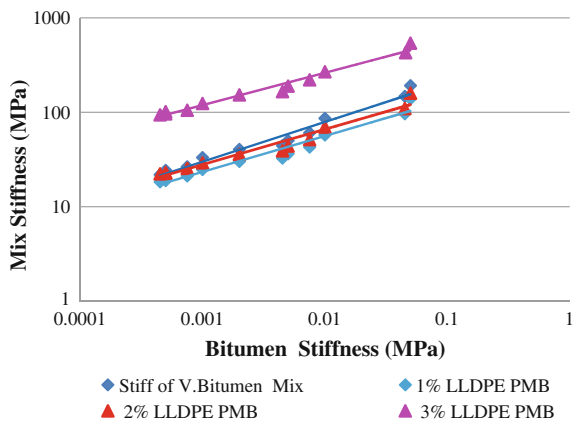
3.4 Dynamic Creep Result

Dynamic creep test was conducted according to British Standard DD 226 on the samples prepared at optimum bitumen content calculated from Marshall Test results. The results are presented in the form of permanent accumulated strain and creep stiffness. The average mix stiffness modulus (S_{mix}) obtained from the creep modulus of mix specimen at optimum binder content for particular bituminous mix is plotted in double logarithmic scale against stiffness modulus of bituminous binder (S_{bit}), evaluated by using Van der Poel’s nomograph as shown in Fig. 1. The $S_{bit} +$ polymer was also determined using Van der Poel’s nomograph considering their penetration, softening point and penetration Index PI. The resistances to permanent deformation obtained from the creep tests by plotting a line in log-log scale. The slope of the line plotted in the log-log scale represents the relationship of mixture stiffness versus binder stiffness, where the slope of the line for each particular mix indicates sensitivity of the mix to loading time and hence bitumen stiffness [13].

Among LLDPE modified bituminous mixes it was observed from Fig. 5, that only 3 % LLDPE bituminous mix offered increased mixture stiffness in comparison to virgin bitumen and rest of the polymer modified bituminous mixes. At higher concentration of polymer (3 %) the increase in viscosity makes the binder rather incompressible while the partially immiscible polymer as observed as helical chain by TEM scanned image considered responsible for the inducing the stiffening affect increasing mixture stiffness. The insignificant behavior of the LLDPE modified bituminous mixture at lower polymer concentration could be attributed due to the failure of formation of proper polymer bitumen network as observed by TEM scanned images as shown in Figs. 2 and 3.

The higher molecular weight of polymer beside the extent of the compatibility of polymer with the bitumen also affects the creep behavior. As higher molecular

Fig. 5 Mixture stiffness versus bitumen stiffness for virgin and LLDPE modified bituminous mixture



weight increases the secondary bonding between polymer chains increases which makes it more creep resistant [14].

The LLDPE PMB mix unable to show better performance at lower polymer concentration but as the polymer chain starts to form network, the deformation was resisted which seems to occur due to reversible slippage of polymer chain. This reversible slippage was considered sufficient enough to overcome the strains induced due to repeated load action.

Thus in case of modified binder where polymer and bitumen play its characteristics individually and collectively, the extent of compatibility becomes the major contributing factor in enhancing the stiffness of the mixture. The interaction of the polymer and bitumen or compatibility starts to play its part when sufficient polymer network was established. In short the combine behavior of LLDPE modified binder at 3 % polymer content shows promising results in terms of rutting when tested.

4 Conclusion

The compatibility of the polymer bitumen has significant effect on the performance behavior of the modified bituminous mixture. Although compatibility between polymer and bitumen was not achieved due to difference in densities and molecular weight, but it does sufficiently changes the physical properties of the bitumen due to modification. The increase in viscosity of the binder makes the aggregate to hold the aggregate-bitumen matrix together while immiscible polymer domains acts as a filler resisting deformation by flexing of the entangled polymer chain. Beside the physical changes in the properties of the virgin bitumen due to modification, the formation of the proper polymer bitumen structure remains unaffected by polymer modification as bitumen being by product of crude oil has similar chemical structure as of polyethylene. Presence of helical polymer network within bitumen was considered responsible for the superior performance behavior of the modified bituminous mixture.

Acknowledgments The authors sincerely thank Universiti Teknologi PETRONAS for financial and technical support. Special thanks for Polyethylene Malaysia and PETRONAS refinery Malacca, Malaysia for providing technical support and material.

References

1. W. Uddin, Viscoelastic characterization of polymer-modified asphalt binders of pavement applications. *Appl. Rheol.* **13**(4), 191–199 (2003)
2. P.G. Redelius, Solubility parameters and bitumen. *Fuel* **79**, 27–35 (2000)
3. C. Giavarini, P.D. Filippis, M.L. Santarelli, M. Scarsella, Production of stable polypropylene modified bitumens. *Fuel* **75**(6), 681–686 (1996)

4. L. Michon, M. Didier, J.P. Planche, B. Hanquet, Estimation of average structural parameters of bitumen by ^{13}C nuclear magnetic spectroscopy. *Fuel* **76**(1), 9–15 (1997)
5. D. Sybilski, New simplified equation for the computation of absolute viscosity of polymer-bitumens. *Mater. Struct.* **30**, 182–187 (1997)
6. American Society for Testing and Materials (ASTM), *Standard Specification*, Sect. 4, Vol. 04.03. (2000)
7. C.D. Whiteoak, *The Shell Bitumen Hand Book* (Thomas Telford Ltd., Surrey, 2003)
8. A.A. Yousefi, A.A. Kadi, Composite asphalt binders: effects of modified RPE on asphalt. *J. Mater. Civil Eng.* **12**, 113–123 (2000)
9. S.N. Bhattacharya, *Rheology Fundamentals and Measurement*, Chap. 1. (Royal Melbourne Institute of Technology, Australia, 1997)
10. O. Gonzalez, M.E. Munoz, A. Santamari, G.M. Morales, F.J. Navarro, P. Partal, Rheology and stability of bitumen/EVA blends. *Eur. Polym. J.* **40**(10), 2365–2372 (2004)
11. F.A. Cristina, J.A. Sandoval, A. Jerez, F.J. Navarro, B.F.J. Martinez, P. Partal, C. Gallegos, Evaluation of thermal and mechanical properties of recycled polyethylene modified bitumen. *Polym. Testing* **27**, 1005–1012 (2008)
12. J.F. Masson, G.M. Polomark, Bitumen microstructure by modulated differential scanning calorimetry. *Thermochim. Acta* **374**, 105–114 (2001)
13. I. Kamruddin, The properties and performance of polymer fibre reinforced hot—rolled asphalt. Ph.D. thesis, Civil Engineering Department, University of Leeds, 1998
14. B. Stuart, *Polymer Analysis* (Wiley, United Kingdom, 2002)

Effects of Residual Carbon on Microstructure and Surface Roughness of PIM 316L Stainless Steel

Muhammad Rafi Raza, Faiz Ahmad, Norhamidi Muhamad, Abu Bakar Sulong, M.A. Omar, Majid Niaz Akhtar, Muhammad Shahid Nazir, Ali S. Muhsan and Muhammad Aslam

Abstract Powder injection molding (PIM) offers an attractive method for producing smart and intricate shapes components. PIM process is cost effective and equally applicable for metals and ceramics. Debinding process is the most critical step among all PIM steps and any residual during debinding can change the composition of sintered product resulting change in final properties. In this research work, the injection molded samples were thermally debound and sintered in various atmospheres. The results showed that the sintered samples with improper thermal debinding resulted the carbide formation at the surface and across the grain boundaries that caused to increase the roughness value.

Keywords 316L stainless steel · PIM · Residual carbon · SEM · Shrinkage · Surface roughness

M.R. Raza (✉) · N. Muhamad · A.B. Sulong · M.N. Akhtar
Department of Mechanical and Materials Engineering, Faculty of Engineering and Built Environment, Universiti Kebangsaan Malaysia, Bangi, Selangor, Malaysia
e-mail: rafirazamalik@gmail.com

F. Ahmad · A.S. Muhsan · M. Aslam
Department of Mechanical Engineering, Universiti Teknologi PETRONAS, Tronoh, Perak, Malaysia

M.A. Omar
Advanced Materials Research Centre (AMREC) SIRIM, Kulim, Kedah, Malaysia

M.N. Akhtar
Department of Physics, COMSATS Institute of Information Technology, Lahore, Pakistan

M.S. Nazir
Department of Chemical Engineering, COMSATS Institute of Information Technology, Lahore, Pakistan

1 Introduction

Powder injection molding (PIM) offers an attractive method for producing smart, complex shape components cost effectively and it is equally applicable for metals and ceramics [1, 2]. PIM process consists of feedstock preparation, injection molding, debinding and sintering [2]. A binder should have the following features of: non reactive with powder provide handling strength. Among all the challenges for PIM, binder composition and its removal is important for the success of PIM process [3].

Debinding is the most important processing step in PIM, and most defects occurred during debinding process [4]. Suitable debinding parameters are those in which the part retains its shape after debinding. Surface finishing is very important for certain applications such as micro heat exchangers, medical tools and parts, and chemical mixers. The surface finish affects the wear and friction properties of the parts.

Therefore, several studies were carried out to control these critical steps. For instance, Liu et al. [5] used water atomized 316L SS of the particle size 3 μm with a multi binder system to investigate the effects of the heating rate during debinding on the surface roughness. It was observed that more weight loss was occurred in the sintered parts at higher heating rates and it gave a lower value of 'Ra' (roughness value), which is responsible for better surface finishing. Levenfeld et al. [6] found that the presence of residual carbon in stainless steel enhanced the sintering densification rate and was able to achieve higher density at low sintering temperature. Microstructural study showed a uniform distribution of carbides within the matrix.

Currently, the corrosion resistant alloys, such as austenitic stainless steels components are widely used in medical tools, marine components and some other applications and are able to be manufactured by PIM technique. The previous research works were mainly focusing on investigating the effects of various processing parameters on the physical, mechanical and corrosion resistive properties of the fabricated PIM parts. However, limited work has studied the effects of these parameters on the surface roughness and surface finishing. Therefore, the objective of the present work is to study the effects of debinding and sintering parameters on the surface roughness of PIM 316L stainless steel. In the current study, the experimental work i.e. thermal debinding and sintering was performed by using lab scale and commercial furnaces and investigated the effects on microstructure and surface roughness.

2 Experimental Materials and Methods

2.1 Materials and Preparation of Green Samples

Water atomized stainless steel 316L (PF-10R) was supplied by PACIFIC SOWA Japan. The morphology and mean particle size are shown in Figs. 1 and 2, respectively. The chemical composition of the steel powder provided by the supplier is given in Table 1.

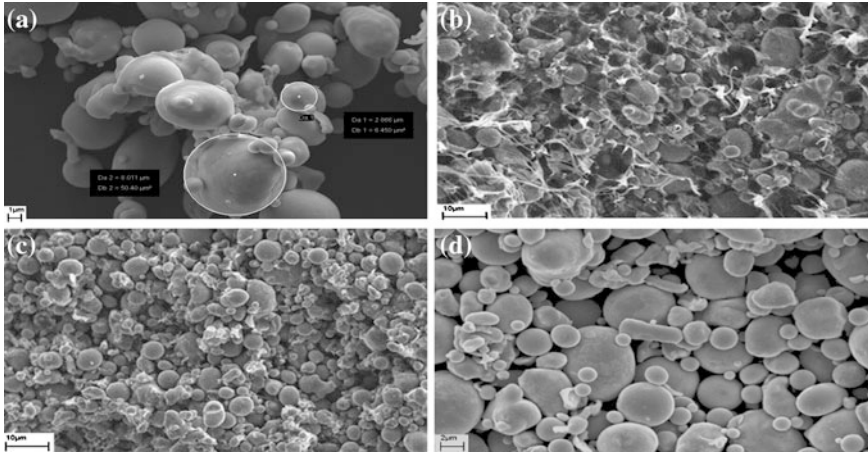


Fig. 1 SEM analysis of a 316L SS powder, b molded sample, c after solvent extraction, d after thermal debinding

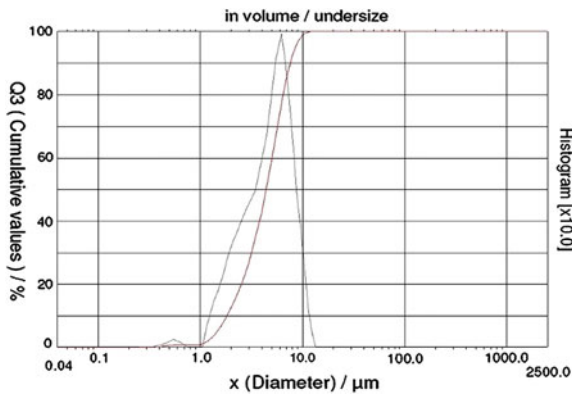


Fig. 2 Particle size distribution of 316L SS

The particle size distribution measurement of the steel powder was performed using the Cilas 1190 particle size distribution analyzer. The particle size measurement was according to the ISO13320 standard.

During this research work four formulations were prepared and molded by using wax based binder system. The procedure to prepared feedstocks and physically defects free molding is given in previous published work [7].

Table 1 Chemical composition of 316L SS

Element	wt%
C	0.024
Si	0.36
Mn	0.07
P	0.029
S	0.002
Ni	10.53
Cr	16.57
Mo	2.1
Cu	0.1

2.2 Debinding and Sintering Process

Debinding was completed into two consecutive steps [8]. After the solvent extraction the test samples were thermally debound at 450 °C for 1 h and sintered at 1,325 °C for 2 h by using lab scale and commercial furnaces [7]. Finally, the debound test samples were sintered in different sintering atmospheres i.e. vacuum, hydrogen, nitrogen and mixture of hydrogen with nitrogen (9:1).

2.3 Characterization of Sintered samples

The percentage shrinkage was calculated by using the following equation:

$$\% \text{ Shrinkage} = \frac{L_g - L_s}{L_g} \times 100$$

Scanning Electron Microscopy (SEM) was performed to study the morphology of the molded 316L SS powder, distribution of binder within molded sample, binder removal after the solvent extraction and thermal debinding. For microstructural analysis test samples were hot mounted using the SimpliMet® 1000 Automatic Mounting Press manufactured by Buehler. The mounted samples were polished and etched according to ASTM standard. The surface roughness of the sintered samples was measured using SURFTEST SV-3000 MITUTOYO.

3 Results and Discussion

3.1 Characterization of 316L Stainless Steel Powder and Molded Samples

Figure 1 showed that the particles are spherical as well as irregular in shape. The test samples are successfully molded and debound as show in Fig. 1. The chemical composition is given in Table 1.

The particle distribution result showed that 80 % of the particles size distribution is between 1.43 and 7.63 μm . The remaining 20 % was divided into two equal parts (i.e. below 1.43 μm and above 7.63 μm). The results in graphical form are shown in Fig. 2. The chemical composition of the 316L SS powder provided by the supplier is given in Tables 1 and 2.

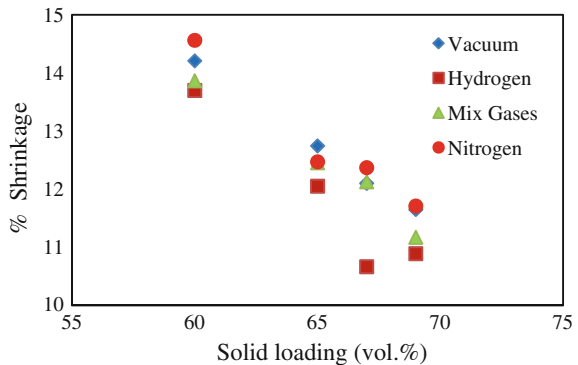
3.2 Effects of Sintering Atmosphere on Shrinkage

The shrinkage noted in samples is shown in Fig. 3. Results showed that the shrinkage is higher in vacuum sintered test samples as compared to the gas atmospheres, which is due to the gas trapped within the pores. The trapped gas generated pressure within these pores that hindered grain growth resulting in the reduction in the shrinkage [9]. In vacuum atmosphere, there is no air inside the furnace, to trap within the pores because the furnace pressure is less as compared to the pressure inside the pores; that caused the increase in shrinkage. The results also

Table 2 Particle size distribution of 316L SS

Particle distribution	D ₁₀	D ₅₀	D ₉₀
Particle size (μm)	1.43	4.42	7.63

Fig. 3 Effects of sintering atmosphere on shrinkage



showed that the shrinkage is also reduced by increasing the solid loading. It is due to the excess amount of the steel powder that increase the green density of the test sample [10]. The achieved shrinkage value is in the range recommended for PIM.

3.3 Effects of Sintering Atmosphere on Microstructure

For vacuum sintered samples the grain boundaries are prominent and pores are irregular in shape and distributed across the grain boundaries as well as within the matrix shown in Fig. 4. The grain growth was responsible for the mechanical properties.

For performing the atmosphere sintering, the solvent extracted test samples were thermally debound and sintered in a commercially available furnace. Figures 5 and 6 show the SEM micrographs of the PIM 316L SS sintered in H_2 and a mixture of H_2/N_2 atmosphere. These SEM micrographs show the presence of porosity as well as the formation of chromium carbides across the grains boundaries that made the grain

Fig. 4 SEM micrograph of vacuum sintered test samples showing distribution of porosity

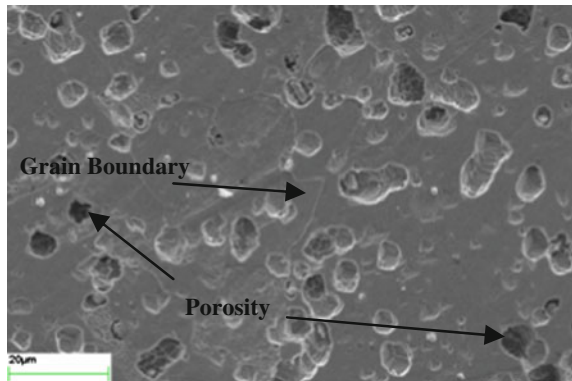


Fig. 5 SEM micrograph of H_2 sintered test samples showing carbide formation

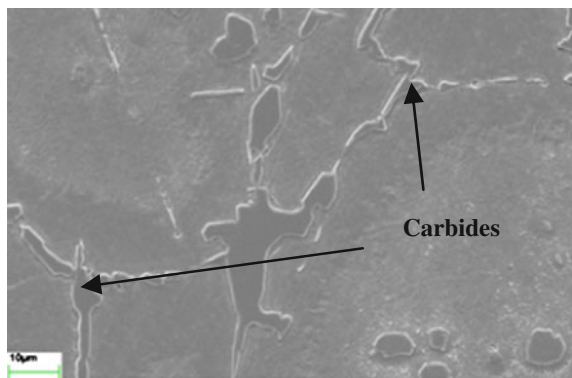
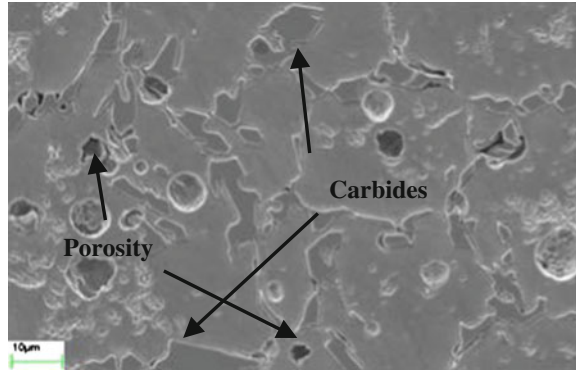


Fig. 6 SEM micrograph of H_2/N_2 sintered test samples showing distribution carbides



boundaries thick. The presence of these carbides was confirmed by the XRD analyses [7]. These carbides were irregular in shape and large in size for the samples sintered in mixed gases. This concludes that change in atmosphere has remarkable effects on morphology of chromium carbides as shown in Figs. 5 and 6. These carbides have significant effect on the mechanical properties of the PIM 316L SS [11].

These carbides may have been formed due to the presence of carbon residue during the unsuitable thermal debinding process [12]. The formation of carbides can be controlled by using an appropriate debinding process followed by proper sintering. Overall, the structure is homogeneous in all the formulations. The carbides were distributed uniformly. The presence of the porosity depends upon the solid loading as well as presence of porosity due to trapped gas between the metal particles that hindered the mass transportation during sintering [6, 13].

SEM micrograph of the samples sintered in N_2 is shown in Fig. 7. The Figure showed the presence of a needle like structure. Needle like structure was in the form of colonies and across the grain boundaries. The presence of residual carbon is an evidence of the carbide formation that encouraged the formation of the sigma phase, which is formed during the slow cooling rate after the sintering [11, 14]. The absorption of N_2 probably helped to form the carbides in the form of colonies

Fig. 7 SEM micrograph of N_2 sintered test samples showing carbide in the form of colonies

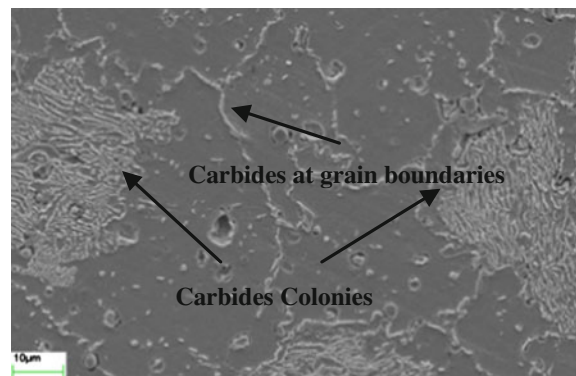


Table 3 Effects of debinding on surface roughness (μm) of PIM 316L SS

Composition (vol%)	Vacuum	H ₂	N ₂
60	17.468	19.243	27.188
65	13.958	31.407	20.341
67	15.095	19.104	18.744
69	13.125	21.885	20.718

because the role of N₂ is still not clear [15]. The presence of carbides changed the final properties of the 316L SS dramatically. It improved the mechanical properties but reduced its ductility because these carbides are hard and brittle. The increase in the mechanical properties of the samples sintered in N₂ was due to the formation of nitrides and the presence of carbides in the form of colonies.

3.4 Effects of Sintering Atmosphere on Surface Roughness

The SURFTEST SV-3000 MITUTOYO was used, having capability to measure the surface roughness up to 100 mm in length and the average surface roughness values are given in Table 3. It was noted that the roughness values are different at same debinding and sintering parameters. The variation in roughness values was probably due to the formation of carbides, which is due to the improper removal of binder residue during thermal debinding, and during sintering the residual carbon reacts with metals and formed the carbides as clearly shown in the SEM micrograph of Figs. 5 and 7. This finding was also confirmed through XRD in previous published work [7]. From the results it is also confirmed that the vacuum atmosphere gave better surface finish as compare to the gas atmosphere in the absence of residual carbon. García et al. [15] investigated the corrosion resistance of stainless steel and reported that the sintering atmosphere also influence the formation of precipitates.

4 Conclusions

The proper thermal debinding process is very essential to obtain final PIM parts with smooth surfaces. Presence of residual carbon during thermal debinding changes the content of stainless steel and caused the formation of carbides at the outer surface of test samples as well as across the grain boundaries that has influenced the surface roughness. In the presence of residual carbon the atmosphere sintering showed double surface roughness as compared to the vacuum sintering (with no residual carbon).

Acknowledgments The authors acknowledge the “Universiti Teknologi PETRONAS, AMREC SIRIM Kulim Kedah”, and “UKM-ICONIC-2013-003 and UKM-DIP-2012-29” for providing technical and financial support.

References

1. A. Bose, I. Otsuka, T. Yoshida, H. Toyoshima, Faster sintering and lower costs with ultra-fine MIM powders. *Met. Powder Rep.* **62**, 18–25 (2007)
2. R.M. German, *Powder Injection Molding: Metal Powder Industries Federation* (Princeton, USA, 1990)
3. A. Bose, The technology and commercial status of powder-injection molding. *JOM* **47**, 26–30 (1995)
4. S.T. Lin, R.M. German, Extraction debinding of injection molded parts by condensed solvent. *Int. J. Powder Metall.* **21**, 19–24 (1989)
5. L. Liu, N.H. Loh, B.Y. Tay, S.B. Tor, Y. Murakoshi, R. Maeda, Effects of thermal debinding on surface roughness in micro powder injection molding. *Mater. Lett.* **61**, 809–812 (2007)
6. B. Levenfeld, A. Varez, J.M. Torralba, Effect of residual carbon on the sintering process of M2 high speed steel parts obtained by a modified metal injection molding process. *Metall. Mater. Trans. A* **33**, 1843–1851 (2002)
7. M.R. Raza, F. Ahmad, M. Omar, R. German, A.S. Muhsan, Role of debinding to control mechanical properties of powder injection molded 316L stainless steel. *Adv. Mater. Res.* **699**, 875–882 (2013)
8. R.M. Rafi, F. Ahmad, M.A. Omar, R.M. German, Effects of cooling rate on mechanical properties and corrosion Resistance of vacuum sintered powder injection molded 316L stainless steel. *J. Mater. Process. Technol.* **212**, 164–170 (2012)
9. C.H. Ji, N.H. Loh, K.A. Khor, S.B. Tor, Sintering study of 316L stainless steel metal injection molding parts using Taguchi method: final density. *Mater. Sci. Eng.* **A311**(311), 74–82 (2001)
10. R.M. German, A. Bose, *Powder Injection Molding of Metal and Ceramics: Metal Powder Industries Federation* (Princeton, NJ, 1997)
11. B. Berginc, Z. Kampus, B. Sustarsic, The influence of MIM and sintering-process parameters on the mechanical properties of 316L SS. *Materiali in Tehnologije* **40**, 193–198 (2006)
12. S. Krug, S. Zachmann, Influence of sintering conditions and furnace technology on chemical and mechanical properties of injection molded 316L. *Powder Injection Moulding Int.* **3**, 66–70 (2009)
13. H.Ö. Gülsoy, S. Salman, Microstructures and mechanical properties of injection molded 17-4PH stainless steel powder with nickel boride additions. *J. Mater. Sci.* **40**, 3415–3421 (2005)
14. P. Vieira Muterlle, *Microstructural and Mechanical Properties of Co and Ti Alloys for Biomedical Applications Produced by Metal Injection Molding (MIM)*, Ph.D. Materials Engineering, University of Trento, 2010
15. C. García, F. Martín, P. de Tiedra, L.G. Cambronero, Pitting corrosion behaviour of PM austenitic stainless steels sintered in nitrogen—hydrogen atmosphere. *Corros. Sci.* **49**, 1718–1736 (2007)

Structural, Optical and Electrical Properties of Nano-structured Sn-doped ZnO Thin Film via Sol Gel Spin Coating Technique

I. Saurdi, M.H. Mamat, A. Ishak and M. Rusop

Abstract In this work, the Sn-doped ZnO thin films were prepared by Sol gel Spin coating technique on glass substrates at different concentrations of Sn 0, 0.5, 1.5, 1, 2.0 and 3 at.%. The surface morphology reveals that the average particle size of nano-structured Sn-doped ZnO thin films become smaller as the Sn concentrations increased as well as decreasing of average roughness. The optical band gaps were increased, while the resistivity of Sn-doped ZnO thin films were decreased when the Sn concentrations increased. The films doped with 2 at.% exhibited the best properties of average transmittance; RMS average roughness and resistivity were 96 %, 1.850 nm and $7.7 \times 10^2 \Omega \text{ cm}$, respectively.

Keywords Zinc oxide · Sn doping · Structural properties · Optical properties · Electrical properties

1 Introduction

Zinc oxide (ZnO) is an attractive semiconductor that has been widely studied for various applications such as gas sensors, dye sensitized solar cell and optoelectronic electronic devices etc. [1–4]. It has a unique properties with wide conductivity

I. Saurdi (✉) · M.H. Mamat · A. Ishak · M. Rusop
NANO-ElecTronic Centre (NET), Faculty of Electrical Engineering,
Universiti Teknologi MARA (UiTM), Shah Alam, Selangor, Malaysia
e-mail: saurdy788@gmail.com

M. Rusop
e-mail: nanouitm@gmail.com

M. Rusop
NANO-SciTech Centre (NST), Institute of Science, Universiti Teknologi MARA (UiTM),
Shah Alam, Selangor, Malaysia

I. Saurdi · A. Ishak
Faculty of Electrical Engineering, UiTM Sarawak Kampus Kota Samarahan Jalan Meranek,
Kota Samarahan, Sarawak, Malaysia

range, non-toxic, high surface activities, highly transparent in the visible region and also economical material with good thermal stability [5–7]. Furthermore, ZnO a well known II–IV compound semiconductor has a direct band gap 3.37 eV and 60 meV of free-exciton excitation energy at room ambient with chemical inertness makes it useful for dye-sensitized solar cell application [8]. Moreover, ZnO thin film that has good crystalline structure has been used to grow variety of structures such as nanowires, nanorods, and etc. [9, 10]. Besides that, in dye sensitized solar cell it has been used as a template for nanostructures growth as well as blocking layer. However, ZnO needs to modify its electrical, structural and optical properties in order to fulfill the requirement of various applications. Introducing other element in ZnO by doping process is a very useful to enhance the ZnO properties. Moreover, the ZnO doped with group elements III, IV, V and VI elements such as Al, Ga, In and Sn have shown its electrical, structural and optical properties improved. The ZnO that has been doped with other elements can be deposited using different techniques like Pulse laser deposition, chemical vapor deposition (CVD), Spray pyrolysis, RF sputtering [11] and sol-gel [12] etc. Among these techniques, sol-gel has the advantages such as good uniformity of thin film, low temperature synthesis and toward economical production.

In the present work, we have deposited various Sn concentrations on glass substrates. The effect of various Sn concentrations on the structural, optical and electrical properties of nano-structured ZnO thin films is highlighted in this work and towards the application in dye sensitized solar cell. To our best of knowledge, there are studies on Sn doping with ZnO but lack of study on various concentrations of small amount of Sn and understanding their properties that possibly to be applied in solar cell application such as dye sensitized solar cell. We have achieved good properties of optical as well as resistivity with sol gel technique at low heat treatment and thin films annealed in air. The nano-structured Sn-doped ZnO films deposited at different Sn concentrations are systemically investigated by I–V measurements, field emission scanning electron microscopy (FESEM), atomic force microscopy (AFM) and UV-Vis-NIR spectrophotometer, respectively.

2 Experimental Details

Microscopes glass was used as substrates were cleaned in the acetone, methanol and deionised water using ultrasonic cleaner in order to remove all the contamination. The nitrogen gas was used to dry the cleaned glass substrates before the deposition process by Sol gel spin coating techniques.

The nano-structured ZnO thin films were prepared using 0.4 M zinc acetate dehydrate as a precursor, 2-methoxyethanol as a solvent and monoethanolamine (MEA) as a stabilizer with molar ratio 1:1. Then appropriate amounts of tin (Sn) doping were achieved by adding tin (IV) chloride pentahydrate to the precursor solution. In order to study an effect of the Sn-doped concentration on structural, optical and electrical properties of the Sn-doped ZnO thin films, there were 6

solutions with doped concentration of Sn/Zn = 0, 0.5, 1, 1.5, 2, 3 at.% respectively, were used. The solution was stirred and heat for 3 h before aged for 24 h at room ambient. Then, the Sn-doped ZnO thin films were spin-coated on glass at a speed of 3,000 rpm for 1 min. Then, each layer of deposited thin film was preheated in air at 150 °C to evaporate the solvent. The coating procedure was repeated a few times to increase the film thickness. After that, the thin films were finally post-heated at 500 °C for 1 h in air using an electronic furnace. The film thicknesses were measured using the Veeco/D 150+ surface profiler. The structural, optical and electrical properties were characterized by field emission scanning electron microscopy (FESEM, JOEL), Park system XE-100 atomic force microscope (AFM), UV-Vis-NIR spectrophotometer (V-670EX) and I-V measurement, respectively.

3 Results and Discussion

3.1 Structural Properties

Figure 1 shows FESEM images of the nano-structured Sn-doped ZnO thin films deposited on glass substrates at various Sn concentrations of 0, 0.5, 1, 1.5, 2.0 and 3 at.%. The images reveal that the nano-structured ZnO thin films morphologies had a smaller particle size as the Sn concentration increased. The average particles size of Sn-doped ZnO thin film estimated from FESEM images at different concentrations of 0, 0.5, 1, 1.5, 2.0, 3 at.%, were 36, 30, 28, 26, 20 and 25 nm, respectively. Therefore, with the increasing of Sn dopant into ZnO by substitutional doping might reduced the average particle size due to a smaller radius of Sn⁴⁺ ions (0.069 nm) than ion Zn²⁺ (0.074 nm) that retarded the growth process of ZnO crystallization [13]. From the FESEM images, the surface flatness of thin film was observed as the Sn concentrations increase to 2 at.% that correlated to the uniformity of thin films as be confirmed from Fig. 1a undoped ZnO and Fig. 1e Sn doped ZnO with 2 at.%. We can conclude that Sn doping might improves the surface flatness as well as the uniformity of films. However, as the Sn increase to 3 at.% the film had different of particle size, which may be due to the ZnO structure deterioration occurred with increasing of doping concentration [14].

AFM images with the scan size of 10 μm × 10 μm of Sn-doped ZnO films are shown in Fig. 2. As observed from AFM images and RMS roughness results in Table 1 there are interrelation between the Sn doping to the surface roughness of films, in which the surface roughness decrease as the Sn concentrations increased. Besides that, in consequence of decreased the average particle size of Sn-doped ZnO, it possibly reduce the surface roughness as supported by average particle size that discussed earlier. Table 2 shows the average roughness of nano-structured Sn-doped ZnO films whereby the average roughness decreased with Sn concentrations. The Sn concentrations with 2 at.% has the smallest of RMS roughness (1.85 nm) slightly smaller than reported by Tsay et al. [15] that uses the scan size of 1 μm × 1 μm. However, when the Sn concentration more than 2 at.% average

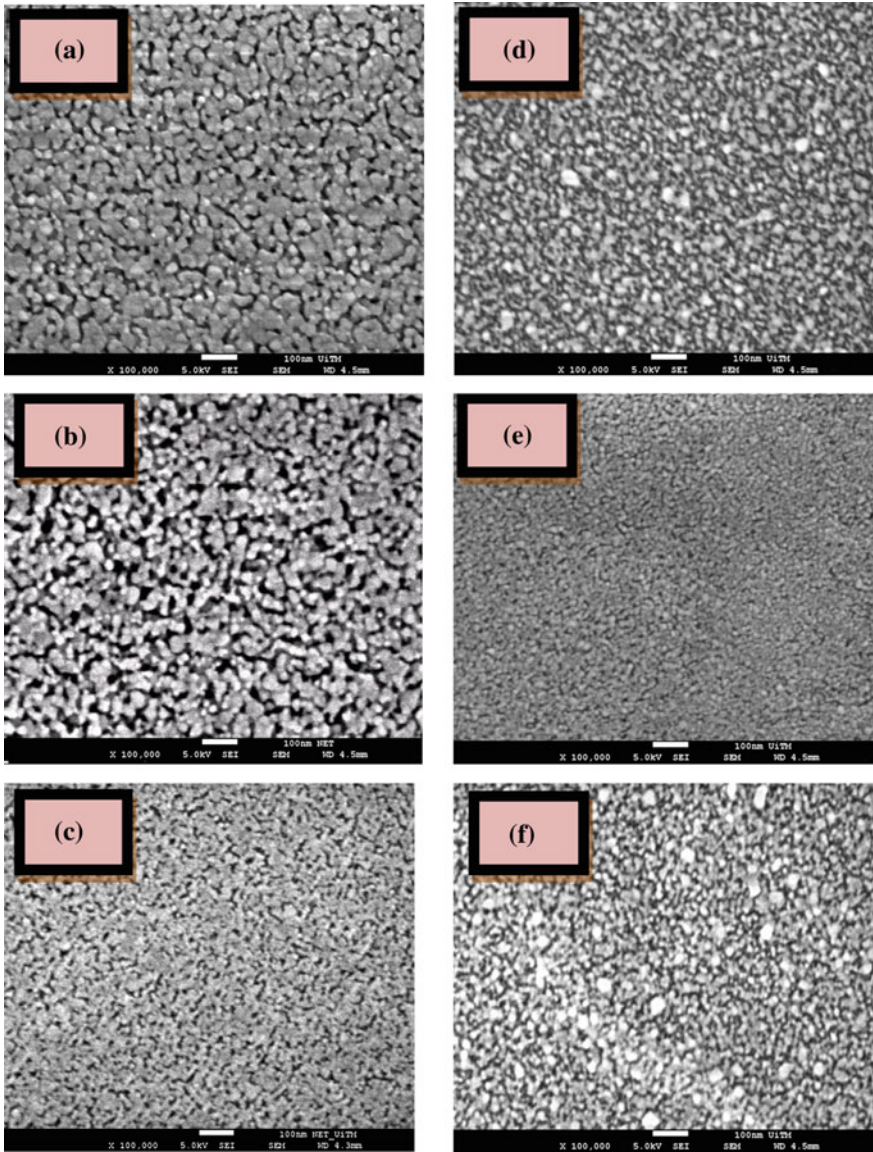


Fig. 1 FESEM images of Sn-doped ZnO thin films at **a** 0, **b** 0.5, **c** 1, **d** 1.5, **e** 2, **f** 3 at.% by magnification of 100 k and 5.0 kV

roughness increased, might be due to the increased of average particle size at 3 at.% Sn-doped ZnO films. Furthermore, a small surface roughness reduced the scattering effect and might improve the optical properties.

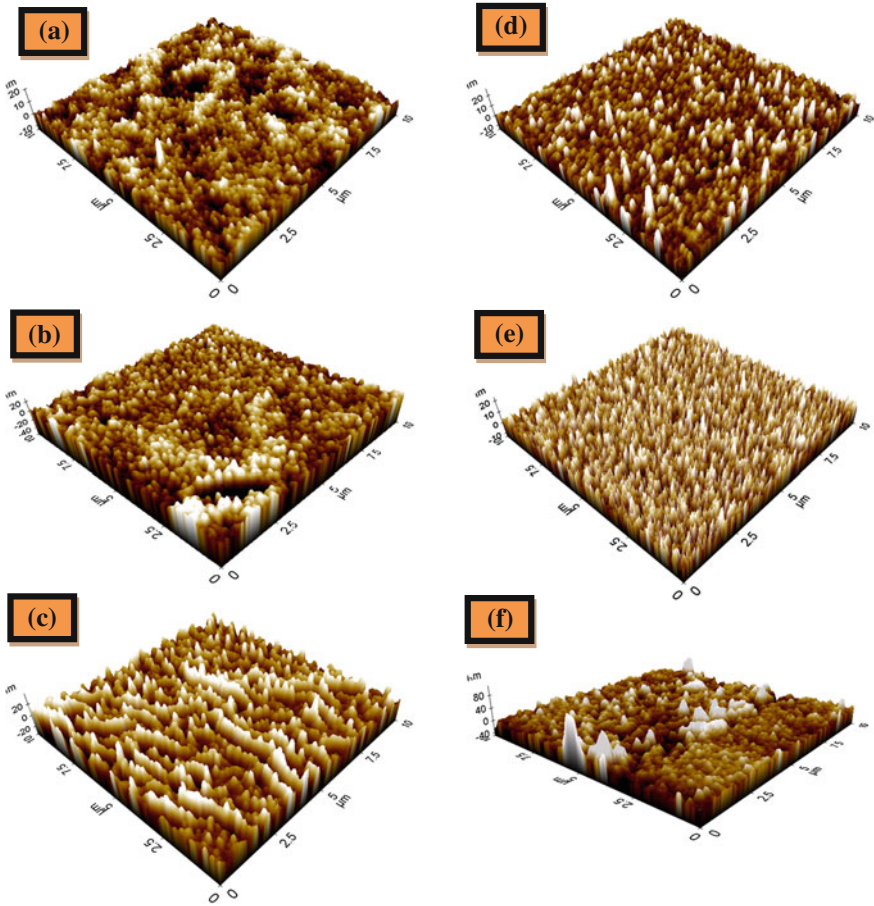


Fig. 2 AFM images of Sn-doped ZnO thin films at **a** 0 at.%, **b** 0.5 at.%, **c** 1 at.%, **d** 1.5 at.%, **e** 2 at.%, and **f** 3 at.%

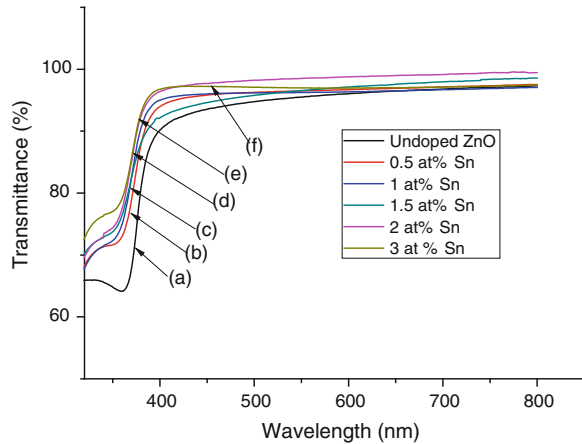
Table 1 Average roughness of nano-structured Sn-doped ZnO at different Sn concentrations

Tin (Sn) concentrations	RMS roughness R_q (nm)
0 at.%	2.995
0.5 at.%	2.755
1 at.%	2.530
1.5 at.%	2.055
2 at.%	1.850
3 at.%	2.850

Table 2 Optical band gap energy of nano-structured Sn-doped ZnO at different Sn concentrations

Tin (Sn) concentrations	Optical band gap energy E_g (eV)
0 at.%	3.23
0.5 at.%	3.26
1 at.%	3.28
1.5 at.%	3.29
2 at.%	3.30
3 at.%	3.32

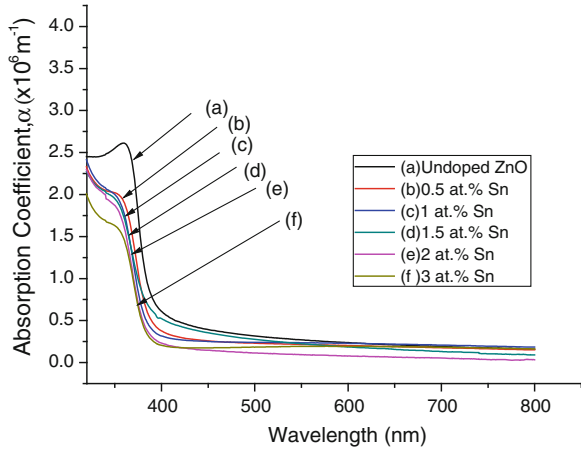
Fig. 3 Transmission spectra of Sn-doped ZnO thin films



3.2 Optical Properties

Figure 3 shows the transmittance spectra of nano-structured Sn-doped ZnO thin films. All the thin films exhibit high transparency between visible wavelengths of 400–800 nm and high absorption edges in UV region. The undoped ZnO shows the average optical transmittance about 90 % with absorption edge at a wavelength about 370 nm. Meanwhile, the Sn-doped up to 2 at.% had higher transmittance as compared to undoped ZnO. However, as the Sn concentration increased further up to 3 at.% average transmittance was lower than other Sn-doped thin films. This result is correlated and supported by the surface roughness measurement in Table 2, which the surface roughness could affect the transmittance of thin film. Furthermore, the lower of transmittance Sn-doped thin film was attributed to the scattering effect at higher doping concentration and might be due to the increasing of ratio metal to oxygen [16, 17]. The average transmittance of 96 % had been achieved in this work that comparable and slightly higher than average transmittance reported by Pan et al. [18]. Moreover, the thin films that allow high percentage of spectrum of light to penetrate in the visible region wavelength might be useful for solar cell application such as dye sensitized solar cell [19].

Fig. 4 Absorption coefficient of Sn-doped ZnO thin films

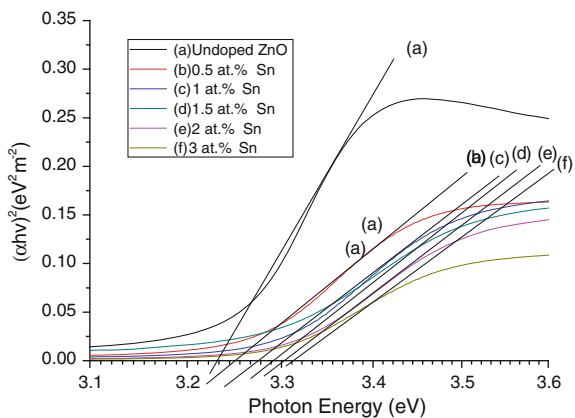


The absorption coefficient of Sn-doped ZnO films at different Sn doping concentration is shown in Fig. 4. The absorption coefficients which is indicated using transmittance data by applying Lambert’s law as shown in Eq. (1):

$$\alpha = \frac{1}{t} \ln \left(\frac{1}{T} \right) \tag{1}$$

where, t is the thickness of thin film, α is the absorption coefficient, and T is the transmittance value at respective wavelength. The result show all films exhibit high absorption in UV region due to the wide band gap properties. Beside that, the optical band gap values of the nano-structured Sn-doped ZnO could be obtained using transmittance data and plotting $(\alpha h\nu)^2$ versus photon energy graphs that also called as Tauc’s plot. The Tauc’s plot is shown Fig. 5 and the resulting optical gap values indicated in Table 2.

Fig. 5 Optical band gap energy estimation using Tauc’s plot



The optical band gaps energy were found to be increased from 3.23, 3.26, 3.28, 3.29, 3.30 and 3.32 eV for nano-structured Sn-doped ZnO thin films deposited at different Sn concentrations of 0 at.%, 0.5, 1, 1.5, 2 and 3 at.% respectively. The optical band gap energy of Sn-doped ZnO thin film was in the range of wide band gap region. This phenomenon due to the electron that has adequate energy supplied from photon energy will jump from the valence band to the conduction band. Therefore, at higher Sn concentration the Sn-doped ZnO thin film had broader the band gap energies compared to undoped ZnO film. Shelke et al. [20] reported that the broadening of optical band gap energy which may be attributed to Burstein-Moss shift.

3.3 Electrical Properties

Figure 6 shows the I-V curve of Sn-doped ZnO thin films at applied voltage -10 to 10 V. In order to study the I-V characteristics of ZnO thin films the 2 probes system measurement have been used. From this figure, all the thin films show a good contact with Au as a metal contact. Furthermore, the ZnO thin film doped at 2 at.% Sn shows the highest current intensity among all Sn-doped ZnO thin films, which reflecting the best of electrical properties, while the undoped ZnO film shows the lowest of current intensity that indicating poor of electrical properties. In Fig. 7, the results show the resistivity ZnO thin films decreases as doping concentration increases from 0 to 2 at.% with the lowest of resistivity is $7.7 \times 10^2 \Omega \text{ cm}$. However, at 3 at.% the resistivity slightly increased. Furthermore, the lower of resistivity of Sn-doped thin film from 0 to 2 at.% of resistivity was due to successfully of substitutional doping into ZnO structure. Therefore, 2 free electrons produces from the substitutional doping which increased carrier concentration in the films. As the Sn concentration increase further up to 3 at.%, it was believed that carrier concentration become higher due to the substitutional doping that might increase more free electron in the thin films as well as the increment of optical band gap energy. However, the resistivity slightly increased

Fig. 6 I-V curves of ZnO thin films at different Sn doping concentrations

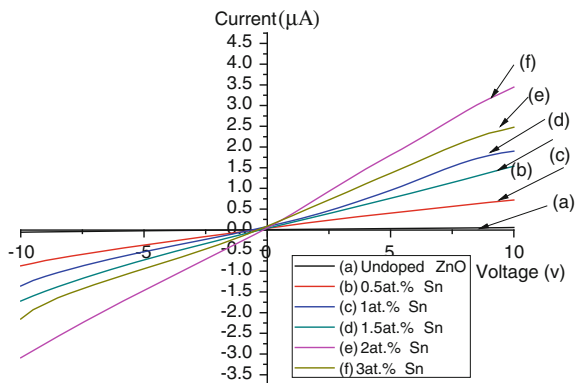


Fig. 7 Resistivity of ZnO thin films at different Sn doping concentrations

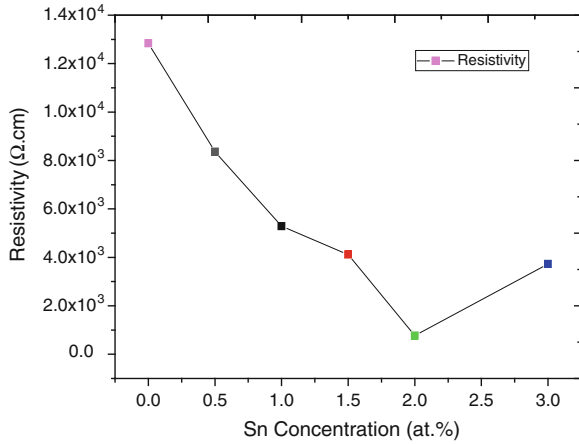
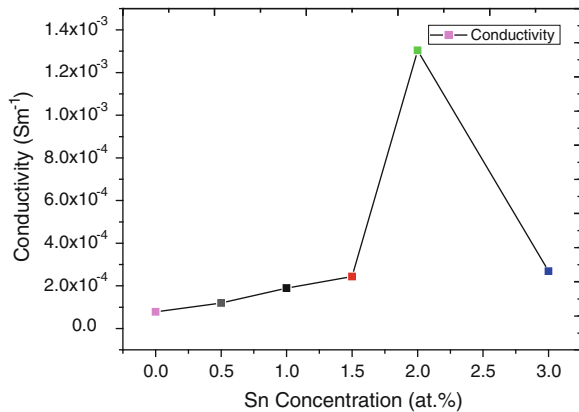


Fig. 8 Conductivity of ZnO thin films at different Sn doping concentrations



and the conductivity decreased this phenomenon due to decrement of electron mobility and the deterioration of ZnO structure [21]. Meanwhile, the conductivity of Sn-doped ZnO thin films is calculated by the reciprocal of resistivity values. Figure 8 shows the conductivity of ZnO thin films increases as doping concentration increases from 0 to 2 at.%, whereas the at 3 at.% shows reduction pattern and this conductivity behavior vice versa of resistivity and the highest of conductivity is $1.3 \times 10^{-3} \text{ S cm}^{-1}$. Moreover, understanding the resistivity and conductivity behavior of thin films is important in order to explore the potential of thin films for various applications. The Sn-doped thin film which the best properties in this work has a potential application for a nanostructure growth as well as the active layer in dye-sensitized solar cell (DSSC).

4 Conclusions

The influences of different Sn doping concentration on the structural, optical and electrical properties of nano-structured ZnO thin films have been investigated. The surface morphology reveals that nano-structured Sn-doped ZnO thin films has reduction of average particle size as the Sn concentrations increased as well as decreasing of average roughness. The results show all films are transparent in the visible region with average transmittance above 90 % and exhibit high UV absorption properties. Meanwhile, the optical band gaps and conductivity were increased as the Sn concentrations increased. However, at 3 at.% the conductivity of Sn-doped ZnO thin films changed. Among all of Sn-doped ZnO thin films, films doped with 2 at.% exhibited the optimum properties of transmittance, RMS average roughness and resistivity were 96 %, 1.850 nm and $7.7 \times 10^2 \Omega \text{ cm}$, respectively.

Acknowledgments Authors are grateful for the financial support from Research Management Institute (RMI) and the Ministry of Education. The authors are also thankful to the staffs of NANO-ElecTronic Center (NET), NANO-SciTech Centre of Universiti Teknologi MARA and UiTM for equipment and facilities.

References

1. M. Liao, C. Hsu, D. Chen, Preparation and properties of amorphous titania-coated zinc oxide nanoparticles. *J. Solid State Chem.* **179**, 2020–2026 (2006)
2. R. Bhatt, H. Sankaranarayanan, C.S. Ferekides, D.H. Morel. 2, (eds.), in *Proceedings of the 26th PVSC*, vol. 171 (Anaheim, California, 1997), pp. 383
3. M.S. Arnold, P. Avouris, Z.W. Pan, Z.L. Wang, Field-effect transistor based on single semiconducting oxide nanobelts. *J. Phys. Chem.* **107**, 659–663 (2003)
4. D. wei, Dye-sensitized solar cell review. *Int. J. Mol. Sci.* **2** **11**, 1103–1113 (2010)
5. H. Wang, Z. Wu, Y. Liu, Z. Sheng, The characterization of ZnO-Anatase-Rutile three components semiconductor and enhanced photocatalytic activity of nitrogen oxides. *J. Mol. Catal. A: Chem.* **287**, 176–181 (2008)
6. R. Velmurugan, M. Swamination, An efficient nanostructured ZnO for dye-sensitized degradation of reactive red 120 dye under solar light. *Sol. Energy Mater. Sol. Cells* **95**, 942–950 (2011)
7. M. Giannouli, F. Spiliopoulau, Effects of the morphology of nanostructured ZnO films on the efficiency of dye-sensitized solar cells. *Renew. Energy* **41**, 115–122 (2012)
8. X.D. Wang, J.H. Song, Z.L. Wang, Nanowire and nanobelt arrays of zinc oxide from synthesis to properties and to novel devices. *J. Mater. Chem.* **17**, 711–720 (2007)
9. Y. Tao, M. Fu, A. Zho, D. He, Y. Wang, The effect of seed layer on morphology of ZnO nanorod arrays grown by hydrothermal Method. *J. Alloy. Compd.* **489**, 99–102 (2010)
10. H.K. Lee, M.S. Kim, J.S. Yu, Effect of AZO seed layer on electrochemical growth and optical properties of ZnO nanorod arrays on ITO glass. *Nanotechnology* **22**, 445602 (8 pp) (2011)
11. S.H. Jeong, J.W. Lee, S.B. Lee, J.H. Boo, Deposition of aluminum-doped zinc oxide films by RF Magnetron sputtering and study of their structural, electrical and optical properties. *Thin Solid Films* **435**, 78–82 (2003)
12. D. Raoufi, T. Raoufi, The effect of heat treatment on the physical properties of sol-gel derived ZnO thin films'. *Appl. Surf. Sci.* **255**, 5812–5817 (2009)

13. M.S. Ghamsari, A.R. Bahramian, High transparent sol-gel derived nanostructured TiO₂ thin films. *Mater. Lett.* **255**, 361–364 (2008)
14. K.J. Chen, F.Y. Huang, Y.T. Chen, S. Jin, Surface characteristic, optical and electrical on sol-gel synthesis Sn-doped ZnO thin film. *Mater. Trans.* **51**, 1340–1345 (2010)
15. C.-Y. Tsay, H.-C. Cheng, Y.-T. Tung, W.-H. Tuan, C.-K. Lin, Effect of Sn-doped on microstructural and optical properties of ZnO thin films deposited by sol-gel method. *Thin Solid Films* **517**, 1032–1036 (2008)
16. Y.S. Kim, W.P. Tai, Electrical and optical properties of Al-doped ZnO thin films by sol-gel process. *Appl. Surf. Sci.* **253**, 4911–4916 (2007)
17. T.V. Vimalkumar, N. Poornima, K.B. Jinesh, C.S. Kartha, K.P. Vijayakumar, Effect of Sn-doped on microstructural and optical properties of ZnO thin films deposited by sol-gel method. *Appl. Surf. Sci.* **257**, 8834–8840 (2011)
18. Z. Pan, X. Tian, W. Shaokun, C. Xiao, Z. Li, J. Deng, H. Guanhui, Z. Wei, Effect of Al and Sn dopants on the structural and optical properties of ZnO thin films. *Superlatticed Microstruct.* **54**, 107–117 (2013)
19. D.I. Suh, S.Y. Lee, T.H. Kim, J.M. Chun, E.K. Suh, O.B. Yang, S.K. Lee, The fabrication and characterization of dye-sensitized solar cells with a branched structure of ZnO nanowires. *Chem. Phys. Lett.* **442**, 348–352 (2007)
20. V. Shelke, B.K. Sonawane, M.P. Bhole, D.S. Patil, Electrical and optical properties of transparent conducting tin doped ZnO thin films. *J. Mater. Sci.* **23**, 451–456 (2012)
21. P. Sagar, M. Kumar, R.M. Mehra, Electrical and optical properties of sol-gel derived ZnO: Al thin films. *Mater. Sci.-Pol.* **23**, 686–696 (2005)

Part VII
Sustainable Environment

Stakeholder Roles in Building Integrated Photovoltaic (BIPV) Implementation

Aaron Boon Kian Yap, Kai Chen Goh, Ta Wee Seow
and Hui Hwang Goh

Abstract Malaysia construction sector has been known to be a sector that pollutes the environment through its land clearing process to its harvesting of raw material from the environment to be used in construction process. Part of this construction process involves building the energy sectors. Mega power plant projects are important to sustain the Malaysian businesses and operations. However, it cannot be halted totally due to the inevitable necessity to meet the needs of the population. Therefore, the Malaysian government has shown effort to balanced sustainable environment and human advancement through exploration of renewable energy through the introduction and renewable energy (RE) policies and Feed-in-Tariff (FiT). Malaysia's strategic locality in the equator proves prospective for untapped solar energy, in which can be harnessed through Building Integrated Photovoltaic (BIPV). However, the BIPV implement is relatively slow although it has been introduced for more than 10 years although it has so much potential. To address this problem, this paper identifies the five major BIPV stakeholders in Malaysia which are the Government, Tenaga Nasional Berhad (TNB), Developers, Consumers and Research and Development (R&D) together with the problem that these stakeholders face in BIPV implementation. The objective of this research is to suggest focus adding value to rectify the developers' setback that will help expedite BIPV implementation in Malaysia using the Iskandar Region, Johor as case study.

Keywords BIPV · Developers' perspective · Iskandar Johor · Solar energy

A.B.K. Yap (✉) · K.C. Goh · T.W. Seow · H.H. Goh
Department of Construction Management, Universiti Tun Hussein Onn Malaysia,
Parit Raja, Batu Pahat, Johor, Malaysia
e-mail: aaronypbk@gmail.com

K.C. Goh
e-mail: kaichen@uthm.edu.my

T.W. Seow
e-mail: tawee@uthm.edu.my

H.H. Goh
e-mail: hhgoh@uthm.edu.my

1 Introduction

Malaysia strategic locality and geographical terrain conditions enable four major forms of renewable energy, namely Hydro, Solar, Wind and Biomass, can be considered as ideal; therefore other criteria must be included in determining most suitable renewable energy with maximized capacity to be selected. Aspects such as technical, political, economy, social and environmental must be taken into consideration. The current policies on renewable energy in Malaysia are deployed under the 8th, 9th and 10th Malaysian Plan to achieve 5.5 % renewable energy mix in Malaysia, displacing a staggering amount of 985 MW worth of fossil fuel energy by 2015 [1].

However, the application of Building Integrated Photovoltaic (BIPV) in Malaysia is still weak. Previous researches show that BIPV still faces plenty of challenges in Malaysia despite being in the market for quite a number of years [2]. In pursuit of sustainable development frontier, Malaysia has been backing the development of BIPV indirectly through the governance of renewable energy by through the Sustainable Energy Development Authority (SEDA) of Malaysia. Though the 8th, 9th and 10th Malaysian plan did highlight renewable energy in general, there is no policy that governs BIPV implementation specifically. This leads to investors especially the major stakeholders remaining skeptical about the actual potential for investment in BIPV. These stakeholders hold the capacity and liquidity in investing large scale into the BIPV implementation that could lead to potential blooming of the BIPV market. However, construction stakeholders are more to business based investment and expect monetary returns from their investments [3]. Furthermore, there is also a capped quota 9.86 MW in 2012 with additional of 2 MW the same year and expected quota of 6 MW the following year. This capped hampers any investment interest of these stakeholders into BIPV thus slowing down the BIPV implementation. Feed-in-Tariff (FiT) rates given by the SEDA does not encourage economy to scale investment and with relatively cheap electricity provided through fossil fuel due to heavy government subsidies, this position BIPV to be even less competitive in terms of pricing and longer payback period in the investment.

2 Literature Review

2.1 *Building Integrated Photovoltaic*

Malaysia's potential is high due to the strategic geographic location near the equator averaging 4.96 kWh/m² annual solar irradiance and with the range of 4.8–6.3 kWh/m² irradiance monthly except for December due to the monsoon season [4]. Malaysia is said to have solar potential about four time of the world's fossil fuel reserve [5]. Solar power can be regarded as the cleanest technology for electricity production.

Nonetheless, there is scarcity in the availability of material for higher efficiency solar cells and the solar cell production poses environmental hazards if the production process is not handled appropriately. The detailed production involves higher costs which increased the price of the solar panels. On the other hand, the price for solar panels has decreased from (Malaysian Ringgit) MYR 31,410 per kilowatt peak (kWp) in 2005 to MYR 20,439 kWp in 2009 [6]. The latest pricing offered in 2013 sees a further drop to an estimated MYR 10,000 kWp. Though the decrementing in prices looks promising in lowering the CAPEX for solar investment, yet the rates for return on investment are seen as low competitiveness against the conventional fossil fuel with heavily subsidized natural gas [7]. However, two-thirds of Malaysia land area is tropical forest, hence to build major solar power plant is not environmentally viable. Thus BIPV for rooftops to harness solar power is the best option [6].

2.2 BIPV and BAPV

BIPV and BAPV have almost similar in description but it totally different type of system. BIPV is defined as Building Integrated Photovoltaic system involves integration of the system into the skin of the building and is considered in the conceptual phase of the project before the building is actually developed. BAPV is defined as Building Applied Photovoltaic which involves retrofitting the system into the building after the building is completed, upon the requirement of the owner. However, in Malaysia, both BIPV and BAPV are categorized under the same category to ease procedures and avoid confusion [8].

2.3 BIPV Stakeholders Roles

Fossil fuel, steel forging, heavy machineries and land clearing are a major part of modern day construction process. These are an inevitable factor which contributes huge amount of greenhouse gas (GHG) emission especially CO₂, notwithstanding with the wastage and inefficient usage of it. The need to give back to the environment is there, not just for the sake of profiting but to create a sustainable development for the future. There are five major influencers in that could affect the BIPV market directly. They are the Government, Tenaga Nasional Berhad (TNB), Developers, Consumers and the Research and Development (R&D).

2.3.1 Government

Malaysia is still over dependent on fossil fuel especially natural gas and coal to generated electricity. The price for supply of natural gas and coal are very escalates to sensitivities such as appreciation of exchange rates, tighter demands, production

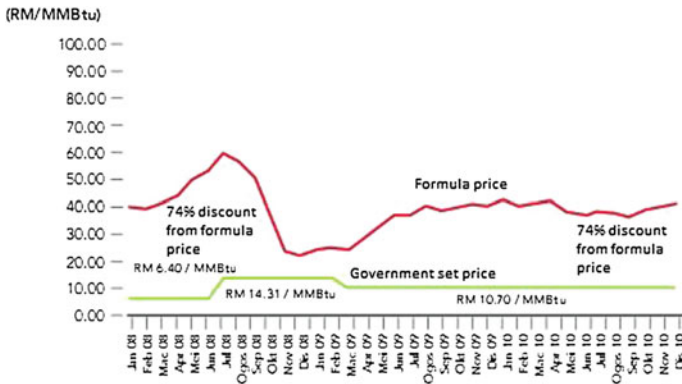


Fig. 1 Price of natural gas in Malaysia [10]

cost, inflation rate and limited stocks in the market, in which this does not side the Malaysia present day economy [9]. The government is still heavily subsidizing the fossil fuel for energy sector as shown in the earlier Fig. 1. With these sensitivities escalation, the risks and challenges for the Malaysian government are great and could be unpredictably disastrous should the supply is disrupted. Nevertheless, these heavy subsidies given on the fossil fuel electricity can be relocated into short term assistance of BIPV projects, reliving the government of long term subsidy burden plus driving the BIPV implementation even further, reducing the risks from the volatile sensitivities. Moreover, the government has currently given many incentives to help create this sustainable development such as the FiT especially for BIPV.

Countries with high technology frontier like Germany, France and Australia has been adopting the solar energy and the FiT policy with various incentives and abandoning nuclear energy after the Fukushima accident in Japan [2]. Japan has also adopted solar BIPV through their NEDO project. Even Malaysia’s neighbor, Singapore is looking into the prospect of solar energy harnessing through BIPV which is projected to supply 28 % of the current electricity demand and reduce approximately 8 % of the CO₂ released with the 30 % margin above peak set by their government. It is estimated that solar can meet the electricity generation up to 65 % in the morning by 2050 [11]. Therefore, the prospect for Malaysia government to invest into solar energy especially BIPV is bright and promising. Other than that, the government has a general policy that does not specifically highlight any of the RE. However, BIPV still lacks of overarching solar policy framework that could actually guide BIPV implementation exclusively and could serve as the BIPV push factor [12]. Besides that, the government’s hesitant in implementation hence creating the lack of information flow and cooperation between the private sector and the government which hampers the RE and BIPV efforts [11]. With the introduction of the SEDA portal, clarification and application can be done online easing the information flow and showing the government intention to support RE and BIPV [13]. Furthermore, the government also has allocation for quota for each RE under SEDA to make it looks lucrative but also at the same time adversely making it

difficult for the investors who are keen to invest. These factors from the government's role on BIPV can have significant impact on BIPV advancement or adverse effect of retardation for BIPV implementation.

2.3.2 Tenaga National Berhad (TNB)

TNB is another key influencer in BIPV implementation and is a direct stakeholder of BIPV. TNB is the largest privatized electricity utility company in Malaysia after the Electricity Supply (Successor Company) Act 1990 [Act 448] was instated to replace the National Electricity Board of the States of Malaya (NEB). TNB manages and operates the National Grid of Malaysia, a comprehensive transmission network that links TNB power stations and the Independent Power Producers (IPPSs) to the distribution network [14]. This means that TNB plays a significant role in the implementation of BIPV, as the provider for interconnection from the BIPV system to the National Grid.

The construction of new RE plants by TNB such as biomass and hydropower requires months if not years to complete where as solar can be assembled and disassembled for relocation in days, hence increases the versatility of solar electricity. This will help TNB turnover even quicker recover economically plus lessen the burden government on fossil fuel subsidy though the cost per kilowatt-hour (kWh) is not as attractive in comparison. TNB has piloted project coastal wind energy in Pulau Perhentian, Terengganu and Pulau Banggi, Sabah and found it not viable due the insufficient substantial wind to create large capacity electricity plus the cost of construction is subjected to accessibility and the forces of nature [6]. TNB has RM 99 billion worth of assets and major parts are the three hydroelectric schemes and six thermal stations but with approximately 8.4 million customer base and ever increasing electricity demand, alternatives must be looked into to supply the excess from demand and maintain a reserve ratio more than 30 % as required [14]. Existing fossil fuel or RE power plants could be put at minimum capacity inside the reserve ratio as energy storage to supply during intermittent weather and night fall should the BIPV electricity is not sufficient, a move with not only prolongs fossil fuel from depletion but also prolong the lifespan of RE power plants without modification to existing infrastructures, making it a sustainable development due to its ability to co-exist towards the present infrastructures [11]. BIPV can help keep these existing energy infrastructures while able to apply the RE in Malaysia. These factors mention are not included in the price per kWh generated which makes solar non competitive compare to other RE when assessed against fossil fuel electricity generation.

2.3.3 Research and Development (R&D)

The most ideal source to be exploited in Malaysia is solar due to the abundance in comparison with the other sources. Moreover, BIPV does not require modification to the current Malaysia power infrastructure unlike the hydropower, wind and

biomass which is much isolated and requires building a new supporting connector power infrastructure [15]. This makes BIPV literally 'plug and play', versatile and availability for quick implementation and installation [1]. Being the second largest solar photovoltaic producer, Malaysia has the capability not only to produce and assemble solar photovoltaic modules but also in large solar capacity installation, dispelling the myth of lacking of expertise in this area. This is proven through the construction of several government building such as Centre of Environment, Technology and Development, the Green Energy Office (GEO) of Pusat Tenaga Malaysia (PTM) and Monash University (Sunway) along with a few residential building in Cheras, Semenyih, Bukit Sebukor (Malacca), Setia Eco Park, Putrajaya and Bangsar [16]. The concern of BIPV is also on the productivity of electricity generation especially during intermittent weather and the night fall, yet the fully utilization of BIPV does not mean fully abandoning other existing RE or fossil fuel power plants infrastructures. Though the electricity generated cannot be stored due to the non-existent of a very large enough capacity electricity storage system but BIPV can be used to meet the demand of the electricity which usually peaks in the morning and afternoon due to business and office consumption with occasionally at night fall for events [11]. The other concern is whether BIPV can support the air-conditioner is almost essential many buildings and houses due to the power surge required to start up the air-conditioner [17]. However, with the new inverter air-conditioner which does not require much electricity to start up makes BIPV more viable to support the air conditioning system.

2.3.4 Consumers

Consumer plays a major role because they are the end user and owner of the property where BIPV is installed. They are the one benefiting the most and have the capacity to invest into RE. FiT are directly paid to them from TNB and can help them out with expenses or loan in this inflating economy. However, the aesthetic valuation of BIPV implementation is based individually. Nevertheless there has been a study made on general public awareness for RE conducted show positive Malaysian public perspective in the RE and especially an exceptionally high response for solar [1]. The high response for solar shows that the public begin to have a certain level of knowledge for solar and its profitability value in the future. The results are still very encouraging despite many barriers that have to be tackled. There is some limitation financially where financial institution are still skeptical about BIPV to approve loans because PV modules are still considered a detachable fittings and are not consider as a fixture as one of a pre-requisite for large amount of investment or housing loan that poses a risk to is not worth taking for them [12]. The interest rates are relatively high, extending the long payback period nearer to the lifespan of solar modules which makes it not lucrative enough plus the FiT rates are not "economic to scale" friendly with a capping in stage as the PV watt peak

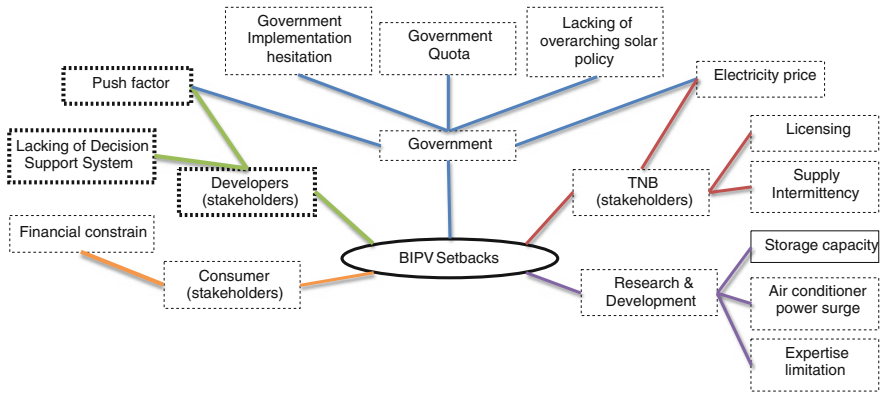


Fig. 2 Summary of stakeholders’ relationship and setbacks

capacity increases. On the other hand, BIPV has no mechanical parts makes it easy to maintain and very reliable, implying relatively minimal OPEX as compared to the other RE power plants and also beneficial towards to consumers [18]. They would not need to fork extra to maintain and minimum cleaning is needed, hence making the month payback a significant amount.

2.3.5 Developers

The existing stakeholders for implementation of BIPV do not include developers into play the role. However, the response for BIPV implementation is slow due to long paperwork trail for application and inability to finance BIPV projects on the consumer side. Therefore, the developers are introduced to play a part as the BIPV push factor for the government where they will facilitate implementation and the end user are consumers [16]. The whole process will be taken over by the developers as illustrated in the proposed stakeholders’ relationship in Fig. 2. BIPV adds value to the building, making it more marketable as one of the green development plus adds incentive to the consumer where the BIPV is package into the overall house price that can be included into the housing loan and from the FiT incentives given out that could help housing loan repayment. Besides that, the initial CAPEX will be boreed by the developers who have financial capacity to build the houses until it is completed and compliance to the SEDA requirement. Then the consumers can apply for housing loan to pay for the house upon purchase of the house, together with the BIPV installed in the house. The payment for FiT can then be transferred to the consumers according to the lot ownership purchase.

3 Research Methodology

3.1 Research Design

In order to rectify the research problems, a research project is undertaken at the Iskandar Region, Johor. This research aims to create a stakeholders' relationship model that includes the developers as one of the major influencer. The research goes through 4 stages which are:

1. Identification of problem
The problem of the research is identified. Research objective and a methodological approach is being sketch up as a guideline for the whole research.
2. Literature Review
Past research on the topic is being looked into and the roles of each stakeholder are being identified. Industry report are being used generate more information on the stakeholders and strengthens the roles of the stakeholders involved at the present moment.
3. Data Analysis
Extensive literature review and industry reports are being used as tools to collect data for data analysis. A general summary of framework is being used to link up the roles and build relationship between the stakeholders. The data is then further analyzed according to the significance of the information and an existing theoretical framework model is on the stakeholder's relationship. Then a proposed model is being build that will include developers according to the roles played by the stakeholders. The model is then put though a case study to evaluate and validate whether the model can be applied in projects.
4. Results
The findings are being discussed and evaluate in the findings section. Figures are being used to help ease understanding between the roles and relationship of the stakeholders.

4 Results

Figure 2 shows the summary of stakeholders and setbacks faced in BIPV implementation in Malaysia. However, this research focuses on the developer because the value that Developer can play an important role in the implementation of BIPV in Malaysia. However, there are two major setbacks that are faced by developers in BIPV implementations. The first is the push factor among developers and lacking of actual decision support system that could assist developers make decisions on whether to invest into BIPV or not. The push factor is mainly because of the lacking of interest among the developers, the government's quota and the non-economic to

scale FiT incentives which does not motivate the developers to actually adopt BIPV into construction projects. The developers also are hesitant to invest because there is the lack of decision support system that could help the developers to actually see the profit and value for BIPV implementation in their construction projects. Therefore, adoption of BIPV into construction project is important with the help of a dependable decision support system model to ensure BIPV implementation among the developers. There are a few propose mechanism that could be proposed among the developers to help the implementation. For adoption, BIPV needs a better marketing strategy with a good interest for housing loan to ensure affordability of the consumers. Besides that, the project can be included as a green building project which creates good reputation for the developers. Moreover, the decision support system must take in consideration the relative efficiency of the BIPV system and also could calculate the return on investment for the project as a whole. Other than that, if the decision support system can compare among PV module to find the most suitable PV module for BIPV is definitely an additional effective tool to expedite implementation. The additional role of the developers in BIPV implementation is illustrated in Fig. 3.

The most recent push for BIPV implementation was the proposal to start a community-based solar power project in the Iskandar Region Economic Corridor in Johor instead of leaving the rooftop bare by the Iskandar Regional Development Authority (IRDA). This is following the property bloom in the Iskandar Region by the influx of foreign investment especially from China [19]. This is an excellent opportunity to maximize investment by developers in adopting BIPV with property project especially residential. Johor is still a developing economic state with a

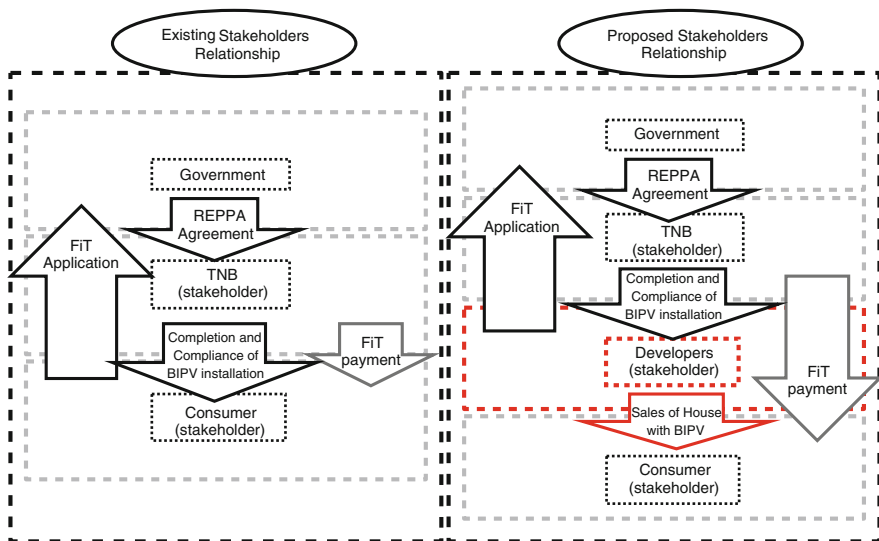


Fig. 3 Stakeholders' relationship model

relatively flat terrain among the other state terrains in Malaysia, minimizing the concerns of nature's shading from surrounding mountains or hills. However, there is still the lapse of proper decision support system that can assist these developers to make sound and accurate decision for the adoption of BIPV into their projects [16]. The adoption of BIPV into construction project gives the developers a significant role to play, given the capacity and liquidity of investment is present for these developers.

5 Conclusion

In pursuit of a sustainable future, the Malaysian government has shown effort to balanced sustainable environment and human advancement through exploration of renewable energy through the introduction and renewable energy (RE) policies and (FiT). Malaysia's strategic locality in the equator proves prospective for untapped solar energy, in which can be harnessed though BIPV. All five major BIPV stakeholders in Malaysia which are the Government, TNB, Developers, Consumers and Research and Development (R&D) together must address and tackle as much setbacks as possible to ensures a more smooth and successful implementation. However, the developer plays significant role as "push factor" in the BIPV implementation. The case study in Iskandar Region, Johor is a good start because of influx of prospective investment into the property development which gives developers the opportunity to further push BIPV implementation. This research gives better insight into the value of BIPV and expedites BIPV implementation in future sustainable development.

Acknowledgments The authors express gratefully acknowledgment to the industry stakeholders for their valuable contributions towards the success of this research. This research is fully funded by Ministry of Education (Malaysia) and Universiti Tun Hussein Onn Malaysia (UTHM) under Vot: E043, Exploratory Research Grant Scheme (ERGS) Phase 1/2013.

References

1. N. Gomesh, I. Daut, M. Irwanto, Y.M. Irwan, M. Fitra, Study on Malaysian's perspective towards renewable energy mainly on solar energy. In *TerraGreen 13 International Conference 2013—Advancement in Renewable Energy and Clean Environment, Energy Procedia*, vol. 36, pp. 303–312 (2013)
2. H. Fayaz, N.A. Rahim, R. Saidur, K.H. Solangi, H. Naiz, M.S. Hossain, Solar energy policy: Malaysia vs developed countries. In *2011 IEEE Conference on Clean Energy and Technology, CET* (2011)
3. K.C. Goh, J. Yang, Importance of sustainability-related cost components in highway infrastructure: perspective of stakeholders in Australia. *J. Infrastruct. Syst.* **20**, 04013002 (2013)

4. A.W. Azhari, K. Sopian, A. Zaharim, M.A. Ghoul, A new approach for predicting solar radiation in tropical environment using satellite images: case study in Malaysia. *WSEAS Trans. Environ. Dev.* **4**(4), 373–378 (2008)
5. T.H. Oh, Carbon capture and storage in potential coal-fired plant in Malaysia. *Renew. Sustain. Energy Rev.* **14**, 2697–2709 (2010)
6. S. Ahmad, R.M. Tahar, Selection of renewable energy sources for sustainable development of electricity generation system using analytic hierarchy process: a case of Malaysia. *Renew. Energy* **47**, 458–466 (2014)
7. K.S. Cheng, G. Lalchand, A review on sustainable power generation in Malaysia to 2030, historical perspective, current assessment and future strategies. *Renew. Sustain. Energy Rev.* **29**, 952–960 (2014)
8. Greentech Media Inc, *Building-Integrated Photovoltaics: An Emerging Market*, July 2010 edn. (Greentech Media Inc, United Kingdom, 2010)
9. A. Rosnazri, D. Ismail, S. Taib, A review on existing and future energy sources for electrical power generation in Malaysia. *Renew. Sustain. Energy Rev.* **16**, 4047–4055 (2012)
10. Suruhanjaya Tenaga. *Laporan Tahunan 2010*. (2010)
11. M. Wagner, K. Schönsteiner, T. Hamacher, Impacts of photovoltaics and electromobility on the Singaporean energy sector. *PV Asia Pac. Conf. Energy Procedia* **25**, 126–134 (2012)
12. K.H. Solangi, T.N.W. Lwin, N.A. Rahim, M.S. Hossain, R. Saidur, H. Fayaz, Development of solar energy and present policies in Malaysia. In *IEEE Conference on Clean Energy and Technology CET*, pp. 115–120 (2011)
13. Sustainable Energy Development Authority (SEDA) of Malaysia. *Sustainable Energy Development Authority (SEDA)* (2011)
14. Tenaga Nasional Berhad (TNB). *Annual Report 2013* (2014)
15. M.A.H. Ahmed, N.J. Priscilla, M. Shawal, Optimal configuration assessment of renewable energy in Malaysia. *Renew. Energy* **36**, 881–888 (2011)
16. S.N. Kamaruzzaman, H. Abdul-Rahman, C. Wang, S.B. Karim, T.Y. Lee, Solar technology and building implementation in Malaysia: a national paradigm shift. *Maejo Int. J. Sci. Technol. Energy Procedia* **6**(02), 196–215 (2012)
17. M.S. Hossain, N.A. Rahim, K.H. Solangi, R. Saidur, H. Fayaz, N.A. Madlool, Global solar energy use and social viability in Malaysia. In *IEEE Conference on Clean Energy and Technology CET*, pp. 187–192 (2011)
18. S. Mekhilef, A. Safari, W.E.S. Mustafa, R. Saidur, R. Omar, M.A.A. Younis, Solar energy in Malaysia: current state and prospects. *Renew. Sustain. Energy Rev.* **16**, 386–396 (2012)
19. The Star. *Iskandar solar power project in the works* (2014)

Removal of Oil from Water by Column Adsorption Method Using Microwave Incinerated Rice Husk Ash (MIRHA)

Alina. M. Faizal, Shamsul Rahman Mohamed Kutty
and Ezerie Henry Ezechi

Abstract This paper addressed the potential use of microwave incinerated rice husk ash (MIRHA) as an adsorbent for the treatment of oily wastewater generated from an oil and gas industry. Presence of total petroleum hydrocarbon (TPH) in oil and gas wastewaters hinders the potential reuse of such wastewaters. The adsorbent MIRHA was produced by burning rice husk at two temperatures of 500 and 800 °C, designated as MIRHA500 and MIRHA800, respectively. The adsorbent was found to be highly porous, light weight with a very high external surface area and consist of 87–97 % silica. Adsorption of oil onto MIRHA500 and MIRHA800 was investigated in this study. Effect of contact time, adsorbent dose and concentration of MIRHA on adsorption process was determined by means of column adsorption study. X-Ray diffraction (XRD) and scanning electron microscopy (SEM) were used to determine the physical properties of MIRHA. MIRHA800 was found to be more effective with a removal ratio of 0.94 as compared with MIRHA500 (0.74) and higher throughput volume to exhaustion and breakthrough at increasing bed depth due to its larger surface area. Theoretically, contact time, adsorbent dose and concentration of MIRHA affect the adsorption process.

Keywords MIRHA · Breakthrough curve · Column adsorption

A.M. Faizal
Petroleum Engineering Department, Universiti Teknologi PETRONAS, Tronoh
Perak, Malaysia
e-mail: alinabalan91@gmail.com

S.R.M. Kutty (✉) · E.H. Ezechi
Civil Engineering Department, Universiti Teknologi PETRONAS, Tronoh, Perak, Malaysia
e-mail: shamsulrahman@petronas.com.my

E.H. Ezechi
e-mail: honhenry2k5@gmail.com

1 Introduction

Oil in water can be a potential source of environmental pollution and can cause some ecological problems. It can represent severe danger for animal, plant and benthic communities as well as a source of fire hazard in waterways. Potential reuse of water sources polluted by oil is hindered by several toxicology issues and can result to scarcity of water for manufacturing industries, irrigation in arid areas or public consumption.

Therefore efficient and economic techniques are required for effective removal of oil from water.

Adsorption technique is commonly used for the removal of pollutants from wastewater. It is useful and present several advantages over few treatments methods due to the availability of adsorbents at low cost, simplicity of operation and high removal efficiency [1, 2]. The most commonly used commercial adsorbents were activated carbon, synthetic polymer and silica based adsorbents. Utilization of these adsorbents are widely hindered by their attendant cost and the challenges synonymous with their regeneration [2]. As a result, several non-conventional adsorbents mainly from agricultural wastes have been investigated and developed over the years. These non conventional adsorbents possess various active groups which enhance their activity for effective separation of mixtures. Solvent polarity is also an important factor that affects the adsorbents. The adsorption capacity of the adsorbents are considered effective and rapid when the polarity of the solvent is high and vice versa. Batch studies are effective techniques but are affected by high cost due to classical alternation of process variables. However, columnar study can present significant understanding of the effects of process variables and the possibility of a full size scale up of such process [3]. Column adsorption process provides effective interaction between the adsorbate in bulk volume with the adsorbent bed. Such interactions results in the decrease of adsorbate concentration due to the continuous movement of the solvent towards the adsorbent bed. At equilibrium, the adsorbent becomes saturated.

In many rice producing nations, rice husk is a common agricultural wastes. It is a large volume production and have little utilization significance. Therefore, it is mostly disposed as waste. However, disposal of rice husk and other waste compounds are costly due to the scarcity of landfills. Due to high volume production of waste, most landfill sites are already full and developing new ones are hindered by its environmental consequences [4]. Rice husk mainly consist of organic matters such as cellulose, lignin and mineral components including silica, alkalis and trace elements [5]. The major adsorptive compound of rice husk ash (RHA) is silica. RHA has good adsorbent properties because of its high silica (about 20 %) content [6]. Rice husk ash has been successfully used as adsorbent for several lipid components such as phospholipids [7], lute in [8], palmitic and oleic acids [9], carotene [10] and saturated fatty acids. Recent studies have shown that RHA can be used as a carrier material for biomass in the removal of heavy metal [11] and also as an oil spill adsorbent [5], because RHA can be considered slightly impure silica [12].

The objective of this study is to investigate the removal efficiency of TPH from produced water using RHA designated as MIRHA500 and MIRHA800. Effects of adsorbent dose, concentration and contact time on the column adsorption process were also investigated.

2 Methodology

2.1 Preparation of MIRHA

Rice husk was obtained from Bernas Rice Mill in Manjung Perak, Malaysia without pretreatment except for sieving to remove very fine particles. A microwave incinerator was used to incinerate the rice husk at two different temperatures (500 and 800 °C) designated as MIRHA500 and MIRHA800, respectively. The fine powder produced was then grinded to a particle size of 75–150 µm.

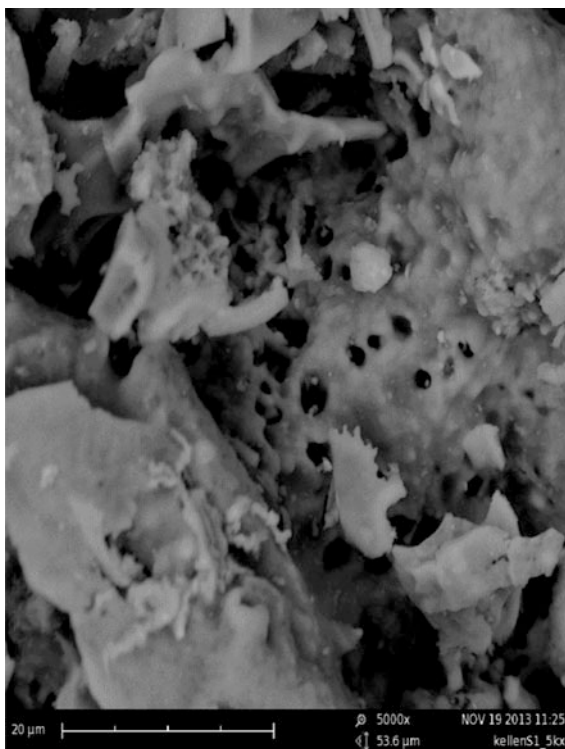
2.2 Column Adsorption Experiment

Three different columns having a height of 40 cm and diameter of 4.3 cm were used for the adsorption study with corresponding MIRHA bed heights of 10, 20 and 25 cm respectively. Experiments were conducted simultaneously for MIRHA500 and MIRHA800. Real wastewater from an oil and gas refinery containing 265 mg/L of TPH was collected and used for the experiment. A constant flowrate of 8 mL/min was maintained during the study using a peristaltic pump. Residual TPH concentration was measured using a TPH analyser until breakthrough.

3 Results and Discussion

3.1 Characteristics of MIRHA

The granular structure and insoluble properties of rice husk enhances its chemical stability and improves its mechanical strength [13]. The surface of rice husks contains various functional groups such as hydroxyl groups (OH), silanol groups (Si-OH) and carbonyl groups which supports its adsorption capacity [14, 15]. Other constituents properties of rice husks that enhances its adsorption capacity include Fe, Mn and Al due to their wide availability in plants [16]. It is reported that a mass loss of 0.43 and 5.8 mg were respectively observed when rice husk was heated at low temperatures of 250–360 °C. However, when the temperature was increased to 950 °C, no mass loss was observed [17]. Rice husk ash (RHA) has a surface area of about 36.44 m²/g with a single point total pore volume of 0.0388 cm³/g. Pore size

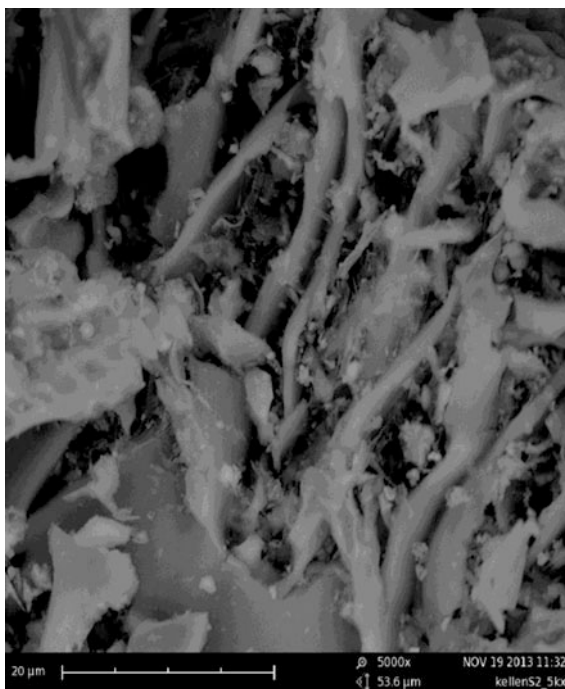
Fig. 1 SEM for MIRHA500

was distributed between micropores (20 %), mesopores (78 %), and macropores (2 %) [18]. Silica (SiO_2) content of rice husk ash increased when heating temperature was increased from 500 to 800 °C. The silica (SiO_2) content of RHA was 83.66 and 92.90 wt(%) at 500 and 800 °C respectively [19]. Based on the above literature surveys, RHA was produced at two different temperatures of 500 and 800 °C respectively.

Figures 1 and 2 shows SEM morphology of MIRHA500 and MIRHA800 at 5000x magnification respectively. The morphology of MIRHA500 and MIRHA800 shows a beehive structure with smoother surface and ridges at 500 °C (Fig. 1). However, when the temperature was increased to 800 °C, the beehive structure was shattered resulting in more pores being formed on the surface of the adsorbent (Fig. 2).

3.2 The Breakthrough Curve

A breakthrough curve represent a plot of relative concentration against time. Relative concentration can be described as effluent concentration (C)/influent concentration (C_0). The breakthrough point represent the time required for a given

Fig. 2 SEM for MIRHA800

concentration to attain its discharge allowable limit. The exhaustion point represent the time at which the bed is fully saturated, resulting to low residual concentration in the effluent.

The measured and modelled breakthrough curves for adsorption of TPH onto MIRHA500 and MIRHA800 at different time and bed depths are represented in Figs. 3 and 4 respectively. At bed depth of 25 cm and after 288 h, a C/C_0 ratio of 0.78 was obtained for MIRHA500 as shown in Fig. 3. However, at the same bed depth and after 384 h, a C/C_0 of 0.94 was obtained for MIRHA800 as shown in Fig. 4. The difference in C/C_0 ratio for both adsorbents can be attributed to the larger surface area of MIRHA800 in terms of physical properties and more silica content. This is also supported by the time requirement of both adsorbents to attain equilibrium. Whereas MIRHA500 required 288 h to reach equilibrium, MIRHA800 required about 384 h. The higher time of MIRHA800 can be attributed to the larger surface area which requires longer detention period.

In addition, the breakthrough curves can also be represented by the plot of (C/C_0) versus volume of water treated (L). Figures 5 and 6 show the relationship between the ratios of concentration with the volume of water treated for MIRHA800 and MIRHA500 respectively.

Both Figs. 5 and 6 follow the characteristic “S” shaped profile produced in ideal adsorption systems. Results indicate that the breakthrough volume varies with bed depth. The throughput volume to breakthrough and exhaustion points for

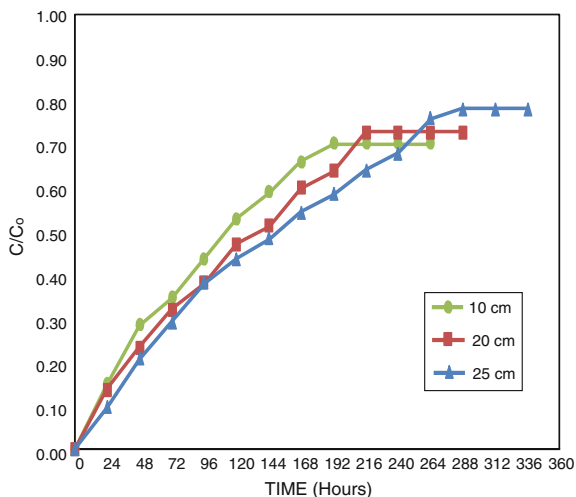
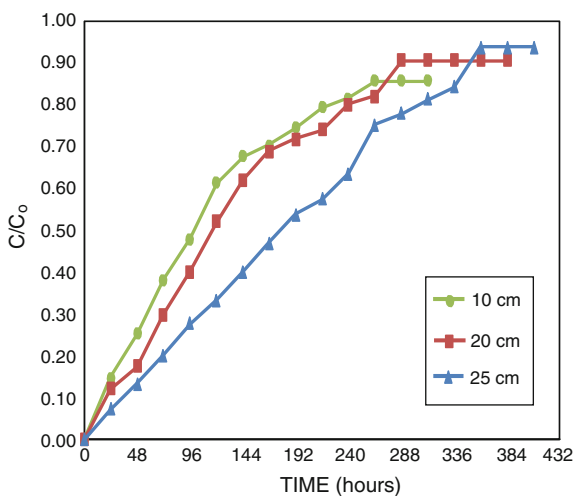


Fig. 3 Measured and modeled breakthrough curves (C/C_0) for adsorption of TPH onto MIRHA500 at different time and bed depths

Fig. 4 Measured and modeled breakthrough curves (C/C_0) for adsorption of TPH onto MIRHA800 at different time and bed depths



MIRHA800 and MIRHA500 can be determined by taking 5–10 % and 90–95 % of the initial concentration value respectively for each bed heights. The throughput volume to breakthrough and exhaustion points are presented in Table 1.

As shown in Table 1, increased in bed depths resulted in reduction of throughput volume to exhaustion and breakthrough. It was also observed that MIRHA500 has lower throughput volume to exhaustion and throughput volume to breakthrough if compared to MIRHA800 at increasing bed depth.

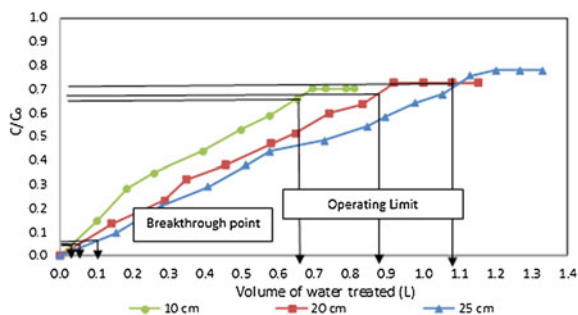


Fig. 5 C/C_0 versus volume of water treated (L) for different bed heights of MIRHA 800

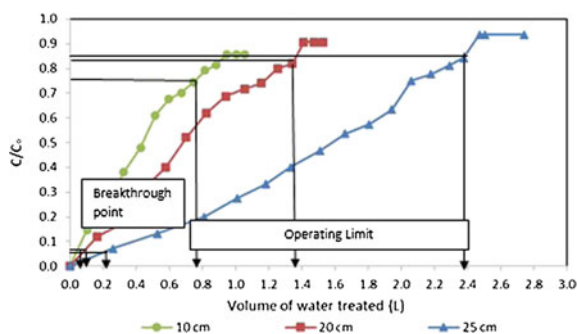


Fig. 6 C/C_0 versus volume of water treated (L) for different bed heights of MIRHA800

3.3 Effect of Different Bed Heights of MIRHA at Various Time

Among all the results presented, significant increase in the adsorption of TPH was mostly observed when bed depth was increased. This can be attributed to provision of more adsorption pores and saturation of the adsorbents due to the continuous movement of the adsorbate as the bed height was increased [20]. In addition, more specific surface area is available when bed depth is increased and improves the adsorption capacity of the adsorbent. This therefore implies that a delayed breakthrough of the TPH onto MIRHA could lead to an increase in the volume of solution treated. Thus, the increase in adsorption rate when the bed depth was increased could be due to the increase in adsorbent doses in larger beds which provide greater surface area [21].

Table 1 Throughput volume to exhaustion and breakthrough for different type of MIRHA and at different bed heights

Types of MIRHA	Bed heights (cm)	Throughput volume to breakthrough, V_B (L)	Throughput volume to exhaustion, V_E (L)
MIRHA800	10	0.08	0.79
	20	0.10	1.39
	25	0.21	2.40
MIRHA500	10	0.03	0.63
	20	0.05	0.89
	25	0.10	1.19

3.4 Effect of Particle Size of MIRHA on Adsorption Rate

In this study, MIRHA800 was more efficient for the adsorption of TPH when compared to MIRHA500. As shown in Fig. 4, the highest ratio of TPH removal (0.94) was obtained with MIRHA800. This has been attributed to the characteristics of MIRHA and its particle size. MIRHA800 has finer particle size than MIRHA500. Decrease in particle size lead to increase in surface area and increase in the adsorption tendencies at the outer surface of the adsorbent materials. Factors such as diffusional path length or mass transfer resistance, contact time, and blockage of some diffusional path may hinder the effective adsorption of internal surface of the particle and consequently decrease adsorption efficiency.

4 Conclusion

MIRHA was successfully used to remove TPH from produced water. MIRHA800 and MIRHA500 was compared and results show that MIRHA800 has a higher removal ratio of 0.94 after 384 h. MIRHA500 highest removal ratio was 0.78 after 288 h. Increase in bed depth resulted in higher removal ratio. MIRHA800 has a finer particle size than MIRHA500. This study has shown that MIRHA can be used as a suitable adsorbent for the removal of oil from water.

Acknowledgments The authors would like to thank Universiti Teknologi PETRONAS for her support in this study.

References

1. E. Malkoc, Y. Nuhoglu, Fixed bed studies for the sorption of chromium (VI) onto tea factory waste. Chem. Eng. Sci. **61**, 4363–4372 (2006)

2. A.H. Mahvi, Application of agricultural fibers in pollution removal from aqueous solution. *Int. J. Environ. Sci. Technol.* **5**, 275–285 (2008)
3. A. Bhatnagar, M. Sillanpää, Utilization of agro-industrial and municipal waste materials as potential adsorbents for water treatment—a review. *Chem. Eng. J.* **157**, 277–296 (2010)
4. E.H. Ezechi, M.H. Isa, S.R. Kutty, N.B. Sapari, Boron recovery, application and economic significance: a review. National Postgraduate Conference (NPC), pp. 1–6 (2011)
5. K.M. Ajay kumar, D. Kumar, O. Parkash, Properties and industrial applications of rice husk: a review. *Int. J. Emerg. Technol. Adv. Eng.* **2**, 2250–2459 (2012)
6. D.B.M. Lakshman Velupillai, J.W. Warshaw, E.J. Wailes, J. Tarver, H. Dr, Rouse Caffey, *A Study of the Market for Rice Husk-To-Energy Systems and Equipment* (Louisiana State University Agricultural Centre, USA, 1997)
7. H.E.S.H.G. Brown, Factors affecting phospholipid on silica from soya oil miscella. *J. Am. Oil Chem. Soc.* **66**, 209–217 (1989)
8. A. Proctor, X-ray diffraction and scanning electron microscope studies of processed rice hull silica. *J. Am. Oil Chem. Soc.* **67**, 576–584 (1990)
9. T. Ooi, W. Leong, Adsorption of palm oil monoglycerides using rice husk ash. *Elaeis* **3**, 317–323 (1991)
10. K. Liew, A. Yee, M. Nordin, Adsorption of carotene from palm oil by acid-treated rice hull ash. *J. Am. Oil Chem. Soc.* **70**, 539–541 (1993)
11. S. Kutty, E. Ezechi, S. Khaw, C. Lai, M. Isa, Evaluation of copper removal using MIRHA as an adsorbent in a continuous flow activated sludge system. *Water Pollut.* **182**, 233 (2014)
12. L. Sun, K. Gong, Silicon-based materials from rice husks and their applications. *Ind. Eng. Chem. Res.* **40**, 5861–5877 (2001)
13. T. Chuah, A. Jumariah, I. Azni, S. Katayon, S. Thomas Choong, Rice husk as a potentially low-cost biosorbent for heavy metal and dye removal: an overview. *Desalination* **175**, 305–316 (2005)
14. S.R. Kamath, A. Proctor, Silica gel from rice hull ash: preparation and characterization. *Cereal Chem.* **75**, 484–487 (1998)
15. C. Pasquali, H. Herrera, Pyrolysis of lignin and IR analysis of residues. *Thermochim. Acta* **293**, 39–46 (1997)
16. A. Swarup, S. Anand, Transformation and availability of iron and manganese in submerged sodic soils in relation to yield and nutrition of rice. *Fert. News* **34**, 21–23 (1989)
17. C.R. Teixeira Tarley, S.L. Costa Ferreira, M.A. Zezzi Arruda, Use of modified rice husks as a natural solid adsorbent of trace metals: characterisation and development of an on-line preconcentration system for cadmium and lead determination by FAAS. *Microchem. J.* **77**, 163–175 (2004)
18. V.C. Srivastava, I.D. Mall, I.M. Mishra, Characterization of mesoporous rice husk ash (RHA) and adsorption kinetics of metal ions from aqueous solution onto RHA. *J. Hazard. Mater.* **134**, 257–267 (2006)
19. N. Yalcin, V. Sevinc, Studies on silica obtained from rice husk. *Ceram. Int.* **27**, 219–224 (2001)
20. Z. Saadi, R. Saadi, R. Fazaeli, Fixed-bed adsorption dynamics of Pb (II) adsorption from aqueous solution using nanostructured γ -alumina. *J. Nanostruct. Chem.* **3**, 48 (2013)
21. Y. Long, D. Lei, J. Ni, Z. Ren, C. Chen, H. Xu, Packed bed column studies on lead(II) removal from industrial wastewater by modified *Agaricus bisporus*. *Bioresour. Technol.* **152**, 457–463 (2014)

Biomass as Low-Cost Adsorbents for Removal of Heavy Metals from Aqueous Solution: A Review of Some Selected Biomass

Salihi Ibrahim Umar, Shamsul Rahman Mohamed Kutty, Mohamed Hasnain Isa, Nasiru Aminu, Ezerie Henry and Ahmad Fitri B. Abd Rahim

Abstract Low cost adsorbents have become a major area of consideration to many researchers due to the expense nature of the available activated carbon. Although commercial activated carbon is the most sufficient and efficiently used carbon for the removal of heavy metals ions coming from wastewater, it is faced with a lot of setback such as; the higher the quality of the activated carbon the more expensive it is, the regeneration of the used carbon tends to be very difficult especially in large volume. Due to this different biomass from agricultural by-products have been investigated to replace the commercial activated carbon and most of the findings have indicated a significant removal in terms of heavy metals in synthetic aqueous solution. This study have looked into and reviewed the various low cost adsorbents that have been employed for the treatment of wastewater laden with heavy metals.

Keywords Biomass · Heavy metals · Adsorbents · Aqueous solution

1 Introduction

The occurrence of heavy metals in wastewater has drawn public attention due their toxic impacts when discharge directly to the receiving environment and also to the entire efficiency of the biological treatment plants [1]. Also, the efficiency of the method employed in the treatment of heavy metals has become paramount important because it allows to evaluate the amount of heavy metals discharged into the bodies of water, this is particularly more sensitive in areas where recycling of

S.I. Umar (✉) · S.R.M. Kutty · M.H. Isa · N. Aminu · E. Henry · A.F.B.A. Rahim
Civil Engineering Department, Universiti Teknologi PETRONAS (UTP), Tronoh
Perak, Malaysia
e-mail: Salihi_g02656@utp.edu.my

the used water is mainly practiced. Due to this, the elimination of heavy metals coming from industrial wastewater has become a matter of argument [2].

Heavy metals are found to be among the major environmental pollutants due to the direct discharge of industrial wastewater into water bodies without given proper treatment. To some extent these heavy metals find their way into human bodies through food, drinking water and air [3]. The nature and the type of heavy metals present in a particular wastewater depends upon its source [4].

The increased in heavy metals in wastewater is mainly due to some activities associated with human and the operating industries. Weakening of surface area accumulation relating to metals nutrient debris, runoff via agricultural area as well as rainfall associated with acidic rain coming from the ambiance, all attributes to the buildup of chemical toxins in wastewater in a normal kind [5].

Various approaches had been formulated intended for the elimination of chemical toxins coming from wastewater. Conventional techniques commonly applied for the removal of heavy metals from wastewater include chemical and physical methods. Chemical techniques include chemical precipitation, coagulation, oxidation, advanced oxidation, ion exchange, adsorption, chemical neutralization, solvent extraction and stabilization [6]. Physical techniques are sedimentation, screening, aeration, filtration, floatation, degasification, adsorption, membrane separation and equalization [7]. Biological treatment includes aerobic or anaerobic techniques.

On the other hand, these techniques possess substantial drawbacks, such as partial metal elimination, generating huge amount of sludge, demands for costly tools as well as tracking programs, excessive reagent or perhaps power demands along with creation of harmful sludge which need removing. Innovative are anticipated which may minimize heavy metal levels in ecosystem to an appropriate degree with regards to economical expenses [8].

Adsorption process is an affective option for the removal of heavy metals from wastewater. An economical and easily available adsorbent would make the adsorption-based process an attractive alternative for the removal of heavy metals from wastewaters [9].

In the presence situation a lot of biomass from agricultural by-products has been examined and their performance as alternative adsorbent was found to be very significant and reliable. Our purpose with this particular effort has been in evaluating the scientific functionality connected with some few chosen inexpensive adsorbents pertaining to the treatment of volatile organic compounds and focused on current studies.

2 Low Cost Adsorbents for Heavy Metal Removal

2.1 Sugarcane Bagasse

Sugarcane bagasse is an agricultural by-product, which is a waste product from sugarcane farming that is mainly obtained from the production of cane sugar after

all the juice has been extracted from it. The waste is normally burnt in the fields or dumped for disposal. Almost every ten loads of sugarcane smashed, the carbohydrates manufacturing plant generates almost three loads of waste bagasse [10].

The particular characteristics of sugarcane bagasse depends largely on some parameters amid several others, such as the properties of the soil used as well as the condition of the climate in which the sugarcane has been harvested [11]. But in general sugarcane bagasse possesses a chemical composition that primarily matches to the following: Cellulose (45–50 %), total lignin (20–25 %), mineral compound (2–5 %), carbon (60–65 %), moisture (70–75 %), and ash (25–30 %) [12]. Apart from the qualities identified, the bio-adsorbent are usually discovered in substantial volumes in a lower price. Sugarcane bagasse has presently been utilized as the primary way to obtain the energy needed basically by ethanol and sugar mills and also for producing electrical power to be marketed [11]. Nevertheless, typically the main constraint with sugarcane bagasse usage is, it has excessive level of intricacy due to the fact that it's combined structure is associated with hemicellulose, celluloses, along with lignin within enormously and nonhomogeneous materials [13]. Various researches were conducted on the use of sugarcane bagasse as low cost adsorbent in recent time with the hope of finding an efficient and cost effective adsorbent that will replace the commercial activated carbon.

An exploration into the utilization of sugarcane bagasse pertaining to the adsorption of methyl blue and Rhodamine was completed by [14]. The adsorption ability of the prepared bagasse was examined in contrast to its distinct surface areas. The result revealed that a modest increase in dye removal was achieved with an increase in the surface area of the bagasse from 0.57 to 1.81 m²/g. Methyl blue appeared to be significantly less sensitive to surface area changes as compared to Rhodamine. The isotherm model studies show that Rhodamine blue fitted well into Freundlich isotherm whereas methyl blue fits to Langmuir isotherm model.

Another study was conducted by Pehlivan et al. [15] for the removal of Arsenic (V) from aqueous solution using bagasse treated with hydrated ferric oxide as an adsorbent, in the study various adsorption parameters were investigated such as pH, contact time, initial Arsenic concentration, adsorbent dosage and ionic strength. The report shows that the adsorption capacity of sugarcane bagasse treated with hydrated ferric oxide was 22.1 mg/g under the influence of adsorption parameters at optimum conditions, the optimum pH was 4.0, contact time 3 h and at temperature of 22 °C. The study also reveals that 17 % desorption was achieved when 30 % hydrochloric acid was used and 85 % with 1 M NaOH solution.

Gusmao et al. has investigated the use of modified sugarcane bagasse for the adsorption of etherdiamine. The modification was done with succinic anhydride and EDTA dianhydride so as to obtain SCB 2 and EB adsorbents respectively [16]. The findings reveal that the maximum adsorption capacities of the prepared adsorbents for etherdiamine are 869.6 and 1203.5 mg/g for SCB 2 and EB respectively. The equilibrium conditions were attained at 90 min time at a pH of 10.0. Kinetic study shows that data fitted well into pseudo-second-order model.

In a recent study by Esfandiar et al. [17] on the removal of Mn (II) through a comparative study using sugarcane bagasse and activated carbon as an adsorbent employed the use of Box-Behnken design, effect of pH, adsorbent dosage and initial metal concentration was considered in the study, the optimum adsorption efficiency was attained at pH of 4.5, 12 mg/l metal ion concentration with adsorbent dosage of 15 g/l at 23 ± 2 °C. The increase in initial metal concentration reduced the efficiency of adsorption, maximum removal efficiency was found to be 63 and 97 % for sugarcane bagasse and activated carbon respectively but when sugarcane bagasse was treated with HCl its removal efficiency was enhanced up to 99 %.

Based on this sugarcane bagasse was found to possess the sorption capabilities to adsorb heavy metals from aqueous solution and hence can be used as an alternative adsorbent to a greater extent especially if it undergoes certain modifications with acidic treatment.

2.2 Rice Husk

Rice husk is an agricultural by product that is reported to possess the ability to absorb heavy metals and basic dyes having 20 % silica as its content [18]. It has a granular composition, together with a substantial physical durability, not soluble in water, and it offers a chemical balance and in addition makes up about 20 % of the entire grain. It is made up of 3 % raw protein, 20 % silica, 21 % lignin, 32 % cellulose and 21 % hemicelluloses [19]. Additionally, it consist of many useful classes which includes hydroxyl, carboxyl as well as amidogen, etc., and also consist of ample floristic fiber content, that represents a good characteristics of rice husk becoming a feasible adsorbent product [20]. It has been employed as lime-pozzolana blinds, in addition it might become acceptable to some extent as an alternative to Portland cement [21].

As per the discoveries with the Ministry of Agriculture, Malaysia, nearly 408,000 loads of rice husk happens to be generated yearly within the nation [22]. Perhaps, it will certainly not be financially feasible to haul large quantity of rice husk from the originating mill to a recycle location especially if such locations are sited in a far distance away from the mill [23]. Rice husk that needed to be transported to a short distance tends to be expensive and competitive especially when using an imported diesel gas that can equally be enough to remove the debris to a far distance within the nation. As a result, in the event that effective approach will be accessible, the actual rice husk could be changed to a valuable sort of power in order to fulfill the mechanical and thermal energy demands of the rice mill and also the electric energy requirement of the surrounding settlement [23]. Also, the grain husk may end up being produced directly into a good triggered carbon to be utilized as adsorbent for the elimination of heavy metals originating from industrial sectors. Numerous studies had been completed on the particular usage of rice husk as adsorbent and also several scientists include further search straight into the potentialities of this particular affordable adsorbent pertaining to heavy metal elimination within current period.

Microwave incinerated form of rice husk was used by Kutty et al. [24] for copper removal in a continuous flow sludge activated system. The modified adsorbent exhibit the ability to increase the concentration threshold of inhibitory effect of heavy metals on microorganisms from 1.0 to 2.0 mg/L. The efficiency of the biological treatment has significantly improved in terms of total chemical oxygen demand, biochemical oxygen demand, copper removal and also improves the growth of microbes in the activated sludge when 2000 mg/L of the adsorbent was added to the aeration chamber of the bench scale biological reactor.

A new approach for activated carbon preparation was done by Li and Zhu [25] The adsorbent was prepared through rice husk pyrolyzation with a combination of carbon dioxide activation and then boiled in a sodium hydroxide solution. This adsorbent has been employed intended for the particular elimination of methylene blue coming from aqueous solution. The particular product was discovered to get a higher surface area 899 m²/g, additionally; the treatment performance had been considerably higher compared to Ninety nine Percent, which often may become in contrast together with that relating to the actual commercial triggered carbon.

A study was conducted by Junaid et al. [26] for the removal of dyes present in a solid waste of cotton that has been produced from sport industries in Pakistan, employing rice husk as an adsorbent. Various adsorption parameters were examined and optimum removal efficiency was achieved at pH 3.0, contact time of 240 min, adsorbent dosage 8.0 g, revolution speed of 300 rpm and dye solution of 200 mL and there corresponding removal efficiency of 91, 93, 92, 90 and 93 % respectively.

Gupta and Mote [27] has carried out a comparative study for the removal of hexavalent chromium from aqueous solution using rice husk (dried and ash), orange peel, and sugarcane bagasse. The result revealed that dried rice husk possessed a higher efficiency for chromium adsorption than the other used adsorbents. The documented sorption capabilities happen to be; dehydrated rice husk (16.94 mg/g), lemon skins (12.65 mg/g), grain husk ashes (11.11 mg/g), sugarcane bagasse (5.12 mg/g), saw dust (4.56 mg/g) almost all during room temperatures.

This indicates that rice husk can be applied as adsorbent in a large scale application for the treatment of different heavy metals in aqueous solution in order to replace the commercial activated carbon in terms of economical perspective, since its application on biological studies has shown an improvement of the treatment plant but still not efficient than the frequently used carbon.

2.3 Banana Peels

Banana plants are considered to belong to the family of Musaceae. It is among the most valuable crop after corn, wheat and rice. It has a reasonable amount of vitamins in it especially vitamins B and C and also some mineral elements of the kind of calcium and potassium. It has a higher level of starch normally during its premature period [28]. This plant is mainly grown specifically for its fruits and to a lesser degree for the development of fibre and ornamental plants. The peel is waste

material that contains abundant carbohydrate along with additional standard nutrients which might assist microbial development. The prospective financial advantages that can be derived through the utilization of banana peel low cost natural material as a substrate for the generation of useful micro fungal biomass and also as a source of mycological medium for investigation have increased the assessment of the development efficiency and generation of biomass regarding the two species on banana peels substrate [29]. Depending upon the type of specie some can grow up to a height of 8 m. Averagely each fruit weigh about 125 g with its 25 % being dry matter and the remaining is water. Banana qualifies to be one of the most consume fruit in the world but at the same time tends to produce waste of peels that becomes a solid waste problem to the living environment. The production of banana was estimated to be roughly around 72.5 million tons in the world and in which Thailand alone contributes 10.4 million tons [30]. This huge production tends to create large amount of garbage from market places and households that leads to environmental nuisance and disposal problem. The presence of different chemical toxins of hydroxyl, carboxyl and amide group have been proven to play a vital role during the sorption process [31]. Due to this some investigation were carried out by different researchers in trying to convert this solid waste to a renewable waste especially in the treatment of wastewater. The peels are mainly converted into low cost adsorbents [32].

The used of banana peels for the treatment of biologically treated palm oil mill effluent (POME) was evaluated by [33]. The peels were modified through chemical and thermal treatment. Perfect elimination effectiveness with regards to coloration, TSS, COD, BOD as well as tan plus lignin had been identified being (95.96, 100, 100, 97.41 and 76.74 %) within the stability situation of pH of 2.0, contact time 30 h and adsorbent dose of 30 g/100 mL. The sorption removal enhanced with the use of acidified methanol and potassium hydroxide as well for the adsorbent modification. The intense action of the used chemical on the adsorbent has increased the pore size as well as the porosity of the adsorbent.

In a similar study by Abdulfatai et al. [34] using banana peel as an adsorbent on the remediation of heavy metals of Pb, Zn and Cr in wastewater. The potentiality of treated and untreated adsorbent was compared; the activation was achieved using 0.5 M sulphuric acids and gave a better removal efficiency of about 88.9 % in terms of chromium. Adsorbent particle showed negative influence on the adsorption of zinc and also reduced the efficiency of removal of lead and chromium with an increasing adsorbent particle size. The biochemical oxygen demand as well as the chemical oxygen demand of the wastewater increase when untreated adsorbent was employed.

Also, Krishni et al. [35] investigated into the use of banana leaves as low cost adsorbent for the removal of methyl blue in aqueous solution. Adsorption parameters such as initial metal concentration, contact time and solution pH were examined, methyl blue removal efficiency is directly proportional to the initial metal concentration and solution pH, the efficiency of methyl blue removal increases with an increase in metal concentration and pH. Optimum monolayer adsorption was found to be 109.89 mg/g.

Cr (VI) removal from aqueous solution using banana peel was also examined by [36]. Sorption efficiency increases with an increase in equilibrium metal concentration. 77 % removal efficiency was achieved when metal concentration in the solution is 100 mg/L but when the concentration level was decrease to a lower level of 20 mg/L the percentage removal was found to be 95 % with adsorbent dosage of 1.5 g.

Banana peels as an adsorbent exhibit the property to remove heavy metals from aqueous solution and can also be employed in a large scale treatment especially in biological treatment system.

2.4 Water Treatment Sludge

Drinking-water treatment sludge is actually a by-product created through the processing of standard water in which aluminum as well as iron based mostly salts are usually utilized as coagulants in order to get rid of colour, turbidity and also humic substances. Existing legislation classified water treatment sludge as waste materials in most cases this is usually chemically conditioned as well as mechanically dewatered before disposal in landfills [37]. A lot of option for its disposal, re-use as well as its regeneration has been explored in the past [38]. The quest for cost efficient as well as eco-friendly disposable alternative offers a sudden precedence as a result of more restrictive environmental legislation, decreasing general public approval regarding landfill options, escalating disposal expenses and decrease in landfill capability [37]. Characteristics of the sludge depends largely upon the source of the drinking water (ground or surface) as well as the type of treatment the water undergoes, it mainly consist of alum hydroxides and colloidal irons, dissolved or colloidal organic matter, silt, clay and microorganisms [39]. In general it falls into kaolinite type of waste generated by industries and in the recent time many researchers have focused on the use of kaolinite based industrial waste into a useful material especially its conversion into pozzolanic material when it undergo thermal activation process [40]. A drinking water treatment plant having a capacity of 1 m³/s volume normally generates a waste sludge amounting to 8300 kg/day [39]. The presence of sludge generated by drinking water treatment at wastewater treatment plant is very vital as the efficiency of the residual coagulating might be utilized to assist the phosphorus abatement, to enhance the sludge dehydration stage as well as to speed up its settling effectiveness. The combined sludge from wastewater and drinking water treatment plant can be utilized for agricultural purposes. At present time there is no limitation on the application of drinking water treatment sludge for ecological purposes.

The use of the produced sludge as an adsorbent for the treatment of wastewater in biological treatment system has also been explored by a number of researchers in order to investigate the effectiveness of the sludge in the treatment system.

The elimination of chemical oxygen demand from leachate using adsorbent prepared from sewage sludge was investigated by [41]. The adsorbent was mixed with corn stalk and pyrolysed with zinc chloride. End result unveils how the

inclusion of corn stalk to sewer gunged get boosted the surface area regarding the adsorbent that improved its sorption ability. Removal efficiency in terms of chemical oxygen demand reached almost 85 % at pH of 4.0, adsorbent dosage of 2 g/mL and at a contact time of 40 min. The result also fitted well into Langmuir and Freudlich isotherm models.

In similar study by Bousba and Meniai [42] adsorbent prepared from sewage sludge was utilized for the removal of 2-chlorophenol from aqueous solution. In the study, the adsorbent was triggered with sulphuric acid in a ration of 1:1 and pyrolysed at 650 °C for a period of one hour. Batch adsorption parameters considered were pH, contact time, adsorbent dosage and concentration of 2-chlorophenol. The result shows that maximum sorption capacity was 47.98 mg/g at a temperature of 20 °C. The data's obtained fitted well into Freudlich isotherm model and also follows pseudo-second order kinetic model.

Untreated anaerobically digested sludge was used by Hawari [43], for the removal of phenol from aqueous solution. The outcome demonstrates the sorption potential involving the adsorbent is definitely relied on the actual pH associated with the aqueous solution as well as the best possible elimination performance had been identified being ninety percent during 2 h connected with get in touch with time. 1.8 g/L of adsorbent dosage indicates optimum dosage for removal of phenol. The result fitted well into Langmuir and Freundlich isotherm model as well as pseudo-second order kinetic model.

Zaini et al. [44] in his study used palm oil effluent sludge ash for the elimination of methyl blue dye from aqueous solution. The ash adsorbent was impregnated with hydrochloric acid and was found to possess a surface area of about 218 m²/g and optimum adsorption was 50.7 mg/g at an initial concentration of 200 mg/L at a pH of 5.8. The result fitted into pseudo-second order kinetic model.

This shows that activated sludge possess the ability to remove heavy metals ion in aqueous solution and their performance is mainly attributed to the pH of the aqueous solution.

2.5 Citrus Peel off

Citrus fruit are members of Rutaceae group such as Lemon or lime berries reticulate (sugary mandarin), Citrus fruit sinensis (sugary lemon), Citrus fruit paradisi (a melon), as well as Citrus fruit limon (lemon), every one of these have a tendency among the majority of broadly utilized fresh fruits upon earth especially in tropical as well as sub-tropical nations [45]. Significant kinds of citrus fruit are generally produced in lots of countries inside Southeast Asia [45]. Citrus is definitely the greatest pure origin of Vitamin C (ascorbic acid) and folic acid, apart from being the superb source of fiber [46]. The primary objective of citrus fruits is to generate citrus juice; nevertheless, the particular waste materials from the citrus industry including peel, seeds and pulps tend to be also a prospective origin of by-products [45]. Citrus contain high polyphenolic compounds with 96 % of the fruit harvested

is being process into drinking juice [47]. The existence of some active dietary fibers as well as antioxidants makes it possible to be utilized as food processing material [47]. The major set-back on the use of citrus peel off is the excessive time commitment required to gather hundreds and thousands of specie for applications that require a particular plant type [48]. Due to this waste generated by the citrus industry, some investigation on the conversion of the waste by product especially the peel has been carried out by some researchers.

Gönen and Serin [49] have completed a study about the utilization of lemon stem just as inexpensive adsorbent with regard to the therapy involving Nickel (II) ions via aqueous solution. The optimum removal pH was found to be 5.0 and the percentage of removal was observed to increase with decrease in initial metal ion concentration. The information fixed nicely into Langmuir as well as Freundlich isotherm models, kinetics research have also been performed and discovered that this adheres to pseudo-second order kinetic mode having a relationship in excess of 0.99. It was concluded that orange peel can be used as a low cost adsorbent for the removal of Nickel (II) from aqueous solution.

In another study by Mohamed, on the removal of Uranium (VI) from aqueous solution also employed the use of orange peel as an adsorbent [50]. The performance of the orange peel is mainly dependent on pH, contact time, initial metal ion concentration as well as adsorbent dosage. Uranium (VI) optimal adsorption was achieved at a pH of 4.0 with a contact time of 60 min. The result also revealed that Langmuir model fitted well into adsorption data than Freundlich isotherm model. It also indicates that an adsorbent prepared using orange peel is a good material for the elimination of Uranium (VI) from aqueous solution.

Mafra et al. [51] in their study also prepared a novel orange peel adsorbent obtained from agricultural waste material and was used for the elimination of Remazol Brilliant blue from a synthetic solution of textile-dye effluent. The result indicates that the capacity of adsorbing Remazol Brilliant decreased with the increase in temperature from 9.7 mg/L at 20 °C to 5.0 mg/L at 60 °C. Langmuir and Freundlich isotherm models fitted well into the adsorption data and the nature of adsorption showed that it is endothermic and spontaneous. The prepared adsorbent was also found to be able to absorb Remazol Brilliant blue from synthetic solution.

2.6 Coconut

The coconut palm, *Cocoas nucifera* L. (*Arecales: Arecaceae*), is amongst the twenty most significant plant varieties [52]. Presently, it is actually in a commercial sense cultivated within more than ninety nations, masking an overall area of roughly twelve million hectares. South America along with Brazil tends to be the main producers of coconut in the Americas [53]. Most of the waste materials that are produced after the utilization of coconut tends to become source pollution to the environment and triggers environmental sustainability. Coconut shell consists of mainly 65–75 % moisture and volatile matter that are often removed during the

process of carbonization. With the increased in the cost of natural gas, oil and electricity, coconut shell has become a source of energy rather than disposable waste. It has been proven to be an outstanding material for its application for the treatment of odor, taste and dissolved organic chemical from water containing suspended matter. For this reason, the waste produced is being utilized for many different applications including preparation of low cost adsorbent for the removal of heavy metals from wastewater. The potentiality of the coconut waste and its applicability has been investigated under different conditions.

A study by Ong et al. [54] on the use of treated coconut coir for the adsorption of cationic and Anionic dye from aqueous solution has been investigated and the outcome of the result revealed that coconut coir treated with acid exhibits better adsorption capacity on cationic dye MB than its counterpart Anionic dye A07. Adsorption data is well defined by both Langmuir and Freundlich isotherm models. An optimum adsorption capacity was found to be 121 and 10 mg/g for MB and A07 respectively. Pseudo second order and first order Langmuir models described the adsorption behavior. Coconut coir was found to be a good adsorbent of cationic dye MB and Anionic dye A07.

Ahmad et al. [55] has used a desiccated coconut waste sorbent (DCWS) which is a byproduct of coconut milk processing and produce a sorbent out of it. The adsorbent was used for the sorption of Hg (II). Maximum sorption capacity was found to be 500 mg/g and the kinetic study followed pseudo-second order kinetic model. Also, column sorption experiment showed that as sorption capacity improves the breakthrough time decreases with an increase in initial Hg (II) concentrations. It also reveals that the regeneration as well as the reused of DCWS is possible. Hence, DCWS can be used as an adsorbent for the removal of Hg (II) from aqueous solution.

The adsorption of lead from aqueous solution by coir-pith activated carbon was also studied by [56]. The coir pith was impregnated with sulphuric acid and the optimum sorption capacity was attained at pH 5.0, dosage 1 g/L, lead concentration of 200 mg/L and a contact time of 4 h. The adsorption data follows pseudo-second order kinetic models.

This indicates that coir-pith impregnated with acid tends to have higher adsorption capacity than its original form and can be employed successfully in the treatment of lead from aqueous solution.

Subha and Namasivayam [57, 58] investigated into the potential application of zinc chloride activated coir pith carbon for the adsorption of phenol from aqueous solution. The adsorption capacity using Langmuir was found to be 92.58 mg/g of the used adsorbent. Adsorption also indicates physical process and endothermic.

2.7 Moringa Oleifera

Moringa oleifera falls within the family of shrub and trees; it is believed to have its origin from North West India, around mountain of Himalaya to the south. The Indians have the possesses lots of values; they usually used it for medicinal purposes.

All parts of Moringa tree is found to be edible and has since being consumed by human for many centuries. It can grow in a hot dry land or humid region with a mean height ranging between 5 to 10 m; It might as well grow in a harsh climatic condition and is not being affected by drought [59]. It can withstand a high amount of rainfall ranging from 250 up to 3000 mm at a pH of 5.0 to 9.0 [60].

However, Moringa according to Meneghel et al. has being used by different means which include: biogas (from leaves), honey- and sugar cane juice-clarifier (powdered alley cropping (biomass generation), blue dye (wood), foliar nutrient (juice expressed from the leaves), fencing (living trees), gum (from tree trunks), honey (flower nectar), medicine (all plant parts), ornamental plantings, biopesticides (soil incorporation of leaves to prevent seedling damping off), pulp (wood), rope (bark), tannin for tanning hides (bark and gum), and water purification (powdered seeds) [61]. Apart from the mentioned uses it is also been applied both in domestic and industrial wastewater treatment especially for the removal of heavy metals coming from industrial wastewater. The disadvantages of using Moringa oleifera in water treatment is the increase in the growth of bacteria wherever the seed is in water or solution, minimum temperature for decantation tends to be difficult and higher dosage is required than the normal aluminium sulphate during the process of coagulation. Water with poor bacteriological quality has to be treated with further addition of chlorine instead.

A study on the adsorption of lead (II) using Moringa oleifera Lam seed was investigated by [62]. It was found out that maximum adsorption capacity was 12.24 mg/g. For effectiveness, a comparative study was conducted in parallel with commercial activated carbon under the same optimal sorption parametric condition. The result reveals that though the adsorption behavior of Moringa is less compared with activated carbon but was concluded that Moringa can be considered as an effective and feasible adsorbent for the biosorption of lead (II) in aqueous solution.

Meneghel et al. [63] used Moringa oleifera Lam seeds as low cost adsorbent for the removal of Cadmium (Cd) from polluted water. Optimum adsorption conditions were attained at pH 7.0, contact time of 160 min and 400 mg of adsorbent dosage. The result fitted well into Freundlich and D-R models for Cd adsorption. Optimum adsorption was found to be 7.864 mg/g. A comparative study was also carried out using activated carbon under the same tested conditions and its capacity was found to be 32.884 mg/g.

Also in a similar study by Marques et al. [64] Moringa oleifera seed was used for the removal of manganese ions from aqueous solution. The seed was initially treated with 0.1 M NaOH. A monolayer sorption capacity of 5.61 mg/g was achieved by applying Langmuir model using 3 g of adsorbent dosage in 50 mL solution and 95 % removal efficiency was realized (Table 1).

Table 1 Comparison of adsorption capacity of the adsorbents

S/N	Performances		
	Biosorbent	Removal capacity (mg/g)	References
1	Sugarcane bagasse	22.1	[15]
2	Rice husk	16.94	[27]
3	Banana peels	109.89	[35]
4	Water treatment sludge	50.7	[44]
5	Citrus peel off	62.3	[49]
6	Coconut	500	[55]
7	Moringa oleifera	12.24	[61]

3 Conclusion

Economical, productive, easily accessible resources work extremely well in preference to activated carbon with regard to the elimination involving heavy metals coming from aqueous solution. An array of low-cost sorbents has long been researched. Evaluations regarding the sorbents tend to be challenging because of disparities with data demonstration. Nevertheless, among the few literature reviewed on sorbents most has shown a great potentiality of adsorption and also exhibits a greater capacity of removal which can be employed to be used in a larger use. As a result of deficiency regarding reliable expense information and facts, expense evaluations tend to be complicated to generate. Despite the fact that very much continues to be achieved within the subject regarding low-cost sorbents, great efforts are essential to improve to comprehend low-cost adsorption techniques as well as in order to show the technological know-how.

Acknowledgments The authors acknowledge the research grant provided by Fundamental Research Grant Scheme (FRGS) that leads to the realization of this article and also Universiti of Teknologi PETRONAS (UTP) for supporting this work. Moreover, we are thankful to Dr. Amirhossein Malakahmad for his guidance.

References

1. M.E. Hodson, Effects of heavy metals and metalloids on soil organisms, in *Heavy Metals in Soils*, ed. by B.J. Alloway. (Springer, Berlin, 2013), pp. 141–160
2. S.Y. Chen, Q.Y. Huang, Heavy metals recovery from wastewater sludge of printed circuit board industry by thermophilic bioleaching process. *J. Chem. Technol. Biotechnol.* (2013)
3. S. Morais, F. Costa, M. Pereira, Heavy metals and human health, in *Environmental Health*, 1st edn., ed. by J. Oosthuizen (InTech Open Sci), pp. 227–246 (2012)
4. D. Kar, P. Sur, S. Mandai, T. Saha, R. Kole, Assessment of heavy metal pollution in surface water. *Int. J. Environ. Sci. Technol.* **5**, 119–124 (2008)
5. J.G. Dean, F.L. Bosqui, K.L. Lannouette, Removing heavy metals from wastewater. *Environ. Sci. Technol.* **6** (1977)

6. M. Barakat, New trends in removing heavy metals from industrial wastewater. *Arab. J. Chem.* **4**, 361–377 (2011)
7. Y.-J. Liang, L.-Y. Chai, X.-B. Min, C.-J. Tang, H.-J. Zhang, Y. Ke et al., Hydrothermal sulfidation and floatation treatment of heavy-metal-containing sludge for recovery and stabilization. *J. Hazard. Mater.* **217**, 307–314 (2012)
8. B. Atkinson, F. Bux, H. Kasan, Considerations for application of biosorption technology to remediate metal-contaminated industrial effluents. *Water S. A.* **24**, 129–135 (1998)
9. M. Corapcioglu, C. Huang, The adsorption of heavy metals onto hydrous activated carbon. *Water Res.* **21**, 1031–1044 (1987)
10. M. Kim, D.F. Day, Composition of sugar cane, energy cane, and sweet sorghum suitable for ethanol production at Louisiana sugar mills. *J. Ind. Microbiol. Biotechnol.* **38**, 803–807 (2011)
11. C.G. da Silva, S. Grelier, F. Pichavant, E. Frollini, A. Castellan, Adding value to lignins isolated from sugarcane bagasse and *Miscanthus*. *Ind. Crops Prod.* **42**, 87–95 (2013)
12. B.T. Guan, P.A. Latif, T.Y. Yap, Physical preparation of activated carbon from sugarcane bagasse and corn husk and its physical and chemical characteristics (2013)
13. L.D. Khuong, R. Kondo, R. De Leon, T. Kim Anh, K. Shimizu, I. Kamei, Bioethanol production from alkaline-pretreated sugarcane bagasse by consolidated bioprocessing using *Phlebia* sp. MG-60. *Int. Biodeterior. Biodegradation* **88**, 62–68 (2014)
14. Z. Zhang, I.M. O'Hara, G.A. Kent, W.O. Doherty, Comparative study on adsorption of two cationic dyes by milled sugarcane bagasse. *Ind. Crops Prod.* **42**, 41–49 (2013)
15. E. Pehlivan, H.T. Tran, W.K.I. Ouedraogo, C. Schmidt, D. Zachmann, M. Bahadir, Sugarcane bagasse treated with hydrous ferric oxide as a potential adsorbent for the removal of As(V) from aqueous solutions. *Food Chem.* **138**, 133–138 (2013)
16. K.A.G. Gusmão, L.V.A. Gurgel, T.M.S. Melo, CdF Carvalho, L.F. Gil, Adsorption studies of etherdiamine onto modified sugarcane bagasses in aqueous solution. *J. Environ. Manage.* **133**, 332–342 (2014)
17. N. Esfandiari, B. Nasernejad, T. Ebadi, Removal of Mn(II) from groundwater by sugarcane bagasse and activated carbon (a comparative study): application of response surface methodology (RSM). *J. Ind. Eng. Chem.*
18. R. Suemitsu, R. Uenishi, I. Akashi, M. Nakano, The use of dyestuff-treated rice hulls for removal of heavy metals from waste water. *J. Appl. Polym. Sci.* **31**, 75–83 (1986)
19. B.S. Ndazi, S. Karlsson, J.V. Tesha, C.W. Nyahumwa, Chemical and physical modifications of rice husks for use as composite panels. *Compos. A Appl. Sci. Manuf.* **38**, 925–935 (2007)
20. H. Jaman, D. Chakraborty, P. Saha, A study of the thermodynamics and kinetics of copper adsorption using chemically modified rice husk. *Clean Soil Air Water* **37**, 704–711 (2009)
21. K. Sakr, Effects of silica fume and rice husk ash on the properties of heavy weight concrete. *J. Mater. Civ. Eng.* **18**, 367–376 (2006)
22. K. Wong, C. Lee, K. Low, M. Haron, Removal of Cu and Pb by tartaric acid modified rice husk from aqueous solutions. *Chemosphere* **50**, 23–28 (2003)
23. E. Natarajan, A. Nordin, A. N. Rao, Overview of combustion and gasification of rice husk in fluidized bed reactors. *Biomass Bioenergy* **14**, 533–546 (1998)
24. S.G.K.S.R.M. Kuty, C.L. Lai, M.H. Isa, Removal of copper using microwave incinerated rice husk ash (MIRHA) in continuous flow activated sludge system, in *2012 International Conference on Civil, Offshore and Environmental Engineering (ICCOEE2012)*, 2012
25. D.W. Li, X.F. Zhu, Preparation and methylene blue adsorption characteristics of highly mesoporous rice husk active carbon prepared by an Alkali-saving and equipment-friendly method. *Appl. Mech. Mater.* **448**, 182–187 (2014)
26. M. Junaid, M.U. Khan, F. Ahmad, R.N. Malik, Z.K. Shinwari, Rice husk as dyes removal from impregnated cotton wastes generated in sports industries of sialkot, pakistan. *Pak. J. Bot.* **46**, 293–297 (2014)
27. A. Gupta, S. Mote, A comparative study and kinetics for the removal of hexavalent chromium from aqueous solution by agricultural, timber and fruit wastes. *Chem. Process Eng. Res.* **19**, 49–56 (2014)

28. M.P. Cano, B. de Ancos, M.C. Matallana, M. Cámara, G. Reglero, J. Tabera, Differences among Spanish and Latin-American banana cultivars: morphological, chemical and sensory characteristics. *Food Chem.* **59**, 411–419 (1997)
29. J.P. Essien, E.J. Akpan, E.P. Essien, Studies on mould growth and biomass production using waste banana peel. *Bioresour. Technol.* **96**, 1451–1456 (2005)
30. C.S. Chooklin, S. Maneerat, A. Saimmai, Utilization of banana peel as a novel substrate for biosurfactant production by halobacteriaceae archaeon AS65. *Appl. Biochem. Biotechnol.* **173**, 624–645 (2014)
31. C. Liu, H.H. Ngo, W. Guo, K.-L. Tung, Optimal conditions for preparation of banana peels, sugarcane bagasse and watermelon rind in removing copper from water. *Bioresour. Technol.* **119**, 349–354 (2012)
32. J. Anwar, U. Shafique, Z. Waheed uz, M. Salman, A. Dar, S. Anwar, Removal of Pb(II) and Cd(II) from water by adsorption on peels of banana. *Bioresour. Technol.* **101**, 1752–1755 (2010)
33. R.R. Mohammed, M.F. Chong, Treatment and decolorization of biologically treated Palm Oil Mill Effluent (POME) using banana peel as novel biosorbent. *J. Environ. Manage.* **132**, 237–249 (2014)
34. J. Abdulfatai, A.A. Saka, A.S. Afolabi, O. Micheal, Development of adsorbent from banana peel for wastewater treatment. *Appl. Mech. Mater.* **248**, 310–315 (2013)
35. R. Krishni, K. Foo, B. Hameed, Adsorptive removal of methylene blue using the natural adsorbent-banana leaves. *Desalin. Water Treat.* 1–9 (2013)
36. U.N. Murthy, Experimental study on biosorption of Cr (VI) from water by banana peel based biosorbent. *Res. Rev. J. Eng. Technol.* **2** (2013)
37. M. Razali, Y. Zhao, M. Bruen, Effectiveness of a drinking-water treatment sludge in removing different phosphorus species from aqueous solution. *Sep. Purif. Technol.* **55**, 300–306 (2007)
38. A. Babatunde, Y. Zhao, Constructive approaches toward water treatment works sludge management: an international review of beneficial reuses. *Crit. Rev. Environ. Sci. Technol.* **37**, 129–164 (2007)
39. P. Verlicchi, L. Masotti, Reuse of drinking water treatment plants sludges in agriculture: problems, perspectives and limitations
40. D.F. Lin, L.S. Huang, H.L. Luo, R.S. Weng, Effects on cement after partial replacement with burned joss paper ash. *Environ. Technol.* **33**, 2595–2601 (2012)
41. Y. He, X. Liao, L. Liao, W. Shu, Low-cost adsorbent prepared from sewage sludge and corn stalk for the removal of COD in leachate. *Environ. Sci. Pollut. Res.* 1–10 (2014)
42. S. Bousba, A.H. Meniai, Adsorption of 2-chlorophenol onto sewage sludge based adsorbent: equilibrium and kinetic study. *Chem. Eng.* **35** (2013)
43. A.H. Hawari, Application of dried anaerobic digested sewage sludge as phenol biosorbent. *Int. J. Environ. Eng.* **6**, 29–42 (2014)
44. M.A.A. Zaini, T.Y. Cher, M. Zakaria, M.J. Kamaruddin, S.H. Mohd. Setapar, M.A. Che Yunus, Palm oil mill effluent sludge ash as adsorbent for methylene blue dye removal. *Desalin. Water Treat.* 1–9 (2013)
45. F. Anwar, R. Naseer, M. Bhangar, S. Ashraf, F.N. Talpur, F.A. Aladedunye, Physico-chemical characteristics of citrus seeds and seed oils from Pakistan. *J. Am. Oil. Chem. Soc.* **85**, 321–330 (2008)
46. B. Matthaus, M. Özcan, Chemical evaluation of citrus seeds, an agro-industrial waste, as a new potential source of vegetable oils. *Grasas y Aceites* **63**(3), 313–320 (2012)
47. H.J. Kang, S.P. Chawla, C. Jo, J.H. Kwon, M.W. Byun, Studies on the development of functional powder from citrus peel. *Bioresour. Technol.* **97**, 614–620 (2006)
48. S.S. Voo, B.M. Lange, Sample preparation for single cell transcriptomics: essential oil glands in citrus fruit peel as an example, in *Plant Isoprenoids* (Springer, 2014), pp. 203–212
49. F. Gönen, D.S. Serin, Adsorption study on orange peel: removal of Ni (II) ions from aqueous solution. *Afr. J. Biotechnol.* **11**, 1250–1258 (2014)
50. M.M. Ahmed, Removal of uranium (VI) from aqueous solution using low cost and eco-friendly adsorbents. *J. Chem. Eng. Process Technol.* **4**, 169 (2013)

51. M. Mafra, L. Igarashi-Mafra, D. Zuim, É. Vasques, M. Ferreira, Adsorption of remazol brilliant blue on an orange peel adsorbent. *Braz. J. Chem. Eng.* **30**, 657–665 (2013)
52. F. Howard, D. Moore, R. Giblin-Davis, R. Abad, The animal class Insecta and the plant family Palmae, in *Insects on Palms*, pp. 1–32 (2001)
53. D.J. Mead, Forests for energy and the role of planted trees. *BPTS* **24**, 407–421 (2005)
54. S.-A. Ong, L.-N. Ho, Y.-S. Wong, A. Zainuddin, Adsorption behavior of cationic and anionic dyes onto acid treated coconut coir. *Sep. Sci. Technol.* **48**, 2125–2131 (2013)
55. M. Ahmad, S.S. Lee, X. Dou, D. Mohan, J.-K. Sung, J.E. Yang et al., Effects of pyrolysis temperature on soybean stover-and peanut shell-derived biochar properties and TCE adsorption in water. *Bioresour. Technol.* **118**, 536–544 (2012)
56. P. Kumar, R. Rao, S. Chand, S. Kumar, K. Wasewar, C.K. Yoo, Adsorption of lead from aqueous solution onto coir-pith activated carbon. *Desalin. Water Treat.* **51**, 2529–2535 (2013)
57. R. Subha, C. Namasivayam, Kinetics and isotherm studies for the adsorption of phenol using low cost micro porous ZnCl₂ activated coir pith carbon. *Can. J. Civ. Eng.* **36**(1), 148–159 (2013). doi:[10.1139/S08-039](https://doi.org/10.1139/S08-039)
58. R. Subha, C. Namasivayam, Kinetics and isotherm studies for the adsorption of phenol using low cost micro porous ZnCl₂ activated coir pith carbon. *J. Environ. Eng. Sci.* **8**, 23–35 (2013)
59. F. Farooq, M. Rai, A. Tiwari, A.A. Khan, S. Farooq, Medicinal properties of *Moringa oleifera*: an overview of promising healer. *J. Med. Plants Res.* **6**, 4368–4374 (2012)
60. J. Animashaun, A. Toye, Feasibility analysis of leaf-based moringa oleifera plantation in the nigerian guinea savannah: case study of university of ilorin moringa plantation. *Agrosearch* **13**, 218–231 (2014)
61. S. Sreelatha, A. Jeyachitra, P. Padma, Antiproliferation and induction of apoptosis by *Moringa oleifera* leaf extract on human cancer cells. *Food Chem. Toxicol.* **49**, 1270–1275 (2011)
62. A.P. Meneghel, A.C. Gonçalves Jr, C.R. Teixeira Tarley, J.R. Stangarlin, F. Rubio, H. Nacke, Studies of Pb²⁺ adsorption by *Moringa oleifera* Lam. seeds from an aqueous medium in a batch system. *Water Sci. Technol.* **69** (2014)
63. A.P. Meneghel, A.C. Gonçalves Jr., F. Rubio, D.C. Dragunski, C.A. Lindino, L. Strey, Biosorption of cadmium from water using moringa (*moringa oleifera* lam.) seeds. *Water Air Soil Pollut.* **224**, 1–13 (2013)
64. T.L. Marques, V.N. Alves, L.M. Coelho, N.M. Coelho, Assessment of the use of moringa oleifera seeds for removal of manganese ions from aqueous systems. *BioResources* **8** (2013)

Partly Decomposed Empty Fruit Bunch Fiber as a Potential Adsorbent for Ammonia-Nitrogen from Urban Drainage Water

A.Y. Zahrim, L.N.S. Ricky, Y. Shahril, S. Rosalam, B. Nurmin, A.M. Harun and I. Azreen

Abstract The removal of ammonia-nitrogen from aqueous solution by using partly decomposed oil palm empty fruit bunch (EFB) fibers has been investigated in this study. The unmodified EFB fiber was superior than highly concentrated sodium hydroxide (1.25 M) modified EFB for ammonia-nitrogen removal. The biosorption isotherm data for ammonia-nitrogen on unmodified EFB fibers were well fitted by Freundlich isotherm model that suggesting the heterogeneous adsorption behavior of the adsorption process ($R^2 = 0.991$). The adsorption kinetic modeling of the adsorption data indicated pseudo-second-order model is the better to describe the predicting a chemisorption process ($R^2 = 0.9875$).

Keywords Ammonia-nitrogen removal · Urban drainage · Biosorption isotherm · Adsorption kinetic modelling

A.Y. Zahrim (✉) · L.N.S. Ricky · S. Rosalam · I. Azreen
Chemical Engineering Programme, Faculty of Engineering, Universiti Malaysia Sabah,
Jalan UMS, 88400 Kota Kinabalu, Sabah, Malaysia
e-mail: zahrim@ums.edu.my

Y. Shahril
Medical, Faculty of Medicine and Health Science, Universiti Malaysia Sabah,
Jalan UMS, 88400 Kota Kinabalu, Sabah, Malaysia

B. Nurmin
Civil Engineering Programme, Faculty of Engineering, Universiti Malaysia Sabah,
Jalan UMS, 88400 Kota Kinabalu, Sabah, Malaysia

A.M. Harun
Electrical Engineering Programme, Faculty of Engineering, Universiti Malaysia Sabah,
Jalan UMS, 88400 Kota Kinabalu, Sabah, Malaysia

1 Introduction

Polluted drainage water which flows into rivers would diminish the aesthetic value, dirty and smelly, kill aquatic life such as fish and prawns, and destroy marine ecology. To protect the human and environment as well to sustain the ecotourism, the drainage water with minimum pollutant is considered to be very important in this regard. The pollution in the river could be minimized if the drainage water is properly treated. It has been reported that particularly in Kota Kinabalu, Sabah, the main pollutant in drainage is the ammonia-nitrogen [1]. There are several techniques to remove ammonia-nitrogen such as coagulation, sand filtration, chlorination, UV and ozone ion exchange (IE), reverse osmosis (RO), nanofiltration, electrodialysis (ED), activated carbon adsorption, and biological treatment [1–3]. Each method has their own advantages and limitations [3, 4].

Malaysia is one of the world largest palm oil exporters, and about 3.0 million tons of oil palm empty fruit bunch (EFB) fibers are produced every year [5]. Empty fruit bunch has ability to adsorb nutrients, color and other pollutants onto their fiber. In the palm oil mill industry, it was reported that EFB able to retain nutrients from palm oil mill effluent [6]. Recently, Sajab et al. [5] reported EFB fibers as a media for dye removal. Previously, EFB also reported to be able to adsorb phenol with adsorption capacity 1 mg/g [7]. In this study, the EFB fibers were employed for removal of ammonia-nitrogen from synthetic solution.

2 Materials and Methods

2.1 Biosorbent Preparation

The partly decomposed (naturally) shredded EFB fibers were collected from Tawau, Sabah (latitude: 4.282457 N, longitude: 117.914787 E). These shredded EFB fibers were firstly washed with tap water in order to remove residual salinity and dirtiness such as sand particles and soils. After that, they were again washed with distilled water before they dried under the room temperature for 3 days. Modification of these EFB fibers were carried out by the treatment with 5 % (1.25 mol/L) of NaOH (Analar NORMAPUR) into the 1,000 mL of distilled water at the time (1, 6, 12, 24, and 72) h in room temperature to remove contaminants such as oil and waxy impurities [5]. Then, the modified EFB fibers were again washed with distilled water. The washed fibers were dried in an oven at 60 °C for 48 h until a constant weight [8].

2.2 Ammonium Solution Preparation

Synthetic ammonium chloride solutions were used through the biosorption tests. First, prepare a 157 mg/L of ammonium chloride solutions by dissolving ammonium

chloride pellets in distilled water in order to produce 50 mg/L of ammonia nitrogen solution. As for pH adjustment, HCl and NaOH solutions (0.1 M) were used.

2.3 Batch Biosorption Experiments

Adsorption experiments were carried out in batch process to analysis the effect of ammonia-nitrogen concentration on ammonia biosorption by unmodified EFB fibers at room temperature. The biosorbent of 0.5 g EFB fibers was added into a beaker containing 500 mL of ammonium solution (157 mg/L). Each experiment was made at least in two times. The initial pH of ammonia-nitrogen solution was adjusted using 0.1 M NaOH or 0.1 M HCl. The solution was stirred for 1 h in order to obtain equilibrium concentration with the pH of 7.

The effect of the initial ammonia-nitrogen residual concentration on its biosorption (EFB fibers) was carried out through kinetics and equilibrium studies [8]. The ammonium chloride concentration was fixed to 157 mg/L which is approximately equivalent to 50 mg/L of ammonia-nitrogen concentration. Their progress in time was checked at 12 contact times as follows: 0.5, 1, 5, 10, 15, 20, 30, 40, 60, 90, 120 and 180 min.

2.4 Analysis

The ammonia-nitrogen concentration were determined according to the volumetric method based on Nessler method [9].

2.5 Estimation of the Amount of Adsorbed Ammonia-Nitrogen

At a giving time (t), the amount of ammonia-nitrogen adsorbed per unit mass of EFB fibers, q_t (mg/g) was obtained from the decrease of the ammonia-nitrogen concentrations as follows:

$$Q_t = \frac{(C_0 - C_t)V}{M} \quad (1)$$

where C_0 and C_t (mg/L) are respectively the initial and at time t of ammonia-nitrogen concentrations, V is the volume of the ammonia-nitrogen solutions (L) and M is the mass of biosorbent used (g).

The absorbance value obtained in each contact time was then used to calculate the percent of ammonia-nitrogen removal, by using the following equation:

$$\% \text{ of ammonia-nitrogen} = \frac{C_0 - C_e}{C_0} \times 100 \% \quad (2)$$

2.6 Biosorption Isotherms

The equilibrium of sorption was defined as the solute distribution between the liquid and solid phases after the sorption reaction reaches equilibrium. The amount of sorbed solute onto the solid phase (mg/g) versus the solute concentration in the aqueous phase (mg/L) at equilibrium that called sorption isotherm. In this research, Langmuir, Freundlich and Tempkin isotherms, which described and investigated to fit most of the adsorption data.

The Langmuir isotherm is expressed as:

$$Q_e = \frac{x}{m} = \frac{abC_e}{1 + bC_e} \quad (3)$$

where Q_e is the amount of ammonia-nitrogen per adsorbed unit mass of EFB fibers in equilibrium (mg/g), C_e is the ammonia-nitrogen liquid phase concentration on the EFB fibers in equilibrium after adsorption (mg/L), a is the empirical constant and b is the Langmuir constant related to the adsorption energy (L/mg). The linear form of Langmuir isotherm equation is represented by the following:

$$\frac{C_e}{Q_e} = \frac{1}{ab} + \frac{1}{a}C_e \quad (4)$$

The maximum adsorption capacity and Langmuir constant were determined from the gradient and the intercepts of the plots of $\frac{C_e}{Q_e}$ versus C_e . The essential features of Langmuir isotherm can be expressed as a dimensionless constant separation factor R_L , which is obtained as follows [5, 8, 10]:

$$R_L = \frac{1}{1 + bC_0} \quad (5)$$

The Freundlich isotherm is expressed as [11]:

$$Q_e = \frac{x}{m} = K_f C_e^{1/n} \quad (6)$$

where K_f is the freundlich capacity factor (mg of ammonia-nitrogen/g of EFB fibers) (L water/mg adsorbate) $^{1/n}$, $1/n$ is the Freundlich intensity parameter or also

known as heterogeneity factor [10]. The linear form of Freundlich isotherm equation is represented by the following:

$$\log Q_e = \log \left(\frac{x}{m} \right) = \log K_f + \frac{1}{n} \log C_e \quad (7)$$

In order to find out the K_f and n values from the intercepts and the slope, the linear plots of $\log Q_e$ versus $\log C_e$ was plotted respectively. The magnitude of the exponent n , indicates whether the adsorption is good ($2 < n < 10$), moderately difficult ($1 < n < 2$) or poor ($n < 1$) [5, 8, 10].

The Temkin isotherm is expressed as [10]:

$$Q_e = \frac{RT}{b} \ln(K_T C_e) \quad (8)$$

where K_T is the equilibrium binding constant (L/g), corresponding to the maximum binding energy and constant $B_1 = RT/b$ is related to the heat of adsorption. The linear form of Temkin isotherm equation is obtained:

$$Q_e = B_1 \ln K_T + B_1 \ln C_e \quad (9)$$

2.7 Biosorption Kinetic Modeling

Adsorption kinetics modeling is important for the mechanisms of the adsorption of ammonia-nitrogen on biosorbent to better understanding of ammonia-nitrogen adsorption mechanisms onto EFB fibers [5]. The pseudo-first-order, pseudo-second-order and intraparticle models were used to fit the ammonia-nitrogen adsorption experimental data and can be expressed as [8, 12].

The pseudo-first-order model equation:

$$\frac{dQ_t}{dt} = K_1(Q_e - Q_t) \quad (10)$$

where dQ_t (mg/g) is the amount of adsorbate absorbed at time, t (min), dQ_e is the adsorption capacity in equilibrium, and k_1 (min^{-1}) is the rate constant for pseudo-first-order model. The integration of Eq. (10) and by applying the initial conditions $Q_t = 0$ at $t = 0$ and $Q_t = Q_t$ at $t = t$ becomes to [10]:

$$\log(Q_e - Q_t) = \log Q_e - \left(\frac{K_1}{2.303} \right) t \quad (11)$$

The pseudo-first-order model is assumed that the rate of change of adsorbed solute with time is proportional to the difference in equilibrium biosorption capacity and the adsorbed amount [8, 13, 14].

The pseudo-second-order model equation:

$$\frac{dQ_t}{dt} = k_2(Q_e - Q_t)^2 \quad (12)$$

where k_2 is the rate constant of pseudo-second-order model (g/mg min) and Q_e is the maximum adsorption capacity (mg/g). By integrating the Eq. (12) and noting that $Q_t = 0$ at $t = 0$, the following Eq. (13) is obtained:

$$\frac{t}{Q_t} = \frac{1}{k_2 Q_e^2} + \left(\frac{1}{Q_e}\right)t \quad (13)$$

where Q_t is the amount of ammonia-nitrogen adsorbed on adsorbent per unit mass of the adsorbent (EFB fibers). The pseudo-second-order model is involved chemisorption that the adsorbate on the adsorbent was assumed to be the rate-limiting steps [8, 15, 16].

The intraparticle diffusion model equation:

$$Q_t = k_p \sqrt{t} \quad (14)$$

where k_p is the rate constant of intraparticle diffusion model (g/mg min). The intraparticle diffusion model describes that applied the threefold of mass transport of the ammonia-nitrogen transport from the solution to the interior of the EFB fibers [8].

3 Results and Discussion

3.1 Preliminary Tests

In the control, the ammonia-nitrogen biosorption experimental data, blank ammonia-nitrogen solution was carried out. They consisted the distilled water with 50 mg/L of ammonia-nitrogen concentration was shaken without biosorbent (EFB fibers) in order to determine the ammonia-nitrogen losses through volatilization to the air due to stirring or pH variations. As a result, it is showed that the EFB fibers did not contain free nitrogen in which the percentage of ammonia-nitrogen removal in percentage is 0.23 %, less than 1 %. Apart from that, the ammonia-nitrogen losses is due to the stirring of the ammonia-nitrogen solution, without EFB fibers. Besides that, the pH variation between 7 and 10 did not cause significant ammonium chloride volatilization (<1 %). Similar findings were found by Jellali et al. [8] when they studied ammonium adsorption onto the *P. oceanica* fibers.

Figures 1 and 2 shows the percentage ammonia-nitrogen removal based onto unmodified and modified EFB fibers of the various weight for the unmodified EFB fibers (0.5, 1, 5, 12, and 15 g) at equilibrium from a ammonium chloride solution containing 50 mg/L of ammonia-nitrogen. The comparison for the unmodified (raw) and modified EFB fibers showed that lower amount of

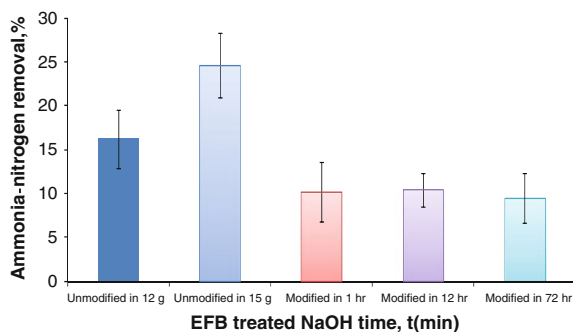


Fig. 1 Ammonia-nitrogen removal based onto unmodified and modified EFB fibers at initial ammonia-nitrogen concentration of 50 mg/g (contact time: 40 min, modified EFB fibers weight: 15.71 g/L temperature: 25.9–28.3 °C, pH: 7)—error bar deviation for duplicate measurements

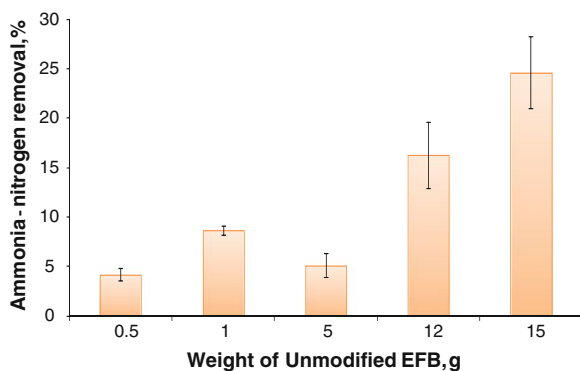


Fig. 2 Ammonia-nitrogen removal based onto unmodified EFB fibers at initial ammonia-nitrogen concentration of 50 mg/g (contact time: 40 min, EFB fibers weight: 0.5, 1, 5, 12, 15 g, temperature: 25.9–28.3 °C, pH: 7)—error bar deviation for duplicate measurements

percentages ammonia-nitrogen removal for the modified EFB fibers (treated with NaOH solutions in 1, 12 and 72 h), which 10.21, 10.45 and 9.48 % are presented in Fig. 1. The higher percentage ammonia-nitrogen removal onto the unmodified EFB fibers between 12 and 15 g, which 16.27 and 24.64 % as shown in Fig. 2.

3.2 Batch Equilibrium Studies

Langmuir, Freundlich and Temkin isotherms are the most widely used for fitting of solid-liquid adsorption data.

3.2.1 Langmuir Isotherm

Figure 3 shows the plots of C_e/Q_e against C_e for the linearized form of Langmuir isotherm. The Langmuir constant were calculated from the plots and distributed graph was obtained. The Langmuir constant for $a = -0.57215$ and $b = -0.016594$ were calculated from the slope and intercept. The Langmuir isotherm was assumed a fixed number of accessible sites are available on the biosorbent (EFB fibers) surface which have the similar energy and the adsorption is reversible [11].

The R_L value is needed to indicate the isotherm whether the adsorption is favorable ($0 < R_L < 1$), unfavorable ($R_L > 1$) or linear ($R_L = 1$). The value of R_L obtained from Fig. 3 is 5.872 have been found to be above 1.0 for the whole EFB fibers range of mass used confirming that the adsorption of ammonia-nitrogen is unfavorable. The Langmuir isotherm model is not suitable for the adsorption of ammonia-nitrogen solution onto the EFB fibers due to the plot is curvilinear [11]. The adsorption results were not fitted by the Langmuir isotherm model, as showed in Fig. 3 by the lower correlation coefficients ($r^2 = 0.1187$) in the linear form.

3.2.2 Freundlich Isotherm

To estimate the n and K_f values from the slope and intercept of the plot $\text{Log } Q_e$ versus $\text{Log } C_e$ from Fig. 4 respectively. The Freundlich coefficient, n and K_f was calculated to be -0.95 and 49.22 . The n value of the Freundlich coefficient is less than 0, which indicated that the ammonia-nitrogen is poor adsorption by EFB fibers.

3.2.3 Temkin Isotherm

Linear plots of Q_e versus $\ln C_e$ permit to determine the isotherm constants K_T and B_1 from the intercepts and slope. As shown in Table 1, the $K_T = 0.0171$ and

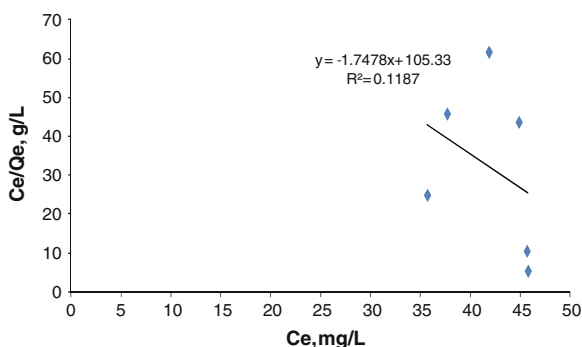


Fig. 3 Langmuir isotherm plots for the ammonia-nitrogen removal by unmodified EFB fibers (contact time: 40 min, temperature: 25.9–28.3 °C, pH: 7)

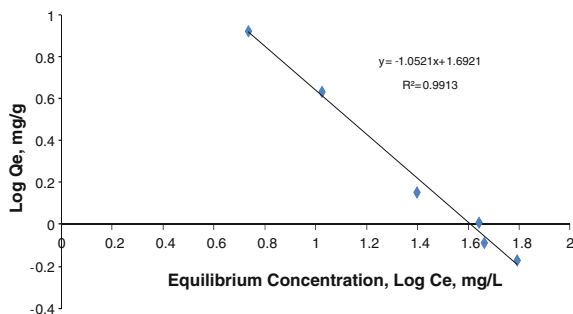


Fig. 4 Freundlich isotherm plots for the ammonia-nitrogen removal by unmodified EFB fibers (contact time: 40 min, temperature: 25.9–28.3 °C, pH: 7)

Table 1 Langmuir, Freundlich and Temkin isotherms constants for the adsorption of ammonia-nitrogen on unmodified EFB fibers (contact time: 40 min, temperature: 25.9 to 28.3 °C, pH: 7)

Langmuir	Q_m (mg/g) = 8.435
	b (L/mg) = -0.0166
	$R^2 = 0.119$
Freundlich	$K_f = 49.215$
	$n = -0.951$
	$R^2 = 0.991$
Temkin	$B_1 = -7.091$
	$K_T = 0.0171$
	$R^2 = 0.910$

$B_1 = -7.091$. Meanwhile, for the regression correlations coefficients of the three models, which Langmuir model was relatively low compare to the other two models. The highest regression correlations coefficient (0.991) was observed for Freundlich model that indicated this model was the most suitable for fitting the biosorption equilibrium of ammonia-nitrogen onto EFB fibers. It also suggests a multilayer adsorption process with the heat of adsorption was distributed in non-uniform over the surface of EFB fibers (Fig. 5).

3.3 Kinetics Studies

The coefficients k_1 and Q_e experiment (exp.) and calculated (cal.) for the pseudo-first-order, k_2 and Q_e for the pseudo-second-order and k_p and Q_e for intraparticle diffusion models, which these adsorption kinetic models formulas were mentioned in Sect. 2.7 and calculated as shown in Table 2. The biosorption of EFB fibers data

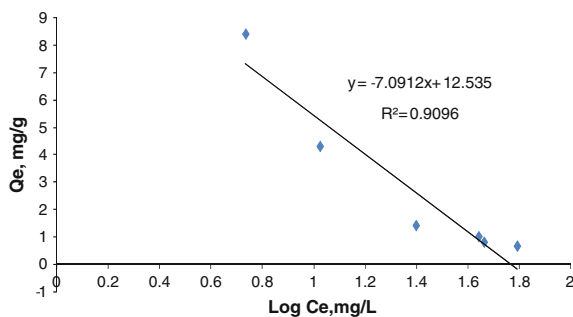


Fig. 5 Temkin isotherm plots for the ammonia-nitrogen removal by unmodified EFB fibers (contact time: 40 min, temperature: 25.9–28.3 °C, pH: 7)

were analyzed according to the first-pseudo-order, the correlation coefficients, R^2 are very low in which lying between 0.0792 and 0.4411. Besides that, the difference between experimental and theoretical calculated adsorbed ammonia-nitrogen at equilibrium state is very high and critically proportional increasing with the mass of EFB fibers used. The experimental values are sudden increasing from more than 0.04 to 10 times than the calculated data. There was no data was obtained for 1 g of EFB fiber used and the Q_e calculated and so the R^2 . From Fig. 6, only 1 value data was obtained in the 1 min while the rest is negative values in other minutes, which unable to log these negative values. This shown a bad fitting between the model and the experimental data and consolidate the results obtained by Jellali et al. for ammonium adsorption onto the *P. oceanica* [8].

For the pseudo-second-order model, the equilibrium biosorption Q_e , rate constant k_2 and correlation coefficients, R^2 were calculated from the slope and intercept of the plots in Fig. 7 and shown in “Table 2” for all different weights of EFB fibers used are very high that is between 0.9165 and 0.9875. In addition, the difference between the experimental data and the calculated data adsorbed masses at equilibrium state is small (15.7 and 32.7 %). Hence, the adsorption of ammonia-nitrogen onto EFB fibers is suitable to fit into the pseudo-second-order.

Table 2 Kinetic model for the adsorption of ammonia-nitrogen on unmodified EFB fibers (contact time: 180 min, temperature: 25.9–28.3 °C, pH: 7)

Weight of the EFB fibers (g)	Pseudo-first-order				Pseudo-second-order			Intraparticle diffusion	
	Q_e exp. (mg/g)	Q_e cal. (mg/g)	k_1 (1/min)	R^2	Q_e (mg/g)	k_2 (g/mg min)	R^2	K_p (mg/gh ^{1/2})	R^2
0.5	8.435	8.076	0.008	0.4411	7.112	-0.030	0.9875	0.1753	0.0117
1	4.325	N/A	N/A	N/A	6.427	0.243	0.9165	0.1869	0.1345
5	1.026	0.082	-0.0078	0.3010	0.792	-0.360	0.9538	-0.0445	0.3050
12	0.678	0.059	-0.0046	0.0792	0.518	-0.352	0.9778	-0.0004	0.0002
15	0.821	0.024	-0.014	0.3876	0.595	-0.262	0.9855	-0.0196	0.3185

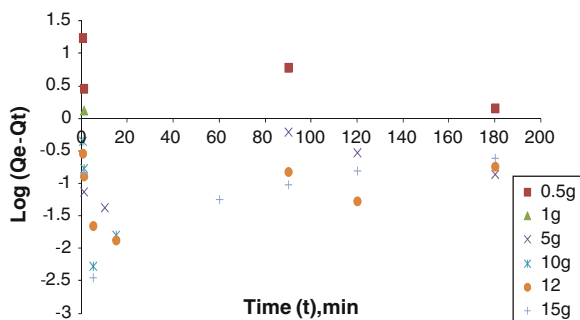
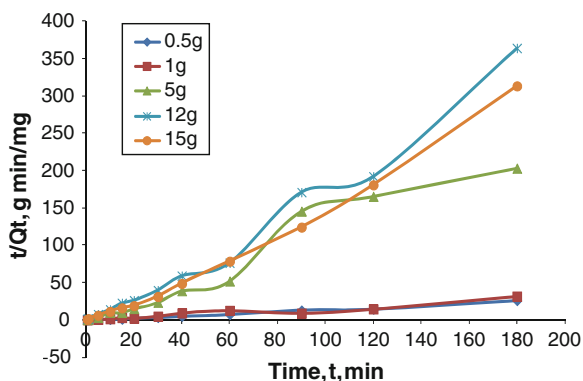


Fig. 6 Pseudo-first-order plots for the ammonia-nitrogen removal by unmodified EFB fibers (contact time: 180 min, temperature: 25.9–28.3 °C, pH: 7)

Fig. 7 Pseudo-second-order plots for the ammonia-nitrogen removal by unmodified EFB fibers (contact time: 180 min, temperature: 25.9–28.3 °C, pH: 7)



Consequently, this adsorption is mainly governed by chemical process involving cations sharing or exchange between EFB fibers and ammonia-nitrogen in the solution [17]. It was showed that pseudo-second-order model describes correctly the biosorption kinetics modeling as compared to pseudo-first-order, which the pseudo-first-order model be successful to explain the biosorption kinetic. This is because pseudo-first-order kinetic model obtained the lower values of R^2 were determined in Fig. 6 and Fig. 7 and listed in Table 2 as compared to the pseudo-second-order kinetic model and the difference equilibrium sorption of experimental and calculated were showed the pseudo-second-order model suitable to describe the biosorption kinetics onto the EFB fibers, yield higher $0.9165 < R^2 < 0.9875$ than the pseudo-first-order.

On the other hand, the intraparticle diffusion analysis of ammonia-nitrogen solution adsorption onto EFB fibers shows the three kinetics modeling (see Sect. 2.7) and play a role of in the biosorption process of ammonia-nitrogen that shown in Fig. 8, plots of Q_t versus $t^{1/2}$ are clearly explained. For the 0.5 and 1.0 g of EFB fibers in Fig. 8, these two lines (0.5 and 1.0 g) indicated by high slopes

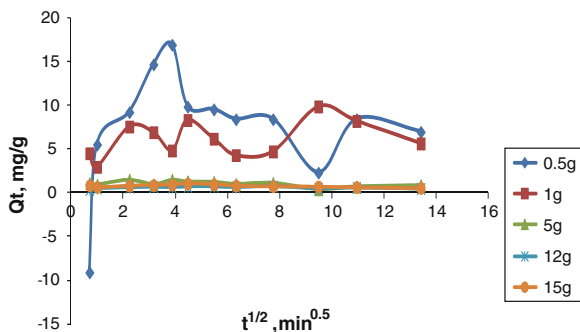


Fig. 8 Intraparticle diffusion kinetic plots for the ammonia-nitrogen removal by unmodified EFB fibers (contact time: 180 min, temperature: 25.9–28.3 °C, pH: 7)

($t^{1/2}$ between 0.707 to 1.342 $\text{min}^{1/2}$), shows the presence of film diffusion. For the 5, 12 and 15 g of EFB fibers in Fig. 8, these three lines (0.5 and 1.0 g) indicated by lower slopes ($t^{1/2}$ between 0.707 to 1.342 $\text{min}^{1/2}$), represents the intraparticle diffusion process.

4 Conclusion

The present study shows that the EFB fibers are potentially to be used as biosorbent for the ammonia-nitrogen removal. The adsorption of ammonia-nitrogen on the EFB fibers achieved equilibrium in the time of 40 min. The experimental data of the adsorption of ammonia-nitrogen onto the EFB fibers fitted the Freundlich isotherm which provided the highest R^2 regression coefficient among the experimental data have been modeled and evaluated by using three different biosorption isotherms model used. The biosorption kinetics obeyed preferably the pseudo-second-order kinetics that gives the best correlation of the experimental data for ammonia-nitrogen onto unmodified EFB fibers.

Acknowledgment The authors appreciate and acknowledge to Universiti Malaysia Sabah for the financial support given under the research Project Grants SGI0013. Special thanks also to the Ministry of Higher Educational, the Department of MyBrain15 scholarship for this study and research fees support.

References

1. N.J. Xiang, *Water of Life from Muddy Microbes* (Insight Sabah, Kota Kinabalu, 2013)
2. A.Y. Zahrim, C. Tizaoui, N. Hilal, Coagulation with polymers for nanofiltration pre-treatment of highly concentrated dyes: a review. *Desalination* **266**(1–3), 1–16 (2011)

3. W.T. Mook, M.H. Chakrabarti, M.K. Aroua, G.M. Khan, B.S. Ali, M.S. Islam, M.A. Abu Hassan, Removal of total ammonia nitrogen (TAN), nitrate and total organic carbon (TOC) from aquaculture wastewater using electrochemical technology: A review. *Desalination* **285**, 1–13 (2012)
4. P. Nigam, G. Armour, I.M. Banat, D. Singh, R. Marchant, Physical removal of textile dyes from effluents and solid-state fermentation of dye-adsorbed agricultural residues. *Bioresour. Technol.* **72**(3), 219–226 (2000)
5. M.S. Sajab, C.H. Chia, S. Zakaria, P.S. Khiew, Cationic and anionic modifications of oil palm empty fruit bunch fibers for the removal of dyes from aqueous solutions. *Bioresour. Technol.* **128**, 571–577 (2013)
6. A.Y. Zahrim, T. Asis, Production of non shredded empty fruit bunch semi-compost. *The Institution of Engineers, Malaysia* **71**, 11–17 (2010)
7. M.Z. Alam, S.A. Muyibi, M.F. Mansor, R. Wahid, Activated carbons derived from oil palm empty-fruit bunches: application to environmental problems. *J. Environ. Sci.* **19**(1), 103–108 (2007)
8. S. Jellali, M.A. Wahab, M. Anane, K. Riahi, N. Jedidi, Biosorption characteristics of ammonium from aqueous solutions onto *Posidonia oceanica* (L.) fibers. *Desalination* **270**(1–3), 40–49 (2011)
9. HACH, *Spectrophotometer Handbook* (USA, 2012)
10. A.M. Yusof, L.K. Keat, Z. Ibrahim, Z.A. Majid, N.A. Nizam, Kinetic and equilibrium studies of the removal of ammonium ions from aqueous solution by rice husk ash-synthesized zeolite Y and powdered and granulated forms of mordenite. *J. Hazard. Mater.* **174**(1–3), 380–385 (2010)
11. E. Metcalf, *Wastewater Engineering Treatment and Reuse*, 4th edn. (McGraw-Hill Companies, USA, 2003) pp. 1138–1149
12. Y.S. Ho, G. McKay, Kinetic models for the sorption of dye from aqueous solution by Wood. *Process Saf. Environ. Prot.* **76**(2), 183–191 (1998)
13. S. Lagergren, About the theory of so-called adsorption of soluble substances. *Kungliga Svenska Vetenskapsakademiens Handlingar* **24**(4), 1–39 (1898)
14. M. El Haddad, R. Slimani, R. Mamouni, M.R. Laamari, S. Rafqah, S. Lazar, Evaluation of potential capability of calcined bones on the biosorption removal efficiency of safranin as cationic dye from aqueous solutions. *J. Taiwan Inst. Chem. Eng.* **44**(1), 13–18 (2013)
15. Q. Qin, J. Ma, K. Liu, Adsorption of anionic dyes on ammonium-functionalized MCM-41. *J. Hazard. Mater.* **162**(1), 133–139 (2009)
16. Y.S. Ho, G. McKay, Pseudo-second order model for sorption processes. *Process Biochem.* **34**(5), 451–465 (1999)
17. M.C. Ncibi, B. Mahjoub, M. Seffen, Investigation of the sorption mechanisms of metal-complexed dye onto *Posidonia oceanica* (L.) fibres through kinetic modelling analysis. *Bioresour. Technol.* **99**(13), 5582–5589 (2008)

A Study on Artificial Hexavalent Chromium Removal by Using Zero Valent Iron Reactor and Sand Filter in Electrochemical Reduction Process

Babby Freskayani Izyani Kaliwon

Abstract Hexavalent Chromium (Cr(VI)) is found in industrial discharges and must be removed before being discharged into receiving waters. Removing Cr(VI) means removing risk of cancer and other ill-health effects associated with it. This research describe column experiment in laboratory which quantify the rate of Cr(VI) removal by zero valence Ion (ZVI) reactor and sand filter from an artificial Cr(VI) waste-water using electrochemical reduction process. The main goal for this study are to study the effectiveness of ZVI in removing Cr(VI) and sand filter for polishing Cr(VI) remaining in ZVI reactor. Test of Cr(VI) were conducted under the following conditions: Cr(VI) concentration for experiments 1, 2, 3 and 4 for feed solution in 1–10 mg/l range; 3 cases of column experiment; The flow rate decided is 2 ml/min and pH adjusted at 7.7 for the feed solution. Three cases of column experiment are column ZVI (1 column), Column ZVI and Sand Filter (2 columns) and Column ZVI mixed with sand (1 column). The result indicate ZVI reduces Cr(VI) to Cr(III) under alkaline conditions. The removal rate efficiencies for all of cases in range 80.33–100 %. The most effective experiment column (individually or in combination) has been chosen for removing Cr(VI) is Column ZVI and sand filter in two columns which is satisfied all of parameters (Cr(VI), iron total and pH) with standard of drinking and river water. The Cr(VI) removal attained for this two columns case is range from 99.8 to 100 %. In conclusion, All of the results in this case were found that the concentration of Cr(VI) effluent lower than the threshold limit 0.05 mg/l except for case of ZVI mixed with sand in one column.

Keywords Hexavalent chromium (Cr(VI)) · Zero valence iron (ZVI) · Sand filter · Electrochemical reduction process

B.F.I. Kaliwon (✉)

Civil Engineering Department, Politeknik Kota Kinabalu, Kota Kinabalu, Sabah, Malaysia
e-mail: izeyani@polikk.edu.my

1 Introduction

Water is a resource that has many uses, including for recreational, transportation, hydroelectric power, agricultural, domestic, industrial, and commercial uses. Water also supports all forms of life, affects our health, lifestyle, and economic well-being. Water is one of the resources required to sustain life and has long been suspected of being the source of many human illnesses. It was not until approximately 150 years ago that a concrete proof of disease transmission through water was established. For examples, in Malaysia a few rivers had been identified as highly polluted. The assessments have shown that, the impact of industrial area was the main contribution factor to the problem [1].

Certain industrial wastewaters contain toxic metals such as Chromium(VI) in increasing concentrations. Wastewater polluted with toxic hexavalent chromium result from sources such as textile mills, the pigment industry, metal finishing industries, drug and organic chemical industries and plant cooling systems where chromate is used as a corrosion inhibitor. Problem with Chromium(VI) is that it is a carcinogenic (cancer risks) heavy metal with possible hazardous effects. It can produce serious hazardous effects like disorder, nose bleeding and perforation of nasal septum [2].

The objectives are to study the effectiveness of zero valence iron in removing Chromium(VI) and sand filter for polishing Chromium(VI) remaining in the zero valence iron (ZVI) reactor. Otherwise, it is also to collect data for the development of a simple, effective technology for removing Chromium(VI) and other metals in water and wastewater treatment.

The study scopes are to construct two columns which are zero valence iron (ZVI) column and sand filter. This study is focusing to feed the reactors with varying concentrations of artificial Chromium(VI) wastewater. The scopes are include to study the effect of the feed wastewater pH, retention time, and pore volume on the metal removal and to compare the Cr(VI) effluent concentration achievable with available effluent quality standards.

2 Literature Review

2.1 Hexavalent Chromium (Cr(VI))

Chromium is a transition metal exhibiting valence states from 2- to 6+, although the 3+ and 6+ species are generally the only ones of interest. It is commonly present as Chromium(VI) in the chromate (CrO_4^{2-}) and dichromate ($\text{Cr}_2\text{O}_7^{2-}$) forms, and as Chromium(III) in the chromic (Cr^{3+}) state. Chromium(VI) compounds are generally soluble in water, whereas Cr(III) compound are insoluble. Chromium is used primarily in metal plating because of its resistance to acid attack and as pigment, but it is also used in leather tanning, as a catalyst in chemical processes, and in the manufacture

of electronic equipment. Chromic and chromate salts are irritating to exposed tissues. Some chromium compounds are known carcinogens. Because of their toxicity, the total chromium concentration is limited to 0.1 mg/l in drinking water [3].

Hexavalent Chromium (Cr(VI)) receives the most public scrutiny, as a carcinogen. Chromium(VI) is a carcinogenic agent which is highly soluble in water. Hexavalent compounds have been shown to be carcinogenic by inhalation and are corrosive to tissue. The chromium guidelines for natural water are linked to the hardness or alkalinity of the water (i.e., the softer the water, the lower the permitted level for chromium) [4].

2.2 Zero-Valence Iron

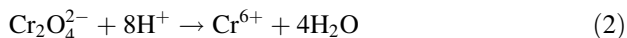
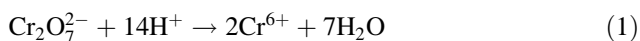
ZVI is an effective and economic reagent for removal of heavy metals and for destruction of chlorinated organic compounds in water because of its high electrochemical reduction potential. Zero-valence iron has been used to recover copper, silver, and mercury in water by reduction and iron cementation.

Zero-valence iron in powder, granular, and fibrous forms can be used in batch reactors, column filters, and permeable reactive barriers installed in groundwater aquifers for water treatment and metal recovery [5].

Zero-valence iron has been used to recover copper, silver, and mercury in water by reduction and iron cementation. Other heavy metals such as lead (Pb), nickel (Ni), cadmium (Cd), chromium (Cr), arsenic (As), selenium (Se), UO_2^{2+} , and TcO_4 can be removed from water by zero-valence iron through reduction and precipitation [6].

3 Methodology

Artificial contaminate water will prepare by dissolving Potassium dichromate ($\text{K}_2\text{Cr}_2\text{O}_7$) or Potassium chromate (K_2CrO_4) add with DIW in Water Quality Lab.



There have four different concentrations of Cr(VI) as feed solution; 1, 3, 5 and 10 mg/l have been utilised for experiment. The reactor column was made of a PVC pipe with an inside diameter of 30 and 180 mm height. The column was packed with 150–450 g iron fillings. The volume of reactor column is 0.1272 l. Total Cr (VI) measured using DR/2010 and DR/4000 to get the effectiveness result.

For two columns experiment model, the column model built up with two columns; column ZVI and sand filter. The diameter of sand filter is 60 mm with 180 mm height.

The volume of sand filter is 0.5089 l. The feed solution was pump through the column ZVI and then through sand filter. There have two samples will be taken to test the concentration of Cr(VI) and ZVI.

For one column experiment model only used one column that it has two cases. Case 1, ZVI Column; the reactor that used in the column is iron fillings only. The weight of iron fillings is 386 g. Case 2, ZVI mixed with sand; the reactive material in the column was composed of 50 % sand and 50 % iron fillings by weight. The sum of weight is 295 g.

Cr(VI) concentration will measure by DR/2010 and the pH is in range 5–9 before running the column experiment. For study the various acidic condition of the feed wastewater, the pH of feed solution adjusted 7.7 at the beginning. Since reactor effluent will be acidic, acid adjustment of the effluent is necessary before the effluent is discharged to the receiving water. The effluent pH below 5 or greater than 9 has damaging effects on most aquatic creatures. pH is important in the removal process of chromium. The flow rate of peristaltic pump that used to pump the feed solution is adjusted in 2 ml/min, the lowest flow rate.

4 Result and Discussion

The summary of result for all parameter in four experiments will be shown in Table 1 for ZVI column case, Table 2 for ZVI and sand in two columns and Table 3 for mixed ZVI and sand in one column.

The analysis of the result based on three cases of two models column created in this project. As expected, the proportion of Cr(VI) removed, decreased by using ZVI reactor and sand as filter. Test of Cr(VI) were conducted under the following conditions: Cr(VI) concentration for four experiments in 1–10 mg/l; 3 cases of column experiment; the flow rate was set 2 ml/min and the pH adjusted at 7.7 for

Table 1 Summary of result for all of parameter in experiments 1, 2, 3 and 4 for one column (ZVI mixed with sand)

Table head	Experiment no.			
	1	2	3	4
Feed				
• Concentration Cr(VI) (mg/l)	1.0	3.0	5.0	10.0
• Concentration Fe (mg/l)	0.05	0.08	0.06	0.10
• pH	7.7	7.7	7.7	7.7
Effluent				
• Lowest concentration Cr(VI) alterable (mg/l)	0.0	0.0	0.0	0.1
• Concentration Fe (mg/l)	10.16	0.20	0.22	0.25
• pH	8.3	8.54	9.3	9.2
% Cr(VI) removed	100	100	100	99.9
Retention time (min)	52.5	49	42.5	40.5

Table 2 Summary of result for all of parameter in experiments 1, 2, 3 and 4 for two columns (column ZVI and sand filter)

Table head	Experiment no.			
	1	2	3	4
Feed				
• Concentration Cr(VI) (mg/l)	1	3	5	10
• Concentration Fe (mg/l)	0.05	0.08	0.06	0.1
• pH	7.7	7.7	7.7	7.7
Effluent				
• Lowest concentration Cr(VI) alterable (mg/l)	0	0	0.01	0.02
• Concentration Fe (mg/l)	0.19	0.21	0.25	0.29
• pH	7.02	7.42	7.79	7.95
% Cr(VI) removed	100	100	99.8	99.8
Retention time (min)	52.5	49	42.5	40.5

Table 3 Summary of result for all of parameter in experiments 1, 2, 3 and 4 for one column (ZVI mixed with sand)

Table head	Experiment no.			
	1	2	3	4
Feed				
• Concentration Cr(VI) (mg/l)	1.0	3.0	5.0	10.0
• Concentration Fe (mg/l)	0.06	0.08	0.10	0.12
• pH	7.7	7.7	7.7	7.7
Effluent				
• Lowest concentration Cr(VI) alterable (mg/l)	0.15	0.59	0.75	0.45
• Concentration Fe (mg/l)	0.20	0.24	0.35	0.44
• pH	7.02	7.42	7.79	7.95
% Cr(VI) removed	85.0	80.33	85	85.5
Retention time (min)	52.5	49	42.5	40.5

the feed solution. The Cr(VI) was removed by the ZVI fillings through electrochemical reduction. After adequate mixing and reduction of aqueous, feed solutions leave the reactor column. The volume that decreased from PV1 to PV2 shows that the ZVI reactor occupied the feed solution in the column in order to remove Cr(VI). The overall pore volume of Cr(VI) range for three of case that occupied is 1–5 ml. The highest volume that occupied in the column is ZVI fillings column.

The process of running each column experiment has been repeated until desired water quality is reached. In this process, the reactive material in column should be replaced after a certain time, as the material will reach the lowest effluent concentration Cr(VI) alterable. The results show that ZVI reduces Cr(VI) to Cr(III) under alkaline conditions. It shows that the concentration Cr(VI) of effluent for overall result are lower than the standard values for drinking water and river water (sewage and industrial effluents); 0.05 mg/l.

From the analysis of all cases, when the concentration of the feed solution increases, the pH of effluent also increases. The most effective column to remove Cr(VI) is ZVI in one column. It is because the three experiments has been running show the percentage 100 % but the range of pH is 8.3–9.2. Two columns (column ZVI and sand filter) model was chosen that satisfied all of parameters. It was also the effective column to remove Cr(VI) in highest percentage is 100 % equal with percent ZVI in one column but the pH is in range 6.5–8.5. It was the sand column that caused the neutrality of pH. The concentration of the total dissolved iron is rather low from standard of drinking water and river water for both cases.

5 Conclusion

From the analysis in this study, this research shows that the feed solution before treated by ZVI reactor and sand filter is 7.7, but after treated by the column it was range 7.02–9.2. This research shows that ZVI reactor and sand filter had the abilities to remove Cr(VI) in dissolving water. Removal of Cr(VI) has been achieved that the efficiencies for Cr(VI) removal as high as 80.33–100 % range by the three of column cases.

From the experiments carried out, it was understood that industrial wastewater treatment could economically and efficiently achieved by employing ZVI reactor and sand filter. By using of this system, industrial wastewaters often contain toxic metals such as Cr(VI) and other metals in increasing concentrations which are being discharged to lakes, rivers or sea could be treated. Result of this study would be used as pilot data for further study on the development of a suitable reactor configuration for Cr removal in water treatment as well as for biological wastewater treatment. The reactive materials used as filter could also become suitable for refractory industries that produce such metals include textile mills, pigment industry, metal finishing, drug, organic chemicals and plant cooling systems where chromate (Cr^{6+}) is applied as corrosion inhibitor. Combining ZVI reactor with sand filter may prove the effective for Cr(VI) removal in drinking water and wastewater that requires biological treatment. As a conclusion, the most effective experiment column (individually or in combination) has been chosen for removing Cr(VI) in this study is two columns experiment model (column ZVI and sand filter) which is satisfied all of parameters (Cr^{6+} , iron total and pH) with standard of drinking and river water.

References

1. N.M. Noor, K.M. Nor, S.A.S. dan Ragnathan Santiago, *Introduction to Environmental Engineering* (Penerbit UniMAP, Universiti Malaysia Perlis, Kangar, Perlis, 2009), pp. 4–97
2. C.H Yap, N. Mohamad, *Reduction of Hexavalent Chromium by Galvanic Cell*, vol. 59. (Universiti sains Malaysia, 2003)

3. P.L. Bishop, *Pollution Prevention: Fundamentals and Practice* (McGraw Hill Higher Education, Singapore, 2000)
4. R.W. Gilham, S. F. O'Hannesin, Enhanced degradation of halogenated aliphatics by zero-valent iron. *Groundwater* **32**, 958–967 (1994)
5. T.E. Shokes, G. Moller, Removal of dissolved heavy metals from acid rock drainage using iron metal. *Environ. Sci. Technol.* **33**, 282–287 (1999)
6. K.J. Cantrell, D.I. Kaplan, T.W. Wietsma, Zero valent iron for the in situ remediation of selected metals in groundwater. *Hazard. Mat.* **42**, 201–212 (1995)

Antibiotic Resistance Bacteria in Coastal Shrimp Pond Water and Effluent

Marfiah Ab. Wahid, Zummy Dahria Mohamed Basri,
Azianabiha A. Halip, Fauzi Baharudin, Janmaizatulriah Jani
and Mohd Fozi Ali

Abstract The rapid growth of shrimp farm activities began since last 40 years. It is due to high demands and can generate economy to the country. In Malaysia, thousands tonnes of shrimp were produced every year for local demand and export as well. However high demand in this industry, causes problem of water pollution in shrimp ponds which subsequently contaminated discharge from the pond due to presence of bacteria. In this study, it was found that shrimp farm water and effluent containing pathogenic bacteria which is resistant to certain antibiotic. These antibiotic resistance bacteria could be harmful to human. *Vibrio alginolyticus*, *Vibrio parahaemolyticus*, *Shigella flexneri* and *E. coli* were detected in the water and effluent from the shrimp farm. Total of *Vibrio* in 3 and 6 months pond were higher than allowable limit, which is 1625 and 2650 cfu/ml, respectively. *E. coli* in this study was recorded at low concentration, however dramatically increased in 4 months pond (438 cfu/ml) before plunging to 13 cfu/ml in 6 months pond. It can be concluded that the higher number of

M.A. Wahid · Z.D.M. Basri (✉) · A.A. Halip · F. Baharudin · J. Jani · M.F. Ali
Faculty of Civil Engineering, UiTM, Shah Alam, Malaysia
e-mail: zummy.d@gmail.com

M.A. Wahid
e-mail: marfi851@salam.uitm.edu.my

A.A. Halip
e-mail: azianabiha@salam.uitm.edu.my

F. Baharudin
e-mail: fauzi1956@salam.uitm.edu.my

J. Jani
e-mail: janmaizatulriah@salam.uitm.edu.my

M.F. Ali
e-mail: mohdfozi@salam.uitm.edu.my

M.A. Wahid
FCRC, UiTM, Shah Alam, Malaysia

J. Jani · M.F. Ali
IIESM, UiTM, Shah Alam, Malaysia

pathogenic bacteria (>1000 cfu/ml of *Vibrio*) were detected in shrimp pond water and effluent can cause illness to human health.

Keywords Pathogenic bacteria · Antibiotic resistance bacteria · Water and wastewater · Shrimp farm · Aquaculture

1 Introduction

Coastal shrimp farming activities became a fastest growing food producing in many countries [1–3]. It is due to high demands and helps to generate income in the country. However, there is negative impact on the environment if this activity release untreated effluent. The untreated effluent will be discharged directly into the receiving water bodies. Therefore, river water will be polluted and can increase human health risk due to chemical, physical and biological contaminants in wastewater.

Antibiotic resistance bacteria is one of the major health risks associated with shrimp pond water and the wastewater. In this study, the antibiotic resistance bacteria is categorized as pathogenic to human. *Pseudomonas aeruginosa* is one of the leading nosocomial pathogens worldwide. *P. aeruginosa* represents a phenomenon of bacterial resistance and practically is known as mechanisms of antimicrobial resistance [4]. *P. aeruginosa* is an extremely adaptive organism and it can grow on a wide range of substrates and quickly responds to environment alterations.

There are many types of bacterias could be found in shrimp ponds water and their effluent. Previous studies showed that *Vibrios* are the most commonly species found in shrimp farms. Table 1 shows the types of bacterias commonly found in shrimp water and their effluent.

The main objective of this study is to investigate the concentration of antibiotic resistance bacteria presence in the coastal shrimp pond water and their effluent.

Table 1 Bacteria commonly found in shrimp pond water and effluent

No.	Bacteria	References
1	<i>Vibrio</i> and <i>Photobacterium</i>	[14]
2	<i>Vibrio</i>	[15, 16]
3	<i>Vibrio parahaemolyticus</i>	[21, 22]
4	<i>Vibrio harveyi</i>	[23]
5	<i>Vibrio nigripulchritudo</i>	[24]
6	<i>V. alginolyticus</i> , <i>V. Parahaemolyticus</i> , <i>V. Alginolyticus</i>	[17]
7	<i>Salmonella</i> and <i>Vibrio</i>	[18]
8	<i>E. coli</i> , <i>Salmonella</i> , <i>Shigella</i> , <i>Vibrio</i>	[13]

Table 2 Characteristics of the shrimp farm

Pond criteria	Farm details
Shrimp type	Tiger shrimp
Total of ponds	14
Pond in operation	6
Total land area	12 ha
Total pond area	8 ha
Age of farm	7 year
Shrimp production (each pond)	6 tonnes
Source of water	Brakish river water
Use of probiotics	Yes
Nearby farm	No

2 Materials and Methods

2.1 Sampling Area

Water samples were collected from a selected coastal shrimp farm in Selangor, Malaysia from November 2013 to January 2014. Table 2 shows the characteristics of the identified farm.

2.2 Sampling

Water samples were collected in 500 ml sterilized bottles and stored at 4 °C until analysed process is been done in the laboratory. The bottles were labelled and the measurement processes were conducted within 24 h. Samples were collected in each pond, including detention pond, inlet and outlet. Sampling was conducted during a fine day.

2.3 Water Quality Analysis

On-site measurement of water quality parameters such as pH, turbidity, Dissolved Oxygen (DO), temperature and salinity were conducted using a portable water quality probe (HORIBA). Biochemical oxygen demand (BOD₅), ammonium nitrogen (NH₄⁺-N) and Total Suspended Solid (TSS) were analysed in laboratory in accordance to Standard Methods [5].

2.4 Microbial Sample and Analysis

Identification of *Shigella flexneri* and *E. coli* showed that 1–2 mm pink and yellow of colonies on XLD agar, respectively. Identification of *Vibrio* was using TCBS agar (OXOID). *Vibrio alginolyticus* was appeared on the media in yellow colonies while *Vibrio parahaemolyticus* was appeared in green colonies. One loopful of sample was streaked on the agar, sealed, labeled and incubated invertedly at 37 °C for 24 h [6]. The concentration of antibiotic resistance bacteria was calculated as colony forming unit (cfu) per milliliter (ml).

3 Result and Discussion

3.1 Water Quality Analysis

The most important activity for the control of noxious crisis in the shrimp farming system is water quality assessment [6]. The Dissolved Oxygen value in the water indicates the growth situation for pollution conditions and aquatic organisms. As shown in Table 3, DO in 3 months pond showed the lowest concentration compared to other ponds. Detrimental to aquatic life happened when the DO is low [7]. Low DO conditions can be attributed to the presence of numerous microorganisms in 3 months pond.

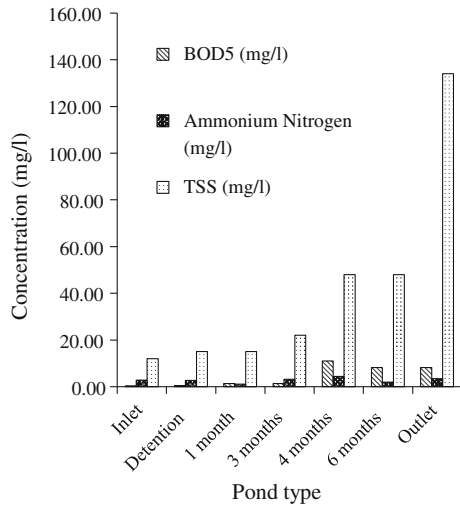
Detention pond was recorded the lowest pH compared to other ponds. The pH range between 6.5 and 9.0 is suitable for aquaculture production [6]. It is showed that water condition in detention pond still not quite suitable yet to being route to the other ponds. The extreme low or high of pH will affect the survival rate of shrimps in the pond.

Temperature recorded in all ponds were found suitable as it is still in the range between 28 and 32 °C where is within the optimum water temperature for the growth of shrimp [6]. The average water temperature recorded during day time in the black tiger shrimp pond is 28 °C [8]. Salinity recorded in Bangladesh shrimp farm wastewater was under 9 psu [3] while in this study, the salinity is ranging between 1.82 and 3.11 psu.

Table 3 Water quality parameter

Parameter	Inlet	Det.	1 month	3 months	4 months	6 months	Outlet
pH	6.76	6.20	8.61	7.88	8.05	7.92	7.91
Turbidity (ntu)	13.00	14.00	18.50	23.34	53.84	43.33	94.67
DO (mg/l)	5.14	8.08	7.57	4.86	7.29	7.56	6.31
Temperature (°C)	29.64	31.52	30.87	30.54	30.95	31.15	30.94
Salinity (psu)	1.82	2.10	2.10	3.06	3.11	3.04	2.88

Fig. 1 BOD₅, ammonium nitrogen and TSS

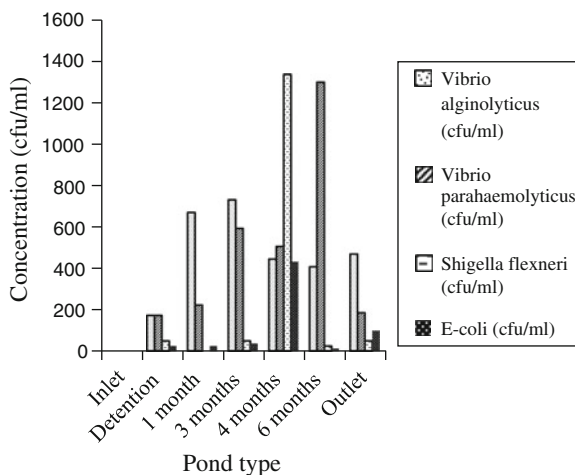


Aquatic life also need nitrogen. They get the required nitrogen by eating plants or by consuming other animals that eat the plants. If the level of ammonium nitrogen in surface waters are too high, they could be toxic to some aquatic organisms. Figure 1 shows that 1.06–4.4 mg/l of ammonium nitrogen were generated. Shrimp farming produced 0.5–1.8 g ammonium/kg shrimp [9]. It shows that the concentration of ammonium nitrogen in the wastewater was considerably low. When more concentration of ammonium nitrogen, it will accelerate the corrosion of pipelines and it causes the chlorination process becomes complicated due to existence of chloramines [10].

The growth of plant and algae usually rise as much nitrogen can be found as nutrient. This occurred when the ammonium nitrate was moderate. This will have a ripple effect on other properties of water quality, such as improving biochemical oxygen demand levels and significantly decreased dissolved oxygen. Increased amount of nitrification will occurred if the level of dissolved oxygen decreased when ammonium nitrogen is high. The BOD₅ of the inlet, 1, 3 months and detention pond were low with the range between 0.36 and 1.38 mg/l. However it was increased for 4 and 6 months pond and outlet with 11.04, 8.22 and 8.16 mg/l, respectively. It was suggested the BOD₅ in shrimp farm is 9.4 mg/l [11].

Total suspended solid discharges during the harvest draining process was 134 mg/l. The average of TSS produced in shrimp pond outlet is 138.5 mg/l [9]. The TSS significantly higher in outlet but still under the limit. The range of TSS were found between 121 and 147 mg/l from shrimp farm wastewater in Ha-Long Bay [12].

Fig. 2 Pathogenic bacteria detected in shrimp farm



3.2 Bacteria Identification

Shigella flexneri, *E. coli* and *Vibrio parahaemolyticus* are life-threatening bacteria and the leading cause of foodborne illness associated with the consumption of seafood. *Shigella flexneri*, *E. coli* and *Vibrio parahaemolyticus* are pathogenic bacteria and a major cause food-borne illness related to seafood intake [13].

Vibrio was known as pathogenic to human and can cause disease through food consumption. Many studies have been done on occurrence and prevalence of *Vibrio* in shrimp farm [2, 14–18]. Figure 2 shows the *Vibriosis* found in this study were ranged between 350 and 1726 cfu/ml. Optimal level for water quality parameters for *Vibrio* is <1000 cfu/ml [6]. It's indicated that the total of *Vibrio* in 3 and 6 months pond are higher than allowable limit.

A total of 11.4 % strains isolated from wastewater were *E. coli* [19]. The presence of *E. coli* in this study were recorded at low concentration, however dramatically increased in 4 months pond (438 cfu/ml) before plunging to 13 cfu/ml in 6 months pond. *E. coli* normally produced from feces of warm-blooded animal and used as an indicator of water pollution. The concentration should be below than 1000 MPN/ml in wastewater analysis [20]. This result indicated that antibiotic resistance bacteria which also pathogenic could be released to the environment and produced potential harm to human health.

4 Conclusion

Based on the findings of this study, it can be concluded that the higher number of pathogenic bacteria (>1000 cfu/ml of *Vibrio*) were detected in shrimp pond water and effluent. These were supported by the increasing of the turbidity level and

E. coli concentration towards harvesting time. Although if quality met the standard of shrimp farm activities, but it still can be harmful to human if the effluent is excessively discharge to the water bodies.

Acknowledgments Authors thank to *Dana Kecemerlangan* (RIF) 04/2012: 600-RMI/DANA 5/3/ RIF (9/2012), Research Management Institute, Universiti Teknologi MARA for financial support in this study.

References

1. L.S. Herbeck, D. Unger, Y.W. Tim, T.C. Jennerjahn, Effluent, nutrient and organic matter export from shrimp and fish ponds causing eutrophication in coastal and back-reef waters of NE Hainan, tropical China. *Continental Shelf Res. (Elsevier)* **57**, 92–104 (2013)
2. S. Nimrat, S. Suksawat, P. Maleeweach, V. Vuthiphandchai, Effect of different shrimp pond soil treatments on the change of physical characteristics and pathogenic bacteria in pond bottom soil. *Aquaculture (Elsevier)* **285**, 123–129 (2008)
3. M.S. Islam, M.J. Sarker, T. Yamamoto, M.A. Wahab, M. Tanaka, Water and sediment quality, partial mass budget and effluent N loading in coastal brackishwater shrimp farm in Bangladesh. *Mar. Pollut. Bull. (Elsevier)* **48**, 471–485 (2004)
4. T. Strateva, D. Yordanov, *Pseudomonas aeruginosa*—a phenomenon of bacterial resistance. *J. Med. Microbiol.* **58**, 1133–1148 (2009)
5. APHA, *Standard methods for examination of water and wastewater*, 22nd edn. (American Public Health Association/American Water Works Association/Water Environment Federation, Washington D.C., 2005)
6. J.J. Carbajal-Hernandez, L.P. Sanchez-Fernandez, L.A. Villa-Vargas, J.A. Carrasco-Ochoa, J. F. Martinez-Trinidad, Water quality assessment in shrimp culture using an analytical hierarchical process. *Ecol. Indic. J.* **29**, 148–158 (2013)
7. Y. Qi, Z. Wang, Y. Pei, Evaluation of water quality and nitrogen removal bacteria community in Fuhe River. *Procedia Environ. Sci.* **13**, 1809–1819 (2012)
8. D.M. Smith, M.A. Burford, S.J. Tabrett, S.J. Irvin, L. Ward, The effect of feeding frequency on water quality of the black tiger shrimp (*Penaeus monodon*). *Aquacult. (Elsevier)* **207**, 125–136 (2002)
9. R. Casillas-Hernandez, H. Nolasco-Soria, T. Garcia-Galano, O. Carrillo-Farnes, F. Paez-Osuna, Water quality, chemical fluxes and production in semi-intensive Pacific white shrimp (*Litopenaeus vannamei*) culture ponds utilizing two different feeding strategies. *Aquacult. Eng. (Elsevier)* **36**, 105–114 (2007)
10. O. Ewa, J. Lach, M. Kacprzak, E. Neczaj, The removal of manganese, iron and ammonium nitrogen on impregnated activated carbon. *Desalination* **206**, 251–258 (2006)
11. A. Sebastian, Development of safety and quality management system in shrimp farming, Ph.D thesis, School of industrial fisheries. Cochin University of Science and Technology, Kerala, 2009
12. T.D. Bui, J. Luong-Van, C.M. Austin, Impact of shrimp farm effluent on water quality in coastal areas of the World Heritage-Listed Ha Long Bay. *Am. J. Environ. Sci.* **8**(2), 104–116 (2012)
13. B.S.M. Mahmoud, Effect of X-ray treatments on inoculated *Escherichia coli* O157:H7, *Salmonella enterica*, *Shigella flexneri* and *Vibrio parahaemolyticus* in ready-to-eat shrimp. *Food Microbiol. J.* **26**, 860–864 (2009)
14. L. Ruangpan, Luminous bacteria associated with shrimp mortality, ed. by Flegel (*Advances in Shrimp Biotechnology*, Bangkok, 1998)

15. J.D. Souza, S.M. Menezes, N.S. Souza, Investigations on the water quality of shrimp farms in Goa with respect to culture practices, 44–69 (2011)
16. J.W.M. David, Disease control in shrimp aquaculture with probiotic bacteria, in *Proceedings of the 18th International Symposium on Microbiol Ecology* (1999)
17. S. Banerjee, T.N. Devaraja, M. Shariff, F.M. Yusoff, Comparison of four antibiotics with indigenous marine bacillus spp. In controlling pathogenic bacteria from shrimp and artemi. *J. Fish Dis.* **30**, 383–389 (2007)
18. S. Banerjee, M.C. Ooi, M. Shariff, H. Khatoon, Antibiotic Resistant *Salmonella* and *Vibrio* associated with farmed *Litopenaeus vannamei*, *Sci. World J.* (2012)
19. F. Matyar, A. Kaya, S. Dincer, Antibacterial agents and heavy metal resistance in Gram-negative bacteria isolated from seawater, shrimp and sediment in Iskenderun Bay, Turkey. *Sci. Total Environ.* **407**, 270–285 (2008)
20. C. Boyd, Water composition and shrimp pond management. *Glob. Aquacult. Advoc* **3**(5), 40–41 (2000)
21. K.M. Alagappan, B. Deivasigamani, S.T. Somasundaram, S. Kumaran, Occurrence of *Vibrio parahaemolyticus* and its specific phages from shrimp ponds in East Coast of India. *Curr. Microbiol.* **61**, 235–240 (2010)
22. D. Rekha, P.K. Surendran, K. Chakraborty, Antibiotic resistance and plasmid profiling of *Vibrio parahaemolyticus* isolated from shrimp farms along the southwest coast of India. *World J. Microbiol. Biotechnol.* **25**, 2005–2012 (2009)
23. M. Saori, B. Raj, Effect of organic acids on shrimp pathogen, *Vibrio harveyi*. *Curr. Microbiol.* **63**, 1–7 (2011)
24. L. Yannick, P. Laurane, A. Dominique, H. Jose, W. Billy, L.R. Frederique, Pathotyping of vibrio isolates by multiplex PCR reveals a risk of virulent strain spreading in new caledonian shrimp farms. *Environ. Microbiol. J.* **63**, 127–138 (2012)

Assessment and Reduction of Carbon Footprint: An Approach via Best Management Practices in a Construction Site

Amirhossein Malakahmad, Nur Arinah Binti Hisham Albakri
and Nasir Shafiq

Abstract Global attention to carbon emissions that are perturbing the environment causing grievous global warming and associated consequences is turning to an individual's contribution or "carbon footprint". Carbon footprint is commonly expressed as the total amount of greenhouse gases (GHG) produced directly or indirectly as a result of an activity. It has become an indicator for sustainable development in numerous sectors including the construction industry. Several literatures studied the calculators estimating the carbon footprint of individual sectors. But, there are limited calculators for estimation of carbon footprint in construction activities. This paper presents assessment and reduction of carbon emission in a construction site via carbon calculator developed by the Environment Agency. The carbon calculator has been utilized to be fed by primary data collected from an actual construction activity dealing with demolition and reconstruction of building. Based on the outcomes from the calculator, the selection of appropriate Best Management Practices (BMPs) have been implemented to reduce the carbon emission in at the mentioned construction activity.

Keywords BMPs · Carbon calculator · Greenhouse gases · Construction industry

A. Malakahmad (✉) · N.A.B.H. Albakri · N. Shafiq
Civil Engineering Department, Universiti Teknologi PETRONAS,
31750 Tronoh, Perak, Malaysia
e-mail: amirhossein@petronas.com.my

N.A.B.H. Albakri
e-mail: arinah.albakri@gmail.com

N. Shafiq
e-mail: nasirshafiq@petronas.com.my

1 Introduction

The world has witnessed a dramatic increase in environmental concerns and issues related to global climate change over the past decade, and the consequences are highly associated with emissions of greenhouse gases (GHG). Due to that, it is agreed by industrialized nations to decrease their GHG emissions. Specifically, since construction operations are highly energy-intensive, they account for significant environmental impacts, including emission of GHG and other engine exhaust associated with material procurement or delivery and on-site construction activities [1]. Thus, all industries including the construction industry should join the efforts to reduce GHG emissions.

The role of construction sectors to improve the environmental performance of buildings and infrastructure is doubtless [2] and construction industries support environmental benefits both through daily job site practices and also lasting structural improvements. Construction industries can be considered as an important economic sector engaged in the preparation of land, repair of buildings and construction alterations [2].

On the other hand, construction industries contribute considerably to environmental footprint, especially in terms of GHG emissions and energy consumption. Extensive amounts of GHG are emitted from activities such as production, installation, maintenance, and end-of-life disposal of construction materials. Site preparation (land clearing and grubbing), earthmoving (grading, trenching, soil compaction, cut and fill operations including hauling of material), paving of roadway surfaces, the erection of buildings and structures, and the application of architectural coatings are among construction activities contribute to carbon emission [3]. Apart from that, some buildings may also entail the demolition of buildings prior to site preparation. All of which contribute to the implication of GHG emissions unless they are controlled and minimized by optimizing the utilization of construction resources. This could be achieved by adjusting the available construction crews and materials and minimizing construction cost and duration.

Carbon footprint is the result of total amount of GHG emissions produced by an organization, event, or product [4]. It serves as an assessment tool to measure the quantitative expression of GHG emissions from an activity. Consequently, it helps management of emission and evaluation of mitigation measures [5]. Similarly, by having a clear picture of quantified emissions, the important sources of emissions can be identified and therefore emission reductions and increasing efficiencies can be prioritized [6].

The objectives of this project are to reduce the amount of CO₂ (embodied carbon in tonnes) with the intervention of green innovation. The carbon footprint of the constructed model was assessed by proportional CO₂ calculations of a construction activities. The guidelines to reduce the emission have been identified by selecting the appropriate Best Management Practices (BMPs).

2 Definition of Key Terms

2.1 Greenhouse Gases

Based on Kyoto Protocol (KP) adopted in 1997, six types of GHGs were defined, namely Carbon dioxide (CO₂), Methane (CH₄), Nitrous oxide (N₂O), Hydrofluorocarbons (HCFs), Perfluorocarbons (PFCs) and Sulphur hexafluoride (SF₆), all of which are related to global warming potentials which must be reduced. However, the most abundant GHGs in the atmosphere are water vapor (H₂O), CO₂, CH₄, N₂O and ozone (O₃) [7]. These gases absorb some of the energy being radiated from the surface of the Earth and trap it in the atmosphere, essentially acting like a blanket that makes the Earth's surface warmer than it would be otherwise [8].

Of all the GHGs, CO₂ has the largest share, forming around 77 % of total GHGs [8]. Hence, emissions of other GHGs are converted in units of CO₂ equivalent (CO₂e), using the warming potential related to each gas [9]. Global Warming Potential (GWP) which was developed by Intergovernmental Panel on Climate Change (IPCC) is a concept to compare the potential of each greenhouse gas to trap heat in the atmosphere relative to another gas. Likewise, IPCC defines the GWP of a greenhouse gas as the ratio of the time-integrated radiative forcing from the instantaneous release of 1 kg of a trace substance relative to that 1 kg of a reference gas [10]. Direct radiative effects occur when the gas itself is a GHG. Since the reference gas used is CO₂, thus GWP-weighted emissions are measured in CO₂e.

2.2 CO₂ Emission

Carbon dioxide is known as the main gas within the context of GHG emissions. CO₂ is also the most abundant gas in the atmosphere and has a high calorific power [11]. CO₂ also is the primary GHG that is contributing to current climate change. As part of the carbon cycle, CO₂ is absorbed and emitted naturally through animals and plants respiration, volcanic eruptions, and ocean-atmosphere exchange. In addition to that, human activities including diversion of land uses and burning of fossil fuels resulted in release of large amounts of carbon and CO₂ concentrations rise in the atmosphere.

Construction activities as a whole, ranked the third highest contributing industrial sector for GHG emissions (just behind the oil and gas and the chemical manufacturing sectors) by producing 8 % of total GHG emissions [8]. This is due to significant consumption of energy and generating considerable levels of CO₂ and other diesel exhaust emissions [1].

Besides that, the atmospheric lifetime of a gas is another key factor in GHG emission. It is defined as the period of time a mass of particular gas remains in the atmosphere before removing by chemical reaction [11].

2.3 Carbon Footprint

The term “carbon footprint” can be traced back to as a subset of “ecological footprint” [12]. According to Pandey et al. [6] ecological footprint refers to the biologically productive land and sea area required to sustain a given human population expressed as global hectares. Therefore, based on this concept, carbon footprint refers to the land area required to absorb the entire CO₂ produced by the mankind during its lifetime. Furthermore, the concept began to be publicized independently, referring to the impact of human activities on the environment and especially on the climatic conditions, in terms of GHG emissions; or briefly called “carbon emissions” [9]. In other words, carbon footprint is a measure of an individual’s contribution to global warming in terms of GHG amount produced by an individual [13]. Carbon footprint as the total amount of GHGs emissions is resulted in directly or indirectly by an activity, organization and event or is accumulated over the life stages of a product [14]. Other terms used associated or sometimes as a synonym of carbon footprint are embodied carbon, carbon content, embedded carbon, carbon flows, virtual carbon, GHG footprint as well as climate footprint [6].

It is good to know that, with growing awareness on climate change, a remarkable responsibility over the emissions of GHG has grown not only among the industrialist, but in individuals as well. This led to the surge of personal carbon footprinting facilities (consultancies and online calculators) particularly in developed countries [15]. Similarly, many websites have been formed for calculation of an individual’s carbon footprint, or estimate the carbon dioxide emissions a person is responsible for over a given period of time [16].

Therefore, carbon footprint calculation assists as a valuation tool in terms of GHG emissions and serves to control and lessen these emissions. Its detailing helps to identify weaknesses such as areas of high emissions that can be eliminated or improved upon calculating the carbon footprint. Thus, carbon footprint is an indicator of sustainable development.

2.4 Carbon Calculators

Numerous methods and models for calculating carbon footprint have been developed globally. Among those are Life Cycle Assessment (LCA); Process Analysis (PA) and Environmental Input-Output Analysis (EIO) [14]. The methods for carbon footprint calculations are still developing and it is emerging as an important tool for GHG management. The concept of carbon footprinting has infused and is being commercialized in all areas of life and economy. Similarly, calculators that estimate an individual’s CO₂ emissions have become more prevalent. However, there is little consistency in definitions and calculations of carbon footprints among the studies. Since carbon footprinting is proposed to be a tool to guide associated emission cuts, its standardization at international level is required [6].

Carbon calculators commonly work by accepting user inputs characteristic of individual behavior and by returning an amount of CO₂ emitted as a direct result of such behavior in the form of a user's carbon footprint [16].

Most of carbon calculators require users to input data manually. This makes the calculations less accurate and causes poor user experience [4]. The recent rise in carbon calculators has been accompanied, however, by variation in output values given similar inputs for individual behavior. The disparity in outputs may be due to different calculating methodologies or conversion factors. In addition, most of calculators claim to be based on recommended guidelines, but rarely any two of them yield similar outputs for the same set of inputs [15]. In an individual study, values can vary as much as several metric tons per annum per activity [16]. These variations in output could influence both the types of steps individuals take and the overall level of effort.

Moreover, carbon calculators use quantitative models to estimate carbon emissions caused by user's activities. These calculators are provided by government agencies, non-governmental organizations, and private companies. Some of these carbon calculator providers also promote methods for mitigating CO₂ emissions through offsets or investments in renewable energy technology. Although they can promote public awareness regarding carbon emission due to individual's behavior, there are concerns about the accuracy and credibility of these existing CO₂ calculators as they are static and fail to take into account the dynamic behavior of human nature [4].

In addition, Carbon calculators reveal lack of uniformity [16]. Similarly, there are no standards or codes of practice associated among carbon calculators, thus, leading to potentially significant differences and inconsistencies between them [15]. Therefore, it creates a gap between its definition and its application in practice.

To overcome this issue, three elements for the selection of appropriate carbon calculators based on the suitability of its uses in respective industries are suggested [15]. These elements are:

- (i) *Complexity and relevance*. The selected model needs to include as many sources of CO₂ as possible in relating to the construction activities. The calculation methods are construction activities oriented rather than business oriented.
- (ii) *Reliability*. The model has to be developed by an expert team or organization with resourceful references.
- (iii) *Recommendation*. The selected model is recommended or developed by a Government Department, State Energy or Environmental Agency.

In the given case study, the main objective is to evaluate the reduction path in carbon footprint of a constructed model by proportional carbon emission calculations through assessment of greenhouse gases impacts from construction activities in terms of CO₂ emissions using carbon calculation and suggestion of appropriate Best Management Practices (BMPs) to be implemented in construction site.

3 Procedures and Techniques

The research procedures are divided into two sections based on reduction path of carbon footprint in a specified construction activity and offering of a conceptual approach to minimize the carbon footprint via BMPs. Figure 1 depicts the methods of carbon footprint calculations based on the carbon calculator developed by the Environment Agency. It describes the step-by-step procedure in attaining the overall carbon footprint of a project.

4 Findings

A project of demolition of an old office building that was then renovated to a new laboratory located in Selangor state, Malaysia, was selected as the focus of this

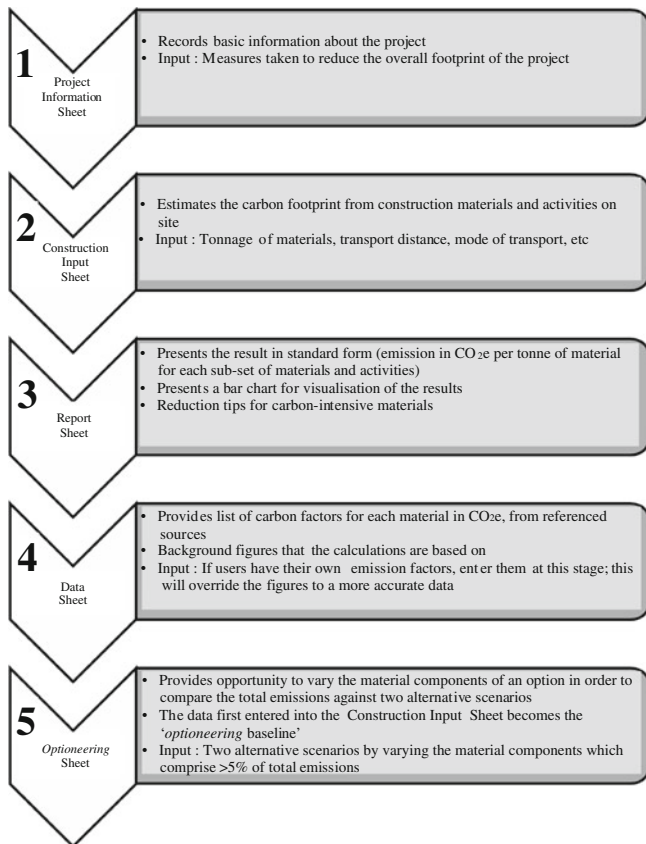


Fig. 1 Methodology of carbon footprint calculation

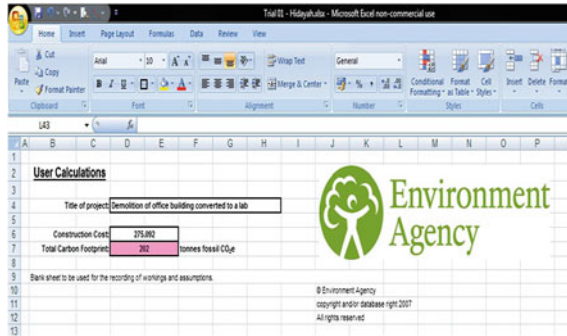


Fig. 2 Screenshot of the total carbon footprint of the project

research. All the data collected during construction stage was then input into the software which returned a total carbon footprint of 202 tCO₂e for the whole project. However, it was noted that some inputs were not included due to limited access of the data. Figure 2 depicts the screenshot of the end result of the total carbon footprint for the said project.

After the acquired data was included into the software, the result can be obtained in the *Report Sheet*. This *Report Sheet* presented the result in standard form. The distribution of the total carbon emission in tons of carbon dioxide equivalence and its percentage is tabulated in Table 1 while Fig. 3 represents the result visually.

From the results obtained, the major contributor of carbon emission was the final stage of construction which is the finishing, coatings and adhesives, with 108.8 tCO₂e contributing more than half of the total carbon footprint of the project with 54 %. Epoxide resin paint was used extensively for the finishing of the floors and painting of steelworks surfaces.

In general, epoxides are known for their excellent adhesion, chemical and heat resistance and dries quickly providing a tough, protective coating with excellent hardness and durable surfaces [17]. Their low volatility and water cleanup makes them useful to be used in laboratories. Though epoxide paint doubled the carbon footprint in the aesthetic value as compared to its counterpart such as waterborne paint which is a more ‘greener’ option—its material compatibility is unsuitable to be used in floorings of laboratories, thus making epoxide resin paint to be selected and used throughout the project as depicted in Fig. 4.

Apart from that, the usage of plastics emitted 42.0 tCO₂e and contributed 21 % of the overall carbon footprint. Polyvinyl chloride (PVC) pipes were used as the rain water down pipe (RWDP) in the gutter system. A ‘greener’ option to reduce the carbon footprint of plastics would be the usage of High Density Polyethylene (HDPE) pipes.

Table 1 The percentage distribution of total carbon emission

Sub-totals	%
Quarried material	9
Timber	0
Concrete, mortars and cement	4
Metals	3
Plastics	21
Glass	9
Miscellaneous	0
Finishing, coatings and adhesives	54
Plant and equipment emissions	0
Waste removal	0
Portable site accommodation	0
Material transport	0
Personnel travel	0

HDPE has demonstrated its effectiveness through its durability, leak-free performance, corrosion resistance, and ductility [18]. Its greater resilience and flexibility make it less susceptible than PVC to surges, damages from digging, and shifting soils during earthquakes.

Besides that, glass and quarried material contributed an equal percentage of its own with 9 % of the total carbon footprint for the whole project. Primary glass was used to construct explosion proof glass windows with clear visibility including reinforcement with all necessary connection to glass wall which emitted 18.2 tCO₂e. On the other hand, 17.3 tCO₂e came from quarried material such as bricks. Bricks walls were constructed for partitions in the laboratory and the gas compressor house as depicted in Figs. 5 and 6.

Meanwhile, concrete, mortars and cement emitted 8.1 tCO₂e which contributed 4 % of the overall carbon footprint of the project. Reinforced concrete G25 was used as the ground floor slab and ramp for the gas compressor house. Mortar of 1:½:4½ cement:lime:sand mix and ordinary Portland cement were used throughout the construction stage. Furthermore, the usage of metals emitted 6.5 tCO₂e which is equivalent to 3 % of the whole project's carbon footprint. Stainless steel was used as the gas compressor house roof and its metal grille panel. In order to minimize the carbon footprint for metals, recycled steel can be used instead, provided it is still in good condition.

In addition, the metal section emitted more carbon footprint than the recorded footprint. Aluminium was used in the compressor house louvers doors, metal decks to cover the cement bricks and glass frames. However, due to limited access of the data input, aluminium was excluded in the overall assessment of carbon footprint of the project.

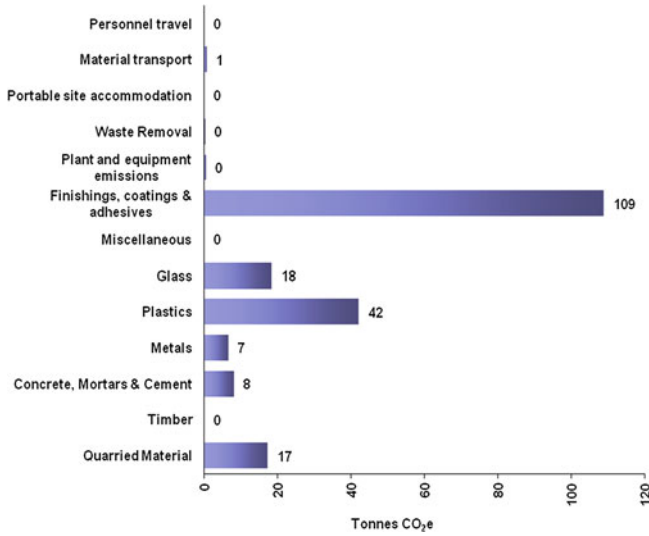


Fig. 3 The visual distribution of total carbon emission in tCO₂e



Fig. 4 Epoxide resin paint used as finishing for the laboratory’s floorings

On the other hand, material transport, plant and equipment emission, and waste removal are amongst the least contributor in the total carbon footprint of the project with only 0.6 tCO₂e, 0.4 tCO₂e and 0.2 tCO₂e respectively. Hence, these values are negligible. In a nutshell, the carbon footprint of the demolition of an old office building that was then renovated to a new laboratory was analyzed and assessed by the carbon calculator developed by the Environment Agency and a set of guidelines based on Best Management Practices (BMP) were established (Table 2) to be practiced at the construction site.

Fig. 5 Construction of brick walls



Fig. 6 Pouring of G25 concrete to gas compressor house ground floor slab



5 Conclusion

It has been found that a total carbon footprint of 202 tCO₂e was produced for changing of an old office building to a laboratory. Based on the provided information from the project consultant, finishing, coating and usage of adhesives had the highest contribution in total CO₂ emission. This was followed by use of plastics, glass and quarried materials. If full access to project information was possible, the carbon emission contribution from some activities such as miscellaneous, personnel travel and material transport could be higher than those have been reported in this study.

Table 2 Guidelines based on BMP

Element	Guidelines (BMP)	Reference
Finishing, coatings and adhesives	<ul style="list-style-type: none"> • Ventilate the working area to prevent accumulation of flammable or noxious fumes • All paints, thinners, chemicals, resins, etc. must be kept in their original containers with product labels in place and disposed of accordingly to prevent contamination to the environment 	[19]
Concrete curing	<ul style="list-style-type: none"> • Protect drain inlets prior to application of cure. Avoid over-spraying cure, allowing it to become airborne • Ensure cure water does not flow to inlets or watercourses but rather to collection areas for infiltration or other means of removal • Ensure that cure is stored, handled, and used properly. Ensure the cure containers are leak-free and spray nozzles are clean 	[20]
Stockpile management	<ul style="list-style-type: none"> • Install temporary barriers (berms, dikes, silt fences, straw bales or sandbag barriers) around stockpile perimeters to prevent contact with storm water when required • During rainy season, cover inactive soil stockpiles or protect them with soil stabilization at all times • During non-rainy season, cover inactive soil stockpiles or protect them with linear barriers prior to rain events 	
Solid waste management	<ul style="list-style-type: none"> • Solid waste storage areas should be located in an area with little potential for flooding and at least 15 m from drainage facilities and receiving waters. During foul weather, waste should be stored in watertight dumpsters or securely covered. Salvage or recycle waste as appropriate • Provide adequate trash receptacles in the yard, field trailer areas, and resting areas for workers. Do not place litter receptacles near drainage inlets or receiving waters. All litter within the construction site is to be collected weekly, regardless of the litter's origin • Provide an adequate number of watertight dumpsters to collect the anticipated volume of construction waste. Plan for additional dumpsters and dumpster pickups during demolition phases. Full dumpsters are to be removed from the site and disposed of outside the highway right-of-way • Separate potentially hazardous waste from non-hazardous waste. Do not dispose of toxic liquid wastes in dumpsters designated for construction wastes. Dispose of hazardous wastes accordingly 	

Acknowledgments The authors are thankful to the Ministry of Education, Malaysia for providing fund for this research via Malaysia Research Assessment grant scheme (MyRA 0153AB-J13).

References

1. C.R. Ahn, P. Lewis, M. Golparvar-Fard, S. Lee, Integrated framework for estimating, benchmarking, and monitoring pollutant emissions of construction operations. *J. Constr. Eng. Manag.* **139**, A4013003 (2013)
2. United States Environmental Protection Agency (USEPA), Potential for reducing greenhouse gas emissions in the construction sector [Online] (2009), Available: <http://www.epa.gov/sectors/pdf/construction-sector-report.pdf>
3. Sacramento Metropolitan Air Quality Management District, Construction-Generated Criteria Air Pollutant and Precursor Emissions [Online] (2013), Available: <http://www.airquality.org/ceqa/cequguideupdate/Ch3Construction-GeneratedCAPsFINAL.pdf>
4. F. Rahman, C. O'Brien, S.I. Ahamed, H. Zhang, L. Liu, Design and implementation of an open framework for ubiquitous carbon footprint calculator applications. *Sustain. Comput. Inform. Sys.* **1**, 257–274 (2011)
5. Carbon Trust, Carbon footprinting [Online] (2012), Available: http://www.carbontrust.com/media/44869/j7912_ctv043_carbon_footprinting_aw_interactive.pdf
6. D. Pandey, M. Agrawal, J.S. Pandey, Carbon footprint: current methods of estimation. *Environ. Monit. Assess.* **178**, 135–160 (2011)
7. S.-J. Lee, I.-S. Ryu, B.-M. Kim, S.-H. Moon, A review of the current application of N₂O emission reduction in CDM projects. *Int. J. Greenhouse Gas Control* **5**(1), 167–176 (2011)
8. United States Environmental Protection Agency (USEPA), Causes of climate change [Online] (2013). Available: <http://www.epa.gov/climatechange/science/causes.html>
9. A.L. Radu, M.A. Scricciu, D.M. Caracota, Carbon footprint analysis: towards a projects evaluation model for promoting sustainable development. *Procedia Econ. Finance* **6**, 353–363 (2013)
10. Intergovernmental Panel on Climate Change (IPCC), *Climate Change 2001: The Scientific Basis*. (Cambridge University Press, Cambridge, 2001)
11. S.E. Hosseini, M.A. Wahid, N. Aghili, The scenario of greenhouse gases reduction in Malaysia. *Renew. Sustain. Energ. Rev.* **28**, 400–409 (2013)
12. M. Wackernagel, W.E. Rees, *Our Ecological Footprint: Reducing Human Impact on the Earth* (New Society Publishers, Gabriola Island, 1996)
13. M. Lynas, *Carbon Counter* (Happer Collins Publishers, Glasgow, 2007)
14. T. Wiedmann, J. Minx, A definition of carbon footprint. *Ecol. Econ. Res. Trends* **1**, 1–11 (2008)
15. T. Kenny, N.F. Gray, Comparative performance of six carbon footprint models for use in Ireland. *Environ. Impact Assess. Rev.* **29**, 1–6 (2009)
16. J.P. Padgett, A.C. Steinemann, J.H. Clarke, M.P. Vandenbergh, A comparison of carbon calculators. *Environ. Impact Assess. Rev.* **28**, 106–115 (2008)
17. Advanced Environmental Services Inc., Benefits of using an epoxy floor coating product [Online] (n.d.). Available: <http://www.epoxyflooringandconcretestain.com/benefits-of-epoxy-floor-coating.html>
18. Build It Green, HDPE (High Density Polyethylene) pipe [Online] (2006). Available: <http://www.builditgreen.org/attachments/wysiwyg/22/HDPE-Pipe.pdf>
19. Sacramento Marina, Best Management Practices (BMP) [Online] (n.d.). Available: http://www.cityofsacramento.org/ccl/sacmarina/pdf/news/SacMarina_BMPs.pdf
20. State of California Department of Transportation, Construction Site Best Management Practices (BMP) field manual and troubleshooting guide [Online] (2003). Available: http://www.dot.ca.gov/hq/construc/stormwater/BMP_Field_Master_FullSize_Final-Jan03.pdf

Effect of Kenaf Water Retting Process by *Bacillus Macerans* ATCC 843 on the pH of Retting Water

Mohd Nazrin Othman, Ramlah Mohd Tajuddin and Zakiah Ahmad

Abstract pH plays a very critical role in kenaf retting process. The aim of this study was to observe the changes in the pH of the retting water with and without the use of *Bacillus macerans* ATCC 843. The duration for retting period was set to one week. The changes of pH was taken daily in both tank. Both of the reading was then compared.

Keywords Kenaf · Water retting · *Bacillus macerans* · pH

1 Introduction

Kenaf (*Hibiscus cannabinus* L.) is one of multi-purpose plant that has gained popularity recently. Kenaf has been used as cordage crops and as livestock feed for more than 6000 years [1]. In the water retting process, kenaf stalks were cut and either tied in bundles with the bark still attached to the stalk or the bark was removed completely and tied together [2]. The kenaf bundles were then placed in ponds, slow moving streams or tanks to allow the degradation process to take effect. Water retting

Universiti Teknologi MARA (600-RMI/DANA 5/3/RIF (776/2012)).

M.N. Othman
Faculty of Civil Engineering, UiTM, Shah Alam, Malaysia
e-mail: nazrinoh88@yahoo.com

R. Mohd Tajuddin (✉)
Faculty of Civil Engineering, Universiti Teknologi MARA UiTM, Shah Alam, Selangor, Malaysia
e-mail: ramlah160@salam.uitm.edu.my; ramlah2007@gmail.com

Z. Ahmad
Institute for Infrastructure and Sustainable Engineering Management, Faculty of Civil Engineering, UiTM, Shah Alam, Malaysia
e-mail: zakiah@salam.uitm.edu.my

process is actually a biochemical process of decomposing biopolymers such as hemicelluloses, pectin and mucilaginous substances that hold the bast fiber to the plant stem [3]. Biological retting was known to be the cheapest, cost-effective, and universally practiced method for the commercial extraction of kenaf fibers [4].

Water retting process was used mainly to degrade substance called pectin. Pectin is the main cementing agent in plant which composed of a heteropolysaccharide made of α -1, 4 linked galacturonate chains with a high percentage of methyl esterification [5]. During microbiological retting, the depolymerization of pectin is operated by an enzyme called pectinases, which primarily comprising a mixture of 4 enzymatic activities: Polygalacturonase (PG), pectin lyase (PL), pectate lyase, and pectin esterase [5]. However, PG [6] and PNL [7] are the primary retting enzymes. Pectic enzymes are produced by many groups and species of microorganisms [8].

Bacillus sp was known as plant pathogen which secretes pectinolytic enzymes. Previous study showed that large numbers of Firmicutes bacteria of the genus *Bacillus* have been isolated from retting water [9]. Previous study also showed that PG activities produced by *Bacillus* sp strains were higher than those produced by *Aspergillus niger* [10], *Aspergillus* sp and *A. niger* ATCC20107 [11], *Aureobasidium pullulans* [12] and *Tubercularia vulgaris* [13]. Thus, *Bacillus* sp was able to reduce the time taken for retting.

Although many researches had been done with kenaf, most of them were regarding the strength of kenaf fiber and the use of kenaf fiber as building materials. There was so little information regarding the quality of water after kenaf water retting process. Thus, this paper was dedicated to study the impact of water retting process on water bodies especially pH changes.

2 Method

2.1 Media Preparation

Bacillus macerans ATCC843 was bought from Next Gene. The *B. macerans* ATCC843 was first activated for 24 h before starting the lab works. 500 ml of Luria-Bertani (LB) broth, Miller (AMRESCO) was prepared. The *B. macerans* was aseptically transferred into the LB nutrient broth. The LB broth containing *B. macerans* was put in the incubator with shaker. The shaker was set at 120 rpm and the *B. macerans* was incubated for a week at room temperature.

2.2 Retting Tank and pH Measurement

Two retting tank measuring 42 cm \times 24.5 cm \times 30 cm was used in the retting process. The fresh kenaf plant was obtained from National Kenaf and Tobacco Board (LKTN). The stalk of kenaf was measured up to 40 cm before it was cut. The

kenaf weight for each tank was ± 1.250 kg. 24.5 L and 500 mL of nutrient broth containing *B. macerans* ATCC843 was added on one tank and 25 L of tap water was added into the other tank. The kenaf stalk was immersed and retted for a week. The pH was checked using HORIBA Water Checker U-10, Type 440–220, HORIBA Ltd. The readings were then recorded.

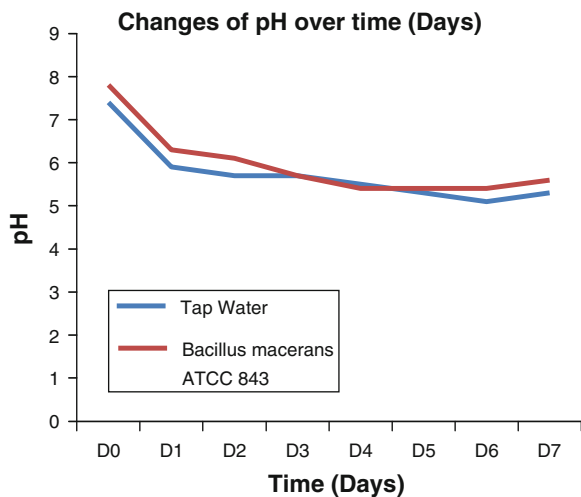
3 Result and Discussion

The recordings showed that there were changes in pH in both tanks during water retting period. Table 1 showed the reading of pH during one week of water retting. From the table, we can see that the pH of water in both retting tank decreasing during the retting period. After 24 h of retting, the pH decreased by 20.27 % for tap water and 19.23 % for *B. macerans* ATCC843 seeded water. From Day 1 to 2, the pH drops by 3.39 % for tap water and 3.17 % for *B. macerans* ATCC843 seeded water. From the Day 2 to 3 the pH remain unchanged for tap water and the pH decreased by 6.56 % for *B. macerans* ATCC843 seeded water. From Day 3 to 4 the pH started to drop by 3.51 % for tap water and 5.26 % in *B. macerans* ATCC843 seeded water. From Day 4 to 6 the pH remained unchanged in *B. macerans* ATCC843 seeded water while the pH drop by 3.64 % from Day 4 to 5 and 3.77 % from Day 5 to 6 for tap water. From Day 6 to 7 the pH increased in both tank by

Table 1 Data of pH in both tanks during the retting period

Water type	Day								
	D0	D1	D2	D3	D4	D5	D6	D7	
Tap water	7.4	5.9	5.7	5.7	5.5	5.3	5.1	5.3	
Tap water + <i>Bacillus macerans</i> ATCC843	7.8	6.3	6.1	5.7	5.4	5.4	5.4	5.6	

Fig. 1 Changes of pH for tap water and *B. macerans* ATCC843 seeded water during retting period



3.92 % for tap water and 3.7 % for *B. macerans* ATCC843 seeded water. The trends of the changes can be seen clearly in Fig. 1.

The reason behind the decreased of pH was caused by the activity of pectinolytic enzyme known as Exo-PGases which produce digalacturonic acid as the main end product of digestion [14, 15]. The production, activity, and stability of the enzymes are dependent on different carbon sources and pH [16]. In the experiment done on certain *Bacillus* sp isolated from jute retting water showed most of PG activities have maximum activity at pH 8.0 and some of it at pH 5.0 [17]. From the data it showed that the drop of pH in tap water was huge compare to *B. macerans* ATCC843 seeded water after 24 h of retting. By the time the retting end, the pH of tap water was lower than pH in *B. macerans* ATCC843 seeded water. This suggested that the natural flora on kenaf itself may produce an even more effective pectinolytic enzyme. However, the microorganism that live on the kenaf are yet to be known [4]. As showed in Fig. 1, there were not much different in the pH between tap water and *B. macerans* ATCC843 seeded water. In term of enzymology, a slight change of pH can determine the efficiency of the enzyme as the enzyme could have its conformation changed or denature at different pH [4].

4 Conclusion

The pH of water become acidic in retting process regardless the types of water used. The pH in tap water drop faster than the pH in *B. macerans* ATCC843 seeded water. Further study on optimum pH for kenaf water retting process is highly suggested.

Acknowledgment This research was financially supported by the Universiti Teknologi MARA, Malaysia (600-RMI/DANA 5/3/RIF (776/2012) is thankfully acknowledged.

References

1. J.M. Dempsey, *Fiber Crops* (The University Presses of Florida, Gainesville, 1975)
2. C.L Webber III, V.K Bledsoe, in *Kenaf Yield Components and Plant Composition*, ed. by J. Janick and A Whipkey. Reprinted from Trends in new Crops and New Uses (ASHS Press, Alexandria, 2002), pp. 348–357
3. M.S. Haque, A. Zakaria, K.B. Adhir et al. Identification of *Micrococcus* sp. responsible for the acceleration of jute retting. *Pak. J. Biol. Sci.* **6**, 686–687 (2003)
4. O.M. Nazrin, R.M. Tajuddin, Z. Ahmad, Effect of kenaf water retting process by *Bacillus cereus* on pH of retting water. *Adv. Mater. Res.* **905**, 339–342 (2014)
5. D.A.S. Biwaspriya, Ashis Chakraborty, Sagarmoy Ghosh, Kalyan Chakrabarti, Studies on the effect of pH and carbon sources on enzyme activities on some pectinolytic bacteria isolated from jute retting water. *Turk J. Biol* **35**, 671–678 (2011)
6. J. Zhang, G. Henriksson, G. Johansson, Polygalacturonase is the key component in enzymatic retting of flax. *J. Biotechnol* **81**, 85–89 (2000)

7. M. Soriano, P. Diaz, F.I.J. Pastor, Pectinolytic systems of two aerobic sporogenous bacterial strains with high activity on pectin. *Curr. Microbiol.* **50**, 114–118 (2005)
8. M.M.C.N. Soares, R. Da Silva, E.C. Carmona, E. Gomes, Pectinolytic enzyme production by *Bacillus* species and their potential application on juice extraction. *World J. Microbiol. Biotechnol.* **17**, 79–82 (2001)
9. Z. Ahmed, F. Akhter, Jute retting :an overview. *Online J. Biol. Sci.* **1**, 685–688 (2001)
10. E.F. Ss Pereira, G.V.Gonzales Torres, M.G. Rojas, Effect of different carbon sources on synthesis of pectinase by *Aspergillus niger* in submerged and solid fermentations. *Appl. Microbiol. Biotechnol.* **39**, 36–41 (1993)
11. G. Larios, J.M. Garcia, C. Huiton, Endopolygalacturonase production from untreated lemon peel by *Aspergillus* sp CH-Y-1043. *Biotechnol. Lett.* **11**, 729–734 (1989)
12. F. Federici, M. Petruccioli, Growth and polygalacturonase production by *Aureobasidium pullulans* on orange peel waste. *Microb. Alim. Nutri* **3**, 39–46 (1885)
13. M.J.V. Fonseca, S. Said, The pectinase produced by *Tubercularia vulgaris* in submerged culture using pectin or orange-pulp pellets as inductor. *Appl. Microbiol. Biotechnol.* **42**, 32–35 (1995)
14. T. Sakai, T. Sakamoto, J. Hallaert, E.J. Vandamme, Pectin, pectinase and protopectinase: production, properties and applications. *Adv. Appl. Microbiol.* **39**, 231–294 (1993)
15. R.S. Jayani, S. Saxena, R. Gupta, Microbial pectinolytic enzyme: a review. *Process Biochem.* **40**, 2931–2944 (2005)
16. D. Voet, J.G. Voet, *In: Biochemistry*, 2nd edn. (Wiley, New York, 1995), pp. 360–362
17. D.A.S. Biwaspriya, C. Ashis, G. Sagarmoy, C. Kaylan, Studies on the effect of pH and carbon sources on enzyme activities of some pectinolytic bacteria isolated from jute retting water. *Turk. J. Biol.* **35**, 671–678 (2011)

Pollutants Removal in Storm Water Pond

Z. Mohd-Zaki, N. Manan, A. Amir and A. Baki

Abstract Storm water ponds are a common feature of the urban landscape in many countries with storm water management. Built to control the impacts of urbanisation in the form of increased runoff flows, volumes and pollution loads, storm water ponds are exposed to strong anthropogenic pressures. This paper presents the ability of storm water pond to self-purify the runoff water. In this study, selected chemical parameters (pH, BOD₅, COD, zinc and lead) and physical parameters (turbidity, colour and suspended solid) of the inlet and outlet runoff waters were measured. From this study, the percentage of reduction in BOD₅, COD, zinc and lead were 15, 16, 15 and 8 % respectively. The percentage of reduction in turbidity, colour and suspended solid was 11, 19 and 11 % respectively. Storm water pond has a greater capacity to remove soluble nutrients and biochemical compounds from storm water runoff. Overall, storm water pond has the ability to purify water contained.

Keywords Runoff · Storm water pond · Chemical parameters · Physical parameters · Pollutants

1 Introduction

Most in urban area, rainwater that cannot percolate into the ground will flow on the surface and then create a surface runoff, which flows directly into surface or is channeled into storm drains. This kind of water cycle is repeated and if not taken care of, it will cause an extreme event such as flash flood. A study conducted by

Z. Mohd-Zaki (✉) · N. Manan · A. Amir
Faculty of Civil Engineering, Universiti Teknologi MARA, 40450 Shah Alam,
Selangor Darul Ehsan, Malaysia
e-mail: cezuhaida@salam.uitm.edu.my

A. Baki
Department of Civil Engineering, University of Tabuk, 71491 Tabuk,
Kingdom of Saudi Arabia

Gromaire-Mert et al. [1] has shown that traditional drainage system seems inadequate and too expensive to manage wet weather flows and it has become essential to intrude the urban runoff cycle to reduce the runoff volume.

Storm water ponds have been used for decades to mitigate the increase of runoff rates that is typical consequences of urbanization. This is done by detaining storm water runoff for a period of hours or days, while releasing it slowly to receiving streams and lakes. Although designed primarily for control of water quantity increase, these ponds are now also being used to reduce pollution [2].

Urban storm water runoff has been identified as a significant source of pollution for many water bodies. Washing off road surfaces, parking area, vehicles, building materials and surface runoff contain a broad spectrum of pollutants. These pollutants lead to adverse effect on receiving waters include oxygen depletion, eutrophication and toxicity. Heaney [3] reported that storm water runoff has become a major problem as it contains high levels of many pollutants including suspended solids and heavy metals. Hence, to improve the quality of urban runoff before discharge, some method of treatment is required. Several studies have documented that storm water ponds effectively removed suspended solids, heavy metals, soluble nutrients and biochemical compounds from storm water runoff [4, 5].

This paper presents the ability of storm water pond to remove pollutants from storm water runoff. Selected chemical parameters (BOD₅, COD, zinc and lead) and physical parameters (total suspended solids, turbidity and colour) were measured at the inlet and outlet of a storm water pond. Pollutants removed by storm water pond were calculated based on the pollutants reduced at the outlet from the initial concentration at the inlet.

2 Materials and Methods

2.1 Collection of Samples

The study area for this project was at Tasek Seksyen 2, Shah Alam. Samples were taken at the inlet and outlet of the storm water pond. Three (3) samples (at different day) were taken at each inlet and outlet with an approximate of 1500 mL of each sample. Grab sampling method was used to take the samples. The duration for collecting the sample was about a day and was measured for average values with 3 replicates. The samples were transported immediately to the laboratory for analysis.

2.2 Sample Analysis

All the samples were tested in the Environmental Laboratory, Faculty of Civil Engineering, UiTM. The laboratory tests were Biological Oxygen Demand (BOD), Chemical Oxygen Demand (COD), zinc, lead, Total Suspended Solids (TSS),

turbidity and colour. BOD test is conducted to measure the dissolved oxygen for the samples. COD test is conducted to estimate the amount of organic matter in waste water. All tests were conducted using the standard method [6].

3 Results and Discussions

Figure 1 indicates the removal of chemical characteristics in the storm water runoff. The error bars indicate 95 % confidence in mean values for three replicates of sample measurement. Removals were 14 and 15 % for BOD₅ and COD respectively. Removal efficiency for zinc and lead were recorded at 15 and 8 % respectively. The presence of zinc and lead may due to the nearby commercial area.

Figure 2 indicates the removal efficiency for physical characteristics namely turbidity, colour and total suspended solids. The error bars indicate 95 % confidence in mean values for three replicates of sample measurement. Storm water pond was able to remove 11 % turbidity, 19 % colour and 12 % total suspended solids.

Based on the result from both physical and chemical characteristics, storm water pond was likely to be favourable for the removal of soluble nutrients and

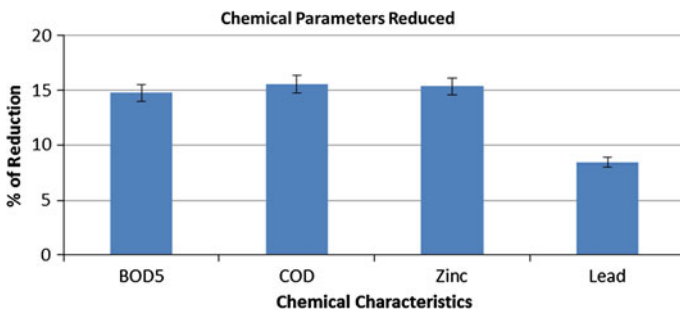


Fig. 1 Reduction of chemical parameters in storm water runoff

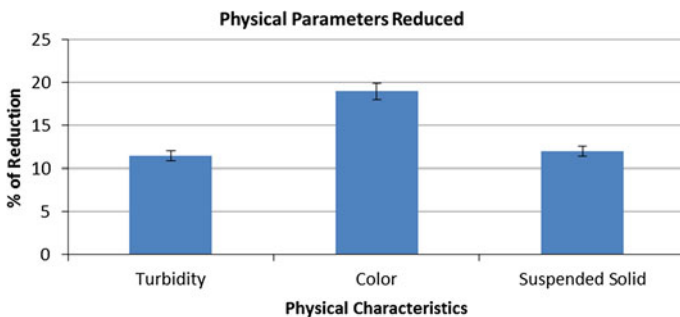


Fig. 2 Reduction of physical parameters in storm water runoff

biochemical compounds from storm water runoff. As the storm water pond is an earth-pond (not cemented and no lining), biological process may occur in the pond. Although no direct measurement of microbial population was conducted in this study, the presence of living organisms such as fish, tortoise and frog were observed in the pond. The soluble nutrients and biochemical compounds may be degraded by the small living organisms that presence in the pond as their food supply. Thus, the declining of nutrient levels is positively correlated to species richness of microorganisms in pond [7]. Leibold [7] stated that the absorption by soil or sediment at the bottom of the pond may also contribute to removal of dissolved nutrients.

Comings et al. [8] discussed that removal efficiency is related to the 'age' of the pond. A relatively new pond tends to remove soluble nutrient with its 'clean' sediment. Clean sediment has a greater capacity to absorb soluble nutrients than older sediment [9].

4 Conclusion

From this study, it can be concluded that the storm water pond in Tasek Seksyen 2, Shah Alam has the ability to remove pollutants in the storm water runoff. All selected parameters measured in this study were observed to have reduction. This obviously can be seen from the result section that all selected parameters have shown minimum of 8 % reduction (in lead) and maximum of 19 % reduction that monitored in colour. More parameter (as such listed in Malaysia Water Quality Standard) may be included in further observation. Further investigation on factors affecting the removal rate e.g. retention time, runoff flow rate may help to understand better the capability of storm water pond to remove pollutants.

References

1. M.C. Gromaire-Mert, S. Garraud, A. Gonzalez, G. Chebbo, Characterisation of Urban runoff pollution in Paris. *Water Sci. Technol.* **39**, 1–8 (1999)
2. W. Wipple Jr, Dual-purposes detention basins. *J. Water Resour. Plann. Manag. Div. ASCE* **105** (2), 403–412 (1979)
3. J.P. Heany, Research needs in urban storm water pollution. *J Water Resour. Plann. Manag. Div. ASCE* **112**(1), 403–412 (1986)
4. R.H. McCuen, S.G. Walesh, W.J. Rawls, *Control of Urban Storm Water Runoff by Detention and Retention* (USDA, ARS, Washington, 1983) Misc. Publ. no 1428
5. T. O'Connor, J. Rossi, Monitoring of a Retention Pond Before and After Maintenance World Environmental and Water Resources Congress 2006 (United States American Society of Civil Engineers, Omaha, 2006), pp. 1–11
6. APHA, *Standard methods for the examination of water and wastewater*, 20th edn. (American Public Health Association, Washington DC, 1998)
7. M.A. Leibold, Biodiversity and nutrient enrichment in pond plankton communities. *Evol. Ecol. Res.* **1**, 73–95 (1999)

8. K.J. Comings, D.B. Booth, R.R. Horner, Storm water pollutant removal by two wet ponds in Bellevue. Washington. J. Environ. Eng. **126**(4), 321–330 (2000)
9. A.E. Maristany, Long-term performance of wet detention ponds, in Proceedings of the 20th Anniversary Conference Water. Management in '90s: A Time for Innovation (ASCE, New York, 1993) pp. 138–141

Removal of Nitrate by *Eichhornia crassipes* sp. in Landfill Leachate

N. Jaya, A. Amir and Z. Mohd-Zaki

Abstract Removal of nitrate (NO_3^-) by *Eichhornia crassipes* sp. in landfill leachate was investigated in this study. Characterization study on the leachates collected from Jeram Sanitary Landfill (young landfill) and Ayer Hitam Sanitary Landfill (old landfill) show interesting pattern in concentration of NO_3^- . This study shows that concentration of NO_3^- was higher in young landfill (27 mg/L) than that in old landfill (9 mg/L) at neutral pH. Finding of these results indicate that *Eichhornia crassipes* sp. has the ability to remove NO_3^- at different concentrations in three days. Approximately 69 and 64 % of NO_3^- that present in leachate from young landfill was removed in sample without dilution and 50 % dilution, respectively. While approximately 28 and 33.6 % of NO_3^- present in leachate collected from old landfill was removed in similar dilution samples. This study is very significant to identify the capability of *Eichhornia crassipes* sp. to remove NO_3^- in landfill leachate.

Keywords Nitrate · *Eichhornia crassipes* sp. · Leachate · Landfill

1 Introduction

Nowadays, the awareness of nitrate (NO_3^-) contamination in water has become a worldwide problem. It can cause serious issues when NO_3^- contamination has caused severe problem to surface water and ground water due to point sources and nonpoint sources of nitrogen leaching usually from landfill activities [1, 2]. Previous studies revealed that high concentration of inorganic nitrogen compounds such as NO_3^- and numerous organic-N compounds present in leachate [3–5]. Indeed, leachate generated from landfills can cause considerable contamination that

N. Jaya · A. Amir (✉) · Z. Mohd-Zaki
Faculty of Civil Engineering, Universiti Teknologi MARA,
40450 Shah Alam, Selangor Darul Ehsan, Malaysia
e-mail: amnorzahira@gmail.com

can be transmitted from environment into soils, surface water and groundwater [6, 7]. Thus, appropriate treatment of landfill leachate is urgently required.

Literatures show that NO_3^- can be degraded by microorganisms through nitrification or/and denitrification processes in aerobic conditions [8, 9]. However, biological nitrogen removal in landfill leachate is a critical environmental problem due to the formation of ammonium (NH_4^+). NH_4^+ may inhibit the degradation process and produce bad smell and organic materials such as volatile fatty acids, phenolics and humic acids which can inhibit degradation of NO_3^- [5]. Since the ammonium-nitrogen strength is high, it could pose microbial inhibition problem [10]. The efficiency of denitrification may also reduce due to the limited level of particular biodegradable organics in old/mature landfills [11]. Another concern that may rise is incomplete degradation when N compound exist in high concentration that leads to toxic by-products [12, 13].

Previous study has reported that removal of NO_3^- by plant shows significant removal efficiency and no additional chemical was added during the treatment [8]. Literatures show that plants can be used to treat most classes of contaminants including excess nutrients, chlorinated solvents, petroleum hydrocarbons, pesticides, metals and landfill leachates [14–16]. The plant uptake plays an important role in the enhancement of nitrogen (N) removal based on reaction mechanisms in wetlands containing fast growing plants [17]. Hence, *Eichhornia crassipes* sp. is the example of fast growing perennial aquatic plant which is widely distributed throughout the world that can be used to treat NO_3^- contaminants [18–20]. Evidences from the previous studies show that there are lot of advantages of applying plant based remediation in treating contaminated sites where it provides low cost treatment methods which usually carried out at the landfill site and it is an environmentally friendly treatment [21].

2 Method

2.1 Material

To conduct this study, materials to be utilized include raw leachate from young and old landfills, *Eichhornia crassipes* sp., open batch reactors and aerators.

2.2 Experimental Procedures

The initial pH of landfill leachate was measured as in situ during leachate sampling at Ayer Hitam and Jeram Sanitary landfills using portable multiparameter. The pH of raw leachate was determined according to its characteristic which is based on young and old landfill leachate.

Determination of the capability of NO_3^- uptake by *Eichhornia crassipes* sp. during leachate treatment was conducted in an aerobic reactor (glass container, 10 L). All treatments were conducted in the reactors based on the original condition of landfill leachate for both landfills such as pH and cations. *Eichhornia crassipes* sp. with height between 10 and 12 cm and roots length between 16 and 17 cm were selected and hydroponically grown in tap water in reactor for one week acclimatization period before being exposed to NO_3^- contaminants. The plants *Eichhornia crassipes* sp. was separated from mud soil and the roots were washed thoroughly with tap water to remove all dirt and dead plant biomass. Then, the plants were rinsed with deionized water to remove any unnecessary compound adsorbed on the surface of plant root. In this study, about six plants of *Eichhornia crassipes* sp. were occupied for each reactor for leachate treatment.

The landfill treatment was conducted in different leachate concentrations based on its dilution rate either 50 % dilution or without dilution for both Ayer Hitam and Jeram landfills. The treated leachate sample was taken and tested every day using Spectrophotometer HACH DR 2800 during the treatment for determination of NO_3^- removal until the nutrient uptake was stopped by plant. After the treatment was terminated, plant used during treatment was dried at 45 °C for 24 h and grounded in order to get the plant tissue for NO_3^- accumulation determination. Acid digestion was done to extract NO_3^- out from the plant and finally the extracted solution containing NO_3^- was measured again by using Spectrophotometer HACH DR 2800.

2.3 Analytical Analysis

Instruments to be utilized in characteristics analysis of NO_3^- in leachates include Spectrophotometer HACH DR 2800 and ICP-MS were used to detect NO_3^- in leachate before and after harvesting. Portable Multiparameter to measure pH of leachate.

For detail characteristics study of leachate, spectrophotometer HACH DR 2800, ICP-MS, YSI 5000 and YSI 5100, HACH COD Reactor, and 220 VAC, 50/60 Hz were used to measure conductivity, dissolved oxygen (DO), turbidity, biochemical oxygen demand (BOD), chemical oxygen demand (COD) and other parameters.

3 Result and Discussion

3.1 Characterization of Leachate in Ayer Hitam and Jeram Landfills

Landfill leachate characterization study was conducted at two types of landfill in Selangor. Ayer Hitam landfill leachate represent of old landfill and Jeram landfill leachate represent of young landfill were selected in this study. Table 1 shows detail

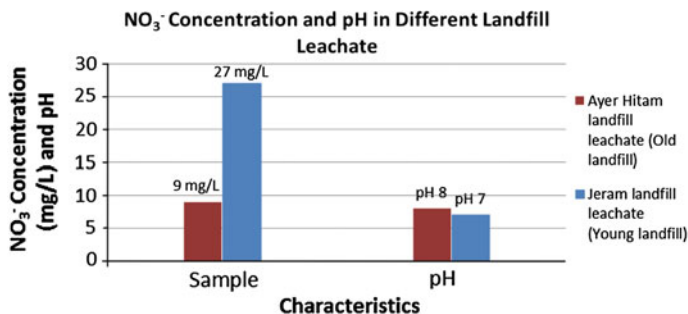
Table 1 Physical and chemical characteristics of leachate in Ayer Hitam and Jeram Landfills

Constituents	Jeram sanitary landfill (young landfill)	Ayer Hitam sanitary landfill (old landfill)
Physical characteristics		
pH	7	8
Conductivity	25.2	18.31
DO	2.31	6.86
TDS	14.96	10.58
Turbidity	1,545	145
Chemical characteristics		
BOD	3,864	1,786
COD	7,598	3,000
Nitrate (NO ₃ ⁻)	27	9
Ammonia nitrogen (NH ₃ -N)	55.8	20.7

characterization study of both landfill leachates. This results indicate that pH of leachate in both leachates were in neutral condition. However measurements of turbidity, DO, BOD, COD, NO₃⁻ and NH₃-N show significant difference characteristics in both leachates, indicating that biogeochemical of old and young landfills probably influence physical and chemical characteristics of these leachates.

3.2 NO₃⁻ Concentration in Ayer Hitam and Jeram Landfill S Leachate

Figure 1 shows the results of NO₃⁻ concentration and pH in Ayer Hitam landfill leachate (old landfill, A) and Jeram landfill leachate (young landfill, B). Sampling results shows that the NO₃⁻ concentration at old landfill and young landfill were 9

**Fig. 1** NO₃⁻ concentration and pH in different types of landfill leachate

and 27 mg/L, respectively at neutral pH. This result indicates that NO_3^- concentration at young landfill was 66.7 % higher than that at old landfill. Literatures have reported that concentration of NO_3^- was strongly influenced by the nitrification process by nitrifying bacteria (e.g., nitrobacter, nitrosomonas and nitrococcus, $\text{NH}_3 + \text{O}_2 \rightarrow \text{NO}_2^- + 3\text{H}^+ + 2\text{e}^-$, $\text{NO}_2^- + \text{H}_2\text{O} \rightarrow \text{NO}_3^- + 2\text{H}^+ + 2\text{e}^-$) [4–6]. Previous study also reported that the existence of organic matter (e.g., humic and fulvic-like fractions) may inhibit formation of NO_3^- by nitrifying bacteria [22]. This result suggests that high population of nitrifying bacteria probably present at young landfill than that at old landfill due to the existence of niche environment at young landfill that promote growth rate of nitrification bacteria (e.g., pH, organic matter and soil properties) [4, 5, 23, 24].

Figure 1 also shows the pH of leachate at Ayer Hitam landfill and Jeram landfill were at pH 8 and 7, respectively. This result indicates that pH level of both landfill leachate areas was under neutral condition. This result suggests that the pH of leachate from these landfills were not critical and may not significantly harmful to human health and environment.

3.3 NO_3^- Removal by *Eichhornia crassipes* sp. in Landfill Leachate at Ayer Hitam and Jeram Sanitary Landfills

Figure 2 demonstrates the removal of NO_3^- by *Eichhornia crassipes* sp. at different concentration of NO_3^- in Ayer Hitam landfill leachate. Approximately 69 and 64 % of NO_3^- was removed in sample 1 (Initial concentration of NO_3^- : 9 mg/L (no dilution)) and sample 2 (Initial concentration of NO_3^- : 6.6 mg/L (50 % dilution)), respectively, in 3 days. This experimental result indicates that *Eichhornia crassipes* sp. has strong capability to uptake difference concentration of NO_3^- at pH 8. Literatures have reported that NO_3^- was one of the important nutrients for *Eichhornia crassipes* sp. to promote the growth of leafy green plant via photosynthesis process [25, 26].

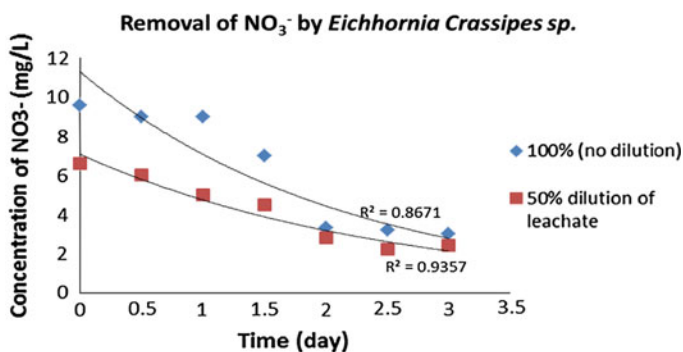


Fig. 2 NO_3^- removal in Ayer Hitam landfill leachate at pH 8

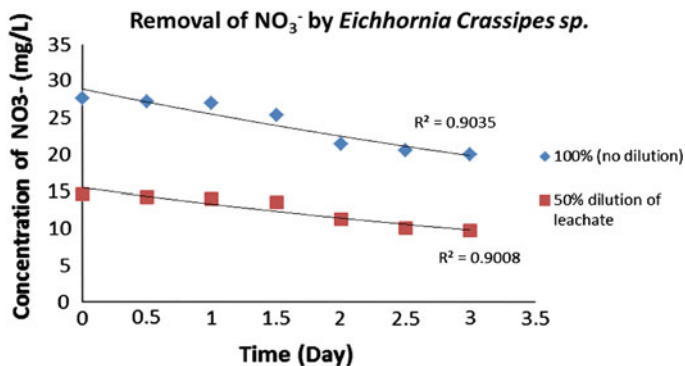


Fig. 3 NO₃⁻ removal by *Eichhornia crassipes* sp. in Jeram landfill leachate at pH 7

Removal kinetic rate of NO₃⁻ in sample 1 (0.469 d⁻¹) was faster than that in sample 2 (0.402 d⁻¹), indicating that *Eichhornia crassipes* sp. in sample 1 probably more fertile than that in sample 2. Previous studies have proved that fertile plant such as *Eichhornia crassipes* sp., *Pistia stratiotes* L., *Vetiveria zizanioides* L., *Australis* P. and *Salix viminalis* grows well in high concentration of NO₃⁻ [27–29]. Literatures show that size of leaf, branch and root were measured to verify the efficiency of NO₃⁻ uptake in the plant for optimal plant growth [13, 30–33]. Finding of this results demonstrate that *Eichhornia crassipes* sp. can be used as one of plant in the treatment of NO₃⁻ in leachate at neutral condition.

Figure 3 shows the removal of NO₃⁻ by *Eichhornia crassipes* sp. at different concentration of NO₃⁻ in Jeram landfill leachate at pH 7. Approximately 28 and 33.6 % of NO₃⁻ in sample 1 [Initial concentration of NO₃⁻: 27 mg/L (no dilution)] and sample 2 (Initial concentration of NO₃⁻: 14 mg/L (50 % dilution)), respectively, were removed in 3 days.

This result shows that *Eichhornia crassipes* sp. has the capability to uptake high concentration of NO₃⁻ in leachate. Removal kinetic rate of NO₃⁻ in sample 1 (0.126 d⁻¹) was slower than that in sample 2 (0.154 d⁻¹).

This result suggests that NO₃⁻ uptake by *Eichhornia crassipes* sp. in sample 1 probably was interfered by excessive amount of NO₃⁻ which limit the capability of plant to uptake the nutrients [25] and high concentration of NO₃⁻ uptake in *Eichhornia crassipes* sp may lead to phytotoxicity [30].

Figure 4 shows the elevation of NO₃⁻ concentration due to nitrification process in Ayer Hitam landfill leachate and Jeram landfill leachate at neutral condition (pH 7–8). Approximately 3.3 and 8.8 % of NO₃⁻ was increased in leachate from Ayer Hitam and Jeram landfills, respectively, without any plant in 3 days. This result indicate that nitrifying bacteria present in the leachate and actively produced NO₃⁻ through nitrification process. This finding is consistent with the previous results reported in the literatures [4–6, 33, 34]. Therefore, it can be concluded that natural nitrification process occurred in landfill leachate was one of the factor that promote

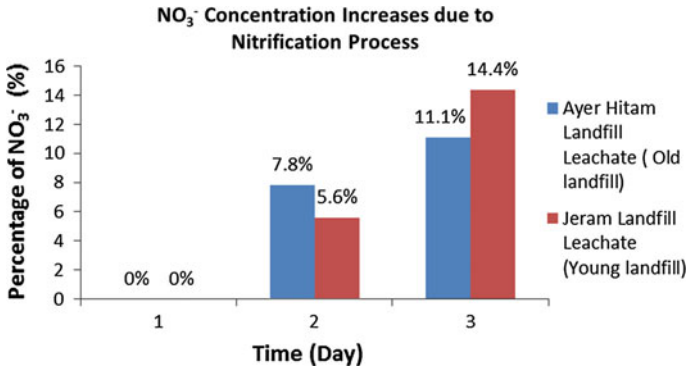


Fig. 4 Effect of nitrification process on the concentration of NO₃⁻ at Ayer hitam landfill leachate and Jeram landfill leachate at neutral pH

increasing of NO₃⁻ concentration in leachate sample particularly in Jeram landfill leachate than that at Ayer Hitam landfill.

The nutrients uptake by *Eichhornia crassipes* sp. mainly distributed in leaves stems and roots [30]. Therefore, analysis on the NO₃⁻ accumulation in plant tissue was carried out in order to determine the capability of NO₃⁻ uptake by *Eichhornia crassipes* sp. Figure 5 shows the NO₃⁻ accumulation in *Eichhornia crassipes* sp. at different concentration of NO₃⁻ at neutral condition (pH 7–8). NO₃⁻ accumulation was approximately 0.15 and 0.16 mg/L in *Eichhornia crassipes* sp. extracted from sample 1 (50 % dilution) and sample 2 (without dilution) for leachate collected from Ayer Hitam landfill. This results shows that there was no significant accumulation of NO₃⁻ in *Eichhornia crassipes* sp. in 3 days. This is probably due to low concentration of NO₃⁻ (9 mg/L) present in leachate collected from Ayer Hitam landfill.

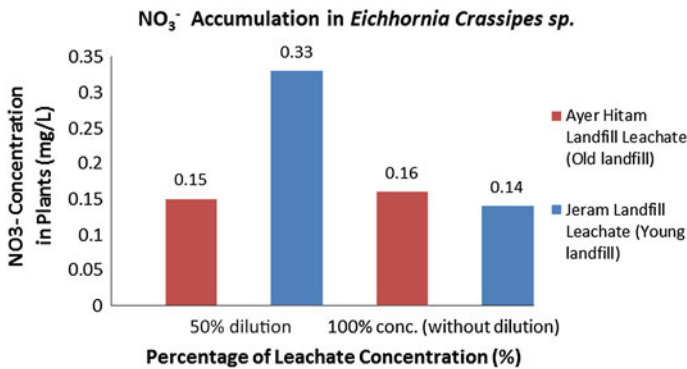


Fig. 5 NO₃⁻ accumulation in *Eichhornia crassipes* sp. after treatment of Ayer Hitam landfill leachate and Jeram Landfill at neutral pH

NO_3^- accumulation in *Eichhornia crassipes* sp. extracted from leachate Jeram Landfill shows contradict pattern than that from leachate Ayer Hitam. Approximately 0.33 mg/L of NO_3^- was accumulated in *Eichhornia crassipes* sp. in sample 1 (50 % dilution), while only 0.14 mg/L of NO_3^- was accumulated in sample 2 (without dilution) in 3 days. High concentration was observed at day 2 was probably due to intensive production of NO_3^- through nitrification process by nitrifying bacteria present in leachate. However, approximately 57.6 % of NO_3^- was leached back into the leachate. This is probably due to the fatality effect of *Eichhornia crassipes* sp [35, 36]. This results imply that *Eichhornia crassipes* sp. can be used to remove NO_3^- in leachate however it should be harvested before its fatality to prevent NO_3^- from plants leach back into the system.

4 Conclusions

This study investigated removal of NO_3^- by *Eicchorhia crassipes* sp. in leachate collected from Ayer Hitam and Jeram landfills. Removal kinetic of NO_3^- by *Eicchorhia crassipes* sp. in leachate collected from Ayer Hitam landfill was greater than that collected from Jeram landfill at neutral condition (pH 7–8). High removal kinetic rate of NO_3^- by *Eicchorhia crassipes* sp. was observed at low concentration of NO_3^- in leachate. Therefore, concentration of NO_3^- in leachate significantly influenced removal kinetic of NO_3^- by *Eicchorhia crassipes* sp. However, removal rate of NO_3^- by *Eichhornia crassipes* sp. need to be done before its fatality to prevent NO_3^- leaching back into the leachate. Another factor that significantly effect concentration of NO_3^- in landfill leachate is natural nitrification process by nitrifying bacteria in leachate. These findings may provide basic understanding on the capability of *Eichhornia crassipes* sp. to remove NO_3^- . However, further study on the characteristic of *Eichhornia crassipes* sp. need to be investigated to provide better understanding on the reaction mechanisms that involve in the removal of NO_3^- in landfill leachate.

References

1. F.M. Anayah, M.N. Almasri, Trends and occurrences of nitrate in the groundwater of the West Bank, Palestine. App. Geo. **29**, 588–601 (2009)
2. R. Dandautiya, Comparative study of existing leachate treatment methods. International conference on recent trends in engineering & technology, 2012
3. R. Matthews, M. Winson, J. Scullion, Treating landfill leachate using passive aeration trickling filter; effects of leachate characteristics and temperature on rates and process dynamics. Sci. Total Environ. **407**, 2557–2564 (2009)
4. A. Białowiec, L. Davies, A. Albuquerque, P.F. Randerson, The influence of plants on nitrogen removal from landfill leachate in discontinuous batch shallow constructed wetland with recirculating subsurface horizontal flow. Ecol. Eng. **40**, 44–52 (2012)

5. J.C. Mangimbulude, N.M.V. Straalen, W.F. Roling, Microbial nitrogen transformation potential in surface run-off leachate from a tropical landfill. *Waste Manag.* **32**, 77–87 (2012)
6. S.D. Parkes, D.F. Jolley, S.R. Wilson, Inorganic nitrogen transformation in the treatment of landfill leachate with a high ammonium load: a case study. *Environ. Monit. Assess.* **124**, 51–61 (2007)
7. H.A. Qdais, Selection of landfill leachate management strategy using decision support system. *J. Solid Waste Technol. Manage.* **36**(4), 246–257 (2010)
8. S. Renou, J.G. Givaudan, S. Poulain, F. Dirassouyan, P. Moulin, Landfill leachate treatment: review and opportunity. *J. Hazard. Mater.* **150**(3), 468–493 (2008)
9. A.H. Lee, H. Nikraz, Hung, Y.T. *Characterization of Acetogenic and Methanogenic Leachates Generated from a Sanitary Landfill Site*, vol. 43 (World Academy of Science, Engineering and Technology, 2010)
10. J.M. Lema, R. Mendez, R. Blazquez, Characteristics of landfill leachates and alternatives for their treatment: a review. *Water Air Soil Pollut.* **40**, 223–250 (1988)
11. J. Wiszniewski, D. Robert, J. Surmacz-Gorska, K. Miksch, J.V. Weber, Landfill leachate treatment methods: a review. *Environ. Chem. Lett.* **4**, 51–61 (2006)
12. G. Dave, E. Nilsson, Increased reproductive toxicity of landfill leachate after degradation was caused by nitrite. *Aquat. Toxicol.* **73**, 11–30 (2005)
13. Y.Q. Zhao, J.B. Lu, L. Zhu, Z.H. Fu, Effects of nutrient levels on growth characteristics and competitive ability of water hyacinth (*Eichhornia Crassipes*), an aquatic invasive plant. *Biodivers. Sci.* **14**, 159–164 (2006)
14. A.A. Basel, J.C. Richard, A.K. Timothy, I.S. Sunil, Phytoremediation-the natural pump-and-treat and hydraulic barrier system. *Pract. Period Hazard. Toxic Radioact. Waste Manage.* **4**, 73–77 (2000)
15. M. Greenway, The role of constructed wetlands in secondary effluent treatment and water reuse in subtropical and Arid Australia. *Ecol. Eng.* **25**, 501–509 (2005)
16. J. Vymazal, Removal of nutrients in various types of constructed wetlands. *Sci. Total Environ.* **380**, 48–65 (2007)
17. P.F. Randerson, Constructed wetlands and vegetation filters: an ecological approach to wastewater treatment. *Environ. Biotechnol.* **2**, 78–89 (2006)
18. A. Malik, Environmental challenge Vis a opportunity: the case of water hyacinth. *Environ. Int.* **33**(1), 22–38 (2007)
19. C.C. Gunnarsson, P.C. Metersen, Water hyacinths as a resource in agriculture and energy production: a literature review. *Waste Manag.* **27**, 117–129 (2007)
20. C. Isarankura-Na-Ayudhya, T. Tantimongcolwat, T. Kongpanpee, P. Prabkate, V. Prachayasittikul, Appropriate technology for the bioconversion of water hyacinth (*eichhornia crassipes*) to liquid ethanol: future prospects for community strengthening and sustainable development. *EXCLI J.* **6**, 167–176 (2007)
21. Y. Lei, Phytoremediation: an ecotechnology for treating contaminated sites. *Pract. Period Hazard. Toxic Radioact. Waste Manage.* **12**, 290–298 (2008)
22. D. Kulikowska, E. Klimiuk, The effect of landfill age on municipal leachate composition. *Bioresour. Technol.* **99**, 5981–5985 (2007)
23. X.Y. Wu, Y.J. Hao, Y. Ding, Y.X. Chen, Denitrification capacity in response to increasing nitrate loads and decreasing organic carbon contents in injected leachate of a simulated landfill reactor. *Process Biochem.* **44**, 486–489 (2009)
24. Z. Fu, F. Yang, Y. An, Y. Xue, Characteristics of nitrite and nitrate in situ denitrification in landfill bioreactors. *Bioresour. Technol.* **100**, 3015–3021 (2009)
25. J.E. Rakocy, M.P. Masser, T.M. Losordo, Recirculating aquaculture tank production systems: aquaponics-integrating fish and plant culture, *SRAC Publi.* 454 (2006)
26. Q. Lu, Z.L. He, D.A. Graetz, P.J. Stoffella, Y. Yang, Phytoremediation to remove nutrients and improve eutrophic stormwaters using water lettuce (*Pistia stratiotes* L.). *Environ. Sci. Pollut. Res.* **17**(1), 94–96 (2009)

27. G.R. Alker, A.R. Godley, and J.E. Hallett, Landfill leachate management by application to short rotation willow coppice, in *Proceedings of the 9th international waste management and Landfill symposium*, Environmental Sanitary Engineering Centre, Italy (2003)
28. S. Katayon, Z. Fiona, M.J.M.M. Noor, G.A. Halim, J. Ahmad, Treatment of mild domestic wastewater using subsurface constructed wetlands in Malaysia. *Inter. J. Environ. Studies* **1**, 87–102 (2008)
29. C.O. Akinbile, M.S. Yusoff, A.Z.A. Zuki, Landfill leachate treatment using sub-surface flow constructed wetland by *Cyperus*. *Haspan. Waste Manag.* **32**, 1387–1393 (2012)
30. P. Gupta, S. Roy, A.B. Mahindrakar, Treatment of water using water hyacinth, water lettuce and vetiver grass—a review. *Res. Env.* **2**(5), 202–215 (2012)
31. S.H. Thian *Leachate Treatment by Floating Plants in Constructed Wetlands*, Masters thesis, (Universiti Teknologi Malaysia, Faculty of Civil Engineering 2005), pp. 57
32. G. De Foe, Performance of vegetated and non-vegetated vertical flow reed beds in the treatment of dilute leachate. *J. Environ. Sci. Health* **42**, 1013–1020 (2007)
33. J.L. Faulwetter, V. Gagnon, C. Sundberg, F. Chazarenc, M.D. Burr, J. Brisson, A.K. Camper, O.R. Stein, O. R. Microbial processes influencing performance of treatment wetlands: a review. *Ecol. Eng.* **35**, 987–1004 (2009)
34. D.L. Jones, K.L. Williamson, A.G. Owen, Phytoremediation of landfill leachate. *Waste Manage.* **26**, 825–837 (2006)
35. A.E. EL-Leboudi, E.M. Abd-Elmoniem, E.M. Soliman, O.F. El-Sayed. Removal of some heavy metals from treated waste water by aquatic plants in *3rd international conference on water resources and Arid environments and the 1st Arab water forum*, (Riyadh, Saudi Arabia, 2008)
36. P.M. Ayyasamy, S. Rajakumar, M. Sathishkumar, K. Swaminathan, K. Shanthi, P. Lakshmanaperumalsamy, S. Lee, Nitrate removal from synthetic medium and groundwater with aquatic macrophytes. *Desalination* **242**, 286–296 (2009)
37. N.D. Berge, D.R. Reinhart, T.G. Townsend, the fate of nitrogen in bioreactor landfills. *Crit. Rev. Env. Sci. Technol.* **35**, 365–399 (2005)
38. R. Li, *Management of Landfill Leachate* (TAMK University of Applied Sciences, Thesis, 2009)

Building Facilities for Autistic Children in Malaysia

Nurul Aida Nazri and Zulhabri Ismail

Abstract The number of children diagnosed with autism has been increasing since 1980s. Generally, autistic children having difficulties with both social interactions and verbal communication skills. All the difficulties that they are facing will give an impact to their daily life especially on their learning process where they cannot concentrate or focus on their learning. Therefore, appropriate building facilities and design can reduce a negative impact to the autistic children where they will be more focus as well as imitate so as to have better development. The aim of this research is to identify the gap in guidelines in providing facilities needed for autistic children in order to enhance their daily life as well as their learning process; from there, guidelines of building facilities for autistic children will be formulated. This paper represents the detail about the relationship between building facilities and Autistic Spectrum Disorder (ASD) through a literature review.

Keywords Autism · Building facilities · Guidelines

1 Introduction

Autism or Autism Spectrum Disorder (ASD) is general terms used for a group of people who suffering from complex disorders of neural development. These disorders can be characterized in different symptoms, by repetitive or restricted behavior, by impaired social interaction and communication [1]. All the difficulties that they are facing will give an impact to their daily life especially on their learning process where they cannot concentrate or focus on the learning. Therefore, it is

N.A. Nazri (✉) · Z. Ismail
Faculty of Architecture, Planning and Surveying Universiti Teknologi MARA (UiTM),
40450 Shah Alam, Selangor, Malaysia
e-mail: noroule_eyeda@yahoo.com

Z. Ismail
e-mail: zulhabri@salam.uitm.edu.my

important to develop their concentration in order to improve their learning process. This is because, improvement in learning can help to maintain behaviors, reduce inappropriate actions and also formulate desired behaviors [2].

In order to promote the development of autistic children, learning environment has become an important factor. This is because, their interest will be attracted and stimulate by the environment [3]. According to Sarah Komendat, when designing an environment for learning, it is important that the needs of the students is to take into consideration [4]. Built environment has a profound effect on learning and behaviour [5]. Since, the autistic children have behavioural problems that may lead to aggressive conduct, the elements in the built environment have to be designed, chosen and implemented by taking into account the potential bouts of aggression [6]. The needs of good design features is important in order to ensure that the children get better learning environment and hence decrease their undesirable behaviour. The publication of “Evaluating Provision for Autistic Spectrum Disorder in Schools”, United Kingdom outlined three performance indicators for consideration [7], there are:

- (i) The learning environment which supportive for the child with autism: lighting, sound and colouring are sufficient in order to encourage the child to relax and settle the work.
- (ii) There is personal space which sufficient for the child with autism to find comfort and to distress when necessary.
- (iii) The areas of high interest are contains in the learning environment where it reflect the particular interests of the child with autism.

Inadequate or inappropriate building facilities may contribute and give a negative impact on the autistic children where they will experience the difficulties in the learning process. It is essential to create a positive impact on the learning environment for the autistic children through a good design. Therefore, the purpose of this paper is to revise a literature on the relationship between building facilities and the autistic children.

2 Building Facilities and Autistic Children

2.1 Autistic Spectrum Disorder

Autism is neurodevelopmental syndrome which is defined by deficits in social reciprocity and communication and by unusual restricted repetitive [8]. Generally, the signs or symptoms of autism can be noticed as the child reached the age of 2–3 years of age. However, the early detection are varies where it depends on the types of autism spectrum disorder which autism being diagnosed 5 months earlier than Pervasive Developmental Disorder—Not otherwise specified or Asperger Syndrome [9].

Autism is a lifelong developmental disability where it results in severe cognitive disabilities that adversely affect their development and also everyday life. Generally, the autistic children have problem with non-verbal communication and social interaction. The autistic children also have other learning limitation and condition such as imaginative thinking, sensory perception, repetition behaviour, learning ability and physical development [10]. The autistic children also shows an attitude or behaviours that are either excessive or in deficit. Most of the individuals with autism also experience other developmental disabilities such as intellectual disabilities. According to Deputy Commissioner of the Department of Intellectual and Development Disabilities, it was found out that 19.2 % of autistic children had an intellectual disability where as a more recent study carried out by CDC on 2012 was found out that 38 % of autistic children had an intellectual disability [11].

Each of autistic children is defined by a certain set of behaviours where some of them share certain difficulties. However, the level of development for each child is different from one another where it depends tremendously in their severity. Parents and clinicians may see the development of symptoms which associated with attention-deficit and disruptive behaviour disorders as the autistic children move towards adolescence [12]. However, some of children with autism also experience improvements. Living or teaching the autistic children can be very challenging where we need to understand their condition and also require tremendous patience. Usually, the autistic children exhibit unusual behaviours causing by the difficulties facing by them to respond to their environment in order to communicate their feeling or to cope with the situation.

2.2 Causes and Characteristics of Autism

Male is commonly diagnosed to have autism, but there are a higher proportion of secondary cases in the biological relatives of female than male probands reportedly [13]. The causes of autism are not known. Although, there are no exact causes of autism have been find out so far but there are many different theories proposed on the causes of autism. Among the causes of autism are genetics, epigenetics, possible environmental influences; certain types of infection, problem of prenatal environment, prenatal environment and postnatal environment [14–16].

Autism involves abnormalities of brain development of a child where it becomes apparent before the child reach the age of 3 years old. The brains of autistic individuals have several differences in term of structural and functional compared to the brains of normal individuals. These structural and functional abnormalities consist of neural basis for the cognitive impairments underlying the behaviour of autism [17]. It is a complex lifelong and severe disorder where they generally have common behaviour or characteristics. When a child is diagnosed to have autism it

will bring some problem especially to the child itself, family, schooling and also community. One of the obvious characteristics facing by the autistic children is they are having language delay where it make them unable to communicate with others. It seems to separate children with autism from the world because of the inability to communicate and establish a relationship with others.

2.3 Effects of Autism on Learning

Autistic child have different degrees of learning ability where it depends on the severity whether it belongs to the categories of mild, moderate, severe or profound. There is a close relationship between autistic child and learning disability. They have a psycho-educational profile which is different from other normal individuals. Some autistic child may have a problem of managing themselves and some are able to live independently. Autism also increases learning disability of a child where it affects the ability of the child to communicate, socialize, learn and also carry out everyday tasks. Learning disabilities often refer to lack of intelligence, chromosome disorder and other clinical abnormalities [18]. According to Department of Health in England, learning disability includes [19]:

- (i) A significantly reduced ability to understand new or complex information in order to learn new skills (impaired intelligence), with;
- (ii) A reduced ability to cope independently (impaired social functioning);
- (iii) Which started before adulthood, with a lasting effect on development.

Autism and learning disability are close related where it give an impacts on learning especially among more severely affected individuals [20]. The development in term of learning ability for autistic children was significantly below the normal developing children [21]. It is crucial therefore to develop the autistic children in terms of learning to ensure that they can cope with what being taught to them. According to the Autism Education Trust (AET) London, that was established in November 2007, the impacts of autism on learning in the classroom are (Table 1):

Overall, autism had negative impacts on behavioural characteristics where it fall into four categories; social interaction, communication, challenging behaviour characteristics and sensory input. All of these characteristics have an impact on learning and behaviour. Based on the research conducted by some researchers, challenging behaviour can have a significant negative impact on the lives of individuals with Autism and their caregivers [22].

Table 1 Effects of autism on learning and behaviour in the classroom

Behavioural characteristics of autism	Possible impacts upon learning and behaviour
<i>Qualitative difficulties in social interaction shown by</i>	
• The use of non-verbal behaviours is limited such as eye gaze and body posture to regulate social interaction	• Difficulties in order to form reciprocal peer relationships and friendships
• Problems developing peer relationships	• Difficulties in picking up on non-verbal or emotional cues
• Limited spontaneous showing and sharing of interests	• Taking what is said to them literally
• Limited social emotional reciprocity	• Difficulties in picking up on social cues, particularly in group activities • Unpredictable emotional responses (e.g., anxiety, outbursts) for no apparent reason
<i>Qualitative difficulties in social communication shown by</i>	
• Delayed language development without non-verbal compensation	• Problems to understand spoken language/verbal instructions
• Problems starting/sustaining conversations	• No respond when spoken to
• Repetitive and stereotyped language	• Poor comprehension of written text even if reading decoding is good
• Limited imaginative and imitative play	• Solo or parallel play in place of group play
<i>Restricted repertoire of interests, behaviours and activities shown by</i>	
• Over-focus on particular topics	• Preference for only one or a few activities
• Rigid adherence to routines/rituals	• Difficulty with transitions, changes in routine and unexpected events
• Repetitive, stereotyped motor mannerisms	• Difficulties maintaining attention without external structure/support
• Preoccupation with object parts rather than whole	• Difficulties moving from one activity to another • Less likely to pick up on the ‘gist’ of a situation or activity
<i>Hyper- or hypo-reactivity to sensory input or unusual interest in sensory aspects of the environment</i>	
• Aversive responses to particular environmental stimuli (e.g., lights, colours, sounds, patterns, smells, touch)	• Shuts eyes or blocks ears
• Sensory seeking behaviour	• Removes self from the source by leaving a room or people • Needs one person/thing at a time • Fascination with (looking, smelling, licking) objects or people

2.4 Concept of Environment

Environment is surrounding or anything that affect any living things especially human during its lifetime. Environment is one of the important aspect that need to be consider in order to enable the autistic children to learn and be self-motivated to do things since they are having complicated disorder and sensitivities within the spectrum. A good environment could enhance and also improve the learning development of autistic children. Various environment designs can attract and increase their interest during the process of learning. The environment should be structured in order to give consistency and also clarity, so that the child know what is expected of them in specific situation, where things belong and can anticipate what comes next [23]. Architects or designers of the building should consider the physical and sensory aspect when designing living and learning spaces for autistic children. Simon Humphreys, an Architect who design building for individuals with autistic suggests ten principles that should be considered when designing the building for autism. The principles that was listed by Humphreys [24] are (Table 2):

To sum up, Simon Humphreys was design an architectural concept which gives an advantage to the autistic children. Therefore, the needs of building facilities is

Table 2 Principles of design

Features	Characteristics
A sense of calm and order	Complexity can cause stress; it is not harmonious. Basically, people with Autistic Spectrum Disorder are unable to discriminate separate noises, shapes and space easily; it can cause them discomfort. An environment that has a calm sense of clarity and order can be easy to use and therefore can reduce tension
Good levels of natural light and ventilation	Good natural light levels uplift, low natural light levels can depress and create gloom. Visual understanding of a space can be achieved by having a high even level of natural light. This ease can help to reduce frustration and anxiety for people with ASD. Natural ventilation is healthier than artificial means and therefore provides a more balanced healthier environment
Reduction of detail (complex detail may be too visually stimulating for people with Autism)	Buildings can be complex in detail. People with ASD can sometimes be absorbed and sometimes obsessed with this sometimes 'picking' at small junctions. If the design of a building reduces the need for complex visual detail it will be more restful. A broad bold detailing approach using a limited pallet of materials and solutions could reduce stimulation and obsessive behaviour

(continued)

Table 2 (continued)

Features	Characteristics
Good proportion	The Greeks developed a system of proportion from mathematical equation that provides a proportion that human beings find pleasing. This proportional system is known as the ‘Golden Proportion’. It is this proportion that can be found in nature abundantly. It is possible to introduce these proportional systems into buildings at no extra cost and people with ASD may benefit from this pleasure of proportion and it may manifest in their behavior
Proxemics (the amount of space that people feel it necessary to set between themselves)	Proxemics deals with the amount of space that people feel it necessary to set between themselves. Proximity is the condition of being close or can also be termed as personal space around the body. A person with autistic spectrum disorder can be more guarded about this space and any infringement is seen as a potential threat. They need more space. Movement around a building requires space; therefore the space should be as large as possible to reduce this perceived threat which can create a sense of unrest
Containment (ensuring that people with ASD are safe and secure in their environment)	It is essential at times to ensure that people with ASD are safe and secure in their environment. This can mean secure boundaries. It is how these boundaries are designed that is important. If they are subtle, natural but secure it will allow possibilities for the person to wander at ease and also allow staff and careers to be more relaxed when this happens. Freedom of movement can be extremely liberating
Easily managed, durable materials	People with ASD can be extremely demanding on buildings. Therefore it is important that the specification of materials reflect this without resorting to an institutionalized feel. It is perfectly possible to detail a building using a limited pallet of materials to meet this demanding need
Good observation	It is useful to be able to observe the movement of people with ASD without them feeling constantly under surveillance. Therefore, a design should be such that observation is possible without it being obvious. Good observation will put the career at rest, which will help their well-being and this can only benefit the person with ASD

(continued)

Table 2 (continued)

Features	Characteristics
Good quality of acoustics	People with ASD are extremely sensitive noise and at times unable to discriminate different noises. It is possible to design a space that has good sound qualities through good proportion as well as detail materials that assist in good acoustic

crucial in order to ensure that the children with autism can adapt with the surrounding environment as well as develop their skill. This is because, children learn well in the environment that is design according to the interests of the children [25].

2.5 Impacts of Building Facilities on Autistic Children

The understanding and knowledge on how the autistic children experience and adapt to the environment is essential to be explore first before designing the areas for them. Even though designing physical environment for autistic children needs a good understanding of autism and individuals requirements, some principles of design can be applied in order to improve their responses to learning and therapies [26]. There are various impacts of building facilities that have been found out by some researcher in term of their behaviours and also learning. If universal design is to achieve its goal of making settings that are usable by all people it must be simply or primarily eliminating physical obstructions or barriers for people with sensory and physical impairments and it must also address the cognitive barriers that effects the decisions making process of individual with brain impairments [27].

Generally, individual with autism having behavioural problems where they might be aggressive, and therefore element present in the built environment must be designed and chosen by the possibility of eventual abuses [28]. A research and development officer at Sunfield School had carried out a research on the impact of building design on children with autistic spectrum disorder. She described the main features of new building created as a residential living space for 12 autistic children and hence she came out with the findings on the impacts to the autistic children. Among the findings were:

2.5.1 Outdoor Space

The creation of an enclosed courtyard incorporating covered areas provides a safe outdoor environment for the children. It is also located centrally so that the children can play independently while the staff still can observe the children. The covered areas consist of hanging canopies which are in effect the continuation of the roof

either side of the courtyard. This allows the children to play freely and essentially unsupervised. This had a significant impact on children and staff where they could offer minimal supervision on the children. One child in particular got upset when he could not go out on his bike where it needed direct supervision from the staff. This problem was solved by this design.

2.5.2 Curved Walls

The creation of curved wall reduces the need for harsh corners, where it is not only making the environment safer but helping the children to move easily to various area of the building. Children at sunfield have been observed having difficulties with right angles. So by adding curves to the design was the natural progression to aid the children with their visual-spatial and cue the child to move. Staff at Sunfield observed that curved walls gave some benefit where it create a less institutionalised feel to the building and made it more aesthetically pleasing. The curved walls facilitate the movement of the children through the environment. Besides that, the curved walls in the circulation space were identified to have orientation value. Therefore, children were guided into the space once they enter the building and were not met by harsh right angles which were visually difficult to navigate.

2.5.3 High-Level Windows

Are provided in addition to low-level openings in all bedrooms and some communal areas in order to give additional daylight and ventilation. It also reduces the risk of a child to climb out of the windows. The abundance of large low-set windows gave the children a view of a space which was now accessible to them. In previous accommodation the children had climbed onto the radiators to look through windows to areas outside which they had not been able to access. Hence it reduces the possibility of children to jump and climb.

2.6 Impacts on Learning

Most of the children with autism facing the problem in learning where they are unable to achieve a significant level of understanding. Basically, people can learn through seeing, hearing, touching or manipulating an object [29]. The earning environment which comprehensible will enable the child to knows what is expected, what will happen next and also allow the child to generalize newly learned skills [30]. Therefore, by providing a good accommodation and environment it will enhance the learning development of the autistic children. Colour surrounding the physical learning environment must be considered because it give the effect on learning and behaviour [31]. The layout and tone of the classroom is

one of the most important in order to help children with ASD understand expectations, and access the curriculum [32].

John Dewey stated that stimulating environment that is designed based on the interest of the children in classroom is good for children to learn [25]. Generally, children with autism do not like multi-space as it can cause confusion to them. Audio and visual interfering, thus spaces should be calming, have less distractions and low stimulating to enhance greatest learning potential [33]. Therefore, good design is essential in order to create a positive impact on learning environment.

Acknowledgments The Authors would like to express their gratitude for the financial support from MOHE (Minister of Higher Education) under the Niche Research Grant Scheme (NRGS), 600-RMI/NRGS 5/3 (12/2013) given to this research.

References

1. J.C. Kelleher, *Anxiety Symptoms in Individuals with High Functioning Autism* (University of Connecticut, 2013)
2. N. Noiprawat, N. Sahachaiseri, The model of environments enhancing autistic children's development. *Procedia. Soc. Behav. Sci.* **5**, 1257–1261 (2010)
3. A. Karahoca, D. Karahoca, L. Yengin, Computer assisted active system development for critical thinking in history of civilization. *Cypriot J. Educ. Sci.* **5**, 4–25 (2010)
4. S. Komendat, *Creative Classroom Designs* (State University of New York, New York, 2010)
5. K.S. Gaines, S. Sancibrian, R. Lock, National Conference and Exposition, in *The Impact of Classroom Design on Students with Autism Spectrum Disorders* (2011), pp. 1–4
6. F.S. Vazquez, A.S. Torres, Autism and architecture. *Recent Adv. Autism Spectr. Disord.* **II** (2009), 178–186 (2013)
7. J. Hunter, *Evaluating Provision for Autistic Spectrum Disorder in Schools* (United Kingdom, 2005)
8. Centers for Disease Control and Prevention, *Autism Spectrum Disorder, Autism and Developmental Disabilities Monitoring (ADDM) Network Publications* (2014) [Online]. Available: <http://www.cdc.gov/ncbddd/autism/hcp-dsm.html>. Accessed 15 Apr 2014
9. J.L. Matson, R.D. Rieske, K. Tureck, Additional considerations for the early detection and diagnosis of autism: review of available instruments. *Res. Autism Spectr. Disord.* **5**(4), 1319–1326 (2011)
10. N. Noiprawa, N. Sahachaisaeree, Interior environment enhancing child development. *Asian J. Environ. Stud.* **2**, 43–51 (2011)
11. D. Wright, *Autism in Tennessee: Part 3—Health* (Tennessee, 2012)
12. L.A. Leblanc, A.R. Riley, T.R. Goldsmith, *Autism Spectrum Disorder: A Lifespan Perspective* (Western Michigan University, 2007), pp. 65–87
13. M.-C. Lai, M.V. Lombardo, S. Baron-Cohen, Autism. *Lancet* **383**(9920), 896–910 (2014)
14. R.R. Dietert, J.M. Dietert, J.C. Dewitt, Environmental risk factors for Autism. *Emerg. Heal. Treats J.* **1**, 1–11 (2011)
15. W.H. James, An update on the hypothesis that one cause of autism is high intrauterine levels of testosterone of maternal origin. *J. Theor. Biol.* **355**, 33–39 (2014)
16. R. Muhle, S.V. Trentacoste, I. Rapin, *The Genetics of Autism* (Pediatrics, 2011), pp. 472–486
17. N.J. Minshew, G. Goldstein, Autism as a Disorder of Complex Information Processing. *Ment. Retard. Dev. Disabil. Res. Rev.* **136**, 129–136 (1998)
18. C.D. Rittey, Learning difficulties: What the neurologist needs to know. *J. Neurol. Neurosurg Psychiatry* **74**(suppl 1), 1–8 (2014)

19. Department of Health, *Valuing People: A New Strategy for Learning Disability for the 21st Century* (United Kingdom, 2001)
20. G. O'Brien, J. Pearson, Autism and learning disability. *Autism* **8**(2), 125–140 (2004)
21. A. Gupta, N. Singhal, Language and learning skill and symptoms in children with autistic spectrum disorder. *Asia Pac. Disabil. Rehabil. J.* **20**(2), 59–83 (2009)
22. A. Sawyer, J.K. Lake, Y. Lunskey, S. Liu, P. Desarkar, *Research in Autism Spectrum Disorders Psychopharmacological Treatment of Challenging Behaviours in Adults with Autism and Intellectual Disabilities: A Systematic Review*, vol. 8 (Elsevier, 2014), pp. 803–813
23. Department of Education, *Teaching Student with Autism Spectrum Disorder (Inclusive Programming for ASD Students in New Brunswick Schools)* (New Brunswick, 2005) pp. 1–146
24. S. Humphreys, Autism and architecture. *Hastings Cent. Rep.* **44**(3), 48 (2005)
25. I. Teaching Strategies, *Research Foundation: The Creative Curriculum* (2010) [Online]. Available: <http://teachingstrategies.com/content/pageDocs/Research-Foundation-Creative-Curriculum.pdf>. Accessed 15 Apr 2014
26. R. Khare, A. Mullick, Educational spaces for children with autism; design development process, *CIB W084 Build. Comf. Liveable Environ. All*, no. May (2008), pp. 66–7
27. M. Calkins, J. Sanford, M. Proffitt, Design for dementia: challenges and lessons for universal design. *Univers. Des. Handb.* 1–54 (2001)
28. P.A. Sánchez, F.S. Vázquez, L.A. Serrano, *Autism and the Built Environment*, 1st edn. (Europe: InTech, 2001), pp. 363–380
29. S.M. Edelson, *Learning Styles and Autism* (Autism Research Institute, 2014) [Online]. Available: http://www.autism.com/understanding_learning. Accessed 12 Apr 2014
30. C. Project, *A Summary of Current Best Practices for Educating Autistic Children* (ECONorthwest, 2008). [Online]. Available: <http://chalkboardproject.org/wp-content/uploads/2011/11/Educating-Autistic-Children.pdf>. Accessed 15 Apr 2014
31. K.S. Gaines, Z.D. Curry, The inclusive classroom: the effects of color on learning and behavior. *J. Fam. Consum. Sci. Educ.* **29**(1), 46–57 (2011)
32. S. McCanney, J. Drysdale, L. Scott, C. O'Flaherty, M.L. Hughes, K. Doherty, J. Greeves, A. Laverty, G. Kearney, L. Hughes, M. Greenwood, *The Autistic Spectrum in Resource File for Special Education Needs* (United Kingdom, Department of Education, 2008) pp. 195–256
33. K. Martinez, *Innovative Learning Environments : Design Awards Meets Research Evidence* (American Institute of Architects Committee, 2012), pp. 4–196

Adsorption of Metals (Zn, Ca and B) in Used Engine Oil by Using Microwave Incinerated Rice Husk Ash (MIRHA)

Amir Izzuddin Habib, Shamsul Rahman Mohd Kutty, Nasir Shafiq and Mohd Fadil Nuruddin

Abstract Microwave Incinerated Rice Husk Ash (MIRHA), produced from the rice husk was proven as one of the low-cost materials that can be used as an adsorbent for heavy metal in aqueous solution. Used engine oil is one of the wastes that contain heavy metals, metals and other contaminants. Most are non-biodegradable and can harm living creatures and human being if not properly disposed. The aim of this research was to study the feasibility of using MIRHA as adsorbent for the removal of heavy metal, metals and other contaminants from used engine oil. The chemical composition of the used engine oil was determined based on ASTM D6595. A series of jar tests were conducted by varying the contact time at fixed concentration of MIRHA and varying the concentration of MIRHA at specified contact time. All the samples were conducted in triplicates. It was observed that the optimum contact time for zinc, calcium and boron removals at fixed concentration of adsorbent of 625,000 mg/L of MIRHA were found to be 4, 4 and 24 h, respectively. The percentage removals of zinc, calcium, and boron were found to be 38.24, 29.39 and 52.27 %, respectively. It was also observed that the optimum adsorbent dosage for Zn, Ca and B removals were at 450,000 mg/L of MIRHA with percentage removals of 55.12, 29.33 and 62.11 %, respectively.

Keywords Used engine oil · Metals · Heavy metals and contaminants · Adsorption · Microwave incinerated rice husk ash (MIRHA)

A.I. Habib · S.R.M. Kutty (✉) · N. Shafiq · M.F. Nuruddin
Civil Engineering Department, Universiti Teknologi PETRONAS, Seri Iskandar, Malaysia
e-mail: shamsulrahman@petronas.com.my

A.I. Habib
e-mail: amerdeen89@gmail.com

N. Shafiq
e-mail: nasirshafiq@petronas.com.my

M.F. Nuruddin
e-mail: fadhilnuruddin@petronas.com.my

1 Introduction

Wastes are unwanted material or any substance which constitutes a scrap material or an effluent or other unwanted surplus substances arising from the application of any process. The process may come from the industrial, commercial, household or any other process that has no economical demand and necessary to be disposed of properly [1].

Approximately 1.35 billion gallons of used oil are generated yearly and approximately 800 million gallons are collected by recyclers for reuse. Hence, only 59 % of the used engine oil were reused and 41 % were dumped away to the environment [2]. Used engine oil are composed of heavy metals that can caused hazards. The formation of hazards resulted from various additives used in its manufacture and from heavy metal contaminants picked up from internal combustion of engines. Used engine oil poured into household drains or directly onto the ground may lead into waterways and groundwater cause pollution [3]. According to Chevron, used motor oils do not present a significant inhalation health hazard. However, it can present a problem if they come in contact with the eyes or skin, triggering an allergic skin reaction or eye irritation. Long-term effects from repeated contact include a higher risk of developing skin cancer [4].

Rice Husk is a commonly available agriculture waste in Malaysia. It is estimated that, in South East Asia approximately 150 million tonnes (25 % of world production) of rice husk are being produced annually, 95 % of the production were used within the region and the remaining 5 % was exported to other countries [5]. Meanwhile, in Malaysia it is estimated that rice husk takes account for about 20 % of the whole rice produced [6]. According to the statistics compiled by the Department of Statistics Malaysia, [7] the production of Malaysia paddy in 2010 is 2,464,831 tonnes. Therefore, it is estimated that more than 400,000 tonnes of rice husk produced annually in Malaysia. The potential use of rice husk ash in the adsorption of metal ions has been widely investigated [8–10]. Microwave Incinerated Rice Husk Ash (MIRHA) obtained from burning the rice husk at controlled temperature using microwave incinerator have been studied and can be utilized as alternative adsorbent for removal of metal ions [11, 12].

Adsorption is considered as an efficient and economically feasible method to remove or treat heavy metals present in used engine oil. The use of rice husk as adsorbents is an option for cheap and readily available sources than activated carbon, since rice husk are one of the agricultural waste which are abundant in Malaysia. The aim of this research was to study the feasibility of using MIRHA as an adsorbent for the removal of heavy metal and other contaminants from used engine oil.

Table 1 Typical chemical composition of MIRHA [13]

Chemical composition	Weight %
Na ₂ O	0.0195
MgO	0.5885
Al ₂ O ₃	0.3572
SiO ₂	86.3115
P ₂ O ₅	3.008
K ₂ O	6.3366
CaO	0.9996
TiO ₂	0.0191
Fe ₂ O ₃	0.7227
SO ₃	1.5145
MnO	0.1301

2 Methodology

2.1 Preparation of Microwave Incinerated Rice Husk Ash

Rice Husk was collected from BERNAS Rice Mill in Seberang Perak, Malaysia. The rice husk was burned at 500 °C (MIRHA) temperature for 8 h. Table 1 illustrates the chemical composition of MIRHA [13].

2.2 Source of Raw Used Engine Oil and Initial Analysis

Raw used engine oil was collected from several car service centres in Perak, Malaysia. All of the raw used engine oil was mixed and the initial elemental analysis of raw used engine oil was analyzed. Table 2 illustrates the elemental analysis of raw used engine oil.

2.3 General Experimental Procedure

The chemical composition of the used engine oil was determined based on ASTM D6595 (Standard Test Method for determination of wear metals and contaminants in used lubricating oils or used hydraulic fluids by rotating disc electrode atomic emission spectrometry). Two sets of jar tests were conducted using the used engine oil. The final chemical composition or wear metals of the used engine oil after the jar tests were measured based on ASTM D6595 procedure. For each metal, optimum contact time and optimum dosage of MIRHA to be added for the adsorption process was evaluated.

Table 2 Initial elemental analysis of raw used engine oil

Type of elements	Metals elements in ppm unit
Iron (as Fe)	26.5
Chromium (as Cr)	1
Lead (as Pb)	2
Copper (as Cu)	9
Tin (as Sn)	<1
Aluminium (as Al)	6.5
Nickel (as Ni)	<1
Silver (as Ag)	<1
Silicon (as Si)	16
Boron (as B)	47.5
Sodium (as Na)	102
Magnesium (as Mg)	99
Calcium (as Ca)	1581.5
Barium (as Ba)	2
Phosphorous (as P)	567
Zinc (as Zn)	944
Molybdenum (as Mo)	33.5
Titanium (as Ti)	<1
Vanadium (as V)	1.5
Manganese (as Mn)	2.5
Cadmium (as Cd)	<1

2.4 Procedure on Effect of Contact Time at Fixed Adsorbent Dosage

In this jar test, a constant concentration of MIRHA at 625,000 mg/L were stirred with 800 mL of used engine oil at contact times of 4, 8, 14 and 24 h. Three jars were prepared for each contact time.

2.5 Procedure on Effect of Adsorbent Dosage (Concentration) at Fixed Contact Time

In this jar test, the adsorbent (MIRHA) was varied at 0.20, 0.28, 0.36, 0.40, 0.44, 0.52, 0.60 kg and stirred with 800 mL of used engine oil at a constant contact time of 24 h. Three jars were prepared for each weight of adsorbent.

3 Results and Discussion

3.1 Effect of Contact Time at Fixed Adsorbent Dosage

Based on the experiment, total of 21 metals which consist of Fe, Cr, Pb, Cu, Sn, Al Ni, Ag, Si, B, Na, Mg, Ca, Ba, P, Zn, Mo, Ti, V, Mn, Cd were found in raw used engine oil. Out of these, 10 types of metals were recognized to be significantly affected by MIRHA. The metals adsorbed were Fe, Al, Si, B, Na, Mg, Ca, P, Zn, and Mn. Table 3 show the removals for the 10 elements. It was observed that some elements increased in concentration while some are removed. The elements

Table 3 Behaviour for the affected elements due to contact time variation

Type of elements	Contact time (hour)	Final conc. of element (ppm)	Initial conc. of element (ppm)	Difference between initial and final conc. (ppm)	Effect of MIRHA to the elements based on contact time variation	Reasons of differences between the initial and final conc. of elements
Iron (as Fe)	24	107.00	26.5	+80.5	Slightly affected	Occurrence of Fe ₂ O ₃ in MIRHA
Aluminium (as Al)	24	21.67	6.5	+15.17	Slightly affected	Occurrence of Al ₂ O ₃ in MIRHA
Silicon (as Si)	24	3339.33	16	+3323.33	Much affected	Occurrence of SiO ₂ in MIRHA
Boron (as B)	24	22.67	47.5	-24.83	Slightly affected	Adsorbed by MIRHA
Sodium (as Na)	24	88.00	102	-18.33	Slightly affected	Adsorbed by MIRHA
Magnesium (as Mg)	24	329.00	99	+230	Affected	Occurrence of MgO in MIRHA
Calcium (as Ca)	4	1116.67	1581.5	-464.83	Affected	Adsorbed by MIRHA
Phosphorous (as P)	14	1882.67	567	+1315.67	Affected	Occurrence of P ₂ O ₅ in MIRHA
Zinc (as Zn)	4	583.00	944	-361	Affected	Adsorbed by MIRHA
Manganese (as Mn)	14	53.67	2.5	+51.67	Slightly affected	Occurrence of MnO in MIRHA

increased in concentration due to their presence in the adsorbent (MIRHA). The elements that were significantly adsorbed were Ca, Zn and B.

3.2 Effect of Adsorbent Dosage at Fixed Contact Time

Based on the experiment, total of 21 elements of metals which consist of Fe, Cr, Pb, Cu, Sn, Al Ni, Ag, Si, B, Na, Mg, Ca, Ba, P, Zn, Mo, Ti, V, Mn, Cd were found in raw used engine oil. Out of these 10 metals were significantly affected by MIRHA. The metals affected were Fe, Al, Si, B, Na, Mg, Ca, P, Zn, and Mn. Table 4 show

Table 4 Behaviour for the affected elements due to concentration variation

Type of elements	MIRHA concentration (mg/L)	Final conc. of element (ppm)	Initial conc. of element (ppm)	Difference between initial and final conc. (ppm)	Effect of MIRHA to the elements based on contact time variation	Reasons of differences between the initial and final conc. of elements
Iron (as Fe)	750,000	137.3	26.5	+110.8	Affected	Occurrence of Fe ₂ O ₃ in MIRHA
Aluminium (as Al)	750,000	48.33	6.5	+41.83	Slightly affected	Occurrence of Al ₂ O ₃ in MIRHA
Silicon (as Si)	650,000	3268.7	16	+3253	Much affected	Occurrence of SiO ₂ in MIRHA
Boron (as B)	450,000	18	47.5	-47.18	Slightly affected	Adsorbed by MIRHA
Sodium (as Na)	250,000 and 750,000	76 and 140.33	102	-26, and +38.33	Slightly affected	Adsorbed by MIRHA
Magnesium (as Mg)	750,000	630	99	+531	Affected	Occurrence of MgO in MIRHA
Calcium (as Ca)	450,000	1117.7	1581.5	-463.8	Affected	Adsorbed by MIRHA
Phosphorous (as P)	750,000	2744.7	567	+2177.7	Much affected	Occurrence of P ₂ O ₅ in MIRHA
Zinc (as Zn)	750,000	423.7	944	-520.3	Much affected	Adsorbed by MIRHA
Manganese (as Mn)	450,000	149.7	2.5	+147.2	Affected	Occurrence of MnO in MIRHA

the behaviour for the 10 affected elements at various adsorbent dosage. It was observed that some of the elements increased in concentration while some are removed through adsorption. The elements that were significantly adsorbed were Ca, Zn and B.

3.3 Removal Efficiency of Zn, Ca and B at Fixed Adsorbent Dosage (625,000 Mg/L) and Variation of Contact Time

From the 10 affected elements it was observed that only Zn, Ca, B were significantly adsorbed by MIRHA. The removals of the metals through adsorption of MIRHA was plotted in Fig. 1. It was also observed that the optimum contact time for zinc, calcium and boron removals at fixed concentration of adsorbent of 625,000 mg/L of MIRHA were found to be 4, 4 and 24 h, respectively. The removals of Zn, Ca, and B were found to be 38.24, 29.39 and 52.27 %, respectively.

3.4 Removal Efficiency of Zn, Ca and B at Fixed Contact Time and Variation of Adsorbent Dosage

From the 10 affected elements it was observed that only Zn, Ca, B were significantly adsorbed by MIRHA. The removals of the metals through adsorption of MIRHA was plotted in Fig. 2. It was also observed that the optimum adsorbent dosage for zinc, calcium and boron removals were at 450,000 mg/L of MIRHA with removals of 55.12, 29.33 and 62.11 %, respectively.

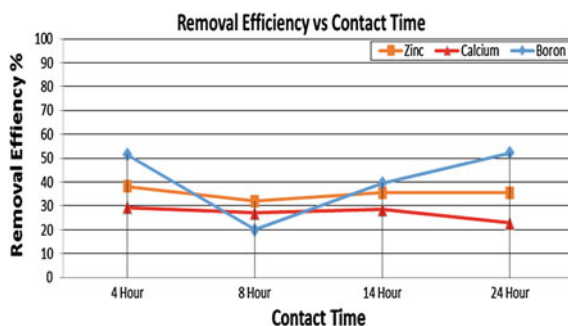


Fig. 1 Removal efficiency versus contact time

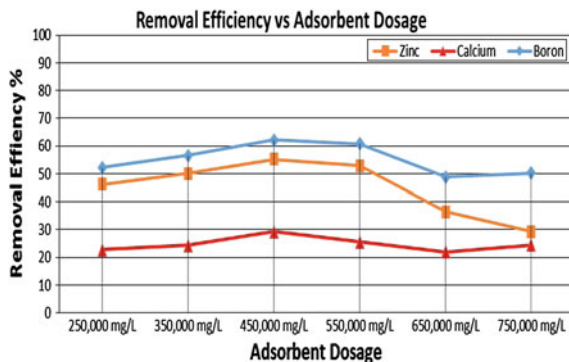


Fig. 2 Removal efficiency versus adsorbent dosage

4 Conclusion

From the study, it can be concluded that MIRHA has the ability to adsorb metals such as Zn, Ca, and B in used engine oil. The removals of these metals will further improve in recycling of used engine oil as a potential superplasticizer in concrete.

Acknowledgments The authors would like to forward his deepest appreciation and extend their acknowledgement to the Universiti Teknologi PETRONAS and Cradle Fund Sdn. Bhd. for providing the funding and resources and to all persons who have given supports for the accomplishments of this research.

References

1. R.G.P. Hawkins, H.S. Shaw, *The Practical Guide to Waste Management Law: With a List of Abbreviations and Acronyms, Useful Websites and Relevant Legislation* (Thomas Telford, London, 2004)
2. Utah Department of Quality, *Division of Solid and Hazardous Waste. Used Oil Section: Used Oil Statistics*. Retrieved Feb 2012, from http://www.hazardouswaste.utah.gov/Used_Oil_Section/UsedOilStatistics.htm (n.d.)
3. S.C. Chin, N. Shafiq, M.F. Nuruddin, Effects of used engine oil in reinforced concrete beams: the structural behaviour. Paper presented at the proceedings of world academy of science, engineering and technology (2012)
4. Chevron, *Used Motor Oils*. Retrieved Feb 2012, from http://psglubricants.chevron.com/PSG%5CChevron_ProdSafetyGds%5C7a_UsedMotorOils_Chevron.pdf (2007)
5. E. Mutert, T.H. Fairhurst, Developments in rice production in Southeast Asia. *Better Crops Int.* **15**, 12–17 (2002)
6. T.G. Chuah, A. Jumariah, I. Azni, S. Katayon, S.Y. Thomas Choong, Rice husk as a potentially low-cost biosorbent for heavy metal and dye removal: an overview. *Desalination*, **175**(3), 305–316 (2005)

7. Malaysia, *Department of Statistics. Paddy Data Series*. Retrieved Feb 2012, from http://www.statistics.gov.my/portal/download_Economics/files/DATA_SERIES/2011/pdf/08Padi.pdf (2012)
8. M. Ajmal, R. Ali Khan Rao, S. Anwar, J. Ahmad, R. Ahmad, R. Adsorption studies on rice husk: removal and recovery of Cd (II) from wastewater. *Bioresour. Technol.* **86**(2), 147–149 (2003)
9. S. Mohan, G. Sreelakshmi, Fixed bed column study for heavy metal removal using phosphate treated rice husk. *J. Hazard. Mater.* **153**(1), 75–82 (2008)
10. V.C. Srivastava, I.D. Mall, I.M. Mishra, Competitive adsorption of cadmium (II) and nickel (II) metal ions from aqueous solution onto rice husk ash. *Chem. Eng. Process.* **48**(1), 370–379 (2009)
11. M.H. Isa, S.R.M. Kutty, S.R. Mohd, N.M.D. Hussin, A. Malakahmad, *Cadmium (Cd) Removal from Aqueous Solution Using Microwave Incinerated Rice Husk Ash (MIRHA)* (2010)
12. N.A. Johan, S.R.M. Kutty, M.H. Isa, N.S. Muhamad, H. Hashim, Adsorption of copper by using microwave incinerated rice husk ash (MIRHA). *Int. J. Civil Environ. Eng.* **3**, 211–215 (2011)
13. M.F. Nuruddin, N. Shafiq, N.L.M. Kamal, The effects of types of rice husk ash on the porosity of concrete. Paper presented at the APSEC-EACEF 2009, Awana Porto Malai, Langkawi (2009)

Influence of Indoor Microclimate Distribution on Mould Infestation in a University Library

Maisarah Ali, Majeed Oladokun, Samsul Baharin Osman,
Niza Samsuddin, Hairul Aini Hamzah and Md Noor Salleh

Abstract Indoor mould contamination portends grave consequence to the stored components as well as inhabitants of infested dwellings. Such defilement, which is due to favourable growth environment for micro-organisms, is often associated with Sick Building Syndrome (SBS) and other Building Related Illness (BRI). As the economic development of Malaysia continues, increase numbers of air-tight, fully air conditioned buildings are evolving. Currently limited guidelines exists on Indoor Air Quality (IAQ) in Malaysia and its knowledge amongst the public is lacking. Hence, diagnosing the aggravating factors favouring indoor mould becomes beneficial as earlier detection is often difficult until growth has advanced. The study aimed at investigating mould infestation in a mechanically ventilated library building in Malaysia. Microclimate parameter and mould sampling were carried out. The microbial investigation results in 72 isolates whose distribution were 86 % mould, 13 % yeast and 1 % bacterial. It is found that *Aspegillus* sp. and *Onychocola* sp. were most common. The library internal microclimate distribution is characterised by

M. Ali (✉) · S.B. Osman

Department of Manufacturing and Material Engineering, International Islamic University, Malaysia (IIUM), P.O. Box 10, 50728 Kuala Lumpur, Malaysia
e-mail: maisarah@iium.edu.my

S.B. Osman

e-mail: irsam747@yahoo.com

M. Oladokun

Department of Architecture, Building Services Engineering, IIUM, Kuala Lumpur, Malaysia
e-mail: majeed.olaide@live.iium.edu.my

N. Samsuddin

Department of Community Medicine, IIUM, Kuantan, Malaysia
e-mail: niza_shamsuddin@iium.edu.my

H.A. Hamzah

Department of Basic Medical Sciences, IIUM, Kuantan, Malaysia
e-mail: hairulaini@iium.edu.my

M.N. Salleh

Department of Biotechnology Engineering, IIUM, Kuala Lumpur, Malaysia
e-mail: mdnoor@iium.edu.my

uneven hygrothermal profile which results in high level of cellulolytic mould species that are highly detrimental to books and other archival materials. It is recommended that the HVAC system operations and set-points be critiqued to bring the ambient to the preservation requirements. In addition, load balancing for thermal and hygric distribution analysis should be executed to eliminate dead-spots in temperature and moisture distributions.

Keywords Mould contamination • Microbial assessment • Indoor microclimatic parameters • Hygrothermal profile • Indoor air quality • Time-series data

1 Introduction

Moulds are pervasive in nature as they are primary decomposer of organic materials from plants and animal remains. Their importance in organic cycle (carbon and nitrogen) cannot be over emphasised. As a results of mould pervasiveness, they are assumed to be omnipresent in indoor environment as microbiologically clean buildings do not exist [1]. Therefore, total elimination of mould spores remains almost impossible. Despite their ecological importance, mould may be harmful to not only the indoor stored collections but also the occupants' health [2]. The concentrations of outdoor moulds outnumbered that of indoor with the outdoor-indoor route classified as environmental and biological [3]. While the environmental routes include: ventilation systems, cracks, cervices and other openings, water leakage, the biological ones are: animal dander and human transport. Mould feeds on their substrates and emits secondary metabolites [4, 5]. While their consumption of the substrates results in discolouration and deterioration [6, 7] (Fig. 1), the secondary metabolites is associated with health related issues in the occupants [8]. Previous studies exist on investigating the relationship between indoor mould exposure and health related issues [9–12] but no conclusive evidence exists [13, 14].

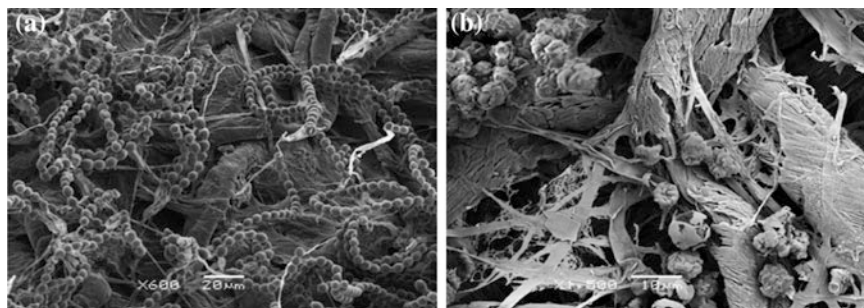


Fig. 1 SEM image of: **a** Biofilm formation by mould fungi on aged paper (600×). Bar = 20 µm. **b** Detail showing deteriorated cellulose fibres (1500×). Bar = 10 µm [6]

This according to [15] is as a result of the difficulty in the determination of health risks due to mould exposure and that human responses are a function of a number of factors: types of moulds, the degree and length of exposure, previous history of exposure, and immune status.

1.1 Mould Growth Factors

Mould thrives when the favourable biotic and abiotic factors exist [5]. While the biotic factors are related to the mould (presence and viability of spores, nature of specie, competition between mould and other organisms), abiotic factors relate to the environmental parameters (moisture, temperature, nutrients, pH, light, oxygen etc.). Nevertheless, it appears there exists a poor understanding of fungal ecology in indoor environment. For instance, oxygen, nutrients and pH are required for mould fungi to carrying out their routine physiologic and metabolic activities. While these factors are of utmost concern in the mycological consideration of mould, they are of less importance in indoor environment. The oxygen requirement by the indoor occupants is more than the range needed by mould to survive hence oxygen will always be present and its reduction becomes indoor air quality issue. Equally, nutrients is found indoor in abundance from the building components made of cellulose and other glucose based materials (furniture, books, paints and other finishes). The pH is a function of aqueous solutions hence, it becomes of less concern where appropriate lid is kept on indoor moisture level.

In addition, insufficient sunlight penetration into the building interiors is considered as factor that promote growth. On this, it should be noted that although the ultra violet component of the light spectrum are found to be detrimental to growth of microbes [5], the same is identified [16] as one of the deteriorating factors of stored collections of books and archives. More so, the heat from sunlight increases the ambient temperature and hence inhibit the growth of some species [2, 17]. Nevertheless, excessive heat intrusion into the buildings remains a contributory factor to an increase in cooling loads on HVAC systems—an energy efficiency issue. Therefore, light, oxygen and pH are practically of less significance as limiting growth factor for indoor mould development and reproduction [5].

Although moisture remains an active contributor to indoor microbial growth, there exists maximal and minimal moisture threshold conditions for microbes to develop on different materials [18]. Regarding the consensus that condensation must be present before mould growth can occur, Clarke [19] submitted that this appears invalid as some species are highly xerophilic (dry loving). He further concluded that the most critical control factors of mould growth remains relative humidity and temperature hence an appropriate moisture level in humid air is sufficient for colonisation. The species that best adapted to the prevailing conditions predominate when the environmental conditions become less favourable and as such an elevated indoor mould levels coupled with the occurrence of certain species are indicative of excessive moisture [20].

1.2 Mould and Ventilation Systems

The ventilation systems create a balance of thermal comfort and indoor air quality [21] to not only the occupants of the indoor environment but also the stored components. In mechanically ventilated buildings, the system contributes on the contrary [15] most especially the Air Handling Units (AHU) which in its distribution of the conditioned air to the downstream possess potential to circulate mould spores throughout a structure thereby support mould growth. In addition, indoor hygrothermal fluctuations due to inadequate ventilation over a long periods of time results in faster deposition of spores on the material surfaces. These spores continue the life-cycle of mould by growing to form hyphae that promote material deterioration.

In naturally ventilated buildings, the risk of mould infestation is lower when compare to mechanically ventilated ones. Study have demonstrated [18] that fungal general appear in low concentration in naturally ventilated building (in a hot and humid climate of Cuba). This according to the study is due to natural ventilation that facilitate movement of particles in the air thereby making spores deposition difficult. On the contrary, in the hot and humid climate, to which Malaysia belongs, mechanical ventilation systems play an important role in maintaining an indoor hygrothermal condition. Cases of microbial infestation of mechanically ventilated buildings had been reported in Malaysia public buildings [22, 23]. Therefore, adequate consideration needs to be given to the mechanical ventilation system in maintaining the hygrothermal gradients in a way to keep a lid on the microbial proliferations. Failure in this regards poses potential risks to not only the stored collections but also the occupants' health.

1.3 Mould Sampling and Identification

Mould sampling and identification can be classified into materials and aerosol sampling. Mould infested materials are investigated by surface or bulk sampling [24]. According to the standard, surface sampling involves the use of contact plate, tape-lift or swab to obtain the spores which are further analysed by direct microscopy or processed and cultured using appropriate culture media [25]. In the remediation and/or investigation of mould infestation, where the affected area and extent of damage is severe, bulk sampling is employed. It involves taking a part or whole of materials for laboratory analysis of not only the causative species of mould but also the extent of damages on the materials. Aerosol sampling on the other hand requires samples to be taken by the exposure of a suitable culture media i.e. agar to the ambient air. Various approach exists in aerosol method of mould sampling and identification—direct/settled plate or sedimentation method [6, 26], filtration method [27] and impaction [28]. The impaction methods involves sampling of particles suspended in air by inertial separation on culture media.

The culture media for mould inoculation varies in their nutrients' composition. Common types of culture media include: Dichlorane 18 % Glycerol Agar (DG18 agar), Malt-extract agar, Potato dextrose agar (PDA), Sabouraud Dextrose Agar (SDA) etc. In addition, moulds are identified by direct microscopy [20] where airborne mould spores are either collected on filters or directly on an adhesive-coated microscope slide, followed by staining and later by microscopic observation. In all the various sampling methods of mould sampling and identification, the choices are determined by the objective of the investigation [20].

1.4 Study Aim and Objectives

This study reports the case of a mould infested library located in Kuala Lumpur Malaysia. The aim is to investigate, isolate and identify the predominant mould species in the library on one hand the contribution of the microclimate distribution to the mould growth. The objective of the study is to identify the mould specie and evaluate the indoor microclimate profile supporting mould growth in a typical mechanical ventilated building in Malaysia.

2 Methodology

2.1 Description of the Case Study

The library building (about 80 m above mean sea level) is located on one of the campuses of a public university in the peninsular Malaysia. The library was commissioned in 1989 with (presently) a total collection of about 150,000 volumes of books and other print media comprising both historic and present day anthologies. There had been a growing concern by the library's staff over the microclimate in the level that housed the manuscript in its ability to properly preserve the collections due to the presence of visible mould growth. Hence, the manuscripts collections (rare books & scholars section) level was selected as the case study in this study. The overall size is 35.33 m × 6.05 m × 3.2 m high (Area = 213.75 m², Volume = 684 m³, and A/V ratio = 0.31). Three of the boundary walls are located adjacent to other indoor spaces, hence only one wall is exposed to the external ambient weather with 12 single panel metal window (Fig. 2). It is also located in the middle floors and as such, has reinforced concrete suspended slab above and below it. The ventilation system comprises of all-air central air conditioning system which controls both air temperature (T) and relative humidity (RH). It also includes split systems as buffer in situation where the central HVAC system is not in operation. Operation hours are between 8:30 am and 7:30 pm (weekdays) and closed (on weekends and public holidays).

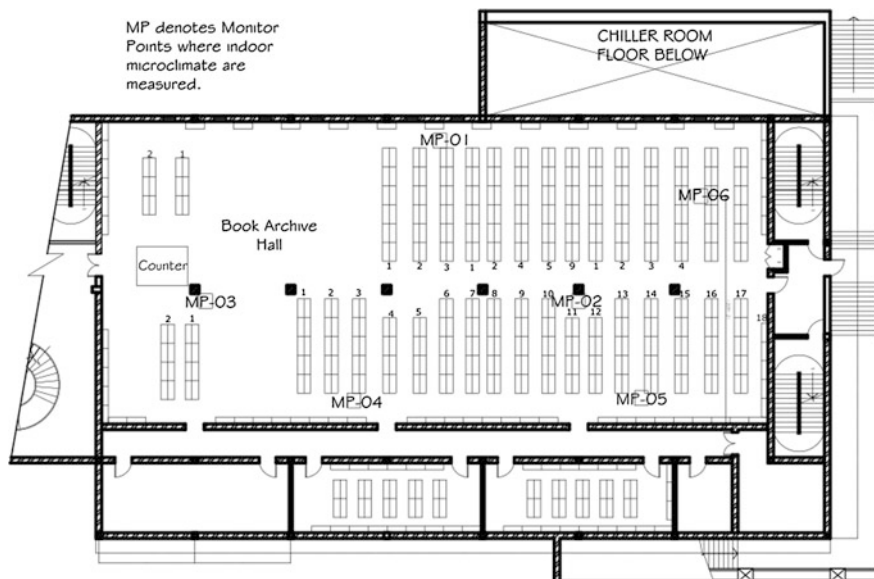


Fig. 2 Layout of the case study library—MP-01 to MP-06 represents the monitoring points where the indoor microclimatic parameters and mould samples were taken

2.2 Microclimate Sampling

The methodology involves microclimate measurement with array of data loggers mounted in the indoor space. The data loggers were installed close to the areas of visible mould growth to best capture the local conditions of the infested areas. Six (6) data loggers were installed within the library for a period of eight (8) days from 27/9/2013 to 4/10/2013. The data loggers were HOBO U12 from Onset Computer Corp. They were calibrated before and after measurements to ensure measurement consistency and reliability. The uncertainty of the measured T and RH were in accordance with the data logger manufacturer specifications. The measurement accuracy are ± 0.35 °C, T and ± 2.5 %, RH with precision 0.03 °C, T and 0.03 %, RH. To reduce the measurement error and improve the data representativeness, time-weighted average is employed as time-averaging reduces measurement errors—BS 6069-5.1 [29]. The sensors logged data at every 10 min result in six time-steps data per hour to give a total of 1,152 (i.e. 6 datapoints \times 24 h/day \times 8 days) rows of microclimatic parameters.

The study presents time-series plots of days against the indoor temperature (T) and relative humidity (RH). As a further check on the microclimate performance, the data is plotted on psychrometric chart where the mean indoor T and RH of the monitor points were shown in relation to the ASHRAE [30] comfort zone (Class A) for archival materials (value ranges: T = 15–25 °C; RH = 40–60 %). In addition, the

distribution of microclimatic condition of the library is presented as a contour plot, the procedure of which had been previously reported in [31].

2.3 Microbial Sampling

The study adopts a combination of material and aerosol sampling protocols. The material sampling involves the swabbing of sterile cotton (swab) over the surfaces of the infested books. The swab were rubbed against the culture media surface. The culture media were of two types: potato dextrose agar (PDA-potato starch 4.0 g; Dextrose 20.0 g; and Agar 15.0 g) and sabouraud dextrose agar (SDA-mycological peptone 10.0 g; glucose 40.0 g; and Agar 15.0 g). In the aerosol sampling, the agar was exposed on the book shelves for about 1 h in a similar manner to [26]. The petri dish holding agar were quickly sealed with paraffin tape immediately after the sampling to prevent secondary contaminants. All the agar plates were sealed in plastic bags to protect the samples during transport for subsequent laboratory analysis. In the laboratory, the agar plates were incubated for 7 days at 25 ± 2 °C. The microbes were identified to their specific genus by macroscopic and microscopic examinations. For microscopic examinations, lactophenol cotton blue (LPCB) staining was used for mould identification and Gram staining was used for bacteria and yeast identification [4, 5].

3 Results and Discussion

3.1 Microclimatic Assessment

The most controllable of all the limiting growth factors of indoor mould fungi are the thermal (temperature) and hygric (humidity) parameters [2]. Figure 3 revealed the indoor hygrothermal profile for T (Fig. 3a) and RH (Fig. 3b). The results show

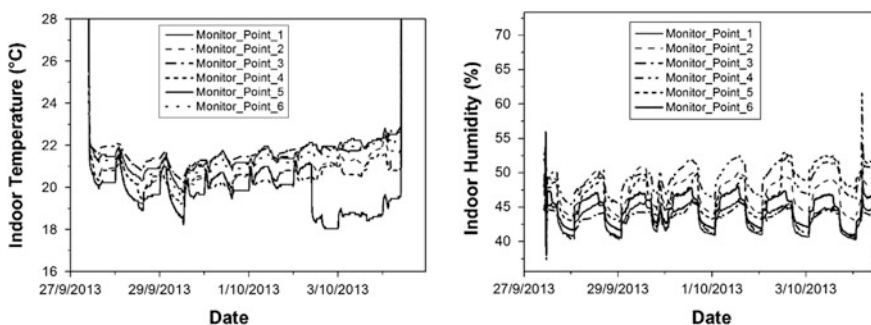


Fig. 3 Time series plot of indoor microclimate (T and RH)

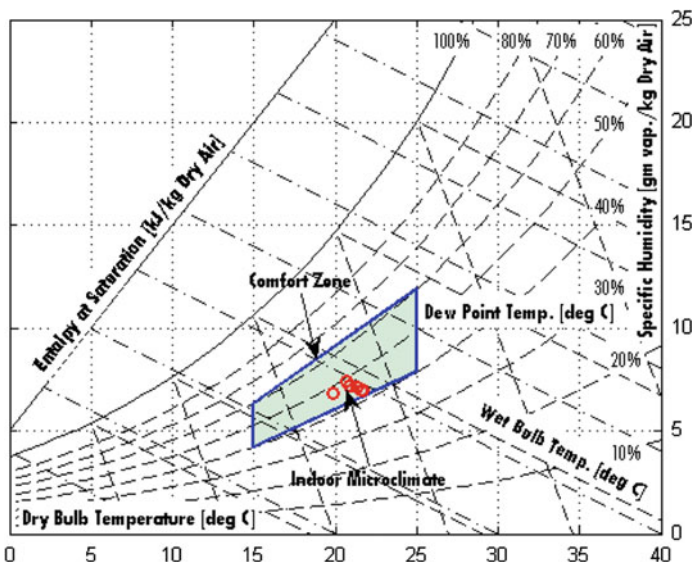


Fig. 4 The psychrometric chart showing the mean (monitor points) microclimatic parameters of the library relative to ASHRAE operative conditions

that both T and RH along the time axis are parallel for all the monitored points save MP5 with variation between 2nd to 4th October. On the psychrometric chart (Fig. 4), values of T and RH revealed that the indoor environment operates at a lower extreme when benchmarked against ASHRAE conservation operative conditions.

Results of the contour plots (Figs. 5 and 6) revealed uneven distribution of the hygrothermal profile in the book archive. Generally, low temperature and high humidity characterises the book shelf area. At 8:00 am, the archive shows a relatively cold interior with the corresponding higher humidity (Fig. 5). In the afternoon (Fig. 6) when the external ambient condition is thermally critical, hot region is revealed around the external wall yet the book shelf area remain relatively cold a situation that results in higher humid condition. These hygrothermal stratifications in the library provides a safe haven for mould to thrive. The observed conditions of the microclimate monitoring suggest poor performance of the

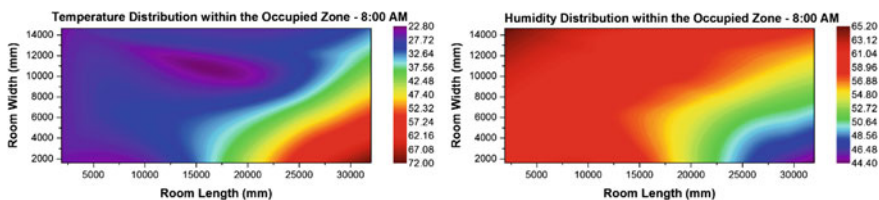


Fig. 5 Indoor microclimate distribution within the book archive at 8:00 am

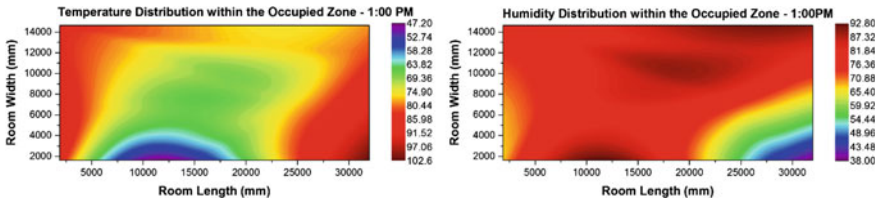


Fig. 6 Indoor microclimate condition within the library at 1:00 pm

ventilation systems and hence the mould proliferation. Good air distribution is an excellent way of preventing microbial infestation [7].

3.2 Microbial Assessment

The microbial investigation results in 72 isolates whose distribution were 86 % mould, 13 % yeast and 1 % bacteria. This revealed that about 99 % of the identified microbes were fungi with only 1 % bacteria. This goes in tandem with the statement of [6] that “fungi are the most harmful microorganisms to paper as they have the ability to grow at lower water activity (*Aw*) than bacteria.” From the isolated fungi, 86 % were mould while the remaining 13 % were yeast. This shows that the indoor space is highly infested with mould. Figure 7 shows the specie distribution of the microbes. It is found that *Aspergillus* sp. and *Onychocola* sp. were most common having 26 and 22 % of the total isolates respectively.

Conversely, the smallest group of the isolates were *Paecilomyces* amounting to 6 % of the total isolates. Other species of mould as identified are: *Lecythophora* sp. (8 %), *Microsporium* sp. (14 %), and *Penicillium* sp. (10 %). Some of the fungi isolated from

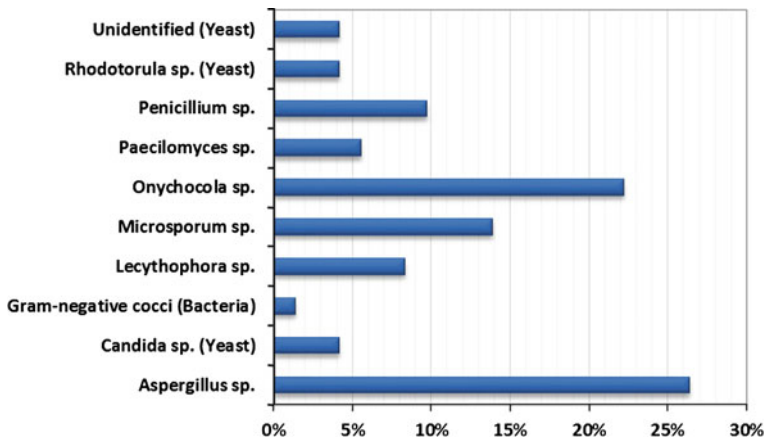


Fig. 7 Distribution of the identified species of microbes in the library



Fig. 8 Samples of book from the library with biofouling due to visible mould growth

the air inside the library may be harmful to the books as *Aspergillus* and *Penicillium* species are found to be among the fermentative organisms that excrete many organic acids resulting in biodeterioration [3, 6]. *Aspergillus* sp., *Penicillium* sp., and some other major mould fungi genera isolated from archival environments (libraries, museums etc.) exhibit cellulolytic, proteolytic, and/or amyolytic activities, producing acids, excreting different pigments onto the substrata, and contributing to the formation of biofilms that stimulate the base materials' deterioration [6]. This according to the authors, is due to the microbes exhibiting cellulolytic, proteolytic, and/or amyolytic activities, producing acids, excreting different pigments onto the substrata, and contributing to the formation of biofilms that stimulate the base materials' deterioration. Figure 8 shows samples of books from the library with visible mould growth.

The results further revealed that some species preferred the nutrients of SDA to PDA and vice versa. The ratio of percentage distribution of isolates based on SDA: PDA from the dominant species are 19:47 (swab) and 14:23 (Aerosol) for *Aspergillus* sp.; 23:21 (swab), 21:23 (Aerosol) for *Onychocola* sp. In addition, some species grow on either of the two media. This results relates to the submission of [3] that a direct relationship exists between the type of culture media and the species composition of microbes isolated from air due to the variation in the available nutrients to the sampled and cultured microbes.

4 Conclusions

The microbial investigation of the infested library results in 72 isolates whose distribution were 86 % mould, 13 % yeast and 1 % bacterial. It is found that *Aspegillus* sp. and *Onychocola* sp. were dominant species having 26 and 22 % of the total

isolates respectively. Other species of mould as identified are: *Lecytophora* sp., *Microsporium* sp., *Paecilomyces* sp. and *Penicillium* sp. It was found that the indoor space is highly infested with mould. The results of the microclimate revealed a highly stratified indoor hygrothermal distribution. This indicates poor air distribution and invariably poor performance of HVAC systems in the library. The internal microclimate is negatively impacting the hygrothermal profile which provides a safe haven for mould to thrive hence, a high level of *Aspegillus* and other species in the library which are found to be highly detrimental to books and other archival materials. It is therefore recommended that the HVAC system operations and set-points be reviewed to bring the ambient conditions to the preservation requirements. In addition, load balancing for thermal and hygric distribution analysis should be carried out to eliminate dead-spots in temperature and moisture distributions.

Acknowledgment The results presented in this study is part of a multidisciplinary research project (FRGS12-067-0126) engineered towards indoor mould growth prediction using thermal characteristics in the tropical climate buildings by the Ministry of Higher Education (MOHE) Malaysia. The financial supports is gratefully acknowledged.

References

1. P. Elumalai, E. Elumalai, E. David, Fungi associated with deteriorations of painted wall surfaces: isolation and identification. *Eur. J. Acad. Essays* **1**, 48–50 (2014)
2. M. Steeman, M. De Paepe, A. Janssens, Impact of whole-building hygrothermal modelling on the assessment of indoor climate in a library building. *Build. Environ.* **45**, 1641–1652 (2010)
3. R. Ogórek, A. Lejman, K. Matkowski, Influence of the external environment on airborne fungi isolated from a cave. *Pol. J. Environ. Stud.* **23**, 435–440 (2014)
4. K. Hess-Kosa, *Indoor air quality: the latest sampling and analytical methods* (CRC Press, USA, 2012)
5. C.S. Yang, P.A. Heinsohn, *Sampling and analysis of indoor microorganisms* (Wiley-Interscience, Hoboken, NJ, 2007)
6. P. Lavin, S.G. Gomez de Saravia, P.S. Guiamet, An environmental assessment of biodeterioration in document repositories. *Biofouling* **30**, 561–569 (2014)
7. S. Borrego, P. Lavin, I. Perdomo, S. Gomez de Saravia, P. Guiamet, Determination of indoor air quality in archives and biodeterioration of the documentary heritage, *ISRN Microbiol* **2012**, 680598 (2012)
8. AIHA, *Facts About Mold* (online, 15th October). Available: <http://www.aiha.org/get-involved/VolunteerGroups/Documents/BiosafetyVG-FactsAbout%20MoldDecember2011.pdf>
9. D. Mudarri, W.J. Fisk, Public health and economic impact of dampness and mold. *Indoor Air* **17**, 226–235 (2007)
10. C. Palatya, M. Shum, *Health Effects from Mould Exposure in Indoor Environments* (2009, 18th August). Available: http://www.ccnse.ca/sites/default/files/Mould_and_Health_Effects_Nov_2009.pdf
11. D.C. Straus, Molds, mycotoxins, and sick building syndrome. *Toxicol. Ind. Health* **25**, 617–635 (2009)
12. G.T. Christina, H. Joachim, Exposure assessment of residential mould, fungi and microbial components in relation to children's health: achievements and challenges. *Int. J. Hyg. Environ. Health* **216**, 109–114 (2013)

13. H. Altamirano-Medina, M. Davies, I. Ridley, D. Mumovic, T. Oreszczyn, Guidelines to avoid mould growth in buildings. *Adv. Build. Energy Res.* **3**, 221–235 (2009)
14. AIHA, *Position Statement on Mold and Dampness in the Built Environment* (American Industrial Hygiene Association, USA, 2013, online)
15. S.C. Wilson, R.N. Palmatier, L.A. Andriychuk, J.M. Martin, C.A. Jumper, H.W. Holder et al., Mold contamination and air handling units. *J Occup. Environ. Hyg.* **4**, 483–491 (2007)
16. O.M. Bankole, A review of biological deterioration of library materials and possible control strategies in the tropics. *Libr. Rev.* **59**, 414–429 (2010)
17. H. Janssen, J.E. Christensen, Hygrothermal optimisation of museum storage spaces. *Energy Build.* **56**, 169–178 (2013)
18. S. Borrego, I. Perdomo, Aerobiological investigations inside repositories of the National Archive of the Republic of Cuba. *Aerobiologia* **28**, 303–316 (2011)
19. J.A. Clarke, *Energy Simulation in Building Design* (Butterworth-Heinem, Oxford, 2001)
20. British Standard Institution, BS ISO 16000-19:2012 Indoor air—Part 19: Sampling strategy for moulds, ed: BSI (2012)
21. J. Hensen, R. Lamberts, *Building performance simulation for design and operation* (Taylor & Francis, UK, 2011)
22. A.F. Cruz, Keeping a lid on superbugs. *New Straits Times* (online, 12th September 2013). Available: <http://blis2.bernama.com.ezproxy.psz.utm.my/getArticle.do?id=147876&tid=79&cid=3>
23. A.F. Cruz, Sick Hospital Ready to Serve. *New Straight Times* (online, 12th September 2013). Available: <http://blis2.bernama.com.ezproxy.psz.utm.my/getArticle.do?id=21492&tid=49&cid=3>
24. British Standard Institution, BS ISO 16000-21:2013 Indoor air—Part 21: detection and enumeration of moulds—Sampling from materials, ed: BSI (2013)
25. British Standards Institution, BS ISO 16000-17:2008 Indoor air—Part 17: detection and enumeration of moulds—Culture-based method, ed: BSI (2008)
26. F. Pinzari, M. Montanari, Mould growth on library materials stored in compactus-type shelving units, in *Sick Building Syndrome: In Public Buildings and Workplaces*, ed. by S.A. Abdul-Wahab (Springer, Heidelberg, 2011), pp. 193–206
27. British Standards Institution, BS ISO 16000-16:2008 Indoor air—Part 16: detection and enumeration of moulds—sampling by filtration, ed: BSI (2008)
28. British Standard Institution, BS ISO 16000-18:2011 Indoor air—Part 18: detection and enumeration of moulds—Sampling by impaction, ed: BSI (2011)
29. British Standards Institution, BS 6069-5.1-1994 Characterization of air quality—Handling of temperature, pressure and humidity data, ed: BSI (1994)
30. ASHRAE, Chapter 21: Museums, galleries, archives, and libraries, in *ASHRAE, Applications Handbook (SI)*, ed. M. S. Owen (American Society of Heating, Refrigerating and Air Conditioning Engineers, Atlanta, USA, 2010) pp. 21.1–21.3
31. M. Ali, M.O. Oladokun, S. Osman, An improved method to evaluate indoor microclimatic data: case study of a book archive in a hot and humid climate, in *13th International Conference on Indoor Air Quality and Climate, Indoor Air*, Hong Kong, 2014

Palm Oil Fuel Ash and Ceramic Sludge as Partial Cement Replacement Materials in Cement Paste

Nurliyana Ismail, Mohd Fadzil Arshad, Hamidah Mohd Saman and Mazni Mat Zin

Abstract Palm oil fuel ash (POFA) and ceramic sludge (CS) are waste materials that found produced abundantly in the palm oil and the porcelain industrial sectors respectively. However, these waste materials are improperly managed that proved can give adverse impacts to the environment and human's health. This research was carried out in order to identify the potential of POFA and CS as partial cement replacement materials in cement paste. POFA was prepared at 10, 20, 30 and 40 % replacement of Ordinary Portland cement (OPC) and CS was prepared at 60 % substitution of the cement paste. The effects of POFA and CS in the cement paste in term of compressive strength at 1, 3, 7, and 28 days of curing were also determined. The results indicated that the optimum compressive strength of cement paste was achieved by P2 containing 10 % POFA: 30 % OPC: 60 % CS. As a result, the utilisation of POFA and CS as partial cement replacement materials can significantly reduce the high amount of OPC usage apart of reducing the environmental problems and human's health problems.

Keywords Waste materials · Cement replacement · Compressive strength · Blended binder · Sustainable environment

N. Ismail (✉) · H.M. Saman · M.M. Zin
Faculty of Civil Engineering, Universiti Teknologi MARA, Shah Alam, Malaysia
e-mail: nurliyana_ismail@ymail.com

H.M. Saman
e-mail: hmohdsaman@salam.uitm.edu.my

M.M. Zin
e-mail: maznimatzin@yahoo.com

M.F. Arshad
Faculty of Civil Engineering, Institute of Infrastructure Engineering and Sustainable Management (IIESM), Universiti Teknologi MARA, Shah Alam, Malaysia
e-mail: fadiil2013@yahoo.com

1 Introduction

Palm oil fuel ash (POFA) is an agro-waste ash which its production is increasing throughout years.

This is same goes to the sludge that is abundantly produced in the ceramic industrial sectors. Due to this problem, large land areas for disposing these waste materials are required as well as increasing the cost for transportation and maintenance of the waste materials [1]. Apart of that, the generation of these waste materials caused a lot of environmental problems such as polluting the air and contaminating the sub-surface water resulted to human's health problems when expose to it [2, 3]. However, the problems can be solved by properly consumption or recycle of these waste materials.

Recycling the waste materials such as POFA and ceramic sludge (CS) can be very beneficial. POFA as one of the pozzolanic materials can be used for many applications such as cement replacement [4] or even used as renewable energy resource [5]. Pozzolanic material is fine materials which containing silica and/or alumina react to form cementitious materials in the presence of calcium oxide (CaO_2) or calcium hydroxide ($\text{Ca(OH}_2\text{)}$) [6]. As a result, more calcium silicate hydrate (C-S-H) gel compounds are developed hence reducing the amount of $\text{Ca(OH}_2\text{)}$ that tends to lower down the strength of the end products. Based on this, silicon dioxide (SiO_2) is a major composition of POFA. POFA when used as cement replacement material can exhibit high strength concrete that is even higher as compared using the normal cement [7]. In addition, the fineness of the POFA can also assist in developing good strength of the end products. The fineness the POFA particles the highest the strength developed. Meanwhile, ceramic products such as bricks and tiles are having the heterogeneous composition whereby those materials are being formed by clay raw materials with a very wide range composition [8]. Specifically, CS is a siliceous material as SiO_2 is the major compound in the sludge and believed can also contribute to strength development [9].

Many attempts in terms of utilising the waste materials have been done, but there is no identified utilisation of POFA and CS together as partial cement replacement in cement paste. Therefore, usage of POFA and CS as binder for cement paste would represent approaches in solving its disposal problems as well as providing cost-effective cement replacement materials. The objective of this research was to identify the potential of POFA and CS as partial cement replacement materials in cement paste. The effectiveness of POFA and CS as to reduce the use of OPC was assessed by analysis the compressive strength at different days.

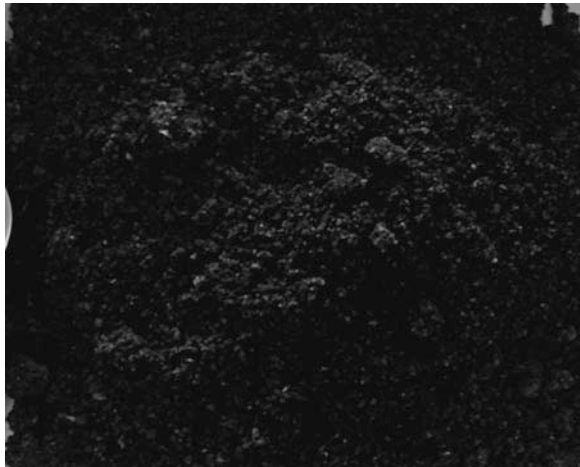
2 Materials and Method

Ordinary Portland cement (OPC) conforming to MS 522: Part 1: 1989 was used as the binder system. POFA used in this research was collected from Kilang Sawit Jengka 21, Pahang, Malaysia. CS was collected from sedimentation tank located in

Fig. 1 Ordinary portland cement (OPC)



Fig. 2 Palm oil fuel ash (POFA)



Johan Ceramic Berhad, Senawang Industrial Estate, Malaysia. The OPC, POFA and CS were shown in Figs. 1, 2 and 3 respectively. Table 1 presented the chemical compositions of OPC, POFA and CS.

For this research, five (5) mixtures were prepared. P1 was a control sample containing standalone OPC added with 60 % CS. The rest of mixtures containing 10, 20, 30 and 40 % of POFA to replace OPC added with 60 % CS. All of the mixtures are as presented in Table 2. Water/binder ratio of 0.5 was used. The mixtures were casted in cube steel mould size of 50 mm × 50 mm × 50 mm, de-mould after 24 h and left under sheltered area for 1, 3, 7 and 28 days before tested. The compressive strength test was carried out as accordance to BS 1881: Part 1: 1983.

Fig. 3 Ceramic sludge (CS) in sedimentation tank



Table 1 Chemical compositions of OPC, POFA and CS

Chemical composition	OPC (%)	POFA (%)	Sludge (%)
CaO	63	3.05	11.41
SiO ₂	20	43.5	53.35
Al ₂ O ₃	5.7	3.19	7.87
MgO	0.99	–	–
Fe ₂ O ₃	2.9	–	–
SO ₃	3.5	–	–
Na ₂ O	0.08	–	–
K ₂ O	1.2	5.67	2.61
LOI	2.63	–	–
Others	–	31.22	24.76

Table 2 OPC:POFA:CS mix proportions

Mixtures	OPC:POFA:CS
P1	40:0:60
P2	30:10:60
P3	20:20:60
P4	10:30:60
P5	0:40:60

3 Results and Discussions

Figure 4 presents the compressive strength of cement paste containing POFA and CS at day 1, 3, 7, and 28 days as cement replacement material. Control sample which is P1 containing OPC and CS showed that there was increasing in early

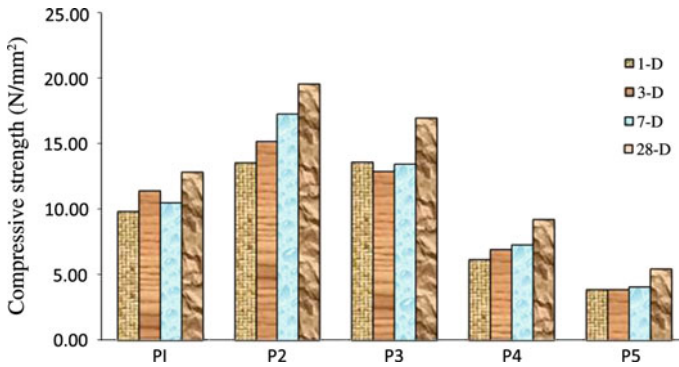


Fig. 4 Compressive strength for P1, P2, P3, P4 and P5

strength. But, the strength decreased at day 7 and continuously increased for day 28. It is known that when 40 %OPC is used for cement paste preparation, the strength of cement paste is keeps on increasing no matter for how long days of curing. So, it is cleared that the CS added gives an effect to the solidification of cement paste. As referred to the other mixtures, the addition of sludge at 60 % replacement of cement definitely tends to decrease the compressive strength. The highest the amount of sludge added the lowest the compressive strength achieved [10].

P2 is a mixture contained 10 %POFA: 30 %OPC: 60 %CS. It was found that the strength of cement paste continuously increased up to 20 MPa for 28 days of curing. Based on this, it can be said that 10 %POFA was strongly assists in the strength development as compared to P1. Although the sludge added can enhance the strength development of the cement paste, the strength development was not consistent. So, the addition of POFA in the mixture had overcome the condition.

POFA and CS contain 43.50 and 53.35 % of SiO₂ respectively. Since CaO in OPC is about 63.0 %, the hydration between SiO₂ and CaO formed the C–S–H assists in the strength development. However, the excess SiO₂ may substitute part of the cementitious material and consequently cause a reduction in strength [11]. This is what happened to P3, P4 and P5 mixtures. The strength of P3, P4 and P5 were decreased with a relative increased either in POFA or CS. When POFA was added at 20 %, 30 % and 40 % replacement of cement, the compressive strengths achieved at 28-day were lower than using 10 %POFA. The compressive strength achieved was even lowered to 5 MPa that was four times lower than using 10 % POFA with 60 %CS.

Furthermore, P3, P4 and P5 did not harden sufficiently as the mixtures did not have ample CaO. CaO is required in order to sustain strength development throughout the curing periods [12]. In this case, the reduction of strength for P3, P4 and P5 may be due to higher POFA and CS weight substitution. This is because POFA and CS is less in CaO as compared to OPC. Therefore, the optimum percentage replacement of cement is 10 % for this type of POFA with 60 %CS.

4 Conclusion

It is found that POFA and CS are the potential waste materials that can be utilized as partial cement replacement materials in cement paste. At specific weight percentage replacement, POFA and CS able to produce hardened cement paste at an appropriate strength. In this research, the optimum percentage replacement of POFA is 10 % with the addition of 60 % of CS for the cement paste production. The compressive strength achieved by utilising 10 % POFA in the mixture is approximately 20 MPa. It is hoped that the problems generated to the environment and human's health can be solved apart of reducing the cost of consuming OPC by fully utilising POFA and CS.

Acknowledgments The first author is a PhD candidate of Faculty of Civil Engineering, Universiti Teknologi MARA, Malaysia and this paper is part of her research.

References

1. D. Ivšić-Bajčeta, Ž. Kamberović, M. Korać, M. Gavrilovski, A solidification/stabilization process for wastewater treatment sludge from a primary copper smelter. *J. Serb. Chem. Soc.* **78** (5), 725–739 (2013)
2. B.C. McLellan, R.P. Williams, J. Lay, A. Van Riessen, G.D. Corder, Costs and carbon emissions for geopolymer pastes in comparison to ordinary portland cement. *J. Clean. Prod.* **19**, 1080–1090 (2011)
3. K. Celik, M.D. Jackson, M. Mancio, C. Meral, A.-H. Emwas, P.K. Mehta, P.J.M. Monteiro, High-volume natural volcanic pozzolan and limestone powder as partial replacements for portland cement in self-compacting and sustainable concrete. *Cement Concr. Compos.* **45**, 136–147 (2014)
4. S.O. Bamaga, M.W. Hussin, M.A. Ismail, Palm oil fuel ash: promising supplementary cementing materials. *KSCE J. Civil Eng.* **17**(7), 1708–1713 (2013)
5. S. Yusoff, Renewable energy from palm oil—innovation on effective utilization of waste. *J. Clean. Prod.* **14**, 87–93 (2006)
6. H.M. Owaid, R. Hamid, M.R. Taha, A review of sustainable supplementary cementitious materials as an alternative to all-portland cement mortar and concrete. *Aust. J. Basic Appl. Sci.* **6**(9), 287–303 (2012)
7. M.R. Karim, M.F.M. Zain, M. Jamil, M.N. Islam, Strength of concrete as influenced by palm oil fuel ash. *Aust. J. Basic Appl. Sci.* **5**(5), 990–997 (2011)
8. C. Martínez-García, D. Eliche-Quesada, L. Pérez-Villarejo, F.J. Iglesias-Godino, F.A. Corpas-Iglesias, Sludge volarization form wastewater treatment plant to its application on the ceramic industry. *J. Environ. Manage.* **95**, S343–S348 (2012)
9. F. Dellisanti, P.L. Rossi, G. Valdrè, Mineralogical and chemical characterization of joule heated soil contaminated by ceramic industry sludge with high Pb contents. *Int. J. Mineral. Process* **83**, 89–98 (2007)
10. E.E. Hekal, W.S. Hegazi, E.A. Kishar, M.R. Mohamed, Solidification/stabilization of Ni(II) by various cement pastes. *Constr. Build. Mater.* **25**, 1109–1114 (2011)
11. P. Fongsatikul, P. Elefsiniotis, D. Kitkaew, C. Rungsipanodom, Use of rice husk ash as an admixture to remove chromium from a tannery waste. *Water Air Soil Pollut.* **220**, 81–88 (2011)
12. C.Y. Yin, W.S.W. Ali, Y.P. Lim, Oil palm ash as partial replacement of cement for solidification / stabilization of nickel hydroxide sludge. *J. Hazard. Mater.* **150**, 413–418 (2008)

Part VIII
Timber Engineering

Analysis of Pre-fabricated Timber Roof Truss

Khairul Salleh Baharudin, Zakiah Ahmad, Azmi Ibrahim and Mohamed Rassam

Abstract Pre-fabricated timber roof truss made of glued laminated timber (glulam) may deem more efficient in supporting the load compared to similar truss made of solid timber. An analysis was conducted on single and double Fink trusses made of solid and glulam timber from selected Malaysian tropical timber with similar configurations. For solid timber truss, the timber used was Kempas from strength grouping SG2 whilst glulam, Mengkulang from SG5 was used since the glulam technology enhanced the strength properties of solid timber into two grades higher. Comparisons were made on the optimum sections designed for the trusses to support similar loadings. Various load patterns were also applied to the trusses to observe the worst-case scenario that resulted in the selection of the optimum sizes of each truss elements. The different combinations of load patterns, namely load applied on member and on node, with and without wind loads, and, symmetric and asymmetric loadings were analyzed. Two significant findings were observed in this analysis. First, glulam truss from a lower stress grade material can be of comparable structural performance to a solid truss from a higher-grade material. This can provide a cost-effective measure as alternative to solid truss since the differences in

K.S. Baharudin (✉)

Faculty of Civil Engineering, UiTM, Shah Alam, Malaysia
e-mail: khairul@iukl.edu.my

Z. Ahmad · A. Ibrahim

Faculty of Civil Engineering, Institute for Infrastructure Engineering and Sustainable Management (IIESM), UiTM, Shah Alam, Malaysia
e-mail: zakiah@salam.uitm.edu.my

A. Ibrahim

e-mail: azmii716@salam.uitm.edu.my

M. Rassam

Infrastructure University Kuala Lumpur (IUKL), Kajang, Malaysia
e-mail: rassam2075@gmail.com

volume are small. Second, the worst-case scenario of load pattern for the truss for designed consideration is when the truss is symmetrically loaded on both nodes and members of the top chords and without the inclusion of wind load.

Keywords Truss · Glulam · Kempas · Mengkulang

1 Introduction

Typical prefabricated timber roof truss may come in various configurations. The arrangement of members in the truss will vary the amount of timber used for the truss due to load distribution and supports given by the truss elements. The lesser amount of timber usage for the truss reflects the efficiency of the truss members in supporting the loads. The behavior of members made of solid timber is expected to be different from that of glulam under the same truss configuration and with the same load pattern. The load patterns in combination with or without wind loads, with symmetrical or asymmetrical loadings, and with the loads applied on members or on nodes, require different member sizes to support the loads. The requirement for the optimum sizes of different materials, either solid or glulam, in supporting the loads under different truss configurations and load patterns are yet to be investigated. Furthermore, the worst-case scenario in which the requirement for the amount of timber among various configurations and load patterns need to be evaluated.

2 Literature Review

Timber structures need to be carefully analyzed as their significance and constant presence in construction especially roof truss. If there exists misunderstanding of their behavior, the risk is, in few years, they can disappear. The structural designers must understand the material properties and must be able to interpret the structural system performance as well as global behavior of timber structures. The misunderstanding could lead to unacceptable stress distribution in the members.

Trusses are a series of girders which have been reduced to an assembly of simple struts connected by pin connections. Struts are stressed either in compression or in tension. The size of compression members are controlled by buckling, while the size of tension members is dictated by tensile stresses at the weakest points which are generally at the connections. Hence, the cross sectional area of a member need to be increased in order to get a convenient connecting surface at connections. The top chords of a truss are designed against buckling by lateral bracing [1].

Shaeffer [2] stated that strength is the ability of the selected materials to resist the stresses generated by loads and shapes of the structure. When designing a roof structure, the main consideration is, what is the most economical solution to span the roof and its dead load over the span of varying degrees. Therefore, the problem in

designing long span roof structure is to get the ratio of dead load to live load to be as low as possible with respect to other factors relating to the design as a whole [3]. In solving these problems there are two important factors to be considered namely; (i) characteristic of the material used and (ii) the design of the roof structure.

Tomusiak [4] studied on the application of different types of roof trusses in wooden constructions. He analyzed four different configurations of timber trusses, namely the Fink type, truss with vertical posts, truss with four diagonals and the “M” type with trusses spans of 8, 10 and 12 m and 19° slopes. He concluded that Fink type truss required the least amount of timbers. Götz et al. [5] claimed that trussed rafters can have span up to 10 m, fink truss up to 10 m, double fink truss between 5 and 14 m. Branco [6] surveyed several timber roofs structures in Portugal in order to collect common values and ranges of geometry, timber species, type of connections, and load parameters. He found that the span defines the truss configuration used. For common Portuguese timber roof structures, trusses with an average span of 6 m, mostly following a king-post configuration were used [7]. Al-Chaar and Issa [8] developed a comprehensive structural evaluation procedure for wood trusses. He observed the moments, displacements, deflection, and shear forces for different semi-rigid models in order to determine a critical scenario.

Numerous reseachers showed that the strength of timber changed even within a single species [9, 10]. The density and strength of timbers depends very much on the thickness of tracheid walls and percentage of latewood. The presence of inherent defects can also affect the strength. Therefore to overcome the variability in properties of solid timber, engineered timber product such as glulam can be an alternative materials. Glulam is an engineered stress rated timber product that consists of two or more layers of timber glued together to form a solid member. Wayne [11] suggested that basicly glulam is not stronger than lumber, because gluing does not have an effect on strength, but wisely selected laminations the bending strength exceeds that of the lumber.

3 Methodology

3.1 Software

Prokon software was used in the analysis of the trusses. The software was used to design the selection of optimized sections for the trusses after assigning the various loading patterns and materials to the assigned trusses.

3.2 Truss Configurations

Two different truss configurations were analysed. Single and double Fink trusses of 8-m span with 2-m high and angle slope of 1:2 (26.57°) were selected as shown in Fig. 1.

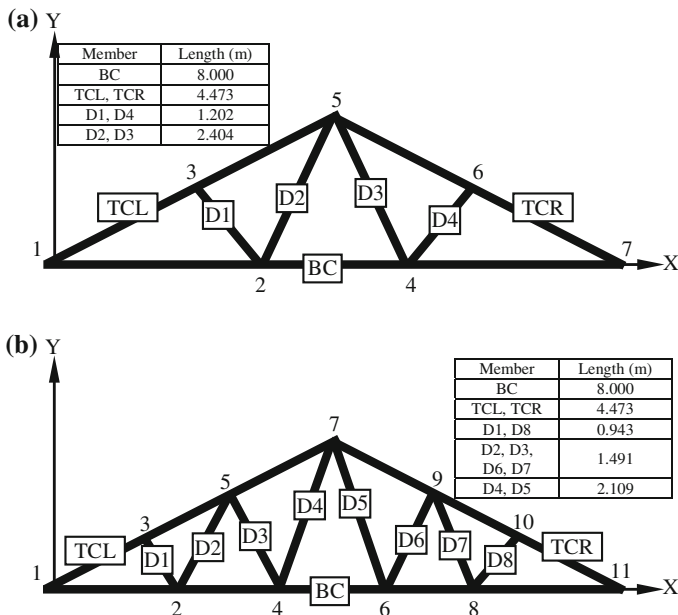


Fig. 1 Truss configurations: **a** Fink truss, and **b** double fink truss

Both trusses are statically determinate. The truss members are designated as bottom chord (BC), top chord left (TCL), top chord right (TCR), and diagonal chords (D). Diagonal chords are numbered D1 to D4 for single Fink truss, and D1 to D8 for double Fink truss. They are numbered from left to right of the truss. Both top and bottom chords are considered continuous member. Each single and double Fink trusses were then assigned as solid and glulam trusses for evaluation.

3.3 Materials

Two types of materials were assigned to evaluate the trusses. Kempas species of grade SG2 [11] were used in the solid truss, whilst Mengkulang species of structural grade D40 [12] were used in the analysis of glulam truss. Mengkulang, as solid member, under MS544: Part 2:2001 belongs to grade SG5, which is three grades lower than Kempas. The properties of the two species are as shown in Table 1.

3.4 Load Pattern

Eight different combinations of load patterns as shown in Table 2 were used in this study for each single and double Fink truss using solid and glulam members. The different

Table 1 Property of timber species

Grade	Mengkulang (D40) [13]	Kempas (SG2) [12]
Bending parallel to grain (N/mm ²)	15.9	14.6
Tension parallel to grain (N/mm ²)	9.5	8.8
Compression parallel to grain (N/mm ²)	14.9	15.6
Shear perpendicular to grain (N/mm ²)	3.6	3.12
Shear parallel to grain (N/mm ²)	1.7	1.58
Modulus of elasticity (N/mm ²)	14,300	17,700
Density (kg/m ³)	700	910

Table 2 Load patterns

Load pattern number (LP)	Loads applied on	Wind	Symmetric or asymmetric
1	Members	Yes	Symmetric
2			Asymmetric
3		No	Symmetric
4			Asymmetric
5	Nodes	Yes	Symmetric
6			Asymmetric
7		No	Symmetric
8			Asymmetric

combination load patterns were loads applied with and without wind load, applied at node points only and applied both on members, which are symmetric or asymmetric. The asymmetric loads were loads applied at only one side of the truss. Figure 2 illustrates the load patterns applied in nodes and on members described earlier.

In the analysis, a dead load of 0.85 kN/m², a live load of 0.75 kN/m² and a wind load of 0.85 kN/m² were used. The windward C_{pe} of -0.44, leeward C_{pe} of -0.6 and internal pressure coefficient C_{pi} of -0.212 were adopted.

4 Result and Discussion

4.1 Optimized Cross Sections

Table 3 summarizes the optimized cross section designed for different load patterns. A total of 32 combinations of trusses are designed based on the combination of 8 different load patterns for a Fink and Double Fink trusses, and from two different materials. Comparisons are focused on the optimized sections required between Mengkulang glulam and Kempas solid trusses.

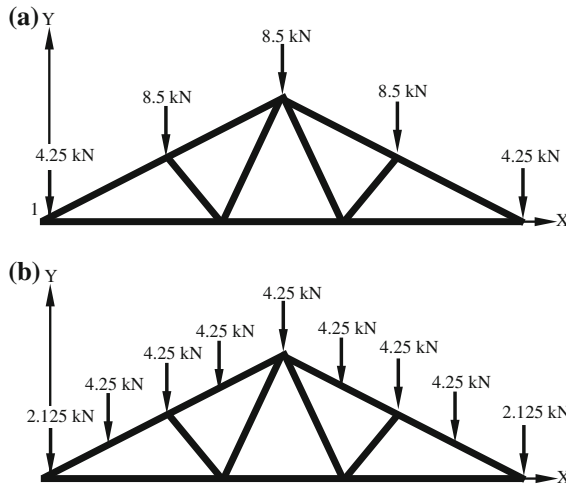


Fig. 2 Load applied on truss: **a** Applied on nodes only, and **b** loads applied on members and nodes

Table 3 Summary of optimised section properties of truss members and total volume

Combination		OPTIMIZED SIZE																Total Volume	Diff. %	
Combo. No.	Load Pattern	Configuration	Loads Applied on	Wind	Symmetric or Asymmetric	Type of timber	BC	TCL	TCR	D1	D2	D3	D4	D5	D6	D7	D8	(m ³)		
1	1				Symmetric	Mengkalang	63x175	75x200	75x200	38x125	38x75	38x75	50x100						0.24889	
2	1			Yes	Symmetric	Kempas	63x175	75x175	75x175	38x125	38x75	38x75	38x125						0.23177	7.4
3	2				Asymmetric	Mengkalang	63x175	75x175	75x150	38x125	38x75	38x75	38x100						0.22204	0.5
4	2				Asymmetric	Kempas	63x175	75x175	75x150	38x125	38x75	38x75	38x100						0.22103	
5	3				Symmetric	Mengkalang	63x175	75x225	75x225	50x100	38x75	38x75	50x100						0.26602	
6	3				Symmetric	Kempas	63x175	75x200	75x200	38x125	38x75	38x75	38x125						0.24854	7.0
7	4			No	Asymmetric	Mengkalang	63x175	75x200	75x150	50x100	38x75	38x75	38x100						0.23078	3.9
8	4				Asymmetric	Kempas	63x175	75x175	75x150	38x125	38x75	38x75	38x100						0.22204	
9	5				Symmetric	Mengkalang	63x175	75x150	75x150	38x100	38x75	38x75	38x125						0.21365	
10	5				Symmetric	Kempas	63x175	63x175	63x175	38x100	38x75	38x75	38x100						0.21030	1.6
11	6				Asymmetric	Mengkalang	63x175	63x150	63x150	38x100	38x75	38x75	38x75						0.19487	0.0
12	6				Asymmetric	Kempas	63x175	63x150	63x150	38x100	38x75	38x75	38x75						0.19487	
13	7				Symmetric	Mengkalang	63x175	75x150	75x150	38x125	38x75	38x75	38x125						0.21500	
14	7				Symmetric	Kempas	63x175	75x150	75x150	38x100	38x75	38x75	38x100						0.21231	1.3
15	8			No	Asymmetric	Mengkalang	63x175	75x150	63x175	38x125	38x75	38x75	38x75						0.21131	4.7
16	8				Asymmetric	Kempas	63x175	63x175	63x150	38x100	38x75	38x75	38x75						0.20191	
17	1				Symmetric	Mengkalang	50x175	63x175	63x175	38x75	38x75	38x125	38x75	38x75	38x100	38x75	38x75	38x75	0.20718	
18	1				Symmetric	Kempas	50x175	63x175	63x175	38x75	38x75	38x100	38x75	38x75	38x75	38x75	38x75	38x75	0.20576	0.7
19	2				Asymmetric	Mengkalang	38x125	63x175	50x175	38x75	38x75	38x125	38x75	38x75	38x75	38x75	38x75	38x75	0.16359	
20	2				Asymmetric	Kempas	38x125	63x150	50x150	38x75	38x75	38x100	38x75	38x75	38x75	38x75	38x75	38x75	0.14954	9.4
21	3				Symmetric	Mengkalang	50x175	63x175	63x175	38x75	38x75	38x125	38x75	38x75	38x125	38x75	38x75	38x75	0.20859	
22	3				Symmetric	Kempas	50x175	63x175	63x175	38x75	38x75	38x125	38x75	38x75	38x125	38x75	38x75	38x75	0.20859	0.0
23	4			No	Asymmetric	Mengkalang	50x175	63x175	63x150	38x75	38x75	38x125	38x75	38x75	38x75	38x75	38x75	38x75	0.19872	1.6
24	4				Asymmetric	Kempas	50x175	63x175	50x175	38x75	38x75	38x125	38x75	38x75	38x125	38x75	38x75	38x75	0.19559	
25	5				Symmetric	Mengkalang	50x175	50x200	50x200	38x75	38x75	38x125	38x75	38x75	38x100	38x75	38x75	38x75	0.19601	
26	5				Symmetric	Kempas	50x175	50x175	50x175	38x75	38x75	38x100	38x75	38x75	38x100	38x75	38x75	38x75	0.18541	6.8
27	6				Asymmetric	Mengkalang	38x125	50x175	50x150	38x75	38x75	38x125	38x75	38x75	38x75	38x75	38x75	38x75	0.14782	
28	6				Asymmetric	Kempas	38x125	50x150	50x125	38x75	38x75	38x100	38x75	38x75	38x75	38x75	38x75	38x75	0.13523	9.3
29	7				Symmetric	Mengkalang	50x175	63x175	63x175	38x75	38x75	38x125	38x75	38x75	38x125	38x75	38x75	38x75	0.20859	
30	7				Symmetric	Kempas	50x175	63x175	63x175	38x75	38x75	38x125	38x75	38x75	38x125	38x75	38x75	38x75	0.19943	4.6
31	8			No	Asymmetric	Mengkalang	50x175	63x150	50x150	38x75	38x75	38x125	38x75	38x75	38x75	38x75	38x75	38x75	0.18295	
32	8				Asymmetric	Kempas	50x175	50x175	50x150	38x75	38x75	38x125	38x75	38x75	38x75	38x75	38x75	38x75	0.17982	1.7

The colored cells in Table 3 highlighted the different sectional sizes required between the two materials for the same member of the same load pattern, whilst the un-highlighted ones indicate no difference in optimized sizes. For example, Fink truss of load pattern LP1, 3 members (i.e. TCL, TCR and D4 as highlighted) from Mengkalang glulam require slightly larger cross-sectional sizes compared to Kempas solid, while the other 4 members (BC, D1, D2 and D3) shows no size differences.

Similar type of comparison can be made from Table 3 for the two materials based on other load patterns.

General observation from the 8 load patterns in Table 3, Mengkulang glulam trusses (Fink and Double Fink) require slightly larger sectional sizes (about one size higher) compared to Kempas solid. In many cases, the top chords (TCL and TCR) are likely to be different in sizes between the two materials since these members are the ones directly supporting the vertical loads. For the Fink trusses, the number of size differences between two materials ranges from 1 to 4 out of 7 members in the truss, where load pattern LP3 having the highest number. For Double Fink trusses, out of 11 members, only up to 3 members are of different sizes, and load pattern LP2, LP5 and LP6 share the highest number. Comparatively, this observation indicates that Mengkulang, which originally 3 stress grade lower than Kempas in solid form, if designed as glulam, can be as comparable to Kempas in structural performance. This may also reflect that Mengkulang glulam may deem efficient in supporting the loads compared to the same Mengkulang truss of solid members, which undeniably will result in having more members in larger sizes due to its much lower stress grade.

It is also observed from Table 3 that Fink truss of load pattern LP6 and Double Fink truss of load pattern LP3, show no differences in member sizes between the two materials. Across the board, load pattern LP3 for both configurations (Fink and Double Fink), as well as in both materials requires the largest optimized sizes in particular for the top chords (TCL and TCR) compared to the other load patterns. This indicates that load pattern LP3 is the worst-case scenario for truss loading where designed consideration should focus on truss symmetrically loaded on both nodes and members of the top chords and without the inclusion of wind load.

4.2 Volume

For economical purposes, the truss needs to have optimum strength as well as minimum amount of timber used. Table 3 also summarizes the total volume of the sections based on the optimized design section properties of the truss. In most cases, Mengkulang trusses require slightly bigger volume compared to Kempas trusses. The volume differences between the two materials for Fink and Double Fink ranges from 0 to 7.4 %, and 0 to 9.4 %, respectively, which are reasonably small.

Table 4 summarizes the volume based on truss configurations. In all cases, Double Fink trusses require less volume compared to Fink trusses, even though there is more number of sections in the trusses. The percentage differences between Fink and Double Fink for Mengkulang and Kempas trusses ranges from 3 to 26.3 %, and 6.1 to 32.3 %, respectively. It is again evident that load pattern LP3 for both configurations (Fink and Double Fink) and materials (Mengkulang and Kempas) is the worst-case scenario where the volumes are the highest.

Table 4 Summary of volume based on truss configurations (in m³)

Combination Combo. number	Type of timber	Loads applied on	Wind	Symmetric or asymmetric	Volume (cubic meters)			Load pattern (LP)
					Fink	Double fink	% difference	
1	Mengkulang	Members	Yes	Symmetric	0.24889	0.20718	16.8	1
2				Asymmetric	0.22204	0.16359	26.3	2
3		Nodes	No	Symmetric	0.26602	0.20859	21.6	3
4				Asymmetric	0.23078	0.19872	13.9	4
5	Kempas	Members	Yes	Symmetric	0.21365	0.19801	7.3	5
6				Asymmetric	0.19487	0.14782	24.1	6
7		Nodes	No	Symmetric	0.21500	0.20859	3.0	7
8				Asymmetric	0.21131	0.18295	13.4	8
9	Kempas	Members	Yes	Symmetric	0.23177	0.20576	11.2	1
10				Asymmetric	0.22103	0.14954	32.3	2
11		Nodes	No	Symmetric	0.24854	0.20859	16.1	3
12				Asymmetric	0.22204	0.19559	11.9	4
13	Kempas	Members	Yes	Symmetric	0.21030	0.18541	11.8	5
14				Asymmetric	0.19487	0.13523	30.6	6
15		Nodes	No	Symmetric	0.21231	0.19943	6.1	7
16				Asymmetric	0.20191	0.17982	10.9	8

Table 5 Summary of maximum nodal displacement

Combination		Configuration	Loads applied on	Wind	Symmetric or asymmetric	Max displacement X (mm)			Max Displacement Y (mm)			
Load pattern (LP)	Members					Nodes	Node	Mengkulang	Kempas	Node	Mengkulang	Kempas
1		Fink	Members	Yes	Symmetric	6	-0.6		4	-3.21	-2.59	
2				No	Asymmetric	3	0.47		2	-2.39	-1.93	
3				Yes	Symmetric	6	-0.7		2	-3.73	-3.01	
4				No	Asymmetric	3	0.58		2	-3.01	-2.43	
5			Nodes	Members	Yes	Symmetric	6	-0.57		4	-3.05	-2.46
6					No	Asymmetric	3	0.43		2	-2.24	-1.81
7					Yes	Symmetric	3	0.66		2	-3.57	-2.88
8					No	Asymmetric	3	0.55		2	-2.87	-2.32
1		Double fink	Members	Yes	Symmetric	3	0.67		4	-3.17	-2.56	
2				No	Asymmetric	3	0.56		5	-2.46	-1.99	
3				Yes	Symmetric	10	-0.8		6	-3.82	-3.08	
4				No	Asymmetric	3	0.69		5	-3.11	-2.49	
5			Nodes	Members	Yes	Symmetric	3	0.65		4	-3.09	-2.5
6					No	Asymmetric	3	0.5		5	-2.18	-1.76
7					Yes	Symmetric	10	-0.78		6	-3.74	-3.02
8					No	Asymmetric	3	0.63		5	-2.8	-2.26

(23.9 %)

(24.0 %)

4.3 Displacement

Table 5 summarizes the maximum nodal displacement of the trusses for different types of timber. Observation is focused in particular to the maximum vertical Y-displacement of the trusses. In all cases, Mengkulang trusses have higher vertical Y-displacement than Kempas for both configurations (Fink and Double Fink).

For Mengkulang, the vertical displacement in Fink and Double Fink ranges from -2.18 to -3.73 mm, and -2.46 to -3.82 mm, respectively. Whilst for Kempas, the vertical displacement in Fink and Double Fink ranges from -1.81 to -3.01 mm, and -1.76 to -3.08 mm, respectively.

The differences in maximum vertical displacement between Mengkulang and Kempas in Fink and Double Fink are 23.9 and 24.0 %, respectively. These differences may be considered reasonably low and are within the acceptable serviceable limit of the design. Furthermore, all the maximum displacement mentioned earlier is associated to load pattern LP3 in which indicated the worst-case scenario of loading.

5 Conclusions

From the analysis on the roof truss using different types of timbers, truss configuration and loading patterns, the following conclusions can be drawn:

- (a) Based on optimized section
 - Mengkulang glulam truss requires about one size larger of sectional sizes compared to Kempas.
 - The structural performance of Mengkulang glulam truss can be as comparable to Kempas, even though its stress grade is 3 grades lower in solid form.
 - Mengkulang glulam may deem efficient in supporting the loads compared to similar Mengkulang truss of solid members.
 - Load pattern LP3 is the worst-case scenario for truss loading since it has the most number of different sizes.
- (b) Based on volume
 - Mengkulang truss require slightly bigger volume compared to Kempas, however the volume differences are reasonably small within 10 %.
 - Double Fink truss requires less volume compared to Fink trusses, even though it has more number of sections.
 - Load pattern LP3 in both configurations (Fink and Double Fink) and materials (Mengkulang and Kempas) is the worst-case scenario where the volumes are the highest.

(c) Based on displacement

- Mengkulang trusses have higher vertical displacement than Kempas for both configurations (Fink and Double Fink) which is below 25 % but within acceptable serviceable design limit.
- Maximum vertical displacement of the trusses are all associated to load pattern LP3 in which indicated the worst-case scenario of loading.

(d) Overall findings

Two significant findings can be concluded in this analysis.

First, glulam truss from a lower stress grade material can be of comparable structural performance to a solid truss from a higher-grade material. This can provide a cost-effective measure as alternative to solid truss since the differences in volume are small.

Second, the worst-case scenario of load pattern for the truss for designed consideration is when the truss is loaded symmetrically on both nodes and members of the top chords and without the inclusion of wind load.

References

1. M. Vandenberg, *AJ Handbook of Building Enclosure* (The Architectural Press, London, 1974)
2. R.E. Shaeffer, *Building Structures: Elementary Analysis and Design* (Prentice Hall Inc, Eaglewood Cliffs, New Jersey, 1980)
3. J.S. Foster, *Structure and Fabric, Part 1 and Part 2* (The Mitchell Publishing Company Limited, London, 1983)
4. A. Tomusiak, *Study on the Application of Different Types of Roof Trusses in Wooden Constructions*, vol. 72. Annals of Warsaw University of Life Sciences—SGGW, Forestry and Wood Technology, pp. 378–381 (2010)
5. K.H. Götz, D. Hoor, K. Möhler, J. Natterer, *Timber Design and Construction Sourcebook* (Mc Graw Hill Publishing Company, New York, 1989)
6. J.M. Branco, Influence of the joints stiffness in the monotonic and cyclic behavior of traditional timber trusses. Assessment of the efficacy of different strengthening techniques, Bi-National Ph.D thesis, University of Minho and University of Trento (2008)
7. J.M. Branco, P.J.S. Cruz, M. Piazza, H. Varum, Behaviour of Traditional Portuguese Timber Roof Structure. *J. Constr. Build. Mater.* **24**, 371–383 (2010)
8. M. Al-chaar, G.A. Issa, *Structural Evaluation Procedures for Heavy Wood Truss Structures*. USACERL Technical Report 98/89 (1998)
9. D.N. Izekorl, J.A. Fuwape, A.O. Oluyeye, Effects of density on variations in the mechanical properties of plantation grown *Tectona grandis* wood *Arch. Appl. Sci. Res.* **2**(6), 113–120 (2010)
10. E. Allen, *Fundamentals of Building Construction: Materials and Methods* (Wiley, Toronto, 1999)
11. W.W. Wayne, *Wood As a Building Material: A Guide for Designers and Builders* (Wiley, New York, 1991)
12. MS544: Part 2: 2001: Code of Practice for Structural Use of Timber: Part 2: Permissible Stress Design of Solid Timber, Department of Standards Malaysia
13. MS544: Part 3: 2001: Code of Practice for Structural Use of Timber: Part 3: Permissible Stress Design of Glued Laminated Timber, Department of Standards Malaysia

Charring Rate of Glued Laminated Timber (Glulam) Made from Selected Malaysian Tropical Timber

Atikah Fatma Md Daud, Zakiah Ahmad and Rohana Hassan

Abstract Besides strengths requirement for safety, fire resistance is also an important factor for safety of timber structure. During the exposure to fire, a charred layer forms on the external part of the timber element that protects the underlying layers against the action of fire. Charring rate value is required in the design of timber structures. Currently the charring rate for glued laminated timber (glulam) made from Malaysian tropical timber is not available. Malaysian standard, MS 544 Part 9 only provides the charring rate value for solid timbers. Therefore a series of glulam were made and have been exposed to fire in accordance with BS EN 1363-1:2012 in order to determine the charring rate values. The results indicate that the charring rate of glulam is smaller than the charring rate of solid timber.

Keywords Glulam · Charring rates · Moisture content · Density

1 Introduction

The behavior of timber structures exposed to fire is an issue of major importance. How structures behave in the first and second phases of fire development is termed its reaction to fire. The reaction to fire of a structure is a measure of how easy it is to ignite that structure and also how easy that structure contributes to the fire development and

A.F. Md Daud (✉)

Faculty of Civil Engineering, Universiti Teknologi MARA, Shah Alam, Selangor, Malaysia

e-mail: fatikah@psa.edu.my; fatikah5488@gmail.com

Z. Ahmad · R. Hassan

Institute for Infrastructure Engineering and Sustainable Management, Universiti Teknologi MARA, Shah Alam, Selangor, Malaysia

e-mail: zakiah@salam.uitm.edu.my

R. Hassan

e-mail: rohan742@salam.uitm.edu.my

spread. This may be important for the intended use of the structure or the influence of the fire on the structure's surroundings. Once the fully developed fire phase has been reached, it is assumed that all combustible materials present are burning.

Fire resistance is defined in BS 4422:2005 [1] as "the ability of an item to fulfill, for a stated period of time, the required fire stability and/or integrity and/or thermal insulation and/or expected duty specified in a standard fire resistant test". Fire resistance is therefore a property of the elements of an item and not its materials.

To assess safety characteristics, variability in fire endurance should be taken into account through consideration of variability in the properties of the member (e.g., charring rate, strength, and stiffness), variability in anticipated applied load, and variability in fire severity [2].

Large timber members have been acknowledged to be able to maintain the structural integrity during fire exposure due to the charring characteristics of timber. In general, timber products with larger cross-sections have greater flame retardancy. Fire reduces the extent of the cross-section as well as the mechanical properties of the heated timber in proximity to the char line.

Fire tests for timber-based products are mainly concerned with their surface properties because their early fire behavior is important to many aspects of fire safety [3]. Timber, like all organic materials, chemically decomposes when subjected to high temperatures and produces char and pyrolysis vapors and gases. Timber has excellent natural resistance to fire penetration due to its low thermal conductivity and to the characteristics of forming an insulating layer of charcoal while burning. The timber beneath the char still retains most of its original strength properties. The remaining uncharred timber supplies the load-carrying capability [4]. During fire exposure, the height and width of timber decreases at a rate dependent on the charring rate of the species, and the remaining uncharred timber contributes to the load-carrying capability. Consequently, the charring rate is the most important property of timber with respect to fire resistance and fire integrity.

In estimating a minimum value for post-flash over-burning duration of the room fire, the charring rate value is commonly used [5]. Mikkola [6] has developed models for calculating charring rate by combining the measurements of timber density, oxygen concentration, moisture content, and heatflux. He validated the model using the cone calorimeter method. In a study conducted by Njankouo et al. [7] on the relationship between the density and charring rate, he found that the relationship was a linearly decreasing correlation.

For glulam utilization as structural member, it is very important to know the mechanical properties of glulam members exposed to fire. Yang et al. [8] studied the temperature distribution within the glulam, the charring depth, and the charring rate of the glulam during fire exposure. Schaffer [9] found some differences in char development rate in the three species studied, Douglas-fir, southern pine and white oak, charring rate decreased with increase in dry specific gravity and with increase in moisture content. However the application of glulam specifically and timber in general, in Malaysian construction is very limited.

Fire tests for timber are mainly concerned with their surface properties because their early fire behavior is important to many aspects of fire safety [10]. This

concern can be seen in the Malaysian Building by Law. It is a requirement to show proves on fire resistance performance if timbers are used for construction in government projects. Currently, the construction of timber structures in Malaysia is limited and facing difficulty in getting approval from fire department as timber is considered as combustible materials. In order to promote the use of timber and engineered timber product as structural member and be accepted as safe material under fire, the timber structures need to be design by incorporating the charring rate values. In Malaysian standard MS 544 Part 9 [11] provides charring rate values only for solid timber but not engineered timber product such as glulam or LVL. BS 5268: Part 4 [12] provides information on charring rate values for solid timber, glulam and laminated veneer lumber (LVL) for softwood timbers for different densities of timbers.

Therefore the main purpose of this study was to investigate the charring rates of glulam made from different densities of Malaysian tropical timber using a standard fire test in accordance with BS EN 1363-1:2012 [13].

2 Experimental Procedures

2.1 Preparation of Specimens

The species used to manufacture the glulam specimens are keruing and malagangai. The glulam beams were manufactured in accordance with MS 758 [14] and the fabrication was done at Woodsfield Glulam Sdn. Bhd., Pasir Gudang, Johor.

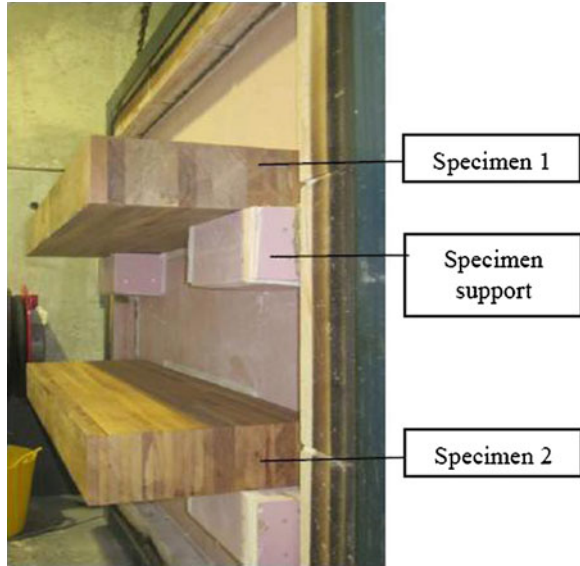
Prior to glulam manufacturing, all timbers were visually graded according to MS 1714:2003 [15] by a certified timber grader. The timbers were graded into Hardwood Structural (HS) grade, the grade specifically used for manufacture structural glulam using Malaysian hardwoods. Timber used was dried to the required moisture content in the range of 8–15 %. Once graded, the individual timber pieces were end jointed into full length laminations. Phenol Resorcinol Formaldehyde (PRF) adhesive and hardener obtained from Dynea NZ Limited (Prefere 4001-2 and Prefere 5837) were used to forming the finger joint and laminate the glulam beams.

The glulam specimens were fabricated using mono species with lamination thickness of 35 mm. The glulam were prepared with dimensions of 1,330 mm (length) \times 440 mm (width) \times 130 mm (thick). Three (3) replicates were prepared for each species.

2.2 Experimental Methods

Fire resistance test were done according to BS EN 1363-1:2012 [13]. The test was conducted at Chilternfire Testing Lab, TRADA, United Kingdom. The glulam beams were mounted onto 1.5 m \times 1.5 m steel frame as shown in Fig. 1 with a

Fig. 1 Exposed face prior to fire test



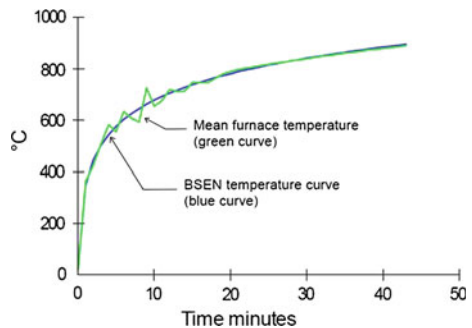
series of thermocouples attached to the beams. Then the frame was connected to the furnace. For the test conditions, the ambient temperature of the test area at commencement of test was 14 °C and at other time were monitored.

The pressure reading inside the furnace was also recorded. The temperature of the furnace was controlled to follow the temperature/time relationship specified in BS EN 1363-1:2012 [13] as shown in Fig. 2.

The temperature of each specimens was monitored by means of thermocouples positioned at different parts of the specimens as shown in Fig. 3.

The glulam beams were exposed to fire inside the furnace for 60 min (Fig. 4a). Once the test completed, the frame was removed from the furnace (Fig. 4b) and the fire was extinguished using fire extinguisher. Then the charred layer was abraded

Fig. 2 Furnace temperature during testing



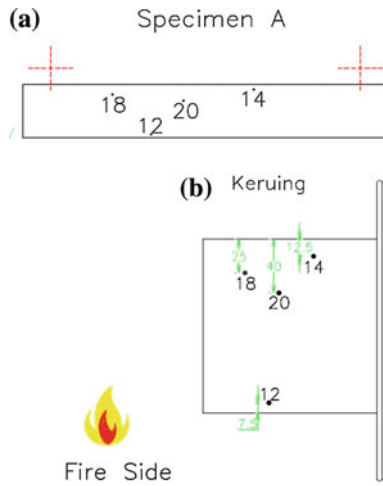


Fig. 3 Position of thermocouple on the beams, a top view and b side view

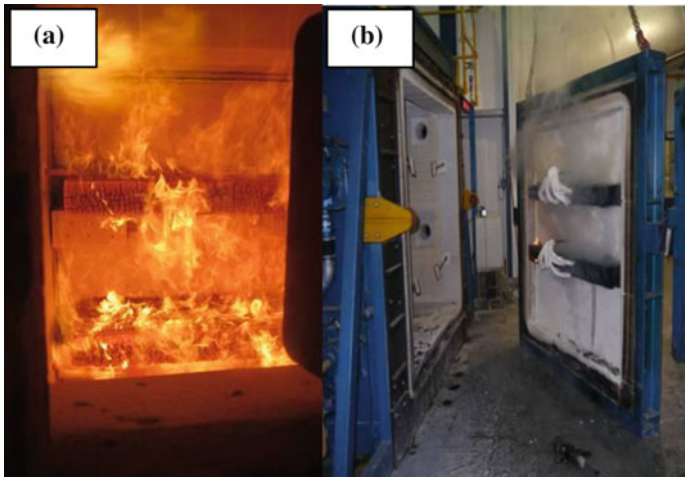


Fig. 4 Fire test specimens: a just after fire test and b after removed the fire

(Fig. 5b) and the resulting thickness was compared with that of the initial sample (Fig. 5b). The moisture content and density of glulam were also measured in accordance with MS 758.

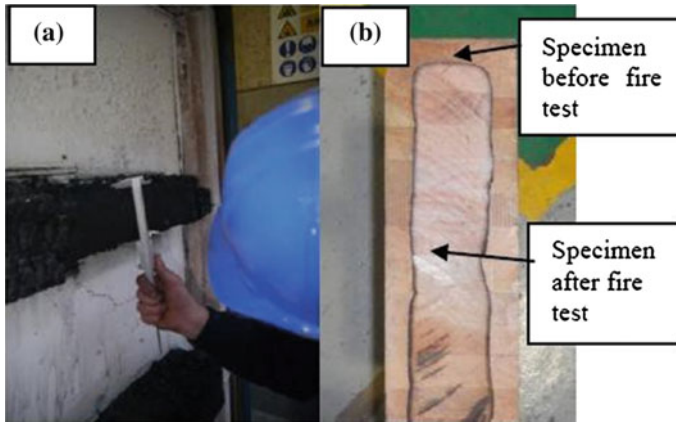


Fig. 5 Fire test specimens: **a** measuring the uncharred sample and **b** specimen before and after fire test

3 Results and Discussions

The results of test are illustrated in Table 1 covering the exposure period of 0–60 min. Within tables, samples of other parameters were also mentioned namely strength group, density and moisture content (MC).

Charring rates were determined by the time taken to reach 300 °C (shown in Table 1). Charring rates were also determined by scrapping away the charred timber and measuring the average depth remaining, to determine the amount lost through charring measured in mm. This was divided by the exposure time. The charring rate in both methods agreed to within 1–12 % after 60 min exposure.

The 1-h samples which were instrumented with thermocouples at various depths are listed in Table 1 and Fig. 6 shows the time-temperature responses for the samples from which charring rate was calculated (on the basis of having exceeded 300 °C).

Table 1 Charring depth of glulam beams

Specimen	Char depth (mm)	Time (min)	Charring rate (mm/min)	Average charring rate
Keruing	5	15.5	0.32	0.440
Density: 823 kg/m ³	10	26.5	0.37	
SG: 5	20	33.3	0.45	0.446
MC: 8.2 %	15	33.3	0.49	
	25	46.1	0.54	
Malagangai	30	63.0	0.47	0.446
Density: 800 kg/m ³	5	13.3	0.38	
	10	25.6	0.41	0.446
	20	43.4	0.46	

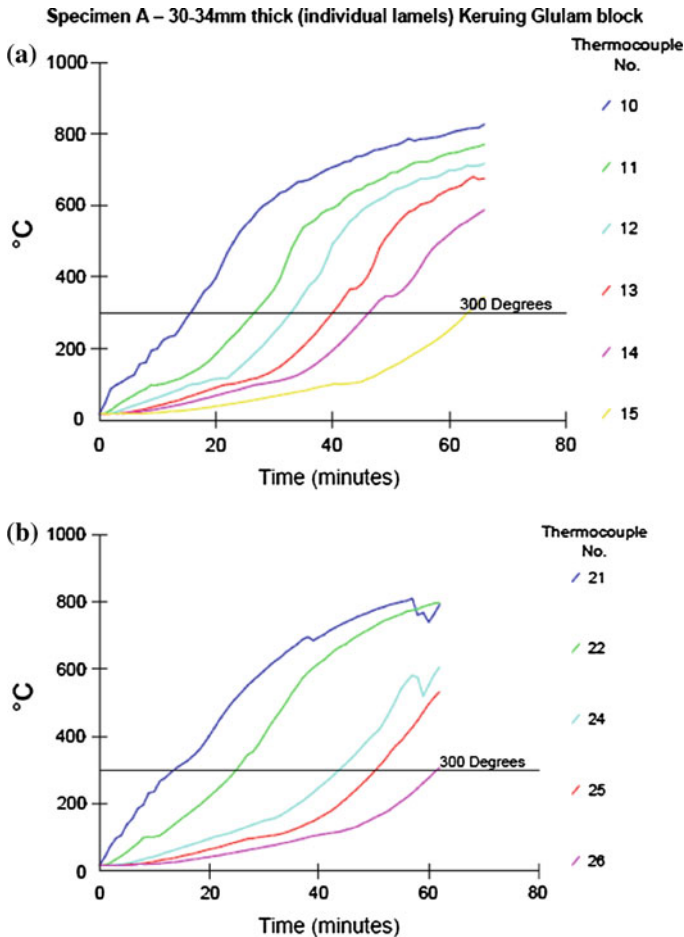


Fig. 6 Temperatures response of internal thermocouples for glulam beams during fire test; **a** keruing and **b** malagangai

Two of the thermocouples at 30 mm depth (thermocouple 15 and 26 for Keruing and Malagangai respectively) had not reached a temperature 300 °C within 1 h.

From Table 1, it can be seen that there is no much different in charring rate between Keruing and Malagangai glulam beam. This may be because both timbers have density around 800 kg/m³ although they came from different strength groupings. The charring rate is 0.44 mm/min.

Measured char rates for these glulam were compared with charr rates of solid timber of similar density or strength grouping as shown in Table 2.

The charr rates of glulam made from timber in SG3 and SG5 were lower than charr rate of solid timber in the same strength groupings as seen in Table 2 based on MS 544 Part 9 [11]. This shows that by converting the solid timber into glulam

Table 2 Notional charring rates of timber for various standards

Standard/timber species	Density (kg/m ³)	Charring rate (mm/min)
<i>EC 5</i> [16]		
Solid or glulam	450	0.50
<i>BS 5268</i> [12]		
Hardwood	>640	0.55
Softwood glulam	–	0.7
<i>MS 544 part 9</i> [11]		
Hardwood in SG1 to SG3	750–1,200	0.5
Hardwood in SG4 to SG5	600–1,000	0.7

improves the resistance to fire. The glue used in the glulam samples, PRF, is one which performs well under fire condition [17].

Trada (1971) [17] concluded that, the overall average of charring rate for structural timbers for exposure under standard time-temperature conditions, is usually 0.6 mm/min, ranging between 0.8 and 0.5 mm/min. Higher rates may be expected for timber species with densities less than 400 kg/m³. Furthermore, char rates are not affected significantly by temperatures normally occurring in building fires.

In Eurocode (EC) 5 [16], the limit for charring rate is 0.5 mm/min for density larger than 450 kg/m³ (refer Table 2). As for AS 1720.4 [18], the charring for timbers with density more than 600 kg/m³ is 0.65. Again, the char rate of glulam made from Malaysian tropical timber is better since most of Malaysian hardwood timber have density much higher than European timbers. The EC5 [16] recommendation is generally on the safe side.

The charred sections of glulam for both species are shown in Fig. 7. The charred sections were not perfectly rectangular. There were variations in charred sections in individual laminations. This is probably due to density variations, which appear to be related to whether the particular laminate is from heartwood or sapwood. Other

Fig. 7 Charred cross-section of glulam after 1 h exposure; **a** keruing and **b** malangangai



factors that may influence charring performance are the presence of knots, ring orientation and presence of glue lines. The trends observed were consistent with trends published in the literature [19].

4 Conclusion

The main conclusions that can be drawn from this research study are:

1. The charring rate of glulam does not depend on strength groupings but on the density of timber. Up to this point, the charring rate of glulam made with 800 kg/m^3 is 0.44 mm/min .
2. Fire performance of glulam differs to that of solid timber of same density/strength groupings. The charring rate of glulam made from timber in SG3 increased by 13.6 % and glulam made from timber in SG5 increased by 59 % compared with the charring rate of solid timber.
3. It is recommended that the charring rate of glulam to be included in MS 544 Part 9.

Acknowledgment The funding of this project was from Malaysian Timber Industry Board (Grant no: 100-RMI/MTIB 16/6/2 (47/2009)) and Universiti Teknologi Mara. We wish to thank the technicians of Civil Engineering Faculty and TRADA for their assistance and support.

References

1. BS 4422:2005, Fire vocabulary. BSI British Standard
2. E.L. Schaffer, *Structural Fire Design: Wood*. Forest Product Laboratory, FPL 450, US Department of Agriculture, Madison, pp. 1–16 (1984)
3. B.A.L. Ostman, L.D. Tsantaridis, Heat release and classification of fire retardant wood products. *Fire Mater. J.* **19**, 253–258 (2007)
4. A. Firmanti, B. Subiyanto, S. Takino, S. Kawai, The critical stress in various stress levels of bending member on fire exposure for mechanical graded lumber. *J. Wood Sci.* **50**(5), 385–390 (2005)
5. V. Babrauskas, Charring rate of wood as a tool for fire investigations. *Fire Saf. J.* **40**, 528–554 (2005)
6. E. Mikkola, *Charring of Wood*. VTT research report 689, Espoo (1990)
7. J.M. Njankouo, J.C. Dotreppe, J.M. Franssen, Experimental study of the charring rate of tropical hardwoods. *Fire Mater.* **28**, 15–24 (2004)
8. T.H. Yang, S.Y. Wang, M.J. Tsai, C.Y. Lin, Temperature distribution within glued laminated timber during a standard fire exposure test. *Mater Des.* **30**, 518–525 (2009)
9. E.L. Schaffer, U.S. For. Serv. Res. Pap. FPL 69, For. Prod. Lab., Madison, Wis (1995)
10. B.A.L. Ostman, L.D. Tsantaridis, Heat release and classification of fire retardant wood products. *Fire Mater. J.* **19**, 253–258 (1995)
11. MS 544:2001: Part 9: Section 1, Code of practice for structural use of timber: Part 9: Fire resistance of timber structures: Section 1: Method of calculating fire resistance of timber members. SIRIM Bhd., Malaysia

12. BS 5268-4.2:1990, Structural use of timber. Fire resistance of timber structures. Recommendations for calculating fire resistance of timber stud walls and joisted floor constructions. BSI British Standard
13. BS EN 1363-1:2012, Fire resistance tests. General requirements. BSI Standard
14. MS 758:2001, Glued laminated timber—Performance requirements and minimum production requirements. SIRIM Bhd., Malaysia
15. MS 1714:2003, Specification for visual strength grading of tropical hardwood timber. SIRIM Bhd., Malaysia
16. BS EN 1995-1:2004, General. Structural fire design. BSI Standard
17. Timber Research and Development Association, TRADA, *The Fire Performance of Timber, A Literature Survey* (High Wycombe, England, 1971)
18. AS 1720.4-2006, Timber structures—Fire resistance for structural adequacy of timber members. Australian Standard
19. P.C.R. Collier, *Charring Rates of Timber*. Building Research Association of New Zealand, Study report SR 42, Judgeford, New Zealand (1992)

Derivation of Grade Stresses of Malaysian Tropical Timber in Structural Size

M.B.F.M. Puaad, Z. Ahmad and S.A.K. Yamani

Abstract The strength data for timbers established in British and European standards (BSEN 5268 and EC5 respectively) are based on large size specimens. However the strength data of Malaysian timbers are based on small clear specimens. This study attempts to compare data on the bending strength properties of timbers in structural size and small clear specimens. Eight selected Malaysian timbers from different strength groupings were used in this study. The results of bending strength from small clear specimens were statistically correlated with the results from the structural size specimens. Based on large size specimens, the strength groupings of some of the timbers are not in the same strength groupings based on small clear specimens.

Keywords Bending strength · Structural size · Malaysian tropical timber

1 Introduction

Sawn timber from log, regardless of species and size, has its variability in mechanical properties. Pieces may differ in strength by several hundred percent. For simplicity and economies use, pieces of sawn timbers of similar mechanical properties are placed in categories called stress grades. The stresses are derived so that the designer can confidently design structures with safety, economy and beauty according to the timber species suitability.

In early day, the Malaysian tropical timber were divided into four different strength groups, A, B, C and D by referring to the compressive and bending

M.B.F.M. Puaad (✉)

Faculty of Civil Engineering, Universiti Teknologi MARA Pasir Gudang, Bandar Seri Alam, 81750 Masai, Malaysia

e-mail: bfaliq86@gmail.com

Z. Ahmad · S.A.K. Yamani

Institute of Infrastructure Engineering and Sustainable Management (IIESM), Universiti Teknologi MARA, 40500 Shah Alam, Malaysia

strength of the timber [1, 2]. Then the strength grouping system were upgraded by using the basic stresses and grade stresses in order to have much accurate strength grouping of Malaysian tropical timber [2, 3]. This basic stress, characteristic strength and grade stresses are the basis for the development of strength groupings where the timbers species were grouped into seven strength groupings namely SG1–SG7 (from higher grades to lower grades) [4]. These new systems of strength grouping are still used by the engineer for structural timber work by referring to the codes of practice for structural use of timber MS 544: Part 2 (2001): Permissible stress design of solid timber [5].

However, the grade stresses in Tables 2 and 3 given in MS 544 Part 2: 2001 such as tension, compression and bending stresses were obtained as a factor of small clear timber stresses.

Other countries such as United Kingdom, the concept of basic stresses has been abandoned and the new approach for assessing the strength of timber appears to be in line with the limit ‘limit stress’ design philosophy [5, 6]. Furthermore the mechanical properties of timber in European standard (EN 338) are derived from the structural size specimen [2] for in-grade testing.

Most structural size sawn timbers have sloping grain and defects and will behave differently to clear wood. Clear wood is stronger in tension than in compression, but the reverse is true for sawn timber containing sloping grain or knots. The strength properties obtained from small clears testing are generally higher than those obtained from structural size testing [7].

The main advantage of small clears testing is that the small test specimens are easily obtained and tested. The test results are useful for comparing one species with another but a big disadvantage is the great difficulty in predicting the lower strength of commercial structural sizes. The main advantage of structural size testing is that the test results can be used directly to derive code values for structural purposes.

The statistical treatment of the test results from small clear specimens was predicated upon the assumption that the population has a normal distribution. However, it has been found that strength distributions of commercial material, to which the allowable stresses are applied, are not necessarily normally distributed [8]. Studies was also found that the distribution of structural size timber from commercial line was positively skewed and followed a three parameter Weibull distribution [9]. When normal and Weibull distributions were compared for data from structural size timbers, it was found that 5th % level would fit better and this is the reason for the 5th % level has been chosen as the characteristic value. It can be concluded that it is important to have direct measurements of the mechanical properties of structural timber [10] for correct design.

This paper reports only part of the investigation made on the bending strength properties of selected Malaysian tropical timbers in structural size. The bending strength properties of structural size timbers and small clear specimens have been

published in Puaad and Ahmad [11]. This paper only present the comparison in the derivation of grade stresses of these timbers.

2 Methodology

2.1 Materials

Eight timber species were used in this experimental study (Table 1). All timber materials used in this project were selected on one occasion in order to obtain a test material without too high a variation in strength which could be arisen from different growth condition. The timbers used for this study were sourced from reserved forest in UiTM Jengka. These species are in the different strength groups [12]. The total number of specimens in structural size was 160 (20 sample for each species) and the total number of specimens for small clear was 240 (30 sample for each species). These specimens were kiln dried to attain dried timber condition as according to the Malaysian standard, and the timbers used are in the category of dry timbers with moisture content less than 19 %.

The timbers were visually graded in accordance with MS1714 [13] by certified grader.

2.2 Specimens Preparations and Test Method

2.2.1 Small Clear Specimens

Timbers with dimensions; 20 mm thick, 20 mm wide and 400 mm long were prepared. The specification of the specimen and test method is in accordance with British Standard BS 373: 1957 Test methods for small clear specimens of timber [14]. The beams were subjected to third point loading. The load was applied using the Instron 3383 testing instrument equipped 100 kN load cell with crosshead of

Table 1 Timber species

Species	Family	Strength grouping (SG)
Kapur	Dipterocarpaceae	SG 4
Merpauh	Anacardiaceae	SG 4
Resak	Dipterocarpaceae	SG 4
Bintangor	Guthiferea	SG 5
White meranti	Dipterocarpaceae	SG 5
Jelutong	Apocynaceae	SG 6
Kelampayan	Rubiaceae	SG 7
Sesendok	Euphorbiaceae	SG 7

0.11 mm/s. The density and moisture content of the specimens were also determined.

2.2.2 Large Size Specimen

Timber beams of size 50 mm × 90 mm × 1,800 mm were prepared in accordance with ASTM D198 [15]. The beams were subjected to four point bending using 2,500 kN Universal Testing Machine (UTM). Load as applied by a hydraulic cylinder at a constant rate of 0.06 mm/s to achieved the ultimate load in about 10 min but not less than 5 min or more than 20 min. The density and moisture content of the specimens were also determined.

3 Analysis Method

3.1 Bending Strength Properties of Small Clear and Large Size Specimens

The discussion on the bending strength properties of all the timber studied can be found in Puaad and Ahmad [11]. The next discussion just focus on the characteristics strengths and strength derivation of grade stresses of those timbers.

3.2 Derivation of Grade Stresses of Timber Strength

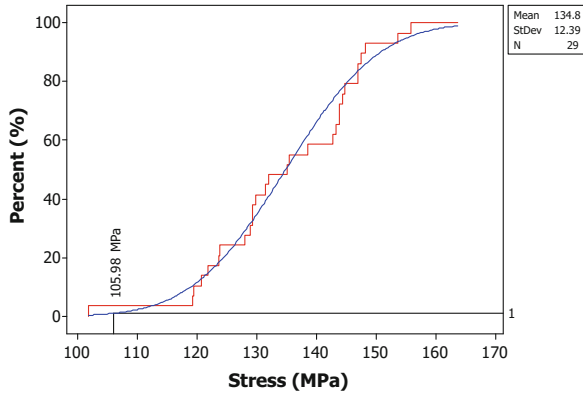
The efficient use of timbers for structural purposes can best be attained by classifying timbers into structural grades to which definite working stresses can readily be applied.

3.2.1 Small Clear Specimen

In Malaysia, probability of 1 in 100 (1 %) that the minimum strength is exceeded is chosen for bending, tension, compression parallel to the grain shear and modulus of elasticity (small clear specimen) [16]. In performing cumulative distribution function, the set of data for mean bending strength were arranged in the ascending order to produce the s-curve graph and from the graph, the 1 % value can be determined. The cumulative distribution functions were plotted using Minitab v 16.0 software as shown in Fig. 1.

In order to compare the strength grouping of the timber studied with the strength grouping published in MS 544 Part 2, the basic stress and grade stress need to be

Fig. 1 Cumulative distribution function graph showing the stress at 1 %



determined. Basic stress is the stress that would be safely permanently sustained by the timbers. For different types of stress, MS 544 Part 2 used different probability value as given in Table 2. From basic stress to characteristics strength, the values were determined using different safety factor as given in Table 2.

To determine the grade stress, the basic stress was multiplied by the strength ratio which related to the percentage of defects in the timbers. There are three stress grades of timber that are associated with the different limits of strength reducing characteristics they are; Common, Standard and Select [16].

The strength ratios for the three grades of each strength property are given in Table 3. Design engineer are supposed to make use of the design values correspond to the stress grade of timber in their calculations. For this study the grade is standard and better. Therefore the strength ratio used was 63 %.

Table 2 Formula for determining basic stresses [16]

Property	Probability value	Factor of safety	Formula
Bending and shear	1 in 100	2.5	$\frac{\bar{X}}{2.5}$
Compression parallel to the grain	1 in 100	1.5	$\frac{\bar{X}}{1.5}$
Compression perpendicular to the grain	1 in 20	1.3	$\frac{\bar{X}}{1.3}$

*This stress is called characteristic stress where \bar{X} = Strength value at 1 or 5 %

Table 3 Strength ratio

Property	Select (%)	Standard (%)	Common (%)
Bending, tension and compression to grain	80	63	50
Shear	72	56	45
Modulus of elasticity	Same as the basic values for all grades	Same as the basic values for all grades	Same as the basic values for all grades

3.2.2 Structural Size Specimen

For structural size specimens, the timbers were not sorted to select, standard or common categories as need for determining the grade stress for small clear specimen. The grade stresses for structural size specimens will be based on timbers visually graded as standard and better which denoted as HS grade [13, 17, 18]. This is the reason why the grade stresses for small clear specimen studied here were chosen from standard and better grade.

For the structural size specimen, the % used is not 1 % as for small clear specimens. This is because for the large size specimen, the confidence level for free from defects is less than small clear specimen. The probability of 1 in 20 (5th %) that the minimum strength is chosen for structural size specimens [19–21]. Those values of characteristic strengths were determined directly from the s-curve graph (without multiplying with reduction factor in Table 3).

4 Results and Discussions

4.1 Bending Strength Characteristics for Small Clear Specimens

The value of one percentile for bending parallel to the grain is shown in Fig. 2 which sorting the data from weakest to strongest, plotted as a cumulative distribution function. It shows that the strength of Resak and Merpauh have greater separation from the distribution of strength Kapur although they are in the same strength group published in MS 544 Part 2.

The strength distribution of Kelempayan, Jelutong and Sesendok are similar and very close to each other which confirm that they are in the same strength group. As for Bintangor, the distribution of strength moves towards the SG 6 timbers which

Fig. 2 Cumulative distributions of bending strength parallel to the grain for small clear specimens

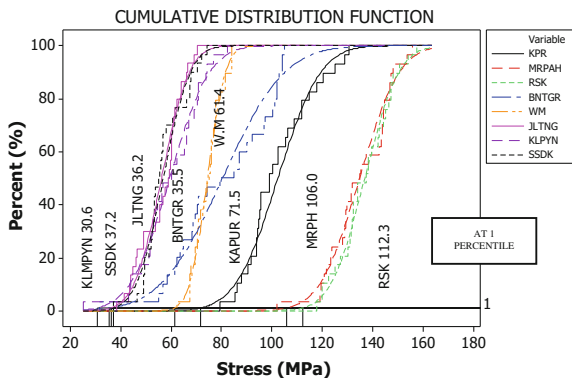


Table 4 Moisture content and density for compression parallel to the grain for small clear specimen

Species	Strength group	Moisture content (%)	Density (kg/m)
Kapur	SG 4	12.87	770
Merpauh	SG 4	11.47	853
Resak	SG 4	11.51	914
Bintangor	SG 5	12.89	650
White meranti	SG 5	12.01	571
Jelutong	SG 6	11.56	431
Kelempayan	SG 7	11.71	425
Sesendok	SG 7	11.67	468

means lower in strength grouping. Table 4 shows the moisture content and density of the small clear specimen.

The density of Resak and Merpauh were higher compared to Kapur even though they are in the same strength grouping (SG 4). This might explain why Kapur were out of the group when referring to Fig. 2 and also, Resak and Merpauh have the strength in the range of 35–43 % higher than the stresses given by MS: Part 2.

The variation in the bending strength of all the beams may be also due to the failure modes. In authors’ paper Puaad and Ahmad [11], all the beams failed in tension except for Bintangor. The beams failed in horizontal shear which may contributed to the reduction of bending strength and this resulted in reduction of strength by 1/16 of the actual bending strength [11, 22]. Due to this reduction, it has placed Bintangor to lower grade as shown in Fig. 2.

4.2 Bending Strength Characteristics for Structural Size Specimens

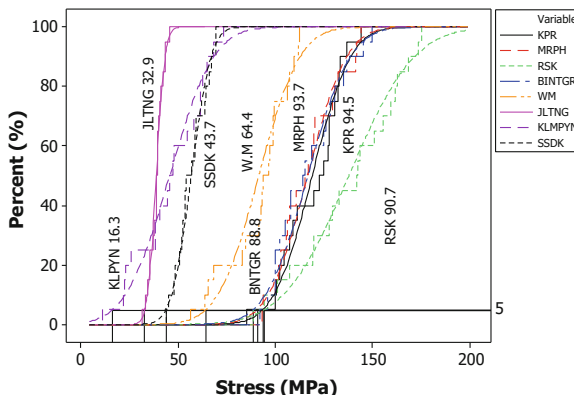
Table 5 shows the moisture content and density of the structural size specimen. All the mean values of moisture content for all species are in the range 9–13 %. Since all mean values of moisture content are lower than 19 %, the samples can be classified as dried samples. For practical use, it is difficult to dry structural timber in Malaysia to 12 % moisture content by air-drying because of the very humid climate. More so, if the recorded strengths could be derived at such high moisture contents, then higher strengths will be obtained when the timber species are in use.

Figure 3 shows the data plotted as a cumulative distribution functions for large size specimens and it shows that the Resak, Bintangor and Sesendok have greater separation in the distribution of the species in their strength group. Bintangor distribution of strength tends to move towards the SG 4 species which mean higher in strength grouping.

Table 5 Moisture content and density for compression parallel to the grain for structural size specimen

Species	Strength group	Moisture content (%)	Density (kg/m)
Kapur	SG 4	10.37	776
Merpauh	SG 4	12.65	875
Resak	SG 4	11.01	915
Bintangor	SG 5	8.92	725
White meranti	SG 5	11.31	594
Jelutong	SG 6	11.44	487
Kelempayan	SG 7	11.59	547
Sesendok	SG 7	9.87	483

Fig. 3 Cumulative distributions of bending strength parallel to the grain for large size specimens



On the other hand, Resak distribution of strength is greater than Kapur and Merpauh, but since the highest strength group had been tested is the SG 4, it cannot be specified in what strength group that Resak shifted to. As for the Sesendok it tends to shift towards SG 5 strength group which higher than Kelempayan and Jelutong.

It shows that there are changes in strength distribution where Kelempayan is tend to shift to the lowest strength distribution due to the presence of defect in the samples. From this investigation, it can be said that the strength properties of large size specimen should be done in order to safely design the timber structure. The cumulative distribution function provides initial information on the strength groupings of the timbers.

Table 6 Summary statistic for bending strength

Species	Small clear specimen		Species	Large size specimen	
	MOR (MPa)	Grade stress = $\frac{\text{Stress at 1 percentile} \times 0.63}{2.5}$		MOR (MPa)	Grade stress = $\frac{\text{Stress at 5th percentile} \times 0.63}{2.5}$
Kapur	102.4	18.0	Kapur	119.1	37.8
Merpauh	134.8	26.7	Merpauh	116.7	37.4
Resak	136.9	28.3	Resak	138	36.2
Bintangor	80.4	8.9	Bintangor	116.9	35.5
White meranti	74.5	15.4	White meranti	91.65	25.7
Jelutong	56.2	9.1	Jelutong	38.8	13.1
Kelempayan	59.4	7.7	Kelempayan	45.7	6.5
Sesendok	56.9	9.3	Sesendok	56.9	17.4

4.3 Grade Stresses

Table 6 shows the comparison of mechanical properties in bending parallel to the grain between structural size and small clear specimens. From Table 6, it can be seen that the MOR values for timbers in structural size are much higher than small clear specimens except for Merpauh, Jelutong and Kelempayan. These results indicate good agreement with Branco et al. [23] where the bending strength of the structural specimens have greater value than the strength based on the small clear specimens. The reduction of MOR in structural size for Merpauh and Kelempayan can be due to the influence of knot where it did cause the reduction MOR. Other than that, it might be because the timber microfibril structure that can cause the reduction of MOR. According to Fonselius [24] and Piter [25] the MOR for structural size Douglas Fir and Pine (which the physical properties of these species are about the same with SG 6 and SG 7 timber) is much lower than the small size. So, for future study, the study regarding microfibril of timber is a need in order to provide better understanding in properties of timbers.

Kapur, Merpauh, Resak and Bintangor give the highest value of bending strength of 37.48, 36.31, 37.86 and 35.54 MPa respectively. Meanwhile, Kelempayan has the lowest values of bending strength of 6.54 MPa. As for Sesendok, the grade strength (17.49 MPa) of the large size specimen is higher than Jelutong (13.14 MPa) although Sesendok is lower in strength group [12].

One difficulty in predicting the strength of Malaysia timbers, under the same species the density may varies in wide range. The grade stress stated in MS 544 Part 2 are group with minimum properties including the density. The density of each species for structural size specimen in bending is about the same with the density of small clear specimen.

5 Conclusion

The investigation on the grade stresses of the timber used in this study will not be able to provide the overall strength grouping since more information are needed such as tensile strength and shear strength parallel to the grain as well as compression perpendicular to the grain. As the aim of the study is to compare the grade stresses for timbers using small clear specimens and large size specimens, the following conclusions can be derived;

- For small clear specimens, based on cumulative distribution function for bending strength, there exist some differences in the strength groupings for Resak, Merpauh and Kapur. Kapur seems to have shifted towards lower grade.
- Kelempayan, Jelutong and Sesendok are in the same strength grouping but Bintangor seems to have shifted to lower grouping.
- For large size specimens, the timbers are arranged in different groupings than small clear specimens. Resak is still has highest strength but Kelampayan have

shifted towards lower groupings. Meanwhile Bintangor tends to move towards the SG 4 species which mean higher in strength grouping.

- The bending strength (MOR) for large size specimens are higher than the MOR using small clear specimens. Except for Kelempayan. The differences are in the range of 20–30 %.
- The results suggest that the strength grouping given in MS 544 Part 2 may need to be re examined as the data established was conducted using the small clear specimen.

Acknowledgments We wish to thank the technicians of Faculty of Civil Engineering and Faculty of Mechanical Engineering, Universiti Teknologi Mara for their assistance and support. The work reported here was financially supported by grant from Malaysian Timber Industry Board.

References

1. H.J. Burgess, Strength grouping of Malayan timbers. *Malayan Forester* **19**(1), 33–36 (1956)
2. M.J.A. Wahab, M.Z. Jumaat, M.O.M. Khaidzir, Statistical technique for grouping tropical timbers into similar strength groups. *Mod. Appl. Sci.* **6**(3), 73 (2012)
3. Z. Ahmad, R. Hassan, *Timber Properties using Dielectric Constant in Low Frequency Technique* (VDM Verlag Dr. Muller GmbH & Co., Saarbrucken, 2012)
4. C. Engku Abdul Rahman, Basic and grade stresses for some Malaysian timbers. *Malayan Forester* **34**(4), 131–134 (1971)
5. R. Hassan, Z. Ahmad, A. Ibrahim, M.S. Noh, *Compressive strength properties of structural size timber made from selected Malaysian tropical timber* (Institute Penyelidikan, Pembangunan Dan Komersilan, Universiti Teknologi Mara, Shah Alam, 2004)
6. C. Arya, *Design of structural elements* (E & FN SPON, London, 1994)
7. R. Hassan, Z. Ahmad, A. Ibrahim, M.S. Noh, *Compressive strength properties of structural size timber made from selected Malaysian tropical timber* (Institute Penyelidikan, Pembangunan Dan Komersilan, Universiti Teknologi Mara, Shah Alam, 2004)
8. D.E. Allen, Limit states design—a probabilistic design. *Can. J. Civ. Eng.* **2**(1), 36–49 (1975)
9. B. Madsen, Duration of load tests for dry lumber subjected to bending. *For. Prod. J.* **23**(2), 21–28 (1971)
10. A. Baltrušaitis, V. Pranckevičienė, Strength grading of the structural timber. *Mater. Sci. (MEDŽIAGOTYRA)* **9**(3), 2003 (2003)
11. M.B.F.M. Puaad, Z. Ahmad, Bending strength properties of Malaysian tropical timber in structural size. in *Proceedings of the IEEE Symposium on Humanities, Science and Engineering Research (SHUSER)*, Penang, 23–26 Jun 2013
12. MS 544 Part 2: 2001. Code of practice for structural use of timber. department of standard. Malaysia. Department of Standard. Malaysia
13. MS 1714: 2003. Specification for visual strength grading of tropical hardwood timber
14. BS 373: 1957. Standard test methods for small clear specimens of timber
15. ASTM D198: 2009. Standard test method for static test of lumber in structural sizes : annual book of ASTM standard, vol. 04. 10
16. Y.P. Chu, K.S. Ho, M.S. Midon, A.R.A. Malik, *Timber design handbook* (FRIM, Kepong, 1997)
17. BS 5268-2: 2002, Structural use of timber-Part 2: Code of practice for permissible stress design, materials and workmanship

18. MS 544 Part 3: 2001. Code of practice for the structural use of timber Part 3: Permissible stress design of glued laminated timber
19. H.P San, Basic engineering properties of laminated veneer lumber (LVL) produced from tropical hardwood species. Doctor of Philosophy Thesis. Faculty of Forestry Universiti Putra Malaysia. Selangor, 2003
20. NZW, Information sheet. grading systems for structural timber (2007)
21. H. Säl, B. Källsner, A. Olsson, Bending strength and stiffness of aspen sawn timber. Paper presented at the COST E 53 conference—quality control for wood and wood products. Warsaw, 15–17th Oct 2007
22. J. Bodig, B.A. Jayne, *Mechanics of woods and wood composite* (Van Nostrand Reinhold Company Inc., New York, 1982)
23. J. Branco, H. Varum, P. Cruz, Structural grades of timber by bending and compression tests. *Mater. Sci. Forum* **514–516**, 1663–1667 (2006)
24. M. Fonselius, Effect of size on the bending strength of laminated veneer lumber. *Wood Sci. Technol.* **31**, 399–413 (1997)
25. J.C. Piter, Size effect on bending strength in sawn timber of fast-growing Argentinean *Eucalyptus grandis*. Analysis according to the criterion of European standards. *Eur. J. Wood Prod.* **70**, 17–24 (2010)

Bending Strength Performance of Selected Timber Species with Different GFRP Strips Pattern

Rohana Hassan, Norilmi Ghazali
and Abdullah Omar Abdullah Zamli

Abstract This paper presents an experimental research aimed in increasing the bending strength performance of selected timber members made from Yellow Meranti and Bintangor species. A series of glass fiber reinforced polymer (GFRP) strips are glued on the timber face with different pattern alignment, which is diagonal (45°) and straight (90°) that is bonded using epoxy resins in order to increase the bending strength. The bending strength test under three-point loading was conducted for solid timber member for the respective species accordance to ASTM D143-09: 1992. The results shown the timber member reinforced with the GFRP strips slightly improved by 2 and 5 % of the bending strength. The failure modes of the selected timber specimen were also observed. Both controlled specimens shown visible damage that is cracking at mid-span for Yellow Meranti specimen and shear failure for Bintangor specimen. While, for reinforced specimens, some of the specimens possess no visible damage and some possess the shear failure.

Keywords Yellow Meranti species · Bintangor species · Bending strength · Glass fibre reinforced polymer (GFRP) strip

1 Introduction

Nowadays, the usage of concrete and steel as construction materials seem to take over the construction market and cause reduction in the usage of timber material. However, the current construction material does not reduce the problems when it

R. Hassan (✉)

Institute Infrastructure Engineering for Sustainable Management (IIESM), Universiti Teknologi MARA, 40450 Shah Alam, Selangor Darul Ehsan, Malaysia
e-mail: rohan742@salam.uitm.edu.my

N. Ghazali · A.O.A. Zamli

Faculty of Civil Engineering, Universiti Teknologi MARA, 40450 Shah Alam, Selangor Darul Ehsan, Malaysia

produces high carbon emission and next gave hazards impact toward environment and human being [1]. Due to that reason, some construction players become aware to the sustainable issues and take immediate action by implementing construction based on timber product which can be renewed and less environmental impact.

Major important properties in solid timber are strength where it is referring to ability of the timber to resist the external forces or maximum load capacity. A lot of research has been done regarding the strength properties and its behaviour especially in flexural for building application either in the same or different species of softwood and hardwood [2]. The failure modes that commonly happen to solid structure are bending and tension parallel to grain, shear failure and failure due to high tensile stresses perpendicular to grain [3].

2 Fibre Reinforced Polymer (FRP) in Timber Applications

Recently, a new composite material has been applied in order to increase the strength of the structure to their maximum level [4]. Glass fibre reinforced polymer (GFRP) has given a new life to the timber structure. The implementation of GFRP is easy whereby it only need to be bonded in between the laminates with good adhesive. The production of fibre reinforced polymer (FRP) is available in laminates, sheets, bars or strips. Just as importantly, FRP offer excellent corrosion resistance to environmental agents as well as the benefits of high stiffness to weight and strength to weight ratio. The coupling of composite materials with wood is extremely interesting because it gives more structural strength and stiffness compared to the performance of the wood alone [5].

Even though, timber has huge opportunity to be used widely but due to lack of research in this area, it is left unexplored. Timbers are proved to be able to carry load capacity similar to the steel or concrete and it provides a lighter and more economical material. Therefore, in order to have similar load carrying capacity, strengthening method by using FRP sheet is developed. FRP are proved to enhance the strength of the timber member but the problem is that the established design rules and information available for construction player and other decision maker are very limited [6]. This reason is one of the major factors contributing to the reluctance of industry to utilise FRP for timber strengthening application. Nevertheless the usage of FRP as a strengthening material could be the great option to most traditional techniques. Previous research have also shown that FRP can be a viable alternative of metallic fasteners in timber connection [7]. The GFRP in the form of rods has also proven to be as an alternative to steel dowels for the mortise and tenon connection loaded in shear [8]. Surprisingly little research has been conducted on the strengthening of timber with FRP as opposed to the much more widely researched strengthening of concrete. Studies have been made so far on the application of In order to determine the best choice and optimum enhancement of strength that can be achieved by different alignment which is diagonal (45°) and

straight (90°), therefore the bending strength performance of selected timber species with different GFRP strip pattern were investigated.

The main objective for this study is to observe the significant bending strength performance which includes the maximum load carrying capacity, modulus of elasticity (MOE) and modulus of rupture (MOR) of selected timber species with different GFRP strips pattern. The significant effects of different GFRP pattern and failure modes were also observed.

3 Materials and Methods

3.1 Timber Species

Two timber species, Yellow Meranti and Bintangor were used in this experimental study. All timber materials used in this study were selected on occasion in order to obtain test materials that are not too high a variation in strength which could be arisen from different growth condition. Based on MS 544: Part 2, these timber species are in the strength group of SG5 and SG6. The total number of specimens was 30.

3.2 Bonding Adhesive

In this research, epoxy resins and hardener was used which is suitable for bonding wood to wood as well as wood to FRP. The primer coat was applied by using Epo bond primer. The primer coat is important to ensure that the surface is clean from dust, better bonding between wood and GFRP and provide additional protection to the material. As a bonding agent, the epoxy resins are capable of curing at room temperature and providing strong adherents. The curing time required is 24 h. A total of 20 % are allowed for wastage. The mixing ratio for Part A and hardener (Part B) is 2.5:1 by weight. The adhesive are manually mixed until well blended for about 5 min using steel knife at a constant rate in order to avoid entrapment of air bubbles. The adhesive spread must be uniform and in sufficient quantity in accordance with the recommendations of the adhesive manufacturer.

3.3 Glass Fiber Reinforced Polymer (GFRP) Strip

The strips that were used in this study were glass fiber reinforced polymer (GFRP) strips produced by a local manufacturer. A total numbers of 100 samples of GFRP with dimensions of 50 mm × 30 mm were required for different pattern alignment.

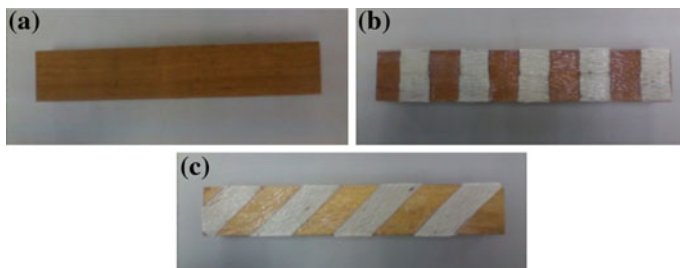


Fig. 1 Small clear specimen with different GFRP strips pattern. **a** Control sample. **b** Straight (90°). **c** Diagonal (45°)

3.4 Preparation of Specimens

The small clear specimen sizes of 300 mm (length) \times 50 mm (width) with the depth of 40 mm were prepared. The sample preparation include control specimen and two different GFRP strip pattern for straight (90°) and diagonal (45°) with 5 samples for each timber specimen. Thus the total of 30 samples was prepared as shown in Fig. 1. Those samples were then tested under three-point bending.

3.5 Small Clear Specimen Method

Three-point bending tests were performed using 100 Ton Capacity Universal Testing Machine (UTM) (Fig. 2). The samples were positioned and the static loads were applied at constant speed rate of 1.0 mm/min accordance to ASTM D143-09 (secondary methods) until the specimen failed completely (Fig. 3). The samples were supported by roller support at both ends so that it is free to follow the bending action. Load-deflection curves were recorded up to maximum load. The modes of failure were observed. The parameters investigate in this test were the type of timber and the pattern alignment of GFRP which is diagonal (45°) and straight (90°). Prior to testing, the alignment of the setup was checked to ensure no eccentricity of loading will take place. Small eccentricity may cause twisting to the samples and failure may occur before the samples achieve it full capacity.

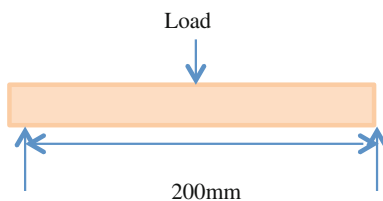


Fig. 2 Configuration of three-point bending test

Fig. 3 Three-point bending test



The modulus of elasticity (MOE) and modulus of rupture (MOR) were computed in order to determine the bending strength performance of the specimens. The MOR and MOE in three-point bending were calculated based on the following Eqs. 1 and 2 [9].

$$\text{MOR} = \frac{3P_{\max}l}{2bd^2} \quad (1)$$

$$\text{MOE} = \frac{P_p l^3}{4\delta b d^3} \quad (2)$$

where P_{\max} is the maximum applied load (kN), P_p is the applied load at the proportionality limit (kN), l is the bending span (mm), δ is the deflection (mm), b is the width of the specimen (mm) and d is the depth of the specimen (mm).

4 Results and Discussions

4.1 Bending Strength of Small Scale Specimens

A total numbers of 30 samples were tested for bending strength test which includes control specimen and two different GFRP strips pattern for 5 samples each for Yellow Meranti and Bintangor species. The samples were prepared with the dimensions of 300 mm × 50 mm × 40 mm of each sample. The result showed that the strength possesses by the reinforced specimen with GFRP strip pattern is slightly higher compared to unreinforced specimen.

Table 1 shows the average of maximum load with their standard deviation and coefficient of variance while Tables 2 and 3 shows the average MOE and MOR with their standard deviation and coefficient of variance of the Yellow Meranti and

Table 1 The average of maximum load, standard deviation and coefficient of variance of Yellow Meranti and Bintangor specimen

Species		Maximum load (kN)		
		Average	SD	COV (%)
Yellow Meranti	Control	22.880	1.135	4.96
	45°	23.530	1.728	7.34
	90°	22.870	1.716	7.50
Bintangor	Control	35.835	4.548	12.69
	45°	37.286	4.460	11.96
	90°	35.890	5.422	15.11

Bintangor specimen. The coefficient of variance of overall specimens is within 4–21 %. The coefficients of variance for Yellow Meranti specimens are less than 10 % which is within the acceptance limit while the Bintangor specimen achieved beyond the acceptance limit which is more than 10 %.

The minimum average load carrying capacity of the specimens was 22.870 kN for 90° GFRP strip pattern and the maximum average load carrying capacity was 37.286 kN for 45° GFRP strip pattern. The average percentage increment of load carrying capacity for Yellow Meranti between control specimen and 45° strip pattern specimen is 2.84 %. While for Bintangor specimen, the average percentage increment of load carrying capacity between control specimen and 45° strip pattern specimen is 4.05 %.

The highest MOE and MOR is average of 15.212 and 0.210 kN/mm² respectively for Bintangor specimen reinforced with diagonal (45°) pattern of GFRP strips. From Table 2, it is shown that the MOE for control specimen is higher than 90° GFRP strips pattern specimen. While, it is shown that the MOR value for control specimen is the same with 90° GFRP strips pattern specimen as tabulated in Table 3. It seems that reinforcing using 90° GFRP strips pattern was not efficient to enhance the stiffness when compared to the control specimen.

4.2 Bending Behavior of Timber Specimens

The bending behavior of the timber specimens are shown in Figs. 4 and 5 respectively. At the early stage, the entire samples behaved linearly elastic and

Table 2 The average of MOE, standard deviation and coefficient of variance of Yellow Meranti and Bintangor specimen

Species		MOE (kN/mm ²)		
		Average	STD	COV (%)
Yellow Meranti	Control	7.199	1.447	20.10
	45°	7.588	0.605	7.97
	90°	6.473	0.825	12.75
Bintangor	Control	13.966	1.989	14.24
	45°	15.212	2.289	15.05
	90°	13.207	2.627	19.89

Table 3 The average of MOR, standard deviation and coefficient of variance of Yellow Meranti and Bintangor specimen

Species		MOR (kN/mm ²)		
		Average	STD	COV (%)
Yellow Meranti	Control	0.129	0.007	5.43
	45°	0.132	9.930e-3	7.52
	90°	0.129	9.654e-3	7.48
Bintangor	Control	0.202	0.026	12.87
	45°	0.210	0.025	11.90
	90°	0.202	0.030	14.85

Fig. 4 Typical load-displacement curve for Yellow Meranti specimen

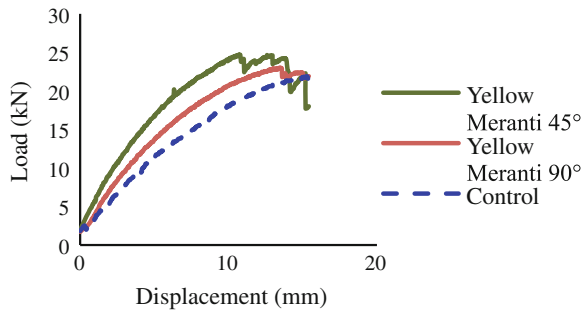
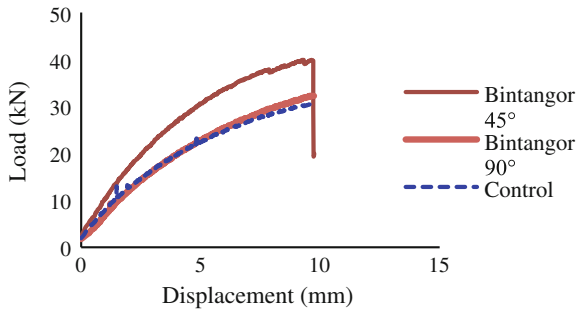


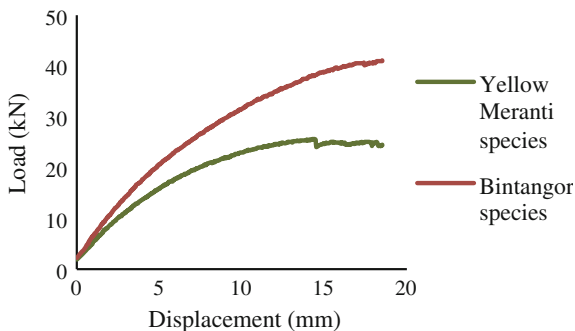
Fig. 5 Typical load-displacement curve for Bintangor specimen



when the loads were increased, the samples exhibited non-linearity until failure occurs. There are some slight drops observed in the curve as a result of small cracking during testing when it achieved its maximum load. The load-displacement curve was typical for most specimens of the bending tests for Yellow Meranti and Bintangor specimen. The 90° pattern improves the deformability of the samples by a small margin but it is not effective in improving the stiffness (MOE).

Figure 6 shows that the load-displacement curves for both species for 45° strips pattern. Since the specimens for Yellow Meranti and Bintangor with 45° strips patterns attained the highest bending strength, therefore the failure patterns were observed. The Bintangor specimen with 45° GFRP strip pattern produce lower deflection than the Yellow Meranti specimen with 45° GFRP strip pattern.

Fig. 6 The load-displacement for Yellow Meranti and Bintangor species for 45° strip patterns



Bintangor species were in strength group (SG5) which are stronger than Yellow Meranti species which in strength group (SG6). Therefore, the Bintangor species can resist slightly higher applied load than Yellow Meranti species and produce lower deflection. The entire reinforced specimens with 45° GFRP strip pattern showed better load-deflection characteristic than the control specimens. In this situation, the longer the composite, the lower the failure loads. Therefore, it was concluded that the strengthening scheme with 45° GFRP strips performed well and lower the deformation in timber specimens.

4.3 Failure Modes of Specimens Under Bending Controlled Specimens

Almost all the specimens for Yellow Meranti and Bintangor controlled specimens failed. Initial cracking sound can be heard and this characteristic has made timber a suitable construction material where it showing sign before failure occurred. There is no visible damage observed on the initial stage. The cracking sound were then continues until the failure load was reached. Failure normally occurs at ultimate load and the specimens' breaks into separate pieces in a brittle manner for traditional sawn timber [10]. The sounds of cracking become louder when the load reached to maximum load. There is visible damage on both timber species of the controlled specimens.

The failure modes of Yellow Meranti and Bintangor species controlled specimens are shown in Figs. 7 and 8. For Yellow Meranti specimens, the failure and cracking were seen at the mid-span which is at the tension zone of the specimen as shown in Fig. 7. It is observed that cracks at the lower section are much longer than the upper section. While for the Bintangor specimens, the failure occurred at the side of the timber, which is in shear where this phenomenon is due to the separation between heartwood and sapwood as shown in Fig. 8.

Fig. 7 Cracking at the tension zone



Fig. 8 Shear failure at the side



4.4 Straight (90°) and Diagonal (45°) Specimens

A total of 20 samples were tested and some of the sample possess no visible damage. For Yellow Meranti specimen with 90° GFRP strips pattern, some of the sample are not damage and some tend to have visible cracks and some of the failure occurred at the side of the timber. For Yellow Meranti specimen with 45° GFRP strips pattern, it show that the failure occurred also at the side of the timber.

When the specimens are loaded beyond the failure load, the specimens still can resist the load applied. It shows that the application of GFRP strips as strengthening material for the timber structure can reduce the risk of failure at the mid- span which is known as the critical area. This happened as the GFRP strips restrained the bending of the timber. The greater flexural stiffness posses by GFRP strips allow the increases of strength.

Therefore, the failure mode of this pattern is mainly in shear. Regardless how the specimen failed, the GFRP strips were still strongly intact with the timber for all specimens and the bonding agent was not cracked.

The difference of failure mode for the selected timber species namely Yellow Meranti and Bintangor specimen are shown in Fig. 9. From the observation, both unreinforced control specimen failed in shear while some of the reinforced specimen with GFRP strips for 90° and 45° pattern shown no visible failures. Even- though not all the reinforced specimen did not possess any damage or failure but it



Fig. 9 Mode of failure between Yellow Meranti and Bintangor specimen

prove that the GFRP strips as the strengthening material is efficient and affordable to be implemented. The risk of failure due to applied load can be resisted by the implementation of GFRP strips.

4.5 Moisture Content of Selected Timber Species

The specimens for both timber species were cut for moisture content determination with dimension of 50 mm × 50 mm × 40 mm for record purposes. The result showed that the moisture content did not vary between Yellow Meranti and Bintangor species. The average percentage of moisture content for Yellow Meranti and Bintangor species was 13.99 and 13.64 % respectively. Both species is considered dry. Hence, the variation in strength of the timber due to moisture content can be eliminated.

5 Conclusions

The maximum load carrying capacity, the modulus of elasticity (MOE) and the modulus of rupture (MOR) were observed. The average maximum load carrying capacity for Yellow Meranti specimen of control, 45° and 90° specimen are 22.880, 23.530 and 22.870 kN respectively. While for Bintangor specimen, the values are 35.835, 37.286 and 35.890 kN respectively. The reinforced specimens have shown only a small increment in bending for Yellow Meranti (45° strips pattern) and Bintangor (45° and 90° strips pattern), which is 2.84, 4.05 and 0.15 % respectively. Average increases in MOE (stiffness) of 5–10 % and MOR (strength) of 2–5 % were achieved.

The significant effects of different GFRP strips pattern toward the bending strength performance of the selected timber specimen were observed. The result showed that Bintangor specimen with diagonal (45°) pattern has slightly high in

bending strength compared to Yellow Meranti specimen. However, the significant effect of 45° and 90° GFRP strips pattern compared to control specimen is significantly too small of Therefore further research should be conducted in order to improve the result.

The failure modes of the selected timber specimen were observed. Both controlled specimens shown visible damage which is cracking at mid-span for Yellow Meranti specimen and shear failure for Bintangor specimen. While, for reinforced specimen, some of the specimen possess no visible damage and some possess the shear failure. The strength of the timber specimen has curbed the failure mode since no rupture occurred to the GFRP strips. Epoxy resins showed good performance as a bonding agent jointing the timber and GFRP strips. Therefore, it is shown that GFRP strips are effective mechanism to reduce the risk of failure.

Acknowledgments The authors would like to thank Universiti Teknologi MARA for funding the research through 600-RMI/DANA 5/3/CIFI (92/2013) from Research Management Institute (RMI), UiTM.

References

1. A. Abd. Jalil, Z. Ahmad and W. Wan Mohamad, Bending Strength of Glulam from Selected Malaysian Hardwood Timber, *AMR* **879**, 237–244 (2014)
2. A. Bakar, S. Saleh, M. Zainai, Factors Affecting Ultimate Strength of Solid and Glulam Timber Beams. *Jurnal Kejuruteraan Awam* **16**(1), 38–47 (2004)
3. S. Thelandersson, H. Larsen (ed.), *Timber Engineering* (J. Wiley, New York, 2003), pp. 68–77
4. T.C. Triantafillou, N. Plevris, FRP—Reinforced Wood as Structural Material. *J. Mate. Civ. Eng. ASCE*. **4**(3), 300–317 (1992)
5. E. Speranzini, S. Agnetti, Structural performance of natural fibres reinforced timber beams. World conference on timber engineering, Riva del Garda, Trento, Italy, pp. 1–8 (2010)
6. F.T. Shin, Bending behavior of GFRP pultruded composite beams. Bachelor in Civ. Eng. UTM (2003)
7. D. Brandon, A. Thomson, R. Harris, P. Walker, Stiffness modelling of non-metallic timber connections with pultruded dowels. R. Hassan et al. (eds.), *InCIEC 2013*. doi:[10.1007/978-981-4585-02-6_4](https://doi.org/10.1007/978-981-4585-02-6_4), (© Springer Science+Business Media Singapore) 2014 pp 37–49
8. R. Hassan, I. Azmi, Z. Ahmad, Shear capacity of dowelled mortise and tenon in tropical timber. *IOP conference ser: material science engineering*. (2011). doi: [10.1088/1757-899X/17/1/012012](https://doi.org/10.1088/1757-899X/17/1/012012)
9. A.W. Jamil, J. Zamin, M.K. Omar, Strength assessment of Malaysian timbers in structural size. *Proceedings of the international civil and infrastructure engineering conference* (2013) pp. 15–26
10. D. Raj, R. Surumi, Shear strengthening of reinforced concrete beams using near surface mounted glass fibre reinforced polymer. *Asian J. Civ. Eng. (Build. Hous.)* **13**, 679–690 (2012)

Computational Approach for Timber and Composite Material Connection Using Particle Swarm Optimization

Marina Yusoff, Ili Izdhar Roslan, Anizahyati Alisibramulisi
and Rohana Hassan

Abstract Timber and composite material connection are currently a popular combination in construction industry. Although composite timber connection has been studied previously, it was based on traditional experimental laboratory work, which led to a higher cost and more time consuming. Therefore, this paper studies the tensile load carrying capacity of the composite connections by using Particle Swarm Optimization (PSO) which has the capability of finding optimal solutions. From the results, it can be concluded that even though the PSO fitness functions has not exactly matched the brittle behavior of the load-displacement response for both single and double shear connections, their overall tensile performance and capacity of the connections are well predicted. Therefore, the findings from this research will be benefited by timber engineers in predicting the timber composite connections behavior and capacity, particularly single and double shear connections.

Keywords Load deformation · Particle swarm optimization · Timber connection · Single and double shear

M. Yusoff (✉) · I.I. Roslan
Faculty of Computer and Mathematical Sciences, Universiti Teknologi MARA,
40450 Shah Alam, Selangor, Malaysia
e-mail: marinay@tmsk.uitm.edu.my

M. Yusoff · A. Alisibramulisi · R. Hassan
Institute for Infrastructure Engineering and Sustainable Management (IIESM),
Universiti Teknologi MARA, 40450 Shah Alam, Selangor, Malaysia

A. Alisibramulisi · R. Hassan
Faculty of Civil Engineering, Universiti Teknologi MARA, 40450 Shah Alam,
Selangor, Malaysia

1 Introduction

Nowadays it is common to use timber material in construction. It is important to assure that the type of timber material being used is durable. In some cases, the chosen timber material can cause the timber structure to collapse. This is due to the lack of knowledge on determining performance and properties of timber. In addition, the safety and behavior of timber structures also depends on the connection's performance itself. In order to identify the best approaches on timber connection, a longer time of testing and several experiments are needed. Eventually, this will increase the cost, time consuming and the timber joint efficiency might still not being identified.

2 Related Work

2.1 Behavior of Timber and Composite Material Connection

In order to promote wood-based construction, several projects had claimed environmental and climate-based advantages [1]. Timbers are small dead weight and have good thermal characteristic that enable heat absorption. Most importantly, this will lead to overall cost reduction for timber building [2]. It is evident that the use of timber can also improve insulation and fire resistance [3]. This is due to the mechanical properties of the timber itself.

There are four categories of timber which are softwood, medium hardwood, heavy hardwood and light hardwood [4]. The failures in timber structures can give negative effects towards the competitiveness in construction market. Poor manufacturing is one of the factors for the collapsed structure of timber. Besides that, inaccurate strength design of structure also leads to the failure [5].

Timbers have also been used as composite structure for upgrading the existing structures [6, 7]. Timber concrete composite structures consist of timber joints interconnected to a concrete slab cast on top of the timber members [6]. This method resists compression, timber joists resist tension and bending, and the connection system transmits shear forces between the two components. Since wood originated from rainforest had been increasingly limited, new approach on timber and composite material connection are being introduced and further research.

2.2 Behavior of Timber and Composite Material Connection

As this study is focusing on the connection of timber and composite material connection, the experimental result of timber and composite material have been collected. Based on the collected data, the load capacity and the performance of nails wrapped with composite material of GFRP were determined. The experiments were

Fig. 1 Tensile test result of single-shear with GFRP

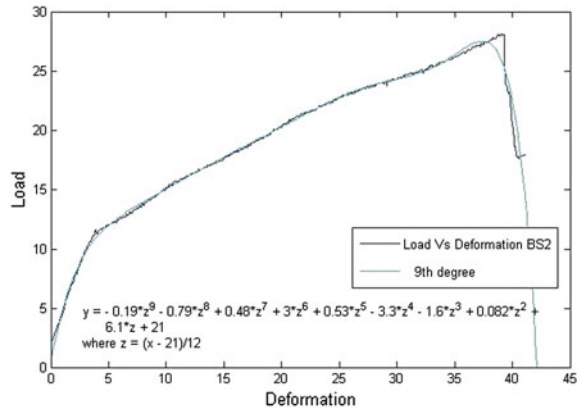
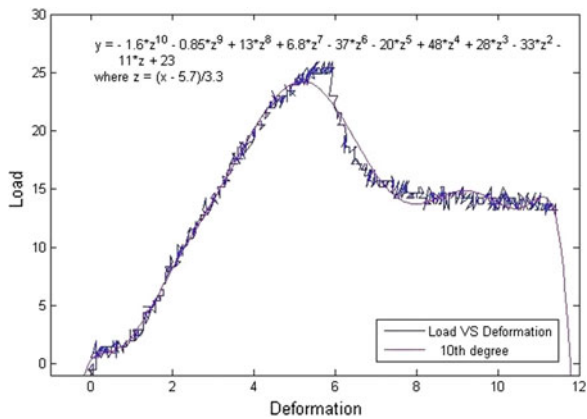


Fig. 2 Tensile test result for double-shear strength with GFRP



done by using tensile test in which the relationship of load and deformation had been obtained and formed into a graph of single shear and double shear connections as shown in Figs. 1 and 2, respectively. Comparison results of the study with the previous researches are shown in Table 1. It shows that the tensile behavior of joint connected with a common steel fastener contributes to a ductile failure.

3 Particle Swarm Optimization

Particle Swarm Optimization (PSO) was developed in 1995 by Kennedy and Eberhart based on birds flocking and fish schooling’s social behavior. In PSO, entities called as particles are placed in a search space. The movements of particles within the search space are evaluated to get the best results [11, 12]. In addition, the claimed that the original idea of particle swarm optimization comes from the

Table 1 Results comparisons with related journals

Author	Tensile result	Finding
Blass et al. [8]	Behavior of nails reinforced is ductile and the large ductility	Large ductility
Jason [9]	5 % offset yield and capacity presented	Increase resistance and
Ahmad et al. [10]	Tension parallel to grain test. The grade stresses for timber are higher rather than grade stresses for structure size	Tensile stress distribution is normal

observation of bird flocks searching for food and particle swarm optimization is now increasing to be widely used in solving many computing problems. Bai [13] mentioned that, according to three principles which are to keep its inertia, to change the condition to its most optimist position and to change the condition according to the swarm's most optimist position, the particles will change it condition. Besides that, particles move through the search space using a combination of an attraction to the best solution.

The original procedure of Particle Swarm Optimization implementation is:

1. Initialize a random population of particle, position and velocity in the problem space.
2. Velocity and position update.
3. Evaluation and update of best location.
4. Repeat until termination condition is met.

Essentially, PSO algorithm is just similar with other existing evolutionary algorithms, it is a population based on search algorithm with random initialization. The concept of PSO is distinct with other evolutionary algorithm where a PSO is based on particle flies through the solution space and have capability to remember its previous best location and survives until the next generation to another. PSO algorithm and its variants can be reviewed in many articles [14–16].

There are few factors that will affect the performance of PSO. These factors are called PSO parameters. These parameters that involve in PSO are velocity, swarm size, inertia weight, cognitive parameter and social parameter. Each of this parameter contains specific function in PSO.

4 Data Acquisition

4.1 Datasets Preparation

The timber and composite material connections were tested to make a comparison between the connection using GFRP material and without the GFRP material. Type of timber joints that have been tested are single-shear and double-shear. The

Table 2 Single-shear strength data

Load (kN)	Deformation (mm)
1.26	0.0
1.09	0.5
1.24	0.7
1.27	0.9
1.26	1.0
1.31	1.1
1.27	1.1
1.34	1.2
1.39	1.3
1.54	1.3
1.53	1.4
1.65	1.4
1.64	1.5
1.77	1.5

strengthening material used for jointing the timber was the GFRP wrapper with 250 mm × 500 mm dimension. The timber has been fastened with 1.5 times diameter (1.5D) end distance where the diameter of the dowel is 20.6 mm. The single shear connection has been tested using Bintangor species whilst double shear connections were tested using Kapur species.

- Single-Shear Strength

There are five (5) samples of data and each contains two variables. The variables shown in Table 2 are load and deformation. Test on single-shear strength data for this project only focuses on two variables which are load (kN) and actuator deformation (mm). Thus, the maximum load of this timber joint connection has been obtained.

- Double shear

There are six (6) samples of data and each contains five variables. The variables shown in Table 3 are time, load, actuator deformation, stress, and actuator strain. However, the test of double-strength on this project only focuses on two variables which are load (kN) and actuator deformation (mm). The result of experiment has determined the strength of timber joint connection. Meanwhile the results shown in Table 4 are maximum and breakpoint value of load and actuator deformation.

4.2 Analysis and Pre-processing

Essentially, collected data of timber joint and composite material were analyzed and pre-processed in a way of identifying the equation for fitness function. The raw data were first coordinated for load over displacement into a graph in excel as shown in

Table 3 Double-shear strength data

Time (s)	Load (kN)	Actuator deformation (mm)	Stress (kPa)	Actuator strain (%)
0.4	0.4884	0	0.023	0
0.8	0.9768	0	0.046	0
1.2	0.9768	0	0.046	0
1.6	1.9536	0.06105	0.092	0.0305
2	1.4652	0.06105	0.069	0.0305
2.4	1.4652	0.06105	0.069	0.0305
2.8	0.9768	0.06105	0.046	0.0305
3.2	1.4652	0.06105	0.069	0.0305
3.6	1.4652	0.06105	0.069	0.0305
4	1.9536	0.18315	0.092	0.0916
4.4	1.9536	0.18315	0.092	0.0916
4.8	1.4652	0.1221	0.069	0.0611

Table 4 Fitness function in PSO

Strength	Fitness function
Double-shear	$y = -1.5z^9 - 0.93z^8 + 9.7z^7 + 4.3z^6 - 21z^5 - 4.8z^4 + 17z^3 - 0.93z^2 + 2.5z + 10;$ where $z = (x - 4.3)/2.5$
Single-shear	$y = 0.28z^{10} - 0.056z^9 - 2.1z^8 + 0.61z^7 + 5.6z^6 - 1.5z^5 - 6.2z^4 + z^3 + 2.2z^2 + 4.7z + 19;$ where $z = (x - 17)/9.5$

Figs. 3 and 4 for the single shear and double shear respectively. Both figures show results of yield behavior of the connections under the tensile loading. The connections yield at proportionate, continues with a constant yielding until it reached

Fig. 3 Tensile test result of single-shear with GFRP

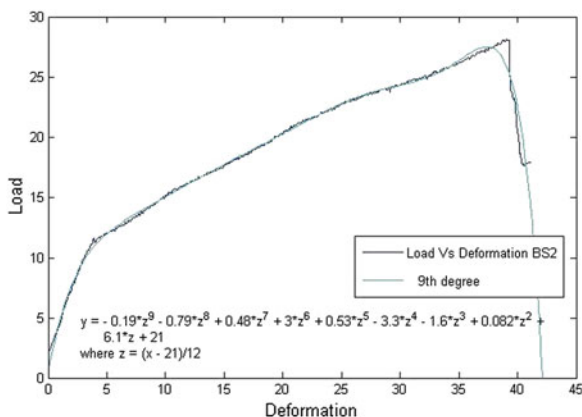
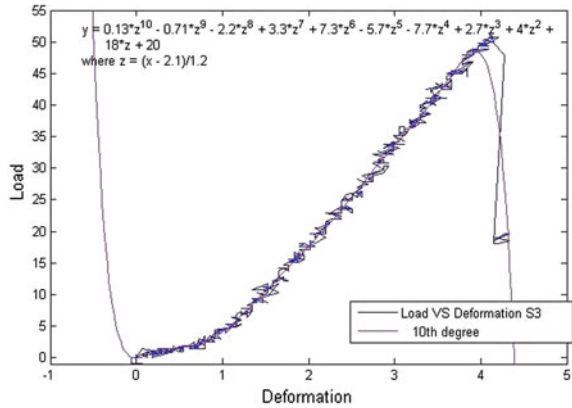


Fig. 4 Tensile test result for double-shear strength with GFRP



their maximum capacity and failed abruptly. Similar brittle failures were found for single and double connections from the effects of the GFRP brittleness right after they reached their maximum capacity.

The graphs were then converted into polynomial for the equations. The resulted equations were used as the fitness function and to be evaluated in the particle swarm optimization. Below are the coordinated graph of load over displacement that have been converted to polynomial for sample one (1), two (2), three (3), four (4), five (5), and six (6) which were obtained through the experiments of tensile test.

5 Computational Results and Findings

5.1 Fitness Function

This system has been tested based on load and deformation of double-shear strength and single-shear strength of timber connection with composite material experiment. The fitness equations that are used in this PSO implementation are based on load over displacement in both double-shear strength and single-shear strength of timber with GFRP as the strengthening material. Table 4 show the fitness function for both double-shear strength and single-shear strength of timber with the GFRP.

5.2 Computational Setup

The technique of PSO has a parameter such as velocity, inertia weight, constant value of social and cognitive behavior and also number of random population. As for the testing process on single-shear strength dataset, the parameter value of PSO has been initialized as follows:

Table 5 Tuning result for single-shear strength (A)

Swarm size	Velocity	Iteration	pBest deformation (mm)	pBest load (kN)	Maximum value of load (kN)
30	-1 to 1	5	33.29	24.71	24.71
30	-1 to 1	10	32.69	24.50	24.50
30	-2 to 2	5	32.84	24.55	24.55
30	-2 to 2	10	28.98	23.17	23.17
30	-3 to 3	5	33.12	24.65	24.65
30	-3 to 3	10	32.83	24.55	24.55
30	-4 to 4	5	33.04	24.62	24.62
30	-4 to 4	10	32.08	24.27	24.27
30	-5 to 5	5	32.36	24.38	24.38
30	-5 to 5	10	32.46	24.41	24.41

- (i) Velocity, $V = -1$ to 1
- (ii) Inertia weight, $W = -1.0$ to 1.0
- (iii) Positive constant, $C1$ and $C2 = 2.0$
- (iv) Random population $X = 0.0 - 36.41$
- (v) Random population $Y = 1.09 - 24.65$
- (vi) Swarm size = 30 population
- (vii) Iteration size = 10 iteration

The highlighted results in the Tables 5, 6 and 7 are among the most optimum value in comparison with different value of parameter specifically in terms of swarm size.

Whereby, from the top three of optimum result that has been identified for single-shear strength as shown in Table 8.

Table 6 Tuning result for single-shear strength (B)

Swarm size	Velocity	Iteration	pBest deformation (mm)	pBest load (kN)	Maximum value of load (kN)
40	-1 to 1	5	31.73	24.14	24.14
40	-1 to 1	10	32.51	24.43	24.43
40	-2 to 2	5	32.84	24.55	24.55
40	-2 to 2	10	33.16	24.66	24.66
40	-3 to 3	5	30.16	23.56	23.56
40	-3 to 3	10	32.04	24.26	24.26
40	-4 to 4	5	32.28	24.35	24.35
40	-4 to 4	10	31.56	24.08	24.08
40	-5 to 5	5	32.90	24.57	24.57
40	-5 to 5	10	32.38	24.38	24.38

Table 7 Tuning result for single-shear strength (C)

Swarm size	Velocity	Iteration	pBest deformation (mm)	pBest load (kN)	Maximum load (kN)
50	-1 to 1	5	33	24.61	24.61
50	-1 to 1	10	32.29	24.71	24.71
50	-2 to 2	5	32.84	24.55	24.55
50	-2 to 2	10	32.87	24.56	24.56
50	-3 to 3	5	32.93	24.58	24.58
50	-3 to 3	10	33.3	24.71	24.71
50	-4 to 4	5	33.01	24.61	24.61
50	-4 to 4	10	30.44	23.66	23.66
50	-5 to 5	5	32.01	24.24	24.24
50	-5 to 5	10	33.22	24.68	24.68

Table 8 Optimum result of single-shear strength

swarm size	Velocity	Iteration	pBest deformation (mm)	pBest load (kN)	Maximum load (kN)
30	-1 to 1	5	33.29	24.71	24.71
40	-2 to 2	10	33.16	24.66	24.66
50	-3 to 3	10	33.3	24.71	24.71

Table 9 Fitness function for double-shear strength

Fitness function	$y = 0.13 * z^{10} - 0.71 * z^9 - 2.2 * z^8 + 3.3 * z^7 + 7.3 * z^6 - 5.7 * z^5 - 7.7 * z^4 + 2.7 * z^3 + 4 * z^2 + 18 * z + 20$ where $z = (x - 2.1)/1.2$
------------------	--

As a result for single-shear strength, from several tuning processes that had been made by changing the parameter value, the best value for deformation (X) is 33.3 and load (Y) is 24.71. The better result is obtained at the tenth iteration with swarm size of 50, positive constant of C1 and C2 is 4 and the velocity is valued from -3 to 3. Whereby, in a way of identifying the better result for double-shear strength, the tuning results are shown in Tables 10, 11 and 12 by using the fitness function in Table 9.

The highlighted results in the above Tables 10, 11 and 12 are among the most optimum value in with different value of parameter specifically in terms of swarm size. Whereby, from the top three of optimum result that has been identified for double-shear strength as shown in Table 13.

As a result for double-shear strength, from several tuning processes that had been made by changing the parameter value, the best value for deformation (X) is 3.83 and load (Y) is 46.74. The better result is obtained at the tenth iteration with swarm size of 40, positive constant of C1 and C2 is 3 and the velocity is valued from -1 to 1.

Table 10 Tuning result for double-shear strength (A)

Swarm size	Velocity	Iteration	pBest deformation (mm)	pBest load (kN)	Maximum value of load (kN)
30	-1 to 1	5	3.69	45.67	45.67
30	-1 to 1	10	3.52	42.89	42.89
30	-2 to 2	5	3.99	43.33	43.33
30	-2 to 2	10	3.69	45.62	45.62
30	-3 to 3	5	3.73	46.16	46.16
30	-3 to 3	10	3.67	45.38	45.38
30	-4 to 4	5	3.66	45.14	45.14
30	-4 to 4	10	4.08	37.05	37.05
30	-5 to 5	5	3.6	44.23	44.23
30	-5 to 5	10	3.76	46.46	46.46

Table 11 Tuning result for double-shear strength (B)

Swarm size	Velocity	Iteration	pBest deformation (mm)	pBest load (kN)	Maximum value of load (kN)
40	-1 to 1	5	3.83	46.74	46.74
40	-1 to 1	10	3.81	46.71	46.71
40	-2 to 2	5	3.78	46.57	46.57
40	-2 to 2	10	3.85	46.67	46.67
40	-3 to 3	5	3.94	45.47	45.47
40	-3 to 3	10	3.98	44.13	44.13
40	-4 to 4	5	3.68	45.48	45.48
40	-4 to 4	10	3.71	45.94	45.94
40	-5 to 5	5	3.35	39.94	39.94
40	-5 to 5	10	3.83	46.74	46.74

Table 12 Tuning result for double-shear (C)

Swarm size	Velocity	Iteration	pBest deformation (mm)	pBest load (kN)	Maximum value of load (kN)
50	-1 to 1	5	3.88	46.44	46.44
50	-1 to 1	10	3.88	46.5	46.5
50	-2 to 2	5	3.8	46.67	46.67
50	-2 to 2	10	3.84	46.73	46.73
50	-3 to 3	5	3.82	46.74	46.74
50	-3 to 3	10	3.81	46.72	46.72
50	-4 to 4	5	3.76	46.44	46.44
50	-4 to 4	10	3.83	46.74	46.74
50	-5 to 5	5	3.78	46.57	46.57
50	-5 to 5	10	3.86	46.66	46.66

Table 13 Optimum result for double-shear strength

Swarm size	Velocity	Iteration	pBest deformation (mm)	pBest load (kN)	Maximum load (kN)
30	-5 to 5	10	3.76	46.46	46.46
40	-1 to 1	5	3.83	46.74	46.74
50	-3 to 3	5	3.82	46.74	46.74

6 Conclusion

The goal of this project is to find optimal solution for timber with composite material connection, particularly single-shear and double-shear strength. The prototype developed will help expert in determining the optimum value of load in an automated way. Even though the PSO fitness functions has not sharply matched the brittle behaviour of the load-displacement of the tensile behavior for both single and double shear connections, their overall tensile performance and capacity of the connections are well predicted. Therefore, the findings from this research will be beneficial to timber engineers in predicting the timber composite connections design capacity. The appropriate computational approaches that identified from this research may help in implementing the best approach to support timber joint design using composite material as compared to the conventional experimental test. Eventually, it can reduce the cost, time and efficiently determining the tensile strength capacity for the composite timber connections.

Acknowledgments The authors would like to thank Faculty of Computer and Mathematical Sciences, Faculty of Civil Engineering, University Teknologi MARA and Ministry of Education (MOE) through RAGS grant, (600-RMI/RAGS 5/3 (61/2013 for all supports in establishing this research.

References

1. A. Roos, L. Woxblom, D. McCluskey, The influence of architects and structural engineers on timber in construction—perceptions and roles. *Silva Fennica* **44**(5), 871–884 (2010)
2. S.G.C. Timmer, Feasibility of tall timber buildings, Master Thesis, Faculty of Civil Engineering and Geosciences, Delft University of Technology, 2011
3. P. Dietsch, S. Winter, Robustness of secondary structures in wide-span timber structures, in *Proceedings WCTE* (2010)
4. W. Toong, J. Ratnasingam, M.K.M. Roslan, R. Halis, The prediction of wood properties from anatomical characteristics: the case of common commercial Malaysian timbers. *BioResources* **9**(3), 5184–5197 (2014)
5. E. Frühwald Hansson, Analysis of structural failures in timber structures: typical causes for failure and failure modes. *Eng. Struct.* **33**(11), 2978–2982 (2011)
6. M. Fragiaco, E. Lukaszewska, Development of prefabricated timber–concrete composite floor systems. *Proc. ICE Struct. Build.* **164**(2), 117–129 (2011)

7. R. Hassan, A. Ibrahim, Z. Ahmad, M. Ahmad, Dowel-bearing strength properties of two tropical hardwoods, in *InCIEC 2013* (Springer, Singapore, 2014) pp. 27–36
8. H.J. Blass, M. Schmid, H. Litze, B. Wagner, Nail plate reinforced joints with dowel-type fasteners, in *Proceedings of the 6th World Conference on Timber Engineering*, July 2000
9. J.V. Smart, Capacity resistance and performance of single-shear bolted and nailed connections: an experimental investigation, Doctoral dissertation, Virginia Polytechnic Institute and State University, 2002
10. Z. Ahmad, Y.C. Bon, E.A. Wahab, Tensile strength properties of tropical hardwoods in structural size testing. *Int. J. Basic Appl. Sci.* **10**(03), 1–6 (2010)
11. D.P. Rini, S.M. Shamsuddin, S.S. Yuhaniz, Particle swarm optimization: technique, system and challenges. *Int. J. Comput. Appl.* **14**(1), 19–26 (2011)
12. D. Bratton, J. Kennedy, Defining a standard for particle swarm optimization, in *Swarm Intelligence Symposium, 2007. SIS 2007* (IEEE, New York, 2007) pp. 120–127
13. Q. Bai, Analysis of particle swarm optimization algorithm. *Comput. Inf. Sci.* **3**(1), 180 (2010)
14. M. Yusoff, J. Ariffin, A. Mohamed, An improved discrete particle swarm optimization in evacuation planning, in *International Conference of Soft Computing and Pattern Recognition, 2009. SOCPAR'09*. (IEEE, New York, 2009) pp. 49–53
15. M. Yusoff, J. Ariffin, A. Mohamed, A multi-valued discrete particle swarm optimization for the evacuation vehicle routing problem, in *Advances in Swarm Intelligence* (Springer, Berlin, 2011) pp. 182–193
16. M. Yusoff, S.M. Shalji, R. Hassan, Particle swarm optimization for single shear timber joint simulation, in *InCIEC 2013* (Springer, Singapore, 2014) pp. 117–126

A Review of Dowel Connection for Glulam Timber Strengthening with GFRP

Nurul Atikah Seri, Rohana Hassan and Shaharin Hamid

Abstract Glued laminated timber also known as glulam had been widely used as construction materials. As the demands are increasing, the research to optimize the strength of glulam timber also increasing. It is known from previous study that glass fibre reinforced polymer (GFRP) is significantly increased the strength of timber. It could be also an essential material in rehabilitation process of glulam timber in terms of cost reducing. This paper mainly review on the previous study in determining the flexural performances of timber by using GFRP which clearly indicates from the results that GFRP is one of the favor materials in enhancing the timber strength. Overall, most of the study focusing on the application of GFRP together with connectors in glulam timber. There is also significant value of timber strength in the review researches that only layered or wrapped by GFRP and timber strength that used together with GFRP and strengthened with connector. Hence further research should be focus on finding flexural performances of glulam timber with GFRP strengthened with connector.

Keywords Flexural strength · Glass fibre reinforced polymer · Glulam timber · Dowel connection

1 Introduction

Glulam timber nowadays had been used in many types of construction such as school, new buildings, multi-storey car parks, electricity masts and many other projects. Glulam become favourite in construction materials for its flexible size and

N.A. Seri · R. Hassan (✉)
Faculty of Civil Engineering, UiTM, 40450 Shah Alam, Selangor Darul Ehsan, Malaysia
e-mail: rohan742@salam.uitm.edu.my; rohan742@yahoo.com

S. Hamid
Institute for Infrastructure Engineering and Sustainable Management (IIESM), UiTM,
40450 Shah Alam, Selangor Daru Ehsan, Malaysia

strength. Compared to concrete and steel, timber had higher strength to weight ratio. With the same size of beam and load bearing capacity for glulam and steel, glulam has approximately 1.5–2 times the strength to weight ratio of steel [1]. Other advantage of glulam is it can perform very well in fires due to the way in which timber chars at a known rate and does not deform like steel.

This last decade, Fiber-reinforced Polymer (FRP) composites have commonly used in combination with masonry and concrete structural elements. It combined with structural adhesives have been used as the reinforcement timber members to increase strength or stiffness. It is also used in the strengthening of old timber structures mainly to deal with local damage due to biological attack or to excessive loading [2].

In order to increase the strengthening efficiency in bending strength capacity of the timber connection, there were several researches in developing new material called Glass Fibre Reinforcement Polymer (GFRP). GFRP were chosen as the strengthening materials because it has good flexural strength performance. FRP was a suitable components if is apply in many structural applications such as rehabilitation, reinforcement, and development of wooden members based on its several important qualities including corrosion resistance, high strength, low weight, electromagnetic neutrality, as well as high elastic modulus and high resistance against the environmental degradation agents [1]. Wrapping glulam beam with GFRP will enhance the shear strength and flexural performance.

Connections are widely applied in timber engineering for numerous of structural applications. However the design rules for the connection are lacking in many parts which often limit the use of the connections which is essential for the design of economically efficient structures.

The successful strengthening or repair of timber structures with connections is depending on the joint itself and the effectiveness of the adhesive used. Epoxy-based structural adhesives have emerged as a critical component for bonding connector with other materials because of their excellent adhesion properties, high mechanical strength, and good chemical properties. Structural adhesives are load-bearing materials with high modulus and strength that can transmit stress without a loss of structural integrity. Compared with other joining methods, such as welding or bolting, epoxy-based structural adhesives provide exceptional advantages including redistributing stresses uniformly over a large area while minimizing peak stress concentrations, joining dissimilar materials, and reducing the overall weight and manufacturing costs [3].

Glulam with larger structure need to provide with connector to strengthen the structure. The success of timber structures depends on the details of the joints such as shape and size. However the area of the joint or connection in glulam structure also known as the weakest area. It is therefore important to select the correct choice of joint type in the early development of glulam structure [4].

2 Glass Fiber Reinforced Polymer (GFRP)

Over the past few decades, the used of Fibre Reinforced Polymer (FRP) has been studied which the performances of this fibres when combined with other structural materials such as concrete and wood were investigated. Many studies about the application of FRP into timber were conducted regarding the relations between GFRP and glulam. Alshurafa [5] were investigated the performance of GFRP reinforced the glued laminated curved beams. As a result, the GFRP can be considered as an effective and economically practical solution to strengthen and stiffened the glulam arches without any addition of substantial weight to the structure [5].

GFRP also has high fatigue endurance limits, it can absorb large impact energy, potential of the corrosive is reduced as well as it can provide maximum. It is suitable to use GFRP as enhancement material to the glulam timber. This maybe can help to improve the performance of glued laminated timber strengthened with GFRP fabric in terms of flexural performance.

3 Structural Performances of Glued Laminated Timber with GFRP

The strengthening of glulam beam using fibre reinforced polymers (FRPs) together with had been common practice for this past 20 years. The used of FRPs had been always in the traditional strengthening methods which refer to externally bonded steel plates or a new solution that has recently gained great favour concerns the use of externally bonded fiber reinforced polymer (FRP). FRPs are known for their low modulus of elasticity, high strength and as a favor for rehabilitation projects.

Studied done by Micelli and Scialpi, 2005 using Carbon FRP (CFRP) showed an improvement as the reinforced beams demonstrated an increase in ultimate capacity and stiffness. Several researchers have also studied the effect of applying FRP sheets on the tensile face of beams, increasing their flexural strength and stiffness [6].

The use of fibre as one of the reinforcement materials in timber products were first introduced in an article from Forest Products Journal in 1964 [7]. As provided by Gentry [8] study which focus on flexural performances on Glued-Laminated Timbers with FRP shear, there is significant improvement on timber beam shear strength. The results shows an increment of 50 % of allowable shear stress [8]. Furthermore the application of FRP at the tension area of timber member had been under research for some time.

For last few decades researcher turn into GFRP as timber reinforcement material which increase the structural strength and the efficiency of beams. Research done by Akbiyik et al., they proposed the idea of repairing heavy timber beams that used for railway bridges by GFRP. The use of GFRP in the timber managed to increase the shear strength by 60 % [9].

Gentile et al. [10] tested on 22 of timber beam samples were reinforced with GFRP bars where seven of it were controlled samples. The experiment used four point loading bending method. As a result the strength of samples increased to 18 to 46 % from controlled samples. When the testing applied to full scaled timber beams, the strength increased 5 % until to 7 % [10].

Silva-Henriquez et al. [11] used 45 Douglas fir timber beam samples to test prestressed performances of glulam timber with GFRP. The samples were tested under three conditions which are controlled samples without any reinforcement, samples that prestressed with GFRP laminated at the tension area and reinforced samples with GFRP without prestressed at tension area. Each samples are tested with servo-hydraulic Instron machine with a 245-kN actuator. Overall responses of the study are as in Figs. 1, 2 and 3.

Fig. 1 Load displacement of controlled beams [11]

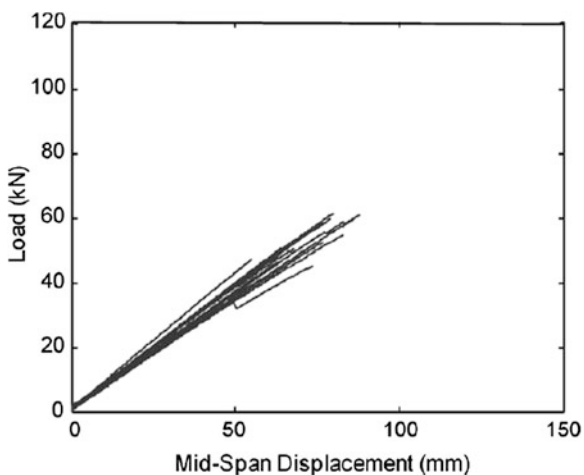


Fig. 2 Load displacement of prestressed beams [11]

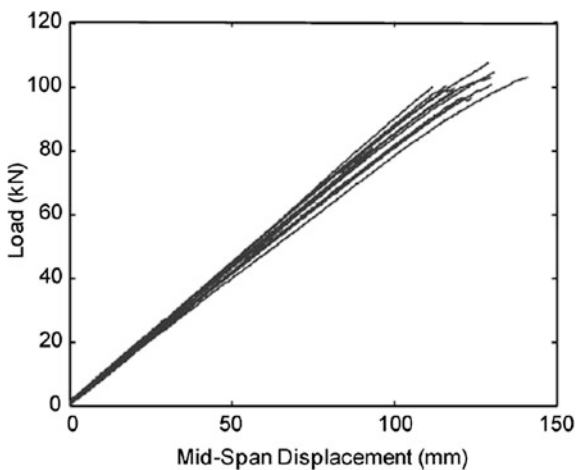
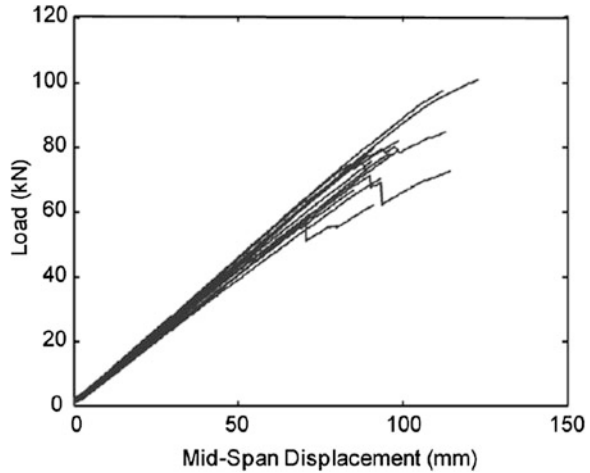


Fig. 3 Load displacement of reinforced beams [11]



The results indicate of increasing the prestressing of the GFRP laminated beam strength by 95 % while for the conventionally reinforced beams, the strength increased by 38 % [11].

Alhayek and Svecova [12] used 20 sample of Douglas Fir beams and were laminated by 5 × 50 mm GFRP to test flexural stiffness and strength of the beams. All the beam were simply supported on rollers and tested in three-point bending. The samples are tested based on two condition which are reinforced with GFRP in the tension zone only (T) and reinforced with GFRP both in tension and compression zone (TC). The result of the study depending on the comparing predicted increasing beam strength by formula as no control beams were tested and compared with experimental value. Formula formulated by Buchanan [13] was used to calculate the strength of unreinforced beams which is;

$$f_m = \left[\frac{k_3 + 1}{c} \right]^{1/k_3} f_{tu} \tag{1}$$

where f_m = bending strength, k_3 = stress distribution parameter, c = ratio of the depth of the neutral axis to the overall depth and f_{tu} = axial tensile strength. While for the reinforced beams for flexure only, formula developed by Gentil et al. [10] which is;

$$f_m = \alpha \left[\frac{k_3 + 1}{c} \right]^{1/k_3} f_{tu} \tag{2}$$

where α = adjustment factor to account for FRP reinforcement (Tables 1 and 2).

Based on the results, both groups increased by 36 and 31 % in strength on average. It is clearly indicates that laminated GFRP increased the flexural capacity of timber beams.

Table 1 Experimental and analytical results of ultimate loads for group T [12]

Bean	NLGA grade	P_{ult}^{theo} (control) (kN)	P_{ult}^{exp} (reinf.) (kN)	P_{ult}^{theo} (reinf.) (kN)	Strength increase (%)	$\frac{P_{ult}^{theo} (reinf.)}{P_{ult}^{exp} (reinf.)}$
1	2	3	4	5	$(4 - 3)/4$	$5/4$
T1	No. 1	74.31	143.86	80.74	48.34	0.56
T4	No. 2	56.97	101.58	88.39	43.91	0.87
T5	No. 2	106.49	100.59	150.29	-5.87	1.49
T6	No. 2	65.54	100.48	95.59	34.78	0.95
T7	No. 2	52.76	125.70	80.71	34.78	0.64
T8	Standard	68.38	100.99	99.05	32.29	0.98
T10	No. 2	68.48	114.70	94.95	40.30	0.83
Average					35.97	0.90
Standard deviation					18.85	0.28

Table 2 Experimental and analytical results of ultimate loads for group T [12]

Bean	NLGA grade	P_{ult}^{theo} (cont.) (kN)	P_{ult}^{exp} (reinf.) (kN)	P_{ult}^{theo} (reinf.) (kN)	Strength increase (%)	$\frac{P_{ult}^{theo} (reinf.)}{P_{ult}^{exp} (reinf.)}$
1	2	3	4	3	$(4 - 3)/4$	$5/4$
TC2	No. 2	48.50	62.56	69.75	22.48	1.11
TC6	No. 2	99.52	148.3	134.03	32.89	0.90
TC7	Utility	65.03	83.58	101.90	22.19	1.22
TC8	Utility	57.58	107.96	86.33	46.67	0.80
Average					31.06	1.02
Standard deviation					9.99	0.17

As for Hay et al. [14] also study about the GFRP sheets but to test the shear strength of GFRP wrapped timber. 20 stringer samples were tested with three different conditions. Ten without GFRP stringers as controlled samples (C), five stringer samples with GFRP wrapped diagonally at the bottom (D) and the other five with GFRP wrapped vertically at the bottom of the samples (V). The samples were tested by linear variable displacement transducers (LVDTs) for deflection and strain gauges for strains.

Figure 4 shows the load deflection of the samples. The load failure load in average for samples with diagonal GFRP sheets was 137.5 kN, which is an increase over 34.1 % the control samples and 15.3 % over the samples with vertical sheets. From the study GFRP diagonally wrapped timber showed a good number in terms of ultimate load capacity. The value of ultimate load capacity was higher than the GFRP vertically wrapped timber and controlled samples. Whereas from the study also, GFRP vertically wrapped timber sheets were easy to tear up.

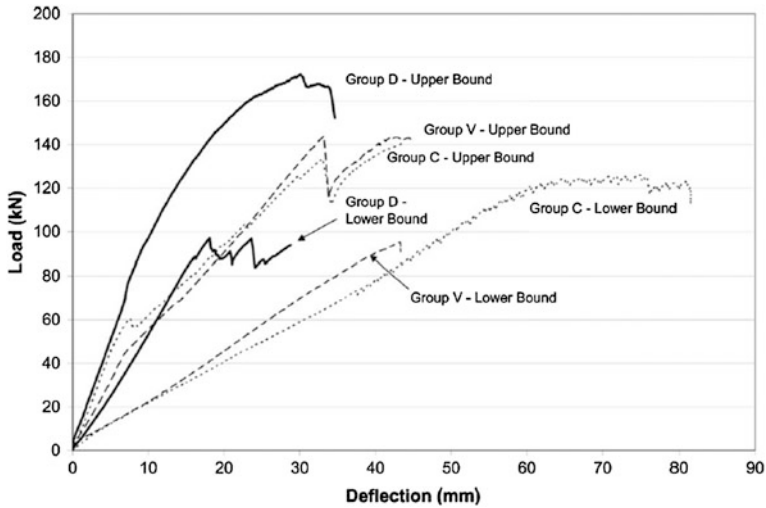


Fig. 4 Load-deflection curves of tested beams [14]

The result shows that the diagonal GFRP sheets are more effective than vertical sheets however to ensure better performances of the sheets, the sheets need to be anchored or wrapped at the bottom of the timber [14].

Recently there is study done by Osmannezhad et al. [15] to examine the effects of applying GFRP between the glulams timber layers. The main aim of this study is to evaluate the properties of flexural in unreinforced and reinforced glulam timber. The glulam timber were made of five layers and 12 were unreinforced while 24 were reinforced with GFRP with two species of wood, poplar and beech. The samples with reinforced by GFRP were divided by four categories for each samples species (Fig. 5).

1. Glulams, reinforced by layer of GFRP at bottom (U1).
2. Glulams, reinforced by two layers of GFRP at bottom (U2).
3. Glulams, reinforced by two layers of GFRP between last two bonding-line at tensile side (B2).
4. Glulams, reinforced by four layers of GFRP between last two bonding line at tensile side (B4).

Load was applied by three-point loading bending test to the centre of tangential surface of samples by bearing block. The result of the study are as below.

From Table 3, glulam beam for both of the species with four layers of GFRP resulted the highest and stiffness of bending test and the highest ultimate strength. However, using four layers of GFRP to enhance the strength of glulam could be cost consuming.

Flexural strength or also known as bending strength is the strength where the specimen tends to failed when certain amount of load is applied on it. A study on the

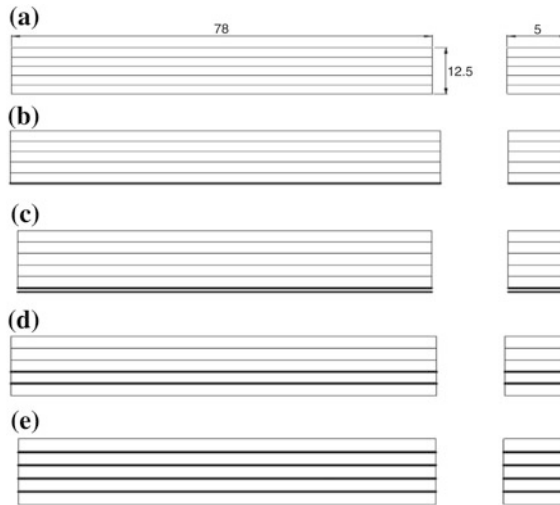


Fig. 5 Various GFRP reinforcement configurations in reinforced timbers [15] and one controlled sample. **a** Non-reinforced glulam, **b** reinforced glulam by one GFRP layer at, **c** reinforced glulam by two GFRP layer at, **d** reinforced glulam by two GFRP layer at between timber's layer (B_2), **e** reinforced glulam by four GFRP layer at between timber's layer (B_4)

Table 3 The percent of increasing for modulus of elasticity, MOE and modulus of rupture, MOR in glulams (reinforced and non-reinforced) timbers in compare with sawn timber for each species [15]

Samples	MOR increase %		MOE increase %		Failure mode
	Beech	Poplar	Beech	Poplar	
Species	Beech	Poplar	Beech	Poplar	–
Glulam with epoxy	11	14	4.9	5.3	Brittle failure in tensile side
Glulam with PVA	8	12	2.6	2.7	Brittle failure in tensile side
Glulam + 1 layer GFRP at bottom	17.9	22	7.4	7	Ductile failure in tensile side
Glulam + 2 layer GFRP at bottom	35.8	40.7	12.3	13	Ductile failure in tensile side
Glulam + 2 layer GFRP at between	29.8	33.3	12	11.9	Ductile failure in tensile side
Glulam + 4 layer GFRP at between	38.4	59.2	15.4	15.8	Ductile failure in compression side

bending properties of wood had been conducted by Andre [16]. They used wood specimens with the dimensions of $100 \times 160 \times 2,600$ mm. The specimen was tested under four point bending at a constant loading rate of 0.100 kN/s. The results showed that the specimens have great significance in successful timber utilization [16].

The previous study conducted by Yusof and Saleh [17] focused on the bending characteristics of glulam timber from selected Malaysian hardwood timber. The dimensions of the specimens were $300 \times 150 \times 6,000$ mm. The specimens were tested under four point loading at a constant loading rate of 0.5 mm/s. From the results, which were load-displacement graph, they concluded that the bending strength for different strength groupings of timber was the same. They also determined that the maximum bending strength of glulam timber was greater compared to allowable bending strength. This shows that the glulam timber is suitable to be used as structural member [17].

Previous study conducted by Svecova and Eden [18] was to investigate the bending behavior of timber beams strengthened with glass fibre reinforced polymer (GFRP) rods. They studied used seven (7) timber samples beams of Yellow Meranti species with the dimensions of $100 \times 200 \times 3,000$ mm and tested under four point bending with constant loading rate of 2.0 kN/min. One of the beams was used as a control beam (unstrengthened) while the remaining six were strengthened before test to failure. The bending behavior of the beams was studied through their load-deflection characteristics and strain distribution across the depth of the beam upon loading and also the failure modes. The results showed that the strengthened beams performed better than the control beam. The ultimate load has increased between 20 and 30 % for the strengthened beams when compared to the control beam. The stiffness increased between 24 and 60 % for the strengthened beams [18].

The bending strength was found to be higher with the use of timber made up from glued laminated and with the present of GFRP as a tool to increase the strength of the timber.

Hence for further study on flexural performances of glued laminated timber layer by GFRP at the bottom should be used as from previous study it give the highest value compared to the previous study. The glulam timber also will strengthened by dowel connection to reduce the GFRP cost and compare the result with of four layers GFRP from Osmannezhad et al. [15] study.

4 Conclusion

Most of research paper focusing on GFRP rods inserted inside the glulam timber. Fewer on the GFRP sheets. Furthermore, the GFRP rods itself acts as connector to two glulam member. There is also significant value of timber strength in study that only layered or wrapped by GFRP and timber strength that used together with GFRP whether wrapped or layered and strengthened with connector.

Acknowledgments Authors express utmost gratitude to RAGS grant: 600-RMI/RAGS 5/3 (51/2012), Research Management Institute, Universiti Teknologi MARA for financial support.

References

1. D. Yeboah, S. Taylor, D. Mcpolin, R. Gilfillan, Pull-out behaviour of axially loaded Basalt Fibre Reinforced Polymer (BFRP) rods bonded perpendicular to the grain of glulam elements. *Constr. Build. Mater.* **38**, 962–969 (2013)
2. N. Maamor, *Composite Tensile Resistance Timber Connection Fastened Using Nails and GFRP Fabric*. Unpublished manuscript. Postgraduate. Universiti Teknologi MARA (n.d.)
3. Z. Ahmad, M. Ansell, D. Smedley, P.M. Tahir, Creep behavior of epoxy-based adhesive reinforced with nanoparticles for bonded-in timber connection. *J. Mater. Civ. Eng.* **24**(7), 825–831 (2012)
4. M. Batchelar, K. Mcintosh, Structural joints in glulam, pp. 17–20 (1998)
5. S. Alshurafa, *Development of Meteorological Towers Using Advanced Composite Materials* (University of Manitoba, Winnipeg, 2012)
6. F. Micelli, V. Scialpi, A. La Tegola, Flexural reinforcement of glulam timber beams and joints with carbon fiber-reinforced polymer rods. *J. Compos. Constr.* **9**(4), 337–347 (2005)
7. F.F. Wangaard, Elastic deflection of wood-fiberglass composite beams. *For. Prod. J.* **14**(6), 256–260 (1964)
8. T. Gentry, Performance of glued-laminated timbers with FRP shear and flexural reinforcement. *J. Compos. Constr.* **15**(5), 861–870 (2011)
9. A. Akbiyik, A.J. Lamanna, W.M. Hale, Feasibility investigation of the shear repair of timber stringers with horizontal splits. *Constr. Build. Mater.* **21**(5), 991–1000 (2007)
10. C. Gentile, D. Svecova, S.H. Rizkalla, Timber beams strengthened with GFRP bars: development and application. *J. Compos. Constr.* **6**(1), 11–20 (2002)
11. R. Silva-Henriquez, H. Gray, H. Dagher, W. Davids, J. Nader, Strength performance of prestressed glass fiber-reinforced polymer, glued-laminated beams. *For. Prod. J.* **60**(1), 33–39 (2010)
12. H. Alhayek, D. Svecova, Flexural stiffness and strength of GFRP-reinforced timber beams. *J. Compos. Constr.* **16**(3), 245–252 (2012)
13. A. Buchanan, Bending strength of lumber. *J. Struct. Eng.* **116**(5), 1213–1229 (1990)
14. S. Hay, K. Thiessen, D. Svecova, B. Bakht, Effectiveness of GFRP sheets for shear strengthening of timber. *J. Compos. Constr.* **10**(6), 483–491 (2006)
15. S. Osmannezhad, M. Faezipour, G. Ebrahimi, Effects of GFRP on bending strength of glulam made of poplar and beech. *Constr. Build. Mater.* **51**, 34–39 (2014)
16. A. Andre, *Fibres for Strengthening of Timber Structures*, vol. 3 (Forest and Wood Product Research and Development Corporation, Australia, 2006), pp. 1–91
17. A. Yusof, A.L. Saleh, Flexural strengthening of timber beams using glass fibre reinforced polymer. *Electron. J. Struct. Eng.* **10**, 2010 (2010)
18. D. Svecova, R. Eden, Flexural and shear strengthening of timber beams using glass fibre reinforced polymer bars an experimental investigation. *Can. J. Civ. Eng.* **31**(1), 45–55 (2004)

A Review of Connections for Glulam Timber

Nurain Rosdi, Rohana Hassan and Mohd Hanafie Yasin

Abstract The use of timber as structural member have come under serious review and study recently as good quality logs are alarmingly becoming scarce besides the chronic problems of traditional sawn timber. Many researches regarding the use of timber are needed to strengthen or repair old timber structures as well as to improve the mechanical properties of new timber structures. Connection is one of the important parts in wood-based products. It can help the structure to increase their strength performance. A detailed and proper connection must be designed properly in order to make sure that the structure can transfer design loads to and from a structural glulam without causing localized stress concentrations that can cause any failure at the joint. This paper reviewed about the performance of glulam with connection, glulam as a replacement of solid timber since it have been proved by some researchers that it give better strength compared to solid timber and the best connection type that can be used to strengthen the structural glulam member.

Keywords Glulam timber · Bolt and nut connection · Dowel connection

1 Introduction

More research has been studied on the connections of timber. Most of the study focused on the type of connections that will improve the strength of the timber. Bolted and dowel connections in wood structures are categorized as one of the extensive research. Most published work on the behavior of these connections involves in simple geometry joints, subjected to uniaxial load in double shear. However, little research has been done on these connections in wood subjected to bending and tension loading.

N. Rosdi · R. Hassan (✉) · M.H. Yasin
Faculty of Civil Engineering, UiTM, 40450 Shah Alam, Selangor Darul Ehsan, Malaysia
e-mail: rohan742@salam.uitm.edu.my; rohan742@yahoo.com

Glued laminated timber, also called glulam, is a type of structural timber product comprising a number of layers of dimensioned timber bonded together with durable, moisture-resistant structural adhesives. By laminating a number of smaller pieces of timber, a single large, strong, structural member is manufactured from smaller pieces. These structural members are used as vertical columns or horizontal beams, as well as curved, arched shapes. Glulam is readily produced in curved shapes and it is available in a range of species and appearance characteristics to meet varied end-use requirements.

Common uses of timber or glulam in residential construction include ridge beams, garage door headers, door and window headers, and columns. High strength and stiffness make glulam beams ideal for long-span girders and beams needed for commercial construction. Glulam arch systems and trusses further increase the aesthetic and structural possibilities when using laminated timber construction. The size of structural glued laminated timber members is limited only by transportation and handling constraints.

For most construction that were made up from wood-based products, there will be some type of connection being used in order to increase the strength of the wood. Since before, connections were found to be the most crucial engineered aspects of light-frame wood construction as it was part of the weakest link in the construction. It was due to the need for ductile performance of a structure.

There are two types of connection that are common used by the researchers these days such as dowel type connection and bolted connection. There are some different between these two fasteners which are the effect from the drilling clearance where for bolts may be below than 1 mm and zero for dowels.

2 Bolt and Nut Connections

As reported by Sotelo and Pellican [1], many researchers had been studying the strength capabilities of bolts and nuts as fasteners. The ductility of joints becomes important in order to make sure that the integrity of the structures is maintain especially during loading events like wind and earthquakes [2].

As for the bolts, together with the use of three-dimensional nuts and washers, it produces a normal load within the bolt, called rope effect. Whereas, even though the dowel connections reduce the initial sliding, however it does not ensure that the connected members will not split. The reason why bolted connections was popular also because bolted connections are quick and easy to install, allows field assembly with no surface preparation and is insensitive to most environmental variables. One only needs to be able to drill properly aligned holes, install the bolts and provide finger tightening of the nut. Although the bolted joint is simple in appearance, its behavior under load was quite complex. As a result, the bolted connections are more preferred to use than dowel connections [3].

There are many types of round pin that are usually used to attach the structural members. That round pins are usually made up from several different materials.

Fundamental to an efficient utilization of bolted joints is an understanding of their mechanical behavior under load. Particularly germane are the effects of stress concentrations resulting from the presence of a load applied to a localized region in a member containing a hole. This behavior is a function of material and geometric factors such as wood species, bolt diameter, and distance, edge distance, spacing and number of bolts [4].

Studied has been conducted by Tan and Smith [5] to predicts the capacity for a row of bolts and whether the global failure at a connection will appear to be brittle or ductile for both single shear arrangement and double shear arrangement. Figure 1 showed the assembling of the bolts and the results were tabulated in Table 1 showed that they were both ductile and brittle for double shear arrangement (steel-timber-steel). While for single shear arrangement (timber-timber), they were ductile only. The bolt spacing and the end distance spacing extremely affected the performance of the connections.

Fig. 1 Arrangements and geometric notation for double-shear connection with bolts in a row (steel side plates and timber main member) [5]

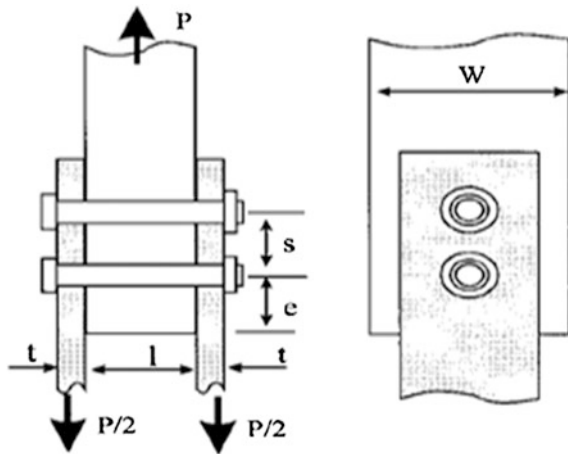


Table 1 Connection capacities and failure modes from hybrid elasto-plastic model and experiments [5]

n	Arrangement/ materials	d (mm)	s/d	e/d	l/d	Experimental P_{ut} mode (kN)	Model P_{ut} mode (kN)	Source
2	d-shear, st-tim-st	3/4" (19.05)	4	7	4.2	98 ductile	100 ductile	Mohammad et al. [6]
4	d-shear, st-tim-st	3/4"(19.05)	4	7	4.2	138 brittle	144 brittle	Mohammad et al. [6]
4	d-shear, st-tim-st	3/4"(19.05)	7	10	6.7	166 brittle	160 brittle	Masse et al. [7]
2	s-shear, tim-tim	1"(25.4)	4	7	1.5	49 ductile	52 ductile	Daneff [8]

Note *d-shear* double shear arrangement; *s-shear* single shear arrangement; *st* steel member; *tim* timber member; P_{ut} ultimate (peak) load

There are also other factors that may govern the performance of the bolts. Some variables such as member width, member thickness, fabrication tolerances, moisture content of the timber or timber-based product, preservative or fire-retardant treatment of the timber or timber-based product, and species of timber may influence the connection performance [9].

From the previous study conducted by David and Claisse [10], their focused is on the positioning of the bolted connection on the glue line in terms of the performance of the structures. They compared to both glued laminated timber and solid timber. It was found that the positioning of a bolted connection on the glue line of a glulam member does not detrimentally affect the joint's performance.

However, there were only a few studies about the performance of bolt and nut connections on glulam subjected to bending or tension. A studied had been conducted also by Sotelo and Pellican [1] to determine the performance of bolt and nut connection of wood under bending or tension loading. They only tested on a single bolt based on four (4) aspects that is wood species from low and high specific gravity, moisture content, and specimens' width as well as washer size.

Their findings showed that the wood species with high specific gravity is stronger therefore, the bending or tension performance is less influential to that species. They also found that, as the dimensions of the washer increases, the joints become more stiffs. It was also reported that the specimen's width does not affected by the increasing of washer dimensions.

Hence, the study on the performance of bolted connections shall be conducted more often in order to enhance its effectiveness so that it can be used to produce good timber-based construction products in the future. The sizes of bolt and nut that can be used are depends on the design. The size of washer also must adequate with the size of bolt based on the size according to Malaysian Standard MS544: Part 5.

3 Dowel Connections

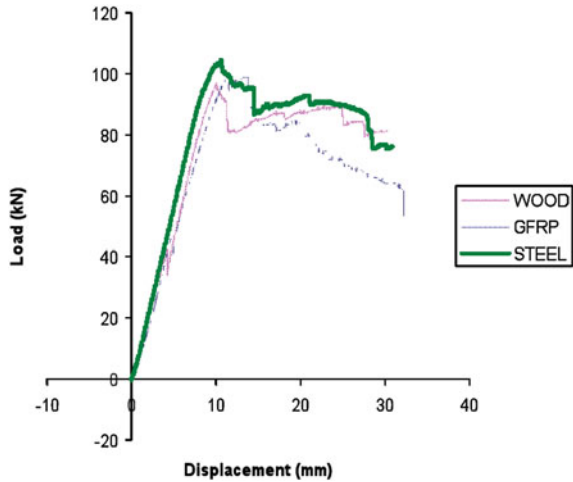
It was a common application in timber engineering to use dowel type connection for large structure. Nevertheless, the current design of dowel connection is lacking in mechanical foundation which limit the application and potential of the connector. Thus, further research to optimize the usage of dowel connection is important [11]. Sansalone and White [12] studied for dowel connection and the end grain method provide full fixity between the dowel and timber structure. Their research also indicates that the end grain connection provide consistent value and sustained loads (Fig. 2).

Hassan et al. [13] study on the shear capacity of dowelled mortise and tenon connection on timber which focus on obtaining the load carrying capacity of connections and dowelled by using steel, GFRP and wood. Ten (10) mortise and tenon connection samples for each type of dowels were tested by Linear Voltage Displacement Transducers (LVDT).

Fig. 2 Example of dowel connection



Fig. 3 Typical load versus displacement for steel, GFRP and wood dowel



As seen result from the study in Fig. 3, steel dowel showed higher value in load displacement as the physical behavior of steel is stiffer than the other dowels.

Table 2 also indicates the summary of proportional limit, 5 % diameter offset and ultimate load for steel, GFRP and wood dowel. The results showed that steel most favor as a dowel to mortise and tenon connection. According to [13] the shear capacity of mortise and tenon connection with single steel, GFRP and wood dowel does not indicate the capacity of the dowel.

An experimental investigation done by Svecova and Eden [15] focused on evaluate strength of timber reinforced with GFRP bars or rods. The study is to optimize the strength of timber bridge stringers. The study was carried out by using specimens that cut from existing bridge. The details of the sample used in this study are as in Table 3.

As in Table 3, the samples are divided into three group which are controlled samples, samples with shear steel dowels only, group S and samples reinforced both with shear and flexural, SF. The results of reinforced beam compared with the controlled samples. The results of samples tested in terms of modulus of rupture (MOR) calculated by using equation and the ultimate bending moment for each samples are summarize in Table 4.

Table 2 Nominal limit states values of steel, GFRP and wood dowel of mortise and tenon [13]

Type of dowel (nos. of test)	Ave. proportional limit (kN)	Different of Prop. limit of GFRP and wood to steel (%)	Ave. Max. load (experiment) (kN)	Different of Max. load of GFRP and wood to steel (%)	Ave. Max. load [14] (kN)	Ave. 5 % Dia. offset (kN)	Different of Max. load to 5 % Dia. offset (%)	Failure mode (EYM)
Steel (3)	127.28	–	135.75	–	–	126.78	6.6	Mode I _m
GFRP (4)	85.76	32.62	96.37	29.01	–	95.47	0.9	Mode I _m
Wood (3)	99.33	21.96	114.04	16.00	35–71	108.83	4.6	Mode III _s

Table 3 Beam description [15]



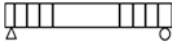
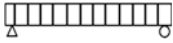
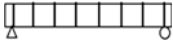
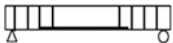



Notation	Schematic representation of strengthening scheme	No. of beams	Description
Control		9	No reinforcement used
<i>Group S</i>			
S-S150 (S)		5	Steel dowels (S) in shear span with 150 mm spacing
S-S150		5	GFRP dowels in shear span only with spacing of 150 mm
S-C150		6	GFRP dowels over the entire length at 150 mm spacing
S-C300		5	GFRP dowels over the entire length at 300 mm spacing
<i>Group SF</i>			
SF-S150		5	GFRP dowels in shear span only and flexural reinforcement
SF-S300		5	GFRP dowels in shear span only and flexural reinforcement
SF-C150		5	GFRP dowels plus flexural reinforcement
SF-C300		5	GFRP dowels plus flexural reinforcement

Table 4 The effect of strengthening on modulus of rupture (MOR)

Notation	Minimum MOR (MPa)	Average MOR (MPa)	Standard deviation (MPa)	Coefficient variation (%)	Increase (%)
Control	10.1	23.08	8.26	35.8	–
<i>Group S</i>					
SS150 (S)	23.2	28.96	6.94	24.0	25
S-S150	21.0	26.95	4.35	16.1	17
S-C150	23.9	31.10	5.77	18.6	35
S-C300	21.2	30.70	8.86	28.9	33
<i>Group SF</i>					
SF-S150	30.6	34.85	4.20	12.1	51
SF-S300	29.8	34.30	3.12	9.1	49
SF-C150	32.1	34.98	2.62	7.5	52
SF-C300	28.4	33.86	5.00	14.8	47

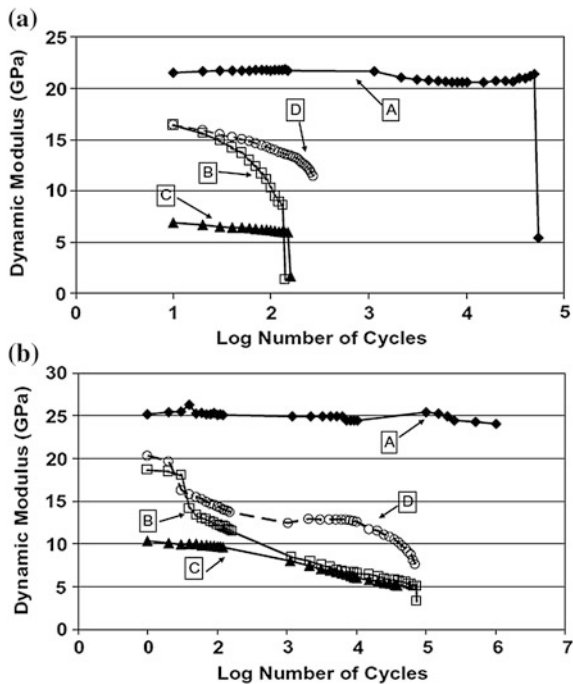


Fig. 4 Dynamic modulus versus log number of cycles for beam samples at the 75 and 50 % stress level [17]

$$f_b = \frac{M}{S} \tag{1}$$

From the equation above, f_b represents the modulus of rupture in megapascal, M represents ultimate bending moment in newton millimetres, and S represents section modulus in cubic millimetres. Based on Table 4, the results will be discussed based on three factors which are effect of dowel spacing, effect of reinforcement type and flexural reinforcement. However, this paper only focusing result based on the effect of reinforcement type. In sample S, five samples were reinforced with steel dowels. From the results, it clearly indicates an increasing of MOR by 25 % compared to GFRP dowels with only 17 %. Steel dowel can be used for further research in the future. Svecova and Eden [15] also found that both shear and flexural strengthened of timber strength increase [12].

Other than that, Svecova and Eden [15] also found that by using epoxy bond of Kemko® 040 epoxy did not perform well with steel dowel. For the next research, it should be taken note to use another type of epoxy resin and more suitable to bond the steel dowel.

Experiment done by Santos et al. [16] investigated the suitable technique to adhesively bond for dowel wood connections. They proposed two techniques for

dowel wood connection which are metal dowel was inserted into wood and strengthened with epoxy adhesive while the second technique was to laminate both faces of timber member glued carbon fibre reinforced polymer (CFRP). The efficiency of proposed technique based on experiment tests on T-connections. Through the study, it is found that the technique of laminating CFRP on both faces timber member proved to be more efficient than metal dowel. In this study also two types of adhesives were used and tested which are the ARALDITE 2011 and the HITRE 500. The result showed HIT-RE 500 adhesive was more efficient at joining the steel insert to wood.

Laminating the CFRP proven more efficient that metal dowel however if using dowel type connection more practical and lessen the time consuming, both of the technique should be combine and analysis for it should be done in the future. Madhoushi and Ansell [17] studied about the behavior of timber connections using GFRP rods. They used two solid laminated veneer lumber (LVL) beams that connected by GFRP rods bonded by epoxy. The samples divided into two, LVL beams without fasteners (A) and fastened samples with different conditions such as different glued-length and different glue thickness (B), (C), (D). The samples were tested under fatigue test and the results of were analysed with Dynamic modulus versus log number at 75 and 50 % maximum stress level as shown in Fig. 4.

From the results, solid LVL beams without reinforcement show higher fatigue strength than LVL beams that strengthened with GFRP rods. It indicates that GFRP rods did increase the static strength.

4 Glued Laminated Timber

Through years timber had been one of construction materials used in construction industry other than concrete and steel. This materials is popular because of the weight ratio which is have high strength, therefore, this materials were chosen to be used as it was easy to construct and move also because there is no framework required. Therefore, due to the unnecessary requirement of heavy machinery, it reduced the budget of construction. Nevertheless construction time can be shortened because they do not require extra time for hardening which in turn, is needed for concrete structures. In addition, due to its insulation from sound and electricity, as well as resistance to corrosion and oxidation, timber is also popular in light construction [18].

Furthermore, from the previous researches, the application of timber materials had been improved from day to day. Most of the countries in the world like London prefer to use timber in their building constructions because they want to prevent and reduce the pollution in their country. However, timber structures may also encounter problems due to the cross-sectional dimensions and lengths of some structural members are limited by the size of the trees available to produce it [19]. Besides, there were also other problems related such as design failure, excessive

loading, and infestation by termites. Therefore, glulam was introduced and been used during the last few decades to improve the timber based structures [20].

Glued laminated timber or also known as glulam was used since middle of the 19th century in Europe [21]. In Malaysia, the one and first glulam building was built by using Malaysian timber like Resak and Keruing. This was introduced by Malaysian Timber Industry Board (MITB). The building was named as Glulam Gallery and was located in Tampoi, Johor [22]. Glulam also is an engineered products produced by structurally glued up individual graded sawn timber laminations. The thickness of individual laminations shall not more than 50 mm. The benefit of glulam is shorter lengths of commercially available sawn timber can be structurally end jointed with adhesives to produce the required full-length laminations.

Davis and Claisse [10] also investigated the performance of bolted connection in glulam and structural timber composites. From the test that they had done, they found that the position of the bolted joint seems to have no effect on the performance of the connection for all specimens.

Hence, further research shall be conducted in order to improve the effectiveness of glulam product. The study may be focused on the lamination thickness of the glulam timber as it believed that it may affect the bending strength performance of the glulam.

5 Conclusion

As a conclusion, based on the literature reviews that had been done, there should be some improvement that can be done in order to produce a better product of glulam timber in the future. Bolted connection is believed to be the best type of glulam connection as it can give higher strength performance compared to dowel connection based on some tests that had been done by researchers. However, further study about this topic shall be conducted for better results.

Acknowledgments Authors express utmost gratitude to ERGS grant: 600-RMI/ERGS 5/3 (25/2012), Research Management Institute, Universiti Teknologi MARA for financial support.

References

1. R.D. Sotelo, P.J. Pellicane, Bolted connection in wood under bending or tension loading. *J. Struct. Eng.* **118**(4) (1992)
2. B.J. Tucker, D.G. Pollock, K.J. Fridley, J.J. Peters, Governing yield modes for common bolted and nailed wood connection. *Pract. Periodical Struct. Design Constr.* **5**(1) (2000)
3. M. Audebert, D. Dhima, M. Taazount, A. Bouchair, Behavior of dowelled and bolted steel-to-timber connections exposed to fire. *Eng. Struct.* **39**(2012), 116–125 (2012)

4. P.M. Mallory, P.J. Pellicane, F.W. Smith, Modeling bolted connections in wood: review. *J. Struct. Eng.* **123**(8), 1054–1062 (1997)
5. D. Tan, I. Smith, Failure in-the-row model for bolted timber connections. *J. Struct. Eng.* **125** (7) (1999)
6. M.A.H. Mohammad, P. Quenneville, I. Smith, *Bolted timber connections: Investigation on failure mechanism*. Proc., Int. Union of Forestry Res. Orgs.: S5.02 Timber Engrg. Group Mtg. (Technical University of Denmark, Lingby, Denmark, 1997), 211–226
7. D.I. Masse, J.J. Salinas, J.E. Turnbull, *Lateral strength and stiffness of single and multiple bolts in Glue-laminated timber loaded parallel to grain*. Unpublished Contract No. C-029, Eng. And Stat. (Research Centre, Research Branch, Agriculture, Ottawa, ON, Canada, 1998)
8. G. Daneff, *Response of bolted connections to pseudo-dynamic (cyclic) loading*. MSc thesis, (University of New Brunswick, Fredericton, Canada, 1997)
9. American Society of Testing and Materials, *Standard Test Methods for Bolted Connections in Wood and Wood-based Products*. West Conshohocken, ASTM D 5652-95 (2007)
10. T.J. Davis, P.A. Claisse, Bolted joints in glulam and structural timber composites. *Constr. Build. Mater.* **14**(2000), 407–417 (2000)
11. M. Dorn, K. de Borst, J. Eberhardsteiner, Experiments on dowel-type timber connections. *Eng. Struct.* **47**, 67–80 (2013)
12. M. Sansalone, R. White, End-grain dowel connections for laminated timber. *J. Struct. Eng.* **9**, 2093–2108 (1986)
13. R. Hassan, A. Ibrahim, Z. Ahmad, Shear capacity of dowelled mortise and tenon in tropical timber, vol. 17(1) (2011), p. 012012
14. J.D. Shanks, Developing rational design guidelines for traditional joints in oak frame construction. PhD Thesis. (University of Bath, 2002)
15. D. Svecova, R. Eden, Flexural and shear strengthening of timber beams using glass fibre reinforced polymer bars an experimental investigation. *Can. J. Civ. Eng.* **31**(1), 45–55 (2004)
16. C. Santos, A. de Jesus, J. Morais, B. Fontoura, An experimental comparison of strengthening solutions for dowel-type wood connections. *Constr. Build. Mater.* **46**, 114–127 (2013)
17. M. Madhoushi, M. Ansell, Behaviour of timber connections using glued-in GFRP rods under fatigue loading. Part I: in-line beam to beam connections. *Compos. B Eng.* **39**(2), 243–248 (2008)
18. A. Yusof, A.L. Saleh, Flexural strengthening of timber beams using glass fibre reinforced polymer. *Electron. J. Struct. Eng.* **10**, 2010 (2010)
19. S. Osmannezhad, M. Faecipour, G. Ebrahimi, Effects of GFRP on bending strength of glulam made of poplar (*Populus deltoids*) and beech (*Fagus orientalis*). *Constr. Build. Mater.* **51** (2014), 34–39 (2014)
20. L.D. Lorenzis, V. Scialpi, A.L. Tegola, Analytical and experimental study on bonded-in CFRP bars in glulam timber. *Compos. B* **36**(2005), 279–289 (2005)
21. A. Andre, *Fibres for Strengthening of Timber Structures*, vol. 3 (Forest and Wood Product Research and Development Corporation, Australia, 2006), pp. 1–91
22. H.I. Amaruddin, R. Hassan, N.M. Amin, N.J.A. Malek, Finite element model of mortise and tenon joint fastened with wood dowel. *InCIEC.* **1**, 3–14 (2013)

Part IX
Transportation Systems Infrastructure
and Intelligent Transport

Investigation of Patching Road Defect with Relation to Soil and Pavement Parameter: A Case Study at Bukit Beruntung

Ab. Mughni B. Ab Rahim, Muhammad Akram Adnan, Norliana Sulaiman and Mohd Azda B. Nordin

Abstract Pavement distress is one of the main issues currently faced by the Road Authorities in this country that often being raised by the public due to the unsatisfactory condition of the road and continuously deteriorate without addressing the issues effectively. Many road authorities especially in the municipality area which have less number of road expertise to conduct a proper maintenance program are not equipped with available indicator to identify when is the time a road will start to deteriorate or when is the right time to do the road rehabilitation without having problem to deal with insufficient allocation. There are several types of pavement distress encountered on a flexible pavement in this country and some of them have very significant relation with the contributing factors which are frequently affecting the pavement condition. One of the main contributing factors that are commonly known to the public is the impact of traffic volume with regards to heavy vehicle. However this issue will have no further to debate if there is no evidence to show the relationship between the pavement distress and the contributing factors and to proof the impact of heavy vehicle due to heavily using the road. It is difficult to explain the relationship between pavement distress and all the contributing factors without having a strong supporting analysis. In this study, there are many types of pavement distress occurred on flexible pavement however patching road defect was selected to be analyzed in order to find a relationship with the combination of few significant factors. The relation between pavement performance due to patching and the reaction towards it can clearly be described based on soil and pavement parameter equation. These parameters are the factors used in developing intensity patching road defect. Calculating the intensity patch can determine the category of patching

Ab.M.B. Ab Rahim (✉) · M.A. Adnan · N. Sulaiman · M.A.B. Nordin
Faculty of Civil Engineering, Universiti Teknologi Mara, Shah Alam, Selangor, Malaysia
e-mail: abmughni8636@yahoo.com

M.A. Adnan
e-mail: akram@salam.uitm.edu.my

degree. The findings are hoped to be a bench marked towards a proper way of road maintenance using established models as an indicator to predict the pavement deterioration and the contributing factors.

Keywords Pavement performance • Patching • Intensity • Road defect

1 Introduction

Malaysia has recorded a high number of fatalities due to transportation crashes. One of the major factors of the crashes is roadway condition and quality in terms of geometric design, and structural pavement condition [1]. Based on the problem encountered, the study is to developed and to investigate the pavement performance due to its characteristic as well as ground characteristic. The objectives of this study are to perform ground and pavement data collection within case study area at Bukit Beruntung, to ascertain the effects of ground and pavement characteristic towards patches on pavement, and to develop model that relates ground and pavement characteristic with patches road defect.

The location involved in this study is Bukit Beruntung with road length of approximately 1,208.33 m for Section A, 833.33 m for Section B and 1,166.67 m for Section C where there are a lot of defects occur on that road. Those defects may lead to road accident and increase the fatalities among road users. Therefore, this study is conducted to analyse one of the road defects which is patching. The road needs to have rehabilitation in order to achieve comfortability to users. Also, determination on category of patching may results in action to be taken due to severity of it. Inconvenience that faced by traffic user can also be eliminated [2, 3]. Thus, decrease the transportation crashes. Therefore, in situ test like skid resistance, sand patch, outflow, and Falling Weight Deflectometer (FWD) were conducted. JKR Probe test and Pavement Coring were conducted to measure the characteristics of pavement and soil. The Automatic Traffic Control (ATC) was installed to evaluate the traffic on three stretch of road under study.

2 Literature Review

Patching is an area of pavement that has been replaced with new material to repair the existing pavement. The factor may lead to patches are inadequate tack coat before the placement of upper layer, weak and loose layer below underlying seal and also seepage of water through asphalt which breaks the bond between surface and lower layer [4]. Replacing the wearing course or by thin bituminous overlay, the reconstruction of weak layer and re-lay upper layer are the treatment methods to

repair patching. The size of patching can be reduced by making regular and detailed inspection of the pavement.

There are many materials for patching and all of them have their purpose, strength and limitations. These materials are hot mix asphalt, cold mix, bitumen emulsion, and crack filling materials [5]. Hot mix asphalt is commonly used because it is higher than cold products placed for pavement repairs. The quality of the mix and adequate thickness of layer influenced the strength, serviceability and durability of hot mix asphalt. The other influenced factor is sufficient compaction whilst still hot. The second material used as patching is cold mix. After the storage in stockpiles for long periods, the mixture made will remain effective even if it is kept in the stockpile for long term storage because of the cold mix binder permits it. Once initial compaction is done, the mixture mainly relies on matrix interlocking physical and patches side in order to keep maintain the shape. The curing rate relies on its thickness, surrounding air temperature, as well as binder type. The cold mix needs a few days to harden in situ. Therefore, pothole patching and massive patching is suit to use cold mix as the material and also the replacement must be as fast as possible like hot mix asphalt [5]. Other materials to be used in patching are bitumen emulsion that usually can be found easily. Potholes patching can be done through the construction of aggregate and bitumen emulsion layer. This technique is beneficial if there are no plant mix materials. The last patching material is cracking filling whereby pavement cracks are filled with several products such as liquid latex, rubber, a filler and bitumen blend. At first, the crack has to be clearly cleaned in order to maintain the performance. There are four steps involve in patching operation which are preparation, priming, placing, and compaction [5]. These steps must be done correctly in order for the pavement is patched perfectly and the similar problem will not occur at the same location in the future. The technique as well as the apparatus that is used for patching purpose relies on the size of patching area that varies. Despite, the principles of patching technique is still similar (Fig. 1).

Fig. 1 Patching on road



3 Research Methodology

See Fig. 2.

In situ tests that were conducted were then grouped in three which are pavement assessment, soil assessment, and traffic data collection strategy. Skid Resistant Test, Sand Patch Test, Outflow Meter Test and Falling Weight Deflectometer (FWD) are used to assess the pavement. JKR Probe and pavement coring were conducted to make an assessment of soil while Automatic Traffic Control (ATC) equipment was installed to collect the traffic data. Skid resistant test, sand patch test, and outflow meter test were conducted to measure the condition of the pavement surface which for its friction force, texture depth and the ability measurement of the pavement to relieve pressure from vehicle' tire that will result in hydroplaning under wet condition. Meanwhile, JKR Probe measured the n-value of penetration depth. The n-value determines the consistency of soil. It will stop when it reaches 12.5 mm depth or 400 blows whichever first [6]. The ATC device was installed to determine and calculate the volume, speed, class and gap for each vehicle that passed the road using four inches spacing tube [7]. Meanwhile, FWD test determines the Young Modulus of pavement and also the ground. Coring was conducted to determine the thickness of the pavement. All information is vital in order to determine the most significant variable that contributing to patching. Only JKR Probe, FWD and coring give the most impact to patching defect. Figures 3, 4 and 5 shows the test had been performed at 3 sites.

Fig. 2 Flowchart of patching model development

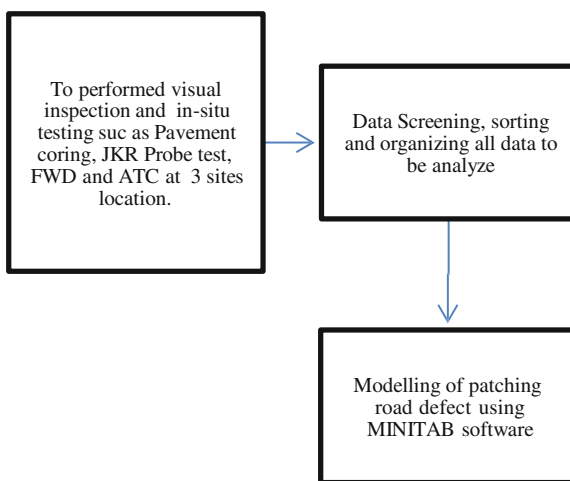


Fig. 3 FWD test



Fig. 4 JKR Probe test



Fig. 5 Coring test



4 Discussion Result for Intensity Patching Defect

Based on all of the data collected, the comprehensive data was established in a table. The summary of overall data as shown in Table 1 was developed containing all data and information such as the percentage of heavy vehicles (%HV), time mean speed (TMS), average daily traffic (ADT), annual average daily traffic (AADT), flowrate, total area, and intensity patch. The number of vehicle passed the road was calculated in one hour interval. The percentage of the heavy vehicle was calculated by total number of heavy vehicle in one hour divided by total number of vehicle in one hour. Time mean speed for heavy vehicle is then calculated as total speed of all heavy vehicles in one hour divided by total number of vehicle in one hour. Total number of vehicle in one day is divided by number of day, the ADT. Meanwhile, AADT was calculated by total number of vehicle times 365 days.

Based on the comprehensive table developed, the highest and lowest number of each parameter can be determined and show the usage of road by both heavy and light vehicles at each location. The traffic range speed and also traffic flowrate in one hour interval can be determined. Overall, Section C showed a heavy traffic flow based on the evaluation and calculation done. Section A had recorded zero value of traffic at certain time. Section B recorded the least traffic number but high number of heavy vehicles. In contrast, the road at Section C recorded high number of traffic that consists of various classes of vehicles. After taking into accounts all of the information and character, Section C showed that it was affected most by traffic and resulted in large patching area. The descriptive statistics are as shown in Table 1.

Intensity patch (IP) was calculated by dividing the total area of patching with total area of road. The value then used in Minitab software to develop the model of patching as in Eqs. 1 and 2. Based on collected data from various tests, the intensity patch equation is obtain as Eqs. 1 and 2.

$$IP = (4.8 \times 10^{-3})M_R - (1.62 \times 10^{-2})E_G - 0.762$$

With $R^2 = 90.1$ (1)

Table 1 Descriptive statistic table of each variable

Var.	Mod	Med	Mean	Std. dev	Max	Min	p-value
%HV	0	4.9	11.1	15.4	77.8	0	<0.005
TMS	48	48.0	46.4	12.5	91.0	0	<0.005
ADT	3,210	4734.0	5,085	3,298	10,502	709	<0.005
AADT	7,823	4,060.0	4,686	2,788	7,823	1,542	<0.005
Flowrate	18	163.0	259.1	249.1	1405.0	1.0	<0.005
Thick coring	0.07	0.07	0.07	0.004	0.08	0.07	<0.005
JKR Probe	3.6	4.5	4.6	1.0	6.0	3.6	<0.005
E_p	185	198.0	206.1	25	244.0	185.0	<0.005
E_G	5	7.0	8.8	4.7	16.0	5.0	<0.005

$$IP = (4.09 \times 10^{-2})P - 1.36 T - (6.82 \times 10^{-3})$$

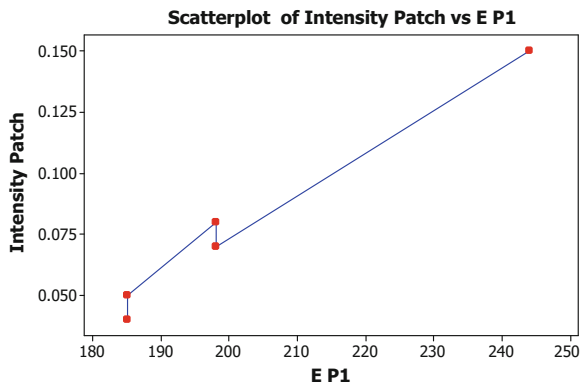
(2)

With $R^2 = 92.1$

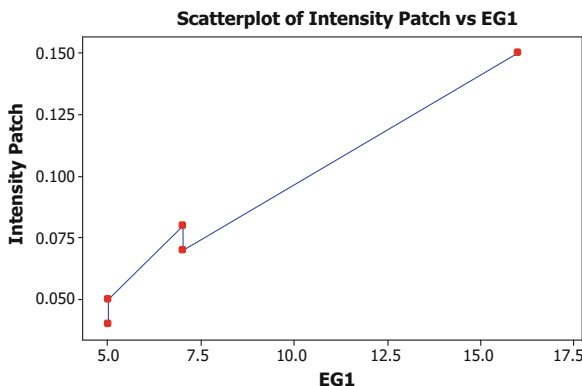
Equations 1 and 2 are developed from four variables which are Resilient Modulus (M_R), Young Modulus of Elasticity for ground (E_G), thickness of pavement (T), and penetration depth of JKR Probe (P). These models are the final and the best result obtained after many trials done to get the best fit of regression and to get the highest value of R^2 . Both model are developed using Minitab software that calculated the accuracy match of various variable such as percentage of heavy vehicle, time mean speed, flowrate (f/t), ADT, AADT, skid resistant value (SRV), texture depth (T.Dep), outflow (O/f), thickness of pavement, depth of penetration, and Young Modulus (E) for both pavement and soil. Each variable were matched to each other to achieve R^2 value of more than 50 %. Only four variables developed were the best fits which are Resilient Modulus (M_R), Young Modulus for soil (E_G), thickness of pavement (T), and penetration depth of JKR Probe (P).

Based on Eq. 1, the intensity patch is directly proportional to Resilient Modulus and inversely proportional to Young Modulus for soil. Resilient modulus is actually an estimation of pavement Young Modulus. The correlation between these three variables is clearly described in Graphs 1 and 2. The pavement that has high elasticity of bonding is able to resist the force from repetitive traffic as long as it is under the limit of elasticity. It is not the same to soil because the modulus of elasticity is not a measure of strength but how well the material returns to its original condition. The Young Modulus for soil is much lower than the Young Modulus for pavement which is Resilient Modulus. M_R and E_G factor have p -value less than 0.05 whereby the value determined the accuracy and suitability for both variables is the best factor contributes to patching. The p -value for both responses, M_R and E_S is less than 0.005 that shows both factors as predictor parameters. Also, the R^2 value for Eq. 1 is 90.1 % which indicates the best fit line can be achieved. When hot mix asphalt (HMA) is used as the surface course, it is the stiffest as measured by the resilient modulus and may contribute as the most depending upon thickness to pavement strength.

Graph 1 Graph of intensity patch against resilient modulus



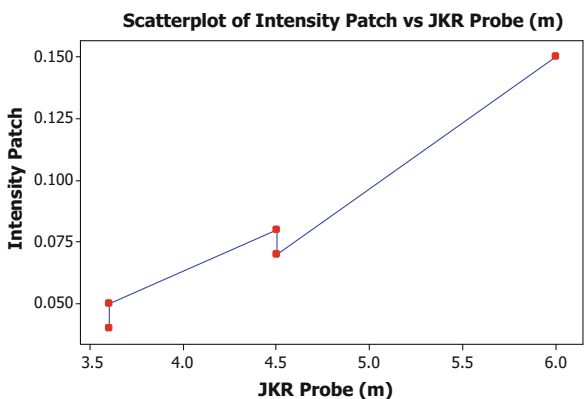
Graph 2 Graph of intensity patch against young modulus



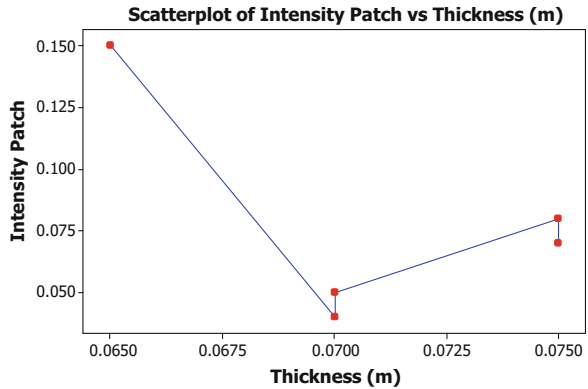
Equation 2 indicates that the intensity of the patch increased due to the decrease in thickness of pavement. It is clearly shown that the intensity patch of pavement is inversely proportional to pavement thickness whereby the lower pavement thickness affected intensity patch. It is because the lower thickness of pavement would not able to cater loads from vehicle. Therefore, the tendency to pavement defect will increase. In contrast, intensity patch will increase with the increasing of penetration depth of JKR Probe. Graph 3 and 4 clearly show the correlation of the three variables. The predictor, IP is depending on both responses which is P and T due to p -value of both responses which is less than 0.05. The p -value of both responses is less than 0.005 that show the accuracy of Eq. 2. The R^2 value shows the best fit line with 92.1 %. The increasing penetration depth of JKR Probe means the soil is softer than the upper soil layer which it would not able to cater loads from the above layer. It shows that the intensity patch is directly proportional to the penetration depth of JKR Probe.

The SRV, texture depth, and outflow meter are minor factors of patching. Their presences are not affected much on patching as a road defect. The intensity of patch

Graph 3 Graph of intensity patch against penetration depth



Graph 4 Graph of intensity patch against pavement thickness



can be categorized into two conditions which are less than 0.1 is regular patch and more than 0.1 is severe patch for Eqs. 1 and 2 and all the dimensions in SI unit.

It is important to measure the intensity of patch in order to decrease the number of crashes due to road defect. The severity of patching can be reduced by the determination of factors contributing toward it and maintenance work can be carried out before it become worst thus, the pavement performance can be improves and repair due to the deteriorations process.

5 Conclusion

This study has achieved the objectives such as to perform ground and pavement data collection within case study area at Bukit Beruntung, to ascertain the effects of ground and pavement characteristic toward patches on pavement and also to develop model that relates ground and pavement characteristic with patches road defect. All data and information about the roads at Bukit Beruntung were tabulated in comprehensive table to develop model of patching which are $IP = 0.0048 M_R - 0.0162 E_G - 0.762$ and $IP = 0.0409 P - 1.36 T - 0.00682$. The value of R^2 for both equations is 90.1 and 92.1 % respectively. The study can conclude that the most influence factor are Resilient Modulus (M_R), Young Modulus for soil (E_G), thickness of pavement (T), and penetration depth of JKR Probe (P) rather than other factors. These four variables are among the significant factor that may be contribute most in patching according to p -value which is less than 0.005 for all these variables. The predictor, IP is depending on four responses, M_R , E_G , T , and P based on p -value and R^2 best fitting line. Determination of IP is important in order to decrease the number of crashes due to road defect. The severity of patching can be reduced by the determination of factors contributing on it and maintenance work can be carried out before it become worst. Thus, lower the pavement performance and provides better riding comfort to road user.

Acknowledgments The authors would like to thank Authorities from Faculty of Civil Engineering, Universiti Teknologi MARA (UiTM) for their constant support and encouragement. Appreciation goes to the Research Management Institute (RMI, UiTM) and Ministry of Higher Education Malaysia (MOHE) for financial supports file no: 600-RMI/ERGS 5/3 (36/2012). Thank you is also extended to all individuals and organization that have made this study possible.

References

1. S.A. Sharad, A.K. Gupta, Pavement deterioration and its causes. IOSR J. Mech. Civ. Eng. 9–15 (n.d)
2. N.A. Kamaluddin, *Highway and Traffic Engineering* (Universiti Teknologi Mara, Shah Alam, 2012)
3. N.J. Garber, L.A. Hoel, *Traffic and Highway Engineering*, 4th edn. (Cengage Learning, Bostan, 2010)
4. N.E. Kordi, I.R. Endut, B. Baharom, Types of damages on flexible pavement for Malaysian Federal Road, in Proceeding of Malaysian Universities Transportation Research Forum and Conferences 2010, pp. 421–432
5. Australian Asphalt Pavement Association, in *Pavement Maintenance and Rehabilitation* (2010)
6. Jabatan Kerja Raya (JKR), JKR Probe, in *Guidelines for Planning Scope of Site Investigation Works for Road Project* (2004)
7. Federal Highway Administrative (FHWA), in *Pavement Surface Analysis Laboratory* (2005)

Rheological Evaluation of High Reclaimed Asphalt Content Modified with Warm Mix Additive

Lillian Gungat and Meor Othman Hamzah

Abstract High temperature for producing reclaimed asphalt mixture becomes the main concern in recycling as this will further age the reclaimed asphalt binder. Highly stiff binder causes workability and compatibility problems, hence affects the desirable performance of pavement. Warm mix asphalt additive is able to decrease the production temperature by reducing the binder viscosity. The synergy of warm mix asphalt and reclaimed asphalt mixtures resulted in a more environmental and energy savings benefits. The effects of a warm mix additive on the rheological properties of conventional asphalt binder containing a high proportion of recovered reclaimed asphalt binder were evaluated. Reclaimed asphalt were obtained from two sources and modified with a warm mix additive named RH. The recovered binders were blended with conventional binder at proportion of 0, 30 and 40 % and then tested for viscosity, stiffness and frequency dependency. Fuel usage and greenhouse gas emission were estimated based on the required fuel to heat up the aggregate and binder from ambient temperature up to the mixing temperature. The addition of RH improves the flow of binders by reducing the viscosity, thus decreases the construction temperature. The initial stiffness of reclaimed asphalt binders influences the effects of RH on the complex modulus and phase angle. The complex modulus increases while the phase angle decreases as the frequency increases, which indicates the binders have become stiffer. The differences in the magnitude of complex modulus are more noticeable at lower frequency and it gets close to each other at the higher frequency. This indicates that in the long run, the

L. Gungat (✉) · M.O. Hamzah
School of Civil Engineering, Engineering Campus, Universiti Sains Malaysia (USM),
Nibong Tebang, Penang, Malaysia
e-mail: liliangungat@gmail.com

M.O. Hamzah
e-mail: cemeor@yahoo.com

performance of modified reclaimed asphalt binders will be slightly better than the conventional hot mix asphalt. The warm mix additive and reclaimed asphalt composite in this study has the potential to reduce the fuel usage and green house gas (GHG) emission by 21 %.

Keywords Reclaimed asphalt • Viscosity • Construction temperature • Stiffness • Frequency-dependence

1 Introduction

The awareness of environmental and sustainability issues of road construction materials in asphalt industry has led to the widespread recycling of secondary materials. The reuse of valuable old asphalt pavement can be considered as cost effective approach for new road construction or rehabilitation. The cost saving will be more on the materials as 70 % of the cost to produce hot mix asphalt (HMA) are from materials [1]. Based on comparative life cycle assessment (LCA) studies on reclaimed asphalt (RA) the materials that were used in pavement for base and sub-base layers could potentially reduce global warming (20 %), energy consumption (16 %), water consumption (11 %), life-cycle costs (21 %) and hazardous waste generation (11 %) [2]. It was reported that the total expenditure for road maintenance program in Malaysia had increased to 2.16 billion in the year 2008 [3]. The author highlighted that pavement recycling is quite new in Malaysia, but has grown dramatically over the last few years as the preferred way for rehabilitation of an existing pavement. The pavement could be recycled partially or fully with the aid of recycling agents depending on the existing road defect. The performances of reclaimed asphalt (RA) pavement incorporated into new HMA are comparable with virgin HMA [4].

Nevertheless, increased stiffness of RA needs higher production temperature and this is the main concern in recycling as this will further age the RA binder. High production temperatures are needed to allow the asphalt binder to become viscous enough to completely coat the aggregate, have good workability during laying and compaction as well as durability during traffic exposure. To compensate the further aging of RA binder, utilization of additives, rejuvenator and lower grade of binder has been suggested [5]. Too stiff binder leads to workability and compactibility problems and causes fatigue failure in the long run. Warm mix asphalt (WMA) additive is able to reduce the production temperature as the result of viscosity reduction. The combination of WMA and RA technology leads to more environmental and energy saving benefits especially during the asphalt production. The incorporation of WMA additive allows more RA content to be incorporated into the mixtures due to improved blending and workability, despite lower production temperature [6, 7]. Various WMA technologies such as organic (wax based), chemical and foamed can be selected to be added with RA [8].

2 Literature Review

In the past, a number of researches had been conducted related to the integration of WMA technology to RA. There are two main effects of WMA additive to the RA mixtures namely: reduction of the production temperature and improved blending and workability. The benefits of lower production temperature in the RA-WMA mixtures are: minimized the further aging of RA due to heating temperature, aid in compaction, fewer emission during the production and paving, shorter construction duration and cost saving. Workability refers to the ease of compaction of the RA-WMA mixture. The workability of RA-WMA to produce porous asphalt based on Compaction Energy Index (CEI) concept was evaluated [9]. The WMA additives decreases the energy used during the production of RA mixture. The workable WMA produced a better degree of blending of RA with virgin binder [10].

The incorporation of RA into WMA mixtures can improve the moisture sensitivity [11, 12]. Other researchers indicated that low production temperature did not exhibit any negative effects on the water sensitivity. Therefore, addition of high percentage of RA to WMA mixtures might be an alternative to reduce the moisture susceptibility regardless of WMA technology and pavement layer [13]. The stiffness of the RA-WMA mixture at various percentages (10, 20, 30, 40, and 50 %) of RA with different penetration grades of binders were blended with organic, chemical and foaming WMA additives [14]. Generally, the Marshall quotient (MQ) values increased linearly with RA percentage, while the organic WMA additive exhibited high MQ values indicating a high stiffness. Investigation on the permanent deformation of surfactant additive with 50 % RA for mixtures consisting RA-HMA, HMA and WMA using wheel tracking tests investigated in [12]. The RA-WMA mixture improved rutting resistance as demonstrated by lowest rut depth.

The type of WMA additives affects the rheological and mixture's performance. Generally, commercial waxes are use as a flow improver which can reduce the viscosity. Therefore a lower construction temperature can be achieved [15–17]. Nevertheless, it has different effects on rheological properties of asphalt binder and mixture performance. RH is a new type of wax additive which was produced from cross-linked polyethylene. It is designed to reduce the viscosity of asphalt binder at high temperature while strengthening the asphalt crystalline structure at low temperature.

Most studies in the past related to RA incorporating WMA additive focused on mixture performance due to high cost of extracting and recovering the RA binder. The incorporation of high RA content will affect the rheological properties and mixture performance. Therefore, the study on the rheological properties as the results of binder modification will enhance the knowledge related to application of RA and WMA. This paper presents the rheological evaluation of conventional binder containing high proportion of recovered RA binder modified with a WMA additive. The effects of WMA wax additive on the source and amount of RA binder added have been evaluated using Dynamic Shear Rheometer (DSR) and rotational viscometer (RV).

3 Materials and Methods

3.1 Materials

1. Asphalt Binder

Conventional asphalt binder 80/100 pen which equivalent to PG64 was used in this study. This type of asphalt is normally used for local road construction in Malaysia. The asphalt binder was supplied by SHELL Sdn. Bhd. The rheological properties of the virgin binder are shown in Table 1.

2. Reclaimed Asphalt Binder

Reclaimed asphalt (RA) was obtained from the milled roads of Jabatan Kerja Raya (JKR) and Projek Lebuhraya Utara Selatan (PLUS). The recovered binder from RA was extracted by means of solvent to separate the binder from the aggregate, followed by recovery using the rotary evaporator. To make sure the consistency of binder's recovery, the penetration of every extracted RA binder were tested. The recovered binder from the RA was blended with the virgin binder at 140 °C in proportion of 30 and 40 % by mass of asphalt binder. The fundamental properties of the blended RA binder are indicated in Table 1. A designation was adopted to simplify the identification of the asphalt blend. The first number denotes the percentage of RA content followed by the source of the RA. For example, 30JKR means that 30 % RA content from the JKR road.

Table 1 Fundamental properties of binders

Binder	Source of RA	Fundamental rheological properties	
		Penetration	Viscosity at 135 °C (Pa s)
Virgin	–	86	0.400
Virgin + RH	–	92	0.270
RA	JKR	12	–
	30 %	42	0.615
	40 %	31	0.735
	PLUS	20	–
	30 %	49	0.580
	40 %	38	0.685
RA + RH	JKR	–	–
	30 %	53	0.440
	40 %	46	0.500
	PLUS	–	–
	30 %	63	0.420
	40 %	54	0.480

3. Additive

WMA additive named RH was supplied by Universal Pave Sdn. Bhd. Malaysia. The addition of additive was based on the mass of asphalt binder. The selected percentage of RH to be blended with RA binder was 3 % and decided based on the performance from basic properties test.

3.2 Tests Program

1. Preparation of RA and WMA additive

The required amount of asphalt binder and RH were blended using mechanical mixer at 145 °C for 15 min in order to obtain a homogenous blend. Meanwhile, 160 °C temperature was used for blending the RA with RH. The blending temperature of RH was recommended by the manufacturer.

2. Brookfield Rotational Viscometer

Viscosity of asphalt binder describes its resistance to flow which related to the handling characteristics. Brookfield RV was used to determine the viscosity of the unaged binders in accordance to AASHTO T316 [18]. Viscosity readings were taken every one hour from 120 to 160 °C at 10 °C increment using spindle number 27.

3. Dynamic Shear Rheometer

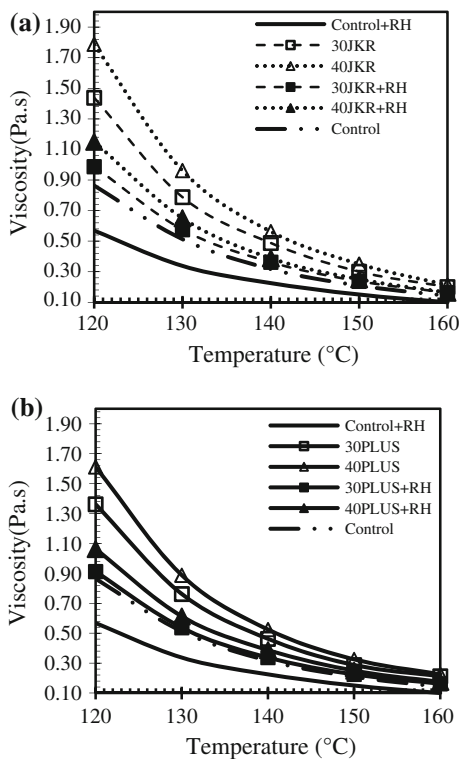
Rheological properties of the RA and RH blends were evaluated by means of dynamic mechanical methods consisting of temperature and frequency sweep of unaged samples. The oscillatory tests performed within the region of linear viscoelastic (LVE) using DSR as outlined in AASHTO T315 [19]. Two parallel plate testing geometries consisting of 8 mm diameter plates with a 2 mm gap and 25 mm diameter plates with a 1 mm testing gap were used. The rheological properties of the binders were determined with reference to their complex shear modulus (G^*) and phase angle (δ). Complex shear modulus indicates the stiffness and resistance to deformation, while phase angle represents viscoelastic balance of rheological behavior. The temperature sweeps were performed from 46 to 82 °C at 6 °C increments on 25 mm diameter plate. The applied loading frequency was 1.59 Hz which simulates the shear stress on pavement when traffic speed approximately 100 km/h. Frequency sweep were carried out at temperature ranging from 5 to 65 °C at 10 °C increments with frequencies ranging from 0.1 to 10 Hz. The amplitude sweeps using stress sweeps were undertaken at 10 °C and 40 °C for 8 mm plate and 25 mm plate respectively for determination of the limit of LVE response.

4 Results and Discussion

4.1 Rotational Viscosity of Reclaimed Asphalt Modified Binder

The ability of asphalt binder to flow at certain temperature that enables sufficient coating and bonding of aggregates can be indicated through measurement of viscosity. The viscosities of RA binder with and without addition of RH were plotted against temperature as shown in Fig. 1. The amount of RA addition affects the stiffness of the modified binder. A higher proportion of RA produced a harder binder as indicated in the penetration value and initial viscosity. It can be observed that the decrement of viscosity at lower temperature (120 °C) was notable as compared to decrement at higher temperature. This is due to the lower melting point of wax additive. The decrease in viscosity due to the addition of RH is more pronounced when virgin binder blended with 40 % RA content. The average reduction for both RA sources with 30 % and 40 % RA content are 47.4 % and 53.6 % respectively. When the temperature increases to 160 °C, the viscosity values are almost similar despite differences in binder content and RA source.

Fig. 1 Relationship between temperature and viscosity of RA binder from JKR and PLUS road. **a** JKR RA. **b** PLUS RA



4.2 Effect of RH on the Construction Temperature

The construction temperature of RA modified with RH were determined based on the recommendation by Asphalt Institute whereby mixing and compaction temperatures correspond to viscosity ranges from 170 ± 20 and 289 ± 30 mPa s respectively. However, this recommendation cannot be directly applied to the modified binder [20]. The addition of RH additive can reduce the construction temperature by about 15 °C lower than the recommended by the Asphalt Institute. The construction temperatures of the RA modified with and without RH are identical and tabulated in Table 2. RA needs higher construction temperature due to its stiffness as the result of aged binder. Higher construction temperature requires more time to cool down, thus can prolong the pavement opening to traffic after the construction completed. The addition of RH to the 30 % RA and 40 % RA content can reduce the construction temperature by 15.7 and 15.4 % respectively. The construction temperatures of RA modified binders are lower than the conventional construction temperature of HMA which benefits the asphalt production plant and road contractors.

4.3 Effects of Reclaimed Asphalt Binder Modification on Stiffness

The complex modulus (G^*) and phase angle (δ) in the previous studies of WMA binder have been used as rutting resistance indicator [21]. In addition, the G^* and δ also used to determine the performance grade (PG) of binder at high temperature. The PG indicates the stiffness of the asphalt binder and the critical value for PG determination stipulated in SHRP for the unaged is 1.0 kPa. Table 3 presents the effects of RA binder modification on the PG. The effects of incorporating RH to the

Table 2 Construction temperatures of virgin and RA modified binders

Binder	Source of RA	Construction temperature (°C)
Virgin	–	160
		130
RA	30JKR	162
	40JKR	165
	30PLUS	162
	40PLUS	165
RA + RH	30JKR	140
	40JKR	143
	30PLUS	140
	40PLUS	143

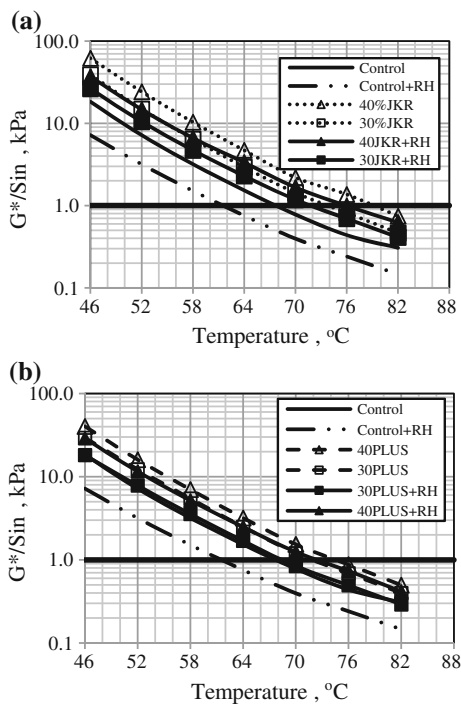
Table 3 Effect of RA binder modification of the performance grade (PG)

Binder	PG		Failure temperature °C	
	0 % RH	3 % RH	0 % RH	3 % RH
Control	64	58	67	61
30JKR	70	70	74	73
40JKR	76	76	79	76
30PLUS	70	64	72	69
40PLUS	70	70	75	72

RA binders on PG at high temperature are not significant. The change of PG can be seen in the control and 30PLUS binder. The penetration of binder (Table 1) influences the change of PG. Softer binder indicates changes in PG while the harder binder remains in the same grade. Nevertheless, the addition of RH reduces the failure temperature for all binders.

Figure 2 shows the stiffness-temperature relationship of the RA modified binders. The 40JKR binder has higher $G^*/\sin \delta$ which denotes the stiffness and resistance to permanent deformation. At high temperature, this binder is expected to perform the best to resist rutting. Past studies highlighted that rutting is the main concern in WMA especially in hot climate region [22].

Fig. 2 Stiffness-temperature relationship of unaged virgin and modified binder of JKR and PLUS RA. **a** JKR RA. **b** PLUS RA



4.4 Frequency Dependence of Modified Binders

The effect of the RA binder modification on frequency dependence can be plotted in master curve shown in Fig. 3. The master curve demonstrates the rheological properties of a bitumen in terms of $|G^*|$ and δ . The complex modulus increases linearly with frequency. As the frequency increases (longer service duration of the binder), the binder becomes stiffer. The RA content and addition of RH affects the stiffness. Significant reductions of complex modulus due to addition of RH are observe for RA from the JKR road. However, very minimum difference of complex modulus value indicated by the 30PLUS, 40PLUS and control. The binder obtained from the JKR road was stiffer than the binder from the PLUS road. Therefore, the stiffness of the RA binders could be one of the reasons for the significant difference in the complex modulus value. The difference of complex modulus is more noticeable at lower frequency and it become close to each other at the high frequency. This implies that in the long run the performance of the binders will be slightly better than the conventional HMA. The phase angles plots are closer at the lower frequency and become wider as the frequency increase. Similar trend was reported in other studies on the WMA additive with aged binders [23]. This suggests that phase angle is more sensitive to the speed rates than the complex modulus [23]. Generally, the phase angle is considered to be more sensitive to the chemical structure and therefore implies significant changes as compared to complex modulus [24].

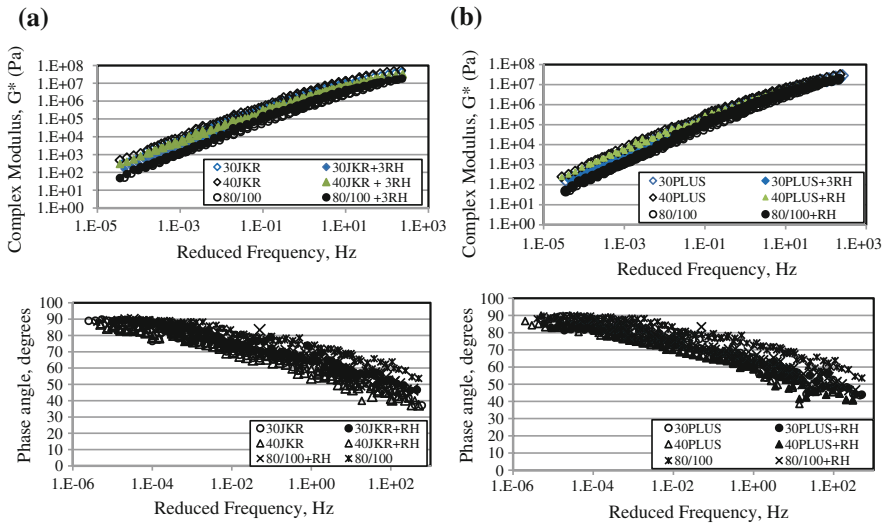


Fig. 3 Master curve of complex modulus and phase angle for RA from JKR and PLUS. **a** JKR RA. **b** PLUS RA

4.5 Environmental Evaluation

Environmental implications on the green house emissions (GHG) as the result of construction temperature reduction are estimated by adopting the method proposed by [25–27] as described in the Eq. (1).

$$Q = \sum_{i=n}^{j=n-1} mc\Delta\theta \quad (1)$$

where Q is the sum of required heat energy (J), m is the mass of material (kg), c is the specific heat capacity coefficient [J/(kg/°C)], $\Delta\theta$ is the difference between the ambient and mixing temperature (°C), and i and j indicate different materials types. Previous researchers also calculated the fuel requirements and GHG emissions with respects to the selection of the source of RA [28]. The estimation of environmental effects was calculated based on the required amount of fuel to heat up the aggregate from ambient temperature up to the expected mixing temperature. The assumed ambient temperature for this estimation was 27 °C. The volumetric properties, mixed density and materials required were estimated based on 10 km dual carriageway with 3 lanes per direction, 5 cm thick wearing course and 5 % optimum binder content. The results of the calculations presented in Table 4. The addition of RH reduces the fuel usage approximately by 32.0 % for the control as compared to without RH. The fuel usage decreases about 21.0 % and 20.3 % for 30 % RA and 40 % RA contents respectively. The reduction in fuel usage indicates positive cost savings in the asphalt mixture production plant. The average reduction of GHG emission due to the addition of RH into the RA binders is approximately 21.0 %. The construction temperature increased linearly with RA content and this result in more fuel usage and emissions. RH as a flow improver reduced the construction temperature which is lower than the control. Consequently, it reduces the fuel usage and GHG emissions. Emission can be seen visually through the volume of fumes

Table 4 Fuel requirement and GHG emission for various RA content

Mixture	Q _T (TJ)	Fuel (Ton)	Reduction	
			Fuel usage (%)	GHG emission (%)
Virgin	3.39	74		
Virgin + RH	2.57	56	32.1	32.0
30JKR/30PLUS	3.44	75		
40JKR/40PLUS	3.53	77		
30JKR + RH /30PLUS + RH	2.84	62	21.0	21.4
40JKR + RH/40PLUS + RH	2.92	64	20.3	20.8

Q_T: Required energy to heat up the aggregate and asphalt binder; type of fuel: Diesel

Assumed laboratory ambient temperature: 27 °C

Specific heat capacity of binder (PG64): 920 J/kg/°C

Specific heat capacity of granite aggregate: 790 J/kg/°C

produced at asphalt plant and paving site. The fumes contain polycyclic aromatic hydrocarbons (PAHs) and some are carcinogenic which can be hazardous to the paving crew.

5 Conclusions

From the test results on the materials used in this study, the addition of RH improves the flow of binders by reducing the viscosity. Hence, the construction temperature can be reduced to a value that is lower than the control. This reduction will compensate the further aging of aged RA binders. Binder modification with RH affects the stiffness of the RA binders by reducing the failure temperature. The change of PG is influenced by the stiffness of the binders, and changes of PG occurred on control and 30PLUS binder. Incorporation of RH also reduces the complex modulus and increases the phase angle as the frequency increase. The differences of complex modulus are more noticeable at lower frequency and it become closer to each other at the higher frequency. These indicate that in the long run, the performance of the RA modified binder will be slightly better than the conventional HMA. Environmental evaluation indicates reduction of fuel usage and GHG emissions by 21 % with the addition of RH additive.

Acknowledgments The authors would like to acknowledge the Malaysian Ministry of Higher Education for financially supporting this research work. Many thanks also due to the technicians of Highway Engineering Laboratory at the Universiti Sains Malaysia for their kind assistance.

References

1. A. Copeland, Reclaimed asphalt pavement in asphalt mixtures: state-of-the-practice (Report No. FHWA-HRT-11-021), Federal Highway Administration, 2011
2. J.C. Lee, T.B. Edil, J.M. Tinjum, C.H. Benson, Quantitative assessment of environmental and economic benefits of recycled materials in highway construction. *Transp. Res. Rec. J. Transp. Res. Board* **2158**(1), 138–142 (2010)
3. R.B. Razali, The effect of reclaimed asphalt pavement (RAP) proportion on strength properties of a full depth recycling pavement, Msc. thesis, Civil Engineering, Universiti Teknologi Mara, Malaysia, 2010
4. I. Widyatmoko, Mechanistic-empirical mixture design for hot mix asphalt pavement recycling. *Constr. Build. Mater.* **22**, 77–87 (2008)
5. R. Hassan, Feasibility of using high RAP contents in hot mix asphalt. Paper presented at the 13th international flexible pavements conference, Gold Coast, Australia, 2009
6. J.A. D'Angelo, E.H. Eric, C.B. John, L.B. Gaylon, R.C. Matthew, E.C. Jack, P.H. Thomas et al., Warm-mix asphalt: European practice. No. FHWA-PL-08-007 (2008)
7. M. Tao, R.B. Mallick, Effects of warm-mix asphalt additives on workability and mechanical properties of reclaimed asphalt pavement material. *Transp. Res. Rec. J. Transp. Res. Board* **2126**(1), 151–160 (2009)

8. S.D. Capitão, L.G. Picado-Santos, F. Martinho, Review on the use of warm-mix asphalt. *Constr. Build. Mater.* **36**, 1016–1024 (2012)
9. S. Goh, Z. You, Mechanical properties of porous asphalt pavement materials with warm mix asphalt and RAP. *J. Transp. Eng.* **138**(1), 90–97 (2012)
10. L. Gaitan, Evaluation of the degree of blending of reclaimed asphalt pavement (RAP) binder for warm mix asphalt. Master Science, Rowan University, 2012
11. X. Shu, B.S. Huang, E.D. Shrum, X.Y. Jia, Laboratory evaluation of moisture susceptibility of foamed warm mix asphalt containing high percentages of RAP. *Constr. Build. Mater.* **35**, 125–130 (2012)
12. J.R. Oliveira, H.M. Silva, L.P. Abreu, J.A. Gonzalez-Leon, The role of a surfactant based additive on the production of recycled warm mix asphalts—less is more. *Constr. Build. Mater.* **35**, 693–700 (2012)
13. S. Zhao, B. Huang, X. Shu, M. Woods, Comparative evaluation of warm mix asphalt containing high percentages of reclaimed asphalt pavement. *Constr. Build. Mater.* **44**, 92–100 (2013)
14. B. Sengoz, J. Oylumluoglu, Utilization of recycled asphalt concrete with different warm mix asphalt additives prepared with different penetration grades bitumen. *Constr. Build. Mater.* **45**, 173–183 (2013)
15. N. Wasiuddin, R. Saha Jr.W. King, Effects of a wax-based warm mix additive on lower compaction temperatures, in *Geo-Frontiers 2011@ Advances in Geotechnical Engineering*. (ASCE 2011), pp. 4614–4623
16. M.O. Hamzah, A. Jamshidi, K. Kanitpong, M.A. Yusri, Parameters to characterize the effects of Sasobit content on the rheological properties of unaged and aged asphalt binders. *J. Road Mater. Pavement Des.* **13**(2), 368–375 (2012)
17. A. Jamshidi, M.O. Hamzah, Z. You, Performance of warm wix asphalt containing Sasobit®: state-of-the-art. *Constr. Build. Mater.* **38**, 530–553 (2013)
18. AASHTO T316 2004, Standard method of test for viscosity determination of asphalt binder using rotational viscometer, in *AASHTO Standards*, American Association of State and Highway Transportation Officials, Washington, D.C. (2004)
19. AASHTO T315 2004, Determining the rheological properties of asphalt binder using a dynamic shear rheometer (DSR). American Association of State Highway and Transportation Officials, Washington, D.C. (2004)
20. Y. Yildirim, M. Solaimanian, T. Kennedy, Mixing and compaction temperatures for superpave mixes. *J. Assoc. Asphalt Paving Technol.* **69**, 34–71 (2000)
21. Z. Arega, A. Bhasin, A. Motamed, F. Turner, Influence of warm-mix additives and reduced aging on the rheology of asphalt binders with different natural wax contents. *J. Mater. Civ. Eng.* **23**(10), 1453–1459 (2011)
22. M.H. Rashwan, Characterization of warm mix asphalt (WMA) performance in different asphalt applications, Ph.D. dissertation, Iowa State University, Ames, 2012
23. H. Kim, S.J. Lee, S.N. Amirghanian, Rheology of warm mix asphalt binders with aged binders. *Constr. Build. Mater.* **25**, 183–189 (2011)
24. G.D. Airey, Rheological evaluation of ethylene vinyl acetate polymer modified bitumens. *Constr. Build. Mater.* **16**(8), 473–487 (2002)
25. M.O. Hamzah, A. Jamshidi, Z. Shahadan, Evaluation of the potential of sasobit to reduce required heat energy and CO₂ emission in the asphalt industry. *J. Clean. Prod.* **18**, 1859–1865 (2010)
26. M.O. Hamzah, A. Jamshidi, Z. Shahadan, Effects of sasobit® on the required heat energy and CO₂ emission on blended asphalt binder incorporated with aged binder. *Eur. J. Sci. Res.* **42**(1), 16–24 (2010)
27. Department for Environment, Food and Rural Affairs (DEFRA), Guidelines to GHGs calculation, Version 1.2.1. (2010)
28. M.O. Hamzah, A. Jamshidi, Z. Shahadan, Selection of reclaimed asphalt pavement sources and contents for asphalt mix production based on asphalt binder rheological properties, fuel requirements and greenhouse gas emissions. *J. Clean. Prod.* **23**, 20–27 (2012)

Effect of Aging on the Resilient Modulus of Stone Mastic Asphalt Incorporating Electric Arc Furnace Steel Slag and Copper Mine Tailings

**Ebenezer Akin Oluwasola, Mohd Rosli Hainin,
Md. Maniruzzaman A. Aziz and Santokh Singh A/L Mahinder Singh**

Abstract Currently, the cost of production of stone mastic asphalt (SMA) is relatively high for paving roads and highways. One means of reducing the cost is to use relatively low cost by-products as aggregates and fillers. The main purpose of this study is to appraise the effect of aging on resilient modulus of SMA incorporating electric arc furnace (EAF) steel slag and copper mine tailing (CMT) as binary industrial waste materials. To achieve this aim, four mix designs consisting of EAF steel slag and CMT at various percentages were investigated. Marshall stability, drain down and indirect tensile resilient modulus tests were conducted. The indirect tensile resilient modulus test was carried out to assess the stiffness of SMA mixture at 25 and 40 °C. Stiffness variation in asphalt mixtures play a vital role in inflicting cracking and rutting in pavement. While some samples were unaged, equal numbers of samples were subjected to short term and long term oven aging. The results show

E.A. Oluwasola
Department of Geotechnics and Highway, Faculty of Civil Engineering,
Universiti Teknologi Malaysia, Johor Bahru, Malaysia
e-mail: eaoluwasola2@live.utm.my

M.R. Hainin · Md.M.A. Aziz (✉)
Faculty of Civil Engineering, Universiti Teknologi Malaysia, Johor Bahru, Malaysia
e-mail: mzaman@utm.my

M.R. Hainin
e-mail: mrosli@utm.my

M.R. Hainin · Md.M.A. Aziz
UTM Construction Research Centre (CRC), Universiti Teknologi Malaysia,
Johor Bahru, Malaysia

S.S.A/L. Mahinder Singh
Malaysia Marine and Heavy Engineering Sdn. Bhd., Kuala Lumpur, Malaysia
e-mail: Santokh.singh@mmhe.com.my

that incorporating EAF steel slag and CMT into SMA mixture has a substantial positive effect on the drain down and resilient modulus of SMA. Thus, the study has contributed to the reuse of economical and environmentally friendly metallurgical and mining by-products in roads and highway industries.

Keywords Stone mastic asphalt • Industrial waste • Aging • Copper mine tailings • EAF steel slag

1 Introduction

Stone mastic asphalt (SMA) was initially developed in the 1960s in Germany. It is widely used in Europe for surfacing of harbor areas, trafficked roads and airfields [1–3]. A typical SMA mixture composed of 65–75 % coarse aggregate, 12–18 % mineral filler, 5–7 % bitumen binder and at times 0.3 % fiber [4]. The high percentage of coarse aggregate results in a stone-on-stone contact that produces a mixture that is highly resistant to permanent deformation and rutting [5]. After its application in Europe in the middle 1960s and the successful completion of many trials in Australia, America and many other countries, SMA has risen to a level that it is now regarded as the premium and valuable pavement surfacing for high speed highways and motorways, heavy traffic roads and other highways with characteristic high volumes of truck traffic [6, 7].

The advantages of SMA being a unique asphalt pavement include the ability to withstand the heavy truck loading and resist the wear of the super side, single truck tyres and studded tyres. It has 30–40 % higher durability compared to conventional dense graded hot mix asphalt. SMA also provides safety and friendly features by improving skid resistance due to the high percentage of fractured aggregate particularly on wet pavement [1]. It equally has a similar surface texture characteristics with open graded aggregate, so that the noise generated by traffic is lower than that on dense graded asphalt [8, 9]. It also provides anti-splash features during wet condition, thus reducing hydroplaning which results from water draining through the voids in the matrix. SMA surfacing may also provide reduced reflections cracking from underlying cracked pavement due to the flexible mastic [10–12].

In terms of short comings, SMA requires higher mixing temperature and longer mixing time at the plant where the time taken to add extra filler may result in reducing productivity. Another potential construction problems with SMA mixtures is drainage and bleeding of asphalt binder [13, 14]. Storage and placement temperatures cannot be reduced to control the problem of drainage and bleeding because of the difficulty in attaining the required compaction [15, 16]. Also, the possible delay before opening to traffic since SMA mix should be cooled to 40 °C to prevent sticking to the tyre surface. Another disadvantage of the SMA is the increase of material cost connected with higher binder and filler contents [17–19].

In order to reduce the cost of SMA due to its outstanding benefits, this research has been articulated towards the use of by-product as aggregate and filler. A series of studies had been conducted on hot mix asphalts produced with steel slag with knowledge of SMA mixtures incorporating electric arc furnace steel slag and copper mine tailings as the binary base material. Hence, the present study concentrates on the effect of aging on resilient modulus of stone mastic asphalt incorporating EAF steel slag and copper mine tailings.

2 Materials and Methods

2.1 Materials

SMA 14 mix designation was used. The grade of bitumen binder used in this study was PG 76, which was obtained from Shell, Singapore. Granite, EAF steel slag and copper mine tailings were obtained from Ulu choh sdn Bhd Quarry Pulai, Bhd respectively. The investigated bitumen binder characteristics were reported in Table 1. Table 2 presents the properties of the granite, EAF steel slag and CMT. The surface texture of the EAF steel slag, CMT and granite were observed through the field emission scanning electron microscope (FESEM) technique. The Zeiss supra 35vp FESEM model was used and the test was performed in accordance with ASTM E 2090 [20]. As shown in Fig. 1, the EAF steel slag and CMT were more porous than the aggregate. Also, in terms of surface texture, the EAF steel slag and CMT were rougher than the granite aggregate.

2.2 Sample Preparations

Three different types of aggregate were used in preparing the SMA 14 mixtures. Table 3 presents the mix design composition of the mixtures. The PG 76 and the aggregates were heated separately in an oven at a specified temperature. The aggregates were heated to remove any inherent moisture. The bitumen binder was

Table 1 Bitumen binder properties

Parameter	PG 76	Standards
Penetration @ 25 °C	48	ASTM D5
Softening point (°C)	64	ASTM D36
Viscosity @ 135 °C (cP)	1,800	ASTM D44
Viscosity @ 60 °C (cP)	36,200	
Specific gravity	1.031	
Mixing temperature	170–185 °C	
Compacting temperature	140–160 °C	ASTM D70

Table 2 Some of the properties of the aggregates used

Testing	Standard	Granite	EAF steel slag	Copper tailings	Specification (%)
Los Angeles abrasion	ASTM C 131	10.276	5.1	–	≤25
Flakiness	MS 30	7 %	5 %	–	≤25
Soundness	AASHTO T 104	3.5 %	0.71 %	–	≤18
Polished stone value	BS 812	52.3 %	55.3 %	–	≥40
Water absorption	MS 30	0.756 %	3.896 %	4.17 %	≤2
Stripping	AASHTO T 182	>95 %	>95 %	–	≥95
<i>Specific gravity</i>					
Coarse aggregate	ASTM C 127	2.594	2.816	–	–
Fine aggregate	ASTM C 128	2.585	3.051	3.578	–
pH	BS 1377	10.22	11.42	6.42	–

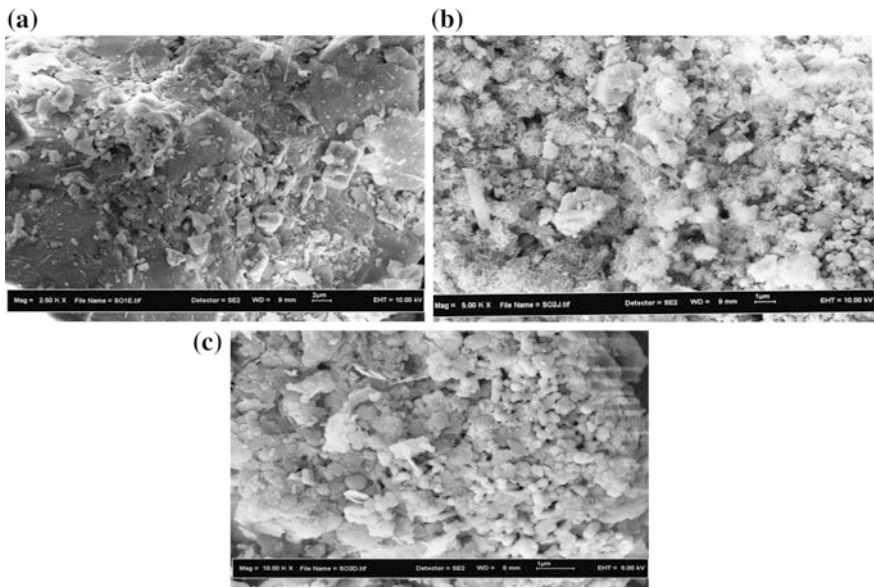


Fig. 1 a FESEM micrographs of granite. b FESEM micrograph of EAF steel slag. c FESEM micrograph of EAF copper tailing

Table 3 Mix design composition

Fraction (mm)	Mix 1	Mix 2		Mix 3		Mix 4		
	Granite (%)	Granite (%)	Copper tailing (%)	EAF slag (%)	Copper tailing (%)	Granite (%)	EAF slag (%)	Copper tailing (%)
9.50	22.0	22.0	–	22.0	–	11.0	11.0	–
4.75	48.0	48.0	–	48.0	–	24.0	24.0	–
2.36	13.0	13.0	–	13.0	–	6.5	6.5	–
0.60	9.0	–	9.0	–	9.0	–	–	9.0
0.30	2.0	–	2.0	–	2.0	–	–	2.0
0.075	4.0	–	4.0	–	4.0	–	–	4.0
Filler (cement)	2.0	2.0		2.0		2.0		

later added to the aggregates. The resulting mixture was mechanically mixed for about 60 s. Prior to mixing, the Marshall stability test had been conducted according to ASTM D 5581 [21] and the theoretical maximum density test was performed as stated in ASTM D 2041 [22] to obtain the optimum bitumen binder (OBC), which was the amount of bitumen binder added to the aggregates of individual mix. The OBC for Mixes 1, 2, 3 and 4 were 5.49, 5.69, 5.84 and 5.90 % respectively.

2.3 Aging Methods

The short term oven aging (STOA) used was conducted according to AASHTO R30-02 [23]. The method consists of $4 \text{ h} \pm 5 \text{ min}$. The mix samples were stirred every $60 \pm 5 \text{ min}$ to ensure uniform conditioning. After curing, the samples were brought to a compaction temperature and compacted using a gyratory compaction.

The long term oven aging (LTOA) was carried out according to AASHTO R30-02 [23]. The procedure was conducted on compacted specimens that have been subjected to short term oven aging. The specimens were positioned in a force-draft oven, conditioned to $85 \pm 1 \text{ }^\circ\text{C}$ for $5 \text{ days} \pm 5 \text{ min}$. After the aging period, the oven was turned off and left to cool room temperature. The specimens were then removed from the oven and were tested not less than 24 h later.

3 Test Method

3.1 Binder Drain-Down Test

Similar to porous asphalt mixture, SMA is encountered with binder drainage problems. In the process of mixing, transporting and laying, drainage problem may occur due to high optimum bitumen content of SMA. The binder drain-down test

was carried out as stated in AASHTO T305 [24], using the wire basket method. A sample of the SMA of approximately mass of 1.1 kg was prepared in the laboratory. The sample was put in a wire mesh basket that was placed on a pre-weighed paper plate. The plate, basket and the sample were placed in a forced air oven for $3 \text{ h} \pm 5 \text{ min}$ at a temperature of $170 \pm 2 \text{ }^\circ\text{C}$. At the end of three hours, the basket containing the sample was removed from the oven along with the paper plate. Then, paper plate was weighed to determine the amount of the binder drain-down that occurred.

3.2 Resilient Modulus Test

The resilient modulus test was conducted using Universal Testing Machine (UTM) in accordance with ASTM D 6931–12 [25] standard. It was carried out at a temperature of 25 and 40 °C by applying repetitive applications of compressive loads in a haversine waveform on the sample. Prior to testing, the specimens were conditioned at the selected temperature for $4 \text{ h} \pm 5 \text{ min}$. A haversine load of 1 kN peak force was applied with a pulse width of 0.1 s along with a rest period of 0.9 s with an assumed Poisson's ratio of 0.40. The compressive load was applied vertically along the curved plane of a cylindrical sample of asphalt mixture. The resulting horizontal and vertical deformations of the samples were measured. The resilient modulus was calculated automatically from the machine using recoverable vertical and horizontal deformations.

4 Results and Discussion

4.1 Drain Down

The result of the drain down test is displayed in Fig. 2. The drain down value of the mixes incorporated EAF steel slag and CMT was lower than the drain down value of the control mix. The reduction in drain down value can be as a result of the rough surface texture (as observed in Fig. 1) of EAF steel slag and CMT compared to the granite aggregate. Also, it was observed in Fig. 1 that both EAF steel slag and CMT are more porous than the granite aggregate. The rough surface area and the porosity of EAF steel slag and CMT enhanced the interlocking and stronger bond with the bitumen binder. This would stabilize and hold the binder on their surface and decrease the rate of binder drain down. The binder drain down value for all the mixes is within the stipulated limit as noticed in Fig. 3, thus, it was not necessary to add stabilizing materials, which are usually added to the conventional bitumen binder in order to avoid the risk of drain down of bitumen binder.

Fig. 2 Drain down value of the mixes

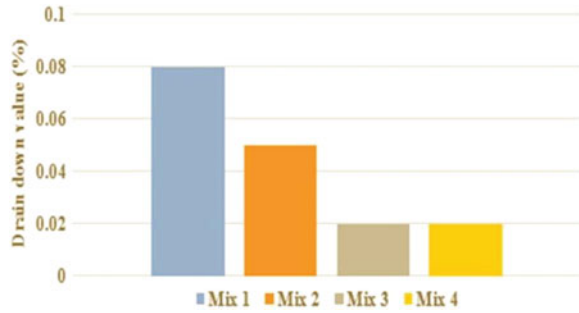
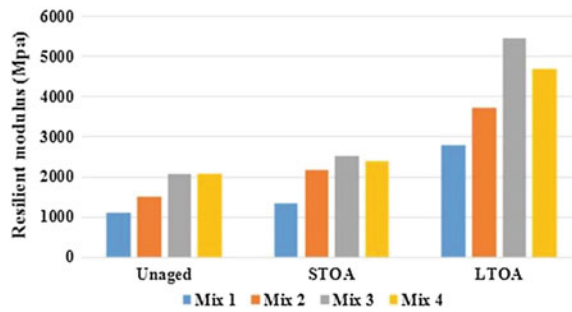


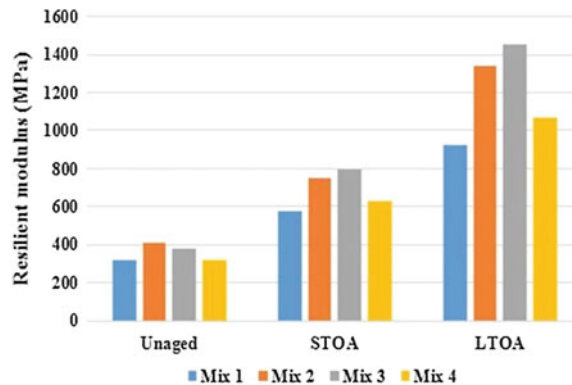
Fig. 3 Resilient modulus of the mixes at 25 °C



4.2 Resilient Modulus

Figures 3 and 4 clearly illustrate the resilient modulus value at 25 and 40 °C for the unaged, short term oven aged and long term oven aged samples for the four mixes. As the Fig. 4 shows, the resilient modulus value at 25 °C for the unaged mixture increased by 36, 89 and 87 % respectively for Mixes 2, 3 and 4 respectively. The same trend is observed in the STOA and LTOA mixtures. The resilient modulus

Fig. 4 Resilient modulus of the mixes at 40 °C



values of mixtures containing the EAF steel slag and CMT are generally greater than the control mix (100 % granite). As noticed in Fig. 3, the aging process increased the resilient modulus of SMA mixtures. The resilient modulus of the SMA Mixes 1, 2, 3 and 4 at 25 °C increases by 22, 44, 20 and 15 % after STOA and 151, 147, 161 and 126 % respectively after LTOA. Interestingly, the level of increment is even higher at 40 °C as displayed in Fig. 4. After STOA the resilient modulus value of the Mixes 1, 2, 3 and 4 increases by 84, 82, 112 and 97 % respectively, and increases by 193, 227, 286 and 233 % respectively after LTOA. The conventional mix (mix 1) has the least value of resilient modulus at both temperatures for the unaged and aged samples.

The rough surface, pH and other tested physical properties of the EAF steel slag and CMT contributed to higher resilient value of mixes 2, 3 and 4 as compared to the conventional sample. The higher the resilient modulus of the aging samples may be attributed to bitumen binder hardening which makes the mix to be stiffer. In addition, higher resilient modulus value is recorded at lower temperature. This is because at low temperature, bitumen binder is more brittle and the asphalt mixture tends to crack. At cooled surface of the asphalt mix, stresses are more pronounced. Due to the flowing asphalt binder in the asphalt mix, the induced stress can be reduced. As then temperature rises, the bitumen binder viscosity decreases and thus enhances the flow within the mix and reduces the stress. At elevated temperatures, bitumen binder may lose its tendency to effectively bind the aggregates together. Hence, the recoverable strain increases with temperature and this would result in lower resilient modulus of the mixes.

5 Conclusion

This research concentrated on the laboratory evaluation of the effect of aging on the resilient modulus of stone mastic asphalt using EAF steel slag and CMT as aggregate materials. This section summarizes the findings of this study as follows:

- Apart from water absorption, all the properties of the aggregates used met the JKR specifications [26]. The degree of porosity of EAF steel slag and CMT accounted for their high water absorption.
- The role of EAF steel slag and CMT was significant in reducing the drain down of the SMA mixture. The drain down values of the mixes containing EAF steel slag and CMT were lower than that of the control mix.
- The indirect tensile resilient modulus value was higher in the mixtures containing EAF steel slag and CMT compared to the conventional mixture at the low and elevated temperatures.
- Though, the aging process improves the resilient modulus of all the mixtures, the effect is more significant in the mixes containing EAF steel slag and CMT. For instance, the resilient modulus value for mix 3 at 40 °C was increased by 112 and 286 % after STOA and LTOA respectively.

- To cap it all, based on the findings of this research, the use of industrial by-products such as EAF steel slag and CMT as aggregates in the production of asphalt concrete mixtures should be encouraged. Apart from alleviating the problems of solid waste disposal, it also reduces the construction cost of road and highway projects.

Acknowledgments The authors gratefully acknowledge the Universiti Teknologi Malaysia (UTM) for providing financial support for conducting this research through the university research grant vote 09H33 GUP, Tier 1. In addition, we are grateful to Malaysia Marine and Heavy Engineering (MMHE), Antara Steel in Malaysia and Shell Singapore for providing copper tailings, EAF steel slag and bitumen respectively.

References

1. E. Ahmadinia, M. Zargar, M.R. Karim, M. Abdelaziz, P. Shafigh, Using waste plastic bottles as additive for stone mastic asphalt. *Mater. Des.* **32**(10), 4844–4849 (2011)
2. J. Behbehani, H. Nowbakht, S. Fazaeli, H. Rahmani, Effect of fiber type and content on the performance of stone mastic asphalt. *J. Appl. Sci.* **9**(10), 1980–1984 (2009)
3. U.R.S. Muniandy, R. Ishak, S.B. Radin, Study on the use of oil palm fiber in rubberized stone mastic asphalt. *Road Saf. Resour. Cent. REAAA* **7**(1), 19–24 (2001)
4. G. Rusbintardjo, M.R. Hainin, N.I.M. Yusoff, Fundamental and rheological properties of oil palm fruit ash modified bitumen. *Constr. Build. Mater.* **49**, 702–711 (2013)
5. R. Hainin, W.F. Reshi, H. Niroumand, The importance of stone mastic asphalt in construction. *EJGE* **2150**, 49–56 (1995)
6. T. Moghaddam, T.B. Karim, M.R. Syammaun, Dynamic properties of stone mastic asphalt mixtures containing waste plastic bottles. *Constr. Build. Mater.* **34**, 236–242 (2012)
7. J. Judycki, Influence of low-temperature physical hardening on stiffness and tensile strength of asphalt concrete and stone mastic asphalt. *Constr. Build. Mater.* **61**, 191–199 (2014)
8. A. Karakuş, Investigating on possible use of Diyarbakir basalt waste in stone mastic asphalt. *Constr. Build. Mater.* **25**(8), 3502–3507 (2011)
9. J. Ahmad, N.I.M. Yusoff, M.R. Hainin, M.Y.A. Rahman, M. Hossain, Investigation into hot-mix asphalt moisture-induced damage under tropical climatic conditions. *Constr. Build. Mater.* **50**, 567–576 (2014)
10. R. Muniandy, B.K.H. Bujang, Laboratory diametral fatigue performance of stone matrix asphalt with cellulose oil palm fiber (Ratnasamy Muniandy and Bujang B . K . Huat Department of Civil Engineering, University Putra Malaysia). *Am. J. Appl. Sci.* **3**(9), 2005–2010 (2010)
11. I.M. Asi, Laboratory comparison study for the use of stone matrix asphalt in hot weather climates. *Constr. Build. Mater.* **20**(10), 982–989 (2006)
12. L.C.A. Chiu, C.T. Lu, Laboratory study on stone matrix asphalt using ground rice rubber. *Constr. Build. Mater.* **21**, 1027–1033 (2007)
13. R. Muniandy, N.A.B.C.M. Akhir, S. Hassim, D. Moazami, Laboratory fatigue evaluation of modified and unmodified asphalt binders in stone mastic asphalt mixtures using a newly developed crack meander technique. *Int. J. Fatigue* **59**, 1–8 (2014)
14. E. Ahmadinia, M. Zargar, M.R. Karim, M. Abdelaziz, E. Ahmadinia, Performance evaluation of utilization of waste polyethylene terephthalate (PET) in stone mastic asphalt. *Constr. Build. Mater.* **36**, 984–989 (2012)

15. D. Casey, C. McNally, A. Gibney, M.D. Gilchrist, Development of a recycled polymer modified binder for use in stone mastic asphalt. *Resour. Conserv. Recycl.* **52**, 1167–1174 (2008)
16. L.-C. Chiu, C.-T. Lu, Laboratory study on stone matrix asphalt using ground tire rubber. *Constr. Build. Mater.* **21**, 1027–1033 (2007)
17. Y. Xue, H. Hou, S. Zhu, J. Zha, Utilization of municipal solid waste incineration ash in stone mastic asphalt mixture: pavement performance and environmental impact. *Constr. Build. Mater.* **23**(2), 989–996 (2009)
18. R. Muniandy, E. Aburkaba, L. Mahdi, S.D. Ehsan, Effects of mineral filler particle size and type on permanent deformation of stone mastic asphalt mixtures. *G.J. P&A Sc and Technol.* pp. 50–64 (2012)
19. R. Muniandy, E.E. Aburkaba, H. Bin Hamid, R.B.T. Yunus, An initial investigation of the use of local industrial wastes and by-products as mineral fillers in stone mastic asphalt pavements. *J. Eng. Appl. Sci.* **4**(3), 54–63 (2009)
20. ASTM E 2090, Standard test method for size—differentiated counting of particles and fibres released from cleanroom fibres using optical and scanning electron microscopy (2012)
21. ASTM D 5581, Standard test method for resistance to plastic flow of bituminous mixtures using Marshall apparatus (Philadelphia U.S., 2013)
22. ASTM D 7369, Standard test method for theoretical maximum specific gravity and density of bituminous paving mixtures (Philadelphia, 2011)
23. AASHTO R30, Method for mixture conditioning of hot mix asphalt (2002)
24. AASHTO M92, Method for determining drain-down characteristics in an uncompacted bituminous mixture using wire mesh basket (1990)
25. ASTM D 7369, Standard test method for determining the resilient modulus of bituminous mixtures by indirect tension test (Philadelphia U.S., 2011)
26. Jabatan Kerja Raya Malaysia, Standard specification for road works, section 4: flexible pavement. Kuala Lumpur, Malaysia, JKR/SP/2008, S4-58–S4-59 (2008)

A Comparative Study on the Behaviour of Motorcyclists on Exclusive Motorcycle Lane at Merging Section Under Different Configuration of Road Marking

Muhammad Hazmi Bin Ilias and Muhammad Akram Adnan

Abstract The exclusive motorcycle lane (EML) at merging section in Federal Highway heading towards Kuala Lumpur at KM 28.4 has been segregated into two lanes via road marking. This study researches on the effect of the road marking by comparing the speed and gap of the exclusive motorcycle lane before and after road marking installation by using a TruSpeed Laser Speed Gun, a TDC Ultra Hand-held Traffic Data Collector and a Sony Hdr Videocam. The results show that there have been significant differences in the speed and gap of motorcyclists in the exclusive motorcycle lane after the installation of road marking. These differences can make a difference in the safety and health of motorcyclists using the exclusive motorcycle lane. The need for further research regarding motorcyclists and exclusive motorcycle lane in Malaysia may help the community with a design standard for exclusive motorcycle lanes.

Keywords Exclusive motorcycle lane • Merging section • Road marking • Speed • Gap

1 Introduction

A motorcyclist is defined as someone who rides, pushes or propel a two or three wheeled motor vehicle with less than four wheels, and the unladen weight of which does not exceed 450 kg along a road [1]. A motorcycle lane is used to describe a special roadway that is specifically designated for smaller vehicles like motorcycles, scooters, trishaws, and bicycles [2]. Currently there are 2 types of motorcycle lanes, exclusive motorcycle lane and non-exclusive motorcycle lane.

M.H.B. Ilias (✉) · M.A. Adnan
Faculty of Civil Engineering, Universiti Teknologi MARA, Selangor, Malaysia
e-mail: hazmiilias@hotmail.com

M.A. Adnan
e-mail: akram@salam.uitm.edu.my

The difference between an exclusive motorcycle lane and a non-exclusive motorcycle lane is that motorcyclists on exclusive motorcycle lanes are separated from other motorists and they have a wider right of way, while a non-exclusive motorcycle lane does not get separated from other motorists [3]. Exclusive motorcycle lanes are used to increase the safety of motorcyclists and reduce the fatalities of motorcyclists as road users. Motorcycle lanes can be commonly found in Asian countries especially South East Asian countries due to a motorcycle's availability, low cost, and maneuverability. The Federal Highway Route 2(R2) in Malaysia is the first ever in the world to have its own exclusive motorcycle lane during the 1970s. It was then extended in 1992 and completed ahead of schedule in November 1993, whereby it was then opened for the public [2] (Table 1).

Exclusive motorcycle lanes are the main subject of the study, specifically the exclusive motorcycle lane at merging section towards Kuala Lumpur at KM 28.4 on the Federal Highway Route 2, Malaysia. This study comprises of the behaviour of motorcyclists and traffic performance on exclusive motorcycle lane before and after implementation of road marking. The road marking is intended to improve safety of motorists on exclusive motorcycle lane, by simply segregating the lane into two whilst maintaining the width of the lane.

The focus of this comparative study is an attempt to investigate the relationship of a road marking that maintains the width of the lane but divides it into two, with the behaviour of motorcyclist on exclusive motorcycle lane approaching merging section under different configurations of road markings. We studied the behaviour of motorcyclists and traffic performance before the implementation of road marking and after the implementation of road marking. The objectives of this study are:

- To perform data collection strategy on exclusive motorcycle lane before and after implementation of road surface marking at merging section.
- To analyse traffic performance on exclusive motorcycle lane at merging section under different configuration of road surface marking.
- To compare the differences of the behaviour of motorcyclists on exclusive motorcycle lane under different configurations of road surface marking.

Table 1 Basic features of a motorcycle lane along federal highway route 2 [2]

Motorcycle lane features	Design parameter
Track length (extension)	14 km
Track width	2.5–3.5 m
Verge	1–2 m
Distant from main carriageway	Varies with maximum 3 m
Access control	Full
Guardrail type	Single face
Wearing course formulation	50 mm Asphaltic concrete
Road base formulation	150 mm Wet Mix Macadam
Sub-base formulation	250 mm CBR > 30 %
Interchange	TypeGrade-separated

2 Problem Statement

In Malaysia, motorcyclists contribute to 48 % of the total vehicle population. That is almost half the whole population of vehicles, with an average of 468,054 new motorcycles registered from the year of 2005 to 2009 [4]. In 1996, according to Radin study the total accidents that occurred in Malaysia contributed by motorcyclists were almost 60 % and the injuries sustained by road users were more than 60 % contributed by motorcyclist. In 2009, the total fatalities contributed by motorcyclists fatalities were 4,067 or 60 % of total recorded road fatalities, which is an increment of 9 % from the year of 2002 [5]. Since the construction of the exclusive motorcycle lane in 70s, it has been widely used by motorist to get from point A to point B. As such, there have been cases of accidents involving motorist. To counter this several steps have been taken to ensure the safety of motorists, and one of the simplest and easiest steps is to implement road markings on exclusive motorcycle lane specifically at merging section (Fig. 1).

There have been many studies done regarding motorcyclist and motorcycle lanes especially in Malaysia, partly because motorcycles are a common mode of transportation of the people. Therefore, it is necessary for us to study on the behaviour of motorcyclists on exclusive motorcycle lanes, to reduce the fatality of motorcyclists.

3 Literature Review

An exclusive motorcycle lane is a completely segregated lane separated from other motorist with a complete separate right-of-way established solely for the use of motorcyclists. It does not come to exist from an existing carriageway of a wide road. Exclusive motorcycle lanes greatly help to reduce conflicts at intersections with the provision of underpasses and other related facilities. The width of an exclusive motorcycle lane is normally in the range of 2.0–3.5 m.

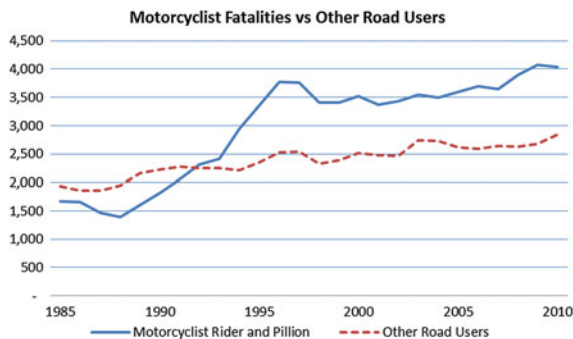


Fig. 1 Motorcyclist fatalities versus other road users (MIROS 2011)

3.1 Merging Section

The merging section of an EML is used by motorcyclists from the main carriage-way to enter the EML via the merging lane. It is very important as without it the motorcyclist cannot enter the EML and will not be excluded from other vehicles which increase the risks of an accident (Figs. 2 and 3).

3.2 Study Area

The location of the study is the Exclusive Motorcycle Lane and its Merging Section at Federal Highway Route 02 at KM 28.4 headed towards Kuala Lumpur.

Fig. 2 Merging section of exclusive motorcycle lane on study location



Fig. 3 Dimensions of exclusive motorcycle lane after road marking



3.3 Data Collection

There were two data collection in this study, the first was taken prior to the installation of road surface markings and the other was after the installation of road surface marking. However the data for before the road marking implementation were obtained from automatic traffic counter. After arriving at the Federal Highway Route 02 at KM 28.4, we set up the instrument into position. The TRUSpeed laser speed gun has to be set in place within range and at a hidden location so as to not affect the reaction of motorcyclists. The laser speed gun can be operated easily by pointing the gun towards the motorcyclists using the scope provided for pinpoint accuracy and pressing the button. Then we set up the video recorder into place. The video recorder must have a clear view of motorcyclists entering the merging section without any obstruction. The TDC Ultra had to be operated by another operator; it can be used to collect gap data just by the press of a button every time a motorcyclist passes through a certain point. Data collection occurred at the merging influence area of the exclusive motorcycle lane. Additionally weather data and pavement conditions were taken into consideration. Data was only collected during dry pavement conditions as to avoid having a biased results. The data was collected for 5 days with 2 weekends and 2 weekdays. Each day was divided into 4 categories Am Peak, Am Non- Peak, Pm Non-Peak and Pm Peak. Each category was collected for each lane at an interval of 15 min. There is a total of 3 lanes making the total time for each category 45 min. Am Peak is strictly between 7 a.m. and 9 a.m. while Pm Peak is between 5 p.m. and 7 p.m.

3.4 Data Analysis

The gap data was obtained from the TDCUltra handheld traffic data controller by downloading into a computer using the PETRAPro software, and the speed data was obtained from the Tru Speed laser speed gun using the Trulogger software. The data is then compared accordingly using the Minitab 16 software, which allows us to analyse data using a paired sample t-test together with a histogram. The gap data was further divided from am, pm, non-peak and peak into 2–3, 4–5, and 6–7 s. Any gap data more than 8 s can be considered as part of another horde of motorcyclists and will not be used. The gap is compared just once, before and after road marking installation. A whole day of gap data before road marking was installed was compared with a whole day of data after road marking was installed, a whole day of data consist of Am Peak, Am Non-Peak, Pm Non-Peak and Pm Non-Peak. Speed is compared twice, the first comparison is between before and after road marking installation, the data is compared between Am Peak, Am Non-Peak, Pm Non-Peak and Pm Peak respectively. Secondly, the speed is compared for just after road marking installation; the 5 days data is again compared by Am Peak respectively. The data analysis will allow us to interpret whether implementation of road surface marking makes any difference to the

data obtained, speed in particular. The analysis also takes into account weather, pavement and other conditions to try and minimize errors.

4 Analysis of Data and Results

The results of the study were compared using a paired sample t-test with α equals to 0.05. EML (3.5 m) is the exclusive motorcycle lane before road marking while L1 and L2 are after road marking implementation. L3 is the merging section of the exclusive motorcycle lane (Figs. 4 and 5).

The gap data is a type of group data collected at 4 different times of the day. The gap data is then compiled into a whole day data. Table 2 shows the 2–3 s gaps being compared, the first comparison showed that the 2–3 s mean gap is slightly higher in EML (3.5 m) compared to L1 although it is not a significant difference since p-value is more than 0.05. It can be said that the nature of the EML (3.5 m) and L1 is almost the same. However it is also important to note that motorcyclist prefer to ride on L1 than L2, because L2 merges with L3 which disrupts the motorcyclists riding in L2.

The next comparison is between EML (3.5 m) and L2, the EML (3.5 m) has a larger 2–3 s mean gap, which is significant because the p-value is higher than the

Fig. 4 Sketch of EML before road marking

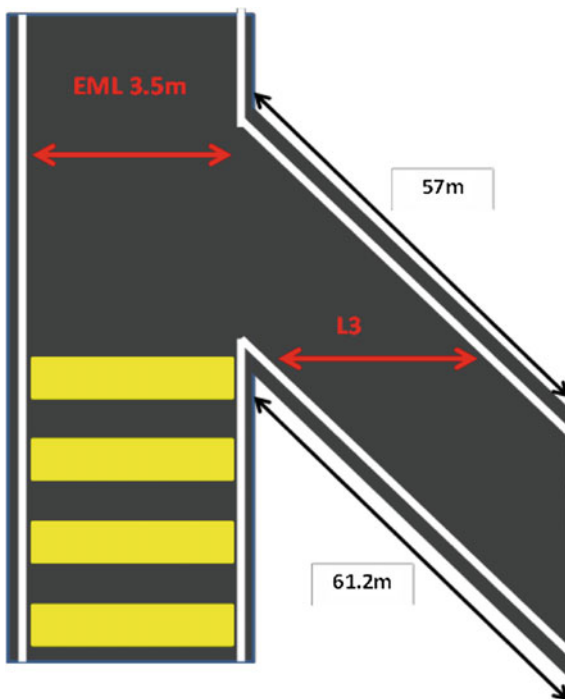


Fig. 5 Sketch of EML after road marking

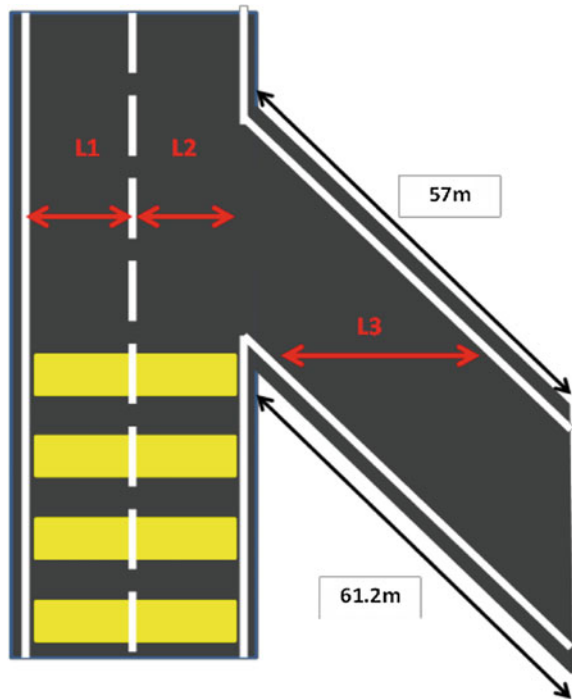


Table 2 Comparison of 2–3 s gap according to lanes

2–3 s	Mean	StDev	SE mean
GAP(3/4/13) EML(3.5 m)	76.3	25.0	12.5
GAP(12/3/14) L1	64.3	30.8	15.4
Difference	-12	26.6	13.3
95 % CI for mean difference: (-30.4, 54.4)			
P-value = 0.434			
GAP(3/4/13) EML(3.5 m)	76.3	25.0	12.5
GAP(12/3/14) L2	23.5	20.9	10.4
Difference	-52.8	20.3	10.1
95 % CI for mean difference: (25.0, 85.0)			
P-value = 0.014			
GAP(3/4/13) L3	92.75	17.37	8.68
GAP(12/3/14) L3	28.75	9.64	4.82
Difference	-64	21.3	10.6
95 % CI for mean difference: (30.2, 97.8)			
P-value = 0.009			

alpha value. This also proves that motorcyclist prefer to ride in L1 than L2, since there are less motorcyclists in L2 than L1.

The last comparison is between L3 before road marking and L3 after road marking. The results show that there is a significant difference after road marking implementation which shows fewer motorcyclists within the 2–3 s gap in L3. This is because when the EML (3.5 m) is segregated into two lanes more motorcyclists prefer to ride along L1 than L2 to avoid possible collision with incoming motorcyclists from the merging lane which is L3. Therefore the road marking effect allows motorcyclists from L3 to merge into the exclusive motorcycle lane via L2 easier compared to before road marking implementation. Furthermore, before the road marking installation the EML (3.5 m) was being treated as a single lane, making it harder for motorcyclists from the merging lane L3 to enter the EML (3.5 m). The alpha value α equals to 5 % or 0.05. The p-value has to be below 0.05 in order to prove that there is a significant difference, the lower the p-value the higher probability that there is a significant difference.

The speed data comparison for before and after road marking installation was analysed using a paired sample t-test. The paired sample t-test is chosen because it is more accurate for us to use a paired sample t-test compared to an independent (unpaired) sample t-test. Table 3 shows the speed of each lane being compared before and after road marking installation during Am Peak, and Table 4 shows is during Pm Peak. The EML (3.5 m) stands for the exclusive motorcycle lane before road marking was installed, while L1 and L2 are both the exclusive motorcycle lane after being segregated by the road marking. L3 simply means the merging section

Table 3 Comparison of speed during AM peak according to lanes

AM peak	85th percentile (km/h)	Mode (km/h)	Median (km/h)	Mean (km/h)
3/4/13 EML (3.5 m)	61.5	51	53	51.568
12/3/14 L1	68	55, 57, 62, 68	57	58.297
Difference	6.5	–	4	6.73
P-value = 0.000		95 % CI for mean difference: (–9.04, –4.42)		
3/4/13 EML (3.5 m)	61.5	51	53	51.63
12/3/14 L2	71	57, 59	57	60.00
Difference	9.5	–	4	8.37
P-value = 0.001		95 % CI for mean difference: (–12.83, –3.91)		
3/4/13 EML (3.5 m)	61.5	51	53	53.419
12/3/14 L1 & L2	68	57	57	58.645
Difference	7.5	–	4	5.23
P-value = 0.000		95 % CI for mean difference: (–7.40, –3.06)		
3/4/13 L3	61	50, 60	53	49.15
12/3/13 L3	55.9	46, 48	46	46.51
Difference	–5.9	–	–7	–2.64
P-Value = 0.086		95 % CI for mean difference: (–0.39, –5.67)		

Table 4 Comparison of speed during PM non peak according to lanes

PM peak	85th percentile (km/h)	Mode (km/h)	Median (km/h)	Mean (km/h)
3/4/13 EML (3.5 m)	58	48	50	50.77
12/3/14 L1	67	55, 56, 57	56.5	57.42
Difference	9	–	6.5	6.65
P-value = 0.000		95 % CI for mean difference: (-9.70, -3.60)		
3/4/13 EML (3.5 m)	58	48	50	52.36
12/3/14 L2	69.2	64, 67	64	63.45
Difference	11.2	–	14	11.09
P-value = 0.008		95 % CI for mean difference: (-18.57, -3.61)		
3/4/13 EML (3.5 m)	58	48	50	50.11
12/3/14 L1 & L2	67.2	67	58	58.35
Difference	9.2	–	8	8.24
P-value = 0.000		95 % CI for mean difference: (-11.16, -5.32)		
3/4/13 L3	56	47	48	49.67
12/3/14 L3	52	47	46	44.38
Difference	-4	–	-2	-5.30
P-value = 0.000		95 % CI for mean difference: (2.58, 8.01)		

of the exclusive motorcycle lane. The first comparison is between EML (3.5 m) and L1, the second comparison is between EML (3.5 m) and L2, the third comparison is between EML (3.5 m) and L1 including L2, the last comparison is between L3 before road marking and L3 after the road marking. The p-value is only relevant for the mean speed since it is compared using a paired sample t-test.

Currently the speed limit for motorcyclists on the Federal Highway Exclusive Motorcycle Lane is 90 km/h. The mode or modal speed is the speed that has the highest frequency. The 85th percentile speed can be used to determine the speed limit. The median speed is the middle speed of the data that is arranged in an increasing order. It is another method of measuring average speed. The mean speed is derived from the paired sample t-test using a confidence interval of 95 % and an α alpha value of 5 %. During Am Peak and Pm Peak the mean speed for the first, second and third comparison shows that the mean speed has increased significantly (p-value is less than 5 %). The reason for the increase in speed is due to the road segregation which provides motorcyclist with their own space and boundary to travel at a higher speed, whereas before the segregation the exclusive motorcycle lane can cater to fewer motorcyclists. During Am Peak motorcyclists mean speed decreased insignificantly while during Pm Peak it decreased significantly. The reason for the decrease of speed in the fourth comparison is because once the exclusive motorcycle lane has been segregated, motorcyclists in L3 would have to

Table 5 Summary of gap

GAP (s)	EML and L1	EML and L2	L3 and L3
2–3	Mean decrease by 12	Mean decrease by 52.8	Mean decrease by 64
4–5	Mean decrease by 14.25	Mean decrease by 27.25	Mean decrease by 26.5
6–7	Mean decrease by 8	Mean decrease by 12.25	Mean decrease by 7.5

Table 6 Summary of speed

Speed	EML and L1	EML and L2	L3 and L3
AM peak	Mean increase by 6.73 km/h	Mean increase by 8.37 km/h	Mean decrease by 2.64 km/h
AM non-peak	Mean increase by 5.71 km/h	Mean increase by 3.71 km/h	Mean decrease by 6.66 km/h
PM non-peak	Mean increase by 6.63 km/h	Mean increase by 12.7 km/h	Mean decrease by 3.27 km/h
PM peak	Mean increase by 6.65 km/h	Mean increase by 11.09 km/h	Mean decrease by 5.30 km/h

enter the exclusive motorcycle lane slower because there are more motorcyclists in the exclusive motorcycle lane that are travelling at a higher speed.

5 Conclusion

The annual statistics of road accidents contributed by motorcyclists in Malaysia has caused a need for more research to be done regarding motorcyclist and safety. This research has contributed to that need by analyzing the effect of road marking on speed and gap of motorcyclists. The overall summary of this research concludes that there has been a significant difference in terms of speed and gap of motorcyclists in each lane after installing a road marking. The speed and gap increased and decreased according to lanes. The speed results are also consistent at 4 different times of a day, which solidifies the accuracy of the results. Below is a table of summary for both gap and speed. Although the speed of the motorcyclists has increased, it is still within the speed limit which is 90 km/h [1]. It can also be said that the road marking has actually made the exclusive motorcycle lane a much safer environment for motorcyclists (Tables 5 and 6).

Acknowledgments The authors would like to express our gratitude to the management from Faculty of Civil Engineering, Universiti Teknologi MARA (UiTM) for their constant support and encouragement. Our appreciation goes to the Research Management Institute (RMI, UiTM) and Ministry of Higher Education Malaysia (MOHE) for financial supports Ref. File Code: 600-RMI/ERGS 5/3 (36/2012). Our utmost thanks is also extended to Muhammad Aiman and Muhammad Akmal and all individuals and organization that have made this study possible.

References

1. Laws of Malaysia, Road Transport Act 1987, ACT 333, Malaysia (1987)
2. R.S. Radin Umar, M.G. Mackay, B.L. Hills, Preliminary analysis of exclusive motorcycle lanes along the federal highway F02, Shah Alam, Malaysia. *IAATSS Res.* **1.9**(2), 93–98 (1995)
3. R.S. Radin Umar, T.H. Law, Determination of comfortable safe width in an exclusive motorcycle lane. *J. East. Asia Soc. Transp. Stud.* **6**, 3372–3385 (2005)
4. Road Transport Department of Malaysia, Statistik Pendaftaran Motosikal, Jabatan Pengangkutan Malaysia (2011)
5. Royal Malaysian Police (PDRM), Statistical report of road accidents in Malaysia. (Traffic Branch, Bukit Aman, Kuala Lumpur, 2010)

Differences in Pedestrian Profile Pattern During Weekdays and Weekends in Central Business District Kuala Lumpur

Noor Iza Bahari, Ahmad Kamil Arshad and Zahrullaili Yahya

Abstract Good, safe and well maintained pedestrian sidewalk facilities that are comfortable to be used by all groups of pedestrians could encourage people to travel by walking. However, due to lack of information on the pedestrian travel trends or pedestrian profile's pattern local authorities have to face many challenges in providing facilities that are suitable to be used by each group of pedestrians. Pedestrians' characteristics such as gender, age and abilities usually influence the pedestrian preference and affect the pedestrian volume. Since each pedestrian have different characteristics, Level of Service (LOS) of a sidewalk may be affected by different pedestrian profile composition, pattern or volume during weekday and weekends. Therefore, the objective of this paper is to look on how does the pedestrian profile pattern differs by number of trips made during weekdays and weekends in one of the Central business district within Kuala Lumpur City Center that are known to have highest pedestrian volume with adequate pedestrian facilities. The objective is achieved through pedestrian classification count on afternoon peak-hour for one whole week in two different locations within Central Business District in Kuala Lumpur City Centre. In overall, similar pedestrian profile pattern for afternoon peak period were observed during a weekend which is on Monday to Thursday for both count location and the number of trips made increased on weekends.

Keywords Pedestrian classification count · Pedestrian profile pattern · Pedestrian travel behavior · Pedestrian volume · Sidewalk facilities · Walkability

N.I. Bahari (✉) · A.K. Arshad · Z. Yahya
Department of Highway and Transportation, Faculty of Civil Engineering,
UiTM, Shah Alam, Malaysia
e-mail: izabahari@gmail.com

A.K. Arshad
e-mail: drahadkamil@salam.uitm.edu.my

Z. Yahya
e-mail: zahrull@salam.uitm.edu.my

1 Introduction

Pedestrian preference and decision to walk usually influence by the urban environment and sidewalk facilities provided for them. This is because each pedestrian could hear, smell, felt and sees the surrounding environment [1, 2]. Good, safe and well maintained pedestrian sidewalk facilities that are comfortable to be used by all groups of pedestrians could encourage people to travel by walking and increased walkability in a city. The likelihood of walking is also affected by the path context and the quality of walk path [3, 4]. From previous literature, it is found that walking is popular for short trips distance [5, 6]. People tend to walk further and more frequently in high sidewalk qualities environment [7–10].

The walking distance and pedestrian preference to walk may be closely related to personal factors and socio-demographic characteristics such as age, gender, income, choice to choose mode of transport and etc. [11–13]. This is because satisfaction of pedestrian is strongly associated with emotional perception rather than physical components [14]. Difference type of facilities provided will attract different group of pedestrian for using the sidewalk [15]. Zacharias stated that variety of sensation experienced by pedestrian once they are exposed to the public environment which will cause them to make a series of decision and judgments for navigating the environment during their journey [2]. This means that even with the same general design criteria that have specific sidewalk design element and components different pedestrian perception may be experienced by pedestrians under the various environments [10].

Pedestrian volumes and number of trips made by pedestrian were also influenced by Pedestrians' characteristics such as gender, age and limitation. Different group of pedestrian will react differently to the sidewalk facilities provided [16, 17]. Different group of pedestrian also required different type of facilities to assists them during their journey. For example people with disability and the elderly would prefer sidewalk facilities that fulfill their requirement and female pedestrian will travel more by walking at a safer sidewalk [16]. Higher number of female pedestrian can be observed at location that has adequate and safer sidewalk facilities [17]. These conditions may lead to different volume in pedestrian group pattern observed within the same area.

A lot of research was done to estimate the pedestrian volume such as regional traffic volume models, sketch-plan method or overlay mapping technique, regression modeling technique, regional household survey data and space syntax models [18]. These models have its' own advantages and disadvantages depending on what purpose that is desire to be accomplished. For example, regional traffic volume models, sketch-plan method are useful for derivation of quantitative estimates of demand [19]. However, these models could not be used to calculate the pedestrian volume by the pedestrian characteristic which is gender, age and limitations. Pedestrian characteristics usually incorporated in research that involved walking speed and sidewalk level of service, LOS [20]. Since each pedestrian have different

characteristics, walking speed and LOS of a sidewalk may be affected by different pedestrian profile composition, pattern or volume and during what day in a week.

Therefore this paper aims to assess on the different of pedestrian profile pattern during weekdays and weekends at one of the sidewalk that to have highest pedestrian volume with adequate pedestrian facilities in Central business district within Kuala Lumpur City Center. The aim is accomplished by conducting Pedestrian Classification Count during afternoon peak hour for the whole week.

2 Methodology

Pedestrian profile pattern were assessed through pedestrian classification count on two different sidewalk segments within Kuala Lumpur City Center. Jalan Tuanku Abdul Rahman that is located within City Center Commercial was selected as study location. This area were identified to have the potential in supporting Malaysia economic growth as it promotes broad range of services such as business center, heritage interest area, shopping complex, education center and public transport station within walking distance. This area have high pedestrian volume due to high pedestrian activities that its offer. The method for conducting pedestrian classification count were modify from previous study and Austroad Manual, Part 3 [21]. The counts were carried out during afternoon peak hour for the duration of 2 h at two locations within the sidewalk network of Jalan Tuaku Abdul Rahman for one whole week.

2.1 Study Area

The fastest developing city and the capital of Malaysia which is Kuala Lumpur was chosen in this study. Kuala Lumpur has the fastest growth in term of population and economic compared to other metropolitan region within the country. The commercial areas that are in line with the distribution of urban center in Kuala Lumpur Structure Plan 2020 as identified in Draft KL City Plan 2020. It is known as City Center Commercial (CCC) that has the potentials to support Kuala Lumpur's economic growth. Broad range of commercial activities was allowed to be conducted in the commercial zones within the CCC which contribute towards pioneering highest order of commercial activities [22]. One study area that has the densest pedestrian activity within CCC of Kuala Lumpur was selected as the study area.

Sidewalk segment in Jalan Tuanku Abdul Rahman was selected as the study area is shown in Fig. 1. This sidewalk segment that has a mixed-use development characteristic with high numbers of building of interest (13) as stated by KL Heritage Center and high pedestrian activities zone is chosen as the study area [23].

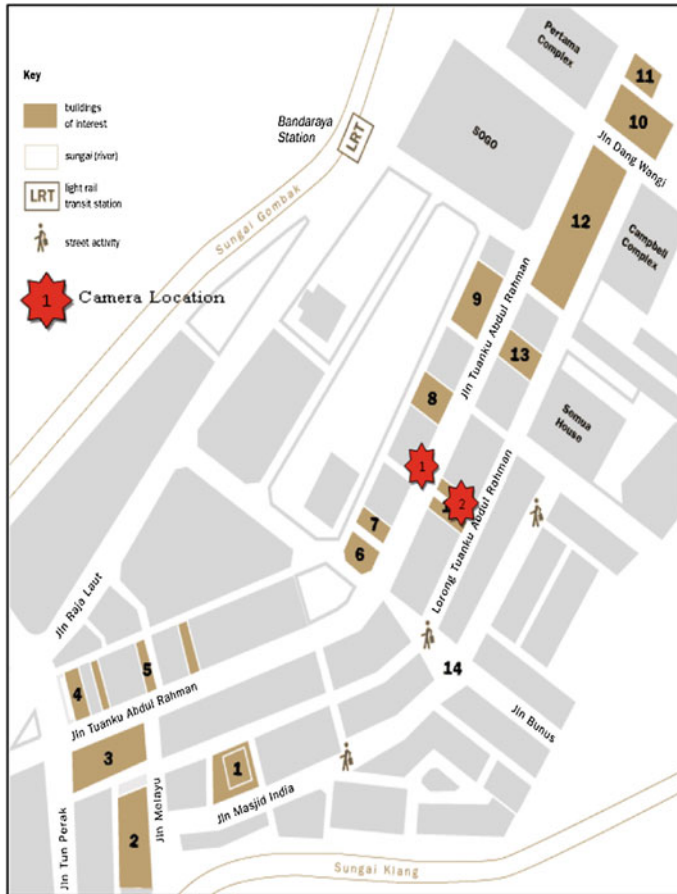


Fig. 1 Study location in Jalan Tuanku Abdul Rahman, Kuala Lumpur [23]

This area consist of shopping complex, business center, heritage interest area, education center and public transport station within walking distance. This area offers a wide range of pedestrians’ activities which is from transit commute, shopping, leisure and education center. Therefore, the pedestrian profile pattern while using the existing sidewalk facilities during afternoon peak hour can be assessed every day for whole week.

2.2 Pedestrian Classification Count

The method for conducting pedestrian classification were modify from previous study and Austroad Manual, Part 3 [21]. Manual count using video camera method was used because of small error rate or approaching zero as the video can be

Fig. 2 Pedestrian profile pattern in Location 1 from 12.00 noon to 1.00 p.m.

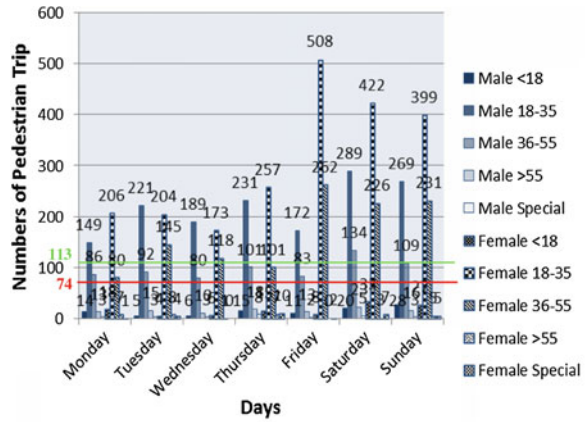


Table 1 Pedestrian group classification

No.	Age group	Gender	
		Male group name	Female group name
1	Less than 17 years old	M1	F1
2	Between 18 and 35 years old	M2	F2
3	Between 36 and 55 years old	M3	F3
4	Above 55 years old	M4	F4
5	Person with disabilities or person with baby prams	M5	F5

repeated [24]. A camera was set at two different locations, opposite the road as shown in Fig. 2. Two mid-blocks sidewalk were selected within the area. The recordings were made during the afternoon peak hour with 2 h duration from 12.00 noon to 2.00 p.m. for one week from Monday to Sunday. The camera is set to start the recordings at the same time for all of the location. Then, the video recordings that were taken were analyzed. The pedestrian are classified into 10 groups according to their characteristics which is gender, age and ability limitation as shown in Table 1. Special Groups include person with disabilities or prams.

2.3 Data Analysis

Screenline method was used in analyzing the video recordings. Pedestrian classification counts were analyzed by counting the total and average numbers of trips made by the pedestrian passing the imaginary screen line at each location.

The pedestrian are classified according to their characteristics and were groups accordingly. The average numbers of pedestrian were count differently on weekdays and on weekends. The findings were than plotted in graphs so that the difference in the pedestrian profile pattern for each weekdays and weekends can be observed more clearly.

3 Results and Discussions

Existing sidewalk segment within Kuala Lumpur City Center which Jalan Tuanku Abdul Rahman was selected as the study location It is found that even though the sidewalk segment were identified as mixed-use development, different numbers and pattern of pedestrian using the sidewalk can be observer when the count is analyzed according to pedestrian characteristics. The results are shown in Figs. 2, 3, 4 and 5. The average numbers of pedestrian trips on weekdays was shown in red line and number and average on weekends are shown in green for all of the figures.

During 28 h of data collection, a total of 29,979 pedestrian were recorded for 2 h of afternoon peak hour in one week. This location is proven to be high pedestrian activity area as stated in NBPD (2010) where pedestrians volume that is more than 100 ped/h consider as high pedestrian activity area [25].

Afternoon peak hour were chosen is because pedestrian volume is higher than vehicle volume during that time compared with morning and evening peaks as supported by Yannie Carrasco and Santana Miranda [26]. Since the manual with videotape count method was used, error consideration can be neglected as stated by Schweizer [24] and Diogenes et al. [27].

Fig. 3 Pedestrian profile pattern in Location 1 from 1.00 p.m. to 2.00 p.m.

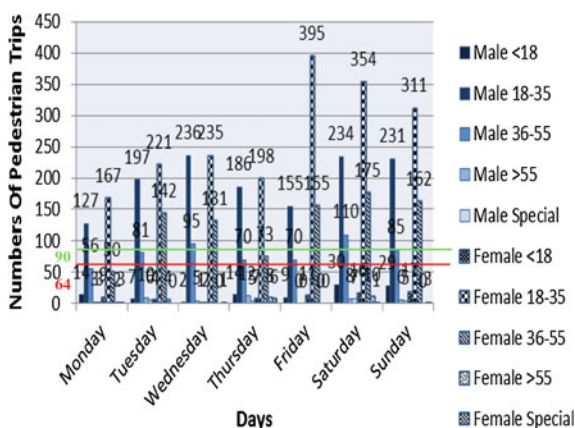


Fig. 4 Pedestrian profile pattern in Location 2 from 12.00 noon to 1.00 p.m.

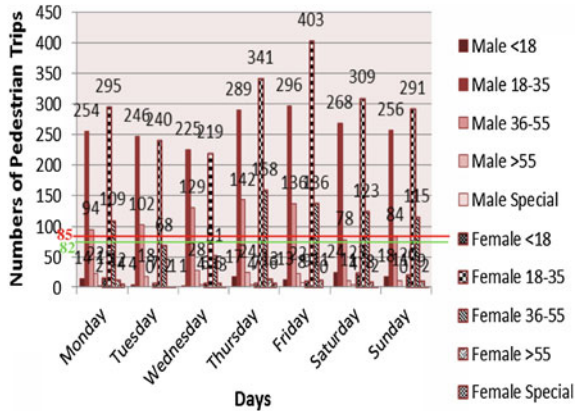
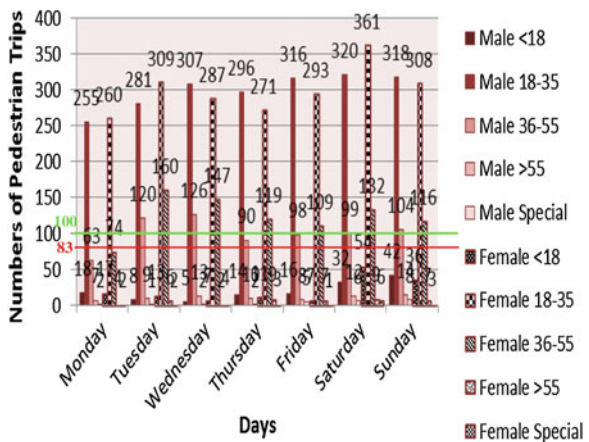


Fig. 5 Pedestrian profile pattern in Location 2 from 1.00 p.m. to 2.00 p.m.



3.1 Pedestrian Travel Pattern During Weekdays

Similar pedestrian profile pattern can be observed from Monday to Thursday and the numbers of trips made increased on Friday for both location during both peak hour. The highest numbers of pedestrian were observed from female and male within the same age group which is between age 18 to years-old group (F2 and M2) for all location and both peak hours.

Only slight differences can be observe in which either female or male group are in lead for the day during weekdays. The highest numbers of pedestrians were recorded on Friday with group F2 are the highest.

From the graphs, the average number of trips made for location 1 first and second afternoon peak hours and location 2 first and second peak hours are 100, 74, 64, 85 and 83 respectively. Location 2 has higher average numbers of pedestrian

trips than Location 1. It is obvious that pedestrian from group M2, M3, F2, and F3 numbers of trips made were higher than the average pedestrian trip numbers for both peak hour and location throughout the weekdays. Pedestrian trip from group M2 and F2 doubled and triple the average value. On the other hand, other groups of pedestrians made far less pedestrian trips which can be seen clearly in graphs that their numbers are below the average numbers.

3.2 Pedestrian Travel Pattern During Weekends

Almost similar pedestrian profile pattern can be seen during the weekends. Except that total numbers of pedestrian trip made were higher during the weekends if to compare with the weekdays. Similarly with the weekdays, pedestrians from group M2, M3, F2 and F3 were among the highest group that made the numbers of pedestrian. Pedestrian from Group F2 recorded the highest number in the entire graph on Saturday and Sunday except on second peak hour at location 2 on Sunday where group M2 show higher number of pedestrian trips.

From the graphs, the average number of trips made for location 1 first and second afternoon peak hours and location 2 first and second peak hours are 113, 90, 82 and 100 respectively. The average numbers of pedestrian trip on weekends were higher than on weekdays for both peak hours on location 1 and location 2 s peak hour. Only during the first peak hour on second location the numbers of pedestrian trips were slightly higher on weekday (85) than on weekends (82).

4 Conclusion

Pedestrian classification counts were carried out in order to assess pedestrian profile pattern in CBD, Kuala Lumpur. In conclusion, the area selected is a high pedestrian volume area with more than 100 ped/h. In overall total, the female pedestrian used the existing pedestrian facilities more than male for group two and three except for minority group of pedestrian including elderly person with disabilities/with prams. On the other hand, similar pedestrian profile pattern for afternoon peak period were observed during a weekend which is on Monday to Thursday for both count location and the number of trips made increased on weekends.

Findings from this research are expected to assist the transport planners and traffic engineers to understand the current pedestrian profile and travel pattern in Kuala Lumpur city. Finding are also expected to assists in providing adequate pedestrian facilities that are safe and comfortable to be used for all groups of pedestrian and cost effective for the infrastructure providers. Therefore a sustainable city that promotes safe walking as main modes of transportation can be created.

Acknowledgments The author would like to express gratitude to all volunteers involves in this research study. The author also would like to express special thanks to the Faculty of Civil Engineering at UiTM for all support rendered. Last but not least, valuable comments from supervisor and referees for are very much appreciated. This research is supported by Ministry of Science, Technology and Innovation (MOSTI) under eScienceFund with reference number 100-RMI/SF 16/6/2 (29/2012) and Research Management Institute, Universiti Teknologi MARA.

References

1. S.L. Handy, Urban form and pedestrian choices. *Transp. Res. Rec.* **1552**, 135–144 (1996)
2. J. Zacharias, Pedestrian behavior and perception in urban walking environment. *J. Plann. Lit.* **16**, 3–18 (2001)
3. M. Southworth, Designing the walkable city. *J. Urban Plann. Dev.* **131**(4), 246–257 (2005)
4. S. Lotfi, J. Koohsari, Neighborhood walkability in a city within a developing country. *J. Urban Plann. Dev.* **137**(4), 402–408 (2011)
5. Z.-M. Fang, W.-G. Song, X. Liu, W. Lv, J. Ma, X. Xiao, A continuous distance model (CDM) for the single-file pedestrian movement considering step frequency and length. *Physica A* **391** (1–2), 307–316 (2012)
6. R.L. Mackett, Policies to attract drivers out of their cars for short trips. *Transp. Policy* **8**(4), 295–306 (2001)
7. C.E. Kelly, M.R. Tight, F.C. Hodgson, M.W. Page, A comparison of three methods for assessing the walkability of the pedestrian environment. *J. Transp. Geogr.* **19**(6), 1500–1508 (2011)
8. K. Gardner, J. Tim, B. Keith, P. Tim, Developing a pedestrian strategy for London. *Transport policy and its implementation* (1996)
9. V.P. Sisiopiku, D. Akin, Pedestrian behaviors at and perceptions towards various pedestrian facilities: an examination based on observation and survey data. *Transp. Res. Part F: Traffic Psychol. Behav.* **6**(4), 249–274 (2003)
10. K.R. Rahaman, J.M. Lourenco, J.M. Viegas, Perceptions of pedestrians and shopkeepers in European medium-sized cities: study of Guimaraes. *Portugal J. Urban Plann. Dev.* **138**(1), 26–34 (2012)
11. P.P. Koh, Y.D. Wong, Comparing pedestrians' needs and behaviours in different land use environments. *J. Transp. Geogr.* **26**, 43–50 (2013)
12. A.B. Weinstein, V. Irvin, K.M. Schlossberg, How far, by which route and why? A spatial analysis of pedestrian preference. *J. Urban Des.* **13**(1), 81–98 (2007)
13. R. Daniels, C. Mulley, Explaining walking distance too public transport: the dominance of public transport supply. Paper presented at the World symposium on transport and land use research, Whistler, Canada, 28–30 July 2011
14. W. Wang, P. Li, W. Wang, M. Namsung, Exploring determinants of pedestrians' satisfaction with sidewalk environments: a case study in Korea. *J. Urban Plann. Dev.* **138**, 199–172 (2012)
15. N.I. Bahari, A.K. Arshad, Z. Yahya, Assessing the pedestrians' perception of the sidewalk facilities based on pedestrian travel purpose. Paper presented at the 2013 IEEE 9th International Colloquium on Signal Processing and Its Applications (CSPA), 2013, pp. 27–32
16. N.I. Bahari, A.K. Arshad, Z. Yahya, Assessing pedestrian profile according to age and gender in Central Business District, Kuala Lumpur, Malaysia, in *Advanced Materials Research* (2014), pp. 768–772
17. N.I. Bahari, A.K. Arshad, Z. Yahya, Assessing pedestrians' perspective on the walkability of pedestrian environment under mixed-use development, in *InCIEC 2013* (Springer, Singapore, 2014), pp. 355–367
18. R.J. Schnieder, L.S. Arnold, D.R. Ragland, A pilot model for estimating pedestrian intersection crossing volume. *J. Transp. Res. Board* (2009)

19. U.S. Department of Transportation's Federal Highway Administration—Research, Development, and Technology (FHWA), in *Guidebook on Methods to Estimate Non-Motorized Travel: Overview of Methods* (July 1999)
20. R. Rastogi, S. Chandra, J. Vamsheedhar, V.R. Das, Parametric study of pedestrian speeds at midblock crossings. *J. Urban Plann. Dev.* **137**, 381–389 (2011)
21. Austroads, *Guide to Traffic Engineering Practice, Part 3—Traffic Studies* (Austroads Publication, Australia, 2004)
22. Dewan Bandaraya Kuala Lumpur, DBKL: Kuala Lumpur Structure Plan 2020 (2004), http://www.dbkl.gov.my/pskl2020/english/urban_design_and_landscape/index.htm. Access on 11 Mei 2013
23. www.badanwarisan.org.my. Access on 26 May 2013
24. T. Schweizer, Method for Counting Pedestrians, Walk21-IV “Everyday Walking Culture”, in *The 6th International Conference on Walking in the 21st Century*, Zurich, Switzerland, 22–23 Sept 2005
25. Alta Planning and Design, National Bicycle and Pedestrian Documentation Project (NBPDP): Instruction Manual (2010)
26. J.G. Yannie Carrasco, E.A. Santana Miranda, *Pedestrian Volume Study: A Case Study in the City of Gothenburg*. Department of Civil and Environmental Engineering, Chalmers University of Technology, Goteborg, Sweden, 2011
27. M.C. Diogenes, R. Green-Roesel, L.S. Arnold, D.R. Ragland, *Pedestrian Counting Method at Intersection: A Comparative Study, Recent Work*. Safe Transportation Research and Education Center, Institute of Transportation Studies, UCB (2007)

Performance Tests of Porous Asphalt Mix—A Review

K.A. Masri and A.K. Arshad

Abstract This paper reviews the overall performance tests for porous asphalt from the material properties until the field evaluation. The material properties are consisting of both aggregate and binder tests. Those tests are the same with material properties evaluation for dense graded asphalt. The tests for binder involved a latest technology for evaluating the rheological properties and microstructural structures such as dynamic shear modulus, rotational viscosity, atomic force microscopy and X-ray diffraction. To evaluate the performance of porous asphalt in lab, the mechanical tests of mixture are very crucial and effective. Among the tests are stability test, indirect tensile strength test, permeability test, rutting resistance, resilient modulus, compression test and imaging analysis. Then, to further monitor the performance of porous asphalt during service life, the field tests are conducted. Among the tests are grain size analysis, hydrometer analysis, compaction parameter, skid resistance, sound adsorption test and flow characterization test. Thus, in order to evaluate the overall performance of PA, the evaluation is done at the initial stage which is the material properties evaluation, the mixture tests and lastly the final stage which is the field tests. The recommendations are also given on the new potential areas to be explored for this topic.

Keywords Porous asphalt · Aggregate tests · Binder tests · Mixture tests · Field tests

K.A. Masri (✉) · A.K. Arshad
Faculty of Civil Engineering, Universiti Teknologi Mara, Shah Alam,
Selangor, Malaysia
e-mail: khairilazmanmasri@yahoo.com

A.K. Arshad
e-mail: drahadkamil@salam.uitm.edu.my

1 Introduction

Porous asphalt (PA) is one type of flexible mixture that is design to solve the problem of stormwater and rainfall especially at the parking lot and other low traffic density areas. PA permits incipient rainfall and local runoff to flow through the pavement surface course of open graded asphalt mix. Then, it tends to accumulate in a porous base consisting of large open graded gravel from which the water would percolate into the natural ground below [1]. PA is first created in the 1970s at the Franklin Institute in Philadelphia, Pennsylvania. PA is consisting of the standard bituminous asphalt in which the usage of fine aggregate have been reduced, which allow the water to flow through the asphalt [2]. PA is an asphalt mixture with little or no fine aggregate. The reduced amount of fines creates interconnected, stable air pockets in the asphalt mix that allow water to flow through the mix [3]. The other definition of PA is that PA is an asphalt paving mixture which the fine particles in the gravel mix have been kept to a minimum. It will permit rainfall to drain through the pavement, rather than dense or ordinary asphalt concrete that only permit the water to flow off of the surface [4]. Figure 1 shows the PA.

PA is an open-graded asphalt that has been used as a wearing surface since the 1970s. In Malaysia, the application of PA was started on 1990s. PA first major use in Australia was about 1973 and in Japan was in 1987. PA is designed in order to form a surface with a voids content of more than 20 % after laying and compacting [1, 5]. The excellent service performance of PA comes from the connected porous structure. The air voids is the inherent feature of asphalt mixture, and it affects the road performance and service performance of pavement directly [6].

PA has a few advantages like the capability to reduce the total amount of impervious area on a site, reducing peak rate of runoff, reducing the runoff volume and reducing the nonpoint source pollutant load [4]. Besides that, PA is also used to reduce the noise and glare [1]. PA is used for two main applications which are as wearing courses on high speed roadways and for stormwater management [3, 7]. Noise levels can be reduced by using a few methods but the greatest and most cost effective reductions can be obtained by using PA [8]. PA is one of the safest pavement surfacing materials used as a friction course by enhancing friction resistance, minimizing hydroplaning, reducing splash and spray, improving night

Fig. 1 Porous asphalt



Fig. 2 PA at parking lot

visibility and lowering pavement noise levels [9–11]. Figure 2 shows the application of PA at the parking lot.

However, PA also has a few disadvantages. One of it is PA is very sensitive to raveling. Raveling is the loss of aggregates at the top layer of pavement surface. Raveling has a negative effect on the noise reduction capacity of PA and requires early maintenance [12]. Raveling occurred due to the combination of traffic loading and severe climate conditions. This problem contributes to the major damage of PA and affect the service life of PA [9]. Raveling is mainly caused by the increment of stiffness reduction of relaxation capacity and formation of micro cracks in the binder due to ageing [12]. There are a few factors that contribute to raveling of PA, one of them is ageing which is believed to be the main factor that contribute to raveling failure of PA. Ageing will increase the chance of damage development due to the applied traffic loading and thermal stresses at low temperature [10, 13–16]. The contaminant from surround environment will also lead to clogging problem of PA [17]. PA usually has shorter service life (sometimes only half) compare to dense graded asphalt mix [11, 18, 19].

Due to the disadvantages and shortcomings of PA, certain tests are required to be carried out to ensure the performance and durability of the mix. These tests should be conducted during the materials selection stage (aggregate and binder), during the mixing stage and also for field performance. These tests are discussed in detail in the following sections.

2 Aggregate Tests

Quantitative evaluation of the existence of stone-on-stone contact in the coarse aggregate fraction of the compacted PA is needed to ensure the design of a mixture with adequate resistance to both permanent deformation and disintegration [20]. Other aggregate testing for PA mix is the same with the other asphalt mix which are specific gravity test, water absorption test, soundness test, aggregate impact value, aggregate crushing value, Los Angeles abrasion value and sieve analysis.

3 Binder Tests

3.1 Penetration Test

The result of penetration test will indicate the capability of binder in resisting the permanent deformation due to temperature changes [11]. This test is an empirical test methods that is used to describe the viscosity characteristics of binder. The penetration results are expressed as the distance in tenths of a millimeter (10 mm) that a standard needle of 100 g penetrates vertically into a sample of the material (binder) at a temperature of 25 °C for loading duration of 5 s [16].

3.2 Softening Point Test

The result of softening point test will indicate the temperature susceptibility the binder [11]. The softening point is the mean of the temperatures at which the two discuss often enough to allow each ball, enveloped in bituminous binder, to fall a distance of 25 mm [11, 16].

Apart from the traditional penetration test and the softening point test, there are other tests that have been used to test the binder performance for PA. This include DSR, short term aging, long term aging, FT IR, DTT and WPT. These tests are discussed in the following sections.

3.3 Dynamic Shear Rheometer (DSR) Test

The DSR test is one of the fatigue test for binder. During this test, the value of torque is measured as well as the phase angle [8]. The critical high temperature of the binder is defined as the temperature, at which the stiffness value, $G^*/\sin I$, of the binder just exceeds 1.0 and 2.2 kPa on the original condition and RTFO condition, respectively. The stiffness value of binder will indicate the resistance behavior of binder towards permanent deformation under the condition of high pavement temperature [11]. Usually, actual pavement condition will gives much higher stiffness compare to the virgin and laboratory aged specimens [8].

The DSR test is conducted to determine the viscoelastic properties of binder such as the response or dependence of the materials on temperature and loading time. This test is carried out in a temperature controlled chamber where the temperature is controlled with air or nitrogen gas. The liquid nitrogen usage is kept to a minimum by switching from gas to liquid nitrogen only when cooling is required. The controlling mechanism and data analysis is performed by a computer connected to the DSR equipment [16].

3.4 Short and Long Term Aging Tests

The laboratory aging is carried out on the binder by using rolling thin film oven test (RTFOT) to simulate short term aging and using pressure aging vessel (PAV) aging test to simulate the long term aging of binder [8]. For RTFOT, each sample is consisting of 35 g of binder. The duration of the test is 75 min [8].

3.5 Fourier Transform Infrared Spectroscopy (FTIR) Test

The FTIR test is carried out to indicate the chemical composition of binder. This test is important as chemical composition could contribute a major influence on the rheological, mechanical and adhesion characteristics of the binder [8]. Infrared spectroscopy is a commonly used technique to identify the functional groups in organic compounds. This equipment is an effective method to investigate the chemical composition of the materials. FTIR is a valuable tool to identify the chemical composition of materials at molecular level. FTIR spectroscopy is using the infrared part of the electromagnetic spectrum. The absorption of this lower energy radiation causes vibrational and rotational excitation of groups of atoms within the molecule [16].

3.6 Direct Tensile Test (DTT)

DTT on binder is performed at constant elongation rates. This test observes the fracture structure of the specimen. The stress and strain in the bituminous specimen is also calculated. The maximum stress is considered as the failure stress and the corresponding strain is the failure strain of the binder [8, 16]. PA mixtures are tested to ensure their performances. Among the tests are discussed in the following section.

4 Mixture Tests

4.1 Cantabro Test

The durability assessment of PA mixtures has been primarily based on phenomenological approaches. One of the approach is the cantabro los s test or known as cantabro test [20]. This test was developed in the 1990s in Spain for assessing PA mixtures [20]. This test is develop to evaluate and control the raveling los s of PA under dry condition and soaked condition. The cantabro test is the laboratory test

most commonly used to evaluate durability for mix design and evaluation and to conduct research on PA mixtures. The design procedures of PA in many countries overlook the influence of aging and temperature on the raveling. Therefore, it is necessary to investigate the raveling characteristic of PA in order to ensure the durability of PA. The cantabro test is viewed as the best test method for investigating the raveling behavior of PA. The test conditions consisted of standard condition, soaked condition, low temperature condition and freeze-thaw condition [21].

In the cantabro test, a compacted marshall specimen is placed in the Los Angeles abrasion machine (without steel ball) and subjected to 300 revolutions. The cantabro loss, expressed in percentage, corresponds to the ratio of lost weight to initial weight of the compacted specimen. This test is also important to investigate the particle loss of PA mixture [12, 20]. In addition, cantabro test can be used to evaluate the performance of PA [3, 22]. Lastly, this test will indicate the lower limit of binder content for optimum binder content (OBC) determination for PA.

4.2 Binder Draindown Test

Binder draindown test is performed to measure the binder lost from the loose mix placed in a drain down basket (No. 4 mesh size) and conditioned at the mixing temperature for 3 h with the draindown being measured every hour. This test shows the amount of binder draindown relative to the total weight of the mix. A maximum draindown of 0.3 % by weight of total mix is typically the maximum value for draindown of PA mix [3]. The drained binder will drop onto the tray below the basket. The mass of retained of binder is calculated by the value of initial mass minus the mass of drained binder. This test will indicate the upper limit of binder content for optimum binder content (OBC) determination of PA.

The irregular distribution of binder generated by its draindown can lead to raveling of zones with low binder content and reduce the permeability in the zones with accumulated binder [20]. The occurrence of binder draindown through the specimen will reduce the permeability of mix.

4.3 Stability Test

Stability is one of the parameter to indicate the strength of asphalt mixture. It can be obtained by performing the marshall properties test. PA mixture will experience a lot of erosion from water along its service operation. The capability of water eroded the PA mixture with different air voids to resist desquamation can be confirmed by conducting the immersed marshall test. This test is also evaluating the relationship between the stability of PA with different value of air voids and particle fracture [6].

4.4 Indirect Tensile Strength Test (ITS)

The indirect tensile strength test (ITS) is carried out to provide an indication of the mechanical performance of asphalt mixtures [23]. The ITS test is the test to evaluate the moisture susceptibility for asphalt mixture. Due to porous nature of PA specimens, it is impossible to archived the level of saturation required by typical test procedures similar to AASHTO T283 standards. Therefore, the saturation step is omitted when testing the PA mix due to the PA specimen becoming easily saturated just by soaking in the water bath [3]. This test is essential to indicate how well the binder can bond with aggregate and evaluate the adhesion between those materials [12]. Figure 3 illustrates the ITS machine.

In addition to assessing the strength of the mixtures, the potential for moisture induced damage is also determined based on the tensile strength ratio (TSR). The TSR is calculated as the ratio of the wet ITS to the dry ITS ($ITS_{wet}/ITS_{dry} \times 100\%$). The minimum value for the T SR of PA mixtures differs according to the requirements of road authorities, but typically the required TSR value is to be greater than or equal to 80 % [3]. Besides that, the stiffness characteristics of indirect tensile stiffness modulus (ITSM) is also can be determine to evaluate the load spreading ability of mixtures in pavement. After compaction and cooling, the specimens will be tested at 30 °C with Nottingham asphalt tester (NU-10). The test results will established the value of ITSM [11]. The evaluation of moisture susceptibility based on the retained tensile strength ratio (TSR) is determined using the modified Lottman method was recommended in 2002 for PA mix design [20].

Fig. 3 ITS machine



4.5 Permeability Test

Drainability is one of the most important characteristics of PA, since it is closely related to several of the advantages exhibited by PA especially under wet weather. However, most agencies do not specify the direct or actual measurement of the coefficient of permeability or permeability value. Thus, most common approaches in determining the permeability are targeting a minimum total air void (AV) content value as an indirect index of adequate permeability and the optional measurement of permeability on laboratory compacted specimens [20]. For these optional measurements, a minimum permeability value of 100 m/day was suggested by NCAT and ASTM international (D 7064-04). However, the selection of minimum values of permeability should be conducted based on the actual rainfall events expected at the project location or country due to different countries are having different rainfall period and intensity for different countries [20].

The permeability of PA is measured using the falling—head procedure. The first step is to prepare a specimen where the specimen is wrap in plastic around the sides to force the water to exit through the bottom of the specimen instead of the perimeter of the specimen. After the specimen is secured in the standpipe, the specimen is initially saturated with water by filling the outlet pipe. The standpipe is then filled with water. The effective porosity is used due to the fact that only the accessible voids will contribute to the permeability of the specimens [3, 15].

4.6 Repeated Load Indirect Tensile Test (RLITT)

Repeated load indirect tensile test (RLITT) is performed to determine the resilient modulus of the asphalt specimens. This test is conducted at low stress levels not exceeding 10 % of the failure stress to ensure linear response of the materials [16]. The RLITT is performed using universal testing machine (UTM). This equipment has a temperature controlled chamber for maintaining constant temperature during the test. During testing, the loading are applied along the vertical diameter of the specimen and the resulting deformations along the horizontal diameters are measured [9, 16]. Figure 4 shows the UTM machine.

4.7 Rutting Resistance

Rutting is one of the permanent deformation of asphalt pavement. It is occurred along the wheel path on the surface of pavement. The asphalt pavement analyzer (APA) is used to evaluate the potential for rutting of PA mixes in accordance with AASHTO T340. This wheel tracking test is conducted to simulate the load

Fig. 4 UTM machine



Fig. 5 APA machine



associated with permanent deformation of PA [4, 14]. Figure 5 illustrates the APA machine.

Besides APA test, the Hamburg wheel tracking test is used for determining the rut resistance of PA. Due to the open-graded proportion of the PA mix, rutting potentials related to scattering and instability will be the major problem. In this test, the specimens are separated into two groups, respectively in a 60 °C air bath and a 40 °C water bath. The pre-heat time is 4 h for the 60 °C air bath and 2 h for the 40 °C water bath [24].

The rut resistance of PA mix can also be carried out for the specimens that have been immersed in the water for a long period. This is called the immersion rutting test. For this test, the specimens are put into a water bath of 60 °C for 48 h. The result from this study will indicate the stripping rate of the PA mix [25].

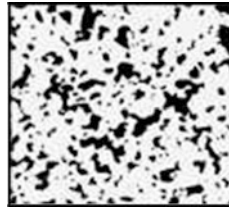


Fig. 6 Scanned and cleaned image of PA

4.8 Compression Test

The triaxial compression test is the test that can reflect the actual road conditions of the asphalt mixture. The unconfined uniaxial tests may underestimate the strength of PA. The shear strength indexes can be obtained from this test and used for road design based on a shear strength criterion. The specimen is made by either a gyratory machine or marshall compactor process [6, 24].

4.9 Aging Effects

The aging test for short term oven aging and long term oven aging are implemented using marshall compacted specimens. The comparison of PA mixture properties subjected to these two aging tests proved inconclusive [20]. Additional work on PA mixtures should be conducted in order to obtain more conclusive results [26].

4.10 Image Analysis

To quantify the vertical pore distribution of PA, the areal porosity where the ratio of the area of the pores to the total area of the sample is used. However, the larger an area used, the less resolution of the porosity distribution. The smallest area that yields a representative porosity value for that location in the PA sample is called the representative elemental area (REA). Figure 6 shows scanned and cleaned image of PA sample where pores are shown as black in the image. One of the equipment that is capable in capturing this image is COSMOS image analysis software [6, 27].

Based on the X-ray computed tomography (X-ray CT) and image analysis techniques, it can be concluded that the interconnected air void content for PA mixtures can be defined as the proportion of air void forming connected pathways for water and air transport throughout the PA mixture. Both equipments are used to evaluate the porosity of PA [20, 28].

5 Field Tests

The first type of test for testing PA at field is the grain size analysis. Usually, sieve and hydrometer analyses in accordance to ASTM D422-63 are performed to obtain the grain size distribution of the vacuumed sediments [5]. These sediments are then classified according to the unified soil classification system. Then, the percentage of organics is determined by loss of ignition testing in accordance to ASTM D7348-08 [5]. The third test is the compaction parameter. The estimation of field compaction of PA pavement is crucial in order to ensure the PA is achieving the targeted density, at the same time to predict the construction costs. This test is also important for the design optimization of PA pavements [29]. Next test is skid resistance test. This test is important to indicate the drainability performance of PA can reduce the road surface water, which means that aquaplaning at high speed is not likely to occur. In addition, air voids can permit the surface water to drain quickly out the road surface, thus reducing spray and enhance the drivers' visibility [10]. Sound absorption coefficient value from sound adsorption test can characterize the sound absorption properties of PA [10]. The flow characterization test, water quality measurement, sediment analysis and rainfall characterization are also can be done in order to determine flow characteristics of PA at certain area like parking lot [30].

6 Conclusions

In order to evaluate the overall performance of PA, the evaluation is carried out at the initial stage which is the material properties evaluation, the mixture tests and lastly the final stage which is the field tests. Studies have been carried out to evaluate the effect of the material properties on the performance of PA. One of the latest development is introducing nanotechnology to enhance the properties of binder. This shows that material properties is very crucial in determining the performance of PA mixture. Although several issues related to PA is still not perfectly solved today, the mechanical performance of PA is adequate to withstand the water sensitivity issue. Furthermore, functional performance results are favorable and the tests performed are crucial to monitor the performance of PA especially its drainage capability properties. PA must be maintained gradually in order to keep the pores paces open and infiltration rates high. Thus, continuous development and latest technology should be applied for PA in order to enhance its performance at the same time preserve its special capabilities.

7 Recommendations

The simulation of rainfall scenario for particular countries should be further enhanced to replicate the actual condition more accurately in order to evaluate the performance of PA. This is due to the performance of PA is related to the rainfall intensity and different countries have different rainfall behavior. Besides that, the application of nanotechnology to enhance the performance of PA should be further studied since nanomaterial has good potential to improve the binder properties.

Acknowledgments The author would to thanks his supervisor, for his opinions and guidance in completing this Review Paper. A big appreciation is also express to family and friends for the continuous support and motivation.

References

1. C. Yalcinkaya, Porous asphalt, Department of Civil Engr, Univ. of Dokus Eylul, Tech. Rep. (2009)
2. C.A. Michele, H.C. Thomas, *Infiltration BMPs-Porous Asphalt Pavement and Beyond* (World Water & Environmental Resources Congress, ASCE Library, 2004), pp. 1–13
3. K.R. Lyons, B.J. Putman, Laboratory evaluation of stabilizing methods for porous asphalt mixtures. *Constr. Build. Mater.* **49**, 772–780 (2013)
4. M.C. Adams, T.H. Cahill, A.E. Mullock, S.J. Burgo, *Porous Bituminous Pavement: A Stormwater Best Management Practice* (World Water Congress, ASCE Library, 2004), pp. 1–5
5. A.L. Welker, J.K. Gilbert, J.L. McCarthy, E. Nemirovsky, Examination of the material found in the pore spaces of two permeable pavements. *J. Irrig. Drainage Eng.* **139**, 278–284 (2013)
6. Y. Xiaoping, W. Xuan, Z. Xin, Y. Yi, Relationship between void feature and road performance of porous asphalt mixture based on image technique. *ICTE*, ASCE Library (2011)
7. A.A. Rowe1, M.B. Thomas, P.O. Connor, Pervious Pavement System Evaluation, in *Proceedings of LID* (ASCE Library, 2008)
8. A.A.A. Molenaar, E.T. Hagos, M.F.C. Van de Ven, Effects of aging on the mechanical characteristics of bituminous binders in PAC. *J. Mater. Civ. Eng.* **22**(8), 779–787 (2010)
9. Y. Zhang, M.F.C. Van de Ven, A.A.A. Molenaar and S. Wu, Increasing the service life of porous asphalt with rejuvenators. *Sustain. Constr. Mater.* **22**, 316–328 (2012)
10. J. Fu, L. Jianming, Z. Hongduo, Test and analysis on performances of drainage asphalt pavement, in *International Conference on Transportation Engineering* (ASCE Library, 2007), pp. 822–827
11. X. Qiu, W. Wong, C. Hu, Laboratory performance evaluation on polymer modified porous asphalt concrete, in *GeoHuman International Conference* (ASCE Library, 2009)
12. Q.T. Liu, E. Schlangen, V.D.V. Martin, M. Poot, Mechanical properties of sustainable, self-healing porous asphalt concrete. *J. Wuhan Univ. Technol.* **32**(17) (2011)
13. J. Wurst, Evaluation of warm mix open graded friction course mixtures. M. Eng. Thesis, Clemson University, 2011
14. J. Sansalone, L. Wang, J. Teng, X. Kuang, M.S., Properties, mechanisms and application of porous pavement as an environmentally-conscious construction material for the built environment, in *World Water Congress* (ASCE Library, 2004), pp. 1–8
15. J.R. Hernandez, D.C. Fresno, Characterization of infiltration capacity of permeable pavements with porous asphalt surface using cantabrian fixed infiltrometer. *J. Hydrol. Eng.* **17**(5), 597–603 (2012)

16. Y. Jemere, Development of a laboratory ageing method for bitumen in porous asphalt. M. Eng. Thesis, Delft Univ. of Tech., Netherland, August 2010
17. C. Syrrakou, J. Fitch, T. Elliasen, W. Ahearn, G. Pinder, *Porous Pavement Hydrology* (World Environmental and Water Resources Congress, ASCE Library, 2010), pp. 994–1001
18. B.A. Dempsey, D.M. Swisher, *Evaluation of Porous Pavement and Infiltration in Centre County* (World Water and Environmental Resources Congress, ASCE Library, 2003)
19. Q. Liu, Induction healing of porous asphalt concrete. M. Eng. Thesis, Delft Univ. of Tech., Netherland, October 2012
20. A.E. Alvarez, A.E. Martin, C. Estakhri, A review of mix design and evaluation research for permeable friction course mixtures. *Constr. Build. Mater.* **25**, 1159–1161 (2011)
21. D. Shaowen, L. Shanshan, The raveling characteristic of porous asphalt mixture, in *ICTE*, pp. 1880–1885 (2011)
22. Y. Wang, G. Wang, *Improvement of Porous Pavement* (2011)
23. F.G. Praticol, R. Vaiana, M. Giunta, Pavement sustainability: permeable wearing courses by recycling porous european mixes. *J. Archit. Eng.* **19**(3), 186–192 (2013)
24. Y. Jun, Y. Chaoen, Laboratory study of porous asphalt mixture made with rubber bitumen, in *GeoHuman International Conference* (ASCE Library, 2009)
25. Q. Liu, D. Cao, Research on material composition and performance of porous asphalt pavement. *J. Mater. Civ. Eng.* **21**(4), 135–140 (2009)
26. M. Xiang, N. Fujian, C. Rongsheng, W. Yan, Evaluation of low-temperature performance of porous asphalt mixture. *J. Highw. Transp.* **4**, 33–37 (2010)
27. W.D. Martin, B.J. Putman, N.B. Kaye, Using image analysis to measure the porosity distribution of a porous pavement. *Constr. Build. Mater.* **48**, 210–217 (2013)
28. J. Sansalone, X. Kuang, V. Ranieri, Permeable pavement as a hydraulic and filtration interface for urban drainage. *J. Irrig. Drainage Eng.* **134**, 666–674 (2008)
29. M. Guler, P.J. Bosscher, M.E. Plesha, A porous elasto-plastic compaction model for asphalt mixtures with parameter estimation algorithm. *J. Mater. Charact. Model. Pavements Syst.* **25**, 126–143 (2011)
30. B. Rushton, Enhanced parking lot design for stormwater treatment. *J. Urban Drainage* (2004)

Assessing Pedestrian Behavioral Pattern at Rail Transit Terminal: State of the Art

Masria Mustafa and Yasmin Ashaari

Abstract An Increasing amount of literature is devoted to discuss about the pedestrian movement pattern in indoor or outdoor environment. A better understanding of human behavior is the key to plan and manage the pedestrian flow especially in a transit terminal. Pedestrians visiting a public space have different motivations and therefore may behave differently. In order to determine the pedestrian behavior, some parameters should be measured such as walking speed, spatial use and person counts. The planners have generated a need to understand the pedestrian movement which behavior could be represented in collective form. A comprehensive review of the existing method in looking at the influencing parameters of the pedestrian behavior to the routes choice and pedestrians flow in relation to the level of service (LOS) and interaction of pedestrian in rail transit terminal is still lacking. Therefore, this paper aims to review the pedestrian movement characteristic in a rail transit terminal. Considering the differences of space requirements among different types of pedestrians and owing to the diverse characteristics of their stature, behavior and surroundings, immediate action on planning the rail based infrastructure is needed.

Keywords Pedestrian flow characteristic · Rail transit terminal

1 Introduction

Walking is an inexpensive mode of transportation and, mobility is a basic and indispensable human activity that is essential for us to be able to lead independent lives on a daily basis [1]. With good pedestrian mobility, walking can also can be

M. Mustafa (✉) · Y. Ashaari

Faculty of Civil Engineering, Universiti Teknologi MARA, Shah Alam, Malaysia
e-mail: masria@salam.uitm.edu.my

Y. Ashaari

e-mail: Yasmin@salam.uitm.edu.my

Fig. 1 Pedestrian movement after train alighting at Masjid Jamek LRT Station, Kuala Lumpur



convenient and time efficient. Urban transport problems of the developing world have changed in the last decade and the progress shows the widespread in mass transit analysis with some good planning and public transport practices in a smaller number of cities [2]. With the rapid growth of the city especially in Malaysia, there has been an extensive capacity to build a multi-transfer transit terminal that handle the passenger efficiently. Therefore, to support the rapid engagement in building transit terminal focusing in rail, the movement patterns of the pedestrian in such facility has to be understood. The understanding somehow requires the true understanding of pedestrian flow characteristic. The increasing number of pedestrians in the infrastructures creates problems of interaction. The pedestrians are influence by each other in their walking behavior either with mutual or reciprocal action. They need to avoid or overtake each other in order to maintain the speed but it is hard to do especially in narrow lane or bottleneck area [3] (Fig. 1).

2 The State of Arts

2.1 *Pedestrian Characteristic at Transit Terminal*

Pedestrians visiting a transit terminal, might have different intentions, not only taking the public transportation, but might do other things and thus may behave differently. Seer et al. [4] renewed interest in discussing the design of the transit terminal facilities related to crowd management for major events such as football match by taking into consideration the main key elements; doors and staircases. Owing to a wide range of services in spite of the main function of the terminal as a public transport hub, a growing amount of information is provided within transit terminal building. This may indirectly force the passengers to filter out relevant information within limited time. This is reflected in the research of [5] where they had focused on the investigation of motion behavior and activities of passengers

under time pressure in a transit infrastructure. Some indicators, for example unusual speed levels of the pedestrian, frequent stops and uncertainties in route choice were used to measure the pedestrian behavior.

Besides, as in previous study of [6], the behavioral patterns of passengers visiting the facilities in transit terminal was carried out and analyzed using market basket analysis to grasp the characteristics of behavioral patterns. Moreover, [7] had demonstrated an intimate knowledge to estimate how pedestrians choose their routes in a complicated multilayered space on the basis of Space Syntax theory. Shibuya station, a huge multilevel complex with a lot of lines, was dealt with as a model of case study. In addition, [8] came out with a methodology for determining equivalent factors in heterogeneous pedestrian flows where it can be used to determine the appropriate width of a corridor when traffic is composed of a mix of commuters and other pedestrians experiencing similar conditions (such as in airport terminals, bus or rail terminals, etc.). Their methodology was derived from vehicle traffic methodologies.

A number of research works have suggested that the analysis of pedestrian behavior can be divided into several categories. For example, the movement of pedestrian can be determined at the staircase, platform and also concourse area. Previous study on pedestrian movement pattern at staircase were found of such carried out by Jianga et al. [9], Yi-fan et al. [10] and Bertuccio and Cesari [11]. Yi-fan et al. [10] for example, found that the effects of the stair effective width on evacuation were evaluated by the combination of the total evacuation time and the stairway level of service which cause the “bottleneck” effect. Effect of different stair width was studied and results show that with the decrease of the stairs effective evacuation width, the crowded degree in the stairway during the subway emergency evacuation process can be obtained. Besides, [12] give an overview of modeling the speed- flow, speed-density and flow-density at the staircase to illustrate behavior of pedestrian stream. They concluded that with the presence luggage, pedestrian’s walking speed may reduced.

Hu et al. [13] suggested an approach which relies on pedestrian monitoring in order to address requirements pedestrian traffic management. Their rules are based on pedestrian counting. Besides, a study by [14] emphasized locations at platforms and concourses were developed as pedestrian areas. As in previous work of [15], the corridors and stairways in transport terminal were chosen as the observation entities to study the relationship of pedestrians flow, density, and speed. The most interesting of their findings relates to pedestrian flow-density relation curves where the data fitted the curve and models are established for corridors, upstairs, and downstairs.

2.2 Factors Influencing Pedestrian Characteristic

In normal conditions, pedestrian is moving naturally and tends to shows some basic attributes while walking to their desired destination. Previous empirical research has shown that under free-flow condition, pedestrian walking speed tends to be

Table 1 Mean walking speed for Asian and Europe countries [16]

No.	Country	Mean walking speed (m/s)
<i>Asia</i>		
1.	Riyadh, Saudi Arabia	1.08
2.	Madras, India	1.20
3.	Hong Kong	1.20
4.	Thailand	1.22
5.	Singapore	1.23
6.	Colombo, Sri Lanka	1.25
7.	Israel	1.31
8.	Malaysia	1.39
9.	England	1.31
<i>United State</i>		
1.	Columbia	1.32
2.	New York	1.35
3.	Pittsburg	1.47
4.	Calgary, Canada	1.40
5.	Jordan	1.34

approximately normally distributed. In the other research, [16] have shown that there are some differences in pedestrian mean walking speed for Asian countries and Europe countries. Mostly, the Europe countries have greater walking speed compare to Asian countries. In Asian country, Malaysian recorded the highest pedestrian mean walking speed (1.39 m/s) as compared to other Asian country such as Singapore, Thailand, Hong Kong. One of the reasons is because due to the physical differences among pedestrians such as the pedestrian height. The taller pedestrian will have greater walking speed and larger footstep as compared to a shorter pedestrian. Table 1 represents the differences of mean walking speed for Asian and Europe countries during normal situation.

A useful introduction to assess pedestrian characteristic especially in terms of their walking speed has been emphasized by Shah et al. [12] where pedestrian flow characteristics are influenced by number of attributes of pedestrian and other attributes such as space availability and direction of movement. Rastogi et al. [17] study has clearly illustrates that characteristics of the pedestrian such as age and gender also influence in the walking speed.

There are important significant relationship between age and pedestrian walking speed, although it can be expected that the young pedestrian are walking faster than the elderly pedestrian. In normal situation, [18] found that the mean walking speed for young pedestrians is 1.51 m/s (4.95 ft/s) and is 1.25 m/s (4.11 ft/s) for elderly pedestrians. An elegant argument for this is the young pedestrians are more energetic and active to act as compared to the older pedestrian. Table 2 shows the mean walking speed for different age and gender during normal situation.

The other factor which influences the pedestrian walking speed is gender. A thorough examination by Knoblauch et al. [18] found that the young male pedestrians

Table 2 The mean and 15th percentile walking speeds (m/s) for different age and gender [18]

Site/environmental factors	Number		Mean		Significance
	Young ped.	Older ped.	Young ped.	Older ped.	
All pedestrians	3,458	3,671	151 (4.95)	1.25 (4.11)	Age
Pedestrian sex					Age, Site, Age × Site
Male	1,701	940	1.56 (5.11)	1.31 (4.31)	
Female	1,757	1,729	1.46 (4.79)	1.19 (3.89)	

have the fastest walking speeds (1.56 m/s) and older females have the slowest (1.19 m/s). A lucid explanation for this would be male pedestrians are more tough than female. Their excessive muscles help them to react proactively while walking.

3 Methodological Framework

3.1 Modelling the Pedestrian Flow

After [19] introduced the principle of fluid dynamics into pedestrian characteristics analysis, a lot of other researchers around the world started to conduct a thorough research in pedestrian flow characteristics. Theories on pedestrian flow are referred to several fields such as walking behavior, route choice, boarding and alighting or interaction between public transport vehicle and walking as and access mode and also activity behavior for example decision making and waiting [20]. Walking speed, delay and density are among the key elements in defining the movement pattern of the pedestrian in transit terminal [8, 15]. As an important phenomenon of transfer activities inside a transit terminal, pedestrians weaving flow generally exists. This was emphasized in the comprehensive study of [21]. The weaving pedestrian show special characteristics during spatial constraint (limited internal space) and also during time constraint (rushing). Generally, the focus on pedestrian flow characteristic will help us in evaluating the pedestrian flow during different scenarios such as in panic situation [22–24].

Several methods were introduced, ranging from statistical updating to simulation exercise to measure the interactions between pedestrians. Micro simulation technique, for example, is used to closely mimic real world dynamic operations. This includes the reproduction of events to imitate the movement of individual pedestrians. Modeling a wide range of pedestrian behaviors is not simple and some model developed from discrete choice and social force can describe how pedestrians deviate from their free flow behaviors due to the presence of other pedestrians [20].

There are several types of Microscopic Pedestrian Simulation Model (MPSM) and to be precise are the Benefit Cost Cellular Model, Magnetic Force Model, Queuing Network Model, Cellular Automata Model and Social Force Model. Using all these models, the impact of facility types on pedestrian movement was not deeply considered, which causes a blank in identifying the response of pedestrian micro-characteristics and macro-characteristics. Furthermore, very few studies reported the research on pedestrian flow characteristics to calibrate parameters of simulation model.

Simulation models can be used to predict the pedestrian movement and to verify the result gained from the empirical technique so that pedestrian interactions problems can be solve effectively. To date, a lot of computer simulation model that have been introduce to investigate the pedestrian movement. The improvement of computer technology allows the researcher to examine the movement of individual pedestrian from one coordinate to another coordinate until they reach at their destination. According to [25], simulation model for can be divided into two (2) main groups which are macroscopic and microscopic model. In macroscopic model, pedestrians are analyzed in groups and pedestrians are generally described by mass densities, flow and average velocity. In Microscopic models, on the other hand, each pedestrian is represented separately as an individual agent and their behaviors will be explored independently [26].

3.2 Modelling Approach

Microscopic model is getting more attention compare to the macroscopic model. It is because microscopic model is able to represent individual pedestrian as individual agent in the model. In addition, microscopic model is also capable to reflect the basic behaviors and interactions between individuals pedestrian. Therefore, a lot of studies have been utilizing the microscopic simulation model to observe the behavior of pedestrian [27].

However, microscopic model are computationally more expensive than macroscopic model [28] as each individual is represented separately by an ordinary differential equation to be solved at each time step, and as the number of individuals increases. Social Force Model (SFM) for examples describes the behavior of pedestrian regarding their interaction with other people and also environment through attractive and repulsive forces. The greatest advantage of the SFM which distinguishes it from the other microscopic pedestrian simulation model is the ability in representing the interactions between pedestrians in a more realistic way [29]. Table 3 shows the advantage and disadvantages of other microscopic models while Fig. 2 depicted the example of floor plan in SIMWALK Software.

SFM was used by most well-known microsimulation software such as VISSIM and SIMWALK SFM tracked the pedestrian movement as an individual which are influence by external and internal forces. An external force is about forces from any

Table 3 Advantages and disadvantages of other type of microscopic pedestrian simulation models [29]

Model	Advantages	Disadvantages
Benefit coast cellular model	Simple and fast	Arbitrary scoring of the cells and pedestrian makes the model difficult to be calibrated in the real world
Cellular automata model	Simple	Heuristic approach of updating rules is undesirable
Magnetic force model	Has force to avoid collision	The validation can only be done by visual inspection
Queuing network model	Evacuation concept	Behavior not clearly shown, collisions are possible



Fig. 2 Example of floor plan in SIMWALK Software

obstacles or other pedestrian in that particular area that can affect their walking path. While an internal force is forces within pedestrian which are encourage them to walk towards their direction.

4 The Results

The results contributed from a number of studies related to pedestrian modeling had drawn our attention to the importance of pedestrian modeling study. The importance of studying the pedestrian movement at a rail transit terminal is demonstrated by the fact that simulation can be used to perform the analysis. Galiza et al. [14] clearly pointed out the qualitative measures of congestion on the train platforms which represent the complexity of pedestrian conditions at public transport terminal. Besides, [24] observed the effect of density on evacuation time where with the increase of the occupant density, the evacuation efficiency would decline. An agent based software FDS + Evac was used to simulate the pedestrian evacuation scene.

Additional support in discussing the contribution of simulation model comes from [15] where they analyzed the pedestrian flow characteristics in order to determine the parameters in pedestrian simulation models. For pedestrian flow-density relation, a quadratic equation in corridor was discovered. In addition, for the flow-space relation, a quadratic equation was observed and for the speed-density relation, a linear equation was revealed. Zhang et al. [30] on the other hand, focused on the study of simulating the alighting and boarding behavior for Beijing metro station. The simulation results show the ability of cellular automata model to capture the characteristics of alighting and boarding movement and the t- test results show no obvious differences between field data and simulation results.

5 Conclusions

Pedestrian can cause congestion especially in a crowded space. There has been a tendency to emphasize the importance of studying the pedestrian movement behavior. However, it is not well known how well the pedestrian move in a public space over time especially in a rail transit terminal environment. A lucid exploration focusing on the fundamental element of a sustainable transportation system which is the pedestrian is important because walking is accessible to all social groups, ages, religions and cultures. It is a free means of travel that can provide access to most facilities and promotes equality and reduces social exclusion. From the literatures, it is important to understand the way of pedestrian move for any design processes of facilities in transit terminal. By knowing the movement pattern and appropriate walking network of pedestrian in a rail transit facility, we can help in enabling the pedestrians/passenger to reach their destinations at shortest time and distance. It is interesting to know the relationship between pedestrian flow parameter models in different facilities at the transfer station for rail transit terminal.

Acknowledgments This study is funded by Research Management Institute (RMI), Universiti Teknologi MARA (UiTM) under the Research Acculturation Grant Scheme (RAGS).

References

1. K. Kayama, I.E. Yairi, S. Igi, Semi-autonomous outdoor mobility support system for elderly and disabled people, in *Proceedings of IEEE/RSJ International Conference on Intelligent Robots and Systems (IROS 2003)*, vol 3, pp. 2606–2611
2. K. Gwilliam, Cities on the move—ten years after. *Res. Transp. Econ.* **40**(1), 3–18 (2013)
3. K. Teknomo, Microscopic pedestrian flow characteristics: development of an image processing data collection and simulation model, Graduate School of Information Sciences, Tohoku University, Japan, 2002
4. S. Seer, D. Bauer, N. Brandle, M. Ray, Estimating pedestrian movement characteristics for crowd control at public transport facilities, in *11th International IEEE Conference on Intelligent Transportation Systems* (2008), pp. 742–747

5. A. Millonig, G. Maierbrugger, Identifying unusual pedestrian movement behaviour in public transport infrastructures. Workshop on movement pattern analysis (2010)
6. Y. Yamashita, N. Hibino, H. Uchiyama, A behavioral analysis of passengers' railway station facilities visiting characteristics. *J. Eastern Asia Soc. Transp. Stud.* **7** (2007)
7. J. Ueno, A. Nakazawa, T. Kishimoto, An analysis of pedestrian movement in multilevel complex by space syntax theory—In the case of Shibuya station, in *7th International Space Syntax Symposium* (2009)
8. R. Galiza, L. Ferreira, A methodology for determining equivalent factors in heterogeneous pedestrian flows. *Comput. Environ. Urban Syst.* **39**, 162–171 (2013)
9. C.S. Jianga, Y.F. Deng, C. Hu, H. Ding, W.K. Chow, Crowding in platform staircases of a subway station in China during rush hours. *Saf Sci* **47**, 931–938 (2009)
10. L.L. Yi-fan, C. Jun-min, J.I. Jie, Z. Ying, S.U.N. Jin-hua, Analysis of crowded degree of emergency evacuation at “Bottleneck” position in subway station based on stairway level of service. *Procedia Eng.* **11**, 242–251 (2011)
11. M. Bertucco, P. Cesari, Dimensional analysis and ground reaction forces for stair climbing: effects of age and task difficult. *Gait Posture* **29**, 326–331 (2009)
12. J. Shah, G.J. Joshi, P. Parida, Behavioral characteristics of pedestrian flow on stairway at railway station. *Procedia—Soc. Behav. Sci.* **104**, 688–697 (2013)
13. X. Hu, W. Wang, W. Wang, H. Zheng, A novel approach for crowd video monitoring of subway platforms. *Optik—Int. J. Light Electron Opt.* **124**(22), 5301–5306 (2013)
14. R.J. Galiza, I. Kim, L. Ferreira, J. Laufer, Modelling pedestrian circulation in rail transit stations using micro-simulation, in *Proceedings of the 32nd Australasian Transport Research Forum (ATRF)*, 2009
15. H. Jia, L. Yang, M. Tang, Pedestrian flow characteristics analysis and model parameter calibration in comprehensive transport terminal. *J. Transp. Syst. Eng. Inf. Technol.* **9**(5), 117–123 (2009)
16. B.H. Goh, K. Subramaniam, Y.T. Wai, A.A. Mohamed, Pedestrian crossing speed: the case of Malaysia. *Int. J. Traffic Transp. Eng.* **2**(4), 323–332 (2012)
17. R. Rastogi, I. Thaniarasu, S. Chandra, Design implications of walking speed for pedestrian facilities. *J. Transp. Eng.* **137**(10), 687–696 (2011)
18. R.L. Knoblauch, M.T. Pietrucha, M. Nitzburg, Field studies of pedestrian walking speed and start-up time. *Transp. Res. Rec.* **1538**, 27–38 (1996)
19. D. Helbing, P. Molnár, Social force model for pedestrian dynamics. *Phys. Rev. E* **51**(5), 4282–4286 (1995)
20. M.C. Campanella, S.P. Hoogendoorn, W. Daamen, A methodology to calibrate pedestrian walker models using multiple-objectives, in *Pedestrian and Evacuation Dynamics*, ed. by R. D. Peacock, E.D. Kuligowski, J.D. Averill (Springer, USA, 2011), pp. 755–759
21. L. Yao, L. Sun, Z. Zhang, S. Wang, J. Rong, Research on the behavior characteristics of pedestrian crowd weaving flow in transport terminal. *Math. Probl. Eng.* (2012)
22. H. Cheng, X. Yang, Emergency evacuation capacity of subway stations. *Procedia—Soc. Behav. Sci.* **43**, 339–348 (2012)
23. D. Helbing, A. Johansson, Pedestrian, crowd and evacuation dynamics. *Encyclopedia of complexity and systems science. Encycl. Complex. Syst. Sci.* **16**, 6476–6495 (2010)
24. W. Lei, A. Li, R. Gao, X. Hao, B. DengLei, Simulation of pedestrian crowds' evacuation in a huge transit terminal subway station. *Physica A* **391**(22), 5355–5365 (2012)
25. E.-W. Augustijn-Beckers, J. Flacke, B. Retsios, Investigating the effect of different pre-evacuation behavior and exit choice strategies using agent-based modeling. *Procedia Eng.* **3**, 23–35 (2010)
26. S. Sahaleh, M. Bierlaire, B. Farooq, A. Danalet, F. Hänseler, Scenario analysis of pedestrian flow in public spaces, in *12th Swiss Transport Research Conference (STRC)*, 2012, Monte Verità, Ascona, Switzerland
27. A. Conca, M.G. Vignolo, Pedestrian flow analysis in emergency evacuation, in *15th Edition of the Euro Working Group on Transportation International Scientific Conference* (2012)

28. R.M. Colombo, P. Goatin, M.D. Rosini, *A Macroscopic Model for Pedestrian Flows In Panic Situations*. GAKUTO International Series Mathematical Sciences and Applications (2010), pp. 43–60
29. Z. Zainuddin, K. Thinakaran, I.M. Abu-Sulyman, Simulating the circumambulation of the Ka'aba using SimWalk. *Eur. J. Sci. Res.* **38**, 454–464 (2009)
30. Q. Zhang, B. Han, D. Li, Modeling and simulation of passenger alighting and boarding movement in Beijing metro stations. *Transp. Res. Part C: Emerg. Technol.* **16**(5), 635–649 (2008)

Pedestrian Behaviour at Stairways and Escalator: A Review

Mohd Khairul Afzan Mohd Lazi and Masria Mustafa

Abstract The pedestrian walking speed is prime importance in a study of design, function and provision of pedestrian facilities. It is quite difficult for the designers to understand the relationship between pedestrian flow characteristic and pedestrian movement by only using their experience and senses. The interactions between pedestrian is hard to understand. Therefore, this paper to review studies from others to better understand the pedestrian flow characteristic, focusing on the pedestrian behavior at stairways and escalator at public transport terminal. This paper addressed the pedestrian movement which includes the walking speed and the relationship between their demographic variables such as age, pedestrian characteristics and also physical characteristic of stairways and escalator.

Keywords Pedestrian behaviour · Walking speeds · Stairways

1 Introduction

Walking is usually considered as transportation mode where it is the most effective and efficient mode of transportation in order to reach a short destination directly or after using other modes of transportation. Walking is the traditional mode of movement between places, irrespective of cities and countries. People walk with different purposes and in large numbers especially in developing countries.

Today, there are a lot of large urban spaces and complicated architectural have been built around the world. In general, within the last 40 years, a wide variety of tools aimed and sophisticated methods in understanding urban mobility. However, only a few of them were designed dealing with pedestrian movement [1, 2]

M.K.A.M. Lazi (✉) · M. Mustafa
Faculty of Civil Engineering, Universiti Teknologi MARA (UiTM), Shah Alam, Malaysia
e-mail: tmm_afzan@yahoo.com

M. Mustafa
e-mail: masria@salam.uitm.edu.my

concluded that, pedestrian behavior is better to understand if knowledge about pedestrian behavior, perceptions and behaviors are discovered and learned. Besides, it is important to improve pedestrian safety. There are many pedestrian patterns that we can see, such as walking speed, pedestrian attitudes, perceptions, behavior, injuries and others.

Walking is our most basic form of transportation. Every trip we make, even by car, we begin and end as pedestrians. In case of mass transit to be effective, passengers must be able to walk between transit stops and multiple destinations of interest. Many people do not have access to automobiles or even bicycles, and must walk to reach important destinations. Walking can also be a pleasant way to exercise, relax, and socially interact with others in the community. The safety and convenience of pedestrian travel are an important factor in our quality of life.

2 State of Arts

2.1 Pedestrian Movement Versus Traffic Flow

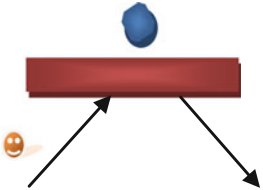
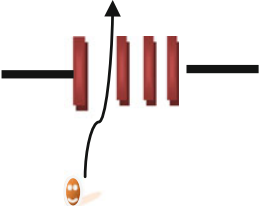
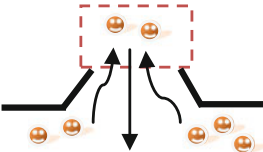
The movements of pedestrians are more complex as compared to vehicular flow. They can simply choose an optimum route by themselves. Their movements are not limited to the “lanes” as vehicular flow. They have more freedom in changing directions. In addition, the slight bumping is acceptable and need not to be absolutely avoided as in traffic flow models. The consideration of these differences must be the priority in developing model for pedestrian movement. To date, only a few special characteristic of pedestrian movement is being considered and most of pedestrian movement models are established based on the rules that being used for traffic flow [3].

2.2 Reliance of Pedestrian Movement Pattern

Short trips and intermodal transportation in cities depends on the vital means of locomotion, walking, which is impossible to duplicate. The constantly increasing air pollution, urban population and urbanization, along with the constraints on the increment of vehicles, have served in order to popularize the mode of transportation.

In least developing countries, however, poor traffic management, the scarcity of transportation, and less ability to bear transportation fares forced the people to walk long distances. Thus, pedestrianization has become a part of sustainable modern urban design, where convenient, safe, pollution-free and comfortable pedestrian facilities are ensured [4].

Table 1 Three types of movement in queue spaces [5]

Type	Type of movement in queue spaces	
	Movement	Description
1		<p>Pedestrian form queues in front of a counter. Pedestrian approach to the queues => stand in the queue => move forward => get the service => get out of the queue. This type of movement can be seen at the reception counters in stations, hotels, department stores, bank and others</p>
2		<p>Pedestrians form queues in front of gates through after they get services. This type of movement can be seen at the entrances of ratchet in railway stations, museums and others</p>
3		<p>Pedestrians form queues in front of the vehicle's door. When a vehicle arrived, pedestrian will wait for the inside passengers to get off vehicle and then will get on it. This type of movement can be seen at platforms of railway stations, at elevator halls, bus stops and others</p>

2.3 Types of Pedestrian Movement

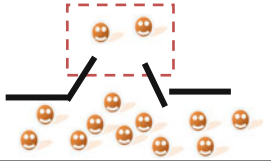

For subway station, queuing is one of the elements of pedestrian movement that occur. In queues spaces, waiting time and the number of waiting people can be calculated by using Queuing Theory. However, Queuing Theory cannot deal with complicated movement of pedestrians and extremely heavy congestion of pedestrian. A lot of pedestrian movement are intersecting and merging in large urban spaces. Some pedestrian form a queue and others only pass through queue spaces. Even during forming a queue, several steps of movement can be observed such as standing in queues, approaching to queues, getting services, moving forward and getting out of queues [5].

Three types of queuing behavior in Table 1 were classified on the basis of observation of pedestrian movement at railway stations, department stores, airport and office buildings. In addition to these three types, Type 3 can be classified into two type (Type 3a and Type 3b) as in Table 2.

2.4 Pedestrian Movement Simulated as Magnetic Forces

The movement for the pedestrians is simulated as the motion of magnetic field whereby each pedestrian simulated by the motion of magnetized object [5]. Each

Table 2 Two types of movement in platform of vehicle [5]

Type	Type of movement in queue spaces	
	Movement	Description
3a		Pedestrian gathers in front of the entrance without give a way for inside passengers to get off the vehicle
3b		Pedestrians give the way for inside passengers to get off the vehicle

pedestrian take a role as positive magnetic pole, same role as obstacle such as columns and walls. Each pedestrian moves to their goals whereby negative magnetic pole from goals attracting positive magnetic pole from pedestrians. Obstacles like columns and walls that plays a positive magnetic pole will make repulsive forces to the pedestrian and also between the pedestrians themselves.

Magnetic forces which acts on pedestrians’ magnetic pole is basically calculated by Coulomb’s Law accordance as in (1) whereas F is magnetic force (vector), K is constant value, Q is the intensity of magnetic load of a pedestrian following by q is intensity of magnetic pole while r is vector from a pedestrian to a magnetic pole following by r , the length of r .

$$F = (k * Q * q/r^3) * r \tag{1}$$

To avoid the collision among the pedestrian, another force acts on pedestrians. Equation (2) is used for Pedestrian X avoiding a collision with Pedestrian Y, the force exerts acceleration a on pedestrian X. Acceleration a calculated according to equation below:

$$a = VA * \cos a * \tan b. \tag{2}$$

3 Pedestrian Behavior at Stairways and Escalator

3.1 Pedestrian Flow Characteristic from Different Studies

Different country has different pattern of pedestrian flow due to different pedestrian behavior and different type of topography. Weather of the country can also affect the flow of pedestrian. Table 3 shows the comparison of pedestrian flow characteristic as in [6].

Table 3 Comparison of pedestrian flow characteristic from different studies [6]

Source	Country	Type	Free-flow speed, μf , m/min	Traffic jam density, kJ , ped/m ²	Max flow rate (q_{max}), ped/m/min
Gerilla (1995)	Philippines	Mixed	83.23	3.60	74.94
Yu (1993)	China	Mixed	75.45	5.10	95.97
Fruin (1971)	United States	Commuter	81.4	3.99	81.2
Tanaboriboon et al. (1986)	Singapore	Mixed	73.9	4.83	89.24
Navin and Wheeler (1969)	United States	Students	97.6	2.70	65.79
Older (1968)	Britain	Shoppers	78.64	3.89	76.54
Oeding (1963)	Germany	Mixed	89.9	3.98	89.10

Imran M. et al. (2012)

3.2 Pedestrian Walking Speeds in Different Studies

Pedestrian walking speeds are different according to the countries or location studies. Average walking speed for pedestrian is influenced by their age and gender. Environment factors will also determine how fast the pedestrian can walk. The comparison of pedestrian speed can be seen in Table 4.

From Table 4, it is noticeable that the American and Asian pedestrians were found to have free-flow walking speed ranging from 79 to 88 m/min, and 73 to 74 m/min respectively. The author analyzed the data of pedestrian speed, pedestrian flow, pedestrian area module and pedestrian density at each study location. Curves were plotted between speed and flow, speed and density, flow and area module and flow and density. The scattered data plot points suggested a straight line relationship between pedestrian speed and density, quadratic relationship between pedestrian speed and flow, and pedestrian flow and density, and polynomial relationship between pedestrian flow and area module [6]. Average walking speeds on stairways in different country also shows a various results especially in Asia. However, in Eastern Asia, stairways usually constructed next to the escalator. People use escalator for ascending and stairs for descending. Table 5 shows the average walking speed on stairways [7].

It is shown that Singapore has the lowest speed of pedestrian walking on stairways. In general, the descending walking speed is higher as compared to ascending. Pedestrian in Singapore and China use stairways for descending purpose.

Table 4 Comparison walking speeds in different countries [6]

No.	Author (s)	City, Country	Mean Speed (m/min)
		<i>Asian Countries</i>	
1	Gerilla (1995)	Metro manila, Philippines	70.6
2	Arasan et al. (1994)	Tiruchirappalli, India	74.0
3	Yu (1993)	Shanghai, China	72.0
4	Koushki and Ali (1993)	Kuwait city, Kuwait	71.0
5	Tanaboriboon and Guyano [36]	Bangkok, Thailand	73.0
6	Poei et al. (1995)	Yogyakarta, Indonesia	52.0
7	Koushi (1998)	Riyadh, Saudi Arabia	65.0
8	Tanaboriboon et al. (1986)	Singapore	74.0
9	Victor (1989)	Madras, India	72.0
10	Laxman et al. (2010)	Roorkee, India	84.0
11	Gupta (1986)	Delhi, India	72.0
12	Kamino (1980)	Tokyo, Japan	93.6
13	Kamino (1980)	Osaka, Japan	90.0
14	Kamino (1980)	Fukushima, Japan	69.6
15	Kamino (1980)	Fukuoka, Japan	81.0
		<i>American and European</i>	
1	Hoel (1968)	Pittsburgh, United States	88.0
2	Older (1968)	London, England	79.0
3	Navin and Wheeler (1969)	Columbia, United States	79.0
4	Fruin (1971)	New York, United States	81.0
5	Kamino (1980)	Paris, France	87.6

Imran M. et al. (2012)

Table 5 Average walking speed on stairways in different countries [7]

No.	Author	Country	Stairways	
			Ascending	Descending
1	Xiang Z. (2009)	Singapore		0.45
2	Liu and Yu [28]	China		0.82
3	Zhang R. (2009)	Beijing, China	0.71	0.90
4	Lam et al. [27]	Hong Kong	0.62	0.74
5	Tanaborinoon and Guyano [36]	Bangkok, Thailand	0.52	0.60
6	Fruin (1987)	USA	0.54	0.72

Jiten S. et al. (2013)

3.3 Relationship Between the Walking Speeds and Age at Stairs

As we know, different age group will have different result in terms of walking speeds. We believed that younger people have a strong leg that able for them to

Table 6 Comparison between Taku F. and Fruin study

Comparison			Taku and Nick [8, 35]				Fruin [9] (1971)	
			Stair gradient				Stair gradient	
			38.8	35.0	30.5	24.6	32	27
Ascending	E	M	0.41	0.50	0.56	0.68	0.43	0.41
		F	0.46	0.53	0.60	0.76	0.39	0.45
	Y	M	0.50	0.57	0.65	0.77	0.69	0.81
		F	0.47	0.56	0.62	0.75	0.51	0.65
Descending	E	M	0.46	0.60	0.64	0.80	0.57	0.60
		F	0.48	0.57	0.64	0.80	0.47	0.56
	Y	M	0.61	0.62	0.72	0.82	0.69	0.81
		F	0.57	0.67	0.76	0.91	0.51	0.65

E Elder, Y Younger, M Male, F Female

move faster as compared to the elders. Table 6 shows the comparison of walking speeds (m/s) between Taku and Nick [8] and Fruin [9] study at London City.

From the comparison, the younger and elder pedestrians have different speed not more than 10 m/s. Due to that, the Threshold model for pedestrian depicted in Fig. 1 is true. Figure 1 shows the Threshold model.

This model shows the leg strength relationship and the walking speeds. When the strength of leg is higher, then the walking speed is also higher. However, it not shows that age is the main factor that affects the walking. The correlation coefficient between walking speeds, age and leg extensor power is shown in Table 7 [8].

From Table 7, age has fewer coefficients or negatively correlated with walking speeds. But LEP that represent the strength of legs has a higher coefficient as compared to walking speeds. However, comparing the ages, the younger people have high LEP as compared to elders.

Fig. 1 Threshold model

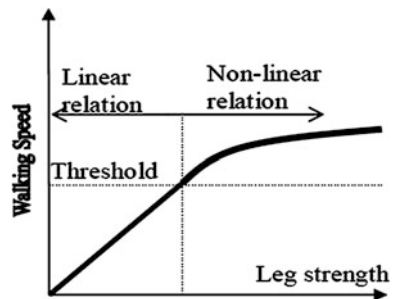


Table 7 Correlation coefficient between walking speeds, age and leg extensor power (LEP) (Watt)

Speed on stairs	Younger		Elder	
	Age (year)	LEP (W)	Age	LEP (W)
Normally ascending	-0.34	0.79	-0.23	0.23
Normally descending	-0.37	0.68	-0.07	-0.05
Fast ascending	-0.14	0.76	-0.43	0.37
Fast descending	-0.32	0.71	-0.20	0.36

3.4 Relationship Between the Walking Speed and Pedestrian Characteristic at Stairs

Taku and Nick [8] proved that the pedestrian physical characteristic have less contribution to correlate between the walking speeds. The height and weight of pedestrians will give a low impact onto the speeds of walking as shown in Table 8.

Table 8, shows that walking speed do not relate to weight and height or physical characteristic of pedestrians. Another interesting study was carried out by [10] focusing on relationship between pedestrian emotion and walking speeds. Table 9 and Fig. 2 show the study result.

Kholshvnikov et al. [10] proved that emotions will also give an effect in walking speeds of pedestrians. When the pedestrian have comfortable and peaceful emotion, they will have slower walking speeds.

Table 8 Correlation coefficient between physical characteristic and walking speeds on stairs speed on stairs

Speed on stairs	Younger		Elder	
	Weight	Height	Weight	Height
Normally ascending	0.03	0.08	-0.25	0.12
Normally descending	0.04	-0.09	-0.60	-0.29
Fast ascending	0.18	-0.02	-0.07	0.29
Fast descending	0.25	0.09	-0.22	0.17

Table 9 Categories of movement, walking speeds and emotional state level

Categories of movement	Level of emotional state	Walking speeds	
		Stairs downward	Stairs upward
Comfortable	0.00	<0.82	<0.45
Quiet	0.45	0.82–1.10	0.45–0.63
Active	0.68	1.11–1.50	0.64–0.92
High activity	0.70	1.51–2.00	0.93–1.25

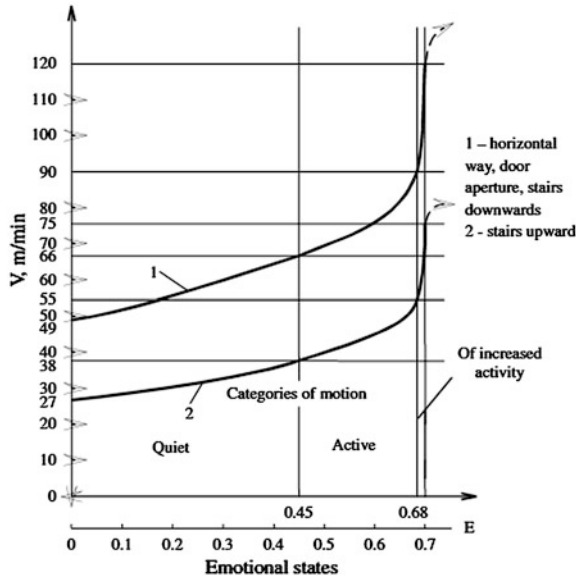


Fig. 2 Relation between walking speed and psychological stress level

3.5 Relationship Between Stairways Characteristics and Walking Speeds

Pedestrian has an intention to walk faster in order to arrive at the destination earlier. The size of the stairways can also give an advantage for the pedestrian to move faster. The 6 inch riser has a higher walking speed as compared to 7 inch riser [11]. Another study carried out by [12] has also emphasized the pedestrian distribution on stairs between the narrow width and large width. Figures 3 and 4 show the differences between these stairs.

From Figs. 3 and 4, the pedestrian will walk through the middle of the stairs if the width is narrow. But, when the stairs width is large, pedestrians prefer to walk aside stairs near the handrail. One of the reasons is because the stability awareness. Pedestrian feel safer to be near the handrail when the width is large and pedestrian more convenient to use middle area of the stairs with narrow width.

3.6 Escalator Versus Stairways

In East Asia, stairways are usually designed together with the escalators. The normal design is for stairs to go down and escalators to go up. However, it is more convenient to have escalator both going up and down. Kone [13] came out with

Fig. 3 Pedestrian distribution with narrow width stairs

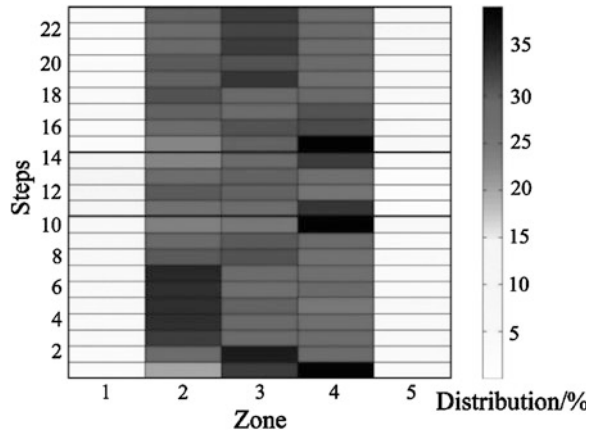
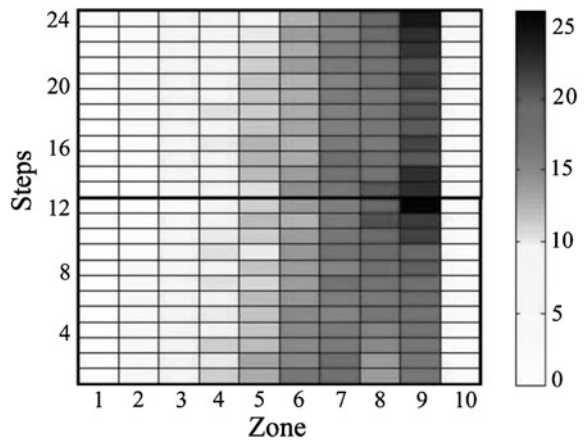


Fig. 4 Pedestrian distribution with large width stairs



statistics shows in Table 10 where the case study was conducted in England while Table 11 shows a case study conducted in Hong Kong and London [14].

From Tables 9 and 10 above, we can see that pedestrian prefer to use escalator as compared to stairways regardless in Asia or Western cities. People will mainly use escalators rather than stairways if both are available at that particular location. In some places, non-working escalator also can be used as stairs.

Table 10 Passenger flow using the devices

	Percentages	Person/h
Escalators, 0.5 m/s	80	5760
Stairs	15	1080
Elevators	5	360
Total	100	7200

Table 11 Comparison capacities in Hong Kong and London

Pedestrian facility	Capacity	
	Hong Kong (MTR)	London (LU)
Stairway (up) (peds/m/min)	70	62
Escalator (up) (peds/esc/min)	92	86
Stairway (down) (peds/m/min)	80	68.3
Escalator (down) (peds/esc/min)	120	120

4 Conclusion

People use escalators or stairways to arrive at their destination when the stairways react as a connection between two levels. Pedestrian behavior while using stairways and escalators are different according to the topography of the location, the physical characteristic of the pedestrian, mental situation of the pedestrians and also characteristic of the facilities. Improper design of pedestrian facilities can caused pedestrian delay, jammed capacities of pedestrian, unstable emotion and will indirectly reduced the use of public transportation system. This review has sheds some light on understanding the behavior of pedestrian while using stairways and escalator. To promote the pedestrian safety, the design of stairways and escalator should take into consideration domestic factor and type of pedestrian that are using such facility.

Acknowledgments This study is funded by Research Management Institute (RMI), Universiti Teknologi MARA (UiTM) under the Research Acculturation Grant Scheme (RAGS).

References

1. B. Arnaud, C. Angele, Simulating pedestrian behavior in subway stations with agent, in *4th European Social Simulation Association Toulouse*, France, 10–14 Sept 2007, pp. 611–621
2. E. Papadimitriou, A. Theofilatos, G. Yannis, Patterns of pedestrian attitudes, perceptions and behavior in Europe. *Saf. Sci.* **53**, 114–122 (2013)
3. W. Xiaoge, M. Xu, L. Wei, S. Weiguo, *Microscopic Character and Movement Consistency of Pedestrian Group: An Experimental Study in Campus* (State Key Laboratory of Fire Science, University of Science and Technology of China, Hefei 230026, PR China, 2014)

4. K. Rahman, A.G. Ghani, A.A. Kamil, A. Mustafa, M.A.K. Chowdhury, *Modelling Pedestrian Travel Time and the Design of Facilities: A Queuing Approach* (School of Distance Education, School of Mathematical Sciences, University Sains Malaysia and School of Physical Sciences, Shahjalal University of Science and Technology, Sylhet, Bangladesh, May 2013)
5. O. Shigeyuki, M. Satoshi, *A Study of Simulation Model For Pedestrian Movement With Evacuation and Queuing* (Department of Architecture and Environmental Design, Architecture and Environmental Engineering, Kyoto University, Yoshidahonmachi, Kyoto, Japan)
6. M.N. Imran, S.J. Adhikary, Q.S. Hossain, S.A. Ali, *Pedestrian Flow Characteristics in Khulna Metropolitan City*, in 2nd Conference of Transportation Research Group of India (2nd CTRG) at Science Direct (Bangladesh, 2012)
7. S. Jiten, G.J. Joshib, P. Purnima, *Behavioral Characteristic of Pedestrian Flow on Stairway at Railway Station* (National Institute of Technology, Surat, 2013)
8. F. Taku, T. Nick, *An Explicit Study on Walking Speeds of Pedestrians on Stairs* (Centre of Transport Studies, University Colledge London, United Kingdom, 2004)
9. J.J. Fruin, *Designing for Pedestrian*, Chapter 8
10. V.V. Kholshchikov, T.J. Shileds, K.E. Boyce, D.A. Samoshin, *Recent Developments in Pedestrian Flow Theory and Research in Russia* (2007)
11. D. Navin, C. Steven, A. Provost, R. Vukan, M. Vuchic, J. Federick, A. Wegmann, *Characteristic and Services Requirements of Pedestrians and Pedestrian Facilities*, ITE Technical Council Committee 5-R, 1976
12. M. Yi, W.J. Na, W.H. Hong, G.Y. Jeon, *Pedestrian Walking Characteristics at Stairs According to Width Change for Application of Piezoelectric Energy Harvesting* (School of Architecture and Civil Engineering, Kyungpook National University, Daegu, South Korea, 2012)
13. C. Kone, *Planning Guide for, People Flow in Transit Stations* (2009)
14. C. Cheung, *Pedestrian Flow Characteristics in the Hong Kong Mass Transit Railways Stations* (Department of Civil and Structural Engineering, The Hong Kong Polytechnic University, Hong Kong, 1998)
15. O. Ayse, P. John, S. Brian, *Modelling Street Connectivity, Pedestrian Movement and Land-use According to Standard GIS Street Network Representations: A Comparative Study*, (2006)
16. D. Charitha, S. Majid, S. Nirajan, E. Omid, *Experimental Study on Pedestrian Walking Characteristics through Angled Corridors* (Institute of Transport Studies, Department of Civil Engineering, Monash University, Australia, 2013)
17. G. Dietrich, Frequency distributions of pedestrians in a rectangular grid. *J. Transp. Econ. Policy* **IV**, 66–88 (1970)
18. H. Dirk, J.F. Illes, M. Peter, V. Tamas, *Simulation of pedestrian crowds in normal and evacuation situations*
19. H. Dirk, M. Peter, J.F. Illes, B. Kai, Self-organizing pedestrian movement. *Environ. Planning B* **28**, 361–383 (2001)
20. V. Ellen, *Portland Pedestrian Design Guide* (City of Portland, Office of Transportation, Engineering and Development, Pedestrian Transportation Program, 1998)
21. H. Flurin, F. Bilal, M. Thomas, B. Michel, *An Aggregated Dynamic Flow Model for Pedestrian Movement in Railway Stations* (Transport and Mobility Lab, EPFL, Switzerland, 2013)
22. K. Hirota, M. Akinori, I. Tadashi, K. Tomohiko, *Studies on the Characteristics Differences of Pedestrian Behaviors among Cities and between City Districts such as Downtown and Suburban Shopping Centre* (Department of Civil Engineering Utsunomiya University, Japan, 2002)
23. D. Jake, D. Elspeth, W. John, S. Andrew, *Pedestrian demand modelling of large cities: an applied example from London*, Centre for Advanced Spatial Analysis, University College London, Paper 62, 2003
24. S. Jiten, J. Gaurang, P. Purnima, *Walking Speed of Pedestrian on Stairways at Intercity Railway Station in India* (National Institute of Technology, Surat, Gujarat, India, 2013)

25. Z. Jun, S. Armin, *Empirical Characteristic of Different Types of Pedestrian Streams*, (Computer Simulations for Fire Safety and Pedestrian Traffic, Wuppertal University, Pauluskirchstrasse 11, 42285 Wuppertal, Germany, 2012)
26. T. Kardi, *Microscopic Pedestrian Flow Characteristics: Development of an Image Processing Data Collection and Simulation Model* (Department of Human Social Information Sciences, Graduate School of Information Sciences, Tohoku University, Japan, 2002)
27. H.K. Lam, J.F. Morrall, H. Ho, *Pedestrian Flow Characteristics in Hong Kong*. Transp. Res. Rec. (1995)
28. W.S. Liu, C.W. Yu, *Analyzing to characteristics of pedestrians flow on stairways at metro transfer stations basing on data fitting* (2008)
29. Y. Liya, L. Sun, Z. Zhang, S. Wang, J. Rong, *Research on the behavior Characteristics of Pedestrian Crowd Weaving Flow in Transport Terminal* (Beijing Institute of Technology, Beijing, 2012)
30. M.I. Nazir, K.A. Sajal, Q.S. Hossain, S.A. Ali, *Pedestrian Flow Characteristic in Khulna Metropolitan City, Bangladesh* (Department of Civil Engineering, Khulna University of Engineering and Technology, Bangladesh, 2012)
31. D. Neil, *Modelling Train and Passenger Capacity* (Transport for NSW, New South Wales, 2012)
32. K. Rahman, N.A. Ghani, A.A. Kamil, A. Mustafa, *Weighted Regression Method for the Study of Pedestrian Flow Characteristics in Dhaka, Bangladesh* (Universiti Sains Malaysia, Penang, 2013)
33. R. Rajat, T. Ilango, C. Satish, *Pedestrian Flow Characteristics for Different Pedestrian Facilities and Situations* (Department of Civil Engineering, Indian Institute of Technology Roorkee, Roorkee)
34. J. Ronald, K. Inhi, F. Luis, L. Julian, *Modelling Pedestrian Circulation in Rail Transit Stations Using Micro-Simulation* (Intelligent Transport System Laboratory, University of Queensland, Brisbane, 2009)
35. F. Taku, T. Nick, *Bridging Characteristics of a Pedestrian and the Facility the Pedestrian Uses: Prediction of the Walking Speed of a Pedestrian on Stairs* (Centre for Transport Studies, Department of Civil, Environmental and Geomatic Engineering, University College London, London, 2004)
36. Y. Tanaboriboon, J.A. Guyano, *Level of Services Standard for Pedestrian Facilities in Bangkok: A Case Study* Transportation Research Board (1991)
37. F.L. Zampieri, D. Rigatti, C. Ugalde, *Evaluated Model of Pedestrian Movement Based on Space Syntax, Performance Measures and Artificial Neural Nets*, Ref 135 (2009)
38. X. Zhou, K.W. Foong, H.C. Chin, *Pedestrian Speed-flow Model on Escalators and Staircases in Singapore MRT Stations* (Department of Civil Engineering, National University of Singapore, Singapore, 2013)

Federal Road Profile Model Generation Based on Road Scanner Data

Rosnawati Buhari, Azali Akhbar Seblan, Munzilah Md Rohani and Saifullizam Puteh

Abstract In Malaysia, the application of Mechanistic-Empirical approach in pavement design guide is still in early stage of introduction and many more researches need to improve it. One of the task needs is generating road profile model to evaluate the dynamic axle loads from vehicles. Therefore, this study aims to generate a few models of road profiles based on the real road profile data called reference road profiles model using mathematical method. The reference road profiles data are a measurement of new paved federal road in Malaysia. A profiles of two section roads (300 m length each) measured by road scanner were determined from Malaysia Public Work Institute (IKRAM). The Profile Viewing and Analysis software (ProVAL) was used to filter unwanted wavelength, visualized the measured road profile data and obtained the road profile International Roughness Index (IRI). Meanwhile, Matrix Laboratory software (MATLAB) was used to generate road profiles based on Dodds and Robson Power Spectral Density (PSD) approximation equation. The calibration between generated and reference road profiles were examined by correlation coefficient value. From the results, all generated road profiles with correlation coefficient value ranges between $-1 < \rho < -0.7$ or $0.7 < \rho < 1$, gives different IRI values with the reference road profile. However, the differences of IRI values are acceptable (less than 5 %). Therefore, all 56 models of generated road profiles are applicable for long term pavement performance.

R. Buhari (✉) · M.M. Rohani
Faculty of Civil Engineering, Smart Driving Research Centre,
Universiti Tun Hussein Onn Malaysia, Batu Pahat, Johor, Malaysia
e-mail: rosna@uthm.edu.my

M.M. Rohani
e-mail: munzilah@uthm.edu.my

A.A. Seblan
Department of Infrastructure and Geomatic Engineering,
Universiti Tun Hussein Onn Malaysia, Batu Pahat, Johor, Malaysia

S. Puteh
Faculty of Technical and Vocational Education,
Universiti Tun Hussein Onn Malaysia, Batu Pahat, Johor, Malaysia
e-mail: saifull@uthm.edu.my

Although, a road profile model with the same IRI value with a reference profile is the most applicable for long term pavement performance.

Keywords Road profiles • International roughness index • Profile viewing and analysis software (ProVal) • Power spectral density

1 Introduction

The Mechanistic-Empirical Pavement Design Guide (MEPDG) is a latest concept in road design approach that uses empirical relationships between cumulative damage and pavement distress to determine the adequacy of a pavement structure to carry the expected traffic load on the pavement by using new Whole-life Pavement Performance Model (WLPPM) method which has been developed that is capable of making deterministic pavement damage predictions. This method also has been implemented in developing MEPDG for several countries around the world. Meanwhile, in Malaysia, application of MEPDG is in the early stage of introduction and many more researches to establish this guide is needed. It is including a study on road profiles that is significantly influenced the dynamic loading of the traffics especially for heavy good vehicles. Knowing that loading from vehicles is the main factor contributing to the pavement damage, a study on road profile should be seriously undertaking to ensure the predicting on the long term pavement performance is more realistic. Therefore, this study focused on generating a few road profiles to represent the real new paved federal road profiles in Malaysia that is valuable for WLPPM as the support input data.

2 Power Spectral Density Approximation

Power Spectral Density (PSD) of the profile height is used to characterize the amplitude and wavelength of roads where the road is considered a homogeneous, isotropic random process with a Gaussian distribution [1]. An adequate description of road profile spectra can often be given as follow:

$$G_d(n) = Cn^{-w} \quad (1)$$

where, G_d is PSD displacement, n is the wavenumber, $w = 2.5$ and C is the roughness coefficient. Using IRI, Hardy and the IRI as follows:

$$C = 1.69 \times 10^{-8} (\text{IRI})^2 m^{1/2} \text{cycle}^{3/2} \quad (2)$$

2.1 Inverse Fast Fourier Transform

Two-dimensional random profiles may be generated by applying a set of random phase angles, uniformly distributed between 0 and π to a series of coefficients derived from the desired direct spectral density. The corresponding series of spot heights u_x at regular intervals along the track is obtained by taking the inverse Discrete Fourier Transform (DFT) of the spectral coefficients. Typical samples are measured at a series of regularly spaced times. The time series analysis is used to determine the spectral estimates of the original function by analyzing the discrete time series obtained by sampling a finite length of a sample function and employing a Fourier transform. The discrete value of the series is carried out by using an Inverse Fourier Transform [2].

$$u_x = \sum_{k=0}^{N-1} \sqrt{S_k} e^{i(\theta_k + \frac{2\pi kx}{N})} \quad k = 0, 1, 2, \dots, (N - 1) \quad (3)$$

where, θ is a set of independent random phase angles uniformly distributed between 0 and 2π which is for this research will be using multiplicative congruential method in MATLAB to generating a sequence of numbers that approximates the properties of uniform random seed number.

3 Multiplicative Congruential Method

The MATLAB command *rand* is based on a popular deterministic algorithm called multiplicative congruential method. It uses the following equation [3];

$$u_i + 1 = Ku_i(\text{mod } M), i = 1, 2, 3, \dots \quad (4)$$

where K and M are usually integers and $\text{mod } M$ is the operation that gives the remainder of division by M (The remainder is a number between 0 and M). To apply this method, one chooses suitable constants K and M (MATLAB use $K = 75$ and $M = 231 - 1$) and an initial value u_i , called the *seed*, a number to base the Random Number generation needed by the random number generation algorithms.

4 Statistical Concept

Base on Huang [4], the correlation coefficient, between random variable x and y is defined as:

$$\rho(x, y) = \frac{Cov[x, y]}{\sqrt{V[x]V[y]}} \quad (5)$$

where, Cov is covariance, V is variance. A covariance of two random variables x and y is defined as the expected value of the product of the deviation of x and y in their expected value:

$$Cov[x, y] = E[xy] - E[x]E[y] \quad (6)$$

The variance of a random variable x is defined as the expected value of the square of the deviation from its expectation:

$$V[x] = E[x^2] - (E[x])^2 \quad (7)$$

The expectation, or mean, of random variable are defined as follows:

$$E[x] = \frac{\sum_{i=1}^n x_i}{n} \quad (8)$$

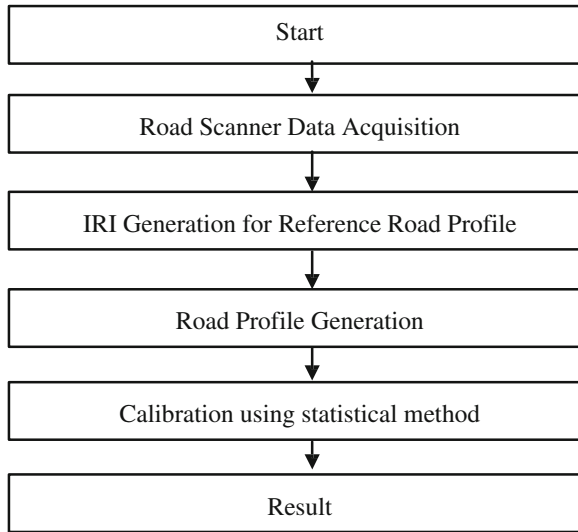
where, n = the number of data of x , and $i = 1, 2, \dots, n$.

5 Methodology

A summary of the research methodology can be seen in Fig. 1. The data of road profiles for new paved federal road in Malaysia was obtained from KUMPULAN IKRAM Sdn. Bhd. The instrument used for data measurement is High speed IKRAM Road Scanner (IRS). The data obtained is then filtered and processed through 250 mm low pass moving average filter method using ProVAL software to remove unneeded wavelength. The data filtered is then segregated into sections of 300 m length measured road profile (named reference road profile) to be used for calibration with the generated road profile.

The IRI of all sections named Model 1 and Model 2 were calculated. The IRI value of Model 1 and Model 2 ranges between 1.5 and 3.5 m/km that meets the criteria of the IRI ranges for new pavement and referred as references road profile. Mathematical approach of Inverse Fast Fourier Transform on the power spectral density approximate equation based on the Dodds and Robson [1] theory with Hardy and Cebon [5] roughness coefficient is used in the generation process of road profile model. The generation process of road profile model is carried out in MATLAB refer to studies of Collop [6]. Where MATLAB was used to generate a sequence of numbers that approximates the properties of uniform random seed numbers for generating a set of independent random phase angle, θ , uniformly distributed between 0 and π . Next step is the calibration process to check whether

Fig. 1 Flow chart research methodology



the generated road profiles model is closer with reference road profile in terms of features and characteristics of spatial similarity by using statistical methods, coefficient correlation. For this calibration, the accepted values of correlation coefficient ranged from -0.7 to -1 and 0.7 to 1 . Where, the generated profile with the correlation coefficient within the limits of -0.7 to -1 and 0.7 to 1 is approaching or has a similarity with the reference road profile data. The IRI values of the generated profiles are then calculated using ProVAL software.

6 Results and Discussions

Model 1 generated 48 road profiles with about the similarity in its characteristic as reference road profile with a seed number ranges from 1 to 1,000. While Model 2 generated 8 road profiles with a seed number range from 1 to 10,000. Table 1 shows all 56 model of road profiles that had been generated within the correlation coefficient range of $-1 < \rho < -0.7$ or $0.7 < \rho < 1$ and its IRI value. Five examples of the road profile modal generated with the highest correlation coefficient chosen from each model as to represent the generated profile closer to the measured profile characteristic are shown on the Figs. 2, 3, 4, 5, 6, 7, 8, 9, 10 and 11.

Table 1 Result of generated road profile based on reference road profile

Model	Seed number	Correlation coefficient	Generated profile IRI	Measured profile IRI	Figures
1	66	0.75	2.01	2.02	
	283	0.72	1.97	2.02	
	357	0.77	1.99	2.02	
	384	-0.73	1.96	2.02	
	420	0.77	2.00	2.02	Fig. 2
	510	-0.73	1.99	2.02	
	521	-0.79	2.00	2.02	Fig. 3
	573	-0.71	1.96	2.02	
	584	-0.81	1.98	2.02	Fig. 4
	611	0.75	1.96	2.02	
	647	-0.75	1.99	2.02	
	674	0.75	1.96	2.02	
	685	0.74	1.99	2.02	
	701	-0.71	1.98	2.02	
	710	-0.71	1.96	2.02	
	737	0.74	1.96	2.02	
	748	0.74	2.03	2.02	
	764	-0.70	1.99	2.02	
	775	-0.75	2.00	2.02	
	811	0.78	2.00	2.02	Fig. 5
	838	-0.82	2.00	2.02	Fig. 6
	874	0.73	1.99	2.02	
	901	-0.73	2.00	2.02	
928	0.70	1.98	2.02		
975	-0.72	2.01	2.02		
991	0.73	2.00	2.02		
2	3	0.70	1.96	2.01	
	1765	-0.70	1.93	2.01	
	2764	-0.71	1.95	2.01	
	3727	0.74	2.01	2.01	Fig. 7
	3774	-0.72	1.98	2.01	Fig. 8
	4964	-0.71	1.97	2.01	Fig. 9
	5117	0.72	1.93	2.01	Fig. 10
6006	-0.72	1.96	2.01	Fig. 11	

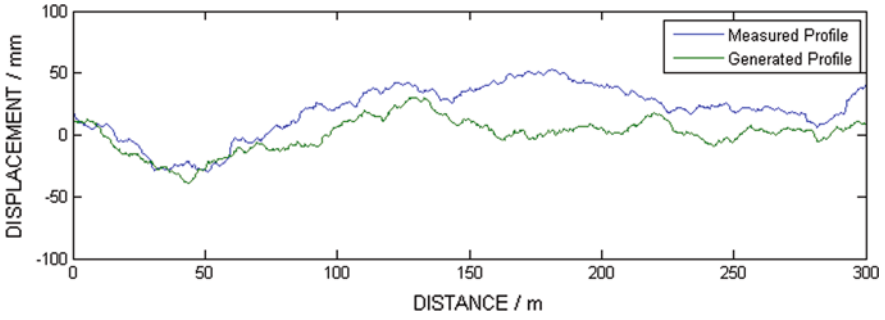


Fig. 2 Model 1 with seed number 420

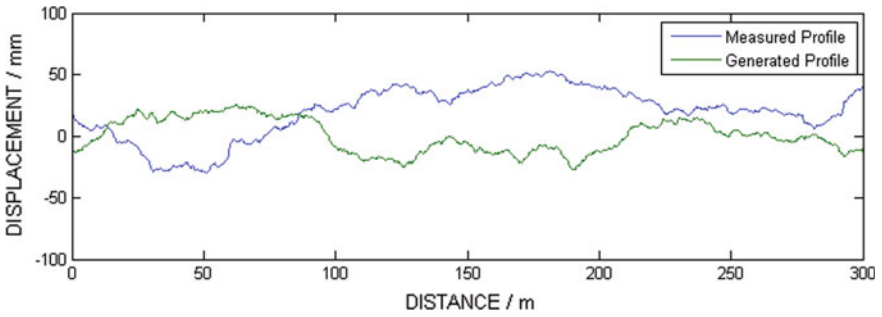


Fig. 3 Model 1 with seed number 521

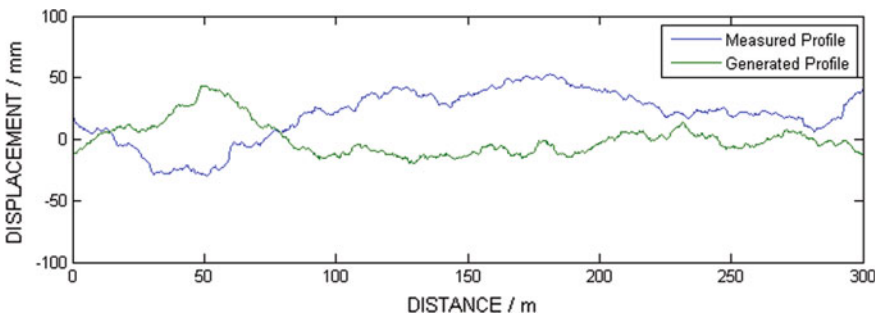


Fig. 4 Model 1 with seed number 584

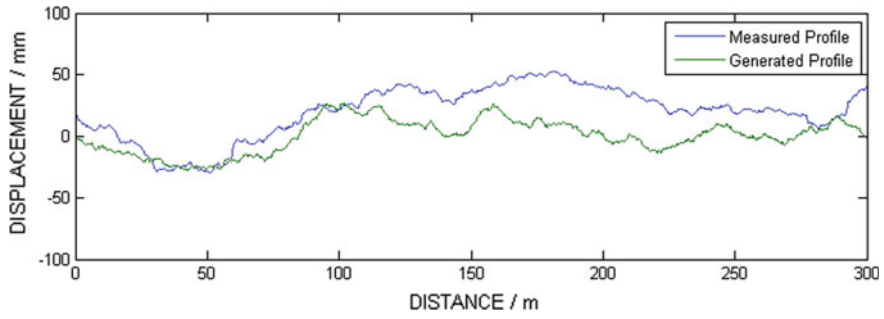


Fig. 5 Model 1 with seed number 811

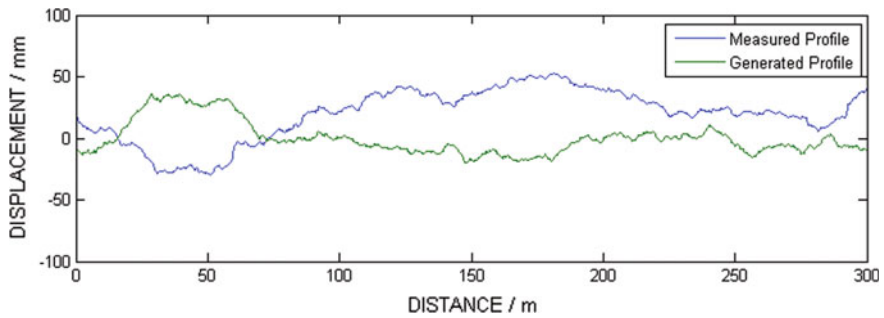


Fig. 6 Model 1 with seed number 838

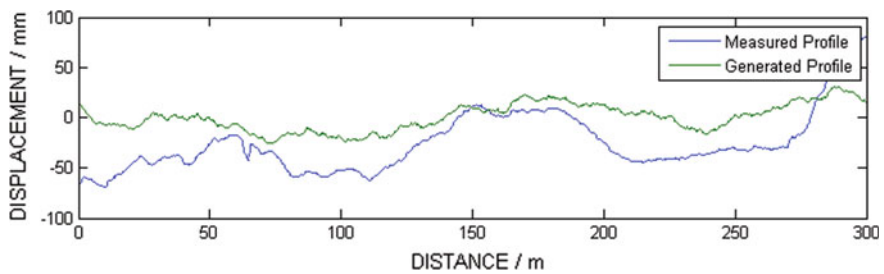


Fig. 7 Model 2 with seed number 3,727

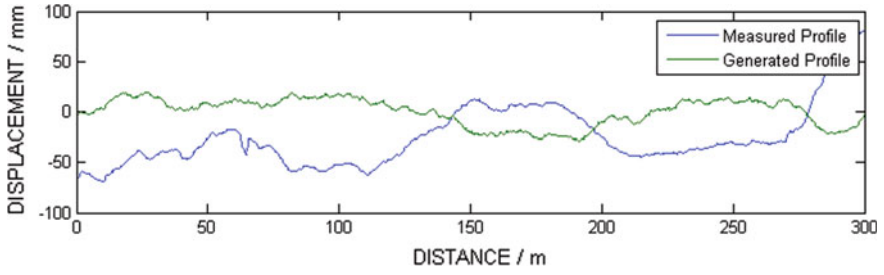


Fig. 8 Model 2 with seed number 3,774

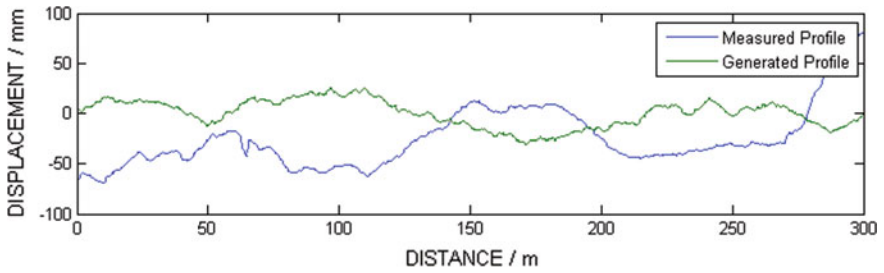


Fig. 9 Model 2 with seed number 4,964

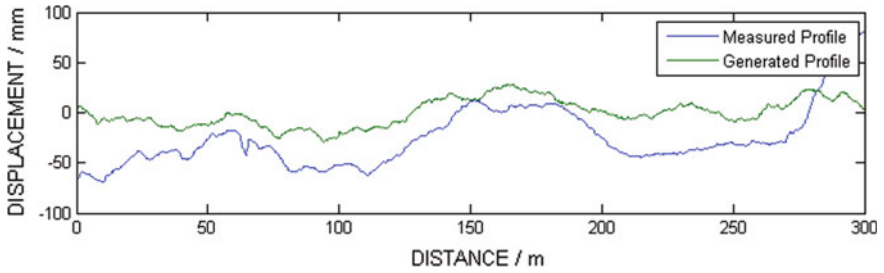


Fig. 10 Model 2 with seed number 5,117

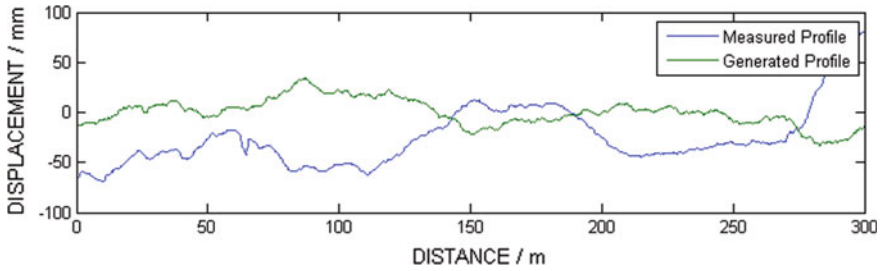


Fig. 11 Model 2 with seed number 6,006

7 Conclusion

All 56 road profiles that had been generated are applicable to be use in WLPPM. Although, Model 2 with seed number of 3,727 produced the same IRI as the reference profile, is mainly suggested to be used. It represents the new road profile for respecting IRI value. Otherwise, Model 1 with seed number 838 have the closest correlation coefficient to 1 compare to Model 2 (seed number of 3,727) is suggested due to it more duplicating the reference road profile characteristic. This is because the nearer the correlation coefficient to -1 or 1 , the closer the shape of generating road profile to measured road profile is produced. Thus, there is no much variation of dynamic loading will be simulated when it used compare when the reference road profile is used.

Acknowledgments The authors wish to thank the KUMPULAN IKRAM Sdn. Bhd. for the supplied of road scanner data measurement and in particular, their staff who assisted the research. Also thanks to the Universiti Tun Hussein Onn Malaysia for giving the Short Term Grant to doing this research.

References

1. C.J. Dodds, J.D. Robson, The description of road surface roughness. *J. Sound Vibr.* **31**(2), 175–183 (1973)
2. D. Cebon, *Handbook of Vehicle—Road Interaction* (Taylor & Francis Group, London, 2006), pp 22–25
3. D.Y. Downham, F.D. Roberts, Multiplicative congruential pseudo-random number generators. *Comput. J.* **10**(1), 74–77 (1967)
4. Y.H. Huang, *Pavement Analysis and Design*, 2nd edn. (Prentice Hall Inc, New Jersey, 2012)
5. M. Hardy, D. Cebon, An investigation of anti-lock braking strategies for heavy goods vehicles. *J. Automobile Eng.* **209**(4), 263–271 (1995)
6. A.C. Collop, Effect of traffic and temperature on flexible pavement wear, Ph.D thesis, Cambridge University Engineering Department, Cambridge (1994)

Author Index

A

Ab Rahim, Ab. Mughni B., 1177
Abd Rahim, Ahmad Fitri B., 973
Abduh, Muhamad, 137
Abdul Awal, Abu Sufian Muhammad, 109
Abdul Ghani, Abdul Halim, 905
Abdul Samad, A.A., 589
Abdullah, Ahmad Sharim, 219
Abdullah, Maureena Jurliel, 51
Abdullah, Noraspalela, 17
Adnan, Azlan, 821
Adnan, Muhammad Akram, 1177, 1209
Ahmad, Asmalia Che, 301
Ahmad, Faiz, 831, 927
Ahmad, Farah Hafifee, 577
Ahmad Jalani, Ahmad Zulfaris, 905
Ahmad, Juhaizad, 727
Ahmad, Juraidah, 873
Ahmad, Sabarinah Sh., 231
Ahmad, Zakiah, 51, 741, 855, 1031, 1095, 1107, 1117
Akasah, Zainal Abidin, 177, 273, 313
Akbar, Anis Rosniza Nizam, 149
Akhir, Nor Solehah Md, 199
Akhtar, Majid Niaz, 927
Albakri, Nur Arinah Binti Hisham, 1019
Alferjani, M.B.S., 589
Ali, Maisarah, 333, 1075
Ali, Mohd Fozi, 1011
Ali, Ridzuan Mohd, 703
Alisibramulisi, Anizahyati, 779, 1141
Almanar, I.P., 681
Al Sanjery, K.A., 801
Alwee, Sharifah Nur Aina Syed, 321
Amin, Norliyati Mohd, 605, 713, 779
Aminu, Nasiru, 973
Amir, A., 1037, 1043
Ariff, Nor Rima Mohd, 219

Arshad, Ahmad Kamil, 873, 1221, 1231
Arshad, Mohd Fadzil, 87, 439, 727, 741, 905, 1087
Asan, Amran, 273
Ashaari, Yasmin, 447, 1245
Aslam, Muhammad, 927
Awang, Haryati, 469, 557
Azdarpour, Amin, 417
Aziz, Hammad, 831
Aziz, Md. Maniruzzaman A., 1199
Aziz, S., 577
Azmi, A., 577
Azrae, Afifah, 741
Azreen, I., 989

B

Bahari, Noor Iza, 1221
Baharudin, Fauzi, 407, 439, 501, 1011
Baharudin, Khairul Salleh, 1095
Bakar, Afidah binti Abu, 605
Bakar, Ilyani Akmar Abu, 779
Bakar, Ismail Bin, 533
Baki, A., 1037
Bakir, A.A., 681
Basri, Zummy Dahria Mohamed, 1011
Bery, Andy Anderson, 459
Bilong, Benard, 905
Buhari, Rosnawati, 1269
Burhanudin, Mohd Khairy, 691

C

Chan, Chee-Ming, 427
Chik, Tuan Norhayati Tuan, 3

D

Daud, Atikah Fatma Md, 51
David, Alicia, 469

Dayana, K., 895
Doraisamy, Sunitha V., 313

E

Elrawaff, Blkasem S., 589
Elzaroug, Omer, 589
Endut, Intan Rohani, 243, 253
Ezechi, Ezerie Henry, 963

F

Faizal, Alina. M., 963
Feng, Yuantian, 625

G

Ghani, Abdul Halim Abdul, 439
Ghazali, Norilmi, 1129
Goh, Hui Hwang, 189, 951
Goh, Kai Chen, 189, 951
Gungat, Lillian, 1187

H

Habib, Amir Izzuddin, 1065
Habib, Noor Zainab, 915
Hadi, Basharudin Abdul, 567
Hainin, Mohd Rosli, 1199
Halip, Azianabiha A., 1011
Hamdi, Mohd Maiziz Bin Fishol, 37
Hamid, Abdul Rahim Abdul, 727
Hamidah, M.S., 613
Hamid, Hanizah Ab., 767, 821
Hamidi, Hossien, 417
Hamid, Nur Amalina Abdul, 87
Hamid, Shaharin, 1153
Hammad, Dabo Baba, 789
Hamzah, Hairul Aini, 333, 1075
Hamzah, Meor Othman, 1187
Hamzah, Nor Hanisah, 427
Hamzah, Siti Hawa, 17, 29, 37, 605
Haniff, Mohammad, 865
Harun, A.M., 989
Harun, Mohd Shafee, 407, 501
Hashim, Mohd Hisbany Bin Mohd, 37
Hashim, Soenita, 577
Hasim, Sulaiman, 779
Hassan, Rohana, 1107, 1129, 1141, 1153, 1163
Henry, Ezerie, 973
Hussein, Edelin, 301
Hyie, Koay Mei, 811

I

Ibrahim, Aniza, 545
Ibrahim, Azmi, 767, 821, 1095
Ibrahim, Siti Halipah, 211
Ilias, Muhammad Hazmi Bin, 1209

Imran Ghazali, Mohd., 3
Isa, Che Maznah Mat, 121, 287
Isa, Mohamed Hasnain, 973
Ishak, Annuar, 895, 937
Ismail, Faridah, 321
Ismail, Mohd Fauzi, 681
Ismail, Mohd Nasrul Naim, 691
Ismail, Norsalisma, 219
Ismail, Nurliyana, 1087
Ismail, Rozaina, 79, 767, 821
Ismail, Wan Zuriea Wan, 231
Ismail, Zulhabri, 1053
Ithnin, Zarina, 231

J

Jaafar, Hidayani, 885
Jaafar, Othman, 545
Jaini, Zainorizuan Mohd, 97, 625, 691
Jani, Janmaizatulriah, 1011
Jaya, N., 1043
Jeni, Mohamad Luthfi Ahmad, 691
Junin, Radzuan, 417

K

Kadir, Mariyana Aida Ab, 109
Kaliwon, Babby Freskayani Izyani, 1003
Kamaruddin, Ibrahim, 915
Kamarudin, Faizah, 439, 873, 905
Kamarudin, Hikmah, 231
Kamarun, Dzraini, 873
Kassim, A.S.M., 347
Khalid, Norazlan, 439, 501, 577, 905
Krishnamoorthy, Renga Rao, 703
Kutty, Shamsul Rahman Mohamed, 963, 973, 1065

L

Lazi, Mohd Khairul Afzan Mohd, 1255
Lee, Hsiu Eik, 387
Lee, Mai Woon, 865
Lee, Wei-Koon, 359, 373
Liew, Mohd Shahir, 387, 639
Ly, Heng, 263
Lynna Juliana, J., 397

M

Madun, Aziman, 477
Mahat, Noor Aisyah Asyikin, 321
Mahbub, Rohana, 163
Mahinder Singh, Santokh Singh A/L, 1199
Mahmood, Mohamad Rusop, 821
Maisham, Mysarah, 149
Makhtar, Ahmad Mahir, 525
Malakahmad, Amirhossein, 1019

- Malek, Marlinda Abdul, 387
 Mamat, Mohamad Hafiz, 937
 Manan, N., 1037
 Mansor, Siti Hajar Binti, 515
 Mardi, Nurul Hani, 387
 Marto, Aminaton, 525
 Masri, Khairil Azman, 1231
 Masrom, Md Asrul Nasid, 189
 Md. Noor, M.J., 447
 Md Daud, Atikah Fatma, 1107
 Memon, Aftab Hameed, 199
 Memon, Neelam, 109
 Mohamad Ezad Hafez, M.P., 613
 Mohamad, Habib Musa, 487
 Mohamed Jais, I.B., 447
 Mohamad, Mazlina, 87
 Mohamad, N., 589
 Mohamad, Syed Burhanuddin Hilmi Syed, 177
 Mohammadian, Erfan, 417
 Mohammad, Mohammad Fadhil, 149, 163, 301
 Mohammad, Shahrin, 651
 Mohd Faizal, Md Jaafar, 613
 Mohd Sani, Mohd Syahrul Hisyam, 651
 Mohd Yusof, Noorsuhana, 845
 Mohd-Zaki, Z., 1037, 1043
 Mokhtar, Shahrul Niza, 625, 691
 Motamedi, Shervin, 567
 Muftah, Fadhlhartini, 651
 Muhamad, Norhamidi, 927
 Muhamad, Nurul Huda, 301
 Muhammad Habibuddin, A., 397
 Muhd Norhasri, Muhd Sidek, 613
 Muhsan, Ali S., 927
 Mukhlisin, Muhammad, 545
 Mukri, Mazidah, 439, 577, 905
 Murad, Mardziah Che, 811
 Musa, Muhamad Faiz, 163
 Mustafa, Masria, 1245, 1255
 Mustaffa, Nur Kamaliah, 51
- N**
 Nagapan, Sasitharan, 199
 Najib, Latifah Mohd, 779
 Napiah, Madzalan, 915
 Naru, Noor Akma Mohd, 557
 Nasir, Siti Rashidah Mohd, 121
 Nawi, Mohd Nasrun Mohd, 211
 Nazir, Muhammad Shahid, 927
 Nazri, Nurul Aida, 1053
 Nifa, Faizatul Akmar Abdul, 211
 Nik Roselina, Nik Roseley, 811
 Noorli, Ismail, 613
- Noor, Mohd Jamaludin Md, 567
 Noor, N.M., 347
 Nordin, Mohd Azda B., 1177
 Nur Fadzeelah, Abu Kassim, 397
 Nurmin, B., 989
 Nuruddin, Muhd Fadhil, 789, 1065
- O**
 Oladokun, Majeed, 333, 1075
 Oluwasola, Ebenezer Akin, 1199
 Omar, M.A., 927
 Osman, Ahmad Rasidi, 651
 Osman, Samsul Baharin, 333, 1075
 Othman, Mohd Nazrin, 1031
- P**
 Peansupap, Vachara, 263
 Pothan, L.A., 855
 Pratama, Aditya, 137
 Preece, Christopher Nigel, 121, 287
 Puaad, M.B.F.M., 1117
 Puteh, Saifullizam, 1269
- R**
 Rahim, Jamilah Abd., 29
 Rahim, Nor Azira Abd., 97
 Rahman, Ismail Abdul, 65, 199
 Rahman, Mohammad Ashraf Abdul, 177
 Rahman, Norashidah Abd., 97
 Rajhan, Nurul Husna, 767
 Rajisha, K.R., 855
 Ramlah Mohd, Tajuddin, 1031
 Ramli, Norain, 845
 Rani, Nur Izzati Ab., 121, 287
 Rashid, Amirul Abd, 865
 Rashid, Robiah Abdul, 219
 Rasid, Zainudin A., 667
 Rassam, Mohamed, 1095
 Razak, Siti Aisyah Abd., 97
 Raza, Muhammad Rafi, 927
 Razlan, Mohd Azran, 651
 Ricky, Lee Nyuk San, 989
 Rohani, Munzilah Md, 1269
 Rosalam, S., 989
 Rosdi, Nurain, 1163
 Roslan, Ili Izzahar, 1141
 Roslee, Nur Syafiqah, 407
 Rusop, Mohamad, 895, 937
- S**
 Saad, Nor Hayati, 681, 865
 Saad, Rosli, 459

Saedon, Nursyahidah Binti, 533
 Saffari, Pooya, 567
 Said, Mohd Jazlan Mad, 477
 Salim, Wan Safizah Wan, 639
 Salleh, Md Noor, 333, 1075
 Saman, Hamidah Mohd, 29, 65, 121, 287, 1087
 Samsuddin, Niza, 333, 1075
 Saurdi, Ishak, 895, 937
 Seblan, Azali Akhbar, 1269
 Seman, Mazlan Abu, 625
 Seow, Ta Wee, 189, 951
 Seri, Nurul Atikah, 1153
 Shaffie, Ekarizan, 873
 Shafie, A'fza, 639
 Shafiq, Nasir, 789, 1019, 1065
 Shahril, Y., 989
 Shazni, Muhammad Aniq, 865
 Sheng, Daniel Bien Chia, 865
 Shih, Teh Aun, 865
 Shuib, N.A., 681
 Shukor, M.S.M., 757
 Sia, J.Y., 801
 Sidek, Norbaya, 905
 Sobri, Mohd Suhelmiey, 17
 Sofwan, Nurzawani Binti Md, 253
 Sulaiman, Norliana, 1177
 Suliman, Nurul Huda binti, 605
 Sulong, Abu Bakar, 927
 Sunar, Norshuhaila Mohamed , 347
 Suraya Hani, Adnan, 65

T

Talib, Noor Amalia, 149
 Tamim, Nur Nabila Mohd, 219
 Tan, Choy Soon, 525
 Tey, Jia Sin, 189
 Thomas, Sabu, 855
 Tongthong, Tanit, 263
 Tuan Resdi, Tuan Asmaa, 359

U

Umar, Salihi Ibrahim, 973

W

Wahid, Marfiah Ab., 1011
 Wahid, Mohamad Firdaus Abdul, 811
 Wen, Ung Shu, 525

Y

Yabi, Shurl, 3
 Yahya, Zahrullaili, 1221
 Yamani, Shaikh Abdul Karim, 1117
 Yap, Aaron Boon Kian, 189, 951
 Yasin, Mohd Hanafie, 1163
 Yee, Lim Lion, 109
 Yen, Lim Mei, 525
 Yunus, Riduan, 313
 Yusoff, Marina, 1141
 Yusoff, Nor Azizi, 3
 Yusof, Mohd Reeza, 163
 Yusof, Zulina Mohd, 501
 Yusuf, Ahmad Idzwan, 713

Z

Zaharuddin, NurHidayah Aqilla binti, 373
 Zahrim, A.Y., 989
 Zaini, Afzan Ahmad, 243, 253
 Zainorabidin, Adnan, 477, 487, 515, 533
 Zamahidi, Nurul Fasiah, 79
 Zamli, Abdullah Omar Abdullah, 1129
 Zia-ul-Mustafa, Muhammad, 831
 Zin, Mazni Mat, 1087
 Zolkefle, Siti Nurul Aini, 487
 Zoolfakar, Md Redzuan, 757
 Zubair, Ahmad Faiz, 681
 Zulkifli, Assrul Reedza, 727